Data quality metrics and time series methods for health surveillance systems

A dissertation submitted by

Ryan Benner Simpson

in partial fulfillment of the requirements

for the degree of

Doctor of Philosophy

in

Nutrition Epidemiology and Data Science

TUFTS UNIVERSITY

June 2022

THESIS COMMITTEE CHAIR

Elena N. Naumova, Ph.D.

THESIS COMMITTEE MEMBERS

Alexandra V. Kulinkina, Ph.D.

Fernando Ona, Ph.D.

José M. Ordovás, Ph.D.

Summary

One in six Americans experience foodborne or waterborne illnesses each year. In 2018 alone, these illnesses culminated in ~$17.6 billion in medical costs, food waste, and retailer lost revenue with expenses growing by ~2-3% annually. Despite fiscal and health burdens, federal agencies have not refined data collection and reporting protocols to ensure its timeliness, usability, and granularity for monitoring, tracking, and predicting emerging and seasonal illnesses and outbreaks. In addition, published literature underutilize time series methods that harness the full potential of time-referenced surveillance data. These studies fail to explain how data quality limitations impact the reliability of temporal trend and seasonality estimations of illnesses.

As digital technologies curate data at ever-faster speeds, health surveillance systems face growing volumes of records on persistent and emerging health threats. This emphasizes the importance of well-defined criteria to collect, harmonize, store, and disseminate data for public reuse. These standards must ensure the granularity, usability, and longevity of data throughout its lifecycle. Concurrently, data curators must disseminate records in a structure conducive for external users to describe, explain, and predict spatiotemporal patterns of health outcomes; data curation must be part of a broader strategic plan to leverage data for real-time monitoring and near-term forecasting of recurring and emerging health threats. This calls for a standardized data workflow facilitating collaboration between data curators and modelers conducting public health surveillance.

My overarching objective was to create an assemble of data quality metrics and time series methods to describe, explain, and predict foodborne and waterborne illnesses and outbreaks using time-referenced, publicly available surveillance data. This objective stems from a systematic literature review demonstrating that public health agencies have few comprehensive strategies for conducting data credibility checks and standardized analyses on enteric illnesses. To achieve this goal, I produced three collections of works conducted on international, national, regional, and local publicly available health surveillance databases.

My first collection proposed quality metrics for time-referenced data to enhance modelers' comprehension of limitations in describing illness trends and seasonality. I demonstrated the utility of metrics using global virological influenza records reported by the World Health Organization's (WHO's) FluNet in 1995-2022. In my second collection, I adopted and refined existing methods for estimating seasonal signatures and synchronization of temporal patterns for enteric illnesses. I demonstrated methods' utility using illnesses and outbreaks reported by the United States (US) Centers for Disease Control and Prevention's (CDC's) Foodborne Diseases Outbreak Surveillance Network (FoodNet) in 1996-2017 and National Outbreak Reporting System (NORS) in 2009-2019. In my final collection, I adapted methods to examine temporal patterns of non-seasonal outbreak threats for *Vibrio cholerae* in emergency settings. These works explored spatiotemporal patterns of cholera illnesses across Yemeni governorates in 2016-2019 using a variety of harmonized data streams.

This data curation-to-visualization systematic workflow assists public health professionals to translate data into actionable information while recognizing its limitations and usability for modeling purposes. Understanding and predicting seasonal and emerging infections' spatiotemporal patterns allow for early outbreak detection and improve the timeliness and effectiveness of proactive management strategies. This approach emphasizes the importance of data quality, usability, and longevity in the era of precision public health.

Acknowledgements

This work would not have been possible without the mentorship, support, collaboration, and love of countless advisors, faculty members, colleagues, friends, and family members.

Dr. Elena Naumova, my advisor and Thesis Committee Chair, you have offered countless hours of mentorship, guidance, and wisdom over our many years together. Since the moment I entered your office, you have fostered an environment welcome to questions, problem solving, and curiosity. You sparked a curiosity for how the world works and operates through the lens of biostatistics and mathematics while delving into crucial principles of data ethics, morals, and human philosophy. Your training as a researcher and teacher has provided countless opportunities for my future career, where I hope to model your leadership, mentorship, and strength. I am forever grateful for your guidance, encouragement, support, and incredible friendship.

I am grateful for the support of my Thesis Committee members, including Dr. Alexandra V. Kulinkina, Dr. Fernando Ona, and Dr. José M. Ordovás. Throughout my doctoral process, you have provided new perspectives on ways to approach the complex and multifaceted topic of public health data and modeling. Your comments have pushed my works to consider larger real-world implications of data quality and credibility imperative for my future professional career. Furthermore, I appreciate your consistent flexibility in scheduling our meetings amidst international travels and across numerous time zone differences.

The following research would not have been possible without the collaboration of numerous fellow researchers at the Tufts University Friedman School. The presented manuscripts were developed in partnership with Dr. Tania Alarcon Falconi, Dr. Meghan Hartwick, Lieutenant Colonel Jarrod McGee, Ms. Bingjie Zhou, Ms. Jordyn Gottlieb, Ms. Emily Sanchez, Ms. Lauren Sallade, Ms. Yutong Zhang, Ms. Amy Gelfand, Ms. Maia Tarnas, Ms. Sofia Babool, Ms. Paulina Kaminski, Ms. Brianna Lauren, Mr. Michael Perkins, Mr. Kees Schipper, Mr. James McCann, and Mr. Kyle Monahan. Research efforts were also performed in close discussion and collaboration with Ms. Aishwarya Venkat, Ms. Xu Jiang, Ms. Abigail Larson, Ms. Alissa Ebel, Ms. Sirjana Shakya, and Ms. Ziming Dou. I cannot express how thankful I am for your support, feedback, guidance, and friendship throughout this process.

A warm-hearted thank you goes out to my dearest friends, Max, Allec, Kees, Emily, Kristin, Maia, and the FC Hammer soccer community, for providing a sounding board of reason in my most challenging of times. You have helped me, knowingly and unknowingly, embrace more than I ever thought was possible just by the nature of your kindness, work ethic, and dedication. Our shared laughs, hopes, dreams, tears, and memories have defined some of the most rewarding years of my life.

Finally, a very special thank you goes out to my family, Paulina, Jon, Katie, Tim, and Cheryl, for their endless compassion, motivation, guidance, and love. Six years ago, I was terrified of life-long challenges with reading, vision, and memory. You have consistently supported my recovery process and provided the encouragement needed to help on this road of self-discovery. None of this would have been possible without you. Here’s to making the improbable become possible.

Financial Support and Declarations

The research presented in this dissertation were based upon works supported in part by:

1. *The Office of the Director of National Intelligence (ODNI), Intelligence Advanced Research Projects Activity (IARPA)*, via 2017-17072100002. The views and conclusions contained herein are those of the authors and should not be interpreted as necessarily representing the official policies, either expressed or implied, of ODNI, IARPA, or the U.S. Government. The U.S. Government is authorized to reproduce and distribute reprints for governmental purposes notwithstanding any copyright annotation therein.

2. *The United States Department of Agriculture (USDA) National Institute of Food and Agriculture (NIFA)* Cooperative State Research, Education, and Extension Service Fellowship, via 2020-38420-30724.

3. *The United States Agency for International Development (USAID), Strategies to Prevent (STOP) Spillover Project*. The contents are the responsibility of STOP Spillover and do not necessarily reflect the views of USAID or the United States Government.

4. *The National Science Foundation (NSF)* Innovations of Graduate Education Program's SOLution-oriented, Student-Initiated, Computationally-Enriched (SOLSTICE) approach, via 1855886.

5. *The Tufts University Data Intensive Science Center (DISC)* Seed Grant on Real-Time Forecasts for COVID-19 Laboratory Confirmed Cases via N306204.

I declared no conflicts of interest for all submitted, accepted, and published manuscripts. I used only publicly available data sources to conduct research and provide references for each data source at the end of each chapter. I did not require permissions of the Tufts Institutional Review Board for the use of human or animal test subjects.

Abbreviations

A(H1)	Influenza A(H1) Strain Positive Cases
A(H1N1)	Influenza A(H1N1) Pandemic 2009 Strain Positive Cases
A(H3)	Influenza A(H3) Strain Positive Cases
A(H5)	Influenza A(H5) Strain Positive Cases
A(UNS)	Influenza A Strain, Unsubtyped Strain Positive Cases
ACLED	Armed Conflict Location and Event Data Project
ACTOR	Availability, Capacity, Timeliness, Operability, and Reliability Principles
AFRO	African Region of the World Health Organization
AIC	Akaike's Information Criterion
AMP	Amplitude
API	Application Programming Interface
ARI	Acute Respiratory Illness
ARIMA	Autoregressive Integrated Moving Average
B(YAM)	Influenza B(Yamagata) Strain Positive Cases
B(VIC)	Influenza B(Victoria) Strain Positive Cases
B(UND)	Influenza B Strain, Undetermined Strain Positive Cases
BAC	*Bacillus* Outbreaks
BIC	Bayesian Information Criterion
CA	California
CAM/CAMP	*Campylobacter* Infections or Outbreaks
CDC	United States Centers for Disease Control and Prevention
CI	Confidence Interval
CID	Citation Identifier
CIG	*Ciguatoxin* Outbreaks
CO	Colorado
COVID-19	Novel Coronavirus 2019 Pandemic
CLO	*Clostridium* Outbreaks
cph	Cases Per 100,000 Persons
cpm	Cases Per 1,000,000 Persons
CSO	Central Statistical Organization
CSSE	Center for Systems Science and Engineering
CT	Connecticut
CRY/CRYP	*Cryptosporidium* Infections or Outbreaks
CYC/CYCL	*Cyclospora* Infections or Outbreaks
DALY	Disability Adjusted Life Year
DFWED	Division of Foodborne, Waterborne, and Environmental Diseases
DHEPC	Domestic General Government Health Expenditure Per Capita
DoW	Day-of-the-Week
dpm	Deaths Per 1,000,000 Persons
DTM	Displacement Tracking Matrix
ECOL	Shiga-Toxin Producing *Escherichia Coli* Infections
eDEWS	Electronic Disease Early Warning System
eFORS	Electronic Foodborne Outbreak Reporting System
EMR	Electronic Medical Records
EMRO	Eastern Mediterranean Region of the World Health Organization
ER	Emergency Room
ES	Effect Size
ESC	*Escherichia* Outbreaks

ETSL	Effective Time Series Length
EURO	European Region of the World Health Organization
FDA	US Food and Drug Administration
FDOSS	Foodborne Disease Outbreak Surveillance System
FERG	Foodborne Disease Burden Epidemiology Reference Group
FLUA	Influenza A Virus Positive Cases
FLUB	Influenza B Virus Positive Cases
FoodNet	Foodborne Disease Active Surveillance Network
FPM	Influenza Health Facilities Per Million Persons
FSIS	Food Safety Inspection Service
GA	Georgia
GAO	US Government Accountability Office
GISN	Global Influenza Surveillance Network
GISRS	Global Influenza Surveillance and Response System
GLM	Generalized Linear Model
GNIPC	Gross National Income Per Capita
GTFCC	Global Task Force on Cholera Control
HEP	*Hepatitis* Outbreaks
HumData	Humanitarian Data Exchange
ICD	International Classification of Diseases and Related Health Problems
IDB	US Census Bureau International Data Base
Iden	Identity Distribution
ILI	Influenza-Like Illness
Insee	Institut national de la statistique et des etudes economiques
IOM	International Organization of Migration
IQR	Interquartile Range
IRR	Incidence Risk Ratio
JHU	John Hopkins University
KZ	Kolmogorov Zurbenko
LIS/LIST	*Listeria* Infections or Outbreaks
ln	Natural Logarithm
LOESS	Locally Estimated Scatterplot Smoothing
M&E	Monitoring & Evaluation
MA	Massachusetts
MD	Maryland
MDPH	Massachusetts Department of Public Health
MN	Minnesota
MOH	Ministry of Health
NBHR	Negative Binomial Harmonic Regression
NCEZID	National Center for Emerging and Zoonotic Infectious Diseases
NEG	Influenza Total Negative Cases
NIC	National Influenza Centre
NM	New Mexico
NOR	*Norovirus* Outbreaks
NORS	National Outbreak Reporting System
NPST	Non-Parametric Seasonality Tests
NY	New York
OCHA	Office for the Coordination of Humanitarian Affairs
OOPHE%	% Out-of-Pocket Health Expenditure
OR	Oregon

PAHO	Regions of the Americas of the World Health Organization
PCR	Polymerase Chain Reaction
pFORS	Paper-Based Foodborne Outbreak Reporting System
POS	Influenza Total Positive Cases
PRISMA	Preferred Reporting Items for Systematic Reviews and Meta Analyses
PT	Peak Timing
R^+	Set of All Positive Real Numbers
RMSE	Root Mean Square Error
RR	Relative Risk
SAL/SALM	*Salmonella* Infections or Outbreaks
SAP	*Sapovirus* or Outbreaks
SARI	Severe Acute Respiratory Illness
SARIMA	Seasonal Autoregression Integrated Moving Average
SDGs	Sustainable Development Goals
SEARO	Southeastern Asian Region of the World Health Organization
SHI/SHIG	*Shigella* Infections or Outbreaks
SPE	Influenza Specimens Collected
STA	*Staphylococcus* Oubreaks
STEC	Shiga Toxin-Producing *Escherichia Coli* Infections
STL	Seasonal Trend Decomposition
TC	Trend Component
TES	Influenza Specimens Processed or Tests
TN	Tennessee
tpm	Tests Per 1,000,000 Persons
Tran	Natural Logarithm Transformed Distribution
TRI	*Trichinella* Outbreaks
TSL	Time Series Length
UN	United Nations
US/USA	United States of America
USD	United States Dollars
USDA	US Department of Agriculture
VIB or VIBR	*Vibrio* Infections or Outbreaks
WASH	Waster, Sanitation, and Hygiene
WDOSS	Waterborne Disease and Outbreak Surveillance System
WFP	World Food Programme
WHO	World Health Organization
WPRO	Western Pacific Region of the World Health Organization
YDP	Yemen Data Project
YERS	*Yersinia* Infections

Table of Contents

Summary ii

Acknowledgements iii

Financial Support and Declarations iv

Abbreviations v

List of Figures x

List of Tables xii

Chapter 1. Health Surveillance and Data Quality 2

1.1. Public health surveillance and data longevity 2

1.2. Research objectives: Data access to action 5

1.3. References 8

Chapter 2. A Review of Time Series Methods in Nutrition Literature 11

2.1. Foodborne illness burdens and surveillance gaps 11

2.2. Investigating seasonal patterns in enteric infections: a systematic review of time series methods 13

2.3. Conclusion: Greater attention needed on data quality and usage 14

2.4. References 14

Chapter 3. Data Quality for Modeling Purposes 17

3.1. Influenza surveillance: A gold standard for data quality metrics 17

3.2. The ACTOR Principles for assessing time series data quality 20

3.3. Case Study – An example using FluNet in 1995-2021 31

3.4. Completeness of open access FluNet influenza surveillance data for Pan-America in 2005-2019 53

3.5. Conclusions: Socioeconomic and geographic patterns of data quality and seasonality 54

3.6. References 59

Chapter 4. Trends and Seasonality Features of Foodborne Illnesses and Outbreaks 69

4.1. Standardizing analytical workflows for modeling seasonality features 69

4.2. Seasonal synchronization of foodborne outbreaks in the United States, 1996–2017 70

4.3. An analecta of visualizations for foodborne illness trends and seasonality 70

4.4. Modeling outbreak severity and its temporal patterns 71

4.5. Case Study – An example using CDC NORS in 2009-2019 74

4.6. Conclusions: Further research for emerging health threats 89

4.7. References 90

Chapter 5. Adapting Time Series Methods for Emerging Threats 95

5.1. Challenges of modeling aperiodic emerging health threats 95

5.2. Dynamic mapping of cholera spread and conflict severity during the Yemeni Civil War, 2016-2019 98
5.3. Signatures of cholera outbreak during the Yemeni Civil War, 2016-2019 99
5.4. Conclusion: Applications of methods beyond enteric infections 99
5.5. Critical periods, critical time points and day-of-the-week effects in COVID-19 surveillance data: an example in Middlesex County, Massachusetts, USA 100
5.6. References 100

Chapter 6. Steps Towards Precision Public Health 105

Appendices 108

A. Supplementary Tables S1-S41 and Supplementary Figures S1-S8 from the case study evaluating *ACTOR* data quality principles and metrics using FluNet in 1995-2021 108

B. Supplementary Tables S1-S7 and Supplementary Figure S1 from the case study evaluating disease outbreak severity using CDC NORS in 2009-2019 223

Manuscripts 239

M.1. Simpson, R. B., et. al. "Investigating seasonal patterns in enteric infections: a systematic review of time series methods." *Epidemiology and Infection* (2022): 1-25. 239
M.2. Simpson, R. B., et. al. "Completeness of open access FluNet influenza surveillance data for Pan-America in 2005-2019." *Scientific Reports* 11, no. 1 (2021): 1-17. 252
M.3. Simpson, R. B., et al. "Seasonal synchronization of foodborne outbreaks in the United States, 1996–2017." *Scientific Reports* 10, no. 1 (2020): 1-16. 269
M.4. Simpson, R. B., et. al. "An analecta of visualizations for foodborne illness trends and seasonality." *Scientific Data* 7, no. 1 (2020): 1-15. 285
M.5. Simpson, R. B., et al. "Dynamic mapping of cholera spread and conflict severity during the Yemeni Civil War, 2016-2019." *Journal of Public Health Policy* (2022). 300
M.6. Simpson, R.B., et. al. "Signatures of cholera outbreak during the Yemeni Civil War, 2016-2019." *International Journal of Environmental Research and Public Health* 19, no. 1 (2021): 378. 318
M.7. Simpson, R. B., et. al. "Critical periods, critical time points and day-of-the-week effects in COVID-19 surveillance data: an example in Middlesex County, Massachusetts, USA." *International Journal of Environmental Research and Public Health* 19, no. 3 (2022): 1321. 347

List of Figures

Figure 1. A shared axis, multi-panel plot of the relationship between log-transformed values of Member State 2021 population estimates, influenza testing facilities, and testing facilities per million persons. 37

Figure 2. A shared axis, multi-panel heatmap of the *extent* for 6 WHO-defined regions and worldwide for 14 influenza variables, including 6 testing outcomes (specimens collected (SPE), specimens processed or tests (TES), influenza A positives (FLUA), influenza B positives (FLUB), total positives (POS), and total negatives (NEG)) and 8 influenza strains and subtypes (A(H1), A(H1N1)pdm09, A(H3), A(H5), A(Unsubtyped), B(Yamagata), B(Victoria), and B(Undetermined) positives). 39

Figure 3. A shared axis, multi-panel heatmap of the *average completeness* for 6 WHO-defined regions and worldwide for 14 influenza variables. 42

Figure 4. A shared axis, multi-panel heatmap of the *annual completeness* for 6 WHO-defined regions and worldwide for total positives and negatives. 43

Figure 5. A shared axis, multi-panel heatmap of the *annual completeness* for 6 WHO-defined regions and worldwide for A(Unsubtyped) and A(H5) positives. 44

Figure 6. A shared axis, multi-panel heatmap of the *seasonal completeness* for 6 WHO-defined regions and worldwide for total positives. 45

Figure 7. A shared axis, multi-panel heatmap of the *reporting lag* for 6 WHO-defined regions and worldwide for 14 influenza variables. 48

Figure 8. Shared axis, multi-panel plot describing Member States' latitude, seasonal peak timing of influenza tests, GNIPC, and *average completeness* using FluNet data reported in 1995-2022. 56

Figure 9. Shared axis, multi-panel plot describing Member States' latitude, seasonal peak timing of total influenza positives, GNIPC, and *average completeness* using FluNet data reported in 1995-2022. 56

Figure 10. Shared axis, multi-panel plot describing Member States' latitude, seasonal peak timing of Influenza A positives, GNIPC, and *average completeness* using FluNet data reported in 1995-2022. 57

Figure 11. Shared axis, multi-panel plot describing Member States' latitude, seasonal peak timing of Influenza B positives, GNIPC, and *average completeness* using FluNet data reported in 1995-2022. 57

Figure 12. Shared axis, multi-panel plot describing Member States' influenza testing facilities per million persons by latitude, average total positives' *completeness*, and GNIPC (left) and by latitude, WHO-defined region, and national population (right) in 1995-2022. 58

Figure 13. A multi-panel plot where pyramids describe the interrelationship between case volume, outbreak duration, and illness intensity to define foodborne outbreak severity. 77

Figure 14. Multi-panel, shared-axis plot of outbreak severity scores for 16 contaminants using the National Outbreak Report System (NORS) in 2009-2019. 83

Figure 15. Multi-panel, shared-axis plot of median outbreak severity score by Gregorian calendar year (left panel) and month (right panel). 85

List of Tables

Table 1. Four common principles of Big Data (Volume, Value, Variety, Value), their definition in the context of public health surveillance, and data quality challenges in application to time-referenced health surveillance data. 3

Table 2. A description of the attributes for all publicly-available international, national, regional, and local administrative level datasets used within this dissertation. 6

Table 3. An overview of commonly-cited World Health Organization (WHO) curation quality principles and metrics for the time-referenced global virological influenza surveillance database FluNet. 17

Table 4. Indicators and metrics associated with the *availability* principle for evaluating time-referenced surveillance data quality. 20

Table 5. Indicators and metrics associated with the *capacity* principle for evaluating time-referenced surveillance data quality. 23

Table 6. Indicators and metrics associated with the *timeliness* principle for evaluating time-referenced surveillance data quality. 25

Table 7. Indicators and metrics associated with the *operability* principle for evaluating time-referenced surveillance data quality. 28

Table 8. Indicators and metrics associated with the *reliability* principle for evaluating time-referenced surveillance data quality. 29

Table 9. Cumulative and per Member State National influenza centers (NICs) as well as cumulative, per Member State, and per capita testing facilities reporting data to the WHO's FluNet in 6 regions and 17 influenza transmission zones. 35

Table 10. Descriptions and units of 12 metrics considered for the creation of a foodborne outbreak severity index (11 used; deaths excluded) using data from the National Outbreak Reporting System (NORS) in 2009-2019. 76

Table 11. Summary of 12 metrics considered for the creation of a foodborne outbreak severity index (11 used; deaths excluded) using data from the National Outbreak Reporting System (NORS) in 2009-2019. 79

Table 12. Outbreak severity scores for 16 contaminants using the National Outbreak Report System (NORS) in 2009-2019. 81

Data quality metrics and time series methods for health surveillance systems

Chapter 1. Health Surveillance and Data Quality

1.1. Public health surveillance and data longevity

Public health surveillance is defined as "the ongoing, systematic collection, analysis, and interpretation of health-related data essential to the planning, implementation, and evaluation of public health practice" [1-3]. When monitoring infectious diseases, health surveillance systems aim to inform decision makers on best programming strategies and policy practices to manage, mitigate, and prevent illnesses and outbreaks [4-5]. The modeling of surveillance data informs early outbreak detection, timely intervention strategies, informative health communications, and preemptive health safety protocols to reduce illness morbidity and mortality [6-10]. The extensive time, personnel, and monetary costs required for data curation incentivizes population-level surveillance of infectious diseases. These systems report the frequency of persons having the same illness case definition in the same location per interval of time [10].

Precise public health programming, planning, and responses require high quality data defined by consistent, complete recordkeeping [11]. The timeliness, frequency, and spatial extent of records dictate the specificity of health responses to assist susceptible and infected subpopulations. Data quality also influences the generalizability and reliability of statistical models and findings using longitudinal surveillance systems [12]. Effective management of curated data permits harmonization of multiple data streams such that health outcomes across systems or indicators across disciplines can be linked by time interval and geographic location. To inform the usability of data for modeling purposes, data curators evaluate and report its fidelity and quality using metadata documentation [13-14].

Data modelers utilize metadata summaries to inform modeling assumptions and limitations using information such as sampling techniques, data completeness, and case definitions. Modelers interpret and manipulate data's structure, organization, and contents to answer targeted research hypotheses, yet rarely engage in primary data collection themselves. At the population level, modelers investigate spatiotemporal patterns of illnesses and outbreaks including annual trends, properties of epidemic or pandemic curves, or the timing and intensity of seasonal peaks of infections [15]. These characteristics define signatures or attributes of epidemic curves such as seasonality features (i.e., peak timing, amplitude, duration, etc.) or critical points and

periods (i.e., outbreak onset, peak, resolution, acceleration phases, deceleration phases, etc.). To describe these temporal patterns, modelers must estimate outbreak features and attributes, done most precisely using frequent and timely records reported over long study periods [16-17].

In recent decades, the introduction of digital technologies has accelerated the speed and quantity of computational capacities for information generation [18-20]. Rapid data processing complemented with widespread transition from paper- to electronic-based recordkeeping has increased the lifespan of generated data [21]. This increased longevity introduces newfound discussions about the sustainability of surveillance recordkeeping; public health agencies must structure surveillance systems in a way that promotes growth and expansion as public health concerns change over time. However, data's longevity threatens to exceed the processing capacity of traditional surveillance systems; while public health agencies continue to collect data, health professionals allocate fewer resources and attention to data's fidelity, usability, and sustainability for modeling purposes [22-23]. These challenges have been cited more recently during the emergence of Big Data in public health [24-28]. While Big Data was initially purposed for business and finance analytics, its principles are useful for highlighting data quality challenges of public health surveillance systems (Table 1) [29-30].

Table 1. Four common principles of Big Data (Volume, Value, Variety, Value), their definition in the context of public health surveillance, and data quality challenges in application to time-referenced health surveillance data [24-30].

Principle	Definition for Public Health Surveillance	Data Quality Challenges
Volume	The amount of data that a public health agency can effectively manage and analyze	• Duration of collected/reported surveillance records • Aggregation of spatial or temporal information • Time and monetary expenses of data curation
Velocity	The speed at which a health agency receives, processes, manages, and disseminates surveillance data for public reuse	• Timeliness and thoroughness of credibility checks • Aggregation of spatial or temporal information • Time and monetary expenses of data curation
Variety	The diversity of health outcomes examined within a surveillance system as well as the differences in how these data are structured	• Harmonization of records across data structures • Availability of clear, comprehensive metadata • Replication of data collected for same outcomes
Value	The expected insights and relationships that can be drawn from using surveillance data	• Reliability of models with limited data volumes • Usability of data for modeling over coarse velocities • Interoperability of differing varieties of data types

For example, as the *volume* of data collected and stored increases, public health agencies must consider for how long they will continue reporting on specific outcomes. Maintaining surveillance records requires additional personnel, time, and

storage allocations that increase the expense of data management. These expenses have rippling effects throughout subnational health systems, who are often charged with conducting passive surveillance and distributing data to federal agencies. Yet, shortening the historical duration of available records reduces the *value* of reported data, particularly its reliability, usability, and generalizability for modeling purposes. The removal of historic records reduces sample size when conducting time series analyses, inhibiting modelers' ability to differentiate between true patterns and random noise. Reduced data longevity also removes imperative institutional memory on less common outbreak occurrences like epidemics or pandemics critical for real-time decision-making by health agencies and professionals.

For many infectious disease morbidity-related outcomes, data *volume* and *velocity* go hand in hand. Faster speeds of data collection require personnel-intensive teams to conduct rapid laboratory testing diagnostics and on-the-ground outbreak investigations. Similarly, curation data curators undergo time-intensive data management, organization, and credibility checks as more outbreaks are reported, increasing the cost of surveillance, or delaying its dissemination for public reuse. Public health organizations rely on highly specialized and costly computation software and expertise to maintain refined spatial and temporal data quality. In their absence, cost reduction techniques include aggregating data over coarser spatial domains and time intervals, reducing data's *value* for informing targeted health interventions. Data compression also minimizes the quantity of usable observations, influencing the effective power of time series analyses. Thus, data's *value* for modeling purposes oppositely relates to the *velocity* of data curation and expense of resources needed to manage increased data *volume*.

In addition, *variety* refers to the types of data collected including the diversity of outcomes and their organizational structure within a dataset. Increased ease in collecting data on a diversity of public health topics calls into question reporting standards and protocols for surveillance systems. In fact, this ease often results in many health organizations collecting near-identical data but with unique formats and structures. These decentralized reporting systems become ever-more challenging to align and harmonize records across health outcomes [31]. Furthermore, in the absence of thorough metadata, modelers lack transparency on what outcomes are reported within downloaded data and the intentions of their collection by data curators [32].

This leads to replication of data collection efforts by health agencies, wasting both time and fiscal resources within the public health community [6].

1.2. Research objectives: Data access to action

Data management and analysis plans rarely facilitate collaborations between curators and modelers despite their importance in planning, implementing, and evaluating health practices. While metadata can establish a baseline of information exchange, few surveillance systems providing publicly available data report such summaries. Of those reporting metadata, data quality information often consists of metrics designed for curators' purposes only rather than provide information imperative for model specification. Yet even in industries beyond academia, biostatisticians, data analysts, and research scientists rarely design the sampling strategies and collect the data they analyze. This disconnect undermines the purpose of public health surveillance by dividing data collection and its analysis into two concurrent yet mutually exclusive processes.

My overarching research objective was to create a standardized data workflow to facilitate collaboration between the curators and modelers of public health surveillance data. To achieve this, I proposed an assemble of data quality metrics and refined time series methods to describe, explain, and predict patterns of infectious disease illnesses and outbreaks while accounting for data limitations and usability. This workflow establishes a systematic approach for translating data into actionable information to inform health policies, programs, and strategies while promoting the transparency of data's management, completeness, and fidelity. I achieved this objective through three collections of works conducted on international, national, regional, and local publicly available health surveillance systems. I describe the research aims, data sources, and structure of my dissertation below.

Chapter 2 describes the importance of public health surveillance for monitoring enteric illnesses and outbreaks. First, I describe challenges related to the quality and usability of health surveillance data for monitoring enteric infections, with a specific emphasis to foodborne and waterborne illnesses. This summary describes ongoing and expected economic and human health burdens of these infections internationally and domestically. Next, I provide a systematic review of time series methods in nutrition literature and their limitations for describing, comparing, explaining, and predicting the seasonality of enteric infections. From this review, I illustrate how few

works examine and report on data quality and usability limitations of public health surveillance systems and emphasize the need for greater adoption of time series methods to assess spatiotemporal patterns of enteric illnesses and outbreaks.

Subsequent chapters respond to these knowledge gaps by proposing metrics for estimating the quality and usability of surveillance data (Chapter 3) and discussing the importance of adopting time series methods for illnesses with periodic and aperiodic patterns (Chapters 4 and 5). In each chapter, I use 1-2 public health surveillance systems to conduct my research beginning with internationally reported data in Chapter 3 and later more spatially refined, locally reported data in Chapter 5 (Table 2). I chose publicly available data for secondary analyses to promote the generalizability and reproducibility of proposed metrics and methods. Additionally, I selected surveillance systems of varying spatial resolutions to illustrate the applicability of my analytical workflow for modeling health outcomes across all administrative levels and population sizes. This workflow can be adopted and adapted to a wide range of surveillance systems on non-enteric illnesses such as respiratory infections as well as in humanitarian emergency contexts so long as data are collected, reported, and analyzed using time referenced records.

Table 2. A description of the attributes for all publicly-available international, national, regional, and local administrative level datasets used within this dissertation. Attributes of datasets include its appearance within the dissertation, geographic extent, data curating organization, name of the database, type of pathogen, administrative areas, start date, end date, and temporal resolution of data.

Chapter	Extent	Host	Database	Disease	Locations	Start Date	End Date	Time Unit
3	Global	World Health Organization (WHO)	FluNet	Influenza	173 WHO Member States	02 Jan. 1995	20 Jun. 2021	Weekly
3	Global	World Health Organization (WHO)	FluNet	Influenza	29 WHO Member States	03 Jan. 2005	29 Dec. 2019	Weekly
4	National	US Centers for Disease Control and Prevention (CDC)	FoodNet	Foodborne/ Waterborne Illnesses	10 of 50 US States	01 Jan. 1996	31 Dec. 2019	Monthly
4	National	US Centers for Disease Control and Prevention (CDC)	NORS	Foodborne/ Waterborne Illnesses	50 US States & 4 US Territories	01 Jan. 2009	31 Dec. 2019	Daily
5	Regional	World Health Organization (WHO)	EMRO Bulletins	Cholera	20 Yemeni Governorates	04 Sep. 2016	29 Dec. 2019	Weekly
5	Local	John Hopkins University (JHU)	CSSE	SARS-CoV-2	Middlesex County, MA	02 Mar. 2020	07 Nov. 2021	Daily

In Chapter 3, I propose quality metrics for time-referenced data to enhance modelers' comprehension of data limitations for describing illness trends and seasonality features. These metrics, referred to as the *ACTOR* principles, provided 25 quantitative metrics for understanding the *availability*, *capacity*, *timeliness*, *operability*, and *reliability* of longitudinal surveillance data. I demonstrate how metrics' estimates can provide an easily adapted and updated metadata report to accompany publicly disseminated surveillance summaries. I apply these metrics using global virological influenza records reported by the World Health Organization's (WHO's) FluNet in 1995-2022. I chose influenza as my outcome of interest due to the longer duration and more comprehensive reporting standards for respiratory infections compared to enteric infections. Thus, FluNet serves as a gold standard for public health surveillance and an example of how data quality metrics can be developed with broad generalizability for other infectious diseases, like enteric illnesses. I conclude this chapter with a series of case studies demonstrating how data quality limitations reflect global socioeconomic inequities in surveillance capacity following unique spatial patterns.

In Chapter 4, I apply the δ-method for estimating periodic illness and outbreak signatures and propose techniques for evaluating the synchronicity of seasonal patterns of foodborne and waterborne illnesses across pathogen etiologies and geographic locations. First, I emphasize the importance of data completeness for drawing statistical comparisons between time series. Next, I describe the analytical workflow to examine distributional properties and seasonality features for time series of health outcomes. This includes assessing serial, phase-phase, and phase-amplitude synchronization for comparing seasonality features. My works also propose standardized data visualization templates to communicate complex spatiotemporal relationships using non-dynamic graphics clearly and comprehensively. All works analyze national surveillance data reported by the United States (US) Centers for Disease Control and Prevention's (CDC's) Foodborne Diseases Outbreak Surveillance Network (FoodNet) in 1996-2017 and National Outbreak Reporting System (NORS) in 2009-2019.

In Chapter 5, I adapt time series methods to examine aperiodic temporal patterns of epidemic and pandemic outbreak threats in humanitarian emergency settings. I describe challenges of extracting spatiotemporal surveillance records in locations with limited health infrastructure due to environmental- or conflict-related disasters. I

describe techniques for harmonizing records of varying spatial and temporal resolution and propose techniques for dynamic mapping to investigate spatiotemporal relationships between disease patterns and related risk factors. Next, I describe analytical approaches for defining outbreak signatures in the absence of clearly defined disease seasonality. This includes application of Kolmogorov Zurbenko adaptive filters for estimating critical points and periods of epidemic curves. I conduct these works using regional cholera illnesses across Yemeni governorates in 2016-2019. I conclude this chapter by recommending application of analytical methods for modeling local SARS-CoV-2 tests, cases, and deaths in Middlesex County, Massachusetts, US.

My final chapter provides recommendations for a data-centric approach towards precision public health. I advocate that improvement in research precision starts with better time, personnel, and monetary investment in strategies for systematic, frequent, and granular data collection. By prioritizing data quality and credibility, public health professionals can ensure improved precision of real-time modeling and near-term forecasts as well as develop more comprehensive and dynamic data visualizations. To accommodate increased surveillance data longevity, I encourage the global health community to proactively consider novel techniques for data generation, collection, management, and reporting. I further implore health agencies to establish feedback loops between curators and modelers to preserve the integrity and sustainability of surveillance system records. These changes enable public health surveillance to transition towards more proactive, preventative health policies and programs aimed at early detection and mitigation of infectious disease outbreaks.

1.3. References

1. United States. Department of Health and Human Services, Centers for Disease Control and Prevention (CDC). “Introduction to Public Health Surveillance.” 2018. https://www.cdc.gov/training/publichealth101/surveillance.html.
2. Thacker, S. B., and R. L. Berkelman. “Public Health Surveillance in the United States.” *Epidemiologic Reviews* 10, no. 1 (1988): 164–190.
3. Choi, B. C. “The past, present, and future of public health surveillance.” *Scientifica* (2012).
4. Nsubuga, P., White, M. E., Thacker, S. B., Anderson, M. A., Blount, S. B., Broome, C. V., Chiller, T. M., Espitia, V., Imtiaz, R., Sosin, D., Stroup, D. F., Tauxe, R. V., Vijayaraghavan, M., and Trostle, M. “Chapter 53: Public health surveillance: a tool for targeting and monitoring interventions.” In *Disease Control Priorities in Developing Countries. 2nd edition*, edited by Dean T Jamison, Joel G Breman, Anthony R Measham, George Alleyne, Mariam Claeson,

David B Evans, Prabhat Jha, Anne Mills, and Philip Musgrove (New York: Oxford University Press, 2006), 997-1015.

5. Groseclose, S. L., and Buckeridge, D. L. "Public health surveillance systems: recent advances in their use and evaluation." *Annual Review of Public Health* 38 (2017): 57-79.
6. United States. Department of Health and Human Services, Centers for Disease Control and Prevention (CDC), Office of Public Health Scientific Services (OPHSS). "Public Health Surveillance: Preparing for the Future." 2018. https://www.cdc.gov/surveillance/pdfs/Surveillance-Series-Bookleth.pdf.
7. United States. Department of Health and Human Services, Centers for Disease Control and Prevention (CDC). "Public Health Data Modernization: Listening Session on Real-World Testing of 21st Century Cures Act Requirements." 2020. https://www.cdc.gov/surveillance/pdfs/20_319521-D_DataMod-Initiative_901420.pdf.
8. United States. Department of Health and Human Services, Centers for Disease Control and Prevention (CDC). "Modernizing for New and Complex Threats." 2021. https://www.cdc.gov/surveillance/pdfs/Modernizing-for-New-and-Complex-Threats.pdf.
9. United States. Department of Health and Human Services, Centers for Disease Control and Prevention (CDC). "It's time to build pandemic-ready IT systems." 2021. https://www.cdc.gov/surveillance/pdfs/PRIME_1-sheet_single-page.pdf.
10. Murray, J., and Cohen, A. L. "Infectious Disease Surveillance." *International Encyclopedia of Public Health* (2017): 222–229.
11. Chen, H., Hailey, D., Wang, N., and Yu, P. "A Review of Data Quality Assessment Methods for Public Health Information Systems." *International Journal of Environmental Research and Public Health* 11, no. 5 (2014): 5170-5207.
12. Zhang, R., Indulska, M., and Sadiq, S. "Discovering Data Quality Problems." *Business and Information Systems Engineering* 61, no. 5 (2019):575–593.
13. Higgins, S. "Metadata and Digital Curation." 2007. https://www.dcc.ac.uk/guidance/briefing-papers/standards-watch-papers/what-are-metadata-standards.
14. University of California, Santa Cruz. "Metadata Curation." 2022. https://guides.library.ucsc.edu/c.php?g=618773&p=4306381.
15. Simpson, R. B., Kulinkina, A. V., and Naumova, E. N. "Investigating seasonal patterns in enteric infections: a systematic review of time series methods." *Epidemiology and Infection* (2022): 1-25.
16. Alarcon Falconi, T. M., Estrella, B., Sempértegui, F., and Naumova, E. N. "Effects of Data Aggregation on Time Series Analysis of Seasonal Infections." *International Journal of Environmental Research and Public Health* 17, no. 16 (2020): 5887.
17. Bhaskaran, K., Gasparrini, A., Hajat, S., Smeeth, L., and Armstrong, B. "Time series regression studies in environmental epidemiology." *International Journal of Epidemiology* 42, no. 4 (2013): 1187-1195.
18. Savel, T. G., Foldy, S., and Centers for Disease Control and Prevention. "The role of public health informatics in enhancing public health surveillance." *Morbidity and Mortality Weekly Report Surveillance Summaries* 61, no. 2 (2012): 20-24.
19. Mooney, S. J., and Pejaver, V. "Big data in public health: terminology, machine learning, and privacy." *Annual Review of Public Health* 39 (2018): 95-112.

20. Benke, K., and Benke, G. “Artificial intelligence and big data in public health.” *International Journal of Environmental Research and Public Health* 15, no. 12 (2018): 2796.
21. Friedman, D. J., Parrish, R. G., and Ross, D. A. “Electronic health records and US public health: current realities and future promise.” *American Journal of Public Health* 103, no. 9 (2013): 1560-1567.
22. del Pilar Angeles, M., and García-Ugalde, F. “A data quality practical approach.” *International Journal on Advances in Software* 1, no. 2-3 (2009).
23. D’Andrea, J. “Improvements in Data Quality Could Yield Up to $42.1 Million for Healthcare Organizations.” *BusinessWire*, January 12, 2022. https://www.businesswire.com/news/home/20220112005031/en/Improvements-in-Data-Quality-Could-Yield-Up-to-42.1-Million-for-Healthcare-Organizations.
24. Ristevski, B., and Chen, M. “Big data analytics in medicine and healthcare.” *Journal of Integrative Bioinformatics* 15, no. 3 (2018): 20170030.
25. Dolley, S. “Big data’s role in precision public health.” *Frontiers in Public Health*, (2018): 68.
26. Gall, C., and Suzuki, E. “5 Big data: A new dawn for public health?.” *Health in the 21st Century* (2019): 146.
27. Prosperi, M., Min, J. S., Bian, J., and Modave, F. “Big data hurdles in precision medicine and precision public health.” *BMC Medical Informatics and Decision Making* 18, no. 1 (2018): 1-15.
28. Khoury, M. J., and Ioannidis, J. P. “Big data meets public health.” *Science* 346, no. 6213 (2014): 1054-1055.
29. “What are the 5 V’s of Big Data?.” *Teradata*, 2022. https://www.teradata.com/Glossary/What-are-the-5-V-s-of-Big-Data.
30. McAfee, A., Brynjolfsson, E., Davenport, T. H., Patil, D. J., and Barton, D. “Big data: the management revolution.” *Harvard Business Review* 90, no. 10 (2012): 60-68.
31. Simpson, R. B., Babool, S., Tarnas, M. C., Kaminski, P. M., Hartwick, M. A., Naumova, E. N. “Dynamic mapping of cholera spread and conflict severity during the Yemeni Civil War, 2016-2019.” *Journal of Public Health Policy* (2022).
32. Edelstein, M., Lee, L. M., Herten-Crabb, A., Heymann, D. L., and Harper, D. R. “Strengthening global public health surveillance through data and benefit sharing.” *Emerging Infectious Diseases* 24, no. 7 (2018): 1324.

Chapter 2. A Review of Time Series Methods in Nutrition Literature

2.1. Foodborne illness burdens and surveillance gaps

The WHO estimates that >600 million persons, or 1 in 10 worldwide, experience foodborne illness annually culminating in ~420,000 deaths of whom one-third are children <5 years of age [1-2]. These values likely underestimate the true health burden, as many diarrheal illnesses, which account for >550 million illnesses and ~230,000 deaths annually, share similar symptomology and are unreported by ill persons [2]. Morbid cases result in ~33 million years of life lost annually with burdens greatest in the African and Southeast Asian regions [2]. Low- and middle-income countries face the highest burdens given limited access to treated water, sanitation, and hygiene (WASH) resources, and limited food storage infrastructure [2-3]. Additionally, incomplete surveillance introduces extensive data gaps impeding reliable estimation of global health burdens [3]. These data gaps are so extensive that the WHO devised key performance indicators in the Sustainable Development Goals (SDGs) to strengthen foodborne illness surveillance globally [4].

Immense economic burdens complement these health burdens. In 2016, the WHO's Foodborne Disease Burden Epidemiology Reference Group (FERG) estimated that foodborne illnesses and productivity-associated losses attributed to ~$95.2 billion in low- and middle-income countries annually [5]. Even among middle-upper- and upper-income countries, the annual burden attributed to productivity losses and illness morbidity and mortality was ~$50.8 billion [5]. These cost estimates are expected to rise by ~$15 billion per year in 2020-2050 [5]. Some reports suggest the overall impact of foodborne illnesses across all stages of the global food system spans as large as $8 trillion per year [1]. This falls well above worldwide annual cost estimates for hypertension (~$370 billion), diabetes (~$825 billion), and obesity (~$2 trillion) [6-8].

In the US, 1 in 6 Americans experience foodborne illness culminating in ~48 million cases, ~128,000 hospitalizations, and ~3,000 deaths annually [9]. Roughly 91% of illnesses are attributed to *Norovirus*- (58%), *Salmonella*- (11%), *Clostridium*- (10%), *Campylobacter*- (9%), and *Staphylococcus*-associated (3%) outbreaks. Similarly, ~88% of hospitalizations and deaths are attributed to *Salmonella*- (35% and 28%), *Norovirus*- (26% and 11%), *Campylobacter*- (15% and 6%), *Toxoplasma* (8% and 24%), *Escherichia*- (4% and <6%), and *Listeria*-associated (<4% and 19%,

respectively) outbreaks [9]. In 2018, these outbreaks surmounted to ~$17.6 billion in medical costs and revenue losses, and estimates suggest economic burdens of illnesses and outbreaks will increase by ~2-3% annually [10]. Per a 2010 estimate, medical expenses alone for treatment of a foodborne illness surmount to ~$2000 per case with higher costs in eastern seaboard states [11].

However, these financial burdens omit "unseen" costs throughout the production, processing, and retail arms of the supply chain. A 2011 report estimates ~$10 million per food recall with 23% of recalls exceeding $30 million per recall when accounting for government fines, health and hygiene trainings, and food safety sanctions [12-13]. These valuations exclude expenses associated with the time and personnel resources required to identify, track, collect, and destroy contaminated foods. Similarly, costs exclude those faced by retailers including indirect expenses like lawsuits, lost sales, and damaged brand reputation – all of which influence future earning potential [12-16]. Despite these growing expenses, the US Government Accountability Office (GAO) and Food and Drug Administration (FDA) have reported limited Congressional funding to strengthen foodborne illness surveillance systems and outbreak response strategies [17-23].

In fact, the GAO has reported limited strengthening of national surveillance systems for over a decade demonstrated by poor data quality and unclear analytical strategies for utilizing surveillance records [18-23]. In 2012-2013, the GAO reported that FDA and USDA foodborne illness, outbreak, and recall surveillance systems were unreliably, inconsistently, and incompletely reporting data, preventing its usage for real-time monitoring, tracking, and controlling of foodborne and waterborne disease outbreaks [18-20]. The GAO also noted limited capacity for harmonizing data across public health agencies or evaluating quality protocols in the absence of centralized data dictionaries and reporting standards [19]. In 2016, the GAO again determined that federal public health agencies conducted inconsistent and non-standardized data collection and reporting, recommending collaboration with non-federal agencies [21].

In recent years, the GAO has noted concerns over strategies for data usage to inform food safety policies and standards. In 2018, agency officials emphasized disorganization and disconnect between data curation and usage strategies including no transparent process for analyzing data to inform food safety and consumption guidelines [22]. Officials also reported no formal timelines or prospective planning of

data collection strategies to expand surveillance capacities. This included a lack of analytical plans and research pipelines to review and revise federal policies [22].

As of 2020, these surveillance limitations remain unmet with federal funding provisions plateauing at ~$30 million per year for all CDC-sponsored foodborne disease programs [23]. This most recent report also cites ~3-4-year delays in data reporting due to quality and reliability concerns, a continued lack of clear data usage goals and plans within agencies, and limited standardization of analytical workflows across agencies [23]. Stakeholder testimonials stated that data reporting delays and limited analytical strategic planning rendered much reported data no longer usable or timely for policy decision making once becoming available [23]. Despite identifying these gaps, the GAO has neither provided alternative data reporting protocols nor proposed data usage, management, and analysis workflows to streamline policy decision making using surveillance records.

2.2. Investigating seasonal patterns in enteric infections: a systematic review of time series methods

Despite global and national surveillance gaps, I found no reviews that summarized common data quality limitations and statistical methodologies for describing patterns of foodborne illnesses using surveillance data. As a result, I conducted a systematic review of time series methodologies applied to surveillance data to estimate disease trends and seasonality features such as peak timing [24]. This review directly responds to the GAO's recommendations for improved data quality and usage strategies; my primary research goals were to describe time series methodologies for estimating seasonality features and explain how researchers report data quality, reliability, and completeness limitations. This included summarizing how researchers reported information on study duration, data missingness, and terms like "seasonality", "seasonal trends", or "seasons". Rather than report the frequency of studies using each analytical technique, I described the advantages and limitations of time series methods. In doing so, I described the variety of analytical workflows for modeling time-referenced data for data modelers to reference when describing, comparing, explaining, or predicting patterns of foodborne illnesses and outbreaks.

Manuscript M1. Simpson, R. B., Kulinkina, A. V., and Naumova, E. N. "Investigating seasonal patterns in enteric infections: a systematic review of time

series methods." *Epidemiology and Infection* (2022): 1-25. https://doi.org/10.1017/S0950268822000243.

2.3. Conclusion: Greater attention needed on data quality and usage

Public health professionals frequently omit information on data quality when reporting research findings from time series analyses. Failure to report the quantity and patterns of missing data inhibits the reproducibility of analytical techniques and workflows by other researchers. Reporting omissions question the fidelity of analyzed data, the appropriateness of time series methods used, or the flexibility of analytical techniques for dealing with missing data. Without greater clarity on the attributes of extracted data and steps taken to manipulate, transform, or otherwise manage these data, research conducted on public health surveillance have uncertain generalizability, accuracy, and precision.

The responsibility to improve data quality falls equally on data curators and modelers. Together, this pair must create data quality protocols that improve the transparency of data's attributes when reported for public reuse (contribution of curators) and assess data quality limitations requiring additional accommodation during analytical workflows (contribution of modelers). For example, by curators reporting information on fluctuations in surveillance capacity and timeliness, modelers can better distinguish between artificial spikes in data and true periodic or aperiodic processes of infections. Similarly, by modelers reporting the quantity and patterns of missing data and its effects on precisely estimating disease outbreak dynamics and signatures, curators can better allocate persons, equipment, and monies to improve data collection in lower surveillance capacity populations.

To facilitate collaboration between curators and modelers, I propose standardized data quality metrics for assessing the usability and fidelity of time series data. These metrics can be compiled to form a metadata for describing the attributes of surveillance data and standardizing its reporting for public reuse. Improved transparency of data limitations informs modelers of potential limitations when performing time series analyses.

2.4. References

1. World Health Organization (WHO). "WHO steps up action to improve food safety and protect people from disease." June 7, 2021.

https://www.who.int/news/item/07-06-2021-who-steps-up-action-to-improve-food-safety-and-protect-people-from-disease.

2. World Health Organization (WHO). "WHO's first ever global estimates of fooborne diseases find children under 5 account for almost one third of deaths." December 3, 2015. https://www.who.int/news/item/03-12-2015-who-s-first-ever-global-estimates-of-foodborne-diseases-find-children-under-5-account-for-almost-one-third-of-deaths.
3. World Health Organization (WHO). "WHO estimates of the global burden of foodborne diseases: foodborne disease burden epidemiology reference group 2007-2015." Switzerland: ISBN-9789241565165. 2016. https://apps.who.int/iris/bitstream/handle/10665/199350/9789241565165_eng.pdf?sequence=1.
4. Codex Alimentaurius. "Sustainable Development Goal food safety indicator – plans explained in World Food Safety Day / Health Talks webinar. Food and Agriculture Organization." June 16, 2021. https://www.fao.org/fao-who-codexalimentarius/news-and-events/news-details/en/c/1412102/.
5. Jaffee, S., Henson, S., Unnevehr, L., Grace, D., and Cassou, E. "The Safe Food Imperative: Accelerating Progress in Lowand Middle-Income Countries." Agriculture and Food Series. Washington, DC: World Bank. doi:10.1596/978-1-4648-1345-0. License: Creative Commons Attribution CC BY 3.0 IGO. (2019).
6. Wierzejska, E., Giernaś, B., Lipiak, A., Karasiewicz, M., Cofta, M., and Staszewski, R. "A global perspective on the costs of hypertension: a systematic review." Archives of Medical Science 16, no. 5 (2020): 1078–1091.
7. Harvard T.H. Chan School of Public Health. "Cost of diabetes hits 825 billion dollars a year." April 06, 2016. https://www.hsph.harvard.edu/news/press-releases/diabetes-cost-825-billion-a-year/.
8. Berenson, T. "Obesity now costs the world $2 trillion a year." TIME. November 20, 2014. https://time.com/3597407/obesity-global-cost-report/.
9. United States. Department of Health and Human Services, Centers for Disease Control and Prevention (CDC), National Center for Emerging and Zoonotic Infectious Diseases (NCEZID), Division of Foodborne, Waterborne, and Environmental Diseases (DFWED). "Burden of Foodborne Illness: Findings." November 05, 2018. https://www.cdc.gov/foodborneburden/2011-foodborne-estimates.html.
10. United States Department of Agriculture (USDA), Economic Research Service (ERS). "Cost Estimate of Foodborne Illnesses." March 04, 2022. https://www.ers.usda.gov/data-products/cost-estimates-of-foodborne-illnesses/.
11. The Pew Charitable Trusts. "Health-Related Costs from Foodborne Illness in the United States." March 03, 2010. https://www.pewtrusts.org/en/research-and-analysis/reports/0001/01/01/healthrelated-costs-from-foodborne-illness-in-the-united-states.
12. Tyco Integrated Security. "Recall: The Food Industry's Biggest Threat to Profitability." *Food Safety Magazine*. October 11, 2012. https://www.food-safety.com/articles/2542-recall-the-food-industrys-biggest-threat-to-profitability.
13. Marel. "Product recalls: How recalls damage your brand and bottom line." *Marel*. July 05, 2021. https://marel.com/en/news/food-recalls-true-cost.
14. SmartSense | Food Safety. "The true cost of food recalls." *SmartSense*. July 11, 2019. https://blog.smartsense.co/costs-of-food-recalls.

15. Heneghan, C. “More than money: What a recall truly costs.” *Food Dive*. September 26, 2016. https://www.fooddive.com/news/more-than-money-what-a-recall-truly-costs/426855/.
16. Koeris, M. “The true costs you endure during a food recall.” *Food Safety Tech*. September 04, 2018. https://foodsafetytech.com/column/the-true-costs-you-endure-during-a-food-recall/.
17. Nixon, R. “Funding gap hinders law for ensuring food safety.” *New York Times*. April 7, 2015. https://www.nytimes.com/2015/04/08/us/food-safety-laws-funding-is-far-below-estimated-requirement.html.
18. United States. Government Accountability Office (GAO). “Information Technology: FDA needs to fully implement key management practices to lessen modernization risks.” Washington, DC: GAO-12-346. March 2012. https://www.gao.gov/assets/gao-12-346.pdf.
19. United States. Government Accountability Office (GAO). “Food Safety: FDA’s food advisory and recall process needs strengthening.” Washington, DC: GAO-12-589. July 2012. https://www.gao.gov/products/gao-12-589.
20. United States. Government Accountability Office (GAO). “Food Safety: More disclosure and data needed to clarify impact of changes to poultry and hog inspections.” Washington, DC: GAO-13-775. August 2013. https://www.gao.gov/products/gao-13-775.
21. United States. Government Accountability Office (GAO). “Food Safety: FDA coordinating stakeholders on new rules but challenges remain and greater tribal consultation needed.” Washington, DC: GAO-16-425. May 2016. https://www.gao.gov/products/gao-16-425.
22. United States. Government Accountability Office (GAO). “Food Safety: USDA should take further action to reduce pathogens in meat and poultry products.” Washington, DC: GAO-18-272. March 2018. https://www.gao.gov/products/gao-18-272.
23. United States. Government Accountability Office (GAO). “Food Safety: CDC could further strengthen its efforts to identify and respond to foodborne illnesses.” Washington, DC: GAO-21-23. October 2020. https://www.gao.gov/products/gao-21-23.
24. Simpson, R. B., Kulinkina, A. V., and Naumova, E. N. “Investigating seasonal patterns in enteric infections: a systematic review of time series methods.” *Epidemiology and Infection* (2022): 1-25.

Chapter 3. Data Quality for Modeling Purposes

3.1. Influenza surveillance: A gold standard for data quality metrics

Real-time monitoring and near-term forecasting of infectious diseases requires frequent and consistent collection, maintenance, and dissemination of surveillance data [1-4]. In the advent of emerging outbreak threats, such as the 2019 novel coronavirus (COVID-19) pandemic, surveillance systems are vital in guiding health safety communications, laboratory resource management, and travel restrictions [5-6]. Rapid testing diagnostics, daily reporting, and public data dissemination throughout COVID-19 has emphasized the importance of data quality for precise and specific early outbreak warnings [7-8]. Yet, recent studies note concerns that case volumes and reporting demands have decreased data's reliability and completeness [9-12]. Public health modelers have called for more descriptive metadata to best leverage surveillance data for modeling purposes [2,7].

Data quality concerns have instigated World Health Organization (WHO) directives to strengthen global disease surveillance capacity for infections of epidemic and pandemic potential [2,13-15]. Directives prioritize joint virological surveillance of SARS-CoV-2 and seasonal influenza with an emphasis on severe acute respiratory illnesses (SARI) and A(H5) subtypes such as A(H5N1) Asian Influenza Virus [7,16-18]. To monitor capacity improvements, national, regional, and sentinel laboratory testing facilities that comprise global surveillance reporting are assessed for data quality principles. These principles, established after the 2009 A(H1N1) pandemic and privately tracked by the WHO, evaluate facilities' thoroughness of testing collected specimens, reliability of testing diagnoses, and regularity of data dissemination (Table 3) [14,19-21]. These principles articulate important attributes of the data collection and curation process from identifying and collecting specimens of ill persons through the reliable reporting of surveillance data. For each principle, the WHO defines quantitative metrics to ensure transparent and systematic testing procedures for all collected data from correctly diagnosing an individual's disease status to publishing weekly summaries of case frequencies [14,19-21].

Table 3. An overview of commonly-cited World Health Organization (WHO) curation quality principles and metrics for the time-referenced global virological influenza surveillance database FluNet [14,19-21]. Principles describe larger data quality and credibility areas of concern during data curation while metrics provide quantitative measures for estimating the efficiency and effectiveness of data collection, management, and reporting.

Principle	Description	Metrics for Assessment
Timeliness	The frequency and regularity of laboratory specimen testing and reporting of testing results to the WHO's FluNet	• Percentage of time that a reporting site achieves target date for data reporting • Percentage of time that an administrative level achieves target date for data reporting • Percentage of time that a site ships specimens by the target number of days after collection • Percentage of time that a laboratory has test results available within target time frame • Percentage of time that a facility reports results to a surveillance site within target time frame
Completeness	How thoroughly health facilities complete all available data reporting fields when reporting health records	• Percentage of reports received from each surveillance site with complete data • Percentage of data reports that are received by data curating organization • Percentage of sampled cases that have complete data collected
Consistency	The presence of aberrations in data records driven by changes in data collection and reporting methods	• Number of unexpected or sudden increases or decreases in the number of reported cases • Unexpected or sudden changes in the percentage of specimens testing positive for influenza • Changes in the distribution of risk factors or age groups testing positive for influenza
Representativeness	The generalizability of patients accessing healthcare at health facilities compared to the population of interest	• Do patients in the capture area of a health facility reflect the age, sex, ethnicity, socioeconomic status, education, and healthcare access of the population • Are patients tested at a health facility more likely to be sampled due to receipt of specialized care • Do all cases of the catchment area have equal likelihood of being infected with illness • Does reported data consist of cases from a variety of climatic areas where cases could originate from

For example, one of the most cited WHO data quality principles is *timeliness*, or the frequency and regularity of specimen collection, shipment, testing, processing, and the reporting [14,19]. The WHO defines a standard measure of practice that 80% of health facilities or testing laboratories provide specimen shipments, test shipments, or report data within 48 hours of sample or data receipt [14]. *Timeliness* metrics evaluate the percentage of facilities within an administrative area or for a specific health outcome (e.g., SARI, ARI, ILI, etc.) meeting this target timeframe. Metrics are calculated using external audits completed by national or regional influenza surveillance officers to minimize facility evaluation biases [14].

Other well-cited principles include *completeness*, or the thoroughness of individual health records, and *consistency*, or the presence of aberrations in reported data [14,21]. *Completeness* tracks the distribution of cases received from various health facilities. This includes both the regularity of reported records over time (i.e., are records available for all weeks of a given year) and omissions of patient

information in extracted and curated records (i.e., are all data fields collected for all patients) [7,14,19-21]. Records' *completeness* relates closely to data *consistency*, as changes in collection protocols, standards, or testing techniques can create artificial spikes or drops in reported cases independent from biological disease processes [14,20]. The evaluation of *consistency* metrics tests for the overall fidelity of reported data as well as public health professionals' ability to perform early outbreak detection of epidemic or pandemic prone influenza subtypes using surveillance data [7,14,20].

Additional principles cited by the WHO include *representativeness* and factors influencing the reliability of laboratory testing such as *sensitivity*, *specificity*, *accuracy*, and *bias*. The WHO commonly references *representativeness* to describe if a health facility reflects the population of an administrative area [14,19-21]. This metric also evaluates whether cases are equally distributed across various climate zones or regions where an infection strain or subtype has been previously identified [20]. Climatic *representativeness* permits close inspection of global viral activity, subtype diversification, and early detection of emerging subtypes with epidemic or pandemic potential. The remaining metrics measure the fidelity of laboratory testing and are evaluated for each testing facility. These classical quality measures (i.e., *sensitivity, specificity, positive predictive value, accuracy, bias*) are commonly conducted in epidemiological research but are not easily scaled for time-referenced population level surveillance, such as with the WHO's global virological surveillance system FluNet [14,20].

While informative, these metrics focus solely on the effectiveness and efficiency of data curation from specimen collection to surveillance reporting. Metadata give little attention to the quality of data for public reuse and its limitations for modeling influenza patterns to inform pandemic preparedness plans. Without detailed metadata, modelers can easily overlook how data's frequency or completeness influence the precision of peak timing, amplitude, outbreak duration, or outbreak severity estimates [22]. Limited information on the generalizability and reliability of reported data inhibits modeling accuracy and precision. These data limitations can lead to imprecise recommendations for vaccine scheduling, laboratory resource and personnel demands, and peak timing of seasonal surges [23-24].

In the sections that follow, I propose 5 data quality principles accompanied by 25 standardized quantitative metrics for assessing the Availability, Capacity, Timeliness, Operability, and Reliability (*ACTOR*) of time series surveillance data. Unlike existing

principles and metrics proposed by the WHO, the *ACTOR* principles and metrics describe data's usability and fidelity for modeling purposes *after* it has been curated and publicly reported. I begin by explaining the importance of these metrics for informing model selection, applying appropriate time series analytical techniques, and understanding patterns of time-dependent disease outcomes. I then provide a series of case studies demonstrating the calculation and application of metrics using global surveillance data.

3.2. The ACTOR Principles for assessing time series data quality

I propose 5 principles for evaluating time-referenced data's quality at various stages of a researcher's analytical workflow. I divide each principle into 1-3 qualitative indicators (10 total) that define key attributes or characteristics of that principle. For each indicator, I propose 4-7 quantitative metrics (25 total) that measure each indicator for the entire surveillance system or by a combination of health outcomes, geographic locations, and time intervals. I describe each principle, its indicators, and associated metrics below. For all metrics except *reporting delay*, higher scores indicate better data quality.

3.2.1. Availability

Availability characterizes data attributes inherent to the design of a surveillance system. Indicators and metrics describe the contents of reported data, which aligns closely with the earliest stages of a modelers' analytical planning: identifying data suitable for research purposes. The *Resolution* indicator describes health records' spatiotemporal granularity, or the most refined time intervals and administrative levels that health outcomes are reported. The *Comparability* indicator describes the variety of health outcomes reported per geographic location. I separate health outcomes by case definitions (e.g., SARI, ARI, ILI, etc.), testing outcomes (e.g., tests, positives, negatives, etc.), and disease strains and subtypes (Table 4).

Table 4. Indicators and metrics associated with the *availability* principle for evaluating time-referenced surveillance data quality. I provide definitions of indicators and calculations for scoring quantitative metrics. *Score Range* is provided for WHO's FluNet, the data source used later in this chapter as a case study for demonstrating metric calculations. *Calculated by* describes how the metric is calculated for FluNet data including for the entire surveillance system or by any combination of Member State, study week, calendar year, week of year, or health outcome.

Indicator	Indicator Definition	Metric	Metric Calculation or Scoring	Score Range	Calculated By…

Resolution	The granularity of spatiotemporal information.	Frequency	Temporal resolution of reported data: 1=Yearly, 2=Quarterly, 3=Monthly, 4=Biweekly/Dekad, 5=Weekly, 6=Daily	1-6	Surveillance System
		Representativeness	Geographic resolution of reported data: 1=Region, 2=Nation, 3=Province/State, 4=City/Town/Village, 5=Postal Code, 6=Latitude/Longitude	1-6	Surveillance System
Comparability	The case definitions, testing outcomes, and strains or subtypes reported.	Case Variety Score	Count of case definitions reported by a surveillance system *(FluNet: ILI, SARI, ARI, pneumonia, cases, and deaths)*	0-6	Member State
		Outcome Variety Score	Count of testing outcomes with ≥1 non-missing time point *(FluNet: specimens collected, specimens processed (tests), positives, negatives, influenza A positives, and influenza B positives)*	0-6	Member State
		Subtype Variety Score	Count of subtypes with ≥1 non-missing time point *(FluNet: A(H1), A(H1N1)pdm09, A(H3), A(H5), A(Unsubtyped), B(Yamataga), B(Victoria), and B(Undetermined) positives)*	0-8	Member State
		Total Variety Score	Sum of all case definition, testing outcome, and strain or subtype variety scores	0-20	Member State

The *frequency* metric scores a surveillance system based on the time unit of health record aggregation. Coarser annual records receive lower scores compared to granular daily and weekly records, as the former limits the usability of data for detecting temporal trends or seasonal patterns. More granular temporal information permits more precise estimation of time-varying patterns such as seasonal peaks, disease outbreak onset, or critical points and periods of outbreak signatures [25-26]. In contrast, coarsely reported annual, quarterly, or monthly records reduce a study period's sample size. Fewer observations reduce statistical power and inhibit inspection of within-year periodic or aperiodic patterns of illnesses [27]. A modelers' knowledge of data's temporal resolution is also pertinent to specify periodic functions when modeling disease seasonality using harmonic regression models [28].

Like WHO internal metrics, the *representativeness* metric provides information on the generalizability and geographic extent of reported records. However, geographic extent reflects not a capture area of cases but rather the spatial aggregation of cases in reported data. This metric scores the spatial resolution of data from coarser regional and national records to granular postal code or geocoded records. In the absence of a detailed estimate of a health facility's capture area, this metric allows modelers to roughly approximate the population size per administrative area collecting and reporting health records. Modelers require this information to extract population estimates to calculate case rates or use as offset terms in regression modeling. Given more cases are expected in larger populations, these adjustments are necessary for comparing disease patterns across spatial domains [26,29].

The *comparability* indicator is divided into 4 *variety score* metrics, each describing the availability and types of health outcomes reported within a geographic location. *Case variety scores* describe the number of symptoms (with FluNet for example: ILI, SARI, ARI, pneumonia), morbidity-related outcomes (i.e., primary cases, secondary cases, hospitalizations, etc.), and mortality outcomes (i.e., death) reported. *Outcome variety scores* sum the number of testing outcomes with ≥1 non-missing time point within a geographic location. This includes both testing results for human specimens (i.e., specimens collected, tests, total positives, total negatives) and any common disease etiologies, such as Influenza A and B positives. *Subtype variety scores* list the number of disease strains or subtypes with ≥1 non-missing time point per geographic location. I sum these three scores to estimate the *total variety score*, as the number of case definitions, testing results, strains, and subtypes may differ greatly between locations due to testing capacities, resource scarcities, etc.

Variety scores assist modelers in research hypothesis formulation and exploratory data analyses. Comparative studies often examine relationships of a single health outcome across multiple locations (e.g., examining regional hotspots of infection) or multiple outcomes within a single location (e.g., examining synchronicity or coinfection of diseases) [22,30]. Variety scores provide clarity on if and how researchers can leverage surveillance data to conduct these analyses. These scores also demonstrate how information on disease morbidity and mortality vary by the surveillance capacity of health facilities reporting to global surveillance systems.

3.2.2. Capacity

Once selecting data with the desired resolution and health outcomes, modelers may inquire about the scope and precision of surveillance reporting and viral testing. *Capacity* describes the ability of laboratory testing facilities to conduct quality reporting and trustworthiness of health records. The *Coverage* indicator estimates the frequency of national centers reporting to data curating organizations and laboratory testing facilities processing human specimens. The *Rigor* indicator parallels existing WHO metrics and evaluates testing diagnostics like precision, accuracy, and bias. All *Rigor* metrics assess how sampling strategies and testing quality varies over time, heavily influenced by the availability of skilled personnel and laboratory testing equipment of health facilities (Table 5).

Table 5. Indicators and metrics associated with the *capacity* principle for evaluating time-referenced surveillance data quality. I provide definitions of indicators and calculations for scoring quantitative metrics. *Score Range* is provided for WHO's FluNet, the data source used later in this chapter as a case study for demonstrating metric calculations. *Calculated by* describes how the metric is calculated for FluNet data including for the entire surveillance system or by any combination of Member State, study week, calendar year, week of year, or health outcome.

Indicator	Indicator Definition	Metric	Metric Calculation or Scoring	Score Range	Calculated By…
Coverage	The quantity of health centers, facilities, or laboratories testing human cultures and specimens.	Reporting Coverage	Count and per capita rate of national reporting centers *(FluNet: National Influenza Centres (NICs))*	R^+	Member State
		Diagnostic Coverage	Count and per capita rate of laboratory testing facilities *(FluNet: influenza testing facilities, centres, and hospitals)*	R^+	Member State
Rigor	The thoroughness of sampling and testing techniques in accordance with international standards.	Sampling Rigor	Laboratory sampling technique for reporting cases: 1=Modified Convenience Sampling, 2=Interval Sampling, 3=Alternate Day Sampling, 4=All Samples	1-4	Member State; Week
		Testing Rigor	Testing technique for human cultures/specimens: 1=Rapid point-of-care tests, 2=Enzyme linked immunoassay, 3=Indirect immunofluorescence, 4=Direct immunofluorescence, 5=Reverse transcriptase PCR, 6=Viral culture	1-6	Member State; Week
		Case Compliance	Surveillance system's usage of international case definition standards (scored 1 if 'Yes' and 0 if 'No') *(FluNet: case definitions for ARI, SARI, and Pneumonia)*	0-3	Member State; Year

Reporting and *diagnostic coverage* metrics estimate the number of national reporting centers and laboratory testing facilities, respectively, within a geographic location. To adjust for populations of scale, modelers can calculate these metrics both as raw counts and as per capita rates. Scores range the set of all positive real numbers (R^+) and vary as surveillance systems mature, capture areas expand, and population sizes grow. These metrics provide a proxy for surveillance capacity, as locations with fewer facilities per capita will likely underestimate illness burdens. Modelers can use *coverage* metrics to better understand why reporting gaps or aberrations appear within reported data. This helps distinguish whether time series patterns reflect issues of data quality or true biological processes of illness. Modelers can also include these metrics as parameters in time series models to approximate surveillance capacity [22]. Data curators or curating organizations benefit from calculating *coverage* metrics as they can inform strategies for resource allocation distributions, like vaccine scheduling, and public health financing of health infrastructure and personnel.

As personnel availability, reporting timeliness, and testing capacities fluctuate seasonally, the number of samples reported, quality of conducted tests, and standards for defining cases may also vary. The *Rigor* indicator and associated metrics evaluate the thoroughness and trustworthiness of data over time. S*ampling rigor* assesses the

number of samples tested and reported to a data curating organization. As laboratory testing requires extensive time and fiscal resources, facilities use differing pooling or stratification techniques to expedite reporting or minimize costs. The WHO encourages facilities to perform 1 of 4 sampling techniques, including modified convenience, interval, alternate day, or all case sampling [14]. By reporting only a subset of cases, such as with modified convenience sampling, surveillance data may have less accurate records than all-case sampling. The underreporting of cases can lead modelers to incorrectly estimate average disease burdens as well as outbreak signatures such as outbreak onset, peak timing, and amplitude.

As with sampling strategies, the WHO provides a list of preferred viral tests for human culture specimens ranked from the highest (viral culture and reverse transcriptase PCR) to lowest (rapid point-of-care tests) sensitivity and specificity [21]. Unlike WHO data quality metrics, *testing rigor* evaluates the precision of testing for each epidemiological week of a researcher's study period. Seasonally, testing facilities may become overwhelmed by case volumes during outbreaks and shift to more rapid but less precise testing techniques. Alternatively, facilities may utilize rapid testing during early stages of an epidemic or pandemic then transition to more comprehensive techniques as they become available. These changes are imperative for data modelers to understand the variability and reliability of case estimates throughout a time series. Using this information, modelers can adjust confidence intervals during times of less precise testing to reliably forecast periodic and aperiodic patterns. These adjustments for uncertainty at different times of the year permit more comprehensive outbreak preparedness plans that account for under- or over-reporting.

The third rigor metric, *case compliance*, evaluates if and how closely a geographic location's case definition aligns with WHO standards. While diagnosis protocols like the International Classification of Diseases and Related Health Problems (ICD) attempt to standardize medical classifications, countries and territories are permitted to adapt case definitions in accordance with federal or subnational health standards, available medical equipment, and personnel training and skills [31-32]. Differences in standards call into question whether the same health outcome is comparable in two locations or at two time points. Fewer diagnostic criteria increase the generalizability of case definitions and capture rate of suspected cases. This in turn increases the number of specimens processed, tests conducted, and reported negatives within surveillance data. In contrast, stricter criteria may result in

far fewer specimens tested but a much higher positivity rate and more severe morbidity- or mortality-related outcomes associated with each case. By understanding these differences, modelers can evaluate the generalizability of model findings and study results using these data.

3.2.3. Timeliness

Whereas *availability* and *capacity* describe the structure and trustworthiness of data, respectively, the *timeliness* principle assesses the usability of records for conducting time series analyses. This differs from the WHO-defined metric of the same name as this principle assesses the frequency of time intervals in reported data with usable records. Data modelers require this information when performing descriptive, explanatory, and predictive models, as effective sample size can influence the reliability of the temporal trends, outbreak signatures, and early outbreak forecasts conducted. This principle consists of 3 indicators: i) *Duration*, or a surveillance system's overall time series length; ii) *Completeness*, or the time series length adjusted for missing records; and iii) *Lag*, or reporting delays between data download dates and the most recently reported records (Table 6).

Table 6. Indicators and metrics associated with the *timeliness* principle for evaluating time-referenced surveillance data quality. I provide definitions of indicators and calculations for scoring quantitative metrics. *Score Range* is provided for WHO's FluNet, the data source used later in this chapter as a case study for demonstrating metric calculations. *Calculated by* describes how the metric is calculated for FluNet data including for the entire surveillance system or by any combination of Member State, study week, calendar year, week of year, or health outcome.

Indicator	Indicator Definition	Metric	Metric Calculation or Scoring	Score Range	Calculated By…
Duration	The unadjusted length of a time series; all available records reported by a surveillance system.	Time Series Length (TSL)	Total number of time points reported by a surveillance system within a downloaded time series or longitudinal dataset.	R^+	Surveillance System
		Extent	Total number of time points reported by a surveillance system from the first to the last time point of non-missing records	R^+	Member State; Outcome
Completeness	Time series length adjusted for the quantity and patterns of missing records.	Average Completeness	Number of time points with non-missing records per time series length and multiplied by 100	0-100%	Member State; Outcome
		Annual Completeness	Number of time points with non-missing records per total Gregorian calendar year time points and multiplied by 100	0-100%	Member State; Outcome; Year
		Seasonal Completeness	Number of calendar years with non-missing records for a specific day, week, or month per total study years that day, week, or month occurred and multiplied by 100	0-100%	Member State; Outcome; Week-of-Year
Lag	The speed of data processing and reporting for reuse.	Reporting Delay	Number of time points from the date of data download to the most recent time point when records are not missing	R^+	Member State; Outcome

Time series length (TSL) refers to the total number of time points reported by a surveillance system. This duration metric is defined by i) the starting date when curating organizations begin collecting and/or reporting historical records; and ii) the ending date when modeler's extracted data. *TSL* reflects the total number of records available for conducting statistical analyses per location-outcome dyad. Longer *TSL* is driven by surveillance system maturity, data's temporal resolution, and a researcher's study period duration of interest.

Like *TSL*, *extent* estimates time series length of location-outcome dyads but in accordance with the first and last reported non-missing record. Here, I differentiate between incomplete or missing records (blanks) and zero counts (0) in reported data. Reasons for missing records may reflect planned or unexpected closures of health facilities, limited resources for conducting laboratory testing, delays in the establishment or expansion of surveillance coverage, or the emergence of a disease strain or subtype previously not isolated or identified. *Extent* revises the historical reference period feasible for analytical purposes and assists modelers with hypothesis generation to determine study periods with available, usable data.

The *Completeness* indicator consists of the *average*, *annual*, and *seasonal completeness* metrics, which estimate the effective sample size of time intervals with usable data relative to a pre-specified duration of time. All metrics are scored from 0-100% where higher scores indicate more records with usable data. *Average completeness* estimates the percentage of time points within a time series that have non-missing records. This metric describes the quantity of usable data within the historical reference period of interest. Data usability dictates the sample size and power of time series models; analyses conducted with limited usability will produce less reliable estimates of disease patterns such as peak timing and amplitude [25,27,33]. Modelers can also compare *average completeness* measures with other metrics (i.e., *reporting* and *diagnostic* coverage) or external data sources (e.g., socioeconomic status, healthcare access, etc.) to explain reasons for incomplete reporting.

In contrast, *annual* and *seasonal completeness* metrics provide more granular information on structural missingness, or patterns of missing data within a time series. As their names suggest, *annual completeness* estimates the percentage of missing data within one year (often a Gregorian calendar year) while *seasonal completeness* estimates the number of years with non-missing records for a specific day, week, or

month of the year within a study period. *Annual completeness* estimates are pertinent when conducting annualized regressions, as the usability of time intervals each year greatly influence a modeler's ability to precisely estimate disease outbreak signatures or compare annual shifts in disease seasonality [28]. For example, if specific years have fewer usable records, modelers' trend estimates within or across those years may underestimate the true infection burden. By tracking this metric over time, modelers can also evaluate the maturity of surveillance capacity within reporting locations.

Seasonal completeness describes more systematic patterns of data missingness, also referred to as structural missingness, such as seasonal facility closures or alternative resource allocations [34]. Laboratory facilities may halt testing at certain times of the year to prioritize testing for other infections and conserve already scarce laboratory testing equipment. When modeling periodic processes of infections, increased missing data can decrease the precision of estimating outbreak features, such as peak timing and amplitude. This especially holds true when *seasonal completeness* estimates show systematically missing data in close alignment with seasonal peaks. Unreliable assessment of peak timing each year also inhibits investigations of peak timing shifts over time and examination of relationships between peak timing and amplitude for a location-outcome dyad. Incomplete records surrounding peaks and nadirs inhibit precise estimation of seasonal amplitude, absolute intensity, and relative intensity, as the minimum and maximum case rates per outbreak season are not well understood [22,32].

Reporting delay assists modelers in understanding the reliability of time series models particularly in the context of disease forecasting. This metric estimates the number of time points between the dates of data download and the most recently reported non-missing record. Unlike all other metrics, lower *reporting delay* scores are optimal and reflect the most timely updating of surveillance records. Longer delays suggest less efficient specimen collection, processing, and reporting during the data curation process. These delays extend the forecast horizon for modelers; when performing near-term forecasts, modelers must predict values for time points both before and after the date of data extraction. Longer prediction intervals decrease the precision of model estimates, as missing data fail to provide the most recent trends or patterns of infection. As with *completeness* metrics, *reporting delays* are subject to vary by time-of-year of data download, frequency of historical record modifications or updates, and resource constraints of laboratory testing facilities.

3.2.4. Operability

The *completeness* metrics above evaluate data usability for each outcome and location, ideal for describing annual trends, seasonality features, and outbreak signatures of illnesses. However, if modelers aim to compare disease features by outcomes, locations, or other risk factors, they must evaluate the shared usability of records across time series. The *operability* principle explains the percentage of time points where two time series have non-missing records within a study period. To achieve these comparisons, data must be properly harmonized across all sources, suggesting the importance of the *Alignment* indicator (Table 7). Metrics evaluate shared completeness between health outcomes in the same location (*outcome interoperability*), between locations for the same outcome (*location interoperability*), or between one time series of a health surveillance system and another time series of an external dataset (*external interoperability*). External data include time-dependent risk factors influencing disease patterns like temperature, precipitation, humidity, socioeconomic status, or vaccine supplies.

Table 7. Indicators and metrics associated with the *operability* principle for evaluating time-referenced surveillance data quality. I provide definitions of indicators and calculations for scoring quantitative metrics. *Score Range* is provided for WHO's FluNet, the data source used later in this chapter as a case study for demonstrating metric calculations. *Calculated by* describes how the metric is calculated for FluNet data including for the entire surveillance system or by any combination of Member State, study week, calendar year, week of year, or health outcome.

Indicator	Indicator Definition	Metric	Metric Calculation or Scoring	Score Range	Calculated By…
Alignment	The number of jointly usable observations when comparing outcomes, locations, and variables within or between datasets.	Outcome Interoperability	Number of time intervals that 2 testing outcomes in the same location have jointly non-missing records per total time points within a study period and multiplied by 100	0-100%	Member State
		Location Interoperability	Number of time intervals that 2 locations for the same testing outcome have jointly non-missing records per total time points within a study period and multiplied by 100	0-100%	Outcome
		External Interoperability	Number of time intervals that a time series variable and variable of an external dataset have jointly non-missing records per time points within a study period	0-100%	Member State; Outcome

Interoperability metrics estimate the percentage of time intervals when pairs of outcomes, locations, or time series have reported health records. Metrics evaluate effective sample size for modelers to understand statistical power when conducting comparison tests. When assessed across outcomes, modelers require effective sample size for assessing the synchronicity of disease outbreak signatures including traveling waves of infections or the potential for coinfections of multiple etiologies or subtypes.

When assessed across locations, modelers require effective sample size to identify geographic hotspots of infection prone to seasonal, epidemic, or pandemic outbreaks. If facing low *location interoperability* metric scores, modelers can identify data-rich time series useful for triangulating disease signatures in data-sparse locations or impute missing values.

While the proposed *ACTOR* principles are for health surveillance data quality, modelers may also conduct interdisciplinary research requiring the use of non-health data streams. *External interoperability* evaluates the alignment and usability of records appended to extracted surveillance records. To achieve this, modelers must ensure that data streams have identical spatial and temporal resolution. As much epidemiological research using time series analyses compare illness trends to biological, climatic, or environmental processes, this metric allows modelers to evaluate the expected effective sample size for explanatory analyses between disease incidence and associated risk factors.

3.2.5. Reliability

The final principle examines the fidelity of reported data by examining the concordance of reported records within and between data downloads. As both data collection and analytics are iterative processes, surveillance records may be modified and updated over the course of a modelers' analysis. The *Correctness* indicator describes concordance between health outcomes within a dataset to determine the reliability of data reporting. This includes that the number of reported specimens collected, tests conducted, total negatives, total positives, and subtypes' and strains' positives fall within expected and biologically plausible bounds. In contrast, the *Variability* indicator examines the concordance of reported records across multiple download dates to monitor modifications made to historical records in the most recent extraction dates (Table 8).

Table 8. Indicators and metrics associated with the *reliability* principle for evaluating time-referenced surveillance data quality. I provide definitions of indicators and calculations for scoring quantitative metrics. *Score Range* is provided for WHO's FluNet, the data source used later in this chapter as a case study for demonstrating metric calculations. *Calculated by* describes how the metric is calculated for FluNet data including for the entire surveillance system or by any combination of Member State, study week, calendar year, week of year, or health outcome.

Indicator	Indicator Definition	Metric	Metric Calculation or Scoring	Score Range	Calculated By…

Correctness	The validity of testing outcomes relative to one another within a dataset.	Specimens Correctness	Percentage of time intervals when the specimens processed are less than or equal to the specimens tested	0-100%	Member State; Outcome
		Tests Correctness	Percentage of time intervals when specimens tested are equal to the sum of positive and negative test outcomes	0-100%	Member State
		Positives Correctness	Percentage of time intervals when total positives are equal to the sum of strain specific (e.g., influenza A and B) positives	0-100%	Member State
		Strain Correctness	Percentage of time intervals when strain-specific positives are equal to the sum of subtype positives for that strain	0-100%	Member State; Strain
Variability	The historical modification of reported health records.	Consistency	Percentage of time intervals when records from one download date equal the same values as records from another download date	0-100%	Member State; Outcome

Specimens' correctness refers to the percentage of time points where specimens collected are correctly less than or equal to the number of tests performed. Lower values suggest limited surveillance capacity, as health facilities were unable to successfully test all specimens sampled at a time point, while values >100% indicate reporting errors. *Tests' correctness* refers to the percentage of time points when tests conducted equal the sum of all positive and negative outcomes. As these health outcomes are mutually dependent, tests and testing results should be equivalent if all tests were conclusively processed. Lower correctness values suggest either that tests were not completely evaluated, leading to over- or under-estimation of true disease burden, or otherwise reported incorrectly.

Both *positives'* and *strains' correctness* metrics are specific to the etiologies of pathogens evaluated by a surveillance system. Etiologies are clearly specified within FluNet data where positives are first disaggregated by strain (influenza A and B positives) and then further by subtypes (e.g., A(H1), A(H1N1)pdm09, B(Victoria), etc.). Under a clear taxonomy, *positives' correctness* evaluates the percentage of time points when total positives are equal to the sum of all strain- and genus-specific positives. *Strains' correctness* further evaluates the percentage of time points where the sum of all strain positives equals that of all subtype- and species-specific positives. The construction of alternative or additional *correctness* metrics depends on the genome sequencing technologies available to health facilities when processing tests.

The *consistency* metric allows modelers to evaluate expected fluctuations in model results based on historical updates to surveillance data. As quality control checks are performed by data curating organizations, surveillance records may be revised with limited formal announcement to data users. The *consistency* metric

evaluates the percentage of time points with discordant records between data extraction dates to better acknowledge these changes during statistical analyses. Differences between extraction dates inform the robustness of researchers' models to revisions in historical records and assess possible variability in model results. Modelers can also use this metric to gain clarity on data quality changes as an outbreak evolves and time series models are routinely performed.

3.3. Case Study – An example using FluNet in 1995-2021

Below, I provide a case study that estimates the 25 *ACTOR* metrics for 14 influenza outcomes across 173 Member States publicly reporting weekly records to the WHO's FluNet from Week 1 of 1995 (02 January 1995) through Week 24 of 2021 (20 June 2021). I describe and compare metrics across 6 WHO-defined regions and 17 influenza transmission zones. The study demonstrates how *ACTOR* principles and metrics can provide metadata for modelers to assess data quality limitations before conducting spatiotemporal analyses. Findings identify global disparities in FluNet surveillance capacity requiring more extensive and complete data reporting. The study also informs modelers of data limitations imperative for reliable, generalizable, and reproducible real-time trend analyses and near-term forecasts produced by using FluNet data.

3.3.1. Influenza data source

The WHO's FluNet publicly reports weekly influenza virological surveillance data on 14 health outcomes for 173 Member States beginning Week 1 1995 [35]. Records include 6 testing outcomes (specimens collected, tests, total positives, total negatives, influenza A positives, influenza B positives) and 8 disease subtypes (A(H1), A(H1N1)pdm09, A(H3), A(H5) A(Unsubtyped), B(Yamagata), B(Victoria), and B(Undetermined) positives). FluNet differentiates between incomplete records (blanks) and 0 counts in reported data.

I first extracted data on 13 June 2020. At this time, FluNet reported extensively missing data from Week 1 1995 through Week 52 2007. I extracted the remaining 626 weeks of available data from Week 1 2008 through Week 52 2019. I next extracted data on 15 June 2021, where I retrieved 1381 weeks of data from Week 1 1995 through Week 24 2021. My second download had more available records for all Member States in 1995-2008. I found no explanation for revised historic records,

however the FluNet website underwent significant maintenance between extraction dates. I used data from the second extraction date to calculate data quality metrics.

3.3.2. Calculating ACTOR metric scores

I used ordinal ranking for *Resolution* (including *frequency* and *representativeness*) and *Comparability* (including *case*, *outcome*, *subtype*, and *total variety scores*) indicators. Low scores (ranging 0-1) suggested coarse spatiotemporal resolution and little variety of case definitions, health outcomes, and disease subtypes. High scores (ranging 6-8) suggested granular resolution and diverse definitions, outcomes, and subtypes per Member State. I estimated *variety scores* using numerous WHO and national influenza reports [36-91].

I scored *reporting* and *diagnostic coverage*, *time series length*, *extent*, and *reporting delay* metrics using values ranging all positive real numbers (R^+). While most Member States reported few national influenza centers (NICs), I saw great variation in influenza facilities; I calculated facilities per million persons (FPM) using 2021 population estimates from the United States Census Bureau International Data Base (IDB) and the Institut national de la statistique et des etudes economiques (Insee) [92-93]. High *reporting* and *diagnostic coverage* indicated greater capacity for capturing and reporting confirmed infections. Higher *time series length* and *extent* scores indicated more usable data per Member State-outcome dyad. In contrast, low *reporting delay* scores suggested shorter lags between data download dates and the most current complete records.

Maximum *extent* scores were 1381 weeks for all outcomes except A(H1N1)pdm09 positives (651 weeks). Though GISRS collected A(H1N1) records since 1978, the pandemic variant appeared in September 2008 [94]. Active reporting of A(H1N1)pdm09 positives in FluNet began Week 1 2009. Ten Member States (Mexico, Cambodia, France, Ghana, Jamaica, Malaysia, Pakistan, Paraguay, Philippines, Slovenia, Ukraine) implausibly reported 0 cases in Week 1 2008, resulting in infeasible scores >651 weeks. I corrected estimates by calculating *extent* as the weeks from the first available record on or after Week 1 2009 to the most recent week of non-missing records.

I scored remaining metrics for *Completeness*, *Alignment*, *Correctness*, and *Variability* indicators using percentages (ranging 0-100%). I calculated percentages as the ratio of weeks meeting a definition criterion divided by total study period or

annual weeks and multiplied by 100%. *Annual* and *seasonal completeness* illustrated structural missingness of data. Higher *outcome* or *location interoperability* indicated greater joint completeness between 2 outcomes or locations. High *correctness* indicated greater concordance between mutually-dependent testing outcomes. High *consistency* indicated greater concordance between datasets, which I calculated using the 626 overlapping weeks (Week 1 2008 to Week 52 2019) from extracted data on my two download dates.

I was unable to estimate scores for 4 of 25 metrics including *testing rigor*, *sampling rigor*, *case compliance*, and *external interoperability*. While *Rigor* metrics are regularly reported by data-curating public health institutions, the WHO does not publicly disseminate this information in metadata files. I did not examine *external interoperability* as no external datasets (i.e., population data) harmonized with FluNet had missing records.

3.3.3. Comparisons by geographic location and population

I compared metrics by 6 WHO-defined regions and 17 influenza transmission zones. I excluded the South African zone, as only 1 country (South Africa) reported data to FluNet during the study period (Appendix A, Supplementary Table S1). I reported median and average metrics' scores with interquartile range and 95% confidence intervals, respectively. I compared scores across regions and zones using Dunn's tests with Bonferroni corrections ($\alpha < 0.05$) to account for score skewness.

I compared *annual* and *seasonal completeness* by study year and calendar week, respectively, using tobit regression models:

$$C_{j,k,t} = \beta_0 + \beta_1(y) \quad \textbf{(1)}$$

$$C_{j,k,t} = \beta_0 + \beta_2\left(\sin\left[\frac{2\pi m}{52.25}\right]\right) + \beta_3\left(\cos\left[\frac{2\pi m}{52.25}\right]\right) \quad \textbf{(2)}$$

where $C_{j,k,t}$ – *completeness* score for *j*-Member State, *k*-outcome, and *t*-study time point; y – study year ranging 1-27; m – calendar week ranging 1-53; and $sin\left[\frac{2\pi m}{52.25}\right]$ and $cos\left[\frac{2\pi m}{52.25}\right]$ – sinusoidal and cosinusoidal harmonic terms adjusted for the length of the annual cycle (52.25 weeks). I constructed models for each Member State, region, and zone. I estimated *annual completeness* using linear trend terms as defined by β_1 and the presence of seasonality for *seasonal completeness* as defined by the significance of either β_2 or β_3.

I performed data extraction, alignment, management, and cleaning using Excel 2016 Version 2103 and Stata SE/16.1 software. I conducted statistical analyses and created data visualizations using Stata SE/16.1, PowerPoint (Version 2112), and R (3.6.3) software (see Supplementary Materials).

3.3.4. Resolution Indicator

FluNet scored 5 of 6 points for the *frequency* metric, as daily records were aggregated and reported weekly. However, FluNet scored only 2 of 6 points for the *representativeness* metric, as records were provided nationally and regionally only (Appendix A, Supplementary Table S1). More spatially-refined records would be reported by population coverage areas of NICs or testing facilities in each Member State.

3.3.5. Comparability Indicator

Most Member States collected specimens for laboratory-confirmed influenza cases and hospitalizations (n=168; 97%), influenza-like-illnesses (n=137; 80%), and severe acute respiratory illnesses (n=110; 64%) but few collected specimens for pneumonia (n=19; 11%) or mortality (n=25; 14%) (Appendix A, Supplementary Tables S2-S8). Nearly all Member States reported tests and total, influenza A, and influenza B positives (n=168-169; 97-98%), yet just two-thirds reported specimens collected (n=116; 67%) and negatives (n=102; 59%). Among subtypes, most Member States reported A(H1N1)pdm09, A(H3), A(Unsubtyped), and all influenza B subtypes (n=154-168; 89-97%) while only 65% (n=112) reported A(H5) positives. Three Caribbean islands (Montserrat, Saint Barthelemy, and Saint Martin) reported no health records to FluNet during the study period.

The AFRO region and corresponding transmission zones monitored significantly more varieties of cases, outcomes, and subtypes than other regions and zones. AFRO had higher median total variety scores than EURO and PAHO; SEARO also had higher total scores than EURO. All regions had higher median outcome variety scores than EURO, as few European Member States reported negatives (n=4, 7.84%) or specimens (n=22, 43.14%). WPRO and AFRO had significantly higher median subtype variety scores than both EURO and PAHO (7.00 [3.00,8.00]; $p<0.001$).

Across transmission zones, Western Africa had higher median outcome variety scores than Northern, Southwestern, and Eastern Europe and Central Asia. Eastern

and Western Africa had higher median total variety scores and subtype variety scores than Central America and the Caribbean.

3.3.6. Coverage Indicator

Worldwide, I identified 152 NICs and 34886 testing facilities with approximately 0.89 NICs [0.74,1.05] and 258.41 facilities per Member State [133.27,383.56], as well as 37.78 FPM [17.28,58.28] (Table 9; Appendix A, Supplementary Table S9). I was unable to estimate facilities in 35 Member States, most located in Central America and the Caribbean (n=9) and Western Asia (n=8). Canada reported the greatest number of NICs (11) while Norway reported the greatest number of facilities (5846) and FPM (1061.06). Fifty Member States, many located in PAHO (22) and AFRO (16), reported 0 NICs. I was unable to estimate total facilities or FPM for the Oceania Melanesia Polynesia zone, as I found no sources that estimated total influenza testing facilities in Australia, New Zealand, Fiji, and New Caledonia.

Table 9. Cumulative and per Member State National influenza centers (NICs) as well as cumulative, per Member State, and per capita testing facilities reporting data to the WHO's FluNet in 6 regions and 17 influenza transmission zones. I reported average (with 95% confidence intervals) and median (with interquartile ranges) NICs and facilities per Member State as well as the average NICs and facilities per million persons (FPM) with 95% confidence intervals using 2021 population estimates [92-93]. Values of *NR* for Oceania Melanesia Polynesia indicate where I could not determine the number of facilities for all Member States in that zone. I report regions and zones in descending order by average NICs per Member State.

Region	NICs			Facilities			FPM	
	Sum	Average	Median	Sum	Average	Median	Average	Median
WPRO	19	1.27 [0.86, 1.67]	1.00 [1.00, 2.00]	1505	167.22 [-36.57, 371.02]	24.00 [15.00, 169.00]	10.39 [-3.00, 23.77]	0.87 [0.22, 1.93]
EURO	54	1.06 [0.89, 1.23]	1.00 [1.00, 1.00]	26342	516.51 [223.95, 809.07]	162.00 [44.00, 478.00]	80.07 [29.57, 130.58]	19.53 [8.93, 35.44]
EMRO	18	0.95 [0.77, 1.13]	1.00 [1.00, 1.00]	1266	140.67 [-2.72, 284.05]	30.00 [9.00, 110.00]	4.85 [0.92, 8.78]	1.52 [1.01, 9.31]
SEARO	10	0.91 [0.42, 1.40]	1.00 [0.00, 1.00]	347	31.55 [18.64, 44.45]	27.00 [13.00, 54.00]	4.40 [0.29, 8.51]	0.92 [0.12, 9.19]
PAHO	36	0.82 [0.31, 1.33]	0.50 [0.00, 1.00]	5154	166.26 [-35.69, 368.20]	17.00 [9.00, 44.00]	23.08 [0.98, 45.18]	3.87 [1.21, 11.39]
AFRO	15	0.50 [0.30, 0.70]	0.00 [0.00, 1.00]	272	11.33 [6.98, 15.69]	8.00 [5.50, 11.50]	4.82 [-3.61, 13.25]	0.48 [0.20, 0.84]
Zone								
North America	12	4.00 [0.00, 10.88]	1.00 [0.00, 11.00]	3247	1623.50 [-1270.39, 4517.39]	1623.50 [147.00, 3100.00]	6.56 [1.29, 11.84]	6.56 [3.87, 9.25]
Temperate South America	6	1.50 [0.52, 2.48]	1.00 [1.00, 2.00]	184	46.00 [21.09, 70.91]	44.00 [30.50, 61.50]	5.14 [-0.14, 10.42]	3.33 [1.65, 8.63]
Northern Europe	12	1.20 [0.81, 1.59]	1.00 [1.00, 1.00]	7727	772.70 [-337.82, 1883.22]	143.00 [94.00, 478.00]	188.73 [-17.74, 395.20]	35.05 [16.96, 265.36]
Northern Africa	6	1.20 [0.81, 1.59]	1.00 [1.00, 1.00]	645	161.25 [-62.97, 385.47]	70.00 [18.50, 304.00]	5.91 [-0.78, 12.60]	4.80 [0.22, 11.59]
Eastern Asia	6	1.20 [0.81, 1.59]	1.00 [1.00, 1.00]	1320	330.00 [-96.25, 756.25]	144.50 [77.00, 583.00]	15.95 [-12.23, 44.14]	2.01 [1.32, 30.59]
Oceania Melanesia	6	1.20	1.00	0	*NR*	*NR*	*NR*	*NR*

Polynesia		[0.06, 2.34]	[0.00, 2.00]					
Eastern Europe	13	1.18 [0.74, 1.63]	1.00 [1.00, 1.00]	7023	638.45 [21.51, 1255.40]	213.00 [158.00, 536.00]	69.37 [8.57, 130.18]	22.74 [9.94, 141.34]
Southwest Europe	21	1.11 [0.85, 1.36]	1.00 [1.00, 1.00]	8039	423.11 [139.14, 707.07]	168.00 [45.00, 650.00]	53.24 [-7.76, 114.23]	20.7 [14.11, 24.09]
Southeast Asia	11	1.10 [0.75, 1.45]	1.00 [1.00, 1.00]	351	39.00 [5.11, 72.89]	18.00 [13.00, 33.00]	4.67 [-1.54, 10.88]	0.87 [0.18, 1.72]
Southern Asia	9	1.00 [0.43, 1.57]	1.00 [1.00, 1.00]	738	92.25 [-35.99, 220.49]	25.00 [13.50, 54.00]	6.34 [0.49, 12.19]	0.94 [0.18, 13.71]
Western Asia	15	0.83 [0.66, 1.01]	1.00 [1.00, 1.00]	462	46.20 [4.04, 88.36]	26.00 [8.00, 40.00]	7.85 [-3.04, 18.74]	2.36 [1.22, 3.76]
Tropical South America	7	0.78 [0.14, 1.41]	1.00 [0.00, 1.00]	372	62.00 [-15.69, 139.69]	25.00 [11.00, 46.00]	2.77 [-0.61, 6.16]	1.13 [0.94, 1.43]
Central Asia	3	0.60 [0.12, 1.08]	1.00 [0.00, 1.00]	3162	632.40 [-570.49, 1835.29]	12.00 [4.00, 57.00]	69.76 [-64.30, 203.82]	1.99 [0.36, 2.96]
Eastern Africa	6	0.60 [0.28, 0.92]	1.00 [0.00, 1.00]	118	13.11 [3.50, 22.72]	9.00 [6.00, 10.00]	11.93 [-10.57, 34.43]	0.22 [0.19, 0.47]
Central America and Caribbean	11	0.39 [0.21, 0.58]	0.00 [0.00, 1.00]	1351	71.11 [-30.64, 172.85]	10.00 [6.00, 21.00]	35.01 [-0.30, 70.32]	6.11 [1.64, 13.96]
Western Africa	4	0.36 [0.07, 0.66]	0.00 [0.00, 1.00]	97	9.70 [5.45, 13.95]	7.00 [4.00, 15.00]	0.55 [0.37, 0.74]	0.52 [0.40, 0.74]
Middle Africa	2	0.29 [0.00, 0.65]	0.00 [0.00, 1.00]	50	12.50 [-0.04, 25.04]	8.00 [4.00, 21.00]	0.67 [0.24, 1.10]	0.74 [0.33, 1.01]
Worldwide	**152**	**0.89 [0.74, 1.05]**	**1.00 [0.00, 1.00]**	**34886**	**258.41 [133.27, 383.56]**	**31.00 [10.00, 162.00]**	**37.78 [17.28, 58.28]**	**3.50 [0.87, 19.53]**

In contrast to *variety score*s, the EURO region and corresponding zones had significantly greater *reporting* and *diagnostic coverage* than other locations (Figure 1). EURO reported the most NICs (n=54) and facilities (n=26342) with 1.5-times more NICs and 5.11-times more facilities than next highest PAHO (NICs=36; facilities=5154). WPRO and EURO had greater median NICs per Member State (1.00 [1.00,2.00] and 1.00 [1.00,1.00], respectively) than AFRO (0.00 [0.00,1.00]; $p \leq 0.003$) and PAHO (0.50 [0.00,1.00]; $p \leq 0.005$). EURO also had higher median FPM (19.53 [8.93,35.44]) compared to all other regions (ranging 0.12-11.39; $p \leq 0.039$).

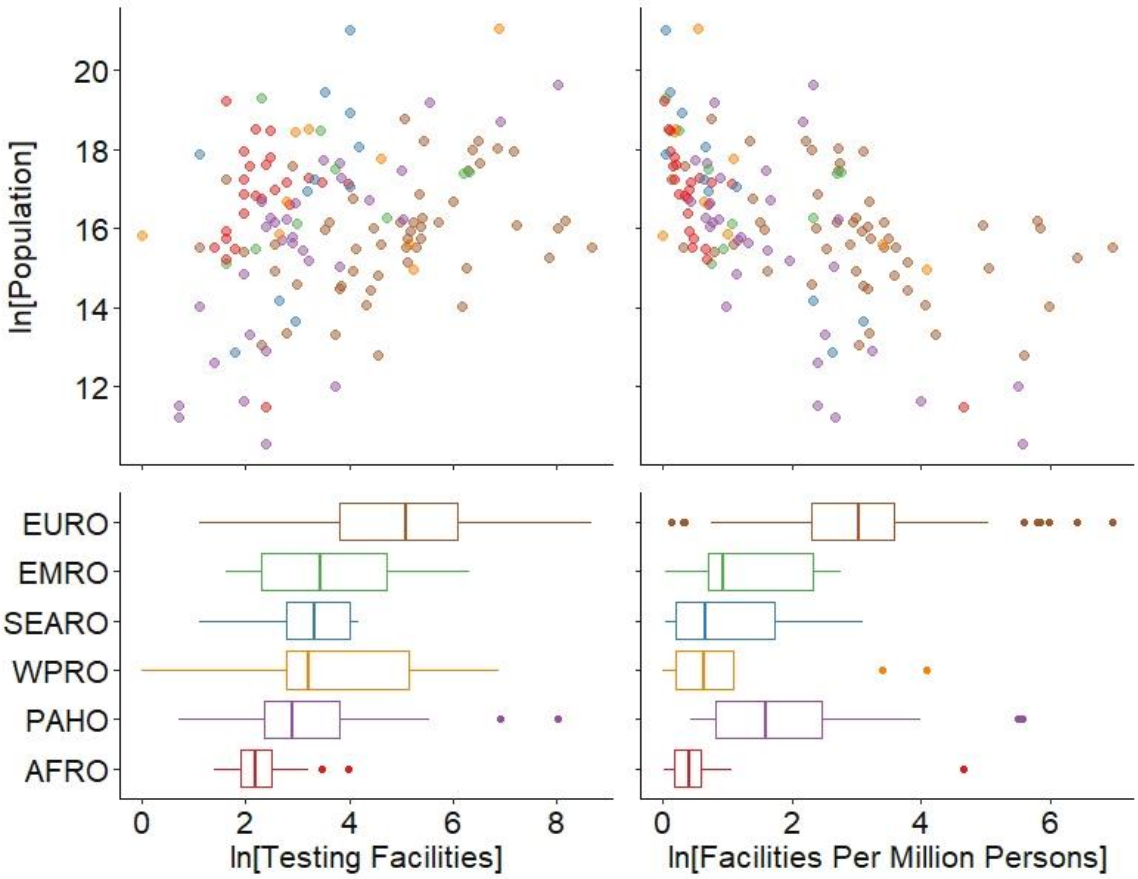


Figure 1. A shared axis, multi-panel plot of the relationship between log-transformed values of Member State 2021 population estimates, influenza testing facilities, and testing facilities per million persons. I extracted Member State population estimates from the United States Census Bureau International Data Base (IDB) and the Institut national de la statistique et des etudes economiques (Insee) [92-93]. I estimated testing facilities using numerous sources [36-91], and calculated facilities per million persons by dividing facilities by population estimates and multiplying by 1,000,000. Scatterplot marker colors (top panel) depict WHO-defined regions (bottom panel) and correspond to the European (EURO), Eastern Mediterranean (EMRO), Southeastern Asia (SEARO), Western Pacific (WPRO), Pan-American (PAHO), and African (AFRO) regions. I report regions in descending order by median testing facilities per Member State.

Northern and Southwestern Europe had greater median NICs (1.00 [1.00,1.00]) and facilities (143.00 [94.00,478.00] and 168.00 [45.00,650.00], respectively) per Member State than Central America and the Caribbean (0.00 [0.00,1.00] and 10.00 [6.00,21.00], respectively; $p \leq 0.043$). Eastern Europe also had greater median facilities per Member State (213.00 [158.00,536.00]; $p=0.001$) than Central America and the Caribbean (Appendix A, Supplementary Figure S1). Northern, Southwestern, and Eastern Europe had greater median facilities per Member State and FPM than both Eastern Africa (9.00 [6.00,10.00] and 0.22 [0.19,0.47], respectively; $p \leq 0.011$) and Western Africa (7.00 [4.00,15.00] and 0.52 [0.40,0.74], respectively; $p \leq 0.002$).

Northern Europe also had greater median FPM than Middle Africa (0.74 [0.33,1.01]; p=0.031).

3.3.7. Duration Indicator

Median *extent* scores for tests and total, influenza A, and influenza B positives (697.00-703.50 [336.00,1224.00] of 1381 weeks) were ~3-times greater than negatives (242.00 [191.00,296.00] weeks). Similarly, median *extent* scores for A(Unsubtyped), A(H1), A(H3), and B(Undetermined) positives (699.00-714.00 [385.00,1198.50] weeks) were ~2-times greater than A(H5) positives (438.50 [194.00,596.50] weeks). Member States reported A(H1N1)pdm09 positives in ~90% of weeks (588.50 [385.00, 631.00] of 651 weeks) since the strain's emergence in 2009 (Appendix A, Supplementary Tables S10-S13).

Like with *reporting* and *diagnostic coverage*, EURO had higher median *extent* for total, influenza A, and influenza B positives and tests (1265.00 [634.00,1274.00], 1265.00 [634.00,1274.00], 1169.00 [613.00,1272.00], and 1075.00 [631.00,1225.00] weeks, respectively; $p \leq 0.015$) than AFRO, EMRO, and PAHO (Figure 2). EURO also had higher median *extent* for A(H3), A(Unsubtyped), A(H1), and B(Undetermined) positives than AFRO and EMRO ($p \leq 0.011$) as well as A(H3), B(Undetermined), and A(H1N1)pdm09 positives compared to PAHO ($p \leq 0.022$). WPRO had higher median *extent* for total, influenza A, and influenza B positives and tests (1016.00 [767.00,1275.00], 1016.00 [767.00,1275.00], 939.00 [754.00,1269.00], and 984.00 [767.00,1230.00] weeks, respectively; $p \leq 0.016$) than EMRO.

All Member States in North America, Northern Europe, Eastern Europe, and Central Asia failed to report any weekly records on negatives. Central Asian Member States (Kazakhstan, Kyrgyzstan, Tajikistan, Turkmenistan, Uzbekistan) also failed to report records on specimens processed. Northern, Southwestern, and Eastern Europe had higher median *extent* for total, influenza A, and influenza B positives than Central America and the Caribbean and Western Asia ($p \leq 0.031$). These European zones also had significantly higher median *extent* for A(H1), A(H3), A(Unsubtyped), and B(Undetermined) positives than Western Asia ($p \leq 0.031$; Appendix A, Supplementary Figure S2).

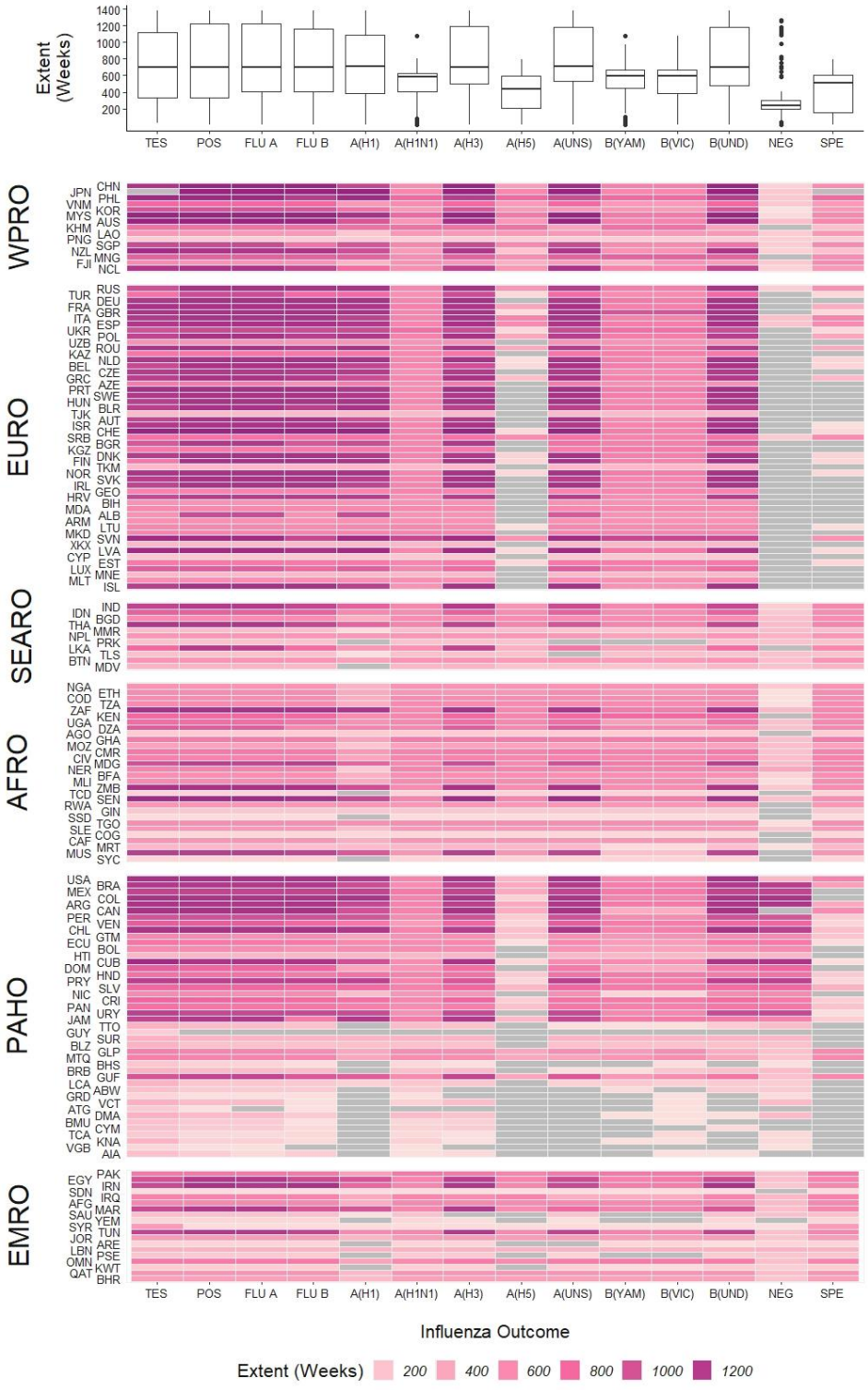


Figure 2. A shared axis, multi-panel heatmap of the *extent* for 6 WHO-defined regions and worldwide for 14 influenza variables, including 6 testing outcomes (specimens collected (SPE), specimens processed or tests (TES), influenza A positives (FLUA), influenza B positives (FLUB), total positives (POS), and total negatives (NEG)) and 8 influenza strains and subtypes (A(H1), A(H1N1)pdm09, A(H3), A(H5), A(Unsubtyped), B(Yamagata), B(Victoria), and B(Undetermined) positives). I calculated *extent* as the time series length from the first to the last week with non-missing records in the study period. A boxplot depicts worldwide *extent* while heatmaps describe *extent* by region in descending order by Member State population. Light pink indicates low extent (~200 weeks) while

dark purple indicates high extent (~1200 weeks). Grey color indicates Member States having missing observations for all weeks with the time series.

3.3.8. Completeness Indicator

The median *average completeness* was ~10-times greater for tests, and total, influenza A, and influenza B positives (41.42% [20.93, 53.66], 40.04% [18.90, 55.32], 39.79% [18.90, 54.96], 35.88% [18.90, 47.86]) compared to negatives (3.48% [0.00, 16.51]). Despite moderate *variety*, *coverage*, and *extent* scores, WPRO had greater median *completeness* for total, influenza A, and influenza B positives (57.71% [39.90, 82.48], 56.92% [39.90, 82.19], and 55.10% [39.90, 60.46], respectively; $p \leq 0.008$) than AFRO, EMRO, and PAHO (Figure 3; Appendix A, Supplementary Tables S14-S17). Across subtypes, WPRO had higher median *completeness* for A(H1N1)pdm09, A(H3), A(Unsubtyped), and all influenza B positive subtypes than EMRO and PAHO ($p \leq 0.011$). WPRO also had higher median *completeness* for A(H1) positives compared to AFRO and SEARO and A(H5) positives compared to EURO.

I found few differences in *average completeness* by zone (Appendix A, Supplementary Figure S3). Northern Europe had greater median *completeness* for positives, influenza A positives, tests, and influenza B positives than Central America and the Caribbean and Western Asia ($p \leq 0.030$). Northern Europe had greater median *completeness* scores for all disease subtypes except A(H5) positives compared to Central America and the Caribbean ($p \leq 0.011$). Southern Asia had greater median *completeness* for all subtypes except A(H1) and A(Unsubtyped) positives compared to Central America and the Caribbean ($p \leq 0.039$). In addition, Northern Europe had greater median *completeness* scores for all subtypes except A(H1N1)pdm09 and A(H5) positives compared to Western Asia ($p \leq 0.034$).

Annual completeness increased by ~2-3% per year for tests and total, influenza A, and influenza B positives (2.93 [2.74,3.12], 2.77 [2.59,2.94], 2.72 [2.54,2.89]), and 2.32 [2.15,2.49], respectively; $p<0.001$). However, these outcomes demonstrated slight declines since the onset of the novel SARS-CoV-2 pandemic in 2019 (COVID-19). In contrast, negatives and specimens collected decreased by ~6% per year, roughly halving since the onset of the COVID-19 pandemic (-6.31 [-7.20,-5.41] and -6.43 [-7.19,-5.66], respectively; $p<0.001$; Figure 4; Appendix A, Supplementary Figures S4-S5; Supplementary Table S18).

All subtypes increased by lesser magnitude per year with prominent improvements in A(H3), B(Undetermined), and A(Unsubtyped) positives'

completeness in 1995-2011 (2.47 [2.29,2.65], 2.15 [1.97,2.32], and 2.13 [1.93,2.33], respectively; $p<0.001$). Since the conclusion of the 2009 A(H1N1) pandemic, completeness of these subtypes plateaued at ~60% worldwide. While few Member States reported A(H5) positives in 1995-2009, *annual completeness* reached ~40% during the A(H1N1) pandemic in 2009-2011. Since then, A(H5) positives' reporting has nearly halved (~40% to ~20% completeness) worldwide by ~6.76%/year [-7.66,-5.86] ($p<0.001$; Figure 5; Appendix A, Supplementary Figure S6).

WPRO had the greatest annual increase for tests and all positive testing outcomes (ranging 4.05-6.96%/year; $p<0.001$) while EMRO had the least increase for these outcomes (ranging 0.13-1.75%/year; $p\leq0.023$). In contrast, EURO had the greatest annual decline for negatives (-23.86%/year [-35.60, -12.11]; $p<0.001$) while PAHO had the greatest decline for specimens collected (-20.93%/year [-27.13,-14.73]; $p<0.001$).

I found the presence of *seasonal completeness* for testing outcomes and disease subtypes worldwide ($p<0.001$) except specimens processed, negatives, and A(H5) positives (Figure 6; Appendix A, Supplementary Figure S7). All outcomes and subtypes had consistently lower completeness during calendar Weeks 26-38 (Appendix A, Supplementary Table S19). EMRO and EURO similarly had significant seasonality ($p\leq0.027$) for all testing outcomes and disease subtypes except specimens processed, negatives, and A(H5) positives.

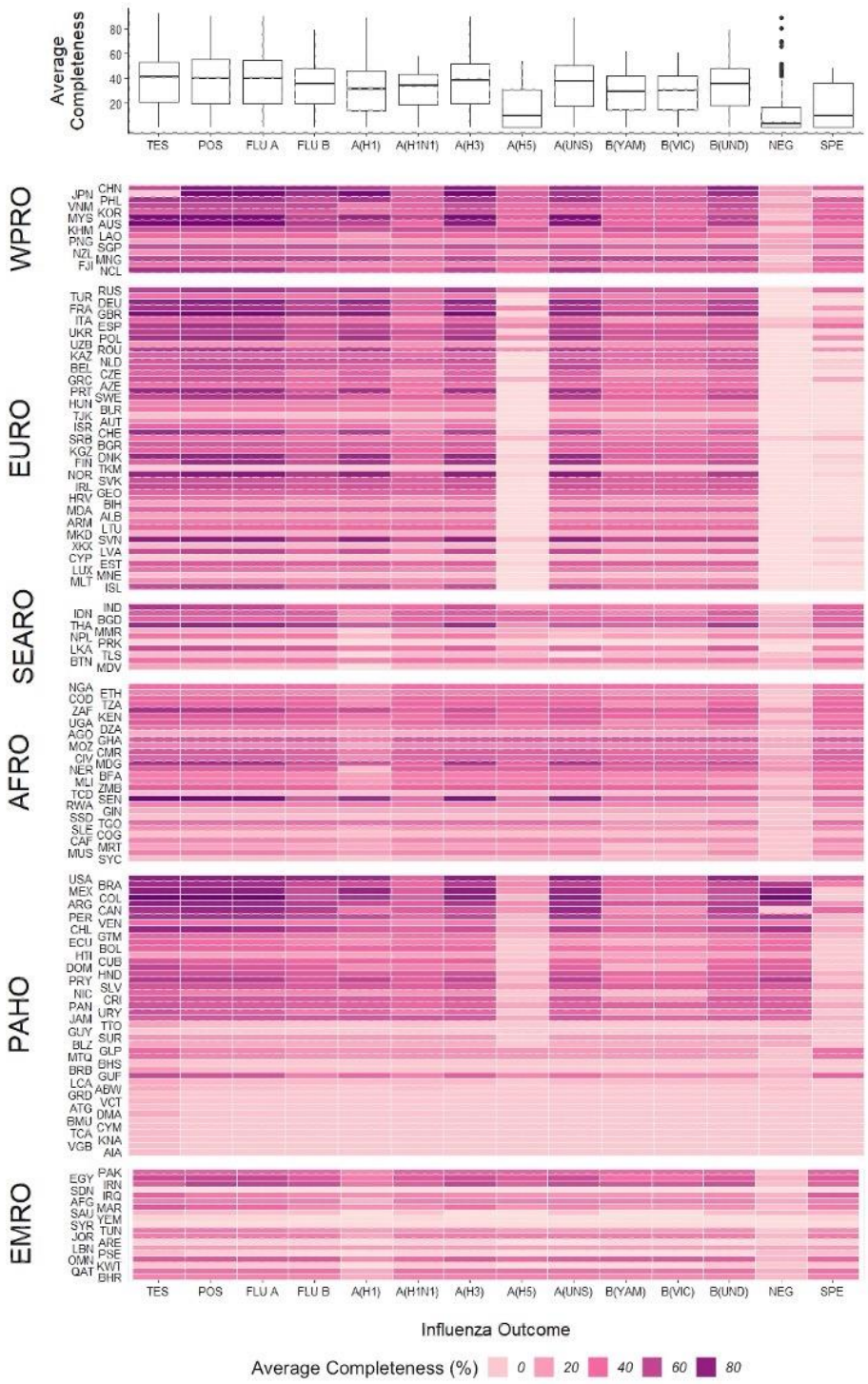


Figure 3. A shared axis, multi-panel heatmap of the *average completeness* for 6 WHO-defined regions and worldwide for 14 influenza variables. I calculated *completeness* as the number of weeks with non-missing records (i.e., counts ≥ 0) in the overall time series and multiplied by 100. A boxplot depicts worldwide *completeness* while heatmaps describe *completeness* by region in descending order by Member State population. Light pink indicates low completeness (~0%) while dark purple indicates high completeness (~80%).

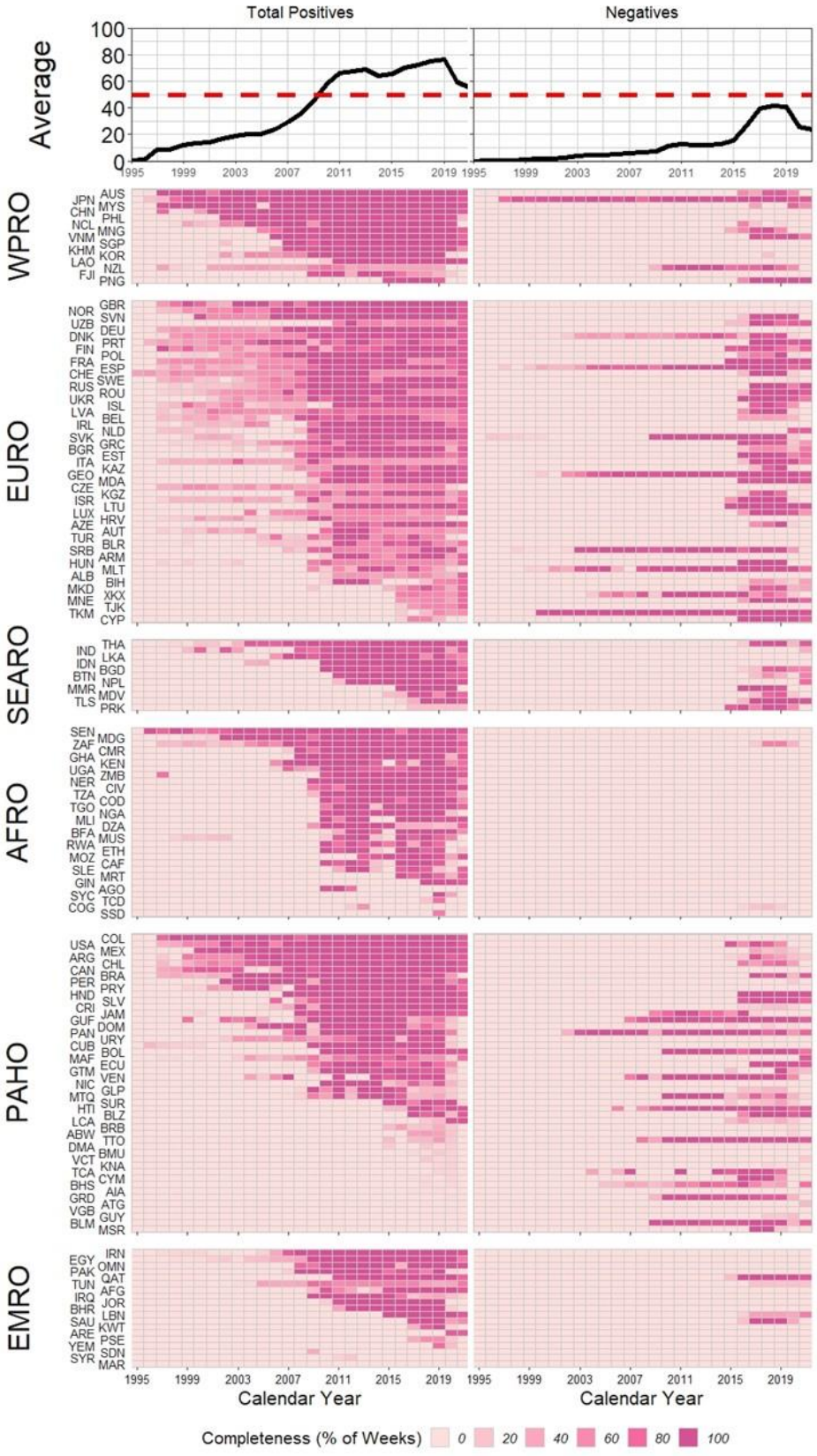


Figure 4. A shared axis, multi-panel heatmap of the *annual completeness* for 6 WHO-defined regions and worldwide for total positives and negatives. I calculated *annual completeness* as the number of weeks with non-missing records (i.e., counts ≥ 0) per total Gregorian calendar year (52 or 53 weeks) and multiplied by 100. I provide a time series plot (top panel) for each variable depicting average worldwide *annual completeness* as well as heatmaps by region (bottom panels) in descending order by

total positives *completeness*. Light pink indicates ~0% while dark purple indicates ~100% completeness per year.

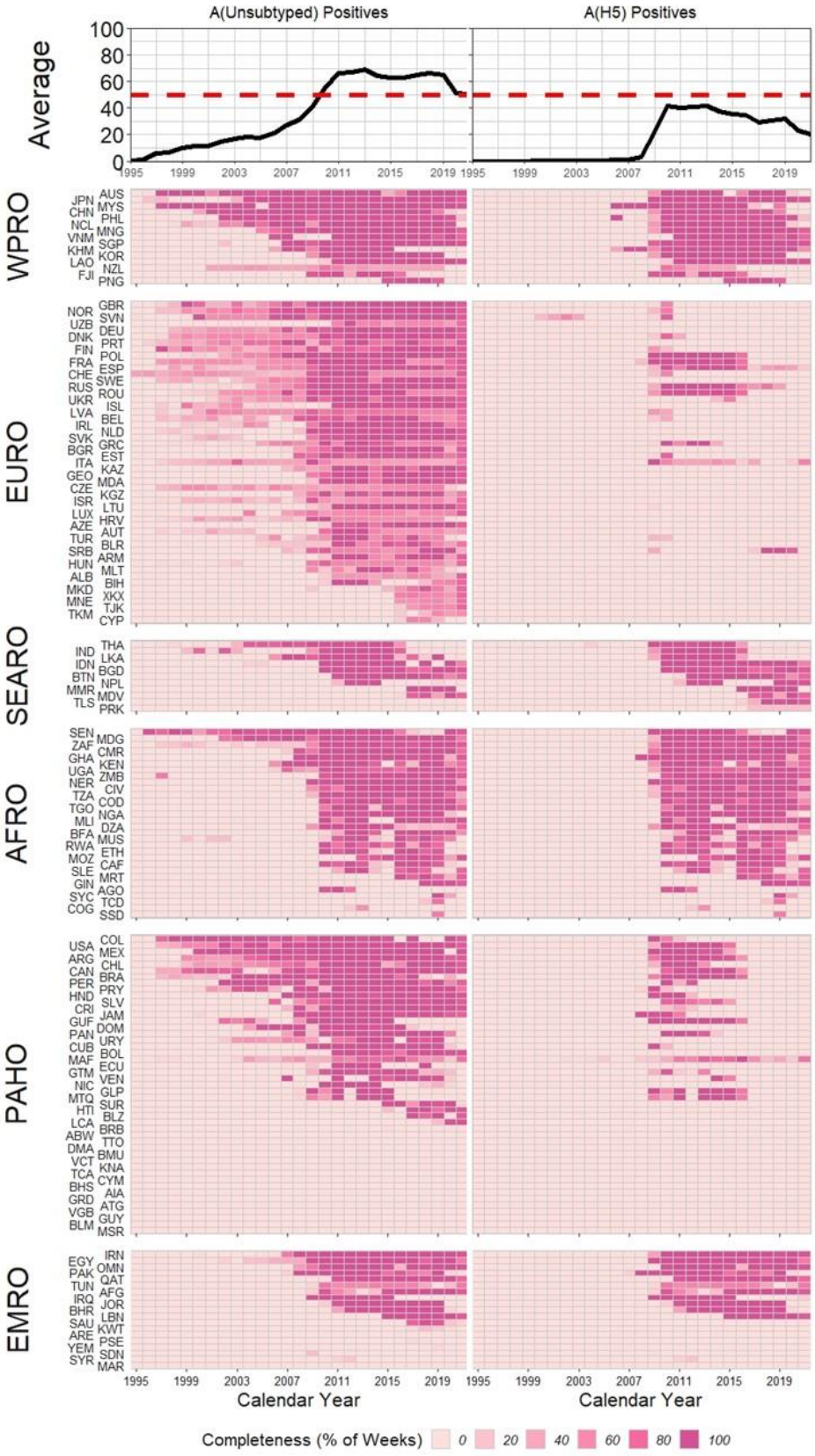


Figure 5. A shared axis, multi-panel heatmap of the *annual completeness* for 6 WHO-defined regions and worldwide for A(Unsubtyped) and A(H5) positives. I calculated *annual completeness* as the

number of weeks with non-missing records (i.e., counts ≥ 0) per total Gregorian calendar year (52 or 53 weeks) and multiplied by 100. I provide a time series plot (top panel) for each variable depicting average worldwide *annual completeness* as well as heatmaps by region (bottom panels) in descending order by total positives *completeness*. Light pink indicates ~0% while dark purple indicates ~100% completeness per year.

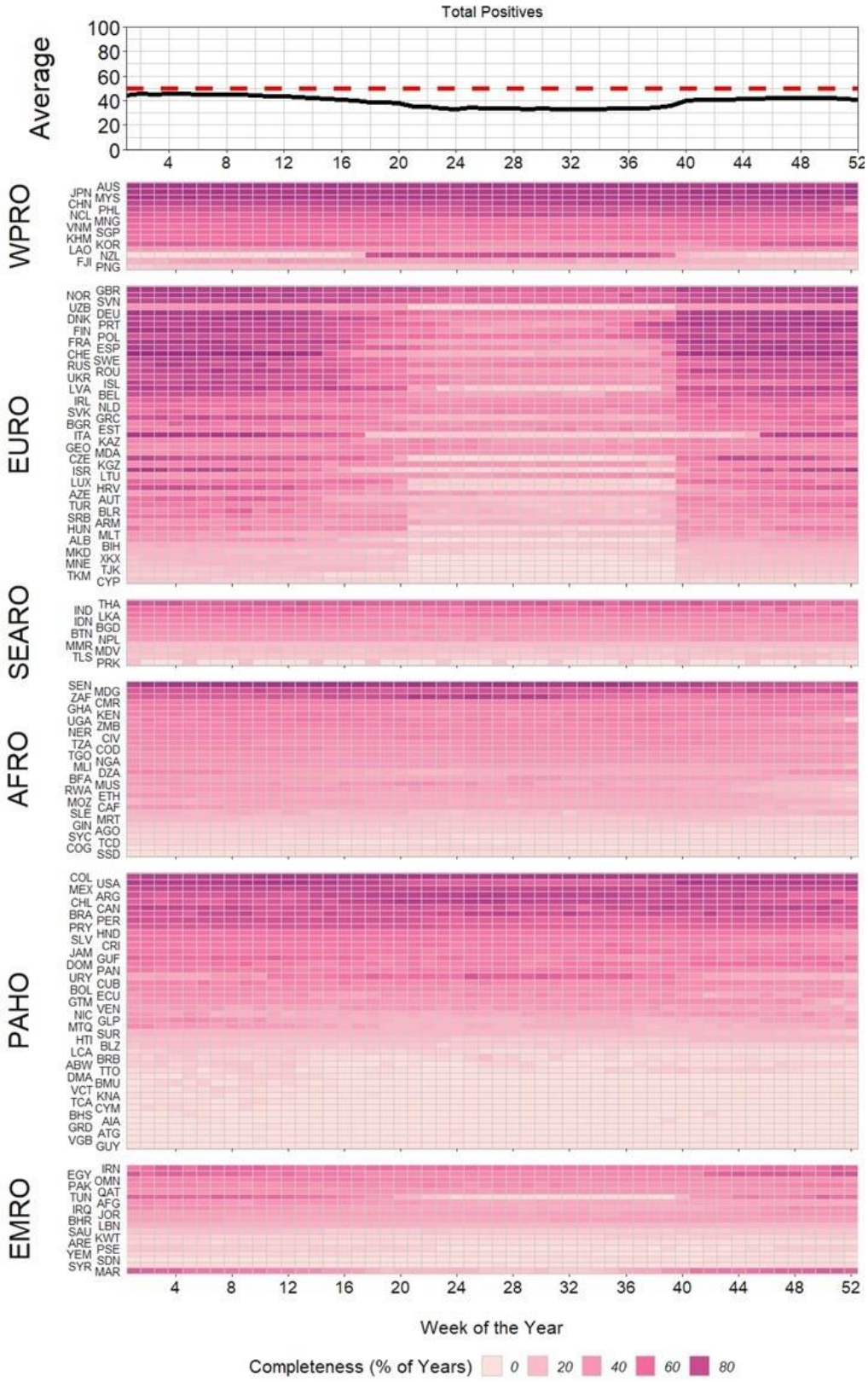


Figure 6. A shared axis, multi-panel heatmap of the *seasonal completeness* for 6 WHO-defined regions and worldwide for total positives. I calculated *seasonal completeness* as the number of calendar years with non-missing records (i.e., counts ≥ 0) for each week of the year per total study years that week occurred (26 or 27) and multiplied by 100. I provide a time series plot (top panel) for each variable depicting average worldwide *seasonal completeness* as well as heatmaps by region (bottom panels) in descending order by total positives *completeness*. Light pink indicates ~0% while dark purple indicates ~100% completeness per year.

3.3.9. Lag Indicator

Median *delays* were shortest for tests, all positive outcomes, and all disease subtypes except specimens processed, A(H1) positives, and A(H5) positives (36.00 [4.00,305.50], 67.50 [2.00,247.00], and 77.00 [4.50,342.00] weeks, respectively; Figure 7; Appendix A, Supplementary Tables S20-S24). While PAHO had shorter tests' *delays* than other regions (1.00 [1.00, 1.00] week; p≤0.026), PAHO and EURO had 8-10 times longer *delays* for specimens processed (395.00 [110.00,494.50] and 550.00 [245.00,564.00] weeks, respectively; p≤0.004). Similarly, while EURO had shorter A(H1) positives' *delays* than other regions (3.00 [2.00,5.00] weeks; p≤0.005), EURO and PAHO had ~5-100 times longer A(H5) positives' *delays* (548.00 [245.00,562.00] and 380.00 [258.00,462.00] weeks, respectively; p≤0.001).

Central America and the Caribbean had shorter tests' *delays* (1.00 [1.00,1.00] weeks) than Southwest Europe, Northern, Eastern, and Middle Africa, Western Asia, and Oceania Melanesia Polynesia (p≤0.012) (Appendix A, Supplementary Figure S8). In contrast, Western Africa, Southern Asia, and Southeastern Asia had shorter specimens processed *delays* (4.00 [2.00,12.00], 2.00 [1.00,4.00], and 3.00 [1.00,8.00] weeks, respectively; p≤0.031) than Northern Europe (562.00 [552.00,576.00] weeks) and Central America and the Caribbean (407.00 [309.00,479.00] weeks). While Northern Europe had shorter A(H1) positives' *delays* (2.00 [2.00,3.00] weeks) than all African zones, Southern Asia, and Oceania Melanesia Polynesia (p≤0.033), Northern Europe and Central America and the Caribbean had longer A(H5) positives' *delays* (562.00 [552.00,576.00] and 393.50 [309.00,462.00] weeks, respectively) than Eastern Africa, Western Africa, Southern Asia, and Southeastern Asia (p≤0.037).

3.3.10. Alignment, Correctness, and Variability Indicators

Median *outcome* and *location interoperability* were greatest between A(H1N1)pdm09 positives and all other testing outcomes (Appendix A, Supplementary Table S25-S33). WPRO had the highest *outcome interoperability* (≥84.64%) between A(H1N1)pdm09 and all other outcomes except A(H1) positives

(~58.37%) whereas PAHO had the lowest scores (≤53.92%). Similarly, Southeastern Asia and Oceania Melanesia Polynesia had the highest scores (≥78.49%) whereas Central America and the Caribbean had the lowest scores (≤19.66%). High scores (≥80.72%) occurred between A(H1N1)pdm09 and all other outcomes except A(H5) positives (≤9.92%) in Temperate South America, Northern Europe, and Eastern Europe. The lowest scores for all *outcome interoperability* comparisons were in Middle Africa (≤21.51%). *Location interoperability* was strongest between Member States in the same region and zone.

Regions and zones had >95% *correctness* for all metrics except *tests' correctness* (Appendix A, Supplementary Tables S34-S37). Across zones, only Eastern and Southwestern Europe had <95% *correctness* for specimens processed (36.06% [3.92,78.29] and 81.78% [50.56,98.00]). Tests had significantly lower *correctness* (29.11% [10.81,89.70]) than other metrics except in PAHO (100.00% [100.00,100.00]) and its corresponding Central, Tropical South, and Temperate South American zones (100.00% [100.00,100.00], 100.00% [85.90,100.00], and 98.03% [95.44,100.00]; respectively). Lower *tests' correctness* was attributed to 70 Member States failing to report any negatives and/or tests in the study period.

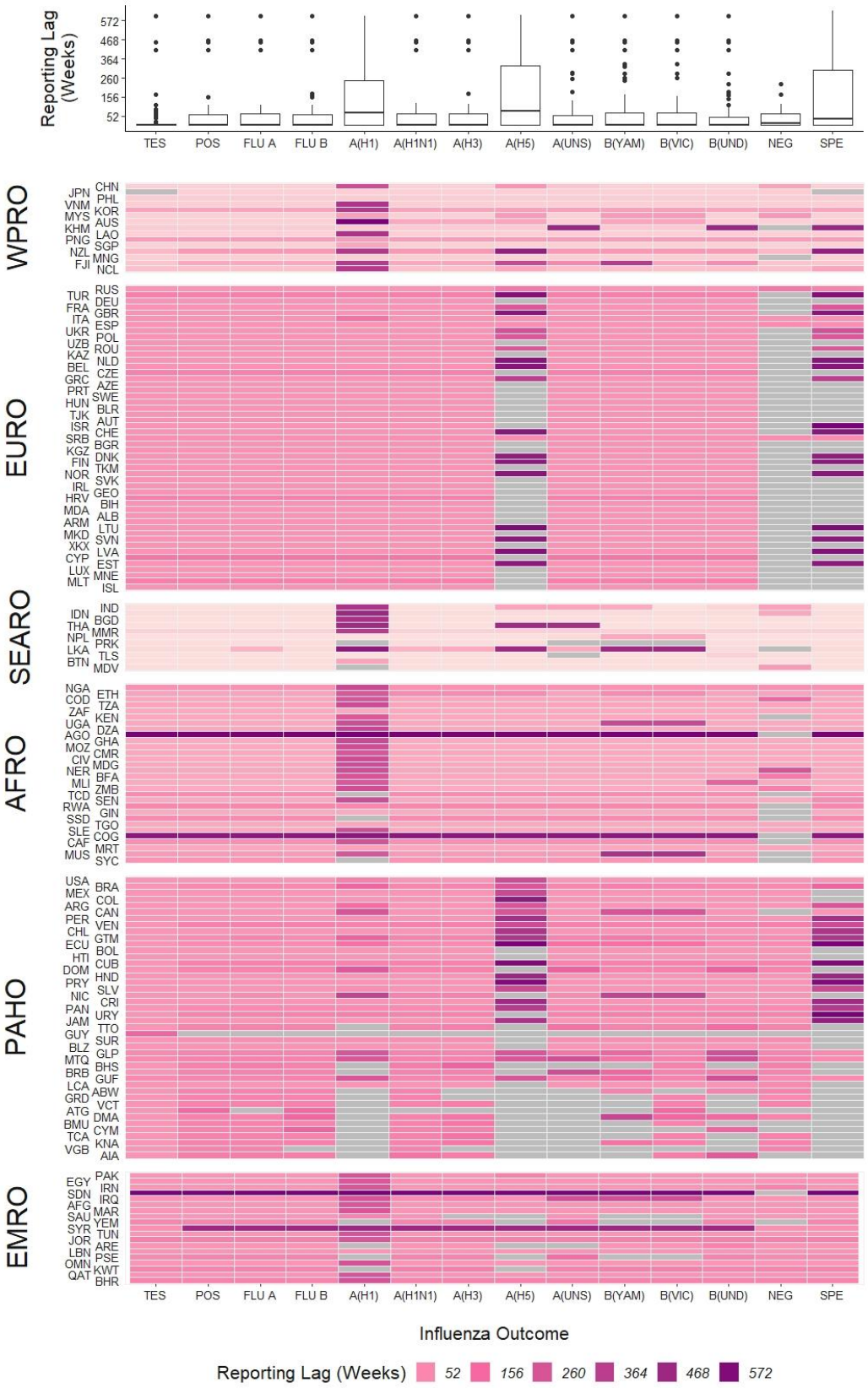


Figure 7. A shared axis, multi-panel heatmap of the *reporting lag* for 6 WHO-defined regions and worldwide for 14 influenza variables. I calculated *reporting lag* as the number of weeks from the date of data download to the most recent week when records are not missing. I provide a boxplot (top panel) for each variable depicting worldwide *reporting lag* as well as heatmaps by region (bottom panels) in

descending order by Member State population. Light pink indicates ~52 weeks while dark purple indicates ~572 weeks.

Interestingly, when replacing missing records with 0 counts, I found no difference in median *specimens'*, *positives'*, and *strains' correctness* scores. However, median *tests' correctness* improved 3-fold to 98.86% [87.76,100.00]. Within this sub-analysis, I could not calculate *tests' correctness* for only 2 Member States (Guyana and Japan), who failed to report any tests in the study period. This suggested that most Member States did not differentiate between incomplete records and 0 counts particularly when reporting negatives.

I estimated *consistency* metrics for all influenza health outcomes and disease subtypes to compare concordance of data records downloaded on 13 June 2020 and 15 June 2021 (Appendix A, Supplementary Tables S38-S41). I found ~100% median *consistency* between data download dates worldwide for all outcomes and subtypes with ~95% median *consistency* per region and zone.

3.3.11. Discussion

The ACTOR data-driven metrics establish metadata repeatable for any time-referenced disease surveillance records. Metrics guide data curators in improving surveillance system data quality and assist modelers in understanding data quality limitations before conducting spatiotemporal analyses. Metadata improve both the precision of data reporting (by curators) and real-time surveillance and near-term forecasting (by modelers) of diseases with pandemic potential, such as seasonal influenza or SARS-CoV-2 [95-96].

3.3.11.1. Improve Spatiotemporal Data Resolution

I encourage data curators to disseminate daily records with representativeness granular to the reporting coverage areas of NICs and testing facilities. Increased data resolution will extend the usability of surveillance data for conducting complex network analyses and utilizing advanced data visualization techniques to monitor traveling waves of infection. More specific spatial information enhances disease transmission tracking, increases precision when investigating population-level transmission-related risk factors, and facilitates the alignment and harmonization of environmental sub-national data streams such as temperature, precipitation, and relative humidity. Additionally, population estimates of these smaller geographic extents permit more precise estimation of disease incidence.

While FluNet offers weekly records, daily records can improve the precision of seasonal peak timing and amplitude estimates as well as detection and characterization of outbreak signatures [25,30]. Daily data permits closer inspection of day-of-the-week effects of data reporting, improves precision of near-term forecasts, and offers flexibility when aggregating data during statistical modeling [97]. If the WHO established an international precedent to disseminate high-resolution spatiotemporal surveillance data, it would redefine real-time infectious disease surveillance by ensuring the continuity of ongoing curation practices during COVID-19 [98].

3.3.11.2. Expand Reporting of Case Definitions

The WHO collects influenza records predominantly on cases, hospitalizations, ILI, and SARI, yet does not disaggregate disseminated data by symptom or case severity. These data streams would permit early warning detection of novel influenza strains or emerging outbreak threats in accordance with SARS-CoV-2 and seasonal influenza joint surveillance directives [8,99-100]. Reporting of patient symptoms permits ongoing efforts for global infectious disease syndromic surveillance, pushing the global health agenda towards preventative intervention strategies. Morbidity and mortality case definitions allow closer examination into seasonal outbreak severity signatures, which can complement estimates on the timing, duration, and magnitude of seasonal case volumes [101]. Together, increased variety of reported health outcomes can inform the quantities, types, and optimal timing of fiscal and in-kind resources to reduce case volumes and infection severity for emerging and recurrent health threats.

3.3.11.3. Balance Data Quality and Data Quality

Only two-thirds of Member States reported specimens collected, negatives, and A(H5) positives with ~10-times lower average completeness than tests and total, influenza A, and influenza B positives. Completeness decreased by ~6% per year after the conclusion of the 2009 A(H1N1) pandemic in 2011. These 3 outcomes also had 5-100-times longer reporting delays than other testing outcomes. Data on specimens processed and negatives can inform modelers of the annual capacity, consistency, and frequency of influenza testing to regulate vaccine and test stockpiling [2,99,102]. Deficiencies in reporting negatives stems from inconsistent differentiation between

blanks and 0 count records; I recommend that FluNet provide a description for the reasons of incomplete records in public data downloads. Greater information and inspection of the quantity, patterns, and reasons for missing data will improve uniformity in modelers' interpretation and manipulation of blanks, promoting research reproducibility.

Remarked as the next strain likely of pandemic potential, A(H5) positives requires immediate improvement in reporting by the global community [102]. Time series analyses require extensive historical records to ensure sufficient statistical power to precisely model disease trends and seasonality features. Longer durations of historical records also enable modelers to examine how outbreak patterns shift, drift, or vary over time. The absence of complete A(H5) positives data inhibits the detection of aberrations in annual and seasonal trends to serve as alarms for potential outbreak events. Until timely and complete surveillance has been established, I recommend Member States utilize real-time surveillance of A(Unsubtyped) and B(Undetermined) positives as markers for early outbreak warnings. These outcomes have high completeness, limited reporting delays, and reflect the limited genus and species identification likely of emerging threats.

While EURO had 1.5-times the NICs and 5.11-times more facilities than the next highest region, few Member States reported negatives, specimens, or A(H5) positives. Furthermore, despite the median FPM in EURO exceeding all other regions, the completeness of these 3 outcomes halved in 2011-2019. EURO and PAHO, having this extensive diagnostic coverage and the highest public health spending Member States worldwide, should establish a strong precedent for international surveillance standards. By diverting resources to improve the monitoring of A(H5) positives, these regions can help drive the international agenda towards more comprehensive, data-driven pandemic preparedness planning. Furthermore, improved A(H5) testing capacities within these regions' NICs can establish outposts for processing global specimen samples for emerging A(H5) subtypes.

In contrast, AFRO monitored a wider variety of cases, outcomes, and subtypes despite ~50% and ~5% of the NICS and facilities, respectively, than EURO and PAHO. Regional differences illustrate the interdependency of surveillance data quantity and quality; while a broader capture of influenza subtypes, AFRO collects poorer quality data on all outcomes. Yet, AFRO's higher total variety scores despite minimal health infrastructure exemplifies positive deviance for improving the

efficiency of data curation amidst limited public health spending [103]. This demonstrates that African nations excel at decentralized influenza testing by establishing a network of diagnostic facilities without overwhelming the fiscal or human resources available in any one location. This technique could be adopted by lower-income countries to maintain longitudinal influenza surveillance. However, closing the gap in public health expenditure between higher- and lower-income countries must be a top priority to boost data completeness and usability in AFRO and EMRO.

3.3.11.4. Assess Near-Term Forecast Accuracy

The WHO privately monitors the *sampling rigor*, *testing rigor*, and *case compliance* of facilities and NICs using various internal reports. This ensures the timeliness of specimen processing as well as the precision and representativeness of reported records. However, these reports are not publicly available and unlikely to be produced on a weekly basis. While *sampling rigor* can assess the degree of underreporting expected in surveillance data, *testing rigor* provides a proxy for weekly test accuracy based on sampling sensitivity and specificity. I encourage the public reporting of weekly *rigor*-related metrics to better understand how testing capacity fluctuates in response to increased or decreased case volumes. Modelers can utilize these metrics to assess the precision and accuracy of real-time surveillance models and near-term forecasts they produce.

In addition, modelers require information on *reporting delay* to assess the precision of near-term forecasts. Shorter *delays* suggest narrower intervals between the last reported record and last time point of a modeler's forecast horizon. This narrow interval permits more precise predictions of expected trends in incidence. In contrast, longer *delays* produce less precise forecasts, as models are developed using more historic data with longer durations of missing records between available records and the forecast horizon. The effect of *reporting delays* on real-time surveillance and near-term forecasting emphasizes the importance of timely, consistent, and complete surveillance reporting. I encourage modelers to use this metric as a tool for describing and evaluating forecast precision.

3.3.11.5. Case Study Limitations

While I extracted NICs and facilities from various sources, I have no means of validating these estimates using FluNet data downloads. I encourage data curators to report information on the population catchment of NICs and facilities by Member State. These metrics can determine data's representativeness and the generalizability of modeler recommendations based on analytical findings. Furthermore, improved *reporting coverage* would allow modelers to estimate case rates and incidence more precisely without relying on annual national population estimates.

I did not calculate a composite score across metrics to emphasize the importance of each metric in informing statistical models and procedures. Coarsely summarizing a surveillance system's data quality undermines the utility of these metrics as a metadata file for assisting modelers. My results articulated the accomplishments and areas of improvement for future FluNet surveillance efforts across WHO regions and zones. I also described how each metric can inform modelers analytical workflow and decision-making when performing time series analyses, for which a composite score has no use.

Worldwide, and specifically within EURO and EMRO, I found *seasonal completeness* nadirs between the summer solstice and autumnal equinox (Weeks 26-38). Member States from these regions consistently reported seasonal peaks of numerous influenza subtypes and influenza-like illnesses during Weeks 45-13 [104-105]. Lower *seasonal completeness* suggests that these regions may diversify laboratory testing resources to monitor other infections during times of expected seasonal nadirs. Yet, seasonal completeness may greatly impact the precision of seasonal peak timing estimates. Future works must evaluate the relationship between data completeness and seasonal estimates of influenza strains and subtypes.

3.4. Completeness of open access FluNet influenza surveillance data for Pan-America in 2005-2019

In the second case study, I explore relationships between public health surveillance data and socioeconomic factors, such as health expenditure and infrastructure, that have been shown to influence the quality and quantity of surveillance data [106]. This case study demonstrates the role that global and national financing must play in creating greater equity and quality of infectious disease surveillance data. Strong associations between health expenditure and data completeness illustrate how data longevity, sustainability, and usability directly

correlates with available funding resources. For this study, I again use FluNet data but with a narrower study interval (2005-2019) and PAHO regional focus. I selected PAHO as it reflects the global variability in surveillance capacity ranging from high-quality data of developed, high-income countries in North America and Southern Tropical and Temperate America to low-quality data of developing, low- and middle-income countries in Central America and the Caribbean.

By harmonizing external data streams reported by the World Bank, this case study also illustrates the importance of the *external interoperability* metric for drawing comparisons between health surveillance capacity and associated risk factors. Works utilize national-level socioeconomic factors like gross national income per capita (GNIPC) and public health expenditure per capita. I compare these metrics to *average* and *annual completeness* metrics to evaluate how surveillance capacity changed before and after the 2009 influenza A(H1N1) pandemic. However, I note that the study's primary limitation is a lack of joint completeness between health and socioeconomic time series during comparative regression analyses.

Manuscript M2. Simpson, R. B., Gottlieb, J., Zhou, B., Hartwick, M. A., and Naumova, E. N. "Completeness of open access FluNet influenza surveillance data for Pan-America in 2005-2019." *Scientific Reports* 11, no. 1 (2021). 1-17. https://doi.org/10.1038/s41598-020-80842-9.

3.5. Conclusion: Socioeconomic and geographic patterns of data quality and seasonality

The *ACTOR* metrics provide an analytical framework for evaluating the quality and fidelity of time series data. I encourage data curating organizations to produce summary tables of these metrics to serve as metadata accompanying data downloads. Additional metadata information pertinent for FluNet reporting includes: i) definitions of health and testing outcomes; ii) explanations of differences between 0 values and blanks; and iii) the capture area of reporting facilities for each geographic location. These same data quality challenges have been well documented for COVID-19 pandemic surveillance systems; even with emerging digital technologies to improve the volume and velocity of disease monitoring, data curating organizations fail to assess the quality of their data for modeling purposes. I encourage the application of *ACTOR* metrics for time-referenced surveillance data on respiratory illnesses, such as

rotavirus, Zika virus, or coronavirus, and less-established enteric illness surveillance systems such as for foodborne and waterborne diseases, outbreaks, and recalls. The creation of a statistical programming package could promote the generalizability of applying these metrics broadly across disease surveillance systems.

The second case study demonstrated important associations between socioeconomic risk factors and surveillance capacity at the regional level. These relationships inform future strategies for public health financing and resource management at the global and regional levels. Public health expenditure must be increased to improve health surveillance capacity, especially by lower- and lower-middle-income countries. This includes improving capacity and quantity of laboratory testing facilities and establishing consistent, year-round surveillance on epidemic-prone illnesses. Integration of multiplex testing to screen for a wide variety of infections will permit greater capture of emerging infections and more extensive assessment of coinfections. However, more intensive testing diagnostics must not lead to poorer sampling strategies, like pooled testing, in resource constrained locations.

Future research should consider non-economic risk factors to compare to spatiotemporal trends of diseases including vaccine supplies, environmental and climatic risk factors, or syndromic surveillance on influenza symptomology. Additional research is also needed to evaluate associations between data quality, socioeconomic risk factors, and the global health community's assumptions of global influenza seasonality patterns. Prior research has documented strong associations between seasonal peak timing and a geographic location's latitude or distance from the equator [107-108]. These associations are driven by the relationship between country latitude and environmental and climatic processes such as temperature, precipitation, humidity, and photoperiods. Studies show that Northern Hemisphere locations tend to have seasonal peak timing later or earlier in the calendar year while Southern Hemisphere locations peak near the year's midpoint [108]. Yet, many studies have concluded no stable seasonality exists in Tropical latitudes near the equator due to a confluence of environmental drivers. These findings come after nearly 2 decades of limited to no research at these latitudes, as too little data were available to conduct time series analyses.

My preliminary findings from exploratory data visualizations using various data sources suggest a different story: Member States within the Tropics do not lack influenza seasonality, but rather sufficient data quality to estimate outbreak signatures

precisely and accurately [109-111]. I found strong visual relationships for influenza tests and total, Influenza A, and Influenza B positives between average completeness, GNIPC, seasonal peak timing, and Member State latitude (Figure 8-11). For many EURO Member States, I found that countries and territories at higher latitudes often had higher average incomes, more data completeness, and clustered seasonal peak timing at Weeks 46-5. For many WPRO and South American Member States with similar data quality and wealth, seasonal peak timing clustered, as expected, at Weeks 23-36.

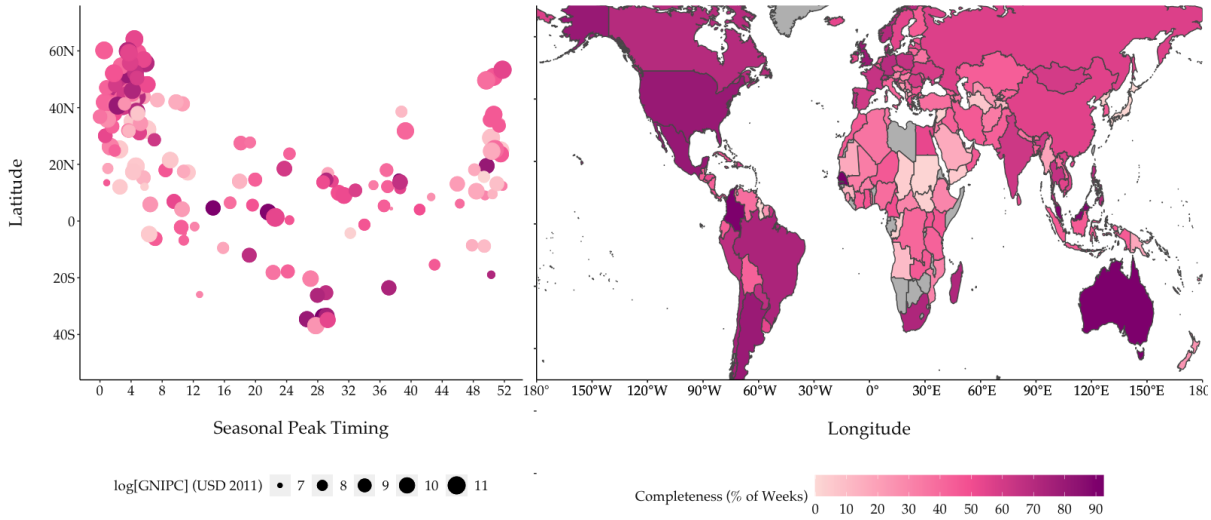


Figure 8. Shared axis, multi-panel plot describing Member States' latitude, seasonal peak timing of influenza tests, GNIPC, and *average completeness* using FluNet data reported in 1995-2022. Marker color reflects *average completeness*, or the percentage of weeks with complete records to the entire study period, where pink indicated lower values (~0%) and purple indicated higher values (~80%). Marker size reflects the natural logarithm transformation of GNIPC reported in USD PPP current international.

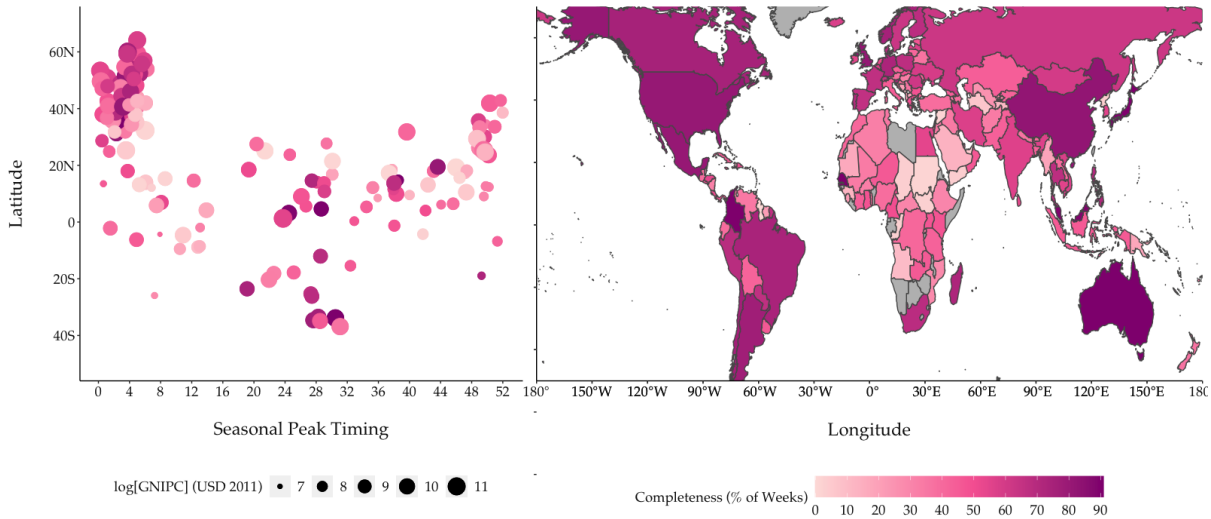


Figure 9. Shared axis, multi-panel plot describing Member States' latitude, seasonal peak timing of total influenza positives, GNIPC, and *average completeness* using FluNet data reported in 1995-2022.

Marker color reflects *average completeness*, or the percentage of weeks with complete records to the entire study period, where pink indicated lower values (~0%) and purple indicated higher values (~80%). Marker size reflects the natural logarithm transformation of GNIPC reported in USD PPP current international.

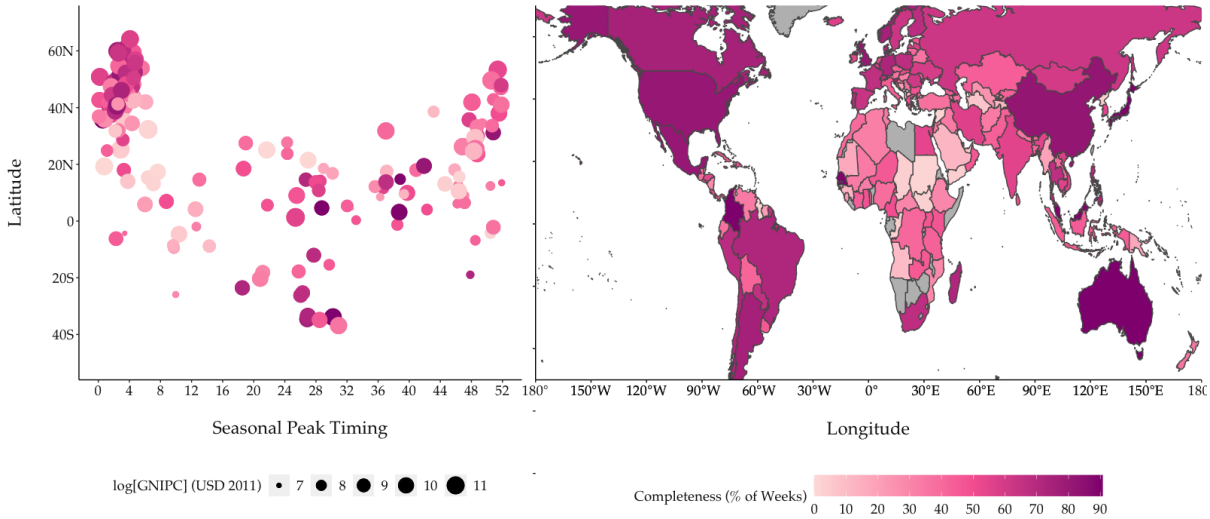


Figure 10. Shared axis, multi-panel plot describing Member States' latitude, seasonal peak timing of Influenza A positives, GNIPC, and *average completeness* using FluNet data reported in 1995-2022. Marker color reflects *average completeness*, or the percentage of weeks with complete records to the entire study period, where pink indicated lower values (~0%) and purple indicated higher values (~80%). Marker size reflects the natural logarithm transformation of GNIPC reported in USD PPP current international.

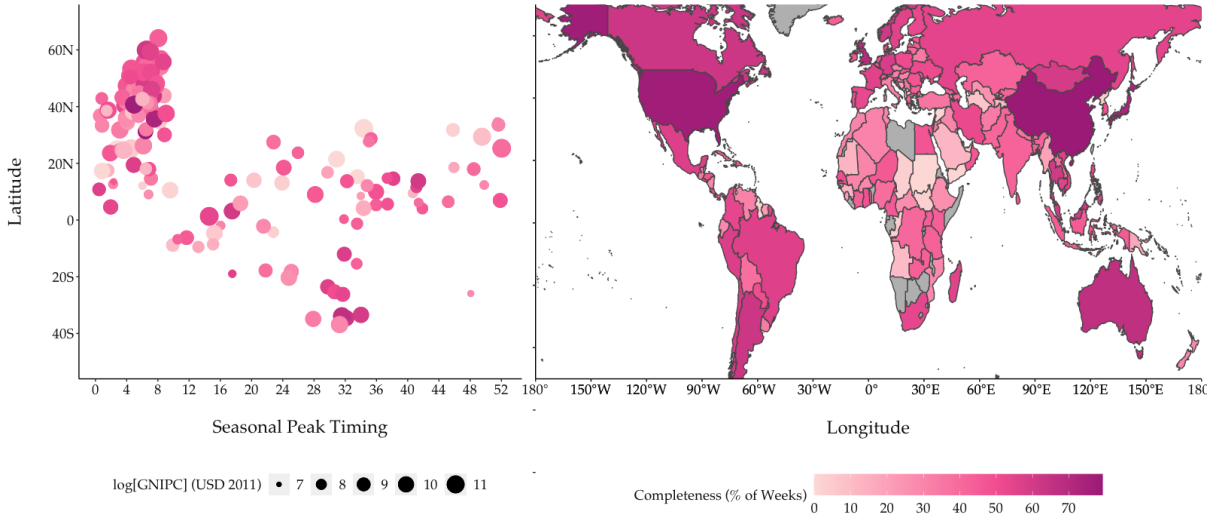


Figure 11. Shared axis, multi-panel plot describing Member States' latitude, seasonal peak timing of Influenza B positives, GNIPC, and *average completeness* using FluNet data reported in 1995-2022. Marker color reflects *average completeness*, or the percentage of weeks with complete records to the entire study period, where pink indicated lower values (~0%) and purple indicated higher values (~80%). Marker size reflects the natural logarithm transformation of GNIPC reported in USD PPP current international.

Yet, PAHO, EMRO, and AFRO Member States near the equator have lower GNIPC and completeness but widely varying seasonal peak timing. These locations

also had very broad confidence interval bounds for seasonal peak timing estimates where estimate uncertainty spanned the entire calendar year. Exploratory visuals demonstrated associations between Member States' latitude, average completeness of positives, and *diagnostic* and *reporting coverage* (Figure 12). As shown, more wealthy Member States had higher quantities of health facilities and facilities per million persons, paralleling a similar effect as shown with GNIPC. This suggests that wealthy Member States with greater public health expenditure also have greater surveillance capacity for reporting influenza cases. Improved surveillance increases the number of time points with complete records, ensuring sufficient sample size and power for modeling outbreak signatures using harmonic regressions.

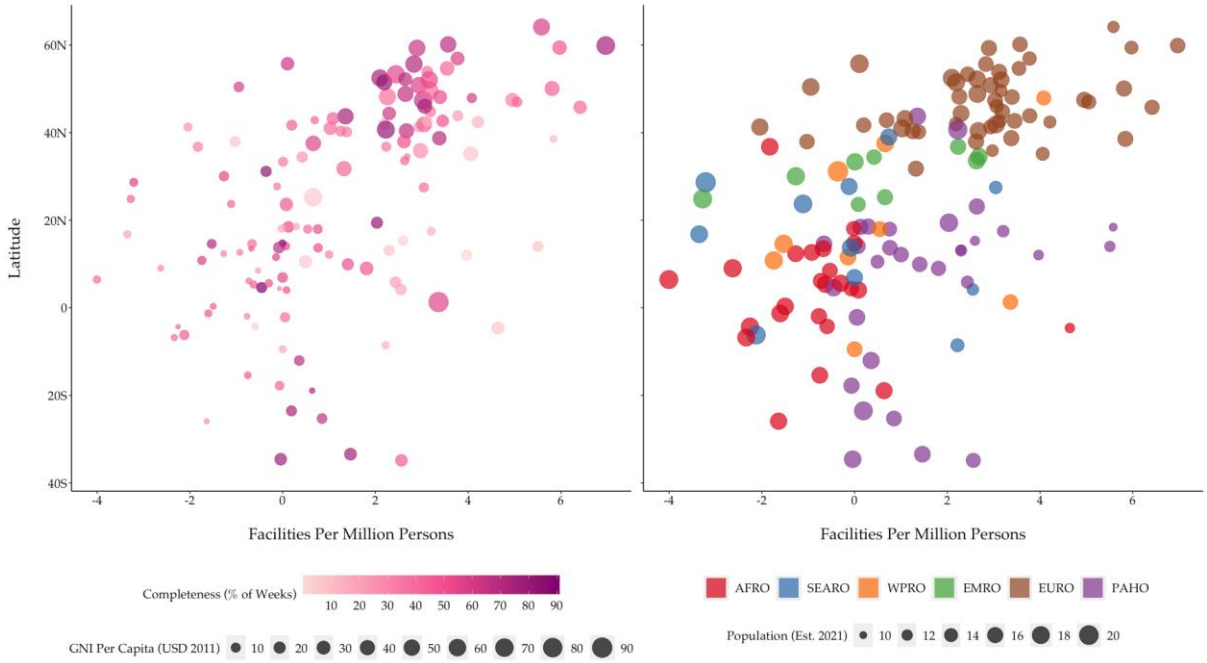


Figure 12. Shared axis, multi-panel plot describing Member States' influenza testing facilities per million persons by latitude, average total positives' *completeness*, and GNIPC (left) and by latitude, WHO-defined region, and national population (right) in 1995-2022. In the left panel, marker color reflects *completeness* ranging in value from 0% (light pink) to 100% (dark purple) while marker size reflects ln-transformed GNIPC in USD PPP current international. In the right panel, marker color reflects WHO-defined region (AFRO, SEARO, WPRO, EMRO, EURO, PAHO) while marker size reflects ln-transformed 2021 Member State population estimates in persons.

Finally, I encourage data curators and modelers to modify and adapt *ACTOR* metrics for new surveillance systems. As calculations are data driven, metrics can be applied more broadly to time-referenced surveillance records to meet the goals of public health organizations and data hosts. Future applications must consider how data quality informs statistical methodology for time series analyses and influences the reliability of estimating outbreak signatures. Emphasis should be placed on data

completeness and *interoperability* metrics for describing and comparing disease patterns within and across time series. Analytical workflows must also provide sufficient examination of distributional properties of disease outcomes to best inform modeling approaches for estimating seasonality features.

3.6. References

1. Gerberding, J. "A Blueprint for Preventing Another Pandemic: We Need to Create an International Pandemic-Surveillance Network. Here's How." *TIME*. June 09, 2021. https://time.com/6072104/pandemic-surveillance-network/.
2. World Health Organization (WHO). "WHO public health research agenda for influenza." *WHO Headquarters*. Geneva: WHO/WHE/IHM/GIP/2017.5. Accessed June 19, 2021. https://apps.who.int/iris/handle/10665/259892.
3. World Health Organization (WHO). "Global influenza strategy 2019-2030." *WHO Headquarters*. Geneva: ISBN: 9789241515320. Accessed June 19, 2021. https://apps.who.int/iris/handle/10665/311184.
4. Fefferman, N, and Naumova, E. N. "Innovation in observation: a vision for early outbreak detection." *Emerging Health Threats Journal* 3, no. 1 (2010): 7103.
5. LaFaro, A. "The importance of COVID-19 data collection and transmission." *UNC Research*. October 01, 2020. https://research.unc.edu/2020/10/01/the-importance-of-covid-19-data-collection-and-transmission/#:~:text=Reporting%20COVID%2D19%20data%20is,which%20treatments%20are%20most%20effective.
6. World Health Organization (WHO). "Public health surveillance for COVID-19: interim guidance, 16 December 2020." *WHO Headquarters*. Geneva: WHO/2019-nCoV/SurveillanceGuidance/2020.8. Accessed June 19, 2021. https://apps.who.int/iris/handle/10665/337897.
7. World Health Organization (WHO). "Maintaining surveillance of influenza and monitoring SARS-CoV-2 – adapting Global Influenza surveillance and Response System (GISRS) and sentinel systems during the COVID-19 pandemic: Interim guidance." *Global Influenza Programme WEP*. Geneva: WHO/2019-nCoV/Adapting_GISRS/2020.1. Accessed June 19, 2021. https://www.who.int/publications/i/item/maintaining-surveillance-of-influenza-and-monitoring-sars-cov-2-adapting-global-influenza-surveillance-and-response-system-(gisrs)-and-sentinel-systems-during-the-covid-19-pandemic.
8. World Health Organization (WHO). "Operational considerations for COVID-19 surveillance using GISRS: interim guidance, 26 March 2020." *WHO Headquarters*. Geneva: WHO/2019-nCoV/Leveraging_GISRS/2020.1. Accessed June 19, 2021. https://apps.who.int/iris/handle/10665/331589.
9. Yiannakoulias, N., Slavik, C. E., Sturrock, S. L., and Darlington, J. C. "Open government data, uncertainty and coronavirus: An infodemiological case study." *Social Science & Medicine* 265 (2020): 113549.
10. Pearce, N., Vandenbroucke, J. P., VanderWeele, T. J., and Greenland, S. "Accurate statistics on COVID-19 are essential for policy guidance and decisions." *American Journal of Public Health* 110, no. 7 (2020), 949-951.
11. Wu, S. L., Mertens, A. N., Crider, Y. S., Nguyen, A., Pokpongkiat, N. N., Djajadi, S., Seth, A., Hsiang, M. S., Colford, J. M., Reingold, A., Arnold, B.

F., Hubbard, A., and Benjamin-Chung, J. “Substantial underestimation of SARS-CoV-2 infection in the United States.” *Nature Communications* 11, no. 1 (2020): 1-10.

12. Rosenbaum, J. E., Stillo, M., Graves, N., and Rivera, R. “Timeliness of provisional United States mortality data releases during the COVID-19 pandemic: delays associated with electronic death registration system and weekly mortality.” *Journal of Public Health Policy* 42, no. 4 (2021): 536-549.
13. World Health Organization (WHO). “Pandemic influenza preparedness and response: a WHO guidance document.” *WHO Headquarters*. Geneva: WHO/CDS/CSR/GIP/2005.5. Accessed June 19, 2021. https://apps.who.int/iris/handle/10665/44123.
14. World Health Organization (WHO). “Global epidemiological surveillance standards for influenza.” *Global Influenza Programme WEP*. Geneva: ISBN: 9789241506601. Accessed June 19, 2021. https://www.who.int/publications/i/item/9789241506601.
15. World Health Organization (WHO). “A checklist for pandemic influenza risk and impact management: building capacity for pandemic response.” *Global Influenza Programme WEP*. Geneva: ISBN: 978-92-4-151362-3. Accessed June 19, 2021. https://www.who.int/publications/i/item/9789241513623.
16. World Health Organization (WHO). “Global influenza strategy 2019-2030.” *WHO Headquarters*. Geneva: ISBN: 9789241515320. Accessed June 19, 2021. https://apps.who.int/iris/handle/10665/311184.
17. Briand, S., Mounts, A., and Chamberland, M. “Challenges of global surveillance during an influenza pandemic.” *Public Health* 125, no. 5 (2011): 247-256.
18. World Health Organization (WHO). “Critical preparedness, readiness and response actions for COVID-19.” *WHO Headquarters*. Geneva: WHO/2019-nCoV/Community_Actions/2021.1. Accessed June 19, 2021. https://www.who.int/publications/i/item/critical-preparedness-readiness-and-response-actions-for-covid-19.
19. Ortiz, J. R., Sotomayor, V., Uez, O. C., Oliva, O., Bettels, D., McCarron, M., Bresee, J. S., and Mounts, A. W. “Strategy to enhance influenza surveillance worldwide.” *Emerging Infectious Diseases* 15, no. 8 (2009): 1271.
20. World Health Organization (WHO). “WHO global technical consultation: global standards and tools for influenza surveillance, Geneva, Switzerland, 8-10 March 2011.” *WHO Headquarters*. Geneva: WHO/HSE/GIP/2011.1. Accessed June 19, 2021. https://apps.who.int/iris/handle/10665/70724.
21. World Health Organization (WHO). “A manual for estimating disease burden associated with seasonal influenza.” *WHO Headquarters*. Geneva: ISBN: 9789241549301. Accessed June 19, 2021. https://apps.who.int/iris/handle/10665/178801.
22. Simpson, R. B., Gottlieb, J., Zhou, B., Hartwick, M. A., and Naumova, E. N. “Completeness of open access FluNet influenza surveillance data for Pan-America in 2005–2019.” *Scientific Reports* 11, no. 1 (2021): 1-17.
23. World Health Organization (WHO). “PIP Framework Critical Path Analysis: From Detection to Protection.” *PIP Framework*. Geneva: WHO/HSE/PED/GIP/PIP/2015.1. Accessed June 19, 2021. https://www.who.int/publications/i/item/pip-framework-critical-path-analysis-from-detection-to-protection.

24. World Health Organization (WHO). “Pandemic influenza preparedness framework for the sharing of influenza viruses and access to vaccines and other benefits.” *PIP Framework*. Geneva: ISBN: 9789240024854. Accessed June 19, 2021. https://www.who.int/publications/i/item/9789240024854.
25. Alarcon Falconi, T. M., Estrella, B., Sempértegui, F., and Naumova, E. N. “Effects of data aggregation on time series analysis of seasonal infections.” *International Journal of Environmental Research and Public Health* 17, no. 16 (2020): 5887.
26. Moorthy, M., Castronovo, D., Abraham, A., Bhattacharyya, S., Gradus, S., Gorski, J., Naumov, Y. N., Fefferman, N. H., and Naumova, E. N. “Deviations in influenza seasonality: odd coincidence or obscure consequence?.” *Clinical Microbiology and Infection* 18, no. 10 (2012): 955-962.
27. Bhaskaran, K., Gasparrini, A., Hajat, S., Smeeth, L., and Armstrong, B. “Time series regression studies in environmental epidemiology.” *International Journal of Epidemiology* 42, no. 4 (2013): 1187–1195.
28. Simpson, R. B., Zhou, B., and Naumova, E. N. “Seasonal synchronization of foodborne outbreaks in the United States, 1996–2017.” *Scientific Reports* 10, no. 1 (2020): 1-16.
29. Wenger, J. B., and Naumova, E. N. “Seasonal synchronization of influenza in the United States older adult population.” *PLoS One* 5, no. 4 (2010): e10187.
30. Simpson, R. B., Kulinkina, A. V., and Naumova, E. N. “Investigating seasonal patterns in enteric infections: a systematic review of time series methods.” *Epidemiology and Infection* (2022): 1-25.
31. World Health Organization (WHO). “International Statistical Classification of Diseases and Related Health Problems (ICD).” *WHO Headquarters*. Accessed May 10, 2022. https://www.who.int/standards/classifications/classification-of-diseases#:~:text=International%20Statistical%20Classification%20of%20Diseases%20and%20Related%20Health%20Problems%20(ICD)&text=ICD%20serves%20a%20broad%20range,and%20coded%20with%20the%20ICD.
32. Simpson, R. B., Gottlieb, J., Zhou, B., Liang, S., Jiang, X., Hartwick, M. A., and Naumova, E. N. “Navigating global public influenza surveillance systems for reliable forecasting.” In *Integrated Science of Global Epidemics*, ed. (Under Review).
33. Naumova, E. N., Jagai, J. S., Matyas, B., DeMaria, A., MacNeill, I. B., and Griffiths, J. K. “Seasonality in six enterically transmitted diseases and ambient temperature.” *Epidemiology and Infection* 135, no. 2 (2007): 281-292.
34. Naumova, E. N. “Public health inequalities, structural missingness, and digital revolution: time to question assumptions.” *Journal of Public Health Policy* (2021): 1-5.
35. World Health Organization (WHO). “FluNet.” Accessed June 20, 2021. https://www.who.int/tools/flunet.
36. World Health Organization (WHO). “Influenza Surveillance in the WHO African Region Epi Weeks 1 to 52, 2016.” Accessed October 07, 2021/ https://www.afro.who.int/sites/default/files/2017-06/afr-influenza-surveillance_epi-weeks-1-to-52.pdf.
37. Radin, J. M., Katz, M. A., Tempia, S., Talla Nzussouo, N., Davis, R., Duque, J., Adedeji, A., Adjabeng, M. J., Ampofo, W. K., Ayele, W., and

Bakamutumaho, B. “Influenza surveillance in 15 countries in Africa, 2006–2010.” *The Journal of Infectious Diseases* 206, no. suppl_1 (2012): S14-S21.

38. World Health Organization (WHO). “Algeria Action Plan.” Accessed October 07, 2021. https://www.fondation-merieux.org/wp-content/uploads/2017/11/8th-mena-2018-algeria-fawzi-derrar.pdf.
39. Njouom, R., Monamele, C. G., Munshili Njifon, H. L., Kenmoe, S., and Ripa Njankouo, M. “Circulation of influenza virus from 2009 to 2018 in Cameroon: 10 years of surveillance data.” *PLoS One* 14, no. 12 (2019): e0225793.
40. Manirakiza, A., Ketta, M. Y., Vickos, U., Komoyo, G. F., Garba-Ouangole, S., Bangue, C., Djimbele, E., Pasotti, O., Kanga, E., Mboufoungou, E. N., and Yambiyo, B. M. “Sentinel surveillance of influenza-like illness in the Central African Republic, 2010–2015.” *Archives of Public Health* 75, no. 1 (2017): 1-7.
41. Steffen, C., Debellut, F., Gessner, B. D., Kasolo, F. C., Yahaya, A. A., Ayebazibwe, N., Bassong, O., Cardoso, Y., Kebede, S., Manoncourt, S., and Vandemaele, K.A. “Improving influenza surveillance in sub-Saharan Africa.” *Bulletin of the World Health Organization* 90 (2012): 301-305.
42. World Health Organization (WHO). “Disease Surveillance Department, Protocol for Human Influenza Surveillance in Ghana.” Accessed October 07, 2021. https://www.afro.who.int/sites/default/files/2017-10/Ghana_National_Influenza_Sentinel_Surveillance%20%20Final%20Art%20work.pdf.
43. United States. Department of Health and Human Services, Centers for Disease Control and Prevention (CDC). “International Influenza Report FY 2016–2017.” Accessed October 07, 2021. https://www.cdc.gov/flu/about/season/flu-season-2016-2017.htm.
44. Simusika, P., Tempia, S., Chentulo, E., Polansky, L., Mazaba, M. L., Ndumba, I., Mbewe, Q. K., and Monze, M. “An evaluation of the Zambia influenza sentinel surveillance system, 2011–2017.” *BMC Health Services Research* 20, no. 1 (2020): 1-12.
45. Kadjo, H. A., Ekaza, E., Coulibaly, D., Kouassi, D. P., Nzussouo, N. T., Kouakou, B., Ouattara, A., Adjogoua, E. V., Akoua–Koffi, C. G., Elia, G. A., and Victoir, K. “Sentinel surveillance for influenza and other respiratory viruses in Côte d’Ivoire, 2003–2010.” *Influenza and Other Respiratory Viruses* 7, no. 3 (2013): 296-303.
46. Katz, M. A., Muthoka, P., Emukule, G. O., Kalani, R., Njuguna, H., Waiboci, L. W., Ahmed, J. A., Bigogo, G., Feikin, D. R., Njenga, M. K., and Breiman, R. F. “Results from the first six years of national sentinel surveillance for influenza in Kenya, July 2007–June 2013.” *PLoS One* 9, no. 6 (2014): e98615.
47. World Health Organization (WHO). “Pandemic Influenza Preparedness, Regional and Country Implementation.” Accessed October 07, 2021. https://www.who.int/influenza/pip/partnership_contribution/hlipi_final_report_reg_cntry.pdf?ua=1.
48. Nzussouo, N. T., Duque, J., Adedeji, A. A., Coulibaly, D., Sow, S., Tarnagda, Z., Maman, I., Lagare, A., Makaya, S., Elkory, M. B., and Adje, H. K. “Epidemiology of influenza in West Africa after the 2009 influenza A (H1N1) pandemic, 2010–2012.” *BMC Infectious Diseases* 17, no. 1 (2017): 1-8.

49. World Health Organization (WHO). “Influenza Update N335.” Accessed October 07, 2021. https://www.who.int/influenza/surveillance_monitoring/updates/2019_02_18_surveillance_update_335.pdf?ua=1.
50. Maïnassara, H. B., Lagare, A., Tempia, S., Sidiki, A., Issaka, B., Sidikou, B. A., and Oukem-Boyer, O. O. “Influenza sentinel surveillance among patients with influenza-like-illness and severe acute respiratory illness within the framework of the National Reference Laboratory, Niger, 2009-2013.” *PLoS One* 10, no. 7 (2015): e0133178.
51. Heraud, J. M., Njouom, R., Rousset, D., Kadjo, H., Caro, V., Ndiaye, M. N., Victoir, K., Collard, J. M., Orelle, A., Yekwa, E. L., and Ekaza, E. “Spatiotemporal circulation of influenza viruses in 5 African countries during 2008–2009: a collaborative study of the Institut Pasteur International Network.” *The Journal of Infectious Diseases* 206, no. suppl_1 (2012): S5-S13.
52. Al Awaidi, S., Abusrewil, S., AbuHasan, M., Akcay, M., Aksakal, F. N. B., Bashir, U., Elahmer, O., Esteghamati, A., Gahwagi, M., Mirza, Y. K., Grasso, C., Kassianos, G., Khris, M., Mardani, M., Maltezou, H., Nourlil, J., Oumzil, H., Oserthaus, A., Picot, V., Pehlivan, T., Saadatian-Elahi, M., Tali, I., Tarraf, H., Ugur, B., Zaraket, H., and 7th MENA-ISN Study Group. “Influenza vaccination situation in Middle-East and North African countries: Report of the 7th MENA Influenza Stakeholders Network (MENA-ISN).” *Journal of Infection and Public Health* 11, no. 6 (2018): 845-850.
53. Elhakim, M., Rasooly, M. H., Fahim, M., Ali, S. S., Haddad, N., Cherkaoui, I., Hjaija, D., Nadeem, S., Assiri, A., Aljifri, A., and Elkholy, A. “Epidemiology of severe cases of influenza and other acute respiratory infections in the Eastern Mediterranean Region, July 2016 to June 2018.” *Journal of Infection and Public Health* 13, no. 3 (2020): 423-429.
54. Caini, S., El-Guerche Séblain, C., Ciblak, M. A., and Paget, J. “Epidemiology of seasonal influenza in the Middle East and North Africa regions, 2010-2016: Circulating influenza A and B viruses and spatial timing of epidemics.” *Influenza and Other Respiratory Viruses* 12, no. 3 (2018): 344-352.
55. Abusrewil, S., Algeer, A., Aljifri, A., Al Slail, F., Andrew, M. K., Awad Tag Eldin, M., Al Awaidy, S., Ben Alaya, N., Ben Khelil, J., Dbaibo, G., and Derrar, F. “Influenza surveillance in Middle East, North, East and South Africa: Report of the 8th MENA Influenza Stakeholders Network.” *Influenza and Other Respiratory Viruses* 13, no. 3 (2019): 298-304.
56. Yazidi, R., Aissi, W., Bouguerra, H., Nouira, M., Kharroubi, G., Maazaoui, L., Zorraga, M., Abdeddaiem, N., Chlif, S., El Moussi, A., and Kacem, M. A. “Evaluation of the influenza-like illness surveillance system in Tunisia, 2012–2015.” *BMC Public Health* 19, no. 1 (2019): 1-9.
57. Tunisia. Ministry of Health, Sante Tunisie. “Guide de Surveillance de la Grippe en Tunisie, 1ere Edition.” April 2016. http://www.santetunisie.rns.tn/images/docs/anis/guidegripf6102016.pdf.
58. Horton, K. C., Dueger, E. L., Kandeel, A., Abdallat, M., El-Kholy, A., Al-Awaidy, S., Kohlani, A. H., Amer, H., El-Khal, A. L., Said, M., and House, B. “Viral etiology, seasonality and severity of hospitalized patients with severe acute respiratory infections in the Eastern Mediterranean Region, 2007–2014.” *PLoS One* 12, no. 7 (2017): e0180954.

59. Hosseini, S., Karami, M., Farhadian, M., and Mohammadi, Y. “Seasonal activity of influenza in Iran: application of influenza-like illness data from sentinel sites of healthcare centers during 2010 to 2015.” *Journal of Epidemiology and Global Health* 8, no. 1 (2018): 29-33.
60. World Health Organization (WHO). “Strengthening Iraq's Influenza Surveillance System.” December 5, 2019. http://www.emro.who.int/pandemic-epidemic-diseases/news/strengthening-iraqs-influenza-surveillance-system.html.
61. Al-Abdallat, M., Dawson, P., Haddadin, A. J., El-Shoubary, W., Dueger, E., Al-Sanouri, T., Said, M. M., and Talaat, M. “Influenza hospitalization epidemiology from a severe acute respiratory infection surveillance system in Jordan, January 2008–February 2014.” *Influenza and Other Respiratory Viruses* 10, no. 2 (2016): 91-97.
62. Republic of Lebanon. Ministry of Public Health. “Influenza Surveillance Bulletin.” Accessed February 15, 2020. https://www.moph.gov.lb/en/Pages/0/11339/influenza-surveillance.
63. World Health Organization (WHO). “Surveillance, Forecasting and Response: Morocco.” Accessed February 15, 2020. http://www.emro.who.int/surveillance-forecasting-response/pandemic-influenza/pip-morocco.html.
64. Noreen, N., Khan, A., Badar, N., Khan, F. K., Khudaidad, F., Khan, N., Riaz, S., and Malik, T. “Evaluation of Lab-based Influenza Surveillance System in Pakistan, 2017.” *Global Biosecurity* 1, no. 2 (2019).
65. Al-Romaihi, H. E., Smatti, M. K., Ganesan, N., Nadeem, S., Farag, E., Coyle, P. V., Nader, J. D., Al-Khatib, H. A., Elmagboul, E. B., Al Dhahry, S., and Al-Marri, S. A. “Epidemiology of respiratory infections among adults in Qatar (2012-2017).” *PLoS One* 14, no. 6 (2019): e0218097.
66. European Center for Disease Control (ECDC), and World Health Organization (WHO). “Influenza Surveillance Country, Territory and Area Profiles 2019.” Accessed February 15, 2020. https://apps.who.int/iris/handle/10665/346334.
67. Saudi Arabia. Ministry of Health, Assistant Agency for Preventive Medicine. “Influenza Surveillance in Saudi Arabia.” Accessed February 15, 2020. https://www.moh.gov.sa/CCC/healthp/regulations/Documents/ISSA%20Protocol.pdf.
68. Hassan, M. B. H. “Influenza Control UAE Experience.” *United Arab Emirates, Ministry of Health and Prevention*. Accessed February 15, 2020. https://www.fondation-merieux.org/wp-content/uploads/2017/11/8th-mena-2018-uae-mohamed-hassan.pdf.
69. Bangladesh. Institute of Epidemiology, Disease Control and Research (IEDCR). “Hospital Based Influenza Surveillance: Reports.” Accessed February 15, 2020. https://iedcr.gov.bd/surveillances/5153e158-157b-4305-8786-f9e29b2a7342.
70. United States. Department of Health and Human Services, Centers for Disease Control and Prevention (CDC). “International Activities Report: Fiscal Years 2014–2015.” Accessed February 15, 2020. https://www.cdc.gov/flu/pdf/international/program/2014-15/2014-2015-intl-program-report_061416.pdf.
71. Australian Government. Department of Health. “Australian Influence Surveillance Report and Activity Updates.” Accessed February 15, 2020.

https://www1.health.gov.au/internet/main/publishing.nsf/Content/cda-surveil-ozflu-flucurr.htm.

72. Australian Government. Department of Health, Australian Sentinel Practices Research Network (ASPREN), and Victorian Sentinel Practitioners Influenza Network (VicSPIN). "National Primary Care Infectious Diseases: Sentinel Surveillance Fortnightly Report: No. 23, 2021." Accessed February 15, 2020. https://aspren.dmac.adelaide.edu.au/documents/20714/604700/ASPREN+Update+23+2021/2b291d2e-201f-40bd-866b-b878d54e1773?version=1.0.
73. Kool, J. L., Pavlin, B. I., Musto, J., and Dawainavesi, A. "Influenza surveillance in the Pacific Island countries and territories during the 2009 pandemic: an observational study." *BMC Infectious Diseases* 13, no. 1 (2013): 1-8.
74. World Health Organization (WHO). Western Pacific Region. "Bi-weekly Influenza Situation Update: 12 August 2020." Accessed February 15, 2020. https://apps.who.int/iris/bitstream/handle/10665/330699/Influenza-20200812.pdf?sequence=17&isAllowed=y.
75. Nguyen, Y. T., Graitcer, S. B., Nguyen, T. H., Tran, D. N., Pham, T. D., Le, M. T., Tran, H. N., Bui, C. T., Dang, D. T., Nguyen, L. T., and Uyeki, T. M. "National surveillance for influenza and influenza-like illness in Vietnam, 2006− 2010." *Vaccine* 31, no. 40 (2013): 4368-4374.
76. United States. Department of Health and Human Services, Centers for Disease Control and Prevention (CDC). "International Division International Activities: Annual Report." Accessed February 15, 2020. https://www.cdc.gov/flu/pdf/international/program/2011-intl-program-report.pdf.
77. Hishamuddin, P. "Evaluation of the Influenza Sentinel Surveillance System in Singapore 2011-2012." *Online Journal of Public Health Informatics* 6, no. 1 (2014).
78. Babakazo, P., Kabamba-Tshilobo, J., Wemakoy, E. O., Lubula, L., Manya, L. K., Ilunga, B. K., Disasuani, W., Nkwembe, E., Kavunga-Membo, H., Changachanga, J. C., and Muhemedi, S. "Evaluation of the influenza sentinel surveillance system in the Democratic Republic of Congo, 2012–2015." *BMC Public Health* 19, no. 1 (2019): 1-12.
79. Australian Government. Department of Health. "Data Considerations for the Australian Influenza Surveillance Report, 2020." Accessed June 19, 2021. https://www1.health.gov.au/internet/main/publishing.nsf/Content/cda-surveil-ozflu-flucurr.htm/$File/Data-considerations-AISR-2020.pdf.
80. Australian Government. Department of Health, Australian Sentinel Practices Research Network (ASPREN), and Victorian Sentinel Practitioners Influenza Network (VicSPIN). "National Primary Care Infectious Diseases: Sentinel Surveillance Fortnightly Report: No. 13, 2020." Accessed February 15, 2020. https://aspren.dmac.adelaide.edu.au/documents/20714/469323/ASPREN+Update+13+2020/67f4d74f-3d35-4cf6-a201-cd7b8ddf0df6?version=1.0.
81. Kool, J. L., Pavlin, B. I., Musto, J., and Dawainavesi, A. "Influenza surveillance in the Pacific Island countries and territories during the 2009 pandemic: an observational study." *BMC Infectious Diseases* 13, no. 1 (2013), 1-8.
82. World Health Organization (WHO). Western Pacific Region. "Biweekly Influenza Situation Update: 18 May 2022." Accessed June 19, 2021. https://www.who.int/docs/default-source/wpro---

documents/emergency/surveillance/seasonal-influenza/influenza-20200701.pdf?sfvrsn=b3fcfc77_30.

83. Vietnam. Ministry of Health. "Influenza Division International Activities: Fiscal Year 2011 Annual Report: Surveillance." *World Health Organization (WHO). Western Pacific Region (WPR).* Accessed June 19, 2021. https://espanol.cdc.gov/flu/pdf/international/program/2011-12/vietnam.pdf.
84. Hishamuddin, P. "Evaluation of the Influenza Sentinel Surveillance System in Singapore 2011-2012." *Online Journal of Public Health Informatics* 6, no. 1 (2014).
85. Babakazo, P., Kabamba-Tshilobo, J., Wemakoy, E. O., Lubula, L., Manya, L. K., Ilunga, B. K., Disasuani, W., Nkwembe, E., Kavunga-Membo, H., Changachanga, J. C., Muhemedi, S., Muyembe Tamfum, J. J., and Tempia, S. "Evaluation of the influenza sentinel surveillance system in the Democratic Republic of Congo, 2012–2015." *BMC Public Health* 19, no. 1 (2019), 1-12.
86. Darwish, A., Rahhal, Y., and Jafar, A. "A comparative study on predicting influenza outbreaks using different feature spaces: application of influenza-like illness data from Early Warning Alert and Response System in Syria." *BMC Research Notes* 13, no. 1 (2020), 1-8.
87. World Health Organization (WHO). Pan American Health Organization (PAHO). "2017 Edition Health in the Americas+: Summary: Regional Outlook and Country Profiles." ISBN: 978-92-75-11966-2. Accessed June 19, 2021. https://www.paho.org/salud-en-las-americas-2017/wp-content/uploads/2017/09/Print-Version-English.pdf.
88. Sanicas, M., Forleo, E., Pozzi, G., and Diop, D. "A review of the surveillance systems of influenza in selected countries in the tropical region." *The Pan African Medical Journal* 19 (2014).
89. Now Grenada. Health Press Release. "Ministry of Health reports increase in influenza-like cases." March 29, 2018. https://www.nowgrenada.com/2018/03/ministry-of-health-reports-increase-in-influenza-like-cases/.
90. World Health Organization (WHO). "COVID-19 Weekly Epidemiological Update: Data as received by WHO from national authorities, as of 7 March 2021, 10 am CET." Accessed June 19, 2021. https://apps.who.int/iris/bitstream/handle/10665/340087/nCoV-weekly-sitrep9Mar21-eng.pdf?sequence=1.
91. Government of the Virgin Islands. "Health Emergency Operations Centre: National Action Plan Against COVID-19 Pandemic." Accessed June 19, 2021. https://bvi.gov.vg/sites/default/files/resources/virgin_islands_covid-19_action_plan_v.1_march_2020.pdf.
92. United States. Census Bureau, International Programs Center. "International Database (IDB): Population estimates and projects for 227 countries and areas." Accessed June 20, 2021. https://www.census.gov/data-tools/demo/idb/#/country?YR_ANIM=2021.
93. Institut national de la statisique et des etudes economiques (Insee). Population estimate as of January 1, 2022: Series by region, department, sex, and age from 1975 to 2022. Accessed June 20, 2021. https://www.insee.fr/fr/statistiques/1893198.
94. Ziegler, T., Mamahit, A., and Cox, N. J. "65 years of influenza surveillance by a World Health Organization-coordinated global network." *Influenza and Other Respiratory Viruses* 12, no. 5 (2018), 558-565.

95. Costa-Santos, C., Neves, A. L., Correia, R., Santos, P., Monteiro-Soares, M., Freitas, A., Ribeiro-Vaz, I., Henriques, T. S., Rodrigues, P. P., Costa-Pereira, A., Pereira, A. M., and Fonseca, J. A. "COVID-19 surveillance data quality issues: a national consecutive case series." *BMJ Open* 11, no. 12 (2021), e047623.
96. Aliabadi, A., Sheikhtaheri, A., and Ansari, H. "Electronic health record–based disease surveillance systems: a systematic literature review on challenges and solutions." *Journal of the American Medical Informatics Association* 27, no. 12 (2020), 1977-1986.
97. Simpson, R. B., Lauren, B. N., Schipper, K. H., McCann, J. C., Tarnas, M. C., and Naumova, E. N. "Critical periods, critical time points and day-of-the-week effects in COVID-19 surveillance data: an example in Middlesex County, Massachusetts, USA." *International Journal of Environmental Research and Public Health* 19, no. 3 (2022): 1321.
98. Dong, E., Du, H., and Gardner, L. "An interactive web-based dashboard to track COVID-19 in real time." *The Lancet Infectious Diseases* 20, no. 5 (2020): 533–534.
99. World Health Organization (WHO). "Interpreting influenza surveillance data in the context of the COVID-19 pandemic." *Weekly Epidemiological Record* 95, no. 35 (2020): 409-415.
100. World Health Organization (WHO). "Surveillance strategies for COVID-19 human infection: interim guidance, 10 May 2020." *WHO Headquarters*. Geneva: WHO/2019-nCoV/National_Surveillance/2020.1. Accessed June 19, 2021. https://apps.who.int/iris/handle/10665/332051.
101. Sanchez, E., Simpson, R. B., Zhang, Y., Sallade, L. E., and Naumova, E. N. "Exploring risk factors of recall-associated foodborne disease outbreaks in the United States, 2009–2019." *International Journal of Environmental Research and Public Health* 19, no. 9 (2022): 4947.
102. World Health Organization (WHO). "Preparing GISRS for the upcoming influenza seasons during the COVID-19 pandemic - practical considerations: interim guidance, 26 May 2020." *WHO Headquarters*. Geneva: WHO/2019-nCoV/Preparing_GISRS/2020.1. Accessed June 19, 2021. https://apps.who.int/iris/handle/10665/332198.
103. Igboh, L. S., Mcmorrow, M., Tempia, S., Emukule, G. O., Talla Nzussouo, N., Mccarron, M., Williams, T., Weatherspoon, V., Moen, A., Fawzi, D., Njouom, R., Nakoune, E., Dauoda, C., Kavunga-Membo, H., Okeyo, M., Heraud, J. M., Mambule, I. K., Sow, S. O., Tivane, A., Lagare, A., Adebayo, A., Dia, N., Mmbaga, V., Maman, I., Lutwama, J., Simusika, P., Walaza, S., Mangtani, P., Nguipdop-Djomo, P., Cohen, C., Azziz-Baumgartner, E., and ANISE Network Working Group. "Influenza surveillance capacity improvements in Africa during 2011-2017." *Influenza and Other Respiratory Viruses* 15, no. 4 (2020): 495-505.
104. Caini, S., Alonso, W. J., Séblain, C. E. G., Schellevis, F., and Paget, J. "The spatiotemporal characteristics of influenza A and B in the WHO European Region: can one define influenza transmission zones in Europe?." *Eurosurveillance* 22, no. 35 (2017): 30606.
105. Khan, W., El Rifay, A. S., Malik, M., and Kayali, G. "Influenza research in the Eastern Mediterranean Region: a review." *Oman Medical Journal* 32, no. 5 (2017), 359.

106. Oshitani, H., Kamigaki, T., and Suzuki, A. “Major issues and challenges of influenza pandemic preparedness in developing countries.” *Emerging Infectious Diseases* 14, no. 6 (2008): 875.
107. Alonso, W. J., Yu, C., Viboud, C., Richard, S. A., Schuck-Paim, C., Simonsen, L., Mello, W. A., and Miller, M. A. “A global map of hemispheric influenza vaccine recommendations based on local patterns of viral circulation.” *Scientific Reports* 5, no. 1 (2015), 1-6.
108. Bloom-Feshbach, K., Alonso, W. J., Charu, V., Tamerius, J., Simonsen, L., Miller, M. A., and Viboud, C. “Latitudinal variations in seasonal activity of influenza and respiratory syncytial virus (RSV): a global comparative review.” *PLoS One* 8, no. 2 (2013): e54445.
109. SimpleMaps.com. “World Cities Database.” Accessed July 31, 2021. https://simplemaps.com/data/world-cities.
110. The World Bank, DataBank. “World Development Indicators.” Accessed July 31, 2021. https://databank.worldbank.org/source/world-development-indicators.
111. Naumova, E. N., Simpson, R. B., Zhou, B., and Hartwick, M. A. “The use of longitudinal analysis to reveal the global seasonal and pandemic patterns in influenza.” *International Statistical Review* (Under Review).

Chapter 4. Trends and Seasonality Features of Foodborne Illnesses and Outbreaks

4.1. Standardizing analytical workflows for modeling seasonality features

As demonstrated in Chapter 2, much research on temporal trends of foodborne and waterborne illnesses compares seasonal features and spatiotemporal patterns of illnesses across locations, pathogens, subpopulations, or other risk factors [1]. Such analyses require harmonization of data streams by their spatiotemporal information and investigation of the joint completeness across time series. Structural missingness of one and especially both time series can impede reliable description and comparison of illness patterns. For example, missing data at or near seasonal peaks can decrease the reliability of peak timing and amplitude estimates. Non-overlapping missingness of two or more time series can significantly reduce effective sample size, rendering statistical analyses imprecise, impractical, or inhibiting them altogether. Furthermore, higher quantities of missing data can obscure patterns of illnesses and lead modelers to confuse random outbreak events with stable periodic patterns of illness.

In addition to assessing data quality limitations, modelers rely on comprehensive analytical workflows for assessing time series distributional properties before performing longitudinal models. Comparisons of time series require careful consideration of count-based distributions so that modeling approaches adequately account for outliers and skewness. These properties define and justify modeling assumptions such as the family of distributions and link functions selected to estimate temporal patterns. As discussed in Chapter 2, I encourage public health professionals to consider standardized approaches to ensure the reproducibility of estimating seasonality features. This includes models that do not rely on subjective definitions of seasons and instead estimate seasonality features and their uncertainty across time series [1]. The δ-method extracts periodic terms of harmonic regression models and serves as a data-driven technique to estimate seasonal peak timing and amplitude. By also calculating measures of uncertainty, the δ-method assists modelers in comparing seasonality features across pathogens, locations, and over time [2-6].

Perhaps most importantly, data visualizations serve as the final stage of standardized analytical workflows for modeling seasonality features. Modelers must place careful attention to how they communicate complex spatiotemporal patterns and relationships like peak timing and amplitude. By creating graphical templates,

modelers can clearly demonstrate patterns across geographic locations, health outcomes, subpopulations, or other risk factors with minor modifications in programming software. When created for annualized estimates, these templates permit investigation of dynamic processes such as shifts or drifts in peak timing and amplitude using animated visualizations. Modelers can easily adapt graphical templates for evaluating a variety of longitudinal outcomes.

In the works that follow, I define an analytical framework for conducting standardized time series analyses of periodic seasonality features. My first manuscript demonstrates applications of the δ-method for measuring seasonality features of enteric infections [7]. While this tool is well-established, I provide additional investigation of time series distributional properties using L-moments. I examine L-skewness and L-kurtosis values to justify distributional assumptions of harmonic regression models. Once estimating seasonality features, I propose techniques for investigating seasonal synchronization through serial, phase-phase, and phase-amplitude correlations. My second manuscript expands on these works to provide templates for visualizing relationships between time series, peak timing, amplitude, and the relationship between peak timing and amplitude [8]. Together, these studies establish an analytical framework for examining outbreak signatures for infectious diseases following stable periodic patterns over time.

4.2. Seasonal synchronization of foodborne outbreaks in the United States, 1996-2017

Manuscript M3. Simpson, R. B., Zhou, B., and Naumova, E. N. "Seasonal synchronization of foodborne outbreaks in the United States, 1996–2017." *Scientific Reports* 10, no. 1 (2020): 1-16. https://doi.org/10.1038/s41598-020-74435-9.

4.3. An analecta of visualizations for foodborne illness trends and seasonality

Manuscript M4. Simpson, R. B., Zhou, B., Alarcon Falconi, T. M., and Naumova, E. N. "An analecta of visualizations for foodborne illness trends and seasonality." *Scientific Data* 7, no. 1 (2020): 1-15. https://doi.org/10.1038/s41597-020-00677-x.

4.4. Modeling outbreak severity and its temporal patterns

While many studies have modeled temporal patterns of enteric illnesses, fewer studies evaluate disease outbreaks. An outbreak, often defined as ≥2 illnesses from the same contaminated food source, require event-based surveillance systems that summarize properties of outbreaks as they occur [9]. Temporal patterns of outbreak events have differing interpretations compared to enteric illnesses. For example, seasonal peaks reflect the timing that illnesses become most extreme while seasonal amplitude illustrates differences in resource needs between most and least severe illnesses. Furthermore, how researchers define severity has great importance, as this may refer to the intensity of case definitions, the geographic distribution of cases, the length of time a person is ill, or the number of medical resources required to treat infected persons. As few analytical workflows exist to measure disease severity, I develop a standardized, data-driven approach for estimating and comparing severity scores across outbreaks.

Few approaches have utilized national reporting systems to conduct real-time surveillance of outbreak severity [10-12]. The Centers for Disease Control and Prevention's (CDC's) *Data Modernization Initiative* has begun exploring applications for real-time surveillance to anticipate and respond to infectious outbreaks more precisely and efficiently [13-16]. The initiative centers on data-driven approaches to investigate emerging public health threats by improving the accountability, quality, timeliness, and harmonization of surveillance data [13-16]. In doing so, the CDC will establish a feedback loop where health agencies automate hospital and health facility data reporting then produce standardized summaries to inform facilities of emerging outbreak threats [13-16]. This call to action introduces a new era of precision public health by emphasizing predictive, real-time analytics for measuring the severity of emerging outbreaks, reducing the lag time between collecting and analyzing data, and promoting more efficient mobilization of health resources to mitigate the most severe threats [15-16].

To achieve these aims, the CDC has called for innovative and reproducible surveillance tools to describe and compare outbreak severity [13]. Historically, health agencies have used Disability Adjusted Life Years (DALYs), which perform comprehensive systematic reviews of published literature to summarize years of 'healthy' life lost per illness per outbreak [17-19]. Researchers calculate DALY

scores using a combination of metrics including average incident cases, illness duration, expected life lost, and disability weights [17]. Average incidence is often estimated using comprehensive meta-analyses and conducted by pathogen, age group, and other demographic information expected to influence disease transmissibility and infectiousness [17-19]. To quantify qualitative differences in disease disability, experts define disability weights that estimate the expected loss of life based on illness severity. For these calculations, severity is often described by disease morbidity and mortality while disability refers to the expected impairment of years lost due to premature death or injury associated with illness.

DALYs provide an effective means of quantifying the economic burden of illnesses at national and global population levels. Yet, this approach requires many subjectively calculated estimates based on researchers' expert opinions. For example, disability weights, life expectancy approximations, and average incidence estimates are not data-driven [20-21]. Instead, metrics' precision depends on the completeness of data during analytical models, publication reporting biases, the generalizability of reviewed literature, and the thoroughness of analytical methods in extracted citations. While systematic reviews and meta-analyses estimate average incidence, they are extremely time intensive and face the same limitations of data availability; while the highest global burdens of illness are in lower- and middle-income countries, these locations have the least available data, poorest health surveillance systems, and least published literature. Missing data requires extensive imputation techniques, calling into question DALY score reliability and the predictive power of studies for more granular sub-national spatial scales [20-21]. Furthermore, DALYs do not investigate a broad spectrum of health burdens that make up disease severity such as the geographic extent or duration of outbreaks.

In contrast, indices describing health burdens of disease provide opportunities for more spatially granular policies, programs, and strategies for mitigating outbreak severity. For example, suppose a health agency establishes a rapid detection tool to estimate the timing of more severe annual outbreaks. Using this information, agencies can inform hospitals and healthcare facilities when more medical resources are needed. This facilitates timelier mobilization of medical staff, laboratory testing personnel, and testing equipment for rapid detection and processing of incident cases. Understanding outbreak severity timing also helps identify geographic hotspots of disease, allowing health agencies to inform food safety agencies when and where

additional inspections are most needed. These examples demonstrate how health severity indices can assist public health and food safety agencies in alerting, detecting, and anticipating severe enteric illness outbreaks rather than retrospectively alarming the public after outbreaks occur.

Indices of health burdens have been poorly explored for enteric infections, especially those using publicly available surveillance data. Studies often describe metrics of severity including the geographic extent (e.g., number of locations where ill persons resided and exposed), morbidity/mortality (e.g., cases, hospitalizations, deaths), and duration (e.g., days from first to last illness or exposure) of illnesses per outbreak [22-26]. Researchers compare metrics by the type of food retailer associated with an outbreak [24], geographic locations [25], years and seasons [25-26], or other characteristics. However, these approaches neglect ratios of metrics such as cases per outbreak duration (speed of infection), morbidity and mortality case ratios (illness intensity), and geographic extent per duration (infection transmissibility). These composite metrics introduce new parameters for public health professionals to define severity.

Below, I propose a data-driven index for evaluating outbreak severity using publicly available data collected by the CDC's National Outbreak Reporting System (NORS) from 01 January 2009 through 31 December 2019. I identified 67 metrics related to the extent, morbidity, mortality, and duration of foodborne outbreaks. I estimated metrics' completeness then examined their identity, natural log-transformed, and calibrated (normalized from 0 to 1) distributions. I selected 12 metrics to create a severity index score, which I estimated by averaging available metric estimates per outbreak. I compared scores by contaminant, study year, and calendar month using Dunn's tests with Bonferroni corrections and tobit regression models. The index establishes data-driven methodology for real-time assessment of outbreak severity signatures to strengthen surveillance capacity, inform outbreak emergency strategies, and evaluate economic burdens of disease outbreaks at refined spatiotemporal scales.

4.5. Case Study – An example using CDC NORS in 2009-2019

4.5.1. Data extraction and management

The NORS electronic surveillance system has captured foodborne outbreak data in the United States since 01 January 2009. Surveillance began under the Waterborne Disease and Outbreak Surveillance System (WDOSS) and Foodborne Disease Outbreak Surveillance System (FDOSS) in 1971 and 1973, respectively [27]. FDOSS began under the paper-based Foodborne Disease Outbreak Reporting System (pFORS) in 1973-1997 before transitioning to an electronic system (eFORS) in 1998-2008 [27]. The CDC established NORS in 2009 to integrate reporting under one centralized system and expand coverage to outbreaks associated with food, water, person-to-person, animal contact, environmental, and unknown modes of transmission [27].

State and local health authorities voluntarily report NORS data using passive surveillance, attributing to well-documented underreporting of outbreak frequency and milder forms of illnesses nationally [28]. Despite this, NORS personnel closely review all traceback investigations to ensure the accuracy of data before public circulation [29]. As an event-based surveillance system, outbreaks are reported on the day exposure events began.

I obtained data for 01 January 2009 through 31 December 2019 from the NORS Foodborne and Animal Contact Team. As of 01 January 2021, data were unavailable for 2020 and 2021. I received data disaggregated into 65 individual data tables each with unique information on the time, geographic location, contaminant, case definition, setting of consumption, food ingredients, and food inspection methods associated with outbreaks. I merged all tables into a single, event-based dataset by aligning and merging variables using outbreak identification numbers. While data were available for eFORS in 1998-2008, I excluded these records due to a lack of conformability with NORS (2009-2019) records.

The compiled dataset consisted of repeated observations for every contaminant, state, and county associated with an outbreak. I removed repeated observations by reshaping data tables from long to wide format and creating binary variables for each contaminant, county, and state. Contaminants included 29 pathogens, 7 toxins, and 5 other contaminants while states included all US mainland states as well as Guam,

Puerto Rico, the Republic of Palau, and Washington D.C. I created binary indicator variables for those outbreaks attributed to multiple contaminants, states, or counties.

NORS records did not provide a variable describing the duration of outbreak events. However, records did provide information on the date of first and last reported illness and exposures. I calculated illness and exposure duration as the difference in days from the date of last to first illness or exposure event, respectively. I added one to this difference to account for onset starting date. I set duration estimates equal to missing if either date had incomplete information. As duration-related information reported counts of time and time units (e.g., hours, days, months) separately, I generated a new variable to estimate duration in days (assuming 30.437 days per month).

4.5.2. Selecting severity metrics

I extracted 19 variables as metrics to define outbreak severity with respect to the geographic extent, case definition, and duration of exposure or illness events per outbreak (Appendix B, Supplementary Table S1). I generated an additional 48 metrics using the ratio of extent to duration metrics (infection transmissibility), case to duration metrics (speed of infection), and morbidity and mortality cases to total cases (illness intensity) (Appendix B, Supplementary Table S2). I examined the completeness of all 67 metrics estimated as the ratio of outbreaks with non-missing records to total outbreaks (N=9407) and multiplied by 100. I differentiated between missing records (i.e., information does not exist) and values of nothingness (i.e., value equals 0) for all metrics. I provided a more comprehensive assessment of NORS data completeness and a detailed summary of temporal outbreak trends elsewhere [30-31]

I examined metrics' distributional characteristics, specifically population mean (with 95% confidence intervals), median (with interquartile range), L-skewness, and L-kurtosis statistics. I chose L-skewness and L-kurtosis rather than conventional product moments due to their superiority in estimating distribution parameters particularly for smaller sample sizes [32]. I estimated population means using generalized linear models (GLM) with negative binomial distributions and logarithmic link functions to account for biologically implausible non-negative distributions.

Due to severe skewness of metric distributions, I created a ceiling for all metrics such that values between the 95^{th}-100^{th} percentiles were set equal to the 95^{th} percentile

value. This adjustment reduced bias of influential observations in constructing the index score. I also added 1 to all metrics prior to natural logarithm (ln) transformation to derive a more symmetrical distribution and prevent undefined estimates for values of zero.

Next, I calibrated metrics using Equation 1:

$$C_{i,j} = \frac{\left(\ln(Y_{i,j}+1) - min(\ln(Y_{i,j}+1))\right)}{\left(max(\ln(Y_{i,j}+1)) - min(\ln(Y_{i,j}+1))\right)} \quad \textbf{(1)}$$

where $C_{i,j}$ is the calibrated estimate for *j*-metric of *i*-outbreak; *min()* is the minimum value function; and *max()* is the maximum value function. This normalization procedure ensured metrics had identical value ranges from 0 to 1 (minimum to maximum value). I then examined distributional properties of ln-transformed and calibrated metrics using the descriptive summary statistics described above.

4.5.3. Creating severity index

I identified 12 metrics for creating the severity index (Table 10). Selection criteria included: i) high completeness (> ~75%); ii) low-to-moderate L-skewness (< ~0.60); and iii) limited redundancies across metrics. I used high completeness criteria to ensure I scored outbreaks with similar data availability. Low-to-moderate L-skewness and L-kurtosis values suggested a reduced impact of influential observations on the final severity index score. I minimized metric redundancies by emphasizing metrics corresponding to more severe morbidity and mortality conditions. The combination of these metrics defined severity as the interrelationship between outbreak duration length, volume of cases, and composition of illness intensity among cases (Figure 13). To estimate a severity score, I averaged all available metrics per outbreak and divided by the total number of completely reported metrics. This averaging technique ensured that I did not penalize severity score estimates for outbreaks with incomplete information.

Table 10. Descriptions and units of 12 metrics considered for the creation of a foodborne outbreak severity index (11 used; deaths excluded) using data from the National Outbreak Reporting System (NORS) in 2009-2019. *All Visits* refer to the sum of primary cases who visited a healthcare provider, hospital, or emergency room (ER). The deaths metric was excluded in the final averaging step when calculating index scores do to fear of diluting score estimates, as only 3.13% of outbreaks in the study period reported > 0 deaths.

Metric	Description	Units

Total Primary Cases	Total primary cases; count of laboratory-confirmed and probable primary cases per outbreak	Cases
Hospital/ER Visits	Total hospitalizations and emergency room (ER) visits; count of primary cases who visited a hospital or ER per outbreak	Visits
Healthcare Visits	Total outpatient healthcare visits; count of primary cases who visited a healthcare provider per outbreak	Visits
Deaths*	Number of total primary cases who died	Deaths
Healthcare Visits per Total Primary Cases	Average number of healthcare visits per primary cases of an outbreak; reported in visits per case	Visits/Cases
Hospital/ER Visits per Total Primary Cases	Average number of hospitalizations and emergency room visits per primary cases of an outbreak; reported in visits per case	Visits/Cases
Exposure Duration	Days primary cases were exposed to a foodborne exposure; days from first to last exposure event of an outbreak	Days
Illness Duration	Days primary cases were ill; days from first person to last person to present with illness symptoms	Days
Total Primary Cases per Exposure Duration	Average number of primary cases per duration from the first to the last outbreak exposure event; reported in cases per day	Cases/Day
All Visits per Exposure Duration	Average number of healthcare, hospital, and emergency room visits per exposure event duration; reported in visits per day	Visits/Day
Total Primary Cases per Illness Duration	Average number of primary cases per duration from the first to the last outbreak illness symptom; reported in cases per day	Cases/Day
All Visits per Illness Duration	Average number of healthcare, hospital, and emergency room visits per illness symptom duration; reported in visits per day	Visits/Day

* I excluded the *death* metric from the index score calculation due to its distributional properties across outbreaks

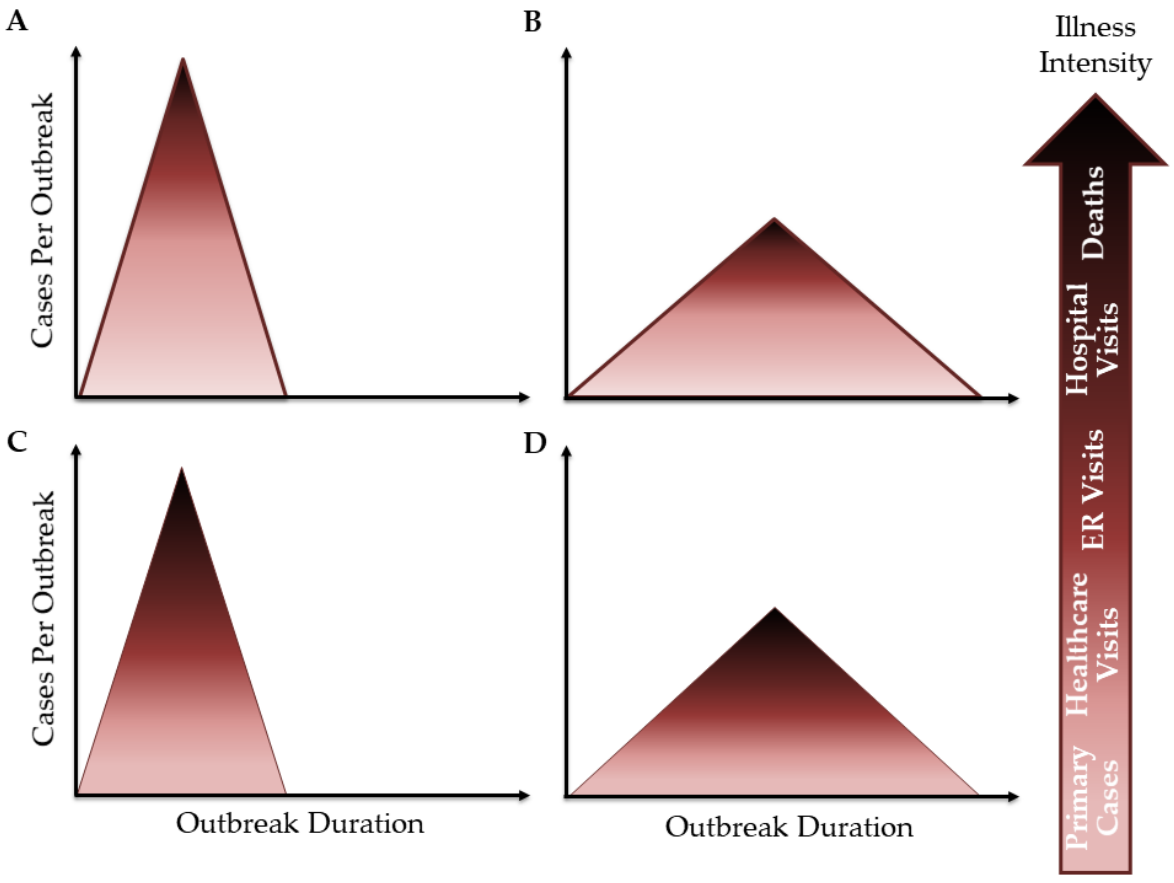


Figure 13. A multi-panel plot where pyramids describe the interrelationship between case volume, outbreak duration, and illness intensity to define foodborne outbreak severity. Each panel plots cases per outbreak (vertical axis) by outbreak duration (horizontal axis). Pyramid fill color ranges from less morbid (light red) to more morbid (dark red) illness conditions. I provide four examples of outbreaks with identical severity but for differing reasons. **Panel A** represents outbreaks with a high speed of infection indicative of many cases, largely of less morbid conditions, over a short duration. **Panel B** reflects an outbreak with less volume of cases but over a much longer duration, which promotes greater severity through increased secondary infections. **Panel C** parallels Panel A but with a higher proportion of more intense illnesses reflecting the infectiousness of contaminants for this severe outbreak. Finally, **Panel D** parallels Panel B but illustrates the increased morbidity and mortality of outbreak severity over a long duration of time.

Total primary cases included both confirmed (contaminant identified with laboratory testing) and probable (no contaminant identified but an epidemiological linkage to a confirmed case or exposure) cases [28-29]. NORS estimated morbidity and mortality case counts by identifying the number of primary cases visiting healthcare providers, hospitals, and emergency rooms (ERs). Cases were not mutually exclusive – the same individual could be reported as a primary case, healthcare, hospital, ER visit, or death as illness worsened. I did not replace or interpolate incomplete records to preserve metrics' underlying distribution. To improve sample size, I created one metric aggregating hospital and ER visits and one metric aggregating healthcare, hospital, and ER visits.

I estimated cases and visits per illness and exposure duration to capture the speed of infection by varying degrees of case morbidity. Higher case volumes over short outbreak durations suggested more rapid disease transmission (Figure 13). I also estimated ratios of healthcare, hospital, and ER visits per primary cases to capture the intensity of illness as a fraction of the total cases identified per outbreak (Figure 13). A higher proportion of more intense illnesses per primary cases reflected the infectiousness of outbreak contaminants.

4.5.4. Comparing index scores

I excluded outbreaks with missing contaminant information (n=2346) and multi-contaminant outbreaks (n=150), as case- and visit-related metrics were not reported per contaminant per outbreak. Using the remaining 6911 outbreaks, I described and compared median severity index scores by 16 outbreak-associated contaminants using Dunn's tests with Bonferroni corrections. I selected these contaminants because they contributed to ~95% (n=6556) of the 6911 outbreaks and had an average of >1 outbreak per study year.

I examined annual trends and seasonality of scores using tobit regression models:

$$S_{k,y} = \beta_0 + \beta_1(y) \quad \textbf{(3)}$$

$$S_{k,m} = \beta_0 + \beta_1\left[\sin\left(\frac{2\pi m}{12}\right)\right] + \beta_2\left[\cos\left(\frac{2\pi m}{12}\right)\right] \quad \textbf{(4)}$$

where $S_{k,y}$ and $S_{k,m}$ - severity index scores of *k*-contaminant in *y*-year or *m*-month, respectively (values ranging from $0 \leq S_{k,y}$; $S_{k,m} \leq 1$); *y* - study year (ranges 1-11); *m* - Gregorian calendar month (ranges 1-12); and $sin\left(\frac{2\pi m}{12}\right)$ and $cos\left(\frac{2\pi m}{12}\right)$ - harmonic trend terms adjusted for the length of the year in months. I used tobit regression models due to their superiority in modeling scores ensuring that the estimated values are within prespecified values of 0 and 1. This technique was employed in other studies to forecast levels within censored detectable quantification limits [33-34]. I assessed model fit using log-likelihood estimates and defined significance as $\alpha < 0.05$.

I performed data extraction, alignment, management, and cleaning using Excel 2016 Version 2103 and Stata SE/16.1 software. I conducted statistical analyses using Stata SE/16.1 software and created data visualizations using R (3.6.3) software.

4.5.5. Metric Selection

Out of 67 available metrics representing 9407 outbreaks, I selected 12 metrics with completeness ranging from 67.83% (healthcare, hospitalizations, and ER visits per exposure duration) to 100.00% (primary cases) (Table 11, Appendix B Supplementary Tables S3-S5). As expected, median total primary cases (7.00 cases [4.00, 17.00]) exceeded median healthcare visits and hospital/ER visits (0.00 visits [0.00, 2.00]) per outbreak, with all 3 metrics having >86% completeness. Despite high completeness (98.47%), median deaths per outbreak was 0.00 deaths [0.00, 0.00] with only 290 of 9263 outbreaks (3.13%) having ≥ 1 deaths. As a result, all mortality-related metrics had near-zero estimates.

Table 11. Summary of 12 metrics considered for the creation of a foodborne outbreak severity index (11 used; deaths excluded) using data from the National Outbreak Reporting System (NORS) in 2009-2019. Summary statistics include observations (with percent completeness), median estimates per outbreak (with interquartile ranges), and L-moments (including L-skewness and L-kurtosis). I estimated completeness as the ratio of outbreaks with available records to total outbreaks in the study period (N=9407) and multiplied by 100. I report interquartile range (IQR) bounds at the 25th and 75th percentiles. Summary statistics are provided for identity, ln-transformed, and calibrated metric estimates. I provide L-skewness and L-kurtosis for identity (*Iden.*) and ln-transformed (*Tran.*) metrics. Product moments do not vary between transformed and calibrated metrics. While listing deaths, I

excluded this metric when calculating severity index scores. I was unable to estimate L-skewness and L-kurtosis for deaths (denoted *NR*), as all observations for transformed metrics were equal to 0.

		Median [IQR] Summary Statistics			L-Skewness		L-Kurtosis	
Metric	**Counts [Completeness]**	**Identity**	**Transformed**	**Calibrated**	**Iden.**	**Tran.**	**Iden.**	**Tran.**
Total Primary Cases	9407 [100.00]	7.00 [4.00, 17.00]	2.08 [1.61, 2.89]	0.33 [0.17, 0.60]	0.62	0.13	0.43	0.03
Hospital/ER Visits	8098 [86.08]	0.00 [0.00, 2.00]	0.00 [0.00, 1.10]	0.00 [0.00, 0.53]	0.69	0.40	0.46	0.02
Healthcare Visits	8385 [89.14]	0.00 [0.00, 2.00]	0.00 [0.00, 1.10]	0.00 [0.00, 0.50]	0.76	0.42	0.57	0.05
Deaths	9263 [98.47]	0.00 [0.00, 0.00]	0.00 [0.00, 0.00]	0.00 [0.00, 0.00]	0.98	*NR*	0.95	*NR*
Healthcare Visits per Total Primary Cases	8385 [89.14]	0.00 [0.00, 0.02]	0.29 [0.00, 0.69]	0.00 [0.00, 0.26]	0.59	0.23	0.24	-0.05
Hospital/ER Visits per Total Primary Cases	8098 [86.08]	0.00 [0.00, 0.03]	0.22 [0.00, 0.69]	0.00 [0.00, 0.28]	0.61	0.27	0.28	-0.03
Exposure Duration	7119 [75.68]	1.00 [1.00, 2.00]	0.69 [0.69, 1.10]	0.00 [0.00, 0.22]	0.87	0.63	0.73	0.27
Illness Duration	8385 [89.14]	2.00 [2.00, 6.00]	1.10 [1.10, 1.95]	0.13 [0.13, 0.39]	0.83	0.32	0.71	0.13
Total Primary Cases per Exposure Duration	7119 [75.68]	5.00 [2.00, 11.00]	1.79 [1.10, 2.48]	0.49 [0.30, 0.69]	0.56	0.07	0.38	0.08
All Visits per Exposure Duration	6381 [67.83]	0.33 [0.00, 2.00]	0.29 [0.00, 1.10]	0.14 [0.00, 0.53]	0.69	0.31	0.50	0.00
Total Primary Cases per Illness Duration	7119 [75.68]	3.00 [1.50, 5.33]	1.39 [0.92, 1.85]	0.49 [0.32, 0.65]	0.53	0.05	0.40	0.10
All Visits per Illness Duration	7754 [82.43]	0.25 [0.00, 1.00]	0.22 [0.00, 0.69]	0.15 [0.00, 0.46]	0.66	0.32	0.45	0.02

Duration metrics had high completeness (89.14% and 75.68% for illness and exposure, respectively) with the illness duration metric having higher median values (2.00 [2.00, 6.00] days per outbreak) than the exposure duration metric (1.00 [1.00, 2.00] days per outbreak). Among morbidity case definitions, I found higher median total primary cases per exposure duration (5.00 [2.00, 11.00] cases/day) than cases per illness duration (3.00 [1.50, 5.33] cases/day). Median healthcare, hospital, and ER visits per exposure duration were comparable to all visits per illness duration (0.33 [0.00, 2.00] and 0.25 [0.00, 1.00] cases/day, respectively).

The proposed transformation substantially improved the statistical properties of all 11 selected metrics as shown by reductions in L-skewness and L-kurtosis statistics between identified and transformed metrics (Table 11, Appendix B Supplementary Tables S4). However, the 95th percentile ceiling used reduced estimates of deaths for all outbreaks to 0.00 deaths. To prevent dilution, I excluded this metric and all other mortality-related metrics when calculating severity index scores.

Median estimates for calibrated metrics ranged from ~0.01 for exposure duration, health visits and hospital/ER visits per primary cases to ~0.49 for total primary cases per exposure and illness duration suggesting high contribution in final index scores (Appendix B Supplementary Table S5). I identified similarly high contributions for

total primary cases (0.33 [0.17, 0.60]) and low-to-moderate contributions for illness duration (0.13 [0.13, 0.39]) (Table 11). Like with mortality-related metrics, I excluded secondary case-related metrics due to near-zero calibrated metric estimates after transformation. Similarly, I excluded extent-related calibrated metrics as they approached ~1.00 values and would have inflated all severity scores (Appendix B Supplementary Table S5).

Of the 9407 outbreaks in the study period, 2346 outbreaks (24.93%) lacked contaminant information while 150 outbreaks were associated with multiple contaminants (1.59%). Of the remaining 6911 outbreaks, *Norovirus* had the greatest number of outbreaks (n=3088, 44.68%) followed by *Salmonella* (n=1510, 21.85%), *Clostridium* (n=376, 5.44%), *Escherichia* (n=355, 5.14%), and *Campylobacter* (n=314, 4.54%). While *Sapovirus* had the fewest outbreaks (n=15), this contaminant reported the highest average completeness across metrics (96.36 [92.42, 100.00]) followed by *Ciguatoxin* (92.81 [89.86, 95.77]) and *Staphylococcus* (90.91 [86.35, 95.46]) (Appendix B, Supplementary Figure S1). *Listeria* had the lowest completeness across metrics (43.56% [19.56, 67.56]) followed by *Hepatitis* (68.47 [54.25, 82.68]), *Escherichia* (68.66 [53.91, 83.40]), and *Salmonella* (74.76 [63.16, 86.36]). Across metrics, all visits per exposure duration had the lowest completeness (67.83%) followed by exposure duration (75.68%).

Norovirus-associated outbreaks had significantly lower ($p \leq 0.001$) median severity (0.25 [0.15, 0.37]) compared to *Hepatitis* (0.50 [0.37, 0.57]), *Salmonella* (0.47 [0.36, 0.58]), *Shigella* (0.47 [0.30, 0.60]), *Listeria* (0.45 [0.37, 0.49]), *Escherichia* (0.44 [0.35, 0.55]), *Cyclospora* (0.42 [0.33, 0.54]), and *Campylobacter* (0.35 [0.28, 0.45]) (Table 12; Figure 14). Similarly, *Campylobacter*-, *Vibrio*- (0.30 [0.22, 0.38]), *Sapovirus*- (0.26 [0.19, 0.35]), and *Bacillus*-associated (0.21 [0.12, 0.28]) outbreaks had lower severity scores compared to *Hepatitis*, *Salmonella*, *Listeria*, and *Escherichia* ($p \leq 0.032$). I found no differences in scores for *Hepatitis*, *Salmonella*, *Listeria*, and *Escherichia*.

Table 12. Outbreak severity scores for 16 contaminants using the National Outbreak Report System (NORS) in 2009-2019. Statistics include observations (with percent of total outbreaks), average and median scores per contaminant (with 95% confidence intervals and interquartile ranges), minimum and maximum scores, and L-skewness and L-kurtosis statistics. I calculated percent of outbreaks as the ratio of contaminant-specific outbreaks to total outbreaks with complete information pertaining to only 1 contaminant (N=6911) and multiplied by 100. I calculated average estimates per outbreak using

generalized linear models adjusted for negative binomial distributions and the logarithmic link function. I report contaminants by type in descending order by outbreaks.

Pathogen/Toxin	Outbreaks [% Total]	Average [95% CI]	Median [IQR]	Min, Max	L-Skew	L-Kurt
Bacterial Outbreaks						
Salmonella	1510 [21.85]	0.48 [0.47, 0.48]	0.47 [0.36, 0.58]	0.00, 1.00	0.04	0.11
Clostridium	376 [5.44]	0.29 [0.27, 0.30]	0.26 [0.16, 0.37]	0.02, 0.78	0.16	0.10
Escherichia	355 [5.14]	0.45 [0.43, 0.47]	0.44 [0.35, 0.55]	0.05, 0.97	0.02	0.13
Campylobacter	314 [4.54]	0.37 [0.35, 0.38]	0.35 [0.28, 0.45]	0.06, 0.89	0.12	0.13
Staphylococcus	157 [2.27]	0.29 [0.26, 0.32]	0.22 [0.11, 0.49]	0.00, 0.75	0.15	-0.04
Vibrio	139 [2.01]	0.31 [0.28, 0.33]	0.30 [0.22, 0.38]	0.00, 0.69	0.09	0.19
Bacillus	137 [1.98]	0.24 [0.21, 0.26]	0.21 [0.12, 0.28]	0.00, 0.67	0.22	0.14
Listeria	72 [1.04]	0.45 [0.42, 0.48]	0.45 [0.37, 0.49]	0.25, 0.78	0.12	0.13
Shigella	62 [0.90]	0.45 [0.40, 0.50]	0.47 [0.30, 0.60]	0.10, 0.83	0.01	0.06
Viral Outbreaks						
Norovirus	3088 [44.68]	0.28 [0.27, 0.28]	0.25 [0.15, 0.37]	0.00, 0.87	0.16	0.09
Hepatitis	32 [0.46]	0.50 [0.45, 0.55]	0.50 [0.37, 0.57]	0.29, 0.85	0.15	0.10
Sapovirus	15 [0.22]	0.27 [0.21, 0.33]	0.26 [0.19, 0.35]	0.10, 0.54	0.14	0.15
Protozoal Outbreaks						
Cyclospora	91 [1.32]	0.46 [0.42, 0.50]	0.42 [0.33, 0.54]	0.12, 0.90	0.17	0.13
Cryptosporidium	21 [0.30]	0.38 [0.32, 0.44]	0.36 [0.29, 0.43]	0.21, 0.79	0.25	0.26
Trichinella	15 [0.22]	0.40 [0.35, 0.46]	0.43 [0.28, 0.50]	0.24, 0.53	-0.12	-0.13
Toxin-Associated Outbreaks						
Ciguatoxin	172 [2.49]	0.30 [0.28, 0.32]	0.32 [0.22, 0.39]	0.00, 0.61	-0.05	0.13

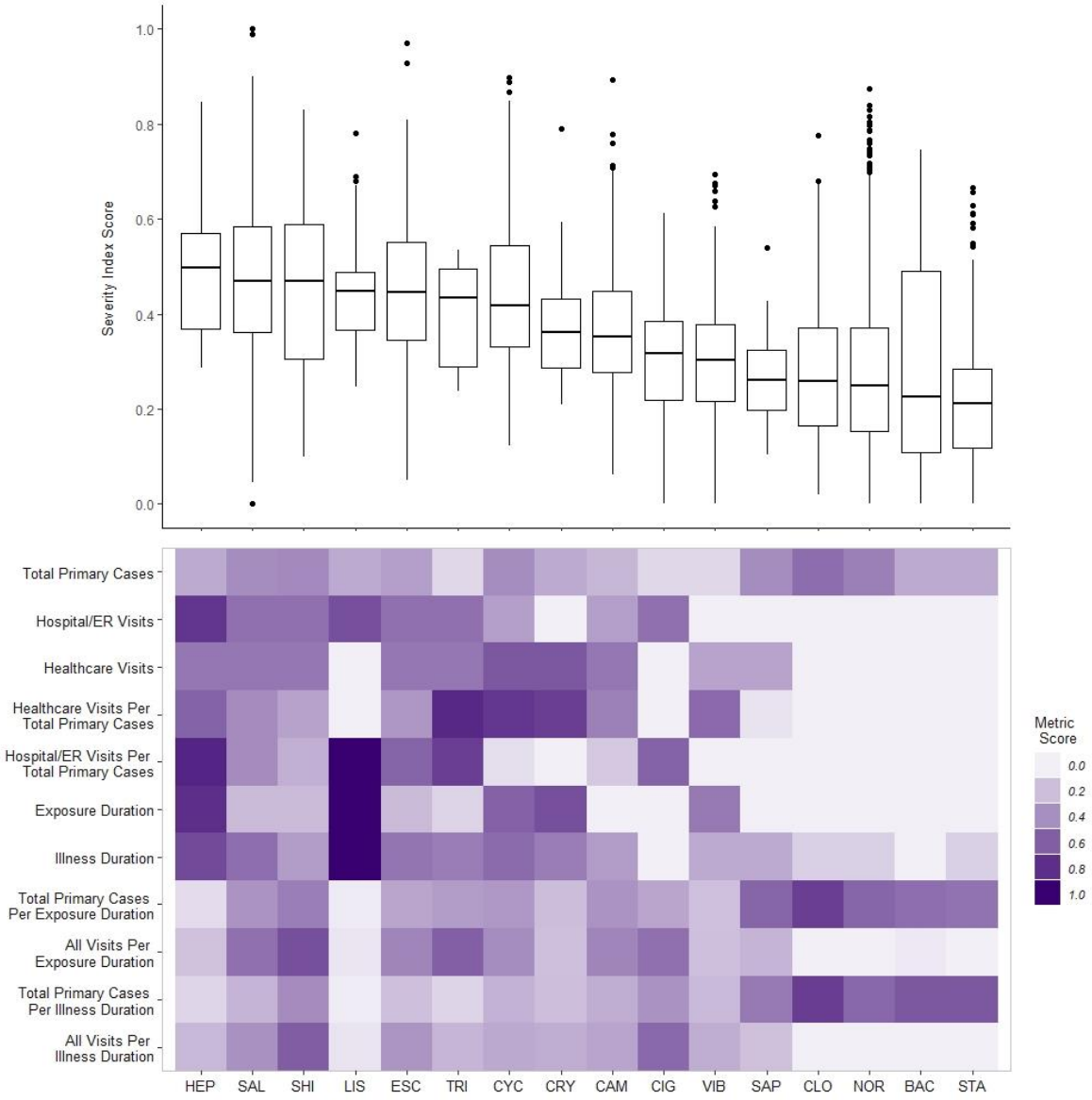


Figure 14. Multi-panel, shared-axis plot of outbreak severity scores for 16 contaminants using the National Outbreak Report System (NORS) in 2009-2019. The top panel provides a boxplot of contaminant-specific severity scores for the 16 contaminants with the greatest number of outbreaks in the study period (n=6556, or 94.9%). I report contaminants in descending order by median severity score. The bottom panel provides a heatmap depicting the median calibrated metric estimate for each of the 11 metrics used to create the severity index score. Scores range from light purple (0.00) to dark purple (1.00). I abbreviate the aggregate of healthcare, hospital, and ER visits as *All Visits*. I abbreviate contaminants as: HEP (*Hepatitis*), SAL *(Salmonella*), SHI (*Shigella*), LIS (*Listeria*), ESC (*Escherichia*), TRI (*Trichinella*), CYC (*Cyclospora*), CRY (*Cryptosporidium*), CAM (*Campylobacter*), CIG (*Ciguatoxin*), VIB (*Vibrio*), SAP (*Sapovirus*), CLO (*Clostridium*), NOR (*Norovirus*), STA (*Staphylococcus*), BAC (*Bacillus*).

I found patterns in metric estimates to explain differences in severity scores by contaminant type with 0.30-unit difference between highest (*Hepatitis*) and lowest (*Staphylococcus*) median scores (Figure 14). Protozoal outbreaks, including *Cyclospora* and *Cryptosporidium*, had high median metric estimates for healthcare

visits per primary cases (0.77 [0.50, 1.00] and 0.74 [0.38, 1.00], respectively) and total healthcare visits (0.63 [0.50, 1.00] and 0.63 [0.50, 0.73], respectively)). However, these contaminants had much lower estimates for primary cases per exposure duration (0.36 [0.16, 0.56] and 0.21 [0.12, 0.57], respectively) and per illness duration (0.25 [0.14, 0.40] and 0.20 [0.14, 0.31], respectively). In contrast, viral outbreaks, including *Norovirus* and *Sapovirus*, had high median metric estimates for primary cases per exposure duration (0.58 [0.44, 0.77] and 0.58 [0.44, 0.75], respectively), per illness duration (0.57 [0.42, 0.73] and 0.49 [0.39, 0.58], respectively), and total (0.47 [0.23, 0.69] and 0.41 [0.17, 0.69], respectively) with near-zero estimates for hospital/ER visits, hospital/ER visits per primary cases, healthcare visits per primary cases, and exposure duration.

Among bacterial contaminants, *Salmonella*, *Campylobacter*, *Escherichia*, and *Shigella* outbreaks had moderate estimates for all metrics. These contaminants had moderately high hospital/ER visits and visits per primary cases, healthcare visits and visits per primary cases, and illness duration. In contrast, outbreaks associated with *Bacillus*, *Clostridium*, and *Staphylococcus* had moderate to high median metric estimates for total primary cases, cases per exposure duration, and cases per illness duration but near-zero estimates for more morbid case definitions. Interestingly, median metric estimates approached 1.00 for *Listeria*-associated outbreaks with respect to illness duration (1.00 [1.00, 1.00]) and hospital/ER visits per primary cases (1.00 [0.96, 1.00]) but low for remaining metrics. These patterns paralleled *Hepatitis*-associated outbreaks (0.69 [0.59, 1.00] and 0.84 [0.51, 1.00], respectively).

All-contaminant outbreak severity scores decreased by 0.10 units (0.006 per year [-0.007, -0.005]) throughout the study period ($p<0.001$) (Appendix B Supplementary Tables S6-S7). *Norovirus*-, *Salmonella*-, *Escherichia*-, and *Clostridium*-associated outbreaks had similar declines of 0.006-0.007 per year. In contrast, *Listeria*-, *Staphylococcus*-, and *Campylobacter*-associated outbreaks had greater declines per year (-0.015 [-0.025, -0.004], -0.013 [-0.024, -0.003], and -0.011 [-0.016, -0.006], respectively; $p\leq0.023$). I detected anomalies in severity scores for specific contaminants (Figure 15) including *Shigella* and *Vibrio* in 2009, *Staphylococcus* in 2012, *Cyclospora* in 2013 and 2015, and *Hepatitis* in 2016.

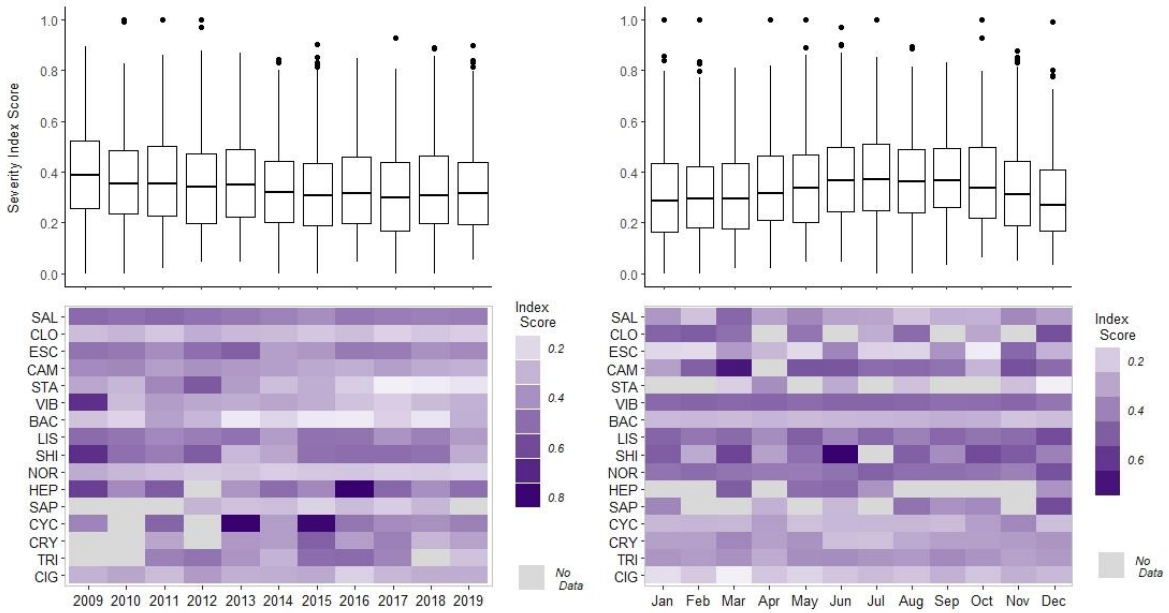


Figure 15. Multi-panel, shared-axis plot of median outbreak severity score by Gregorian calendar year (left panel) and month (right panel). I created plots using the National Outbreak Report System (NORS) in 2009-2019. Top panels provide boxplots of severity scores estimated using outbreaks with complete contaminant information and not associated with multiple contaminants in the study period (N=6911). Bottom panels provide a heatmap for the breakdown of median severity score by year, month, and contaminants. Scores range from light (0.00) to dark purple (1.00) with grey color to indicate years with no data. I abbreviate contaminants as: HEP (*Hepatitis*), SAL *(Salmonella*), SHI (*Shigella*), LIS (*Listeria*), ESC (*Escherichia*), TRI (*Trichinella*), CYC (*Cyclospora*), CRY (*Cryptosporidium*), CAM (*Campylobacter*), CIG (*Ciguatoxin*), VIB (*Vibrio*), SAP (*Sapovirus*), CLO (*Clostridium*), NOR (*Norovirus*), STA (*Staphylococcus*), BAC (*Bacillus*). I report contaminants by type in descending order by outbreaks (as in Table 12).

I found significant seasonality in the all-contaminant severity score ($p<0.001$) with 0.20-unit higher median scores in summer compared to winter months (Figure 15). More specifically, median scores were greatest in June-September compared to November-March. *Norovirus*-, *Clostridium*-, *Vibrio*-, *Bacillus*-, and *Cyclospora*-associated outbreaks also had significant seasonality in scores ($p\leq0.027$). However, *Cyclospora*-associated outbreaks were only reported within the months of March, May-July, and December, resulting in poor model fit relative to other contaminants. Like with trend analyses, I found severity score anomalies for two contaminants: *Shigella* outbreaks in March and *Hepatitis* outbreaks in June.

4.5.6. Discussion

I created a data-driven index for evaluating foodborne outbreak severity using publicly available surveillance data. The index utilized case volumes of varying morbidity and mortality, outbreak duration, and their ratios to describe the speed of

infection and illness intensity of outbreaks. I emphasized the importance of data completeness when selecting metrics for generating index scores and the use of product moments, like L-skewness and L-kurtosis, to monitor reporting anomalies and case influential observations. I performed a standardized 4-step procedure to select, transform, calibrate, and average metric estimates for creating severity scores. This technique provides a systematic and reproducible analytic tool to leverage real-time surveillance data for describing and comparing outbreak severity in accordance with the CDC's *Data Modernization Initiative* [13-16].

As data are collected, public health agencies can estimate health impact metrics and construct severity index scores in real-time. Health agencies can rank scores across ongoing outbreaks to identify which threats are most severe. This precisely determines laboratory testing personnel needs and resource stockpiles to facilitate rapid processing of incident cases. Standardized severity alerts can inform hospitals, health facilities, and other federal agencies which metrics contribute greatest to severity. As outbreaks progress, these patterns inform immediate food safety inspections to minimize multistate outbreak spread, increased personnel and antibiotics to reduce illness intensity, and expedited health communications to limit the transmissibility of infection among exposed persons.

Real-time creation of severity indices allows for the relative ranking of emerging compared to historic outbreaks. Spatial clusters of severe outbreaks illustrate regional hotspots of emerging threats requiring coordination among local, regional, and national health agencies. Annual trends in index scores demonstrate the efficiency of public health intervention strategies in reducing outbreak severity by contaminant. Precise estimation of seasonal severity signatures informs the timing and intensity of peak outbreak severity and the duration of severe outbreak seasons. Spikes in severity scores during specific times-of-the-year can alert health agencies and facilities to when the onset of seasonal severity increases begin, allowing for preemptive public health measures [10].

As a data-driven approach, this index is limited by the availability and usability of surveillance records. Prior works have demonstrated the importance of measuring the quantity and distribution of missing data within surveillance records [35-36]. I found that 18 of 67 metrics had <70% completeness with 13 metrics having <50% completeness. This prevented the use of secondary cases and exposure duration information in creating the index. Additionally, I was forced to remove outbreaks with

no contaminant information or listing multiple contaminants without disaggregated case information. These exclusions and incomplete data reporting resulted in an average of ~43% completeness for *Listeria*-associated outbreaks. As the *Data Modernization Initiative* strengthens the accountability, quality, timeliness, and harmonization of public health surveillance data in the United States, index score precision will only improve [13-14]. I encourage the CDC to improve historic data completeness and standardize the reporting of missing data as part of the *Data Modernization Initiative*.

Prior studies leveraging surveillance data do not consider the speed of infection, illness intensity, and geographic infection transmissibility of outbreaks. Yet, ratios of metrics describe unique features of outbreak signatures not captured by location, case, or duration metrics independently. This study identified 48 relative metrics for inclusion in creating a severity index generated from 19 variables. I encourage researchers to provide clear metric inclusion/exclusion criteria using thorough investigation of distributional characteristics. Product moments, such as L-skewness and L-kurtosis, can help identify metrics with case influential observations or minimal variability across outbreaks. Researchers should prevent diluting scores from metrics with exclusively near-zero values or inflating scores with exclusively near-one values. Future studies could conduct sub-analyses to evaluate outbreaks with non-zero reported deaths, as these were removed from the overall index calculation. Researchers can also consider estimating index scores using a variety of criteria to produce to create an assemble of scores for informing early warning severity alerts.

The severity index analytical workflow faced several limitations with respect to internal and external validity. First, I did not produce measures of uncertainty for estimating severity by outbreak, only when averaging scores across pathogens, years, or months of the year. Future research is required to determine techniques for estimating confidence interval bounds per outbreak. Second, as the calibration step depends on minimum and maximum severity scores across outbreaks, the index has limited external validity. While adaptive to trends in severity over time, scores are subject to change, minimizing their reproducibility and generalizability. Finally, I used no weighting schemes to differentially value metrics during the averaging stage of score calculation. While this limits researchers' subjectivity, I advise researchers to explore applications of weights and clearly specify justification for their need.

I found intense spikes in outbreak severity by contaminant and study year. *Vibrio* severity spiked in 2009, coinciding with the American continent outbreak of *Vibrio parahaemolyticus* in Lima, Peru [37]. Reports also describe isolated outbreaks of *Vibrio* within the Chesapeake Bay in Maryland attributed to the consumption and handling of shellfish and nutrient pollution promoting intense bacterial growth [38]. *Shigella* severity similarly spiked in 2009 attributed to numerous outbreaks nationwide [39-43]. While the locations of outbreaks all pertained to restaurant, day care, and private homes, neither the food vehicle nor mode of transmission was detected. *Staphylococcus* severity spikes in 2012 were attributed to intense food poisoning within a military unit leading to 22 healthcare visits and hospitalizations over the 2-day outbreak [44-45].

I found 2 annual spikes in *Cyclospora* severity scores in 2013 and 2015. Both multistate outbreaks were attributed to contamination of cilantro and salad produce with cases spanning 20+ states per outbreak [46-47]. Lasting 2 weeks in duration, outbreaks reported 631 and 495 primary cases, respectively, with limited information on hospitalizations and deaths [46-47]. Similarly, I found a spike in *Hepatitis* severity in 2016 attributed to an expansive multistate domestic outbreak [48-49]. Originally introduced via food imports of scallops and strawberries in August of 2016, this outbreak has culminated in a mass vaccination campaign in 37 states [48-49]. As of 15 October 2021, this outbreak attributed to ~43,000 cases, ~26,000 hospitalizations and ~400 deaths nationwide [48-49].

Prior works have examined the seasonal signature of bacterial and viral contaminants using publicly and privately available surveillance databases [50-54]. These studies identified consistent summertime peaks of foodborne pathogens, specifically during July and August within the United States. Index scores demonstrated similar seasonality with increased severity in June-September. This emphasizes the need for increased resource allocation, monitoring, and surveillance of foodborne outbreaks during and prior to these months. Future research must explore relationships between seasonal signatures of outbreak incidence and severity considering applications of L-moments to detect change points in the acceleration of outbreak severity towards seasonal peaks.

Future applications of this index include exploring differences in severity by outbreak characteristics. Comparisons by contaminated food products can inform food safety regulations while differences by production, distribution, and retail facilities

illustrate ramifications of outbreaks tied to when hazards are introduced in the supply chain. Seasonal outbreak signatures by supply chain can inform food safety regulatory organizations' scheduling of agricultural and food safety inspections to minimize outbreak severity. Future research investigating differences in severity scores by food preparation techniques, pathogen strains/species, and geographic location will improve the precision of regulation and investigation recommendations.

4.6. Conclusions: Further research for emerging health threats

In this chapter, I proposed a standardized analytical workflow for evaluating seasonality features of enteric infections and their severity. The approach included inspection of the availability and completeness of public health surveillance data, proposing techniques for estimating distributional properties of L-moments, and standardized estimation of seasonality features. As the δ-method provided measures of uncertainty for peak timing and amplitude, I compared these features across locations, pathogens, and time. I also proposed several correlation metrics to examine the synchronicity of disease patterns by pathogen and location. I apply similar techniques for comparing differences in outbreak health burdens, which I estimated using a standardized workflow for selecting, transforming, calibrating, and averaging data-centric metrics. This case study expands on prior research to include composite metrics created from ratios of surveillance variables that estimate illness intensity, speed of infection, and outbreak spread.

Yet, the analytical approaches within this chapter, particularly those related to estimating seasonality features, rely on two assumptions. First, all studies assumed a stable, periodic pattern of infections and severity. Second, all studies utilized public health surveillance data that were available, complete, and frequently reported. These assumptions reflect the characteristics of the geographic location (United States) and data curating organization (CDC) used for this chapter. But what is the applicability of these analytical approaches when investigating aperiodic, emerging outbreak threats in locations with sparse health resources and poor data quality?

To prove the generalizability of these analytical workflows, I conduct further research to demonstrate the adaptability of approaches for aperiodic outbreaks. Like with periodic processes, the workflows should estimate critical points defining outbreak signatures as well as help public health agencies identify the severity of emerging threats over time. Focusing on areas with poor health surveillance, I

demonstrate effects of data quality limitations such as completeness, timeliness, and representativeness on the modeling of these aperiodic illness patterns. This includes assessments of *ACTOR* principles when harmonizing data across multiple surveillance systems or integrating health data with risk factor data expected to drive epidemic or pandemic events.

4.7. References

1. Simpson, R. B., Kulinkina, A. V., and Naumova, E. N. "Investigating seasonal patterns in enteric infections: a systematic review of time series methods." *Epidemiology and Infection* (2022): 1-25.
2. Naumova, E. N., and MacNeill, I. B. "Seasonality assessment for biosurveillance systems." In *Advances in Statistical Methods for the Health Sciences*, ed. Jean-Louis Auget, N. Balakrishnan, Mounir Mesbah, and Geert Molenberghs (Boston: Birkhäuser, 2007), 437-450.
3. Wenger, J. B., and Naumova, E. N. "Seasonal synchronization of influenza in the United States older adult population." *PLoS One* 5, no. 4 (2010): e10187.
4. Naumova, E. N., Jagai, J. S., Matyas, B., DeMaria, A., MacNeill, I. B., and Griffiths, J. K. "Seasonality in six enterically transmitted diseases and ambient temperature." *Epidemiology and Infection* 135, no. 2 (2007): 281-292.
5. Falconi, T. A., Cruz, M. S., and Naumova, E. N. "The shift in seasonality of legionellosis in the USA." *Epidemiology and Infection* 146, no. 14 (2018): 1824-1833.
6. Naumova, E. N. "Mystery of seasonality: getting the rhythm of nature." *Journal of Public Health Policy* 27, no. 1 (2006): 2-12.
7. Simpson, R. B., Zhou, B., and Naumova, E. N. "Seasonal synchronization of foodborne outbreaks in the United States, 1996–2017." *Scientific Reports* 10, no. 1 (2020): 1-16.
8. Simpson, R. B., Zhou, B., Alarcon Falconi, T. M., and Naumova, E. N. "An analecta of visualizations for foodborne illness trends and seasonality." *Scientific Data* 7, no. 1 (2020): 1-15.
9. United States. Department of Health and Human Services, Centers for Disease Control and Prevention (CDC). "Outbreaks of Foodborne Illness." Accessed September 01, 2021. https://www.fda.gov/food/recalls-outbreaks-emergencies/outbreaks-foodborne-illness.
10. Fefferman, N., and Naumova, E. N. "Innovation in observation: a vision for early outbreak detection." *Emerging Health Threats Journal* 3, no. 1 (2010): 7103.
11. Koopmans, M., Vennema, H., Heersma, H., Van Strien, E., Van Duynhoven, Y., Brown, D., Reacher, M., Lopman, B., and European Consortium on Foodborne Viruses. "Early identification of common-source foodborne virus outbreaks in Europe." *Emerging Infectious Diseases* 9, no. 9 (2003): 1136.
12. Chretien, J. P., Tomich, N. E., Gaydos, J. C., and Kelley, P. W. "Real-time public health surveillance for emergency preparedness." *American Journal of Public Health* 99, no. 8 (2009): 1360–1363.
13. United States. Department of Health and Human Services, Centers for Disease Control and Prevention (CDC), Office of Public Health Scientific

Services (OPHSS). “Public Health Surveillance: Preparing for the Future.” 2018. https://www.cdc.gov/surveillance/pdfs/Surveillance-Series-Bookleth.pdf.

14. United States. Department of Health and Human Services, Centers for Disease Control and Prevention (CDC). “Public Health Data Modernization: Listening Session on Real-World Testing of 21st Century Cures Act Requirements.” 2020. https://www.cdc.gov/surveillance/pdfs/20_319521-D_DataMod-Initiative_901420.pdf.
15. United States. Department of Health and Human Services, Centers for Disease Control and Prevention (CDC). “Modernizing for New and Complex Threats.” 2021. https://www.cdc.gov/surveillance/pdfs/Modernizing-for-New-and-Complex-Threats.pdf.
16. United States. Department of Health and Human Services, Centers for Disease Control and Prevention (CDC). “It’s time to build pandemic-ready IT systems.” 2021. https://www.cdc.gov/surveillance/pdfs/PRIME_1-sheet_single-page.pdf.
17. Havelaar, A. H., Kirk, M. D., Torgerson, P. R., Gibb, H. J., Hald, T., Lake, R. J., Praet, N., Bellinger, D. C., De Silva, N. R., Gargouri, N., and Speybroeck, N. “World Health Organization Global Estimates and Regional Comparisons of the Burden of Foodborne Disease in 2010.” *PLoS Medicine* 12, no. 12 (2015): e1001923.
18. Torgerson, P. R., Devleesschauwer, B., Praet, N., Spebroeck, N., Willingham, A. L., Kasuga, F., Rokni, M. B., Zhou, X. N., Fevre, E. M., Sripa, B., and Gargouri, N. “World Health Organization Estimates of the Global and Regional Disease Burden of 11 Foodborne Parasitic Diseases, 2010: A Data Synthesis.” *PLoS Medicine* 12, no. 12 (2015): e1001920.
19. Devleesschauwer, B., Bouwknegt, M., Domy, P., Gabriel, S., Havelaar, A. H., Quoilin, S., Robertson, L. J., Speybroeck, N., Torgerson, P. R., van der Giessen, J. W., Trevisan, C. “Risk ranking of foodborne parasites: state of the art.” *Food and Waterborne Parasitology* 8 (2017): 1-13.
20. Barker, C., and Green, A. “Opening the debate on DALYs.” *Health Policy and Planning* 11, no. 2 (1996): 179-183.
21. Arnesen, T., and Kapiriri, L. “Can the value choices in DALYs influence global priority-setting?” *Health Policy* 70, no. 2 (2004):137-149.
22. Batz, M. B., Hoffmann, S., and Morris Jr., J. G. “Ranking the disease burden of 14 pathogens in food sources in the United States using attribution data from outbreak investigations and expert elicitation.” *Journal of Food Protection* 75, no. 7 (2012): 1278-1291.
23. Cardoen, S., Van Huffel, X., Berkvens, D., Quoilin, S., Ducoffre, G., Saegerman, C., Speybroeck, N., Imberechts, H., Herman, L., Ducatelle, R., and Dierick, K. “Evidence-based semiquantitative methodology for prioritization of foodborne zoonoses.” *Foodborne Pathogens and Disease* 6, no. 9 (2009): 1083-1096.
24. Hoover, E. R., Hedeen, N. Freeland, A., Kambhampati, A., Dewey-Mattia, D., Scott, K. W., Hall, A., and Brown, L. “Restaurant policies and practices related to norovirus outbreak size and duration.” *Journal of Food Protection* 83, no. 9 (2020): 1607-1618.
25. Olsen, S. J., Bleasdale, S. C., Magnano, A. R., Landrigan, C., Holland, B. H., Tauxe, R. V., Mintz, E. D., and Luby, S. “Outbreaks of typhoid fever in the United States, 1960-99.” *Epidemiology and Infection* 130, no. 1 (2003): 13.

26. Grass, J. E., Gould, L. H., and Mahon, B. E. “Epidemiology of foodborne disease outbreaks caused by Clostridium perfringens, United States, 1998–2010.” *Foodborne Pathogens and Disease* 10, no. 2 (2013): 131-136.
27. United States. Department of Health and Human Services, Centers for Disease Control and Prevention (CDC). “About NORS”. Accessed October 20, 2021. https://www.cdc.gov/nors/about.html.
28. United States. Department of Health and Human Services, Centers for Disease Control and Prevention (CDC). “National Outbreak Reporting System (NORS) Guidance”. Accessed January 01, 2021. https://www.cdc.gov/nors/downloads/guidance.pdf.
29. United States. Department of Health and Human Services, Centers for Disease Control and Prevention (CDC). “Using NORS Data”. Accessed January 01, 2021. https://www.cdc.gov/nors/data/using-nors.html.
30. Zhang, Y., Simpson, R. B., Sallade, L. E., Sanchez, E., Monahan, K. M., and Naumova, E. N. “Evaluating completeness of foodborne outbreak reporting in the United States, 1998–2019.” *International Journal of Environmental Research and Public Health* 19, no. 5 (2022): 2898.
31. Sanchez, E., Simpson, R. B., Zhang, Y., Sallade, L. E., and Naumova, E. N. “Exploring risk factors of recall-associated foodborne disease outbreaks in the United States, 2009–2019.” *International Journal of Environmental Research and Public Health* 19, no. 9 (2022): 4947.
32. Hosking, J. “L-Moments: analysis and estimation of distributions using linear combinations of order statistics.” *Journal of the Royal Statistical Society: Series B* 52, no. 1 (1990): 105–124.
33. Davis, B. J., Jacobs, J. M., Zaitchik, B., DePaola, A., and Curriero, F. C. “Vibrio parahaemolyticus in the Chesapeake Bay: operational in situ prediction and forecast models can benefit from inclusion of lagged water quality measurements.” *Applied and Environmental Microbiology* 85, no. 17 (2019): e01007-19.
34. Setty, K. E., Kayser, G. L., Bowling, M., Enault, J., Loret, J. F., Serra, C. P., Alonso, J. M., Mateu, A. P., and Bartram, J. “Water quality, compliance, and health outcomes among utilities implementing Water Safety Plans in France and Spain.” *International Journal of Hygiene and Environmental Health* 220, no. 3 (2017): 513-530.
35. Simpson, R. B., Gottlieb, J., Zhou, B., Hartwick, M. A., and Naumova, E. N. “Completeness of open access FluNet influenza surveillance data for Pan-America in 2005–2019.” *Scientific Reports* 11, no. 1 (2021): 1-17.
36. Lawpoolsri, S., Kaewkungwal, J., Khamsiriwatchara, A., Sovann, L., Sreng, B., Phommasack, B., Kitthiphong, V., Lwin Nyein, S., Win Myint, N., Dang Vung, N., and Hung, P. “Data quality and timeliness of outbreak reporting system among countries in Greater Mekong subregion: Challenges for international data sharing.” *PLOS Neglected Tropical Diseases* 12, no. 4 (2018): e0006425.
37. Gonzalez-Escalona, N., Gavilan, R. G., Toro, M., Zamudio, M. L., and Martinez-Urtaza, J. “Outbreak of Vibrio parahaemolyticus Sequence Type 120, Peru, 2009.” *Emerging Infectious Diseases* 22, no. 7 (2016): 1235-1237.
38. Pelton, T. “Bad Water 2009: The impact on human health in the Chesapeake Bay Region.” *Chesapeake Bay Foundation*. Accessed November 28, 2021. https://www.cbf.org/document-library/cbf-reports/57298_final008c.pdf.

39. Foodborne Illness Outbreak Database (FIOD). "Maryland Other and Workplace Unknown 2009." *Marler Clark LLP, PS*. Accessed October 20, 2021. http://www.outbreakdatabase.com/details/maryland-other-and-workplace-unknown-2009/?organism=Shigella.
40. Foodborne Illness Outbreak Database (FIOD). "Illinois Restaurant Unknown 4 2009." *Marler Clark LLP, PS*. Accessed October 20, 2021. http://www.outbreakdatabase.com/details/illinois-restaurant-unknown-4-2009/?organism=Shigella.
41. Foodborne Illness Outbreak Database (FIOD). "Illinois Restaurant Unknown 4 2009." *Marler Clark LLP, PS*. Accessed October 20, 2021. http://www.outbreakdatabase.com/details/rufus-putnam-day-care-2009/?organism=Shigella.
42. Foodborne Illness Outbreak Database (FIOD). "Florida Private Home Unknown 2009." *Marler Clark LLP, PS*. Accessed October 20, 2021. http://www.outbreakdatabase.com/details/florida-private-home-unknown-2009/?organism=Shigella.
43. Foodborne Illness Outbreak Database (FIOD). "2009 Outbreak of Shigella Infections at Applebee's Restaurant, New York." *Marler Clark LLP, PS*. Accessed October 20, 2021. http://www.outbreakdatabase.com/details/2009-outbreak-of-shigella-infections-at-applebees-restaurant-new-york/?organism=Shigella.
44. Teague, N. S., Grigg, S. S., Peterson, J. C., Gomez, G. A., and Talkington, D. F. "Outbreak of Staphylococcal food poisoning from a military unit lunch party—United States, July 2012." *Morbidity and Mortality Weekly Report* 62, no 50 (2013): 1026.
45. Andrews, J. "Staphylococcal Food Poisoning Hit Military Unit in 2012." *Food Safety News*. December 23, 2013. https://www.foodsafetynews.com/2013/12/staphylococcal-food-poisoning-hit-military-unit-in-2012/#:~:text=A%20total%20of%2022%20people,for%20Disease%20Control%20and%20Prevention.
46. Foodborne Illness Outbreak Database (FIOD). "2013 Multistate Outbreak of Cyclospora cayetanensis." *Marler Clark LLP, PS*. Accessed October 20, 2021. http://www.outbreakdatabase.com/details/2013-multistate-outbreak-of-cyclospora-cayetanensis/?organism=Cyclospora&year=2013&country=US.
47. Foodborne Illness Outbreak Database (FIOD). "2015 Multistate Outbreak of Cyclospora." *Marler Clark LLP, PS*. Accessed October 20, 2021. http://www.outbreakdatabase.com/details/2015-multistate-outbreak-of-cyclospora/?organism=Cyclospora&year=2015&country=US.
48. United States. Department of Health and Human Services, Centers for Disease Control and Prevention (CDC). "Viral Hepatitis." Accessed October 20, 2021. https://www.cdc.gov/hepatitis/outbreaks/hepatitisaoutbreaks.htm.
49. United States. Department of Health and Human Services, Centers for Disease Control and Prevention (CDC). "Widespread outbreaks of hepatitis A across the United States" Accessed October 20, 2021. https://www.cdc.gov/hepatitis/outbreaks/2017March-HepatitisA.htm.
50. Simpson, R. B., Zhou, B., and Naumova, E. N. "Seasonal synchronization of foodborne outbreaks in the United States, 1996–2017." *Scientific Reports* 10, no. 1 (2020): 1-16.

51. Simpson, R. B., Zhou, B., Alarcon Falconi, T. M., and Naumova, E. N. “An analecta of visualizations for foodborne illness trends and seasonality.” *Scientific Data* 7, no. 1 (2020): 1-15.
52. Naumova, E. N., Jagai, J. S., Matyas, B., DeMaria, A., MacNeill, I. B., and Griffiths, J. K. “Seasonality in six enterically transmitted diseases and ambient temperature.” *Epidemiology and Infection* 135, no. 2 (2007): 281-292.
53. Chui, K. K., Webb, P., Russell, R. M., and Naumova, E. N. “Geographic variations and temporal trends of Salmonella-associated hospitalization in the US elderly, 1991-2004: a time series analysis of the impact of HACCP regulation.” *BMC Public Health* 9, no. 1 (2009): 1-10.
54. Naumova, E. N., Chen, J. T., Griffiths, J. K., Matyas, B. T., Estes-Smargiassi, S. A., and Morris, R. D. “Use of passive surveillance data to study temporal and spatial variation in the incidence of giardiasis and cryptosporidiosis.” *Public Health Reports* 115, no. 5 (2000): 436.

Chapter 5. Adapting Time Series Methods for Emerging Threats

5.1. Challenges of modeling aperiodic emerging health threats

Emerging health threats pose unique challenges to public health professionals compared to stable seasonal occurrences of infectious diseases. For epidemic or pandemic events, outbreaks quickly spread nationally or globally, respectively, complicating health professionals' understanding of mechanisms driving transmission [1-2]. As threats unfold, no historical data are available for reference to understand the dynamics of outbreak signatures. Mass hysteria and misinformation complicate the creation and abidance to intervention policies as well as the reliability of models to predict disease spread [2-5]. Furthermore, the geographic extent and speed of infection result in poor data quality, uncertainty of modeling approaches, and potentially misleading visual communications to describe the spatiotemporal patterns of illness [6-8].

For these reasons, epidemic and pandemic preparedness planning has received extensive attention and resources by the global community, only compounded since the emergence of SARS-CoV-2 [9-13]. For decades, the WHO and Western States have prioritized health surveillance of foreign threats both to minimize illness severity and ensure international stability and security as these outbreaks unfold [14-16]. Since the 1990s, Western States have considered human health a cornerstone of national security agendas for ensuring economic and political stability during health responses [14]. This securitization has benefitted many high-income countries that have established international networks of epidemiological surveillance to identify, respond to, and mitigate outbreaks in a timely, efficient manner [15].

Yet, security efforts serve only to mitigate some countries from severe threats and bias global surveillance with well-reported data from wealthier nations. As many low-income countries lack such surveillance capacity, the global community still faces limited ability to detect and routinely monitor outbreaks often originating in these developing nations [17-19]. In the absence of routinely reported data, these nations also struggle to best stockpile and distribute health resources – a challenge equally faced by aid assistance organizations attempting to import medical supplies [20-21]. As most highly infectious pathogens tend to have zoonotic carriers and transmission, lack of OneHealth initiatives and surveillance globally only further complicates public health responses and interventions [22].

Epidemic and pandemic events do not occur in isolation; health threats often emerge in parallel with humanitarian emergencies like natural disasters, internal displacement, overcrowding, war conflict, and food insecurity. For example, the modern era has experienced 6 well-defined cholera pandemics, the most recent beginning in 1961 and still ongoing [1,23]. Cholera reemergence is in part contributed to the long lifespan that the bacteria can survive within environmental ecosystems [24]. Epidemic and pandemic events often originate in locations with access to poor water, sanitation, and hygiene (WASH) resources where environmental reservoirs enter human food and water supplies [1,25-28]. As climate change threatens to increase the volume of disaster events, coastal nations face higher risks of severe flooding. As a result, coastal communities face increased risks of cholera infectivity as stagnant water, sewage overflow, population crowding, and internal displacement increase the likelihood of infection exposure and transmission [29-33].

Similarly, conflict events can disrupt medical supply lines and severely weaken health infrastructure, turning otherwise endemic enteric infections like cholera into large-scale epidemic events [34-36]. Conflict also jeopardizes food and water supply lines resulting in acute or chronic malnutrition conditions [37]. Poor nutrition worsens overall immune response, increasing conflict-affected persons susceptibility to infection [38-39]. With population displacement and migration accompanying these challenges, WASH resources are limited thereby increasing disease susceptibility, exposure, and transmission [40-41].

Together, both environmental (e.g., cyclone, hurricane, landslide, etc.) and humanitarian (e.g., war conflict, political riot, famine, etc.) disasters impede routine infectious disease surveillance. Limited infrastructure impedes data collection, preventing real-time responses needed for emerging threats as well as longitudinal tracking of an outbreaks' spread. This often manifests in unavailable data in low-income or emergency-prone locations that lack laboratory testing facilities. Even if data are available, they often are of coarser temporal, spatial, or demographic resolutions preventing timely, precise, and specific intervention strategies. As much data not collected by national or subnational public health agencies instead come from disparate humanitarian assistance organizations, this can also pose challenges for aligning and harmonizing data from multiple sources. This especially holds true when integrating data from non-health resources, such as on conflict events, climate conditions, or food prices/trade, where data may have a variety of surveillance

reporting structures and standards. The integration of data into a single source brings further challenges of completeness and reliability limitations to answer on questions related to disease outbreak dynamics and signatures.

Amidst data challenges, public health challenges perhaps more than ever need well-established analytical frameworks for evaluating data quality and strategizing its usage to examine complex spatiotemporal disease patterns. This framework expands on my prior research by considering techniques for aligning, harmonizing, and managing data collected from multiple sources, varying geographic extents, and differing temporal frequencies. This includes quantifying the quality of individual and collective data sources with respect to completeness and correctness. Furthermore, public health professionals must design comprehensive data communication tools such as interactive dashboards or dynamic, animated graphics that compress large quantities of information on spatiotemporal patterns clearly, concisely, and comprehensively. These tools will integrate data quality and analytics into a single forum, enabling modelers to collaborate with curators to define outbreak signatures and their changes over time.

Though aperiodic processes, epidemic and pandemic outbreak signatures share many of the same features defined for periodic seasonal patterns. For example, the peak timing of emerging outbreaks remains important to define in real-time or in near-term forecasts to schedule resource allocation and mobilization. Similarly, the amplitude or absolute intensity of infections at local peaks inform the volume of supplies needed. Comparing these features across geographic locations provide important characteristics of the geographic extent and traveling waves of outbreaks, paralleling my prior works on synchronicity [42]. By defining geographic hotspots and staggered waves of infection, health professionals can better identify and target health interventions in locations where outbreaks originate. Additionally, understanding of outbreak severity such as illness intensity, often evaluated using reproductive numbers, provides a greater understand of how rates of infection accelerate or decelerate over time, thereby describing the transmissibility of infections throughout a population [43]. As with periodic processes, all modeling techniques used to estimate epidemic and pandemic outbreak signatures should remain reproducible and generalizable for application across diverse emergency situations.

The establishment of versatile, standardized methodological approaches as part of a complex emergency analytical framework proves difficult as emerging threats lack

any historical context. For periodic seasonal infections, harmonic regressions use sinusoidal and cosinusoidal functions with well-defined properties for estimating seasonality features [42,44-51]. The generalizability of these methods depends on *a priori* understanding and assumption of the annual duration of seasonal cycles. For emerging threats, infection rates have sporadic periods of intense outbreaks followed by gradual or rapid declines in illness intensity. These aperiodic patterns face additional complexities in the presence of poor data quality and credibility, which introduce potential under- and over-reporting of health outcomes. Both volatile spikes in incidence and poor data quality manifest as noise in reported data, which greatly impact the precision of model estimates and forecasts. Thus, modelers must utilize smoothing techniques optimal for pattern recognition yet sufficiently precise to estimate outbreak signature features and their uncertainty.

In the works that follow, I demonstrate how methodologies in prior chapters can be adapted for evaluating outbreak signatures of aperiodic disease patterns of epidemic and pandemic events [52-53]. Using consistent terminology as defined for estimating seasonality features, I demonstrate an analytical workflow for defining, describing, and comparing outbreak signatures using regional and local publicly available health surveillance data. These works emphasize not only the importance of robust, standardized workflows for modeling infections in complex environments but also the extensive data quality challenges and limitations when performing time series modeling for outbreaks in these areas. This includes extensive description of data management steps and credibility checks to align and harmonize interdisciplinary data sources for conducting secondary time series analyses. These works also provide graphical templates for developing animated or dynamic maps ideal for visualizing complex spatiotemporal patterns between time series.

5.2. Dynamic mapping of cholera spread and conflict severity during the Yemeni Civil War, 2016-2019

Manuscript M5. Simpson, R. B., Babool, S., Tarnas, M. C., Kaminski, P. M., Hartwick, M. A., Naumova, E. N. “Dynamic mapping of cholera spread and conflict severity during the Yemeni Civil War, 2016-2019.” *Journal of Public Health Policy* (2022). https://doi.org/10.1057/s41271-022-00345-x.

5.3. Signatures of cholera outbreak during the Yemeni Civil War, 2016-2019

Manuscript M6. Simpson, R. B., Babool, S., Tarnas, M. C., Kaminski, P. M., Hartwick, M. A., and Naumova, E. N. "Signatures of cholera outbreak during the Yemeni Civil War, 2016-2019." *International Journal of Environmental Research and Public Health* 19, no. 1 (2022): 378. https://doi.org/10.3390/ijerph19010378.

5.4. Conclusion: Applications of methods beyond enteric infections

The above works define a generalizable analytical workflow for modeling outbreak signatures of emerging enteric outbreak threats in complex emergency settings. By selecting Yemen as a case study during a time of both civil war and near-famine crisis, I demonstrate how data quality metrics and time series analyses can be applied even when data are sparsely reported from diverse sources. Even here, I utilized data quality measures defined by the *ACTOR* principles previously applied to assessing the quality of international influenza records. I also utilize L-moments to evaluate distributional properties of cholera infections, like seasonal enteric illnesses, and estimate outbreak signatures like local peaks and peak rates, paralleling seasonality features of peak timing and amplitude. Detailed description of critical points permitted estimation of speeds of increase and decline, which proxy for measures of outbreak severity during acceleration and deceleration periods.

Thus, data management and time series analysis methodologies demonstrated in this chapter are adaptable for application in complex emergency settings. The proposed analytical workflow is robust to varying spatial extents, temporal resolutions, and overall, annual, and seasonal completeness of publicly reported surveillance data. Data modelers can apply analytical methods irrespective of the type of infection (e.g., enteric, respiratory, etc.) or its temporal patterns (e.g., aperiodic, periodic). These techniques are also data-driven, provide a diverse analecta of visualizations for communicating research findings, and encourage comparisons of time series by location, pathogen, and risk factors. Overall, this workflow provides the tools necessary for data modelers to conduct real-time monitoring of emerging outbreak threats to inform public health policy planning and intervention strategies during epidemic and pandemic events.

To illustrate this further, the following study demonstrates how the proposed analytical workflow has been applied for an ongoing outbreak event: the COVID-19

pandemic. Here, I demonstrate how data modelers can again utilize KZ adaptive filters to examine outbreak signatures of SARS-CoV-2 tests, cases, and deaths. Unlike prior studies, I conduct this work on high spatiotemporal resolution, publicly available surveillance data conducted at the local administrative level. More specifically, this study evaluates data from Massachusetts state and Middlesex County. Data visualizations, like those used to demonstrate outbreak signatures of cholera in Yemen, are repurposed for modeling SARS-CoV-2 data quality and outbreak signatures at refined scales.

As an expansion of my works in Yemen, this study's use of daily data allows me to investigate a new temporal pattern, day-of-the-week effects, and describe their importance in public health planning and programming [54]. More refined data reporting permits closer inspection of patterns and quantities of data reporting anomalies and credibility checks as well as detailed explanation of techniques for handling incomplete and incorrect records. These works also introduce time-dependent factors, such as health intervention policies, that introduce the complexity of estimating outbreak signatures amidst ongoing health interventions. We conclude these works by discussing the challenges of deciphering how health interventions influence patterns of illness over time.

5.5. Critical periods, critical time points and day-of-the-week effects in COVID-19 surveillance data: an example in Middlesex County, Massachusetts, USA

Manuscript M7. Simpson, R. B., Lauren, B. N., Schipper, K. H., McCann, J. C., Tarnas, M. C., and Naumova, E. N. "Critical periods, critical time points and day-of-the-week effects in COVID-19 surveillance data: an example in Middlesex County, Massachusetts, USA." *International Journal of Environmental Research and Public Health* 19, no. 3 (2022): 1321. https://doi.org/10.3390/ijerph19031321.

5.6. References

1. Piret, J., and Boivin, G. "Pandemics throughout history." *Frontiers in Microbiology* (2021): 3594.
2. Heesterbeek, H., Anderson, R. M., Andreasen, V., Bansal, S., De Angelis, D., Dye, C., Eames, K. T., Edmunds, W. J., Frost, S. D., Funk, S., Hollingsworth, T. D., House, T., Isham, V., Klepac, P., Lessler, J., Lloyd-Smith, J. O., Metcalf, C. J. E., Mollison, D., Pellis, L., Pulliam, J. R. C., Roberts, M. G., Viboud, C., and Isaac Newton Institute IDD Collaboration. "Modeling infectious disease dynamics in the complex landscape of global health." *Science* 347, no. 6227 (2015): aaa4339.

3. Pavelea, A. M., Neamțu, B., and Pavel, A. “Do social media reduce compliance with COVID-19 preventive measures?.” *Policy Studies* (2021): 1-16.
4. John Hopkins University (JHU). “Meeting COVID-19 misinformation and disinformation head-on: The U.S. needs a national strategy to combat health-related misinformation and disinformation.” *Bloomberg School of Public Health*. Accessed on 10 May 2022. https://publichealth.jhu.edu/meeting-covid-19-misinformation-and-disinformation-head-on.
5. Agley, J., and Xiao, Y. “Misinformation about COVID-19: evidence for differential latent profiles and a strong association with trust in science.” *BMC Public Health* 21, no. 1 (2021): 1-12.
6. Glennon, E. E., Bruijning, M., Lessler, J., Miller, I. F., Rice, B. L., Thompson, R. N., Wells. K., and Metcalf, C. J. E. “Challenges in modeling the emergence of novel pathogens.” *Epidemics* 37 (2021): 100516.
7. Naumova, E. N. “Public health response to COVID-19: the forecaster’s dilemma.” *Journal of Public Health Policy* 41, no. 4 (2021): 395-398.
8. Kraemer, M. U., Scarpino, S. V., Marivate, V., Gutierrez, B., Xu, B., Lee, G., Hawkins, J. B., Rivers, C., Pigott, D. M., Katz, R., and Brownstein, J. S. “Data curation during a pandemic and lessons learned from COVID-19.” *Nature Computational Science* 1, no. 1 (2021): 9-10.
9. King, D. A., Peckham, C., Waage, J. K., Brownlie, J., and Woolhouse, M. E. “Infectious diseases: preparing for the future.” *Science* 313, no. 5792 (2006): 1392-1393.
10. Harrington, W. N., Kackos, C. M., and Webby, R. J. “The evolution and future of influenza pandemic preparedness.” *Experimental & Molecular Medicine* 53, no. 5 (2021): 737-749.
11. Kelly-Cirino, C. D., Nkengasong, J., Kettler, H., Tongio, I., Gay-Andrieu, F., Escadafal, C., Piot, P., Peeling, R. W., Gadde, R., and Boehme, C. “Importance of diagnostics in epidemic and pandemic preparedness.” *BMJ Global Health* 4, no. Suppl 2 (2019): e001179.
12. Kentikelenis, A. E., and Seabrooke, L. “Governing and Measuring Health Security: The Global Push for Pandemic Preparedness Indicators.” *Global Policy* (2022).
13. Yellen, J., Ghebreyesus, T. A., Indrawati, S. M. “The next pandemic doesn’t have to hit so hard: Investing in global health security can provide critical insurance against disaster.” *Foreign Policy*. April 21, 2022. https://foreignpolicy.com/2022/04/21/pandemic-covid-19-future-global-health-security-architecture/.
14. Davies, S. E. “Securitizing infectious disease.” *International Affairs* 84, no. 2 (2008): 295-313.
15. Jin, J., and Karackattu, J. T. “Infectious diseases and securitization: WHO's dilemma.” *Biosecurity and Bioterrorism: Biodefense Strategy, Practice, and Science* 9, no. 2 (2011): 181-187.
16. Pereira, R. “Processes of securitization of infectious diseases and Western hegemonic power: a historical-political analysis.” *Global Health Governance* 2, no. 1 (2008): 1-15.
17. Naumova, E. N. “Public health inequalities, structural missingness, and digital revolution: time to question assumptions.” *Journal of Public Health Policy* (2021): 1-5.

18. Quinn, S. C., and Kumar, S. “Health inequalities and infectious disease epidemics: a challenge for global health security.” *Biosecurity and Bioterrorism: Biodefense Strategy, Practice, and Science* 12, no. 5 (2014): 263-273.
19. Mamelund, S. E., and Dimka, J. “Social inequalities in infectious diseases.” *Scandinavian Journal of Public Health* 49, no. 7 (2021): 675-680.
20. Piva, P., and Dodd, R. “Where did all the aid go? An in-depth analysis of increased health aid flows over the past 10 years.” *Bulletin of the World Health Organization* 87 (2009): 930-939.
21. Hitchcock, P., Chamberlain, A., Van Wagoner, M., Inglesby, T. V., and O'Toole, T. “Challenges to global surveillance and response to infectious disease outbreaks of international importance.” *Biosecurity and Bioterrorism: Biodefense Strategy, Practice, and Science* 5, no. 3 (2007): 206-227.
22. Christaki, E. “New technologies in predicting, preventing and controlling emerging infectious diseases.” *Virulence* 6, no. 6 (2015): 558-565.
23. Barua, D. “ History of cholera.” In *Cholera*, ed. Dhiman Barua and William B. Greenough (Boston: Springer, 1992), 1-36.
24. Colwell, R. R. “Global climate and infectious disease: the cholera paradigm.” *Science* 274, no. 5295 (1996): 2025-2031.
25. Baker, R. E., Mahmud, A. S., Miller, I. F., Rajeev, M., Rasambainarivo, F., Rice, B. L., Takahashi, S., Tatem, A. J., Wagner, C. E., Wang, L. F., Wesolowski, A., and Metcalf, C. J. E. “Infectious disease in an era of global change.” *Nature Reviews Microbiology* 20 (2022): 1-13.
26. Hsiao, H. I., Jan, M. S., and Chi, H. J. “Impacts of climatic variability on Vibrio parahaemolyticus outbreaks in Taiwan.” *International Journal of Environmental Research and Public Health* 13, no. 2 (2016): 188.
27. Leckebusch, G. C., and Abdussalam, A. F. “Climate and socioeconomic influences on interannual variability of cholera in Nigeria.” *Health & Place* 34 (2015): 107-117.
28. Dureab, F., Jahn, A., Krisam, J., Dureab, A., Zain, O., Al-Awlaqi, S., and Müller, O. “Risk factors associated with the recent cholera outbreak in Yemen: a case-control study.” *Epidemiology and Health* 41 (2019).
29. Lemaitre, J., Pasetto, D., Perez-Saez, J., Sciarra, C., Wamala, J. F., and Rinaldo, A. (2019). “Rainfall as a driver of epidemic cholera: comparative model assessments of the effect of intra-seasonal precipitation events.” *Acta Tropica* 190 (2019): 235-243.
30. Carrel, M., Emch, M., Streatfield, P. K., and Yunus, M. “Spatio-temporal clustering of cholera: The impact of flood control in Matlab, Bangladesh, 1983–2003.” *Health & Place* 15, no. 3 (2009): 771-782.
31. Moore, S. M., Azman, A. S., Zaitchik, B. F., Mintz, E. D., Brunkard, J., Legros, D., Hill, A., McKay, H., Luquero, F. J., Olson, D., and Lessler, J. “El Niño and the shifting geography of cholera in Africa.” *Proceedings of the National Academy of Sciences* 114, no. 17 (2017): 4436-4441.
32. Alam, M., Islam, A., Bhuiyan, N., Rahim, N., Hossain, A., Khan, G. Y., Ahmed, D., Watanabe, H., Izumiya, H., Faruque, A. G., Akanda, A., Islam, S., Sack, R. B., Huq., A., Colwell, R. R., and Cravioto, A. “Clonal transmission, dual peak, and off-season cholera in Bangladesh.” *Infection Ecology and Epidemiology* 1, no. 1 (2011): 7273.
33. Jutla, A., Whitcombe, E., Hasan, N., Haley, B., Akanda, A., Huq, A., Alam, M., Sack, R. B., and Colwell, R. “Environmental factors influencing epidemic

cholera." *The American Journal of Tropical Medicine and Hygiene* 89, no. 3 (2013): 597.

34. Al-Mekhlafi, H. M. "Yemen in a time of cholera: current situation and challenges." *The American Journal of Tropical Medicine and Hygiene* 98, no. 6 (2018): 1558.
35. Blackburn, C. C., Lenze, P. E., and Casey, R. P. "Conflict and cholera: Yemen's man-made public health crisis and the global implications of weaponizing health." *Health Security* 18, no. 2 (2020): 125-131.
36. Bompangue, D., Giraudoux, P., Piarroux, M., Mutombo, G., Shamavu, R., Sudre, B., Mutombo, A., Mondonge, V., and Piarroux, R. "Cholera epidemics, war and disasters around Goma and Lake Kivu: an eight-year survey." *PLoS Neglected Tropical Diseases* 3, no. 5 (2009): e436.
37. Raad, I. I., Chaftari, A. M., Dib, R. W., Graviss, E. A., and Hachem, R. "Emerging outbreaks associated with conflict and failing healthcare systems in the Middle East." *Infection Control & Hospital Epidemiology* 39, no. 10 (2018): 1230-1236.
38. Richterman, A., Azman, A. S., Constant, G., and Ivers, L. C. "The inverse relationship between national food security and annual cholera incidence: A 30-country analysis." *BMJ Global Health* 4, no. 5 (2019): e001755.
39. Diseases, T. L. I. "Cholera in Yemen: war, hunger, disease… and heroics." *The Lancet Infectious Diseases* 17, no. 8 (2017): 781.
40. Centers for Disease Control and Prevention (CDC). "Cholera epidemic after increased civil conflict--Monrovia, Liberia, June-September 2003." *Morbidity and Mortality Weekly Report* 52, no. 45 (2003): 1093-1095.
41. Golicha, Q., Shetty, S., Nasiblov, O., Hussein, A., Wainaina, E., Obonyo, M., Macharia, D., Musyoka, R. N., Andille, H., Ope, M., Joseph, R., Kabugi, W., Kiogora, J., Said, M., Boru, W., Galgalo, T., Lowther, S. A., Juma, B., Mugoh, R., Wamola, N., Onyango, C., Gura, Z., Widdowson, M. A., DeCock, K. M., and Burton, J. W. "Cholera Outbreak in Dadaab Refugee Camp, Kenya—November 2015–June 2016." *Morbidity and Mortality Weekly Report* 67, no. 34 (2018): 958.
42. Simpson, R. B., Zhou, B., and Naumova, E. N. "Seasonal synchronization of foodborne outbreaks in the United States, 1996–2017." *Scientific Reports* 10, no. 1 (2020): 1-16.
43. Mukandavire, Z., Liao, S., Wang, J., Gaff, H., Smith, D. L., and Morris, J. G. "Estimating the reproductive numbers for the 2008–2009 cholera outbreaks in Zimbabwe." *Proceedings of the National Academy of Sciences* 108, no. 21 (2011): 8767-8772.
44. Naumova, E. N., and MacNeill, I. B. "Seasonality assessment for biosurveillance systems." In *Advances in Statistical Methods for the Health Sciences*, ed. Jean-Louis Auget, N. Balakrishnan, Mounir Mesbah, and Geert Molenberghs (Boston: Birkhäuser, 2007), 437-450.
45. Wenger, J. B., and Naumova, E. N. "Seasonal synchronization of influenza in the United States older adult population." *PLoS One* 5, no. 4 (2010): e10187.
46. Naumova, E. N., Jagai, J. S., Matyas, B., DeMaria, A., MacNeill, I. B., and Griffiths, J. K. "Seasonality in six enterically transmitted diseases and ambient temperature." *Epidemiology and Infection* 135, no. 2 (2007): 281-292.

47. Falconi, T. A., Cruz, M. S., and Naumova, E. N. “The shift in seasonality of legionellosis in the USA.” *Epidemiology and Infection* 146, no. 14 (2018): 1824-1833.
48. Naumova, E. N. “Mystery of seasonality: getting the rhythm of nature.” *Journal of Public Health Policy* 27, no. 1 (2006): 2-12.
49. Sanchez, E., Simpson, R. B., Zhang, Y., Sallade, L. E., and Naumova, E. N. “Exploring risk factors of recall-associated foodborne disease outbreaks in the United States, 2009–2019.” *International Journal of Environmental Research and Public Health* 19, no. 9 (2022): 4947.
50. Naumova, E. N. “The value of not being lost in our digital world.” *Journal of Public Health Policy* 39, no. 1 (2018): 27-29.
51. Naumova, E. N. “On the way to recovery with the help of a keystone species.” *Journal of Public Health Policy* 42, no. 3 (2021): 355-358.
52. Simpson, R. B., Babool, S., Tarnas, M. C., Kaminski, P. M., Hartwick, M. A., and Naumova, E. N. “Signatures of cholera outbreak during the Yemeni Civil War, 2016-2019.” *International Journal of Environmental Research and Public Health* 19, no. 1 (2022): 378.
53. Simpson, R. B., Babool, S., Tarnas, M. C., Kaminski, P. M., Hartwick, M. A., Naumova, E. N. “Dynamic mapping of cholera spread and conflict severity during the Yemeni Civil War, 2016-2019.” *Journal of Public Health Policy* (2022).
54. Simpson, R. B., Lauren, B. N., Schipper, K. H., McCann, J. C., Tarnas, M. C., and Naumova, E. N. “Critical periods, critical time points and day-of-the-week effects in COVID-19 surveillance data: an example in Middlesex County, Massachusetts, USA.” *International Journal of Environmental Research and Public Health* 19, no. 3 (2022): 1321.

Chapter 6. Steps Towards Precision Public Health

The recent paradigm shift towards *Precision Public Health* aims to improve clinical decision-making through evidence-based, data-driven, individualized treatments. From genomics to nutrition, optimizing healthcare delivery and efficiency relies on improved curation, management, and analysis of health surveillance data. The promises of Big Data fuel aspirations for precise treatment recommendations; digital technologies permit faster collection of larger quantities of diverse data streams than ever before. The rapid data generation introduces complex analytical methodologies, such as machine learning and artificial intelligence, for modeling disease trends and patterns. These techniques have become new standards for excellence in both the public and private health sectors.

Yet, Big Data, machine learning, and artificial intelligence serve only to improve the management and analysis of increased volumes, velocities, and varieties of curated data. This defines *Precision Public Health* as a collection of tools for enhancing public health surveillance processing, not a strategy for transforming data into actionable information. In the haste of modernizing the digital capacity of public health surveillance, health professionals have overlooked reductions in data's value and usability over time. By neglecting the interrelationship between data curators and modelers, publicly available surveillance data have less and less utility in creating specific, actionable health policies and recommendations. Furthermore, many health agencies have failed to establish strategies for ensuring data's credibility, usability, and longevity for continued usage years and decades into the future.

I implore the global health community to consider a *Precision Public Health* paradigm shift: precision begins with a collective understanding of data's potential. This concept emphasizes the need for public health agencies to strategize the usability of data before its collection. This task falls equally on data curators, modelers, and policymakers. Curators are responsible for proactive data management in alignment with stakeholders' immediate needs but flexible for future adaptations. Curators ensure that data are specific, comprehensive, timely, and complete to reliably examine disease patterns and relationships. Modelers communicate the importance of data's structure and fidelity to curators prior to collection as well as ensure standardized reporting of both data limitations and their effects on model precision. Transparency between data curators and modelers ensures rapid information generation for advising

policymakers, who can utilize complex visualization techniques to clearly explain health policies, interventions, and programming. By establishing this feedback loop between those who collect data, those who analyze it, and those who inform policies with it, the global health community can improve its precision of delivering medical care and health treatments.

This dissertation demonstrates how standardized analytical workflows can integrate techniques for data curation and management with methodologies for descriptive, comparative, and predictive modeling. These workflows prioritize developing a deeper understanding of surveillance capacity gaps, credibility concerns, modeling intentions, and visualization communications. This holistic approach to managing and analyzing data ensures that surveillance longevity and usability remains the top priority of health professionals regardless of how much, how fast, or how diverse data are. More comprehensive descriptions of data use strategies ensure the reproducibility and generalizability of data generation, analysis, and reporting. This promotes the harmonization and interoperability of data streams and interagency collaborations across health disciplines.

At the core of any analytical workflow must be attention to data's usability. Particularly within the nutrition epidemiology discipline, few studies report basic principles of data's completeness, credibility, and trustworthiness when publishing analytical works. These omissions question whether data quality considerations are sufficiently accounted for during data analysis. We propose the *ACTOR* principles and metrics, which emphasize the importance of evaluating data's completeness both within metadata to accompany health records and in literature for published works. Data quality limitations greatly influence the precision of modeling outbreak signatures thereby describing both the value of data when curated and for analytical purposes. Our ability to detect disease patterns and outbreak signatures begins with knowing that data are suitable for modeling purposes.

As new health threats emerge, data longevity and sustainability are imperative for anticipating disease signatures. I recommend that public health professionals implement data quality reporting protocols and utilize standardized methodologies that are adaptive for these future applications. In designing surveillance systems, curators must collaborate with modelers to conceptualize data streams and structures not only to answer on pertinent crises of today but to prepare for modeling future crises tomorrow. Similarly, modelers must consider flexible and adaptive analytical

techniques to model recurrent and emerging health threats with periodic or aperiodic patterns. Such models require data longevity, as institutional memory ensures sufficient sample size, power, and ultimately understanding of historic illness patterns. In anticipating future threats, modelers must also consider broadening modeling approaches to consider techniques for quantifying and comparing outbreak severity, as this is pertinent for effective early outbreak alarms and warnings.

Overall, collective understanding begins with transparency throughout the entirety of the data lifecycle. The success of the *Precision Public Health* movement begins with clear, comprehensive, and complete communication over the ways that data are managed, analyzed, and visualized. Systematic metadata summaries offer detailed descriptions of surveillance reporting gaps and limitations pertinent for modelers to explain the reproducibility and generalizability of their results. Systematic terminology, statistical methodology, and data visualizations enable expedited transformation of data into actionable information. This includes justifications for distributional assumptions when modeling periodic and aperiodic processes, standardizing calculations of uncertainty for evaluating spatiotemporal relationships, and creating uniformity of terminology for describing critical time points and periods within outbreak signatures.

In essence, the global health community must preserve data's value throughout its entire lifecycle to ensure it remains a catalyst for developing information. Only then can the publicly available data at our disposal become effectively transformed into insights and recommendations to push public health into proactive prevention and mitigation of infectious disease illnesses and outbreaks.

Appendix A.

Supplementary Table S1. The 173 Member States reporting influenza virological data to the World Health Organization's (WHO's) FluNet as of 15 June 2021. We list Member States alphabetically by 6 WHO-defined regions (African Region (AFRO), Eastern Mediterranean Region (EMRO), European Region (EURO), Region of the Americas (PAHO), South-East Asia Region (SEARO), and Western Pacific Region (WPRO)) and 18 influenza transmission zones (North, Central and Caribbean, Temperate South, and Tropical South America; Northern, Southwestern, and Eastern Europe; Northern, Eastern, Middle, Western, and Southern Africa; Western, Central, Eastern, Southern, and Southeastern Asia; and Oceania Melanesia Polynesia).

Regions	Countries and Territories
AFRO	Algeria, Angola, Burkina Faso, Cameroon, Central African Republic, Chad, Congo, Côte d'Ivoire, Democratic Republic of the Congo, Ethiopia, Ghana, Guinea, Kenya, Madagascar, Mali, Mauritania, Mauritius, Mozambique, Niger, Nigeria, Rwanda, Senegal, Seychelles, Sierra Leone, South Africa, South Sudan, Tanzania, Togo, Uganda, Zambia
EMRO	Afghanistan, Bahrain, Egypt, Iran, Iraq, Jordan, Kuwait, Lebanon, Morocco, Oman, Pakistan, Qatar, Saudi Arabia, Sudan, Syrian Arab Republic, Tunisia, United Arab Emirates, West Bank and Gaza Strip, Yemen
EURO	Albania, Armenia, Austria, Azerbaijan, Belarus, Belgium, Bosnia and Herzegovina, Bulgaria, Croatia, Cyprus, Czechia, Denmark, Estonia, Finland, France, Georgia, Germany, Greece, Hungary, Iceland, Ireland, Israel, Italy, Kazakhstan, Kosovo, Kyrgyzstan, Latvia, Lithuania, Luxembourg, Malta, Moldova, Montenegro, Netherlands, North Macedonia, Norway, Poland, Portugal, Romania, Russian Federation, Serbia, Slovakia, Slovenia, Spain, Sweden, Switzerland, Tajikistan, Turkey, Turkmenistan, Ukraine, United Kingdom, Uzbekistan
PAHO	Anguilla, Antigua and Barbuda, Argentina, Aruba, Bahamas, Barbados, Belize, Bermuda, Bolivia, Brazil, British Virgin Islands, Canada, Cayman Islands, Chile, Colombia, Costa Rica, Cuba, Dominica, Dominican Republic, Ecuador, El Salvador, French Guiana, Grenada, Guadeloupe, Guatemala, Guyana, Haiti, Honduras, Jamaica, Martinique, Mexico, Montserrat, Nicaragua, Panama, Paraguay, Peru, Saint Barthelemy, Saint Kitts and Nevis, Saint Lucia, Saint Martin, Saint Vincent and the Grenadines, Suriname, Trinidad and Tobago, Turks and Caicos Islands, United States of America, Uruguay, Venezuela
SEARO	Bangladesh, Bhutan, India, Indonesia, Maldives, Myanmar, Nepal, North Korea, Sri Lanka, Thailand, Timor-Leste
WPRO	Australia, Cambodia, China, Fiji, Japan, Laos, Malaysia, Mongolia, New Caledonia, New Zealand, Papua New Guinea, Philippines, Singapore, South Korea, Viet Nam
Transmission Zones	
North America	Bermuda, Canada, United States of America
Central America and the Caribbean	Anguilla, Antigua and Barbuda, Aruba, Bahamas, Barbados, Belize, British Virgin Islands, Cayman Islands, Costa Rica, Cuba, Dominica, Dominican Republic, El Salvador, Grenada, Guadeloupe, Guatemala, Haiti, Honduras, Jamaica, Martinique, Montserrat, Mexico, Nicaragua, Panama, Saint Barthelemy, Saint Kitts and Nevis, Saint Lucia, Saint Martin, Saint Vincent and the Grenadines, Trinidad and Tobago, Turks and Caicos Islands
Temperate South America	Argentina, Chile, Paraguay, Uruguay
Tropical South America	Bolivia, Brazil, Colombia, Ecuador, French, Guiana, Guyana, Peru, Suriname, Venezuela
Northern Europe	Denmark, Estonia, Finland, Iceland, Ireland, Latvia, Lithuania, Norway, Sweden, United Kingdom
Southwestern Europe	Albania, Austria, Belgium, Bosnia and Herzegovina, Croatia, France, Germany, Greece, Italy, Luxembourg, Malta, Montenegro, Netherlands, North Macedonia, Portugal, Serbia, Slovenia, Spain, Switzerland
Eastern Europe	Belarus, Bulgaria, Czechia, Hungary, Kosovo, Moldova, Poland, Romania, Russian Federation, Slovakia, Ukraine
Northern Africa	Algeria, Egypt, Morocco, Sudan, Tunisia
Eastern Africa	Ethiopia, Kenya, Madagascar, Mauritius, Mozambique, Rwanda, Seychelles, Uganda, Tanzania, Zambia
Middle Africa	Angola, Cameroon, Central African Republic, Chad, Congo, Democratic Republic of the Congo, South Sudan
Western Africa	Burkina Faso, Côte d'Ivoire, Ghana, Guinea, Mali, Mauritania, Niger, Nigeria, Senegal, Sierra Leone, Togo
Southern Africa	South Africa
Western Asia	Armenia, Azerbaijan, Bahrain, Cyprus, Georgia, Iraq, Israel, Jordan, Kuwait, Lebanon, Oman, Qatar, Saudi Arabia, Syrian Arab Republic, Turkey, United Arab Emirates, West Bank and Gaza Strip, Yemen
Central Asia	Kazakhstan, Kyrgyzstan, Tajikistan, Turkmenistan, Uzbekistan
Eastern Asia	China, Japan, Mongolia, North Korea, South Korea
Southern Asia	Afghanistan, Bangladesh, Bhutan, India, Iran, Maldives, Nepal, Pakistan, Sri Lanka
Southeastern Asia	Cambodia, Indonesia, Laos, Malaysia, Myanmar, Philippines, Singapore, Thailand, Timor-Leste, Viet Nam
Oceania Melanesia Polynesia	Australia, Fiji, New Caledonia, New Zealand, Papua New Guinea

Supplementary Table S2. Summary of the average (with 95%CI; top values) and median (with interquartile range; bottom values) *case variety* (CVS), *outcome variety* (OVS), *subtype variety* (SVS), and *total variety* (TVS) scores for 6 WHO-defined regions and 17 influenza transmission zones. We estimated scores using numerous WHO and national influenza reports. We calculated scores by counting the number of case definitions, test outcomes, or subtypes where a Member State reported at least 1 week with complete records. We extracted data from FluNet on 15 June 2021, at which time 173 Member States reported data. We report regions and zones in descending order by average TVS and omit the Southern African zone, as it consisted of only 1 country.

Region	TVS	CVS	OVS	SVS
AFRO	16.77 [16.30, 17.23] 17.00 [16.00, 18.00]	3.20 [2.90, 3.50] 3.00 [3.00, 4.00]	5.67 [5.50, 5.84] 6.00 [5.00, 6.00]	7.90 [7.79, 8.00] 8.00 [8.00, 8.00]
SEARO	16.64 [15.83, 17.44] 17.00 [16.00, 17.00]	3.27 [3.00, 3.55] 3.00 [3.00, 4.00]	5.91 [5.73, 6.00] 6.00 [6.00, 6.00]	7.45 [6.74, 8.00] 8.00 [7.00, 8.00]
WPRO	16.33 [15.71, 16.96] 16.00 [16.00, 17.00]	2.60 [2.14, 3.06] 3.00 [2.00, 3.00]	5.73 [5.43, 6.00] 6.00 [6.00, 6.00]	8.00 [8.00, 8.00] 8.00 [8.00, 8.00]
EMRO	15.58 [14.59, 16.57] 16.00 [14.00, 17.00]	2.58 [2.10, 3.06] 3.00 [2.00, 3.00]	5.89 [5.75, 6.00] 6.00 [6.00, 6.00]	7.11 [6.39, 7.82] 8.00 [6.00, 8.00]
EURO	15.00 [14.64, 15.36] 15.00 [14.00, 16.00]	3.08 [2.85, 3.31] 3.00 [2.00, 4.00]	4.51 [4.33, 4.69] 4.00 [4.00, 5.00]	7.41 [7.28, 7.55] 7.00 [7.00, 8.00]
PAHO	13.62 [12.00, 15.23] 15.00 [9.00, 18.00]	2.98 [2.43, 3.53] 3.00 [1.00, 5.00]	4.87 [4.42, 5.33] 5.00 [5.00, 6.00]	5.77 [4.96, 6.57] 7.00 [3.00, 8.00]
Zone				
Temperate South America	17.25 [15.58, 18.92] 17.50 [16.00, 18.50]	3.50 [2.23, 4.77] 3.50 [2.50, 4.50]	6.00 [6.00, 6.00] 6.00 [6.00, 6.00]	7.75 [7.26, 8.00] 8.00 [7.50, 8.00]
Eastern Africa	17.10 [16.48, 17.72] 17.00 [17.00, 18.00]	3.60 [3.28, 3.92] 4.00 [3.00, 4.00]	5.60 [5.28, 5.92] 6.00 [5.00, 6.00]	7.90 [7.70, 8.00] 8.00 [8.00, 8.00]
Western Africa	17.09 [16.77, 17.41] 17.00 [17.00, 17.00]	3.18 [2.94, 3.42] 3.00 [3.00, 3.00]	5.91 [5.73, 6.00] 6.00 [6.00, 6.00]	8.00 [8.00, 8.00] 8.00 [8.00, 8.00]
Southern Asia	17.00 [16.54, 17.46] 17.00 [17.00, 17.00]	3.22 [2.79, 3.66] 3.00 [3.00, 4.00]	5.89 [5.67, 6.00] 6.00 [6.00, 6.00]	7.89 [7.67, 8.00] 8.00 [8.00, 8.00]
Southeast Asia	17.00 [16.59, 17.41] 17.00 [17.00, 17.00]	3.20 [2.94, 3.46] 3.00 [3.00, 3.00]	5.90 [5.70, 6.00] 6.00 [6.00, 6.00]	7.90 [7.70, 8.00] 8.00 [8.00, 8.00]
Northern Africa	16.80 [15.23, 18.37] 17.00 [17.00, 17.00]	3.00 [1.76, 4.24] 3.00 [3.00, 3.00]	5.80 [5.41, 6.00] 6.00 [6.00, 6.00]	8.00 [8.00, 8.00] 8.00 [8.00, 8.00]
Oceania Melanesia Polynesia	16.40 [15.62, 17.18] 16.00 [16.00, 16.00]	2.40 [1.62, 3.18] 2.00 [2.00, 2.00]	6.00 [6.00, 6.00] 6.00 [6.00, 6.00]	8.00 [8.00, 8.00] 8.00 [8.00, 8.00]
Middle Africa	15.43 [14.16, 16.70] 15.00 [14.00, 17.00]	2.43 [1.59, 3.27] 3.00 [1.00, 3.00]	5.29 [4.92, 5.65] 5.00 [5.00, 6.00]	7.71 [7.35, 8.00] 8.00 [7.00, 8.00]
Tropical South America	15.33 [11.92, 18.74] 17.00 [15.00, 18.00]	3.33 [2.07, 4.60] 4.00 [1.00, 5.00]	5.11 [4.06, 6.00] 6.00 [5.00, 6.00]	6.89 [5.18, 8.00] 8.00 [7.00, 8.00]
Eastern Europe	15.18 [14.31, 16.05] 15.00 [15.00, 16.00]	3.36 [2.82, 3.91] 4.00 [2.00, 4.00]	4.45 [4.05, 4.86] 4.00 [4.00, 5.00]	7.36 [7.07, 7.66] 7.00 [7.00, 8.00]
Northern Europe	15.10 [14.25, 15.95] 15.50 [14.00, 16.00]	2.70 [2.28, 3.12] 3.00 [2.00, 3.00]	4.70 [4.40, 5.00] 5.00 [4.00, 5.00]	7.70 [7.40, 8.00] 8.00 [7.00, 8.00]
North America	15.00 [8.12, 20.00] 18.00 [8.00, 19.00]	3.67 [0.82, 6.00] 4.00 [1.00, 6.00]	5.00 [3.87, 6.00] 5.00 [4.00, 6.00]	6.33 [3.07, 8.00] 8.00 [3.00, 8.00]
Central Asia	15.00 [15.00, 15.00] 15.00 [15.00, 15.00]	4.00 [4.00, 4.00] 4.00 [4.00, 4.00]	4.00 [4.00, 4.00] 4.00 [4.00, 4.00]	7.00 [7.00, 7.00] 7.00 [7.00, 7.00]
Southwest Europe	14.95 [14.27, 15.63] 15.00 [13.00, 16.00]	2.84 [2.47, 3.22] 3.00 [2.00, 4.00]	4.63 [4.29, 4.97] 4.00 [4.00, 5.00]	7.47 [7.24, 7.70] 7.00 [7.00, 8.00]
Eastern Asia	14.80 [13.23, 16.37] 15.00 [13.00, 16.00]	2.20 [1.24, 3.16] 3.00 [1.00, 3.00]	5.40 [4.62, 6.00] 6.00 [5.00, 6.00]	7.20 [5.63, 8.00] 8.00 [8.00, 8.00]
Western Asia	14.78 [13.93, 15.62] 15.00 [14.00, 16.00]	2.61 [2.19, 3.03] 3.00 [2.00, 3.00]	5.39 [5.00, 5.78] 6.00 [5.00, 6.00]	6.78 [6.08, 7.48] 7.00 [6.00, 8.00]
Central America and Caribbean	12.52 [10.44, 14.59] 14.00 [9.00, 17.00]	2.74 [2.05, 3.43] 3.00 [1.00, 4.00]	4.65 [4.05, 5.24] 5.00 [5.00, 6.00]	5.13 [4.11, 6.14] 6.00 [3.00, 8.00]
Worldwide	**15.21 [14.71, 15.72]** **16.00 [15.00, 17.00]**	**2.99 [2.80, 3.17]** **3.00 [2.00, 4.00]**	**5.16 [4.99, 5.32]** **5.00 [5.00, 6.00]**	**7.07 [6.80, 7.34]** **8.00 [7.00, 8.00]**

Supplementary Table S3. Average and median *case variety scores* (CVS) of Member States collecting health records for 6 case definitions (influenza-like illness (ILI), acute respiratory illness (ARI), severe acute respiratory illness (SARI), pneumonia (PNE), influenza confirmed cases and hospitalizations (CASE), and influenza-related mortality (MOR)) in 6 WHO-defined regions and 17 influenza transmission zones. We extracted data from FluNet on 15 June 2021, at which time 173 Member States reported data. We estimated these scores using numerous WHO and national influenza reports. We calculated CVS by counting the number of case definitions reported per Member State. We estimate average scores with 95% confidence intervals (top values) and median scores with lower and upper quartiles (bottom values). We report regions and zones in descending order by average CVS, and omit the Southern African zone, as it only consisted of 1 country (South Africa).

Region	CVS	ILI	ARI	SARI	PNE	CASE	MOR
SEARO	3.27 [3.00, 3.55] 3.00 [3.00, 4.00]	1.00 [1.00, 1.00] 1.00 [1.00, 1.00]	0.18 [0.00, 0.42] 0.00 [0.00, 0.00]	1.00 [1.00, 1.00] 1.00 [1.00, 1.00]	0.09 [0.00, 0.27] 0.00 [0.00, 0.00]	1.00 [1.00, 1.00] 1.00 [1.00, 1.00]	0.00 [0.00, 0.00] 0.00 [0.00, 0.00]
AFRO	3.20 [2.90, 3.50] 3.00 [3.00, 4.00]	0.93 [0.84, 1.00] 1.00 [1.00, 1.00]	0.03 [0.00, 0.10] 0.00 [0.00, 0.00]	0.90 [0.79, 1.00] 1.00 [1.00, 1.00]	0.03 [0.00, 0.10] 0.00 [0.00, 0.00]	1.00 [1.00, 1.00] 1.00 [1.00, 1.00]	0.30 [0.13, 0.47] 0.00 [0.00, 1.00]
EURO	3.08 [2.85, 3.31] 3.00 [2.00, 4.00]	0.96 [0.91, 1.00] 1.00 [1.00, 1.00]	0.65 [0.51, 0.78] 1.00 [0.00, 1.00]	0.49 [0.35, 0.63] 0.00 [0.00, 1.00]	0.02 [0.00, 0.06] 0.00 [0.00, 0.00]	0.96 [0.91, 1.00] 1.00 [1.00, 1.00]	0.00 [0.00, 0.00] 0.00 [0.00, 0.00]
PAHO	2.98 [2.43, 3.53] 3.00 [1.00, 5.00]	0.51 [0.37, 0.66] 1.00 [0.00, 1.00]	0.40 [0.26, 0.55] 0.00 [0.00, 1.00]	0.57 [0.43, 0.72] 1.00 [0.00, 1.00]	0.28 [0.15, 0.41] 0.00 [0.00, 1.00]	0.94 [0.87, 1.00] 1.00 [1.00, 1.00]	0.28 [0.15, 0.41] 0.00 [0.00, 1.00]
WPRO	2.60 [2.14, 3.06] 3.00 [2.00, 3.00]	0.87 [0.69, 1.00] 1.00 [1.00, 1.00]	0.07 [0.00, 0.20] 0.00 [0.00, 0.00]	0.47 [0.21, 0.73] 0.00 [0.00, 1.00]	0.13 [0.00, 0.31] 0.00 [0.00, 0.00]	1.00 [1.00, 1.00] 1.00 [1.00, 1.00]	0.07 [0.00, 0.20] 0.00 [0.00, 0.00]
EMRO	2.58 [2.10, 3.06] 3.00 [2.00, 3.00]	0.63 [0.41, 0.85] 1.00 [0.00, 1.00]	0.11 [0.00, 0.25] 0.00 [0.00, 0.00]	0.68 [0.47, 0.90] 1.00 [0.00, 1.00]	0.05 [0.00, 0.16] 0.00 [0.00, 0.00]	1.00 [1.00, 1.00] 1.00 [1.00, 1.00]	0.11 [0.00, 0.25] 0.00 [0.00, 0.00]
Zone							
Central Asia	4.00 [4.00, 4.00] 4.00 [4.00, 4.00]	1.00 [1.00, 1.00] 1.00 [1.00, 1.00]	1.00 [1.00, 1.00] 1.00 [1.00, 1.00]	1.00 [1.00, 1.00] 1.00 [1.00, 1.00]	0.00 [0.00, 0.00] 0.00 [0.00, 0.00]	1.00 [1.00, 1.00] 1.00 [1.00, 1.00]	0.00 [0.00, 0.00] 0.00 [0.00, 0.00]
North America	3.67 [0.82, 6.00] 4.00 [1.00, 6.00]	0.67 [0.01, 1.00] 1.00 [0.00, 1.00]	0.67 [0.01, 1.00] 1.00 [0.00, 1.00]	0.33 [0.00, 0.99] 0.00 [0.00, 1.00]	0.33 [0.00, 0.99] 0.00 [0.00, 1.00]	1.00 [1.00, 1.00] 1.00 [1.00, 1.00]	0.67 [0.01, 1.00] 1.00 [0.00, 1.00]
Eastern Africa	3.60 [3.28, 3.92] 4.00 [3.00, 4.00]	1.00 [1.00, 1.00] 1.00 [1.00, 1.00]	0.10 [0.00, 0.30] 0.00 [0.00, 0.00]	1.00 [1.00, 1.00] 1.00 [1.00, 1.00]	0.00 [0.00, 0.00] 0.00 [0.00, 0.00]	1.00 [1.00, 1.00] 1.00 [1.00, 1.00]	0.50 [0.17, 0.83] 0.50 [0.00, 1.00]
Temperate South America	3.50 [2.23, 4.77] 3.50 [2.50, 4.50]	0.75 [0.26, 1.00] 1.00 [0.50, 1.00]	0.25 [0.00, 0.74] 0.00 [0.00, 0.50]	1.00 [1.00, 1.00] 1.00 [1.00, 1.00]	0.25 [0.00, 0.74] 0.00 [0.00, 0.50]	1.00 [1.00, 1.00] 1.00 [1.00, 1.00]	0.25 [0.00, 0.74] 0.00 [0.00, 0.50]
Eastern Europe	3.36 [2.82, 3.91] 4.00 [2.00, 4.00]	0.91 [0.73, 1.00] 1.00 [1.00, 1.00]	0.82 [0.58, 1.00] 1.00 [1.00, 1.00]	0.73 [0.45, 1.00] 1.00 [0.00, 1.00]	0.00 [0.00, 0.00] 0.00 [0.00, 0.00]	0.91 [0.73, 1.00] 1.00 [1.00, 1.00]	0.00 [0.00, 0.00] 0.00 [0.00, 0.00]
Tropical South America	3.33 [2.07, 4.60] 4.00 [1.00, 5.00]	0.56 [0.21, 0.90] 1.00 [0.00, 1.00]	0.22 [0.00, 0.51] 0.00 [0.00, 0.00]	0.67 [0.34, 0.99] 1.00 [0.00, 1.00]	0.56 [0.21, 0.90] 1.00 [0.00, 1.00]	1.00 [1.00, 1.00] 1.00 [1.00, 1.00]	0.33 [0.01, 0.66] 0.00 [0.00, 1.00]
Southern Asia	3.22 [2.79, 3.66] 3.00 [3.00, 4.00]	1.00 [1.00, 1.00] 1.00 [1.00, 1.00]	0.11 [0.00, 0.33] 0.00 [0.00, 0.00]	0.89 [0.67, 1.00] 1.00 [1.00, 1.00]	0.11 [0.00, 0.33] 0.00 [0.00, 0.00]	1.00 [1.00, 1.00] 1.00 [1.00, 1.00]	0.11 [0.00, 0.33] 0.00 [0.00, 0.00]
Southeast Asia	3.20 [2.94, 3.46] 3.00 [3.00, 3.00]	1.00 [1.00, 1.00] 1.00 [1.00, 1.00]	0.20 [0.00, 0.46] 0.00 [0.00, 0.00]	0.90 [0.70, 1.00] 1.00 [1.00, 1.00]	0.10 [0.00, 0.30] 0.00 [0.00, 0.00]	1.00 [1.00, 1.00] 1.00 [1.00, 1.00]	0.00 [0.00, 0.00] 0.00 [0.00, 0.00]
Western Africa	3.18 [2.94, 3.42] 3.00 [3.00, 3.00]	1.00 [1.00, 1.00] 1.00 [1.00, 1.00]	0.00 [0.00, 0.00] 0.00 [0.00, 0.00]	1.00 [1.00, 1.00] 1.00 [1.00, 1.00]	0.00 [0.00, 0.00] 0.00 [0.00, 0.00]	1.00 [1.00, 1.00] 1.00 [1.00, 1.00]	0.18 [0.00, 0.42] 0.00 [0.00, 0.00]
Northern Africa	3.00 [1.76, 4.24] 3.00 [3.00, 3.00]	0.80 [0.41, 1.00] 1.00 [1.00, 1.00]	0.20 [0.00, 0.59] 0.00 [0.00, 0.00]	0.80 [0.41, 1.00] 1.00 [1.00, 1.00]	0.20 [0.00, 0.59] 0.00 [0.00, 0.00]	1.00 [1.00, 1.00] 1.00 [1.00, 1.00]	0.00 [0.00, 0.00] 0.00 [0.00, 0.00]
Southwest Europe	2.84 [2.47, 3.22] 3.00 [2.00, 4.00]	0.95 [0.84, 1.00] 1.00 [1.00, 1.00]	0.53 [0.30, 0.76] 1.00 [0.00, 1.00]	0.37 [0.15, 0.59] 0.00 [0.00, 1.00]	0.00 [0.00, 0.00] 0.00 [0.00, 0.00]	1.00 [1.00, 1.00] 1.00 [1.00, 1.00]	0.00 [0.00, 0.00] 0.00 [0.00, 0.00]
Central America and Caribbean	2.74 [2.05, 3.43] 3.00 [1.00, 4.00]	0.45 [0.27, 0.63] 0.00 [0.00, 1.00]	0.45 [0.27, 0.63] 0.00 [0.00, 1.00]	0.52 [0.34, 0.69] 1.00 [0.00, 1.00]	0.19 [0.05, 0.33] 0.00 [0.00, 0.00]	0.90 [0.80, 1.00] 1.00 [1.00, 1.00]	0.23 [0.08, 0.38] 0.00 [0.00, 0.00]
Northern Europe	2.70 [2.28, 3.12] 3.00 [2.00, 3.00]	1.00 [1.00, 1.00] 1.00 [1.00, 1.00]	0.60 [0.28, 0.92] 1.00 [0.00, 1.00]	0.10 [0.00, 0.30] 0.00 [0.00, 0.00]	0.10 [0.00, 0.30] 0.00 [0.00, 0.00]	0.90 [0.70, 1.00] 1.00 [1.00, 1.00]	0.00 [0.00, 0.00] 0.00 [0.00, 0.00]
Western Asia	2.61 [2.19, 3.03] 3.00 [2.00, 3.00]	0.67 [0.44, 0.89] 1.00 [0.00, 1.00]	0.22 [0.02, 0.42] 0.00 [0.00, 0.00]	0.67 [0.44, 0.89] 1.00 [0.00, 1.00]	0.00 [0.00, 0.00] 0.00 [0.00, 0.00]	1.00 [1.00, 1.00] 1.00 [1.00, 1.00]	0.06 [0.00, 0.16] 0.00 [0.00, 0.00]
Middle Africa	2.43 [1.59, 3.27] 3.00 [1.00, 3.00]	0.71 [0.35, 1.00] 1.00 [0.00, 1.00]	0.00 [0.00, 0.00] 0.00 [0.00, 0.00]	0.57 [0.18, 0.97] 1.00 [0.00, 1.00]	0.00 [0.00, 0.00] 0.00 [0.00, 0.00]	1.00 [1.00, 1.00] 1.00 [1.00, 1.00]	0.14 [0.00, 0.42] 0.00 [0.00, 0.00]
Oceania Melanesia Polynesia	2.40 [1.62, 3.18] 2.00 [2.00, 2.00]	1.00 [1.00, 1.00] 1.00 [1.00, 1.00]	0.00 [0.00, 0.00] 0.00 [0.00, 0.00]	0.00 [0.00, 0.00] 0.00 [0.00, 0.00]	0.20 [0.00, 0.59] 0.00 [0.00, 0.00]	1.00 [1.00, 1.00] 1.00 [1.00, 1.00]	0.20 [0.00, 0.59] 0.00 [0.00, 0.00]
Eastern Asia	2.20 [1.24, 3.16] 3.00 [1.00, 3.00]	0.60 [0.12, 1.00] 1.00 [0.00, 1.00]	0.00 [0.00, 0.00] 0.00 [0.00, 0.00]	0.60 [0.12, 1.00] 1.00 [0.00, 1.00]	0.00 [0.00, 0.00] 0.00 [0.00, 0.00]	1.00 [1.00, 1.00] 1.00 [1.00, 1.00]	0.00 [0.00, 0.00] 0.00 [0.00, 0.00]
Worldwide	**2.99 [2.80, 3.17]** **3.00 [2.00, 4.00]**	**0.79 [0.73, 0.85]** **1.00 [1.00, 1.00]**	**0.34 [0.26, 0.41]** **0.00 [0.00, 1.00]**	**0.64 [0.56, 0.71]** **1.00 [0.00, 1.00]**	**0.11 [0.06, 0.16]** **0.00 [0.00, 0.00]**	**0.97 [0.95, 1.00]** **1.00 [1.00, 1.00]**	**0.14 [0.09, 0.20]** **0.00 [0.00, 0.00]**

Supplementary Table S4. The *case variety score* (CVS) for each Member State reporting influenza virological data to the WHO's FluNet as of 15 June 2021. Scores range from 0-6 depending on the number of case definitions collected by a Member State, which include influenza-like-illness (ILI), acute respiratory illness (ARI), severe acute respiratory illness (SARI), pneumonia (PNE), influenza confirmed cases and hospitalizations (CASE), and influenza-related mortality (MOR). We list Member States in descending order by CVS, region, and zone. We estimated scores using numerous WHO and national influenza reports.

Region	Zone	Member State	ILI	ARI	SARI	PNE	CASE	MOR	CVS
PAHO	Central America and Caribbean	Costa Rica	✓	✓	✓	✓	✓	✓	6
PAHO	Central America and Caribbean	Cuba	✓	✓	✓	✓	✓	✓	6
PAHO	Central America and Caribbean	Honduras	✓	✓	✓	✓	✓	✓	6
PAHO	Central America and Caribbean	Nicaragua	✓	✓	✓	✓	✓	✓	6
PAHO	Central America and Caribbean	Panama	✓	✓	✓	✓	✓	✓	6
PAHO	North America	Canada	✓	✓	✓	✓	✓	✓	6
PAHO	Tropical South America	Colombia	✓	✓	✓	✓	✓	✓	6
AFRO	Southern Africa	South Africa	✓	✗	✓	✓	✓	✓	5
EMRO	Northern Africa	Egypt	✓	✓	✓	✓	✓	✗	5
PAHO	Central America and Caribbean	Guatemala	✓	✓	✓	✓	✓	✗	5
PAHO	Central America and Caribbean	Saint Lucia	✓	✓	✓	✗	✓	✓	5
PAHO	Temperate South America	Paraguay	✓	✓	✓	✓	✓	✗	5
PAHO	Tropical South America	Peru	✓	✗	✓	✓	✓	✓	5
PAHO	Tropical South America	Suriname	✓	✓	✓	✓	✓	✗	5
AFRO	Eastern Africa	Kenya	✓	✗	✓	✗	✓	✓	4
AFRO	Eastern Africa	Madagascar	✓	✗	✓	✗	✓	✓	4
AFRO	Eastern Africa	Mozambique	✓	✓	✓	✗	✓	✗	4
AFRO	Eastern Africa	Rwanda	✓	✗	✓	✗	✓	✓	4
AFRO	Eastern Africa	Tanzania	✓	✗	✓	✗	✓	✓	4
AFRO	Eastern Africa	Uganda	✓	✗	✓	✗	✓	✓	4
AFRO	Middle Africa	Democratic Republic of the Congo	✓	✗	✓	✗	✓	✓	4
AFRO	Western Africa	Burkina Faso	✓	✗	✓	✗	✓	✓	4
AFRO	Western Africa	Côte d'Ivoire	✓	✗	✓	✗	✓	✓	4
EMRO	Southern Asia	Afghanistan	✓	✗	✓	✗	✓	✓	4
EMRO	Western Asia	Jordan	✓	✗	✓	✗	✓	✓	4
EURO	Central Asia	Kazakhstan	✓	✓	✓	✗	✓	✗	4
EURO	Central Asia	Kyrgyzstan	✓	✓	✓	✗	✓	✗	4
EURO	Central Asia	Tajikistan	✓	✓	✓	✗	✓	✗	4
EURO	Central Asia	Turkmenistan	✓	✓	✓	✗	✓	✗	4
EURO	Central Asia	Uzbekistan	✓	✓	✓	✗	✓	✗	4
EURO	Eastern Europe	Belarus	✓	✓	✓	✗	✓	✗	4
EURO	Eastern Europe	Czechia	✓	✓	✓	✗	✓	✗	4
EURO	Eastern Europe	Kosovo	✓	✓	✓	✗	✓	✗	4
EURO	Eastern Europe	Moldova	✓	✓	✓	✗	✓	✗	4
EURO	Eastern Europe	Romania	✓	✓	✓	✗	✓	✗	4
EURO	Eastern Europe	Russian Federation	✓	✓	✓	✗	✓	✗	4
EURO	Eastern Europe	Slovakia	✓	✓	✓	✗	✓	✗	4
EURO	Northern Europe	Latvia	✓	✓	✓	✓	✗	✗	4
EURO	South West Europe	Albania	✓	✓	✓	✗	✓	✗	4
EURO	South West Europe	Belgium	✓	✓	✓	✗	✓	✗	4
EURO	South West Europe	Bosnia and Herzegovina	✓	✓	✓	✗	✓	✗	4
EURO	South West Europe	Netherlands	✓	✓	✓	✗	✓	✗	4
EURO	South West Europe	North Macedonia	✓	✓	✓	✗	✓	✗	4
EURO	Western Asia	Armenia	✓	✓	✓	✗	✓	✗	4
EURO	Western Asia	Azerbaijan	✓	✓	✓	✗	✓	✗	4
PAHO	Central America and Caribbean	Dominica	✗	✓	✓	✗	✓	✓	4
PAHO	North America	United States of America	✓	✓	✗	✗	✓	✓	4
PAHO	Temperate South America	Argentina	✓	✗	✓	✗	✓	✓	4
PAHO	Tropical South America	Bolivia	✓	✗	✓	✓	✓	✗	4
PAHO	Tropical South America	Brazil	✓	✗	✓	✗	✓	✓	4
SEARO	South-East Asia	Myanmar	✓	✓	✓	✗	✓	✗	4

SEARO	Southern Asia	Bangladesh	✓	✗	✓	✓	✓	✗	4
SEARO	Southern Asia	Maldives	✓	✓	✓	✗	✓	✗	4
WPRO	Oceania Melanesia Polynesia	Australia	✓	✗	✗	✓	✓	✓	4
WPRO	South-East Asia	Viet Nam	✓	✗	✓	✓	✓	✗	4
AFRO	Eastern Africa	Ethiopia	✓	✗	✓	✗	✓	✗	3
AFRO	Eastern Africa	Mauritius	✓	✗	✓	✗	✓	✗	3
AFRO	Eastern Africa	Seychelles	✓	✗	✓	✗	✓	✗	3
AFRO	Eastern Africa	Zambia	✓	✗	✓	✗	✓	✗	3
AFRO	Middle Africa	Angola	✓	✗	✓	✗	✓	✗	3
AFRO	Middle Africa	Cameroon	✓	✗	✓	✗	✓	✗	3
AFRO	Middle Africa	Chad	✓	✗	✓	✗	✓	✗	3
AFRO	Northern Africa	Algeria	✓	✗	✓	✗	✓	✗	3
AFRO	Western Africa	Ghana	✓	✗	✓	✗	✓	✗	3
AFRO	Western Africa	Guinea	✓	✗	✓	✗	✓	✗	3
AFRO	Western Africa	Mali	✓	✗	✓	✗	✓	✗	3
AFRO	Western Africa	Mauritania	✓	✗	✓	✗	✓	✗	3
AFRO	Western Africa	Niger	✓	✗	✓	✗	✓	✗	3
AFRO	Western Africa	Nigeria	✓	✗	✓	✗	✓	✗	3
AFRO	Western Africa	Senegal	✓	✗	✓	✗	✓	✗	3
AFRO	Western Africa	Sierra Leone	✓	✗	✓	✗	✓	✗	3
AFRO	Western Africa	Togo	✓	✗	✓	✗	✓	✗	3
EMRO	Northern Africa	Morocco	✓	✗	✓	✗	✓	✗	3
EMRO	Northern Africa	Tunisia	✓	✗	✓	✗	✓	✗	3
EMRO	Southern Asia	Pakistan	✓	✗	✓	✗	✓	✗	3
EMRO	Western Asia	Kuwait	✓	✗	✓	✗	✓	✗	3
EMRO	Western Asia	Saudi Arabia	✓	✗	✓	✗	✓	✗	3
EMRO	Western Asia	Syrian Arab Republic	✓	✓	✗	✗	✓	✗	3
EMRO	Western Asia	United Arab Emirates	✓	✗	✓	✗	✓	✗	3
EURO	Eastern Europe	Ukraine	✓	✓	✓	✗	✗	✗	3
EURO	Northern Europe	Estonia	✓	✓	✗	✗	✓	✗	3
EURO	Northern Europe	Finland	✓	✓	✗	✗	✓	✗	3
EURO	Northern Europe	Iceland	✓	✓	✗	✗	✓	✗	3
EURO	Northern Europe	Lithuania	✓	✓	✗	✗	✓	✗	3
EURO	Northern Europe	Norway	✓	✓	✗	✗	✓	✗	3
EURO	South West Europe	Greece	✓	✗	✓	✗	✓	✗	3
EURO	South West Europe	Italy	✓	✓	✗	✗	✓	✗	3
EURO	South West Europe	Luxembourg	✓	✓	✗	✗	✓	✗	3
EURO	South West Europe	Montenegro	✓	✗	✓	✗	✓	✗	3
EURO	South West Europe	Serbia	✓	✓	✗	✗	✓	✗	3
EURO	South West Europe	Slovenia	✓	✓	✗	✗	✓	✗	3
EURO	Western Asia	Cyprus	✓	✓	✗	✗	✓	✗	3
EURO	Western Asia	Georgia	✓	✗	✓	✗	✓	✗	3
EURO	Western Asia	Turkey	✓	✗	✓	✗	✓	✗	3
PAHO	Central America and Caribbean	Barbados	✗	✓	✓	✗	✓	✗	3
PAHO	Central America and Caribbean	Belize	✓	✗	✓	✗	✓	✗	3
PAHO	Central America and Caribbean	British Virgin Islands	✓	✓	✗	✗	✓	✗	3
PAHO	Central America and Caribbean	Dominican Republic	✓	✗	✓	✗	✓	✗	3
PAHO	Central America and Caribbean	El Salvador	✓	✗	✓	✗	✓	✗	3
PAHO	Central America and Caribbean	Haiti	✗	✓	✓	✗	✓	✗	3
PAHO	Central America and Caribbean	Jamaica	✗	✓	✓	✗	✓	✗	3
PAHO	Central America and Caribbean	Mexico	✓	✓	✗	✗	✓	✗	3
PAHO	Central America and Caribbean	Saint Vincent and the Grenadines	✓	✗	✓	✗	✓	✗	3
PAHO	Central America and Caribbean	Trinidad and Tobago	✗	✓	✓	✗	✓	✗	3
PAHO	Temperate South America	Chile	✓	✗	✓	✗	✓	✗	3
PAHO	Tropical South America	Ecuador	✗	✗	✓	✓	✓	✗	3
SEARO	Eastern Asia	North Korea	✓	✗	✓	✗	✓	✗	3
SEARO	South-East Asia	Indonesia	✓	✗	✓	✗	✓	✗	3
SEARO	South-East Asia	Thailand	✓	✗	✓	✗	✓	✗	3
SEARO	South-East Asia	Timor-Leste	✓	✗	✓	✗	✓	✗	3
SEARO	Southern Asia	Bhutan	✓	✗	✓	✗	✓	✗	3

SEARO	Southern Asia	India	✓	✗	✓	✗	✓	✗	3
SEARO	Southern Asia	Nepal	✓	✗	✓	✗	✓	✗	3
SEARO	Southern Asia	Sri Lanka	✓	✗	✓	✗	✓	✗	3
WPRO	Eastern Asia	China	✓	✗	✓	✗	✓	✗	3
WPRO	Eastern Asia	Mongolia	✓	✗	✓	✗	✓	✗	3
WPRO	South-East Asia	Cambodia	✓	✗	✓	✗	✓	✗	3
WPRO	South-East Asia	Laos	✓	✗	✓	✗	✓	✗	3
WPRO	South-East Asia	Malaysia	✓	✗	✓	✗	✓	✗	3
WPRO	South-East Asia	Philippines	✓	✗	✓	✗	✓	✗	3
WPRO	South-East Asia	Singapore	✓	✓	✗	✗	✓	✗	3
AFRO	Middle Africa	Central African Republic	✓	✗	✗	✗	✓	✗	2
EMRO	Southern Asia	Iran	✓	✗	✗	✗	✓	✗	2
EMRO	Western Asia	Iraq	✗	✗	✓	✗	✓	✗	2
EMRO	Western Asia	Lebanon	✗	✗	✓	✗	✓	✗	2
EMRO	Western Asia	Oman	✗	✗	✓	✗	✓	✗	2
EMRO	Western Asia	Qatar	✓	✗	✗	✗	✓	✗	2
EMRO	Western Asia	Yemen	✗	✗	✓	✗	✓	✗	2
EURO	Eastern Europe	Bulgaria	✗	✓	✗	✗	✓	✗	2
EURO	Eastern Europe	Hungary	✓	✗	✗	✗	✓	✗	2
EURO	Eastern Europe	Poland	✓	✗	✗	✗	✓	✗	2
EURO	Northern Europe	Denmark	✓	✗	✗	✗	✓	✗	2
EURO	Northern Europe	Ireland	✓	✗	✗	✗	✓	✗	2
EURO	Northern Europe	Sweden	✓	✗	✗	✗	✓	✗	2
EURO	Northern Europe	United Kingdom	✓	✗	✗	✗	✓	✗	2
EURO	South West Europe	Austria	✓	✗	✗	✗	✓	✗	2
EURO	South West Europe	Croatia	✓	✗	✗	✗	✓	✗	2
EURO	South West Europe	France	✓	✗	✗	✗	✓	✗	2
EURO	South West Europe	Germany	✗	✓	✗	✗	✓	✗	2
EURO	South West Europe	Malta	✓	✗	✗	✗	✓	✗	2
EURO	South West Europe	Portugal	✓	✗	✗	✗	✓	✗	2
EURO	South West Europe	Spain	✓	✗	✗	✗	✓	✗	2
EURO	South West Europe	Switzerland	✓	✗	✗	✗	✓	✗	2
EURO	Western Asia	Israel	✓	✗	✗	✗	✓	✗	2
PAHO	Central America and Caribbean	Grenada	✓	✗	✗	✗	✓	✗	2
PAHO	Temperate South America	Uruguay	✗	✗	✓	✗	✓	✗	2
WPRO	Oceania Melanesia Polynesia	Fiji	✓	✗	✗	✗	✓	✗	2
WPRO	Oceania Melanesia Polynesia	New Caledonia	✓	✗	✗	✗	✓	✗	2
WPRO	Oceania Melanesia Polynesia	New Zealand	✓	✗	✗	✗	✓	✗	2
WPRO	Oceania Melanesia Polynesia	Papua New Guinea	✓	✗	✗	✗	✓	✗	2
AFRO	Middle Africa	Congo	✗	✗	✗	✗	✓	✗	1
AFRO	Middle Africa	South Sudan	✗	✗	✗	✗	✓	✗	1
EMRO	Northern Africa	Sudan	✗	✗	✗	✗	✓	✗	1
EMRO	Western Asia	Bahrain	✗	✗	✗	✗	✓	✗	1
EMRO	Western Asia	West Bank and Gaza Strip	✗	✗	✗	✗	✓	✗	1
PAHO	Central America and Caribbean	Anguilla	✗	✗	✗	✗	✓	✗	1
PAHO	Central America and Caribbean	Antigua and Barbuda	✗	✗	✗	✗	✓	✗	1
PAHO	Central America and Caribbean	Aruba	✗	✗	✗	✗	✓	✗	1
PAHO	Central America and Caribbean	Bahamas	✗	✗	✗	✗	✓	✗	1
PAHO	Central America and Caribbean	Cayman Islands	✗	✗	✗	✗	✓	✗	1
PAHO	Central America and Caribbean	Guadeloupe	✗	✗	✗	✗	✓	✗	1
PAHO	Central America and Caribbean	Martinique	✗	✗	✗	✗	✓	✗	1
PAHO	Central America and Caribbean	Saint Kitts and Nevis	✗	✗	✗	✗	✓	✗	1
PAHO	Central America and Caribbean	Turks and Caicos Islands	✗	✗	✗	✗	✓	✗	1
PAHO	North America	Bermuda	✗	✗	✗	✗	✓	✗	1
PAHO	Tropical South America	French Guiana	✗	✗	✗	✗	✓	✗	1
PAHO	Tropical South America	Guyana	✗	✗	✗	✗	✓	✗	1
PAHO	Tropical South America	Venezuela	✗	✗	✗	✗	✓	✗	1
WPRO	Eastern Asia	Japan	✗	✗	✗	✗	✓	✗	1
WPRO	Eastern Asia	South Korea	✗	✗	✗	✗	✓	✗	1
PAHO	Central America and Caribbean	Montserrat	✗	✗	✗	✗	✗	✗	0

PAHO	Central America and Caribbean	Saint Barthelemy	✗	✗	✗	✗	✗	✗	0
PAHO	Central America and Caribbean	Saint Martin	✗	✗	✗	✗	✗	✗	0
Total Reporting Countries			**137**	**58**	**110**	**19**	**168**	**25**	**173**

Supplementary Table S5. Average and median *outcome variety scores* (OVS) of Member States collecting health records for 6 testing outcomes (specimens collected (SPE), specimens processed or tests (TES), influenza A positives (FLUA), influenza B positives (FLUB), total positives (POS), and total negatives (NEG)) in 6 WHO-defined regions and 17 influenza transmission zones. We extracted data from FluNet on 15 June 2021, at which time 173 Member States reported data. We estimated these scores using numerous WHO and national influenza reports. We calculated OVS by counting the number of test outcomes where a Member States reported at least 1 week with complete records. We estimate average scores with 95% confidence intervals (top values) and median scores with lower and upper quartiles (bottom values). We report regions and zones in descending order by average OVS, and omit the Southern African zone, as it only consisted of 1 country.

Region	OVS	POS	FLUA	FLUB	NEG	SPE	TES
SEARO	5.91 [5.73, 6.00] 6.00 [6.00, 6.00]	1.00 [1.00, 1.00] 1.00 [1.00, 1.00]	1.00 [1.00, 1.00] 1.00 [1.00, 1.00]	1.00 [1.00, 1.00] 1.00 [1.00, 1.00]	0.91 [0.73, 1.00] 1.00 [1.00, 1.00]	1.00 [1.00, 1.00] 1.00 [1.00, 1.00]	1.00 [1.00, 1.00] 1.00 [1.00, 1.00]
EMRO	5.89 [5.75, 6.00] 6.00 [6.00, 6.00]	1.00 [1.00, 1.00] 1.00 [1.00, 1.00]	1.00 [1.00, 1.00] 1.00 [1.00, 1.00]	1.00 [1.00, 1.00] 1.00 [1.00, 1.00]	0.89 [0.75, 1.00] 1.00 [1.00, 1.00]	1.00 [1.00, 1.00] 1.00 [1.00, 1.00]	1.00 [1.00, 1.00] 1.00 [1.00, 1.00]
WPRO	5.73 [5.43, 6.00] 6.00 [6.00, 6.00]	1.00 [1.00, 1.00] 1.00 [1.00, 1.00]	1.00 [1.00, 1.00] 1.00 [1.00, 1.00]	1.00 [1.00, 1.00] 1.00 [1.00, 1.00]	0.87 [0.69, 1.00] 1.00 [1.00, 1.00]	0.93 [0.80, 1.00] 1.00 [1.00, 1.00]	0.93 [0.80, 1.00] 1.00 [1.00, 1.00]
AFRO	5.67 [5.50, 5.84] 6.00 [5.00, 6.00]	1.00 [1.00, 1.00] 1.00 [1.00, 1.00]	1.00 [1.00, 1.00] 1.00 [1.00, 1.00]	1.00 [1.00, 1.00] 1.00 [1.00, 1.00]	0.67 [0.50, 0.84] 1.00 [0.00, 1.00]	1.00 [1.00, 1.00] 1.00 [1.00, 1.00]	1.00 [1.00, 1.00] 1.00 [1.00, 1.00]
PAHO	4.87 [4.42, 5.33] 5.00 [5.00, 6.00]	0.91 [0.83, 1.00] 1.00 [1.00, 1.00]	0.89 [0.80, 0.98] 1.00 [1.00, 1.00]	0.89 [0.80, 0.98] 1.00 [1.00, 1.00]	0.81 [0.69, 0.92] 1.00 [1.00, 1.00]	0.43 [0.28, 0.57] 0.00 [0.00, 1.00]	0.94 [0.87, 1.00] 1.00 [1.00, 1.00]
EURO	4.51 [4.33, 4.69] 4.00 [4.00, 5.00]	1.00 [1.00, 1.00] 1.00 [1.00, 1.00]	1.00 [1.00, 1.00] 1.00 [1.00, 1.00]	1.00 [1.00, 1.00] 1.00 [1.00, 1.00]	0.08 [0.00, 0.15] 0.00 [0.00, 0.00]	0.43 [0.29, 0.57] 0.00 [0.00, 1.00]	1.00 [1.00, 1.00] 1.00 [1.00, 1.00]
Zone							
Temperate South America	6.00 [6.00, 6.00] 6.00 [6.00, 6.00]	1.00 [1.00, 1.00] 1.00 [1.00, 1.00]	1.00 [1.00, 1.00] 1.00 [1.00, 1.00]	1.00 [1.00, 1.00] 1.00 [1.00, 1.00]	1.00 [1.00, 1.00] 1.00 [1.00, 1.00]	1.00 [1.00, 1.00] 1.00 [1.00, 1.00]	1.00 [1.00, 1.00] 1.00 [1.00, 1.00]
Oceania Melanesia Polynesia	6.00 [6.00, 6.00] 6.00 [6.00, 6.00]	1.00 [1.00, 1.00] 1.00 [1.00, 1.00]	1.00 [1.00, 1.00] 1.00 [1.00, 1.00]	1.00 [1.00, 1.00] 1.00 [1.00, 1.00]	1.00 [1.00, 1.00] 1.00 [1.00, 1.00]	1.00 [1.00, 1.00] 1.00 [1.00, 1.00]	1.00 [1.00, 1.00] 1.00 [1.00, 1.00]
Western Africa	5.91 [5.73, 6.00] 6.00 [6.00, 6.00]	1.00 [1.00, 1.00] 1.00 [1.00, 1.00]	1.00 [1.00, 1.00] 1.00 [1.00, 1.00]	1.00 [1.00, 1.00] 1.00 [1.00, 1.00]	0.91 [0.73, 1.00] 1.00 [1.00, 1.00]	1.00 [1.00, 1.00] 1.00 [1.00, 1.00]	1.00 [1.00, 1.00] 1.00 [1.00, 1.00]
Southeast Asia	5.90 [5.70, 6.00] 6.00 [6.00, 6.00]	1.00 [1.00, 1.00] 1.00 [1.00, 1.00]	1.00 [1.00, 1.00] 1.00 [1.00, 1.00]	1.00 [1.00, 1.00] 1.00 [1.00, 1.00]	0.90 [0.70, 1.00] 1.00 [1.00, 1.00]	1.00 [1.00, 1.00] 1.00 [1.00, 1.00]	1.00 [1.00, 1.00] 1.00 [1.00, 1.00]
Southern Asia	5.89 [5.67, 6.00] 6.00 [6.00, 6.00]	1.00 [1.00, 1.00] 1.00 [1.00, 1.00]	1.00 [1.00, 1.00] 1.00 [1.00, 1.00]	1.00 [1.00, 1.00] 1.00 [1.00, 1.00]	0.89 [0.67, 1.00] 1.00 [1.00, 1.00]	1.00 [1.00, 1.00] 1.00 [1.00, 1.00]	1.00 [1.00, 1.00] 1.00 [1.00, 1.00]
Northern Africa	5.80 [5.41, 6.00] 6.00 [6.00, 6.00]	1.00 [1.00, 1.00] 1.00 [1.00, 1.00]	1.00 [1.00, 1.00] 1.00 [1.00, 1.00]	1.00 [1.00, 1.00] 1.00 [1.00, 1.00]	0.80 [0.41, 1.00] 1.00 [1.00, 1.00]	1.00 [1.00, 1.00] 1.00 [1.00, 1.00]	1.00 [1.00, 1.00] 1.00 [1.00, 1.00]
Eastern Africa	5.60 [5.28, 5.92] 6.00 [5.00, 6.00]	1.00 [1.00, 1.00] 1.00 [1.00, 1.00]	1.00 [1.00, 1.00] 1.00 [1.00, 1.00]	1.00 [1.00, 1.00] 1.00 [1.00, 1.00]	0.60 [0.28, 0.92] 1.00 [0.00, 1.00]	1.00 [1.00, 1.00] 1.00 [1.00, 1.00]	1.00 [1.00, 1.00] 1.00 [1.00, 1.00]
Eastern Asia	5.40 [4.62, 6.00] 6.00 [5.00, 6.00]	1.00 [1.00, 1.00] 1.00 [1.00, 1.00]	1.00 [1.00, 1.00] 1.00 [1.00, 1.00]	1.00 [1.00, 1.00] 1.00 [1.00, 1.00]	0.80 [0.41, 1.00] 1.00 [1.00, 1.00]	0.80 [0.41, 1.00] 1.00 [1.00, 1.00]	0.80 [0.41, 1.00] 1.00 [1.00, 1.00]
Western Asia	5.39 [5.00, 5.78] 6.00 [5.00, 6.00]	1.00 [1.00, 1.00] 1.00 [1.00, 1.00]	1.00 [1.00, 1.00] 1.00 [1.00, 1.00]	1.00 [1.00, 1.00] 1.00 [1.00, 1.00]	0.61 [0.38, 0.84] 1.00 [0.00, 1.00]	0.78 [0.58, 0.98] 1.00 [1.00, 1.00]	1.00 [1.00, 1.00] 1.00 [1.00, 1.00]
Middle Africa	5.29 [4.92, 5.65] 5.00 [5.00, 6.00]	1.00 [1.00, 1.00] 1.00 [1.00, 1.00]	1.00 [1.00, 1.00] 1.00 [1.00, 1.00]	1.00 [1.00, 1.00] 1.00 [1.00, 1.00]	0.29 [0.00, 0.65] 0.00 [0.00, 1.00]	1.00 [1.00, 1.00] 1.00 [1.00, 1.00]	1.00 [1.00, 1.00] 1.00 [1.00, 1.00]
Tropical South America	5.11 [4.06, 6.00] 6.00 [5.00, 6.00]	0.89 [0.67, 1.00] 1.00 [1.00, 1.00]	0.89 [0.67, 1.00] 1.00 [1.00, 1.00]	0.89 [0.67, 1.00] 1.00 [1.00, 1.00]	0.89 [0.67, 1.00] 1.00 [1.00, 1.00]	0.56 [0.21, 0.90] 1.00 [0.00, 1.00]	1.00 [1.00, 1.00] 1.00 [1.00, 1.00]
North America	5.00 [3.87, 6.00] 5.00 [4.00, 6.00]	1.00 [1.00, 1.00] 1.00 [1.00, 1.00]	1.00 [1.00, 1.00] 1.00 [1.00, 1.00]	1.00 [1.00, 1.00] 1.00 [1.00, 1.00]	0.33 [0.00, 0.99] 0.00 [0.00, 1.00]	0.67 [0.01, 1.00] 1.00 [0.00, 1.00]	1.00 [1.00, 1.00] 1.00 [1.00, 1.00]
Northern Europe	4.70 [4.40, 5.00] 5.00 [4.00, 5.00]	1.00 [1.00, 1.00] 1.00 [1.00, 1.00]	1.00 [1.00, 1.00] 1.00 [1.00, 1.00]	1.00 [1.00, 1.00] 1.00 [1.00, 1.00]	0.00 [0.00, 0.00] 0.00 [0.00, 0.00]	0.70 [0.40, 1.00] 1.00 [0.00, 1.00]	1.00 [1.00, 1.00] 1.00 [1.00, 1.00]
Central America and Caribbean	4.65 [4.05, 5.24] 5.00 [5.00, 6.00]	0.90 [0.80, 1.00] 1.00 [1.00, 1.00]	0.87 [0.75, 0.99] 1.00 [1.00, 1.00]	0.87 [0.75, 0.99] 1.00 [1.00, 1.00]	0.81 [0.67, 0.95] 1.00 [1.00, 1.00]	0.29 [0.13, 0.45] 0.00 [0.00, 1.00]	0.90 [0.80, 1.01] 1.00 [1.00, 1.00]
Southwest Europe	4.63 [4.29, 4.97] 4.00 [4.00, 5.00]	1.00 [1.00, 1.00] 1.00 [1.00, 1.00]	1.00 [1.00, 1.00] 1.00 [1.00, 1.00]	1.00 [1.00, 1.00] 1.00 [1.00, 1.00]	0.16 [0.00, 0.33] 0.00 [0.00, 0.00]	0.47 [0.24, 0.70] 0.00 [0.00, 1.00]	1.00 [1.00, 1.00] 1.00 [1.00, 1.00]
Eastern Europe	4.45 [4.05, 4.86] 4.00 [4.00, 5.00]	1.00 [1.00, 1.00] 1.00 [1.00, 1.00]	1.00 [1.00, 1.00] 1.00 [1.00, 1.00]	1.00 [1.00, 1.00] 1.00 [1.00, 1.00]	0.09 [0.00, 0.27] 0.00 [0.00, 0.00]	0.36 [0.07, 0.66] 0.00 [0.00, 1.00]	1.00 [1.00, 1.00] 1.00 [1.00, 1.00]
Central Asia	4.00 [4.00, 4.00] 4.00 [4.00, 4.00]	1.00 [1.00, 1.00] 1.00 [1.00, 1.00]	1.00 [1.00, 1.00] 1.00 [1.00, 1.00]	1.00 [1.00, 1.00] 1.00 [1.00, 1.00]	0.00 [0.00, 0.00] 0.00 [0.00, 0.00]	0.00 [0.00, 0.00] 0.00 [0.00, 0.00]	1.00 [1.00, 1.00] 1.00 [1.00, 1.00]
Worldwide	**5.16 [4.99, 5.32]** **5.00 [5.00, 6.00]**	**0.98 [0.95, 1.00]** **1.00 [1.00, 1.00]**	**0.97 [0.95, 1.00]** **1.00 [1.00, 1.00]**	**0.97 [0.95, 1.00]** **1.00 [1.00, 1.00]**	**0.59 [0.52, 0.66]** **1.00 [0.00, 1.00]**	**0.67 [0.60, 0.74]** **1.00 [0.00, 1.00]**	**0.98 [0.95, 1.00]** **1.00 [1.00, 1.00]**

Supplementary Table S6. The *outcome variety score* (OVS) for each Member State reporting influenza virological data to the WHO's FluNet as of 15 June 2021. Scores range from 0-6 depending on the number of case definitions collected by a Member State, which included specimens collected (SPE), specimens processed or tests (TES), influenza A positives (FLUA), influenza B positives (FLUB), total positives (POS), and total negatives (NEG). We list Member States in descending order by CVS, region, and zone. We estimated scores using numerous WHO and national influenza reports.

Region	Zone	Member State	POS	FLUA	FLUB	NEG	SPE	TES	OVS
AFRO	Eastern Africa	Ethiopia	✓	✓	✓	✓	✓	✓	6
AFRO	Eastern Africa	Madagascar	✓	✓	✓	✓	✓	✓	6
AFRO	Eastern Africa	Mozambique	✓	✓	✓	✓	✓	✓	6
AFRO	Eastern Africa	Tanzania	✓	✓	✓	✓	✓	✓	6
AFRO	Eastern Africa	Uganda	✓	✓	✓	✓	✓	✓	6
AFRO	Eastern Africa	Zambia	✓	✓	✓	✓	✓	✓	6
AFRO	Middle Africa	Cameroon	✓	✓	✓	✓	✓	✓	6
AFRO	Middle Africa	Democratic Republic of the Congo	✓	✓	✓	✓	✓	✓	6
AFRO	Northern Africa	Algeria	✓	✓	✓	✓	✓	✓	6
AFRO	Southern Africa	South Africa	✓	✓	✓	✓	✓	✓	6
AFRO	Western Africa	Burkina Faso	✓	✓	✓	✓	✓	✓	6
AFRO	Western Africa	Côte d'Ivoire	✓	✓	✓	✓	✓	✓	6
AFRO	Western Africa	Ghana	✓	✓	✓	✓	✓	✓	6
AFRO	Western Africa	Mali	✓	✓	✓	✓	✓	✓	6
AFRO	Western Africa	Mauritania	✓	✓	✓	✓	✓	✓	6
AFRO	Western Africa	Niger	✓	✓	✓	✓	✓	✓	6
AFRO	Western Africa	Nigeria	✓	✓	✓	✓	✓	✓	6
AFRO	Western Africa	Senegal	✓	✓	✓	✓	✓	✓	6
AFRO	Western Africa	Sierra Leone	✓	✓	✓	✓	✓	✓	6
AFRO	Western Africa	Togo	✓	✓	✓	✓	✓	✓	6
EMRO	Northern Africa	Egypt	✓	✓	✓	✓	✓	✓	6
EMRO	Northern Africa	Morocco	✓	✓	✓	✓	✓	✓	6
EMRO	Northern Africa	Tunisia	✓	✓	✓	✓	✓	✓	6
EMRO	Southern Asia	Afghanistan	✓	✓	✓	✓	✓	✓	6
EMRO	Southern Asia	Iran	✓	✓	✓	✓	✓	✓	6
EMRO	Southern Asia	Pakistan	✓	✓	✓	✓	✓	✓	6
EMRO	Western Asia	Bahrain	✓	✓	✓	✓	✓	✓	6
EMRO	Western Asia	Iraq	✓	✓	✓	✓	✓	✓	6
EMRO	Western Asia	Jordan	✓	✓	✓	✓	✓	✓	6
EMRO	Western Asia	Kuwait	✓	✓	✓	✓	✓	✓	6
EMRO	Western Asia	Lebanon	✓	✓	✓	✓	✓	✓	6
EMRO	Western Asia	Oman	✓	✓	✓	✓	✓	✓	6
EMRO	Western Asia	Qatar	✓	✓	✓	✓	✓	✓	6
EMRO	Western Asia	Saudi Arabia	✓	✓	✓	✓	✓	✓	6
EMRO	Western Asia	Syrian Arab Republic	✓	✓	✓	✓	✓	✓	6
EMRO	Western Asia	United Arab Emirates	✓	✓	✓	✓	✓	✓	6
EMRO	Western Asia	West Bank and Gaza Strip	✓	✓	✓	✓	✓	✓	6
EURO	Eastern Europe	Russian Federation	✓	✓	✓	✓	✓	✓	6
EURO	South West Europe	Italy	✓	✓	✓	✓	✓	✓	6
EURO	South West Europe	Serbia	✓	✓	✓	✓	✓	✓	6
EURO	South West Europe	Spain	✓	✓	✓	✓	✓	✓	6
PAHO	Central America and Caribbean	Costa Rica	✓	✓	✓	✓	✓	✓	6
PAHO	Central America and Caribbean	Cuba	✓	✓	✓	✓	✓	✓	6
PAHO	Central America and Caribbean	El Salvador	✓	✓	✓	✓	✓	✓	6
PAHO	Central America and Caribbean	Guadeloupe	✓	✓	✓	✓	✓	✓	6
PAHO	Central America and Caribbean	Guatemala	✓	✓	✓	✓	✓	✓	6
PAHO	Central America and Caribbean	Honduras	✓	✓	✓	✓	✓	✓	6
PAHO	Central America and Caribbean	Jamaica	✓	✓	✓	✓	✓	✓	6
PAHO	Central America and Caribbean	Martinique	✓	✓	✓	✓	✓	✓	6
PAHO	Central America and Caribbean	Panama	✓	✓	✓	✓	✓	✓	6
PAHO	North America	United States of America	✓	✓	✓	✓	✓	✓	6
PAHO	Temperate South America	Argentina	✓	✓	✓	✓	✓	✓	6

PAHO	Temperate South America	Chile	✓	✓	✓	✓	✓	✓	6
PAHO	Temperate South America	Paraguay	✓	✓	✓	✓	✓	✓	6
PAHO	Temperate South America	Uruguay	✓	✓	✓	✓	✓	✓	6
PAHO	Tropical South America	Brazil	✓	✓	✓	✓	✓	✓	6
PAHO	Tropical South America	Ecuador	✓	✓	✓	✓	✓	✓	6
PAHO	Tropical South America	French Guiana	✓	✓	✓	✓	✓	✓	6
PAHO	Tropical South America	Peru	✓	✓	✓	✓	✓	✓	6
PAHO	Tropical South America	Venezuela	✓	✓	✓	✓	✓	✓	6
SEARO	Eastern Asia	North Korea	✓	✓	✓	✓	✓	✓	6
SEARO	South-East Asia	Indonesia	✓	✓	✓	✓	✓	✓	6
SEARO	South-East Asia	Myanmar	✓	✓	✓	✓	✓	✓	6
SEARO	South-East Asia	Thailand	✓	✓	✓	✓	✓	✓	6
SEARO	South-East Asia	Timor-Leste	✓	✓	✓	✓	✓	✓	6
SEARO	Southern Asia	Bangladesh	✓	✓	✓	✓	✓	✓	6
SEARO	Southern Asia	Bhutan	✓	✓	✓	✓	✓	✓	6
SEARO	Southern Asia	India	✓	✓	✓	✓	✓	✓	6
SEARO	Southern Asia	Maldives	✓	✓	✓	✓	✓	✓	6
SEARO	Southern Asia	Nepal	✓	✓	✓	✓	✓	✓	6
WPRO	Eastern Asia	China	✓	✓	✓	✓	✓	✓	6
WPRO	Eastern Asia	South Korea	✓	✓	✓	✓	✓	✓	6
WPRO	Oceania Melanesia Polynesia	Australia	✓	✓	✓	✓	✓	✓	6
WPRO	Oceania Melanesia Polynesia	Fiji	✓	✓	✓	✓	✓	✓	6
WPRO	Oceania Melanesia Polynesia	New Caledonia	✓	✓	✓	✓	✓	✓	6
WPRO	Oceania Melanesia Polynesia	New Zealand	✓	✓	✓	✓	✓	✓	6
WPRO	Oceania Melanesia Polynesia	Papua New Guinea	✓	✓	✓	✓	✓	✓	6
WPRO	South-East Asia	Laos	✓	✓	✓	✓	✓	✓	6
WPRO	South-East Asia	Malaysia	✓	✓	✓	✓	✓	✓	6
WPRO	South-East Asia	Philippines	✓	✓	✓	✓	✓	✓	6
WPRO	South-East Asia	Singapore	✓	✓	✓	✓	✓	✓	6
WPRO	South-East Asia	Viet Nam	✓	✓	✓	✓	✓	✓	6
AFRO	Eastern Africa	Kenya	✓	✓	✓	✗	✓	✓	5
AFRO	Eastern Africa	Mauritius	✓	✓	✓	✗	✓	✓	5
AFRO	Eastern Africa	Rwanda	✓	✓	✓	✗	✓	✓	5
AFRO	Eastern Africa	Seychelles	✓	✓	✓	✗	✓	✓	5
AFRO	Middle Africa	Angola	✓	✓	✓	✗	✓	✓	5
AFRO	Middle Africa	Central African Republic	✓	✓	✓	✗	✓	✓	5
AFRO	Middle Africa	Chad	✓	✓	✓	✗	✓	✓	5
AFRO	Middle Africa	Congo	✓	✓	✓	✗	✓	✓	5
AFRO	Middle Africa	South Sudan	✓	✓	✓	✗	✓	✓	5
AFRO	Western Africa	Guinea	✓	✓	✓	✗	✓	✓	5
EMRO	Northern Africa	Sudan	✓	✓	✓	✗	✓	✓	5
EMRO	Western Asia	Yemen	✓	✓	✓	✗	✓	✓	5
EURO	Eastern Europe	Poland	✓	✓	✓	✗	✓	✓	5
EURO	Eastern Europe	Romania	✓	✓	✓	✗	✓	✓	5
EURO	Eastern Europe	Ukraine	✓	✓	✓	✗	✓	✓	5
EURO	Northern Europe	Denmark	✓	✓	✓	✗	✓	✓	5
EURO	Northern Europe	Estonia	✓	✓	✓	✗	✓	✓	5
EURO	Northern Europe	Finland	✓	✓	✓	✗	✓	✓	5
EURO	Northern Europe	Latvia	✓	✓	✓	✗	✓	✓	5
EURO	Northern Europe	Lithuania	✓	✓	✓	✗	✓	✓	5
EURO	Northern Europe	Norway	✓	✓	✓	✗	✓	✓	5
EURO	Northern Europe	United Kingdom	✓	✓	✓	✗	✓	✓	5
EURO	South West Europe	Belgium	✓	✓	✓	✗	✓	✓	5
EURO	South West Europe	France	✓	✓	✓	✗	✓	✓	5
EURO	South West Europe	Greece	✓	✓	✓	✗	✓	✓	5
EURO	South West Europe	Netherlands	✓	✓	✓	✗	✓	✓	5
EURO	South West Europe	Slovenia	✓	✓	✓	✗	✓	✓	5
EURO	South West Europe	Switzerland	✓	✓	✓	✗	✓	✓	5
EURO	Western Asia	Israel	✓	✓	✓	✗	✓	✓	5
EURO	Western Asia	Turkey	✓	✓	✓	✗	✓	✓	5

PAHO	Central America and Caribbean	Aruba	✓	✓	✓	✓	✗	✓	5
PAHO	Central America and Caribbean	Bahamas	✓	✓	✓	✓	✗	✓	5
PAHO	Central America and Caribbean	Barbados	✓	✓	✓	✓	✗	✓	5
PAHO	Central America and Caribbean	Belize	✓	✓	✓	✓	✗	✓	5
PAHO	Central America and Caribbean	Dominica	✓	✓	✓	✓	✗	✓	5
PAHO	Central America and Caribbean	Dominican Republic	✓	✓	✓	✓	✗	✓	5
PAHO	Central America and Caribbean	Grenada	✓	✓	✓	✓	✗	✓	5
PAHO	Central America and Caribbean	Haiti	✓	✓	✓	✓	✗	✓	5
PAHO	Central America and Caribbean	Mexico	✓	✓	✓	✓	✗	✓	5
PAHO	Central America and Caribbean	Nicaragua	✓	✓	✓	✓	✗	✓	5
PAHO	Central America and Caribbean	Saint Kitts and Nevis	✓	✓	✓	✓	✗	✓	5
PAHO	Central America and Caribbean	Saint Lucia	✓	✓	✓	✓	✗	✓	5
PAHO	Central America and Caribbean	Saint Vincent and the Grenadines	✓	✓	✓	✓	✗	✓	5
PAHO	Central America and Caribbean	Trinidad and Tobago	✓	✓	✓	✓	✗	✓	5
PAHO	Central America and Caribbean	Turks and Caicos Islands	✓	✓	✓	✓	✗	✓	5
PAHO	North America	Canada	✓	✓	✓	✗	✓	✓	5
PAHO	Tropical South America	Bolivia	✓	✓	✓	✓	✗	✓	5
PAHO	Tropical South America	Colombia	✓	✓	✓	✓	✗	✓	5
PAHO	Tropical South America	Suriname	✓	✓	✓	✓	✗	✓	5
SEARO	Southern Asia	Sri Lanka	✓	✓	✓	✗	✓	✓	5
WPRO	Eastern Asia	Mongolia	✓	✓	✓	✗	✓	✓	5
WPRO	South-East Asia	Cambodia	✓	✓	✓	✗	✓	✓	5
EURO	Central Asia	Kazakhstan	✓	✓	✓	✗	✗	✓	4
EURO	Central Asia	Kyrgyzstan	✓	✓	✓	✗	✗	✓	4
EURO	Central Asia	Tajikistan	✓	✓	✓	✗	✗	✓	4
EURO	Central Asia	Turkmenistan	✓	✓	✓	✗	✗	✓	4
EURO	Central Asia	Uzbekistan	✓	✓	✓	✗	✗	✓	4
EURO	Eastern Europe	Belarus	✓	✓	✓	✗	✗	✓	4
EURO	Eastern Europe	Bulgaria	✓	✓	✓	✗	✗	✓	4
EURO	Eastern Europe	Czechia	✓	✓	✓	✗	✗	✓	4
EURO	Eastern Europe	Hungary	✓	✓	✓	✗	✗	✓	4
EURO	Eastern Europe	Kosovo	✓	✓	✓	✗	✗	✓	4
EURO	Eastern Europe	Moldova	✓	✓	✓	✗	✗	✓	4
EURO	Eastern Europe	Slovakia	✓	✓	✓	✗	✗	✓	4
EURO	Northern Europe	Iceland	✓	✓	✓	✗	✗	✓	4
EURO	Northern Europe	Ireland	✓	✓	✓	✗	✗	✓	4
EURO	Northern Europe	Sweden	✓	✓	✓	✗	✗	✓	4
EURO	South West Europe	Albania	✓	✓	✓	✗	✗	✓	4
EURO	South West Europe	Austria	✓	✓	✓	✗	✗	✓	4
EURO	South West Europe	Bosnia and Herzegovina	✓	✓	✓	✗	✗	✓	4
EURO	South West Europe	Croatia	✓	✓	✓	✗	✗	✓	4
EURO	South West Europe	Germany	✓	✓	✓	✗	✗	✓	4
EURO	South West Europe	Luxembourg	✓	✓	✓	✗	✗	✓	4
EURO	South West Europe	Malta	✓	✓	✓	✗	✗	✓	4
EURO	South West Europe	Montenegro	✓	✓	✓	✗	✗	✓	4
EURO	South West Europe	North Macedonia	✓	✓	✓	✗	✗	✓	4
EURO	South West Europe	Portugal	✓	✓	✓	✗	✗	✓	4
EURO	Western Asia	Armenia	✓	✓	✓	✗	✗	✓	4
EURO	Western Asia	Azerbaijan	✓	✓	✓	✗	✗	✓	4
EURO	Western Asia	Cyprus	✓	✓	✓	✗	✗	✓	4
EURO	Western Asia	Georgia	✓	✓	✓	✗	✗	✓	4
PAHO	Central America and Caribbean	Anguilla	✓	✓	✓	✗	✗	✓	4
PAHO	Central America and Caribbean	British Virgin Islands	✓	✓	✗	✓	✗	✓	4
PAHO	Central America and Caribbean	Cayman Islands	✓	✓	✓	✗	✗	✓	4
PAHO	North America	Bermuda	✓	✓	✓	✗	✗	✓	4
WPRO	Eastern Asia	Japan	✓	✓	✓	✓	✗	✗	4
PAHO	Central America and Caribbean	Antigua and Barbuda	✓	✗	✓	✗	✗	✓	3
PAHO	Tropical South America	Guyana	✗	✗	✗	✗	✗	✓	1
PAHO	Central America and Caribbean	Montserrat	✗	✗	✗	✗	✗	✗	0
PAHO	Central America and Caribbean	Saint Barthelemy	✗	✗	✗	✗	✗	✗	0

PAHO	Central America and Caribbean	Saint Martin	✗	✗	✗	✗	✗	✗	0
	Total Reporting Countries		**169**	**168**	**168**	**102**	**116**	**169**	**173**

Supplementary Table S7. Average and median *subtype variety scores* (SVS) of Member States collecting health records for 8 influenza strains and subtypes (A(H1), A(H1N1)pdm09, A(H3), A(H5), A(Unsubtyped), B(Yamagata), B(Victoria), and B(Undetermined) positives) in 6 WHO-defined regions and 17 influenza transmission zones. We extracted data from FluNet on 15 June 2021, at which time 173 Member States reported data. We estimated these scores using numerous WHO and national influenza reports. We calculated SVS by counting the number of subtypes where a Member State reported at least 1 week with complete records. We estimate average scores with 95% confidence intervals (top values) and median scores with lower and upper quartiles (bottom values). We report regions and zones in descending order by average SVS, and omit the Southern African zone, as it only consisted of 1 country.

Region	SVS	A(H1)	A(H1N1)pdm09	A(H3)	A(H5)	A(Unsubtyped)	B(Yamagata)	B(Victoria)	B(Undetermined)
WPRO	8.00 [8.00, 8.00] 8.00 [8.00, 8.00]	1.00 [1.00, 1.00] 1.00 [1.00, 1.00]	1.00 [1.00, 1.00] 1.00 [1.00, 1.00]	1.00 [1.00, 1.00] 1.00 [1.00, 1.00]	1.00 [1.00, 1.00] 1.00 [1.00, 1.00]	1.00 [1.00, 1.00] 1.00 [1.00, 1.00]	1.00 [1.00, 1.00] 1.00 [1.00, 1.00]	1.00 [1.00, 1.00] 1.00 [1.00, 1.00]	1.00 [1.00, 1.00] 1.00 [1.00, 1.00]
AFRO	7.90 [7.79, 8.00] 8.00 [8.00, 8.00]	0.90 [0.79, 1.00] 1.00 [1.00, 1.00]	1.00 [1.00, 1.00] 1.00 [1.00, 1.00]	1.00 [1.00, 1.00] 1.00 [1.00, 1.00]	1.00 [1.00, 1.00] 1.00 [1.00, 1.00]	1.00 [1.00, 1.00] 1.00 [1.00, 1.00]	1.00 [1.00, 1.00] 1.00 [1.00, 1.00]	1.00 [1.00, 1.00] 1.00 [1.00, 1.00]	1.00 [1.00, 1.00] 1.00 [1.00, 1.00]
SEARO	7.45 [6.74, 8.00] 8.00 [7.00, 8.00]	0.82 [0.58, 1.00] 1.00 [1.00, 1.00]	1.00 [1.00, 1.00] 1.00 [1.00, 1.00]	1.00 [1.00, 1.00] 1.00 [1.00, 1.00]	1.00 [1.00, 1.00] 1.00 [1.00, 1.00]	0.82 [0.58, 1.00] 1.00 [1.00, 1.00]	0.91 [0.73, 1.00] 1.00 [1.00, 1.00]	0.91 [0.73, 1.00] 1.00 [1.00, 1.00]	1.00 [1.00, 1.00] 1.00 [1.00, 1.00]
EURO	7.41 [7.28, 7.55] 7.00 [7.00, 8.00]	1.00 [1.00, 1.00] 1.00 [1.00, 1.00]	1.00 [1.00, 1.00] 1.00 [1.00, 1.00]	1.00 [1.00, 1.00] 1.00 [1.00, 1.00]	0.41 [0.28, 0.55] 0.00 [0.00, 1.00]	1.00 [1.00, 1.00] 1.00 [1.00, 1.00]	1.00 [1.00, 1.00] 1.00 [1.00, 1.00]	1.00 [1.00, 1.00] 1.00 [1.00, 1.00]	1.00 [1.00, 1.00] 1.00 [1.00, 1.00]
EMRO	7.11 [6.39, 7.82] 8.00 [6.00, 8.00]	0.79 [0.60, 0.98] 1.00 [1.00, 1.00]	1.00 [1.00, 1.00] 1.00 [1.00, 1.00]	0.95 [0.84, 1.00] 1.00 [1.00, 1.00]	0.74 [0.53, 0.94] 1.00 [0.00, 1.00]	0.95 [0.84, 1.00] 1.00 [1.00, 1.00]	0.84 [0.67, 1.00] 1.00 [1.00, 1.00]	0.84 [0.67, 1.00] 1.00 [1.00, 1.00]	1.00 [1.00, 1.00] 1.00 [1.00, 1.00]
PAHO	5.77 [4.96, 6.57] 7.00 [3.00, 8.00]	0.62 [0.48, 0.76] 1.00 [0.00, 1.00]	0.89 [0.80, 0.98] 1.00 [1.00, 1.00]	0.83 [0.72, 0.94] 1.00 [1.00, 1.00]	0.45 [0.30, 0.59] 0.00 [0.00, 1.00]	0.66 [0.52, 0.80] 1.00 [0.00, 1.00]	0.72 [0.59, 0.85] 1.00 [0.00, 1.00]	0.85 [0.75, 0.95] 1.00 [1.00, 1.00]	0.74 [0.62, 0.87] 1.00 [0.00, 1.00]
Zone									
Northern Africa	8.00 [8.00, 8.00] 8.00 [8.00, 8.00]	1.00 [1.00, 1.00] 1.00 [1.00, 1.00]	1.00 [1.00, 1.00] 1.00 [1.00, 1.00]	1.00 [1.00, 1.00] 1.00 [1.00, 1.00]	1.00 [1.00, 1.00] 1.00 [1.00, 1.00]	1.00 [1.00, 1.00] 1.00 [1.00, 1.00]	1.00 [1.00, 1.00] 1.00 [1.00, 1.00]	1.00 [1.00, 1.00] 1.00 [1.00, 1.00]	1.00 [1.00, 1.00] 1.00 [1.00, 1.00]
Western Africa	8.00 [8.00, 8.00] 8.00 [8.00, 8.00]	1.00 [1.00, 1.00] 1.00 [1.00, 1.00]	1.00 [1.00, 1.00] 1.00 [1.00, 1.00]	1.00 [1.00, 1.00] 1.00 [1.00, 1.00]	1.00 [1.00, 1.00] 1.00 [1.00, 1.00]	1.00 [1.00, 1.00] 1.00 [1.00, 1.00]	1.00 [1.00, 1.00] 1.00 [1.00, 1.00]	1.00 [1.00, 1.00] 1.00 [1.00, 1.00]	1.00 [1.00, 1.00] 1.00 [1.00, 1.00]
Oceania Melanesia Polynesia	8.00 [8.00, 8.00] 8.00 [8.00, 8.00]	1.00 [1.00, 1.00] 1.00 [1.00, 1.00]	1.00 [1.00, 1.00] 1.00 [1.00, 1.00]	1.00 [1.00, 1.00] 1.00 [1.00, 1.00]	1.00 [1.00, 1.00] 1.00 [1.00, 1.00]	1.00 [1.00, 1.00] 1.00 [1.00, 1.00]	1.00 [1.00, 1.00] 1.00 [1.00, 1.00]	1.00 [1.00, 1.00] 1.00 [1.00, 1.00]	1.00 [1.00, 1.00] 1.00 [1.00, 1.00]
Eastern Africa	7.90 [7.70, 8.00] 8.00 [8.00, 8.00]	0.90 [0.70, 1.10] 1.00 [1.00, 1.00]	1.00 [1.00, 1.00] 1.00 [1.00, 1.00]	1.00 [1.00, 1.00] 1.00 [1.00, 1.00]	1.00 [1.00, 1.00] 1.00 [1.00, 1.00]	1.00 [1.00, 1.00] 1.00 [1.00, 1.00]	1.00 [1.00, 1.00] 1.00 [1.00, 1.00]	1.00 [1.00, 1.00] 1.00 [1.00, 1.00]	1.00 [1.00, 1.00] 1.00 [1.00, 1.00]
Southeast Asia	7.90 [7.70, 8.00] 8.00 [8.00, 8.00]	1.00 [1.00, 1.00] 1.00 [1.00, 1.00]	1.00 [1.00, 1.00] 1.00 [1.00, 1.00]	1.00 [1.00, 1.00] 1.00 [1.00, 1.00]	1.00 [1.00, 1.00] 1.00 [1.00, 1.00]	0.90 [0.70, 1.00] 1.00 [1.00, 1.00]	1.00 [1.00, 1.00] 1.00 [1.00, 1.00]	1.00 [1.00, 1.00] 1.00 [1.00, 1.00]	1.00 [1.00, 1.00] 1.00 [1.00, 1.00]
Southern Asia	7.89 [7.67, 8.00] 8.00 [8.00, 8.00]	0.89 [0.67, 1.00] 1.00 [1.00, 1.00]	1.00 [1.00, 1.00] 1.00 [1.00, 1.00]	1.00 [1.00, 1.00] 1.00 [1.00, 1.00]	1.00 [1.00, 1.00] 1.00 [1.00, 1.00]	1.00 [1.00, 1.00] 1.00 [1.00, 1.00]	1.00 [1.00, 1.00] 1.00 [1.00, 1.00]	1.00 [1.00, 1.00] 1.00 [1.00, 1.00]	1.00 [1.00, 1.00] 1.00 [1.00, 1.00]
Temperate South America	7.75 [7.26, 8.00] 8.00 [7.50, 8.00]	1.00 [1.00, 1.00] 1.00 [1.00, 1.00]	1.00 [1.00, 1.00] 1.00 [1.00, 1.00]	1.00 [1.00, 1.00] 1.00 [1.00, 1.00]	0.75 [0.26, 1.00] 1.00 [0.50, 1.00]	1.00 [1.00, 1.00] 1.00 [1.00, 1.00]	1.00 [1.00, 1.00] 1.00 [1.00, 1.00]	1.00 [1.00, 1.00] 1.00 [1.00, 1.00]	1.00 [1.00, 1.00] 1.00 [1.00, 1.00]
Middle Africa	7.71 [7.35, 8.00] 8.00 [7.00, 8.00]	0.71 [0.35, 1.00] 1.00 [0.00, 1.00]	1.00 [1.00, 1.00] 1.00 [1.00, 1.00]	1.00 [1.00, 1.00] 1.00 [1.00, 1.00]	1.00 [1.00, 1.00] 1.00 [1.00, 1.00]	1.00 [1.00, 1.00] 1.00 [1.00, 1.00]	1.00 [1.00, 1.00] 1.00 [1.00, 1.00]	1.00 [1.00, 1.00] 1.00 [1.00, 1.00]	1.00 [1.00, 1.00] 1.00 [1.00, 1.00]
Northern Europe	7.70 [7.40, 8.00] 8.00 [7.00, 8.00]	1.00 [1.00, 1.00] 1.00 [1.00, 1.00]	1.00 [1.00, 1.00] 1.00 [1.00, 1.00]	1.00 [1.00, 1.00] 1.00 [1.00, 1.00]	0.70 [0.40, 1.00] 1.00 [0.00, 1.00]	1.00 [1.00, 1.00] 1.00 [1.00, 1.00]	1.00 [1.00, 1.00] 1.00 [1.00, 1.00]	1.00 [1.00, 1.00] 1.00 [1.00, 1.00]	1.00 [1.00, 1.00] 1.00 [1.00, 1.00]
Southwest Europe	7.47 [7.24, 7.70]	1.00 [1.00, 1.00]	1.00 [1.00, 1.00]	1.00 [1.00, 1.00]	0.47 [0.24, 0.70]	1.00 [1.00, 1.00]	1.00 [1.00, 1.00]	1.00 [1.00, 1.00]	1.00 [1.00, 1.00]

	7.00 [7.00, 8.00]	1.00 [1.00, 1.00]	1.00 [1.00, 1.00]	1.00 [1.00, 1.00]	0.00 [0.00, 1.00]	1.00 [1.00, 1.00]	1.00 [1.00, 1.00]	1.00 [1.00, 1.00]	1.00 [1.00, 1.00]
Eastern Europe	7.36 [7.07, 7.66] 7.00 [7.00, 8.00]	1.00 [1.00, 1.00] 1.00 [1.00, 1.00]	1.00 [1.00, 1.00] 1.00 [1.00, 1.00]	1.00 [1.00, 1.00] 1.00 [1.00, 1.00]	0.36 [0.07, 0.66] 0.00 [0.00, 1.00]	1.00 [1.00, 1.00] 1.00 [1.00, 1.00]	1.00 [1.00, 1.00] 1.00 [1.00, 1.00]	1.00 [1.00, 1.00] 1.00 [1.00, 1.00]	1.00 [1.00, 1.00] 1.00 [1.00, 1.00]
Eastern Asia	7.20 [5.63, 8.00] 8.00 [8.00, 8.00]	0.80 [0.41, 1.00] 1.00 [1.00, 1.00]	1.00 [1.00, 1.00] 1.00 [1.00, 1.00]	1.00 [1.00, 1.00] 1.00 [1.00, 1.00]	1.00 [1.00, 1.00] 1.00 [1.00, 1.00]	0.80 [0.41, 1.00] 1.00 [1.00, 1.00]	0.80 [0.41, 1.00] 1.00 [1.00, 1.00]	0.80 [0.41, 1.00] 1.00 [1.00, 1.00]	1.00 [1.00, 1.00] 1.00 [1.00, 1.00]
Central Asia	7.00 [7.00, 7.00] 7.00 [7.00, 7.00]	1.00 [1.00, 1.00] 1.00 [1.00, 1.00]	1.00 [1.00, 1.00] 1.00 [1.00, 1.00]	1.00 [1.00, 1.00] 1.00 [1.00, 1.00]	0.00 [0.00, 0.00] 0.00 [0.00, 0.00]	1.00 [1.00, 1.00] 1.00 [1.00, 1.00]	1.00 [1.00, 1.00] 1.00 [1.00, 1.00]	1.00 [1.00, 1.00] 1.00 [1.00, 1.00]	1.00 [1.00, 1.00] 1.00 [1.00, 1.00]
Tropical South America	6.89 [5.18, 8.00] 8.00 [7.00, 8.00]	0.89 [0.67, 1.00] 1.00 [1.00, 1.00]	0.89 [0.67, 1.00] 1.00 [1.00, 1.00]	0.89 [0.67, 1.00] 1.00 [1.00, 1.00]	0.67 [0.34, 0.99] 1.00 [0.00, 1.00]	0.89 [0.67, 1.00] 1.00 [1.00, 1.00]	0.89 [0.67, 1.00] 1.00 [1.00, 1.00]	0.89 [0.67, 1.00] 1.00 [1.00, 1.00]	0.89 [0.67, 1.00] 1.00 [1.00, 1.00]
Western Asia	6.78 [6.08, 7.48] 7.00 [6.00, 8.00]	0.78 [0.58, 0.98] 1.00 [1.00, 1.00]	1.00 [1.00, 1.00] 1.00 [1.00, 1.00]	0.94 [0.84, 1.00] 1.00 [1.00, 1.00]	0.44 [0.21, 0.68] 0.00 [0.00, 1.00]	0.94 [0.84, 1.00] 1.00 [1.00, 1.00]	0.83 [0.66, 1.00] 1.00 [1.00, 1.00]	0.83 [0.66, 1.00] 1.00 [1.00, 1.00]	1.00 [1.00, 1.00] 1.00 [1.00, 1.00]
North America	6.33 [3.07, 8.00] 8.00 [3.00, 8.00]	0.67 [0.01, 1.00] 1.00 [0.00, 1.00]	1.00 [1.00, 1.00] 1.00 [1.00, 1.00]	1.00 [1.00, 1.00] 1.00 [1.00, 1.00]	0.67 [0.01, 1.00] 1.00 [0.00, 1.00]	0.67 [0.01, 1.00] 1.00 [0.00, 1.00]	0.67 [0.01, 1.00] 1.00 [0.00, 1.00]	1.00 [1.00, 1.00] 1.00 [1.00, 1.00]	0.67 [0.01, 1.00] 1.00 [0.00, 1.00]
Central America and Caribbean	5.13 [4.11, 6.14] 6.00 [3.00, 8.00]	0.48 [0.31, 0.66] 0.00 [0.00, 1.00]	0.87 [0.75, 0.99] 1.00 [1.00, 1.00]	0.77 [0.62, 0.92] 1.00 [1.00, 1.00]	0.32 [0.16, 0.49] 0.00 [0.00, 1.00]	0.55 [0.37, 0.73] 1.00 [0.00, 1.00]	0.65 [0.47, 0.82] 1.00 [0.00, 1.00]	0.81 [0.67, 0.95] 1.00 [1.00, 1.00]	0.68 [0.51, 0.84] 1.00 [0.00, 1.00]
Worldwide	**7.07 [6.80, 7.34]** **8.00 [7.00, 8.00]**	**0.84 [0.79, 0.90]** **1.00 [1.00, 1.00]**	**0.97 [0.95, 1.00]** **1.00 [1.00, 1.00]**	**0.95 [0.91, 0.98]** **1.00 [1.00, 1.00]**	**0.65 [0.58, 0.72]** **1.00 [0.00, 1.00]**	**0.89 [0.84, 0.94]** **1.00 [1.00, 1.00]**	**0.90 [0.86, 0.95]** **1.00 [1.00, 1.00]**	**0.94 [0.90, 0.97]** **1.00 [1.00, 1.00]**	**0.93 [0.89, 0.97]** **1.00 [1.00, 1.00]**

Supplementary Table S8. The *subtype variety score* (SVS) for each Member State reporting influenza virological data to the WHO's FluNet as of 15 June 2021. Scores range from 0-8 depending on the number of subtypes reported by a Member State, which included A(H1), A(H1N1)pdm09, A(H3), A(H5), A(Unsubtyped) abbreviated A(Uns), B(Yamagata) abbreviated B(Yam), B(Victoria) abbreviated B(Vic), and B(Undetermined) positives abbreviated B(Und). We list Member States in descending order by SVS, region, and zone. We estimated scores using numerous WHO and national influenza reports.

Region	Zone	Member State	A(H1)	A(H1N1)	A(H3)	A(H5)	A(Uns)	B(Yam)	B(Vic)	B(Und)	SVS
AFRO	Eastern Africa	Ethiopia	✓	✓	✓	✓	✓	✓	✓	✓	8
AFRO	Eastern Africa	Kenya	✓	✓	✓	✓	✓	✓	✓	✓	8
AFRO	Eastern Africa	Madagascar	✓	✓	✓	✓	✓	✓	✓	✓	8
AFRO	Eastern Africa	Mauritius	✓	✓	✓	✓	✓	✓	✓	✓	8
AFRO	Eastern Africa	Mozambique	✓	✓	✓	✓	✓	✓	✓	✓	8
AFRO	Eastern Africa	Rwanda	✓	✓	✓	✓	✓	✓	✓	✓	8
AFRO	Eastern Africa	Tanzania	✓	✓	✓	✓	✓	✓	✓	✓	8
AFRO	Eastern Africa	Uganda	✓	✓	✓	✓	✓	✓	✓	✓	8
AFRO	Eastern Africa	Zambia	✓	✓	✓	✓	✓	✓	✓	✓	8
AFRO	Middle Africa	Angola	✓	✓	✓	✓	✓	✓	✓	✓	8
AFRO	Middle Africa	Cameroon	✓	✓	✓	✓	✓	✓	✓	✓	8
AFRO	Middle Africa	Central African Republic	✓	✓	✓	✓	✓	✓	✓	✓	8
AFRO	Middle Africa	Congo	✓	✓	✓	✓	✓	✓	✓	✓	8
AFRO	Middle Africa	Democratic Republic of the Congo	✓	✓	✓	✓	✓	✓	✓	✓	8
AFRO	Northern Africa	Algeria	✓	✓	✓	✓	✓	✓	✓	✓	8
AFRO	Southern Africa	South Africa	✓	✓	✓	✓	✓	✓	✓	✓	8
AFRO	Western Africa	Burkina Faso	✓	✓	✓	✓	✓	✓	✓	✓	8
AFRO	Western Africa	Côte d'Ivoire	✓	✓	✓	✓	✓	✓	✓	✓	8
AFRO	Western Africa	Ghana	✓	✓	✓	✓	✓	✓	✓	✓	8
AFRO	Western Africa	Guinea	✓	✓	✓	✓	✓	✓	✓	✓	8
AFRO	Western Africa	Mali	✓	✓	✓	✓	✓	✓	✓	✓	8
AFRO	Western Africa	Mauritania	✓	✓	✓	✓	✓	✓	✓	✓	8
AFRO	Western Africa	Niger	✓	✓	✓	✓	✓	✓	✓	✓	8
AFRO	Western Africa	Nigeria	✓	✓	✓	✓	✓	✓	✓	✓	8
AFRO	Western Africa	Senegal	✓	✓	✓	✓	✓	✓	✓	✓	8
AFRO	Western Africa	Sierra Leone	✓	✓	✓	✓	✓	✓	✓	✓	8
AFRO	Western Africa	Togo	✓	✓	✓	✓	✓	✓	✓	✓	8
EMRO	Northern Africa	Egypt	✓	✓	✓	✓	✓	✓	✓	✓	8
EMRO	Northern Africa	Morocco	✓	✓	✓	✓	✓	✓	✓	✓	8
EMRO	Northern Africa	Sudan	✓	✓	✓	✓	✓	✓	✓	✓	8
EMRO	Northern Africa	Tunisia	✓	✓	✓	✓	✓	✓	✓	✓	8
EMRO	Southern Asia	Afghanistan	✓	✓	✓	✓	✓	✓	✓	✓	8
EMRO	Southern Asia	Iran	✓	✓	✓	✓	✓	✓	✓	✓	8
EMRO	Southern Asia	Pakistan	✓	✓	✓	✓	✓	✓	✓	✓	8
EMRO	Western Asia	Bahrain	✓	✓	✓	✓	✓	✓	✓	✓	8
EMRO	Western Asia	Iraq	✓	✓	✓	✓	✓	✓	✓	✓	8
EMRO	Western Asia	Jordan	✓	✓	✓	✓	✓	✓	✓	✓	8
EMRO	Western Asia	Lebanon	✓	✓	✓	✓	✓	✓	✓	✓	8
EMRO	Western Asia	Oman	✓	✓	✓	✓	✓	✓	✓	✓	8
EMRO	Western Asia	Qatar	✓	✓	✓	✓	✓	✓	✓	✓	8
EMRO	Western Asia	Syrian Arab Republic	✓	✓	✓	✓	✓	✓	✓	✓	8
EURO	Eastern Europe	Poland	✓	✓	✓	✓	✓	✓	✓	✓	8
EURO	Eastern Europe	Romania	✓	✓	✓	✓	✓	✓	✓	✓	8
EURO	Eastern Europe	Russian Federation	✓	✓	✓	✓	✓	✓	✓	✓	8
EURO	Eastern Europe	Ukraine	✓	✓	✓	✓	✓	✓	✓	✓	8
EURO	Northern Europe	Denmark	✓	✓	✓	✓	✓	✓	✓	✓	8
EURO	Northern Europe	Estonia	✓	✓	✓	✓	✓	✓	✓	✓	8
EURO	Northern Europe	Finland	✓	✓	✓	✓	✓	✓	✓	✓	8
EURO	Northern Europe	Latvia	✓	✓	✓	✓	✓	✓	✓	✓	8
EURO	Northern Europe	Lithuania	✓	✓	✓	✓	✓	✓	✓	✓	8
EURO	Northern Europe	Norway	✓	✓	✓	✓	✓	✓	✓	✓	8

EURO	Northern Europe	United Kingdom	✓	✓	✓	✓	✓	✓	✓	✓	8
EURO	South West Europe	Belgium	✓	✓	✓	✓	✓	✓	✓	✓	8
EURO	South West Europe	France	✓	✓	✓	✓	✓	✓	✓	✓	8
EURO	South West Europe	Greece	✓	✓	✓	✓	✓	✓	✓	✓	8
EURO	South West Europe	Italy	✓	✓	✓	✓	✓	✓	✓	✓	8
EURO	South West Europe	Netherlands	✓	✓	✓	✓	✓	✓	✓	✓	8
EURO	South West Europe	Serbia	✓	✓	✓	✓	✓	✓	✓	✓	8
EURO	South West Europe	Slovenia	✓	✓	✓	✓	✓	✓	✓	✓	8
EURO	South West Europe	Spain	✓	✓	✓	✓	✓	✓	✓	✓	8
EURO	South West Europe	Switzerland	✓	✓	✓	✓	✓	✓	✓	✓	8
EURO	Western Asia	Turkey	✓	✓	✓	✓	✓	✓	✓	✓	8
PAHO	Central America and Caribbean	Costa Rica	✓	✓	✓	✓	✓	✓	✓	✓	8
PAHO	Central America and Caribbean	Cuba	✓	✓	✓	✓	✓	✓	✓	✓	8
PAHO	Central America and Caribbean	El Salvador	✓	✓	✓	✓	✓	✓	✓	✓	8
PAHO	Central America and Caribbean	Guadeloupe	✓	✓	✓	✓	✓	✓	✓	✓	8
PAHO	Central America and Caribbean	Guatemala	✓	✓	✓	✓	✓	✓	✓	✓	8
PAHO	Central America and Caribbean	Honduras	✓	✓	✓	✓	✓	✓	✓	✓	8
PAHO	Central America and Caribbean	Jamaica	✓	✓	✓	✓	✓	✓	✓	✓	8
PAHO	Central America and Caribbean	Martinique	✓	✓	✓	✓	✓	✓	✓	✓	8
PAHO	Central America and Caribbean	Mexico	✓	✓	✓	✓	✓	✓	✓	✓	8
PAHO	Central America and Caribbean	Panama	✓	✓	✓	✓	✓	✓	✓	✓	8
PAHO	North America	Canada	✓	✓	✓	✓	✓	✓	✓	✓	8
PAHO	North America	United States of America	✓	✓	✓	✓	✓	✓	✓	✓	8
PAHO	Temperate South America	Argentina	✓	✓	✓	✓	✓	✓	✓	✓	8
PAHO	Temperate South America	Chile	✓	✓	✓	✓	✓	✓	✓	✓	8
PAHO	Temperate South America	Paraguay	✓	✓	✓	✓	✓	✓	✓	✓	8
PAHO	Tropical South America	Brazil	✓	✓	✓	✓	✓	✓	✓	✓	8
PAHO	Tropical South America	Colombia	✓	✓	✓	✓	✓	✓	✓	✓	8
PAHO	Tropical South America	Ecuador	✓	✓	✓	✓	✓	✓	✓	✓	8
PAHO	Tropical South America	French Guiana	✓	✓	✓	✓	✓	✓	✓	✓	8
PAHO	Tropical South America	Peru	✓	✓	✓	✓	✓	✓	✓	✓	8
PAHO	Tropical South America	Venezuela	✓	✓	✓	✓	✓	✓	✓	✓	8
SEARO	South-East Asia	Indonesia	✓	✓	✓	✓	✓	✓	✓	✓	8
SEARO	South-East Asia	Myanmar	✓	✓	✓	✓	✓	✓	✓	✓	8
SEARO	South-East Asia	Thailand	✓	✓	✓	✓	✓	✓	✓	✓	8
SEARO	Southern Asia	Bangladesh	✓	✓	✓	✓	✓	✓	✓	✓	8
SEARO	Southern Asia	Bhutan	✓	✓	✓	✓	✓	✓	✓	✓	8
SEARO	Southern Asia	India	✓	✓	✓	✓	✓	✓	✓	✓	8
SEARO	Southern Asia	Nepal	✓	✓	✓	✓	✓	✓	✓	✓	8
SEARO	Southern Asia	Sri Lanka	✓	✓	✓	✓	✓	✓	✓	✓	8
WPRO	Eastern Asia	China	✓	✓	✓	✓	✓	✓	✓	✓	8
WPRO	Eastern Asia	Japan	✓	✓	✓	✓	✓	✓	✓	✓	8
WPRO	Eastern Asia	Mongolia	✓	✓	✓	✓	✓	✓	✓	✓	8
WPRO	Eastern Asia	South Korea	✓	✓	✓	✓	✓	✓	✓	✓	8
WPRO	Oceania Melanesia Polynesia	Australia	✓	✓	✓	✓	✓	✓	✓	✓	8
WPRO	Oceania Melanesia Polynesia	Fiji	✓	✓	✓	✓	✓	✓	✓	✓	8
WPRO	Oceania Melanesia Polynesia	New Caledonia	✓	✓	✓	✓	✓	✓	✓	✓	8
WPRO	Oceania Melanesia Polynesia	New Zealand	✓	✓	✓	✓	✓	✓	✓	✓	8
WPRO	Oceania Melanesia Polynesia	Papua New Guinea	✓	✓	✓	✓	✓	✓	✓	✓	8
WPRO	South-East Asia	Cambodia	✓	✓	✓	✓	✓	✓	✓	✓	8
WPRO	South-East Asia	Laos	✓	✓	✓	✓	✓	✓	✓	✓	8
WPRO	South-East Asia	Malaysia	✓	✓	✓	✓	✓	✓	✓	✓	8
WPRO	South-East Asia	Philippines	✓	✓	✓	✓	✓	✓	✓	✓	8
WPRO	South-East Asia	Singapore	✓	✓	✓	✓	✓	✓	✓	✓	8
WPRO	South-East Asia	Viet Nam	✓	✓	✓	✓	✓	✓	✓	✓	8
AFRO	Eastern Africa	Seychelles	✗	✓	✓	✓	✓	✓	✓	✓	7
AFRO	Middle Africa	Chad	✗	✓	✓	✓	✓	✓	✓	✓	7
AFRO	Middle Africa	South Sudan	✗	✓	✓	✓	✓	✓	✓	✓	7
EURO	Central Asia	Kazakhstan	✓	✓	✓	✗	✓	✓	✓	✓	7
EURO	Central Asia	Kyrgyzstan	✓	✓	✓	✗	✓	✓	✓	✓	7

EURO	Central Asia	Tajikistan	✓	✓	✓	✗	✓	✓	✓	✓	7
EURO	Central Asia	Turkmenistan	✓	✓	✓	✗	✓	✓	✓	✓	7
EURO	Central Asia	Uzbekistan	✓	✓	✓	✗	✓	✓	✓	✓	7
EURO	Eastern Europe	Belarus	✓	✓	✓	✗	✓	✓	✓	✓	7
EURO	Eastern Europe	Bulgaria	✓	✓	✓	✗	✓	✓	✓	✓	7
EURO	Eastern Europe	Czechia	✓	✓	✓	✗	✓	✓	✓	✓	7
EURO	Eastern Europe	Hungary	✓	✓	✓	✗	✓	✓	✓	✓	7
EURO	Eastern Europe	Kosovo	✓	✓	✓	✗	✓	✓	✓	✓	7
EURO	Eastern Europe	Moldova	✓	✓	✓	✗	✓	✓	✓	✓	7
EURO	Eastern Europe	Slovakia	✓	✓	✓	✗	✓	✓	✓	✓	7
EURO	Northern Europe	Iceland	✓	✓	✓	✗	✓	✓	✓	✓	7
EURO	Northern Europe	Ireland	✓	✓	✓	✗	✓	✓	✓	✓	7
EURO	Northern Europe	Sweden	✓	✓	✓	✗	✓	✓	✓	✓	7
EURO	South West Europe	Albania	✓	✓	✓	✗	✓	✓	✓	✓	7
EURO	South West Europe	Austria	✓	✓	✓	✗	✓	✓	✓	✓	7
EURO	South West Europe	Bosnia and Herzegovina	✓	✓	✓	✗	✓	✓	✓	✓	7
EURO	South West Europe	Croatia	✓	✓	✓	✗	✓	✓	✓	✓	7
EURO	South West Europe	Germany	✓	✓	✓	✗	✓	✓	✓	✓	7
EURO	South West Europe	Luxembourg	✓	✓	✓	✗	✓	✓	✓	✓	7
EURO	South West Europe	Malta	✓	✓	✓	✗	✓	✓	✓	✓	7
EURO	South West Europe	Montenegro	✓	✓	✓	✗	✓	✓	✓	✓	7
EURO	South West Europe	North Macedonia	✓	✓	✓	✗	✓	✓	✓	✓	7
EURO	South West Europe	Portugal	✓	✓	✓	✗	✓	✓	✓	✓	7
EURO	Western Asia	Armenia	✓	✓	✓	✗	✓	✓	✓	✓	7
EURO	Western Asia	Azerbaijan	✓	✓	✓	✗	✓	✓	✓	✓	7
EURO	Western Asia	Cyprus	✓	✓	✓	✗	✓	✓	✓	✓	7
EURO	Western Asia	Georgia	✓	✓	✓	✗	✓	✓	✓	✓	7
EURO	Western Asia	Israel	✓	✓	✓	✗	✓	✓	✓	✓	7
PAHO	Central America and Caribbean	Belize	✓	✓	✓	✗	✓	✓	✓	✓	7
PAHO	Central America and Caribbean	Dominican Republic	✓	✓	✓	✗	✓	✓	✓	✓	7
PAHO	Central America and Caribbean	Haiti	✓	✓	✓	✗	✓	✓	✓	✓	7
PAHO	Central America and Caribbean	Nicaragua	✓	✓	✓	✗	✓	✓	✓	✓	7
PAHO	Central America and Caribbean	Saint Lucia	✓	✓	✓	✗	✓	✓	✓	✓	7
PAHO	Temperate South America	Uruguay	✓	✓	✓	✗	✓	✓	✓	✓	7
PAHO	Tropical South America	Bolivia	✓	✓	✓	✗	✓	✓	✓	✓	7
PAHO	Tropical South America	Suriname	✓	✓	✓	✗	✓	✓	✓	✓	7
SEARO	South-East Asia	Timor-Leste	✓	✓	✓	✓	✗	✓	✓	✓	7
SEARO	Southern Asia	Maldives	✗	✓	✓	✓	✓	✓	✓	✓	7
EMRO	Western Asia	Kuwait	✗	✓	✓	✗	✓	✓	✓	✓	6
PAHO	Central America and Caribbean	Barbados	✗	✓	✓	✗	✓	✓	✓	✓	6
PAHO	Central America and Caribbean	Trinidad and Tobago	✗	✓	✓	✗	✓	✓	✓	✓	6
EMRO	Western Asia	United Arab Emirates	✗	✓	✓	✗	✗	✓	✓	✓	5
PAHO	Central America and Caribbean	Dominica	✗	✓	✓	✗	✗	✓	✓	✓	5
EMRO	Western Asia	Saudi Arabia	✓	✓	✗	✗	✓	✗	✗	✓	4
EMRO	Western Asia	West Bank and Gaza Strip	✗	✓	✓	✗	✓	✗	✗	✓	4
EMRO	Western Asia	Yemen	✗	✓	✓	✗	✓	✗	✗	✓	4
PAHO	Central America and Caribbean	Anguilla	✗	✓	✓	✗	✗	✗	✓	✓	4
PAHO	Central America and Caribbean	Saint Kitts and Nevis	✗	✓	✓	✗	✗	✓	✓	✗	4
SEARO	Eastern Asia	North Korea	✗	✓	✓	✓	✗	✗	✗	✓	4
PAHO	Central America and Caribbean	Aruba	✗	✓	✗	✗	✗	✓	✗	✓	3
PAHO	Central America and Caribbean	Bahamas	✗	✓	✓	✗	✗	✗	✓	✗	3
PAHO	Central America and Caribbean	Cayman Islands	✗	✓	✓	✗	✗	✗	✗	✓	3
PAHO	Central America and Caribbean	Saint Vincent and the Grenadines	✗	✓	✓	✗	✗	✗	✓	✗	3
PAHO	Central America and Caribbean	Turks and Caicos Islands	✗	✓	✓	✗	✗	✗	✓	✗	3
PAHO	North America	Bermuda	✗	✓	✓	✗	✗	✗	✓	✗	3
PAHO	Central America and Caribbean	Grenada	✗	✓	✗	✗	✗	✗	✓	✗	2
PAHO	Central America and Caribbean	Antigua and Barbuda	✗	✗	✗	✗	✗	✗	✓	✗	1
PAHO	Central America and Caribbean	British Virgin Islands	✗	✓	✗	✗	✗	✗	✗	✗	1
PAHO	Central America and Caribbean	Montserrat	✗	✗	✗	✗	✗	✗	✗	✗	0
PAHO	Central America and Caribbean	Saint Barthelemy	✗	✗	✗	✗	✗	✗	✗	✗	0

PAHO	Central America and Caribbean	Saint Martin	✗	✗	✗	✗	✗	✗	✗	✗	0
PAHO	Tropical South America	Guyana	✗	✗	✗	✗	✗	✗	✗	✗	0
	Total Reporting Countries		**146**	**168**	**164**	**112**	**154**	**156**	**162**	**161**	**173**

Supplementary Table S9. The *reporting* and *diagnostic coverage* scores for each Member State reporting influenza virological data to the WHO's FluNet as of 15 June 2021. Scores range the set of all positive integers (Z^+). For this surveillance system, reporting coverage ranged from 0-11 national influenza centers (NICs) and diagnostic coverage ranged 0-5846 laboratory testing facilities. We estimated facilities per million persons (FPM) as the number of laboratory testing facilities divided by 2021 population estimates and multiplied by 1,000,000. We denoted Member States where we could not estimate the number of facilities using *NR*. We list Member States in descending order by NICs, facilities, and FPM.

Region	Zone	Member States	NICs	Facilities	Population	FPM
PAHO	North America	Canada	11	147	37943231	3.87
EURO	South West Europe	Spain	3	682	47260584	14.43
EURO	Northern Europe	United Kingdom	3	590	66052076	8.93
PAHO	Tropical South America	Brazil	3	258	213445417	1.21
EURO	Eastern Europe	Romania	3	211	21230362	9.94
SEARO	Southern Asia	India	3	54	1339330514	0.04
PAHO	Temperate South America	Argentina	3	44	45864941	0.96
WPRO	Oceania Melanesia Polynesia	Australia	3	NR	25809973	NR
WPRO	Eastern Asia	China	2	977	1397897720	0.70
EURO	South West Europe	France	2	961	68084217	14.11
EURO	Eastern Europe	Russian Federation	2	158	142320790	1.11
EMRO	Northern Africa	Egypt	2	30	106437241	0.28
WPRO	South-East Asia	Viet Nam	2	18	102789598	0.18
WPRO	Oceania Melanesia Polynesia	New Zealand	2	NR	4991442	NR
WPRO	South-East Asia	Malaysia	2	NR	33519406	NR
AFRO	Southern Africa	South Africa	2	NR	56978635	NR
EURO	Northern Europe	Norway	1	5846	5509591	1061.06
EURO	Eastern Europe	Czechia	1	3570	10702596	333.56
PAHO	North America	United States of America	1	3100	334998398	9.25
EURO	South West Europe	Croatia	1	2570	4208973	610.60
EURO	Eastern Europe	Hungary	1	1375	9728337	141.34
EURO	South West Europe	Italy	1	1317	62390364	21.11
PAHO	Central America and Caribbean	Mexico	1	995	130207371	7.64
EURO	South West Europe	Germany	1	650	79903481	8.13
EMRO	Southern Asia	Afghanistan	1	548	37466414	14.63
EURO	Eastern Europe	Poland	1	536	38185913	14.04
EURO	Eastern Europe	Moldova	1	519	3323875	156.14
EMRO	Northern Africa	Morocco	1	498	35892951	13.87
EURO	Northern Europe	Estonia	1	478	1220042	391.79
EURO	South West Europe	Netherlands	1	409	17337403	23.59
EURO	South West Europe	Portugal	1	301	10263850	29.33
EURO	Western Asia	Turkey	1	230	82482383	2.79
EURO	South West Europe	Belgium	1	222	11778842	18.85
EURO	Eastern Europe	Bulgaria	1	218	6919180	31.51
EURO	Eastern Europe	Belarus	1	213	9441842	22.56
EURO	Northern Europe	Finland	1	198	5587442	35.44
WPRO	Eastern Asia	Mongolia	1	189	3198913	59.08
EURO	Northern Europe	Sweden	1	186	10261767	18.13
EURO	South West Europe	Switzerland	1	175	8453550	20.70
WPRO	South-East Asia	Singapore	1	169	5866139	28.81
EURO	South West Europe	Serbia	1	168	6974289	24.09
EURO	Eastern Europe	Slovakia	1	162	5436066	29.80
PAHO	Central America and Caribbean	Cuba	1	154	11032343	13.96
EURO	South West Europe	Greece	1	145	10569703	13.72
EMRO	Northern Africa	Tunisia	1	110	11811335	9.31
EURO	Northern Europe	Denmark	1	100	5894687	16.96
WPRO	Eastern Asia	South Korea	1	100	51715162	1.93
EURO	Northern Europe	Iceland	1	94	354234	265.36
EURO	Northern Europe	Lithuania	1	94	2711566	34.67
EURO	South West Europe	Austria	1	85	8884864	9.57

EURO	Northern Europe	Latvia	1	81	1862687	43.49
PAHO	Temperate South America	Chile	1	79	18307925	4.32
EURO	Western Asia	Cyprus	1	74	1281506	57.74
SEARO	South-East Asia	Thailand	1	64	69480520	0.92
EURO	Northern Europe	Ireland	1	60	5224884	11.48
EURO	South West Europe	Albania	1	58	3088385	18.78
EURO	Central Asia	Kazakhstan	1	57	19245793	2.96
SEARO	Eastern Asia	North Korea	1	54	25831360	2.09
SEARO	Southern Asia	Bangladesh	1	54	164098818	0.33
AFRO	Eastern Africa	Madagascar	1	52	27534354	1.89
PAHO	Tropical South America	Peru	1	46	32201224	1.43
EURO	South West Europe	Slovenia	1	45	2102106	21.41
PAHO	Temperate South America	Uruguay	1	44	3398239	12.95
EURO	South West Europe	Montenegro	1	41	607414	67.50
EMRO	Western Asia	Iraq	1	40	39650145	1.01
EURO	Western Asia	Israel	1	33	8787045	3.76
SEARO	South-East Asia	Indonesia	1	33	275122131	0.12
PAHO	Tropical South America	Colombia	1	32	50355650	0.64
AFRO	Middle Africa	Cameroon	1	31	28524175	1.09
SEARO	Southern Asia	Nepal	1	27	30424878	0.89
PAHO	Central America and Caribbean	Panama	1	24	3928646	6.11
AFRO	Western Africa	Ghana	1	24	32372889	0.74
WPRO	South-East Asia	Philippines	1	24	110818325	0.22
SEARO	Southern Asia	Sri Lanka	1	23	23044123	1.00
PAHO	Central America and Caribbean	Costa Rica	1	21	5151140	4.08
EURO	South West Europe	North Macedonia	1	19	2128262	8.93
EMRO	Western Asia	United Arab Emirates	1	19	9856612	1.93
PAHO	Tropical South America	Ecuador	1	18	17093159	1.05
PAHO	Central America and Caribbean	Nicaragua	1	17	6243931	2.72
PAHO	Temperate South America	Paraguay	1	17	7272639	2.34
EURO	Eastern Europe	Ukraine	1	17	43745640	0.39
AFRO	Western Africa	Senegal	1	16	16082442	0.99
EURO	South West Europe	Luxembourg	1	15	639589	23.45
WPRO	South-East Asia	Cambodia	1	15	17304363	0.87
AFRO	Western Africa	Côte d'Ivoire	1	15	28088455	0.53
PAHO	Central America and Caribbean	El Salvador	1	14	6528135	2.14
WPRO	South-East Asia	Laos	1	13	7574356	1.72
EURO	Western Asia	Armenia	1	12	3011609	3.98
EURO	Central Asia	Kyrgyzstan	1	12	6018789	1.99
PAHO	Central America and Caribbean	Dominican Republic	1	12	10597348	1.13
AFRO	Eastern Africa	Kenya	1	11	54685051	0.20
PAHO	Central America and Caribbean	Honduras	1	10	9346277	1.07
AFRO	Eastern Africa	Uganda	1	10	44712143	0.22
EURO	South West Europe	Malta	1	9	460891	19.53
PAHO	Central America and Caribbean	Guatemala	1	9	17422821	0.52
AFRO	Eastern Africa	Zambia	1	9	19077816	0.47
EMRO	Southern Asia	Pakistan	1	9	238181034	0.04
EMRO	Western Asia	Lebanon	1	8	5261372	1.52
AFRO	Northern Africa	Algeria	1	7	43576691	0.16
PAHO	Central America and Caribbean	Jamaica	1	6	2816602	2.13
EURO	Western Asia	Georgia	1	6	4933674	1.22
AFRO	Eastern Africa	Tanzania	1	6	62092761	0.10
AFRO	Middle Africa	Central African Republic	1	5	5357984	0.93
EMRO	Western Asia	Oman	1	4	3694755	1.08
AFRO	Western Africa	Nigeria	1	4	219463862	0.02
PAHO	Central America and Caribbean	Trinidad and Tobago	1	2	1221047	1.64
EURO	Central Asia	Turkmenistan	1	2	5579889	0.36
SEARO	South-East Asia	Myanmar	1	2	57069099	0.04
WPRO	Oceania Melanesia Polynesia	Papua New Guinea	1	0	7399757	0.00
AFRO	Eastern Africa	Mauritius	1	NR	1386129	NR

WPRO	Eastern Asia	Japan	1	NR	124687293	NR
EMRO	Northern Africa	Sudan	1	NR	46751152	NR
EMRO	Southern Asia	Iran	1	NR	85888910	NR
PAHO	Tropical South America	Venezuela	1	NR	29069153	NR
EMRO	Western Asia	Bahrain	1	NR	1526929	NR
EMRO	Western Asia	Jordan	1	NR	10909567	NR
EMRO	Western Asia	Kuwait	1	NR	3032065	NR
EMRO	Western Asia	Qatar	1	NR	2479995	NR
EMRO	Western Asia	Saudi Arabia	1	NR	34783757	NR
EMRO	Western Asia	Syrian Arab Republic	1	NR	20384316	NR
EURO	Central Asia	Tajikistan	0	3087	8990874	343.35
EURO	South West Europe	Bosnia and Herzegovina	0	167	3824782	43.66
EURO	Eastern Europe	Kosovo	0	44	1935259	22.74
PAHO	Central America and Caribbean	Saint Lucia	0	41	166637	246.04
EURO	Western Asia	Azerbaijan	0	36	10282283	3.50
SEARO	Southern Asia	Bhutan	0	18	857423	20.99
PAHO	Central America and Caribbean	Haiti	0	15	11198240	1.34
SEARO	South-East Asia	Timor-Leste	0	13	1413958	9.19
AFRO	Western Africa	Niger	0	12	23605767	0.51
PAHO	Tropical South America	Bolivia	0	11	11758869	0.94
AFRO	Middle Africa	Democratic Republic of the Congo	0	11	105044646	0.10
PAHO	Central America and Caribbean	British Virgin Islands	0	10	37891	263.91
AFRO	Eastern Africa	Seychelles	0	10	96387	103.75
PAHO	Central America and Caribbean	Belize	0	10	405633	24.65
AFRO	Western Africa	Mali	0	8	20137527	0.40
AFRO	Eastern Africa	Ethiopia	0	8	110871031	0.07
PAHO	Tropical South America	Suriname	0	7	614749	11.39
PAHO	Central America and Caribbean	Grenada	0	6	113570	52.83
AFRO	Eastern Africa	Rwanda	0	6	12943132	0.46
AFRO	Western Africa	Burkina Faso	0	6	21382659	0.28
AFRO	Eastern Africa	Mozambique	0	6	30888034	0.19
SEARO	Southern Asia	Maldives	0	5	390669	12.80
AFRO	Western Africa	Mauritania	0	4	4079284	0.98
AFRO	Western Africa	Sierra Leone	0	4	6807277	0.59
AFRO	Western Africa	Togo	0	4	8283189	0.48
EURO	Central Asia	Uzbekistan	0	4	30842796	0.13
PAHO	Central America and Caribbean	Barbados	0	3	301865	9.94
AFRO	Middle Africa	Congo	0	3	5417414	0.55
PAHO	Central America and Caribbean	Dominica	0	1	74584	13.41
PAHO	Central America and Caribbean	Saint Vincent and the Grenadines	0	1	101145	9.89
PAHO	Central America and Caribbean	Anguilla	0	NR	18403	NR
PAHO	Central America and Caribbean	Antigua and Barbuda	0	NR	99175	NR
PAHO	Central America and Caribbean	Aruba	0	NR	120917	NR
PAHO	Central America and Caribbean	Bahamas	0	NR	352655	NR
PAHO	Central America and Caribbean	Cayman Islands	0	NR	63131	NR
PAHO	Central America and Caribbean	Guadeloupe	0	NR	375693	NR
PAHO	Central America and Caribbean	Martinique	0	NR	354824	NR
PAHO	Central America and Caribbean	Saint Kitts and Nevis	0	NR	54149	NR
PAHO	Central America and Caribbean	Turks and Caicos Islands	0	NR	57196	NR
AFRO	Middle Africa	Angola	0	NR	33642646	NR
AFRO	Middle Africa	Chad	0	NR	17414108	NR
AFRO	Middle Africa	South Sudan	0	NR	10984074	NR
PAHO	North America	Bermuda	0	NR	72084	NR
WPRO	Oceania Melanesia Polynesia	Fiji	0	NR	939535	NR
WPRO	Oceania Melanesia Polynesia	New Caledonia	0	NR	293608	NR
PAHO	Tropical South America	French Guiana	0	NR	294146	NR
PAHO	Tropical South America	Guyana	0	NR	787971	NR
AFRO	Western Africa	Guinea	0	NR	12877894	NR
EMRO	Western Asia	West Bank and Gaza Strip	0	NR	4906308	NR
EMRO	Western Asia	Yemen	0	NR	30399243	NR

Supplementary Table S10. The average and median *extent* of 173 Member States for 6 test outcomes (specimens collected (SPE), specimens processed or tests (TES), influenza A positives (FLUA), influenza B positives (FLUB), total positives (POS), and total negatives (NEG)) reported by the WHO's FluNet. We downloaded data on 15 June 2021 at which time the total time series length was 1381 weeks. We calculated *extent* as the length of a time series (number of weeks) from the first to last week of complete records. We reported average *extent* with 95% confidence intervals (top values) and median *extent* with lower and upper quartile bounds (bottom values) by 6 regions and 17 influenza transmission zones. We report regions and zones in the order of average *extent* of total positives (POS). We indicate zone-outcome dyads where all Member States had incomplete records using *Missing*. We omit the Southern African zone, as it only consisted of 1 country.

Region	POS	FLUA	FLUB	NEG	SPE	TES
EURO	991.31 [890.05, 1092.57] 1265.00 [634.00, 1274.00]	991.29 [890.04, 1092.55] 1265.00 [634.00, 1274.00]	952.00 [851.21, 1052.79] 1169.00 [613.00, 1272.00]	185.50 [141.40, 229.60] 187.00 [148.00, 223.00]	234.82 [139.73, 329.90] 88.50 [63.00, 405.00]	920.10 [825.64, 1014.55] 1075.00 [631.00, 1225.00]
WPRO	967.27 [803.38, 1131.16] 1016.00 [767.00, 1275.00]	966.40 [802.81, 1129.99] 1016.00 [767.00, 1275.00]	931.07 [771.54, 1090.60] 939.00 [754.00, 1269.00]	251.31 [223.66, 278.96] 263.00 [228.00, 282.00]	553.14 [475.29, 631.00] 592.00 [542.00, 633.00]	942.00 [777.14, 1106.86] 984.00 [767.00, 1230.00]
SEARO	654.82 [417.42, 892.21] 542.00 [261.00, 1194.00]	649.91 [416.70, 883.12] 542.00 [261.00, 1147.00]	592.27 [399.85, 784.70] 542.00 [261.00, 861.00]	244.80 [215.60, 274.00] 243.00 [227.00, 261.00]	472.73 [371.69, 573.76] 542.00 [261.00, 618.00]	611.64 [403.56, 819.71] 542.00 [261.00, 869.00]
PAHO	630.28 [495.87, 764.69] 633.00 [177.00, 1112.00]	640.02 [505.15, 774.90] 635.00 [231.00, 1112.00]	600.43 [463.98, 736.88] 615.00 [165.00, 1011.00]	565.82 [434.07, 697.56] 590.50 [231.00, 822.00]	286.40 [187.77, 385.03] 212.00 [112.00, 523.50]	654.89 [532.94, 776.84] 636.00 [307.50, 1047.50]
AFRO	609.53 [477.66, 741.40] 583.50 [434.00, 791.00]	607.80 [476.84, 738.76] 583.50 [434.00, 791.00]	591.93 [464.07, 719.79] 583.50 [434.00, 703.00]	168.00 [116.21, 219.79] 214.00 [21.00, 241.00]	477.93 [403.54, 552.33] 576.50 [434.00, 620.00]	604.73 [475.21, 734.26] 583.50 [434.00, 791.00]
EMRO	531.16 [335.79, 726.52] 476.00 [128.00, 707.00]	527.58 [333.92, 721.24] 476.00 [126.00, 707.00]	502.79 [325.65, 679.92] 476.00 [128.00, 707.00]	210.47 [172.48, 248.46] 232.00 [191.00, 253.00]	426.26 [321.05, 531.48] 481.00 [191.00, 624.00]	522.00 [360.58, 683.42] 481.00 [191.00, 707.00]
Zone						
Temperate South America	1192.00 [1107.07, 1276.93] 1202.00 [1120.50, 1263.50]	1182.00 [1108.07, 1255.93] 1194.00 [1120.50, 1243.50]	1189.00 [1100.38, 1277.62] 1200.00 [1114.50, 1263.50]	1162.25 [1096.18, 1228.32] 1153.00 [1120.50, 1204.00]	176.75 [13.84, 339.66] 154.50 [43.50, 310.00]	1206.25 [1148.18, 1264.32] 1205.00 [1155.00, 1257.50]
Northern Europe	1155.70 [992.80, 1318.60] 1273.00 [1268.00, 1275.00]	1155.70 [992.80, 1318.60] 1273.00 [1268.00, 1275.00]	1148.00 [984.51, 1311.49] 1272.50 [1267.00, 1275.00]	Missing	64.29 [46.52, 82.05] 65.00 [51.00, 75.00]	1059.10 [891.25, 1226.95] 1179.00 [711.00, 1258.00]
Eastern Europe	1092.55 [895.26, 1289.83] 1269.00 [1063.00, 1273.00]	1092.55 [895.26, 1289.83] 1269.00 [1063.00, 1273.00]	1041.82 [853.75, 1229.89] 1169.00 [954.00, 1266.00]	136.00 [136.00, 136.00] 136.00 [136.00, 136.00]	353.25 [153.89, 552.61] 394.50 [227.00, 479.50]	996.64 [821.59, 1171.68] 1116.00 [958.00, 1175.00]
Southwest Europe	1058.63 [907.45, 1209.81] 1269.00 [740.00, 1275.00]	1058.58 [907.41, 1209.74] 1269.00 [740.00, 1275.00]	1008.11 [851.13, 1165.08] 1209.00 [631.00, 1275.00]	202.00 [159.60, 244.40] 214.00 [160.00, 232.00]	361.44 [203.67, 519.22] 368.00 [90.00, 594.00]	992.26 [842.43, 1142.10] 1110.00 [631.00, 1229.00]
Eastern Asia	919.40 [540.85, 1297.95] 952.00 [856.00, 1275.00]	919.40 [540.85, 1297.95] 952.00 [856.00, 1275.00]	915.60 [538.35, 1292.85] 939.00 [856.00, 1275.00]	223.50 [166.20, 280.80] 234.50 [185.00, 262.00]	509.00 [322.26, 695.74] 592.00 [393.00, 625.00]	804.00 [404.06, 1203.94] 904.00 [541.50, 1066.50]
Northern Africa	916.40 [463.19, 1369.61] 1212.00 [908.00, 1215.00]	916.40 [463.19, 1369.61] 1212.00 [908.00, 1215.00]	754.40 [355.13, 1153.67] 965.00 [623.00, 1057.00]	236.75 [230.18, 243.32] 239.00 [232.50, 241.00]	506.20 [269.28, 743.12] 621.00 [620.00, 623.00]	823.60 [425.57, 1221.63] 1006.00 [908.00, 1068.00]
North America	904.67 [179.81, 1629.53] 1274.00 [165.00, 1275.00]	904.33 [178.82, 1629.85] 1274.00 [164.00, 1275.00]	852.00 [23.92, 1680.09] 1274.00 [7.00, 1275.00]	296.00 [296.00, 296.00] 296.00 [296.00, 296.00]	619.50 [561.68, 677.32] 619.50 [590.00, 649.00]	926.00 [242.95, 1609.05] 1274.00 [229.00, 1275.00]
Oceania Melanesia Polynesia	895.40 [498.62, 1292.18] 1180.00 [585.00, 1183.00]	892.80 [497.79, 1287.81] 1167.00 [585.00, 1183.00]	869.40 [488.37, 1250.43] 1062.00 [584.00, 1180.00]	264.60 [223.32, 305.88] 251.00 [228.00, 284.00]	483.00 [324.18, 641.82] 556.00 [329.00, 628.00]	907.40 [513.66, 1301.14] 1150.00 [628.00, 1230.00]
Tropical South America	890.38 [660.77, 1119.98] 955.00 [649.00, 1167.00]	889.13 [660.50, 1117.75] 955.00 [649.00, 1162.00]	851.25 [625.22, 1077.28] 877.50 [623.00, 1116.50]	760.50 [499.78, 1021.22] 761.50 [448.50, 1078.50]	267.00 [45.77, 488.23] 156.00 [88.00, 457.00]	795.33 [546.89, 1043.78] 896.00 [597.00, 981.00]
Southeast Asia	825.70 [588.45, 1062.95]	825.70 [588.45, 1062.95]	771.30 [557.50, 985.10]	251.56 [226.21, 276.91]	526.00 [411.28, 640.72]	825.70 [588.45, 1062.95]

	836.00 [554.00, 1226.00]	836.00 [554.00, 1226.00]	784.50 [554.00, 1084.00]	263.00 [237.00, 281.00]	572.00 [342.00, 650.00]	836.00 [554.00, 1226.00]
Southern Asia	774.33 [544.92, 1003.75] 610.00 [542.00, 1194.00]	762.89 [544.27, 981.51] 610.00 [542.00, 1147.00]	714.56 [518.85, 910.27] 610.00 [542.00, 788.00]	244.50 [205.99, 283.01] 252.00 [209.50, 270.00]	574.89 [505.60, 644.17] 610.00 [542.00, 624.00]	699.67 [530.01, 869.32] 610.00 [542.00, 798.00]
Eastern Africa	738.90 [504.85, 972.95] 695.50 [511.00, 1156.00]	733.70 [503.41, 963.99] 695.50 [511.00, 1104.00]	725.70 [497.82, 953.58] 665.50 [511.00, 1114.00]	158.67 [61.63, 255.70] 209.00 [8.00, 243.00]	518.30 [414.79, 621.81] 587.50 [511.00, 617.00]	724.30 [499.80, 948.80] 695.50 [511.00, 1010.00]
Western Africa	595.82 [425.02, 766.61] 578.00 [509.00, 648.00]	595.82 [425.02, 766.61] 578.00 [509.00, 648.00]	586.36 [419.34, 753.39] 578.00 [509.00, 646.00]	165.90 [86.88, 244.92] 183.50 [22.00, 239.00]	527.64 [434.16, 621.11] 575.00 [509.00, 638.00]	596.00 [425.18, 766.82] 578.00 [509.00, 650.00]
Central Asia	498.40 [306.31, 690.49] 541.00 [270.00, 696.00]	498.40 [306.31, 690.49] 541.00 [270.00, 696.00]	495.00 [306.51, 683.49] 541.00 [270.00, 696.00]	Missing	Missing	498.40 [306.31, 690.49] 541.00 [270.00, 696.00]
Western Asia	455.89 [296.43, 615.35] 461.00 [166.00, 638.00]	454.83 [295.04, 614.62] 459.50 [166.00, 638.00]	433.28 [285.61, 580.95] 461.00 [153.00, 634.00]	194.18 [138.57, 249.79] 208.00 [128.00, 253.00]	307.14 [187.97, 426.32] 284.00 [75.00, 481.00]	463.50 [326.74, 600.26] 478.50 [191.00, 647.00]
Central America and Caribbean	446.32 [305.45, 587.19] 268.50 [150.50, 733.50]	456.56 [313.05, 600.06] 269.00 [164.00, 754.00]	410.96 [273.41, 548.51] 259.00 [59.00, 700.00]	418.88 [280.08, 557.68] 267.00 [168.00, 693.00]	271.89 [135.41, 408.37] 209.00 [141.00, 342.00]	501.93 [375.22, 628.63] 335.00 [231.50, 754.00]
Middle Africa	309.00 [97.28, 520.72] 143.00 [63.00, 588.00]	309.00 [97.28, 520.72] 143.00 [63.00, 588.00]	308.57 [97.36, 519.78] 143.00 [63.00, 588.00]	119.50 [-93.16, 332.16] 119.50 [11.00, 228.00]	300.43 [98.56, 502.30] 143.00 [63.00, 588.00]	309.00 [97.28, 520.72] 143.00 [63.00, 588.00]
Worldwide	**755.91 [690.51, 821.31]** **701.00 [336.00, 1224.00]**	**757.98 [692.79, 823.16]** **703.50 [385.00, 1224.00]**	**723.58 [659.90, 787.26]** **697.00 [385.00, 1165.50]**	**342.12 [281.42, 402.81]** **242.00 [191.00, 296.00]**	**398.92 [356.30, 441.54]** **510.00 [149.50, 609.00]**	**732.05 [672.67, 791.43]** **701.00 [336.00, 1120.00]**

Supplementary Table S11. The *extent* of 173 Member States for 6 test outcomes (specimens collected (SPE), specimens processed or tests (TES), influenza A positives (FLUA), influenza B positives (FLUB), total positives (POS), and total negatives (NEG)) reported by the WHO's FluNet. We downloaded data on 15 June 2021 at which time the total time series length of reported data was 1381 weeks. We calculated *extent* as the length of a time series (number of weeks) from the first to last week of complete records. We list Member States in descending order by average *extent* across all 6 outcomes (AVG), region, and zone. We denote Member State-outcome dyads where all 1381 weeks had incomplete records using *M*.

Region	Zone	Member States	POS	FLUA	FLUB	NEG	SPE	TES	AVG
EURO	South West Europe	Portugal	1292	1292	1289	M	M	1292	1291
PAHO	Tropical South America	Colombia	1266	1266	1261	1265	M	1267	1265
EURO	South West Europe	Germany	1279	1279	1274	M	M	1227	1265
EURO	Northern Europe	Sweden	1272	1272	1272	M	M	1230	1262
EURO	Northern Europe	Iceland	1275	1275	1275	M	M	1170	1249
EURO	Eastern Europe	Slovakia	1273	1273	1270	M	M	1175	1248
EURO	Eastern Europe	Hungary	1273	1273	1266	M	M	1168	1245
EURO	Northern Europe	Ireland	1271	1271	1270	M	M	1123	1234
EURO	South West Europe	Austria	1265	1265	1261	M	M	1110	1225
EURO	Eastern Europe	Belarus	1269	1269	1162	M	M	1163	1216
EURO	Eastern Europe	Czechia	1209	1209	1206	M	M	1195	1205
EURO	South West Europe	Croatia	1200	1200	1193	M	M	1096	1172
PAHO	North America	Canada	1274	1274	1274	M	590	1274	1137
EURO	South West Europe	Slovenia	1329	1329	1081	M	535	1329	1121
PAHO	Central America and Caribbean	Mexico	1120	1120	1120	1120	M	1120	1120
EURO	South West Europe	Switzerland	1379	1379	1379	M	58	1379	1115
PAHO	Temperate South America	Argentina	1253	1237	1253	1253	382	1254	1105
EURO	South West Europe	France	1275	1275	1275	M	368	1275	1094
EURO	Eastern Europe	Bulgaria	1220	1220	954	M	M	958	1088
PAHO	Tropical South America	Brazil	1222	1212	1222	1178	457	1224	1086
EURO	Eastern Europe	Romania	1271	1271	1211	M	384	1265	1080
PAHO	Temperate South America	Chile	1274	1250	1274	1155	238	1261	1075
PAHO	Central America and Caribbean	Cuba	1262	1262	1261	1262	16	1328	1065
EURO	Northern Europe	Latvia	1328	1328	1273	M	51	1328	1062
EURO	Eastern Europe	Poland	1274	1274	1169	M	405	1116	1048
EURO	South West Europe	Greece	1271	1271	1209	M	281	1165	1039
WPRO	Eastern Asia	Japan	1287	1287	1281	282	M	M	1034
EURO	Northern Europe	United Kingdom	1275	1275	1275	M	63	1264	1030
AFRO	Eastern Africa	Mauritius	1168	1168	1114	M	529	1168	1029
EURO	Northern Europe	Norway	1274	1274	1274	M	65	1258	1029
EURO	South West Europe	Netherlands	1275	1274	1275	M	87	1229	1028
EURO	Northern Europe	Denmark	1268	1268	1267	M	100	1188	1018
WPRO	Oceania Melanesia Polynesia	Australia	1277	1277	1269	337	650	1277	1015
AFRO	Western Africa	Senegal	1327	1327	1277	231	575	1327	1011
EURO	Western Asia	Israel	1271	1271	1271	M	1	1225	1008
PAHO	North America	United States of America	1275	1275	1275	296	649	1275	1008
AFRO	Southern Africa	South Africa	1272	1272	1268	283	625	1272	999
EURO	South West Europe	Belgium	1273	1273	1272	M	90	1075	997
WPRO	South-East Asia	Philippines	1245	1245	1115	292	799	1245	990
WPRO	South-East Asia	Malaysia	1277	1277	1276	176	650	1277	989
EURO	South West Europe	Italy	1269	1269	1268	232	643	1223	984
WPRO	Eastern Asia	China	1275	1275	1275	242	625	1181	979
AFRO	Eastern Africa	Zambia	1276	1276	1258	189	596	1276	979
EURO	South West Europe	Spain	1275	1275	1275	214	594	1229	977
PAHO	Temperate South America	Paraguay	1151	1151	1147	1151	71	1156	971
SEARO	South-East Asia	Thailand	1226	1226	1084	284	650	1226	949
EMRO	Southern Asia	Iran	1271	1222	1271	182	624	1074	941
EURO	Northern Europe	Finland	1275	1275	1275	M	75	711	922
EURO	Eastern Europe	Russian Federation	1273	1273	1270	136	554	1016	920

PAHO	Temperate South America	Uruguay	1090	1090	1082	1090	16	1154	920
EMRO	Northern Africa	Tunisia	1212	1212	1113	238	620	1113	918
SEARO	Southern Asia	Sri Lanka	1201	1147	788	M	618	798	910
SEARO	Southern Asia	India	1194	1194	1092	157	626	1120	897
EMRO	Northern Africa	Egypt	1215	1215	1057	240	644	1006	896
WPRO	Oceania Melanesia Polynesia	New Caledonia	1183	1183	1062	223	556	1150	893
EMRO	Northern Africa	Morocco	1224	1224	965	242	621	1068	891
AFRO	Eastern Africa	Madagascar	1156	1104	1156	278	620	1010	887
WPRO	Oceania Melanesia Polynesia	New Zealand	1180	1167	1180	228	329	1230	886
EURO	South West Europe	Luxembourg	910	910	799	M	M	910	882
PAHO	Tropical South America	Peru	1014	1014	1011	979	156	981	859
EURO	Eastern Europe	Ukraine	1063	1063	1059	M	70	1014	854
PAHO	Central America and Caribbean	Jamaica	1224	1224	700	648	141	1114	842
PAHO	Tropical South America	French Guiana	1112	1112	943	242	608	974	832
PAHO	Central America and Caribbean	Dominican Republic	815	815	815	815	M	882	828
WPRO	Eastern Asia	Mongolia	856	856	856	M	625	856	810
EURO	South West Europe	Albania	1058	1058	550	M	M	550	804
WPRO	South-East Asia	Singapore	1016	1016	754	263	633	1016	783
AFRO	Eastern Africa	Kenya	799	799	799	M	622	799	764
WPRO	Eastern Asia	South Korea	952	952	939	143	559	952	750
EURO	Western Asia	Turkey	1052	1052	793	M	49	748	739
PAHO	Tropical South America	Venezuela	896	896	812	822	88	896	735
PAHO	Central America and Caribbean	El Salvador	805	805	777	805	342	806	723
EURO	Central Asia	Kazakhstan	715	715	698	M	M	715	711
SEARO	South-East Asia	Indonesia	869	869	861	205	590	869	711
AFRO	Northern Africa	Algeria	908	908	623	227	623	908	700
EURO	Central Asia	Kyrgyzstan	696	696	696	M	M	696	696
PAHO	Central America and Caribbean	Costa Rica	828	828	781	693	136	828	682
WPRO	South-East Asia	Cambodia	767	767	767	M	342	767	682
WPRO	South-East Asia	Viet Nam	803	803	802	281	542	803	672
AFRO	Eastern Africa	Uganda	791	791	731	229	617	791	658
EURO	Western Asia	Azerbaijan	690	690	556	M	M	690	657
PAHO	Central America and Caribbean	Honduras	754	754	695	747	172	754	646
PAHO	Central America and Caribbean	Panama	713	713	712	713	215	754	637
EURO	Western Asia	Georgia	634	634	634	M	M	634	634
EMRO	Southern Asia	Pakistan	707	707	707	260	707	707	633
EURO	South West Europe	North Macedonia	631	631	631	M	M	631	631
AFRO	Western Africa	Ghana	701	701	701	239	701	701	624
EURO	South West Europe	Serbia	740	740	730	160	597	740	618
AFRO	Middle Africa	Cameroon	706	706	703	228	646	706	616
EURO	Eastern Europe	Moldova	613	613	613	M	M	613	613
EMRO	Western Asia	Oman	693	693	693	232	626	693	605
AFRO	Western Africa	Niger	638	638	638	410	638	638	600
PAHO	Tropical South America	Ecuador	701	701	701	701	26	736	594
PAHO	Central America and Caribbean	Nicaragua	595	562	595	595	M	597	589
PAHO	Tropical South America	Bolivia	597	597	545	596	M	597	586
AFRO	Western Africa	Côte d'Ivoire	648	648	646	247	650	650	582
EMRO	Western Asia	Iraq	638	638	637	281	647	647	581
EURO	Northern Europe	Estonia	701	701	699	M	74	701	575
EURO	South West Europe	Malta	565	565	565	M	M	565	565
PAHO	Central America and Caribbean	Martinique	637	637	635	210	608	661	565
EURO	Western Asia	Armenia	556	556	556	M	M	556	556
PAHO	Central America and Caribbean	Guadeloupe	633	633	584	219	608	657	556
EMRO	Southern Asia	Afghanistan	610	610	610	280	610	610	555
EURO	South West Europe	Bosnia and Herzegovina	549	549	549	M	M	549	549
WPRO	Oceania Melanesia Polynesia	Fiji	585	585	584	284	628	628	549
EURO	Central Asia	Uzbekistan	541	541	541	M	M	541	541
SEARO	Southern Asia	Bangladesh	596	596	596	249	596	596	538
AFRO	Middle Africa	Central African Republic	528	528	528	M	528	528	528
PAHO	Central America and Caribbean	Guatemala	586	557	586	586	209	615	523

AFRO	Eastern Africa	Rwanda	511	511	511	M	511	511	511
WPRO	South-East Asia	Laos	554	554	554	265	554	554	506
AFRO	Eastern Africa	Tanzania	600	600	600	8	600	600	501
AFRO	Western Africa	Mali	597	597	597	22	597	597	501
EURO	Northern Europe	Lithuania	618	618	600	M	22	618	495
SEARO	Southern Asia	Bhutan	542	542	542	255	542	542	494
EMRO	Western Asia	Qatar	542	542	542	253	542	542	494
AFRO	Middle Africa	Democratic Republic of the Congo	588	588	588	11	588	588	492
SEARO	Southern Asia	Nepal	521	521	520	336	521	521	490
AFRO	Western Africa	Burkina Faso	561	561	561	114	561	561	487
AFRO	Western Africa	Togo	578	578	578	20	578	578	485
AFRO	Eastern Africa	Ethiopia	579	579	579	5	579	579	483
AFRO	Western Africa	Nigeria	534	534	534	166	534	534	473
AFRO	Western Africa	Sierra Leone	509	509	509	201	509	509	458
EMRO	Western Asia	Jordan	476	476	476	208	476	476	431
EMRO	Western Asia	Bahrain	446	443	446	195	446	446	404
AFRO	Eastern Africa	Mozambique	434	434	434	243	434	434	402
EMRO	Western Asia	Lebanon	336	336	336	336	336	336	336
PAHO	Tropical South America	Suriname	315	315	315	301	M	336	316
SEARO	Southern Asia	Maldives	327	327	305	237	330	329	309
PAHO	Central America and Caribbean	Haiti	297	297	297	295	M	297	297
PAHO	Central America and Caribbean	Barbados	269	269	259	269	M	336	280
EURO	Eastern Europe	Kosovo	280	280	280	M	M	280	280
EURO	South West Europe	Montenegro	279	279	279	M	M	279	279
PAHO	Central America and Caribbean	Trinidad and Tobago	266	265	231	266	M	336	273
EURO	Central Asia	Tajikistan	270	270	270	M	M	270	270
EURO	Central Asia	Turkmenistan	270	270	270	M	M	270	270
SEARO	South-East Asia	Myanmar	261	261	261	261	261	261	261
PAHO	Central America and Caribbean	Dominica	268	268	165	267	M	334	260
WPRO	Oceania Melanesia Polynesia	Papua New Guinea	252	252	252	251	252	252	252
PAHO	Central America and Caribbean	Belize	231	231	231	231	M	329	251
SEARO	South-East Asia	Timor-Leste	239	239	239	237	239	239	239
EMRO	Western Asia	Saudi Arabia	229	217	229	232	232	232	229
AFRO	Western Africa	Mauritania	282	282	230	9	282	282	228
SEARO	Eastern Asia	North Korea	227	227	227	227	227	227	227
PAHO	Central America and Caribbean	Saint Vincent and the Grenadines	264	264	1	264	M	331	225
PAHO	Central America and Caribbean	Saint Lucia	177	177	172	141	M	318	197
PAHO	Central America and Caribbean	Aruba	168	168	165	168	M	232	180
AFRO	Western Africa	Guinea	179	179	179	M	179	179	179
EMRO	Western Asia	Syrian Arab Republic	33	33	33	5	481	481	178
EMRO	Western Asia	West Bank and Gaza Strip	166	166	153	191	191	191	176
EURO	Western Asia	Cyprus	173	173	173	M	M	173	173
PAHO	Central America and Caribbean	Cayman Islands	164	164	50	M	M	231	152
PAHO	Tropical South America	Guyana	M	M	M	M	M	147	147
AFRO	Middle Africa	Angola	143	143	143	M	143	143	143
PAHO	North America	Bermuda	165	164	7	M	M	229	141
PAHO	Central America and Caribbean	Anguilla	137	53	137	M	M	226	138
PAHO	Central America and Caribbean	Saint Kitts and Nevis	114	114	49	59	M	327	133
EMRO	Western Asia	Kuwait	128	126	128	128	128	128	128
AFRO	Middle Africa	Chad	99	99	99	M	99	99	99
PAHO	Central America and Caribbean	Bahamas	106	90	17	1	M	176	78
PAHO	Central America and Caribbean	Turks and Caicos Islands	60	54	59	54	M	156	77
AFRO	Eastern Africa	Seychelles	75	75	75	M	75	75	75
EMRO	Western Asia	United Arab Emirates	75	75	75	75	75	75	75
EMRO	Western Asia	Yemen	68	66	68	M	70	70	68
AFRO	Middle Africa	Congo	63	63	63	M	63	63	63
PAHO	Central America and Caribbean	Antigua and Barbuda	1	M	1	M	M	157	53
AFRO	Middle Africa	South Sudan	36	36	36	M	36	36	36
PAHO	Central America and Caribbean	Grenada	2	2	1	36	M	76	23
PAHO	Central America and Caribbean	British Virgin Islands	1	1	M	8	M	76	22

EMRO	Northern Africa	Sudan	23	23	14	M	23	23	21

Supplementary Table S12. The average and median *extent* of 173 Member States for 8 influenza subtypes (A(H1), A(H1N1)pdm09, A(H3), A(H5), A(Unsubtyped), B(Yamagata), B(Victoria), and B(Undetermined) positives) reported by the WHO's FluNet. We downloaded data on 15 June 2021 at which time the total time series length was 1381 weeks. We calculated *extent* as the length of a time series (number of weeks) from the first to last week of complete records. We reported average *extent* with 95% confidence intervals (top values) and median *extent* with lower and upper quartile bounds (bottom values) by 6 regions and 17 influenza transmission zones. We report regions and zones in alphabetical order. We indicate zone-subtype dyads where all Member States had incomplete records using *Missing*. We omit the Southern African zone, as it only consisted of 1 country.

Region	A(H1)	A(H1N1)pdm09	A(H3)	A(H5)	A(Unsubtyped)	B(Yamagata)	B(Victoria)	B(Undetermined)
AFRO	488.63 [373.70, 603.56] 385.00 [266.00, 591.00]	475.87 [401.96, 549.77] 569.50 [434.00, 622.00]	603.77 [473.61, 733.92] 583.00 [434.00, 791.00]	477.43 [402.96, 551.91] 569.50 [434.00, 622.00]	602.20 [474.13, 730.27] 583.50 [434.00, 791.00]	466.93 [382.79, 551.08] 547.50 [237.00, 623.00]	466.43 [382.44, 550.43] 547.50 [237.00, 623.00]	585.90 [457.52, 714.28] 578.50 [416.00, 703.00]
EMRO	416.13 [257.05, 575.22] 366.00 [253.00, 601.00]	393.79 [282.78, 504.80] 476.00 [115.00, 622.00]	534.89 [333.10, 736.67] 509.00 [101.00, 707.00]	483.57 [370.31, 596.83] 596.00 [443.00, 624.00]	482.67 [311.72, 653.61] 459.50 [116.00, 707.00]	435.00 [305.80, 564.20] 509.00 [201.00, 654.00]	438.38 [308.17, 568.58] 509.00 [205.00, 668.50]	498.32 [319.49, 677.14] 476.00 [128.00, 707.00]
EURO	953.84 [858.01, 1049.68] 1116.00 [634.00, 1245.00]	575.82 [544.95, 606.69] 624.00 [557.00, 634.00]	967.78 [866.75, 1068.82] 1202.00 [631.00, 1273.00]	234.33 [133.85, 334.82] 75.00 [49.00, 419.00]	961.96 [862.97, 1060.95] 1175.00 [634.00, 1271.00]	616.43 [574.69, 658.17] 650.00 [578.00, 682.00]	612.12 [570.65, 653.58] 637.00 [565.00, 678.00]	951.65 [850.79, 1052.51] 1169.00 [613.00, 1272.00]
PAHO	762.17 [632.50, 891.85] 771.00 [410.00, 1070.00]	417.14 [344.58, 489.70] 558.00 [177.00, 635.00]	652.92 [517.04, 788.80] 611.00 [231.00, 1106.00]	242.95 [186.63, 299.28] 238.00 [136.00, 382.00]	753.32 [614.66, 891.99] 739.00 [545.00, 1120.00]	454.79 [371.02, 538.57] 523.00 [297.00, 679.00]	399.83 [312.61, 487.04] 513.50 [69.00, 669.50]	682.34 [542.15, 822.54] 700.00 [297.00, 1120.00]
SEARO	475.67 [277.47, 673.86] 521.00 [349.00, 609.00]	465.55 [365.48, 565.61] 542.00 [261.00, 596.00]	639.00 [415.41, 862.59] 542.00 [261.00, 1118.00]	428.27 [329.53, 527.01] 494.00 [239.00, 590.00]	636.33 [442.63, 830.04] 596.00 [512.00, 864.00]	451.80 [344.81, 558.79] 469.50 [239.00, 596.00]	459.30 [346.89, 571.71] 469.50 [239.00, 596.00]	588.91 [396.38, 781.44] 542.00 [261.00, 861.00]
WPRO	822.93 [656.56, 989.31] 856.00 [549.00, 1046.00]	584.80 [534.18, 635.42] 621.00 [559.00, 649.00]	944.80 [788.50, 1101.10] 1016.00 [767.00, 1213.00]	566.33 [489.14, 643.53] 559.00 [534.00, 650.00]	899.20 [723.40, 1075.00] 1008.00 [553.00, 1231.00]	624.20 [547.10, 701.30] 649.00 [554.00, 721.00]	634.93 [563.57, 706.29] 649.00 [554.00, 721.00]	909.93 [739.85, 1080.01] 939.00 [554.00, 1269.00]
Zone								
Central America and Caribbean	592.20 [419.66, 764.74] 431.00 [297.00, 783.00]	343.41 [250.22, 436.60] 268.00 [110.00, 584.00]	480.38 [326.02, 634.73] 414.00 [193.50, 760.00]	256.70 [184.51, 328.89] 249.50 [172.00, 389.00]	545.35 [387.33, 703.37] 580.00 [297.00, 739.00]	373.80 [249.81, 497.79] 420.50 [61.00, 678.00]	314.44 [199.02, 429.86] 231.00 [11.00, 584.00]	476.10 [323.52, 628.67] 418.00 [162.00, 700.00]
Central Asia	498.40 [306.31, 690.49] 541.00 [270.00, 696.00]	464.00 [306.14, 621.86] 541.00 [270.00, 610.00]	498.40 [306.31, 690.49] 541.00 [270.00, 696.00]	Missing	494.80 [306.17, 683.43] 541.00 [270.00, 678.00]	487.20 [306.31, 668.09] 541.00 [270.00, 659.00]	483.60 [306.60, 660.60] 541.00 [270.00, 659.00]	491.40 [306.50, 676.30] 541.00 [270.00, 678.00]
Eastern Africa	603.00 [416.72, 789.28] 550.00 [385.00, 862.00]	512.10 [409.43, 614.77] 562.50 [511.00, 617.00]	721.70 [493.09, 950.31] 695.50 [511.00, 1046.00]	512.10 [409.43, 614.77] 562.50 [511.00, 617.00]	719.10 [498.79, 939.41] 695.50 [511.00, 1010.00]	492.00 [360.85, 623.15] 514.00 [434.00, 600.00]	492.00 [360.85, 623.15] 514.00 [434.00, 600.00]	725.70 [497.82, 953.58] 665.50 [511.00, 1114.00]
Eastern Asia	990.75 [767.31, 1214.19] 951.00 [815.00, 1166.50]	538.40 [382.90, 693.90] 625.00 [559.00, 632.00]	915.80 [537.48, 1294.12] 934.00 [856.00, 1275.00]	517.60 [369.13, 666.07] 553.00 [534.00, 625.00]	981.75 [644.67, 1318.83] 1043.50 [704.50, 1259.00]	690.00 [572.69, 807.31] 665.50 [611.00, 769.00]	685.00 [561.08, 808.92] 665.50 [601.00, 769.00]	915.60 [538.35, 1292.85] 939.00 [856.00, 1275.00]
Eastern Europe	1062.00 [871.46, 1252.54] 1195.00 [1061.00, 1269.00]	587.45 [524.57, 650.34] 625.00 [568.00, 634.00]	1081.09 [886.67, 1275.51] 1220.00 [1059.00, 1273.00]	344.50 [155.78, 533.22] 394.00 [227.00, 462.00]	1006.09 [819.02, 1193.16] 1173.00 [756.00, 1182.00]	621.55 [548.99, 694.10] 656.00 [613.00, 682.00]	621.55 [548.99, 694.10] 656.00 [613.00, 682.00]	1041.82 [853.75, 1229.89] 1169.00 [954.00, 1266.00]
Middle Africa	287.80 [131.06, 444.54] 365.00 [143.00, 372.00]	300.43 [98.56, 502.30] 143.00 [63.00, 588.00]	308.86 [97.30, 520.41] 143.00 [63.00, 588.00]	300.43 [98.56, 502.30] 143.00 [63.00, 588.00]	309.00 [97.28, 520.72] 143.00 [63.00, 588.00]	302.14 [98.37, 505.91] 143.00 [63.00, 588.00]	300.43 [98.56, 502.30] 143.00 [63.00, 588.00]	308.57 [97.36, 519.78] 143.00 [63.00, 588.00]
Northern Africa	642.80 [297.01, 988.59] 642.00 [601.00, 978.00]	506.40 [269.38, 743.42] 622.00 [620.00, 623.00]	905.00 [454.09, 1355.91] 1167.00 [908.00, 1212.00]	492.60 [251.59, 733.61] 599.00 [595.00, 623.00]	782.40 [395.05, 1169.75] 908.00 [813.00, 1057.00]	519.60 [271.59, 767.61] 653.00 [623.00, 654.00]	528.80 [275.40, 782.20] 653.00 [623.00, 654.00]	754.40 [355.13, 1153.67] 965.00 [623.00, 1057.00]
North America	1109.00 [930.64, 1287.36] 1109.00 [1018.00, 1200.00]	448.67 [69.66, 827.68] 635.00 [62.00, 649.00]	888.33 [131.46, 1645.21] 1274.00 [116.00, 1275.00]	344.00 [293.04, 394.96] 344.00 [318.00, 370.00]	1274.50 [1273.52, 1275.48] 1274.50 [1274.00, 1275.00]	492.00 [252.88, 731.12] 492.00 [370.00, 614.00]	330.33 [0.00, 675.96] 370.00 [7.00, 614.00]	1274.50 [1273.52, 1275.48] 1274.50 [1274.00, 1275.00]
Northern Europe	1115.40 [960.35, 1270.45] 1221.00 [1123.00, 1271.00]	620.60 [604.45, 636.75] 629.50 [623.00, 634.00]	1144.20 [981.21, 1307.19] 1272.00 [1217.00, 1275.00]	54.71 [32.42, 77.01] 51.00 [39.00, 75.00]	1155.60 [992.73, 1318.47] 1273.00 [1268.00, 1275.00]	684.00 [613.98, 754.02] 671.50 [631.00, 686.00]	684.00 [613.98, 754.02] 671.50 [631.00, 686.00]	1148.00 [984.51, 1311.49] 1272.50 [1267.00, 1275.00]
Oceania Melanesia	675.60 [384.77, 966.43]	509.00 [381.28, 636.72]	857.60 [487.13, 1228.07]	420.20 [295.16, 545.24]	882.20 [479.70, 1284.70]	517.40 [356.05, 678.75]	553.60 [401.56, 705.64]	861.00 [473.62, 1248.38]

Polynesia	789.00 [401.00, 939.00]	568.00 [537.00, 585.00]	1077.00 [579.00, 1167.00]	427.00 [302.00, 559.00]	1164.00 [535.00, 1183.00]	593.00 [403.00, 665.00]	593.00 [584.00, 665.00]	1062.00 [542.00, 1180.00]
Southeast Asia	654.70 [385.67, 923.73] 688.00 [293.00, 948.00]	550.20 [450.15, 650.25] 628.00 [554.00, 650.00]	801.90 [580.72, 1023.08] 836.00 [554.00, 1115.00]	577.30 [458.12, 696.48] 620.00 [542.00, 721.00]	799.44 [585.76, 1013.13] 864.00 [554.00, 1008.00]	570.40 [445.46, 695.34] 611.50 [542.00, 721.00]	570.40 [445.46, 695.34] 611.50 [542.00, 721.00]	741.60 [518.71, 964.49] 778.00 [492.00, 1084.00]
Southern Asia	547.13 [408.51, 685.74] 492.50 [406.50, 674.50]	559.89 [491.62, 628.16] 596.00 [542.00, 625.00]	761.56 [544.04, 979.07] 610.00 [542.00, 1135.00]	512.11 [422.94, 601.28] 543.00 [494.00, 604.00]	673.67 [504.29, 843.04] 604.00 [542.00, 731.00]	536.67 [437.49, 635.85] 596.00 [445.00, 629.00]	545.00 [441.85, 648.15] 596.00 [445.00, 683.00]	712.89 [518.70, 907.08] 610.00 [542.00, 788.00]
Southwest Europe	1013.00 [872.04, 1153.96] 1116.00 [740.00, 1245.00]	593.26 [555.98, 630.55] 624.00 [565.00, 634.00]	1008.16 [850.75, 1165.57] 1205.00 [631.00, 1275.00]	346.56 [173.36, 519.75] 419.00 [52.00, 594.00]	1047.21 [897.25, 1197.17] 1235.00 [740.00, 1273.00]	642.00 [577.22, 706.78] 658.00 [578.00, 685.00]	629.68 [565.30, 694.07] 637.00 [565.00, 678.00]	1008.11 [851.13, 1165.08] 1209.00 [631.00, 1275.00]
Temperate South America	1134.50 [1067.58, 1201.42] 1121.50 [1083.00, 1186.00]	625.00 [585.41, 664.59] 643.00 [601.00, 649.00]	1092.75 [996.33, 1189.17] 1119.50 [1019.00, 1166.50]	230.33 [54.21, 406.46] 238.00 [71.00, 382.00]	1181.75 [1107.42, 1256.08] 1194.00 [1120.00, 1243.50]	665.25 [624.54, 705.96] 673.00 [631.50, 699.00]	675.50 [641.70, 709.30] 687.50 [652.00, 699.00]	1186.00 [1092.67, 1279.33] 1200.00 [1108.50, 1263.50]
Tropical South America	808.00 [596.65, 1019.35] 815.50 [602.50, 1023.50]	550.25 [476.36, 624.14] 592.00 [530.50, 596.50]	862.38 [632.53, 1092.22] 920.50 [604.00, 1134.50]	192.67 [60.22, 325.11] 137.00 [88.00, 390.00]	850.75 [619.30, 1082.20] 923.00 [576.50, 1113.00]	542.75 [451.54, 633.96] 549.50 [457.50, 664.00]	554.88 [462.28, 647.47] 590.00 [457.50, 667.00]	823.88 [597.58, 1050.17] 768.00 [623.00, 1116.50]
Western Africa	403.73 [253.89, 553.56] 346.00 [264.00, 447.00]	527.64 [435.60, 619.67] 578.00 [509.00, 638.00]	595.82 [425.02, 766.61] 578.00 [509.00, 648.00]	531.91 [437.25, 626.57] 578.00 [509.00, 638.00]	595.82 [425.02, 766.61] 578.00 [509.00, 648.00]	514.36 [388.93, 639.80] 578.00 [509.00, 638.00]	514.36 [388.93, 639.80] 578.00 [509.00, 638.00]	569.91 [400.20, 739.62] 561.00 [416.00, 646.00]
Western Asia	435.79 [265.43, 606.14] 365.00 [253.00, 634.00]	377.50 [273.28, 481.72] 459.50 [166.00, 557.00]	461.65 [292.95, 630.35] 476.00 [165.00, 634.00]	388.25 [224.73, 551.77] 459.50 [188.50, 569.50]	433.47 [281.35, 585.59] 443.00 [173.00, 634.00]	407.47 [291.14, 523.80] 476.00 [173.00, 589.00]	410.13 [293.04, 527.23] 476.00 [173.00, 589.00]	428.56 [279.12, 577.99] 461.00 [153.00, 634.00]
Worldwide	**731.57 [668.32, 794.82]** **708.00 [385.00, 1096.00]**	**491.30 [461.07, 521.53]** **588.50 [385.00, 631.00]**	**754.65 [690.42, 818.88]** **703.00 [492.50, 1198.50]**	**395.73 [353.72, 437.75]** **438.50 [194.00, 596.50]**	**768.71 [705.87, 831.56]** **714.00 [534.00, 1180.00]**	**524.04 [489.58, 558.49]** **596.50 [442.00, 670.00]**	**508.24 [472.08, 544.40]** **591.50 [370.00, 665.00]**	**742.78 [679.36, 806.20]** **699.00 [476.00, 1180.00]**

Supplementary Table S13. The *extent* of 173 Member States for 8 influenza subtypes (A(H1), A(H1N1)pdm09, A(H3), A(H5), A(Unsubtyped) abbreviated A(Uns), B(Yamagata) abbreviated B(Yam), B(Victoria) abbreviated B(Vic), and B(Undetermined) positives abbreviated B(Und)) reported by the WHO's FluNet. We downloaded data on 15 June 2021 at which time the total time series length of reported data was 1381 weeks. We calculated *extent* as the length of a time series (number of weeks) from the first to last week of complete records. We list Member States in descending order by average *extent* across all 8 subtypes (AVG), region, and zone. We denote Member State-outcome dyads where all 1381 weeks had incomplete records using *M*.

Region	Zone	Member States	A(H1)	A(H1N1)	A(H3)	A(H5)	A(Uns)	B(Yam)	B(Vic)	B(Und)	AVG
EURO	South West Europe	Slovenia	1329	627	1329	535	1329	1081	1081	1081	1049
EURO	South West Europe	Portugal	1230	603	1289	M	1292	687	687	1289	1011
EURO	South West Europe	Germany	1269	634	1279	M	1215	704	682	1274	1008
EURO	Northern Europe	Sweden	1225	623	1228	M	1272	681	681	1272	997
EURO	Eastern Europe	Hungary	1265	632	1269	M	1273	619	619	1266	992
EURO	Western Asia	Israel	1225	631	1271	M	1225	631	663	1271	988
WPRO	South-East Asia	Malaysia	1201	651	1277	721	1277	721	721	1276	981
EURO	Northern Europe	Ireland	1123	631	1271	M	1270	631	631	1270	975
EURO	Eastern Europe	Slovakia	1175	634	1273	M	1175	632	632	1270	970
WPRO	Eastern Asia	Japan	1287	649	1287	649	1287	649	649	1281	967
EURO	Northern Europe	United Kingdom	1271	634	1275	39	1275	975	975	1275	965
AFRO	Western Africa	Senegal	1080	649	1327	649	1327	701	701	1277	964
AFRO	Southern Africa	South Africa	1244	625	1272	625	1250	692	689	1268	958
EURO	South West Europe	Spain	1229	634	1275	594	1235	682	682	1275	951
EURO	Eastern Europe	Belarus	1269	555	1163	M	1163	656	656	1162	946
EURO	Northern Europe	Iceland	1151	548	1275	M	1275	548	548	1275	946
EURO	South West Europe	Italy	1144	643	1269	643	1269	650	650	1268	942
EURO	South West Europe	Switzerland	1379	632	1379	52	1379	685	647	1379	942
WPRO	South-East Asia	Philippines	1245	635	1115	799	1008	799	799	1115	939
EURO	Eastern Europe	Russian Federation	1270	625	1273	520	1173	684	684	1270	937
EURO	Eastern Europe	Czechia	1195	568	1202	M	1209	585	585	1206	936
EURO	South West Europe	Austria	1054	578	1205	M	1265	578	578	1261	931
EURO	South West Europe	France	1245	651	1245	419	1275	662	662	1275	929
EURO	South West Europe	Croatia	1195	561	1195	M	1200	579	579	1193	929
EURO	Northern Europe	Latvia	1328	625	1328	51	1328	713	713	1273	920
WPRO	Eastern Asia	China	1046	632	1275	534	1231	682	682	1275	920
EURO	Eastern Europe	Poland	1220	648	1274	404	1180	682	682	1169	907
EURO	Eastern Europe	Romania	1271	622	1266	384	1182	659	659	1211	907
AFRO	Eastern Africa	Zambia	1034	596	1276	596	1276	596	596	1258	904
PAHO	North America	United States of America	1200	635	1275	318	1275	614	614	1275	901
PAHO	Temperate South America	Argentina	1096	637	1160	382	1237	701	701	1253	896
EURO	Northern Europe	Norway	1272	634	1273	65	1274	686	686	1274	896
WPRO	Oceania Melanesia Polynesia	Australia	939	568	1213	559	1277	665	665	1269	894
PAHO	Temperate South America	Chile	1225	649	1173	238	1250	649	678	1274	892
PAHO	Tropical South America	Colombia	1266	649	1266	118	1266	649	649	1261	891
EURO	Northern Europe	Finland	1255	634	1274	75	1275	662	662	1275	889
EURO	Northern Europe	Denmark	1217	631	1217	100	1268	662	662	1267	878
EMRO	Southern Asia	Iran	827	625	1222	624	1070	683	683	1271	876
PAHO	Tropical South America	Brazil	1054	585	1163	390	1212	679	695	1222	875
PAHO	Temperate South America	Uruguay	1070	565	1079	M	1089	614	626	1070	873
EURO	South West Europe	Greece	1060	624	1271	232	1271	658	658	1209	873
EURO	South West Europe	Netherlands	1273	633	1274	1	1270	666	565	1275	870
PAHO	Central America and Caribbean	Mexico	1120	651	1120	389	1120	702	702	1120	866
EMRO	Northern Africa	Egypt	978	644	1167	644	1057	654	700	1057	863
EURO	Eastern Europe	Bulgaria	1061	634	1220	M	756	661	661	954	850
EURO	South West Europe	Belgium	1116	623	1026	46	1273	678	678	1272	839
AFRO	Eastern Africa	Madagascar	862	620	1046	620	1010	696	696	1156	838
SEARO	Southern Asia	India	881	626	1194	543	1051	629	700	1077	838
SEARO	South-East Asia	Thailand	861	650	1118	650	972	650	650	1084	829

WPRO	Oceania Melanesia Polynesia	New Caledonia	789	603	1077	561	1183	674	674	1062	828
PAHO	North America	Canada	1018	649	1274	370	1274	370	370	1274	825
EMRO	Northern Africa	Tunisia	601	620	1212	595	1113	653	653	1113	820
PAHO	Central America and Caribbean	Jamaica	1219	651	1224	281	1084	700	700	700	820
WPRO	Oceania Melanesia Polynesia	New Zealand	997	537	1167	302	1164	593	593	1180	817
PAHO	Temperate South America	Paraguay	1147	649	959	71	1151	697	697	1147	815
EMRO	Northern Africa	Morocco	979	622	1224	599	813	654	654	965	814
EURO	Eastern Europe	Ukraine	1063	651	1059	70	1063	766	766	1059	812
WPRO	Eastern Asia	Mongolia	856	625	856	625	856	856	856	856	798
WPRO	South-East Asia	Singapore	948	650	1016	650	1016	633	633	754	788
EURO	South West Europe	Luxembourg	902	634	805	M	910	699	626	799	768
PAHO	Tropical South America	Peru	993	595	1014	156	1014	595	595	1011	747
PAHO	Central America and Caribbean	Cuba	1016	584	1262	69	584	584	584	1261	743
AFRO	Eastern Africa	Mauritius	938	529	1168	529	1116	237	237	1114	734
AFRO	Eastern Africa	Kenya	591	622	799	622	799	799	799	799	729
PAHO	Tropical South America	French Guiana	913	589	1106	402	950	504	585	724	722
AFRO	Northern Africa	Algeria	642	623	908	623	908	623	623	623	697
SEARO	South-East Asia	Indonesia	609	590	869	590	864	590	590	861	695
PAHO	Central America and Caribbean	El Salvador	783	649	805	289	805	701	701	777	689
WPRO	South-East Asia	Cambodia	767	651	767	767	492	767	767	492	684
EURO	Central Asia	Kazakhstan	715	610	715	M	715	659	659	698	682
EURO	South West Europe	Serbia	740	621	740	597	740	637	637	730	680
WPRO	Eastern Asia	South Korea	774	559	934	553	553	573	553	939	680
EURO	South West Europe	Albania	1058	550	550	M	950	549	549	550	679
EURO	Central Asia	Kyrgyzstan	696	629	696	M	678	696	678	678	679
AFRO	Western Africa	Ghana	447	651	701	701	701	701	701	701	663
PAHO	Central America and Caribbean	Costa Rica	771	635	828	136	739	702	702	781	662
EMRO	Southern Asia	Pakistan	447	650	707	637	707	707	707	707	659
AFRO	Middle Africa	Cameroon	496	646	705	646	706	658	646	703	651
WPRO	South-East Asia	Viet Nam	549	621	803	542	803	542	542	802	651
EURO	Western Asia	Turkey	793	557	1052	41	788	589	589	793	650
PAHO	Tropical South America	Venezuela	718	476	827	88	896	685	685	812	648
PAHO	Central America and Caribbean	Honduras	754	650	754	172	754	695	695	695	646
EMRO	Western Asia	Oman	426	597	693	597	680	693	693	674	632
EURO	Western Asia	Georgia	634	634	634	M	634	622	622	634	631
EURO	South West Europe	North Macedonia	631	631	631	M	631	624	624	631	629
AFRO	Eastern Africa	Uganda	550	617	791	617	791	455	455	731	626
SEARO	Southern Asia	Sri Lanka	522	564	1135	365	731	441	441	788	623
EURO	Western Asia	Azerbaijan	690	556	690	M	690	556	556	556	613
EURO	Eastern Europe	Moldova	613	613	613	M	613	613	613	613	613
PAHO	Central America and Caribbean	Panama	661	589	661	218	713	661	661	712	610
EURO	Northern Europe	Estonia	701	628	701	49	701	682	682	699	605
AFRO	Western Africa	Côte d'Ivoire	401	626	648	623	648	623	623	646	605
AFRO	Western Africa	Niger	163	638	638	638	638	638	638	638	579
EMRO	Southern Asia	Afghanistan	366	610	610	604	604	610	610	610	578
AFRO	Western Africa	Togo	573	578	578	578	578	578	578	578	577
AFRO	Eastern Africa	Tanzania	365	600	600	600	600	600	600	600	571
SEARO	Southern Asia	Bangladesh	349	596	596	596	596	596	596	596	565
EURO	South West Europe	Malta	565	565	565	M	565	552	552	565	561
AFRO	Middle Africa	Democratic Republic of the Congo	372	588	588	588	588	588	588	588	561
EURO	Western Asia	Armenia	556	556	556	M	556	556	556	556	556
EURO	South West Europe	Bosnia and Herzegovina	549	549	549	M	549	548	548	549	549
AFRO	Western Africa	Mali	384	597	597	597	597	597	597	416	548
PAHO	Central America and Caribbean	Dominican Republic	410	530	766	M	698	361	360	697	546
EURO	Central Asia	Uzbekistan	541	541	541	M	541	541	541	541	541
PAHO	Tropical South America	Bolivia	597	597	597	M	545	441	441	545	538
AFRO	Western Africa	Burkina Faso	346	561	561	561	561	561	561	561	534
EURO	Northern Europe	Lithuania	611	618	600	4	618	600	600	600	531
WPRO	South-East Asia	Laos	293	554	554	554	554	554	554	554	521

AFRO	Eastern Africa	Ethiopia	385	517	517	517	579	517	517	579	516
SEARO	Southern Asia	Bhutan	464	542	542	494	542	494	494	542	514
AFRO	Eastern Africa	Rwanda	511	511	511	511	511	511	511	511	511
EMRO	Western Asia	Qatar	289	542	542	542	542	542	542	542	510
AFRO	Western Africa	Nigeria	338	534	534	534	534	534	534	534	510
PAHO	Tropical South America	Ecuador	608	596	611	2	608	474	474	701	509
AFRO	Middle Africa	Central African Republic	365	528	528	528	528	528	528	528	508
WPRO	Oceania Melanesia Polynesia	Fiji	401	585	579	427	535	403	584	542	507
SEARO	Southern Asia	Nepal	521	521	521	521	512	445	445	520	501
PAHO	Central America and Caribbean	Guadeloupe	402	584	584	402	580	480	584	366	498
EMRO	Western Asia	Iraq	394	622	587	638	366	366	366	637	497
PAHO	Central America and Caribbean	Guatemala	431	551	552	209	557	519	553	586	495
PAHO	Central America and Caribbean	Martinique	402	583	584	402	419	527	583	418	490
AFRO	Western Africa	Sierra Leone	264	509	509	509	509	509	509	509	478
EMRO	Western Asia	Jordan	298	476	476	476	476	476	476	476	454
EMRO	Western Asia	Bahrain	253	443	443	443	443	443	443	446	420
AFRO	Eastern Africa	Mozambique	191	434	434	434	434	434	434	434	404
PAHO	Central America and Caribbean	Nicaragua	261	531	531	M	562	79	79	595	377
EMRO	Western Asia	Lebanon	336	336	336	336	336	336	336	336	336
PAHO	Tropical South America	Suriname	315	315	315	M	315	315	315	315	315
PAHO	Central America and Caribbean	Haiti	297	297	297	M	297	297	297	297	297
EURO	Eastern Europe	Kosovo	280	280	280	M	280	280	280	280	280
EURO	South West Europe	Montenegro	279	279	279	M	279	279	279	279	279
EURO	Central Asia	Tajikistan	270	270	270	M	270	270	270	270	270
EURO	Central Asia	Turkmenistan	270	270	270	M	270	270	270	270	270
SEARO	Southern Asia	Maldives	M	305	327	225	250	225	229	305	267
WPRO	Oceania Melanesia Polynesia	Papua New Guinea	252	252	252	252	252	252	252	252	252
PAHO	Central America and Caribbean	Belize	231	231	231	M	231	231	231	231	231
SEARO	Eastern Asia	North Korea	M	227	227	227	M	M	M	227	227
SEARO	South-East Asia	Myanmar	52	261	261	261	209	209	209	261	215
AFRO	Western Africa	Mauritania	266	282	282	282	282	37	37	230	212
SEARO	South-East Asia	Timor-Leste	22	239	239	239	M	239	239	217	205
AFRO	Western Africa	Guinea	179	179	179	179	179	179	179	179	179
EURO	Western Asia	Cyprus	173	173	173	M	173	173	173	173	173
EMRO	Western Asia	Saudi Arabia	1	217	M	M	211	M	M	229	165
PAHO	Central America and Caribbean	Barbados	M	236	262	M	2	13	201	238	159
PAHO	Central America and Caribbean	Saint Lucia	125	177	176	M	125	172	127	159	152
EMRO	Western Asia	West Bank and Gaza Strip	M	166	165	M	96	M	M	153	145
AFRO	Middle Africa	Angola	143	143	143	143	143	143	143	143	143
PAHO	Central America and Caribbean	Aruba	M	168	M	M	M	43	M	162	124
PAHO	Central America and Caribbean	Saint Vincent and the Grenadines	M	107	248	M	M	M	1	M	119
PAHO	Central America and Caribbean	Trinidad and Tobago	M	265	217	M	1	5	8	151	108
PAHO	Central America and Caribbean	Cayman Islands	M	110	158	M	M	M	M	50	106
AFRO	Middle Africa	Chad	M	99	99	99	99	99	99	99	99
PAHO	Central America and Caribbean	Dominica	M	268	211	M	M	3	11	1	99
EMRO	Western Asia	Kuwait	M	115	101	M	116	30	30	128	87
AFRO	Eastern Africa	Seychelles	M	75	75	75	75	75	75	75	75
AFRO	Middle Africa	Congo	63	63	63	63	63	63	63	63	63
PAHO	North America	Bermuda	M	62	116	M	M	M	7	M	62
EMRO	Western Asia	United Arab Emirates	M	75	75	M	M	66	74	9	60
EMRO	Western Asia	Yemen	M	66	21	M	4	M	M	68	40
PAHO	Central America and Caribbean	Turks and Caicos Islands	M	54	1	M	M	M	59	M	38
AFRO	Middle Africa	South Sudan	M	36	36	36	36	36	36	36	36
EMRO	Western Asia	Syrian Arab Republic	33	33	33	33	33	33	33	33	33
PAHO	Central America and Caribbean	Saint Kitts and Nevis	M	114	1	M	M	1	2	M	30
PAHO	Central America and Caribbean	Bahamas	M	53	3	M	M	M	17	M	24
EMRO	Northern Africa	Sudan	14	23	14	2	21	14	14	14	15
PAHO	Central America and Caribbean	Anguilla	M	1	53	M	M	M	1	1	14
PAHO	Central America and Caribbean	Grenada	M	2	M	M	M	M	1	M	2

PAHO	Central America and Caribbean	British Virgin Islands	M	1	M	M	M	M	M	M	1
PAHO	Central America and Caribbean	Antigua and Barbuda	M	M	M	M	M	M	1	M	1
PAHO	Tropical South America	Guyana	M	M	M	M	M	M	M	M	M

Supplementary Table S14. Average and median *effective time series length (ETSL)* for 6 testing outcomes (specimens collected (SPE), specimens processed or tests (TES), influenza A positives (FLUA), influenza B positives (FLUB), total positives (POS), and total negatives (NEG)) in 6 regions and 17 transmission zones. We extracted FluNet data from 173 Member States on 15 June 2021. We calculated *ETSL* as the ratio of the number of time points when records were complete divided by the total time series length (1381 weeks) and multiplied by 100. We report average *ETSL* with 95% confidence intervals (top values) and median *ETSL* with lower and upper quartiles (bottom values). Regions and zones are listed in descending order by average positives *ETSL*, and we omit the Southern African transmission zone, as it consisted of only 1 country.

Region	POS	FLUA	FLUB	NEG	SPE	TES
WPRO	60.28 [49.01, 71.56] 57.71 [39.90, 82.48]	59.88 [48.52, 71.24] 56.92 [39.90, 82.19]	51.68 [43.22, 60.15] 55.10 [39.90, 60.46]	12.46 [8.51, 16.41] 14.77 [6.59, 19.04]	35.03 [27.82, 42.23] 40.04 [24.62, 45.18]	51.31 [38.67, 63.95] 55.25 [36.78, 70.75]
EURO	45.91 [40.56, 51.25] 44.32 [36.86, 62.78]	45.66 [40.35, 50.96] 44.17 [36.78, 62.64]	39.09 [35.09, 43.10] 42.36 [31.35, 49.46]	0.61 [0.00, 1.28] 0.00 [0.00, 0.00]	5.42 [2.60, 8.25] 0.00 [0.00, 5.21]	43.97 [38.95, 48.99] 44.03 [34.18, 56.92]
SEARO	35.89 [24.06, 47.72] 38.52 [16.94, 53.08]	35.11 [23.50, 46.72] 38.52 [15.42, 49.96]	33.24 [22.98, 43.49] 38.23 [15.93, 44.90]	13.32 [9.17, 17.46] 13.40 [10.79, 17.74]	31.39 [22.97, 39.81] 36.42 [18.90, 42.72]	36.75 [24.97, 48.54] 38.96 [18.90, 52.93]
AFRO	35.02 [27.59, 42.45] 33.31 [22.59, 46.05]	34.86 [27.53, 42.20] 33.27 [22.45, 46.05]	31.21 [25.46, 36.96] 30.59 [22.01, 43.88]	6.53 [3.71, 9.34] 1.48 [0.00, 13.54]	30.91 [25.76, 36.05] 34.29 [25.92, 42.51]	35.44 [27.93, 42.94] 34.76 [25.92, 46.13]
PAHO	33.43 [24.80, 42.05] 33.02 [1.67, 51.96]	32.81 [24.24, 41.39] 31.50 [1.41, 51.41]	27.37 [20.36, 34.38] 28.71 [0.47, 48.01]	26.66 [18.69, 34.64] 18.32 [0.72, 46.34]	8.48 [4.30, 12.66] 0.00 [0.00, 11.01]	37.58 [29.65, 45.51] 41.82 [11.19, 55.50]
EMRO	27.21 [18.88, 35.54] 33.82 [6.52, 41.13]	26.88 [18.57, 35.19] 33.82 [6.15, 39.97]	24.79 [16.94, 32.64] 30.05 [5.00, 39.03]	11.79 [8.89, 14.69] 12.96 [8.54, 16.51]	26.30 [18.99, 33.60] 32.30 [8.83, 41.56]	27.84 [19.94, 35.74] 33.74 [8.83, 43.30]
Zone						
Temperate South America	66.64 [52.38, 80.89] 71.65 [56.37, 76.90]	65.01 [51.84, 78.17] 69.23 [55.97, 74.04]	51.54 [38.73, 64.34] 54.92 [42.03, 61.04]	61.93 [49.50, 74.36] 67.31 [54.45, 69.41]	11.24 [1.62, 20.86] 10.68 [3.15, 19.33]	69.17 [57.91, 80.43] 71.61 [60.54, 77.81]
Northern Europe	61.75 [53.85, 69.65] 60.54 [54.38, 71.11]	61.43 [53.56, 69.31] 59.96 [53.51, 71.04]	51.04 [45.44, 56.63] 48.70 [43.88, 55.68]	0.00 [0.00, 0.00] 0.00 [0.00, 0.00]	2.77 [1.32, 4.21] 3.29 [0.00, 4.20]	56.97 [49.21, 64.73] 54.16 [46.85, 70.24]
Eastern Asia	58.31 [28.72, 87.90] 59.74 [55.76, 82.48]	58.03 [28.50, 87.56] 59.74 [54.82, 82.19]	53.02 [26.78, 79.26] 59.59 [49.17, 73.35]	10.14 [2.50, 17.77] 9.05 [3.77, 17.52]	26.89 [6.77, 47.02] 40.26 [3.77, 45.18]	33.09 [7.71, 58.47] 46.05 [3.77, 55.90]
North America	52.59 [2.29, 102.90] 75.31 [1.38, 81.10]	52.52 [2.08, 102.96] 75.31 [1.16, 81.10]	46.80 [0.41, 93.20] 62.78 [0.22, 77.41]	7.14 [0.00, 21.15] 0.00 [0.00, 21.43]	29.79 [0.48, 59.09] 42.36 [0.00, 46.99]	51.80 [5.32, 98.27] 69.95 [4.78, 80.67]
Southeast Asia	51.49 [37.30, 65.68] 55.14 [39.90, 67.78]	51.32 [37.18, 65.46] 55.14 [39.90, 67.27]	46.02 [35.65, 56.39] 54.45 [39.90, 56.48]	12.71 [8.18, 17.23] 13.43 [6.59, 19.04]	36.52 [28.83, 44.22] 41.31 [24.62, 46.63]	51.13 [37.07, 65.19] 54.53 [39.90, 65.89]
Oceania Melanesia Polynesia	49.67 [23.42, 75.93] 36.78 [32.30, 70.31]	48.94 [22.55, 75.32] 35.84 [30.56, 69.51]	38.52 [21.63, 55.41] 29.91 [28.82, 49.24]	14.38 [8.66, 20.10] 14.77 [9.63, 15.50]	30.47 [18.61, 42.33] 37.22 [18.10, 40.04]	48.30 [20.78, 75.82] 36.78 [24.48, 71.47]
Eastern Europe	47.28 [37.85, 56.72] 48.23 [36.86, 61.84]	47.15 [37.74, 56.56] 48.15 [36.78, 61.77]	40.79 [33.57, 48.02] 43.16 [32.08, 51.48]	0.23 [0.00, 0.68] 0.00 [0.00, 0.00]	9.09 [0.17, 18.02] 0.00 [0.00, 27.15]	46.13 [37.24, 55.01] 47.50 [36.57, 58.58]
Tropical South America	46.99 [28.76, 65.22] 42.22 [34.54, 68.79]	46.38 [28.27, 64.49] 42.00 [34.03, 68.50]	35.42 [23.14, 47.69] 32.44 [28.31, 54.02]	40.41 [21.75, 59.06] 37.87 [19.26, 65.53]	10.37 [0.00, 21.16] 1.23 [0.00, 8.62]	48.82 [31.01, 66.63] 44.10 [38.45, 67.78]
Southwest Europe	45.82 [36.71, 54.94] 44.75 [27.59, 66.18]	45.49 [36.47, 54.51] 44.53 [27.59, 65.03]	37.60 [31.11, 44.08] 35.26 [27.59, 49.46]	1.52 [0.00, 3.22] 0.00 [0.00, 0.00]	7.69 [2.54, 12.84] 0.00 [0.00, 13.03]	43.86 [35.04, 52.68] 41.71 [27.59, 64.74]
Southern Asia	42.07 [33.74, 50.40] 42.72 [36.64, 53.08]	41.10 [32.91, 49.29] 41.49 [35.92, 49.96]	38.95 [32.21, 45.69] 41.56 [36.06, 42.72]	14.08 [9.63, 18.53] 13.40 [11.15, 17.74]	37.73 [33.05, 42.40] 39.03 [33.82, 43.23]	42.04 [34.60, 49.47] 42.72 [36.71, 45.62]
Western Africa	38.65 [26.34, 50.96] 38.52 [22.59, 46.05]	38.48 [26.38, 50.58] 38.52 [22.45, 46.05]	33.81 [25.85, 41.77] 38.52 [22.01, 46.05]	9.05 [4.11, 14.00] 8.18 [1.38, 16.58]	34.34 [27.46, 41.21] 38.52 [25.92, 44.39]	39.05 [26.60, 51.50] 38.52 [25.92, 46.13]
Eastern Africa	38.42 [27.56, 49.29] 37.62 [30.05, 47.21]	38.28 [27.53, 49.02] 37.58 [29.76, 47.21]	34.67 [25.91, 43.43] 36.46 [26.43, 43.88]	6.30 [1.25, 11.35] 0.43 [0.00, 13.54]	33.23 [26.13, 40.33] 33.13 [30.05, 42.51]	38.36 [27.71, 49.02] 37.44 [30.63, 47.07]
Northern Africa	32.98 [15.87, 50.08] 35.48 [32.30, 41.13]	32.5 [15.52, 49.48] 34.32 [32.22, 39.97]	27.66 [12.94, 42.38] 30.63 [29.33, 30.77]	9.08 [3.43, 14.74] 9.70 [6.37, 12.02]	29.62 [14.76, 44.47] 34.69 [28.96, 36.28]	34.74 [17.33, 52.15] 36.50 [36.42, 46.13]
Central Asia	26.05 [10.86, 41.25] 25.56 [10.93, 42.80]	26.04 [10.86, 41.22] 25.56 [10.93, 42.80]	25.56 [10.91, 40.21] 25.56 [10.93, 42.07]	0.00 [0.00, 0.00] 0.00 [0.00, 0.00]	0.00 [0.00, 0.00] 0.00 [0.00, 0.00]	26.05 [10.86, 41.25] 25.56 [10.93, 42.80]
Western Asia	25.15 [17.68, 32.62] 33.24 [6.52, 38.52]	24.89 [17.41, 32.37] 33.06 [6.44, 37.87]	23.80 [16.37, 31.23] 30.34 [6.44, 35.70]	7.88 [4.20, 11.57] 6.73 [0.00, 15.57]	14.99 [7.30, 22.67] 7.10 [0.07, 32.30]	26.15 [18.80, 33.51] 33.24 [8.83, 38.96]
Central America and Caribbean	22.27 [13.49, 31.05] 10.25 [0.76, 46.31]	21.74 [12.96, 30.53] 9.88 [0.58, 45.98]	19.25 [11.56, 26.94] 9.92 [0.25, 42.98]	19.30 [10.66, 27.94] 4.63 [0.62, 43.74]	5.20 [1.24, 9.15] 0.00 [0.00, 5.43]	27.93 [19.83, 36.03] 17.89 [6.41, 48.23]
Middle Africa	20.04 [5.16, 34.91] 10.14 [2.68, 41.06]	20.03 [5.16, 34.89] 10.14 [2.68, 41.06]	18.97 [5.06, 32.88] 10.14 [2.68, 40.98]	0.97 [0.00, 2.63] 0.00 [0.00, 0.80]	19.47 [5.46, 33.48] 10.14 [2.68, 41.13]	20.11 [5.29, 34.93] 10.07 [2.68, 41.06]
Worldwide	**39.29 [35.65, 42.93]** **40.04 [18.90, 55.32]**	**38.90 [35.28, 42.52]** **39.79 [18.90, 54.96]**	**33.80 [30.86, 36.74]** **35.88 [18.90, 47.86]**	**11.52 [8.87, 14.16]** **3.48 [0.00, 16.51]**	**17.34 [14.65, 20.03]** **9.23 [0.00, 36.42]**	**39.19 [35.81, 42.56]** **41.42 [20.93, 53.66]**

Supplementary Table S15. The *effective time series length* (*ETSL*) of 173 Member States for 6 test outcomes (specimens collected (SPE), specimens processed or tests (TES), influenza A positives (FLUA), influenza B positives (FLUB), total positives (POS), and total negatives (NEG)) reported by the WHO's FluNet. Data were downloaded on 15 June 2021 at which time the *time series length* (*TSL*) of reported data was 1381 weeks. We calculated *ETSL* as the ratio of the number of time points when records are complete divided by the *TSL* and multiplied by 100. Member States are listed in descending order by average *ETSL* across all 6 outcomes (AVG), regions, and zones. Member State-outcome dyads where all 1381 weeks have incomplete records have an *ETSL* of 0.

Region	Zone	Country/Territory	POS	FLUA	FLUB	NEG	SPE	TES	AVG
PAHO	Tropical South America	Colombia	90.37	90.37	54.02	88.78	0.00	90.66	69.03
WPRO	Oceania Melanesia Polynesia	Australia	90.88	90.66	66.55	24.40	43.23	90.66	67.73
PAHO	North America	United States of America	81.10	81.10	77.41	21.43	46.99	80.67	64.78
PAHO	Temperate South America	Argentina	77.19	75.81	62.78	68.79	22.45	79.65	64.45
PAHO	Central America and Caribbean	Mexico	80.96	80.96	56.99	80.81	0.00	80.96	63.44
AFRO	Western Africa	Senegal	90.59	89.14	49.96	16.58	40.41	92.40	63.18
WPRO	South-East Asia	Malaysia	88.92	88.92	60.46	3.62	47.07	88.92	62.99
PAHO	Tropical South America	Brazil	74.15	72.12	56.41	65.53	33.09	73.79	62.52
PAHO	Temperate South America	Chile	76.61	72.27	59.30	70.02	16.22	75.96	61.73
WPRO	Eastern Asia	China	82.48	82.19	79.22	17.52	45.26	55.90	60.43
PAHO	Tropical South America	Peru	68.79	68.50	57.49	65.68	8.62	67.78	56.14
AFRO	Eastern Africa	Madagascar	73.06	72.12	55.32	19.77	43.81	71.98	56.01
SEARO	South-East Asia	Thailand	67.78	67.27	60.46	20.56	46.63	65.89	54.77
AFRO	Southern Africa	South Africa	68.65	67.41	54.09	20.06	44.68	72.70	54.60
PAHO	North America	Canada	75.31	75.31	62.78	0.00	42.36	69.95	54.28
WPRO	South-East Asia	Philippines	71.33	71.11	55.54	6.59	48.23	70.75	53.92
PAHO	Temperate South America	Paraguay	66.69	66.18	50.54	65.82	5.14	67.27	53.61
EURO	Northern Europe	United Kingdom	81.68	81.10	69.51	0.00	4.20	79.72	52.70
WPRO	Oceania Melanesia Polynesia	New Caledonia	70.31	69.51	49.24	15.50	40.04	71.47	52.68
EURO	South West Europe	Spain	66.18	64.30	52.93	13.61	39.83	60.83	49.61
WPRO	South-East Asia	Viet Nam	57.71	56.92	56.48	19.99	39.17	57.86	48.02
EURO	South West Europe	Slovenia	73.79	73.79	56.70	0.00	10.79	72.63	47.95
EURO	Northern Europe	Norway	75.81	75.74	61.26	0.00	3.69	70.67	47.86
WPRO	Eastern Asia	Mongolia	59.74	59.74	59.59	0.00	45.18	59.74	47.33
EURO	Eastern Europe	Poland	67.70	67.56	51.48	0.00	29.18	65.24	46.86
WPRO	South-East Asia	Singapore	54.96	54.96	53.80	19.04	43.37	53.80	46.66
EURO	Eastern Europe	Russian Federation	62.78	62.64	54.82	2.53	39.83	56.92	46.58
EURO	South West Europe	France	66.69	66.55	55.76	0.00	25.34	64.74	46.51
EURO	South West Europe	Germany	73.50	73.06	58.65	0.00	0.00	69.30	45.75
WPRO	Eastern Asia	Japan	89.79	89.65	73.35	20.35	0.00	0.00	45.52
EMRO	Northern Africa	Egypt	54.45	54.45	46.99	17.31	46.63	53.15	45.50
PAHO	Central America and Caribbean	Honduras	53.73	53.73	47.50	51.92	12.38	53.66	45.49
PAHO	Central America and Caribbean	El Salvador	51.27	51.27	47.86	49.60	20.64	51.34	45.33
SEARO	Southern Asia	India	56.34	55.03	42.22	10.79	44.46	62.13	45.16
EURO	Northern Europe	Denmark	71.11	71.04	49.82	0.00	6.59	70.24	44.80
EMRO	Southern Asia	Iran	57.28	56.41	52.21	12.96	43.88	45.62	44.73
EURO	South West Europe	Portugal	70.31	69.73	49.46	0.00	0.00	70.46	43.33
EURO	Eastern Europe	Romania	61.84	61.77	47.36	0.00	27.15	59.81	42.99
AFRO	Western Africa	Niger	46.05	46.05	46.05	25.05	46.13	46.13	42.58
AFRO	Western Africa	Ghana	48.15	48.15	48.15	14.34	48.15	48.15	42.52
WPRO	Eastern Asia	South Korea	55.76	54.82	49.17	9.05	40.26	46.05	42.52
PAHO	Central America and Caribbean	Panama	47.72	47.43	45.55	47.28	15.06	51.70	42.46
PAHO	Central America and Caribbean	Dominican Republic	51.56	49.82	45.84	45.69	0.00	60.39	42.22
PAHO	Tropical South America	French Guiana	52.35	51.56	32.44	13.11	44.03	57.20	41.78
PAHO	Central America and Caribbean	Costa Rica	50.98	50.83	48.15	46.99	3.19	49.82	41.66
PAHO	Central America and Caribbean	Jamaica	50.62	50.62	48.66	43.16	9.63	46.78	41.58
EURO	South West Europe	Switzerland	65.46	65.03	46.27	0.00	3.62	67.34	41.29
AFRO	Middle Africa	Cameroon	50.04	49.96	45.69	6.01	45.40	50.04	41.19
WPRO	South-East Asia	Cambodia	55.32	55.32	55.10	0.00	24.62	55.25	40.94
AFRO	Eastern Africa	Uganda	47.21	47.21	44.68	15.79	41.71	47.14	40.62

EMRO	Western Asia	Oman	46.49	46.49	46.49	15.57	41.56	46.27	40.48
SEARO	South-East Asia	Indonesia	45.47	45.26	44.90	14.84	42.72	45.40	39.77
AFRO	Western Africa	Côte d'Ivoire	44.32	44.03	43.59	17.89	44.39	44.24	39.74
SEARO	Southern Asia	Sri Lanka	53.08	49.96	47.79	0.00	33.60	52.93	39.56
EURO	Northern Europe	Finland	68.28	68.14	52.93	0.00	3.04	44.68	39.51
AFRO	Eastern Africa	Zambia	45.69	45.55	43.37	13.54	42.80	45.69	39.44
EURO	Northern Europe	Sweden	63.36	62.93	55.68	0.00	0.00	54.60	39.43
EURO	Eastern Europe	Ukraine	59.16	59.02	51.56	0.00	3.84	58.58	38.69
SEARO	Southern Asia	Bangladesh	42.72	41.49	42.72	17.74	42.72	42.72	38.35
EMRO	Southern Asia	Pakistan	43.30	43.30	41.56	11.15	43.23	43.30	37.64
PAHO	Central America and Caribbean	Cuba	44.90	44.53	40.41	44.32	1.16	49.67	37.50
PAHO	Temperate South America	Uruguay	46.05	45.76	33.53	43.08	1.16	53.80	37.23
AFRO	Eastern Africa	Kenya	47.50	47.50	43.88	0.00	35.48	47.07	36.91
WPRO	South-East Asia	Laos	39.90	39.90	39.90	18.83	39.90	39.90	36.39
EURO	Northern Europe	Latvia	57.06	56.77	43.88	0.00	3.55	53.15	35.73
EMRO	Western Asia	Qatar	39.03	39.03	39.03	18.32	39.03	38.96	35.57
AFRO	Eastern Africa	Tanzania	42.51	42.51	42.51	0.58	42.51	42.51	35.52
EURO	Northern Europe	Iceland	57.71	56.99	43.74	0.00	0.00	54.02	35.41
EURO	South West Europe	Belgium	56.55	55.90	46.92	0.00	5.29	46.42	35.18
SEARO	Southern Asia	Bhutan	38.52	38.52	38.23	17.52	39.03	38.96	35.13
EURO	South West Europe	Greece	50.54	49.89	41.49	0.00	18.68	49.96	35.10
EURO	Northern Europe	Ireland	54.38	53.51	47.57	0.00	0.00	54.31	34.96
PAHO	Tropical South America	Bolivia	42.22	42.00	38.16	41.85	0.00	43.16	34.56
AFRO	Middle Africa	Democratic Republic of the Congo	41.06	41.06	40.98	0.80	41.13	41.06	34.35
EURO	South West Europe	Netherlands	52.06	51.77	48.08	0.00	6.30	47.79	34.34
SEARO	Southern Asia	Nepal	36.64	35.92	36.06	24.26	36.42	36.71	34.34
EMRO	Northern Africa	Morocco	41.13	39.97	30.63	12.02	34.69	46.13	34.09
EMRO	Western Asia	Iraq	34.40	34.03	30.05	16.00	45.98	43.16	33.94
PAHO	Central America and Caribbean	Guatemala	38.74	38.45	34.54	38.45	7.68	43.74	33.60
EURO	Eastern Europe	Slovakia	51.19	50.69	47.36	0.00	0.00	51.70	33.49
AFRO	Western Africa	Nigeria	38.52	38.52	38.52	8.18	38.52	38.52	33.47
AFRO	Western Africa	Togo	38.96	38.96	38.96	1.38	38.96	38.96	32.69
EURO	South West Europe	Italy	44.75	44.53	32.30	8.40	23.24	41.71	32.49
EURO	Northern Europe	Estonia	46.85	46.85	45.55	0.00	5.21	46.85	31.89
PAHO	Tropical South America	Ecuador	39.10	37.58	28.31	37.87	1.23	44.10	31.37
EMRO	Southern Asia	Afghanistan	33.82	33.82	33.82	18.90	33.82	33.74	31.32
EURO	Eastern Europe	Bulgaria	48.23	48.15	43.16	0.00	0.00	47.50	31.17
EMRO	Western Asia	Jordan	34.25	34.25	34.25	15.06	34.25	34.25	31.05
WPRO	Oceania Melanesia Polynesia	Fiji	32.30	30.56	29.91	9.63	37.22	36.78	29.40
EURO	Western Asia	Georgia	44.03	44.03	44.03	0.00	0.00	44.03	29.35
PAHO	Tropical South America	Venezuela	34.54	34.03	30.92	31.57	6.37	38.45	29.31
AFRO	Northern Africa	Algeria	32.30	32.22	30.77	6.37	36.28	36.42	29.06
EURO	Central Asia	Kazakhstan	44.10	44.03	42.07	0.00	0.00	44.10	29.05
EMRO	Northern Africa	Tunisia	35.48	34.32	29.33	9.70	28.96	36.50	29.05
EMRO	Western Asia	Bahrain	32.30	32.08	30.63	13.83	32.30	32.30	28.90
EURO	Central Asia	Kyrgyzstan	42.80	42.80	42.36	0.00	0.00	42.80	28.46
EURO	Eastern Europe	Moldova	42.58	42.58	42.58	0.00	0.00	42.58	28.39
AFRO	Western Africa	Burkina Faso	32.59	32.59	28.82	8.25	32.59	32.59	27.90
EURO	South West Europe	Serbia	36.93	36.93	35.26	6.81	13.03	36.93	27.65
EURO	Northern Europe	Lithuania	41.27	41.27	40.41	0.00	1.38	41.49	27.64
AFRO	Western Africa	Mali	33.89	33.89	30.05	1.59	33.09	33.09	27.60
PAHO	Central America and Caribbean	Guadeloupe	29.83	28.96	23.61	3.33	38.74	40.48	27.49
EURO	Eastern Europe	Czechia	44.32	44.17	32.08	0.00	0.00	43.74	27.38
PAHO	Central America and Caribbean	Nicaragua	31.50	27.88	29.11	31.50	0.00	43.23	27.20
PAHO	Central America and Caribbean	Martinique	29.04	28.24	23.82	3.98	37.00	38.81	26.82
AFRO	Eastern Africa	Mozambique	28.46	28.46	28.39	13.03	30.77	30.63	26.62
EURO	Western Asia	Israel	41.64	40.91	34.40	0.00	0.07	41.35	26.39
AFRO	Eastern Africa	Rwanda	31.57	31.57	30.41	0.00	30.77	30.77	25.85
AFRO	Eastern Africa	Mauritius	32.73	32.66	26.43	0.00	28.96	32.37	25.52
EURO	Western Asia	Turkey	38.52	37.65	35.70	0.00	2.75	37.87	25.42

EURO	Western Asia	Azerbaijan	37.87	37.87	37.73	0.00	0.00	37.87	25.22
EURO	South West Europe	Croatia	40.19	39.68	30.20	0.00	0.00	39.61	24.95
AFRO	Middle Africa	Central African Republic	30.20	30.20	27.15	0.00	30.20	30.20	24.66
WPRO	Oceania Melanesia Polynesia	New Zealand	36.78	35.84	28.82	7.60	13.76	24.48	24.55
AFRO	Eastern Africa	Ethiopia	30.05	29.76	26.29	0.29	30.05	30.05	24.41
EURO	South West Europe	Luxembourg	38.52	38.09	31.35	0.00	0.00	38.45	24.40
EURO	Eastern Europe	Belarus	36.86	36.78	34.25	0.00	0.00	36.57	24.08
EMRO	Western Asia	Lebanon	24.33	24.33	24.33	20.56	24.33	24.33	23.70
EURO	South West Europe	Austria	37.73	37.58	31.64	0.00	0.00	29.83	22.80
EURO	Western Asia	Armenia	34.18	34.18	34.18	0.00	0.00	34.18	22.79
EURO	Eastern Europe	Hungary	32.15	32.01	30.77	0.00	0.00	31.43	21.06
AFRO	Western Africa	Sierra Leone	22.59	22.45	22.01	5.79	25.92	25.92	20.78
EURO	South West Europe	Malta	27.59	27.59	27.59	0.00	0.00	27.59	18.39
PAHO	Tropical South America	Suriname	21.36	21.22	21.00	19.26	0.00	24.11	17.83
SEARO	South-East Asia	Myanmar	18.90	18.90	18.90	12.02	18.90	18.90	17.75
SEARO	Southern Asia	Maldives	16.94	15.42	15.93	13.40	22.38	22.23	17.72
WPRO	Oceania Melanesia Polynesia	Papua New Guinea	18.10	18.10	18.10	14.77	18.10	18.10	17.55
EURO	Central Asia	Uzbekistan	25.56	25.56	25.56	0.00	0.00	25.56	17.04
PAHO	Central America and Caribbean	Haiti	17.89	17.89	17.89	17.38	0.00	18.46	14.92
EMRO	Western Asia	Saudi Arabia	13.83	12.02	12.67	16.51	16.51	16.36	14.65
SEARO	South-East Asia	Timor-Leste	14.63	14.63	14.63	11.59	14.63	14.63	14.12
EURO	South West Europe	Albania	21.07	21.07	20.93	0.00	0.00	20.93	14.00
EURO	South West Europe	Bosnia and Herzegovina	20.93	20.93	20.93	0.00	0.00	20.93	13.95
AFRO	Western Africa	Mauritania	16.65	16.65	12.89	0.51	16.65	16.65	13.34
PAHO	Central America and Caribbean	Belize	13.40	13.03	13.11	13.40	0.00	16.51	11.57
AFRO	Western Africa	Guinea	12.89	12.89	12.89	0.00	12.89	12.89	10.74
EURO	South West Europe	North Macedonia	15.86	15.86	15.86	0.00	0.00	15.86	10.57
EURO	Eastern Europe	Kosovo	13.32	13.32	13.32	0.00	0.00	13.32	8.88
EMRO	Western Asia	West Bank and Gaza Strip	6.52	6.15	2.61	12.45	12.45	12.89	8.85
EMRO	Western Asia	Kuwait	8.83	8.62	8.83	8.54	8.83	8.83	8.75
AFRO	Middle Africa	Angola	10.14	10.14	10.14	0.00	10.14	10.07	8.44
EURO	South West Europe	Montenegro	12.02	12.02	12.02	0.00	0.00	12.02	8.01
EURO	Central Asia	Tajikistan	10.93	10.93	10.93	0.00	0.00	10.93	7.29
PAHO	Central America and Caribbean	Barbados	6.30	3.62	3.48	6.30	0.00	21.65	6.89
PAHO	Central America and Caribbean	Saint Lucia	7.10	6.73	6.73	2.32	0.00	13.32	6.03
PAHO	Central America and Caribbean	Trinidad and Tobago	5.58	4.71	1.74	5.07	0.00	17.31	5.73
PAHO	Central America and Caribbean	Aruba	5.94	4.92	2.03	4.20	0.00	14.12	5.20
EMRO	Western Asia	United Arab Emirates	5.00	5.00	5.00	4.92	5.36	5.36	5.10
EURO	Central Asia	Turkmenistan	6.88	6.88	6.88	0.00	0.00	6.88	4.59
AFRO	Eastern Africa	Seychelles	5.43	5.43	5.43	0.00	5.43	5.43	4.53
EURO	Western Asia	Cyprus	6.44	6.44	6.44	0.00	0.00	6.44	4.30
SEARO	Eastern Asia	North Korea	3.77	3.77	3.77	3.77	3.77	3.77	3.77
PAHO	Central America and Caribbean	Dominica	1.96	1.59	0.65	1.59	0.00	13.61	3.23
AFRO	Middle Africa	Chad	3.55	3.55	3.55	0.00	4.13	4.13	3.15
EMRO	Western Asia	Yemen	3.91	3.77	0.87	0.00	5.00	5.00	3.09
AFRO	Middle Africa	Congo	2.68	2.68	2.68	0.00	2.68	2.68	2.23
AFRO	Middle Africa	South Sudan	2.61	2.61	2.61	0.00	2.61	2.61	2.17
PAHO	Central America and Caribbean	Saint Vincent and the Grenadines	1.30	1.23	0.07	0.80	0.00	9.05	2.08
PAHO	Central America and Caribbean	Saint Kitts and Nevis	0.80	0.58	0.22	0.51	0.00	6.59	1.45
PAHO	Central America and Caribbean	Turks and Caicos Islands	0.72	0.58	0.29	0.58	0.00	6.23	1.40
PAHO	North America	Bermuda	1.38	1.16	0.22	0.00	0.00	4.78	1.26
PAHO	Central America and Caribbean	Cayman Islands	0.65	0.51	0.14	0.00	0.00	6.01	1.22
PAHO	Central America and Caribbean	Bahamas	0.51	0.29	0.29	0.07	0.00	5.87	1.17
PAHO	Central America and Caribbean	Anguilla	0.29	0.22	0.14	0.00	0.00	6.08	1.12
EMRO	Northern Africa	Sudan	1.52	1.52	0.58	0.00	1.52	1.52	1.11
PAHO	Central America and Caribbean	Grenada	0.14	0.14	0.07	0.65	0.00	5.50	1.09
EMRO	Western Asia	Syrian Arab Republic	1.16	1.16	1.16	0.14	1.30	1.30	1.04
PAHO	Central America and Caribbean	British Virgin Islands	0.07	0.07	0.00	0.51	0.00	5.50	1.03
PAHO	Central America and Caribbean	Antigua and Barbuda	0.07	0.00	0.07	0.00	0.00	5.65	0.97
PAHO	Tropical South America	Guyana	0.00	0.00	0.00	0.00	0.00	0.14	0.02

Supplementary Table S16. Average and median *effective time series length (ETSL)* for 8 influenza strains and subtypes (A(H1), A(H1N1)pdm09, A(H3), A(H5), A(Unsubtyped), B(Yamagata), B(Victoria), and B(Undetermined) positives) in 6 regions and 17 influenza transmission zones. We extracted FluNet data from 173 Member States on 15 June 2021. We calculated *ETSL* as the ratio of the number of time points when records are complete divided by the total time series length (TSL) and multiplied by 100. The *TSL* was 1381 weeks for all disease subtypes except A(H1N1)pdm09 (651 weeks). We report average *ETSL* with 95% confidence intervals (top values) and median *ETSL* with lower and upper quartiles (bottom values). Regions and zones are listed in descending order by average positives *ETSL*, and we omit the Southern African transmission zone, as it consisted of only 1 country.

Region	A(H1)	A(H1N1)pdm09	A(H3)	A(H5)	A(Unsubtyped)	B(Yamagata)	B(Victoria)	B(Undetermined)
AFRO	23.56 [17.40, 29.71] 22.48 [12.82, 31.35]	30.48 [25.32, 35.63] 33.02 [21.94, 42.51]	34.24 [27.22, 41.26] 33.24 [22.38, 46.05]	30.26 [25.15, 35.37] 33.24 [21.87, 41.71]	33.85 [27.10, 40.60] 33.20 [21.65, 45.98]	27.18 [21.75, 32.61] 27.62 [12.82, 41.93]	27.25 [21.79, 32.70] 27.62 [12.89, 42.36]	30.21 [24.54, 35.88] 29.40 [17.45, 43.59]
EMRO	16.61 [10.41, 22.81] 20.71 [0.07, 28.53]	24.33 [17.00, 31.66] 29.40 [5.29, 39.03]	25.08 [16.42, 33.75] 30.92 [3.91, 39.03]	21.92 [13.74, 30.11] 26.72 [0.00, 39.03]	23.99 [15.48, 32.49] 26.50 [1.16, 39.03]	22.07 [14.10, 30.03] 25.20 [1.16, 38.60]	22.09 [14.12, 30.06] 25.49 [1.16, 38.60]	24.36 [16.44, 32.28] 29.18 [2.61, 39.03]
EURO	42.89 [37.92, 47.85] 43.08 [32.01, 58.73]	34.32 [31.14, 37.50] 37.73 [26.79, 44.03]	43.64 [38.60, 48.68] 43.08 [34.11, 58.00]	4.76 [2.17, 7.34] 0.00 [0.00, 3.55]	44.22 [39.16, 49.27] 44.03 [35.48, 58.65]	34.98 [31.57, 38.40] 37.58 [26.94, 43.74]	34.98 [31.58, 38.38] 37.58 [26.94, 43.74]	39.02 [35.02, 43.01] 41.93 [31.21, 49.46]
PAHO	26.59 [19.38, 33.80] 23.64 [0.00, 46.78]	23.84 [18.20, 29.48] 25.42 [1.12, 42.58]	29.31 [21.47, 37.15] 27.01 [0.33, 50.65]	7.25 [4.33, 10.17] 0.00 [0.00, 14.37]	29.65 [21.38, 37.92] 21.43 [0.00, 50.54]	18.73 [13.68, 23.79] 19.37 [0.11, 33.27]	18.87 [13.81, 23.92] 19.55 [0.29, 33.27]	26.63 [19.69, 33.57] 28.10 [0.11, 47.54]
SEARO	20.49 [10.18, 30.79] 24.84 [1.59, 35.41]	30.12 [21.57, 38.67] 36.28 [14.63, 41.42]	33.99 [22.93, 45.05] 38.52 [14.63, 45.11]	24.81 [17.78, 31.84] 25.85 [14.63, 33.74]	25.96 [15.44, 36.49] 36.06 [12.82, 41.42]	25.69 [17.59, 33.80] 31.21 [14.63, 34.61]	25.26 [17.24, 33.29] 31.28 [14.63, 34.83]	32.19 [22.00, 42.38] 37.15 [15.79, 44.90]
WPRO	48.85 [37.85, 59.85] 50.04 [26.43, 64.81]	41.25 [35.51, 46.98] 43.30 [39.90, 46.99]	58.34 [47.30, 69.39] 55.32 [39.90, 81.82]	38.18 [32.48, 43.89] 39.90 [35.19, 46.13]	54.08 [43.06, 65.11] 54.96 [34.25, 70.67]	41.34 [35.30, 47.37] 44.53 [39.17, 49.38]	41.35 [35.34, 47.37] 44.53 [39.17, 49.38]	49.90 [40.85, 58.96] 53.80 [35.19, 60.46]
Zone								
Central America and Caribbean	18.40 [10.21, 26.58] 9.27 [0.00, 36.35]	18.12 [11.13, 25.12] 9.74 [0.51, 38.27]	19.72 [11.18, 28.27] 9.45 [0.14, 39.79]	5.19 [2.11, 8.27] 0.00 [0.00, 10.25]	19.52 [10.93, 28.11] 9.34 [0.00, 43.05]	13.76 [7.68, 19.84] 6.01 [0.00, 23.64]	14.00 [7.91, 20.10] 6.05 [0.11, 24.73]	18.60 [11.00, 26.20] 9.41 [0.04, 41.49]
Central Asia	25.72 [10.89, 40.55] 25.56 [10.93, 42.29]	24.52 [10.99, 38.05] 25.56 [10.93, 39.10]	25.65 [10.90, 40.40] 25.56 [10.93, 42.22]	0.00 [0.00, 0.00] 0.00 [0.00, 0.00]	25.66 [10.89, 40.44] 25.56 [10.93, 41.49]	25.11 [10.94, 39.29] 25.56 [10.93, 40.19]	24.90 [10.96, 38.83] 25.56 [10.93, 39.97]	25.36 [10.93, 39.79] 25.56 [10.93, 41.49]
Eastern Africa	26.08 [17.19, 34.96] 27.15 [19.99, 31.35]	33.04 [25.89, 40.19] 33.60 [28.96, 42.51]	38.14 [27.42, 48.86] 37.36 [29.62, 47.21]	33.08 [25.92, 40.23] 33.78 [28.96, 42.51]	37.97 [27.46, 48.47] 37.11 [29.76, 47.21]	28.33 [19.86, 36.79] 27.62 [22.16, 42.36]	28.33 [19.86, 36.79] 27.62 [22.16, 42.36]	34.40 [25.56, 43.23] 35.41 [26.43, 43.88]
Eastern Asia	49.95 [20.43, 79.47] 59.67 [36.13, 64.81]	36.34 [20.23, 52.45] 44.90 [40.33, 45.69]	57.52 [28.00, 87.05] 59.59 [52.79, 81.82]	34.69 [19.21, 50.16] 39.39 [38.45, 44.82]	48.30 [22.06, 74.54] 59.52 [39.68, 69.23]	39.09 [18.92, 59.25] 46.99 [39.46, 49.38]	39.04 [18.91, 59.18] 46.99 [39.39, 49.38]	52.95 [26.72, 79.17] 59.30 [49.09, 73.35]
Eastern Europe	46.05 [36.94, 55.16] 46.20 [36.21, 59.96]	37.24 [30.53, 43.95] 42.51 [29.98, 45.40]	46.30 [37.13, 55.47] 47.43 [36.50, 60.10]	8.47 [0.31, 16.62] 0.00 [0.00, 27.08]	45.82 [36.85, 54.79] 44.53 [36.06, 58.58]	37.83 [30.81, 44.84] 41.93 [29.04, 47.50]	37.82 [30.81, 44.83] 41.93 [29.04, 47.43]	40.79 [33.57, 48.02] 43.16 [32.08, 51.48]
Middle Africa	12.87 [3.11, 22.62] 10.14 [0.00, 25.49]	19.42 [5.31, 33.52] 10.14 [2.68, 41.06]	19.71 [5.22, 34.20] 10.14 [2.68, 40.98]	19.41 [5.31, 33.50] 10.14 [2.68, 40.98]	19.99 [5.17, 34.80] 10.14 [2.68, 40.98]	17.81 [5.12, 30.50] 10.14 [2.68, 37.36]	17.75 [5.14, 30.37] 10.14 [2.68, 37.36]	18.09 [5.17, 31.01] 10.14 [2.68, 38.23]
Northern Africa	22.59 [11.22, 33.96] 25.85 [24.19, 27.44]	27.23 [12.95, 41.51] 29.40 [26.94, 31.64]	30.66 [14.22, 47.10] 32.08 [30.92, 37.87]	25.56 [10.93, 40.20] 26.72 [23.75, 30.70]	28.20 [11.92, 44.48] 31.50 [23.90, 31.93]	23.74 [11.27, 36.20] 25.20 [23.90, 30.12]	23.77 [11.29, 36.24] 25.49 [23.82, 29.98]	27.02 [12.45, 41.60] 29.18 [28.60, 29.98]
North America	36.47 [0.00, 79.10] 34.18 [0.00, 75.24]	30.94 [1.12, 60.77] 45.98 [0.51, 46.34]	44.90 [0.00, 90.84] 53.15 [0.80, 80.74]	15.66 [0.30, 31.03] 23.03 [0.00, 23.97]	51.97 [0.92, 103.01] 74.87 [0.00, 81.03]	22.81 [0.00, 47.99] 23.97 [0.00, 44.46]	22.88 [0.00, 47.94] 23.97 [0.22, 44.46]	46.73 [0.19, 93.27] 62.78 [0.00, 77.41]
Northern Europe	56.84 [48.88, 64.8] 51.74 [46.13, 69.23]	42.17 [39.80, 44.53] 42.83 [41.20, 44.82]	58.22 [49.99, 66.45] 53.98 [46.85, 69.88]	2.19 [0.99, 3.40] 2.82 [0.00, 3.55]	59.25 [51.86, 66.65] 58.91 [51.12, 69.30]	44.50 [40.34, 48.67] 44.06 [40.33, 45.26]	44.48 [40.47, 48.48] 44.06 [40.33, 45.33]	50.91 [45.42, 56.40] 48.55 [43.81, 55.61]
Oceania Melanesia Polynesia	35.38 [19.88, 50.88] 26.43 [25.78, 44.97]	30.08 [19.81, 40.35] 29.04 [19.26, 40.70]	45.42 [22.09, 68.74] 33.96 [29.54, 62.49]	26.53 [16.32, 36.75] 27.01 [18.10, 35.19]	46.92 [21.28, 72.57] 34.03 [27.15, 69.08]	30.41 [18.85, 41.97] 26.36 [18.90, 42.51]	30.49 [18.92, 42.05] 26.65 [18.90, 42.51]	37.44 [19.38, 55.50] 29.40 [28.82, 49.02]

Southeast Asia	38.46 [22.41, 54.52] 40.66 [21.00, 54.31]	41.33 [32.58, 50.09] 44.90 [39.90, 47.07]	50.86 [36.88, 64.84] 55.03 [39.90, 65.75]	37.52 [29.60, 45.45] 41.31 [28.53, 46.13]	43.37 [27.63, 59.10] 43.19 [34.25, 54.96]	37.68 [29.33, 46.02] 41.46 [31.43, 44.97]	37.55 [29.24, 45.87] 40.80 [31.43, 45.11]	43.77 [33.25, 54.28] 49.35 [35.19, 56.48]
Southern Asia	25.68 [17.11, 34.26] 31.35 [16.15, 35.41]	36.30 [30.35, 42.26] 38.52 [33.96, 41.42]	39.84 [32.16, 47.52] 41.35 [35.63, 45.11]	31.74 [24.91, 38.57] 33.38 [25.85, 41.35]	35.19 [26.30, 44.08] 37.44 [33.38, 42.65]	33.51 [26.51, 40.51] 34.40 [31.21, 41.06]	33.13 [25.91, 40.35] 33.82 [31.28, 40.98]	37.84 [31.05, 44.63] 38.16 [33.82, 42.29]
Southwest Europe	41.64 [33.27, 50.00] 38.02 [27.59, 59.45]	32.45 [27.59, 37.32] 34.69 [24.84, 42.22]	42.67 [34.26, 51.08] 43.08 [27.59, 58.00]	6.59 [1.87, 11.32] 0.00 [0.00, 13.03]	43.89 [35.33, 52.45] 42.58 [27.59, 62.93]	32.51 [27.42, 37.60] 34.40 [22.30, 40.55]	32.57 [27.48, 37.65] 34.40 [23.17, 40.48]	37.53 [31.05, 44.01] 35.26 [27.59, 49.46]
Temperate South America	51.54 [43.47, 59.61] 51.67 [44.79, 58.29]	41.91 [35.06, 48.75] 44.53 [37.58, 46.23]	56.01 [45.31, 66.71] 57.13 [47.68, 64.34]	11.75 [0.05, 23.45] 9.92 [2.57, 20.93]	60.75 [47.84, 73.67] 63.36 [52.82, 68.68]	37.18 [23.69, 50.67] 40.41 [28.02, 46.34]	37.36 [23.95, 50.78] 40.62 [28.17, 46.56]	50.58 [38.19, 62.97] 53.19 [41.85, 59.30]
Tropical South America	37.69 [23.85, 51.54] 41.71 [23.46, 55.03]	31.21 [21.82, 40.60] 31.72 [26.29, 41.13]	42.07 [26.36, 57.78] 41.78 [32.73, 57.78]	8.87 [1.18, 16.55] 6.37 [0.00, 8.69]	39.91 [22.95, 56.88] 37.94 [20.85, 64.23]	24.64 [16.23, 33.06] 27.95 [20.85, 30.41]	24.43 [15.90, 32.97] 26.29 [20.93, 30.41]	34.26 [22.39, 46.13] 30.92 [27.95, 51.19]
Western Africa	24.76 [13.47, 36.05] 18.90 [12.82, 32.37]	33.78 [26.79, 40.77] 38.52 [21.94, 42.72]	38.15 [26.52, 49.79] 38.52 [22.38, 46.05]	33.26 [26.43, 40.08] 35.26 [21.87, 41.49]	37.48 [26.71, 48.26] 38.52 [21.65, 45.98]	30.12 [21.45, 38.80] 28.82 [21.72, 42.58]	30.43 [21.60, 39.25] 28.82 [21.87, 44.82]	32.06 [23.97, 40.14] 38.52 [17.45, 43.59]
Western Asia	18.71 [11.40, 26.01] 21.04 [0.07, 33.24]	23.08 [16.12, 30.05] 28.75 [6.44, 34.25]	23.20 [15.31, 31.10] 30.77 [5.00, 37.87]	11.13 [3.65, 18.60] 0.00 [0.00, 26.72]	22.93 [14.99, 30.88] 29.29 [2.03, 37.87]	21.52 [13.68, 29.36] 26.36 [2.17, 34.25]	21.55 [13.70, 29.39] 26.47 [2.17, 34.25]	23.47 [15.94, 31.00] 30.34 [6.44, 35.63]
Worldwide	**31.40 [28.06, 34.73]** **31.03 [13.40, 46.34]**	**30.15 [27.78, 32.53]** **34.21 [18.90, 43.16]**	**36.87 [33.41, 40.34]** **38.52 [18.90, 51.85]**	**16.07 [13.52, 18.62]** **9.41 [0.00, 30.70]**	**36.05 [32.55, 39.54]** **37.91 [16.87, 50.83]**	**27.92 [25.43, 30.40]** **29.33 [14.63, 41.93]**	**27.94 [25.46, 30.42]** **29.58 [14.63, 42.22]**	**33.14 [30.21, 36.07]** **35.23 [17.89, 47.36]**

Supplementary Table S17. The *effective time series length* (*ETSL*) of 173 Member States for 8 influenza strains and subtypes (A(H1), A(H1N1)pdm09, A(H3), A(H5), A(Unsubtyped) abbreviated A(Uns), B(Yamagata) abbreviated B(Yam), B(Victoria) abbreviated B(Vic), and B(Undetermined) positives abbreviated B(Und)) reported by the WHO's FluNet. Data were downloaded on 15 June 2021 at which time the *time series length* (*TSL*) of reported data was 1381 weeks for all subtypes except A(H1N1)pdm09 positives (651 weeks). We calculated *ETSL* as the ratio of the number of time points when records are complete divided by the *TSL* and multiplied by 100. Member States are listed in descending order by average *ETSL* across all 8 subtypes (AVG), regions, and zones. Member State-outcome dyads where all weeks have incomplete records have an *ETSL* of 0.

Region	Zone	Country/Territory	A(H1)	A(H1N1)	A(H3)	A(H5)	A(Uns)	B(Yam)	B(Vic)	B(Und)	AVG
WPRO	South-East Asia	Malaysia	78.06	58.36	88.85	45.11	88.85	44.97	45.11	60.46	63.72
WPRO	Eastern Asia	Japan	89.14	46.99	89.65	46.99	69.23	46.99	46.99	73.35	63.67
WPRO	Eastern Asia	China	64.81	45.69	81.82	38.45	73.06	49.38	49.38	79.22	60.23
PAHO	North America	United States of America	75.24	45.98	80.74	23.03	81.03	44.46	44.46	77.41	59.04
EURO	Northern Europe	United Kingdom	76.32	45.91	80.16	2.68	72.63	61.84	60.97	68.79	58.66
WPRO	Oceania Melanesia Polynesia	Australia	61.62	40.70	82.98	35.19	86.24	42.51	42.51	66.55	57.29
WPRO	South-East Asia	Philippines	69.08	47.07	70.09	46.13	70.67	49.96	49.89	54.53	57.18
WPRO	Eastern Asia	Mongolia	59.67	44.90	59.59	44.82	59.52	59.59	59.45	59.30	55.86
EURO	South West Europe	Slovenia	72.63	51.70	72.70	10.21	72.48	54.67	54.67	56.70	55.72
AFRO	Western Africa	Senegal	74.08	39.90	85.95	35.26	79.58	41.56	44.82	43.59	55.59
PAHO	Central America and Caribbean	Mexico	77.05	47.07	80.88	24.04	76.90	40.12	40.12	56.99	55.39
AFRO	Eastern Africa	Madagascar	54.09	43.81	71.76	43.81	70.17	49.31	49.31	55.32	54.70
PAHO	Temperate South America	Argentina	56.12	45.55	67.56	27.15	73.86	50.04	50.04	62.78	54.14
EURO	Eastern Europe	Poland	65.46	46.78	65.75	29.11	66.84	49.24	49.24	51.48	52.99
EURO	Northern Europe	Norway	72.70	45.76	73.14	3.69	75.38	45.76	45.76	61.26	52.93
EURO	South West Europe	Germany	70.02	45.18	71.18	0.00	68.72	47.14	47.14	58.51	50.99
EURO	Eastern Europe	Russian Federation	60.17	45.11	61.12	33.09	56.92	47.50	47.43	54.82	50.77
WPRO	Oceania Melanesia Polynesia	New Caledonia	44.97	43.30	62.49	40.26	69.08	46.20	46.27	49.02	50.20
AFRO	Southern Africa	South Africa	57.64	44.68	56.12	44.68	52.21	45.98	45.26	53.01	49.95
EURO	South West Europe	France	59.45	42.22	60.61	30.05	66.18	42.22	42.22	55.76	49.84
EURO	Northern Europe	Denmark	69.23	44.82	69.88	5.21	69.30	45.11	45.33	49.53	49.80
EURO	South West Europe	Spain	55.76	44.03	57.57	32.08	62.93	46.34	46.34	52.93	49.75
WPRO	South-East Asia	Cambodia	54.31	55.25	55.32	54.02	34.25	54.02	54.02	35.19	49.55
WPRO	South-East Asia	Singapore	50.04	46.49	54.89	46.49	54.96	44.53	44.53	53.80	49.47
PAHO	Tropical South America	Brazil	55.03	41.13	66.04	28.24	64.23	41.64	43.16	55.83	49.41
EMRO	Southern Asia	Iran	36.86	45.11	55.76	44.90	53.66	48.30	48.37	52.21	48.14
PAHO	Tropical South America	Colombia	68.57	46.63	79.94	7.24	79.07	28.75	22.95	51.19	48.04
SEARO	South-East Asia	Thailand	47.72	46.71	65.75	28.53	47.36	43.01	41.71	60.46	47.66
EURO	Northern Europe	Finland	65.46	41.20	66.40	2.97	67.99	41.93	42.29	52.86	47.64
EURO	Eastern Europe	Ukraine	58.73	49.46	58.29	3.84	58.58	49.46	49.46	51.56	47.42
EURO	Eastern Europe	Romania	59.96	39.32	60.10	27.08	59.38	41.93	41.93	47.36	47.13
AFRO	Western Africa	Ghana	32.37	48.15	48.15	47.79	48.01	48.15	48.15	48.08	46.11
EURO	South West Europe	Portugal	66.76	36.71	67.85	0.00	66.69	40.26	40.26	49.46	46.00
PAHO	Temperate South America	Paraguay	60.46	46.92	61.12	5.14	63.22	38.16	38.16	50.54	45.47
PAHO	Temperate South America	Chile	47.21	43.52	53.15	14.70	63.50	42.65	43.08	55.83	45.46
PAHO	Tropical South America	Peru	56.55	40.91	57.78	8.69	68.43	36.13	36.13	55.10	44.97
EMRO	Northern Africa	Egypt	34.90	46.63	51.85	46.49	52.64	38.88	38.96	46.78	44.64
PAHO	Central America and Caribbean	El Salvador	49.60	46.13	51.19	17.38	50.83	45.91	45.91	47.57	44.32
WPRO	South-East Asia	Viet Nam	33.60	43.30	55.18	38.81	46.49	39.17	39.17	56.48	44.03
AFRO	Middle Africa	Cameroon	32.95	45.69	47.94	45.69	49.75	41.93	41.49	42.29	43.46
PAHO	Central America and Caribbean	Jamaica	50.25	49.96	50.11	14.05	50.25	41.93	41.93	46.78	43.16
PAHO	North America	Canada	34.18	46.34	53.15	23.97	74.87	23.97	23.97	62.78	42.90
PAHO	Central America and Caribbean	Honduras	46.34	46.27	53.73	12.38	53.73	40.84	40.84	47.50	42.70
EURO	Northern Europe	Sweden	45.55	43.59	46.85	0.00	62.27	43.74	43.74	55.61	42.67
EMRO	Western Asia	Oman	29.69	40.55	46.49	40.55	45.18	46.42	46.49	45.11	42.56
WPRO	Eastern Asia	South Korea	36.13	40.33	52.79	39.39	39.68	39.46	39.39	49.09	42.03
EURO	Eastern Europe	Slovakia	50.25	45.40	50.62	0.00	50.33	45.26	45.26	47.36	41.81
EURO	Northern Europe	Ireland	50.47	44.39	51.48	0.00	51.41	44.39	44.39	47.57	41.76

AFRO	Eastern Africa	Zambia	28.02	42.80	45.55	42.80	45.47	42.80	42.80	43.37	41.70
AFRO	Eastern Africa	Kenya	36.13	35.99	47.50	35.99	47.43	42.36	42.36	43.88	41.46
EURO	South West Europe	Switzerland	60.03	34.83	58.00	3.48	58.65	34.90	35.48	45.84	41.40
EMRO	Southern Asia	Pakistan	31.35	43.23	43.30	43.01	42.65	41.06	40.98	41.49	40.89
AFRO	Western Africa	Niger	4.71	45.98	46.05	46.05	45.98	46.05	45.91	46.05	40.85
PAHO	Central America and Caribbean	Panama	44.82	40.33	44.75	15.35	46.56	44.68	44.68	45.55	40.84
AFRO	Western Africa	Côte d'Ivoire	25.49	42.72	43.66	41.49	43.66	42.58	42.58	43.59	40.72
EURO	South West Europe	Netherlands	49.09	45.84	50.69	0.07	50.33	40.55	40.48	48.01	40.63
EURO	Northern Europe	Estonia	46.13	42.07	45.91	3.55	46.13	45.26	45.26	45.55	39.98
EURO	Northern Europe	Latvia	53.01	33.16	54.74	3.55	55.54	37.15	37.15	43.81	39.76
SEARO	Southern Asia	Bangladesh	24.84	41.42	41.35	41.35	41.42	42.72	42.72	42.29	39.76
EURO	Northern Europe	Iceland	49.09	39.54	53.22	0.00	51.12	39.54	39.54	43.74	39.47
EURO	Eastern Europe	Bulgaria	46.20	42.51	47.43	0.00	44.53	41.93	41.93	43.16	38.46
AFRO	Eastern Africa	Uganda	30.85	41.64	47.21	41.71	47.21	27.01	27.01	44.68	38.41
EURO	Western Asia	Georgia	44.03	44.03	44.03	0.00	44.03	43.16	43.16	44.03	38.31
EURO	South West Europe	Belgium	43.37	38.38	45.26	2.10	55.10	37.22	37.15	46.92	38.19
AFRO	Middle Africa	Democratic Republic of the Congo	25.49	41.06	40.98	40.98	40.98	37.36	37.36	38.23	37.81
SEARO	Southern Asia	India	39.10	40.04	50.54	28.10	37.44	34.40	33.31	38.16	37.64
WPRO	South-East Asia	Laos	21.00	39.90	39.90	39.90	39.90	39.90	39.90	39.90	37.54
EURO	South West Europe	Greece	45.33	35.63	46.20	15.28	45.47	34.90	35.70	41.49	37.50
SEARO	South-East Asia	Indonesia	25.49	42.72	45.11	42.72	36.06	31.43	31.43	44.90	37.48
EURO	Eastern Europe	Moldova	42.58	42.58	42.58	0.00	42.58	42.58	42.58	42.58	37.26
SEARO	Southern Asia	Sri Lanka	35.41	36.28	45.11	25.85	44.10	31.21	31.28	47.36	37.07
AFRO	Western Africa	Nigeria	24.33	38.52	38.52	38.52	38.52	38.52	38.52	38.52	36.75
EMRO	Western Asia	Qatar	20.71	39.03	39.03	39.03	39.03	38.60	38.60	39.03	36.63
EURO	Central Asia	Kyrgyzstan	42.29	40.12	42.65	0.00	41.49	42.00	41.13	41.49	36.40
EURO	Central Asia	Kazakhstan	42.94	39.10	42.22	0.00	43.45	40.19	39.97	41.93	36.22
SEARO	Southern Asia	Bhutan	33.38	38.52	38.52	33.74	37.36	34.61	34.83	37.15	36.02
AFRO	Eastern Africa	Tanzania	26.29	42.51	42.43	42.51	42.51	24.55	24.55	42.51	35.98
PAHO	Central America and Caribbean	Costa Rica	47.86	43.16	48.44	3.19	49.60	22.45	22.45	48.15	35.66
EURO	Northern Europe	Lithuania	40.48	41.20	40.41	0.29	40.77	40.33	40.33	40.41	35.53
AFRO	Western Africa	Togo	38.60	38.96	38.96	38.96	38.96	22.52	22.52	38.96	34.80
PAHO	Tropical South America	French Guiana	41.85	31.72	45.33	29.11	38.67	27.95	29.69	28.24	34.07
PAHO	Central America and Caribbean	Cuba	42.07	41.93	44.39	4.92	41.93	26.57	26.57	40.41	33.60
EURO	Western Asia	Azerbaijan	37.80	37.73	37.87	0.00	37.87	37.58	37.58	37.73	33.02
PAHO	Tropical South America	Bolivia	41.71	42.00	41.78	0.00	37.94	30.41	30.41	38.16	32.80
EMRO	Western Asia	Jordan	21.36	34.25	34.25	34.25	34.25	34.25	34.25	34.25	32.64
EURO	South West Europe	Serbia	32.01	34.69	36.93	13.03	36.93	34.40	34.40	35.26	32.20
EMRO	Southern Asia	Afghanistan	16.15	33.82	33.82	33.38	33.38	33.82	33.82	33.82	31.50
EURO	South West Europe	Italy	36.71	24.84	43.08	18.97	42.58	22.30	23.17	31.93	30.45
AFRO	Eastern Africa	Rwanda	31.35	31.21	31.14	31.57	31.57	29.04	29.04	27.73	30.33
EURO	Eastern Europe	Belarus	36.21	32.51	36.50	0.00	36.06	33.53	33.53	34.25	30.32
AFRO	Northern Africa	Algeria	25.85	31.64	32.08	30.70	31.50	30.12	29.98	29.98	30.23
EURO	Western Asia	Armenia	34.18	34.18	34.18	0.00	34.18	34.11	34.11	34.18	29.89
EURO	Western Asia	Turkey	33.24	31.21	34.61	2.17	35.48	32.30	32.37	35.63	29.63
EMRO	Western Asia	Bahrain	18.32	32.08	32.08	32.08	32.08	29.76	29.76	30.63	29.60
AFRO	Western Africa	Burkina Faso	17.09	32.59	32.59	32.59	32.59	28.82	28.82	28.82	29.24
EMRO	Northern Africa	Morocco	27.44	29.40	37.87	26.72	31.93	25.20	25.49	28.60	29.08
EURO	Eastern Europe	Czechia	43.08	22.66	43.01	0.00	44.03	22.30	22.30	32.08	28.68
PAHO	Central America and Caribbean	Guatemala	30.63	36.21	35.19	8.11	34.03	24.84	27.08	32.37	28.56
PAHO	Temperate South America	Uruguay	42.36	31.64	42.22	0.00	42.43	17.89	18.18	33.16	28.48
EURO	South West Europe	Croatia	38.02	26.79	37.07	0.00	39.03	27.95	27.88	30.12	28.36
EURO	Western Asia	Israel	36.86	26.29	38.02	0.00	38.23	26.21	26.43	34.25	28.29
EMRO	Western Asia	Iraq	28.53	31.86	29.47	26.72	26.50	26.50	26.50	30.05	28.27
AFRO	Western Africa	Mali	18.90	33.45	33.89	33.89	33.82	26.36	26.36	17.45	28.01
EURO	South West Europe	Austria	31.86	29.54	34.11	0.00	35.84	29.47	29.47	31.64	27.74
WPRO	Oceania Melanesia Polynesia	Fiji	26.43	29.04	29.54	27.01	27.15	26.36	26.65	29.40	27.70
AFRO	Middle Africa	Central African Republic	18.83	30.20	30.12	30.20	30.20	26.43	26.43	27.15	27.44
EURO	South West Europe	Luxembourg	32.66	28.89	32.15	0.00	35.55	29.18	28.17	31.21	27.23

AFRO	Eastern Africa	Mozambique	13.40	28.46	28.46	28.46	28.39	28.24	28.24	28.31	26.49
EURO	Eastern Europe	Hungary	30.56	29.98	30.56	0.00	31.50	29.04	29.04	30.77	26.43
PAHO	Tropical South America	Venezuela	31.21	26.29	32.73	6.37	30.20	26.29	26.29	30.92	26.29
AFRO	Eastern Africa	Ethiopia	20.64	29.62	29.62	29.54	29.76	22.16	22.16	26.29	26.22
EMRO	Northern Africa	Tunisia	24.19	26.94	30.92	23.75	23.90	23.90	23.82	29.18	25.82
EMRO	Western Asia	Lebanon	24.33	24.33	24.33	24.33	24.33	24.33	24.33	24.33	24.33
PAHO	Central America and Caribbean	Dominican Republic	26.29	30.27	28.67	0.00	44.17	11.22	11.37	42.58	24.32
SEARO	Southern Asia	Nepal	14.05	33.96	35.63	21.65	12.82	22.88	20.13	32.30	24.18
AFRO	Eastern Africa	Mauritius	19.99	28.96	32.30	28.96	31.72	12.38	12.38	26.43	24.14
EURO	South West Europe	Malta	27.59	27.59	27.59	0.00	27.59	26.94	26.94	27.59	23.98
WPRO	Oceania Melanesia Polynesia	New Zealand	25.78	19.26	33.96	12.09	34.03	18.90	18.90	28.82	23.97
PAHO	Central America and Caribbean	Guadeloupe	23.82	24.40	25.34	23.82	21.65	22.30	22.88	21.22	23.18
EURO	Central Asia	Uzbekistan	25.56	25.56	25.56	0.00	25.56	25.56	25.56	25.56	22.37
PAHO	Central America and Caribbean	Martinique	22.09	24.55	23.17	22.09	19.91	21.07	22.45	19.84	21.90
AFRO	Western Africa	Sierra Leone	10.93	21.94	22.38	21.87	21.65	21.72	21.87	21.80	20.52
PAHO	Tropical South America	Ecuador	23.46	31.35	33.82	0.14	19.84	9.78	10.35	27.95	19.59
EURO	South West Europe	Albania	21.00	20.93	20.93	0.00	21.00	20.85	20.85	20.93	18.31
PAHO	Tropical South America	Suriname	20.85	20.85	21.22	0.00	20.85	20.85	20.93	20.93	18.31
EURO	South West Europe	Bosnia and Herzegovina	20.93	20.93	20.93	0.00	20.93	20.85	20.85	20.93	18.29
WPRO	Oceania Melanesia Polynesia	Papua New Guinea	18.10	18.10	18.10	18.10	18.10	18.10	18.10	13.40	17.51
PAHO	Central America and Caribbean	Nicaragua	18.90	24.19	24.76	0.00	21.22	5.65	5.65	29.11	16.18
SEARO	South-East Asia	Myanmar	3.77	18.90	18.90	18.90	15.13	15.13	15.13	18.90	15.60
PAHO	Central America and Caribbean	Haiti	16.87	17.89	17.89	0.00	16.87	17.89	17.89	17.89	15.40
EURO	South West Europe	North Macedonia	15.86	15.86	15.86	0.00	15.86	15.57	15.57	15.86	13.80
AFRO	Western Africa	Guinea	12.82	12.82	12.89	12.89	12.89	12.82	12.89	12.89	12.86
SEARO	Southern Asia	Maldives	0.00	14.34	14.55	13.69	13.90	12.60	12.74	15.79	12.20
AFRO	Western Africa	Mauritania	13.03	16.58	16.65	16.51	16.65	2.24	2.24	12.89	12.10
EURO	Eastern Europe	Kosovo	13.32	13.32	13.32	0.00	13.32	13.32	13.32	13.32	11.66
SEARO	South-East Asia	Timor-Leste	1.59	14.63	14.63	14.63	0.00	14.63	14.63	13.03	10.97
PAHO	Central America and Caribbean	Belize	12.24	12.89	12.38	0.00	12.38	12.31	12.96	12.31	10.93
EURO	South West Europe	Montenegro	12.02	12.02	12.02	0.00	12.02	12.02	12.02	12.02	10.52
AFRO	Middle Africa	Angola	10.14	10.14	10.14	10.14	10.14	10.14	10.14	10.14	10.14
EURO	Central Asia	Tajikistan	10.93	10.93	10.93	0.00	10.93	10.93	10.93	10.93	9.57
EURO	Central Asia	Turkmenistan	6.88	6.88	6.88	0.00	6.88	6.88	6.88	6.88	6.02
EURO	Western Asia	Cyprus	6.44	6.44	6.44	0.00	6.44	6.44	6.44	6.44	5.64
PAHO	Central America and Caribbean	Saint Lucia	6.30	6.59	6.52	0.00	6.30	6.37	6.44	6.52	5.63
AFRO	Eastern Africa	Seychelles	0.00	5.43	5.43	5.43	5.43	5.43	5.43	5.43	4.75
EMRO	Western Asia	Saudi Arabia	0.07	10.79	0.00	0.00	11.37	0.00	0.00	12.67	4.36
EMRO	Western Asia	Kuwait	0.00	7.60	6.15	0.00	2.03	2.17	2.17	8.83	3.62
AFRO	Middle Africa	Chad	0.00	3.55	3.55	3.55	3.55	3.55	3.55	3.55	3.10
AFRO	Middle Africa	Congo	2.68	2.68	2.68	2.68	2.68	2.68	2.68	2.68	2.68
EMRO	Western Asia	United Arab Emirates	0.00	5.00	5.00	0.00	0.00	4.34	4.49	0.65	2.43
AFRO	Middle Africa	South Sudan	0.00	2.61	2.53	2.61	2.61	2.61	2.61	2.61	2.27
SEARO	Eastern Asia	North Korea	0.00	3.77	3.77	3.77	0.00	0.00	0.00	3.77	1.88
EMRO	Western Asia	West Bank and Gaza Strip	0.00	5.29	3.91	0.00	0.36	0.00	0.00	2.61	1.52
EMRO	Western Asia	Syrian Arab Republic	1.16	1.16	1.16	1.16	1.16	1.16	1.16	1.16	1.16
PAHO	Central America and Caribbean	Barbados	0.00	2.53	1.74	0.00	0.14	0.29	1.01	2.90	1.08
PAHO	Central America and Caribbean	Trinidad and Tobago	0.00	4.06	1.74	0.00	0.07	0.36	0.36	1.23	0.98
PAHO	Central America and Caribbean	Aruba	0.00	4.92	0.00	0.00	0.00	0.29	0.00	1.74	0.87
EMRO	Northern Africa	Sudan	0.58	1.52	0.58	0.14	1.01	0.58	0.58	0.58	0.70
EMRO	Western Asia	Yemen	0.00	3.69	0.65	0.00	0.29	0.00	0.00	0.87	0.69
PAHO	Central America and Caribbean	Dominica	0.00	1.38	0.29	0.00	0.00	0.14	0.51	0.07	0.30
PAHO	North America	Bermuda	0.00	0.51	0.80	0.00	0.00	0.00	0.22	0.00	0.19
PAHO	Central America and Caribbean	Saint Vincent and the Grenadines	0.00	0.87	0.36	0.00	0.00	0.00	0.07	0.00	0.16
PAHO	Central America and Caribbean	Cayman Islands	0.00	0.43	0.29	0.00	0.00	0.00	0.00	0.14	0.11
PAHO	Central America and Caribbean	Turks and Caicos Islands	0.00	0.51	0.07	0.00	0.00	0.00	0.29	0.00	0.11
PAHO	Central America and Caribbean	Saint Kitts and Nevis	0.00	0.51	0.07	0.00	0.00	0.07	0.14	0.00	0.10
PAHO	Central America and Caribbean	Bahamas	0.00	0.14	0.14	0.00	0.00	0.00	0.29	0.00	0.07
PAHO	Central America and Caribbean	Anguilla	0.00	0.07	0.14	0.00	0.00	0.00	0.07	0.07	0.05

PAHO	Central America and Caribbean	Grenada	0.00	0.14	0.00	0.00	0.00	0.00	0.07	0.00	0.03
PAHO	Central America and Caribbean	Antigua and Barbuda	0.00	0.00	0.00	0.00	0.00	0.00	0.07	0.00	0.01
PAHO	Central America and Caribbean	British Virgin Islands	0.00	0.07	0.00	0.00	0.00	0.00	0.00	0.00	0.01
PAHO	Tropical South America	Guyana	0.00	0.00	0.00	0.00	0.00	0.00	0.00	0.00	0.00

Supplementary Table S18. Tobit regression model results for trend analyses of *annual completeness* using 173 Member States reporting influenza records to the WHO's FluNet as of 15 June 2021. We report annual trend coefficients (Coef.), 95% confidence intervals (LCI and UCI), significance values (p-value), log-likelihood estimates (Log. Lik.), and total Member State-year observations (Obs.). All models adjusted for a linear annual trend and were performed for each of 6 test outcomes (specimens collected (SPE), specimens processed or tests (TES), influenza A positives (FLUA), influenza B positives (FLUB), total positives (POS), and total negatives (NEG)) and 8 disease subtypes (A(H1), A(H1N1)pdm09, A(H3), A(H5), A(Unsubtyped) abbreviated A(Uns), B(Yamagata) abbreviated B(Yam), B(Victoria) abbreviated B(Vic), and B(Undetermined) positives abbreviated B(Und)) for all countries (worldwide), by 6 regions, and by 17 influenza transmission zones. Blank cells suggest that no countries within a region or zone provided records for the testing outcome or disease subtype, preventing the estimation of *annual completeness*. We calculated *completeness* in 1995-2021 as the ratio of weeks with complete records to all weeks within a Gregorian calendar year (52 or 53).

Outcome	Location	Coef.	LCI	UCI	p-value	Log. Lik.	Obs.
SPE	Worldwide	-6.31	-7.20	-5.41	0.000	-5619.64	4590
TES	Worldwide	2.93	2.74	3.12	0.000	-10717.01	4590
POS	Worldwide	2.77	2.59	2.94	0.000	-11387.23	4590
NEG	Worldwide	-6.43	-7.19	-5.66	0.000	-5403.51	4590
FLUA	Worldwide	2.72	2.54	2.89	0.000	-11403.36	4590
FLUB	Worldwide	2.32	2.15	2.49	0.000	-11151.74	4590
A(H1)	Worldwide	0.81	0.57	1.05	0.000	-10154.83	4590
A(H1N1)	Worldwide	1.43	1.17	1.70	0.000	-8595.91	4590
A(H3)	Worldwide	2.47	2.29	2.65	0.000	-11110.93	4590
A(H5)	Worldwide	-6.76	-7.66	-5.86	0.000	-5561.63	4590
A(UNS)	Worldwide	2.13	1.93	2.33	0.000	-10843.05	4590
B(YAM)	Worldwide	0.69	0.41	0.97	0.000	-8531.62	4590
B(VIC)	Worldwide	0.77	0.49	1.04	0.000	-8614.93	4590
B(UND)	Worldwide	2.15	1.97	2.32	0.000	-11006.12	4590
SPE	AFRO	1.31	0.58	2.03	0.000	-1436.28	810
TES	AFRO	2.06	1.44	2.68	0.000	-1608.45	810
POS	AFRO	2.03	1.44	2.63	0.000	-1636.81	810
NEG	AFRO	-8.63	-11.15	-6.12	0.000	-753.44	810
FLUA	AFRO	2.01	1.42	2.60	0.000	-1645.41	810
FLUB	AFRO	1.60	1.02	2.17	0.000	-1630.34	810
A(H1)	AFRO	-2.39	-3.41	-1.36	0.000	-1372.89	810
A(H1N1)	AFRO	1.25	0.55	1.94	0.001	-1464.69	810
A(H3)	AFRO	1.94	1.35	2.53	0.000	-1644.30	810
A(H5)	AFRO	1.19	0.49	1.88	0.001	-1473.91	810
A(UNS)	AFRO	1.90	1.33	2.47	0.000	-1671.72	810
B(YAM)	AFRO	0.06	-0.75	0.87	0.881	-1410.52	810
B(VIC)	AFRO	0.05	-0.77	0.86	0.913	-1405.46	810
B(UND)	AFRO	1.35	0.75	1.95	0.000	-1610.47	810
SPE	EMRO	0.05	-1.06	1.17	0.924	-836.44	513
TES	EMRO	0.94	0.13	1.75	0.023	-971.18	513
POS	EMRO	1.02	0.32	1.72	0.005	-1048.49	513
NEG	EMRO	-4.79	-6.68	-2.90	0.000	-636.93	513
FLUA	EMRO	0.93	0.22	1.64	0.011	-1038.03	513
FLUB	EMRO	0.62	-0.11	1.35	0.098	-1008.46	513
A(H1)	EMRO	-4.15	-5.70	-2.59	0.000	-767.60	513
A(H1N1)	EMRO	-0.34	-1.41	0.73	0.535	-846.48	513
A(H3)	EMRO	0.37	-0.44	1.17	0.370	-986.12	513
A(H5)	EMRO	-2.66	-4.40	-0.93	0.003	-725.79	513
A(UNS)	EMRO	-0.36	-1.36	0.64	0.475	-892.24	513
B(YAM)	EMRO	-1.56	-2.82	-0.30	0.015	-815.03	513
B(VIC)	EMRO	-1.46	-2.68	-0.24	0.019	-825.24	513
B(UND)	EMRO	0.51	-0.23	1.25	0.174	-1002.43	513
SPE	EURO	-14.56	-18.14	-10.97	0.000	-966.55	1377
TES	EURO	3.39	3.20	3.58	0.000	-4152.98	1377
POS	EURO	3.49	3.31	3.67	0.000	-4402.24	1377

NEG	EURO	-23.86	-35.60	-12.11	0.000	-384.56	1377
FLUA	EURO	3.48	3.30	3.65	0.000	-4414.31	1377
FLUB	EURO	3.15	2.98	3.33	0.000	-4196.31	1377
A(H1)	EURO	3.31	3.13	3.49	0.000	-4267.20	1377
A(H1N1)	EURO	2.56	2.26	2.85	0.000	-3093.69	1377
A(H3)	EURO	3.37	3.20	3.55	0.000	-4345.23	1377
A(H5)	EURO	-13.22	-16.43	-10.01	0.000	-952.59	1377
A(UNS)	EURO	3.39	3.22	3.57	0.000	-4362.02	1377
B(YAM)	EURO	2.70	2.43	2.96	0.000	-3251.51	1377
B(VIC)	EURO	2.69	2.42	2.96	0.000	-3238.80	1377
B(UND)	EURO	3.15	2.97	3.33	0.000	-4192.56	1377
SPE	PAHO	-20.93	-27.13	-14.73	0.000	-876.71	1188
TES	PAHO	2.70	2.16	3.24	0.000	-2345.41	1188
POS	PAHO	1.30	0.80	1.80	0.000	-2517.94	1188
NEG	PAHO	-0.21	-0.77	0.35	0.468	-2336.47	1188
FLUA	PAHO	1.20	0.69	1.71	0.000	-2506.63	1188
FLUB	PAHO	0.71	0.24	1.19	0.003	-2486.42	1188
A(H1)	PAHO	-2.02	-2.96	-1.07	0.000	-1959.84	1188
A(H1N1)	PAHO	-0.76	-1.52	0.01	0.052	-1918.34	1188
A(H3)	PAHO	0.46	-0.12	1.04	0.121	-2323.10	1188
A(H5)	PAHO	-18.16	-23.15	-13.17	0.000	-861.68	1188
A(UNS)	PAHO	-0.62	-1.38	0.14	0.112	-2135.93	1188
B(YAM)	PAHO	-3.21	-4.25	-2.16	0.000	-1721.11	1188
B(VIC)	PAHO	-2.48	-3.37	-1.59	0.000	-1806.18	1188
B(UND)	PAHO	0.06	-0.51	0.62	0.844	-2325.64	1188
SPE	SEARO	1.85	0.23	3.47	0.025	-449.08	297
TES	SEARO	2.98	1.84	4.13	0.000	-539.04	297
POS	SEARO	2.77	1.80	3.74	0.000	-588.38	297
NEG	SEARO	-3.89	-6.04	-1.74	0.000	-394.26	297
FLUA	SEARO	2.56	1.61	3.50	0.000	-598.18	297
FLUB	SEARO	2.47	1.47	3.47	0.000	-566.96	297
A(H1)	SEARO	-5.71	-8.74	-2.68	0.000	-408.25	297
A(H1N1)	SEARO	1.55	0.25	2.85	0.019	-495.03	297
A(H3)	SEARO	2.37	1.40	3.34	0.000	-587.74	297
A(H5)	SEARO	-0.62	-2.29	1.05	0.464	-463.57	297
A(UNS)	SEARO	-0.73	-2.21	0.74	0.329	-515.70	297
B(YAM)	SEARO	-0.86	-2.67	0.96	0.354	-452.96	297
B(VIC)	SEARO	-0.56	-2.19	1.07	0.500	-468.75	297
B(UND)	SEARO	2.22	1.25	3.19	0.000	-576.55	297
SPE	WPRO	2.45	1.03	3.86	0.001	-622.21	405
TES	WPRO	4.86	4.05	5.67	0.000	-893.24	405
POS	WPRO	6.17	5.39	6.96	0.000	-907.52	405
NEG	WPRO	-4.67	-6.79	-2.54	0.000	-507.34	405
FLUA	WPRO	6.15	5.36	6.94	0.000	-908.00	405
FLUB	WPRO	4.95	4.41	5.50	0.000	-1006.84	405
A(H1)	WPRO	3.61	2.63	4.60	0.000	-894.31	405
A(H1N1)	WPRO	4.45	3.32	5.58	0.000	-673.83	405
A(H3)	WPRO	5.82	5.04	6.59	0.000	-913.33	405
A(H5)	WPRO	3.32	1.99	4.64	0.000	-644.08	405
A(UNS)	WPRO	5.20	4.37	6.04	0.000	-896.88	405
B(YAM)	WPRO	4.02	2.89	5.15	0.000	-688.51	405
B(VIC)	WPRO	4.11	3.00	5.22	0.000	-692.86	405
B(UND)	WPRO	4.59	4.03	5.16	0.000	-1025.99	405
SPE	North America	-1.57	-9.55	6.41	0.697	-91.68	81
TES	North America	4.61	3.05	6.18	0.000	-205.61	81
POS	North America	4.46	2.73	6.19	0.000	-202.92	81
NEG	North America	-32.62	-80.89	15.66	0.183	-52.83	81
FLUA	North America	4.45	2.72	6.18	0.000	-202.97	81
FLUB	North America	3.72	2.18	5.26	0.000	-207.13	81
A(H1)	North America	0.15	-2.59	2.88	0.916	-165.33	81

A(H1N1)	North America	1.09	-3.30	5.48	0.623	-109.77	81
A(H3)	North America	3.86	1.96	5.77	0.000	-184.12	81
A(H5)	North America	-9.63	-18.95	-0.32	0.043	-90.53	81
A(UNS)	North America	4.19	2.12	6.25	0.000	-185.63	81
B(YAM)	North America	-5.00	-12.15	2.16	0.169	-100.07	81
B(VIC)	North America	-3.59	-9.29	2.11	0.214	-106.27	81
B(UND)	North America	3.64	2.04	5.25	0.000	-202.99	81
SPE	Central America and Caribbean	-21.94	-30.48	-13.41	0.000	-455.26	756
TES	Central America and Caribbean	0.67	-0.16	1.51	0.112	-1307.01	756
POS	Central America and Caribbean	-0.85	-1.63	-0.07	0.032	-1355.95	756
NEG	Central America and Caribbean	-1.77	-2.62	-0.92	0.000	-1287.41	756
FLUA	Central America and Caribbean	-1.05	-1.86	-0.24	0.011	-1333.62	756
FLUB	Central America and Caribbean	-1.48	-2.32	-0.65	0.001	-1285.78	756
A(H1)	Central America and Caribbean	-8.21	-10.99	-5.44	0.000	-891.13	756
A(H1N1)	Central America and Caribbean	-2.09	-3.09	-1.10	0.000	-1178.00	756
A(H3)	Central America and Caribbean	-2.07	-3.06	-1.08	0.000	-1227.19	756
A(H5)	Central America and Caribbean	-18.14	-24.58	-11.70	0.000	-479.99	756
A(UNS)	Central America and Caribbean	-5.26	-7.12	-3.41	0.000	-1007.62	756
B(YAM)	Central America and Caribbean	-4.81	-6.32	-3.31	0.000	-995.61	756
B(VIC)	Central America and Caribbean	-3.89	-5.15	-2.63	0.000	-1050.27	756
B(UND)	Central America and Caribbean	-3.05	-4.25	-1.85	0.000	-1140.51	756
SPE	Temperate South America	-8.15	-14.17	-2.13	0.008	-120.03	108
TES	Temperate South America	6.10	5.45	6.76	0.000	-286.63	108
POS	Temperate South America	5.46	4.82	6.10	0.000	-332.59	108
NEG	Temperate South America	5.05	4.48	5.63	0.000	-335.60	108
FLUA	Temperate South America	5.33	4.72	5.94	0.000	-335.05	108
FLUB	Temperate South America	4.50	3.90	5.09	0.000	-341.76	108
A(H1)	Temperate South America	4.29	3.53	5.05	0.000	-346.53	108
A(H1N1)	Temperate South America	4.45	2.69	6.21	0.000	-193.06	108
A(H3)	Temperate South America	4.87	4.18	5.56	0.000	-311.93	108
A(H5)	Temperate South America	-12.46	-22.65	-2.27	0.017	-104.85	108
A(UNS)	Temperate South America	4.96	4.34	5.59	0.000	-341.82	108
B(YAM)	Temperate South America	3.27	1.45	5.09	0.001	-195.18	108
B(VIC)	Temperate South America	3.41	1.77	5.04	0.000	-204.56	108
B(UND)	Temperate South America	4.42	3.79	5.05	0.000	-337.89	108
SPE	Tropical South America	-32.16	-57.57	-6.75	0.013	-169.23	243
TES	Tropical South America	4.95	3.60	6.31	0.000	-463.27	243
POS	Tropical South America	3.55	2.44	4.65	0.000	-534.47	243
NEG	Tropical South America	2.20	1.21	3.19	0.000	-554.14	243
FLUA	Tropical South America	3.47	2.38	4.56	0.000	-539.25	243
FLUB	Tropical South America	2.52	1.67	3.36	0.000	-567.98	243
A(H1)	Tropical South America	1.33	-0.18	2.83	0.083	-470.26	243
A(H1N1)	Tropical South America	1.14	-0.38	2.66	0.140	-409.10	243
A(H3)	Tropical South America	2.89	1.75	4.04	0.000	-519.33	243
A(H5)	Tropical South America	-23.41	-39.05	-7.77	0.004	-174.30	243
A(UNS)	Tropical South America	1.92	0.54	3.30	0.006	-492.05	243
B(YAM)	Tropical South America	-0.81	-2.49	0.87	0.343	-400.69	243
B(VIC)	Tropical South America	-0.50	-2.01	1.00	0.509	-415.81	243
B(UND)	Tropical South America	2.11	1.19	3.02	0.000	-555.31	243
SPE	Northern Europe	-11.73	-18.50	-4.96	0.001	-147.43	270
TES	Northern Europe	4.81	4.42	5.21	0.000	-778.57	270
POS	Northern Europe	4.92	4.58	5.26	0.000	-847.56	270
NEG	Northern Europe						
FLUA	Northern Europe	4.88	4.55	5.21	0.000	-856.54	270
FLUB	Northern Europe	4.42	4.10	4.74	0.000	-831.33	270
A(H1)	Northern Europe	4.67	4.33	5.02	0.000	-830.90	270
A(H1N1)	Northern Europe	4.09	3.28	4.90	0.000	-531.71	270
A(H3)	Northern Europe	4.74	4.40	5.08	0.000	-844.97	270
A(H5)	Northern Europe	-9.94	-15.58	-4.29	0.001	-145.00	270
A(UNS)	Northern Europe	4.74	4.43	5.06	0.000	-868.33	270

B(YAM)	Northern Europe	4.25	3.61	4.89	0.000	-589.79	270
B(VIC)	Northern Europe	4.25	3.61	4.89	0.000	-589.74	270
B(UND)	Northern Europe	4.42	4.10	4.73	0.000	-831.09	270
SPE	Southwest Europe						
TES	Southwest Europe						
POS	Southwest Europe						
NEG	Southwest Europe						
FLUA	Southwest Europe						
FLUB	Southwest Europe						
A(H1)	Southwest Europe						
A(H1N1)	Southwest Europe						
A(H3)	Southwest Europe						
A(H5)	Southwest Europe						
A(UNS)	Southwest Europe						
B(YAM)	Southwest Europe						
B(VIC)	Southwest Europe						
B(UND)	Southwest Europe						
SPE	Eastern Europe	-15.02	-22.77	-7.27	0.000	-248.27	297
TES	Eastern Europe	3.75	3.37	4.13	0.000	-885.74	297
POS	Eastern Europe	3.82	3.48	4.15	0.000	-964.48	297
NEG	Eastern Europe	-7.39	-14.75	-0.03	0.049	-79.08	297
FLUA	Eastern Europe	3.81	3.47	4.15	0.000	-964.46	297
FLUB	Eastern Europe	3.48	3.09	3.87	0.000	-882.18	297
A(H1)	Eastern Europe	3.76	3.39	4.12	0.000	-918.01	297
A(H1N1)	Eastern Europe	3.03	2.36	3.70	0.000	-648.59	297
A(H3)	Eastern Europe	3.78	3.43	4.13	0.000	-939.49	297
A(H5)	Eastern Europe	-13.82	-20.76	-6.88	0.000	-248.99	297
A(UNS)	Eastern Europe	3.75	3.38	4.12	0.000	-910.03	297
B(YAM)	Eastern Europe	3.14	2.53	3.75	0.000	-678.33	297
B(VIC)	Eastern Europe	3.14	2.53	3.75	0.000	-678.33	297
B(UND)	Eastern Europe	3.48	3.09	3.87	0.000	-882.18	297
SPE	Northern Africa	1.49	0.31	2.66	0.014	-284.16	135
TES	Northern Africa	2.48	1.79	3.16	0.000	-383.65	135
POS	Northern Africa	2.35	1.76	2.94	0.000	-419.13	135
NEG	Northern Africa	-2.33	-4.13	-0.53	0.012	-193.00	135
FLUA	Northern Africa	2.30	1.70	2.90	0.000	-415.09	135
FLUB	Northern Africa	1.86	1.19	2.54	0.000	-381.53	135
A(H1)	Northern Africa	-0.26	-1.37	0.86	0.648	-322.98	135
A(H1N1)	Northern Africa	1.23	0.11	2.35	0.032	-287.48	135
A(H3)	Northern Africa	2.15	1.52	2.79	0.000	-398.95	135
A(H5)	Northern Africa	0.87	-0.32	2.07	0.152	-282.43	135
A(UNS)	Northern Africa	1.61	0.79	2.42	0.000	-344.82	135
B(YAM)	Northern Africa	0.87	-0.06	1.80	0.067	-315.12	135
B(VIC)	Northern Africa	0.92	0.01	1.82	0.047	-319.54	135
B(UND)	Northern Africa	1.78	1.09	2.47	0.000	-377.69	135
SPE	Eastern Africa	1.97	1.03	2.91	0.000	-544.23	270
TES	Eastern Africa	2.68	1.84	3.52	0.000	-601.72	270
POS	Eastern Africa	2.68	1.88	3.49	0.000	-615.52	270
NEG	Eastern Africa	-10.20	-15.55	-4.84	0.000	-233.79	270
FLUA	Eastern Africa	2.66	1.84	3.48	0.000	-610.76	270
FLUB	Eastern Africa	2.22	1.41	3.02	0.000	-602.42	270
A(H1)	Eastern Africa	-1.47	-2.89	-0.06	0.042	-519.08	270
A(H1N1)	Eastern Africa	1.86	0.92	2.81	0.000	-544.25	270
A(H3)	Eastern Africa	2.56	1.74	3.38	0.000	-610.82	270
A(H5)	Eastern Africa	1.87	0.92	2.81	0.000	-544.24	270
A(UNS)	Eastern Africa	2.59	1.81	3.38	0.000	-618.61	270
B(YAM)	Eastern Africa	0.11	-1.16	1.39	0.862	-502.81	270
B(VIC)	Eastern Africa	0.11	-1.16	1.39	0.862	-502.81	270
B(UND)	Eastern Africa	2.15	1.33	2.97	0.000	-598.04	270
SPE	Middle Africa	-3.90	-6.95	-0.84	0.013	-262.61	189

TES	Middle Africa	-3.35	-6.09	-0.60	0.017	-274.28	189
POS	Middle Africa	-3.51	-6.39	-0.64	0.017	-269.34	189
NEG	Middle Africa	-22.72	-48.98	3.54	0.089	-67.01	189
FLUA	Middle Africa	-3.33	-6.06	-0.60	0.017	-274.24	189
FLUB	Middle Africa	-3.01	-5.45	-0.58	0.016	-282.89	189
A(H1)	Middle Africa	-8.63	-13.65	-3.60	0.001	-211.51	189
A(H1N1)	Middle Africa	-3.88	-6.93	-0.84	0.013	-262.58	189
A(H3)	Middle Africa	-3.30	-6.00	-0.59	0.017	-274.00	189
A(H5)	Middle Africa	-3.88	-6.93	-0.84	0.013	-262.57	189
A(UNS)	Middle Africa	-3.32	-6.05	-0.59	0.017	-274.20	189
B(YAM)	Middle Africa	-3.91	-6.78	-1.05	0.008	-264.85	189
B(VIC)	Middle Africa	-4.22	-7.28	-1.17	0.007	-259.14	189
B(UND)	Middle Africa	-3.02	-5.41	-0.64	0.013	-282.26	189
SPE	Western Africa	2.62	1.33	3.91	0.000	-497.18	297
TES	Western Africa	3.19	2.05	4.33	0.000	-545.27	297
POS	Western Africa	3.08	2.00	4.16	0.000	-559.84	297
NEG	Western Africa	-6.02	-8.85	-3.18	0.000	-338.11	297
FLUA	Western Africa	3.06	1.99	4.14	0.000	-559.79	297
FLUB	Western Africa	2.51	1.49	3.53	0.000	-562.85	297
A(H1)	Western Africa	-2.41	-4.34	-0.49	0.014	-472.68	297
A(H1N1)	Western Africa	2.48	1.35	3.61	0.000	-527.03	297
A(H3)	Western Africa	3.03	1.96	4.11	0.000	-559.75	297
A(H5)	Western Africa	2.29	1.19	3.39	0.000	-537.02	297
A(UNS)	Western Africa	2.81	1.80	3.83	0.000	-579.80	297
B(YAM)	Western Africa	1.28	-0.01	2.56	0.052	-511.69	297
B(VIC)	Western Africa	1.32	0.03	2.61	0.045	-511.75	297
B(UND)	Western Africa	1.98	0.87	3.10	0.001	-548.87	297
SPE	Western Asia	-8.98	-12.94	-5.01	0.000	-521.97	486
TES	Western Asia	0.49	-0.33	1.31	0.241	-919.44	486
POS	Western Asia	0.37	-0.43	1.17	0.366	-927.00	486
NEG	Western Asia	-11.32	-15.91	-6.72	0.000	-434.11	486
FLUA	Western Asia	0.34	-0.45	1.13	0.400	-931.14	486
FLUB	Western Asia	0.22	-0.56	1.01	0.579	-928.25	486
A(H1)	Western Asia	-2.30	-3.50	-1.10	0.000	-798.93	486
A(H1N1)	Western Asia	-0.51	-1.53	0.51	0.328	-826.35	486
A(H3)	Western Asia	-0.16	-1.03	0.70	0.708	-902.43	486
A(H5)	Western Asia	-22.89	-34.52	-11.27	0.000	-382.35	486
A(UNS)	Western Asia	-0.39	-1.31	0.52	0.400	-881.73	486
B(YAM)	Western Asia	-1.88	-3.25	-0.51	0.007	-752.37	486
B(VIC)	Western Asia	-1.80	-3.15	-0.46	0.009	-757.87	486
B(UND)	Western Asia	0.14	-0.66	0.93	0.731	-922.60	486
SPE	Central Asia						
TES	Central Asia	1.30	0.40	2.19	0.005	-309.29	135
POS	Central Asia	1.30	0.40	2.19	0.005	-309.29	135
NEG	Central Asia						
FLUA	Central Asia	1.29	0.40	2.19	0.005	-309.28	135
FLUB	Central Asia	1.22	0.30	2.14	0.010	-304.69	135
A(H1)	Central Asia	1.28	0.39	2.17	0.005	-309.10	135
A(H1N1)	Central Asia	1.04	0.06	2.02	0.037	-295.65	135
A(H3)	Central Asia	1.27	0.38	2.17	0.006	-309.14	135
A(H5)	Central Asia						
A(UNS)	Central Asia	1.28	0.39	2.17	0.005	-308.97	135
B(YAM)	Central Asia	1.20	0.28	2.11	0.011	-304.52	135
B(VIC)	Central Asia	1.19	0.27	2.10	0.011	-304.41	135
B(UND)	Central Asia	1.21	0.30	2.13	0.010	-304.55	135
SPE	Eastern Asia	-0.74	-4.70	3.22	0.713	-174.21	135
TES	Eastern Asia	1.94	0.27	3.61	0.023	-261.75	135
POS	Eastern Asia	6.74	4.86	8.63	0.000	-275.28	135
NEG	Eastern Asia	-5.93	-10.47	-1.39	0.011	-151.63	135
FLUA	Eastern Asia	6.73	4.85	8.61	0.000	-275.29	135

FLUB	Eastern Asia	5.40	4.14	6.66	0.000	-316.03	135
A(H1)	Eastern Asia	4.34	2.15	6.52	0.000	-267.92	135
A(H1N1)	Eastern Asia	4.84	1.10	8.57	0.011	-174.82	135
A(H3)	Eastern Asia	6.47	4.69	8.25	0.000	-280.55	135
A(H5)	Eastern Asia	3.06	-0.33	6.45	0.076	-181.62	135
A(UNS)	Eastern Asia	5.25	2.79	7.71	0.000	-231.90	135
B(YAM)	Eastern Asia	4.70	-0.01	9.41	0.051	-164.02	135
B(VIC)	Eastern Asia	4.69	-0.01	9.40	0.051	-164.02	135
B(UND)	Eastern Asia	5.39	4.14	6.65	0.000	-316.02	135
SPE	Southern Asia	3.60	2.38	4.82	0.000	-427.51	243
TES	Southern Asia	4.27	3.21	5.32	0.000	-464.76	243
POS	Southern Asia	3.96	3.14	4.79	0.000	-530.86	243
NEG	Southern Asia	-4.10	-6.68	-1.53	0.002	-317.95	243
FLUA	Southern Asia	3.72	2.89	4.55	0.000	-532.51	243
FLUB	Southern Asia	3.65	2.79	4.51	0.000	-512.50	243
A(H1)	Southern Asia	-2.25	-4.35	-0.16	0.035	-400.14	243
A(H1N1)	Southern Asia	3.10	2.08	4.12	0.000	-466.95	243
A(H3)	Southern Asia	3.50	2.69	4.31	0.000	-542.29	243
A(H5)	Southern Asia	1.72	0.41	3.03	0.010	-435.05	243
A(UNS)	Southern Asia	2.57	1.56	3.57	0.000	-505.31	243
B(YAM)	Southern Asia	2.17	1.00	3.35	0.000	-455.31	243
B(VIC)	Southern Asia	2.21	1.14	3.28	0.000	-474.22	243
B(UND)	Southern Asia	3.40	2.60	4.21	0.000	-531.32	243
SPE	Southeast Asia						
TES	Southeast Asia						
POS	Southeast Asia						
NEG	Southeast Asia						
FLUA	Southeast Asia						
FLUB	Southeast Asia						
A(H1)	Southeast Asia						
A(H1N1)	Southeast Asia						
A(H3)	Southeast Asia						
A(H5)	Southeast Asia						
A(UNS)	Southeast Asia						
B(YAM)	Southeast Asia						
B(VIC)	Southeast Asia						
B(UND)	Southeast Asia						
SPE	Oceania Melanesia Polynesia	0.95	-1.10	2.99	0.361	-228.81	135
TES	Oceania Melanesia Polynesia	3.42	2.22	4.62	0.000	-348.36	135
POS	Oceania Melanesia Polynesia	3.61	2.53	4.69	0.000	-364.93	135
NEG	Oceania Melanesia Polynesia	-1.89	-3.78	-0.01	0.049	-213.37	135
FLUA	Oceania Melanesia Polynesia	3.56	2.48	4.64	0.000	-365.01	135
FLUB	Oceania Melanesia Polynesia	2.73	1.96	3.51	0.000	-390.32	135
A(H1)	Oceania Melanesia Polynesia	0.28	-1.32	1.87	0.730	-312.50	135
A(H1N1)	Oceania Melanesia Polynesia	1.21	-0.27	2.68	0.108	-262.55	135
A(H3)	Oceania Melanesia Polynesia	2.96	1.94	3.99	0.000	-368.42	135
A(H5)	Oceania Melanesia Polynesia	-0.56	-2.80	1.68	0.624	-225.84	135
A(UNS)	Oceania Melanesia Polynesia	3.13	2.11	4.16	0.000	-379.12	135
B(YAM)	Oceania Melanesia Polynesia	0.84	-0.75	2.42	0.298	-262.82	135
B(VIC)	Oceania Melanesia Polynesia	1.13	-0.35	2.61	0.132	-267.96	135
B(UND)	Oceania Melanesia Polynesia	2.53	1.77	3.30	0.000	-394.48	135

Supplementary Table S19. Tobit regression model results for seasonality analyses of *seasonal completeness* using 173 Member States reporting influenza records to the WHO's FluNet as of 15 June 2021. We used sinusoidal and cosinusoidal harmonic terms to estimate the presence of seasonality and report coefficients (Coef.), 95% confidence intervals (LCI and UCI), significance values (p-value), log-likelihood estimates (Log. Lik.), and total Member State-year observations (Obs.). All models were performed for each of 6 test outcomes (specimens collected (SPE), specimens processed or tests (TES), influenza A positives (FLUA), influenza B positives (FLUB), total positives (POS), and total negatives (NEG)) and 8 disease subtypes (A(H1), A(H1N1)pdm09, A(H3), A(H5), A(Unsubtyped) abbreviated A(Uns), B(Yamagata) abbreviated B(Yam), B(Victoria) abbreviated B(Vic), and B(Undetermined) positives abbreviated B(Und)) for all countries (worldwide), by 6 regions, and by 17 influenza transmission zones. Blank cells suggest that no countries within a region or zone provided records for the testing outcome or disease subtype, preventing the estimation of *seasonal completeness*. We calculated *completeness* in 1995-2021 as the ratio of years with complete records for a specific Gregorian calendar week by the total number of years that calendar week appeared in our study period (26 or 27).

Outcome	Location	SIN	LCI	UCI	p-value	SIN	LCI	UCI	p-value	Log. Lik.	Obs.
SPE	Worldwide	0.36	-0.64	1.36	0.479	0.34	-0.66	1.34	0.507	-29477.34	8840
TES	Worldwide	3.05	1.65	4.45	0.000	5.08	3.68	6.49	0.000	-44743.01	8840
POS	Worldwide	3.80	2.31	5.29	0.000	6.65	5.15	8.14	0.000	-42911.25	8840
NEG	Worldwide	1.40	0.41	2.38	0.005	1.14	0.15	2.13	0.024	-24237.98	8840
FLUA	Worldwide	3.67	2.19	5.15	0.000	6.69	5.20	8.17	0.000	-42709.56	8840
FLUB	Worldwide	3.89	2.62	5.17	0.000	4.50	3.22	5.78	0.000	-40990.66	8840
A(H1)	Worldwide	2.94	1.63	4.26	0.000	5.25	3.93	6.58	0.000	-38853.25	8840
A(H1N1)	Worldwide	2.23	1.14	3.33	0.000	3.60	2.49	4.70	0.000	-40176.93	8840
A(H3)	Worldwide	3.23	1.80	4.66	0.000	5.99	4.55	7.43	0.000	-41457.38	8840
A(H5)	Worldwide	0.81	-0.15	1.78	0.098	0.61	-0.36	1.58	0.215	-28187.17	8840
A(UNS)	Worldwide	2.71	1.28	4.15	0.000	5.64	4.19	7.08	0.000	-40608.04	8840
B(YAM)	Worldwide	1.98	0.91	3.05	0.000	3.39	2.31	4.47	0.000	-38591.22	8840
B(VIC)	Worldwide	2.04	0.97	3.12	0.000	3.40	2.32	4.48	0.000	-38700.97	8840
B(UND)	Worldwide	3.58	2.31	4.84	0.000	4.39	3.12	5.66	0.000	-40562.29	8840
SPE	AFRO	1.56	-0.89	4.01	0.212	-1.42	-3.89	1.04	0.258	-7529.50	1560
TES	AFRO	2.65	-0.32	5.63	0.081	-2.24	-5.23	0.76	0.144	-7787.51	1560
POS	AFRO	2.50	-0.45	5.45	0.097	-1.92	-4.89	1.05	0.206	-7748.29	1560
NEG	AFRO	2.24	1.11	3.38	0.000	1.88	0.74	3.03	0.001	-3701.58	1560
FLUA	AFRO	2.38	-0.54	5.30	0.110	-1.95	-4.89	0.99	0.193	-7758.14	1560
FLUB	AFRO	1.48	-1.04	4.01	0.249	-1.78	-4.32	0.76	0.170	-7569.32	1560
A(H1)	AFRO	1.79	-0.45	4.02	0.117	-1.58	-3.83	0.67	0.169	-6799.27	1560
A(H1N1)	AFRO	1.43	-1.00	3.87	0.248	-1.01	-3.46	1.44	0.418	-7483.36	1560
A(H3)	AFRO	2.05	-0.79	4.89	0.156	-2.00	-4.85	0.86	0.170	-7736.89	1560
A(H5)	AFRO	1.56	-0.85	3.98	0.204	-1.10	-3.53	1.33	0.377	-7475.10	1560
A(UNS)	AFRO	2.01	-0.78	4.81	0.158	-1.85	-4.66	0.96	0.197	-7697.01	1560
B(YAM)	AFRO	1.87	-0.42	4.15	0.110	-0.50	-2.81	1.81	0.670	-7240.98	1560
B(VIC)	AFRO	1.87	-0.42	4.17	0.110	-0.42	-2.73	1.90	0.722	-7242.25	1560
B(UND)	AFRO	1.32	-1.13	3.78	0.291	-1.78	-4.25	0.69	0.159	-7520.34	1560
SPE	EMRO	0.84	-2.04	3.73	0.567	2.82	-0.07	5.71	0.056	-4525.47	988
TES	EMRO	1.02	-2.08	4.12	0.520	4.87	1.76	7.98	0.002	-4593.54	988
POS	EMRO	2.83	-0.33	6.00	0.079	6.49	3.33	9.66	0.000	-4490.23	988
NEG	EMRO	1.35	-0.03	2.74	0.055	2.26	0.86	3.65	0.002	-3447.36	988
FLUA	EMRO	2.73	-0.40	5.86	0.087	6.22	3.08	9.35	0.000	-4481.37	988
FLUB	EMRO	3.51	0.48	6.54	0.023	5.66	2.63	8.70	0.000	-4193.45	988
A(H1)	EMRO	1.86	-0.70	4.42	0.153	3.66	1.09	6.22	0.005	-3268.47	988
A(H1N1)	EMRO	2.09	-0.70	4.89	0.142	4.29	1.49	7.09	0.003	-4368.10	988
A(H3)	EMRO	3.19	-0.11	6.49	0.058	6.40	3.10	9.71	0.000	-4041.05	988
A(H5)	EMRO	2.30	-1.09	5.70	0.183	3.84	0.44	7.24	0.027	-3378.63	988
A(UNS)	EMRO	1.41	-1.94	4.75	0.409	6.04	2.69	9.38	0.000	-3770.36	988
B(YAM)	EMRO	1.66	-1.49	4.81	0.301	2.44	-0.71	5.60	0.128	-3676.28	988
B(VIC)	EMRO	1.65	-1.50	4.80	0.304	2.47	-0.68	5.63	0.124	-3676.85	988
B(UND)	EMRO	3.72	0.61	6.83	0.019	6.13	3.02	9.25	0.000	-4023.23	988
SPE	EURO	-0.06	-1.25	1.13	0.918	1.49	0.29	2.68	0.015	-5501.79	2652
TES	EURO	6.74	4.04	9.44	0.000	18.23	15.50	20.96	0.000	-13518.33	2652

POS	EURO	7.83	5.02	10.64	0.000	20.15	17.31	22.99	0.000	-13659.36	2652
NEG	EURO	0.44	-0.38	1.26	0.294	0.93	0.11	1.76	0.027	-2296.84	2652
FLUA	EURO	7.59	4.80	10.39	0.000	19.96	17.14	22.79	0.000	-13651.72	2652
FLUB	EURO	8.72	6.38	11.06	0.000	14.16	11.80	16.53	0.000	-13230.91	2652
A(H1)	EURO	6.43	3.82	9.05	0.000	17.45	14.81	20.09	0.000	-13510.49	2652
A(H1N1)	EURO	4.28	2.25	6.32	0.000	9.96	7.90	12.01	0.000	-12850.80	2652
A(H3)	EURO	6.75	4.08	9.41	0.000	18.48	15.79	21.17	0.000	-13543.89	2652
A(H5)	EURO	0.90	-0.27	2.07	0.133	1.70	0.53	2.88	0.005	-4991.41	2652
A(UNS)	EURO	6.93	4.23	9.62	0.000	18.66	15.93	21.38	0.000	-13578.05	2652
B(YAM)	EURO	4.51	2.43	6.60	0.000	10.77	8.67	12.88	0.000	-12900.82	2652
B(VIC)	EURO	4.48	2.40	6.56	0.000	10.79	8.69	12.90	0.000	-12905.80	2652
B(UND)	EURO	8.67	6.34	11.01	0.000	14.12	11.76	16.48	0.000	-13226.16	2652
SPE	PAHO	-0.03	-1.73	1.67	0.969	-0.52	-2.23	1.18	0.547	-5239.00	2288
TES	PAHO	2.28	-0.46	5.01	0.103	-0.85	-3.60	1.90	0.543	-11751.24	2288
POS	PAHO	3.17	0.01	6.33	0.049	1.64	-1.54	4.82	0.312	-9476.06	2288
NEG	PAHO	2.50	-0.38	5.37	0.089	1.29	-1.61	4.19	0.382	-8568.93	2288
FLUA	PAHO	2.97	-0.18	6.13	0.065	2.11	-1.08	5.29	0.194	-9312.92	2288
FLUB	PAHO	1.97	-0.69	4.64	0.146	0.17	-2.51	2.85	0.901	-8808.22	2288
A(H1)	PAHO	0.90	-1.86	3.65	0.523	-0.42	-3.18	2.35	0.768	-8382.84	2288
A(H1N1)	PAHO	2.03	-0.19	4.25	0.073	1.85	-0.39	4.09	0.105	-8618.86	2288
A(H3)	PAHO	1.81	-1.13	4.75	0.228	0.63	-2.33	3.59	0.678	-8783.85	2288
A(H5)	PAHO	0.06	-1.16	1.28	0.920	-0.33	-1.55	0.90	0.599	-5240.75	2288
A(UNS)	PAHO	0.82	-2.29	3.94	0.604	-0.62	-3.75	2.51	0.697	-8580.31	2288
B(YAM)	PAHO	0.94	-1.01	2.89	0.346	0.47	-1.49	2.43	0.640	-7842.94	2288
B(VIC)	PAHO	1.26	-0.67	3.20	0.201	0.59	-1.36	2.54	0.552	-7942.26	2288
B(UND)	PAHO	0.84	-1.81	3.49	0.533	-0.48	-3.14	2.18	0.723	-8632.81	2288
SPE	SEARO	0.83	-3.34	5.01	0.696	0.12	-4.07	4.31	0.955	-2682.56	572
TES	SEARO	0.95	-4.11	6.01	0.712	0.04	-5.05	5.12	0.988	-2780.98	572
POS	SEARO	0.86	-4.14	5.86	0.736	0.38	-4.64	5.40	0.882	-2762.84	572
NEG	SEARO	0.64	-1.43	2.71	0.543	-0.06	-2.14	2.01	0.951	-2045.58	572
FLUA	SEARO	0.89	-3.99	5.78	0.719	0.25	-4.66	5.16	0.921	-2754.78	572
FLUB	SEARO	0.42	-4.14	4.98	0.856	0.82	-3.76	5.40	0.726	-2718.56	572
A(H1)	SEARO	2.17	-1.50	5.83	0.246	-0.46	-4.15	3.23	0.805	-2207.56	572
A(H1N1)	SEARO	0.70	-3.35	4.75	0.735	0.39	-3.67	4.46	0.850	-2666.31	572
A(H3)	SEARO	0.60	-4.10	5.31	0.801	0.38	-4.35	5.10	0.876	-2738.63	572
A(H5)	SEARO	1.90	-1.68	5.47	0.297	0.41	-3.17	3.99	0.824	-2462.88	572
A(UNS)	SEARO	0.27	-3.87	4.40	0.899	-0.48	-4.63	3.68	0.821	-2389.49	572
B(YAM)	SEARO	1.23	-2.34	4.80	0.499	0.40	-3.19	3.99	0.828	-2548.12	572
B(VIC)	SEARO	1.12	-2.40	4.64	0.532	-0.11	-3.65	3.43	0.951	-2540.27	572
B(UND)	SEARO	0.06	-4.38	4.51	0.977	0.44	-4.02	4.91	0.846	-2704.70	572
SPE	WPRO	-0.34	-4.30	3.63	0.868	-1.06	-5.04	2.92	0.602	-3716.87	780
TES	WPRO	0.41	-5.80	6.61	0.898	-2.63	-8.88	3.62	0.409	-3890.49	780
POS	WPRO	-1.30	-7.79	5.20	0.695	-3.78	-10.31	2.74	0.255	-4303.41	780
NEG	WPRO	-0.27	-2.01	1.47	0.762	-1.21	-2.96	0.53	0.172	-2749.13	780
FLUA	WPRO	-1.59	-8.06	4.88	0.629	-3.72	-10.22	2.79	0.262	-4290.32	780
FLUB	WPRO	-0.62	-6.13	4.90	0.826	-3.37	-8.90	2.17	0.233	-4168.11	780
A(H1)	WPRO	-0.63	-6.02	4.75	0.817	-2.73	-8.14	2.68	0.322	-4150.16	780
A(H1N1)	WPRO	-1.43	-5.87	3.02	0.529	-2.17	-6.62	2.29	0.340	-3897.08	780
A(H3)	WPRO	-1.52	-7.83	4.78	0.635	-3.33	-9.66	3.00	0.303	-4269.93	780
A(H5)	WPRO	-2.00	-6.05	2.06	0.334	-1.47	-5.54	2.60	0.478	-3885.68	780
A(UNS)	WPRO	-2.35	-8.25	3.56	0.435	-4.04	-9.97	1.89	0.181	-4215.62	780
B(YAM)	WPRO	-1.91	-6.26	2.44	0.389	-2.44	-6.80	1.93	0.273	-3974.77	780
B(VIC)	WPRO	-1.86	-6.21	2.49	0.402	-2.41	-6.78	1.95	0.278	-3975.00	780
B(UND)	WPRO	-0.75	-6.13	4.64	0.785	-3.10	-8.51	2.30	0.260	-4149.56	780
SPE	North America	0.74	-9.91	11.38	0.892	-0.26	-10.95	10.44	0.962	-578.86	156
TES	North America	4.05	-10.25	18.36	0.577	7.03	-7.31	21.37	0.334	-842.86	156
POS	North America	11.70	-6.56	29.96	0.208	11.98	-6.32	30.29	0.198	-667.15	156
NEG	North America	-1.46	-8.33	5.42	0.676	3.03	-3.92	9.98	0.391	-271.72	156
FLUA	North America	11.57	-6.70	29.83	0.213	11.91	-6.39	30.22	0.201	-667.17	156
FLUB	North America	12.83	-4.41	30.07	0.144	9.19	-8.07	26.46	0.295	-620.55	156

A(H1)	North America	4.61	-10.04	19.25	0.535	5.40	-9.23	20.03	0.467	-589.63	156
A(H1N1)	North America	3.18	-7.40	13.76	0.554	1.73	-8.93	12.40	0.748	-606.15	156
A(H3)	North America	10.43	-5.79	26.66	0.206	9.10	-7.16	25.35	0.271	-639.55	156
A(H5)	North America	0.12	-5.53	5.78	0.965	-0.80	-6.48	4.89	0.783	-509.62	156
A(UNS)	North America	4.63	-14.87	24.12	0.640	7.04	-12.42	26.51	0.476	-617.48	156
B(YAM)	North America	0.37	-8.13	8.87	0.931	-0.04	-8.58	8.51	0.993	-555.50	156
B(VIC)	North America	1.52	-6.82	9.86	0.719	0.58	-7.83	8.98	0.892	-566.83	156
B(UND)	North America	10.79	-6.82	28.40	0.228	8.09	-9.50	25.68	0.365	-607.47	156
SPE	Central America and Caribbean	0.32	-1.54	2.18	0.737	0.29	-1.58	2.16	0.763	-2598.22	1456
TES	Central America and Caribbean	2.20	-0.37	4.77	0.094	-0.09	-2.68	2.50	0.945	-7231.03	1456
POS	Central America and Caribbean	2.71	-0.37	5.79	0.085	3.10	-0.01	6.22	0.050	-5255.51	1456
NEG	Central America and Caribbean	3.08	0.00	6.15	0.050	3.92	0.81	7.03	0.014	-4789.52	1456
FLUA	Central America and Caribbean	2.20	-0.91	5.32	0.166	3.74	0.59	6.89	0.020	-5111.53	1456
FLUB	Central America and Caribbean	1.78	-1.07	4.63	0.220	1.04	-1.83	3.90	0.478	-4798.50	1456
A(H1)	Central America and Caribbean	0.84	-2.35	4.02	0.606	-0.15	-3.35	3.05	0.929	-4366.15	1456
A(H1N1)	Central America and Caribbean	2.38	-0.24	4.99	0.075	3.27	0.63	5.92	0.015	-4799.25	1456
A(H3)	Central America and Caribbean	0.88	-2.26	4.02	0.583	1.51	-1.66	4.67	0.351	-4688.84	1456
A(H5)	Central America and Caribbean	0.14	-1.24	1.52	0.841	-0.04	-1.42	1.35	0.960	-2790.87	1456
A(UNS)	Central America and Caribbean	0.26	-3.02	3.53	0.878	0.12	-3.17	3.41	0.944	-4479.63	1456
B(YAM)	Central America and Caribbean	0.88	-1.43	3.19	0.456	0.79	-1.53	3.12	0.503	-4237.97	1456
B(VIC)	Central America and Caribbean	1.22	-1.06	3.51	0.294	0.81	-1.49	3.11	0.491	-4331.26	1456
B(UND)	Central America and Caribbean	0.50	-2.35	3.36	0.729	0.22	-2.65	3.09	0.882	-4653.69	1456
SPE	Temperate South America	0.83	-2.42	4.08	0.615	-3.61	-6.89	-0.33	0.031	-736.66	208
TES	Temperate South America	2.24	-11.35	15.84	0.745	-8.85	-22.52	4.83	0.204	-1175.72	208
POS	Temperate South America	0.56	-12.72	13.85	0.933	-11.68	-25.07	1.71	0.087	-1161.25	208
NEG	Temperate South America	-0.25	-12.58	12.09	0.969	-12.00	-24.44	0.45	0.059	-1146.15	208
FLUA	Temperate South America	1.18	-11.70	14.07	0.857	-11.84	-24.83	1.14	0.074	-1159.54	208
FLUB	Temperate South America	-2.64	-12.97	7.68	0.614	-9.15	-19.55	1.26	0.084	-1113.98	208
A(H1)	Temperate South America	0.73	-9.46	10.91	0.888	-6.70	-16.96	3.56	0.199	-1111.07	208
A(H1N1)	Temperate South America	-0.30	-8.65	8.05	0.943	-2.75	-11.20	5.70	0.521	-1053.32	208
A(H3)	Temperate South America	1.87	-9.27	13.01	0.741	-10.46	-21.70	0.77	0.068	-1125.19	208
A(H5)	Temperate South America	0.87	-2.90	4.63	0.651	-0.20	-4.00	3.59	0.917	-701.41	208
A(UNS)	Temperate South America	1.48	-10.66	13.61	0.811	-11.58	-23.81	0.65	0.063	-1142.70	208
B(YAM)	Temperate South America	3.03	-5.34	11.39	0.476	-0.07	-8.46	8.32	0.987	-987.36	208
B(VIC)	Temperate South America	2.74	-5.66	11.14	0.521	0.10	-8.32	8.53	0.981	-988.11	208
B(UND)	Temperate South America	-2.93	-13.06	7.20	0.569	-9.22	-19.43	0.99	0.077	-1110.12	208
SPE	Tropical South America	-1.49	-5.34	2.37	0.449	-1.36	-5.22	2.50	0.490	-1229.20	468
TES	Tropical South America	2.50	-5.39	10.40	0.533	-1.76	-9.67	6.16	0.662	-2280.61	468
POS	Tropical South America	2.99	-4.74	10.71	0.448	-1.39	-9.14	6.36	0.725	-2266.56	468
NEG	Tropical South America	1.63	-5.31	8.57	0.644	-1.86	-8.83	5.10	0.599	-2232.66	468
FLUA	Tropical South America	3.33	-4.30	10.97	0.392	-1.14	-8.80	6.52	0.770	-2261.98	468
FLUB	Tropical South America	1.69	-3.85	7.23	0.550	-0.78	-6.35	4.78	0.782	-2180.57	468
A(H1)	Tropical South America	2.21	-3.89	8.31	0.477	-0.54	-6.65	5.58	0.863	-2175.09	468
A(H1N1)	Tropical South America	1.42	-3.32	6.16	0.556	-0.42	-5.18	4.35	0.864	-2119.80	468
A(H3)	Tropical South America	3.25	-3.60	10.11	0.351	-0.38	-7.25	6.49	0.913	-2218.18	468
A(H5)	Tropical South America	-0.64	-3.60	2.33	0.674	-1.31	-4.29	1.67	0.389	-1219.19	468
A(UNS)	Tropical South America	2.61	-4.10	9.32	0.445	-0.72	-7.45	6.01	0.833	-2210.09	468
B(YAM)	Tropical South America	0.67	-3.17	4.51	0.733	-0.16	-4.03	3.70	0.934	-2028.90	468
B(VIC)	Tropical South America	0.98	-2.86	4.82	0.616	0.09	-3.77	3.95	0.962	-2021.80	468
B(UND)	Tropical South America	1.05	-4.31	6.40	0.701	-1.07	-6.45	4.31	0.696	-2166.79	468
SPE	Northern Europe	-1.86	-2.66	-1.05	0.000	-0.14	-0.94	0.66	0.730	-991.00	520
TES	Northern Europe	3.73	-3.45	10.91	0.308	11.93	4.71	19.15	0.001	-2850.30	520
POS	Northern Europe	7.43	-0.54	15.40	0.068	17.97	9.95	25.99	0.000	-2835.90	520
NEG	Northern Europe										
FLUA	Northern Europe	7.25	-0.68	15.18	0.073	17.81	9.84	25.79	0.000	-2833.39	520
FLUB	Northern Europe	8.09	1.72	14.46	0.013	8.57	2.18	14.97	0.009	-2787.98	520
A(H1)	Northern Europe	4.26	-2.91	11.43	0.243	12.57	5.37	19.78	0.001	-2853.78	520
A(H1N1)	Northern Europe	0.58	-4.60	5.76	0.826	2.72	-2.48	7.92	0.305	-2688.85	520
A(H3)	Northern Europe	5.00	-2.42	12.42	0.186	14.64	7.17	22.11	0.000	-2845.18	520
A(H5)	Northern Europe	0.15	-0.50	0.81	0.642	-0.05	-0.70	0.60	0.879	-926.33	520

A(UNS)	Northern Europe	5.60	-1.93	13.13	0.145	15.58	8.01	23.15	0.000	-2848.04	520
B(YAM)	Northern Europe	1.69	-3.86	7.23	0.550	3.64	-1.93	9.21	0.200	-2708.12	520
B(VIC)	Northern Europe	1.50	-4.02	7.02	0.594	3.66	-1.88	9.20	0.195	-2713.79	520
B(UND)	Northern Europe	7.98	1.62	14.33	0.014	8.57	2.19	14.95	0.009	-2786.59	520
SPE	Southwest Europe										
TES	Southwest Europe										
POS	Southwest Europe										
NEG	Southwest Europe										
FLUA	Southwest Europe										
FLUB	Southwest Europe										
A(H1)	Southwest Europe										
A(H1N1)	Southwest Europe										
A(H3)	Southwest Europe										
A(H5)	Southwest Europe										
A(UNS)	Southwest Europe										
B(YAM)	Southwest Europe										
B(VIC)	Southwest Europe										
B(UND)	Southwest Europe										
SPE	Eastern Europe	0.52	-3.41	4.45	0.794	1.77	-2.19	5.73	0.381	-1181.50	572
TES	Eastern Europe	6.40	0.57	12.24	0.032	17.53	11.62	23.45	0.000	-2937.52	572
POS	Eastern Europe	6.87	0.88	12.86	0.025	18.72	12.65	24.78	0.000	-2955.85	572
NEG	Eastern Europe	-0.06	-0.81	0.69	0.876	0.25	-0.50	1.01	0.512	-460.78	572
FLUA	Eastern Europe	6.70	0.73	12.67	0.028	18.53	12.47	24.58	0.000	-2954.51	572
FLUB	Eastern Europe	7.55	2.41	12.69	0.004	11.95	6.75	17.15	0.000	-2864.00	572
A(H1)	Eastern Europe	6.53	0.66	12.41	0.029	17.21	11.26	23.16	0.000	-2928.27	572
A(H1N1)	Eastern Europe	3.88	-0.82	8.58	0.105	9.30	4.53	14.07	0.000	-2804.08	572
A(H3)	Eastern Europe	6.34	0.48	12.20	0.034	17.68	11.74	23.61	0.000	-2943.92	572
A(H5)	Eastern Europe	0.97	-2.65	4.59	0.598	1.86	-1.78	5.51	0.316	-1165.60	572
A(UNS)	Eastern Europe	5.73	-0.08	11.54	0.053	16.83	10.94	22.72	0.000	-2939.46	572
B(YAM)	Eastern Europe	3.55	-1.25	8.35	0.147	10.62	5.74	15.50	0.000	-2797.17	572
B(VIC)	Eastern Europe	3.54	-1.26	8.34	0.148	10.62	5.74	15.50	0.000	-2797.08	572
B(UND)	Eastern Europe	7.55	2.41	12.69	0.004	11.95	6.75	17.15	0.000	-2864.00	572
SPE	Northern Africa	-0.52	-6.97	5.93	0.874	7.98	1.50	14.47	0.016	-1157.04	260
TES	Northern Africa	-0.90	-8.57	6.76	0.817	15.51	7.79	23.22	0.000	-1187.09	260
POS	Northern Africa	1.14	-6.22	8.49	0.761	16.73	9.33	24.13	0.000	-1178.75	260
NEG	Northern Africa	3.34	0.88	5.81	0.008	7.31	4.81	9.81	0.000	-754.30	260
FLUA	Northern Africa	1.26	-5.99	8.51	0.732	16.15	8.85	23.44	0.000	-1175.60	260
FLUB	Northern Africa	4.13	-2.27	10.52	0.205	12.49	6.05	18.92	0.000	-1087.91	260
A(H1)	Northern Africa	2.27	-2.97	7.52	0.394	10.89	5.62	16.17	0.000	-1036.97	260
A(H1N1)	Northern Africa	0.90	-5.09	6.89	0.768	8.51	2.49	14.52	0.006	-1140.40	260
A(H3)	Northern Africa	4.92	-2.25	12.08	0.178	16.93	9.71	24.15	0.000	-1097.44	260
A(H5)	Northern Africa	6.18	-0.09	12.44	0.053	10.32	4.03	16.61	0.001	-1015.01	260
A(UNS)	Northern Africa	3.22	-3.44	9.89	0.342	13.99	7.27	20.71	0.000	-1077.93	260
B(YAM)	Northern Africa	4.85	-0.75	10.46	0.090	10.43	4.78	16.08	0.000	-1019.22	260
B(VIC)	Northern Africa	4.72	-0.89	10.33	0.099	10.48	4.82	16.14	0.000	-1019.45	260
B(UND)	Northern Africa	3.88	-2.39	10.15	0.224	11.54	5.24	17.85	0.000	-1083.76	260
SPE	Eastern Africa	1.06	-3.22	5.34	0.627	-1.15	-5.46	3.16	0.599	-2585.96	520
TES	Eastern Africa	2.76	-2.49	8.02	0.302	-1.10	-6.38	4.17	0.681	-2628.58	520
POS	Eastern Africa	2.35	-2.79	7.50	0.369	-1.42	-6.59	3.75	0.590	-2673.04	520
NEG	Eastern Africa	1.63	-0.63	3.89	0.156	1.43	-0.83	3.69	0.216	-1088.67	520
FLUA	Eastern Africa	2.30	-2.80	7.41	0.376	-1.54	-6.67	3.60	0.557	-2673.31	520
FLUB	Eastern Africa	1.87	-2.70	6.43	0.422	-1.30	-5.89	3.29	0.578	-2615.03	520
A(H1)	Eastern Africa	1.90	-2.00	5.81	0.339	-2.00	-5.92	1.92	0.317	-2297.46	520
A(H1N1)	Eastern Africa	1.18	-3.09	5.44	0.587	-1.09	-5.38	3.19	0.617	-2583.60	520
A(H3)	Eastern Africa	2.15	-2.94	7.24	0.407	-1.57	-6.69	3.55	0.547	-2671.45	520
A(H5)	Eastern Africa	1.24	-3.03	5.51	0.568	-1.03	-5.33	3.26	0.637	-2584.12	520
A(UNS)	Eastern Africa	2.46	-2.65	7.57	0.345	-1.45	-6.58	3.68	0.579	-2649.95	520
B(YAM)	Eastern Africa	1.66	-2.28	5.59	0.408	-0.26	-4.21	3.69	0.896	-2482.05	520
B(VIC)	Eastern Africa	1.66	-2.28	5.59	0.408	-0.26	-4.21	3.69	0.896	-2482.05	520
B(UND)	Eastern Africa	1.73	-2.80	6.27	0.453	-1.18	-5.74	3.38	0.610	-2611.77	520

SPE	Middle Africa	2.71	-1.44	6.86	0.200	-4.51	-8.73	-0.29	0.036	-1549.00	364
TES	Middle Africa	2.66	-1.71	7.02	0.232	-4.35	-8.78	0.08	0.054	-1558.05	364
POS	Middle Africa	2.00	-2.44	6.43	0.377	-3.51	-8.02	1.00	0.127	-1530.12	364
NEG	Middle Africa	1.21	0.11	2.31	0.031	0.89	-0.22	1.99	0.116	-404.81	364
FLUA	Middle Africa	2.01	-2.42	6.45	0.373	-3.49	-8.00	1.01	0.128	-1529.92	364
FLUB	Middle Africa	1.86	-2.31	6.02	0.382	-3.63	-7.86	0.60	0.093	-1513.89	364
A(H1)	Middle Africa	2.81	-0.64	6.27	0.110	-1.51	-4.97	1.95	0.392	-1157.34	364
A(H1N1)	Middle Africa	2.06	-2.17	6.29	0.339	-3.67	-7.97	0.63	0.094	-1522.22	364
A(H3)	Middle Africa	3.02	-1.51	7.55	0.190	-3.26	-7.85	1.32	0.162	-1488.42	364
A(H5)	Middle Africa	2.06	-2.17	6.29	0.338	-3.69	-7.99	0.60	0.092	-1522.04	364
A(UNS)	Middle Africa	2.07	-2.35	6.49	0.358	-3.51	-8.00	0.99	0.126	-1529.16	364
B(YAM)	Middle Africa	2.08	-1.78	5.93	0.290	-3.39	-7.31	0.52	0.089	-1492.80	364
B(VIC)	Middle Africa	2.23	-1.61	6.07	0.254	-3.48	-7.38	0.42	0.080	-1491.48	364
B(UND)	Middle Africa	1.62	-2.29	5.54	0.415	-3.20	-7.18	0.78	0.114	-1498.18	364
SPE	Western Africa	1.47	-2.80	5.74	0.500	-0.36	-4.67	3.94	0.869	-2817.62	572
TES	Western Africa	2.26	-3.04	7.55	0.403	-1.13	-6.46	4.20	0.677	-2900.76	572
POS	Western Africa	2.41	-2.81	7.62	0.365	-1.03	-6.28	4.22	0.700	-2904.06	572
NEG	Western Africa	3.04	1.25	4.83	0.001	2.14	0.33	3.95	0.020	-1759.36	572
FLUA	Western Africa	2.06	-3.06	7.17	0.430	-1.03	-6.18	4.12	0.695	-2920.49	572
FLUB	Western Africa	1.20	-3.02	5.43	0.576	-0.31	-4.55	3.94	0.887	-2857.33	572
A(H1)	Western Africa	0.90	-2.75	4.54	0.629	-1.12	-4.79	2.54	0.548	-2746.76	572
A(H1N1)	Western Africa	1.58	-2.64	5.80	0.463	-0.15	-4.40	4.10	0.945	-2806.45	572
A(H3)	Western Africa	1.64	-3.34	6.62	0.518	-0.87	-5.89	4.14	0.733	-2932.07	572
A(H5)	Western Africa	1.61	-2.52	5.73	0.444	0.18	-3.96	4.33	0.931	-2824.33	572
A(UNS)	Western Africa	2.10	-2.79	6.99	0.399	-0.91	-5.84	4.01	0.715	-2898.95	572
B(YAM)	Western Africa	2.13	-1.87	6.14	0.296	1.29	-2.76	5.35	0.532	-2712.33	572
B(VIC)	Western Africa	2.02	-2.04	6.08	0.330	1.52	-2.59	5.62	0.469	-2715.34	572
B(UND)	Western Africa	1.10	-2.93	5.14	0.591	-0.50	-4.56	3.55	0.807	-2835.36	572
SPE	Western Asia	1.08	-1.54	3.69	0.419	1.42	-1.20	4.03	0.288	-3162.53	936
TES	Western Asia	2.84	-0.12	5.80	0.060	6.02	3.05	8.99	0.000	-4353.95	936
POS	Western Asia	3.99	1.04	6.95	0.008	7.44	4.48	10.40	0.000	-4229.88	936
NEG	Western Asia	0.98	-0.54	2.50	0.208	0.89	-0.64	2.42	0.253	-2408.15	936
FLUA	Western Asia	3.85	0.92	6.78	0.010	7.30	4.36	10.24	0.000	-4223.90	936
FLUB	Western Asia	4.29	1.37	7.20	0.004	7.00	4.08	9.93	0.000	-4028.56	936
A(H1)	Western Asia	2.90	-0.09	5.90	0.058	5.97	2.96	8.98	0.000	-3228.53	936
A(H1N1)	Western Asia	3.22	0.54	5.89	0.019	5.77	3.09	8.45	0.000	-4140.76	936
A(H3)	Western Asia	3.40	0.33	6.46	0.030	7.30	4.23	10.38	0.000	-3852.89	936
A(H5)	Western Asia	1.02	-2.34	4.38	0.552	2.83	-0.53	6.20	0.099	-2086.99	936
A(UNS)	Western Asia	2.33	-0.91	5.56	0.159	7.94	4.70	11.18	0.000	-3606.59	936
B(YAM)	Western Asia	1.88	-1.18	4.93	0.228	3.90	0.84	6.96	0.013	-3572.54	936
B(VIC)	Western Asia	1.87	-1.18	4.93	0.230	3.92	0.85	6.98	0.012	-3573.20	936
B(UND)	Western Asia	4.54	1.53	7.54	0.003	7.70	4.68	10.71	0.000	-3863.74	936
SPE	Central Asia										
TES	Central Asia	7.96	1.98	13.95	0.009	15.86	9.71	22.02	0.000	-1090.20	260
POS	Central Asia	7.96	1.98	13.95	0.009	15.86	9.71	22.02	0.000	-1090.20	260
NEG	Central Asia										
FLUA	Central Asia	7.94	1.96	13.92	0.009	15.88	9.73	22.03	0.000	-1090.08	260
FLUB	Central Asia	8.31	2.64	13.98	0.004	14.39	8.59	20.19	0.000	-1108.77	260
A(H1)	Central Asia	7.39	1.49	13.29	0.014	15.76	9.70	21.83	0.000	-1087.27	260
A(H1N1)	Central Asia	7.54	2.13	12.94	0.006	13.95	8.42	19.48	0.000	-1098.10	260
A(H3)	Central Asia	7.71	1.88	13.53	0.010	15.68	9.68	21.67	0.000	-1091.84	260
A(H5)	Central Asia										
A(UNS)	Central Asia	7.75	1.92	13.59	0.009	15.52	9.52	21.53	0.000	-1092.29	260
B(YAM)	Central Asia	7.56	2.00	13.12	0.008	14.22	8.52	19.91	0.000	-1104.65	260
B(VIC)	Central Asia	7.24	1.73	12.75	0.010	13.99	8.35	19.63	0.000	-1102.66	260
B(UND)	Central Asia	8.01	2.39	13.64	0.005	14.19	8.44	19.94	0.000	-1106.99	260
SPE	Eastern Asia	-1.06	-8.87	6.76	0.790	0.04	-7.81	7.89	0.992	-931.38	260
TES	Eastern Asia	0.07	-9.80	9.94	0.988	4.34	-5.57	14.25	0.390	-957.70	260
POS	Eastern Asia	1.52	-11.28	14.33	0.815	3.59	-9.29	16.46	0.584	-1272.30	260
NEG	Eastern Asia	0.57	-2.85	4.00	0.743	0.52	-2.90	3.94	0.766	-727.17	260

FLUA	Eastern Asia	1.60	-11.15	14.35	0.804	3.28	-9.54	16.10	0.615	-1271.34	260
FLUB	Eastern Asia	6.10	-5.51	17.72	0.302	3.51	-8.14	15.17	0.553	-1250.82	260
A(H1)	Eastern Asia	1.38	-10.41	13.18	0.818	1.56	-10.29	13.40	0.796	-1193.41	260
A(H1N1)	Eastern Asia	-0.61	-8.32	7.11	0.877	-0.11	-7.86	7.64	0.978	-1169.98	260
A(H3)	Eastern Asia	1.64	-11.02	14.29	0.799	2.88	-9.85	15.60	0.657	-1269.74	260
A(H5)	Eastern Asia	-0.90	-8.28	6.48	0.811	-0.35	-7.76	7.07	0.926	-1160.21	260
A(UNS)	Eastern Asia	-0.97	-12.17	10.23	0.865	0.14	-11.14	11.41	0.981	-1178.50	260
B(YAM)	Eastern Asia	0.02	-8.83	8.87	0.997	0.48	-8.41	9.37	0.915	-1142.60	260
B(VIC)	Eastern Asia	0.05	-8.79	8.89	0.991	0.40	-8.48	9.28	0.929	-1142.36	260
B(UND)	Eastern Asia	6.00	-5.61	17.60	0.310	3.48	-8.17	15.12	0.557	-1250.58	260
SPE	Southern Asia	1.39	-3.56	6.33	0.582	0.26	-4.71	5.24	0.917	-2362.14	468
TES	Southern Asia	2.50	-3.18	8.19	0.388	0.51	-5.20	6.22	0.861	-2398.19	468
POS	Southern Asia	2.43	-3.24	8.10	0.400	-0.01	-5.72	5.70	0.997	-2405.16	468
NEG	Southern Asia	0.89	-1.40	3.17	0.446	0.44	-1.85	2.73	0.707	-1746.73	468
FLUA	Southern Asia	1.97	-3.56	7.49	0.484	0.29	-5.26	5.85	0.917	-2412.75	468
FLUB	Southern Asia	3.12	-2.16	8.40	0.247	0.52	-4.78	5.81	0.849	-2336.16	468
A(H1)	Southern Asia	1.09	-2.88	5.07	0.589	-0.91	-4.91	3.08	0.653	-2046.57	468
A(H1N1)	Southern Asia	1.22	-3.60	6.05	0.619	0.62	-4.24	5.48	0.802	-2346.10	468
A(H3)	Southern Asia	1.65	-3.68	6.98	0.543	0.38	-4.98	5.74	0.890	-2400.24	468
A(H5)	Southern Asia	1.25	-3.04	5.54	0.567	-0.12	-4.44	4.20	0.956	-2295.57	468
A(UNS)	Southern Asia	0.91	-3.93	5.75	0.712	-0.36	-5.23	4.52	0.886	-2351.79	468
B(YAM)	Southern Asia	1.70	-2.83	6.24	0.461	0.21	-4.35	4.77	0.928	-2318.08	468
B(VIC)	Southern Asia	1.70	-2.80	6.21	0.458	-0.25	-4.78	4.27	0.912	-2314.63	468
B(UND)	Southern Asia	2.89	-2.25	8.04	0.270	0.10	-5.06	5.26	0.969	-2324.29	468
SPE	Southeast Asia										
TES	Southeast Asia										
POS	Southeast Asia										
NEG	Southeast Asia										
FLUA	Southeast Asia										
FLUB	Southeast Asia										
A(H1)	Southeast Asia										
A(H1N1)	Southeast Asia										
A(H3)	Southeast Asia										
A(H5)	Southeast Asia										
A(UNS)	Southeast Asia										
B(YAM)	Southeast Asia										
B(VIC)	Southeast Asia										
B(UND)	Southeast Asia										
SPE	Oceania Melanesia Polynesia	-0.95	-7.63	5.73	0.779	-4.02	-10.67	2.63	0.235	-1128.50	260
TES	Oceania Melanesia Polynesia	0.35	-10.60	11.30	0.950	-12.22	-23.30	-1.14	0.031	-1282.82	260
POS	Oceania Melanesia Polynesia	-2.90	-13.86	8.07	0.603	-13.06	-24.07	-2.06	0.020	-1317.84	260
NEG	Oceania Melanesia Polynesia	0.59	-2.70	3.89	0.724	-4.13	-7.43	-0.82	0.015	-953.18	260
FLUA	Oceania Melanesia Polynesia	-3.67	-14.59	7.26	0.509	-12.65	-23.60	-1.71	0.024	-1306.59	260
FLUB	Oceania Melanesia Polynesia	-7.75	-15.57	0.07	0.052	-13.40	-21.24	-5.55	0.001	-1285.00	260
A(H1)	Oceania Melanesia Polynesia	-3.77	-10.90	3.35	0.298	-8.75	-15.90	-1.60	0.017	-1270.48	260
A(H1N1)	Oceania Melanesia Polynesia	-4.90	-10.78	0.99	0.103	-6.08	-11.95	-0.21	0.043	-1208.15	260
A(H3)	Oceania Melanesia Polynesia	-5.32	-15.02	4.39	0.282	-10.67	-20.42	-0.91	0.032	-1318.07	260
A(H5)	Oceania Melanesia Polynesia	-4.36	-9.57	0.84	0.100	-4.29	-9.48	0.91	0.105	-1178.32	260
A(UNS)	Oceania Melanesia Polynesia	-8.65	-18.87	1.56	0.096	-14.36	-24.60	-4.12	0.006	-1319.29	260
B(YAM)	Oceania Melanesia Polynesia	-7.32	-13.79	-0.85	0.027	-6.39	-12.84	0.05	0.052	-1159.96	260
B(VIC)	Oceania Melanesia Polynesia	-7.19	-13.67	-0.71	0.030	-6.49	-12.95	-0.03	0.049	-1160.49	260
B(UND)	Oceania Melanesia Polynesia	-8.02	-15.77	-0.26	0.043	-12.54	-20.32	-4.77	0.002	-1282.93	260

Supplementary Table S20. Average and median *reporting delay* for specimens collected (SPE), tests (TES), total positives (POS), A(H1) positives, and A(H5) positives in 6 regions and 17 influenza transmission zones. We extracted FluNet data from 173 Member States on 15 June 2021. We calculated *delays* as the number of weeks from data download to the most recent complete week of reported data. We report average *delay* with 95% confidence intervals (top values) and median *delay* with lower and upper quartiles (bottom values). Values of *Missing* indicate zones where all Member States had no reported data for that testing outcome or subtype. Regions and zones are listed in ascending order by positives' *delay*, and we omit the Southern African zone, as it consisted of only 1 country.

Region	TES	POS	SPE	A(H1)	A(H5)
SEARO	5.73 [1.77, 9.68] 4.00 [1.00, 8.00]	5.64 [1.67, 9.60] 4.00 [1.00, 8.00]	5.64 [1.67, 9.60] 4.00 [1.00, 8.00]	213.07 [172.53, 253.62] 244.00 [213.00, 249.00]	50.80 [12.02, 89.58] 6.00 [2.00, 64.00]
EURO	11.16 [4.70, 17.61] 3.00 [2.00, 5.00]	11.16 [4.70, 17.61] 3.00 [2.00, 5.00]	403.59 [312.08, 495.10] 550.00 [245.00, 564.00]	263.00 [193.59, 332.41] 257.00 [246.00, 263.00]	95.14 [0.00, 194.54] 7.00 [2.00, 73.00]
WPRO	19.29 [5.00, 33.57] 6.00 [1.00, 24.00]	24.33 [7.19, 41.47] 4.00 [1.00, 63.00]	60.71 [7.13, 114.30] 6.00 [1.00, 71.00]	13.53 [5.65, 21.41] 3.00 [2.00, 5.00]	395.14 [302.90, 487.39] 548.00 [245.00, 562.00]
PAHO	7.75 [0.00, 15.79] 1.00 [1.00, 1.00]	40.02 [29.25, 50.80] 45.00 [2.00, 67.00]	332.60 [238.67, 426.53] 395.00 [110.00, 494.50]	90.59 [52.44, 128.73] 42.00 [2.00, 171.00]	382.57 [330.13, 435.01] 380.00 [258.00, 462.00]
AFRO	48.73 [9.96, 87.51] 6.00 [2.00, 54.00]	48.73 [9.96, 87.51] 6.00 [2.00, 54.00]	51.20 [12.52, 89.88] 8.50 [3.00, 64.00]	180.00 [103.59, 256.41] 245.00 [82.00, 260.00]	59.73 [0.00, 120.22] 6.00 [2.00, 84.00]
EMRO	51.42 [0.00, 112.43] 6.00 [2.00, 59.00]	76.89 [2.69, 151.10] 7.00 [2.00, 70.00]	51.42 [0.00, 112.43] 6.00 [2.00, 59.00]	154.47 [93.73, 215.21] 209.00 [10.00, 254.00]	68.13 [24.05, 112.21] 66.00 [3.00, 86.00]
Zone					
Northern Europe	2.60 [1.93, 3.27] 2.00 [2.00, 3.00]	2.60 [1.93, 3.27] 2.00 [2.00, 3.00]	561.71 [545.42, 578.00] 562.00 [552.00, 576.00]	93.07 [32.13, 154.01] 24.00 [1.00, 233.00]	385.30 [318.91, 451.69] 393.50 [309.00, 462.00]
Southern Asia	3.00 [1.27, 4.73] 2.00 [1.00, 4.00]	2.89 [1.21, 4.57] 2.00 [1.00, 4.00]	2.89 [1.21, 4.57] 2.00 [1.00, 4.00]	5.40 [2.59, 8.21] 5.00 [3.00, 7.00]	*Missing*
Central Asia	5.40 [2.59, 8.21] 5.00 [3.00, 7.00]	5.40 [2.59, 8.21] 5.00 [3.00, 7.00]	*Missing*	218.33 [184.64, 252.03] 244.00 [213.00, 245.00]	29.80 [8.88, 50.72] 11.00 [4.00, 54.00]
Southeast Asia	6.00 [1.53, 10.47] 3.00 [1.00, 8.00]	6.00 [1.53, 10.47] 3.00 [1.00, 8.00]	33.50 [0.00, 88.45] 3.00 [1.00, 8.00]	115.75 [0.00, 244.90] 106.00 [2.50, 229.00]	36.20 [0.00, 75.58] 6.00 [3.00, 77.00]
Eastern Europe	8.82 [0.00, 20.44] 2.00 [2.00, 4.00]	8.82 [0.00, 20.44] 2.00 [2.00, 4.00]	208.00 [111.13, 304.87] 244.50 [152.50, 263.50]	8.82 [0.00, 20.44] 2.00 [2.00, 4.00]	218.50 [141.81, 295.19] 244.50 [173.50, 263.50]
Western Africa	9.55 [0.00, 20.43] 3.00 [2.00, 10.00]	9.55 [0.00, 20.43] 3.00 [2.00, 10.00]	16.27 [0.36, 32.19] 4.00 [2.00, 12.00]	308.00 [206.90, 409.10] 233.00 [226.00, 411.00]	159.29 [18.46, 300.11] 82.00 [10.00, 411.00]
Southwest Europe	11.68 [1.83, 21.54] 3.00 [2.00, 8.00]	11.68 [1.83, 21.54] 3.00 [2.00, 8.00]	322.89 [158.47, 487.31] 370.00 [30.00, 560.00]	167.50 [0.00, 344.88] 167.50 [77.00, 258.00]	278.00 [238.80, 317.20] 278.00 [258.00, 298.00]
Eastern Asia	20.50 [0.00, 53.53] 4.50 [2.50, 38.50]	16.80 [0.00, 43.40] 3.00 [2.00, 6.00]	20.50 [0.00, 53.53] 4.50 [2.50, 38.50]	324.80 [189.64, 459.96] 262.00 [248.00, 270.00]	124.80 [0.00, 357.65] 7.00 [6.00, 7.00]
Temperate South America	1.00 [1.00, 1.00] 1.00 [1.00, 1.00]	18.75 [0.00, 49.02] 4.00 [2.00, 35.50]	466.25 [304.79, 627.71] 498.50 [335.00, 597.50]	2.60 [1.93, 3.27] 2.00 [2.00, 3.00]	561.71 [545.42, 578.00] 562.00 [552.00, 576.00]
North America	1.67 [1.01, 2.32] 2.00 [1.00, 2.00]	23.00 [0.00, 64.16] 2.00 [2.00, 65.00]	2.00 [2.00, 2.00] 2.00 [2.00, 2.00]	234.00 [153.12, 314.88] 247.00 [247.00, 254.00]	147.40 [54.38, 240.42] 84.00 [68.00, 221.00]
Eastern Africa	23.60 [5.88, 41.32] 11.00 [4.00, 42.00]	23.60 [5.88, 41.32] 11.00 [4.00, 42.00]	23.60 [5.88, 41.32] 11.00 [4.00, 42.00]	144.20 [69.94, 218.46] 155.00 [10.00, 260.00]	40.40 [0.00, 90.79] 8.00 [2.00, 24.00]
Tropical South America	24.44 [0.00, 61.24] 1.00 [1.00, 1.00]	30.13 [11.05, 49.20] 29.00 [2.50, 53.50]	313.00 [121.41, 504.59] 302.00 [177.00, 442.00]	202.25 [131.29, 273.21] 247.00 [163.50, 255.50]	48.00 [0.00, 104.67] 4.00 [2.00, 72.00]
Central America and Caribbean	4.00 [0.00, 8.08] 1.00 [1.00, 1.00]	47.71 [33.70, 61.73] 65.00 [2.50, 67.00]	357.56 [230.49, 484.62] 407.00 [309.00, 479.00]	18.05 [2.47, 33.64] 3.00 [2.00, 12.00]	323.11 [158.53, 487.69] 370.00 [30.00, 560.00]
Oceania Melanesia Polynesia	33.80 [6.36, 61.24] 24.00 [20.00, 40.00]	52.40 [18.53, 86.27] 63.00 [24.00, 84.00]	94.80 [0.00, 198.85] 71.00 [20.00, 84.00]	57.00 [0.00, 122.23] 42.00 [4.00, 110.00]	418.00 [232.92, 603.08] 413.00 [257.00, 584.00]
Western Asia	30.50 [13.68, 47.32] 4.50 [2.00, 70.00]	57.39 [7.17, 107.60] 9.00 [2.00, 71.00]	111.50 [0.94, 222.06] 30.50 [2.00, 71.00]	83.50 [20.39, 146.61] 47.00 [12.00, 150.00]	395.17 [273.05, 517.28] 372.00 [249.00, 533.00]
Northern Africa	124.80 [0.00, 357.65] 7.00 [6.00, 7.00]	124.80 [0.00, 357.65] 7.00 [6.00, 7.00]	124.80 [0.00, 357.65] 7.00 [6.00, 7.00]	179.64 [114.75, 244.53] 245.00 [19.00, 249.00]	9.55 [0.00, 20.43] 3.00 [2.00, 10.00]
Middle Africa	159.29 [18.46, 300.11] 82.00 [10.00, 411.00]	159.29 [18.46, 300.11] 82.00 [10.00, 411.00]	159.29 [18.46, 300.11] 82.00 [10.00, 411.00]	145.14 [67.80, 222.49] 92.00 [3.00, 257.00]	152.63 [0.00, 314.98] 43.00 [3.00, 272.00]
Worldwide	**21.79 [11.40, 32.17] 2.00 [1.00, 8.00]**	**33.37 [21.69, 45.06] 4.00 [2.00, 62.00]**	**163.41 [123.38, 203.45] 36.00 [4.00, 305.50]**	**116.11 [95.17, 137.05] 67.50 [2.00, 247.00]**	**186.31 [146.89, 225.73] 77.00 [4.50, 342.00]**

Supplementary Table S21. The *reporting delay* of 173 Member States for 6 test outcomes (specimens collected (SPE), specimens processed or tests (TES), influenza A positives (FLUA), influenza B positives (FLUB), total positives (POS), and total negatives (NEG)) reported by the WHO's FluNet. Data were downloaded on 15 June 2021 at which time the *total time series length* of reported data was 1381 weeks. We calculated *reporting delay* as the number of weeks from the date of data download to the most recent week of complete records. Member States are listed in ascending order by average *reporting delay* across all 6 outcomes (AVG), region, and zone. Member State-outcome dyads where all 1381 weeks for our study period have incomplete records were denoted as *M*.

Region	Zone	Country/Territory	POS	FLUA	FLUB	NEG	SPE	TES	AVG
AFRO	Western Africa	Côte d'Ivoire	1	1	1	1	1	1	1
AFRO	Western Africa	Mali	1	1	1	1	1	1	1
EMRO	Western Asia	Oman	1	1	1	1	1	1	1
PAHO	Central America and Caribbean	Mexico	1	1	1	1	M	1	1
SEARO	South-East Asia	Thailand	1	1	1	1	1	1	1
WPRO	Oceania Melanesia Polynesia	Australia	1	1	1	1	1	1	1
WPRO	South-East Asia	Laos	1	1	1	1	1	1	1
WPRO	South-East Asia	Singapore	1	1	1	1	1	1	1
SEARO	Southern Asia	Nepal	1	1	2	1	1	1	1
PAHO	Tropical South America	Bolivia	1	1	1	2	M	1	1
AFRO	Eastern Africa	Mozambique	1	1	1	3	1	1	1
PAHO	Central America and Caribbean	Haiti	1	1	1	3	M	1	1
PAHO	Central America and Caribbean	Belize	2	2	2	2	M	1	2
PAHO	Tropical South America	Colombia	2	2	2	2	M	1	2
AFRO	Southern Africa	South Africa	2	2	2	2	2	2	2
AFRO	Western Africa	Ghana	2	2	2	2	2	2	2
AFRO	Western Africa	Guinea	2	2	2	M	2	2	2
EMRO	Southern Asia	Pakistan	2	2	2	2	2	2	2
EMRO	Western Asia	Lebanon	2	2	2	2	2	2	2
EMRO	Western Asia	United Arab Emirates	2	2	2	2	2	2	2
EURO	Central Asia	Kazakhstan	2	2	2	M	M	2	2
EURO	Eastern Europe	Bulgaria	2	2	2	M	M	2	2
EURO	Eastern Europe	Moldova	2	2	2	M	M	2	2
EURO	Eastern Europe	Slovakia	2	2	2	M	M	2	2
EURO	Northern Europe	Iceland	2	2	2	M	M	2	2
EURO	South West Europe	Germany	2	2	2	M	M	2	2
EURO	South West Europe	Luxembourg	2	2	2	M	M	2	2
EURO	South West Europe	Portugal	2	2	2	M	M	2	2
EURO	Western Asia	Georgia	2	2	2	M	M	2	2
PAHO	North America	Canada	2	2	2	M	2	2	2
PAHO	North America	United States of America	2	2	2	2	2	2	2
SEARO	Southern Asia	Bangladesh	2	2	2	2	2	2	2
WPRO	Eastern Asia	Japan	2	2	2	3	M	M	2
SEARO	South-East Asia	Timor-Leste	2	2	2	4	2	2	2
EMRO	Southern Asia	Afghanistan	2	2	2	5	2	2	3
EMRO	Western Asia	Saudi Arabia	1	13	1	1	1	1	3
EURO	Central Asia	Tajikistan	3	3	3	M	M	3	3
EURO	South West Europe	Albania	3	3	3	M	M	3	3
EURO	South West Europe	North Macedonia	3	3	3	M	M	3	3
EURO	Western Asia	Armenia	3	3	3	M	M	3	3
EURO	Western Asia	Azerbaijan	3	3	3	M	M	3	3
WPRO	Eastern Asia	Mongolia	3	3	3	M	3	3	3
AFRO	Eastern Africa	Uganda	4	4	4	4	4	4	4
AFRO	Western Africa	Togo	4	4	4	4	4	4	4
EMRO	Western Asia	Qatar	4	4	4	4	4	4	4
EURO	Eastern Europe	Belarus	4	4	4	M	M	4	4
EURO	Eastern Europe	Hungary	4	4	4	M	M	4	4
EURO	Eastern Europe	Kosovo	4	4	4	M	M	4	4
EURO	Northern Europe	Sweden	4	4	4	M	M	4	4

EURO	South West Europe	Bosnia and Herzegovina	4	4	4	M	M	4	4
SEARO	Southern Asia	Bhutan	4	4	4	4	4	4	4
WPRO	South-East Asia	Viet Nam	4	4	4	4	4	4	4
AFRO	Western Africa	Sierra Leone	4	4	4	6	4	4	4
AFRO	Western Africa	Mauritania	3	3	3	12	3	3	5
AFRO	Eastern Africa	Kenya	5	5	5	M	5	5	5
AFRO	Middle Africa	Cameroon	5	5	5	5	5	5	5
EURO	Central Asia	Uzbekistan	5	5	5	M	M	5	5
EURO	Northern Europe	Ireland	5	5	5	M	M	5	5
EURO	South West Europe	Montenegro	5	5	5	M	M	5	5
AFRO	Northern Africa	Algeria	4	4	4	11	4	4	5
SEARO	Eastern Asia	North Korea	6	6	6	6	6	6	6
AFRO	Eastern Africa	Madagascar	7	7	7	7	7	7	7
EMRO	Northern Africa	Egypt	7	7	7	7	7	7	7
EMRO	Northern Africa	Tunisia	7	7	7	7	7	7	7
EURO	Central Asia	Kyrgyzstan	7	7	7	M	M	7	7
EMRO	Northern Africa	Morocco	6	6	6	14	6	6	7
EURO	South West Europe	Italy	8	8	8	8	8	8	8
WPRO	South-East Asia	Philippines	8	8	8	8	8	8	8
PAHO	Central America and Caribbean	Saint Lucia	1	1	1	37	M	1	8
EMRO	Western Asia	Iraq	13	13	14	4	4	4	9
PAHO	Central America and Caribbean	Nicaragua	3	36	3	3	M	1	9
EURO	Central Asia	Turkmenistan	10	10	10	M	M	10	10
EURO	South West Europe	Spain	2	2	2	32	20	2	10
EMRO	Southern Asia	Iran	1	1	1	66	1	1	12
EURO	South West Europe	Austria	12	12	12	M	M	12	12
WPRO	Eastern Asia	China	2	2	2	70	2	2	13
AFRO	Western Africa	Senegal	2	2	2	2	76	2	14
AFRO	Eastern Africa	Tanzania	15	15	15	15	15	15	15
SEARO	Southern Asia	India	1	1	2	88	1	1	16
WPRO	South-East Asia	Malaysia	1	1	1	92	1	1	16
AFRO	Eastern Africa	Ethiopia	19	19	19	19	19	19	19
AFRO	Eastern Africa	Zambia	2	2	2	104	2	2	19
SEARO	Southern Asia	Maldives	4	4	4	97	4	5	20
SEARO	Southern Asia	Sri Lanka	9	63	9	M	9	9	20
EURO	South West Europe	Serbia	15	15	15	30	30	15	20
SEARO	South-East Asia	Indonesia	8	8	8	80	8	8	20
PAHO	Tropical South America	Suriname	22	22	22	36	M	1	21
SEARO	South-East Asia	Myanmar	24	24	24	24	24	24	24
AFRO	Western Africa	Burkina Faso	10	10	10	119	10	10	28
EURO	Eastern Europe	Russian Federation	2	2	2	105	62	2	29
WPRO	Oceania Melanesia Polynesia	New Caledonia	24	24	24	24	71	24	32
AFRO	Middle Africa	Democratic Republic of the Congo	10	10	10	170	10	10	37
WPRO	Oceania Melanesia Polynesia	Fiji	63	63	64	20	20	20	42
AFRO	Eastern Africa	Mauritius	42	42	42	M	42	42	42
PAHO	Temperate South America	Argentina	2	2	2	2	257	1	44
PAHO	Central America and Caribbean	Grenada	66	66	67	38	M	1	48
AFRO	Western Africa	Niger	12	12	12	226	12	12	48
PAHO	North America	Bermuda	65	66	65	M	M	1	49
PAHO	Central America and Caribbean	British Virgin Islands	67	67	M	65	M	1	50
EURO	South West Europe	France	2	2	2	M	245	2	51
EURO	Eastern Europe	Poland	2	2	2	M	246	2	51
PAHO	Central America and Caribbean	Aruba	65	65	66	65	M	1	52
PAHO	Central America and Caribbean	Trinidad and Tobago	65	66	65	65	M	1	52
EURO	Eastern Europe	Romania	5	5	5	M	243	5	53
PAHO	Central America and Caribbean	Barbados	65	65	69	65	M	1	53
PAHO	Central America and Caribbean	El Salvador	2	2	2	2	309	1	53
PAHO	Tropical South America	French Guiana	62	62	66	43	43	43	53
AFRO	Eastern Africa	Seychelles	54	54	54	M	54	54	54
PAHO	Central America and Caribbean	Turks and Caicos Islands	67	67	68	67	M	1	54

PAHO	Central America and Caribbean	Saint Kitts and Nevis	65	65	75	65	M	1	54
EMRO	Western Asia	West Bank and Gaza Strip	67	67	67	42	42	42	55
PAHO	Central America and Caribbean	Dominican Republic	68	68	68	68	M	1	55
PAHO	Central America and Caribbean	Saint Vincent and the Grenadines	68	68	70	68	M	1	55
EURO	Eastern Europe	Ukraine	2	2	2	M	281	2	58
PAHO	Central America and Caribbean	Guadeloupe	67	67	67	66	43	43	59
PAHO	Tropical South America	Brazil	45	48	45	45	177	1	60
PAHO	Central America and Caribbean	Martinique	67	67	68	75	43	43	61
EMRO	Western Asia	Yemen	61	63	61	M	59	59	61
PAHO	Central America and Caribbean	Bahamas	71	87	71	73	M	1	61
AFRO	Western Africa	Nigeria	64	64	64	67	64	64	65
WPRO	South-East Asia	Cambodia	10	10	10	M	285	10	65
PAHO	Central America and Caribbean	Anguilla	90	90	90	M	M	1	68
EURO	Eastern Europe	Czechia	68	68	68	M	M	68	68
AFRO	Middle Africa	Central African Republic	70	70	70	M	70	70	70
PAHO	Temperate South America	Chile	2	2	2	2	413	1	70
EMRO	Western Asia	Bahrain	70	73	70	70	70	70	71
EURO	South West Europe	Malta	71	71	71	M	M	71	71
WPRO	Eastern Asia	South Korea	71	71	71	71	71	71	71
EMRO	Western Asia	Kuwait	71	73	71	71	71	71	71
PAHO	Central America and Caribbean	Dominica	66	66	162	67	M	1	72
EURO	South West Europe	Croatia	75	75	75	M	M	75	75
PAHO	Tropical South America	Peru	3	3	3	3	442	1	76
EMRO	Western Asia	Jordan	77	77	77	77	77	77	77
PAHO	Central America and Caribbean	Cayman Islands	68	68	175	M	M	1	78
PAHO	Central America and Caribbean	Costa Rica	1	1	1	2	462	1	78
EURO	South West Europe	Greece	6	6	6	M	370	6	79
PAHO	Central America and Caribbean	Honduras	1	1	1	3	479	1	81
AFRO	Middle Africa	Chad	82	82	82	M	82	82	82
AFRO	Middle Africa	South Sudan	82	82	82	M	82	82	82
WPRO	Oceania Melanesia Polynesia	Papua New Guinea	84	84	84	85	84	84	84
AFRO	Eastern Africa	Rwanda	87	87	87	M	87	87	87
PAHO	Central America and Caribbean	Jamaica	3	3	3	3	510	1	87
PAHO	Central America and Caribbean	Panama	42	42	42	42	383	1	92
PAHO	Central America and Caribbean	Guatemala	30	59	30	30	407	1	93
PAHO	Tropical South America	Venezuela	70	70	70	75	302	1	98
PAHO	Temperate South America	Paraguay	6	6	6	6	584	1	102
PAHO	Central America and Caribbean	Antigua and Barbuda	157	M	157	M	M	1	105
EURO	Northern Europe	Denmark	3	3	3	M	527	3	108
WPRO	Oceania Melanesia Polynesia	New Zealand	90	90	90	40	298	40	108
EURO	South West Europe	Slovenia	2	2	2	M	548	2	111
EURO	Northern Europe	Finland	2	2	2	M	552	2	112
EURO	Western Asia	Cyprus	112	112	112	M	M	112	112
EURO	Northern Europe	Estonia	2	2	2	M	553	2	112
EURO	South West Europe	Switzerland	2	2	2	M	560	2	114
EURO	Northern Europe	Norway	2	2	2	M	562	2	114
EURO	Northern Europe	United Kingdom	2	2	2	M	564	2	114
EURO	South West Europe	Netherlands	2	2	2	M	564	2	114
EURO	South West Europe	Belgium	4	4	4	M	561	4	115
EURO	Northern Europe	Latvia	2	2	2	M	576	2	117
EURO	Northern Europe	Lithuania	2	2	2	M	598	2	121
PAHO	Tropical South America	Ecuador	36	36	36	36	601	1	124
EURO	Western Asia	Israel	5	5	5	M	625	5	129
PAHO	Central America and Caribbean	Cuba	67	67	67	67	582	1	142
PAHO	Temperate South America	Uruguay	65	65	66	65	611	1	146
PAHO	Tropical South America	Guyana	M	M	M	M	M	170	170
EURO	Western Asia	Turkey	72	72	72	M	584	72	174
EMRO	Western Asia	Syrian Arab Republic	467	467	467	19	19	19	243
AFRO	Middle Africa	Congo	411	411	411	M	411	411	411
AFRO	Middle Africa	Angola	455	455	455	M	455	455	455

EMRO	Northern Africa	Sudan	600	600	600	M	600	600	600

Supplementary Table S22. The *reporting delay* of 173 Member States for 8 influenza strains and subtypes (A(H1), A(H1N1)pdm09, A(H3), A(H5), A(Unsubtyped) abbreviated A(Uns), B(Yamagata) abbreviated B(Yam), B(Victoria) abbreviated B(Vic), and B(Undetermined) positives abbreviated B(Und)) reported by the WHO's FluNet. Data were downloaded on 15 June 2021 at which time the *total time series length* of reported data was 1381 weeks for all subtypes except A(H1N1)pdm09 (651 weeks). We calculated *reporting delay* as the number of weeks from the date of data download to the most recent week of complete records. Member States are listed in ascending order by average *reporting delay* across all 8 subtypes (AVG), region, and zone. Member State-outcome dyads where all weeks for our study period have incomplete records were denoted as *M*.

Region	Zone	Country/Territory	A(H1)	A(H1N1)	A(H3)	A(H5)	A(Uns)	B(Yam)	B(Vic)	B(Und)	AVG
PAHO	Central America and Caribbean	Haiti	1	1	1	M	1	1	1	1	1
PAHO	Central America and Caribbean	Saint Lucia	1	1	1	M	1	1	1	1	1
PAHO	Tropical South America	Bolivia	1	1	1	M	1	1	1	1	1
AFRO	Southern Africa	South Africa	2	2	2	2	2	2	2	2	2
AFRO	Western Africa	Guinea	2	2	2	2	2	2	2	2	2
EMRO	Western Asia	Lebanon	2	2	2	2	2	2	2	2	2
EURO	Central Asia	Kazakhstan	2	2	2	M	2	2	2	2	2
EURO	Eastern Europe	Bulgaria	2	2	2	M	2	2	2	2	2
EURO	Eastern Europe	Moldova	2	2	2	M	2	2	2	2	2
EURO	Eastern Europe	Slovakia	2	2	2	M	2	2	2	2	2
EURO	Northern Europe	Iceland	2	2	2	M	2	2	2	2	2
EURO	South West Europe	Germany	2	2	2	M	2	2	2	2	2
EURO	South West Europe	Luxembourg	2	2	2	M	2	2	2	2	2
EURO	South West Europe	Portugal	2	2	2	M	2	2	2	2	2
EURO	Western Asia	Georgia	2	2	2	M	2	2	2	2	2
PAHO	Central America and Caribbean	Belize	2	2	2	M	2	2	2	2	2
WPRO	Eastern Asia	Japan	2	2	2	2	2	2	2	2	2
EURO	Central Asia	Tajikistan	3	3	3	M	3	3	3	3	3
EURO	South West Europe	Albania	3	3	3	M	3	3	3	3	3
EURO	South West Europe	North Macedonia	3	3	3	M	3	3	3	3	3
EURO	Western Asia	Armenia	3	3	3	M	3	3	3	3	3
EURO	Western Asia	Azerbaijan	3	3	3	M	3	3	3	3	3
WPRO	Eastern Asia	Mongolia	3	3	3	3	3	3	3	3	3
EURO	Eastern Europe	Belarus	4	4	4	M	4	4	4	4	4
EURO	Eastern Europe	Hungary	4	4	4	M	4	4	4	4	4
EURO	Eastern Europe	Kosovo	4	4	4	M	4	4	4	4	4
EURO	Northern Europe	Sweden	4	4	4	M	4	4	4	4	4
EURO	South West Europe	Bosnia and Herzegovina	4	4	4	M	4	4	4	4	4
SEARO	Southern Asia	Maldives	M	4	4	4	4	4	4	4	4
EURO	South West Europe	Spain	2	2	2	20	2	2	2	2	4
AFRO	Western Africa	Togo	9	4	4	4	4	4	4	4	5
AFRO	Western Africa	Mauritania	19	3	3	3	3	3	3	3	5
EURO	Central Asia	Uzbekistan	5	5	5	M	5	5	5	5	5
EURO	Northern Europe	Ireland	5	5	5	M	5	5	5	5	5
EURO	South West Europe	Montenegro	5	5	5	M	5	5	5	5	5
EURO	Western Asia	Israel	5	5	5	M	5	5	5	5	5
SEARO	South-East Asia	Timor-Leste	2	2	2	2	M	2	2	24	5
SEARO	Eastern Asia	North Korea	M	6	6	6	M	M	M	6	6
EURO	Central Asia	Kyrgyzstan	7	7	7	M	7	7	7	7	7
WPRO	South-East Asia	Philippines	8	8	8	8	8	8	8	8	8
WPRO	South-East Asia	Singapore	69	1	1	1	1	1	1	1	10
EURO	Central Asia	Turkmenistan	10	10	10	M	10	10	10	10	10
EURO	South West Europe	Austria	12	12	12	M	12	12	12	12	12
SEARO	Southern Asia	Bhutan	82	4	4	4	4	4	4	4	14
EURO	Eastern Europe	Russian Federation	2	2	2	104	2	2	2	2	15
EMRO	Western Asia	United Arab Emirates	M	2	2	M	M	2	2	68	15
EURO	South West Europe	Serbia	15	15	15	30	15	15	15	15	17
SEARO	Southern Asia	Nepal	1	1	1	1	10	77	77	2	21
PAHO	Tropical South America	Suriname	22	22	22	M	22	22	22	22	22

EURO	South West Europe	Italy	129	8	8	8	8	8	8	8	23
EMRO	Western Asia	Saudi Arabia	66	13	M	M	18	M	M	1	25
AFRO	Eastern Africa	Kenya	213	5	5	5	5	5	5	5	31
AFRO	Eastern Africa	Mozambique	244	1	1	1	1	1	1	1	31
AFRO	Middle Africa	Cameroon	215	5	6	5	5	5	5	5	31
AFRO	Western Africa	Côte d'Ivoire	248	1	1	1	1	1	1	1	32
EMRO	Southern Asia	Iran	248	1	1	1	1	1	1	1	32
AFRO	Eastern Africa	Zambia	244	2	2	2	2	2	2	2	32
EURO	South West Europe	France	2	2	2	245	2	2	2	2	32
EMRO	Southern Asia	Afghanistan	246	2	2	2	2	2	2	2	33
EURO	Eastern Europe	Poland	2	2	2	246	2	2	2	2	33
AFRO	Western Africa	Senegal	249	2	2	2	2	2	2	2	33
SEARO	Southern Asia	Bangladesh	249	2	2	2	2	2	2	2	33
WPRO	South-East Asia	Laos	262	1	1	1	1	1	1	1	34
AFRO	Western Africa	Ghana	256	2	2	2	2	2	2	2	34
EMRO	Western Asia	Oman	268	1	1	1	1	1	1	1	34
AFRO	Western Africa	Sierra Leone	249	4	4	4	4	4	4	4	35
EURO	Eastern Europe	Romania	5	5	5	243	5	5	5	5	35
EMRO	Western Asia	Qatar	257	4	4	4	4	4	4	4	36
WPRO	South-East Asia	Viet Nam	258	4	4	4	4	4	4	4	36
EMRO	Northern Africa	Morocco	248	6	6	6	6	6	6	6	36
EMRO	Northern Africa	Egypt	244	7	7	7	7	7	7	7	37
AFRO	Western Africa	Burkina Faso	225	10	10	10	10	10	10	10	37
EURO	Eastern Europe	Ukraine	2	2	2	281	2	2	2	2	37
AFRO	Middle Africa	Democratic Republic of the Congo	226	10	10	10	10	10	10	10	37
AFRO	Eastern Africa	Madagascar	249	7	7	7	7	7	7	7	37
AFRO	Northern Africa	Algeria	270	4	4	4	4	4	4	4	37
EMRO	Northern Africa	Tunisia	262	7	7	7	7	7	7	7	39
SEARO	South-East Asia	Indonesia	263	8	8	8	8	8	8	8	40
PAHO	Central America and Caribbean	Mexico	1	1	1	314	1	1	1	1	40
AFRO	Western Africa	Niger	245	12	12	12	12	12	12	12	41
WPRO	Eastern Asia	China	209	2	2	93	20	2	2	2	42
WPRO	South-East Asia	Malaysia	77	1	1	86	1	86	86	1	42
PAHO	Central America and Caribbean	El Salvador	24	2	2	309	2	2	2	2	43
EMRO	Southern Asia	Pakistan	262	2	2	72	2	2	2	2	43
AFRO	Eastern Africa	Tanzania	250	15	15	15	15	15	15	15	44
PAHO	North America	United States of America	77	2	2	298	2	2	2	2	48
SEARO	South-East Asia	Myanmar	233	24	24	24	24	24	24	24	50
AFRO	Western Africa	Mali	214	1	1	1	1	1	1	182	50
PAHO	Temperate South America	Argentina	142	2	2	257	2	2	2	2	51
EURO	South West Europe	Greece	6	6	6	370	6	6	6	6	52
PAHO	Temperate South America	Chile	2	2	2	413	2	2	2	2	53
AFRO	Eastern Africa	Seychelles		54	54	54	54	54	54	54	54
PAHO	Central America and Caribbean	Jamaica	3	3	3	422	3	3	3	3	55
WPRO	Oceania Melanesia Polynesia	New Caledonia	247	24	24	66	24	24	24	24	57
PAHO	Central America and Caribbean	Costa Rica	1	1	1	462	1	1	1	1	59
PAHO	Tropical South America	Peru	24	3	3	442	3	3	3	3	61
PAHO	Central America and Caribbean	Honduras	1	1	1	479	1	1	1	1	61
SEARO	Southern Asia	India	245	1	1	84	84	74	2	17	64
PAHO	Central America and Caribbean	Grenada	M	66	M	M	M	M	67	M	67
PAHO	Central America and Caribbean	Aruba	M	65	M	M	M	66	M	69	67
PAHO	Central America and Caribbean	British Virgin Islands	M	67	M	M	M	M	M	M	67
EURO	Eastern Europe	Czechia	68	68	68	M	68	68	68	68	68
PAHO	Tropical South America	Colombia	2	2	2	533	2	2	2	2	68
EURO	Northern Europe	Denmark	3	3	3	527	3	3	3	3	69
EURO	South West Europe	Slovenia	2	2	2	548	2	2	2	2	70
EURO	Northern Europe	Finland	2	2	2	552	2	2	2	2	71
EURO	Northern Europe	Estonia	2	2	2	553	2	2	2	2	71
EURO	South West Europe	Malta	71	71	71	M	71	71	71	71	71

PAHO	Temperate South America	Uruguay	78	65	69	M	66	78	66	78	71
EURO	South West Europe	Switzerland	2	2	2	560	2	2	2	2	72
EURO	Northern Europe	Norway	2	2	2	562	2	2	2	2	72
EURO	Northern Europe	United Kingdom	2	2	2	564	2	2	2	2	72
EURO	South West Europe	Netherlands	2	2	2	566	2	2	2	2	73
EURO	South West Europe	Belgium	4	4	4	561	4	4	4	4	74
EURO	Northern Europe	Latvia	2	2	2	576	2	2	2	2	74
PAHO	Central America and Caribbean	Saint Vincent and the Grenadines	M	68	84	M	M	M	70	M	74
EURO	South West Europe	Croatia	75	75	75	M	75	75	75	75	75
EURO	Northern Europe	Lithuania	2	2	2	598	2	2	2	2	77
EMRO	Western Asia	Yemen	M	63	63	M	123	M	M	61	78
PAHO	Temperate South America	Paraguay	6	6	6	584	6	6	6	6	78
WPRO	South-East Asia	Cambodia	10	10	10	10	285	10	10	285	79
EMRO	Western Asia	Kuwait	M	84	84	M	73	84	84	71	80
PAHO	North America	Bermuda	M	66	114	M	M	M	65	M	82
AFRO	Eastern Africa	Ethiopia	213	81	81	81	19	81	81	19	82
AFRO	Middle Africa	Chad	M	82	82	82	82	82	82	82	82
AFRO	Middle Africa	South Sudan	M	82	82	82	82	82	82	82	82
WPRO	Oceania Melanesia Polynesia	Australia	338	63	64	68	1	68	68	1	84
PAHO	Central America and Caribbean	Turks and Caicos Islands	M	67	117	M	M	M	68	M	84
WPRO	Oceania Melanesia Polynesia	Papua New Guinea	84	84	84	84	84	84	84	84	84
EMRO	Western Asia	West Bank and Gaza Strip	M	67	67	M	136	M	M	67	84
PAHO	Central America and Caribbean	Panama	42	42	42	380	42	42	42	42	84
AFRO	Eastern Africa	Rwanda	87	87	87	87	87	87	87	87	87
AFRO	Western Africa	Nigeria	260	64	64	64	64	64	64	64	89
AFRO	Middle Africa	Central African Republic	233	70	70	70	70	70	70	70	90
PAHO	Central America and Caribbean	Trinidad and Tobago	M	66	82	M	127	65	65	145	92
PAHO	Central America and Caribbean	Saint Kitts and Nevis	M	65	111	M	M	123	75	M	94
PAHO	Tropical South America	Brazil	171	49	62	244	48	75	59	45	94
WPRO	Eastern Asia	South Korea	249	71	71	77	77	77	77	71	96
EMRO	Western Asia	Bahrain	263	73	73	73	73	73	73	70	96
SEARO	South-East Asia	Thailand	260	1	1	260	255	1	1	1	98
AFRO	Eastern Africa	Uganda	245	4	4	4	4	260	260	4	98
PAHO	Tropical South America	Venezuela	70	70	70	302	70	70	70	70	99
EMRO	Western Asia	Jordan	255	77	77	77	77	77	77	77	99
PAHO	Central America and Caribbean	Cayman Islands	M	68	74	M	M	M	M	175	106
PAHO	Central America and Caribbean	Bahamas	M	87	174	M	M	M	71	M	111
EURO	Western Asia	Cyprus	112	112	112	M	112	112	112	112	112
PAHO	Central America and Caribbean	Guatemala	185	65	64	407	59	97	63	30	121
PAHO	Central America and Caribbean	Barbados	M	65	72	M	291	166	69	90	126
PAHO	Central America and Caribbean	Dominican Republic	233	68	72	M	185	68	69	186	126
PAHO	North America	Canada	258	2	2	258	2	258	258	2	130
PAHO	Central America and Caribbean	Cuba	67	67	67	582	67	67	67	67	131
PAHO	Central America and Caribbean	Anguilla	M	123	90	M	M	M	90	226	132
EURO	Western Asia	Turkey	72	72	72	584	72	72	72	72	136
WPRO	Oceania Melanesia Polynesia	New Zealand	254	90	90	298	90	90	90	90	137
AFRO	Eastern Africa	Mauritius	220	42	42	42	42	334	334	42	137
WPRO	Oceania Melanesia Polynesia	Fiji	247	63	69	221	113	245	64	106	141
PAHO	Tropical South America	French Guiana	249	62	68	249	67	147	66	285	149
PAHO	Tropical South America	Ecuador	129	36	36	601	129	129	129	36	153
EMRO	Western Asia	Iraq	257	29	64	13	285	285	285	14	154
PAHO	Central America and Caribbean	Antigua and Barbuda	M	M	M	M	M	M	157	M	157
PAHO	Central America and Caribbean	Guadeloupe	249	67	67	249	120	171	67	285	159
SEARO	Southern Asia	Sri Lanka	285	63	75	262	76	262	262	9	162
PAHO	Central America and Caribbean	Dominica	M	66	117	M	M	324	162	163	166
PAHO	Central America and Caribbean	Nicaragua	337	67	67	M	36	337	337	3	169
PAHO	Central America and Caribbean	Martinique	249	68	67	249	285	124	68	285	174
AFRO	Middle Africa	Congo	411	411	411	411	411	411	411	411	411
AFRO	Middle Africa	Angola	455	455	455	455	455	455	455	455	455

EMRO	Western Asia	Syrian Arab Republic	467	467	467	467	467	467	467	467	467
EMRO	Northern Africa	Sudan	600	600	600	600	600	600	600	600	600
PAHO	Tropical South America	Guyana	M	M	M	M	M	M	M	M	M

Supplementary Table S23. Average and median *reporting delay* for 3 test outcomes (influenza A positives (FLUA), influenza B positives (FLUB), and total negatives (NEG)) in 6 regions and 17 WHO-defined influenza transmission zones. We extracted FluNet data from 173 Member States on 15 June 2021. We calculated *reporting delay* as the number of weeks from the date of data download to the most recent week with complete records. We report average *reporting delay* with 95% confidence intervals (top values) and median *reporting delay* with lower and upper quartiles (bottom values). Regions and zones are listed in alphabetical order, and we omit the Southern African transmission zone, as it consisted of only 1 country.

Region	FLUA	FLUB	NEG
AFRO	10.55 [0.00, 21.55] 4.00 [1.00, 8.00]	5.82 [1.93, 9.71] 4.00 [2.00, 8.00]	30.70 [5.58, 55.82] 5.00 [2.00, 80.00]
EMRO	11.16 [4.70, 17.61] 3.00 [2.00, 5.00]	11.16 [4.70, 17.61] 3.00 [2.00, 5.00]	43.75 [2.34, 85.16] 31.00 [19.00, 68.50]
EURO	24.33 [7.19, 41.47] 4.00 [1.00, 63.00]	24.40 [7.22, 41.58] 4.00 [1.00, 64.00]	32.31 [13.26, 51.35] 20.00 [3.00, 70.00]
PAHO	39.21 [29.63, 48.80] 53.50 [2.00, 67.00]	44.81 [30.96, 58.66] 43.50 [2.00, 68.00]	35.82 [26.42, 45.21] 37.50 [3.00, 65.00]
SEARO	48.73 [9.96, 87.51] 6.00 [2.00, 54.00]	48.73 [9.96, 87.51] 6.00 [2.00, 54.00]	39.00 [10.56, 67.44] 6.50 [2.50, 43.00]
WPRO	77.89 [3.83, 151.96] 7.00 [2.00, 73.00]	76.95 [2.76, 151.14] 7.00 [2.00, 70.00]	23.18 [9.33, 37.03] 7.00 [2.00, 42.00]
Zone			
Central America and Caribbean	2.60 [1.93, 3.27] 2.00 [2.00, 3.00]	2.60 [1.93, 3.27] 2.00 [2.00, 3.00]	Missing
Central Asia	8.89 [0.00, 22.17] 2.00 [1.00, 4.00]	3.11 [1.53, 4.69] 2.00 [2.00, 4.00]	33.13 [3.52, 62.73] 4.50 [2.00, 77.00]
Eastern Africa	5.40 [2.59, 8.21] 5.00 [3.00, 7.00]	5.40 [2.59, 8.21] 5.00 [3.00, 7.00]	Missing
Eastern Asia	6.00 [1.53, 10.47] 3.00 [1.00, 8.00]	6.00 [1.53, 10.47] 3.00 [1.00, 8.00]	23.89 [0.33, 47.45] 4.00 [1.00, 24.00]
Eastern Europe	8.82 [0.00, 20.44] 2.00 [2.00, 4.00]	8.82 [0.00, 20.44] 2.00 [2.00, 4.00]	105.00 [105.00, 105.00] 105.00 [105.00, 105.00]
Middle Africa	9.55 [0.00, 20.43] 3.00 [2.00, 10.00]	9.55 [0.00, 20.43] 3.00 [2.00, 10.00]	44.00 [0.00, 90.46] 5.00 [2.00, 67.00]
North America	11.68 [1.83, 21.54] 3.00 [2.00, 8.00]	11.68 [1.83, 21.54] 3.00 [2.00, 8.00]	23.33 [8.26, 38.40] 30.00 [8.00, 32.00]
Northern Africa	16.80 [0.00, 43.40] 3.00 [2.00, 6.00]	16.80 [0.00, 43.40] 3.00 [2.00, 6.00]	37.50 [0.14, 74.86] 38.00 [4.50, 70.50]
Northern Europe	18.75 [0.00, 49.02] 4.00 [2.00, 35.50]	19.00 [0.00, 49.76] 4.00 [2.00, 36.00]	18.75 [0.00, 49.02] 4.00 [2.00, 35.50]
Oceania Melanesia Polynesia	23.33 [0.00, 65.15] 2.00 [2.00, 66.00]	23.00 [0.00, 64.16] 2.00 [2.00, 65.00]	2.00 [2.00, 2.00] 2.00 [2.00, 2.00]
Southeast Asia	23.60 [5.88, 41.32] 11.00 [4.00, 42.00]	23.60 [5.88, 41.32] 11.00 [4.00, 42.00]	25.33 [0.00, 56.58] 11.00 [4.00, 19.00]
Southern Asia	30.50 [11.25, 49.75] 29.00 [2.50, 55.00]	30.63 [11.07, 50.18] 29.00 [2.50, 55.50]	30.25 [12.13, 48.37] 36.00 [2.50, 44.00]
Southwest Europe	46.59 [34.74, 58.45] 65.00 [2.00, 67.00]	55.26 [36.24, 74.28] 67.00 [2.00, 70.00]	41.68 [30.02, 53.34] 65.00 [3.00, 67.00]
Temperate South America	52.40 [18.53, 86.27] 63.00 [24.00, 84.00]	52.60 [18.67, 86.53] 64.00 [24.00, 84.00]	34.00 [6.21, 61.79] 24.00 [20.00, 40.00]
Tropical South America	58.44 [8.36, 108.53] 13.00 [3.00, 73.00]	57.44 [7.24, 107.65] 9.50 [2.00, 71.00]	26.64 [7.73, 45.54] 4.00 [2.00, 70.00]
Western Africa	124.80 [0.00, 357.65] 7.00 [6.00, 7.00]	124.80 [0.00, 357.65] 7.00 [6.00, 7.00]	9.75 [6.41, 13.09] 9.00 [7.00, 12.50]
Western Asia	159.29 [18.46, 300.11] 82.00 [10.00, 411.00]	159.29 [18.46, 300.11] 82.00 [10.00, 411.00]	87.50 [0.00, 249.20] 87.50 [5.00, 170.00]
Worldwide	**33.57 [21.89, 45.24]** **4.00 [2.00, 63.00]**	**34.55 [22.60, 46.51]** **4.00 [2.00, 62.50]**	**33.70 [25.88, 41.51]** **13.00 [3.00, 66.00]**

Supplementary Table S24. Average and median *reporting delay* for 6 influenza subtypes (A(H1N1)pdm09, A(H3), A(Unsubtyped), B(Yamagata), B(Victoria), and B(Undetermined) positives) in 6 regions and 17 WHO-defined influenza transmission zones. We extracted FluNet data from 173 Member States on 15 June 2021. We calculated *reporting delay* as the number of weeks from the date of data download to the most recent week with complete records. We report average *reporting delay* with 95% confidence intervals (top values) and median *reporting delay* with lower and upper quartiles (bottom values). Regions and zones are listed in alphabetical order, and we omit the Southern African transmission zone, as it consisted of only 1 country.

Region	A(H1N1)pdm09	A(H3)	A(Unsubtyped)	B(Yamagata)	B(Victoria)	B(Undetermined)
AFRO	50.80 [12.02, 89.58] 6.00 [2.00, 64.00]	50.83 [12.06, 89.61] 6.50 [2.00, 64.00]	48.73 [9.96, 87.51] 6.00 [2.00, 54.00]	69.07 [24.38, 113.75] 8.50 [2.00, 81.00]	69.07 [24.38, 113.75] 8.50 [2.00, 81.00]	54.77 [15.18, 94.35] 8.50 [3.00, 64.00]
EMRO	79.32 [5.39, 153.24] 7.00 [2.00, 73.00]	84.94 [7.38, 162.51] 7.00 [2.00, 73.00]	104.67 [24.43, 184.90] 12.50 [2.00, 123.00]	101.25 [10.57, 191.93] 6.50 [2.00, 80.50]	101.25 [10.57, 191.93] 6.50 [2.00, 80.50]	80.42 [6.67, 154.17] 7.00 [2.00, 70.00]
EURO	11.16 [4.70, 17.61] 3.00 [2.00, 5.00]	11.16 [4.70, 17.61] 3.00 [2.00, 5.00]	11.16 [4.70, 17.61] 3.00 [2.00, 5.00]	11.16 [4.70, 17.61] 3.00 [2.00, 5.00]	11.16 [4.70, 17.61] 3.00 [2.00, 5.00]	11.16 [4.70, 17.61] 3.00 [2.00, 5.00]
PAHO	40.93 [30.73, 51.13] 63.50 [2.00, 67.00]	47.18 [32.99, 61.37] 62.00 [2.00, 72.00]	53.10 [25.26, 80.93] 6.00 [2.00, 67.00]	72.32 [41.42, 103.22] 53.50 [2.00, 123.00]	59.30 [37.40, 81.20] 65.00 [2.00, 69.50]	66.69 [36.26, 97.11] 22.00 [2.00, 90.00]
SEARO	10.55 [0.00, 21.55] 4.00 [1.00, 8.00]	11.64 [0.00, 24.66] 4.00 [1.00, 8.00]	51.89 [0.00, 105.76] 10.00 [4.00, 76.00]	45.80 [0.00, 96.30] 6.00 [2.00, 74.00]	38.60 [0.00, 89.36] 4.00 [2.00, 24.00]	9.18 [4.11, 14.25] 6.00 [2.00, 17.00]
WPRO	28.47 [10.96, 45.97] 8.00 [2.00, 63.00]	28.93 [11.16, 46.71] 8.00 [2.00, 69.00]	47.60 [8.83, 86.37] 8.00 [1.00, 84.00]	47.00 [13.66, 80.34] 10.00 [2.00, 84.00]	34.93 [15.96, 53.90] 10.00 [2.00, 77.00]	45.53 [6.75, 84.32] 4.00 [1.00, 84.00]
Zone						
Central America and Caribbean	49.22 [36.41, 62.03] 66.00 [2.00, 67.00]	57.46 [38.38, 76.54] 67.00 [2.00, 83.00]	72.00 [25.43, 118.57] 36.00 [1.00, 120.00]	83.10 [38.52, 127.68] 65.50 [1.50, 123.50]	64.76 [36.41, 93.11] 67.00 [2.00, 70.00]	84.67 [42.34, 126.99] 42 [2.00, 163.00]
Central Asia	5.40 [2.59, 8.21] 5.00 [3.00, 7.00]	5.40 [2.59, 8.21] 5.00 [3.00, 7.00]	5.40 [2.59, 8.21] 5.00 [3.00, 7.00]	5.40 [2.59, 8.21] 5.00 [3.00, 7.00]	5.40 [2.59, 8.21] 5.00 [3.00, 7.00]	5.40 [2.59, 8.21] 5.00 [3.00, 7.00]
Eastern Africa	29.80 [8.88, 50.72] 11.00 [4.00, 54.00]	29.80 [8.88, 50.72] 11.00 [4.00, 54.00]	23.60 [5.88, 41.32] 11.00 [4.00, 42.00]	84.60 [11.58, 157.62] 34.50 [5.00, 87.00]	84.60 [11.58, 157.62] 34.50 [5.00, 87.00]	23.60 [5.88, 41.32] 11.00 [4.00, 42.00]
Eastern Asia	16.80 [0.00, 43.40] 3.00 [2.00, 6.00]	16.80 [0.00, 43.40] 3.00 [2.00, 6.00]	25.50 [0.00, 60.11] 11.50 [2.50, 48.50]	21.00 [0.00, 57.59] 2.50 [2, 40.00]	21.00 [0.00, 57.59] 2.50 [2.00, 40.00]	16.80 [0.00, 43.40] 3.00 [2.00, 6.00]
Eastern Europe	8.82 [0.00, 20.44] 2.00 [2.00, 4.00]	8.82 [0.00, 20.44] 2.00 [2.00, 4.00]	8.82 [0.00, 20.44] 2.00 [2.00, 4.00]	8.82 [0.00, 20.44] 2.00 [2.00, 4.00]	8.82 [0.00, 20.44] 2.00 [2.00, 4.00]	8.82 [0.00, 20.44] 2.00 [2.00, 4.00]
Middle Africa	159.29 [18.46, 300.11] 82.00 [10.00, 411.00]	159.43 [18.71, 300.15] 82.00 [10.00, 411.00]	159.29 [18.46, 300.11] 82.00 [10.00, 411.00]	159.29 [18.46, 300.11] 82.00 [10.00, 411.00]	159.29 [18.46, 300.11] 82.00 [10.00, 411.00]	159.29 [18.46, 300.11] 82.00 [10.00, 411.00]
North America	23.33 [0.00, 65.15] 2.00 [2.00, 66.00]	39.33 [0.00, 112.51] 2.00 [2.00, 114.00]	2.00 [2.00, 2.00] 2.00 [2.00, 2.00]	130.00 [0.00, 380.88] 130.00 [2.00, 258.00]	108.33 [0.00, 259.27] 65.00 [2.00, 258.00]	2.00 [2.00, 2.00] 2.00 [2.00, 2.00]
Northern Africa	124.80 [0.00, 357.65] 7.00 [6.00, 7.00]	124.80 [0.00, 357.65] 7.00 [6.00, 7.00]	124.80 [0.00, 357.65] 7.00 [6.00, 7.00]	124.80 [0.00, 357.65] 7.00 [6.00, 7.00]	124.80 [0.00, 357.65] 7.00 [6.00, 7.00]	124.80 [0.00, 357.65] 7.00 [6.00, 7.00]
Northern Europe	2.60 [1.93, 3.27] 2.00 [2.00, 3.00]	2.60 [1.93, 3.27] 2.00 [2.00, 3.00]	2.60 [1.93, 3.27] 2.00 [2.00, 3.00]	2.60 [1.93, 3.27] 2.00 [2.00, 3.00]	2.60 [1.93, 3.27] 2.00 [2.00, 3.00]	2.60 [1.93, 3.27] 2.00 [2.00, 3.00]
Oceania Melanesia Polynesia	64.80 [42.13, 87.47] 63.00 [63.00, 84.00]	66.20 [43.53, 88.87] 69.00 [64.00, 84.00]	62.40 [20.75, 104.05] 84.00 [24.00, 90.00]	102.20 [28.66, 175.74] 84.00 [68.00, 90.00]	66.00 [43.35, 88.65] 68.00 [64.00, 84.00]	61.00 [20.92, 101.08] 84.00 [24.00, 90.00]
Southeast Asia	6.00 [1.53, 10.47]	6.00 [1.53, 10.47]	65.22 [0.00, 141.37]	14.50 [0.00, 30.66]	14.50 [0.00, 30.66]	35.70 [0.00, 90.27]

	3.00 [1.00, 8.00]	3.00 [1.00, 8.00]	8.00 [1.00, 24.00]	6.00 [1.00, 10.00]	6.00 [1.00, 10.00]	6.00 [1.00, 24.00]
Southern Asia	8.89 [0.00, 22.17] 2.00 [1.00, 4.00]	10.22 [0.00, 26.11] 2.00 [1.00, 4.00]	20.56 [0.00, 42.68] 4.00 [2.00, 10.00]	47.56 [0.00, 104.01] 4.00 [2.00, 74.00]	39.56 [0.00, 96.39] 2.00 [2.00, 4.00]	4.78 [1.40, 8.15] 2.00 [2.00, 4.00]
Southwest Europe	11.68 [1.83, 21.54] 3.00 [2.00, 8.00]	11.68 [1.83, 21.54] 3.00 [2.00, 8.00]	11.68 [1.83, 21.54] 3.00 [2.00, 8.00]	11.68 [1.83, 21.54] 3.00 [2.00, 8.00]	11.68 [1.83, 21.54] 3.00 [2.00, 8.00]	11.68 [1.83, 21.54] 3.00 [2.00, 8.00]
Temperate South America	18.75 [0.00, 49.02] 4.00 [2.00, 35.50]	19.75 [0.00, 51.98] 4.00 [2.00, 37.50]	19.00 [0.00, 49.76] 4.00 [2.00, 36.00]	22.00 [0.00, 58.63] 4.00 [2.00, 42.00]	19.00 [0.00, 49.76] 4.00 [2.00, 36.00]	22.00 [0.00, 58.63] 4.00 [2.00, 42.00]
Tropical South America	30.63 [11.31, 49.94] 29.00 [2.50, 55.50]	33.00 [11.97, 54.03] 29.00 [2.50, 65.00]	42.75 [11.53, 73.97] 35.00 [2.50, 68.50]	56.13 [15.49, 96.76] 46.00 [2.50, 102.00]	44.00 [12.58, 75.42] 40.50 [2.50, 68.00]	58.00 [0.00, 123.76] 29.00 [2.50, 57.50]
Western Africa	9.55 [0.00, 20.43] 3.00 [2.00, 10.00]	9.55 [0.00, 20.43] 3.00 [2.00, 10.00]	9.55 [0.00, 20.43] 3.00 [2.00, 10.00]	9.55 [0.00, 20.43] 3.00 [2.00, 10.00]	9.55 [0.00, 20.43] 3.00 [2.00, 10.00]	26.00 [0.00, 58.41] 4.00 [2.00, 12.00]
Western Asia	59.94 [9.96, 109.93] 21.00 [3.00, 73.00]	64.76 [12.23, 117.30] 63.00 [3.00, 73.00]	85.65 [27.07, 144.22] 72.00 [3.00, 112.00]	79.47 [13.11, 145.82] 5.00 [2.00, 84.00]	79.47 [13.11, 145.82] 5.00 [2.00, 84.00]	61.11 [11.31, 110.91] 37.50 [3.00, 71.00]
Worldwide	**34.89 [23.17, 46.62]** **4.50 [2.00, 64.50]**	**36.74 [24.51, 48.97]** **4.00 [2.00, 65.50]**	**43.78 [29.05, 58.51]** **4.00 [2.00, 59.00]**	**50.53 [34.89, 66.17]** **4.00 [2.00, 70.00]**	**46.56 [32.18, 60.94]** **5.00 [2.00, 68.00]**	**42.60 [28.40, 56.79]** **4.00 [2.00, 45.00]**

Supplementary Table S25. Average and median *outcome interoperability* for 14 influenza test outcomes worldwide and in 2 WHO regions (AFRO - African Region; EMRO – Eastern Mediterranean Region). We extracted FluNet data from 173 Member States on 15 June 2021. We calculated *outcome interoperability* as the number of time points that 2 testing outcomes (defined below as *Outcome 1* and *Outcome 2*) in the same Member State have jointly non-missing records per total time points within a study period and multiplied by 100. Maximal time points included 1381 weeks for all testing outcomes except A(H1N1)pdm09 positives, for which the maximal time points was 651 weeks. We report average and median *outcome interoperability* with 95% confidence intervals (left column) and lower and upper quartiles (right column) for each geographic location.

Outcome 1	Outcome 2	Mean [LCI, UCI] World	Med. [LQR, UQR] World	Mean [LCI, UCI] AFRO	Med. [LQR, UQR] AFRO	Mean [LCI, UCI] EMRO	Med. [LQR, UQR] EMRO
SPE	TES	17.21 [14.74, 20.09]	8.73 [0.00, 36.42]	30.89 [21.47, 44.44]	34.29 [25.92, 42.51]	26.07 [16.49, 41.22]	32.30 [8.83, 41.42]
SPE	A(H1)	11.80 [10.09, 13.80]	4.92 [0.00, 24.19]	19.74 [13.68, 28.49]	22.41 [12.82, 26.29]	14.78 [9.29, 23.52]	18.32 [0.07, 24.76]
SPE	A(H1N1)	35.01 [30.06, 40.77]	17.28 [0.00, 70.05]	64.15 [44.73, 92.00]	69.66 [46.54, 90.17]	51.46 [32.68, 81.03]	62.21 [11.21, 82.8]
SPE	A(H3)	16.38 [14.03, 19.13]	7.02 [0.00, 32.80]	30.35 [21.10, 43.66]	32.84 [22.38, 42.43]	23.21 [14.66, 36.74]	28.89 [3.77, 39.03]
SPE	A(H5)	15.16 [12.98, 17.71]	7.02 [0.00, 29.54]	30.00 [20.85, 43.16]	31.68 [21.87, 41.71]	21.86 [13.81, 34.63]	26.72 [0.00, 39.03]
SPE	A(UNS)	15.69 [13.43, 18.32]	7.02 [0.00, 30.77]	30.10 [20.92, 43.31]	31.93 [21.65, 42.51]	22.68 [14.32, 35.90]	26.50 [1.16, 39.03]
SPE	FLUA	16.77 [14.37, 19.58]	8.62 [0.00, 33.82]	30.47 [21.18, 43.83]	32.84 [22.45, 42.51]	24.65 [15.58, 39.00]	30.20 [6.01, 39.03]
SPE	B(YAM)	14.76 [12.64, 17.24]	5.90 [0.00, 28.24]	26.15 [18.16, 37.66]	27.34 [12.82, 38.52]	21.49 [13.56, 34.04]	24.62 [1.16, 38.60]
SPE	B(VIC)	14.78 [12.66, 17.27]	5.90 [0.00, 28.82]	26.27 [18.24, 37.82]	27.34 [12.89, 38.52]	21.48 [13.56, 34.02]	24.33 [1.16, 38.60]
SPE	B(UND)	15.96 [13.67, 18.64]	8.73 [0.00, 30.63]	28.48 [19.79, 40.99]	29.36 [16.65, 41.85]	23.43 [14.80, 37.08]	26.65 [2.61, 39.03]
SPE	FLUB	16.31 [13.97, 19.04]	8.73 [0.00, 32.22]	29.42 [20.45, 42.34]	30.23 [22.01, 42.51]	23.72 [14.99, 37.54]	27.73 [5.00, 39.03]
SPE	POS	16.87 [14.45, 19.70]	8.73 [0.00, 33.82]	30.53 [21.22, 43.92]	32.84 [22.59, 42.51]	24.87 [15.72, 39.34]	30.77 [6.37, 39.03]
SPE	NEG	5.57 [4.73, 6.56]	0.00 [0.00, 11.88]	6.35 [4.32, 9.33]	1.48 [0.00, 13.03]	11.73 [7.34, 18.74]	12.45 [8.54, 16.51]
TES	A(H1)	30.14 [25.87, 35.12]	29.54 [13.11, 45.04]	23.45 [16.27, 33.80]	22.48 [12.82, 30.77]	16.06 [10.10, 25.53]	20.64 [0.07, 27.66]
TES	A(H1N1)	63.04 [54.17, 73.35]	72.27 [37.94, 90.78]	64.53 [45.00, 92.55]	69.66 [46.54, 90.17]	51.44 [32.67, 81.00]	62.37 [11.21, 82.64]
TES	A(H3)	35.44 [30.43, 41.28]	38.16 [18.10, 48.59]	34.10 [23.72, 49.03]	32.84 [22.38, 46.05]	24.41 [15.43, 38.62]	29.91 [3.91, 38.96]
TES	A(H5)	15.65 [13.40, 18.27]	7.68 [0.00, 30.20]	30.18 [20.98, 43.42]	32.84 [21.87, 41.71]	21.90 [13.83, 34.68]	26.65 [0.00, 38.96]
TES	A(UNS)	34.74 [29.83, 40.47]	37.58 [16.65, 48.01]	33.74 [23.47, 48.51]	32.80 [21.65, 45.98]	23.50 [14.85, 37.20]	26.43 [1.16, 38.96]
TES	FLUA	37.16 [31.91, 43.27]	38.96 [18.10, 51.27]	34.69 [24.13, 49.86]	32.84 [22.45, 46.05]	26.12 [16.52, 41.30]	32.95 [6.15, 39.54]
TES	B(YAM)	27.46 [23.56, 32.00]	29.11 [12.82, 41.93]	27.15 [18.86, 39.08]	27.52 [12.82, 41.93]	21.82 [13.78, 34.56]	25.20 [1.16, 38.52]
TES	B(VIC)	27.48 [23.58, 32.03]	29.25 [12.96, 41.85]	27.22 [18.91, 39.18]	27.52 [12.89, 42.00]	21.85 [13.79, 34.60]	25.49 [1.16, 38.52]
TES	B(UND)	32.02 [27.49, 37.30]	34.69 [15.86, 46.05]	30.11 [20.93, 43.31]	29.36 [16.65, 43.45]	23.87 [15.09, 37.78]	28.60 [2.61, 38.96]
TES	FLUB	32.68 [28.06, 38.07]	35.41 [17.89, 46.85]	31.11 [21.63, 44.75]	30.23 [22.01, 43.52]	24.30 [15.36, 38.45]	29.98 [5.00, 38.96]
TES	POS	37.48 [32.18, 43.65]	38.96 [18.10, 52.21]	34.83 [24.23, 50.06]	32.84 [22.59, 46.05]	26.41 [16.70, 41.75]	33.74 [6.52, 40.70]
TES	NEG	11.39 [9.74, 13.32]	2.93 [0.00, 16.00]	6.53 [4.44, 9.58]	1.48 [0.00, 13.54]	11.74 [7.35, 18.75]	12.96 [8.54, 16.36]
A(H1)	A(H1N1)	52.29 [44.92, 60.85]	55.61 [28.42, 81.87]	41.92 [29.18, 60.20]	47.62 [27.19, 55.76]	31.07 [19.68, 49.06]	38.86 [0.15, 51.61]
A(H1)	A(H3)	30.94 [26.55, 36.04]	30.74 [13.40, 45.91]	23.13 [16.05, 33.33]	22.45 [12.82, 30.92]	16.25 [10.22, 25.82]	20.71 [0.00, 26.79]
A(H1)	A(H5)	12.24 [10.47, 14.31]	5.79 [0.00, 24.26]	19.78 [13.71, 28.54]	22.41 [12.82, 26.29]	14.49 [9.10, 23.07]	18.32 [0.00, 24.33]
A(H1)	A(UNS)	30.41 [26.10, 35.43]	30.20 [13.32, 45.33]	23.09 [16.02, 33.28]	22.48 [12.82, 31.35]	15.71 [9.88, 24.98]	18.32 [0.07, 26.50]
A(H1)	FLUA	31.40 [26.95, 36.58]	31.03 [13.40, 46.34]	23.56 [16.35, 33.94]	22.48 [12.82, 31.35]	16.61 [10.46, 26.39]	20.71 [0.07, 28.53]
A(H1)	B(YAM)	23.96 [20.55, 27.93]	25.42 [12.24, 36.21]	18.50 [12.81, 26.71]	18.79 [10.93, 27.01]	15.12 [9.51, 24.06]	18.18 [0.00, 26.50]
A(H1)	B(VIC)	23.95 [20.55, 27.93]	25.42 [12.24, 36.21]	18.46 [12.79, 26.66]	18.79 [10.93, 27.01]	15.13 [9.51, 24.08]	18.18 [0.00, 26.50]
A(H1)	B(UND)	27.14 [23.29, 31.63]	27.95 [13.32, 40.84]	19.88 [13.78, 28.69]	19.80 [10.93, 27.52]	15.37 [9.66, 24.44]	19.48 [0.07, 27.23]
A(H1)	FLUB	27.43 [23.54, 31.97]	29.65 [13.32, 41.13]	20.20 [14.00, 29.14]	20.60 [10.93, 29.76]	15.5 [9.75, 24.65]	19.62 [0.07, 27.23]
A(H1)	POS	31.40 [26.95, 36.58]	31.03 [13.40, 46.34]	23.56 [16.35, 33.94]	22.48 [12.82, 31.35]	16.61 [10.46, 26.39]	20.71 [0.07, 28.53]
A(H1)	NEG	6.64 [5.65, 7.80]	0.00 [0.00, 2.10]	1.10 [0.67, 1.80]	0.00 [0.00, 0.14]	1.48 [0.83, 2.65]	0.00 [0.00, 0.22]
A(H1N1)	A(H3)	62.91 [54.06, 73.20]	71.66 [40.09, 90.63]	64.43 [44.92, 92.40]	70.05 [46.39, 90.02]	48.95 [31.08, 77.10]	59.45 [6.45, 82.80]
A(H1N1)	A(H5)	33.99 [29.18, 39.59]	19.97 [0.00, 65.13]	64.11 [44.70, 91.95]	70.05 [46.39, 88.33]	46.48 [29.50, 73.22]	56.22 [0.00, 82.80]
A(H1N1)	A(UNS)	60.71 [52.17, 70.64]	69.74 [35.79, 89.55]	64.24 [44.79, 92.14]	69.97 [45.93, 90.17]	47.87 [30.39, 75.40]	56.22 [2.15, 82.80]
A(H1N1)	FLUA	63.96 [54.97, 74.42]	72.58 [40.09, 91.55]	64.65 [45.08, 92.72]	70.05 [46.54, 90.17]	51.61 [32.78, 81.27]	62.37 [11.21, 82.80]
A(H1N1)	B(YAM)	57.00 [48.98, 66.33]	61.60 [31.03, 85.87]	55.82 [38.90, 80.09]	57.99 [27.04, 81.72]	45.57 [28.92, 71.79]	51.92 [2.46, 81.87]
A(H1N1)	B(VIC)	56.97 [48.95, 66.30]	61.60 [31.03, 85.87]	55.93 [38.98, 80.25]	57.99 [27.19, 81.72]	45.53 [28.90, 71.72]	51.61 [2.46, 81.87]
A(H1N1)	B(UND)	61.42 [52.78, 71.47]	71.04 [37.94, 90.32]	60.79 [42.38, 87.20]	62.37 [36.10, 89.40]	49.00 [31.11, 77.17]	55.76 [4.76, 82.80]

A(H1N1)	FLUB	62.49 [53.71, 72.72]	71.27 [39.78, 90.63]	62.56 [43.62, 89.73]	64.36 [46.39, 90.17]	49.56 [31.47, 78.05]	56.53 [10.60, 82.80]
A(H1N1)	POS	63.96 [54.97, 74.42]	72.58 [40.09, 91.55]	64.65 [45.08, 92.72]	70.05 [46.54, 90.17]	51.61 [32.78, 81.27]	62.37 [11.21, 82.80]
A(H1N1)	NEG	19.97 [17.12, 23.30]	5.38 [0.00, 33.03]	13.18 [9.09, 19.10]	3.15 [0.00, 27.50]	21.51 [13.58, 34.08]	22.89 [10.60, 33.03]
A(H3)	A(H5)	16.01 [13.71, 18.69]	9.41 [0.00, 30.70]	30.23 [21.02, 43.50]	33.24 [21.87, 41.71]	21.91 [13.83, 34.70]	26.50 [0.00, 39.03]
A(H3)	A(UNS)	34.71 [29.80, 40.42]	36.71 [16.87, 49.09]	33.68 [23.42, 48.42]	33.20 [21.65, 45.98]	23.12 [14.61, 36.60]	26.50 [0.29, 39.03]
A(H3)	FLUA	36.87 [31.66, 42.94]	38.52 [18.90, 51.85]	34.24 [23.82, 49.23]	33.24 [22.38, 46.05]	25.08 [15.86, 39.68]	30.92 [3.91, 39.03]
A(H3)	B(YAM)	27.82 [23.87, 32.42]	29.25 [14.63, 41.93]	27.09 [18.82, 38.99]	27.62 [12.82, 41.13]	22.07 [13.93, 34.95]	25.20 [1.16, 38.60]
A(H3)	B(VIC)	27.80 [23.85, 32.39]	29.25 [14.63, 41.93]	27.14 [18.85, 39.07]	27.62 [12.89, 42.14]	22.05 [13.93, 34.93]	24.84 [1.16, 38.60]
A(H3)	B(UND)	31.97 [27.45, 37.25]	34.21 [17.89, 46.27]	30.00 [20.85, 43.15]	29.36 [17.45, 43.23]	23.05 [14.56, 36.49]	27.81 [1.16, 39.03]
A(H3)	FLUB	32.49 [27.89, 37.85]	34.76 [18.90, 46.85]	30.85 [21.45, 44.38]	30.38 [21.80, 43.88]	23.45 [14.81, 37.11]	27.88 [1.30, 39.03]
A(H3)	POS	36.87 [31.66, 42.94]	38.52 [18.90, 51.85]	34.24 [23.82, 49.23]	33.24 [22.38, 46.05]	25.08 [15.86, 39.68]	30.92 [3.91, 39.03]
A(H3)	NEG	10.33 [8.83, 12.09]	1.52 [0.00, 15.57]	6.29 [4.28, 9.24]	1.48 [0.00, 12.96]	9.34 [5.82, 15.00]	8.83 [2.68, 15.57]
A(H5)	A(UNS)	15.66 [13.41, 18.28]	8.40 [0.00, 30.70]	30.24 [21.02, 43.51]	33.20 [21.65, 41.71]	21.86 [13.80, 34.62]	26.50 [0.00, 39.03]
A(H5)	FLUA	16.07 [13.76, 18.76]	9.41 [0.00, 30.70]	30.26 [21.03, 43.53]	33.24 [21.87, 41.71]	21.92 [13.84, 34.72]	26.72 [0.00, 39.03]
A(H5)	B(YAM)	15.02 [12.86, 17.54]	8.40 [0.00, 28.24]	26.21 [18.20, 37.74]	27.34 [12.82, 38.52]	21.06 [13.29, 33.37]	24.33 [0.00, 38.60]
A(H5)	B(VIC)	15.03 [12.87, 17.56]	8.40 [0.00, 28.24]	26.22 [18.21, 37.75]	27.34 [12.89, 38.52]	21.05 [13.29, 33.35]	24.33 [0.00, 38.60]
A(H5)	B(UND)	15.53 [13.30, 18.13]	9.41 [0.00, 28.82]	28.62 [19.88, 41.18]	29.33 [17.45, 41.64]	21.59 [13.63, 34.20]	25.20 [0.00, 39.03]
A(H5)	FLUB	15.83 [13.56, 18.48]	9.41 [0.00, 30.05]	29.33 [20.38, 42.20]	30.23 [21.80, 41.64]	21.61 [13.64, 34.23]	25.56 [0.00, 39.03]
A(H5)	POS	16.07 [13.76, 18.76]	9.41 [0.00, 30.70]	30.26 [21.03, 43.53]	33.24 [21.87, 41.71]	21.92 [13.84, 34.72]	26.72 [0.00, 39.03]
A(H5)	NEG	4.70 [3.99, 5.55]	0.00 [0.00, 8.25]	5.98 [4.06, 8.80]	1.48 [0.00, 12.96]	8.24 [5.12, 13.27]	6.81 [0.00, 15.57]
A(UNS)	FLUA	36.05 [30.95, 41.98]	37.91 [16.87, 50.83]	33.85 [23.55, 48.67]	33.20 [21.65, 45.98]	23.99 [15.16, 37.96]	26.50 [1.16, 39.03]
A(UNS)	B(YAM)	27.20 [23.34, 31.70]	29.04 [12.82, 41.42]	27.03 [18.78, 38.92]	27.59 [12.82, 41.71]	21.54 [13.60, 34.11]	24.48 [0.00, 38.60]
A(UNS)	B(VIC)	27.22 [23.35, 31.72]	28.93 [12.89, 41.42]	27.01 [18.76, 38.89]	27.59 [12.89, 41.42]	21.53 [13.59, 34.10]	24.33 [0.00, 38.60]
A(UNS)	B(UND)	31.56 [27.09, 36.77]	34.21 [15.86, 46.05]	29.95 [20.82, 43.10]	29.36 [17.38, 43.01]	22.86 [14.44, 36.18]	26.07 [1.16, 39.03]
A(UNS)	FLUB	31.79 [27.29, 37.03]	34.21 [16.87, 46.05]	30.70 [21.34, 44.17]	30.34 [21.58, 43.23]	22.90 [14.46, 36.25]	26.50 [1.16, 39.03]
A(UNS)	POS	36.05 [30.95, 41.98]	37.91 [16.87, 50.83]	33.85 [23.55, 48.67]	33.20 [21.65, 45.98]	23.99 [15.16, 37.96]	26.50 [1.16, 39.03]
A(UNS)	NEG	9.70 [8.28, 11.36]	0.11 [0.00, 15.06]	6.05 [4.11, 8.91]	1.48 [0.00, 12.89]	8.93 [5.56, 14.35]	10.79 [0.00, 15.57]
FLUA	B(YAM)	27.88 [23.93, 32.49]	29.25 [14.63, 41.93]	27.17 [18.87, 39.11]	27.62 [12.82, 41.93]	22.07 [13.93, 34.95]	25.20 [1.16, 38.60]
FLUA	B(VIC)	27.88 [23.93, 32.49]	29.29 [14.63, 41.93]	27.21 [18.90, 39.17]	27.62 [12.89, 42.36]	22.06 [13.93, 34.94]	24.91 [1.16, 38.60]
FLUA	B(UND)	32.81 [28.17, 38.22]	34.97 [17.89, 46.85]	30.10 [20.92, 43.30]	29.40 [17.45, 43.30]	24.06 [15.21, 38.07]	28.02 [2.24, 39.03]
FLUA	FLUB	33.42 [28.69, 38.92]	35.30 [18.90, 47.79]	31.05 [21.59, 44.67]	30.56 [21.87, 43.88]	24.46 [15.46, 38.70]	29.47 [5.00, 39.03]
FLUA	POS	38.90 [33.41, 45.30]	39.79 [18.90, 54.96]	34.86 [24.25, 50.12]	33.27 [22.45, 46.05]	26.88 [17.00, 42.49]	33.82 [6.15, 39.97]
FLUA	NEG	11.10 [9.49, 12.99]	2.75 [0.00, 15.57]	6.37 [4.34, 9.37]	1.48 [0.00, 13.54]	10.47 [6.54, 16.76]	11.15 [6.01, 15.57]
B(YAM)	B(VIC)	27.72 [23.79, 32.31]	29.25 [14.63, 41.93]	27.08 [18.81, 38.98]	27.62 [12.82, 41.20]	22.01 [13.90, 34.86]	24.55 [1.16, 38.60]
B(YAM)	B(UND)	27.38 [23.50, 31.91]	29.25 [13.32, 41.20]	26.33 [18.28, 37.91]	26.72 [12.82, 39.03]	21.69 [13.70, 34.36]	24.33 [0.58, 38.60]
B(YAM)	FLUB	27.92 [23.96, 32.53]	29.33 [14.63, 41.93]	27.18 [18.88, 39.13]	27.62 [12.82, 41.93]	22.07 [13.93, 34.95]	25.20 [1.16, 38.60]
B(YAM)	POS	27.92 [23.96, 32.53]	29.33 [14.63, 41.93]	27.18 [18.88, 39.13]	27.62 [12.82, 41.93]	22.07 [13.93, 34.95]	25.20 [1.16, 38.60]
B(YAM)	NEG	7.59 [6.47, 8.91]	0.33 [0.00, 13.54]	5.50 [3.73, 8.12]	1.09 [0.00, 8.62]	7.81 [4.84, 12.58]	6.66 [0.00, 15.06]
B(VIC)	B(UND)	27.38 [23.50, 31.91]	29.25 [13.32, 41.71]	26.34 [18.29, 37.92]	26.72 [12.89, 39.25]	21.71 [13.71, 34.38]	24.33 [0.58, 38.60]
B(VIC)	FLUB	27.94 [23.98, 32.56]	29.58 [14.63, 42.22]	27.25 [18.93, 39.23]	27.62 [12.89, 42.36]	22.09 [13.95, 34.99]	25.49 [1.16, 38.60]
B(VIC)	POS	27.94 [23.98, 32.56]	29.58 [14.63, 42.22]	27.25 [18.93, 39.23]	27.62 [12.89, 42.36]	22.09 [13.95, 34.99]	25.49 [1.16, 38.60]
B(VIC)	NEG	7.62 [6.49, 8.94]	0.51 [0.00, 13.54]	5.62 [3.81, 8.28]	1.09 [0.00, 11.88]	7.81 [4.84, 12.58]	6.66 [0.00, 15.06]
B(UND)	FLUB	33.14 [28.45, 38.60]	35.23 [17.89, 47.36]	30.21 [21.00, 43.46]	29.4 [17.45, 43.59]	24.36 [15.40, 38.54]	29.18 [2.61, 39.03]
B(UND)	POS	33.14 [28.45, 38.60]	35.23 [17.89, 47.36]	30.21 [21.00, 43.46]	29.4 [17.45, 43.59]	24.36 [15.40, 38.54]	29.18 [2.61, 39.03]
B(UND)	NEG	9.63 [8.22, 11.28]	0.91 [0.00, 15.57]	5.96 [4.05, 8.78]	1.09 [0.00, 12.82]	9.57 [5.97, 15.36]	9.63 [2.61, 15.57]
FLUB	POS	33.80 [29.02, 39.37]	35.88 [18.90, 47.86]	31.21 [21.70, 44.89]	30.59 [22.01, 43.88]	24.79 [15.67, 39.22]	30.05 [5.00, 39.03]
FLUB	NEG	9.95 [8.50, 11.65]	1.77 [0.00, 15.57]	6.26 [4.26, 9.20]	1.48 [0.00, 12.89]	9.86 [6.15, 15.80]	9.63 [3.55, 15.57]
POS	NEG	11.29 [9.65, 13.20]	2.90 [0.00, 15.79]	6.43 [4.38, 9.44]	1.48 [0.00, 13.54]	10.67 [6.67, 17.07]	11.15 [6.37, 15.57]

Supplementary Table S26. Average and median *outcome interoperability* for 14 influenza test outcomes worldwide and in 2 WHO regions (EURO - European Region; PAHO – Pan-American Region). We extracted FluNet data from 173 Member States on 15 June 2021. We calculated *outcome interoperability* as the number of time points that 2 testing outcomes (defined below as *Outcome 1* and *Outcome 2*) in the same Member State have jointly non-missing records per total time points within a study period and multiplied by 100. Maximal time points included 1381 weeks for all testing outcomes except A(H1N1)pdm09 positives, for which the maximal time points was 651 weeks. We report average and median *outcome interoperability* with 95% confidence intervals (left column) and lower and upper quartiles (right column) for each geographic location.

Outcome 1	Outcome 2	Mean [LCI, UCI] WORLD	Med. [LQR, UQR] WORLD	Mean [LCI, UCI] EURO	Med. [LQR, UQR] EURO	Mean [LCI, UCI] PAHO	Med. [LQR, UQR] PAHO
SPE	TES	17.21 [14.74, 20.09]	8.73 [0.00, 36.42]	5.37 [3.98, 7.24]	0.00 [0.00, 4.20]	8.46 [6.19, 11.57]	0.00 [0.00, 11.01]
SPE	A(H1)	11.80 [10.09, 13.80]	4.92 [0.00, 24.19]	5.04 [3.73, 6.81]	0.00 [0.00, 4.20]	6.75 [4.92, 9.27]	0.00 [0.00, 11.01]
SPE	A(H1N1)	35.01 [30.06, 40.77]	17.28 [0.00, 70.05]	11.28 [8.47, 15.02]	0.00 [0.00, 8.91]	15.99 [11.79, 21.69]	0.00 [0.00, 23.35]
SPE	A(H3)	16.38 [14.03, 19.13]	7.02 [0.00, 32.80]	5.24 [3.89, 7.07]	0.00 [0.00, 4.20]	7.49 [5.47, 10.26]	0.00 [0.00, 11.01]
SPE	A(H5)	15.16 [12.98, 17.71]	7.02 [0.00, 29.54]	4.63 [3.42, 6.26]	0.00 [0.00, 3.55]	6.23 [4.53, 8.56]	0.00 [0.00, 11.01]
SPE	A(UNS)	15.69 [13.43, 18.32]	7.02 [0.00, 30.77]	5.28 [3.92, 7.13]	0.00 [0.00, 4.42]	7.23 [5.27, 9.90]	0.00 [0.00, 11.01]
SPE	FLUA	16.77 [14.37, 19.58]	8.62 [0.00, 33.82]	5.40 [4.01, 7.28]	0.00 [0.00, 5.14]	7.83 [5.72, 10.72]	0.00 [0.00, 11.01]
SPE	B(YAM)	14.76 [12.64, 17.24]	5.9 [0.00, 28.24]	5.00 [3.7, 6.76]	0.00 [0.00, 3.84]	6.78 [4.94, 9.31]	0.00 [0.00, 11.01]
SPE	B(VIC)	14.78 [12.66, 17.27]	5.9 [0.00, 28.82]	5.03 [3.73, 6.80]	0.00 [0.00, 3.84]	6.82 [4.97, 9.36]	0.00 [0.00, 11.01]
SPE	B(UND)	15.96 [13.67, 18.64]	8.73 [0.00, 30.63]	5.21 [3.86, 7.02]	0.00 [0.00, 4.20]	7.20 [5.25, 9.86]	0.00 [0.00, 11.01]
SPE	FLUB	16.31 [13.97, 19.04]	8.73 [0.00, 32.22]	5.21 [3.86, 7.03]	0.00 [0.00, 4.20]	7.42 [5.42, 10.17]	0.00 [0.00, 11.01]
SPE	POS	16.87 [14.45, 19.70]	8.73 [0.00, 33.82]	5.41 [4.01, 7.29]	0.00 [0.00, 5.14]	7.87 [5.75, 10.77]	0.00 [0.00, 11.01]
SPE	NEG	5.57 [4.73, 6.56]	0.00 [0.00, 11.88]	0.61 [0.39, 0.96]	0.00 [0.00, 0.00]	4.64 [3.35, 6.43]	0.00 [0.00, 6.88]
TES	A(H1)	30.14 [25.87, 35.12]	29.54 [13.11, 45.04]	41.89 [31.74, 55.30]	42.94 [32.01, 54.74]	26.28 [19.45, 35.52]	23.32 [0.00, 46.13]
TES	A(H1N1)	63.04 [54.17, 73.35]	72.27 [37.94, 90.78]	72.63 [55.09, 95.75]	78.96 [56.84, 93.39]	50.32 [37.34, 67.82]	53.92 [2.38, 90.32]
TES	A(H3)	35.44 [30.43, 41.28]	38.16 [18.10, 48.59]	42.27 [32.02, 55.80]	42.65 [32.15, 55.61]	28.95 [21.43, 39.10]	27.01 [0.33, 49.35]
TES	A(H5)	15.65 [13.40, 18.27]	7.68 [0.00, 30.20]	4.67 [3.45, 6.32]	0.00 [0.00, 3.55]	7.17 [5.23, 9.82]	0.00 [0.00, 13.54]
TES	A(UNS)	34.74 [29.83, 40.47]	37.58 [16.65, 48.01]	42.66 [32.31, 56.31]	43.74 [34.18, 56.12]	29.23 [21.64, 39.47]	21.43 [0.00, 49.86]
TES	FLUA	37.16 [31.91, 43.27]	38.96 [18.10, 51.27]	43.59 [33.02, 57.54]	44.03 [34.18, 56.92]	32.21 [23.86, 43.49]	30.88 [1.41, 50.54]
TES	B(YAM)	27.46 [23.56, 32.00]	29.11 [12.82, 41.93]	34.89 [26.41, 46.09]	37.58 [26.94, 43.74]	18.63 [13.76, 25.23]	19.37 [0.11, 33.27]
TES	B(VIC)	27.48 [23.58, 32.03]	29.25 [12.96, 41.85]	34.89 [26.41, 46.09]	37.58 [26.94, 43.74]	18.76 [13.85, 25.41]	19.55 [0.29, 33.27]
TES	B(UND)	32.02 [27.49, 37.30]	34.69 [15.86, 46.05]	38.18 [28.91, 50.41]	41.49 [30.41, 47.28]	26.29 [19.45, 35.52]	28.06 [0.11, 47.47]
TES	FLUB	32.68 [28.06, 38.07]	35.41 [17.89, 46.85]	38.25 [28.96, 50.51]	42.07 [30.56, 47.28]	27.02 [20.00, 36.51]	28.67 [0.47, 47.47]
TES	POS	37.48 [32.18, 43.65]	38.96 [18.10, 52.21]	43.76 [33.15, 57.75]	44.03 [34.18, 56.92]	32.76 [24.27, 44.22]	32.30 [1.63, 51.41]
TES	NEG	11.39 [9.74, 13.32]	2.93 [0.00, 16.00]	0.61 [0.39, 0.96]	0.00 [0.00, 0.00]	26.66 [19.73, 36.03]	18.32 [0.72, 46.34]
A(H1)	A(H1N1)	52.29 [44.92, 60.85]	55.61 [28.42, 81.87]	72.09 [54.69, 95.04]	78.34 [56.84, 93.24]	44.19 [32.78, 59.58]	47.24 [0.00, 80.57]
A(H1)	A(H3)	30.94 [26.55, 36.04]	30.74 [13.40, 45.91]	42.33 [32.06, 55.87]	42.8 [31.72, 54.96]	26.06 [19.28, 35.21]	22.19 [0.00, 45.55]
A(H1)	A(H5)	12.24 [10.47, 14.31]	5.79 [0.00, 24.26]	4.62 [3.41, 6.25]	0.00 [0.00, 3.55]	7.25 [5.29, 9.94]	0.00 [0.00, 14.37]
A(H1)	A(UNS)	30.41 [26.10, 35.43]	30.20 [13.32, 45.33]	42.19 [31.96, 55.70]	43.08 [31.72, 55.10]	25.87 [19.14, 34.96]	21.04 [0.00, 45.55]
A(H1)	FLUA	31.40 [26.95, 36.58]	31.03 [13.40, 46.34]	42.89 [32.49, 56.61]	43.08 [32.01, 58.73]	26.59 [19.68, 35.93]	23.64 [0.00, 46.78]
A(H1)	B(YAM)	23.96 [20.55, 27.93]	25.42 [12.24, 36.21]	34.81 [26.35, 45.98]	37.51 [26.94, 43.66]	17.41 [12.85, 23.60]	18.75 [0.00, 31.93]
A(H1)	B(VIC)	23.95 [20.55, 27.93]	25.42 [12.24, 36.21]	34.78 [26.33, 45.94]	37.51 [26.94, 43.66]	17.45 [12.88, 23.65]	19.26 [0.00, 31.93]
A(H1)	B(UND)	27.14 [23.29, 31.63]	27.95 [13.32, 40.84]	37.71 [28.56, 49.81]	40.84 [29.69, 47.36]	22.78 [16.84, 30.81]	21.04 [0.00, 40.19]
A(H1)	FLUB	27.43 [23.54, 31.97]	29.65 [13.32, 41.13]	37.75 [28.59, 49.85]	40.98 [29.69, 47.36]	22.94 [16.97, 31.03]	21.18 [0.00, 40.22]
A(H1)	POS	31.40 [26.95, 36.58]	31.03 [13.40, 46.34]	42.89 [32.49, 56.61]	43.08 [32.01, 58.73]	26.59 [19.68, 35.93]	23.64 [0.00, 46.78]
A(H1)	NEG	6.64 [5.65, 7.80]	0.00 [0.00, 2.10]	0.51 [0.32, 0.82]	0.00 [0.00, 0.00]	21.67 [16.02, 29.32]	16.18 [0.00, 43.85]
A(H1N1)	A(H3)	62.91 [54.06, 73.20]	71.66 [40.09, 90.63]	72.51 [55.01, 95.59]	79.11 [56.84, 93.39]	48.63 [36.08, 65.55]	52.07 [0.23, 88.79]
A(H1N1)	A(H5)	33.99 [29.18, 39.59]	19.97 [0.00, 65.13]	10.08 [7.56, 13.45]	0.00 [0.00, 7.53]	15.16 [11.18, 20.57]	0.00 [0.00, 30.49]
A(H1N1)	A(UNS)	60.71 [52.17, 70.64]	69.74 [35.79, 89.55]	72.57 [55.05, 95.67]	80.03 [56.84, 92.93]	46.22 [34.28, 62.30]	44.78 [0.00, 86.10]
A(H1N1)	FLUA	63.96 [54.97, 74.42]	72.58 [40.09, 91.55]	72.81 [55.23, 95.98]	80.03 [56.84, 93.39]	50.57 [37.52, 68.15]	53.92 [2.38, 90.32]
A(H1N1)	B(YAM)	57.00 [48.98, 66.33]	61.60 [31.03, 85.87]	71.68 [54.37, 94.49]	78.19 [56.84, 91.55]	38.05 [28.21, 51.33]	38.10 [0.08, 69.20]
A(H1N1)	B(VIC)	56.97 [48.95, 66.30]	61.60 [31.03, 85.87]	71.71 [54.40, 94.54]	78.19 [56.84, 91.55]	38.00 [28.17, 51.26]	38.10 [0.23, 69.20]
A(H1N1)	B(UND)	61.42 [52.78, 71.47]	71.04 [37.94, 90.32]	72.38 [54.91, 95.42]	78.34 [56.84, 92.32]	47.03 [34.89, 63.39]	49.08 [0.00, 85.94]
A(H1N1)	FLUB	62.49 [53.71, 72.72]	71.27 [39.78, 90.63]	72.40 [54.92, 95.45]	78.34 [56.84, 92.47]	48.06 [35.65, 64.77]	49.46 [0.46, 88.02]

A(H1N1)	POS	63.96 [54.97, 74.42]	72.58 [40.09, 91.55]	72.81 [55.23, 95.98]	80.03 [56.84, 93.39]	50.57 [37.52, 68.15]	53.92 [2.38, 90.32]
A(H1N1)	NEG	19.97 [17.12, 23.30]	5.38 [0.00, 33.03]	1.30 [0.90, 1.87]	0.00 [0.00, 0.00]	42.47 [31.50, 57.27]	38.40 [0.92, 87.17]
A(H3)	A(H5)	16.01 [13.71, 18.69]	9.41 [0.00, 30.70]	4.75 [3.51, 6.42]	0.00 [0.00, 3.55]	7.08 [5.17, 9.71]	0.00 [0.00, 14.37]
A(H3)	A(UNS)	34.71 [29.80, 40.42]	36.71 [16.87, 49.09]	42.66 [32.31, 56.31]	42.87 [32.51, 56.41]	27.24 [20.17, 36.81]	21.11 [0.00, 49.53]
A(H3)	FLUA	36.87 [31.66, 42.94]	38.52 [18.90, 51.85]	43.64 [33.06, 57.60]	43.08 [34.11, 58.00]	29.31 [21.70, 39.58]	27.01 [0.33, 50.65]
A(H3)	B(YAM)	27.82 [23.87, 32.42]	29.25 [14.63, 41.93]	34.94 [26.45, 46.16]	37.58 [26.94, 43.74]	18.58 [13.72, 25.16]	18.83 [0.00, 33.27]
A(H3)	B(VIC)	27.80 [23.85, 32.39]	29.25 [14.63, 41.93]	34.96 [26.46, 46.18]	37.58 [26.94, 43.74]	18.54 [13.69, 25.11]	19.01 [0.00, 33.27]
A(H3)	B(UND)	31.97 [27.45, 37.25]	34.21 [17.89, 46.27]	37.95 [28.74, 50.12]	40.70 [30.05, 47.72]	24.78 [18.33, 33.50]	24.87 [0.00, 47.14]
A(H3)	FLUB	32.49 [27.89, 37.85]	34.76 [18.90, 46.85]	38.00 [28.78, 50.18]	40.70 [30.05, 47.72]	25.16 [18.62, 34.01]	25.02 [0.04, 47.50]
A(H3)	POS	36.87 [31.66, 42.94]	38.52 [18.90, 51.85]	43.64 [33.06, 57.60]	43.08 [34.11, 58.00]	29.31 [21.70, 39.58]	27.01 [0.33, 50.65]
A(H3)	NEG	10.33 [8.83, 12.09]	1.52 [0.00, 15.57]	0.61 [0.39, 0.95]	0.00 [0.00, 0.00]	23.82 [17.62, 32.20]	18.25 [0.04, 44.17]
A(H5)	A(UNS)	15.66 [13.41, 18.28]	8.40 [0.00, 30.70]	4.76 [3.52, 6.43]	0.00 [0.00, 3.55]	7.07 [5.16, 9.70]	0.00 [0.00, 14.37]
A(H5)	FLUA	16.07 [13.76, 18.76]	9.41 [0.00, 30.70]	4.76 [3.52, 6.43]	0.00 [0.00, 3.55]	7.25 [5.29, 9.94]	0.00 [0.00, 14.37]
A(H5)	B(YAM)	15.02 [12.86, 17.54]	8.40 [0.00, 28.24]	4.75 [3.51, 6.42]	0.00 [0.00, 3.55]	7.05 [5.14, 9.66]	0.00 [0.00, 14.37]
A(H5)	B(VIC)	15.03 [12.87, 17.56]	8.40 [0.00, 28.24]	4.75 [3.51, 6.42]	0.00 [0.00, 3.55]	7.08 [5.16, 9.71]	0.00 [0.00, 14.37]
A(H5)	B(UND)	15.53 [13.30, 18.13]	9.41 [0.00, 28.82]	4.75 [3.51, 6.43]	0.00 [0.00, 3.55]	7.07 [5.16, 9.70]	0.00 [0.00, 14.37]
A(H5)	FLUB	15.83 [13.56, 18.48]	9.41 [0.00, 30.05]	4.75 [3.51, 6.43]	0.00 [0.00, 3.55]	7.13 [5.20, 9.77]	0.00 [0.00, 14.37]
A(H5)	POS	16.07 [13.76, 18.76]	9.41 [0.00, 30.70]	4.76 [3.52, 6.43]	0.00 [0.00, 3.55]	7.25 [5.29, 9.94]	0.00 [0.00, 14.37]
A(H5)	NEG	4.70 [3.99, 5.55]	0.00 [0.00, 8.25]	0.37 [0.22, 0.62]	0.00 [0.00, 0.00]	4.46 [3.21, 6.18]	0.00 [0.00, 6.77]
A(UNS)	FLUA	36.05 [30.95, 41.98]	37.91 [16.87, 50.83]	44.22 [33.50, 58.36]	44.03 [35.48, 58.65]	29.65 [21.96, 40.04]	21.43 [0.00, 50.54]
A(UNS)	B(YAM)	27.20 [23.34, 31.70]	29.04 [12.82, 41.42]	34.91 [26.43, 46.12]	37.58 [26.94, 43.74]	18.13 [13.39, 24.56]	18.65 [0.00, 33.27]
A(UNS)	B(VIC)	27.22 [23.35, 31.72]	28.93 [12.89, 41.42]	34.93 [26.45, 46.15]	37.58 [26.94, 43.74]	18.18 [13.42, 24.62]	18.72 [0.00, 33.27]
A(UNS)	B(UND)	31.56 [27.09, 36.77]	34.21 [15.86, 46.05]	38.37 [29.06, 50.66]	41.49 [30.49, 47.50]	25.29 [18.72, 34.19]	21.07 [0.00, 46.56]
A(UNS)	FLUB	31.79 [27.29, 37.03]	34.21 [16.87, 46.05]	38.39 [29.07, 50.69]	41.49 [30.56, 47.50]	25.46 [18.84, 34.41]	21.07 [0.00, 47.03]
A(UNS)	POS	36.05 [30.95, 41.98]	37.91 [16.87, 50.83]	44.22 [33.50, 58.36]	44.03 [35.48, 58.65]	29.65 [21.96, 40.04]	21.43 [0.00, 50.54]
A(UNS)	NEG	9.70 [8.28, 11.36]	0.11 [0.00, 15.06]	0.60 [0.38, 0.94]	0.00 [0.00, 0.00]	23.54 [17.41, 31.83]	17.60 [0.00, 44.71]
FLUA	B(YAM)	27.88 [23.93, 32.49]	29.25 [14.63, 41.93]	34.98 [26.48, 46.20]	37.58 [26.94, 43.74]	18.68 [13.79, 25.30]	19.37 [0.04, 33.27]
FLUA	B(VIC)	27.88 [23.93, 32.49]	29.29 [14.63, 41.93]	34.97 [26.48, 46.20]	37.58 [26.94, 43.74]	18.74 [13.84, 25.38]	19.41 [0.11, 33.27]
FLUA	B(UND)	32.81 [28.17, 38.22]	34.97 [17.89, 46.85]	38.78 [29.37, 51.21]	41.85 [30.85, 48.88]	26.16 [19.36, 35.35]	26.00 [0.00, 47.54]
FLUA	FLUB	33.42 [28.69, 38.92]	35.30 [18.90, 47.79]	38.84 [29.42, 51.29]	42.36 [30.92, 48.88]	26.76 [19.80, 36.15]	26.14 [0.22, 47.94]
FLUA	POS	38.90 [33.41, 45.30]	39.79 [18.90, 54.96]	45.66 [34.6, 60.26]	44.17 [36.78, 62.64]	32.81 [24.31, 44.29]	31.50 [1.41, 51.41]
FLUA	NEG	11.10 [9.49, 12.99]	2.75 [0.00, 15.57]	0.61 [0.39, 0.96]	0.00 [0.00, 0.00]	26.06 [19.28, 35.22]	18.25 [0.65, 45.51]
B(YAM)	B(VIC)	27.72 [23.79, 32.31]	29.25 [14.63, 41.93]	34.91 [26.42, 46.11]	37.58 [26.94, 43.74]	18.39 [13.58, 24.91]	18.97 [0.00, 33.27]
B(YAM)	B(UND)	27.38 [23.50, 31.91]	29.25 [13.32, 41.20]	34.93 [26.45, 46.15]	37.58 [26.94, 43.66]	18.31 [13.51, 24.79]	18.68 [0.00, 32.08]
B(YAM)	FLUB	27.92 [23.96, 32.53]	29.33 [14.63, 41.93]	34.98 [26.48, 46.21]	37.58 [26.94, 43.74]	18.73 [13.83, 25.37]	19.37 [0.11, 33.27]
B(YAM)	POS	27.92 [23.96, 32.53]	29.33 [14.63, 41.93]	34.98 [26.48, 46.21]	37.58 [26.94, 43.74]	18.73 [13.83, 25.37]	19.37 [0.11, 33.27]
B(YAM)	NEG	7.59 [6.47, 8.91]	0.33 [0.00, 13.54]	0.56 [0.35, 0.88]	0.00 [0.00, 0.00]	15.59 [11.50, 21.15]	10.46 [0.04, 29.25]
B(VIC)	B(UND)	27.38 [23.50, 31.91]	29.25 [13.32, 41.71]	34.95 [26.46, 46.16]	37.58 [26.94, 43.66]	18.32 [13.53, 24.82]	18.68 [0.00, 32.08]
B(VIC)	FLUB	27.94 [23.98, 32.56]	29.58 [14.63, 42.22]	34.98 [26.48, 46.21]	37.58 [26.94, 43.74]	18.87 [13.93, 25.55]	19.55 [0.29, 33.27]
B(VIC)	POS	27.94 [23.98, 32.56]	29.58 [14.63, 42.22]	34.98 [26.48, 46.21]	37.58 [26.94, 43.74]	18.87 [13.93, 25.55]	19.55 [0.29, 33.27]
B(VIC)	NEG	7.62 [6.49, 8.94]	0.51 [0.00, 13.54]	0.57 [0.36, 0.90]	0.00 [0.00, 0.00]	15.67 [11.55, 21.25]	10.83 [0.11, 28.42]
B(UND)	FLUB	33.14 [28.45, 38.60]	35.23 [17.89, 47.36]	39.02 [29.55, 51.52]	41.93 [31.21, 49.46]	26.63 [19.71, 35.98]	28.10 [0.11, 47.54]
B(UND)	POS	33.14 [28.45, 38.60]	35.23 [17.89, 47.36]	39.02 [29.55, 51.52]	41.93 [31.21, 49.46]	26.63 [19.71, 35.98]	28.10 [0.11, 47.54]
B(UND)	NEG	9.63 [8.22, 11.28]	0.91 [0.00, 15.57]	0.57 [0.36, 0.90]	0.00 [0.00, 0.00]	21.37 [15.79, 28.91]	18.14 [0.00, 42.72]
FLUB	POS	33.80 [29.02, 39.37]	35.88 [18.90, 47.86]	39.09 [29.61, 51.62]	42.36 [31.35, 49.46]	27.37 [20.26, 36.98]	28.71 [0.47, 48.01]
FLUB	NEG	9.95 [8.50, 11.65]	1.77 [0.00, 15.57]	0.58 [0.37, 0.91]	0.00 [0.00, 0.00]	21.99 [16.26, 29.75]	18.18 [0.18, 43.56]
POS	NEG	11.29 [9.65, 13.20]	2.90 [0.00, 15.79]	0.61 [0.39, 0.96]	0.00 [0.00, 0.00]	26.51 [19.62, 35.82]	18.32 [0.69, 46.34]

Supplementary Table S27. Average and median *outcome interoperability* for 14 influenza test outcomes worldwide and in 2 WHO regions (SEARO – Southeast Asian Region; WPRO – Western Pacific Region). We extracted FluNet data from 173 Member States on 15 June 2021. We calculated *outcome interoperability* as the number of time points that 2 testing outcomes (defined below as *Outcome 1* and *Outcome 2*) in the same Member State have jointly non-missing records per total time points within a study period and multiplied by 100. Maximal time points included 1381 weeks for all testing outcomes except A(H1N1)pdm09 positives, for which the maximal time points was 651 weeks. We report average and median *outcome interoperability* with 95% confidence intervals (left column) and lower and upper quartiles (right column) for each geographic location.

Outcome 1	Outcome 2	Mean [LCI, UCI] WORLD	Med. [LQR, UQR] WORLD	Mean [LCI, UCI] SEARO	Med. [LQR, UQR] SEARO	Mean [LCI, UCI] WPRO	Med. [LQR, UQR] WPRO
SPE	TES	17.21 [14.74, 20.09]	8.73 [0.00, 36.42]	31.37 [17.21, 57.17]	36.42 [18.90, 42.72]	34.15 [20.44, 57.06]	39.90 [24.62, 45.18]
SPE	A(H1)	11.80 [10.09, 13.80]	4.92 [0.00, 24.19]	16.46 [8.96, 30.26]	24.19 [1.59, 27.44]	26.47 [15.81, 44.32]	26.43 [20.85, 36.21]
SPE	A(H1N1)	35.01 [30.06, 40.77]	17.28 [0.00, 70.05]	62.64 [34.53, 100.00]	71.43 [31.03, 87.86]	72.06 [43.29, 100.00]	84.64 [52.07, 95.24]
SPE	A(H3)	16.38 [14.03, 19.13]	7.02 [0.00, 32.80]	29.51 [16.18, 53.82]	35.34 [14.63, 41.35]	34.14 [20.43, 57.05]	39.90 [24.62, 45.18]
SPE	A(H5)	15.16 [12.98, 17.71]	7.02 [0.00, 29.54]	24.73 [13.53, 45.18]	25.85 [14.63, 33.74]	32.00 [19.14, 53.50]	38.45 [23.32, 40.04]
SPE	A(UNS)	15.69 [13.43, 18.32]	7.02 [0.00, 30.77]	21.82 [11.92, 39.92]	28.10 [12.53, 35.19]	33.69 [20.16, 56.29]	39.61 [23.46, 43.37]
SPE	FLUA	16.77 [14.37, 19.58]	8.62 [0.00, 33.82]	30.03 [16.47, 54.76]	35.63 [15.42, 41.85]	34.58 [20.70, 57.78]	40.04 [24.62, 45.18]
SPE	B(YAM)	14.76 [12.64, 17.24]	5.90 [0.00, 28.24]	24.98 [13.67, 45.63]	25.85 [14.63, 34.61]	32.58 [19.49, 54.46]	39.17 [23.32, 43.37]
SPE	B(VIC)	14.78 [12.66, 17.27]	5.90 [0.00, 28.82]	24.63 [13.48, 45.01]	25.85 [14.63, 34.83]	32.62 [19.51, 54.52]	39.17 [23.32, 43.37]
SPE	B(UND)	15.96 [13.67, 18.64]	8.73 [0.00, 30.63]	29.23 [16.02, 53.31]	33.02 [15.79, 42.29]	34.04 [20.37, 56.89]	39.90 [24.40, 45.18]
SPE	FLUB	16.31 [13.97, 19.04]	8.73 [0.00, 32.22]	30.06 [16.48, 54.81]	35.77 [15.93, 42.72]	34.44 [20.61, 57.55]	39.90 [24.40, 45.18]
SPE	POS	16.87 [14.45, 19.70]	8.73 [0.00, 33.82]	30.64 [16.81, 55.86]	36.35 [16.94, 42.72]	34.70 [20.77, 57.98]	40.04 [24.62, 45.18]
SPE	NEG	5.57 [4.73, 6.56]	0.00 [0.00, 11.88]	13.32 [7.22, 24.58]	13.40 [10.79, 17.74]	10.11 [5.95, 17.19]	9.63 [0.00, 18.83]
TES	A(H1)	30.14 [25.87, 35.12]	29.54 [13.11, 45.04]	20.35 [11.11, 37.27]	24.84 [1.59, 35.41]	39.88 [23.89, 66.58]	40.70 [21.00, 59.67]
TES	A(H1N1)	63.04 [54.17, 73.35]	72.27 [37.94, 90.78]	63.85 [35.2, 115.82]	76.96 [31.03, 87.86]	78.80 [47.36, 100.00]	91.40 [61.60, 96.47]
TES	A(H3)	35.44 [30.43, 41.28]	38.16 [18.10, 48.59]	33.91 [18.62, 61.76]	38.45 [14.63, 45.11]	49.07 [29.43, 81.81]	55.18 [29.54, 61.98]
TES	A(H5)	15.65 [13.40, 18.27]	7.68 [0.00, 30.20]	24.79 [13.57, 45.30]	25.85 [14.63, 33.67]	34.13 [20.43, 57.04]	39.32 [27.01, 45.11]
TES	A(UNS)	34.74 [29.83, 40.47]	37.58 [16.65, 48.01]	25.81 [14.13, 47.14]	36.06 [12.82, 41.42]	46.83 [28.08, 78.09]	46.49 [27.15, 67.41]
TES	FLUA	37.16 [31.91, 43.27]	38.96 [18.10, 51.27]	34.85 [19.14, 63.46]	38.45 [15.35, 49.89]	50.40 [30.23, 84.02]	55.25 [30.56, 67.70]
TES	B(YAM)	27.46 [23.56, 32.00]	29.11 [12.82, 41.93]	25.67 [14.06, 46.89]	31.21 [14.63, 34.54]	37.17 [22.26, 62.08]	42.43 [26.36, 47.79]
TES	B(VIC)	27.48 [23.58, 32.03]	29.25 [12.96, 41.85]	25.25 [13.82, 46.12]	31.28 [14.63, 34.76]	37.20 [22.28, 62.12]	42.43 [26.65, 47.79]
TES	B(UND)	32.02 [27.49, 37.30]	34.69 [15.86, 46.05]	32.09 [17.61, 58.48]	37.07 [15.71, 44.82]	42.00 [25.17, 70.08]	48.30 [29.40, 56.48]
TES	FLUB	32.68 [28.06, 38.07]	35.41 [17.89, 46.85]	33.14 [18.19, 60.37]	38.16 [15.86, 44.82]	43.77 [26.24, 73.02]	52.64 [29.91, 56.48]
TES	POS	37.48 [32.18, 43.65]	38.96 [18.10, 52.21]	35.58 [19.54, 64.78]	38.45 [16.87, 52.93]	50.70 [30.42, 84.52]	55.25 [32.30, 68.28]
TES	NEG	11.39 [9.74, 13.32]	2.93 [0.00, 16.00]	13.32 [7.22, 24.58]	13.40 [10.79, 17.74]	11.08 [6.53, 18.80]	9.63 [3.62, 18.83]
A(H1)	A(H1N1)	52.29 [44.92, 60.85]	55.61 [28.42, 81.87]	35.00 [19.22, 63.72]	51.31 [3.38, 58.22]	68.97 [41.43, 100.00]	58.37 [44.85, 96.16]
A(H1)	A(H3)	30.94 [26.55, 36.04]	30.74 [13.40, 45.91]	20.26 [11.06, 37.11]	24.84 [1.59, 35.34]	48.57 [29.13, 80.98]	49.96 [26.43, 64.45]
A(H1)	A(H5)	12.24 [10.47, 14.31]	5.79 [0.00, 24.26]	16.24 [8.83, 29.85]	24.19 [1.59, 27.44]	31.90 [19.08, 53.34]	27.01 [20.93, 44.82]
A(H1)	A(UNS)	30.41 [26.10, 35.43]	30.20 [13.32, 45.33]	19.37 [10.57, 35.51]	24.84 [0.00, 35.34]	45.03 [27.00, 75.12]	44.90 [26.43, 63.43]
A(H1)	FLUA	31.40 [26.95, 36.58]	31.03 [13.40, 46.34]	20.49 [11.18, 37.52]	24.84 [1.59, 35.41]	48.85 [29.30, 81.45]	50.04 [26.43, 64.81]
A(H1)	B(YAM)	23.96 [20.55, 27.93]	25.42 [12.24, 36.21]	16.31 [8.87, 29.99]	24.26 [0.00, 28.89]	34.01 [20.35, 56.83]	29.98 [21.00, 46.99]
A(H1)	B(VIC)	23.95 [20.55, 27.93]	25.42 [12.24, 36.21]	16.29 [8.86, 29.95]	24.26 [0.00, 28.60]	33.99 [20.34, 56.80]	29.98 [21.00, 46.99]
A(H1)	B(UND)	27.14 [23.29, 31.63]	27.95 [13.32, 40.84]	18.33 [9.99, 33.64]	24.84 [0.00, 30.05]	39.84 [23.87, 66.50]	34.40 [26.43, 53.22]
A(H1)	FLUB	27.43 [23.54, 31.97]	29.65 [13.32, 41.13]	18.68 [10.18, 34.25]	24.84 [1.59, 30.85]	41.52 [24.88, 69.29]	40.41 [26.43, 54.31]
A(H1)	POS	31.40 [26.95, 36.58]	31.03 [13.40, 46.34]	20.49 [11.18, 37.52]	24.84 [1.59, 35.41]	48.85 [29.30, 81.45]	50.04 [26.43, 64.81]
A(H1)	NEG	6.64 [5.65, 7.80]	0.00 [0.00, 2.10]	1.95 [0.94, 4.03]	1.09 [0.00, 1.81]	4.40 [2.51, 7.70]	0.29 [0.00, 7.24]
A(H1N1)	A(H3)	62.91 [54.06, 73.20]	71.66 [40.09, 90.63]	62.58 [34.49, 100.00]	71.43 [31.03, 87.71]	86.98 [52.29, 100.00]	91.71 [84.64, 98.46]
A(H1N1)	A(H5)	33.99 [29.18, 39.59]	19.97 [0.00, 65.13]	52.38 [28.85, 95.12]	53.61 [31.03, 71.58]	80.98 [48.67, 100.00]	84.64 [74.65, 97.70]
A(H1N1)	A(UNS)	60.71 [52.17, 70.64]	69.74 [35.79, 89.55]	46.96 [25.85, 85.33]	59.75 [27.19, 74.65]	82.14 [49.37, 100.00]	84.64 [72.66, 98.62]
A(H1N1)	FLUA	63.96 [54.97, 74.42]	72.58 [40.09, 91.55]	63.89 [35.22, 100.00]	76.96 [31.03, 87.86]	87.50 [52.60, 100.00]	91.86 [84.64, 99.69]
A(H1N1)	B(YAM)	57.00 [48.98, 66.33]	61.60 [31.03, 85.87]	52.55 [28.94, 95.42]	53.61 [31.03, 73.43]	82.79 [49.76, 100.00]	90.63 [74.65, 96.93]
A(H1N1)	B(VIC)	56.97 [48.95, 66.30]	61.60 [31.03, 85.87]	51.81 [28.53, 94.08]	53.61 [31.03, 73.89]	82.83 [49.78, 100.00]	90.78 [74.65, 96.93]
A(H1N1)	B(UND)	61.42 [52.78, 71.47]	71.04 [37.94, 90.32]	61.35 [33.81, 100.00]	75.42 [29.34, 87.40]	83.42 [50.14, 100.00]	90.32 [74.50, 98.62]
A(H1N1)	FLUB	62.49 [53.71, 72.72]	71.27 [39.78, 90.63]	63.02 [34.74, 100.00]	76.34 [31.03, 87.86]	87.01 [52.31, 100.00]	91.71 [84.64, 99.54]

A(H1N1)	POS	63.96 [54.97, 74.42]	72.58 [40.09, 91.55]	63.89 [35.22, 100.00]	76.96 [31.03, 87.86]	87.50 [52.60, 100.00]	91.86 [84.64, 99.69]
A(H1N1)	NEG	19.97 [17.12, 23.30]	5.38 [0.00, 33.03]	26.28 [14.39, 47.99]	25.50 [18.43, 36.10]	24.45 [14.59, 40.98]	31.34 [7.68, 40.40]
A(H3)	A(H5)	16.01 [13.71, 18.69]	9.41 [0.00, 30.70]	24.69 [13.51, 45.12]	24.69 [14.63, 33.74]	38.18 [22.86, 63.74]	39.90 [35.19, 46.13]
A(H3)	A(UNS)	34.71 [29.80, 40.42]	36.71 [16.87, 49.09]	25.63 [14.03, 46.81]	36.06 [12.82, 41.35]	52.95 [31.77, 88.25]	54.89 [34.25, 69.95]
A(H3)	FLUA	36.87 [31.66, 42.94]	38.52 [18.90, 51.85]	33.99 [18.66, 61.90]	38.52 [14.63, 45.11]	58.34 [35.02, 97.20]	55.32 [39.90, 81.82]
A(H3)	B(YAM)	27.82 [23.87, 32.42]	29.25 [14.63, 41.93]	25.30 [13.85, 46.22]	29.98 [14.63, 34.61]	41.27 [24.73, 68.88]	44.46 [39.17, 49.24]
A(H3)	B(VIC)	27.80 [23.85, 32.39]	29.25 [14.63, 41.93]	24.91 [13.63, 45.51]	30.05 [14.63, 34.83]	41.31 [24.76, 68.95]	44.46 [39.17, 49.38]
A(H3)	B(UND)	31.97 [27.45, 37.25]	34.21 [17.89, 46.27]	30.87 [16.94, 56.28]	36.28 [13.90, 41.20]	48.80 [29.27, 81.37]	53.73 [35.19, 60.46]
A(H3)	FLUB	32.49 [27.89, 37.85]	34.76 [18.90, 46.85]	31.78 [17.44, 57.92]	38.23 [14.63, 41.35]	50.52 [30.3, 84.22]	54.02 [39.90, 60.46]
A(H3)	POS	36.87 [31.66, 42.94]	38.52 [18.90, 51.85]	33.99 [18.66, 61.90]	38.52 [14.63, 45.11]	58.34 [35.02, 97.20]	55.32 [39.90, 81.82]
A(H3)	NEG	10.33 [8.83, 12.09]	1.52 [0.00, 15.57]	12.40 [6.71, 22.91]	12.02 [8.18, 17.02]	11.64 [6.87, 19.72]	14.77 [3.62, 18.97]
A(H5)	A(UNS)	15.66 [13.41, 18.28]	8.40 [0.00, 30.70]	21.15 [11.55, 38.72]	24.19 [12.82, 33.74]	36.85 [22.06, 61.54]	39.32 [34.11, 45.11]
A(H5)	FLUA	16.07 [13.76, 18.76]	9.41 [0.00, 30.70]	24.81 [13.58, 45.33]	25.85 [14.63, 33.74]	38.18 [22.87, 63.76]	39.90 [35.19, 46.13]
A(H5)	B(YAM)	15.02 [12.86, 17.54]	8.40 [0.00, 28.24]	22.38 [12.23, 40.95]	25.85 [14.63, 31.43]	37.90 [22.70, 63.29]	39.68 [35.19, 44.97]
A(H5)	B(VIC)	15.03 [12.87, 17.56]	8.40 [0.00, 28.24]	22.39 [12.24, 40.96]	25.85 [14.63, 31.43]	37.96 [22.74, 63.39]	39.75 [35.19, 45.11]
A(H5)	B(UND)	15.53 [13.30, 18.13]	9.41 [0.00, 28.82]	24.58 [13.45, 44.92]	25.42 [13.61, 33.74]	36.47 [21.83, 60.91]	39.39 [34.11, 45.11]
A(H5)	FLUB	15.83 [13.56, 18.48]	9.41 [0.00, 30.05]	24.78 [13.56, 45.28]	25.85 [14.63, 33.74]	38.13 [22.83, 63.66]	39.75 [35.19, 46.13]
A(H5)	POS	16.07 [13.76, 18.76]	9.41 [0.00, 30.70]	24.81 [13.58, 45.33]	25.85 [14.63, 33.74]	38.18 [22.87, 63.76]	39.90 [35.19, 46.13]
A(H5)	NEG	4.70 [3.99, 5.55]	0.00 [0.00, 8.25]	8.56 [4.58, 15.98]	9.27 [1.81, 14.84]	10.30 [6.06, 17.50]	12.45 [0.87, 18.83]
A(UNS)	FLUA	36.05 [30.95, 41.98]	37.91 [16.87, 50.83]	25.96 [14.22, 47.41]	36.06 [12.82, 41.42]	54.08 [32.45, 90.13]	54.96 [34.25, 70.67]
A(UNS)	B(YAM)	27.20 [23.34, 31.70]	29.04 [12.82, 41.42]	21.09 [11.52, 38.62]	27.66 [12.38, 31.43]	39.56 [23.70, 66.03]	42.51 [34.11, 46.13]
A(UNS)	B(VIC)	27.22 [23.35, 31.72]	28.93 [12.89, 41.42]	21.13 [11.54, 38.69]	27.73 [12.38, 31.43]	39.57 [23.70, 66.06]	42.51 [34.11, 46.20]
A(UNS)	B(UND)	31.56 [27.09, 36.77]	34.21 [15.86, 46.05]	24.07 [13.17, 44.00]	29.25 [12.82, 38.60]	46.53 [27.90, 77.59]	48.15 [34.25, 60.46]
A(UNS)	FLUB	31.79 [27.29, 37.03]	34.21 [16.87, 46.05]	24.14 [13.21, 44.12]	29.33 [12.82, 39.03]	46.93 [28.14, 78.27]	48.37 [34.25, 60.46]
A(UNS)	POS	36.05 [30.95, 41.98]	37.91 [16.87, 50.83]	25.96 [14.22, 47.41]	36.06 [12.82, 41.42]	54.08 [32.45, 90.13]	54.96 [34.25, 70.67]
A(UNS)	NEG	9.70 [8.28, 11.36]	0.11 [0.00, 15.06]	5.53 [2.91, 10.51]	2.03 [0.00, 9.41]	11.37 [6.71, 19.28]	14.77 [3.62, 19.04]
FLUA	B(YAM)	27.88 [23.93, 32.49]	29.25 [14.63, 41.93]	25.48 [13.95, 46.54]	31.21 [14.63, 34.61]	41.33 [24.76, 68.97]	44.53 [39.17, 49.38]
FLUA	B(VIC)	27.88 [23.93, 32.49]	29.29 [14.63, 41.93]	25.12 [13.75, 45.89]	31.28 [14.63, 34.83]	41.34 [24.77, 68.99]	44.53 [39.17, 49.38]
FLUA	B(UND)	32.81 [28.17, 38.22]	34.97 [17.89, 46.85]	31.50 [17.28, 57.41]	37.15 [14.34, 44.24]	49.52 [29.70, 82.56]	53.80 [35.19, 60.46]
FLUA	FLUB	33.42 [28.69, 38.92]	35.30 [18.90, 47.79]	32.45 [17.81, 59.13]	38.23 [14.63, 44.68]	51.28 [30.76, 85.47]	55.10 [39.90, 60.46]
FLUA	POS	38.90 [33.41, 45.30]	39.79 [18.90, 54.96]	35.11 [19.28, 63.92]	38.52 [15.42, 49.96]	59.88 [35.95, 99.74]	56.92 [39.90, 82.19]
FLUA	NEG	11.10 [9.49, 12.99]	2.75 [0.00, 15.57]	12.66 [6.85, 23.39]	12.02 [9.56, 17.02]	12.03 [7.10, 20.36]	14.77 [4.34, 19.04]
B(YAM)	B(VIC)	27.72 [23.79, 32.31]	29.25 [14.63, 41.93]	24.93 [13.64, 45.55]	31.21 [14.63, 34.61]	41.25 [24.71, 68.83]	44.53 [39.17, 48.95]
B(YAM)	B(UND)	27.38 [23.50, 31.91]	29.25 [13.32, 41.20]	24.75 [13.55, 45.23]	30.77 [13.03, 33.74]	39.59 [23.72, 66.10]	42.51 [34.11, 46.99]
B(YAM)	FLUB	27.92 [23.96, 32.53]	29.33 [14.63, 41.93]	25.69 [14.07, 46.93]	31.21 [14.63, 34.61]	41.34 [24.77, 68.99]	44.53 [39.17, 49.38]
B(YAM)	POS	27.92 [23.96, 32.53]	29.33 [14.63, 41.93]	25.69 [14.07, 46.93]	31.21 [14.63, 34.61]	41.34 [24.77, 68.99]	44.53 [39.17, 49.38]
B(YAM)	NEG	7.59 [6.47, 8.91]	0.33 [0.00, 13.54]	8.90 [4.77, 16.60]	9.41 [3.77, 16.51]	10.99 [6.48, 18.64]	14.27 [3.48, 18.83]
B(VIC)	B(UND)	27.38 [23.50, 31.91]	29.25 [13.32, 41.71]	24.53 [13.42, 44.82]	30.85 [13.03, 33.74]	39.63 [23.74, 66.15]	42.51 [34.11, 46.99]
B(VIC)	FLUB	27.94 [23.98, 32.56]	29.58 [14.63, 42.22]	25.26 [13.83, 46.15]	31.28 [14.63, 34.83]	41.35 [24.78, 69.01]	44.53 [39.17, 49.38]
B(VIC)	POS	27.94 [23.98, 32.56]	29.58 [14.63, 42.22]	25.26 [13.83, 46.15]	31.28 [14.63, 34.83]	41.35 [24.78, 69.01]	44.53 [39.17, 49.38]
B(VIC)	NEG	7.62 [6.49, 8.94]	0.51 [0.00, 13.54]	8.49 [4.55, 15.86]	7.75 [3.55, 15.57]	11.07 [6.53, 18.78]	14.27 [3.62, 18.83]
B(UND)	FLUB	33.14 [28.45, 38.60]	35.23 [17.89, 47.36]	32.19 [17.67, 58.66]	37.15 [15.79, 44.90]	49.90 [29.93, 83.19]	53.80 [35.19, 60.46]
B(UND)	POS	33.14 [28.45, 38.60]	35.23 [17.89, 47.36]	32.19 [17.67, 58.66]	37.15 [15.79, 44.90]	49.90 [29.93, 83.19]	53.80 [35.19, 60.46]
B(UND)	NEG	9.63 [8.22, 11.28]	0.91 [0.00, 15.57]	12.01 [6.49, 22.21]	12.02 [7.53, 17.31]	11.66 [6.88, 19.75]	10.72 [3.62, 19.04]
FLUB	POS	33.80 [29.02, 39.37]	35.88 [18.90, 47.86]	33.24 [18.24, 60.55]	38.23 [15.93, 44.90]	51.68 [31.01, 86.15]	55.10 [39.90, 60.46]
FLUB	NEG	9.95 [8.50, 11.65]	1.77 [0.00, 15.57]	12.70 [6.88, 23.47]	12.02 [8.69, 17.74]	11.98 [7.08, 20.29]	14.77 [3.77, 19.04]
POS	NEG	11.29 [9.65, 13.20]	2.90 [0.00, 15.79]	13.01 [7.04, 24.02]	12.02 [10.35, 17.74]	12.15 [7.17, 20.56]	14.77 [6.08, 19.04]

Supplementary Table S28. Average and median *outcome interoperability* for 14 influenza test outcomes worldwide and in 3 transmission zones (N-Am – North America; C-Am – Central America and the Caribbean; Te-SAm – Temperate South America). We extracted FluNet data from 173 Member States on 15 June 2021. We calculated *outcome interoperability* as the number of time points that 2 testing outcomes (defined below as *Outcome 1* and *Outcome 2*) in the same Member State have jointly non-missing records per total time points within a study period and multiplied by 100. Maximal time points included 1381 weeks for all testing outcomes except A(H1N1)pdm09 positives, for which the maximal time points was 651 weeks. We report average and median *outcome interoperability* with 95% confidence intervals (left column) and lower and upper quartiles (right column) for each geographic location.

Outcome 1	Outcome 2	Mean [LCI, UCI] N-Am	Med. [LQR, UQR] N-Am	Mean [LCI, UCI] C-Am	Med. [LQR, UQR] C-Am	Mean [LCI, UCI] Te-SAm	Med. [LQR, UQR] Te-SAm
SPE	TES	29.79 [9.43, 94.11]	42.36 [0.00, 46.99]	5.20 [3.47, 7.79]	0.00 [0.00, 5.43]	11.24 [4.04, 31.26]	10.68 [3.15, 19.33]
SPE	A(H1)	21.80 [6.85, 69.34]	23.82 [0.00, 41.56]	4.13 [2.73, 6.24]	0.00 [0.00, 5.43]	10.64 [3.82, 29.67]	10.03 [2.61, 18.68]
SPE	A(H1N1)	62.47 [19.97, 100.00]	89.86 [0.00, 97.54]	8.91 [6.03, 13.18]	0.00 [0.00, 11.52]	23.73 [8.73, 64.54]	22.43 [6.68, 40.78]
SPE	A(H3)	29.79 [9.43, 94.11]	42.36 [0.00, 46.99]	4.17 [2.76, 6.30]	0.00 [0.00, 5.43]	10.72 [3.85, 29.86]	10.21 [2.57, 18.86]
SPE	A(H5)	15.62 [4.86, 50.18]	23.03 [0.00, 23.82]	4.01 [2.65, 6.07]	0.00 [0.00, 5.43]	10.55 [3.79, 29.43]	9.88 [2.57, 18.54]
SPE	A(UNS)	29.79 [9.43, 94.11]	42.36 [0.00, 46.99]	3.94 [2.61, 5.97]	0.00 [0.00, 5.43]	10.84 [3.89, 30.20]	9.88 [3.15, 18.54]
SPE	FLUA	29.79 [9.43, 94.11]	42.36 [0.00, 46.99]	4.44 [2.95, 6.69]	0.00 [0.00, 5.43]	11.22 [4.04, 31.21]	10.64 [3.15, 19.30]
SPE	B(YAM)	22.76 [7.16, 72.33]	23.82 [0.00, 44.46]	4.03 [2.66, 6.09]	0.00 [0.00, 5.43]	10.55 [3.79, 29.43]	9.88 [2.57, 18.54]
SPE	B(VIC)	22.76 [7.16, 72.33]	23.82 [0.00, 44.46]	4.09 [2.70, 6.18]	0.00 [0.00, 5.43]	10.55 [3.79, 29.43]	9.88 [2.57, 18.54]
SPE	B(UND)	29.79 [9.43, 94.11]	42.36 [0.00, 46.99]	3.93 [2.60, 5.96]	0.00 [0.00, 5.43]	10.57 [3.79, 29.47]	9.88 [2.61, 18.54]
SPE	FLUB	29.79 [9.43, 94.11]	42.36 [0.00, 46.99]	4.14 [2.74, 6.26]	0.00 [0.00, 5.43]	10.57 [3.79, 29.47]	9.88 [2.61, 18.54]
SPE	POS	29.79 [9.43, 94.11]	42.36 [0.00, 46.99]	4.48 [2.97, 6.75]	0.00 [0.00, 5.43]	11.22 [4.04, 31.21]	10.64 [3.15, 19.30]
SPE	NEG	7.14 [2.13, 23.92]	0.00 [0.00, 21.43]	2.73 [1.77, 4.21]	0.00 [0.00, 3.22]	11.21 [4.03, 31.16]	10.61 [3.11, 19.30]
TES	A(H1)	36.06 [11.45, 100.00]	32.95 [0.00, 75.24]	18.23 [12.46, 26.66]	9.27 [0.00, 36.35]	51.25 [19.05, 100.00]	51.09 [44.21, 58.29]
TES	A(H1N1)	65.54 [20.96, 100.00]	97.54 [0.77, 98.31]	38.16 [26.22, 55.54]	20.66 [1.08, 81.18]	88.90 [33.18, 100.00]	94.47 [79.72, 98.08]
TES	A(H3)	44.24 [14.09, 100.00]	51.27 [0.80, 80.67]	19.55 [13.37, 28.58]	9.45 [0.14, 39.79]	55.70 [20.72, 100.00]	56.55 [47.10, 64.30]
TES	A(H5)	15.66 [4.88, 50.33]	23.03 [0.00, 23.97]	5.06 [3.37, 7.58]	0.00 [0.00, 9.20]	11.75 [4.23, 32.61]	9.92 [2.57, 20.93]
TES	A(UNS)	50.13 [15.99, 100.00]	69.73 [0.00, 80.67]	19.35 [13.23, 28.29]	9.34 [0.00, 43.05]	59.90 [22.30, 100.00]	61.73 [51.34, 68.46]
TES	FLUA	50.49 [16.11, 100.00]	69.80 [1.01, 80.67]	21.54 [14.75, 31.47]	9.88 [0.58, 45.37]	64.08 [23.87, 100.00]	67.49 [55.97, 72.19]
TES	B(YAM)	22.81 [7.18, 72.48]	23.97 [0.00, 44.46]	13.60 [9.27, 19.97]	6.01 [0.00, 23.57]	37.18 [13.77, 100.00]	40.41 [28.02, 46.34]
TES	B(VIC)	22.81 [7.18, 72.48]	23.97 [0.00, 44.46]	13.85 [9.44, 20.32]	6.05 [0.11, 24.73]	37.36 [13.84, 100.00]	40.62 [28.17, 46.56]
TES	B(UND)	46.20 [14.72, 100.00]	61.19 [0.00, 77.41]	18.44 [12.61, 26.98]	9.41 [0.04, 41.49]	49.75 [18.49, 100.00]	51.63 [41.85, 57.64]
TES	FLUB	46.20 [14.72, 100.00]	61.19 [0.00, 77.41]	19.09 [13.05, 27.91]	9.92 [0.25, 42.65]	50.71 [18.85, 100.00]	53.37 [42.03, 59.38]
TES	POS	50.49 [16.11, 100.00]	69.80 [1.01, 80.67]	22.07 [15.11, 32.23]	10.25 [0.76, 45.55]	65.35 [24.34, 100.00]	69.26 [56.37, 74.33]
TES	NEG	7.14 [2.13, 23.92]	0.00 [0.00, 21.43]	19.30 [13.20, 28.22]	4.63 [0.62, 43.74]	61.93 [23.06, 100.00]	67.31 [54.45, 69.41]
A(H1)	A(H1N1)	48.34 [15.41, 100.00]	58.99 [0.00, 86.02]	34.54 [23.72, 50.29]	19.66 [0.00, 73.73]	79.11 [29.51, 100.00]	77.19 [69.12, 89.09]
A(H1)	A(H3)	36.18 [11.49, 100.00]	33.31 [0.00, 75.24]	18.20 [12.44, 26.62]	9.27 [0.00, 36.28]	48.55 [18.04, 100.00]	47.32 [40.73, 56.37]
A(H1)	A(H5)	15.66 [4.88, 50.33]	23.03 [0.00, 23.97]	5.19 [3.46, 7.78]	0.00 [0.00, 10.25]	11.75 [4.23, 32.61]	9.92 [2.57, 20.93]
A(H1)	A(UNS)	36.37 [11.55, 100.00]	33.89 [0.00, 75.24]	18.15 [12.41, 26.55]	9.27 [0.00, 36.17]	49.15 [18.26, 100.00]	49.46 [42.03, 56.26]
A(H1)	FLUA	36.47 [11.58, 100.00]	34.18 [0.00, 75.24]	18.40 [12.58, 26.91]	9.27 [0.00, 36.35]	51.54 [19.16, 100.00]	51.67 [44.79, 58.29]
A(H1)	B(YAM)	21.00 [6.59, 66.87]	23.97 [0.00, 39.03]	13.03 [8.87, 19.13]	5.97 [0.00, 23.14]	33.27 [12.31, 89.96]	37.55 [27.37, 39.17]
A(H1)	B(VIC)	21.00 [6.59, 66.87]	23.97 [0.00, 39.03]	13.06 [8.89, 19.18]	5.97 [0.00, 23.14]	33.38 [12.35, 90.25]	37.73 [27.59, 39.17]
A(H1)	B(UND)	34.49 [10.94, 100.00]	31.50 [0.00, 71.98]	16.78 [11.46, 24.56]	9.27 [0.00, 35.19]	41.84 [15.52, 100.00]	43.08 [36.60, 47.07]
A(H1)	FLUB	34.49 [10.94, 100.00]	31.50 [0.00, 71.98]	16.91 [11.55, 24.76]	9.27 [0.00, 35.19]	41.85 [15.53, 100.00]	43.12 [36.64, 47.07]
A(H1)	POS	36.47 [11.58, 100.00]	34.18 [0.00, 75.24]	18.40 [12.58, 26.91]	9.27 [0.00, 36.35]	51.54 [19.16, 100.00]	51.67 [44.79, 58.29]
A(H1)	NEG	5.33 [1.55, 18.31]	0.00 [0.00, 16.00]	16.15 [11.03, 23.66]	0.69 [0.00, 36.17]	49.22 [18.29, 100.00]	48.73 [42.69, 55.76]
A(H1N1)	A(H3)	65.39 [20.91, 100.00]	97.54 [0.31, 98.31]	36.28 [24.92, 52.81]	19.74 [0.00, 78.49]	86.64 [32.33, 100.00]	92.32 [75.19, 98.08]
A(H1N1)	A(H5)	33.23 [10.54, 100.00]	48.85 [0.00, 50.84]	10.78 [7.32, 15.88]	0.00 [0.00, 21.74]	24.92 [9.17, 67.71]	21.04 [5.45, 44.39]
A(H1N1)	A(UNS)	65.28 [20.87, 100.00]	97.54 [0.00, 98.31]	35.35 [24.28, 51.47]	19.82 [0.00, 77.11]	83.87 [31.30, 100.00]	89.09 [72.58, 95.16]
A(H1N1)	FLUA	65.64 [20.99, 100.00]	97.54 [1.08, 98.31]	38.45 [26.42, 55.95]	20.66 [1.08, 81.18]	88.90 [33.18, 100.00]	94.47 [79.72, 98.08]
A(H1N1)	B(YAM)	48.39 [15.43, 100.00]	50.84 [0.00, 94.32]	28.08 [19.26, 40.94]	12.75 [0.00, 49.31]	73.31 [27.33, 100.00]	80.72 [54.53, 92.09]
A(H1N1)	B(VIC)	48.39 [15.43, 100.00]	50.84 [0.00, 94.32]	28.22 [19.36, 41.14]	12.67 [0.08, 50.69]	73.35 [27.35, 100.00]	80.80 [54.53, 92.17]
A(H1N1)	B(UND)	65.28 [20.87, 100.00]	97.54 [0.00, 98.31]	35.41 [24.32, 51.56]	19.66 [0.00, 75.58]	83.29 [31.08, 100.00]	89.02 [71.43, 95.16]

A(H1N1)	FLUB	65.28 [20.87, 100.00]	97.54 [0.00, 98.31]	36.25 [24.90, 52.77]	20.12 [0.15, 77.19]	84.45 [31.51, 100.00]	91.32 [73.73, 95.16]
A(H1N1)	POS	65.64 [20.99, 100.00]	97.54 [1.08, 98.31]	38.45 [26.42, 55.95]	20.66 [1.08, 81.18]	88.90 [33.18, 100.00]	94.47 [79.72, 98.08]
A(H1N1)	NEG	15.16 [4.71, 48.75]	0.00 [0.00, 45.47]	33.72 [23.16, 49.11]	6.30 [0.77, 80.65]	87.90 [32.81, 100.00]	94.32 [78.03, 97.77]
A(H3)	A(H5)	15.66 [4.88, 50.33]	23.03 [0.00, 23.97]	5.01 [3.34, 7.52]	0.00 [0.00, 10.25]	11.75 [4.23, 32.61]	9.92 [2.57, 20.93]
A(H3)	A(UNS)	44.53 [14.18, 100.00]	52.93 [0.00, 80.67]	18.61 [12.73, 27.22]	9.27 [0.00, 37.15]	53.55 [19.92, 100.00]	53.73 [44.61, 62.49]
A(H3)	FLUA	44.90 [14.30, 100.00]	53.15 [0.80, 80.74]	19.72 [13.49, 28.83]	9.45 [0.14, 39.79]	56.01 [20.84, 100.00]	57.13 [47.68, 64.34]
A(H3)	B(YAM)	22.81 [7.18, 72.48]	23.97 [0.00, 44.46]	13.58 [9.25, 19.93]	5.97 [0.00, 23.46]	36.93 [13.68, 99.70]	39.93 [27.99, 45.87]
A(H3)	B(VIC)	22.81 [7.18, 72.48]	23.97 [0.00, 44.46]	13.67 [9.31, 20.06]	5.97 [0.00, 24.29]	36.73 [13.60, 99.17]	39.50 [28.02, 45.44]
A(H3)	B(UND)	42.46 [13.51, 100.00]	49.96 [0.00, 77.41]	17.50 [11.96, 25.61]	9.27 [0.00, 35.66]	46.00 [17.08, 100.00]	46.63 [39.03, 52.97]
A(H3)	FLUB	42.46 [13.51, 100.00]	49.96 [0.00, 77.41]	17.73 [12.12, 25.95]	9.34 [0.00, 36.50]	46.56 [17.29, 100.00]	47.76 [40.15, 52.97]
A(H3)	POS	44.90 [14.30, 100.00]	53.15 [0.80, 80.74]	19.72 [13.49, 28.83]	9.45 [0.14, 39.79]	56.01 [20.84, 100.00]	57.13 [47.68, 64.34]
A(H3)	NEG	7.14 [2.13, 23.92]	0.00 [0.00, 21.43]	17.38 [11.87, 25.44]	1.74 [0.00, 39.03]	53.64 [19.95, 100.00]	55.83 [45.47, 61.80]
A(H5)	A(UNS)	15.66 [4.88, 50.33]	23.03 [0.00, 23.97]	5.00 [3.34, 7.51]	0.00 [0.00, 10.25]	11.75 [4.23, 32.61]	9.92 [2.57, 20.93]
A(H5)	FLUA	15.66 [4.88, 50.33]	23.03 [0.00, 23.97]	5.19 [3.46, 7.78]	0.00 [0.00, 10.25]	11.75 [4.23, 32.61]	9.92 [2.57, 20.93]
A(H5)	B(YAM)	15.66 [4.88, 50.33]	23.03 [0.00, 23.97]	4.96 [3.30, 7.44]	0.00 [0.00, 10.25]	11.75 [4.23, 32.61]	9.92 [2.57, 20.93]
A(H5)	B(VIC)	15.66 [4.88, 50.33]	23.03 [0.00, 23.97]	4.99 [3.33, 7.49]	0.00 [0.00, 10.25]	11.75 [4.23, 32.61]	9.92 [2.57, 20.93]
A(H5)	B(UND)	15.66 [4.88, 50.33]	23.03 [0.00, 23.97]	5.00 [3.34, 7.51]	0.00 [0.00, 10.25]	11.75 [4.23, 32.61]	9.92 [2.57, 20.93]
A(H5)	FLUB	15.66 [4.88, 50.33]	23.03 [0.00, 23.97]	5.06 [3.37, 7.59]	0.00 [0.00, 10.25]	11.75 [4.23, 32.61]	9.92 [2.57, 20.93]
A(H5)	POS	15.66 [4.88, 50.33]	23.03 [0.00, 23.97]	5.19 [3.46, 7.78]	0.00 [0.00, 10.25]	11.75 [4.23, 32.61]	9.92 [2.57, 20.93]
A(H5)	NEG	0.00 [0.00, 0.00]	0.00 [0.00, 0.00]	3.44 [2.26, 5.25]	0.00 [0.00, 3.98]	11.73 [4.23, 32.56]	9.88 [2.53, 20.93]
A(UNS)	FLUA	51.97 [16.58, 100.00]	74.87 [0.00, 81.03]	19.52 [13.35, 28.54]	9.34 [0.00, 43.05]	60.75 [22.62, 100.00]	63.36 [52.82, 68.68]
A(UNS)	B(YAM)	22.81 [7.18, 72.48]	23.97 [0.00, 44.46]	13.36 [9.10, 19.61]	5.97 [0.00, 23.43]	36.46 [13.50, 98.45]	38.99 [27.99, 44.93]
A(UNS)	B(VIC)	22.81 [7.18, 72.48]	23.97 [0.00, 44.46]	13.41 [9.13, 19.69]	5.97 [0.00, 23.90]	36.77 [13.62, 99.27]	39.54 [28.06, 45.47]
A(UNS)	B(UND)	46.71 [14.88, 100.00]	62.71 [0.00, 77.41]	17.80 [12.17, 26.05]	9.27 [0.00, 40.91]	48.55 [18.04, 100.00]	50.25 [41.49, 55.61]
A(UNS)	FLUB	46.71 [14.88, 100.00]	62.71 [0.00, 77.41]	17.93 [12.25, 26.23]	9.34 [0.00, 41.06]	48.81 [18.14, 100.00]	50.72 [41.53, 56.08]
A(UNS)	POS	51.97 [16.58, 100.00]	74.87 [0.00, 81.03]	19.52 [13.35, 28.54]	9.34 [0.00, 43.05]	60.75 [22.62, 100.00]	63.36 [52.82, 68.68]
A(UNS)	NEG	7.14 [2.13, 23.92]	0.00 [0.00, 21.43]	17.14 [11.71, 25.09]	0.11 [0.00, 40.12]	57.11 [21.25, 100.00]	60.75 [49.38, 64.84]
FLUA	B(YAM)	22.81 [7.18, 72.48]	23.97 [0.00, 44.46]	13.71 [9.34, 20.12]	6.01 [0.00, 23.64]	37.06 [13.73, 100.00]	40.19 [27.99, 46.13]
FLUA	B(VIC)	22.81 [7.18, 72.48]	23.97 [0.00, 44.46]	13.85 [9.44, 20.33]	5.97 [0.07, 24.51]	37.27 [13.81, 100.00]	40.55 [28.06, 46.49]
FLUA	B(UND)	46.73 [14.89, 100.00]	62.78 [0.00, 77.41]	18.24 [12.47, 26.68]	9.27 [0.00, 40.98]	49.09 [18.24, 100.00]	50.91 [41.60, 56.59]
FLUA	FLUB	46.73 [14.89, 100.00]	62.78 [0.00, 77.41]	18.72 [12.80, 27.38]	9.56 [0.07, 42.07]	49.91 [18.55, 100.00]	52.50 [41.64, 58.18]
FLUA	POS	52.52 [16.76, 100.00]	75.31 [1.16, 81.10]	21.74 [14.89, 31.76]	9.88 [0.58, 45.98]	65.01 [24.22, 100.00]	69.23 [55.97, 74.04]
FLUA	NEG	7.14 [2.13, 23.92]	0.00 [0.00, 21.43]	18.78 [12.84, 27.47]	3.51 [0.40, 43.59]	60.90 [22.67, 100.00	66.44 [54.06, 67.74]
B(YAM)	B(VIC)	22.81 [7.18, 72.48]	23.97 [0.00, 44.46]	13.61 [9.27, 19.97]	5.97 [0.00, 23.61]	36.84 [13.64, 99.46]	39.75 [27.99, 45.69]
B(YAM)	B(UND)	22.81 [7.18, 72.48]	23.97 [0.00, 44.46]	13.45 [9.16, 19.75]	5.97 [0.00, 23.32]	36.46 [13.50, 98.45]	38.99 [27.99, 44.93]
B(YAM)	FLUB	22.81 [7.18, 72.48]	23.97 [0.00, 44.46]	13.76 [9.38, 20.20]	6.01 [0.00, 23.64]	37.18 [13.77, 100.00]	40.41 [28.02, 46.34]
B(YAM)	POS	22.81 [7.18, 72.48]	23.97 [0.00, 44.46]	13.76 [9.38, 20.20]	6.01 [0.00, 23.64]	37.18 [13.77, 100.00]	40.41 [28.02, 46.34]
B(YAM)	NEG	7.14 [2.13, 23.92]	0.00 [0.00, 21.43]	11.72 [7.97, 17.24]	0.80 [0.00, 22.92]	36.60 [13.56, 98.83]	40.19 [27.52, 45.69]
B(VIC)	B(UND)	22.81 [7.18, 72.48]	23.97 [0.00, 44.46]	13.51 [9.20, 19.83]	5.97 [0.00, 23.71]	36.69 [13.59, 99.07]	39.43 [28.02, 45.37]
B(VIC)	FLUB	22.88 [7.20, 72.70]	23.97 [0.22, 44.46]	14.00 [9.54, 20.55]	6.05 [0.11, 24.73]	37.36 [13.84, 100.00]	40.62 [28.17, 46.56]
B(VIC)	POS	22.88 [7.20, 72.70]	23.97 [0.22, 44.46]	14.00 [9.54, 20.55]	6.05 [0.11, 24.73]	37.36 [13.84, 100.00]	40.62 [28.17, 46.56]
B(VIC)	NEG	7.14 [2.13, 23.92]	0.00 [0.00, 21.43]	11.88 [8.08, 17.48]	1.19 [0.07, 23.90]	36.78 [13.62, 99.32]	40.41 [27.66, 45.91]
B(UND)	FLUB	46.73 [14.89, 100.00]	62.78 [0.00, 77.41]	18.60 [12.72, 27.21]	9.41 [0.04, 41.49]	50.58 [18.80, 100.00]	53.19 [41.85, 59.30]
B(UND)	POS	46.73 [14.89, 100.00]	62.78 [0.00, 77.41]	18.60 [12.72, 27.21]	9.41 [0.04, 41.49]	50.58 [18.80, 100.00]	53.19 [41.85, 59.30]
B(UND)	NEG	7.14 [2.13, 23.92]	0.00 [0.00, 21.43]	16.39 [11.19, 24.00]	1.63 [0.00, 38.88]	47.86 [17.78, 100.00]	50.69 [40.70, 55.03]
FLUB	POS	46.80 [14.91, 100.00]	62.78 [0.22, 77.41]	19.25 [13.16, 28.14]	9.92 [0.25, 42.98]	51.54 [19.16, 100.00]	54.92 [42.03, 61.04]
FLUB	NEG	7.14 [2.13, 23.92]	0.00 [0.00, 21.43]	16.88 [11.53, 24.71]	1.92 [0.11, 40.62]	48.82 [18.14, 100.00]	52.43 [40.88, 56.77]
POS	NEG	7.14 [2.13, 23.92]	0.00 [0.00, 21.43]	19.21 [13.14, 28.09]	4.63 [0.54, 43.74]	61.93 [23.06, 100.00]	67.31 [54.45, 69.41]

Supplementary Table S29. Average and median *outcome interoperability* for 14 influenza test outcomes worldwide and in 3 transmission zones (Tr-SAm – Tropical South America; N-Eu – Northern Europe; SW-Eu – Southwestern Europe). We extracted FluNet data from 173 Member States on 15 June 2021. We calculated *outcome interoperability* as the number of time points that 2 testing outcomes (defined below as *Outcome 1* and *Outcome 2*) in the same Member State have jointly non-missing records per total time points within a study period and multiplied by 100. Maximal time points included 1381 weeks for all testing outcomes except A(H1N1)pdm09 positives, for which the maximal time points was 651 weeks. We report average and median *outcome interoperability* with 95% confidence intervals (left column) and lower and upper quartiles (right column) for each geographic location.

Outcome 1	Outcome 2	Mean [LCI, UCI] Tr-SAm	Med. [LQR, UQR] Tr-SAm	Mean [LCI, UCI] N-Eu	Med. [LQR, UQR] N-Eu	Mean [LCI, UCI] SW-Eu	Med. [LQR, UQR] SW-Eu
SPE	TES	10.28 [5.19, 20.38]	1.23 [0.00, 8.62]	2.76 [1.34, 5.69]	3.29 [0.00, 4.20]	7.55 [4.68, 12.19]	0.00 [0.00, 13.03]
SPE	A(H1)	8.16 [4.08, 16.30]	0.14 [0.00, 8.62]	2.47 [1.18, 5.15]	3.11 [0.00, 4.20]	6.86 [4.24, 11.11]	0.00 [0.00, 9.85]
SPE	A(H1N1)	19.08 [9.76, 37.30]	2.61 [0.00, 18.28]	5.78 [2.95, 11.30]	6.91 [0.00, 8.91]	15.80 [9.94, 25.12]	0.00 [0.00, 27.65]
SPE	A(H3)	8.95 [4.50, 17.83]	0.22 [0.00, 8.62]	2.47 [1.18, 5.15]	3.11 [0.00, 4.20]	7.40 [4.58, 11.94]	0.00 [0.00, 13.03]
SPE	A(H5)	8.05 [4.03, 16.10]	0.14 [0.00, 8.62]	2.19 [1.04, 4.63]	2.82 [0.00, 3.55]	6.25 [3.85, 10.15]	0.00 [0.00, 13.03]
SPE	A(UNS)	8.31 [4.16, 16.60]	0.87 [0.00, 8.62]	2.52 [1.21, 5.24]	3.29 [0.00, 4.20]	7.48 [4.64, 12.08]	0.00 [0.00, 13.03]
SPE	FLUA	9.55 [4.81, 18.98]	1.23 [0.00, 8.62]	2.74 [1.33, 5.65]	3.29 [0.00, 4.20]	7.66 [4.75, 12.36]	0.00 [0.00, 13.03]
SPE	B(YAM)	8.34 [4.18, 16.66]	0.14 [0.00, 8.62]	2.39 [1.14, 5.00]	3.26 [0.00, 3.91]	6.80 [4.20, 11.01]	0.00 [0.00, 13.03]
SPE	B(VIC)	8.34 [4.17, 16.64]	0.14 [0.00, 8.62]	2.39 [1.14, 5.00]	3.26 [0.00, 3.91]	6.89 [4.26, 11.14]	0.00 [0.00, 13.03]
SPE	B(UND)	8.32 [4.17, 16.61]	0.29 [0.00, 8.62]	2.43 [1.16, 5.07]	3.26 [0.00, 4.20]	7.31 [4.52, 11.80]	0.00 [0.00, 13.03]
SPE	FLUB	8.79 [4.41, 17.51]	0.29 [0.00, 8.62]	2.43 [1.16, 5.07]	3.26 [0.00, 4.20]	7.32 [4.54, 11.83]	0.00 [0.00, 13.03]
SPE	POS	9.64 [4.85, 19.15]	1.23 [0.00, 8.62]	2.74 [1.33, 5.65]	3.29 [0.00, 4.20]	7.66 [4.75, 12.36]	0.00 [0.00, 13.03]
SPE	NEG	6.84 [3.40, 13.76]	1.23 [0.00, 8.62]	0.00 [0.00, 0.00]	0.00 [0.00, 0.00]	1.52 [0.85, 2.71]	0.00 [0.00, 0.00]
TES	A(H1)	36.99 [19.08, 71.73]	38.96 [22.81, 54.02]	53.98 [28.88, 100.00]	48.99 [45.04, 69.08]	40.80 [25.88, 64.31]	37.29 [27.59, 58.00]
TES	A(H1N1)	65.95 [34.15, 100.00]	67.28 [55.76, 86.79]	89.43 [47.95, 100.00]	90.78 [87.40, 95.08]	68.40 [43.48, 100.00]	73.58 [52.07, 86.64]
TES	A(H3)	41.20 [21.27, 79.81]	41.78 [31.79, 55.25]	54.61 [29.22, 100.00]	50.00 [45.84, 69.15]	41.40 [26.27, 65.26]	40.55 [27.59, 57.86]
TES	A(H5)	8.87 [4.45, 17.66]	6.37 [0.00, 8.69]	2.19 [1.03, 4.62]	2.82 [0.00, 3.55]	6.39 [3.94, 10.36]	0.00 [0.00, 13.03]
TES	A(UNS)	39.37 [20.32, 76.29]	37.94 [20.85, 62.06]	55.07 [29.46, 100.00]	52.06 [46.05, 68.65]	42.17 [26.76, 66.47]	40.33 [27.59, 58.65]
TES	FLUA	45.15 [23.33, 87.41]	42.00 [32.80, 65.89]	56.49 [30.23, 100.00]	53.15 [46.78, 70.17]	43.34 [27.50, 68.30]	41.27 [27.59, 64.59]
TES	B(YAM)	24.64 [12.66, 47.99]	27.95 [20.85, 30.41]	44.49 [23.77, 83.26]	44.06 [40.33, 45.18]	32.30 [20.46, 50.98]	34.40 [22.01, 40.48]
TES	B(VIC)	24.43 [12.55, 47.59]	26.29 [20.93, 30.41]	44.46 [23.76, 83.21]	44.06 [40.33, 45.26]	32.35 [20.49, 51.07]	34.40 [22.88, 40.48]
TES	B(UND)	33.63 [17.33, 65.26]	30.34 [27.88, 51.19]	48.96 [26.18, 91.58]	46.38 [42.58, 51.48]	36.51 [23.15, 57.60]	35.26 [27.59, 49.17]
TES	FLUB	34.79 [17.93, 67.49]	32.44 [28.24, 53.58]	49.09 [26.25, 91.81]	46.38 [42.65, 51.56]	36.58 [23.19, 57.69]	35.26 [27.59, 49.17]
TES	POS	45.64 [23.58, 88.33]	42.22 [33.09, 66.18]	56.71 [30.34, 100.00]	53.58 [46.78, 70.24]	43.55 [27.64, 68.63]	41.35 [27.59, 64.74]
TES	NEG	40.41 [20.86, 78.28]	37.87 [19.26, 65.53]	0.00 [0.00, 0.00]	0.00 [0.00, 0.00]	1.52 [0.85, 2.71]	0.00 [0.00, 0.00]
A(H1)	A(H1N1)	57.33 [29.66, 100.00]	58.37 [47.77, 74.96]	88.83 [47.63, 100.00]	90.02 [85.71, 94.16]	67.31 [42.79, 100.00]	63.13 [44.39, 89.55]
A(H1)	A(H3)	37.15 [19.16, 72.02]	39.17 [23.03, 54.89]	56.36 [30.16, 100.00]	51.16 [45.91, 69.08]	40.78 [25.87, 64.28]	36.93 [27.59, 54.96]
A(H1)	A(H5)	8.87 [4.45, 17.66]	6.37 [0.00, 8.69]	2.17 [1.02, 4.58]	2.68 [0.00, 3.55]	6.24 [3.84, 10.13]	0.00 [0.00, 10.21]
A(H1)	A(UNS)	36.04 [18.58, 69.89]	36.42 [20.85, 54.96]	55.96 [29.94, 100.00]	51.05 [46.13, 68.65]	40.80 [25.88, 64.32]	37.36 [27.59, 55.10]
A(H1)	FLUA	37.69 [19.44, 73.07]	41.71 [23.46, 55.03]	56.84 [30.42, 100.00]	51.74 [46.13, 69.23]	41.64 [26.42, 65.63]	38.02 [27.59, 59.45]
A(H1)	B(YAM)	22.81 [11.70, 44.46]	26.21 [20.85, 30.41]	44.41 [23.73, 83.11]	44.03 [40.33, 45.26]	32.11 [20.34, 50.69]	29.47 [20.85, 40.48]
A(H1)	B(VIC)	22.85 [11.72, 44.54]	26.21 [20.85, 30.41]	44.40 [23.72, 83.09]	44.03 [40.33, 45.26]	32.07 [20.31, 50.63]	29.47 [20.85, 40.48]
A(H1)	B(UND)	29.09 [14.97, 56.53]	30.12 [20.85, 39.25]	48.72 [26.05, 91.12]	45.69 [42.29, 50.76]	35.68 [22.61, 56.28]	30.34 [27.44, 47.43]
A(H1)	FLUB	29.46 [15.16, 57.24]	30.12 [20.85, 39.25]	48.78 [26.08, 91.23]	45.69 [42.36, 50.83]	35.69 [22.63, 56.31]	30.34 [27.52, 47.43]
A(H1)	POS	37.69 [19.44, 73.07]	41.71 [23.46, 55.03]	56.84 [30.42, 100.00]	51.74 [46.13, 69.23]	41.64 [26.42, 65.63]	38.02 [27.59, 59.45]
A(H1)	NEG	32.05 [16.51, 62.22]	29.47 [18.83, 53.22]	0.00 [0.00, 0.00]	0.00 [0.00, 0.00]	1.23 [0.67, 2.26]	0.00 [0.00, 0.00]
A(H1N1)	A(H3)	64.6 [33.44, 100.00]	61.90 [55.76, 86.79]	88.89 [47.66, 100.00]	89.86 [85.71, 94.16]	68.39 [43.48, 100.00]	72.04 [52.07, 89.55]
A(H1N1)	A(H5)	18.43 [9.42, 36.05]	13.52 [0.00, 18.43]	4.64 [2.34, 9.19]	5.99 [0.00, 7.53]	13.99 [8.78, 22.28]	0.00 [0.00, 27.65]
A(H1N1)	A(UNS)	56.92 [29.45, 100.00]	56.68 [44.24, 74.96]	88.97 [47.71, 100.00]	90.09 [86.48, 94.16]	68.50 [43.55, 100.00]	73.43 [51.00, 89.55]
A(H1N1)	FLUA	66.21 [34.28, 100.00]	67.28 [55.76, 87.25]	89.45 [47.96, 100.00]	90.86 [87.40, 95.08]	68.84 [43.77, 100.00]	73.58 [52.69, 89.55]
A(H1N1)	B(YAM)	49.94 [25.82, 96.61]	58.53 [44.24, 64.52]	88.33 [47.36, 100.00]	89.71 [85.56, 94.16]	67.00 [42.59, 100.00]	71.58 [46.39, 85.87]
A(H1N1)	B(VIC)	49.24 [25.45, 95.26]	48.69 [44.24, 64.52]	88.34 [47.37, 100.00]	89.78 [85.56, 94.16]	67.10 [42.65, 100.00]	71.58 [48.23, 85.87]
A(H1N1)	B(UND)	60.97 [31.55, 100.00]	56.22 [50.84, 81.72]	88.76 [47.59, 100.00]	89.78 [85.71, 94.16]	68.12 [43.31, 100.00]	71.89 [48.39, 89.55]
A(H1N1)	FLUB	62.86 [32.54, 100.00]	61.29 [51.15, 86.79]	88.77 [47.60, 100.00]	89.78 [85.71, 94.16]	68.17 [43.34, 100.00]	71.89 [49.16, 89.55]

A(H1N1)	POS	66.21 [34.28, 100.00]	67.28 [55.76, 87.25]	89.45 [47.96, 166.82]	90.86 [87.40, 95.08]	68.84 [43.77, 100.00]	73.58 [52.69, 89.55]
A(H1N1)	NEG	58.59 [30.32, 100.00]	65.75 [39.94, 86.02]	0.00 [0.00, 0.00]	0.00 [0.00, 0.00]	3.21 [1.92, 5.37]	0.00 [0.00, 0.00]
A(H3)	A(H5)	8.58 [4.30, 17.12]	6.37 [0.00, 8.69]	2.17 [1.02, 4.58]	2.68 [0.00, 3.55]	6.59 [4.07, 10.68]	0.00 [0.00, 13.03]
A(H3)	A(UNS)	36.64 [18.90, 71.05]	36.42 [20.85, 57.71]	56.54 [30.26, 100.00]	51.92 [46.42, 68.79]	41.73 [26.48, 65.78]	41.35 [27.59, 56.41]
A(H3)	FLUA	42.07 [21.72, 81.48]	41.78 [32.73, 57.78]	58.22 [31.16, 10.00]	53.98 [46.85, 69.88]	42.67 [27.07, 67.25]	43.08 [27.59, 58.00]
A(H3)	B(YAM)	24.58 [12.62, 47.87]	27.44 [20.85, 30.41]	44.44 [23.75, 83.17]	44.06 [40.33, 45.11]	32.45 [20.56, 51.22]	34.40 [22.30, 40.48]
A(H3)	B(VIC)	24.17 [12.41, 47.08]	26.29 [20.85, 30.41]	44.39 [23.72, 83.07]	44.06 [40.33, 45.18]	32.55 [20.62, 51.38]	34.40 [23.17, 40.48]
A(H3)	B(UND)	32.12 [16.54, 62.36]	30.27 [25.92, 47.72]	49.02 [26.21, 91.69]	45.76 [42.94, 51.41]	36.13 [22.90, 56.99]	35.26 [27.59, 48.30]
A(H3)	FLUB	33.00 [17.00, 64.06]	30.27 [26.21, 50.54]	49.12 [26.26, 91.86]	45.80 [43.01, 51.48]	36.17 [22.93, 57.05]	35.26 [27.59, 48.30]
A(H3)	POS	42.07 [21.72, 81.48]	41.78 [32.73, 57.78]	58.22 [31.16, 100.00]	53.98 [46.85, 69.88]	42.67 [27.07, 67.25]	43.08 [27.59, 58.00]
A(H3)	NEG	36.16 [18.65, 70.12]	32.87 [19.12, 54.74]	0.00 [0.00, 0.00]	0.00 [0.00, 0.00]	1.50 [0.84, 2.68]	0.00 [0.00, 0.00]
A(H5)	A(UNS)	8.58 [4.30, 17.11]	6.37 [0.00, 8.69]	2.19 [1.04, 4.63]	2.82 [0.00, 3.55]	6.59 [4.07, 10.68]	0.00 [0.00, 13.03]
A(H5)	FLUA	8.87 [4.45, 17.66]	6.37 [0.00, 8.69]	2.19 [1.04, 4.63]	2.82 [0.00, 3.55]	6.59 [4.07, 10.68]	0.00 [0.00, 13.03]
A(H5)	B(YAM)	8.58 [4.30, 17.11]	6.37 [0.00, 8.69]	2.19 [1.03, 4.62]	2.82 [0.00, 3.55]	6.59 [4.07, 10.68]	0.00 [0.00, 13.03]
A(H5)	B(VIC)	8.65 [4.34, 17.24]	6.37 [0.00, 8.69]	2.19 [1.03, 4.62]	2.82 [0.00, 3.55]	6.59 [4.07, 10.68]	0.00 [0.00, 13.03]
A(H5)	B(UND)	8.58 [4.30, 17.11]	6.37 [0.00, 8.69]	2.19 [1.04, 4.63]	2.82 [0.00, 3.55]	6.59 [4.07, 10.68]	0.00 [0.00, 13.03]
A(H5)	FLUB	8.65 [4.34, 17.24]	6.37 [0.00, 8.69]	2.19 [1.04, 4.63]	2.82 [0.00, 3.55]	6.59 [4.07, 10.68]	0.00 [0.00, 13.03]
A(H5)	POS	8.87 [4.45, 17.66]	6.37 [0.00, 8.69]	2.19 [1.04, 4.63]	2.82 [0.00, 3.55]	6.59 [4.07, 10.68]	0.00 [0.00, 13.03]
A(H5)	NEG	5.86 [2.89, 11.88]	2.10 [0.00, 7.24]	0.00 [0.00, 0.00]	0.00 [0.00, 0.00]	0.87 [0.45, 1.67]	0.00 [0.00, 0.00]
A(UNS)	FLUA	39.91 [20.60, 77.34]	37.94 [20.85, 64.23]	59.25 [31.72, 100.00]	58.91 [51.12, 69.30]	43.89 [27.85, 69.16]	42.58 [27.59, 62.93]
A(UNS)	B(YAM)	23.29 [11.95, 45.39]	26.29 [20.85, 30.41]	44.29 [23.67, 82.90]	44.06 [40.33, 45.26]	32.48 [20.58, 51.28]	34.40 [22.23, 40.48]
A(UNS)	B(VIC)	23.20 [11.91, 45.22]	26.29 [20.85, 30.41]	44.34 [23.69, 82.98]	44.06 [40.33, 45.26]	32.52 [20.60, 51.34]	34.40 [22.95, 40.48]
A(UNS)	B(UND)	31.13 [16.03, 60.45]	30.05 [20.85, 42.72]	50.01 [26.74, 93.52]	47.68 [43.01, 55.03]	36.74 [23.29, 57.96]	35.26 [27.59, 47.5]
A(UNS)	FLUB	31.43 [16.18, 61.03]	30.05 [20.85, 42.72]	50.06 [26.77, 93.61]	47.79 [43.08, 55.10]	36.77 [23.31, 58.00]	35.26 [27.59, 47.5]
A(UNS)	POS	39.91 [20.60, 77.34]	37.94 [20.85, 64.23]	59.25 [31.72, 100.00]	58.91 [51.12, 69.30]	43.89 [27.85, 69.16]	42.58 [27.59, 62.93]
A(UNS)	NEG	33.99 [17.51, 65.94]	28.60 [18.83, 58.00]	0.00 [0.00, 0.00]	0.00 [0.00, 0.00]	1.47 [0.82, 2.63]	0.00 [0.00, 0.00]
FLUA	B(YAM)	24.61 [12.64, 47.93]	27.73 [20.85, 30.41]	44.49 [23.77, 83.26]	44.06 [40.33, 45.26]	32.50 [20.59, 51.30]	34.40 [22.30, 40.48]
FLUA	B(VIC)	24.35 [12.50, 47.43]	26.29 [20.85, 30.41]	44.46 [23.76, 83.21]	44.06 [40.33, 45.33]	32.56 [20.63, 51.39]	34.40 [23.17, 40.48]
FLUA	B(UND)	33.76 [17.40, 65.51]	30.41 [26.50, 51.19]	50.62 [27.07, 94.65]	48.08 [43.52, 55.18]	37.21 [23.59, 58.68]	35.26 [27.59, 48.88]
FLUA	FLUB	34.81 [17.94, 67.52]	31.64 [26.79, 54.02]	50.72 [27.12, 94.83]	48.23 [43.59, 55.25]	37.26 [23.63, 58.77]	35.26 [27.59, 48.88]
FLUA	POS	46.38 [23.96, 89.76]	42.00 [34.03, 68.50]	61.43 [32.89, 100.00]	59.96 [53.51, 71.04]	45.49 [28.87, 71.67]	44.53 [27.59, 65.03]
FLUA	NEG	39.53 [20.40, 76.60]	36.35 [19.12, 65.03]	0.00 [0.00, 0.00]	0.00 [0.00, 0.00]	1.51 [0.85, 2.70]	0.00 [0.00, 0.00]
B(YAM)	B(VIC)	23.62 [12.12, 46.03]	26.29 [20.85, 30.41]	44.40 [23.72, 83.09]	44.06 [40.33, 45.26]	32.42 [20.54, 51.17]	34.4 [22.01, 40.48]
B(YAM)	B(UND)	23.83 [12.23, 46.43]	26.29 [20.85, 30.41]	44.41 [23.73, 83.11]	44.03 [40.33, 45.26]	32.48 [20.57, 51.27]	34.4 [22.23, 40.48]
B(YAM)	FLUB	24.64 [12.66, 47.99]	27.95 [20.85, 30.41]	44.50 [23.78, 83.29]	44.06 [40.33, 45.26]	32.51 [20.60, 51.32]	34.4 [22.30, 40.55]
B(YAM)	POS	24.64 [12.66, 47.99]	27.95 [20.85, 30.41]	44.50 [23.78, 83.29]	44.06 [40.33, 45.26]	32.51 [20.60, 51.32]	34.4 [22.30, 40.55]
B(YAM)	NEG	21.14 [10.83, 41.25]	24.76 [9.78, 30.05]	0.00 [0.00, 0.00]	0.00 [0.00, 0.00]	1.36 [0.75, 2.45]	0.00 [0.00, 0.00]
B(VIC)	B(UND)	23.65 [12.14, 46.07]	26.29 [20.85, 30.41]	44.40 [23.72, 83.09]	44.03 [40.33, 45.26]	32.53 [20.61, 51.35]	34.4 [22.88, 40.48]
B(VIC)	FLUB	24.43 [12.55, 47.59]	26.29 [20.93, 30.41]	44.48 [23.76, 83.23]	44.06 [40.33, 45.33]	32.57 [20.63, 51.41]	34.4 [23.17, 40.48]
B(VIC)	POS	24.43 [12.55, 47.59]	26.29 [20.93, 30.41]	44.48 [23.76, 83.23]	44.06 [40.33, 45.33]	32.57 [20.63, 51.41]	34.4 [23.17, 40.48]
B(VIC)	NEG	20.89 [10.71, 40.78]	22.66 [10.35, 30.05]	0.00 [0.00, 0.00]	0.00 [0.00, 0.00]	1.40 [0.78, 2.53]	0.00 [0.00, 0.00]
B(UND)	FLUB	34.26 [17.66, 66.47]	30.92 [27.95, 51.19]	50.91 [27.23, 95.20]	48.55 [43.81, 55.61]	37.53 [23.80, 59.19]	35.26 [27.59, 49.46]
B(UND)	POS	34.26 [17.66, 66.47]	30.92 [27.95, 51.19]	50.91 [27.23, 95.20]	48.55 [43.81, 55.61]	37.53 [23.80, 59.19]	35.26 [27.59, 49.46]
B(UND)	NEG	29.83 [15.35, 57.95]	28.82 [18.90, 50.83]	0.00 [0.00, 0.00]	0.00 [0.00, 0.00]	1.41 [0.78, 2.53]	0.00 [0.00, 0.00]
FLUB	POS	35.42 [18.26, 68.70]	32.44 [28.31, 54.02]	51.04 [27.29, 95.43]	48.70 [43.88, 55.68]	37.60 [23.84, 59.29]	35.26 [27.59, 49.46]
FLUB	NEG	30.92 [15.92, 60.05]	28.82 [18.97, 51.92]	0.00 [0.00, 0.00]	0.00 [0.00, 0.00]	1.43 [0.79, 2.56]	0.00 [0.00, 0.00]
POS	NEG	39.94 [20.61, 77.39]	37.87 [19.26, 65.53]	0.00 [0.00, 0.00]	0.00 [0.00, 0.00]	1.51 [0.85, 2.70]	0.00 [0.00, 0.00]

Supplementary Table S30. Average and median *outcome interoperability* for 14 influenza test outcomes worldwide and in 3 transmission zones (E-Eu – Eastern Europe; N-Af – Northern Africa; E-Af – Eastern Africa). We extracted FluNet data from 173 Member States on 15 June 2021. We calculated *outcome interoperability* as the number of time points that 2 testing outcomes (defined below as *Outcome 1* and *Outcome 2*) in the same Member State have jointly non-missing records per total time points within a study period and multiplied by 100. Maximal time points included 1381 weeks for all testing outcomes except A(H1N1)pdm09 positives, for which the maximal time points was 651 weeks. We report average and median *outcome interoperability* with 95% confidence intervals (left column) and lower and upper quartiles (right column) for each geographic location.

Outcome 1	Outcome 2	Mean [LCI, UCI] E-Eu	Med. [LQR, UQR] E-Eu	Mean [LCI, UCI] N-Af	Med. [LQR, UQR] N-Af	Mean [LCI, UCI] E-Af	Med. [LQR, UQR] E-Af
SPE	TES	9.08 [4.87, 16.92]	0.00 [0.00, 27.15]	29.40 [12.06, 71.68]	34.69 [27.88, 36.28]	33.21 [17.70, 62.29]	33.13 [30.05, 42.51]
SPE	A(H1)	9.08 [4.87, 16.93]	0.00 [0.00, 27.15]	18.52 [7.53, 45.55]	19.04 [17.89, 25.63]	20.89 [11.08, 39.40]	24.73 [16.87, 26.29]
SPE	A(H1N1)	19.27 [10.51, 35.33]	0.00 [0.00, 57.60]	57.70 [23.83, 100.00]	62.21 [57.14, 66.97]	69.88 [37.43, 100.00]	70.20 [61.44, 90.17]
SPE	A(H3)	9.09 [4.88, 16.94]	0.00 [0.00, 27.15]	26.89 [11.01, 65.66]	28.89 [26.50, 31.86]	32.94 [17.56, 61.79]	33.09 [28.96, 42.43]
SPE	A(H5)	8.45 [4.52, 15.79]	0.00 [0.00, 27.08]	25.55 [10.45, 62.43]	26.72 [23.75, 30.63]	32.95 [17.56, 61.81]	33.13 [28.96, 42.51]
SPE	A(UNS)	9.09 [4.88, 16.94]	0.00 [0.00, 27.15]	25.85 [10.58, 63.16]	27.01 [23.82, 31.28]	32.95 [17.57, 61.82]	33.13 [28.96, 42.51]
SPE	FLUA	9.09 [4.88, 16.94]	0.00 [0.00, 27.15]	27.53 [11.28, 67.20]	30.20 [27.30, 32.01]	32.97 [17.57, 61.85]	33.13 [28.96, 42.51]
SPE	B(YAM)	9.08 [4.87, 16.92]	0.00 [0.00, 27.08]	23.55 [9.62, 57.63]	24.62 [23.82, 30.05]	26.39 [14.03, 49.61]	26.39 [22.16, 31.21]
SPE	B(VIC)	9.08 [4.87, 16.92]	0.00 [0.00, 27.08]	23.45 [9.58, 57.38]	24.33 [23.75, 29.91]	26.39 [14.03, 49.61]	26.39 [22.16, 31.21]
SPE	B(UND)	9.08 [4.87, 16.92]	0.00 [0.00, 27.08]	25.91 [10.60, 63.30]	26.65 [26.65, 29.91]	31.53 [16.80, 59.17]	30.27 [26.29, 42.51]
SPE	FLUB	9.08 [4.87, 16.92]	0.00 [0.00, 27.08]	26.30 [10.77, 64.24]	27.73 [26.72, 30.70]	31.80 [16.95, 59.68]	30.99 [26.29, 42.51]
SPE	POS	9.09 [4.88, 16.94]	0.00 [0.00, 27.15]	27.73 [11.36, 67.68]	30.77 [27.66, 32.08]	33.00 [17.59, 61.90]	33.13 [28.96, 42.51]
SPE	NEG	0.23 [0.06, 0.90]	0.00 [0.00, 0.00]	9.08 [3.61, 22.87]	9.70 [6.37, 12.02]	6.30 [3.23, 12.28]	0.43 [0.00, 13.54]
TES	A(H1)	45.53 [25.05, 82.74]	46.05 [35.99, 58.22]	22.40 [9.15, 54.88]	25.78 [23.90, 27.37]	25.89 [13.76, 48.69]	27.15 [19.91, 30.77]
TES	A(H1N1)	78.97 [43.57, 100.00]	90.17 [63.59, 96.31]	57.30 [23.67, 100.00]	62.37 [54.99, 66.97]	69.86 [37.42, 100.00]	70.35 [61.29, 90.17]
TES	A(H3)	45.51 [25.04, 82.72]	46.63 [36.35, 58.15]	30.25 [12.41, 73.74]	32.01 [29.91, 37.44]	37.94 [20.25, 71.09]	37.18 [29.62, 47.07]
TES	A(H5)	8.45 [4.52, 15.79]	0.00 [0.00, 27.08]	25.55 [10.45, 62.43]	26.72 [23.75, 30.63]	32.94 [17.56, 61.79]	33.20 [28.89, 42.51]
TES	A(UNS)	45.40 [24.98, 82.50]	44.53 [35.99, 58.00]	28.12 [11.53, 68.62]	31.43 [23.90, 31.93]	37.81 [20.18, 70.85]	37.07 [29.76, 47.07]
TES	FLUA	45.86 [25.24, 83.35]	47.21 [36.50, 58.22]	31.86 [13.08, 77.60]	32.95 [32.15, 39.54]	38.01 [20.29, 71.22]	37.40 [29.76, 47.07]
TES	B(YAM)	37.79 [20.76, 68.76]	41.93 [29.04, 47.21]	23.72 [9.69, 58.04]	25.20 [23.90, 30.05]	28.25 [15.04, 53.09]	27.52 [22.16, 42.00]
TES	B(VIC)	37.78 [20.76, 68.75]	41.93 [29.04, 47.14]	23.75 [9.71, 58.11]	25.49 [23.82, 29.91]	28.25 [15.04, 53.09]	27.52 [22.16, 42.00]
TES	B(UND)	40.44 [22.24, 73.56]	43.16 [31.79, 51.19]	26.72 [10.94, 65.25]	28.60 [28.17, 29.91]	34.23 [18.25, 64.19]	35.34 [26.36, 43.52]
TES	FLUB	40.44 [22.24, 73.56]	43.16 [31.79, 51.19]	27.36 [11.21, 66.78]	30.63 [28.31, 30.70]	34.50 [18.4, 64.70]	36.13 [26.36, 43.52]
TES	POS	45.93 [25.27, 83.47]	47.28 [36.57, 58.36]	32.32 [13.27, 78.71]	34.03 [32.22, 40.70]	38.12 [20.35, 71.43]	37.44 [30.05, 47.07]
TES	NEG	0.23 [0.06, 0.90]	0.00 [0.00, 0.00]	8.92 [3.54, 22.48]	8.91 [6.37, 12.02]	6.30 [3.23, 12.28]	0.43 [0.00, 13.54]
A(H1)	A(H1N1)	78.98 [43.58, 100.00]	90.17 [63.59, 96.31]	39.26 [16.16, 95.38]	40.09 [37.94, 54.53]	44.49 [23.77, 83.25]	53.00 [35.79, 55.76]
A(H1)	A(H3)	45.62 [25.10, 82.91]	45.47 [36.06, 58.73]	21.67 [8.84, 53.10]	25.85 [21.36, 26.65]	25.95 [13.80, 48.81]	27.15 [19.62, 30.92]
A(H1)	A(H5)	8.46 [4.53, 15.80]	0.00 [0.00, 27.08]	18.16 [7.38, 44.68]	18.83 [16.65, 25.71]	21.01 [11.14, 39.62]	24.98 [16.87, 26.29]
A(H1)	A(UNS)	45.36 [24.96, 82.44]	44.53 [35.84, 58.36]	20.17 [8.22, 49.52]	23.68 [16.73, 25.85]	25.89 [13.77, 48.70]	27.12 [19.62, 31.35]
A(H1)	FLUA	46.05 [25.34, 83.68]	46.20 [36.21, 59.96]	22.59 [9.22, 55.33]	25.85 [24.19, 27.44]	26.08 [13.87, 49.04]	27.15 [19.99, 31.35]
A(H1)	B(YAM)	37.83 [20.79, 68.83]	41.93 [29.04, 47.50]	18.45 [7.50, 45.38]	19.48 [16.80, 25.71]	20.92 [11.09, 39.45]	24.51 [13.40, 28.96]
A(H1)	B(VIC)	37.82 [20.78, 68.82]	41.93 [29.04, 47.43]	18.49 [7.52, 45.48]	19.77 [16.73, 25.71]	20.92 [11.09, 39.45]	24.51 [13.40, 28.96]
A(H1)	B(UND)	40.47 [22.25, 73.61]	43.08 [31.79, 51.19]	19.13 [7.78, 47.01]	19.91 [19.48, 25.71]	22.17 [11.77, 41.78]	26.00 [14.27, 28.31]
A(H1)	FLUB	40.47 [22.25, 73.61]	43.08 [31.79, 51.19]	19.35 [7.88, 47.54]	20.71 [19.62, 25.71]	22.44 [11.91, 42.28]	26.00 [14.27, 30.20]
A(H1)	POS	46.05 [25.34, 83.68]	46.20 [36.21, 59.96]	22.59 [9.22, 55.33]	25.85 [24.19, 27.44]	26.08 [13.87, 49.04]	27.15 [19.99, 31.35]
A(H1)	NEG	0.23 [0.06, 0.90]	0.00 [0.00, 0.00]	0.06 [0.00, 2.45]	0.00 [0.00, 0.07]	0.62 [0.23, 1.68]	0.00 [0.00, 0.14]
A(H1N1)	A(H3)	79.00 [43.59, 100.00]	90.17 [63.59, 96.31]	56.37 [23.28, 100.00]	59.45 [55.45, 66.82]	70.03 [37.51, 100.00]	71.12 [61.44, 90.02]
A(H1N1)	A(H5)	17.96 [9.79, 32.96]	0.00 [0.00, 57.45]	54.22 [22.39, 100.00]	56.68 [50.38, 65.13]	70.06 [37.53, 100.00]	71.27 [61.44, 90.17]
A(H1N1)	A(UNS)	79.00 [43.59, 100.00]	90.17 [63.59, 96.31]	54.90 [22.67, 100.00]	57.45 [50.54, 66.51]	70.06 [37.53, 100.00]	71.27 [61.44, 90.17]
A(H1N1)	FLUA	79.00 [43.59, 100.00]	90.17 [63.59, 96.31]	57.76 [23.86, 100.00]	62.37 [57.14, 67.13]	70.09 [37.55, 100.00]	71.27 [61.44, 90.17]
A(H1N1)	B(YAM)	78.31 [43.21, 100.00]	88.17 [61.60, 96.01]	49.89 [20.59, 100.00]	51.92 [50.54, 63.75]	56.07 [30.00, 100.00]	55.99 [47.00, 67.28]
A(H1N1)	B(VIC)	78.31 [43.21, 100.00]	88.17 [61.60, 96.01]	49.52 [20.43, 100.00]	50.84 [50.38, 63.13]	56.07 [30.00, 100.00]	55.99 [47.00, 67.28]
A(H1N1)	B(UND)	78.97 [43.57, 100.00]	90.17 [63.59, 96.31]	54.59 [22.54, 100.00]	55.76 [55.30, 63.59]	66.99 [35.88, 100.00]	64.75 [54.99, 90.17]
A(H1N1)	FLUB	78.97 [43.57, 100.00]	90.17 [63.59, 96.31]	55.08 [22.75, 100.00]	56.53 [55.91, 64.67]	67.57 [36.19, 100.00]	66.74 [54.99, 90.17]

A(H1N1)	POS	79.00 [43.59, 100.00]	90.17 [63.59, 96.31]	57.76 [23.86, 100.00]	62.37 [57.14, 67.13]	70.09 [37.55, 100.00]	71.27 [61.44, 90.17]
A(H1N1)	NEG	0.49 [0.17, 1.37]	0.00 [0.00, 0.00]	15.98 [6.47, 39.43]	16.44 [9.37, 17.36]	13.29 [6.99, 25.27]	0.61 [0.00, 28.73]
A(H3)	A(H5)	8.47 [4.53, 15.81]	0.00 [0.00, 27.08]	25.56 [10.46, 62.46]	26.72 [23.75, 30.70]	33.02 [17.6, 61.94]	33.56 [28.96, 42.43]
A(H3)	A(UNS)	45.32 [24.93, 82.36]	44.53 [35.92, 58.00]	27.56 [11.29, 67.26]	31.50 [23.90, 31.50]	37.89 [20.22, 71.00]	37.04 [29.62, 47.21]
A(H3)	FLUA	46.30 [25.48, 84.13]	47.43 [36.50, 60.10]	30.66 [12.58, 74.71]	32.08 [30.92, 37.87]	38.14 [20.36, 71.46]	37.36 [29.62, 47.21]
A(H3)	B(YAM)	37.83 [20.79, 68.83]	41.93 [29.04, 47.50]	23.72 [9.69, 58.04]	25.20 [23.90, 30.05]	28.33 [15.08, 53.22]	27.62 [22.16, 42.36]
A(H3)	B(VIC)	37.82 [20.78, 68.82]	41.93 [29.04, 47.43]	23.62 [9.65, 57.80]	24.84 [23.82, 29.98]	28.33 [15.08, 53.22]	27.62 [22.16, 42.36]
A(H3)	B(UND)	40.52 [22.28, 73.71]	43.08 [31.86, 51.19]	26.23 [10.74, 64.06]	27.81 [26.57, 29.91]	34.20 [18.24, 64.14]	35.37 [26.36, 43.88]
A(H3)	FLUB	40.52 [22.28, 73.71]	43.08 [31.86, 51.19]	26.71 [10.94, 65.21]	29.18 [26.72, 30.63]	34.48 [18.38, 64.65]	36.28 [26.36, 43.88]
A(H3)	POS	46.30 [25.48, 84.13]	47.43 [36.50, 60.10]	30.66 [12.58, 74.71]	32.08 [30.92, 37.87]	38.14 [20.36, 71.46]	37.36 [29.62, 47.21]
A(H3)	NEG	0.23 [0.06, 0.90]	0.00 [0.00, 0.00]	7.70 [3.03, 19.56]	7.82 [4.56, 8.83]	6.26 [3.21, 12.21]	0.29 [0.00, 13.54]
A(H5)	A(UNS)	8.47 [4.53, 15.81]	0.00 [0.00, 27.08]	25.46 [10.42, 62.22]	26.65 [23.68, 30.70]	33.06 [17.62, 62.02]	33.78 [28.96, 42.51]
A(H5)	FLUA	8.47 [4.53, 15.81]	0.00 [0.00, 27.08]	25.56 [10.46, 62.46]	26.72 [23.75, 30.70]	33.08 [17.63, 62.05]	33.78 [28.96, 42.51]
A(H5)	B(YAM)	8.44 [4.52, 15.77]	0.00 [0.00, 27.01]	23.33 [9.53, 57.10]	24.26 [23.75, 29.83]	26.44 [14.06, 49.71]	26.39 [22.16, 31.72]
A(H5)	B(VIC)	8.44 [4.52, 15.77]	0.00 [0.00, 27.01]	23.23 [9.49, 56.86]	23.90 [23.75, 29.69]	26.44 [14.06, 49.71]	26.39 [22.16, 31.72]
A(H5)	B(UND)	8.45 [4.52, 15.79]	0.00 [0.00, 27.01]	24.91 [10.19, 60.90]	25.20 [23.75, 29.83]	31.61 [16.84, 59.32]	30.52 [25.92, 42.51]
A(H5)	FLUB	8.45 [4.52, 15.79]	0.00 [0.00, 27.01]	25.03 [10.24, 61.18]	25.56 [23.75, 30.05]	31.88 [16.99, 59.83]	31.57 [25.92, 42.51]
A(H5)	POS	8.47 [4.53, 15.81]	0.00 [0.00, 27.08]	25.56 [10.46, 62.46]	26.72 [23.75, 30.70]	33.08 [17.63, 62.05]	33.78 [28.96, 42.51]
A(H5)	NEG	0.20 [0.05, 0.86]	0.00 [0.00, 0.00]	6.84 [2.67, 17.47]	6.66 [3.55, 6.81]	6.26 [3.21, 12.21]	0.29 [0.00, 13.54]
A(UNS)	FLUA	45.82 [25.21, 83.28]	44.53 [36.06, 58.58]	28.20 [11.56, 68.80]	31.50 [23.90, 31.93]	37.97 [20.26, 71.13]	37.11 [29.76, 47.21]
A(UNS)	B(YAM)	37.83 [20.79, 68.83]	41.93 [29.04, 47.50]	23.42 [9.57, 57.31]	24.48 [23.75, 29.98]	28.31 [15.07, 53.19]	27.59 [22.16, 42.36]
A(UNS)	B(VIC)	37.82 [20.78, 68.82]	41.93 [29.04, 47.43]	23.29 [9.51, 57.00]	24.11 [23.68, 29.69]	28.31 [15.07, 53.19]	27.59 [22.16, 42.36]
A(UNS)	B(UND)	40.29 [22.15, 73.28]	43.08 [31.79, 51.19]	25.23 [10.32, 61.66]	26.07 [23.82, 29.91]	34.22 [18.25, 64.18]	35.37 [26.36, 43.88]
A(UNS)	FLUB	40.29 [22.15, 73.28]	43.08 [31.79, 51.19]	25.45 [10.41, 62.18]	26.50 [23.90, 30.27]	34.50 [18.40, 64.69]	36.46 [26.36, 43.88]
A(UNS)	POS	45.82 [25.21, 83.28]	44.53 [36.06, 58.58]	28.20 [11.56, 68.80]	31.50 [23.90, 31.93]	37.97 [20.26, 71.13]	37.11 [29.76, 47.21]
A(UNS)	NEG	0.23 [0.06, 0.90]	0.00 [0.00, 0.00]	6.88 [2.69, 17.58]	6.59 [4.20, 6.81]	6.26 [3.21, 12.21]	0.33 [0.00, 13.54]
FLUA	B(YAM)	37.83 [20.79, 68.83]	41.93 [29.04, 47.50]	23.72 [9.69, 58.04]	25.20 [23.90, 30.05]	28.33 [15.08, 53.22]	27.62 [22.16, 42.36]
FLUA	B(VIC)	37.82 [20.78, 68.82]	41.93 [29.04, 47.43]	23.65 [9.66, 57.87]	24.91 [23.82, 29.98]	28.33 [15.08, 53.22]	27.62 [22.16, 42.36]
FLUA	B(UND)	40.66 [22.36, 73.96]	43.08 [31.93, 51.34]	26.68 [10.92, 65.14]	28.02 [28.02, 29.98]	34.25 [18.26, 64.23]	35.41 [26.36, 43.88]
FLUA	FLUB	40.66 [22.36, 73.96]	43.08 [31.93, 51.34]	27.18 [11.14, 66.36]	29.47 [28.17, 30.70]	34.53 [18.41, 64.74]	36.46 [26.36, 43.88]
FLUA	POS	47.15 [25.95, 85.68]	48.15 [36.78, 61.77]	32.50 [13.35, 79.13]	34.32 [32.22, 39.97]	38.28 [20.43, 71.71]	37.58 [29.76, 47.21]
FLUA	NEG	0.23 [0.06, 0.90]	0.00 [0.00, 0.00]	7.79 [3.07, 19.77]	8.11 [4.63, 8.91]	6.27 [3.22, 12.22]	0.33 [0.00, 13.54]
B(YAM)	B(VIC)	37.82 [20.78, 68.82]	41.93 [29.04, 47.43]	23.48 [9.59, 57.45]	24.55 [23.82, 29.69]	28.33 [15.08, 53.22]	27.62 [22.16, 42.36]
B(YAM)	B(UND)	37.83 [20.79, 68.83]	41.93 [29.04, 47.50]	23.37 [9.55, 57.21]	24.11 [23.75, 29.62]	28.05 [14.93, 52.71]	26.68 [22.16, 42.36]
B(YAM)	FLUB	37.83 [20.79, 68.83]	41.93 [29.04, 47.50]	23.74 [9.70, 58.08]	25.20 [23.90, 30.12]	28.33 [15.08, 53.22]	27.62 [22.16, 42.36]
B(YAM)	POS	37.83 [20.79, 68.83]	41.93 [29.04, 47.50]	23.74 [9.70, 58.08]	25.20 [23.90, 30.12]	28.33 [15.08, 53.22]	27.62 [22.16, 42.36]
B(YAM)	NEG	0.23 [0.06, 0.90]	0.00 [0.00, 0.00]	4.76 [1.82, 12.50]	4.71 [3.04, 6.66]	4.66 [2.36, 9.23]	0.00 [0.00, 12.74]
B(VIC)	B(UND)	37.82 [20.78, 68.82]	41.93 [29.04, 47.43]	23.37 [9.55, 57.21]	24.11 [23.75, 29.62]	28.05 [14.93, 52.71]	26.68 [22.16, 42.36]
B(VIC)	FLUB	37.82 [20.78, 68.82]	41.93 [29.04, 47.43]	23.77 [9.71, 58.15]	25.49 [23.82, 29.98]	28.33 [15.08, 53.22]	27.62 [22.16, 42.36]
B(VIC)	POS	37.82 [20.78, 68.82]	41.93 [29.04, 47.43]	23.77 [9.71, 58.15]	25.49 [23.82, 29.98]	28.33 [15.08, 53.22]	27.62 [22.16, 42.36]
B(VIC)	NEG	0.23 [0.06, 0.9]	0.00 [0.00, 0.00]	4.68 [1.78, 12.29]	4.49 [2.82, 6.66]	4.66 [2.36, 9.23]	0.00 [0.00, 12.74]
B(UND)	FLUB	40.79 [22.43, 74.19]	43.16 [32.08, 51.48]	27.02 [11.07, 65.98]	29.18 [28.60, 29.98]	34.40 [18.34, 64.50]	35.41 [26.43, 43.88]
B(UND)	POS	40.79 [22.43, 74.19]	43.16 [32.08, 51.48]	27.02 [11.07, 65.98]	29.18 [28.60, 29.98]	34.40 [18.34, 64.50]	35.41 [26.43, 43.88]
B(UND)	NEG	0.23 [0.06, 0.90]	0.00 [0.00, 0.00]	6.76 [2.64, 17.30]	6.66 [2.90, 7.75]	6.28 [3.22, 12.24]	0.43 [0.00, 13.54]
FLUB	POS	40.79 [22.43, 74.19]	43.16 [32.08, 51.48]	27.66 [11.33, 67.51]	30.63 [29.33, 30.77]	34.67 [18.49, 65.01]	36.46 [26.43, 43.88]
FLUB	NEG	0.23 [0.06, 0.90]	0.00 [0.00, 0.00]	7.11 [2.79, 18.13]	7.68 [3.62, 7.75]	6.29 [3.22, 12.25]	0.43 [0.00, 13.54]
POS	NEG	0.23 [0.06, 0.90]	0.00 [0.00, 0.00]	7.97 [3.14, 20.19]	8.40 [4.71, 9.41]	6.29 [3.23, 12.26]	0.43 [0.00, 13.54]

Supplementary Table S31. Average and median *outcome interoperability* for 14 influenza test outcomes worldwide and in 3 transmission zones (M-Af – Middle Africa; W-Af – Western Africa; W-As – Western Asia). We extracted FluNet data from 173 Member States on 15 June 2021. We calculated *outcome interoperability* as the number of time points that 2 testing outcomes (defined below as *Outcome 1* and *Outcome 2*) in the same Member State have jointly non-missing records per total time points within a study period and multiplied by 100. Maximal time points included 1381 weeks for all testing outcomes except A(H1N1)pdm09 positives, for which the maximal time points was 651 weeks. We report average and median *outcome interoperability* with 95% confidence intervals (left column) and lower and upper quartiles (right column) for each geographic location.

Outcome 1	Outcome 2	Mean [LCI, UCI] M-Af	Med. [LQR, UQR] M-Af	Mean [LCI, UCI] W-Af	Med. [LQR, UQR] W-Af	Mean [LCI, UCI] W-As	Med. [LQR, UQR] W-As
SPE	TES	19.45 [9.10, 41.57]	10.07 [2.68, 41.06]	34.32 [18.85, 62.51]	38.52 [25.92, 44.24]	14.81 [9.19, 23.87]	7.10 [0.07, 32.30]
SPE	A(H1)	12.43 [5.76, 26.85]	10.14 [0.00, 25.49]	20.59 [11.24, 37.71]	18.10 [12.82, 29.04]	7.86 [4.81, 12.83]	0.04 [0.00, 20.71]
SPE	A(H1N1)	41.1 [19.42, 86.99]	21.51 [5.68, 87.10]	70.56 [38.91, 100.00]	73.27 [46.54, 90.63]	28.06 [17.53, 44.90]	10.91 [0.15, 67.59]
SPE	A(H3)	19.33 [9.04, 41.33]	10.14 [2.68, 40.98]	33.57 [18.43, 61.14]	36.28 [22.38, 43.66]	12.20 [7.55, 19.73]	2.97 [0.00, 29.47]
SPE	A(H5)	19.36 [9.06, 41.39]	10.14 [2.68, 40.98]	32.70 [17.95, 59.57]	33.09 [21.87, 41.49]	11.12 [6.87, 18.02]	0.00 [0.00, 26.72]
SPE	A(UNS)	19.35 [9.05, 41.37]	10.14 [2.68, 40.98]	32.91 [18.07, 59.97]	33.02 [21.65, 43.66]	11.95 [7.39, 19.33]	1.59 [0.00, 26.50]
SPE	FLUA	19.38 [9.06, 41.42]	10.14 [2.68, 41.06]	33.82 [18.57, 61.59]	38.52 [22.45, 44.03]	13.58 [8.41, 21.91]	5.50 [0.07, 32.08]
SPE	B(YAM)	17.67 [8.25, 37.84]	10.14 [2.68, 37.36]	29.29 [16.06, 53.43]	28.82 [21.72, 42.58]	11.38 [7.03, 18.43]	1.67 [0.00, 26.50]
SPE	B(VIC)	17.71 [8.27, 37.92]	10.14 [2.68, 37.36]	29.60 [16.23, 53.97]	28.82 [21.87, 42.58]	11.39 [7.03, 18.44]	1.67 [0.00, 26.50]
SPE	B(UND)	18.03 [8.42, 38.59]	10.14 [2.68, 38.23]	30.76 [16.87, 56.08]	30.12 [16.65, 43.59]	12.73 [7.88, 20.57]	2.57 [0.00, 30.05]
SPE	FLUB	18.81 [8.79, 40.22]	10.14 [2.68, 40.98]	32.51 [17.84, 59.24]	36.50 [22.01, 43.59]	12.97 [8.03, 20.95]	3.80 [0.00, 30.05]
SPE	POS	19.38 [9.06, 41.42]	10.14 [2.68, 41.06]	33.97 [18.65, 61.87]	38.52 [22.59, 44.32]	13.77 [8.53, 22.21]	5.68 [0.07, 32.30]
SPE	NEG	0.97 [0.34, 2.79]	0.00 [0.00, 0.80]	8.57 [4.59, 16.00]	8.18 [1.38, 14.34]	7.88 [4.83, 12.88]	6.73 [0.00, 15.57]
TES	A(H1)	12.86 [5.96, 27.74]	10.07 [0.00, 25.49]	24.68 [13.51, 45.09]	18.10 [12.82, 32.37]	18.67 [11.62, 29.99]	21.00 [0.07, 33.16]
TES	A(H1N1)	41.17 [19.45, 87.13]	21.35 [5.68, 87.10]	71.58 [39.48, 100.00]	81.72 [46.54, 90.63]	48.92 [30.68, 78.02]	60.98 [13.67, 72.66]
TES	A(H3)	19.70 [9.22, 42.09]	10.07 [2.68, 40.98]	38.07 [20.92, 69.27]	38.52 [22.38, 46.05]	23.14 [14.44, 37.09]	30.74 [5.00, 37.73]
TES	A(H5)	19.40 [9.07, 41.46]	10.07 [2.68, 40.98]	33.18 [18.21, 60.44]	35.19 [21.87, 41.49]	11.11 [6.86, 17.99]	0.00 [0.00, 26.65]
TES	A(UNS)	19.98 [9.35, 42.67]	10.07 [2.68, 40.98]	37.40 [20.55, 68.07]	38.52 [21.65, 45.98]	22.89 [14.28, 36.70]	29.25 [2.03, 37.87]
TES	FLUA	20.02 [9.37, 42.76]	10.07 [2.68, 41.06]	38.39 [21.10, 69.86]	38.52 [22.45, 46.05]	24.81 [15.49, 39.74]	33.02 [6.44, 37.87]
TES	B(YAM)	17.80 [8.31, 38.12]	10.07 [2.68, 37.36]	30.12 [16.52, 54.91]	28.82 [21.72, 42.58]	21.50 [13.40, 34.49]	26.32 [2.17, 34.25]
TES	B(VIC)	17.74 [8.29, 37.99]	10.07 [2.68, 37.36]	30.42 [16.68, 55.46]	28.82 [21.87, 44.75]	21.53 [13.42, 34.53]	26.43 [2.17, 34.25]
TES	B(UND)	18.08 [8.45, 38.70]	10.07 [2.68, 38.23]	31.97 [17.54, 58.25]	38.52 [16.65, 43.52]	23.43 [14.62, 37.55]	30.30 [6.44, 35.48]
TES	FLUB	18.96 [8.87, 40.55]	10.07 [2.68, 40.98]	33.72 [18.51, 61.42]	38.52 [22.01, 46.05]	23.76 [14.83, 38.07]	30.30 [6.44, 35.55]
TES	POS	20.03 [9.37, 42.78]	10.07 [2.68, 41.06]	38.56 [21.19, 70.15]	38.52 [22.59, 46.05]	25.07 [15.65, 40.16]	33.24 [6.52, 37.87]
TES	NEG	0.97 [0.34, 2.79]	0.00 [0.00, 0.80]	9.05 [4.86, 16.87]	8.18 [1.38, 16.58]	7.88 [4.82, 12.86]	6.73 [0.00, 15.57]
A(H1)	A(H1N1)	26.38 [12.40, 56.10]	21.51 [0.00, 54.07]	43.61 [23.99, 79.28]	39.17 [27.19, 61.60]	37.27 [23.34, 59.52]	44.62 [0.15, 57.45]
A(H1)	A(H3)	12.77 [5.91, 27.55]	10.14 [0.00, 25.49]	24.66 [13.50, 45.06]	18.90 [12.82, 32.37]	18.50 [11.51, 29.73]	21.04 [0.00, 33.16]
A(H1)	A(H5)	12.43 [5.76, 26.85]	10.14 [0.00, 25.49]	20.58 [11.24, 37.69]	18.90 [12.82, 29.04]	7.68 [4.70, 12.56]	0.00 [0.00, 20.71]
A(H1)	A(UNS)	12.85 [5.95, 27.72]	10.14 [0.00, 25.49]	24.66 [13.50, 45.06]	18.90 [12.82, 32.37]	18.42 [11.46, 29.60]	21.04 [0.07, 32.95]
A(H1)	FLUA	12.87 [5.96, 27.77]	10.14 [0.00, 25.49]	24.76 [13.55, 45.24]	18.90 [12.82, 32.37]	18.71 [11.64, 30.05]	21.04 [0.07, 33.24]
A(H1)	B(YAM)	11.70 [5.41, 25.31]	10.14 [0.00, 24.98]	17.54 [9.55, 32.20]	13.76 [10.93, 24.69]	17.87 [11.11, 28.72]	21.04 [0.00, 29.62]
A(H1)	B(VIC)	11.64 [5.38, 25.18]	10.14 [0.00, 24.98]	17.54 [9.56, 32.21]	13.76 [10.93, 24.69]	17.88 [11.12, 28.74]	21.04 [0.00, 29.69]
A(H1)	B(UND)	11.11 [5.13, 24.08]	10.14 [0.00, 22.74]	20.32 [11.09, 37.23]	15.13 [10.93, 32.37]	18.28 [11.37, 29.37]	21.04 [0.07, 32.59]
A(H1)	FLUB	11.98 [5.54, 25.90]	10.14 [0.00, 25.49]	20.32 [11.09, 37.23]	15.13 [10.93, 32.37]	18.36 [11.42, 29.50]	21.04 [0.07, 32.66]
A(H1)	POS	12.87 [5.96, 27.77]	10.14 [0.00, 25.49]	24.76 [13.55, 45.24]	18.90 [12.82, 32.37]	18.71 [11.64, 30.05]	21.04 [0.07, 33.24]
A(H1)	NEG	0.11 [0.01, 1.16]	0.00 [0.00, 0.00]	0.59 [0.22, 1.55]	0.00 [0.00, 0.58]	1.39 [0.76, 2.54]	0.00 [0.00, 0.07]
A(H1N1)	A(H3)	41.10 [19.42, 86.99]	21.51 [5.68, 86.94]	71.21 [39.27, 100.00]	79.72 [46.39, 90.63]	46.49 [29.15, 74.16]	58.37 [10.6, 72.66]
A(H1N1)	A(H5)	41.17 [19.45, 87.13]	21.51 [5.68, 86.94]	70.42 [38.84, 100.00]	74.81 [46.39, 88.02]	23.58 [14.71, 37.79]	0.00 [0.00, 56.22]
A(H1N1)	A(UNS)	41.15 [19.44, 87.08]	21.51 [5.68, 86.94]	70.67 [38.98, 100.00]	74.96 [45.93, 90.63]	45.85 [28.74, 73.14]	55.91 [2.46, 72.66]
A(H1N1)	FLUA	41.19 [19.46, 87.17]	21.51 [5.68, 87.10]	71.67 [39.53, 100.00]	81.72 [46.54, 90.63]	48.97 [30.71, 78.09]	60.98 [13.67, 72.66]
A(H1N1)	B(YAM)	37.57 [17.74, 79.58]	21.51 [5.68, 79.26]	62.94 [34.69, 100.00]	61.14 [45.93, 90.32]	44.79 [28.08, 71.46]	55.91 [4.61, 72.66]
A(H1N1)	B(VIC)	37.66 [17.78, 79.76]	21.51 [5.68, 79.26]	63.25 [34.86, 100.00]	61.14 [46.24, 90.32]	44.81 [28.09, 71.49]	55.91 [4.61, 72.66]
A(H1N1)	B(UND)	38.34 [18.10, 81.19]	21.51 [5.68, 81.11]	66.09 [36.44, 100.00]	74.96 [36.10, 90.63]	47.10 [29.53, 75.12]	58.91 [13.67, 72.66]
A(H1N1)	FLUB	39.98 [18.89, 84.64]	21.51 [5.68, 86.94]	69.25 [38.19, 100.00]	81.72 [46.39, 90.63]	47.61 [29.85, 75.93]	58.91 [13.67, 72.66]

A(H1N1)	POS	41.19 [19.46, 87.17]	21.51 [5.68, 87.10]	71.67 [39.53, 100.00]	81.72 [46.54, 90.63]	48.97 [30.71, 78.09]	60.98 [13.67, 72.66]
A(H1N1)	NEG	2.06 [0.84, 5.09]	0.00 [0.00, 1.69]	17.83 [9.72, 32.73]	17.36 [2.92, 30.41]	13.72 [8.50, 22.14]	10.52 [0.00, 28.88]
A(H3)	A(H5)	19.38 [9.06, 41.42]	10.14 [2.68, 40.98]	33.26 [18.26, 60.58]	35.26 [21.87, 41.49]	11.12 [6.86, 18.00]	0.00 [0.00, 26.50]
A(H3)	A(UNS)	19.70 [9.22, 42.09]	10.14 [2.68, 40.98]	37.45 [20.58, 68.16]	38.52 [21.65, 45.98]	21.95 [13.69, 35.21]	29.29 [0.87, 36.06]
A(H3)	FLUA	19.71 [9.22, 42.11]	10.14 [2.68, 40.98]	38.15 [20.97, 69.43]	38.52 [22.38, 46.05]	23.20 [14.48, 37.19]	30.77 [5.00, 37.87]
A(H3)	B(YAM)	17.68 [8.26, 37.86]	10.14 [2.68, 37.36]	30.02 [16.47, 54.75]	28.82 [21.65, 42.58]	21.52 [13.41, 34.52]	26.36 [2.17, 34.25]
A(H3)	B(VIC)	17.72 [8.28, 37.94]	10.14 [2.68, 37.36]	30.18 [16.55, 55.02]	28.82 [21.80, 42.58]	21.54 [13.43, 34.55]	26.39 [2.17, 34.25]
A(H3)	B(UND)	18.04 [8.43, 38.62]	10.14 [2.68, 38.23]	31.96 [17.54, 58.24]	38.52 [17.45, 43.23]	22.11 [13.79, 35.46]	29.15 [1.30, 34.25]
A(H3)	FLUB	18.82 [8.80, 40.24]	10.14 [2.68, 40.98]	33.44 [18.36, 60.92]	38.52 [21.80, 46.05]	22.43 [13.99, 35.97]	29.15 [5.00, 34.25]
A(H3)	POS	19.71 [9.22, 42.11]	10.14 [2.68, 40.98]	38.15 [20.97, 69.43]	38.52 [22.38, 46.05]	23.20 [14.48, 37.19]	30.77 [5.00, 37.87]
A(H3)	NEG	0.96 [0.33, 2.77]	0.00 [0.00, 0.80]	8.60 [4.61, 16.06]	8.18 [1.38, 14.34]	5.59 [3.39, 9.23]	1.34 [0.00, 13.61]
A(H5)	A(UNS)	19.40 [9.07, 41.46]	10.14 [2.68, 40.98]	33.22 [18.24, 60.52]	35.26 [21.65, 41.49]	11.12 [6.86, 18.00]	0.00 [0.00, 26.5]
A(H5)	FLUA	19.41 [9.08, 41.48]	10.14 [2.68, 40.98]	33.26 [18.26, 60.58]	35.26 [21.87, 41.49]	11.13 [6.87, 18.02]	0.00 [0.00, 26.72]
A(H5)	B(YAM)	17.71 [8.27, 37.92]	10.14 [2.68, 37.36]	29.40 [16.12, 53.62]	28.82 [21.65, 41.49]	10.96 [6.77, 17.76]	0.00 [0.00, 26.50]
A(H5)	B(VIC)	17.75 [8.29, 38.01]	10.14 [2.68, 37.36]	29.41 [16.12, 53.63]	28.82 [21.80, 41.49]	10.96 [6.77, 17.76]	0.00 [0.00, 26.50]
A(H5)	B(UND)	18.07 [8.44, 38.68]	10.14 [2.68, 38.23]	31.04 [17.03, 56.58]	35.12 [17.45, 41.49]	11.03 [6.81, 17.86]	0.00 [0.00, 26.57]
A(H5)	FLUB	18.85 [8.81, 40.31]	10.14 [2.68, 40.98]	32.21 [17.68, 58.69]	35.12 [21.80, 41.49]	11.03 [6.81, 17.86]	0.00 [0.00, 26.57]
A(H5)	POS	19.41 [9.08, 41.48]	10.14 [2.68, 40.98]	33.26 [18.26, 60.58]	35.26 [21.87, 41.49]	11.13 [6.87, 18.02]	0.00 [0.00, 26.72]
A(H5)	NEG	0.97 [0.34, 2.79]	0.00 [0.00, 0.80]	7.85 [4.19, 14.71]	6.15 [1.38, 13.98]	4.63 [2.78, 7.71]	0.00 [0.00, 13.61]
A(UNS)	FLUA	19.99 [9.35, 42.70]	10.14 [2.68, 40.98]	37.48 [20.6, 68.21]	38.52 [21.65, 45.98]	22.93 [14.31, 36.77]	29.29 [2.03, 37.87]
A(UNS)	B(YAM)	17.78 [8.30, 38.07]	10.14 [2.68, 37.36]	29.83 [16.36, 54.40]	28.82 [21.43, 42.58]	21.08 [13.14, 33.83]	26.36 [0.00, 34.25]
A(UNS)	B(VIC)	17.74 [8.29, 37.99]	10.14 [2.68, 37.36]	29.86 [16.37, 54.45]	28.82 [21.58, 42.58]	21.09 [13.14, 33.83]	26.36 [0.00, 34.25]
A(UNS)	B(UND)	18.07 [8.44, 38.68]	10.14 [2.68, 38.23]	31.89 [17.50, 58.12]	38.52 [17.38, 43.01]	22.33 [13.93, 35.81]	28.46 [2.03, 34.25]
A(UNS)	FLUB	18.93 [8.85, 40.48]	10.14 [2.68, 40.98]	33.08 [18.16, 60.26]	38.52 [21.58, 43.23]	22.33 [13.93, 35.81]	28.46 [2.03, 34.25]
A(UNS)	POS	19.99 [9.35, 42.70]	10.14 [2.68, 40.98]	37.48 [20.6, 68.21]	38.52 [21.65, 45.98]	22.93 [14.31, 36.77]	29.29 [2.03, 37.87]
A(UNS)	NEG	0.97 [0.34, 2.79]	0.00 [0.00, 0.80]	7.99 [4.27, 14.96]	6.37 [1.38, 14.19]	5.38 [3.25, 8.90]	0.00 [0.00, 13.61]
FLUA	B(YAM)	17.81 [8.32, 38.14]	10.14 [2.68, 37.36]	30.10 [16.51, 54.89]	28.82 [21.65, 42.58]	21.52 [13.41, 34.52]	26.36 [2.17, 34.25]
FLUA	B(VIC)	17.75 [8.29, 38.01]	10.14 [2.68, 37.36]	30.32 [16.63, 55.28]	28.82 [21.80, 43.74]	21.54 [13.43, 34.56]	26.43 [2.17, 34.25]
FLUA	B(UND)	18.08 [8.45, 38.70]	10.14 [2.68, 38.23]	31.99 [17.56, 58.3]	38.52 [17.45, 43.30]	23.21 [14.48, 37.21]	30.05 [6.44, 34.76]
FLUA	FLUB	18.96 [8.87, 40.55]	10.14 [2.68, 40.98]	33.64 [18.47, 61.27]	38.52 [21.87, 46.05]	23.54 [14.69, 37.72]	30.05 [6.44, 34.83]
FLUA	POS	20.03 [9.37, 42.78]	10.14 [2.68, 41.06]	38.48 [21.15, 70.02]	38.52 [22.45, 46.05]	24.89 [15.54, 39.87]	33.06 [6.44, 37.87]
FLUA	NEG	0.97 [0.34, 2.79]	0.00 [0.00, 0.80]	8.82 [4.73, 16.46]	8.18 [1.38, 14.77]	6.75 [4.12, 11.08]	5.47 [0.00, 13.61]
B(YAM)	B(VIC)	17.71 [8.27, 37.92]	10.14 [2.68, 37.36]	30.04 [16.47, 54.77]	28.82 [21.72, 42.58]	21.52 [13.41, 34.52]	26.36 [2.17, 34.25]
B(YAM)	B(UND)	16.93 [7.90, 36.29]	10.14 [2.68, 34.61]	28.73 [15.75, 52.41]	28.82 [13.76, 42.58]	21.20 [13.21, 34.01]	26.36 [1.16, 34.25]
B(YAM)	FLUB	17.81 [8.32, 38.14]	10.14 [2.68, 37.36]	30.12 [16.52, 54.93]	28.82 [21.72, 42.58]	21.52 [13.41, 34.52]	26.36 [2.17, 34.25]
B(YAM)	POS	17.81 [8.32, 38.14]	10.14 [2.68, 37.36]	30.12 [16.52, 54.93]	28.82 [21.72, 42.58]	21.52 [13.41, 34.52]	26.36 [2.17, 34.25]
B(YAM)	NEG	0.73 [0.24, 2.29]	0.00 [0.00, 0.80]	8.2 [4.39, 15.34]	8.18 [1.38, 14.34]	4.84 [2.91, 8.03]	0.00 [0.00, 11.44]
B(VIC)	B(UND)	16.98 [7.92, 36.38]	10.14 [2.68, 34.61]	28.75 [15.76, 52.44]	28.82 [13.76, 42.58]	21.22 [13.22, 34.04]	26.39 [1.16, 34.25]
B(VIC)	FLUB	17.75 [8.29, 38.01]	10.14 [2.68, 37.36]	30.43 [16.69, 55.47]	28.82 [21.87, 44.82]	21.55 [13.43, 34.56]	26.47 [2.17, 34.25]
B(VIC)	POS	17.75 [8.29, 38.01]	10.14 [2.68, 37.36]	30.43 [16.69, 55.47]	28.82 [21.87, 44.82]	21.55 [13.43, 34.56]	26.47 [2.17, 34.25]
B(VIC)	NEG	0.78 [0.25, 2.38]	0.00 [0.00, 0.80]	8.51 [4.55, 15.89]	8.18 [1.38, 14.34]	4.84 [2.92, 8.05]	0.00 [0.00, 11.44]
B(UND)	FLUB	18.09 [8.45, 38.73]	10.14 [2.68, 38.23]	32.06 [17.59, 58.42]	38.52 [17.45, 43.59]	23.47 [14.64, 37.61]	30.34 [6.44, 35.63]
B(UND)	POS	18.09 [8.45, 38.73]	10.14 [2.68, 38.23]	32.06 [17.59, 58.42]	38.52 [17.45, 43.59]	23.47 [14.64, 37.61]	30.34 [6.44, 35.63]
B(UND)	NEG	0.97 [0.34, 2.79]	0.00 [0.00, 0.80]	7.85 [4.19, 14.71]	6.37 [0.51, 14.27]	6.10 [3.70, 10.04]	1.59 [0.00, 12.67]
FLUB	POS	18.97 [8.87, 40.57]	10.14 [2.68, 40.98]	33.81 [18.56, 61.58]	38.52 [22.01, 46.05]	23.8 [14.85, 38.14]	30.34 [6.44, 35.70]
FLUB	NEG	0.97 [0.34, 2.79]	0.00 [0.00, 0.80]	8.58 [4.6, 16.03]	8.18 [1.38, 14.34]	6.34 [3.86, 10.42]	3.08 [0.00, 12.67]
POS	NEG	0.97 [0.34, 2.79]	0.00 [0.00, 0.80]	8.94 [4.79, 16.67]	8.18 [1.38, 16.00]	6.92 [4.22, 11.34]	5.65 [0.00, 13.83]

Supplementary Table S32. Average and median *outcome interoperability* for 14 influenza test outcomes worldwide and in 3 transmission zones (C-As – Central Asia; E-As – Eastern Asia; S-As – Southern Asia). We extracted FluNet data from 173 Member States on 15 June 2021. We calculated *outcome interoperability* as the number of time points that 2 testing outcomes (defined below as *Outcome 1* and *Outcome 2*) in the same Member State have jointly non-missing records per total time points within a study period and multiplied by 100. Maximal time points included 1381 weeks for all testing outcomes except A(H1N1)pdm09 positives, for which the maximal time points was 651 weeks. We report average and median *outcome interoperability* with 95% confidence intervals (left column) and lower and upper quartiles (right column) for each geographic location.

Outcome 1	Outcome 2	Mean [LCI, UCI] C-As	Med. [LQR, UQR] C-As	Mean [LCI, UCI] E-As	Med. [LQR, UQR] E-As	Mean [LCI, UCI] S-As	Med. [LQR, UQR] S-As
SPE	TES	0.00 [0.00, 0.00]	0.00 [0.00, 0.00]	26.88 [11.01, 65.63]	40.26 [3.77, 45.18]	37.69 [19.44, 73.07]	38.96 [33.74, 43.23]
SPE	A(H1)	0.00 [0.00, 0.00]	0.00 [0.00, 0.00]	20.54 [8.37, 50.39]	27.44 [0.00, 30.05]	22.02 [11.29, 42.95]	24.84 [16.15, 27.44]
SPE	A(H1N1)	0.00 [0.00, 0.00]	0.00 [0.00, 0.00]	56.93 [23.51, 100.00]	85.41 [7.99, 95.24]	75.22 [38.97, 100.00]	81.72 [71.43, 87.86]
SPE	A(H3)	0.00 [0.00, 0.00]	0.00 [0.00, 0.00]	26.89 [11.01, 65.66]	40.26 [3.77, 45.18]	35.43 [18.27, 68.73]	38.52 [33.82, 41.35]
SPE	A(H5)	0.00 [0.00, 0.00]	0.00 [0.00, 0.00]	25.27 [10.34, 61.77]	38.45 [3.77, 39.32]	31.60 [16.27, 61.35]	33.38 [25.85, 41.35]
SPE	A(UNS)	0.00 [0.00, 0.00]	0.00 [0.00, 0.00]	24.85 [10.16, 60.76]	39.46 [0.00, 39.61]	31.27 [16.10, 60.73]	33.38 [28.17, 41.42]
SPE	FLUA	0.00 [0.00, 0.00]	0.00 [0.00, 0.00]	26.89 [11.01, 65.66]	40.26 [3.77, 45.18]	36.07 [18.60, 69.95]	38.52 [33.82, 41.85]
SPE	B(YAM)	0.00 [0.00, 0.00]	0.00 [0.00, 0.00]	25.95 [10.62, 63.40]	39.32 [0.00, 45.18]	32.05 [16.51, 62.23]	33.82 [25.85, 40.98]
SPE	B(VIC)	0.00 [0.00, 0.00]	0.00 [0.00, 0.00]	25.92 [10.61, 63.33]	39.32 [0.00, 45.04]	31.78 [16.37, 61.71]	33.82 [25.85, 40.98]
SPE	B(UND)	0.00 [0.00, 0.00]	0.00 [0.00, 0.00]	26.89 [11.01, 65.66]	40.26 [3.77, 45.18]	35.05 [18.07, 67.98]	36.28 [33.02, 41.49]
SPE	FLUB	0.00 [0.00, 0.00]	0.00 [0.00, 0.00]	26.89 [11.01, 65.66]	40.26 [3.77, 45.18]	35.88 [18.50, 69.59]	37.94 [33.82, 41.49]
SPE	POS	0.00 [0.00, 0.00]	0.00 [0.00, 0.00]	26.89 [11.01, 65.66]	40.26 [3.77, 45.18]	36.82 [18.99, 71.39]	38.52 [33.82, 42.72]
SPE	NEG	0.00 [0.00, 0.00]	0.00 [0.00, 0.00]	6.07 [2.36, 15.63]	3.77 [0.00, 9.05]	13.96 [7.10, 27.45]	13.40 [11.15, 17.74]
TES	A(H1)	25.72 [10.53, 62.85]	25.56 [10.93, 42.29]	25.98 [10.63, 63.47]	29.54 [0.00, 40.70]	24.61 [12.64, 47.93]	27.66 [16.08, 33.31]
TES	A(H1N1)	52.01 [21.47, 100.00]	54.22 [23.20, 82.95]	57.02 [23.55, 100.00]	85.41 [7.99, 95.24]	76.94 [39.86, 100.00]	81.57 [72.04, 87.86]
TES	A(H3)	25.65 [10.50, 62.67]	25.56 [10.93, 42.22]	32.70 [13.43, 79.62]	44.24 [3.77, 55.90]	38.61 [19.92, 74.83]	41.35 [35.63, 45.04]
TES	A(H5)	0.00 [0.00, 0.00]	0.00 [0.00, 0.00]	25.26 [10.33, 61.73]	38.38 [3.77, 39.32]	31.72 [16.33, 61.58]	33.31 [25.85, 41.35]
TES	A(UNS)	25.66 [10.50, 62.71]	25.56 [10.93, 41.49]	29.76 [12.21, 72.55]	39.61 [0.00, 49.67]	34.11 [17.58, 66.19]	37.29 [33.31, 42.65]
TES	FLUA	26.04 [10.66, 63.61]	25.56 [10.93, 42.80]	32.96 [13.54, 80.24]	45.40 [3.77, 55.90]	39.74 [20.51, 77.00]	41.49 [35.92, 45.55]
TES	B(YAM)	25.11 [10.27, 61.38]	25.56 [10.93, 40.19]	29.34 [12.03, 71.54]	39.32 [0.00, 47.79]	33.01 [17.01, 64.07]	34.40 [31.21, 41.06]
TES	B(VIC)	24.90 [10.18, 60.86]	25.56 [10.93, 39.97]	29.31 [12.02, 71.48]	39.32 [0.00, 47.79]	32.63 [16.81, 63.34]	33.74 [31.28, 40.98]
TES	B(UND)	25.36 [10.38, 61.98]	25.56 [10.93, 41.49]	32.41 [13.31, 78.92]	43.81 [3.77, 55.18]	36.99 [19.08, 71.71]	38.16 [33.74, 42.29]
TES	FLUB	25.56 [10.46, 62.46]	25.56 [10.93, 42.07]	32.47 [13.33, 79.06]	43.81 [3.77, 55.18]	38.10 [19.65, 73.84]	41.56 [36.06, 42.72]
TES	POS	26.05 [10.67, 63.65]	25.56 [10.93, 42.80]	33.09 [13.59, 80.56]	46.05 [3.77, 55.90]	40.61 [20.96, 78.68]	42.72 [36.64, 45.62]
TES	NEG	0.00 [0.00, 0.00]	0.00 [0.00, 0.00]	6.07 [2.36, 15.63]	3.77 [0.00, 9.05]	14.08 [7.16, 27.68]	13.40 [11.15, 17.74]
A(H1)	A(H1N1)	52.01 [21.47, 100.00]	54.22 [23.20, 82.95]	63.59 [26.29, 100.00]	64.67 [58.37, 95.24]	46.80 [24.18, 90.57]	52.69 [34.25, 58.22]
A(H1)	A(H3)	25.55 [10.45, 62.43]	25.56 [10.93, 42.14]	49.46 [20.4, 100.00]	59.59 [34.11, 64.45]	25.46 [13.08, 49.57]	31.35 [16.15, 35.34]
A(H1)	A(H5)	0.00 [0.00, 0.00]	0.00 [0.00, 0.00]	29.75 [12.20, 72.52]	29.91 [27.01, 44.82]	21.63 [11.09, 42.19]	24.84 [15.71, 27.44]
A(H1)	A(UNS)	25.45 [10.41, 62.18]	25.56 [10.93, 41.49]	43.91 [18.10, 100.00]	59.52 [27.37, 63.43]	24.94 [12.81, 48.56]	31.28 [15.71, 35.34]
A(H1)	FLUA	25.72 [10.53, 62.85]	25.56 [10.93, 42.29]	49.95 [20.61, 100.00]	59.67 [36.13, 64.81]	25.68 [13.20, 49.98]	31.35 [16.15, 35.41]
A(H1)	B(YAM)	25.04 [10.24, 61.21]	25.56 [10.93, 40.12]	33.57 [13.79, 81.70]	34.18 [27.08, 46.99]	22.73 [11.66, 44.31]	28.89 [16.15, 29.98]
A(H1)	B(VIC)	24.90 [10.18, 60.86]	25.56 [10.93, 39.97]	33.53 [13.77, 81.60]	34.18 [27.01, 46.99]	22.70 [11.64, 44.25]	28.60 [16.15, 29.98]
A(H1)	B(UND)	25.14 [10.29, 61.45]	25.56 [10.93, 40.84]	45.47 [18.75, 100.00]	59.3 [32.66, 62.27]	23.55 [12.09, 45.89]	29.11 [16.15, 31.28]
A(H1)	FLUB	25.29 [10.35, 61.80]	25.56 [10.93, 40.98]	45.55 [18.78, 100.00]	59.59 [32.73, 62.27]	23.80 [12.22, 46.37]	30.49 [16.15, 31.35]
A(H1)	POS	25.72 [10.53, 62.85]	25.56 [10.93, 42.29]	49.95 [20.61, 100.00]	59.67 [36.13, 64.81]	25.68 [13.20, 49.98]	31.35 [16.15, 35.41]
A(H1)	NEG	0.00 [0.00, 0.00]	0.00 [0.00, 0.00]	5.52 [2.13, 14.31]	0.00 [0.00, 7.24]	1.91 [0.85, 4.27]	0.00 [0.00, 1.67]
A(H1N1)	A(H3)	52.01 [21.47, 100.00]	54.22 [23.20, 82.95]	77.08 [31.90, 100.00]	95.24 [85.56, 96.93]	75.39 [39.06, 100.00]	80.34 [71.43, 87.71]
A(H1N1)	A(H5)	0.00 [0.00, 0.00]	0.00 [0.00, 0.00]	73.55 [30.43, 100.00]	83.56 [81.57, 94.93]	67.16 [34.78, 100.00]	70.81 [53.61, 87.71]
A(H1N1)	A(UNS)	52.01 [21.47, 100.00]	54.22 [23.20, 82.95]	72.75 [30.10, 100.00]	84.64 [84.18, 95.24]	67.45 [34.93, 100.00]	70.81 [59.75, 87.71]
A(H1N1)	FLUA	52.01 [21.47, 100.00]	54.22 [23.20, 82.95]	77.08 [31.90, 100.00]	95.24 [85.56, 96.93]	77.01 [39.90, 100.00]	81.72 [72.04, 87.86]
A(H1N1)	B(YAM)	51.86 [21.40, 100.00]	54.22 [23.20, 82.95]	75.08 [31.07, 100.00]	95.24 [83.56, 96.93]	67.69 [35.05, 100.00]	71.74 [53.61, 86.94]
A(H1N1)	B(VIC)	51.86 [21.40, 100.00]	54.22 [23.20, 82.95]	75.02 [31.05, 100.00]	94.93 [83.56, 96.93]	67.11 [34.75, 100.00]	71.74 [53.61, 86.94]
A(H1N1)	B(UND)	52.01 [21.47, 100.00]	54.22 [23.20, 82.95]	77.08 [31.90, 100.00]	95.24 [85.56, 96.93]	73.82 [38.24, 100.00]	75.73 [71.74, 87.40]
A(H1N1)	FLUB	52.01 [21.47, 100.00]	54.22 [23.20, 82.95]	77.08 [31.90, 100.00]	95.24 [85.56, 96.93]	75.49 [39.11, 100.00]	78.96 [71.74, 87.86]

A(H1N1)	POS	52.01 [21.47, 100.00]	54.22 [23.20, 82.95]	77.08 [31.90, 100.00]	95.24 [85.56, 96.93]	77.01 [39.90, 100.00]	81.72 [72.04, 87.86]
A(H1N1)	NEG	0.00 [0.00, 0.00]	0.00 [0.00, 0.00]	21.51 [8.77, 52.72]	19.20 [7.99, 37.17]	27.46 [14.12, 53.41]	27.50 [20.89, 36.10]
A(H3)	A(H5)	0.00 [0.00, 0.00]	0.00 [0.00, 0.00]	34.69 [14.26, 84.38]	39.39 [38.45, 44.82]	31.60 [16.27, 61.35]	33.38 [24.69, 41.35]
A(H3)	A(UNS)	25.42 [10.40, 62.12]	25.56 [10.93, 41.49]	48.30 [19.92, 100.00]	59.52 [39.68, 69.23]	34.83 [17.95, 67.57]	37.36 [33.38, 42.43]
A(H3)	FLUA	25.65 [10.50, 62.67]	25.56 [10.93, 42.22]	57.52 [23.76, 100.00]	59.59 [52.79, 81.82]	39.84 [20.56, 77.20]	41.35 [35.63, 45.11]
A(H3)	B(YAM)	25.05 [10.25, 61.25]	25.56 [10.93, 39.97]	39.07 [16.08, 94.93]	46.99 [39.46, 49.38]	33.04 [17.02, 64.12]	33.82 [29.98, 41.06]
A(H3)	B(VIC)	24.90 [10.18, 60.86]	25.56 [10.93, 39.97]	39.03 [16.06, 94.82]	46.99 [39.39, 49.38]	32.70 [16.85, 63.47]	33.82 [30.05, 40.98]
A(H3)	B(UND)	25.11 [10.27, 61.38]	25.56 [10.93, 40.70]	52.48 [21.66, 100.00]	59.23 [47.43, 73.21]	36.22 [18.68, 70.24]	37.15 [33.82, 41.20]
A(H3)	FLUB	25.27 [10.34, 61.77]	25.56 [10.93, 40.70]	52.56 [21.69, 100.00]	59.52 [47.50, 73.21]	37.16 [19.17, 72.05]	39.25 [35.26, 41.35]
A(H3)	POS	25.65 [10.50, 62.67]	25.56 [10.93, 42.22]	57.52 [23.76, 100.00]	59.59 [52.79, 81.82]	39.84 [20.56, 77.20]	41.35 [35.63, 45.11]
A(H3)	NEG	0.00 [0.00, 0.00]	0.00 [0.00, 0.00]	10.14 [4.05, 25.41]	9.05 [3.77, 17.52]	12.95 [6.57, 25.50]	12.89 [8.76, 17.02]
A(H5)	A(UNS)	0.00 [0.00, 0.00]	0.00 [0.00, 0.00]	33.92 [13.94, 82.54]	39.32 [38.45, 44.82]	30.53 [15.72, 59.29]	33.38 [24.19, 41.35]
A(H5)	FLUA	0.00 [0.00, 0.00]	0.00 [0.00, 0.00]	34.69 [14.26, 84.38]	39.39 [38.45, 44.82]	31.74 [16.35, 61.63]	33.38 [25.85, 41.35]
A(H5)	B(YAM)	0.00 [0.00, 0.00]	0.00 [0.00, 0.00]	33.93 [13.94, 82.57]	39.39 [38.45, 44.82]	30.59 [15.75, 59.42]	33.38 [25.85, 40.84]
A(H5)	B(VIC)	0.00 [0.00, 0.00]	0.00 [0.00, 0.00]	33.93 [13.94, 82.57]	39.39 [38.45, 44.82]	30.61 [15.76, 59.45]	33.38 [25.85, 40.84]
A(H5)	B(UND)	0.00 [0.00, 0.00]	0.00 [0.00, 0.00]	34.69 [14.26, 84.38]	39.39 [38.45, 44.82]	31.42 [16.18, 61.01]	33.38 [25.42, 41.20]
A(H5)	FLUB	0.00 [0.00, 0.00]	0.00 [0.00, 0.00]	34.69 [14.26, 84.38]	39.39 [38.45, 44.82]	31.49 [16.22, 61.15]	33.38 [25.85, 41.27]
A(H5)	POS	0.00 [0.00, 0.00]	0.00 [0.00, 0.00]	34.69 [14.26, 84.38]	39.39 [38.45, 44.82]	31.74 [16.35, 61.63]	33.38 [25.85, 41.35]
A(H5)	NEG	0.00 [0.00, 0.00]	0.00 [0.00, 0.00]	9.67 [3.85, 24.29]	8.62 [3.77, 15.64]	10.31 [5.20, 20.43]	10.93 [8.25, 15.64]
A(UNS)	FLUA	25.66 [10.50, 62.71]	25.56 [10.93, 41.49]	48.30 [19.92, 100.00]	59.52 [39.68, 69.23]	35.19 [18.14, 68.26]	37.44 [33.38, 42.65]
A(UNS)	B(YAM)	24.91 [10.19, 60.90]	25.56 [10.93, 40.04]	37.87 [15.58, 92.04]	43.59 [39.32, 46.99]	31.10 [16.01, 60.39]	33.38 [27.66, 40.70]
A(UNS)	B(VIC)	24.90 [10.18, 60.86]	25.56 [10.93, 39.97]	37.84 [15.57, 91.97]	43.59 [39.32, 46.99]	31.13 [16.03, 60.45]	33.38 [27.73, 40.70]
A(UNS)	B(UND)	25.34 [10.37, 61.94]	25.56 [10.93, 41.49]	46.55 [19.19, 100.00]	59.16 [39.68, 63.07]	33.07 [17.04, 64.18]	37.15 [29.25, 41.13]
A(UNS)	FLUB	25.34 [10.37, 61.94]	25.56 [10.93, 41.49]	46.60 [19.22, 100.00]	59.45 [39.68, 63.07]	33.15 [17.08, 64.33]	37.22 [29.33, 41.13]
A(UNS)	POS	25.66 [10.50, 62.71]	25.56 [10.93, 41.49]	48.30 [19.92, 100.00]	59.52 [39.68, 69.23]	35.19 [18.14, 68.26]	37.44 [33.38, 42.65]
A(UNS)	NEG	0.00 [0.00, 0.00]	0.00 [0.00, 0.00]	8.95 [3.55, 22.55]	8.54 [0.00, 15.86]	9.39 [4.72, 18.67]	10.79 [0.65, 15.86]
FLUA	B(YAM)	25.11 [10.27, 61.38]	25.56 [10.93, 40.19]	39.09 [16.09, 94.96]	46.99 [39.46, 49.38]	33.25 [17.13, 64.54]	33.82 [31.21, 41.06]
FLUA	B(VIC)	24.90 [10.18, 60.86]	25.56 [10.93, 39.97]	39.04 [16.07, 94.86]	46.99 [39.39, 49.38]	32.96 [16.98, 63.96]	33.82 [31.28, 40.98]
FLUA	B(UND)	25.34 [10.37, 61.94]	25.56 [10.93, 41.49]	52.67 [21.74, 127.60]	59.30 [48.15, 73.21]	36.98 [19.07, 71.69]	37.58 [33.82, 41.49]
FLUA	FLUB	25.55 [10.45, 62.43]	25.56 [10.93, 42.00]	52.74 [21.77, 100.00]	59.59 [48.23, 73.21]	37.98 [19.59, 73.61]	40.91 [35.34, 41.56]
FLUA	POS	26.04 [10.66, 63.61]	25.56 [10.93, 42.80]	58.03 [23.97, 100.00]	59.74 [54.82, 82.19]	41.10 [21.22, 79.61]	41.49 [35.92, 49.96]
FLUA	NEG	0.00 [0.00, 0.00]	0.00 [0.00, 0.00]	10.14 [4.05, 25.41]	9.05 [3.77, 17.52]	13.28 [6.74, 26.14]	12.96 [9.92, 17.02]
B(YAM)	B(VIC)	24.90 [10.18, 60.86]	25.56 [10.93, 39.97]	39.04 [16.07, 94.86]	46.99 [39.39, 49.38]	32.84 [16.92, 63.75]	33.82 [31.21, 40.98]
B(YAM)	B(UND)	24.91 [10.19, 60.90]	25.56 [10.93, 40.04]	39.02 [16.06, 94.79]	46.99 [39.39, 49.38]	32.53 [16.76, 63.14]	33.74 [30.77, 40.98]
B(YAM)	FLUB	25.11 [10.27, 61.38]	25.56 [10.93, 40.19]	39.09 [16.09, 94.96]	46.99 [39.46, 49.38]	33.51 [17.27, 65.03]	34.40 [31.21, 41.06]
B(YAM)	POS	25.11 [10.27, 61.38]	25.56 [10.93, 40.19]	39.09 [16.09, 94.96]	46.99 [39.46, 49.38]	33.51 [17.27, 65.03]	34.40 [31.21, 41.06]
B(YAM)	NEG	0.00 [0.00, 0.00]	0.00 [0.00, 0.00]	9.30 [3.70, 23.39]	8.62 [0.00, 17.52]	10.75 [5.43, 21.28]	10.50 [7.17, 16.51]
B(VIC)	B(UND)	24.90 [10.18, 60.86]	25.56 [10.93, 39.97]	38.99 [16.05, 94.72]	46.99 [39.39, 49.38]	32.41 [16.69, 62.91]	33.74 [30.85, 40.98]
B(VIC)	FLUB	24.90 [10.18, 60.86]	25.56 [10.93, 39.97]	39.04 [16.07, 94.86]	46.99 [39.39, 49.38]	33.13 [17.07, 64.30]	33.82 [31.28, 40.98]
B(VIC)	POS	24.90 [10.18, 60.86]	25.56 [10.93, 39.97]	39.04 [16.07, 94.86]	46.99 [39.39, 49.38]	33.13 [17.07, 64.30]	33.82 [31.28, 40.98]
B(VIC)	NEG	0.00 [0.00, 0.00]	0.00 [0.00, 0.00]	9.30 [3.70, 23.39]	8.62 [0.00, 17.52]	10.40 [5.25, 20.62]	9.20 [7.31, 16.73]
B(UND)	FLUB	25.36 [10.38, 61.98]	25.56 [10.93, 41.49]	52.95 [21.86, 100.00]	59.3 [49.09, 73.35]	37.84 [19.52, 73.35]	38.16 [33.82, 42.29]
B(UND)	POS	25.36 [10.38, 61.98]	25.56 [10.93, 41.49]	52.95 [21.86, 100.00]	59.3 [49.09, 73.35]	37.84 [19.52, 73.35]	38.16 [33.82, 42.29]
B(UND)	NEG	0.00 [0.00, 0.00]	0.00 [0.00, 0.00]	10.14 [4.05, 25.41]	9.05 [3.77, 17.52]	12.41 [6.29, 24.47]	12.67 [9.63, 17.31]
FLUB	POS	25.56 [10.46, 62.46]	25.56 [10.93, 42.07]	53.02 [21.89, 100.00]	59.59 [49.17, 73.35]	38.95 [20.10, 75.48]	41.56 [36.06, 42.72]
FLUB	NEG	0.00 [0.00, 0.00]	0.00 [0.00, 0.00]	10.14 [4.05, 25.41]	9.05 [3.77, 17.52]	13.14 [6.67, 25.88]	12.67 [9.63, 17.74]
POS	NEG	0.00 [0.00, 0.00]	0.00 [0.00, 0.00]	10.14 [4.05, 25.41]	9.05 [3.77, 17.52]	13.70 [6.96, 26.96]	12.96 [11.01, 17.74]

Supplementary Table S33. Average and median *outcome interoperability* for 14 influenza test outcomes worldwide and in 2 transmission zones (SE-As – Southeast Asia; O-M-P – Oceania Melanesia Polynesia). We extracted FluNet data from 173 Member States on 15 June 2021. We calculated *outcome interoperability* as the number of time points that 2 testing outcomes (defined below as *Outcome 1* and *Outcome 2*) in the same Member State have jointly non-missing records per total time points within a study period and multiplied by 100. Maximal time points included 1381 weeks for all testing outcomes except A(H1N1)pdm09 positives, for which the maximal time points was 651 weeks. We report average and median *outcome interoperability* with 95% confidence intervals (left column) and lower and upper quartiles (right column) for each geographic location.

Outcome 1	Outcome 2	Mean [LCI, UCI] SE-As	Med. [LQR, UQR] SE-As	Mean [LCI, UCI] O-M-P	Med. [LQR, UQR] O-M-P
SPE	TES	36.52 [19.49, 68.46]	41.31 [24.62, 46.63]	27.85 [11.41, 67.96]	36.78 [18.10, 39.83]
SPE	A(H1)	24.39 [12.96, 45.90]	23.93 [20.85, 36.21]	21.59 [8.81, 52.93]	22.66 [18.10, 26.43]
SPE	A(H1N1)	77.19 [41.37, 100.00]	87.63 [52.07, 98.92]	58.62 [24.22, 100.00]	61.60 [38.40, 78.96]
SPE	A(H3)	36.43 [19.44, 68.28]	41.31 [24.62, 46.63]	27.99 [11.47, 68.31]	29.54 [18.10, 38.60]
SPE	A(H5)	32.93 [17.55, 61.77]	36.31 [23.32, 42.72]	26.46 [10.83, 64.62]	27.01 [18.10, 35.19]
SPE	A(UNS)	31.91 [17.01, 59.88]	37.00 [23.46, 43.37]	28.07 [11.50, 68.48]	27.15 [18.10, 39.97]
SPE	FLUA	36.52 [19.48, 68.44]	41.31 [24.62, 46.63]	29.14 [11.95, 71.06]	30.56 [18.10, 40.04]
SPE	B(YAM)	33.04 [17.61, 61.98]	36.42 [23.32, 42.94]	26.53 [10.86, 64.79]	26.36 [18.10, 36.57]
SPE	B(VIC)	32.95 [17.56, 61.81]	36.50 [23.32, 41.64]	26.60 [10.89, 64.97]	26.65 [18.10, 36.57]
SPE	B(UND)	36.26 [19.34, 67.96]	41.31 [24.40, 46.56]	27.72 [11.36, 67.65]	29.40 [13.40, 39.39]
SPE	FLUB	36.48 [19.46, 68.38]	41.31 [24.40, 46.56]	28.79 [11.80, 70.22]	29.91 [18.10, 39.54]
SPE	POS	36.52 [19.49, 68.46]	41.31 [24.62, 46.63]	29.49 [12.09, 71.89]	32.30 [18.10, 40.04]
SPE	NEG	12.69 [6.67, 24.16]	13.43 [6.44, 19.04]	11.44 [4.59, 28.54]	12.24 [9.63, 14.77]
TES	A(H1)	38.19 [20.38, 71.55]	40.12 [21.00, 54.24]	32.77 [13.46, 79.79]	26.43 [18.10, 44.68]
TES	A(H1N1)	87.37 [46.85, 100.00]	94.01 [84.64, 99.54]	58.37 [24.11, 100.00]	61.60 [38.40, 86.02]
TES	A(H3)	50.67 [27.10, 94.75]	54.45 [39.90, 65.46]	42.72 [17.60, 100.00]	29.54 [21.14, 61.98]
TES	A(H5)	37.37 [19.94, 70.03]	41.31 [28.46, 45.33]	24.10 [9.85, 58.95]	27.01 [18.10, 35.12]
TES	A(UNS)	43.16 [23.06, 80.80]	43.19 [34.18, 53.80]	44.00 [18.13, 100.00]	27.15 [21.14, 67.41]
TES	FLUA	51.00 [27.27, 95.36]	54.53 [39.90, 65.82]	45.91 [18.93, 100.00]	30.56 [22.66, 67.70]
TES	B(YAM)	37.51 [20.02, 70.29]	41.42 [31.43, 44.97]	27.98 [11.47, 68.27]	26.36 [18.10, 42.43]
TES	B(VIC)	37.40 [19.96, 70.08]	40.77 [31.43, 45.11]	28.05 [11.50, 68.45]	26.65 [18.10, 42.43]
TES	B(UND)	43.51 [23.25, 81.44]	48.73 [35.12, 56.48]	34.60 [14.22, 84.18]	29.40 [15.50, 48.30]
TES	FLUB	45.76 [24.45, 85.62]	53.84 [39.90, 56.48]	35.68 [14.67, 86.78]	29.91 [18.10, 48.52]
TES	POS	51.11 [27.33, 95.56]	54.53 [39.90, 65.82]	46.50 [19.18, 100.00]	32.30 [23.17, 68.28]
TES	NEG	12.69 [6.67, 24.16]	13.43 [6.44, 19.04]	14.35 [5.80, 35.53]	14.77 [9.63, 15.42]
A(H1)	A(H1N1)	61.20 [32.76, 100.00]	55.38 [44.55, 96.16]	45.35 [18.69, 100.00]	44.85 [38.40, 56.07]
A(H1)	A(H3)	38.29 [20.44, 71.74]	40.08 [21.00, 54.31]	35.16 [14.46, 85.53]	26.43 [24.91, 44.75]
A(H1)	A(H5)	28.34 [15.09, 53.25]	26.39 [20.85, 42.65]	20.91 [8.53, 51.29]	20.93 [18.10, 26.43]
A(H1)	A(UNS)	35.19 [18.77, 65.98]	31.35 [21.00, 50.04]	35.08 [14.42, 85.32]	26.43 [24.76, 44.90]
A(H1)	FLUA	38.46 [20.53, 72.06]	40.66 [21.00, 54.31]	35.38 [14.55, 86.05]	26.43 [25.78, 44.97]
A(H1)	B(YAM)	28.08 [14.94, 52.76]	26.10 [20.85, 42.51]	23.06 [9.42, 56.44]	26.29 [18.10, 28.24]
A(H1)	B(VIC)	28.08 [14.94, 52.76]	26.10 [20.85, 42.65]	23.04 [9.41, 56.41]	26.21 [18.10, 28.24]
A(H1)	B(UND)	30.98 [16.51, 58.16]	33.42 [21.00, 48.88]	26.14 [10.70, 63.86]	26.43 [19.33, 31.14]
A(H1)	FLUB	33.16 [17.68, 62.20]	36.78 [21.00, 49.60]	27.08 [11.09, 66.12]	26.43 [19.33, 31.14]
A(H1)	POS	38.46 [20.53, 72.06]	40.66 [21.00, 54.31]	35.38 [14.55, 86.05]	26.43 [25.78, 44.97]
A(H1)	NEG	3.01 [1.47, 6.16]	1.63 [1.09, 2.61]	3.07 [1.12, 8.42]	0.29 [0.00, 0.29]
A(H1N1)	A(H3)	87.16 [46.73, 100.00]	94.39 [84.64, 99.08]	63.32 [26.17, 100.00]	59.60 [40.86, 86.02]
A(H1N1)	A(H5)	79.46 [42.59, 100.00]	87.63 [59.29, 97.70]	56.28 [23.25, 100.00]	57.30 [38.40, 74.65]
A(H1N1)	A(UNS)	72.83 [39.02, 100.00]	78.49 [59.75, 98.62]	61.32 [25.34, 100.00]	57.45 [40.71, 78.34]
A(H1N1)	FLUA	87.68 [47.01, 100.00]	95.24 [84.64, 99.85]	63.81 [26.38, 100.00]	61.60 [40.86, 86.33]
A(H1N1)	B(YAM)	79.03 [42.36, 100.00]	87.94 [66.67, 95.39]	59.42 [24.55, 100.00]	55.91 [38.40, 74.65]
A(H1N1)	B(VIC)	78.85 [42.26, 100.00]	86.56 [66.67, 95.70]	59.42 [24.55, 100.00]	55.76 [38.40, 74.65]
A(H1N1)	B(UND)	82.92 [44.45, 100.00]	91.17 [74.50, 98.62]	60.40 [24.96, 100.00]	57.45 [39.78, 86.02]
A(H1N1)	FLUB	87.57 [46.95, 100.00]	95.16 [84.64, 99.54]	62.55 [25.85, 100.00]	57.76 [39.78, 86.02]

A(H1N1)	POS	87.68 [47.01, 100.00]	95.24 [84.64, 99.85]	63.81 [26.38, 100.00]	61.60 [40.86, 86.33]
A(H1N1)	NEG	26.93 [14.32, 50.62]	28.49 [13.67, 40.40]	24.64 [10.08, 60.25]	31.34 [11.37, 32.87]
A(H3)	A(H5)	37.52 [20.02, 70.30]	41.31 [28.53, 46.13]	26.52 [10.86, 64.76]	27.01 [18.10, 35.19]
A(H3)	A(UNS)	43.22 [23.09, 80.91]	43.19 [34.25, 54.89]	43.69 [18.01, 100.00]	32.66 [27.01, 62.06]
A(H3)	FLUA	50.86 [27.20, 95.10]	55.03 [39.90, 65.75]	45.42 [18.72, 100.00]	33.96 [29.54, 62.49]
A(H3)	B(YAM)	37.60 [20.06, 70.45]	41.46 [31.43, 44.97]	30.40 [12.47, 74.08]	26.36 [18.90, 42.51]
A(H3)	B(VIC)	37.55 [20.04, 70.35]	40.80 [31.43, 45.11]	30.40 [12.47, 74.08]	26.29 [18.90, 42.51]
A(H3)	B(UND)	43.37 [23.17, 81.17]	49.13 [35.19, 54.09]	35.19 [14.47, 85.60]	27.73 [27.23, 47.14]
A(H3)	FLUB	45.56 [24.35, 85.25]	53.87 [39.90, 55.10]	36.21 [14.89, 88.04]	27.88 [27.23, 47.36]
A(H3)	POS	50.86 [27.20, 95.10]	55.03 [39.90, 65.75]	45.42 [18.72, 100.00]	33.96 [29.54, 62.49]
A(H3)	NEG	12.69 [6.66, 24.15]	13.43 [6.44, 18.97]	11.96 [4.80, 29.79]	14.77 [6.52, 15.42]
A(H5)	A(UNS)	32.93 [17.55, 61.78]	37.00 [28.46, 45.11]	26.52 [10.86, 64.76]	27.01 [18.10, 35.19]
A(H5)	FLUA	37.52 [20.02, 70.31]	41.31 [28.53, 46.13]	26.53 [10.86, 64.79]	27.01 [18.10, 35.19]
A(H5)	B(YAM)	35.66 [19.02, 66.86]	39.36 [27.95, 44.97]	26.29 [10.76, 64.20]	26.36 [18.10, 35.19]
A(H5)	B(VIC)	35.76 [19.07, 67.03]	39.36 [27.95, 45.11]	26.27 [10.76, 64.17]	26.21 [18.10, 35.19]
A(H5)	B(UND)	35.37 [18.86, 66.30]	39.36 [28.46, 45.11]	25.36 [10.38, 61.98]	26.57 [13.40, 35.19]
A(H5)	FLUB	37.52 [20.02, 70.30]	41.31 [28.46, 46.13]	26.36 [10.79, 64.38]	26.65 [18.10, 35.19]
A(H5)	POS	37.52 [20.02, 70.31]	41.31 [28.53, 46.13]	26.53 [10.86, 64.79]	27.01 [18.10, 35.19]
A(H5)	NEG	10.78 [5.64, 20.61]	11.80 [3.62, 18.83]	8.47 [3.35, 21.40]	12.45 [0.87, 14.27]
A(UNS)	FLUA	43.37 [23.17, 81.17]	43.19 [34.25, 54.96]	46.92 [19.35, 100.00]	34.03 [27.15, 69.08]
A(UNS)	B(YAM)	32.65 [17.40, 61.26]	36.46 [27.95, 44.53]	30.40 [12.47, 74.08]	26.36 [18.90, 42.51]
A(UNS)	B(VIC)	32.71 [17.43, 61.36]	36.46 [28.17, 44.53]	30.40 [12.47, 74.08]	26.29 [18.90, 42.51]
A(UNS)	B(UND)	38.00 [20.28, 71.20]	40.37 [34.25, 53.80]	35.42 [14.56, 86.16]	26.86 [26.57, 48.15]
A(UNS)	FLUB	38.07 [20.32, 71.34]	40.37 [34.25, 53.80]	36.44 [14.99, 88.59]	26.86 [26.72, 48.37]
A(UNS)	POS	43.37 [23.17, 81.17]	43.19 [34.25, 54.96]	46.92 [19.35, 100.00]	34.03 [27.15, 69.08]
A(UNS)	NEG	8.65 [4.50, 16.65]	6.99 [2.03, 18.83]	11.66 [4.68, 29.06]	14.77 [6.52, 15.50]
FLUA	B(YAM)	37.66 [20.10, 70.57]	41.46 [31.43, 44.97]	30.41 [12.48, 74.12]	26.36 [18.90, 42.51]
FLUA	B(VIC)	37.55 [20.04, 70.37]	40.80 [31.43, 45.11]	30.44 [12.49, 74.19]	26.43 [18.90, 42.51]
FLUA	B(UND)	43.61 [23.30, 81.62]	49.24 [35.19, 55.68]	36.74 [15.11, 89.32]	27.88 [27.88, 48.23]
FLUA	FLUB	45.84 [24.50, 85.78]	54.45 [39.90, 55.68]	37.78 [15.55, 91.83]	28.17 [27.88, 48.44]
FLUA	POS	51.32 [27.45, 95.95]	55.14 [39.90, 67.27]	48.94 [20.19, 100.00]	35.84 [30.56, 69.51]
FLUA	NEG	12.69 [6.67, 24.16]	13.43 [6.44, 19.04]	13.11 [5.28, 32.54]	14.77 [6.52, 15.5]
B(YAM)	B(VIC)	37.32 [19.92, 69.94]	40.19 [31.43, 44.97]	30.38 [12.47, 74.05]	26.21 [18.90, 42.51]
B(YAM)	B(UND)	35.43 [18.90, 66.42]	39.54 [31.43, 44.53]	29.43 [12.07, 71.75]	26.29 [18.90, 42.51]
B(YAM)	FLUB	37.68 [20.11, 70.60]	41.46 [31.43, 44.97]	30.41 [12.48, 74.12]	26.36 [18.90, 42.51]
B(YAM)	POS	37.68 [20.11, 70.60]	41.46 [31.43, 44.97]	30.41 [12.48, 74.12]	26.36 [18.90, 42.51]
B(YAM)	NEG	10.88 [5.69, 20.79]	10.50 [3.77, 18.83]	10.24 [4.09, 25.65]	14.27 [6.52, 14.77]
B(VIC)	B(UND)	35.37 [18.87, 66.32]	39.54 [31.43, 44.53]	29.41 [12.06, 71.72]	26.21 [18.90, 42.51]
B(VIC)	FLUB	37.55 [20.04, 70.37]	40.80 [31.43, 45.11]	30.49 [12.51, 74.29]	26.65 [18.90, 42.51]
B(VIC)	POS	37.55 [20.04, 70.37]	40.80 [31.43, 45.11]	30.49 [12.51, 74.29]	26.65 [18.90, 42.51]
B(VIC)	NEG	10.83 [5.66, 20.69]	10.50 [3.77, 18.83]	10.33 [4.12, 25.86]	14.27 [6.52, 14.77]
B(UND)	FLUB	43.77 [23.38, 81.91]	49.35 [35.19, 56.48]	37.44 [15.40, 90.99]	29.40 [28.82, 49.02]
B(UND)	POS	43.77 [23.38, 81.91]	49.35 [35.19, 56.48]	37.44 [15.40, 90.99]	29.40 [28.82, 49.02]
B(UND)	NEG	12.58 [6.61, 23.95]	13.43 [6.44, 19.04]	12.01 [4.82, 29.89]	10.72 [6.52, 15.28]
FLUB	POS	46.02 [24.59, 86.10]	54.45 [39.90, 56.48]	38.52 [15.85, 93.60]	29.91 [28.82, 49.24]
FLUB	NEG	12.69 [6.67, 24.16]	13.43 [6.52, 19.04]	12.96 [5.22, 32.19]	14.77 [6.52, 15.50]
POS	NEG	12.70 [6.67, 24.18]	13.43 [6.52, 19.04]	13.45 [5.42, 33.37]	14.77 [6.52, 15.50]

Supplementary Table S34. Average and median *correctness* for 5 test outcomes in 6 WHO regions and 17 influenza transmission zones. We extracted FluNet data from 173 Member States on 15 June 2021. We calculated specimens collected (SPE) *correctness* as the percentage of weeks when specimens were less than or equal to tests. We calculated tests' *correctness* (TES) as the percentage of weeks when tests equaled the sum of total positives and negatives. We calculated positives' *correctness* (POS) as the percentage of weeks when positives equaled the sum of influenza A and B positives. We calculated influenza A and B positives' *correctness* (FLUA and FLUB, respectively) as the percentage of weeks where strain positives equaled the sum of all respectively subtypes. We calculated correctness only if all outcomes were complete. We report average *correctness* with 95% confidence intervals (top values) and median *correctness* with lower and upper quartiles (bottom values). Regions and zones are listed in descending order by tests' *correctness*, regions, and zones. We omit the Southern African transmission zone, as it only consisted of 1 country (South Africa). Member State-outcome dyads where weeks had incomplete records were denoted as *Missing*.

Region	SPE	TES	POS	FLUA	FLUB
PAHO	88.95 [79.00, 98.90] 98.71 [91.21, 100.00]	98.81 [97.68, 99.94] 100.00 [100.00, 100.00]	100.00 [100.00, 100.00] 100.00 [100.00, 100.00]	99.44 [98.60, 100.00] 100.00 [100.00, 100.00]	89.40 [81.52, 97.27] 100.00 [91.13, 100.00]
SEARO	98.93 [97.22, 100.65] 99.84 [99.50, 100.00]	91.80 [87.90, 95.70] 92.16 [90.38, 96.10]	100.00 [100.00, 100.00] 100.00 [100.00, 100.00]	99.53 [98.60, 100.00] 100.00 [100.00, 100.00]	86.34 [67.25, 105.43] 97.10 [91.30, 100.00]
AFRO	98.50 [96.98, 100.00] 100.00 [99.78, 100.00]	85.89 [77.46, 94.32] 93.17 [84.42, 96.52]	100.00 [100.00, 100.00] 100.00 [100.00, 100.00]	99.97 [99.90, 100.00] 100.00 [100.00, 100.00]	93.07 [86.82, 99.33] 100.00 [97.12, 100.00]
WPRO	94.98 [88.26, 100.00] 99.76 [98.40, 100.00]	75.89 [59.60, 92.18] 82.81 [70.03, 97.53]	100.00 [100.00, 100.00] 100.00 [100.00, 100.00]	98.95 [97.73, 100.00] 100.00 [99.19, 100.00]	89.56 [75.85, 100.00] 100.00 [98.18, 100.00]
EMRO	98.95 [97.36, 100.00] 99.81 [99.56, 100.00]	75.56 [61.91, 89.21] 89.28 [66.09, 95.02]	100.00 [100.00, 100.00] 100.00 [100.00, 100.00]	100.00 [100.00, 100.00] 100.00 [100.00, 100.00]	91.88 [77.98, 100.00] 100.00 [98.81, 100.00]
EURO	74.40 [59.58, 89.22] 93.34 [64.27, 100.00]	26.98 [0.00, 70.69] 7.45 [0.00, 53.97]	100.00 [100.00, 100.00] 100.00 [100.00, 100.00]	99.97 [99.92, 100.00] 100.00 [100.00, 100.00]	99.94 [99.89, 99.99] 100.00 [100.00, 100.00]
Zone					
Central America and Caribbean	94.28 [88.15, 100.00] 98.83 [91.51, 100.00]	99.91 [99.73, 100.00] 100.00 [100.00, 100.00]	100.00 [100.00, 100.00] 100.00 [100.00, 100.00]	99.76 [99.29, 100.00] 100.00 [100.00, 100.00]	82.90 [68.57, 97.23] 100.00 [65.79, 100.00]
Temperate South America	76.64 [33.51, 100.00] 97.96 [53.98, 99.30]	98.05 [95.84, 100.00] 98.21 [96.11, 100.00]	100.00 [100.00, 100.00] 100.00 [100.00, 100.00]	99.91 [99.74, 100.00] 100.00 [99.73, 100.00]	97.99 [94.06, 100.00] 100.00 [95.99, 100.00]
Tropical South America	84.86 [64.76, 100.00] 96.59 [81.51, 100.00]	96.22 [91.35, 100.00] 100.00 [94.06, 100.00]	100.00 [100.00, 100.00] 100.00 [100.00, 100.00]	100.00 [100.00, 100.00] 100.00 [100.00, 100.00]	94.62 [89.07, 100.16] 99.42 [89.90, 100.00]
Western Africa	99.49 [98.80, 100.00] 99.85 [99.69, 100.00]	95.06 [92.24, 97.89] 94.72 [93.12, 100.00]	100.00 [100.00, 100.00] 100.00 [100.00, 100.00]	99.92 [99.76, 100.00] 100.00 [100.00, 100.00]	89.88 [75.26, 100.00] 100.00 [90.00, 100.00]
North America	99.84 [99.82, 99.85] 99.84 [99.83, 99.85]	94.93 [94.93, 94.93] 94.93 [94.93, 94.93]	100.00 [100.00, 100.00] 100.00 [100.00, 100.00]	95.45 [87.11, 100.00] 95.45 [91.19, 99.70]	100.00 [100.00, 100.00] 100.00 [100.00, 100.00]
Southern Asia	98.73 [96.64, 100.00] 99.83 [99.79, 100.00]	87.31 [80.87, 93.74] 91.49 [82.56, 92.47]	100.00 [100.00, 100.00] 100.00 [100.00, 100.00]	99.59 [98.78, 100.00] 100.00 [100.00, 100.00]	95.93 [92.26, 99.61] 97.45 [94.65, 100.00]
Southeast Asia	97.93 [94.83, 100.00] 99.76 [99.50, 100.00]	85.65 [73.35, 97.95] 96.10 [77.53, 97.46]	100.00 [100.00, 100.00] 100.00 [100.00, 100.00]	99.34 [98.54, 100.00] 100.00 [98.91, 100.00]	84.18 [62.74, 100.00] 100.00 [98.98, 100.00]
Northern Africa	99.84 [99.54, 100.15] 100.00 [100.00, 100.00]	85.52 [73.51, 97.54] 87.89 [77.39, 93.66]	100.00 [100.00, 100.00] 100.00 [100.00, 100.00]	100.00 [100.00, 100.00] 100.00 [100.00, 100.00]	97.63 [94.61, 100.64] 98.70 [95.85, 99.40]
Oceania Melanesia Polynesia	90.30 [71.94, 108.65] 99.82 [98.82, 100.00]	84.59 [72.82, 96.37] 88.10 [75.00, 94.61]	100.00 [100.00, 100.00] 100.00 [100.00, 100.00]	99.92 [99.76, 100.00] 100.00 [100.00, 100.00]	81.06 [44.84, 100.00] 100.00 [98.18, 100.00]
Eastern Africa	96.82 [92.56, 100.00] 99.91 [99.75, 100.00]	80.37 [62.97, 97.76] 84.98 [75.00, 95.53]	100.00 [100.00, 100.00] 100.00 [100.00, 100.00]	100.00 [100.00, 100.00] 100.00 [100.00, 100.00]	95.05 [86.26, 100.00] 100.00 [100.00, 100.00]
Western Asia	98.65 [96.49, 100.00] 99.80 [99.56, 100.00]	69.94 [49.28, 90.60] 88.18 [36.36, 95.67]	100.00 [100.00, 100.00] 100.00 [100.00, 100.00]	100.00 [100.00, 100.00] 100.00 [100.00, 100.00]	92.46 [78.49, 100.00] 100.00 [100.00, 100.00]
Eastern Asia	99.60 [98.81, 100.00] 100.00 [99.20, 100.00]	63.35 [3.15, 100.00] 90.38 [2.07, 97.60]	100.00 [100.00, 100.00] 100.00 [100.00, 100.00]	97.50 [93.11, 100.00] 99.60 [94.99, 100.00]	99.06 [97.21, 100.00] 100.00 [98.11, 100.00]
Middle Africa	98.95 [96.94, 100.96] 100.00 [99.84, 100.00]	55.20 [0.46, 100.00] 55.20 [27.27, 83.13]	100.00 [100.00, 100.00] 100.00 [100.00, 100.00]	100.00 [100.00, 100.00] 100.00 [100.00, 100.00]	93.13 [83.88, 100.00] 100.00 [86.50, 100.00]
Southwest Europe	68.81 [44.55, 93.07] 81.78 [50.56, 98.00]	35.98 [0.00, 92.53] 14.89 [0.00, 93.04]	100.00 [100.00, 100.00] 100.00 [100.00, 100.00]	99.95 [99.85, 100.00] 100.00 [100.00, 100.00]	99.93 [99.84, 100.00] 100.00 [100.00, 100.00]
Eastern Europe	41.11 [0.00, 84.76] 36.06 [3.92, 78.29]	0.00 [0.00, 0.00] 0.00 [0.00, 0.00]	100.00 [100.00, 100.00] 100.00 [100.00, 100.00]	99.93 [99.80, 100.00] 100.00 [99.87, 100.00]	100.00 [100.00, 100.00] 100.00 [100.00, 100.00]
Northern Europe	93.31 [84.24, 100.00] 100.00 [84.21, 100.00]	*Missing*	100.00 [100.00, 100.00] 100.00 [100.00, 100.00]	100.00 [100.00, 100.00] 100.00 [100.00, 100.00]	99.82 [99.66, 99.98] 100.00 [99.67, 100.00]
Central Asia	*Missing*	*Missing*	100.00 [100.00, 100.00] 100.00 [100.00, 100.00]	*Missing*	100.00 [100.00, 100.00] 100.00 [100.00, 100.00]
Worldwide	**91.97 [88.22, 95.73]** **99.83 [97.08, 100.00]**	**86.18 [81.44, 90.93]** **95.86 [87.76, 100.00]**	**100.00 [100.00, 100.00]** **100.00 [100.00, 100.00]**	**99.69 [99.44, 99.95]** **100.00 [100.00, 100.00]**	**93.76 [90.68, 96.83]** **100**.00 **[99.24, 100**.00**]**

Supplementary Table S35. Average and median *correctness* for 5 test outcomes in 6 WHO regions and 17 influenza transmission zones. We extracted FluNet data from 173 Member States on 15 June 2021. We calculated specimens collected (SPE) *correctness* as the percentage of weeks when specimens were less than or equal to tests. We calculated tests' *correctness* (TES) as the percentage of weeks when tests equaled the sum of total positives and negatives. We calculated positives' *correctness* (POS) as the percentage of weeks when positives equaled the sum of influenza A and B positives. We calculated influenza A and B positives' *correctness* (FLUA and FLUB, respectively) as the percentage of weeks where strain positives equaled the sum of all respectively subtypes. We calculated correctness if at least one test, disease, or strain/subtype outcome was complete, and assumed that missing values were equal to 0. We report average *correctness* with 95%CI (top values) and median *correctness* with IQR (bottom values). Regions and zones are listed in descending order by average tests' *correctness*, regions, and zones. Member State-outcome dyads where weeks had incomplete records were denoted as *Missing*.

Region	SPE	TES	POS	FLUA	FLUB
PAHO	88.95 [79.00, 98.90] 98.71 [91.21, 100.00]	92.47 [86.19, 98.74] 100.00 [100.00, 100.00]	100.00 [100.00, 100.00] 100.00 [100.00, 100.00]	99.46 [98.73, 100.00] 100.00 [100.00, 100.00]	100.00 [100.00, 100.00] 100.00 [100.00, 100.00]
SEARO	98.93 [97.22, 100.65] 99.84 [99.50, 100.00]	52.83 [33.58, 72.08] 49.26 [28.93, 90.38]	100.00 [100.00, 100.00] 100.00 [100.00, 100.00]	99.19 [97.86, 100.00] 100.00 [99.87, 100.00]	100.00 [100.00, 100.00] 100.00 [100.00, 100.00]
EMRO	98.95 [97.36, 100.54] 99.81 [99.56, 100.00]	40.36 [28.98, 51.73] 34.11 [24.11, 54.60]	100.00 [100.00, 100.00] 100.00 [100.00, 100.00]	99.95 [99.86, 100.00] 100.00 [100.00, 100.00]	100.00 [100.00, 100.00] 100.00 [100.00, 100.00]
WPRO	94.98 [88.26, 100.00] 99.76 [98.40, 100.00]	28.21 [14.63, 41.79] 25.23 [1.87, 43.77]	100.00 [100.00, 100.00] 100.00 [100.00, 100.00]	99.41 [98.80, 100.00] 100.00 [99.19, 100.00]	100.00 [100.00, 100.00] 100.00 [100.00, 100.00]
AFRO	98.50 [96.98, 100.00] 100.00 [99.78, 100.00]	27.66 [21.04, 34.28] 27.25 [11.07, 38.72]	100.00 [100.00, 100.00] 100.00 [100.00, 100.00]	99.82 [99.57, 100.00] 100.00 [100.00, 100.00]	100.00 [100.00, 100.00] 100.00 [100.00, 100.00]
EURO	74.40 [59.58, 89.22] 93.34 [64.27, 100.00]	14.08 [10.03, 18.14] 9.65 [2.77, 20.15]	100.00 [100.00, 100.00] 100.00 [100.00, 100.00]	99.95 [99.87, 100.00] 100.00 [100.00, 100.00]	100.00 [100.00, 100.00] 100.00 [100.00, 100.00]
Zone					
Central America and Caribbean	94.28 [88.15, 100.00] 98.83 [91.51, 100.00]	98.11 [95.51, 100.00] 100.00 [100.00, 100.00]	100.00 [100.00, 100.00] 100.00 [100.00, 100.00]	99.40 [98.27, 100.00] 100.00 [100.00, 100.00]	100.00 [100.00, 100.00] 100.00 [100.00, 100.00]
Temperate South America	76.64 [33.51, 100.00] 97.96 [53.98, 99.30]	97.72 [95.09, 100.35] 98.03 [95.44, 100.00]	100.00 [100.00, 100.00] 100.00 [100.00, 100.00]	99.98 [99.93, 100.00] 100.00 [99.95, 100.00]	100.00 [100.00, 100.00] 100.00 [100.00, 100.00]
Tropical South America	84.86 [64.76, 100.00] 96.59 [81.51, 100.00]	89.11 [74.91, 100.00] 100.00 [85.90, 100.00]	100.00 [100.00, 100.00] 100.00 [100.00, 100.00]	99.55 [98.95, 100.00] 100.00 [99.25, 100.00]	100.00 [100.00, 100.00] 100.00 [100.00, 100.00]
Oceania Melanesia Polynesia	90.30 [71.94, 100.00] 99.82 [98.82, 100.00]	48.00 [23.47, 72.52] 43.77 [24.48, 55.56]	100.00 [100.00, 100.00] 100.00 [100.00, 100.00]	99.76 [99.44, 100.00] 100.00 [99.60, 100.00]	100.00 [100.00, 100.00] 100.00 [100.00, 100.00]
North America	99.84 [99.82, 99.85] 99.84 [99.83, 99.85]	41.74 [0.00, 100.00] 25.22 [0.00, 100.00]	100.00 [100.00, 100.00] 100.00 [100.00, 100.00]	99.13 [97.53, 100.00] 99.90 [97.50, 100.00]	100.00 [100.00, 100.00] 100.00 [100.00, 100.00]
Southern Asia	98.73 [96.64, 100.00] 99.83 [99.79, 100.00]	38.95 [23.60, 54.30] 39.83 [20.29, 60.55]	100.00 [100.00, 100.00] 100.00 [100.00, 100.00]	99.00 [97.38, 100.00] 100.00 [99.87, 100.00]	100.00 [100.00, 100.00] 100.00 [100.00, 100.00]
Southeast Asia	97.93 [94.83, 100.00] 99.76 [99.50, 100.00]	37.90 [16.23, 59.57] 30.81 [11.87, 46.82]	100.00 [100.00, 100.00] 100.00 [100.00, 100.00]	99.77 [99.52, 100.00] 100.00 [99.69, 100.00]	100.00 [100.00, 100.00] 100.00 [100.00, 100.00]
Western Asia	98.65 [96.49, 100.00] 99.80 [99.56, 100.00]	34.11 [20.63, 47.59] 32.63 [4.77, 42.60]	100.00 [100.00, 100.00] 100.00 [100.00, 100.00]	99.95 [99.86, 100.00] 100.00 [100.00, 100.00]	100.00 [100.00, 100.00] 100.00 [100.00, 100.00]
Western Africa	99.49 [98.80, 100.00] 99.85 [99.69, 100.00]	32.20 [21.79, 42.6] 29.13 [21.40, 38.72]	100.00 [100.00, 100.00] 100.00 [100.00, 100.00]	99.90 [99.79, 100.00] 100.00 [99.84, 100.00]	100.00 [100.00, 100.00] 100.00 [100.00, 100.00]
Northern Africa	99.84 [99.54, 100.15] 100.00 [100.00, 100.00]	31.35 [23.45, 39.25] 28.57 [24.23, 34.11]	100.00 [100.00, 100.00] 100.00 [100.00, 100.00]	100.00 [100.00, 100.00] 100.00 [100.00, 100.00]	100.00 [100.00, 100.00] 100.00 [100.00, 100.00]
Eastern Asia	99.60 [98.81, 100.00] 100.00 [99.20, 100.00]	31.04 [0.00, 72.37] 16.57 [0.93, 61.15]	100.00 [100.00, 100.00] 100.00 [100.00, 100.00]	98.93 [97.11, 100.00] 100.00 [99.39, 100.00]	100.00 [100.00, 100.00] 100.00 [100.00, 100.00]
Middle Africa	98.95 [96.94, 100.00] 100.00 [99.84, 100.00]	24.32 [10.69, 37.96] 16.67 [8.15, 42.45]	100.00 [100.00, 100.00] 100.00 [100.00, 100.00]	100.00 [100.00, 100.00] 100.00 [100.00, 100.00]	100.00 [100.00, 100.00] 100.00 [100.00, 100.00]
Eastern Africa	96.82 [92.56, 100.00] 99.91 [99.75, 100.00]	23.07 [10.09, 36.05] 18.87 [5.18, 35.33]	100.00 [100.00, 100.00] 100.00 [100.00, 100.00]	99.58 [98.84, 100.00] 100.00 [100.00, 100.00]	100.00 [100.00, 100.00] 100.00 [100.00, 100.00]
Central Asia	*Missing*	22.78 [9.81, 35.76] 19.80 [12.63, 28.90]	100.00 [100.00, 100.00] 100.00 [100.00, 100.00]	99.63 [98.9, 100.00] 100.00 [100.00, 100.00]	100.00 [100.00, 100.00] 100.00 [100.00, 100.00]
Southwest Europe	68.81 [44.55, 93.07] 81.78 [50.56, 98.00]	15.20 [7.09, 23.31] 10.24 [5.76, 23.14]	100.00 [100.00, 100.00] 100.00 [100.00, 100.00]	99.97 [99.92, 100.00] 100.00 [100.00, 100.00]	100.00 [100.00, 100.00] 100.00 [100.00, 100.00]
Eastern Europe	41.11 [0.00, 84.76] 36.06 [3.92, 78.29]	11.81 [4.47, 19.15] 6.08 [2.77, 17.92]	100.00 [100.00, 100.00] 100.00 [100.00, 100.00]	99.99 [99.97, 100.00] 100.00 [100.00, 100.00]	100.00 [100.00, 100.00] 100.00 [100.00, 100.00]
Northern Europe	93.31 [84.24, 100.00] 100.00 [84.21, 100.00]	10.98 [4.94, 17.02] 9.57 [2.45, 17.69]	100.00 [100.00, 100.00] 100.00 [100.00, 100.00]	99.99 [99.97, 100.00] 100.00 [100.00, 100.00]	100.00 [100.00, 100.00] 100.00 [100.00, 100.00]
Worldwide	**91.97 [88.22, 95.73]** **99.83 [97.08, 100.00]**	**43.26 [37.65, 48.86]** **29.11 [10.81, 89.70]**	**100.00 [100.00, 100.00]** **100.00 [100.00, 100.00]**	**99.71 [99.49, 99.92]** **100.00 [100.00, 100.00]**	**100.00 [100.00, 100.00]** **100.00 [100.00, 100.00]**

Supplementary Table S36. The *correctness* of 173 Member States for 5 test outcomes reported by the WHO's FluNet. Data were downloaded on 15 June 2021 at which time the total time series length of reported data was 1381 weeks. We calculated specimens collected (SPE) *correctness* as the percentage of weeks when specimens were less than or equal to tests. We calculated tests' *correctness* (TES) as the percentage of weeks when tests equaled the sum of total positives and negatives. We calculated positives' *correctness* (POS) as the percentage of weeks when positives equaled the sum of influenza A and B positives. We calculated influenza A and B positives' *correctness* (FLUA and FLUB, respectively) as the percentage of weeks where strain positives equaled the sum of all respectively subtypes. We calculated correctness only if all outcomes were complete. Member States are listed in descending order by average *correctness* (AVG), region, and zone. We could not calculate *correctness* if any test, disease, or strain/subtype outcome was incomplete, denoted as *M*.

Region	Zone	Country/Territory	SPE	TES	POS	FLUA	FLUB	AVG
AFRO	Eastern Africa	Seychelles	100.00	M	100.00	M	100.00	100.00
AFRO	Middle Africa	Central African Republic	100.00	M	100.00	100.00	100.00	100.00
AFRO	Middle Africa	Chad	100.00	M	100.00	M	100.00	100.00
AFRO	Middle Africa	Congo	100.00	M	100.00	100.00	100.00	100.00
AFRO	Middle Africa	South Sudan	100.00	M	100.00	M	M	100.00
AFRO	Western Africa	Togo	100.00	100.00	100.00	100.00	100.00	100.00
EMRO	Northern Africa	Sudan	100.00	M	100.00	100.00	M	100.00
EMRO	Western Asia	Syrian Arab Republic	100.00	M	100.00	100.00	M	100.00
EURO	Central Asia	Kazakhstan	M	M	100.00	M	100.00	100.00
EURO	Central Asia	Kyrgyzstan	M	M	100.00	M	100.00	100.00
EURO	Central Asia	Tajikistan	M	M	100.00	M	100.00	100.00
EURO	Central Asia	Turkmenistan	M	M	100.00	M	100.00	100.00
EURO	Central Asia	Uzbekistan	M	M	100.00	M	100.00	100.00
EURO	Eastern Europe	Belarus	M	M	100.00	M	100.00	100.00
EURO	Eastern Europe	Bulgaria	M	M	100.00	M	100.00	100.00
EURO	Eastern Europe	Czechia	M	M	100.00	M	100.00	100.00
EURO	Eastern Europe	Hungary	M	M	100.00	M	100.00	100.00
EURO	Eastern Europe	Kosovo	M	M	100.00	M	100.00	100.00
EURO	Eastern Europe	Moldova	M	M	100.00	M	100.00	100.00
EURO	Eastern Europe	Slovakia	M	M	100.00	M	100.00	100.00
EURO	Northern Europe	Estonia	100.00	M	100.00	100.00	100.00	100.00
EURO	Northern Europe	Finland	100.00	M	100.00	100.00	100.00	100.00
EURO	Northern Europe	Iceland	M	M	100.00	M	100.00	100.00
EURO	Northern Europe	Ireland	M	M	100.00	M	100.00	100.00
EURO	Northern Europe	Norway	100.00	M	100.00	100.00	100.00	100.00
EURO	South West Europe	Albania	M	M	100.00	M	100.00	100.00
EURO	South West Europe	Austria	M	M	100.00	M	100.00	100.00
EURO	South West Europe	Bosnia and Herzegovina	M	M	100.00	M	100.00	100.00
EURO	South West Europe	Germany	M	M	100.00	M	M	100.00
EURO	South West Europe	Luxembourg	M	M	100.00	M	100.00	100.00
EURO	South West Europe	Malta	M	M	100.00	M	100.00	100.00
EURO	South West Europe	Montenegro	M	M	100.00	M	100.00	100.00
EURO	South West Europe	Netherlands	100.00	M	100.00	100.00	100.00	100.00
EURO	South West Europe	North Macedonia	M	M	100.00	M	100.00	100.00
EURO	South West Europe	Portugal	M	M	100.00	M	100.00	100.00
EURO	Western Asia	Armenia	M	M	100.00	M	100.00	100.00
EURO	Western Asia	Azerbaijan	M	M	100.00	M	100.00	100.00
EURO	Western Asia	Cyprus	M	M	100.00	M	100.00	100.00
EURO	Western Asia	Georgia	M	M	100.00	M	100.00	100.00
EURO	Western Asia	Israel	100.00	M	100.00	M	100.00	100.00
EURO	Western Asia	Turkey	100.00	M	100.00	100.00	100.00	100.00
PAHO	Central America and Caribbean	Anguilla	M	M	100.00	M	M	100.00
PAHO	Central America and Caribbean	Aruba	M	100.00	100.00	M	M	100.00
PAHO	Central America and Caribbean	Bahamas	M	100.00	100.00	M	M	100.00
PAHO	Central America and Caribbean	Barbados	M	100.00	100.00	M	M	100.00
PAHO	Central America and Caribbean	Belize	M	100.00	100.00	M	100.00	100.00
PAHO	Central America and Caribbean	British Virgin Islands	M	100.00	M	M	M	100.00

PAHO	Central America and Caribbean	Cuba	100.00	100.00	100.00	100.00	100.00	100.00
PAHO	Central America and Caribbean	Dominica	M	100.00	100.00	M	M	100.00
PAHO	Central America and Caribbean	Grenada	M	100.00	100.00	M	M	100.00
PAHO	Central America and Caribbean	Haiti	M	100.00	100.00	M	100.00	100.00
PAHO	Central America and Caribbean	Nicaragua	M	100.00	100.00	M	100.00	100.00
PAHO	Central America and Caribbean	Saint Kitts and Nevis	M	100.00	M	M	M	100.00
PAHO	Central America and Caribbean	Saint Lucia	M	100.00	100.00	M	M	100.00
PAHO	Central America and Caribbean	Saint Vincent and the Grenadines	M	100.00	M	M	M	100.00
PAHO	Central America and Caribbean	Turks and Caicos Islands	M	100.00	100.00	M	M	100.00
PAHO	Tropical South America	Ecuador	100.00	100.00	100.00	100.00	100.00	100.00
PAHO	Tropical South America	Suriname	M	100.00	100.00	M	100.00	100.00
WPRO	Eastern Asia	Japan	M	M	100.00	100.00	100.00	100.00
AFRO	Eastern Africa	Tanzania	99.83	100.00	100.00	100.00	100.00	99.97
AFRO	Eastern Africa	Mauritius	99.75	M	100.00	100.00	100.00	99.94
AFRO	Western Africa	Niger	99.69	100.00	100.00	100.00	100.00	99.94
EURO	Northern Europe	Denmark	100.00	M	100.00	100.00	99.67	99.92
PAHO	North America	Canada	99.83	M	100.00	99.70	100.00	99.88
EURO	Northern Europe	Latvia	100.00	M	100.00	100.00	99.52	99.88
EURO	Northern Europe	Sweden	M	M	100.00	M	99.74	99.87
EMRO	Western Asia	Iraq	100.00	99.04	100.00	100.00	100.00	99.81
PAHO	Central America and Caribbean	Honduras	98.83	100.00	100.00	100.00	100.00	99.77
PAHO	Temperate South America	Paraguay	98.59	100.00	100.00	100.00	100.00	99.72
EURO	South West Europe	Croatia	M	M	100.00	M	99.24	99.62
EURO	South West Europe	Belgium	98.25	M	100.00	100.00	100.00	99.56
WPRO	Eastern Asia	South Korea	100.00	97.60	100.00	100.00	100.00	99.52
WPRO	South-East Asia	Laos	99.64	97.69	100.00	100.00	100.00	99.47
PAHO	Central America and Caribbean	Mexico	M	100.00	100.00	97.59	100.00	99.40
EURO	South West Europe	Switzerland	98.00	M	100.00	100.00	99.58	99.39
WPRO	Oceania Melanesia Polynesia	New Caledonia	99.82	98.59	100.00	100.00	98.18	99.32
PAHO	Tropical South America	Venezuela	96.59	100.00	100.00	100.00	100.00	99.32
EMRO	Western Asia	Yemen	98.55	M	100.00	M	M	99.28
AFRO	Western Africa	Ghana	99.85	97.47	100.00	100.00	98.92	99.25
SEARO	South-East Asia	Indonesia	100.00	96.10	100.00	100.00	100.00	99.22
AFRO	Western Africa	Nigeria	100.00	95.58	100.00	100.00	100.00	99.12
SEARO	South-East Asia	Myanmar	100.00	96.39	100.00	M	100.00	99.10
EMRO	Western Asia	Jordan	99.79	95.67	100.00	100.00	100.00	99.09
AFRO	Western Africa	Guinea	96.07	M	100.00	100.00	100.00	99.02
PAHO	Temperate South America	Uruguay	100.00	95.80	100.00	M	100.00	98.95
AFRO	Eastern Africa	Uganda	99.83	94.50	100.00	100.00	100.00	98.86
WPRO	Eastern Asia	Mongolia	100.00	M	100.00	99.19	96.23	98.85
WPRO	South-East Asia	Viet Nam	99.82	97.46	100.00	96.88	100.00	98.83
EMRO	Western Asia	Lebanon	99.70	94.37	100.00	100.00	100.00	98.81
AFRO	Western Africa	Burkina Faso	100.00	93.86	100.00	100.00	100.00	98.77
PAHO	Central America and Caribbean	El Salvador	96.84	100.00	100.00	100.00	96.69	98.71
SEARO	Southern Asia	Sri Lanka	100.00	M	100.00	96.70	97.45	98.54
SEARO	Southern Asia	Bangladesh	99.83	95.92	100.00	100.00	96.76	98.50
EMRO	Southern Asia	Iran	100.00	92.18	100.00	100.00	100.00	98.44
AFRO	Western Africa	Côte d'Ivoire	99.84	93.12	100.00	99.12	100.00	98.41
EMRO	Southern Asia	Afghanistan	99.79	91.95	100.00	100.00	100.00	98.35
SEARO	South-East Asia	Thailand	100.00	91.55	100.00	100.00	100.00	98.31
AFRO	Eastern Africa	Mozambique	100.00	95.53	100.00	100.00	95.65	98.24
AFRO	Middle Africa	Angola	92.81	M	100.00	100.00	100.00	98.20
PAHO	Central America and Caribbean	Costa Rica	90.91	100.00	100.00	100.00	100.00	98.18
EMRO	Northern Africa	Morocco	100.00	97.69	100.00	100.00	93.10	98.16
EURO	Eastern Europe	Poland	92.31	M	100.00	100.00	100.00	98.08
PAHO	Temperate South America	Chile	97.32	100.00	100.00	100.00	91.97	97.86
PAHO	Tropical South America	Colombia	M	100.00	100.00	100.00	91.13	97.78
EMRO	Western Asia	Qatar	99.81	88.93	100.00	100.00	100.00	97.75
EMRO	Northern Africa	Tunisia	100.00	89.62	100.00	100.00	98.81	97.69
PAHO	Tropical South America	French Guiana	100.00	99.19	100.00	100.00	88.68	97.57

AFRO	Southern Africa	South Africa	99.84	88.45	100.00	100.00	99.30	97.52
EURO	South West Europe	Italy	94.38	93.04	100.00	100.00	100.00	97.48
EMRO	Western Asia	Bahrain	99.78	87.43	100.00	100.00	100.00	97.44
WPRO	Oceania Melanesia Polynesia	Fiji	98.82	88.10	100.00	100.00	100.00	97.38
PAHO	North America	United States of America	99.85	94.93	100.00	91.19	100.00	97.19
AFRO	Eastern Africa	Kenya	88.78	M	100.00	100.00	100.00	97.19
AFRO	Northern Africa	Algeria	100.00	86.15	100.00	100.00	98.59	96.95
PAHO	Central America and Caribbean	Guatemala	91.51	100.00	100.00	100.00	93.10	96.92
SEARO	Eastern Asia	North Korea	100.00	90.38	100.00	M	M	96.79
SEARO	Southern Asia	India	99.84	88.81	100.00	100.00	94.65	96.66
SEARO	Southern Asia	Bhutan	99.07	92.77	100.00	100.00	91.30	96.63
AFRO	Western Africa	Sierra Leone	100.00	91.67	100.00	100.00	90.00	96.33
PAHO	Tropical South America	Bolivia	M	88.93	100.00	M	100.00	96.31
AFRO	Western Africa	Mauritania	99.13	85.71	100.00	100.00	M	96.21
EURO	Northern Europe	Lithuania	84.21	M	100.00	100.00	100.00	96.05
AFRO	Western Africa	Senegal	100.00	93.21	100.00	100.00	85.54	95.75
EURO	South West Europe	Greece	81.78	M	100.00	100.00	100.00	95.45
WPRO	South-East Asia	Philippines	100.00	77.53	100.00	99.52	98.98	95.21
AFRO	Eastern Africa	Madagascar	100.00	75.46	100.00	100.00	100.00	95.09
SEARO	Southern Asia	Nepal	99.80	91.02	100.00	100.00	83.25	94.81
EURO	South West Europe	Slovenia	77.85	M	100.00	100.00	100.00	94.46
PAHO	Central America and Caribbean	Panama	71.15	100.00	100.00	100.00	100.00	94.23
WPRO	South-East Asia	Singapore	96.66	73.38	100.00	100.00	100.00	94.01
EMRO	Southern Asia	Pakistan	100.00	69.48	100.00	100.00	100.00	93.90
AFRO	Middle Africa	Cameroon	99.84	83.13	100.00	100.00	86.50	93.89
EMRO	Northern Africa	Egypt	99.22	68.62	100.00	100.00	100.00	93.57
WPRO	Oceania Melanesia Polynesia	New Zealand	100.00	66.67	100.00	100.00	100.00	93.33
PAHO	Central America and Caribbean	Jamaica	99.25	100.00	100.00	100.00	65.79	93.01
EURO	Northern Europe	United Kingdom	68.97	M	100.00	100.00	99.26	92.06
PAHO	Tropical South America	Peru	81.51	100.00	100.00	100.00	78.29	91.96
PAHO	Central America and Caribbean	Guadeloupe	100.00	100.00	100.00	100.00	58.33	91.67
SEARO	Southern Asia	Maldives	90.23	76.32	100.00	M	100.00	91.64
PAHO	Central America and Caribbean	Dominican Republic	M	100.00	100.00	M	74.07	91.36
AFRO	Eastern Africa	Ethiopia	80.00	75.00	100.00	100.00	100.00	91.00
EURO	Eastern Europe	Romania	64.27	M	100.00	99.73	100.00	91.00
EMRO	Western Asia	Kuwait	100.00	63.56	100.00	M	100.00	90.89
PAHO	Central America and Caribbean	Martinique	100.00	97.73	100.00	100.00	55.56	90.66
AFRO	Eastern Africa	Rwanda	100.00	M	100.00	100.00	54.88	88.72
AFRO	Eastern Africa	Zambia	100.00	41.71	100.00	100.00	100.00	88.34
WPRO	South-East Asia	Cambodia	99.71	M	100.00	100.00	42.83	85.63
WPRO	Oceania Melanesia Polynesia	Australia	52.85	75.00	100.00	100.00	100.00	85.57
PAHO	Tropical South America	Brazil	46.19	81.66	100.00	100.00	98.83	85.34
WPRO	South-East Asia	Malaysia	84.00	42.00	100.00	98.30	100.00	84.86
AFRO	Western Africa	Mali	99.78	100.00	100.00	100.00	24.35	84.83
PAHO	Temperate South America	Argentina	10.65	96.42	100.00	99.73	100.00	81.36
WPRO	Oceania Melanesia Polynesia	Papua New Guinea	100.00	94.61	100.00	99.60	7.14	80.27
EMRO	Western Asia	Oman	84.44	22.33	100.00	100.00	94.38	80.23
AFRO	Middle Africa	Democratic Republic of the Congo	100.00	27.27	100.00	100.00	72.26	79.91
EMRO	Western Asia	West Bank and Gaza Strip	99.42	36.36	100.00	M	M	78.59
WPRO	Eastern Asia	China	98.40	2.07	100.00	90.80	100.00	78.25
EURO	South West Europe	France	10.27	M	100.00	100.00	100.00	77.57
EURO	Eastern Europe	Ukraine	0.00	M	100.00	100.00	100.00	75.00
SEARO	South-East Asia	Timor-Leste	99.50	98.75	100.00	M	0.00	74.56
EMRO	Western Asia	United Arab Emirates	100.00	97.06	100.00	M	0.00	74.26
EURO	South West Europe	Serbia	50.56	14.89	100.00	100.00	100.00	73.09
EMRO	Western Asia	Saudi Arabia	99.56	14.66	100.00	M	M	71.41
PAHO	Central America and Caribbean	Trinidad and Tobago	M	100.00	100.00	M	0.00	66.67
EURO	Eastern Europe	Russian Federation	7.85	0.00	100.00	100.00	100.00	61.57
EURO	South West Europe	Spain	8.18	0.00	100.00	99.55	100.00	61.55
PAHO	Central America and Caribbean	Antigua and Barbuda	M	M	M	M	M	M

PAHO	Central America and Caribbean	Cayman Islands	M	M	M	M	M	M
PAHO	North America	Bermuda	M	M	M	M	M	M
PAHO	Tropical South America	Guyana	M	M	M	M	M	M

Supplementary Table S37. The *correctness* of 173 Member States for 5 test outcomes reported by the WHO's FluNet. Data were downloaded on 15 June 2021 at which time the total time series length of reported data was 1381 weeks. We calculated specimens collected (SPE) *correctness* as the percentage of weeks when specimens were less than or equal to tests. We calculated tests' *correctness* (TES) as the percentage of weeks when tests equaled the sum of total positives and negatives. We calculated positives' *correctness* (POS) as the percentage of weeks when positives equaled the sum of influenza A and B positives. We calculated influenza A and B positives' *correctness* (FLUA and FLUB, respectively) as the percentage of weeks where strain positives equaled the sum of all respectively subtypes. We calculated correctness if at least one test, disease, or strain/subtype was not missing. Member States are listed in descending order by average *correctness* (AVG), region, and zone. We could not calculate *correctness* if all outcomes were incomplete, denoted as *M*.

Region	Zone	Country/Territory	SPE	TES	POS	FLUA	FLUB	AVG
PAHO	Central America and Caribbean	Anguilla	M	100.00	100.00	100.00	100.00	100.00
PAHO	Central America and Caribbean	Antigua and Barbuda	M	100.00	100.00	M	100.00	100.00
PAHO	Central America and Caribbean	Aruba	M	100.00	100.00	100.00	100.00	100.00
PAHO	Central America and Caribbean	Bahamas	M	100.00	100.00	100.00	100.00	100.00
PAHO	Central America and Caribbean	Barbados	M	100.00	100.00	100.00	100.00	100.00
PAHO	Central America and Caribbean	Belize	M	100.00	100.00	100.00	100.00	100.00
PAHO	Central America and Caribbean	British Virgin Islands	M	100.00	100.00	100.00	M	100.00
PAHO	Central America and Caribbean	Cayman Islands	M	100.00	100.00	100.00	100.00	100.00
PAHO	Central America and Caribbean	Dominica	M	100.00	100.00	100.00	100.00	100.00
PAHO	Central America and Caribbean	Dominican Republic	M	100.00	100.00	100.00	100.00	100.00
PAHO	Central America and Caribbean	Grenada	M	100.00	100.00	100.00	100.00	100.00
PAHO	Central America and Caribbean	Haiti	M	100.00	100.00	100.00	100.00	100.00
PAHO	Central America and Caribbean	Nicaragua	M	100.00	100.00	100.00	100.00	100.00
PAHO	Central America and Caribbean	Saint Kitts and Nevis	M	100.00	100.00	100.00	100.00	100.00
PAHO	Central America and Caribbean	Saint Lucia	M	100.00	100.00	100.00	100.00	100.00
PAHO	Central America and Caribbean	Saint Vincent and the Grenadines	M	100.00	100.00	100.00	100.00	100.00
PAHO	Central America and Caribbean	Trinidad and Tobago	M	100.00	100.00	100.00	100.00	100.00
PAHO	Central America and Caribbean	Turks and Caicos Islands	M	100.00	100.00	100.00	100.00	100.00
PAHO	North America	Bermuda	M	100.00	100.00	100.00	100.00	100.00
PAHO	Tropical South America	Colombia	M	100.00	100.00	100.00	100.00	100.00
PAHO	Tropical South America	Suriname	M	100.00	100.00	100.00	100.00	100.00
WPRO	Eastern Asia	Japan	M	M	100.00	100.00	100.00	100.00
PAHO	Central America and Caribbean	Cuba	100.00	100.00	100.00	99.84	100.00	99.97
PAHO	Central America and Caribbean	Jamaica	99.25	100.00	100.00	99.71	100.00	99.79
PAHO	Central America and Caribbean	Honduras	98.83	100.00	100.00	99.87	100.00	99.74
PAHO	Temperate South America	Paraguay	98.59	100.00	100.00	100.00	100.00	99.72
SEARO	South-East Asia	Timor-Leste	99.50	98.51	100.00	100.00	100.00	99.60
PAHO	Tropical South America	Ecuador	100.00	100.00	100.00	97.87	100.00	99.57
SEARO	South-East Asia	Myanmar	100.00	97.70	100.00	100.00	100.00	99.54
PAHO	Temperate South America	Chile	97.32	100.00	100.00	100.00	100.00	99.46
PAHO	Central America and Caribbean	El Salvador	96.84	100.00	100.00	100.00	100.00	99.37
PAHO	Tropical South America	Venezuela	96.59	100.00	100.00	100.00	100.00	99.32
PAHO	Temperate South America	Uruguay	100.00	96.07	100.00	100.00	100.00	99.21
EMRO	Western Asia	United Arab Emirates	100.00	95.65	100.00	100.00	100.00	99.13
EMRO	Western Asia	Lebanon	99.70	94.64	100.00	100.00	100.00	98.87
WPRO	Oceania Melanesia Polynesia	Papua New Guinea	100.00	92.00	100.00	99.60	100.00	98.32
PAHO	Central America and Caribbean	Guatemala	91.51	100.00	100.00	100.00	100.00	98.30
PAHO	Central America and Caribbean	Costa Rica	90.91	100.00	100.00	100.00	100.00	98.18
SEARO	Eastern Asia	North Korea	100.00	90.38	100.00	100.00	100.00	98.08
PAHO	Tropical South America	Bolivia	M	89.02	100.00	100.00	100.00	97.26
PAHO	Tropical South America	Peru	81.51	100.00	100.00	100.00	100.00	96.30
PAHO	Central America and Caribbean	Mexico	M	100.00	100.00	84.44	100.00	96.11
PAHO	Central America and Caribbean	Martinique	100.00	77.18	100.00	100.00	100.00	95.44
EURO	South West Europe	Bosnia and Herzegovina	M	80.62	100.00	100.00	100.00	95.16
PAHO	Central America and Caribbean	Panama	71.15	100.00	100.00	100.00	100.00	94.23
EMRO	Southern Asia	Afghanistan	99.79	70.17	100.00	100.00	100.00	93.99
PAHO	Central America and Caribbean	Guadeloupe	100.00	69.91	100.00	100.00	100.00	93.98

AFRO	Western Africa	Niger	99.69	70.02	100.00	100.00	100.00	93.94
AFRO	Eastern Africa	Mozambique	100.00	62.24	100.00	100.00	100.00	92.45
EMRO	Western Asia	Kuwait	100.00	61.48	100.00	99.16	100.00	92.13
SEARO	Southern Asia	Nepal	99.80	60.55	100.00	100.00	100.00	92.07
WPRO	Oceania Melanesia Polynesia	Fiji	98.82	55.56	100.00	100.00	100.00	90.87
EMRO	Western Asia	West Bank and Gaza Strip	99.42	54.60	100.00	100.00	100.00	90.80
AFRO	Western Africa	Sierra Leone	100.00	52.81	100.00	100.00	100.00	90.56
SEARO	Southern Asia	Maldives	90.23	62.41	100.00	100.00	100.00	90.53
AFRO	Eastern Africa	Seychelles	100.00	52.00	100.00	100.00	100.00	90.40
AFRO	Middle Africa	Chad	100.00	51.02	100.00	100.00	100.00	90.20
SEARO	Southern Asia	Bhutan	99.07	49.26	100.00	100.00	100.00	89.67
WPRO	South-East Asia	Laos	99.64	46.82	100.00	100.00	100.00	89.29
AFRO	Northern Africa	Algeria	100.00	45.73	100.00	100.00	100.00	89.15
EMRO	Western Asia	Bahrain	99.78	42.60	100.00	100.00	100.00	88.48
EMRO	Western Asia	Jordan	99.79	42.07	100.00	100.00	100.00	88.37
EMRO	Western Asia	Qatar	99.81	41.82	100.00	100.00	100.00	88.33
EMRO	Western Asia	Iraq	100.00	41.46	100.00	100.00	100.00	88.29
PAHO	Tropical South America	French Guiana	100.00	41.08	100.00	100.00	100.00	88.22
AFRO	Western Africa	Nigeria	100.00	38.72	100.00	100.00	100.00	87.74
SEARO	Southern Asia	Bangladesh	99.83	39.83	100.00	98.78	100.00	87.69
AFRO	Western Africa	Côte d'Ivoire	99.84	38.20	100.00	99.51	100.00	87.51
AFRO	Middle Africa	Angola	92.81	42.45	100.00	100.00	100.00	87.05
AFRO	Eastern Africa	Uganda	99.83	35.33	100.00	100.00	100.00	87.03
AFRO	Middle Africa	Congo	100.00	35.14	100.00	100.00	100.00	87.03
EMRO	Northern Africa	Morocco	100.00	34.11	100.00	100.00	100.00	86.82
WPRO	South-East Asia	Viet Nam	99.82	34.63	100.00	98.85	100.00	86.66
SEARO	South-East Asia	Indonesia	100.00	32.70	100.00	100.00	100.00	86.54
WPRO	Eastern Asia	South Korea	100.00	31.92	100.00	100.00	100.00	86.38
EURO	Central Asia	Tajikistan	M	45.03	100.00	100.00	100.00	86.26
AFRO	Western Africa	Ghana	99.85	29.17	100.00	100.00	100.00	85.80
SEARO	South-East Asia	Thailand	100.00	28.93	100.00	100.00	100.00	85.79
AFRO	Southern Africa	South Africa	99.84	29.08	100.00	100.00	100.00	85.78
AFRO	Western Africa	Burkina Faso	100.00	28.67	100.00	100.00	100.00	85.73
EMRO	Northern Africa	Sudan	100.00	28.57	100.00	100.00	100.00	85.71
AFRO	Western Africa	Mauritania	99.13	29.13	100.00	99.57	100.00	85.57
EMRO	Western Asia	Syrian Arab Republic	100.00	27.78	100.00	100.00	100.00	85.56
EMRO	Southern Asia	Iran	100.00	27.78	100.00	99.87	100.00	85.53
PAHO	Tropical South America	Brazil	46.19	82.78	100.00	98.49	100.00	85.49
EMRO	Northern Africa	Tunisia	100.00	24.23	100.00	100.00	100.00	84.85
WPRO	Oceania Melanesia Polynesia	New Caledonia	99.82	24.18	100.00	100.00	100.00	84.80
WPRO	Oceania Melanesia Polynesia	New Zealand	100.00	24.48	100.00	99.19	100.00	84.73
EMRO	Northern Africa	Egypt	99.22	24.11	100.00	100.00	100.00	84.67
WPRO	South-East Asia	Singapore	96.66	25.98	100.00	100.00	100.00	84.53
PAHO	North America	United States of America	99.85	25.22	100.00	97.50	100.00	84.51
EURO	South West Europe	Belgium	98.25	24.22	100.00	100.00	100.00	84.49
AFRO	Eastern Africa	Madagascar	100.00	22.56	100.00	99.60	100.00	84.43
AFRO	Western Africa	Guinea	96.07	25.84	100.00	100.00	100.00	84.38
EURO	Western Asia	Azerbaijan	M	37.48	100.00	100.00	100.00	84.37
EURO	Eastern Europe	Moldova	M	37.07	100.00	100.00	100.00	84.27
AFRO	Western Africa	Senegal	100.00	21.40	100.00	99.84	100.00	84.25
SEARO	Southern Asia	India	99.84	20.29	100.00	99.87	100.00	84.00
EMRO	Southern Asia	Pakistan	100.00	19.73	100.00	100.00	100.00	83.95
EURO	South West Europe	Italy	94.38	25.52	100.00	99.67	100.00	83.91
AFRO	Eastern Africa	Zambia	100.00	23.30	100.00	96.18	100.00	83.90
AFRO	Middle Africa	South Sudan	100.00	16.67	100.00	100.00	100.00	83.33
EURO	Northern Europe	Lithuania	84.21	31.75	100.00	100.00	100.00	83.19
EMRO	Western Asia	Saudi Arabia	99.56	15.04	100.00	100.00	100.00	82.92
EURO	Northern Europe	Finland	100.00	13.29	100.00	100.00	100.00	82.66
AFRO	Middle Africa	Cameroon	99.84	13.31	100.00	100.00	100.00	82.63
EURO	Eastern Europe	Kosovo	M	30.43	100.00	100.00	100.00	82.61

WPRO	South-East Asia	Philippines	100.00	11.87	100.00	99.69	100.00	82.31
EURO	Central Asia	Uzbekistan	M	28.90	100.00	100.00	100.00	82.22
AFRO	Eastern Africa	Tanzania	99.83	11.07	100.00	100.00	100.00	82.18
AFRO	Western Africa	Togo	100.00	10.78	100.00	100.00	100.00	82.16
EURO	Northern Europe	Norway	100.00	9.65	100.00	100.00	100.00	81.93
EURO	Northern Europe	Denmark	100.00	9.48	100.00	100.00	100.00	81.90
EURO	South West Europe	North Macedonia	M	27.40	100.00	100.00	100.00	81.85
AFRO	Western Africa	Mali	99.78	9.41	100.00	100.00	100.00	81.84
EURO	Western Asia	Armenia	M	27.33	100.00	100.00	100.00	81.83
EURO	South West Europe	Switzerland	98.00	10.20	100.00	100.00	100.00	81.64
AFRO	Middle Africa	Central African Republic	100.00	8.15	100.00	100.00	100.00	81.63
PAHO	Temperate South America	Argentina	10.65	94.82	100.00	99.90	100.00	81.07
AFRO	Eastern Africa	Rwanda	100.00	5.18	100.00	100.00	100.00	81.04
AFRO	Middle Africa	Democratic Republic of the Congo	100.00	3.53	100.00	100.00	100.00	80.71
EURO	Western Asia	Turkey	100.00	2.49	100.00	100.00	100.00	80.50
EURO	Northern Europe	Latvia	100.00	2.45	100.00	100.00	100.00	80.49
EMRO	Western Asia	Yemen	98.55	3.70	100.00	100.00	100.00	80.45
EURO	South West Europe	Netherlands	100.00	2.12	100.00	100.00	100.00	80.42
EMRO	Western Asia	Oman	84.44	17.21	100.00	100.00	100.00	80.33
EURO	Western Asia	Israel	100.00	1.58	100.00	100.00	100.00	80.32
EURO	Eastern Europe	Poland	92.31	9.10	100.00	100.00	100.00	80.28
AFRO	Eastern Africa	Mauritius	99.75	0.89	100.00	100.00	100.00	80.13
WPRO	Eastern Asia	Mongolia	100.00	1.21	100.00	99.39	100.00	80.12
EURO	South West Europe	Portugal	M	20.15	100.00	100.00	100.00	80.04
EURO	Northern Europe	Estonia	100.00	0.15	100.00	100.00	100.00	80.03
PAHO	North America	Canada	99.83	0.00	100.00	99.90	100.00	79.95
WPRO	South-East Asia	Cambodia	99.71	0.00	100.00	100.00	100.00	79.94
EURO	Northern Europe	Sweden	M	18.30	100.00	100.00	100.00	79.58
EURO	Central Asia	Kyrgyzstan	M	19.80	100.00	98.14	100.00	79.48
EURO	Eastern Europe	Bulgaria	M	17.92	100.00	100.00	100.00	79.48
EURO	Northern Europe	Ireland	M	17.69	100.00	100.00	100.00	79.42
WPRO	Oceania Melanesia Polynesia	Australia	52.85	43.77	100.00	100.00	100.00	79.32
AFRO	Eastern Africa	Ethiopia	80.00	15.18	100.00	100.00	100.00	79.04
WPRO	Eastern Asia	China	98.40	0.65	100.00	95.24	100.00	78.86
SEARO	Southern Asia	Sri Lanka	100.00	0.55	100.00	92.46	100.00	78.60
EURO	South West Europe	Greece	81.78	10.85	100.00	100.00	100.00	78.53
AFRO	Eastern Africa	Kenya	88.78	2.92	100.00	100.00	100.00	78.34
EURO	Central Asia	Turkmenistan	M	12.63	100.00	100.00	100.00	78.16
EURO	South West Europe	Malta	M	11.81	100.00	100.00	100.00	77.95
EURO	South West Europe	Albania	M	11.42	100.00	100.00	100.00	77.85
EURO	South West Europe	Montenegro	M	10.24	100.00	100.00	100.00	77.56
EURO	South West Europe	Luxembourg	M	8.85	100.00	100.00	100.00	77.21
WPRO	South-East Asia	Malaysia	84.00	1.87	100.00	99.19	100.00	77.01
EURO	Central Asia	Kazakhstan	M	7.55	100.00	100.00	100.00	76.89
EURO	South West Europe	Slovenia	77.85	6.08	100.00	100.00	100.00	76.79
EURO	South West Europe	Croatia	M	5.76	100.00	100.00	100.00	76.44
EURO	Eastern Europe	Romania	64.27	17.22	100.00	99.88	100.00	76.27
EURO	Western Asia	Georgia	M	4.77	100.00	100.00	100.00	76.19
EURO	Eastern Europe	Slovakia	M	4.43	100.00	100.00	100.00	76.11
EURO	Eastern Europe	Belarus	M	2.77	100.00	100.00	100.00	75.69
EURO	Western Asia	Cyprus	M	2.25	100.00	100.00	100.00	75.56
EURO	Eastern Europe	Czechia	M	1.49	100.00	100.00	100.00	75.37
EURO	South West Europe	Germany	M	1.15	100.00	100.00	100.00	75.29
EURO	South West Europe	Austria	M	0.97	100.00	100.00	100.00	75.24
EURO	Northern Europe	Iceland	M	0.83	100.00	100.00	100.00	75.21
EURO	Eastern Europe	Hungary	M	0.46	100.00	100.00	100.00	75.12
EURO	Northern Europe	United Kingdom	68.97	6.19	100.00	99.91	100.00	75.01
EURO	South West Europe	Serbia	50.56	23.14	100.00	100.00	100.00	74.74
EURO	South West Europe	Spain	8.18	8.18	100.00	99.66	100.00	63.21
EURO	Eastern Europe	Russian Federation	7.85	2.93	100.00	100.00	100.00	62.15

EURO	South West Europe	France	10.27	0.11	100.00	100.00	100.00	62.08
EURO	Eastern Europe	Ukraine	0.00	6.08	100.00	100.00	100.00	61.22
PAHO	Tropical South America	Guyana	M	M	M	M	M	M

Supplementary Table S38. Average and median *consistency* for 6 testing outcomes (specimens collected (SPE), specimens processed or tests (TES), influenza A positives (FLUA), influenza B positives (FLUB), total positives (POS), and total negatives (NEG)) in 6 regions and 17 transmission zones. We calculated *consistency* as the ratio of weeks when records from one data download were equal to those of another divided by the shared time series length between downloads and multiplied by 100. We downloaded data on 13 June 2020, from Week 1 of 2008 through Week 52 of 2019 and downloaded data again on 15 June 2021 from Week 1 of 1995 through Week 24 of 2021. The shared time series length between downloads consisted of 626 weeks. We report average *consistency* with 95% confidence intervals (top values) and median *consistency* with lower and upper quartiles (bottom values). Regions and zones are listed in ascending order by the average *consistency* of positives, and we omit the Southern African transmission zone, as it consisted of only 1 country (South Africa).

Region	SPE	TES	POS	FLUA	FLUB	NEG
AFRO	100.00 [100.00, 100.00] 100.00 [100.00, 100.00]	100.00 [100.00, 100.00] 100.00 [100.00, 100.00]	99.99 [99.97, 100.00] 100.00 [100.00, 100.00]	100.00 [100.00, 100.00] 100.00 [100.00, 100.00]	99.86 [99.68, 100.00] 100.00 [100.00, 100.00]	100.00 [100.00, 100.00] 100.00 [100.00, 100.00]
EURO	100.00 [100.00, 100.00] 100.00 [100.00, 100.00]	99.92 [99.76, 100.00] 100.00 [100.00, 100.00]	99.91 [99.75, 100.00] 100.00 [100.00, 100.00]	99.92 [99.76, 100.00] 100.00 [100.00, 100.00]	99.92 [99.77, 100.00] 100.00 [100.00, 100.00]	100.00 [100.00, 100.00] 100.00 [100.00, 100.00]
SEARO	99.24 [97.76, 100.72] 100.00 [100.00, 100.00]	99.46 [98.41, 100.00] 100.00 [100.00, 100.00]	99.24 [98.26, 100.00] 100.00 [99.84, 100.00]	99.56 [98.71, 100.00] 100.00 [100.00, 100.00]	98.75 [97.42, 100.00] 100.00 [97.12, 100.00]	100.00 [100.00, 100.00] 100.00 [100.00, 100.00]
WPRO	98.84 [97.40, 100.00] 100.00 [100.00, 100.00]	98.23 [96.55, 99.91] 100.00 [98.88, 100.00]	98.42 [97.02, 99.83] 100.00 [98.08, 100.00]	98.64 [97.37, 99.90] 100.00 [98.24, 100.00]	96.9 [92.25, 100.00] 100.00 [98.88, 100.00]	98.10 [96.43, 99.78] 100.00 [98.24, 100.00]
EMRO	98.53 [96.36, 100.70] 100.00 [100.00, 100.00]	98.53 [96.36, 100.00] 100.00 [100.00, 100.00]	98.29 [96.89, 99.68] 100.00 [98.24, 100.00]	99.44 [98.54, 100.00] 100.00 [100.00, 100.00]	97.40 [95.06, 99.74] 99.44 [97.28, 100.00]	98.58 [96.49, 100.00] 100.00 [100.00, 100.00]
PAHO	99.95 [99.85, 100.00] 100.00 [100.00, 100.00]	99.95 [99.85, 100.00] 100.00 [100.00, 100.00]	95.70 [93.72, 97.67] 99.20 [93.45, 100.00]	94.91 [92.58, 97.24] 99.12 [90.26, 100.00]	91.65 [88.59, 94.71] 96.81 [85.78, 99.20]	96.70 [95.05, 98.36] 99.68 [94.73, 100.00]
Zone						
Eastern Europe	100.00 [100.00, 100.00] 100.00 [100.00, 100.00]	100.00 [100.00, 100.00] 100.00 [100.00, 100.00]	100.00 [100.00, 100.00] 100.00 [100.00, 100.00]	100.00 [100.00, 100.00] 100.00 [100.00, 100.00]	100.00 [100.00, 100.00] 100.00 [100.00, 100.00]	100.00 [100.00, 100.00] 100.00 [100.00, 100.00]
Eastern Africa	100.00 [100.00, 100.00] 100.00 [100.00, 100.00]	100.00 [100.00, 100.00] 100.00 [100.00, 100.00]	100.00 [100.00, 100.00] 100.00 [100.00, 100.00]	100.00 [100.00, 100.00] 100.00 [100.00, 100.00]	99.78 [99.34, 100.00] 100.00 [100.00, 100.00]	100.00 [100.00, 100.00] 100.00 [100.00, 100.00]
Middle Africa	100.00 [100.00, 100.00] 100.00 [100.00, 100.00]	100.00 [100.00, 100.00] 100.00 [100.00, 100.00]	100.00 [100.00, 100.00] 100.00 [100.00, 100.00]	100.00 [100.00, 100.00] 100.00 [100.00, 100.00]	99.77 [99.32, 100.00] 100.00 [100.00, 100.00]	100.00 [100.00, 100.00] 100.00 [100.00, 100.00]
Central Asia	100.00 [100.00, 100.00] 100.00 [100.00, 100.00]	100.00 [100.00, 100.00] 100.00 [100.00, 100.00]	100.00 [100.00, 100.00] 100.00 [100.00, 100.00]	100.00 [100.00, 100.00] 100.00 [100.00, 100.00]	100.00 [100.00, 100.00] 100.00 [100.00, 100.00]	100.00 [100.00, 100.00] 100.00 [100.00, 100.00]
Southwest Europe	100.00 [100.00, 100.00] 100.00 [100.00, 100.00]	100.00 [100.00, 100.00] 100.00 [100.00, 100.00]	99.97 [99.93, 100.00] 100.00 [100.00, 100.00]	100.00 [100.00, 100.00] 100.00 [100.00, 100.00]	99.97 [99.93, 100.00] 100.00 [100.00, 100.00]	100.00 [100.00, 100.00] 100.00 [100.00, 100.00]
Western Africa	100.00 [100.00, 100.00] 100.00 [100.00, 100.00]	100.00 [100.00, 100.00] 100.00 [100.00, 100.00]	99.97 [99.93, 100.00] 100.00 [100.00, 100.00]	100.00 [100.00, 100.00] 100.00 [100.00, 100.00]	99.96 [99.90, 100.00] 100.00 [100.00, 100.00]	100.00 [100.00, 100.00] 100.00 [100.00, 100.00]
Northern Europe	100.00 [100.00, 100.00] 100.00 [100.00, 100.00]	99.58 [98.77, 100.4] 100.00 [100.00, 100.00]	99.58 [98.77, 100.00] 100.00 [100.00, 100.00]	99.58 [98.77, 100.00] 100.00 [100.00, 100.00]	99.62 [98.87, 100.00] 100.00 [100.00, 100.00]	100.00 [100.00, 100.00] 100.00 [100.00, 100.00]
Eastern Asia	99.78 [99.34, 100.00] 100.00 [100.00, 100.00]	99.78 [99.34, 100.21] 100.00 [100.00, 100.00]	99.39 [98.62, 100.00] 100.00 [98.88, 100.00]	99.42 [98.71, 100.00] 100.00 [98.88, 100.00]	99.71 [99.29, 100.00] 100.00 [99.68, 100.00]	99.42 [98.71, 100.00] 100.00 [98.88, 100.00]
North America	99.31 [97.95, 100.00] 100.00 [97.92, 100.00]	99.31 [97.95, 100.66] 100.00 [97.92, 100.00]	99.36 [98.11, 100.00] 100.00 [98.08, 100.00]	99.41 [98.27, 100.00] 100.00 [98.24, 100.00]	98.83 [97.56, 100.00] 98.72 [97.76, 100.00]	99.31 [97.95, 100.00] 100.00 [97.92, 100.00]

Southeast Asia	99.17 [97.54, 100.00] 100.00 [100.00, 100.00]	99.17 [97.54, 100.00] 100.00 [100.00, 100.00]	99.25 [97.78, 100.72] 100.00 [100.00, 100.00]	99.41 [98.25, 100.00] 100.00 [100.00, 100.00]	99.49 [98.49, 100.00] 100.00 [100.00, 100.00]	99.17 [97.54, 100.00] 100.00 [100.00, 100.00]
Western Asia	98.44 [96.15, 100.00] 100.00 [100.00, 100.00]	98.44 [96.15, 100.00] 100.00 [100.00, 100.00]	99.05 [97.74, 100.36] 100.00 [100.00, 100.00]	99.41 [98.46, 100.00] 100.00 [100.00, 100.00]	99.30 [98.56, 100.00] 100.00 [100.00, 100.00]	98.5 [96.28, 100.00] 100.00 [100.00, 100.00]
Northern Africa	100.00 [100.00, 100.00] 100.00 [100.00, 100.00]	100.00 [100.00, 100.00] 100.00 [100.00, 100.00]	98.53 [96.64, 100.42] 99.52 [98.24, 100.00]	100.00 [100.00, 100.00] 100.00 [100.00, 100.00]	94.73 [86.97, 100.00] 97.28 [97.28, 100.00]	100.00 [100.00, 100.00] 100.00 [100.00, 100.00]
Temperate South America	100.00 [100.00, 100.00] 100.00 [100.00, 100.00]	100.00 [100.00, 100.00] 100.00 [100.00, 100.00]	98.32 [95.53, 101.00] 99.60 [96.65, 100.00]	97.88 [94.85, 100.00] 99.04 [95.77, 100.00]	92.29 [86.29, 98.29] 91.69 [87.62, 96.96]	97.4 [92.93, 100.00] 99.52 [94.89, 99.92]
Southern Asia	99.08 [97.27, 100.00] 100.00 [100.00, 100.00]	99.34 [98.06, 100.00] 100.00 [100.00, 100.00]	98.26 [96.65, 99.87] 99.84 [96.65, 100.00]	99.47 [98.42, 100.00] 100.00 [100.00, 100.00]	97.52 [95.58, 99.45] 98.88 [95.21, 100.00]	100.00 [100.00, 100.00] 100.00 [100.00, 100.00]
Tropical South America	100.00 [100.00, 100.00] 100.00 [100.00, 100.00]	100.00 [100.00, 100.00] 100.00 [100.00, 100.00]	97.52 [94.99, 100.00] 99.68 [97.28, 100.00]	96.84 [93.69, 99.99] 99.68 [96.96, 100.00]	91.94 [83.96, 99.92] 99.36 [89.30, 100.00]	97.27 [94.89, 99.64] 99.68 [94.73, 100.00]
Oceania Melanesia Polynesia	98.40 [95.27, 100.00] 100.00 [100.00, 100.00]	96.58 [92.85, 100.00] 99.04 [92.01, 100]	97.38 [94.31, 100.00] 99.04 [96.33, 99.84]	97.67 [94.62, 100.00] 99.04 [97.60, 100.00]	92.01 [78.29, 100.00] 99.04 [97.44, 99.52]	96.55 [92.77, 100.00] 99.04 [92.01, 100.00]
Central America and Caribbean	100.00 [100.00, 100.00] 100.00 [100.00, 100.00]	100.00 [100.00, 100.00] 100.00 [100.00, 100.00]	94.24 [91.32, 97.17] 99.04 [86.58, 100.00]	93.26 [89.81, 96.71] 98.96 [85.78, 100.00]	90.62 [86.63, 94.61] 95.61 [83.55, 99.04]	96.10 [93.64, 98.56] 99.52 [94.25, 100.00]
Worldwide	**99.67 [99.39, 99.96]** 100.00 [100.00, 100.00]	**99.61 [99.31, 99.91]** 100.00 [100.00, 100.00]	**98.51 [97.92, 99.11]** **100**.00 **[99.68, 100**.00**]**	**98.48 [97.80, 99.17]** 100.00 [100.00, 100.00]	**97.21 [96.17, 98.25]** **100**.00 **[98.72, 100**.00**]**	**98.85 [98.31, 99.38]** 100.00 [100.00, 100.00]

Supplementary Table S39. Average and median *consistency* for 8 influenza subtypes (A(H1), A(H1N1)pdm09, A(H3), A(H5), A(Unsubtyped), B(Yamagata), B(Victoria), and B(Undetermined) positives) in 6 regions and 17 transmission zones. We calculated *consistency* as the ratio of weeks when records from one data download were equal to those of another divided by the shared time series length between downloads and multiplied by 100. We downloaded data on 13 June 2020, from Week 1 of 2008 through Week 52 of 2019 and downloaded data again on 15 June 2021 from Week 1 of 1995 through Week 24 of 2021. The shared time series length between downloads consisted of 626 weeks. We report average *consistency* with 95% confidence intervals (top values) and median *consistency* with lower and upper quartiles (bottom values). Regions and zones are listed in alphabetical order, and we omit the Southern African transmission zone, as it consisted of only 1 country (South Africa).

Region	A(H1)	A(H1N1)pdm09	A(H3)	A(H5)	A(Unsubtyped)	B(Yamagata)	B(Victoria)	B(Undetermined)
AFRO	100.00 [100.00, 100.00] 100.00 [100.00, 100.00]	100.00 [100.00, 100.00] 100.00 [100.00, 100.00]	100.00 [100.00, 100.00] 100.00 [100.00, 100.00]	100.00 [100.00, 100.00] 100.00 [100.00, 100.00]	100.00 [100.00, 100.00] 100.00 [100.00, 100.00]	100.00 [100.00, 100.00] 100.00 [100.00, 100.00]	100.00 [100.00, 100.00] 100.00 [100.00, 100.00]	98.99 [98.14, 99.83] 100.00 [99.84, 100.00]
EMRO	100.00 [100.00, 100.00] 100.00 [100.00, 100.00]	99.64 [98.98, 100.00] 100.00 [100.00, 100.00]	99.92 [99.76, 100.00] 100.00 [100.00, 100.00]	100.00 [100.00, 100.00] 100.00 [100.00, 100.00]	99.77 [99.32, 100.00] 100.00 [100.00, 100.00]	100.00 [100.00, 100.00] 100.00 [100.00, 100.00]	100.00 [100.00, 100.00] 100.00 [100.00, 100.00]	97.24 [94.89, 99.59] 98.72 [96.81, 100.00]
EURO	100.00 [100.00, 100.00] 100.00 [100.00, 100.00]	99.94 [99.81, 100.00] 100.00 [100.00, 100.00]	99.93 [99.81, 100.00] 100.00 [100.00, 100.00]	100.00 [100.00, 100.00] 100.00 [100.00, 100.00]	99.93 [99.79, 100.00] 100.00 [100.00, 100.00]	99.94 [99.82, 100.00] 100.00 [100.00, 100.00]	99.97 [99.93, 100.00] 100.00 [100.00, 100.00]	99.90 [99.76, 100.00] 100.00 [100.00, 100.00]
PAHO	100.00 [100.00, 100.00] 100.00 [100.00, 100.00]	99.98 [99.95, 100.00] 100.00 [100.00, 100.00]	99.99 [99.97, 100.00] 100.00 [100.00, 100.00]	100.00 [100.00, 100.00] 100.00 [100.00, 100.00]	99.96 [99.88, 100.00] 100.00 [100.00, 100.00]	100.00 [100.00, 100.00] 100.00 [100.00, 100.00]	99.98 [99.93, 100.00] 100.00 [100.00, 100.00]	91.50 [88.47, 94.54] 96.09 [85.46, 99.20]
SEARO	100.00 [100.00, 100.00] 100.00 [100.00, 100.00]	99.49 [98.50, 100.00] 100.00 [100.00, 100.00]	99.35 [98.07, 100.00] 100.00 [100.00, 100.00]	100.00 [100.00, 100.00] 100.00 [100.00, 100.00]	99.56 [98.71, 100.00] 100.00 [100.00, 100.00]	100.00 [100.00, 100.00] 100.00 [100.00, 100.00]	100.00 [100.00, 100.00] 100.00 [100.00, 100.00]	97.92 [96.27, 99.58] 100.00 [94.25, 100.00]
WPRO	99.98 [99.95, 100.00] 100.00 [100.00, 100.00]	98.86 [97.71, 100.00] 100.00 [98.88, 100.00]	98.95 [97.83, 100.00] 100.00 [98.88, 100.00]	99.98 [99.95, 100.00] 100.00 [100.00, 100.00]	99.56 [99.15, 99.98] 100.00 [99.04, 100.00]	99.65 [99.28, 100.00] 100.00 [99.36, 100.00]	99.56 [99.03, 100.00] 100.00 [99.68, 100.00]	95.73 [90.90, 100.00] 99.84 [96.49, 100.00]
Zone								
Central America and Caribbean	100.00 [100.00, 100.00] 100.00 [100.00, 100.00]	100.00 [100.00, 100.00] 100.00 [100.00, 100.00]	100.00 [100.00, 100.00] 100.00 [100.00, 100.00]	100.00 [100.00, 100.00] 100.00 [100.00, 100.00]	100.00 [100.00, 100.00] 100.00 [100.00, 100.00]	100.00 [100.00, 100.00] 100.00 [100.00, 100.00]	100.00 [100.00, 100.00] 100.00 [100.00, 100.00]	90.42 [86.46, 94.38] 95.05 [83.55, 98.88]
Central Asia	100.00 [100.00, 100.00] 100.00 [100.00, 100.00]	100.00 [100.00, 100.00] 100.00 [100.00, 100.00]	100.00 [100.00, 100.00] 100.00 [100.00, 100.00]	100.00 [100.00, 100.00] 100.00 [100.00, 100.00]	100.00 [100.00, 100.00] 100.00 [100.00, 100.00]	100.00 [100.00, 100.00] 100.00 [100.00, 100.00]	100.00 [100.00, 100.00] 100.00 [100.00, 100.00]	99.94 [99.81, 100.00] 100.00 [100.00, 100.00]
Eastern Africa	100.00 [100.00, 100.00] 100.00 [100.00, 100.00]	100.00 [100.00, 100.00] 100.00 [100.00, 100.00]	100.00 [100.00, 100.00] 100.00 [100.00, 100.00]	100.00 [100.00, 100.00] 100.00 [100.00, 100.00]	100.00 [100.00, 100.00] 100.00 [100.00, 100.00]	100.00 [100.00, 100.00] 100.00 [100.00, 100.00]	100.00 [100.00, 100.00] 100.00 [100.00, 100.00]	99.17 [97.98, 100.00] 100.00 [99.84, 100.00]
Eastern Asia	100.00 [100.00, 100.00] 100.00 [100.00, 100.00]	99.42 [98.71, 100.00] 100.00 [98.88, 100.00]	99.71 [99.29, 100.00] 100.00 [99.68, 100.00]	100.00 [100.00, 100.00] 100.00 [100.00, 100.00]	99.87 [99.69, 100.00] 100.00 [99.84, 100.00]	99.78 [99.34, 100.00] 100.00 [100.00, 100.00]	99.71 [99.29, 100.00] 100.00 [99.68, 100.00]	99.78 [99.34, 100.00] 100.00 [100.00, 100.00]
Eastern Europe	100.00 [100.00, 100.00] 100.00 [100.00, 100.00]	100.00 [100.00, 100.00] 100.00 [100.00, 100.00]	100.00 [100.00, 100.00] 100.00 [100.00, 100.00]	100.00 [100.00, 100.00] 100.00 [100.00, 100.00]	100.00 [100.00, 100.00] 100.00 [100.00, 100.00]	100.00 [100.00, 100.00] 100.00 [100.00, 100.00]	100.00 [100.00, 100.00] 100.00 [100.00, 100.00]	100.00 [100.00, 100.00] 100.00 [100.00, 100.00]
Middle Africa	100.00 [100.00, 100.00] 100.00 [100.00, 100.00]	100.00 [100.00, 100.00] 100.00 [100.00, 100.00]	100.00 [100.00, 100.00] 100.00 [100.00, 100.00]	100.00 [100.00, 100.00] 100.00 [100.00, 100.00]	100.00 [100.00, 100.00] 100.00 [100.00, 100.00]	100.00 [100.00, 100.00] 100.00 [100.00, 100.00]	100.00 [100.00, 100.00] 100.00 [100.00, 100.00]	98.31 [96.40, 100.00] 100.00 [96.49, 100.00]
North America	100.00 [100.00, 100.00] 100.00 [100.00, 100.00]	99.79 [99.37, 100.00] 100.00 [99.36, 100.00]	99.84 [99.53, 100.00] 100.00 [99.52, 100.00]	100.00 [100.00, 100.00] 100.00 [100.00, 100.00]	99.41 [98.27, 100.00] 100.00 [98.24, 100.00]	100.00 [100.00, 100.00] 100.00 [100.00, 100.00]	99.68 [99.05, 100.00] 100.00 [99.04, 100.00]	98.94 [97.67, 100.00] 99.04 [97.76, 100.00]
Northern Africa	100.00 [100.00, 100.00] 100.00 [100.00, 100.00]	100.00 [100.00, 100.00] 100.00 [100.00, 100.00]	100.00 [100.00, 100.00] 100.00 [100.00, 100.00]	100.00 [100.00, 100.00] 100.00 [100.00, 100.00]	100.00 [100.00, 100.00] 100.00 [100.00, 100.00]	100.00 [100.00, 100.00] 100.00 [100.00, 100.00]	100.00 [100.00, 100.00] 100.00 [100.00, 100.00]	94.47 [86.71, 100.00] 96.96 [96.49, 100.00]
Northern Europe	100.00 [100.00, 100.00] 100.00 [100.00, 100.00]	99.68 [99.05, 100.00] 100.00 [100.00, 100.00]	99.66 [99.01, 100.00] 100.00 [100.00, 100.00]	100.00 [100.00, 100.00] 100.00 [100.00, 100.00]	99.63 [98.91, 100.00] 100.00 [100.00, 100.00]	99.70 [99.10, 100.00] 100.00 [100.00, 100.00]	99.87 [99.65, 100.00] 100.00 [100.00, 100.00]	99.60 [98.89, 100.00] 100.00 [99.84, 100.00]
Oceania Melanesia Polynesia	99.97 [99.91, 100.00] 100.00 [100.00, 100.00]	98.21 [95.31, 100.00] 99.68 [99.04, 100.00]	97.76 [94.71, 100.00] 99.04 [98.08, 100.00]	99.97 [99.91, 100.00] 100.00 [100.00, 100.00]	99.01 [97.92, 100.00] 99.04 [99.04, 100.00]	99.30 [98.32, 100.00] 100.00 [99.04, 100.00]	99.78 [99.41, 100.00] 100.00 [99.84, 100.00]	90.58 [77.13, 100.00] 99.04 [90.42, 99.52]

Southeast Asia	99.98 [99.95, 100.00] 100.00 [100.00, 100.00]	99.47 [98.44, 100.00] 100.00 [100.00, 100.00]	99.68 [99.05, 100.00] 100.00 [100.00, 100.00]	99.98 [99.95, 100.00] 100.00 [100.00, 100.00]	99.90 [99.72, 100.00] 100.00 [100.00, 100.00]	99.94 [99.81, 100.00] 100.00 [100.00, 100.00]	99.60 [98.82, 100.00] 100.00 [100.00, 100.00]	98.42 [95.99, 100.00] 100.00 [100.00, 100.00]
Southern Asia	100.00 [100.00, 100.00] 100.00 [100.00, 100.00]	99.38 [98.16, 100.00] 100.00 [100.00, 100.00]	99.20 [97.64, 100.00] 100.00 [100.00, 100.00]	100.00 [100.00, 100.00] 100.00 [100.00, 100.00]	99.47 [98.42, 100.00] 100.00 [100.00, 100.00]	100.00 [100.00, 100.00] 100.00 [100.00, 100.00]	100.00 [100.00, 100.00] 100.00 [100.00, 100.00]	96.49 [94.49, 98.48] 95.69 [93.93, 99.36]
Southwest Europe	100.00 [100.00, 100.00] 100.00 [100.00, 100.00]	100.00 [100.00, 100.00] 100.00 [100.00, 100.00]	100.00 [100.00, 100.00] 100.00 [100.00, 100.00]	100.00 [100.00, 100.00] 100.00 [100.00, 100.00]	100.00 [100.00, 100.00] 100.00 [100.00, 100.00]	100.00 [100.00, 100.00] 100.00 [100.00, 100.00]	100.00 [100.00, 100.00] 100.00 [100.00, 100.00]	99.96 [99.91, 100.00] 100.00 [100.00, 100.00]
Temperate South America	100.00 [100.00, 100.00] 100.00 [100.00, 100.00]	100.00 [100.00, 100.00] 100.00 [100.00, 100.00]	100.00 [100.00, 100.00] 100.00 [100.00, 100.00]	100.00 [100.00, 100.00] 100.00 [100.00, 100.00]	100.00 [100.00, 100.00] 100.00 [100.00, 100.00]	100.00 [100.00, 100.00] 100.00 [100.00, 100.00]	100.00 [100.00, 100.00] 100.00 [100.00, 100.00]	92.29 [86.29, 98.29] 91.69 [87.62, 96.96]
Tropical South America	100.00 [100.00, 100.00] 100.00 [100.00, 100.00]	100.00 [100.00, 100.00] 100.00 [100.00, 100.00]	100.00 [100.00, 100.00] 100.00 [100.00, 100.00]	100.00 [100.00, 100.00] 100.00 [100.00, 100.00]	100.00 [100.00, 100.00] 100.00 [100.00, 100.00]	100.00 [100.00, 100.00] 100.00 [100.00, 100.00]	100.00 [100.00, 100.00] 100.00 [100.00, 100.00]	91.80 [83.89, 99.71] 99.04 [89.30, 99.68]
Western Africa	100.00 [100.00, 100.00] 100.00 [100.00, 100.00]	100.00 [100.00, 100.00] 100.00 [100.00, 100.00]	100.00 [100.00, 100.00] 100.00 [100.00, 100.00]	100.00 [100.00, 100.00] 100.00 [100.00, 100.00]	100.00 [100.00, 100.00] 100.00 [100.00, 100.00]	100.00 [100.00, 100.00] 100.00 [100.00, 100.00]	100.00 [100.00, 100.00] 100.00 [100.00, 100.00]	99.07 [97.37, 100.00] 100.00 [99.84, 100.00]
Western Asia	100.00 [100.00, 100.00] 100.00 [100.00, 100.00]	99.61 [98.92, 100.00] 100.00 [100.00, 100.00]	99.92 [99.75, 100.00] 100.00 [100.00, 100.00]	100.00 [100.00, 100.00] 100.00 [100.00, 100.00]	99.76 [99.28, 100.00] 100.00 [100.00, 100.00]	100.00 [100.00, 100.00] 100.00 [100.00, 100.00]	100.00 [100.00, 100.00] 100.00 [100.00, 100.00]	99.22 [98.48, 99.96] 100.00 [98.56, 100.00]
Worldwide	**100.00 [100.00, 100.00]** **100.00 [100.00, 100.00]**	**99.80 [99.65, 99.95]** **100.00 [100.00, 100.00]**	**99.83 [99.69, 99.97]** **100.00 [100.00, 100.00]**	**100.00 [100.00, 100.00]** **100.00 [100.00, 100.00]**	**99.87 [99.78, 99.97]** **100.00 [100.00, 100.00]**	**99.95 [99.90, 100.00]** **100.00 [100.00, 100.00]**	**99.95 [99.89, 100.00]** **100.00 [100.00, 100.00]**	**96.83 [95.78, 97.88]** **100.00 [97.76, 100.00]**

Supplementary Table S40. The *consistency* of 173 Member States for 6 test outcomes (specimens collected (SPE), specimens processed or tests (TES), influenza A positives (FLUA), influenza B positives (FLUB), total positives (POS), and total negatives (NEG)) reported by the WHO's FluNet. We estimated *consistency* as the ratio of weeks when records from one data download were equal to those of another divided by the shared time series length between downloads and multiplied by 100. We downloaded data on 13 June 2020, from Week 1 of 2008 through Week 52 of 2019 and again on 15 June 2021 from Week 1 of 1995 through Week 24 of 2021. The shared time series length consisted of 626 weeks. Member States are listed in descending order by average *consistency* across all 6 outcomes (AVG), regions, and zones. Member State-outcome dyads with missing records for both data downloads are denoted as *M*.

Region	Zone	Country/Territory	POS	FLUA	FLUB	NEG	SPE	TES	AVG
AFRO	Eastern Africa	Ethiopia	100.00	100.00	100.00	100.00	100.00	100.00	100.00
AFRO	Eastern Africa	Kenya	100.00	100.00	100.00	100.00	100.00	100.00	100.00
AFRO	Eastern Africa	Madagascar	100.00	100.00	100.00	100.00	100.00	100.00	100.00
AFRO	Eastern Africa	Mauritius	100.00	100.00	100.00	100.00	100.00	100.00	100.00
AFRO	Eastern Africa	Mozambique	100.00	100.00	100.00	100.00	100.00	100.00	100.00
AFRO	Eastern Africa	Rwanda	100.00	100.00	100.00	100.00	100.00	100.00	100.00
AFRO	Eastern Africa	Seychelles	100.00	100.00	100.00	100.00	100.00	100.00	100.00
AFRO	Eastern Africa	Tanzania	100.00	100.00	100.00	100.00	100.00	100.00	100.00
AFRO	Eastern Africa	Zambia	100.00	100.00	100.00	100.00	100.00	100.00	100.00
AFRO	Middle Africa	Angola	100.00	100.00	100.00	100.00	100.00	100.00	100.00
AFRO	Middle Africa	Cameroon	100.00	100.00	100.00	100.00	100.00	100.00	100.00
AFRO	Middle Africa	Chad	100.00	100.00	100.00	100.00	100.00	100.00	100.00
AFRO	Middle Africa	Congo	100.00	100.00	100.00	100.00	100.00	100.00	100.00
AFRO	Middle Africa	Democratic Republic of the Congo	100.00	100.00	100.00	100.00	100.00	100.00	100.00
AFRO	Middle Africa	South Sudan	100.00	100.00	100.00	100.00	100.00	100.00	100.00
AFRO	Northern Africa	Algeria	100.00	100.00	100.00	100.00	100.00	100.00	100.00
AFRO	Southern Africa	South Africa	100.00	100.00	100.00	100.00	100.00	100.00	100.00
AFRO	Western Africa	Burkina Faso	100.00	100.00	100.00	100.00	100.00	100.00	100.00
AFRO	Western Africa	Côte d'Ivoire	100.00	100.00	100.00	100.00	100.00	100.00	100.00
AFRO	Western Africa	Ghana	100.00	100.00	100.00	100.00	100.00	100.00	100.00
AFRO	Western Africa	Guinea	100.00	100.00	100.00	100.00	100.00	100.00	100.00
AFRO	Western Africa	Mali	100.00	100.00	100.00	100.00	100.00	100.00	100.00
AFRO	Western Africa	Mauritania	100.00	100.00	100.00	100.00	100.00	100.00	100.00
AFRO	Western Africa	Niger	100.00	100.00	100.00	100.00	100.00	100.00	100.00
AFRO	Western Africa	Senegal	100.00	100.00	100.00	100.00	100.00	100.00	100.00
AFRO	Western Africa	Togo	100.00	100.00	100.00	100.00	100.00	100.00	100.00
EMRO	Northern Africa	Sudan	100.00	100.00	100.00	100.00	100.00	100.00	100.00
EMRO	Southern Asia	Afghanistan	100.00	100.00	100.00	100.00	100.00	100.00	100.00
EMRO	Western Asia	Iraq	100.00	100.00	100.00	100.00	100.00	100.00	100.00
EMRO	Western Asia	Jordan	100.00	100.00	100.00	100.00	100.00	100.00	100.00
EMRO	Western Asia	Kuwait	100.00	100.00	100.00	100.00	100.00	100.00	100.00
EMRO	Western Asia	Oman	100.00	100.00	100.00	100.00	100.00	100.00	100.00
EMRO	Western Asia	Qatar	100.00	100.00	100.00	100.00	100.00	100.00	100.00
EMRO	Western Asia	Syrian Arab Republic	100.00	100.00	100.00	100.00	100.00	100.00	100.00
EMRO	Western Asia	West Bank and Gaza Strip	100.00	100.00	100.00	100.00	100.00	100.00	100.00
EURO	Central Asia	Kazakhstan	100.00	100.00	100.00	100.00	100.00	100.00	100.00
EURO	Central Asia	Kyrgyzstan	100.00	100.00	100.00	100.00	100.00	100.00	100.00
EURO	Central Asia	Tajikistan	100.00	100.00	100.00	100.00	100.00	100.00	100.00
EURO	Central Asia	Turkmenistan	100.00	100.00	100.00	100.00	100.00	100.00	100.00
EURO	Central Asia	Uzbekistan	100.00	100.00	100.00	100.00	100.00	100.00	100.00
EURO	Eastern Europe	Belarus	100.00	100.00	100.00	100.00	100.00	100.00	100.00
EURO	Eastern Europe	Bulgaria	100.00	100.00	100.00	100.00	100.00	100.00	100.00
EURO	Eastern Europe	Czechia	100.00	100.00	100.00	100.00	100.00	100.00	100.00
EURO	Eastern Europe	Hungary	100.00	100.00	100.00	100.00	100.00	100.00	100.00
EURO	Eastern Europe	Kosovo	100.00	100.00	100.00	100.00	100.00	100.00	100.00
EURO	Eastern Europe	Moldova	100.00	100.00	100.00	100.00	100.00	100.00	100.00
EURO	Eastern Europe	Poland	100.00	100.00	100.00	100.00	100.00	100.00	100.00

EURO	Eastern Europe	Romania	100.00	100.00	100.00	100.00	100.00	100.00	100.00
EURO	Eastern Europe	Russian Federation	100.00	100.00	100.00	100.00	100.00	100.00	100.00
EURO	Eastern Europe	Slovakia	100.00	100.00	100.00	100.00	100.00	100.00	100.00
EURO	Eastern Europe	Ukraine	100.00	100.00	100.00	100.00	100.00	100.00	100.00
EURO	Northern Europe	Estonia	100.00	100.00	100.00	100.00	100.00	100.00	100.00
EURO	Northern Europe	Finland	100.00	100.00	100.00	100.00	100.00	100.00	100.00
EURO	Northern Europe	Iceland	100.00	100.00	100.00	100.00	100.00	100.00	100.00
EURO	Northern Europe	Ireland	100.00	100.00	100.00	100.00	100.00	100.00	100.00
EURO	Northern Europe	Latvia	100.00	100.00	100.00	100.00	100.00	100.00	100.00
EURO	Northern Europe	Lithuania	100.00	100.00	100.00	100.00	100.00	100.00	100.00
EURO	Northern Europe	Norway	100.00	100.00	100.00	100.00	100.00	100.00	100.00
EURO	Northern Europe	Sweden	100.00	100.00	100.00	100.00	100.00	100.00	100.00
EURO	Northern Europe	United Kingdom	100.00	100.00	100.00	100.00	100.00	100.00	100.00
EURO	South West Europe	Albania	100.00	100.00	100.00	100.00	100.00	100.00	100.00
EURO	South West Europe	Austria	100.00	100.00	100.00	100.00	100.00	100.00	100.00
EURO	South West Europe	Belgium	100.00	100.00	100.00	100.00	100.00	100.00	100.00
EURO	South West Europe	Bosnia and Herzegovina	100.00	100.00	100.00	100.00	100.00	100.00	100.00
EURO	South West Europe	Croatia	100.00	100.00	100.00	100.00	100.00	100.00	100.00
EURO	South West Europe	France	100.00	100.00	100.00	100.00	100.00	100.00	100.00
EURO	South West Europe	Germany	100.00	100.00	100.00	100.00	100.00	100.00	100.00
EURO	South West Europe	Greece	100.00	100.00	100.00	100.00	100.00	100.00	100.00
EURO	South West Europe	Italy	100.00	100.00	100.00	100.00	100.00	100.00	100.00
EURO	South West Europe	Luxembourg	100.00	100.00	100.00	100.00	100.00	100.00	100.00
EURO	South West Europe	Malta	100.00	100.00	100.00	100.00	100.00	100.00	100.00
EURO	South West Europe	Montenegro	100.00	100.00	100.00	100.00	100.00	100.00	100.00
EURO	South West Europe	Netherlands	100.00	100.00	100.00	100.00	100.00	100.00	100.00
EURO	South West Europe	North Macedonia	100.00	100.00	100.00	100.00	100.00	100.00	100.00
EURO	South West Europe	Portugal	100.00	100.00	100.00	100.00	100.00	100.00	100.00
EURO	South West Europe	Serbia	100.00	100.00	100.00	100.00	100.00	100.00	100.00
EURO	South West Europe	Slovenia	100.00	100.00	100.00	100.00	100.00	100.00	100.00
EURO	South West Europe	Switzerland	100.00	100.00	100.00	100.00	100.00	100.00	100.00
EURO	Western Asia	Armenia	100.00	100.00	100.00	100.00	100.00	100.00	100.00
EURO	Western Asia	Azerbaijan	100.00	100.00	100.00	100.00	100.00	100.00	100.00
EURO	Western Asia	Cyprus	100.00	100.00	100.00	100.00	100.00	100.00	100.00
EURO	Western Asia	Georgia	100.00	100.00	100.00	100.00	100.00	100.00	100.00
EURO	Western Asia	Israel	100.00	100.00	100.00	100.00	100.00	100.00	100.00
EURO	Western Asia	Turkey	100.00	100.00	100.00	100.00	100.00	100.00	100.00
PAHO	North America	Canada	100.00	100.00	100.00	100.00	100.00	100.00	100.00
PAHO	Tropical South America	Colombia	100.00	100.00	100.00	100.00	100.00	100.00	100.00
PAHO	Tropical South America	Venezuela	100.00	100.00	100.00	100.00	100.00	100.00	100.00
SEARO	Eastern Asia	North Korea	100.00	100.00	100.00	100.00	100.00	100.00	100.00
SEARO	South-East Asia	Indonesia	100.00	100.00	100.00	100.00	100.00	100.00	100.00
SEARO	South-East Asia	Myanmar	100.00	100.00	100.00	100.00	100.00	100.00	100.00
SEARO	South-East Asia	Thailand	100.00	100.00	100.00	100.00	100.00	100.00	100.00
SEARO	South-East Asia	Timor-Leste	100.00	100.00	100.00	100.00	100.00	100.00	100.00
SEARO	Southern Asia	Bangladesh	100.00	100.00	100.00	100.00	100.00	100.00	100.00
SEARO	Southern Asia	Bhutan	100.00	100.00	100.00	100.00	100.00	100.00	100.00
SEARO	Southern Asia	Nepal	100.00	100.00	100.00	100.00	100.00	100.00	100.00
WPRO	Eastern Asia	Mongolia	100.00	100.00	100.00	100.00	100.00	100.00	100.00
WPRO	Eastern Asia	South Korea	100.00	100.00	100.00	100.00	100.00	100.00	100.00
WPRO	Oceania Melanesia Polynesia	New Caledonia	100.00	100.00	100.00	100.00	100.00	100.00	100.00
WPRO	South-East Asia	Cambodia	100.00	100.00	100.00	100.00	100.00	100.00	100.00
WPRO	South-East Asia	Laos	100.00	100.00	100.00	100.00	100.00	100.00	100.00
WPRO	South-East Asia	Malaysia	100.00	100.00	100.00	100.00	100.00	100.00	100.00
WPRO	South-East Asia	Singapore	100.00	100.00	100.00	100.00	100.00	100.00	100.00
WPRO	South-East Asia	Viet Nam	100.00	100.00	100.00	100.00	100.00	100.00	100.00
PAHO	Temperate South America	Argentina	100.00	100.00	100.00	99.84	100.00	100.00	99.97
AFRO	Western Africa	Nigeria	99.84	100.00	99.84	100.00	100.00	100.00	99.95
PAHO	Central America and Caribbean	Panama	100.00	100.00	99.68	100.00	100.00	100.00	99.95
AFRO	Western Africa	Sierra Leone	99.84	100.00	99.68	100.00	100.00	100.00	99.92

WPRO	Oceania Melanesia Polynesia	Fiji	99.84	100.00	99.52	100.00	100.00	100.00	99.89
PAHO	Tropical South America	Peru	100.00	100.00	99.36	100.00	100.00	100.00	99.89
PAHO	Central America and Caribbean	Antigua and Barbuda	99.84	99.68	99.84	99.84	100.00	100.00	99.87
EURO	South West Europe	Spain	99.52	100.00	99.52	100.00	100.00	100.00	99.84
PAHO	Central America and Caribbean	Costa Rica	100.00	100.00	99.04	100.00	100.00	100.00	99.84
PAHO	Central America and Caribbean	Bahamas	99.84	99.84	99.36	99.84	100.00	100.00	99.81
PAHO	Central America and Caribbean	El Salvador	100.00	100.00	98.88	100.00	100.00	100.00	99.81
PAHO	Tropical South America	Guyana	99.68	99.68	99.68	99.68	100.00	100.00	99.79
EMRO	Western Asia	Bahrain	100.00	100.00	98.56	100.00	100.00	100.00	99.76
EMRO	Western Asia	Yemen	100.00	100.00	98.56	100.00	100.00	100.00	99.76
AFRO	Middle Africa	Central African Republic	100.00	100.00	98.40	100.00	100.00	100.00	99.73
EMRO	Southern Asia	Iran	99.04	100.00	98.88	100.00	100.00	100.00	99.65
PAHO	Central America and Caribbean	Cayman Islands	99.68	99.36	99.20	99.68	100.00	100.00	99.65
AFRO	Eastern Africa	Uganda	100.00	100.00	97.76	100.00	100.00	100.00	99.63
PAHO	North America	Bermuda	100.00	100.00	97.76	100.00	100.00	100.00	99.63
PAHO	Central America and Caribbean	Jamaica	100.00	100.00	97.12	100.00	100.00	100.00	99.52
SEARO	Southern Asia	India	99.84	100.00	97.12	100.00	100.00	100.00	99.49
PAHO	Central America and Caribbean	Anguilla	99.36	99.20	99.04	99.36	100.00	100.00	99.49
EMRO	Northern Africa	Morocco	99.52	100.00	97.28	100.00	100.00	100.00	99.47
PAHO	Central America and Caribbean	Belize	99.20	99.20	99.20	99.20	100.00	100.00	99.47
PAHO	Central America and Caribbean	Haiti	98.88	98.88	98.88	100.00	100.00	100.00	99.44
PAHO	Central America and Caribbean	Turks and Caicos Islands	99.20	99.04	98.72	99.20	100.00	100.00	99.36
PAHO	Central America and Caribbean	Cuba	100.00	100.00	95.69	100.00	100.00	100.00	99.28
EMRO	Northern Africa	Tunisia	98.24	100.00	97.28	100.00	100.00	100.00	99.25
PAHO	Central America and Caribbean	Mexico	100.00	100.00	95.53	100.00	100.00	100.00	99.25
WPRO	Oceania Melanesia Polynesia	New Zealand	99.04	99.04	99.04	99.04	100.00	99.04	99.20
PAHO	Tropical South America	Brazil	100.00	99.84	100.00	94.73	100.00	100.00	99.09
PAHO	Central America and Caribbean	Honduras	100.00	100.00	94.57	100.00	100.00	100.00	99.09
WPRO	Eastern Asia	Japan	98.08	98.24	99.68	98.24	100.00	100.00	99.04
PAHO	Temperate South America	Paraguay	100.00	100.00	93.93	100.00	100.00	100.00	98.99
WPRO	Eastern Asia	China	98.88	98.88	98.88	98.88	98.88	98.88	98.88
PAHO	Central America and Caribbean	Saint Kitts and Nevis	98.40	98.24	97.76	98.40	100.00	100.00	98.80
SEARO	Southern Asia	Maldives	96.65	100.00	93.93	100.00	100.00	100.00	98.43
PAHO	North America	United States of America	98.08	98.24	98.72	97.92	97.92	97.92	98.14
PAHO	Tropical South America	Suriname	97.28	96.96	96.49	97.28	100.00	100.00	98.00
EMRO	Southern Asia	Pakistan	93.61	100.00	92.49	100.00	100.00	100.00	97.68
PAHO	Temperate South America	Chile	99.20	98.08	89.46	99.20	100.00	100.00	97.66
PAHO	Central America and Caribbean	Guatemala	98.40	98.08	89.78	98.40	100.00	100.00	97.44
EURO	Northern Europe	Denmark	95.85	95.85	96.17	100.00	100.00	95.85	97.28
PAHO	Central America and Caribbean	Saint Vincent and the Grenadines	94.25	94.25	92.17	96.49	100.00	100.00	96.19
PAHO	Tropical South America	Bolivia	98.24	97.76	89.30	90.26	100.00	100.00	95.93
EMRO	Northern Africa	Egypt	94.89	100.00	79.07	100.00	100.00	100.00	95.66
SEARO	Southern Asia	Sri Lanka	95.21	95.21	95.21	100.00	91.69	94.09	95.23
WPRO	Oceania Melanesia Polynesia	Papua New Guinea	96.33	97.60	97.44	92.01	92.01	92.01	94.57
PAHO	Temperate South America	Uruguay	94.09	93.45	85.78	90.58	100.00	100.00	93.98
EMRO	Western Asia	Lebanon	93.77	98.08	94.25	92.65	92.33	92.33	93.90
PAHO	Central America and Caribbean	Aruba	92.33	90.26	84.82	94.25	100.00	100.00	93.61
WPRO	South-East Asia	Philippines	92.49	94.09	94.89	91.69	91.69	91.69	92.76
PAHO	Central America and Caribbean	Dominican Republic	91.21	87.38	82.11	91.21	100.00	100.00	91.99
PAHO	Tropical South America	French Guiana	88.98	87.22	73.00	100.00	100.00	100.00	91.53
PAHO	Central America and Caribbean	Saint Lucia	86.58	85.78	85.78	89.46	100.00	100.00	91.27
PAHO	Tropical South America	Ecuador	93.45	90.10	69.65	93.45	100.00	100.00	91.11
PAHO	Central America and Caribbean	Dominica	85.30	84.50	83.55	87.54	100.00	100.00	90.15
PAHO	Central America and Caribbean	Martinique	82.27	80.83	71.09	100.00	100.00	100.00	89.03
WPRO	Oceania Melanesia Polynesia	Australia	91.69	91.69	64.06	91.69	100.00	91.85	88.50
PAHO	Central America and Caribbean	Trinidad and Tobago	84.82	83.23	76.68	85.46	100.00	100.00	88.37
PAHO	Central America and Caribbean	Guadeloupe	80.67	78.75	67.25	100.00	100.00	100.00	87.78
EMRO	Western Asia	Saudi Arabia	90.10	91.85	96.81	81.79	81.15	81.15	87.14
PAHO	Central America and Caribbean	Nicaragua	83.23	77.16	78.43	83.23	100.00	100.00	87.01
PAHO	Central America and Caribbean	Barbados	76.84	71.09	71.88	77.00	100.00	100.00	82.80

EMRO	Western Asia	United Arab Emirates	M	M	M	M	M	M	M
PAHO	Central America and Caribbean	British Virgin Islands	M	M	M	M	M	M	M
PAHO	Central America and Caribbean	Grenada	M	M	M	M	M	M	M

Supplementary Table S41. The *consistency* of 173 Member States for 8 influenza subtypes (A(H1), A(H1N1)pdm09, A(H3), A(H5), A(Unsubtyped) abbreviated A(Uns), B(Yamagata) abbreviated B(Yam), B(Victoria) abbreviated B(Vic), and B(Undetermined) positives abbreviated B(Und)) reported by the WHO's FluNet. We estimated *consistency* as the ratio of weeks when records from one data download were equal to those of another divided by the shared time series length between downloads and multiplied by 100. We downloaded data on 13 June 2020, from Week 1 of 2008 through Week 52 of 2019 and again on 15 June 2021 from Week 1 of 1995 through Week 24 of 2021. The shared time series length consisted of 626 weeks. Member States are listed in descending order by average *consistency* across all 8 subtypes (AVG), regions, and zones. Member State-outcome dyads with missing records for both data downloads are denoted as *M*.

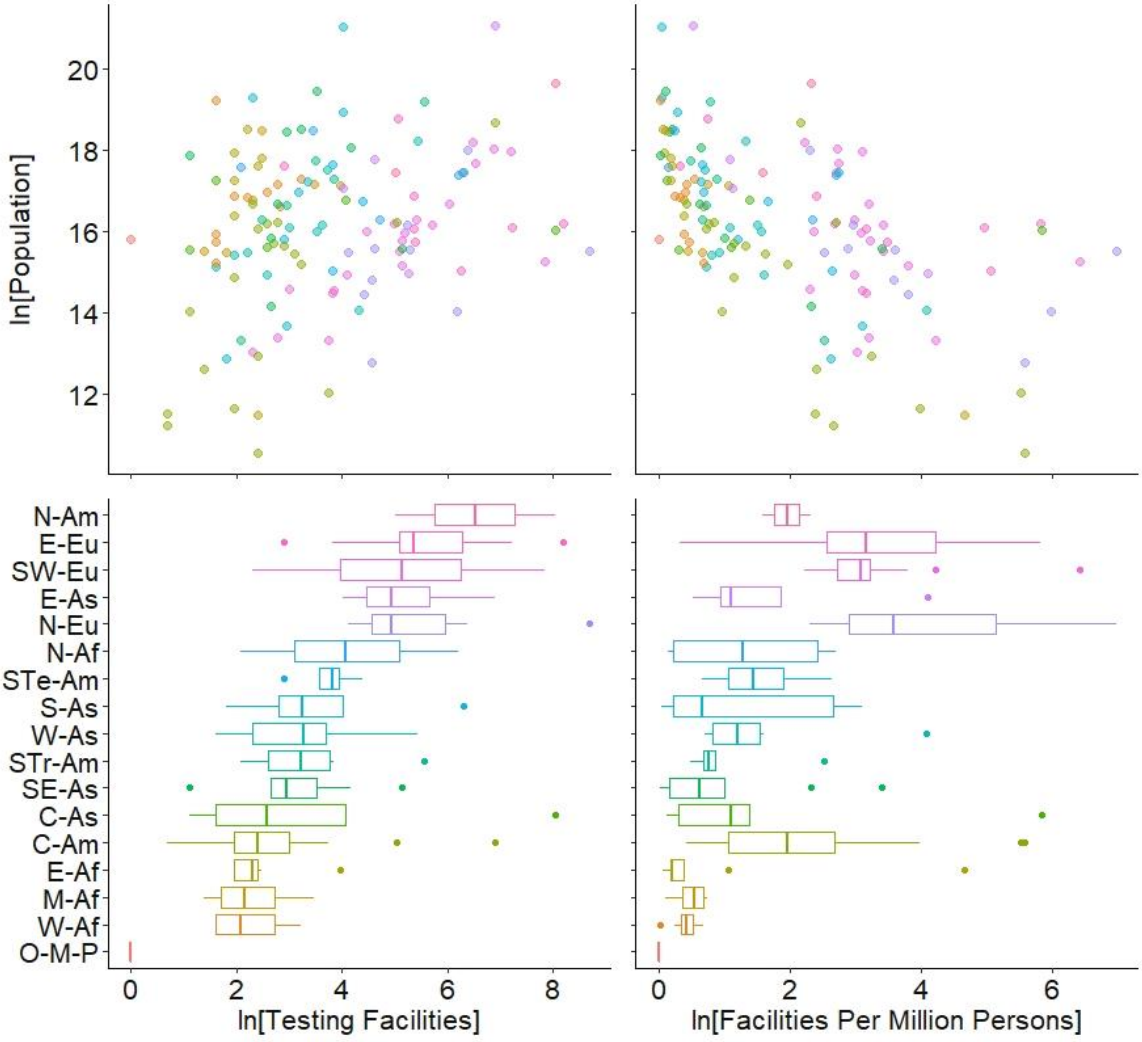
Region	Zone	Country/Territory	A(H1)	A(H1N1)	A(H3)	A(H5)	A(Uns)	B(Yam)	B(Vic)	B(Und)	AVG
AFRO	Eastern Africa	Ethiopia	100.00	100.00	100.00	100.00	100.00	100.00	100.00	100.00	100.00
AFRO	Eastern Africa	Kenya	100.00	100.00	100.00	100.00	100.00	100.00	100.00	100.00	100.00
AFRO	Eastern Africa	Madagascar	100.00	100.00	100.00	100.00	100.00	100.00	100.00	100.00	100.00
AFRO	Eastern Africa	Mauritius	100.00	100.00	100.00	100.00	100.00	100.00	100.00	100.00	100.00
AFRO	Eastern Africa	Seychelles	100.00	100.00	100.00	100.00	100.00	100.00	100.00	100.00	100.00
AFRO	Eastern Africa	Tanzania	100.00	100.00	100.00	100.00	100.00	100.00	100.00	100.00	100.00
AFRO	Eastern Africa	Zambia	100.00	100.00	100.00	100.00	100.00	100.00	100.00	100.00	100.00
AFRO	Middle Africa	Angola	100.00	100.00	100.00	100.00	100.00	100.00	100.00	100.00	100.00
AFRO	Middle Africa	Chad	100.00	100.00	100.00	100.00	100.00	100.00	100.00	100.00	100.00
AFRO	Middle Africa	Congo	100.00	100.00	100.00	100.00	100.00	100.00	100.00	100.00	100.00
AFRO	Middle Africa	South Sudan	100.00	100.00	100.00	100.00	100.00	100.00	100.00	100.00	100.00
AFRO	Northern Africa	Algeria	100.00	100.00	100.00	100.00	100.00	100.00	100.00	100.00	100.00
AFRO	Southern Africa	South Africa	100.00	100.00	100.00	100.00	100.00	100.00	100.00	100.00	100.00
AFRO	Western Africa	Burkina Faso	100.00	100.00	100.00	100.00	100.00	100.00	100.00	100.00	100.00
AFRO	Western Africa	Côte d'Ivoire	100.00	100.00	100.00	100.00	100.00	100.00	100.00	100.00	100.00
AFRO	Western Africa	Ghana	100.00	100.00	100.00	100.00	100.00	100.00	100.00	100.00	100.00
AFRO	Western Africa	Guinea	100.00	100.00	100.00	100.00	100.00	100.00	100.00	100.00	100.00
AFRO	Western Africa	Mauritania	100.00	100.00	100.00	100.00	100.00	100.00	100.00	100.00	100.00
AFRO	Western Africa	Niger	100.00	100.00	100.00	100.00	100.00	100.00	100.00	100.00	100.00
AFRO	Western Africa	Senegal	100.00	100.00	100.00	100.00	100.00	100.00	100.00	100.00	100.00
AFRO	Western Africa	Togo	100.00	100.00	100.00	100.00	100.00	100.00	100.00	100.00	100.00
EMRO	Northern Africa	Sudan	100.00	100.00	100.00	100.00	100.00	100.00	100.00	100.00	100.00
EMRO	Southern Asia	Afghanistan	100.00	100.00	100.00	100.00	100.00	100.00	100.00	100.00	100.00
EMRO	Western Asia	Iraq	100.00	100.00	100.00	100.00	100.00	100.00	100.00	100.00	100.00
EMRO	Western Asia	Jordan	100.00	100.00	100.00	100.00	100.00	100.00	100.00	100.00	100.00
EMRO	Western Asia	Kuwait	100.00	100.00	100.00	100.00	100.00	100.00	100.00	100.00	100.00
EMRO	Western Asia	Qatar	100.00	100.00	100.00	100.00	100.00	100.00	100.00	100.00	100.00
EMRO	Western Asia	Syrian Arab Republic	100.00	100.00	100.00	100.00	100.00	100.00	100.00	100.00	100.00
EMRO	Western Asia	West Bank and Gaza Strip	100.00	100.00	100.00	100.00	100.00	100.00	100.00	100.00	100.00
EURO	Central Asia	Kyrgyzstan	100.00	100.00	100.00	100.00	100.00	100.00	100.00	100.00	100.00
EURO	Central Asia	Tajikistan	100.00	100.00	100.00	100.00	100.00	100.00	100.00	100.00	100.00
EURO	Central Asia	Turkmenistan	100.00	100.00	100.00	100.00	100.00	100.00	100.00	100.00	100.00
EURO	Central Asia	Uzbekistan	100.00	100.00	100.00	100.00	100.00	100.00	100.00	100.00	100.00
EURO	Eastern Europe	Belarus	100.00	100.00	100.00	100.00	100.00	100.00	100.00	100.00	100.00
EURO	Eastern Europe	Bulgaria	100.00	100.00	100.00	100.00	100.00	100.00	100.00	100.00	100.00
EURO	Eastern Europe	Czechia	100.00	100.00	100.00	100.00	100.00	100.00	100.00	100.00	100.00
EURO	Eastern Europe	Hungary	100.00	100.00	100.00	100.00	100.00	100.00	100.00	100.00	100.00
EURO	Eastern Europe	Kosovo	100.00	100.00	100.00	100.00	100.00	100.00	100.00	100.00	100.00
EURO	Eastern Europe	Moldova	100.00	100.00	100.00	100.00	100.00	100.00	100.00	100.00	100.00
EURO	Eastern Europe	Poland	100.00	100.00	100.00	100.00	100.00	100.00	100.00	100.00	100.00
EURO	Eastern Europe	Romania	100.00	100.00	100.00	100.00	100.00	100.00	100.00	100.00	100.00
EURO	Eastern Europe	Russian Federation	100.00	100.00	100.00	100.00	100.00	100.00	100.00	100.00	100.00
EURO	Eastern Europe	Slovakia	100.00	100.00	100.00	100.00	100.00	100.00	100.00	100.00	100.00
EURO	Eastern Europe	Ukraine	100.00	100.00	100.00	100.00	100.00	100.00	100.00	100.00	100.00
EURO	Northern Europe	Estonia	100.00	100.00	100.00	100.00	100.00	100.00	100.00	100.00	100.00
EURO	Northern Europe	Finland	100.00	100.00	100.00	100.00	100.00	100.00	100.00	100.00	100.00
EURO	Northern Europe	Iceland	100.00	100.00	100.00	100.00	100.00	100.00	100.00	100.00	100.00
EURO	Northern Europe	Ireland	100.00	100.00	100.00	100.00	100.00	100.00	100.00	100.00	100.00

EURO	Northern Europe	Latvia	100.00	100.00	100.00	100.00	100.00	100.00	100.00	100.00	100.00
EURO	Northern Europe	Lithuania	100.00	100.00	100.00	100.00	100.00	100.00	100.00	100.00	100.00
EURO	Northern Europe	United Kingdom	100.00	100.00	100.00	100.00	100.00	100.00	100.00	100.00	100.00
EURO	South West Europe	Albania	100.00	100.00	100.00	100.00	100.00	100.00	100.00	100.00	100.00
EURO	South West Europe	Austria	100.00	100.00	100.00	100.00	100.00	100.00	100.00	100.00	100.00
EURO	South West Europe	Belgium	100.00	100.00	100.00	100.00	100.00	100.00	100.00	100.00	100.00
EURO	South West Europe	Bosnia and Herzegovina	100.00	100.00	100.00	100.00	100.00	100.00	100.00	100.00	100.00
EURO	South West Europe	France	100.00	100.00	100.00	100.00	100.00	100.00	100.00	100.00	100.00
EURO	South West Europe	Germany	100.00	100.00	100.00	100.00	100.00	100.00	100.00	100.00	100.00
EURO	South West Europe	Greece	100.00	100.00	100.00	100.00	100.00	100.00	100.00	100.00	100.00
EURO	South West Europe	Italy	100.00	100.00	100.00	100.00	100.00	100.00	100.00	100.00	100.00
EURO	South West Europe	Luxembourg	100.00	100.00	100.00	100.00	100.00	100.00	100.00	100.00	100.00
EURO	South West Europe	Malta	100.00	100.00	100.00	100.00	100.00	100.00	100.00	100.00	100.00
EURO	South West Europe	Montenegro	100.00	100.00	100.00	100.00	100.00	100.00	100.00	100.00	100.00
EURO	South West Europe	Netherlands	100.00	100.00	100.00	100.00	100.00	100.00	100.00	100.00	100.00
EURO	South West Europe	North Macedonia	100.00	100.00	100.00	100.00	100.00	100.00	100.00	100.00	100.00
EURO	South West Europe	Portugal	100.00	100.00	100.00	100.00	100.00	100.00	100.00	100.00	100.00
EURO	South West Europe	Serbia	100.00	100.00	100.00	100.00	100.00	100.00	100.00	100.00	100.00
EURO	South West Europe	Slovenia	100.00	100.00	100.00	100.00	100.00	100.00	100.00	100.00	100.00
EURO	Western Asia	Armenia	100.00	100.00	100.00	100.00	100.00	100.00	100.00	100.00	100.00
EURO	Western Asia	Azerbaijan	100.00	100.00	100.00	100.00	100.00	100.00	100.00	100.00	100.00
EURO	Western Asia	Cyprus	100.00	100.00	100.00	100.00	100.00	100.00	100.00	100.00	100.00
EURO	Western Asia	Georgia	100.00	100.00	100.00	100.00	100.00	100.00	100.00	100.00	100.00
EURO	Western Asia	Israel	100.00	100.00	100.00	100.00	100.00	100.00	100.00	100.00	100.00
EURO	Western Asia	Turkey	100.00	100.00	100.00	100.00	100.00	100.00	100.00	100.00	100.00
PAHO	North America	Canada	100.00	100.00	100.00	100.00	100.00	100.00	100.00	100.00	100.00
PAHO	Temperate South America	Argentina	100.00	100.00	100.00	100.00	100.00	100.00	100.00	100.00	100.00
PAHO	Tropical South America	Venezuela	100.00	100.00	100.00	100.00	100.00	100.00	100.00	100.00	100.00
SEARO	Eastern Asia	North Korea	100.00	100.00	100.00	100.00	100.00	100.00	100.00	100.00	100.00
SEARO	South-East Asia	Indonesia	100.00	100.00	100.00	100.00	100.00	100.00	100.00	100.00	100.00
SEARO	South-East Asia	Myanmar	100.00	100.00	100.00	100.00	100.00	100.00	100.00	100.00	100.00
SEARO	South-East Asia	Thailand	100.00	100.00	100.00	100.00	100.00	100.00	100.00	100.00	100.00
SEARO	South-East Asia	Timor-Leste	100.00	100.00	100.00	100.00	100.00	100.00	100.00	100.00	100.00
SEARO	Southern Asia	Bangladesh	100.00	100.00	100.00	100.00	100.00	100.00	100.00	100.00	100.00
WPRO	Eastern Asia	Mongolia	100.00	100.00	100.00	100.00	100.00	100.00	100.00	100.00	100.00
WPRO	Eastern Asia	South Korea	100.00	100.00	100.00	100.00	100.00	100.00	100.00	100.00	100.00
WPRO	South-East Asia	Laos	100.00	100.00	100.00	100.00	100.00	100.00	100.00	100.00	100.00
WPRO	South-East Asia	Malaysia	100.00	100.00	100.00	100.00	100.00	100.00	100.00	100.00	100.00
WPRO	South-East Asia	Singapore	100.00	100.00	100.00	100.00	100.00	100.00	100.00	100.00	100.00
WPRO	South-East Asia	Viet Nam	100.00	100.00	100.00	100.00	100.00	100.00	100.00	100.00	100.00
AFRO	Eastern Africa	Mozambique	100.00	100.00	100.00	100.00	100.00	100.00	100.00	99.84	99.98
AFRO	Western Africa	Nigeria	100.00	100.00	100.00	100.00	100.00	100.00	100.00	99.84	99.98
EURO	Northern Europe	Sweden	100.00	100.00	100.00	100.00	100.00	100.00	100.00	99.84	99.98
EURO	South West Europe	Croatia	100.00	100.00	100.00	100.00	100.00	100.00	100.00	99.84	99.98
EURO	South West Europe	Switzerland	100.00	100.00	100.00	100.00	100.00	100.00	100.00	99.84	99.98
PAHO	Central America and Caribbean	Antigua and Barbuda	100.00	100.00	100.00	100.00	100.00	100.00	100.00	99.84	99.98
WPRO	Oceania Melanesia Polynesia	New Caledonia	100.00	100.00	100.00	100.00	100.00	100.00	100.00	99.84	99.98
EURO	Northern Europe	Norway	100.00	100.00	100.00	100.00	100.00	100.00	99.84	99.84	99.96
EURO	Central Asia	Kazakhstan	100.00	100.00	100.00	100.00	100.00	100.00	100.00	99.68	99.96
PAHO	Central America and Caribbean	Panama	100.00	100.00	100.00	100.00	100.00	100.00	100.00	99.68	99.96
PAHO	Tropical South America	Colombia	100.00	100.00	100.00	100.00	100.00	100.00	100.00	99.68	99.96
PAHO	Tropical South America	Guyana	100.00	100.00	100.00	100.00	100.00	100.00	100.00	99.68	99.96
AFRO	Western Africa	Sierra Leone	100.00	100.00	100.00	100.00	100.00	100.00	100.00	99.52	99.94
EURO	South West Europe	Spain	100.00	100.00	100.00	100.00	100.00	100.00	100.00	99.52	99.94
WPRO	Oceania Melanesia Polynesia	Fiji	100.00	100.00	100.00	100.00	100.00	100.00	100.00	99.52	99.94
PAHO	Tropical South America	Peru	100.00	100.00	100.00	100.00	100.00	100.00	100.00	99.36	99.92
SEARO	Southern Asia	Bhutan	100.00	100.00	100.00	100.00	100.00	100.00	100.00	99.36	99.92
PAHO	Central America and Caribbean	Bahamas	100.00	100.00	100.00	100.00	100.00	100.00	100.00	99.20	99.90
PAHO	Central America and Caribbean	Belize	100.00	100.00	100.00	100.00	100.00	100.00	100.00	99.20	99.90
PAHO	Central America and Caribbean	Cayman Islands	100.00	100.00	100.00	100.00	100.00	100.00	100.00	99.20	99.90

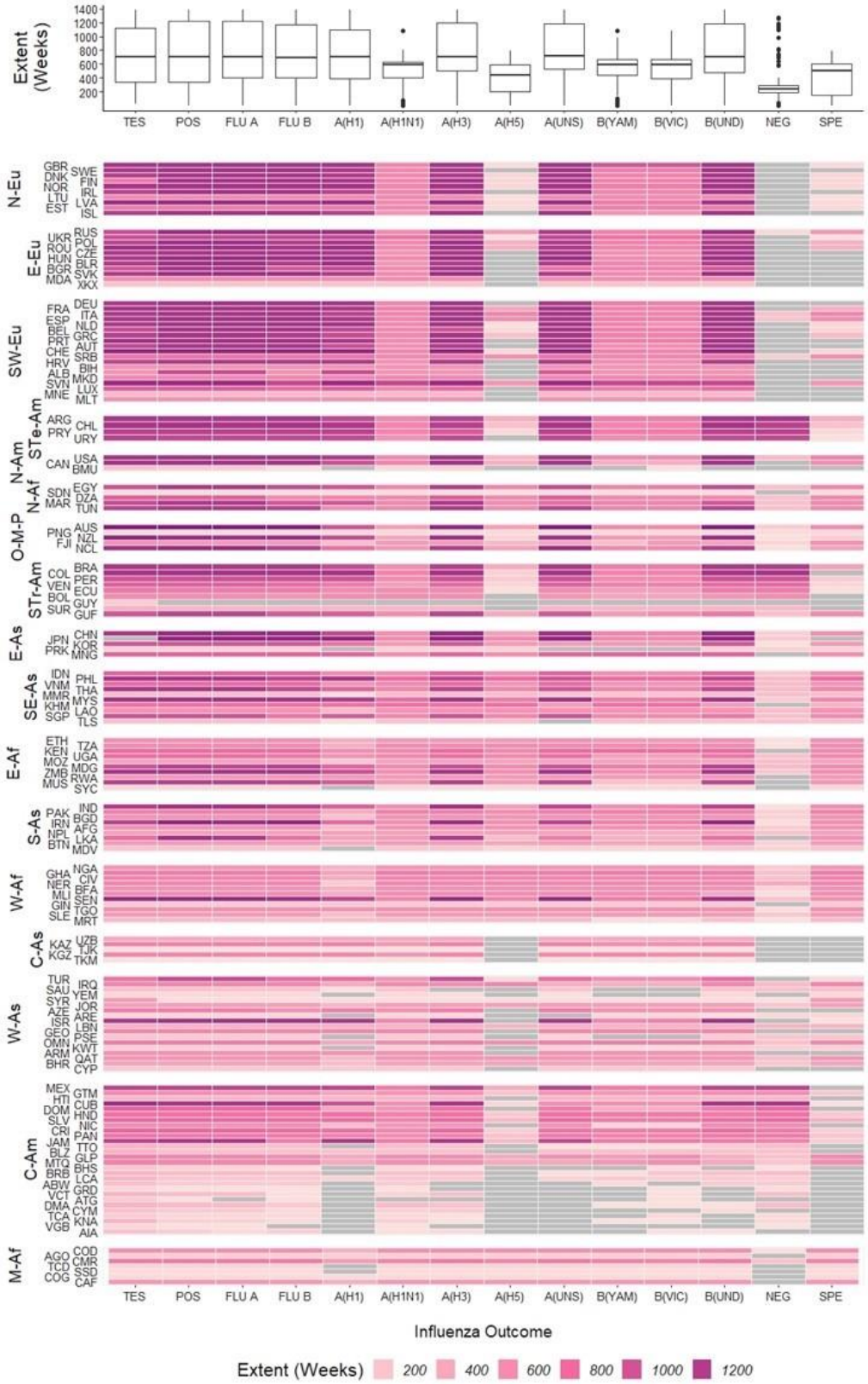
PAHO	Central America and Caribbean	Costa Rica	100.00	100.00	100.00	100.00	100.00	100.00	100.00	99.04	99.88
PAHO	Tropical South America	Brazil	100.00	100.00	100.00	100.00	100.00	100.00	100.00	99.04	99.88
EMRO	Southern Asia	Iran	100.00	100.00	100.00	100.00	100.00	100.00	100.00	98.88	99.86
PAHO	Central America and Caribbean	Anguilla	100.00	100.00	100.00	100.00	100.00	100.00	100.00	98.88	99.86
PAHO	Central America and Caribbean	Haiti	100.00	100.00	100.00	100.00	100.00	100.00	100.00	98.88	99.86
PAHO	Central America and Caribbean	Turks and Caicos Islands	100.00	100.00	100.00	100.00	100.00	100.00	100.00	98.72	99.84
EMRO	Western Asia	Bahrain	100.00	100.00	100.00	100.00	100.00	100.00	100.00	98.56	99.82
EMRO	Western Asia	Oman	100.00	100.00	100.00	100.00	100.00	100.00	100.00	98.56	99.82
EMRO	Western Asia	Yemen	100.00	100.00	100.00	100.00	100.00	100.00	100.00	98.56	99.82
AFRO	Middle Africa	Central African Republic	100.00	100.00	100.00	100.00	100.00	100.00	100.00	98.40	99.80
PAHO	Central America and Caribbean	El Salvador	100.00	100.00	100.00	100.00	100.00	100.00	100.00	98.24	99.78
AFRO	Eastern Africa	Uganda	100.00	100.00	100.00	100.00	100.00	100.00	100.00	97.76	99.72
PAHO	Central America and Caribbean	Saint Kitts and Nevis	100.00	100.00	100.00	100.00	100.00	100.00	100.00	97.76	99.72
PAHO	North America	Bermuda	100.00	100.00	100.00	100.00	100.00	100.00	100.00	97.76	99.72
WPRO	Eastern Asia	Japan	100.00	98.24	99.68	100.00	99.84	100.00	99.68	100.00	99.68
EMRO	Northern Africa	Tunisia	100.00	100.00	100.00	100.00	100.00	100.00	100.00	96.96	99.62
AFRO	Middle Africa	Democratic Republic of the Congo	100.00	100.00	100.00	100.00	100.00	100.00	100.00	96.49	99.56
EMRO	Northern Africa	Morocco	100.00	100.00	100.00	100.00	100.00	100.00	100.00	96.49	99.56
PAHO	Tropical South America	Suriname	100.00	100.00	100.00	100.00	100.00	100.00	100.00	96.49	99.56
PAHO	Central America and Caribbean	Cuba	100.00	100.00	100.00	100.00	100.00	100.00	100.00	95.69	99.46
SEARO	Southern Asia	Nepal	100.00	100.00	100.00	100.00	100.00	100.00	100.00	95.69	99.46
PAHO	Central America and Caribbean	Mexico	100.00	100.00	100.00	100.00	100.00	100.00	100.00	95.53	99.44
PAHO	North America	United States of America	100.00	99.36	99.52	100.00	98.24	100.00	99.04	99.04	99.40
PAHO	Central America and Caribbean	Honduras	100.00	100.00	100.00	100.00	100.00	100.00	100.00	94.57	99.32
WPRO	Oceania Melanesia Polynesia	New Zealand	100.00	99.04	99.04	100.00	99.04	99.04	99.04	99.04	99.28
AFRO	Eastern Africa	Rwanda	100.00	100.00	100.00	100.00	100.00	100.00	100.00	94.09	99.26
WPRO	Eastern Asia	China	100.00	98.88	98.88	100.00	99.52	98.88	98.88	98.88	99.24
PAHO	Temperate South America	Paraguay	100.00	100.00	100.00	100.00	100.00	100.00	100.00	93.93	99.24
SEARO	Southern Asia	India	100.00	100.00	100.00	100.00	100.00	100.00	100.00	93.93	99.24
SEARO	Southern Asia	Maldives	100.00	100.00	100.00	100.00	100.00	100.00	100.00	93.93	99.24
AFRO	Middle Africa	Cameroon	100.00	100.00	100.00	100.00	100.00	100.00	100.00	93.29	99.16
PAHO	Central America and Caribbean	Jamaica	100.00	100.00	100.00	100.00	100.00	100.00	100.00	93.29	99.16
EMRO	Southern Asia	Pakistan	100.00	100.00	100.00	100.00	100.00	100.00	100.00	92.33	99.04
EMRO	Western Asia	Lebanon	100.00	99.52	98.56	100.00	100.00	100.00	100.00	94.25	99.04
PAHO	Central America and Caribbean	Saint Vincent and the Grenadines	100.00	100.00	100.00	100.00	100.00	100.00	100.00	92.17	99.02
AFRO	Western Africa	Mali	100.00	100.00	100.00	100.00	100.00	100.00	100.00	90.42	98.80
PAHO	Central America and Caribbean	Guatemala	100.00	100.00	100.00	100.00	100.00	100.00	100.00	89.78	98.72
PAHO	Temperate South America	Chile	100.00	100.00	100.00	100.00	100.00	100.00	100.00	89.46	98.68
PAHO	Tropical South America	Bolivia	100.00	100.00	100.00	100.00	100.00	100.00	100.00	89.30	98.66
WPRO	South-East Asia	Cambodia	100.00	100.00	100.00	100.00	100.00	100.00	100.00	87.70	98.46
EMRO	Western Asia	Saudi Arabia	100.00	93.93	100.00	100.00	95.85	100.00	100.00	96.81	98.32
PAHO	Temperate South America	Uruguay	100.00	100.00	100.00	100.00	100.00	100.00	100.00	85.78	98.22
PAHO	Central America and Caribbean	Saint Lucia	100.00	100.00	100.00	100.00	100.00	100.00	100.00	85.46	98.18
PAHO	Central America and Caribbean	Aruba	100.00	100.00	100.00	100.00	100.00	100.00	100.00	84.82	98.10
WPRO	Oceania Melanesia Polynesia	Papua New Guinea	99.84	99.68	98.08	99.84	99.04	97.44	99.84	90.42	98.02
PAHO	Central America and Caribbean	Dominica	100.00	100.00	100.00	100.00	100.00	100.00	100.00	83.55	97.94
WPRO	South-East Asia	Philippines	99.84	94.73	96.81	99.84	99.04	99.36	96.01	96.49	97.76
PAHO	Central America and Caribbean	Dominican Republic	100.00	100.00	100.00	100.00	100.00	100.00	100.00	82.11	97.76
EURO	Northern Europe	Denmark	100.00	96.81	96.65	100.00	96.33	96.96	98.88	96.33	97.74
EMRO	Northern Africa	Egypt	100.00	100.00	100.00	100.00	100.00	100.00	100.00	78.91	97.36
PAHO	Central America and Caribbean	Nicaragua	100.00	100.00	100.00	100.00	100.00	100.00	100.00	78.43	97.30
SEARO	Southern Asia	Sri Lanka	100.00	94.41	92.81	100.00	95.21	100.00	100.00	94.25	97.08
PAHO	Central America and Caribbean	Trinidad and Tobago	100.00	100.00	100.00	100.00	100.00	100.00	100.00	76.68	97.08
PAHO	Tropical South America	French Guiana	100.00	100.00	100.00	100.00	100.00	100.00	100.00	73.00	96.63
PAHO	Central America and Caribbean	Barbados	100.00	100.00	100.00	100.00	100.00	100.00	100.00	71.88	96.49
PAHO	Central America and Caribbean	Martinique	100.00	100.00	100.00	100.00	100.00	100.00	100.00	71.09	96.39
PAHO	Tropical South America	Ecuador	100.00	100.00	100.00	100.00	100.00	100.00	100.00	69.65	96.21
PAHO	Central America and Caribbean	Guadeloupe	100.00	100.00	100.00	100.00	100.00	100.00	100.00	67.25	95.91

WPRO	Oceania Melanesia Polynesia	Australia	100.00	92.33	91.69	100.00	96.96	100.00	100.00	64.06	93.13
EMRO	Western Asia	United Arab Emirates	M	M	M	M	M	M	M	M	M
PAHO	Central America and Caribbean	British Virgin Islands	M	M	M	M	M	M	M	M	M
PAHO	Central America and Caribbean	Grenada	M	M	M	M	M	M	M	M	M

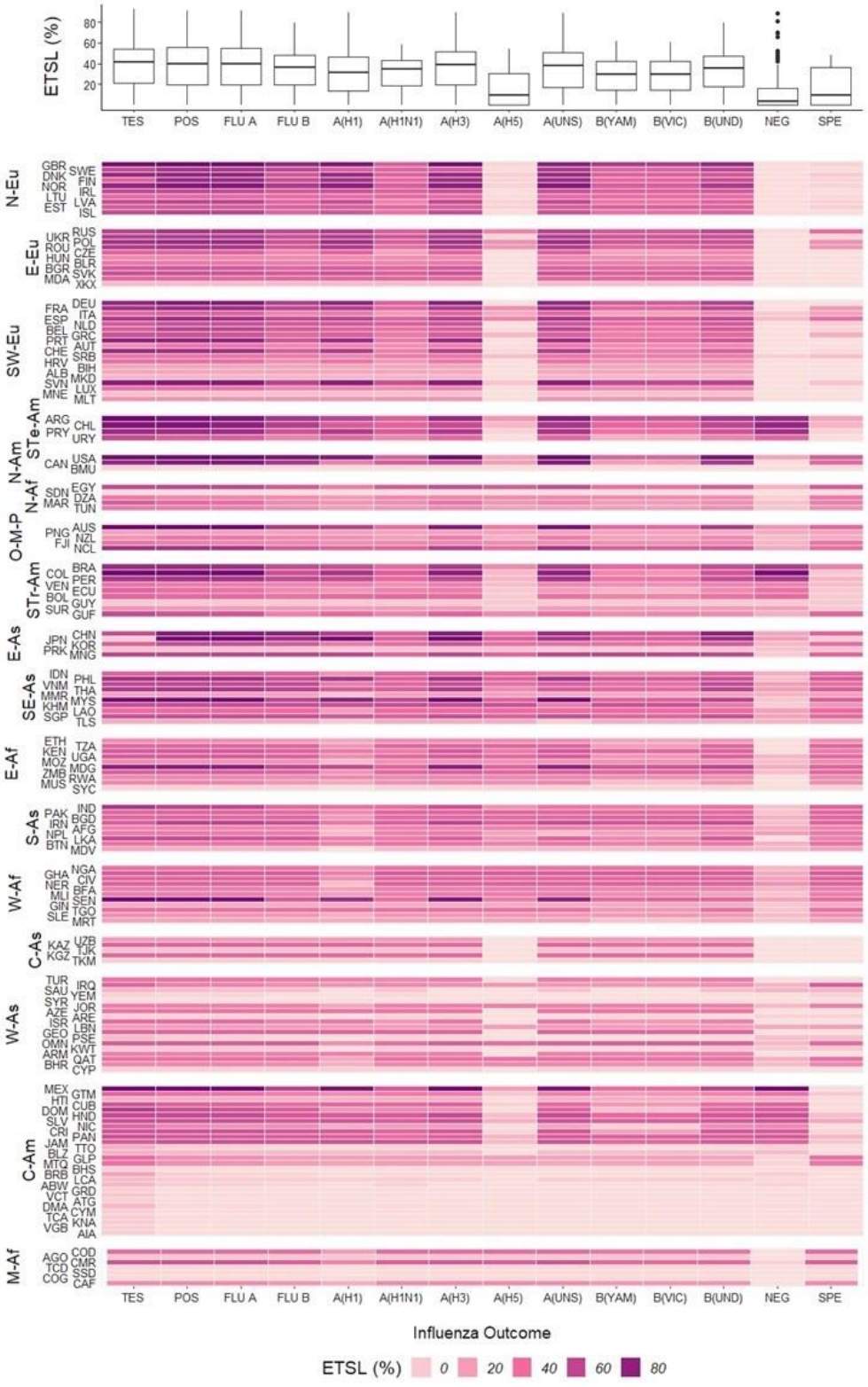
Supplementary Figure S1. A shared axis, multi-panel plot of the relationship between log-transformed values of Member State 2021 population estimates, influenza testing facilities, and testing facilities per million persons. We extracted Member State population estimates from the United States Census Bureau International Data Base (IDB) and the Institut national de la statistique et des etudes economiques (Insee). We estimated testing facilities using numerous sources, and calculated facilities per million persons by dividing facilities by population estimates and multiplying by 1,000,000. Marker colors used in scatterplots (top panel) depict WHO-defined influenza transmission zones used for boxplots (bottom panel) and correspond to the European (EURO), Eastern Mediterranean (EMRO), Southeastern Asia (SEARO), Western Pacific (WPRO), Pan-American (PAHO), and African (AFRO) regions. We report boxplot categories in descending order by median testing facilities per Member State.



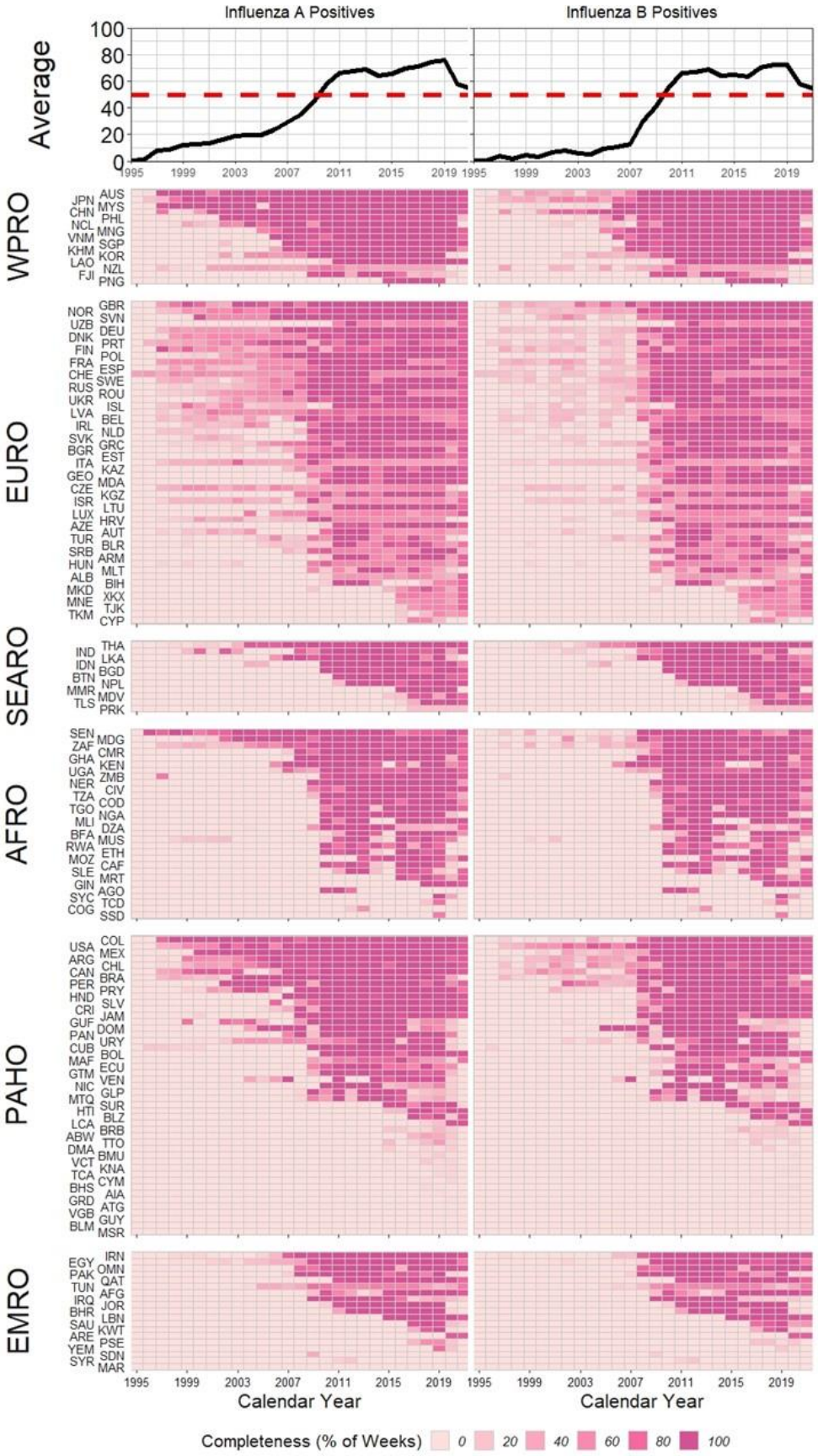
Supplementary Figure S2. This figure is identical to Figure 2 except has been disaggregated by 17 WHO-defined influenza transmission zones (North, Central and Caribbean, Temperate South, and Tropical South America; Northern, Southwestern, and Eastern Europe; Northern, Eastern, Middle, Western, and Southern Africa; Western, Central, Eastern, Southern, and Southeastern Asia; and Oceania Melanesia Polynesia). Zones and Member States are listed in descending order by median extent of total positives and 2021 population estimates, respectively.



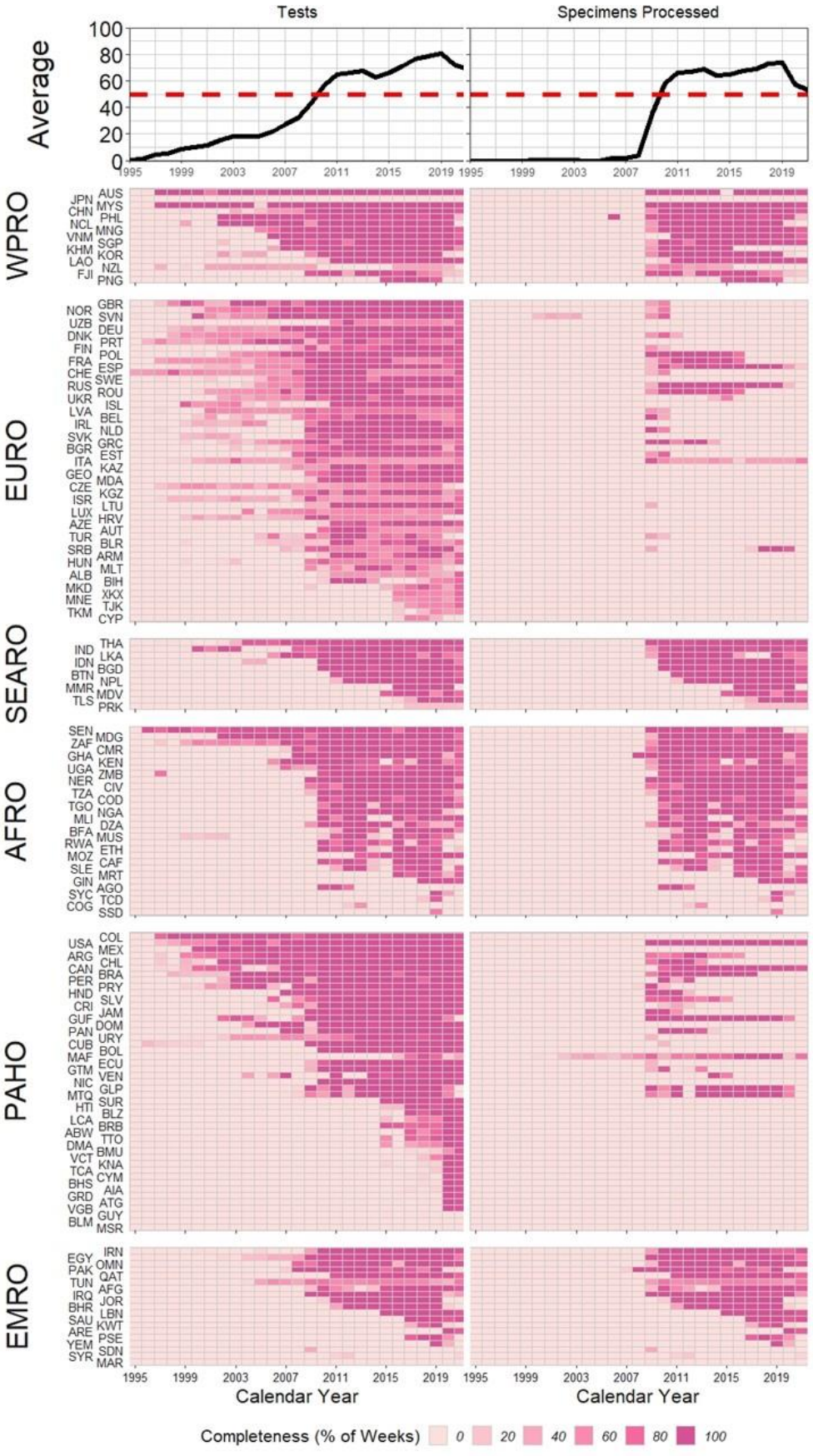
Supplementary Figure S3. This figure is identical to Figure 3 except has been disaggregated by 17 WHO-defined influenza transmission zones (North, Central and Caribbean, Temperate South, and Tropical South America; Northern, Southwestern, and Eastern Europe; Northern, Eastern, Middle, Western, and Southern Africa; Western, Central, Eastern, Southern, and Southeastern Asia; and Oceania Melanesia Polynesia). Zones and Member States are listed in descending order by median effective time series length of total positives and 2021 population estimates, respectively.



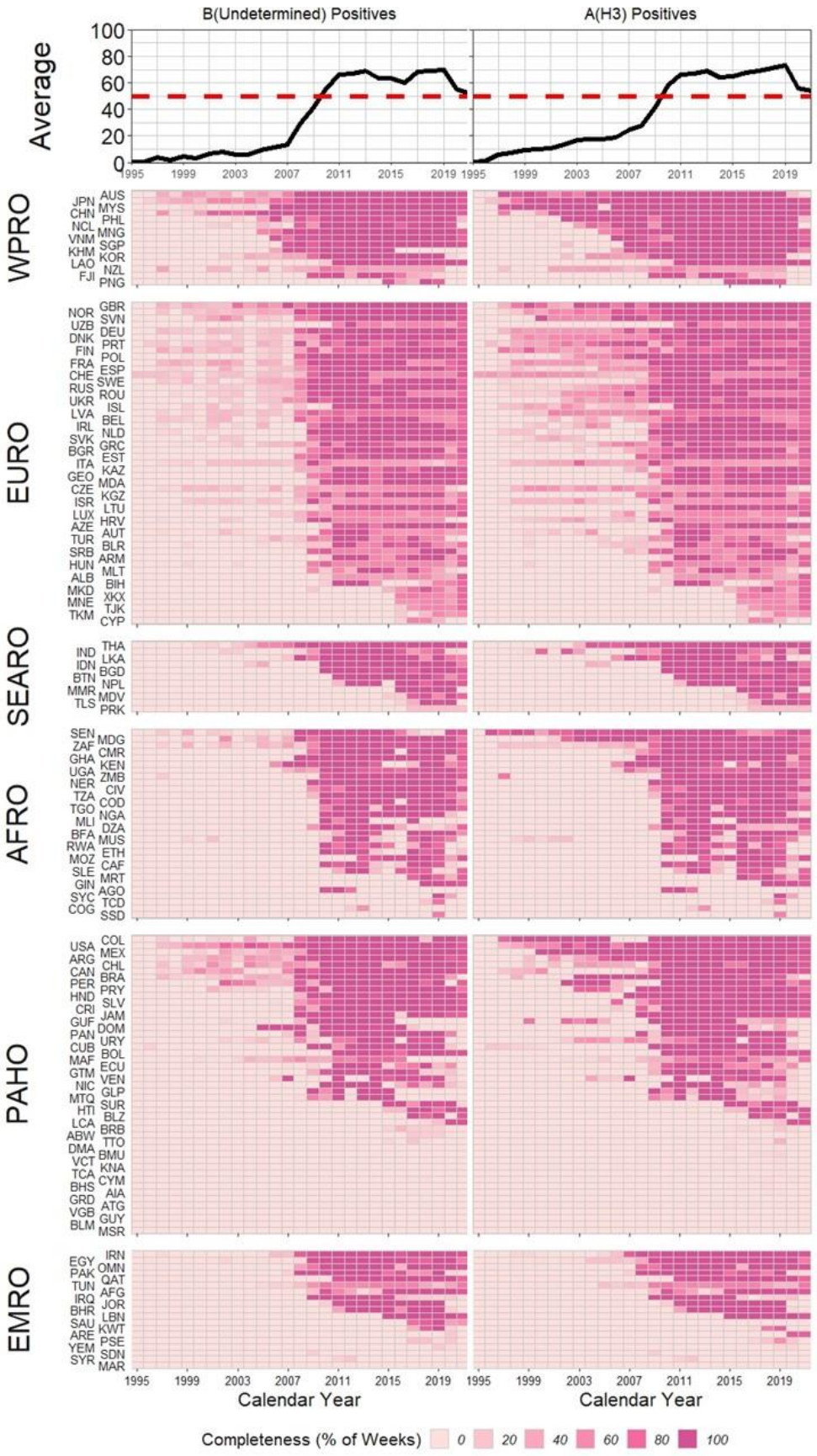
Supplementary Figure S4. This figure is identical to Figure 4 for influenza A and B positives. Member States are listed in descending order by average completeness of total positives.



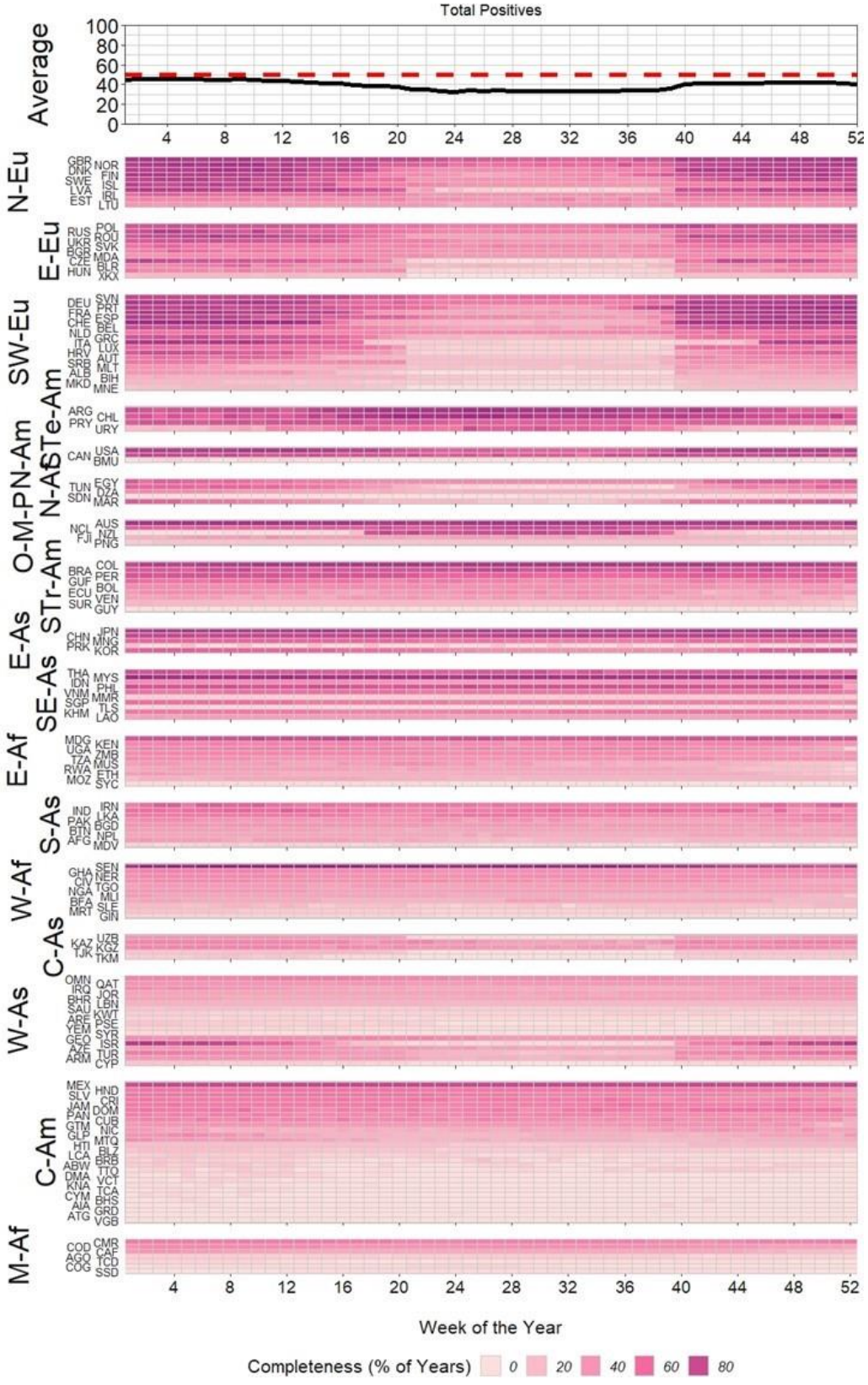
Supplementary Figure S5. This figure is identical to Figure 4 for tests and specimens processed. Member States are listed in descending order by average completeness of total positives.



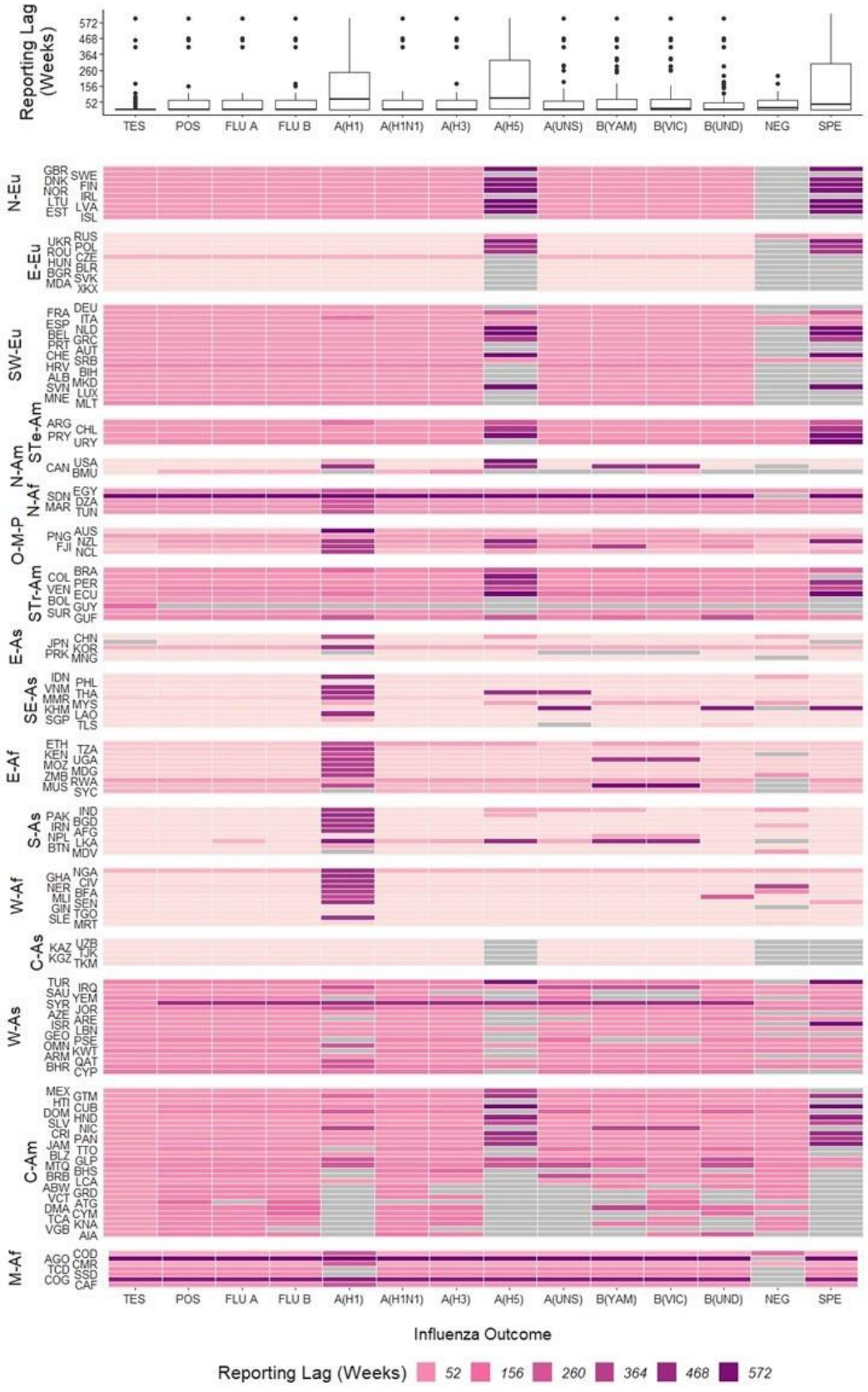
Supplementary Figure S6. This figure is identical to Figure 5 for B(Undetermined) and A(H3) positives. Member States are listed in descending order by average completeness of total positives.



Supplementary Figure S7. This figure is identical to Figure 6 with comparisons across transmission zones. Member States are listed in descending order by 2021 population estimates.



Supplementary Figure S8. This figure is identical to Figure 7 with comparisons across transmission zones. Member States are listed in descending order by 2021 population estimates.



Appendix B.

Supplementary Table S1. Nineteen metrics related to the geographic extent, case definition, and exposure or illness duration of foodborne outbreaks as reported by the National Outbreak Reporting System (NORS) in 2009-2019. *All Visits* refers to the sum of all primary cases who visited a healthcare provider, hospital, or emergency room (ER).

Metric	Description	Units
States of Residence	Number of states where persons exposed to contaminated food vehicle reside	States
States of Exposure	Number of states where persons consumed the contaminated food vehicle responsible for the outbreak	States
Counties of Residence	Number of counties where persons exposed to contaminated food vehicle reside	Counties
Counties of Exposure	Number of counties where persons consumed the contaminated food vehicle responsible for the outbreak	Counties
Primary Confirmed Cases	Number of laboratory-confirmed primary cases	Cases
Primary Probable Cases	Number of probable primary cases	Cases
Total Primary Cases	Number of laboratory-confirmed and probable primary cases	Cases
Secondary Confirmed Cases	Number of laboratory-confirmed secondary cases	Cases
Secondary Probable Cases	Number of probable secondary cases	Cases
Total Secondary Cases	Number of laboratory-confirmed and probable secondary cases	Cases
Total Cases	Sum of all laboratory-confirmed and probable primary and secondary cases	Cases
Healthcare Visits	Number of total primary cases who visited a health care provider	Visits
Hospitalizations	Number of total primary cases who were hospitalized	Visits
ER Visits	Number of total primary cases who visited an emergency room	Visits
Hospital/ER Visits	Number of total primary cases who visited an emergency room and/or were hospitalized	Visits
All Visits	Number of primary cases who visited a health care provider, were hospitalized, and/or visited an emergency room	Visits
Deaths	Number of total primary cases who died	Deaths
Illness Duration	Duration from earliest to latest reported illness symptom	Days
Exposure Duration	Duration from the earliest to latest reported exposure event	Days

Supplementary Table S2. Forty-eight metrics generated using the ratio of extent, case definition, and duration metrics reported in Supplementary Table S1. We extracted 19 metrics describing the severity of foodborne outbreaks as reported by the National Outbreak Reporting System (NORS) in 2009-2019. We generated these additional metrics to describe the speed of infection (case definition per duration), transmissibility of infection (extent per duration), and intensity of illness (morbidity/mortality of cases per total cases). Units suggest the numerator and denominator of ratios. *All Visits* refers to the sum of all primary cases who visited a healthcare provider, hospital, or emergency room (ER).

Metric	Description	Units
Healthcare Visits per Primary Confirmed Cases	Primary cases who visited a healthcare provider per laboratory-confirmed primary cases	Visits/Cases
Healthcare Visits per Total Primary Cases	Primary cases who visited a healthcare provider per laboratory-confirmed and probable primary cases	Visits/Cases
Healthcare Visits per Total Cases	Primary cases who visited a healthcare provider per total cases	Visits/Cases
Hospital Visits per Primary Confirmed Cases	Primary cases who visited a healthcare provider per laboratory-confirmed primary cases	Visits/Cases
Hospital Visits per Total Primary Cases	Primary cases who were hospitalized per laboratory-confirmed and probable primary cases	Visits/Cases
Hospital Visits per Total Cases	Primary cases who were hospitalized per total cases	Visits/Cases
ER Visits per Primary Confirmed Cases	Primary cases who were hospitalized per laboratory-confirmed primary cases	Visits/Cases
ER Visits per Total Primary Cases	Primary cases who visited an emergency room per laboratory-confirmed and probable primary cases	Visits/Cases
ER Visits per Total Cases	Primary cases who visited an emergency room per total cases	Visits/Cases
Hospital/ER Visits per Primary Confirmed Cases	Primary cases who visited an emergency room and/or hospital per laboratory-confirmed primary cases	Visits/Cases
Hospital/ER Visits per Total Primary Cases	Primary cases who visited an emergency room and/or hospital per laboratory-confirmed and probable primary cases	Visits/Cases
Hospital/ER Visits per Total Cases	Primary cases who visited an emergency room and/or hospital per total cases	Visits/Cases
All Visits per Primary Confirmed Cases	Primary cases who visited a healthcare provider, emergency room, and/or hospital per laboratory-confirmed primary cases	Visits/Cases
All Visits per Total Primary Cases	Primary cases visiting a healthcare provider, hospital, and/or emergency room per laboratory-confirmed and probable primary cases	Visits/Cases
All Visits per Total Cases	Primary cases visiting a healthcare provider, hospital, and/or emergency room per total cases	Visits/Cases
Deaths per Primary Confirmed Cases	Primary cases who died per laboratory-confirmed primary cases	Deaths/Cases
Deaths per Total Primary Cases	Primary cases who died per laboratory-confirmed and probable primary cases	Deaths/Cases
Deaths per Total Cases	Primary cases who died per total cases	Deaths/Cases
Exposed States per Exposure Duration	States where persons consumed the contaminated food vehicle responsible for the outbreak per days of reported exposure events	States/Days
Exposed Counties per Exposure Duration	Counties where persons consumed the contaminated food vehicle responsible for the outbreak per days of reported exposure events	Counties/Days
Primary Confirmed Cases per Exposure Duration	Laboratory-confirmed primary cases per days of reported exposure events	Cases/Days

Primary Probable Cases per Exposure Duration	Probable primary cases per days of reported exposure events	Cases/Days
Total Primary Cases per Exposure Duration	Laboratory-confirmed and probable primary cases per days of reported exposure events	Cases/Days
Secondary Confirmed Cases per Exposure Duration	Laboratory-confirmed secondary cases per days of reported exposure events	Cases/Days
Secondary Probable Cases per Exposure Duration	Probable secondary cases per days of reported exposure events	Cases/Days
Total Secondary Cases per Exposure Duration	Laboratory-confirmed and probable secondary cases per days of reported exposure events	Cases/Days
Total Cases per Exposure Duration	Total cases per days of reported exposure events	Cases/Days
Healthcare Visits per Exposure Duration	Primary cases who visited a health care provider per days of reported exposure events	Visits/Days
Hospital Visits per Exposure Duration	Primary cases who were hospitalized per days of reported exposure events	Visits/Days
ER Visits per Exposure Duration	Primary cases who visited an emergency room per days of reported exposure events	Visits/Days
Hospital/ER Visits per Exposure Duration	Primary cases who visited an emergency room and/or were hospitalized per days of reported exposure events	Visits/Days
All Visits per Exposure Duration	Primary cases visiting health care provider, hospital, and/or emergency room per days of reported exposure events	Visits/Days
Deaths per Exposure Duration	Primary cases who died per days of reported exposure events	Deaths/Days
Residing States per Illness Duration	States where persons exposed to contaminated food vehicle reside per days of reported illness symptoms	States/Days
Residing Counties per Illness Duration	Counties where persons exposed to contaminated food vehicle reside per days of reported illness symptoms	Counties/Days
Primary Confirmed Cases per Illness Duration	Laboratory-confirmed primary cases per days of reported illness symptoms	Cases/Days
Primary Probable Cases per Illness Duration	Probable primary cases per days of reported illness symptoms	Cases/Days
Total Primary Cases per Illness Duration	Laboratory-confirmed and probable primary cases per days of reported illness symptoms	Cases/Days
Secondary Confirmed Cases per Illness Duration	Laboratory-confirmed secondary cases per days of reported illness symptoms	Cases/Days
Secondary Probable Cases per Illness Duration	Probable secondary cases per days of reported illness symptoms	Cases/Days
Total Secondary Cases per Illness Duration	Laboratory-confirmed and probable secondary cases per days of reported illness symptoms	Cases/Days
Total Cases per Illness Duration	Total cases per days of reported illness symptoms	Cases/Days
Healthcare Visits per Illness Duration	Primary cases who visited a health care provider per days of reported illness symptoms	Visits/Days
Hospital Visits per Illness Duration	Primary cases who were hospitalized per days of reported illness symptoms	Visits/Days
ER Visits per Illness Duration	Primary cases who visited an emergency room per days of reported illness symptoms	Visits/Days
Hospital/ER Visits per Illness Duration	Primary cases who visited an emergency room and/or were hospitalized per days of reported illness symptoms	Visits/Days
All Visits per Illness Duration	Primary cases visiting health care provider, hospital, and/or emergency room per days of reported illness symptoms	Visits/Days

Deaths per Illness Duration	Primary cases who died per days of reported illness symptoms	Deaths/Days

Supplementary Table S3. Summary statistics to evaluate severity metrics related to geographic extent, case definition, and duration of exposure or illness events in the National Outbreak Reporting System (NORS) in 2009-2019. Statistics include observations (with percent completeness), average estimates per outbreak (with 95% confidence intervals), median estimates per outbreak (with interquartile range), minimum and maximum metric values, and measures of L-skewness and L-kurtosis. We estimated completeness as the ratio of outbreaks with available records to total outbreaks in our study period (N=9,407) and multiplied by 100. We calculated average estimates per outbreak using generalized linear models adjusted for negative binomial distributions and the logarithmic link function. We chose L-skewness and L-kurtosis rather than conventional product moment statistics due to their superiority in estimating distribution parameters particularly for smaller sample sizes [23]. Metrics are listed in descending order by record completeness. *All Visits* refers to the sum of all primary cases who visited a healthcare provider, hospital, or emergency room (ER).

Metric	Counts [% Complete]	Average [95% CI]	Median [IQR]	Min, Max	L-Skew	L-Kurt
States of Residence	9407 [100.00]	0.27 [0.26, 0.28]	0.00 [0.00, 0.00]	0.00, 47.00	0.88	0.73
States of Exposure	9407 [100.00]	1.34 [1.31, 1.38]	1.00 [1.00, 1.00]	1.00, 45.00	0.96	0.90
Counties of Residence	9407 [100.00]	0.46 [0.44, 0.48]	0.00 [0.00, 0.00]	0.00, 22.00	0.75	0.49
Counties of Exposure	9407 [100.00]	1.02 [0.99, 1.05]	1.00 [1.00, 1.00]	0.00, 19.00	0.20	0.81
Total Primary Cases	9407 [100.00]	17.27 [16.92, 17.64]	7.00 [4.00, 17.00]	2.00, 1939.00	0.62	0.43
Total Cases	9407 [100.00]	17.69 [17.33, 18.06]	8.00 [4.00, 18.00]	2.00, 1939.00	0.62	0.43
Primary Confirmed Cases	9298 [98.84]	4.35 [4.26, 4.45]	1.00 [0.00, 3.00]	0.00, 907.00	0.72	0.56
Deaths	9263 [98.47]	0.03 [0.02, 0.03]	0.00 [0.00, 0.00]	0.00, 33.00	0.98	0.95
Deaths per Total Primary Cases	9263 [98.47]	0.00 [0.00, 0.00]	0.00 [0.00, 0.00]	0.00, 1.00	0.99	0.97
Deaths per Total Cases	9263 [98.47]	0.00 [0.00, 0.00]	0.00 [0.00, 0.00]	0.00, 1.00	0.99	0.97
Hospital Visits	9194 [97.74]	1.12 [1.09, 1.16]	0.00 [0.00, 1.00]	0.00, 204.00	0.82	0.63
Hospital Visits per Total Primary Cases	9194 [97.74]	0.08 [0.07, 0.09]	0.00 [0.00, 0.03]	0.00, 1.00	0.73	0.45
Hospital Visits per Total Cases	9194 [97.74]	0.08 [0.07, 0.08]	0.00 [0.00, 0.03]	0.00, 1.00	0.74	0.46
Illness Duration	9116 [96.91]	13.59 [13.30, 13.88]	2.00 [2.00, 6.00]	1.00, 2665.00	0.83	0.71
Residing States per Illness Duration	9116 [96.91]	0.08 [0.08, 0.09]	0.00 [0.00, 0.00]	0.00, 23.50	0.89	0.74
Residing Counties per Illness Duration	9116 [96.91]	0.16 [0.15, 0.17]	0.00 [0.00, 0.00]	0.00, 13.00	0.79	0.55
Total Primary Cases per Illness Duration	9116 [96.91]	5.07 [4.96, 5.19]	3.00 [1.50, 5.33]	0.00, 400.00	0.53	0.40
Total Cases per Illness Duration	9116 [96.91]	5.16 [5.05, 5.28]	3.00 [1.50, 5.50]	0.00, 400.00	0.54	0.39
Primary Confirmed Cases per Illness Duration	9023 [95.92]	0.57 [0.55, 0.59]	0.18 [0.00, 0.88]	0.00, 16.00	0.50	0.22
Deaths per Illness Duration	8999 [95.66]	0.00 [0.00, 0.00]	0.00 [0.00, 0.00]	0.00, 2.00	0.99	0.98
Hospital Visits per Illness Duration	8937 [95.00]	0.14 [0.13, 0.15]	0.00 [0.00, 0.03]	0.00, 30.00	0.81	0.59
Primary Probable Cases	8932 [94.95]	13.00 [12.72, 13.28]	5.00 [2.00, 13.00]	0.00, 1858.00	0.59	0.42

Primary Probable Cases per Illness Duration	8670 [92.17]	4.51 [4.41, 4.62]	2.33 [1.00, 5.00]	0.00, 400.00	0.52	0.38
Healthcare Visits	8385 [89.14]	2.17 [2.12, 2.23]	0.00 [0.00, 2.00]	0.00, 244.00	0.76	0.57
Healthcare Visits per Total Primary Cases	8385 [89.14]	0.16 [0.15, 0.17]	0.00 [0.00, 0.20]	0.00, 1.00	0.59	0.24
Healthcare Visits per Total Cases	8385 [89.14]	0.15 [0.15, 0.16]	0.00 [0.00, 0.19]	0.00, 1.00	0.59	0.25
Healthcare Visits per Illness Duration	8176 [86.91]	0.50 [0.49, 0.52]	0.00 [0.00, 0.50]	0.00, 103.00	0.75	0.54
ER Visits	8130 [86.43]	1.12 [1.09, 1.16]	0.00 [0.00, 1.00]	0.00, 98.00	0.73	0.49
ER Visits per Total Primary Cases	8130 [86.43]	0.12 [0.11, 0.12]	0.00 [0.00, 0.10]	0.00, 1.00	0.67	0.35
ER Visits per Total Cases	8130 [86.43]	0.11 [0.11, 0.12]	0.00 [0.00, 0.10]	0.00, 1.00	0.67	0.35
Hospital/ER Visits	8098 [86.08]	1.79 [1.74, 1.84]	0.00 [0.00, 2.00]	0.00, 133.00	0.69	0.46
Hospital/ER Visits per Total Primary Cases	8098 [86.08]	0.18 [0.17, 0.19]	0.00 [0.00, 0.21]	0.00, 2.00	0.61	0.28
Hospital/ER Visits per Total Cases	8098 [86.08]	0.18 [0.17, 0.19]	0.00 [0.00, 0.20]	0.00, 2.00	0.61	0.28
All Visits	7952 [84.53]	3.71 [3.62, 3.80]	1.00 [0.00, 3.00]	0.00, 239.00	0.68	0.48
All Visits per Total Primary Cases	7952 [84.53]	0.32 [0.31, 0.34]	0.09 [0.00, 0.50]	0.00, 3.00	0.44	0.11
All Visits per Total Cases	7952 [84.53]	0.32 [0.30, 0.33]	0.09 [0.00, 0.50]	0.00, 3.00	0.44	0.11
ER Visits per Illness Duration	7915 [84.14]	0.40 [0.38, 0.42]	0.00 [0.00, 0.25]	0.00, 50.00	0.77	0.55
Hospital/ER Visits per Illness Duration	7886 [83.83]	0.53 [0.51, 0.55]	0.00 [0.00, 0.50]	0.00, 60.00	0.73	0.50
All Visits per Illness Duration	7754 [82.43]	1.00 [0.97, 1.03]	0.25 [0.00, 1.00]	0.00, 103.00	0.66	0.45
Exposure Duration	7119 [75.68]	4.09 [3.98, 4.20]	1.00 [1.00, 2.00]	1.00, 549.00	0.87	0.73
Exposed States per Exposure Duration	7119 [75.68]	0.80 [0.77, 0.83]	1.00 [0.50, 1.00]	0.00, 12.00	-0.51	0.13
Exposed Counties per Exposure Duration	7119 [75.68]	0.78 [0.76, 0.81]	1.00 [0.50, 1.00]	0.00, 6.00	-0.45	0.12
Total Primary Cases per Exposure Duration	7119 [75.68]	10.58 [10.32, 10.84]	5.00 [2.00, 11.00]	0.01, 800.00	0.56	0.38
Total Cases per Exposure Duration	7119 [75.68]	10.81 [10.55, 11.08]	5.00 [2.00, 12.00]	0.01, 800.00	0.56	0.38
Deaths per Exposure Duration	7041 [74.85]	0.00 [0.00, 0.01]	0.00 [0.00, 0.00]	0.00, 4.00	0.99	0.99
Primary Confirmed Cases per Exposure Duration	7037 [74.81]	1.15 [1.12, 1.19]	0.05 [0.00, 2.00]	0.00, 56.00	0.55	0.26
Hospital Visits per Exposure Duration	7002 [74.43]	0.28 [0.27, 0.30]	0.00 [0.00, 0.00]	0.00, 30.00	0.83	0.63
Primary Probable Cases per Exposure Duration	7001 [74.42]	9.18 [8.96, 9.41]	4.00 [2.00, 10.00]	0.00, 800.00	0.56	0.38
Healthcare Visits per Exposure Duration	6697 [71.19]	1.01 [0.98, 1.05]	0.00 [0.00, 1.00]	0.00, 160.00	0.77	0.57
ER Visits per Exposure Duration	6485 [68.94]	0.75 [0.72, 0.77]	0.00 [0.00, 0.50]	0.00, 89.00	0.77	0.56
Hospital/ER Visits per Exposure Duration	6462 [68.69]	1.02 [0.98, 1.05]	0.00 [0.00, 1.00]	0.00, 100.00	0.74	0.52
All Visits per Exposure Duration	6381 [67.83]	1.96 [1.90, 2.02]	0.33 [0.00, 2.00]	0.00, 160.00	0.69	0.50
Deaths per Primary Confirmed Cases	5184 [55.11]	0.01 [0.00, 0.01]	0.00 [0.00, 0.00]	0.00, 1.00	0.98	0.94

Hospital Visits per Primary Confirmed Cases	5145 [54.69]	0.22 [0.21, 0.24]	0.00 [0.00, 0.33]	0.00, 7.00	0.56	0.22
Total Secondary Cases	4542 [48.28]	0.86 [0.83, 0.90]	0.00 [0.00, 0.00]	0.00, 167.00	0.88	0.74
Healthcare Visits per Primary Confirmed Cases	4480 [47.62]	0.72 [0.69, 0.76]	0.33 [0.00, 1.00]	0.00, 58.00	0.55	0.34
Total Secondary Cases per Illness Duration	4455 [47.36]	0.19 [0.18, 0.21]	0.00 [0.00, 0.00]	0.00, 50.00	0.88	0.74
ER Visits per Primary Confirmed Cases	4318 [45.90]	0.43 [0.40, 0.45]	0.00 [0.00, 0.50]	0.00, 60.00	0.65	0.39
Hospital/ER Visits per Primary Confirmed Cases	4305 [45.76]	0.64 [0.61, 0.67]	0.25 [0.00, 1.00]	0.00, 62.00	0.54	0.30
Secondary Confirmed Cases	4254 [45.22]	0.12 [0.11, 0.13]	0.00 [0.00, 0.00]	0.00, 62.00	0.92	0.81
Secondary Probable Cases	4235 [45.02]	0.71 [0.68, 0.74]	0.00 [0.00, 0.00]	0.00, 94.00	0.88	0.74
All Visits per Primary Confirmed Cases	4213 [44.79]	1.31 [1.26, 1.36]	1.00 [0.05, 1.50]	0.00, 62.00	0.47	0.37
Secondary Confirmed Cases per Illness Duration	4185 [44.49]	0.02 [0.01, 0.02]	0.00 [0.00, 0.00]	0.00, 10.33	0.95	0.87
Secondary Probable Cases per Illness Duration	4165 [44.28]	0.16 [0.15, 0.17]	0.00 [0.00, 0.00]	0.00, 25.00	0.87	0.71
Total Secondary Cases per Exposure Duration	3652 [38.82]	0.46 [0.43, 0.48]	0.00 [0.00, 0.00]	0.00, 100.00	0.88	0.74
Secondary Probable Cases per Exposure Duration	3440 [36.57]	0.38 [0.35, 0.40]	0.00 [0.00, 0.00]	0.00, 40.00	0.87	0.71
Secondary Confirmed Cases per Exposure Duration	3416 [36.31]	0.04 [0.04, 0.05]	0.00 [0.00, 0.00]	0.00, 7.00	0.95	0.87

Supplementary Table S4. Sixty-seven natural logarithm-transformed (ln-transformed) metrics used for describing the severity of National Outbreak Reporting System (NORS) in 2009-2019. We added a value of 1 to all metrics prior to performing transformations to prevent undefined estimates for values of nothingness (e.g., ln(0) = undefined). Statistics include observations (with percent completeness), average estimates per outbreak (with 95% confidence intervals), median estimates per outbreak (with interquartile range), minimum and maximum metric values, and measures of L-skewness and L-kurtosis. We estimated completeness as the ratio of outbreaks with available records to total outbreaks in our study period (N=9,407) and multiplied by 100. We calculated average estimates per outbreak using generalized linear models adjusted for negative binomial distributions and the logarithmic link function. We chose L-skewness and L-kurtosis rather than conventional product moment statistics due to their superiority in estimating distribution parameters particularly for smaller sample sizes [23]. *All Visits* refers to the sum of all primary cases who visited a healthcare provider, hospital, or emergency room (ER). We were unable to estimate L-skewness and L-kurtosis for all metrics (denoted *NR*), as all observations for transformed metrics were equal to 0. Metrics are listed in descending order by the absolute value of L-skewness estimates.

Metric	Counts [% Complete]	Average [95% CI]	Median [IQR]	Min, Max	L-Skew	L-Kurt
Primary Probable Cases	8932 [94.95]	1.85 [1.80, 1.90]	1.79 [1.10, 2.64]	0.00, 3.85	0.01	0.07
Primary Probable Cases per Exposure Duration	7001 [74.42]	1.67 [1.62, 1.72]	1.61 [1.10, 2.40]	0.00, 3.51	0.03	0.08
Primary Probable Cases per Illness Duration	8670 [92.17]	1.22 [1.19, 1.26]	1.2 [0.69, 1.79]	0.00, 2.77	0.03	0.06
Total Cases per Illness Duration	9116 [96.91]	1.38 [1.35, 1.42]	1.39 [0.92, 1.87]	0.00, 2.83	0.05	0.10
Total Primary Cases per Illness Duration	9116 [96.91]	1.37 [1.34, 1.41]	1.39 [0.92, 1.85]	0.00, 2.83	0.05	0.10
All Visits per Primary Confirmed Cases	4213 [44.79]	0.61 [0.58, 0.64]	0.69 [0.05, 0.92]	0.00, 1.61	0.07	0.05
Total Primary Cases per Exposure Duration	7119 [75.68]	1.88 [1.82, 1.93]	1.79 [1.10, 2.48]	0.01, 3.61	0.07	0.08
Total Cases per Exposure Duration	7119 [75.68]	1.89 [1.84, 1.95]	1.79 [1.10, 2.56]	0.01, 3.66	0.07	0.08
Total Cases	9407 [100.00]	2.28 [2.22, 2.33]	2.2 [1.61, 2.94]	1.10, 4.09	0.13	0.03
Total Primary Cases	9407 [100.00]	2.26 [2.20, 2.31]	2.08 [1.61, 2.89]	1.10, 4.06	0.13	0.03
Primary Confirmed Cases	9298 [98.84]	0.85 [0.82, 0.87]	0.69 [0.00, 1.39]	0.00, 2.71	0.22	-0.04
Healthcare Visits per Primary Confirmed Cases	4480 [47.62]	0.35 [0.33, 0.37]	0.29 [0.00, 0.69]	0.00, 1.16	0.23	-0.05
All Visits	7952 [84.53]	0.84 [0.81, 0.87]	0.69 [0.00, 1.39]	0.00, 2.71	0.23	-0.02
Hospital/ER Visits per Primary Confirmed Cases	4305 [45.76]	0.33 [0.31, 0.35]	0.22 [0.00, 0.69]	0.00, 1.1	0.27	-0.03
Primary Confirmed Cases per Illness Duration	9023 [95.92]	0.32 [0.31, 0.34]	0.17 [0.00, 0.63]	0.00, 1.1	0.31	-0.02
All Visits per Exposure Duration	6381 [67.83]	0.57 [0.55, 0.59]	0.29 [0.00, 1.10]	0.00, 2.08	0.31	0.00
Illness Duration	9116 [96.91]	1.54 [1.50, 1.58]	1.10 [1.10, 1.95]	0.69, 3.87	0.32	0.13
All Visits per Illness Duration	7754 [82.43]	0.40 [0.38, 0.42]	0.22 [0.00, 0.69]	0.00, 1.50	0.32	0.02
Primary Confirmed Cases per Exposure Duration	7037 [74.81]	0.48 [0.47, 0.51]	0.05 [0.00, 1.10]	0.00, 1.70	0.32	-0.03
All Visits per Total Primary Cases	7952 [84.53]	0.22 [0.21, 0.23]	0.09 [0.00, 0.41]	0.00, 0.76	0.33	-0.02
All Visits per Total Cases	7952 [84.53]	0.22 [0.21, 0.23]	0.09 [0.00, 0.41]	0.00, 0.75	0.33	-0.02

Hospital/ER Visits	8098 [86.08]	0.52 [0.50, 0.54]	0.00 [0.00, 1.10]	0.00, 2.08	0.40	0.02
ER Visits per Primary Confirmed Cases	4318 [45.90]	0.22 [0.20, 0.23]	0.00 [0.00, 0.41]	0.00, 0.92	0.42	0.04
Healthcare Visits	8385 [89.14]	0.51 [0.49, 0.53]	0.00 [0.00, 1.10]	0.00, 2.20	0.42	0.05
Hospital Visits per Primary Confirmed Cases	5145 [54.69]	0.16 [0.15, 0.17]	0.00 [0.00, 0.29]	0.00, 0.69	0.46	0.08
Hospital/ER Visits per Exposure Duration	6462 [68.69]	0.34 [0.32, 0.35]	0.00 [0.00, 0.69]	0.00, 1.61	0.49	0.11
ER Visits	8130 [86.43]	0.37 [0.35, 0.38]	0.00 [0.00, 0.69]	0.00, 1.79	0.50	0.11
Healthcare Visits per Exposure Duration	6697 [71.19]	0.32 [0.30, 0.33]	0.00 [0.00, 0.69]	0.00, 1.61	0.50	0.12
Healthcare Visits per Illness Duration	8176 [86.91]	0.21 [0.20, 0.22]	0.00 [0.00, 0.41]	0.00, 1.10	0.50	0.13
Hospital/ER Visits per Illness Duration	7886 [83.83]	0.23 [0.21, 0.24]	0.00 [0.00, 0.41]	0.00, 1.10	0.51	0.13
Exposed Counties per Exposure Duration	7119 [75.68]	0.55 [0.53, 0.57]	0.69 [0.41, 0.69]	0.00, 0.69	-0.53	0.12
Hospital/ER Visits per Total Primary Cases	8098 [86.08]	0.13 [0.12, 0.14]	0.00 [0.00, 0.19]	0.00, 0.69	0.54	0.17
Hospital/ER Visits per Total Cases	8098 [86.08]	0.13 [0.12, 0.14]	0.00 [0.00, 0.18]	0.00, 0.69	0.54	0.17
Healthcare Visits per Total Primary Cases	8385 [89.14]	0.12 [0.11, 0.13]	0.00 [0.00, 0.18]	0.00, 0.69	0.55	0.19
Exposed States per Exposure Duration	7119 [75.68]	0.56 [0.54, 0.59]	0.69 [0.41, 0.69]	0.00, 0.69	-0.55	0.15
Healthcare Visits per Total Cases	8385 [89.14]	0.12 [0.11, 0.13]	0.00 [0.00, 0.17]	0.00, 0.69	0.56	0.19
ER Visits per Exposure Duration	6485 [68.94]	0.26 [0.24, 0.27]	0.00 [0.00, 0.41]	0.00, 1.39	0.56	0.18
Hospital Visits	9194 [97.74]	0.30 [0.28, 0.31]	0.00 [0.00, 0.69]	0.00, 1.79	0.60	0.23
ER Visits per Illness Duration	7915 [84.14]	0.17 [0.17, 0.19]	0.00 [0.00, 0.22]	0.00, 1.10	0.60	0.24
ER Visits per Total Primary Cases	8130 [86.43]	0.08 [0.08, 0.09]	0.00 [0.00, 0.10]	0.00, 0.51	0.61	0.24
ER Visits per Total Cases	8130 [86.43]	0.08 [0.08, 0.09]	0.00 [0.00, 0.10]	0.00, 0.51	0.61	0.25
Exposure Duration	7119 [75.68]	0.98 [0.95, 1.01]	0.69 [0.69, 1.10]	0.69, 2.56	0.63	0.27
Counties of Residence	9407 [100.00]	0.20 [0.19, 0.21]	0.00 [0.00, 0.00]	0.00, 1.39	0.65	0.30
Hospital Visits per Total Primary Cases	9194 [97.74]	0.06 [0.05, 0.06]	0.00 [0.00, 0.03]	0.00, 0.41	0.67	0.34
Hospital Visits per Total Cases	9194 [97.74]	0.06 [0.05, 0.06]	0.00 [0.00, 0.03]	0.00, 0.41	0.68	0.34
Total Secondary Cases	4542 [48.28]	0.19 [0.18, 0.2]	0.00 [0.00, 0.00]	0.00, 1.39	0.69	0.36
Hospital Visits per Illness Duration	8937 [95.00]	0.08 [0.07, 0.08]	0.00 [0.00, 0.03]	0.00, 0.62	0.70	0.38
Hospital Visits per Exposure Duration	7002 [74.43]	0.11 [0.11, 0.12]	0.00 [0.00, 0.00]	0.00, 0.85	0.70	0.38
Residing Counties per Illness Duration	9116 [96.91]	0.09 [0.08, 0.1]	0.00 [0.00, 0.00]	0.00, 0.69	0.71	0.38
Secondary Probable Cases	4235 [45.02]	0.17 [0.15, 0.18]	0.00 [0.00, 0.00]	0.00, 1.39	0.73	0.43
Total Secondary Cases per Exposure Duration	3652 [38.82]	0.13 [0.12, 0.14]	0.00 [0.00, 0.00]	0.00, 1.10	0.75	0.45
Total Secondary Cases per Illness Duration	4455 [47.36]	0.07 [0.06, 0.08]	0.00 [0.00, 0.00]	0.00, 0.69	0.76	0.48

Secondary Probable Cases per Exposure Duration	3440 [36.57]	0.12 [0.11, 0.13]	0.00 [0.00, 0.00]	0.00, 1.10	0.76	0.48
States of Residence	9407 [100.00]	0.08 [0.07, 0.08]	0.00 [0.00, 0.00]	0.00, 0.69	0.77	0.50
Secondary Probable Cases per Illness Duration	4165 [44.28]	0.07 [0.06, 0.08]	0.00 [0.00, 0.00]	0.00, 0.69	0.78	0.51
Residing States per Illness Duration	9116 [96.91]	0.04 [0.03, 0.04]	0.00 [0.00, 0.00]	0.00, 0.41	0.82	0.59
Counties of Exposure	9407 [100.00]	0.64 [0.62, 0.66]	0.69 [0.69, 0.69]	0.00, 0.69	-0.86	0.67
Secondary Confirmed Cases	4254 [45.22]	0.05 [0.04, 0.05]	0.00 [0.00, 0.00]	0.00, 0.69	0.87	0.69
Secondary Confirmed Cases per Illness Duration	4185 [44.49]	0.00 [0.00, 0.01]	0.00 [0.00, 0.00]	0.00, 0.06	0.88	0.72
Secondary Confirmed Cases per Exposure Duration	3416 [36.31]	0.00 [0.00, 0.00]	0.00 [0.00, 0.00]	0.00, 0.05	0.90	0.76
States of Exposure	9407 [100.00]	0.69 [0.67, 0.72]	0.69 [0.69, 0.69]	0.69, 0.69	*NR*	*NR*
Deaths	9263 [98.47]	0.00 [0.00, 0.00]	0.00 [0.00, 0.00]	0.00, 0.00	*NR*	*NR*
Deaths per Illness Duration	8999 [95.66]	0.00 [0.00, 0.00]	0.00 [0.00, 0.00]	0.00, 0.00	*NR*	*NR*
Deaths per Exposure Duration	7041 [74.85]	0.00 [0.00, 0.00]	0.00 [0.00, 0.00]	0.00, 0.00	*NR*	*NR*
Deaths per Primary Confirmed Cases	5184 [55.11]	0.00 [0.00, 0.00]	0.00 [0.00, 0.00]	0.00, 0.00	*NR*	*NR*
Deaths per Total Primary Cases	9263 [98.47]	0.00 [0.00, 0.00]	0.00 [0.00, 0.00]	0.00, 0.00	*NR*	*NR*
Deaths per Total Cases	9263 [98.47]	0.00 [0.00, 0.00]	0.00 [0.00, 0.00]	0.00, 0.00	*NR*	*NR*

Supplementary Table S5. Sixty-seven calibrated metrics (values ranging 0-1) used for describing the severity of foodborne outbreaks in the National Outbreak Reporting System (NORS) in 2009-2019. We normalized all metric scores by subtracting an outbreak's score by the minimum across all outbreaks and dividing by the difference between maximum and minimum scores across all outbreaks. Statistics include observations (with percent completeness), average estimates per outbreak (with 95% confidence intervals), median estimates per outbreak (with interquartile range), minimum and maximum metric values, and measures of L-skewness and L-kurtosis. We estimated completeness as the ratio of outbreaks with available records to total outbreaks in our study period (N=9,407) and multiplied by 100. We calculated average estimates per outbreak using generalized linear models adjusted for negative binomial distributions and the logarithmic link function. We chose L-skewness and L-kurtosis rather than conventional product moment statistics due to their superiority in estimating distribution parameters particularly for smaller sample sizes [23]. *All Visits* refers to the sum of all primary cases who visited a healthcare provider, hospital, or emergency room (ER). We were unable to estimate L-skewness and L-kurtosis for all metrics (denoted *NR*), as all observations for transformed metrics were equal to 0. Metrics are listed in descending order by median normalized score.

Metric	Counts [% Complete]	Average [95% CI]	Median [IQR]	Min, Max	L-Skew	L-Kurt
Counties of Exposure	9407 [100.00]	0.93 [0.90, 0.96]	1.00 [1.00, 1.00]	0.00, 1.00	-0.86	0.67
Exposed States per Exposure Duration	7119 [75.68]	0.81 [0.79, 0.84]	1.00 [0.58, 1.00]	0.00, 1.00	-0.55	0.15
Exposed Counties per Exposure Duration	7119 [75.68]	0.80 [0.77, 0.82]	1.00 [0.58, 1.00]	0.00, 1.00	-0.53	0.12
Total Primary Cases per Exposure Duration	7119 [75.68]	0.52 [0.50, 0.54]	0.49 [0.30, 0.69]	0.00, 1.00	0.07	0.08
Total Primary Cases per Illness Duration	9116 [96.91]	0.48 [0.47, 0.50]	0.49 [0.32, 0.65]	0.00, 1.00	0.05	0.10
Total Cases per Illness Duration	9116 [96.91]	0.49 [0.47, 0.51]	0.49 [0.32, 0.66]	0.00, 1.00	0.05	0.10
Total Cases per Exposure Duration	7119 [75.68]	0.52 [0.5, 0.54]	0.49 [0.30, 0.70]	0.00, 1.00	0.07	0.08
Primary Probable Cases	8932 [94.95]	0.48 [0.46, 0.50]	0.47 [0.29, 0.69]	0.00, 1.00	0.01	0.07
Primary Probable Cases per Exposure Duration	7001 [74.42]	0.48 [0.46, 0.50]	0.46 [0.31, 0.68]	0.00, 1.00	0.03	0.08
Primary Probable Cases per Illness Duration	8670 [92.17]	0.44 [0.43, 0.46]	0.43 [0.25, 0.65]	0.00, 1.00	0.03	0.06
Hospital Visits per Primary Confirmed Cases	4213 [44.79]	0.38 [0.36, 0.40]	0.43 [0.03, 0.57]	0.00, 1.00	0.07	0.05
Total Cases	9407 [100.00]	0.39 [0.38, 0.41]	0.37 [0.17, 0.62]	0.00, 1.00	0.13	0.03
Total Primary Cases	9407 [100.00]	0.39 [0.38, 0.41]	0.33 [0.17, 0.60]	0.00, 1.00	0.13	0.03
Primary Confirmed Cases	9298 [98.84]	0.31 [0.30, 0.33]	0.26 [0.00, 0.51.00]	0.00, 1.00	0.22	-0.04
All Visits	7952 [84.53]	0.31 [0.30, 0.32]	0.26 [0.00, 0.51.00]	0.00, 1.00	0.23	-0.02
Healthcare Visits per Primary Confirmed Cases	4480 [47.62]	0.31 [0.29, 0.32]	0.25 [0.00, 0.60]	0.00, 1.00	0.23	-0.05
Hospital/ER Visits per Primary Confirmed Cases	4305 [45.76]	0.30 [0.29, 0.32]	0.20 [0.00, 0.63]	0.00, 1.00	0.27	-0.03
Primary Confirmed Cases per Illness Duration	9023 [95.92]	0.29 [0.28, 0.31]	0.15 [0.00, 0.57]	0.00, 1.00	0.31	-0.02
All Visits per Illness Duration	7754 [82.43]	0.27 [0.25, 0.28]	0.15 [0.00, 0.46]	0.00, 1.00	0.32	0.02
All Visits per Exposure Duration	6381 [67.83]	0.27 [0.26, 0.29]	0.14 [0.00, 0.53]	0.00, 1.00	0.31	0.00
Illness Duration	9116 [96.91]	0.27 [0.25, 0.28]	0.13 [0.13, 0.39]	0.00, 1.00	0.32	0.13

All Visits per Total Cases	7952 [84.53]	0.29 [0.28, 0.31]	0.12 [0.00, 0.54]	0.00, 1.00	0.33	-0.02
All Visits per Total Primary Cases	7952 [84.53]	0.29 [0.28, 0.31]	0.11 [0.00, 0.53]	0.00, 1.00	0.33	-0.02
Primary Confirmed Cases per Exposure Duration	7037 [74.81]	0.28 [0.27, 0.30]	0.03 [0.00, 0.64]	0.00, 1.00	0.32	-0.03
States of Residence	9407 [100.00]	0.11 [0.11, 0.12]	0.00 [0.00, 0.00]	0.00, 1.00	0.77	0.50
Counties of Residence	9407 [100.00]	0.15 [0.14, 0.16]	0.00 [0.00, 0.00]	0.00, 1.00	0.65	0.30
Secondary Confirmed Cases	4254 [45.22]	0.07 [0.06, 0.07]	0.00 [0.00, 0.00]	0.00, 1.00	0.87	0.69
Secondary Probable Cases	4235 [45.02]	0.12 [0.11, 0.13]	0.00 [0.00, 0.00]	0.00, 1.00	0.73	0.43
Total Secondary Cases	4542 [48.28]	0.14 [0.13, 0.15]	0.00 [0.00, 0.00]	0.00, 1.00	0.69	0.36
Healthcare Visits	8385 [89.14]	0.23 [0.22, 0.24]	0.00 [0.00, 0.50]	0.00, 1.00	0.42	0.05
Hospital Visits	9194 [97.74]	0.16 [0.16, 0.17]	0.00 [0.00, 0.39]	0.00, 1.00	0.60	0.23
ER Visits	8130 [86.43]	0.21 [0.19, 0.22]	0.00 [0.00, 0.39]	0.00, 1.00	0.50	0.11
ER Visits, Hospital Visits	8098 [86.08]	0.25 [0.24, 0.26]	0.00 [0.00, 0.53]	0.00, 1.00	0.40	0.02
Exposure Duration	7119 [75.68]	0.15 [0.14, 0.16]	0.00 [0.00, 0.22]	0.00, 1.00	0.63	0.27
Residing States per Illness Duration	9116 [96.91]	0.09 [0.08, 0.09]	0.00 [0.00, 0.00]	0.00, 1.00	0.82	0.59
Residing Counties per Illness Duration	9116 [96.91]	0.13 [0.12, 0.14]	0.00 [0.00, 0.00]	0.00, 1.00	0.71	0.38
Secondary Confirmed Cases per Illness Duration	4185 [44.49]	0.06 [0.05, 0.07]	0.00 [0.00, 0.00]	0.00, 1.00	0.88	0.72
Secondary Probable Cases per Illness Duration	4165 [44.28]	0.10 [0.09, 0.11]	0.00 [0.00, 0.00]	0.00, 1.00	0.78	0.51
Total Secondary Cases per Illness Duration	4455 [47.36]	0.10 [0.09, 0.11]	0.00 [0.00, 0.00]	0.00, 1.00	0.76	0.48
Healthcare Visits per Illness Duration	8176 [86.91]	0.19 [0.18, 0.20]	0.00 [0.00, 0.37]	0.00, 1.00	0.50	0.13
Hospital Visits per Illness Duration	8937 [95.00]	0.12 [0.12, 0.13]	0.00 [0.00, 0.04]	0.00, 1.00	0.70	0.38
ER Visits per Illness Duration	7915 [84.14]	0.16 [0.15, 0.17]	0.00 [0.00, 0.20]	0.00, 1.00	0.60	0.24
Hospital/ER Visits per Illness Duration	7886 [83.83]	0.21 [0.19, 0.22]	0.00 [0.00, 0.37]	0.00, 1.00	0.51	0.13
Secondary Confirmed Cases per Exposure Duration	3416 [36.31]	0.05 [0.04, 0.06]	0.00 [0.00, 0.00]	0.00, 1.00	0.90	0.76
Secondary Probable Cases per Exposure Duration	3440 [36.57]	0.11 [0.10, 0.12]	0.00 [0.00, 0.00]	0.00, 1.00	0.76	0.48
Total Secondary Cases per Exposure Duration	3652 [38.82]	0.12 [0.11, 0.13]	0.00 [0.00, 0.00]	0.00, 1.00	0.75	0.45
Healthcare Visits per Exposure Duration	6697 [71.19]	0.20 [0.19, 0.21]	0.00 [0.00, 0.43]	0.00, 1.00	0.50	0.12
Hospital Visits per Exposure Duration	7002 [74.43]	0.13 [0.13, 0.14]	0.00 [0.00, 0.00]	0.00, 1.00	0.70	0.38
ER Visits per Exposure Duration	6485 [68.94]	0.18 [0.17, 0.20]	0.00 [0.00, 0.29]	0.00, 1.00	0.56	0.18
Hospital/ER Visits per Exposure Duration	6462 [68.69]	0.21 [0.20, 0.22]	0.00 [0.00, 0.43]	0.00, 1.00	0.49	0.11
Healthcare Visits per Total Primary Cases	8385 [89.14]	0.18 [0.17, 0.19]	0.00 [0.00, 0.26]	0.00, 1.00	0.55	0.19
Healthcare Visits per Total Cases	8385 [89.14]	0.17 [0.16, 0.18]	0.00 [0.00, 0.25]	0.00, 1.00	0.56	0.19

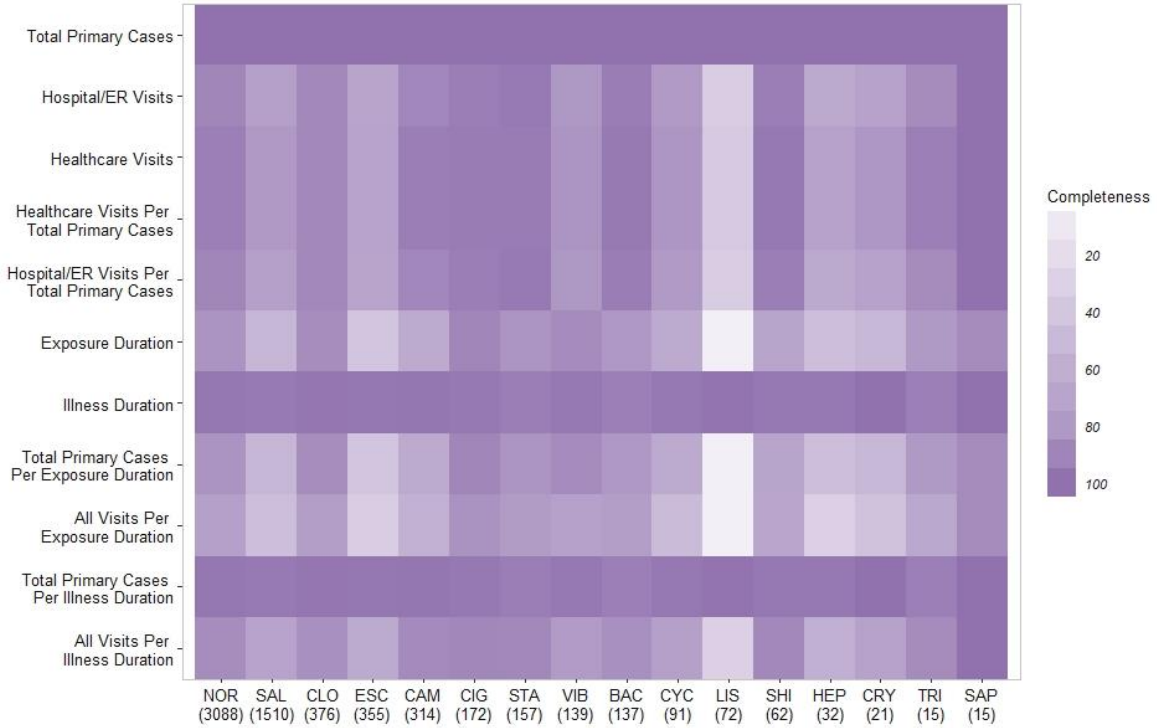
Hospital Visits per Primary Confirmed Cases	5145 [54.69]	0.23 [0.21, 0.24]	0.00 [0.00, 0.42]	0.00, 1.00	0.46	0.08
Hospital Visits per Total Primary Cases	9194 [97.74]	0.14 [0.13, 0.15]	0.00 [0.00, 0.06]	0.00, 1.00	0.67	0.34
Hospital Visits per Total Cases	9194 [97.74]	0.14 [0.13, 0.15]	0.00 [0.00, 0.06]	0.00, 1.00	0.68	0.34
ER Visits per Primary Confirmed Cases	4318 [45.90]	0.24 [0.22, 0.25]	0.00 [0.00, 0.44]	0.00, 1.00	0.42	0.04
ER Visits per Total Primary Cases	8130 [86.43]	0.16 [0.15, 0.17]	0.00 [0.00, 0.19]	0.00, 1.00	0.61	0.24
ER Visits per Total Cases	8130 [86.43]	0.16 [0.15, 0.17]	0.00 [0.00, 0.19]	0.00, 1.00	0.61	0.25
Hospital/ER Visits per Total Primary Cases	8098 [86.08]	0.19 [0.18, 0.20]	0.00 [0.00, 0.28]	0.00, 1.00	0.54	0.17
Hospital/ER Visits per Total Cases	8098 [86.08]	0.19 [0.18, 0.20]	0.00 [0.00, 0.26]	0.00, 1.00	0.54	0.17
States of Exposure	9407 [100.00]	0.00 [0.00, 0.00]	0.00 [0.00, 0.00]	0.00, 0.00	*NR*	*NR*
Deaths	7119 [75.68]	0.00 [0.00, 0.00]	0.00 [0.00, 0.00]	0.00, 0.00	*NR*	*NR*
Deaths per Illness Duration	7119 [75.68]	0.00 [0.00, 0.00]	0.00 [0.00, 0.00]	0.00, 0.00	*NR*	*NR*
Deaths per Exposure Duration	7119 [75.68]	0.00 [0.00, 0.00]	0.00 [0.00, 0.00]	0.00, 0.00	*NR*	*NR*
Deaths per Primary Confirmed Cases	9116 [96.91]	0.00 [0.00, 0.00]	0.00 [0.00, 0.00]	0.00, 0.00	*NR*	*NR*
Deaths per Total Primary Cases	9116 [96.91]	0.00 [0.00, 0.00]	0.00 [0.00, 0.00]	0.00, 0.00	*NR*	*NR*
Deaths per Total Cases	7119 [75.68]	0.00 [0.00, 0.00]	0.00 [0.00, 0.00]	0.00, 0.00	*NR*	*NR*

Supplementary Table S6. Outbreak severity score by study year and Gregorian calendar month using the National Outbreak Report System (NORS) in 2009-2019. Statistics include observations (with percent of total outbreaks), average and median scores per contaminant (with 95% confidence intervals and interquartile range), minimum and maximum scores, and L-skewness and L-kurtosis statistics. We calculated the percent of outbreaks attributed to each year or month as the ratio of outbreaks associated with that year or month to the total number of outbreaks in our study period for which severity scores were calculated (N=6911) and multiplied by 100. We calculated average estimates per outbreak using generalized linear models adjusted for negative binomial distributions and the logarithmic link function.

Year	Outbreaks [% Total]	Average [95% CI]	Median [IQR]	Min, Max	L-Skew	L-Kurt
2009	453 [6.55]	0.39 [0.33, 0.47]	0.38 [0.26, 0.52]	0.00, 0.89	0.04	0.09
2010	588 [8.51]	0.37 [0.31, 0.43]	0.35 [0.24, 0.49]	0.00, 1.00	0.08	0.10
2011	504 [7.29]	0.37 [0.31, 0.43]	0.35 [0.23, 0.49]	0.02, 1.00	0.09	0.09
2012	587 [8.49]	0.35 [0.30, 0.41]	0.33 [0.20, 0.47]	0.05, 1.00	0.10	0.08
2013	615 [8.90]	0.36 [0.31, 0.42]	0.34 [0.22, 0.48]	0.05, 0.87	0.08	0.08
2014	678 [9.81]	0.33 [0.28, 0.38]	0.32 [0.20, 0.44]	0.00, 0.84	0.09	0.08
2015	698 [10.1]	0.32 [0.28, 0.37]	0.31 [0.18, 0.43]	0.00, 0.90	0.12	0.09
2016	661 [9.56]	0.33 [0.28, 0.39]	0.31 [0.18, 0.46]	0.05, 0.85	0.11	0.07
2017	667 [9.65]	0.31 [0.27, 0.37]	0.30 [0.17, 0.44]	0.00, 0.93	0.11	0.07
2018	782 [11.3]	0.33 [0.29, 0.38]	0.31 [0.20, 0.45]	0.00, 0.89	0.15	0.09
2019	678 [9.81]	0.33 [0.28, 0.38]	0.32 [0.20, 0.44]	0.05, 0.90	0.10	0.09
Calendar Month						
January	542 [7.84]	0.31 [0.26, 0.37]	0.28 [0.16, 0.43]	0.00, 1.00	0.13	0.08
February	496 [7.18]	0.31 [0.26, 0.37]	0.29 [0.18, 0.42]	0.00, 1.00	0.14	0.10
March	652 [9.43]	0.32 [0.27, 0.37]	0.30 [0.18, 0.43]	0.02, 0.81	0.13	0.08
April	646 [9.35]	0.34 [0.29, 0.40]	0.32 [0.21, 0.46]	0.02, 1.00	0.11	0.09
May	674 [9.75]	0.34 [0.30, 0.40]	0.33 [0.20, 0.46]	0.05, 1.00	0.10	0.08
June	691 [10.0]	0.37 [0.33, 0.43]	0.36 [0.24, 0.49]	0.05, 0.97	0.08	0.10
July	601 [8.70]	0.38 [0.32, 0.44]	0.36 [0.24, 0.50]	0.00, 1.00	0.07	0.10
August	567 [8.20]	0.37 [0.31, 0.43]	0.36 [0.23, 0.49]	0.00, 0.89	0.05	0.09
September	488 [7.06]	0.37 [0.31, 0.44]	0.37 [0.25, 0.48]	0.03, 0.83	0.04	0.10
October	463 [6.70]	0.36 [0.30, 0.43]	0.33 [0.22, 0.49]	0.06, 1.00	0.11	0.09
November	473 [6.84]	0.33 [0.28, 0.40]	0.32 [0.19, 0.44]	0.05, 0.87	0.12	0.07
December	618 [8.94]	0.30 [0.26, 0.36]	0.28 [0.17, 0.41]	0.03, 0.99	0.14	0.07

Supplementary Table S7. Tobit regression model results reporting trends of severity scores using the National Outbreak Reporting System (NORS) in 2009-2019. We report annual trends (Equation 3) and seasonality as defined by sinusoidal and cosinusoidal harmonic terms (Equation 4). Top rows provide model coefficients, middle rows provide 95% confidence intervals, and bottom rows provide p-values. *Overall* estimates refer to all-contaminant outbreaks with non-missing information and not associated with multiple contaminants. *Diagnostics* report information on the log-likelihood (top value) and number of observations (bottom value) for each model. We report contaminants in descending order by number of outbreaks and defined significance as $\alpha < 0.05$.

Contaminant	Trend Analyses			Seasonality Analyses			
	Year	Intercept	Diagnostics	Sine	Cosine	Intercept	Diagnostics
All Contaminants	-0.006 [-0.007, -0.005] <0.001	0.379 [0.370, 0.389] <0.001	2096.63 6911	-0.024 [-0.030, -0.018] <0.001	-0.027 [-0.033, -0.021] <0.001	0.341 [0.337, 0.345] <0.001	2131.41 6911
Norovirus	-0.006 [-0.007, -0.004] <0.001	0.310 [0.298, 0.322] <0.001	1447.92 3088	0.000 [-0.008, 0.008] 0.981	-0.009 [-0.016, -0.001] 0.027	0.277 [0.271, 0.282] <0.001	1431.20 3088
Salmonella	-0.006 [-0.009, -0.003] <0.001	0.514 [0.496, 0.532] <0.001	596.34 1510	0.005 [-0.007, 0.016] 0.454	-0.006 [-0.019, 0.006] 0.297	0.475 [0.467, 0.484] <0.001	587.07 1510
Clostridium	-0.007 [-0.012, -0.002] 0.004	0.334 [0.298, 0.369] <0.001	167.52 376	-0.011 [-0.033, 0.012] 0.342	0.029 [0.007, 0.051] 0.010	0.289 [0.273, 0.304] <0.001	167.46 376
Escherichia	-0.006 [-0.011, -0.001] 0.020	0.488 [0.452, 0.524] <0.001	140.16 355	-0.009 [-0.034, 0.015] 0.468	0.003 [-0.023, 0.028] 0.826	0.449 [0.431, 0.467] <0.001	137.75 355
Campylobacter	-0.011 [-0.016, -0.006] <0.001	0.435 [0.402, 0.469] <0.001	186.06 314	-0.008 [-0.031, 0.014] 0.458	-0.014 [-0.036, 0.008] 0.212	0.364 [0.348, 0.379] <0.001	177.67 314
Ciguatoxin	-0.001 [-0.007, 0.006] 0.870	0.303 [0.254, 0.351] <0.001	104.52 172	0.015 [-0.012, 0.042] 0.266	0.019 [-0.012, 0.049] 0.224	0.306 [0.285, 0.326] <0.001	105.96 172
Staphylococcus	-0.013 [-0.024, -0.003] 0.015	0.381 [0.301, 0.462] <0.001	19.75 157	-0.029 [-0.077, 0.020] 0.246	-0.008 [-0.053, 0.038] 0.743	0.290 [0.257, 0.323] <0.001	17.55 157
Vibrio	-0.009 [-0.018, -0.001] 0.023	0.380 [0.314, 0.447] <0.001	77.00 139	0.083 [0.043, 0.122] <0.001	-0.015 [-0.064, 0.035] 0.562	0.326 [0.286, 0.367] <0.001	82.86 139
Bacillus	0.001 [-0.007, 0.009] 0.892	0.231 [0.170, 0.292] <0.001	54.78 137	-0.059 [-0.097, -0.021] 0.002	-0.003 [-0.038, 0.033] 0.876	0.244 [0.217, 0.270] <0.001	59.41 137
Cyclospora	-0.015 [-0.033, 0.003] 0.107	0.607 [0.425, 0.789] <0.001	27.94 91	0.127 [0.026, 0.229] 0.014	-0.066 [-0.219, 0.088] 0.396	0.410 [0.268, 0.553] <0.001	29.84 91
Listeria	-0.015 [-0.025, -0.004] 0.006	0.541 [0.472, 0.610] <0.001	51.57 72	-0.001 [-0.043, 0.041] 0.958	0.027 [-0.012, 0.066] 0.171	0.454 [0.425, 0.484] <0.001	48.71 72
Shigella	-0.007 [-0.024, 0.010] 0.406	0.497 [0.375, 0.620] <0.001	9.64 62	0.062 [-0.018, 0.141] 0.125	-0.007 [-0.078, 0.064] 0.847	0.471 [0.414, 0.529] <0.001	10.52 62
Hepatitis	0.000 [-0.018, 0.018] 0.988	0.501 [0.359, 0.643] <0.001	10.06 32	-0.005 [-0.085, 0.075] 0.905	-0.051 [-0.134, 0.032] 0.218	0.491 [0.433, 0.550] <0.001	10.84 32
Cryptosporidium	0.004 [-0.026, 0.033] 0.800	0.357 [0.128, 0.587] 0.004	9.46 21	-0.044 [-0.137, 0.049] 0.331	0.089 [-0.016, 0.193] 0.091	0.363 [0.286, 0.440] <0.001	11.63 21
Trichinella	-0.010 [-0.034, 0.014] 0.394	0.469 [0.302, 0.636] <0.001	10.51 15	0.055 [-0.021, 0.131] 0.142	0.064 [-0.014, 0.142] 0.099	0.421 [0.364, 0.478] <0.001	12.75 15
Sapovirus	-0.010 [-0.042, 0.022] 0.526	0.343 [0.100, 0.586] 0.009	7.72 15	0.061 [-0.060, 0.181] 0.296	-0.022 [-0.118, 0.075] 0.637	0.268 [0.201, 0.335] <0.001	8.66 15



Supplementary Figure S1. A heatmap depicting the completeness of 11 outbreak severity metrics for 16 contaminants using the National Outbreak Report System (NORS) in 2009-2019. These 16 contaminants had the greatest number of outbreaks in our study period (n=6556, or 94.9%) after removing outbreaks with missing contaminant information and multiple contaminants per outbreak. We report contaminants in descending order by outbreak counts. We calculated completeness as the number of outbreaks with available information for a given metric divided by the total number of outbreaks reported by that contaminant and multiplied by 100. Scores range from light blue (0%) to dark blue (100%). We abbreviate the aggregate of healthcare, hospital, and ER visits as *All Visits*. We abbreviate contaminants as: HEP (*Hepatitis*), SAL *(Salmonella*), SHI (*Shigella*), LIS (*Listeria*), ESC (*Escherichia*), TRI (*Trichinella*), CYC (*Cyclospora*), CRY (*Cryptosporidium*), CAM (*Campylobacter*), CIG (*Ciguatoxin*), VIB (*Vibrio*), SAP (*Sapovirus*), CLO (*Clostridium*), NOR (*Norovirus*), STA (*Staphylococcus*), BAC (*Bacillus*).

Epidemiology and Infection

cambridge.org/hyg

Investigating seasonal patterns in enteric infections: a systematic review of time series methods

Ryan B. Simpson[1], Alexandra V. Kulinkina[1,2,3] and Elena N. Naumova[1]

[1]Tufts University Friedman School of Nutrition Science and Policy, Boston, MA 02111, USA; [2]Swiss Tropical and Public Health Institute, Basel, Switzerland and [3]University of Basel, Basel, Switzerland

Review

Cite this article: Simpson RB, Kulinkina AV, Naumova EN (2022). Investigating seasonal patterns in enteric infections: a systematic review of time series methods. *Epidemiology and Infection* **150**, e50, 1–13. https://doi.org/10.1017/S0950268822000243

Received: 9 September 2021
Revised: 31 January 2022
Accepted: 3 February 2022

Key words:
Foodborne infection; gastrointestinal infection; reproducibility; season; seasonality; time series analysis; waterborne infection

Author for correspondence:
Elena N. Naumova,
E-mail: elena.naumova@tufts.edu

Abstract

Foodborne and waterborne gastrointestinal infections and their associated outbreaks are preventable, yet still result in significant morbidity, mortality and revenue loss. Many enteric infections demonstrate seasonality, or annual systematic periodic fluctuations in incidence, associated with climatic and environmental factors. Public health professionals use statistical methods and time series models to describe, compare, explain and predict seasonal patterns. However, descriptions and estimates of seasonal features, such as peak timing, depend on how researchers define seasonality for research purposes and how they apply time series methods. In this review, we outline the advantages and limitations of common methods for estimating seasonal peak timing. We provide recommendations improving reporting requirements for disease surveillance systems. Greater attention to how seasonality is defined, modelled, interpreted and reported is necessary to promote reproducible research and strengthen proactive and targeted public health policies, intervention strategies and preparedness plans to dampen the intensity and impacts of seasonal illnesses.

Introduction

Foodborne and waterborne gastrointestinal infections are caused by the consumption of contaminated food and water, respectively [1, 2]. Food contamination often occurs due to poor health or hygiene practices during food production, processing, distribution or consumption, or cross-contamination between food products [1–3]. Waterborne illnesses and outbreaks are often attributed to ageing infrastructure and severe weather events [4–6]. Outbreaks are commonly defined as the occurrences of two or more infections caused by the same source [1–3]. Infection incubation periods range from a few hours to many months, causing high volumes and broad geographic extent of infected persons per outbreak. This, combined with the habitude of human food and water consumption, the globalisation of food supply chains, and the frequent handling or storage of food and water before consumption, makes sources of gastrointestinal infections difficult to identify and control [3, 7–9].

Public health professionals often use time series analyses, or a collection of methods to describe, explain and predict temporal processes, to assess the patterns of infections [10–12]. Time series analyses examine population-based likelihoods of infections as a function of time and time-varying factors [13]. These methods decompose the temporal distribution of infections into three components: (i) trend or general incidence fluctuation over time; (ii) seasonality or systematic periodic fluctuation in incidence generally observed over 1 year; and (iii) change in incidence driven by other periodic, sporadic or random events [14]. Seasonality can be further characterised by three main features: (i) peak (and nadir) timing or when incidence reaches its maximum (and minimum); (ii) amplitude or the difference in incidence between seasonal peaks and nadirs; and (iii) duration or the time interval when incidence rises above a specified threshold [12, 15]. Most modelling studies detect the presence of seasonality by characterizing peak timing.

Precise estimation of peak timing helps identify differences in seasonal patterns by pathogen, subpopulation and geographic location [12]. Synchronisation of pathogens' peaks suggests possible co-infections and shared food/water- or environmental-drivers of infection [12, 16, 17]. Lags between peaks of infections and their drivers, best assessed with more granular temporal data, inform forecasts of peak incidence for early outbreak warnings [12, 18, 19]. Better characterisation of seasonal patterns in diseases and exposures contributes to refinements of research hypotheses by identifying non-seasonal drivers such as stagnant water, agricultural runoff, livestock migration or sanitation practices [20–22]. Accurate peak timing estimates by subpopulation and geographic location identify when and where vulnerable populations are at the highest risk of infection [12].

© The Author(s), 2022. Published by Cambridge University Press. This is an Open Access article, distributed under the terms of the Creative Commons Attribution licence (http://creativecommons.org/licenses/by/4.0/), which permits unrestricted re-use, distribution and reproduction, provided the original article is properly cited.

CAMBRIDGE UNIVERSITY PRESS

While the concept of seasonality may seem straightforward, its characterisation and quantification are complex. Researchers often detect seasonality and estimate seasonal peak timing by comparing average incidence or cumulative infections by season [23]. Alternatively, researchers can describe seasonality as a continuous temporal process. Researchers model temporal patterns using data-driven methods based on smoothing or polynomial, periodic and other non-linear functions [14]. Researchers detect seasonality with a formal statistical test of periodicity or by assessing model fit [23, 24]. These approaches and their methods have advantages and limitations that have been thoroughly explored for modelling seasonal respiratory infections like influenza and pneumonia [25–28]. However, differences in terminology for defining seasonality and limitations of methods for estimating seasonal peak timing remain largely underexplored within literature related to gastrointestinal infections.

In this systematic review, we demonstrate differences in applied definitions of seasonality when modelling, interpreting and reporting gastrointestinal infections. We extracted and reviewed original research articles that detected and estimated the seasonality features of gastrointestinal infections in humans using disease surveillance systems or hospital health records. We describe advantages and limitations of statistical methods for detecting, estimating and comparing seasonal peak timing. Standardised terminology and reporting requirements can be extended to the field of infectious disease epidemiology.

Methods

Literature search

We conducted a search of published literature in peer-reviewed journals using the National Library of Medicine's National Center for Biotechnology Information bibliographic database *PubMed*. This database identified publications spanning many disciplines related to enteric infections including nutritional, agricultural, environmental, public health, zoonotic and microbiological sciences. *PubMed*'s emphasis on circulating research with innovative analytical approaches prioritised publications that thoroughly reported on statistical methodologies [29].

We used no publishing date restrictions. We conducted our first search on 02 March 2019 with follow-up searches on 18 July 2019, 20 December 2020 and 22 July 2021. For each search, we included the following search terms forming four categories:

- *Disease aetiology*: 'foodborne', 'food borne', 'food-borne', 'waterborne', 'water borne', 'water-borne' and 'gastroenteritis';
- *Notifiable gastrointestinal infections*: '*Campylobacter*', 'campylobacteriosis', '*Salmonella*', 'salmonellosis', '*Vibrio*', 'vibriosis', 'cholera', '*Listeria*', 'listeriosis', '*Cryptosporidium*', 'cryptosporidiosis', '*Shigella*', 'shigellosis', '*Cyclospora*', 'cyclosporiasis', '*Escherichia*', 'e. coli', '*Yersinia*', 'yersiniosis', 'norovirus', '*Giardia*', 'giardiasis', 'rotavirus' and 'rotaviral';
- *Case definitions*: 'illness', 'infection', 'incidence', 'rate' and 'outbreak'; and
- *Key terms*: 'season', 'seasonal', 'seasonality' and 'peak'.

We selected pathogens using nationally notifiable enteric infections reported by the US Centers for Disease Control and Prevention's (CDC's) Foodborne Diseases Active Surveillance Network (FoodNet) and National Outbreak Reporting System (NORS) [9, 30–33]. These notifiable infections represented internationally monitored enteric infections [34, 35].

Exclusion criteria and study abstraction

Our search yielded 2064 publications (Fig. 1). First, we excluded non-English publications ($n = 61$) and duplicates ($n = 849$). Next, we reviewed the abstracts of the remaining 1154 publications and excluded those with: (i) animal, plant or water hosts/reservoirs ($n = 470$); (ii) <1 year of data, case control studies or ecologic studies ($n = 146$); (iii) non-gastrointestinal infections ($n = 82$); (iv) literature reviews, editorials or viewpoints ($n = 82$); and (v) studies examining antimicrobial resistance, genetic diversity, and economic burdens of illness or using simulation-generated data ($n = 24$). We conducted a full-text review on the remaining 350 publications and excluded publications with no estimation of seasonal peak timing ($n = 84$), no reporting on human illnesses or outbreaks ($n = 20$), non-original research ($n = 20$), and no health outcome or surveillance records assessed ($n = 17$).

We reviewed references of the 209 extracted publications for additional manuscripts meeting the above inclusion criteria but not identified in our initial search (Fig. 1). We also reviewed featured publications on FoodNet and NORS websites [36, 37]. We identified 11 additional publications meeting our search criteria that were not identified in our *PubMed* search. We exported and reviewed all 220 citations using EndNote version X7.7.1 software. We report all citations in Supplementary Table S1, which are referenced below using a citation identifier (CID). We designed and created all visualisations using PowerPoint version 14.3.6 and R version 3.6.2 software.

Structure of findings

First, we describe study objectives and rationale for investigating seasonality. Next, we discuss two approaches for detecting and estimating seasonality features: (i) comparisons of discrete time intervals; and (ii) construction of seasonal curves. For comparisons by discrete time intervals, we compare methods used when defining two and four seasons or the use of discrete calendar months. For constructed seasonal curves, we compare common modelling techniques including average smoothers, cubic splines, seasonal trend decomposition (STL), seasonal autoregressive integrated moving averages (SARIMA), harmonic regression models and spectral analyses. For each method, we outline advantages and limitations for detecting seasonality and estimating seasonal peak timing.

Results

Motivation and rationale for investigating seasonality

Studies investigating seasonality aimed to: (i) describe trends in infections over time; (ii) compare trends and seasonality features by pathogen, subpopulation, geographic location or other risk factors; and/or (iii) explain associations between seasonal infections and their environmental drivers. Descriptive studies often defined seasonality using discrete seasons or calendar months (Table 1). Comparative and explanatory studies examined the seasonality of common pathogens like *Salmonella* and *Campylobacter* by constructing seasonal curves. For example, *Norovirus* studies compared seasonal peak timing by strain/subtype while *Escherichia coli*, *Cryptosporidium* and *Vibrio* studies compared peak timing across geographic locations or subpopulations using both discrete seasons and seasonal curves (Table 1).

https://doi.org/10.1017/S0950268822000243 Published online by Cambridge University Press

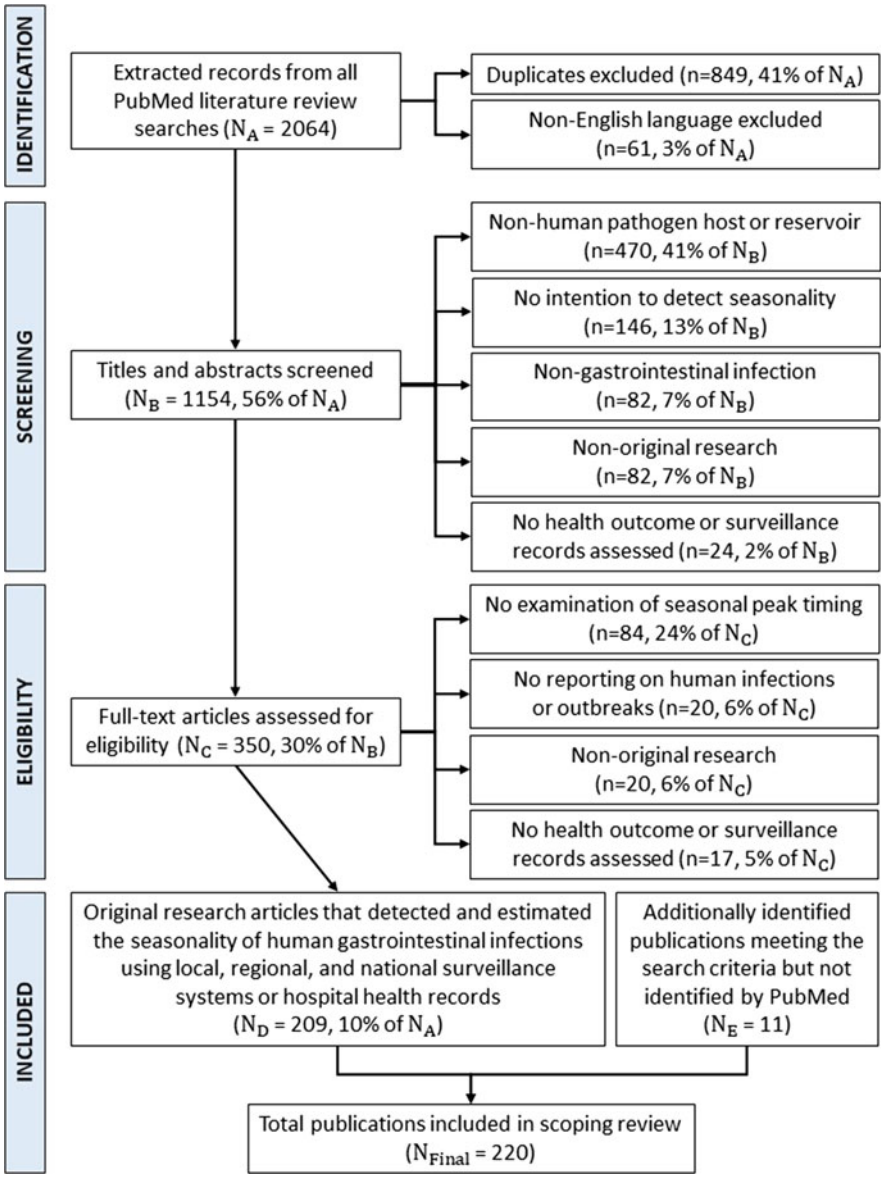


Fig. 1. PRISMA flow diagram detailing the identification, screening, eligibility and inclusion of articles for our systematic review. Included studies (n = 220) were original research articles that detected and estimated the seasonality of human gastrointestinal infections using local, regional and national surveillance systems or hospital health records.

Describing trends in infections over time

Descriptive studies often reported linear fluctuations in mean and median incidence over time or the sum and percentage of infections by consecutive seasons or months (CID 1–11). Studies frequently estimated seasonal peak timing by identifying the calendar month or season with the highest sum, percentage or average incidence of infections (CID 12–18). Study rationales aimed to understand trends in infection severity for creating, modifying or evaluating public health interventions. Researchers stated that linear trends and seasonal peak timing estimates informed when, where and for which pathogen health safety policies were most needed (CID 13, 19–21). Researchers equated reductions in infections or dampening of seasonal peak intensities to positive benefits of enacted health policies or programmes (CID 12, 22).

Additional study rationales included reviewing surveillance system capacity and preparing public health institutions for seasonal hospitalisation peaks (CID 23–30). Many early studies described trends and seasonality features to assist public health laboratories in detecting, monitoring and tracking infections (CID 23–28). Peak timing estimates aided public health institutions in: (i) managing personnel and supplies (CID 30); and (ii) communicating risks of gastrointestinal infections to travellers or residents in high-risk areas during outbreak seasons (CID 29). Studies often emphasised the importance of improving the spatial and temporal resolution of surveillance records to permit more precise, accurate and reliable estimation of seasonality features.

Comparing seasonal peak timing by subgroups

Comparative studies estimated seasonality features by pathogen strain, subpopulation, geographic location or other risk factors (CID 31–38). Surveillance systems collected and reported cases by pathogen subtype as serotyping technologies became available. Many studies compared *Norovirus* and *Salmonella* strains to demonstrate the utility of advanced laboratory testing capabilities (CID 1, 4, 39–43). Studies identified which strains were most severe, required greatest allocation of laboratory resources and needed continued surveillance during outbreak seasons (CID 1, 42, 43). Descriptive assessments of seasonal peak timing by

https://doi.org/10.1017/S0950268822000243 Published online by Cambridge University Press

https://doi.org/10.1017/S0950268822000243 Published online by Cambridge University Press

Table 1. A summary of time series methods for describing, comparing and explaining the seasonality of the 14 most cited gastrointestinal infections from our review

		Discrete seasons			Seasonal curves as continuous processes					
Pathogen	Total citations	Two seasons	Four seasons	Monthly records	Average smoothers	Cubic splines	STL models	SARIMA models	Harmonic regressions	Spectral analyses
Salmonella	66	5	25	22	1			2	12	
Campylobacter	45	2	20	9	1	1	1		9	2
Gastroenteritis	38	1	15	15		1		2	4	
Vibrio	20	2	7	4		1		2	4	
Norovirus	19	3	9	6						
E. coli	18		14	1			1		2	
Cryptosporidium	17	2	1	10		1			3	
Yersinia	11		7	3					1	
Shigella	11		7	2					2	
Giardia	10	1	3	3				1	2	
Listeria	9		6	2					1	
Cyclospora	6	1	1	4					1	
Rotavirus	6	2	1						3	1
Clostridium	2			2						
Total	215	17	76	74	2	4	2	7	31	2

We ranked pathogens in descending order by total citations. We divided methods by comparisons of discrete seasons and the construction of seasonal curves. Discrete seasons methods included comparisons by two seasons, four seasons or calendar months. Seasonal curve methods included average smoothers, cubic splines, seasonal trend decomposition (STL), seasonal autoregressive integrated moving average (SARIMA) models, harmonic regression models and spectral analyses. Column and row totals are less than the sum of all rows and columns, respectively, as many publications investigated multiple pathogens and used multiple methodologies to describe, compare and explain seasonality features.

enteric species' subtypes informed the circulation patterns of common strains and their epidemiological or clinical characteristics, which can improve the specificity of lab methods used for pathogen detection (CID 39). Researchers also compared peak timing by strain to forecast disease burden in upcoming outbreak seasons (CID 4, 40, 41).

Comparisons by subpopulation and geographic location identified who and where was at the highest risk of infection (CID 44–50). Study rationales aimed to provide information for developing infection prevention and management guidelines in future outbreaks (CID 46–48, 51). Studies investigating subpopulations compared trends and seasonality by sex, age group or place where infection was acquired (domestic- *vs.* travel-related) (CID 46, 52). Geographical comparisons attempted to identify the hotspots of infection vulnerable to multi-county or multi-state outbreaks (CID 47, 53). Many comparison studies lacked formal statistical tests for detecting significant peak timing differences.

Explaining associations between infections and risk factors

Few studies investigated associations between seasonal infections and environmental factors such as ambient temperature, precipitation and relative humidity (CID 54–60). These studies often extracted daily or weekly time series data and explored seasonal patterns using harmonic regression models (CID 18, 37, 61–65). Studies quantified associations between health and environmental variables using lags, which varied in length according to data's temporal resolution (CID 66–76). Study findings informed early warning forecasts or evaluated the effect of extreme weather events on the amplification or dampening of incidence in human infections (CID 55, 58, 64, 66, 67, 69). Researchers noted that their understanding of associations between environmental drivers and human infections improved the reliability of peak timing forecasts (CID 55, 66, 68). Studies encouraged continued examination of associations between environmental drivers and gastrointestinal infections considering ongoing climate changes globally (CID 58, 59, 77).

Describing seasonality with discrete seasons

Most studies detected seasonality and examined seasonality features using discrete seasons (Table 1). Researchers defined seasons either analytically using surveillance data (e.g. high/low incidence) (CID 78–82) or using external biological, environmental, physical, physiological or other assumptions (e.g. wet/dry, warm/cool, summer/fall/winter/spring) (CID 3, 18, 33, 37, 80, 81, 83–86). This approach closely reflected layman definitions of season: 'a period normally characterised by a particular kind of weather' or 'a period marked by special activity especially in some field' [38]. Seasons had equal or unequal lengths and were defined by pre-determined dates or known patterns of disease incidence. To detect seasonal peak timing, researchers identified one season with significantly higher incidence than all others. While we only describe applications of two and four seasons below, studies might also define three, five or more seasons [39–42].

Two seasons

Studies often defined two seasons with equal 6-month lengths that spanned either a single calendar year such as two semesters (e.g. January–June *vs.* July–December) or two adjacent calendar years (e.g. October–March *vs.* April–September) (Supplementary Table S2; CID 48, 78, 79). Studies defined unequal season lengths when analytically deriving seasons based on incidence, which often consisted of a ~3-month high-incidence season compared to a ~9-month low-incidence season (CID 58, 80, 81). Unequal season lengths varied by genus, strain or serotype of the pathogen(s) assessed (CID 81).

Studies defining seasons with environmental factors used meteorological patterns like coolness and warmness, wetness and dryness, or their combination. Cool and warm seasons varied by climate region and hemisphere (CID 37, 87). Some studies defined seasons by extreme temperature events, such as heatwaves, whose dates varied by annual cycle (CID 84). Other studies defined cool and warm seasons by aggregating times-of-the-year with similar temperatures such as spring/summer and fall/winter (CID 79). Researchers defined wet and dry seasons using precipitation or relative humidity and often examined associations between flooding events and incidence (CID 58, 60, 88, 89). These studies aimed to investigate the effects of seasonal surface water flooding dynamics on human health (CID 88, 89).

Statistical analyses for detecting seasonality with two seasons are computationally straightforward. However, in the absence of formal comparison tests, differences in incidence by season could be spurious. While studies used terminology like 'seasonal peaks' or 'greater incidence' to imply formal inferences, seasonality was undetermined without test results. Studies applied pairwise Student's *t*-tests, Mann–Whitney rank-sum tests or χ^2-tests to compare average incidence, median incidence or cumulative infections, respectively (CID 37, 79, 89). Statistical power depended on the number of study years assessed as seasons occurred only once per year.

Recent studies conducted formal comparisons using binary variables within logistic regression models (CID 37, 48, 58, 60, 80, 82–84). Models compared seasons using odds ratio (OR) and incidence rate ratio (IRR) measures of association. Studies applying these models had the advantage of adjusting for additional confounding factors expected to influence seasonality (CID 80, 82–84).

When comparing two seasons, peaks and nadirs ideally fall at the centre of each season in each year (Fig. 2a). Equal season lengths neatly divide time points of the highest and lowest incidence into each season. However, many enteric infections exhibit irregularities when long periods of low incidence alternate with short bursts of infections, or when extended periods of high incidence are replaced with intermittent declines. This complicates analytically deriving season intervals and can lead to misclassification when *a priori* assigned seasons align poorly (Fig. 2b) or not at all (Fig. 2c) with actual data. Poor alignment will result in more similar average or median incidence between seasons, decreasing a researcher's ability to detect seasonality. If peak timing falls near or at the boundary between seasons, differences will be indistinguishable, and researchers will not detect seasonality, resulting in misclassification bias (Fig. 2c).

Seasons defined using exogenous environmental or biological assumptions could align well with seasonal peaks or nadirs and demonstrate strong correlations as in Figure 2a. However, environmental seasons and infection seasonality could be misaligned resulting in low (Fig. 2b) or no correlation (Fig. 2c). Low or no correlation does not indicate the absence of disease seasonality but rather a potential lag in peak timing from the centre of the season compared to an environmental factor's seasonal peak.

In general, the precision for estimating seasonal peak timing is low using this method. Coarse aggregation of seasons suggests that peak timing could occur anytime within a ~6-month interval. This inhibits informative public health policies and prevents

https://doi.org/10.1017/S0950268822000243 Published online by Cambridge University Press

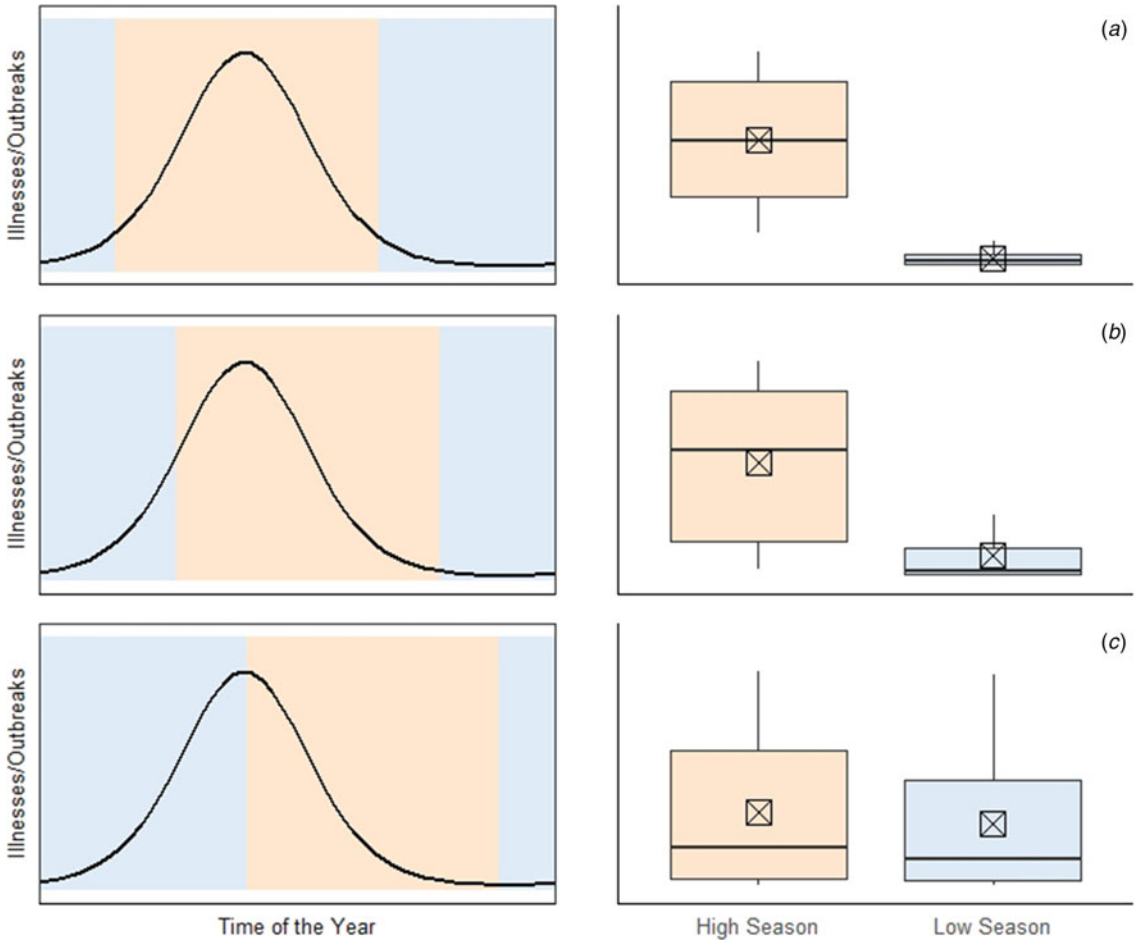


Fig. 2. An illustration of detecting seasonality and estimating seasonal peak timing using two discrete seasons. Scenarios include (a) when peak and nadir timing align with the centre of each season, as expected for incidence-based definitions of seasons; (b) when peak and nadir timing is shifted from the centre of each season; and (c) when peak timing aligns with the boundary between seasons and results in substantial misclassification bias.

investigating possible trends, drifts or instantaneous shifts of seasonal curves over time. Data compression also underutilises daily, weekly and monthly surveillance system records that could more precisely estimate peak timing.

Four seasons

Studies often defined four seasons with equal 3-month lengths and were described as: 'one of the 4 quarters into which the year is commonly divided' [38]. Studies consistently named seasons 'summer', 'fall', 'winter' and 'spring' despite seasons' start and end dates differing by geographic locations and climatic zones (Supplementary Table S3). Nearly all studies used monthly surveillance data, which inferred that seasons spanned from the first day of the first month to the last day of the third month (CID 17, 36). Studies using daily or weekly surveillance data occasionally selected dates to start and end mid-month (CID 90). Studies used unequal season lengths when analytically defining a high-incidence season (commonly referred to as summer) of 4 rather than 3 months (CID 91–95). Few studies defined high-incidence seasons using environmental factors such as rainfall, temperature or their combination (CID 18, 77, 96).

Quarterly seasons are historically defined by the photoperiod and align with agricultural production schedules [43]. Seasons vary by the relative durations of daylight and depend on a location's position relative to the equator [43]. Since meteorological patterns in each season vary by geographic location, so does the influence of environmental drivers on the peak timing of gastrointestinal infections. As expected, we found that studies conducted in the Southern Hemisphere defined summer/highest-incidence seasons from December to March while studies in the Northern Hemisphere defined summer/highest-incidence seasons from April to September (CID 16, 97–100).

Definitions of seasons also varied within the same geographic location. For example, we identified 10 studies conducted using the FoodNet surveillance system in the United States in 1996–2013 (CID 91, 101–109). Seven studies described seasonal peaks in summer months defined as June to August (CID 101–107). Two studies defined summertime peaks from July to September while one study used a broader 4-month interval from June to September (CID 91, 108, 109). Variation in definitions of summer results in less precise peak timing estimates; when comparing these studies, peak timing ranges from June to September despite most studies having a 3-month season length.

The use of four seasons follows similar analytical advantages and limitations as two seasons. The fixed number of seasons allows researchers to detect seasonality with straightforward statistical analyses that adjust for multiple comparisons. Researchers can incorporate indicator variables in regression models that

https://doi.org/10.1017/S0950268822000243 Published online by Cambridge University Press

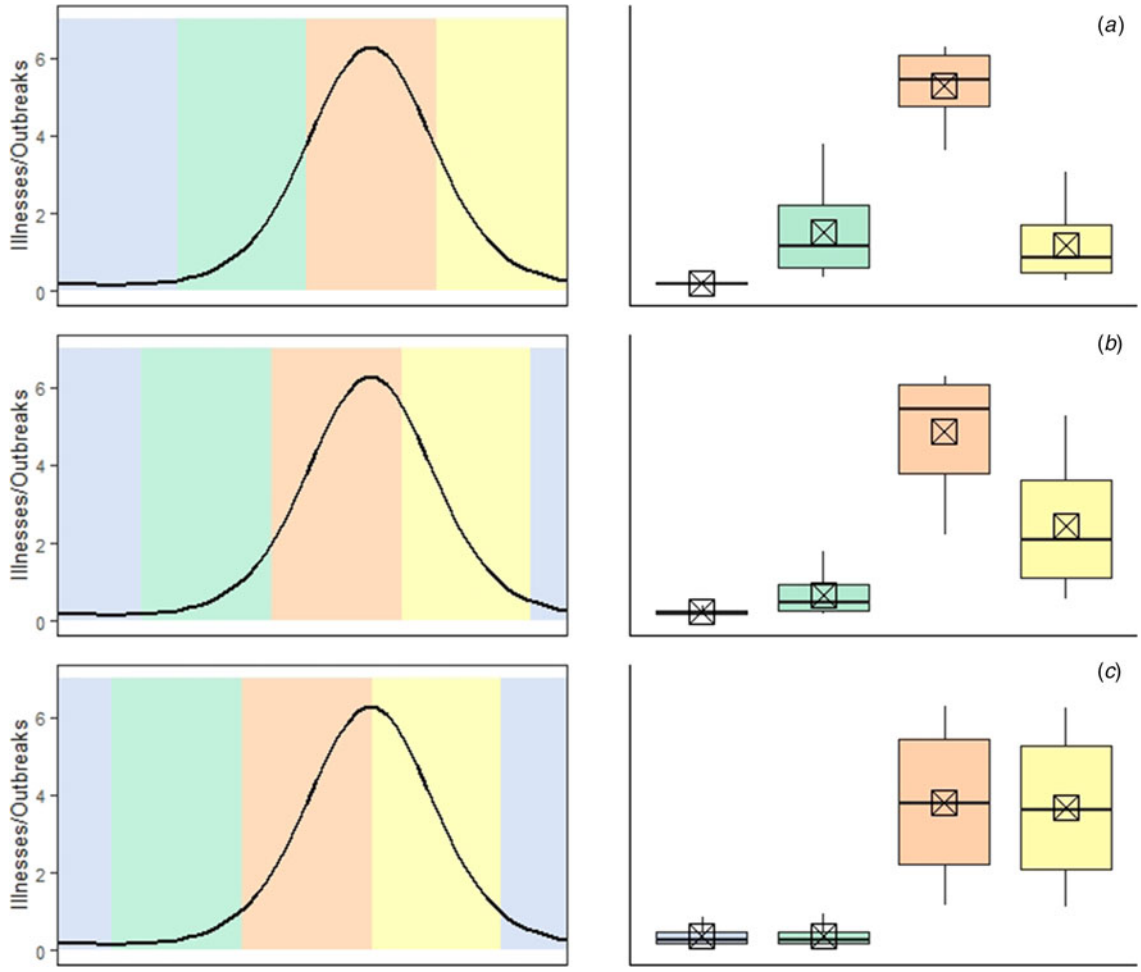


Fig. 3. An illustration of detecting seasonality and estimating seasonal peak timing using four discrete seasons. Scenarios include (a) when peak timing is well aligned with the centre of a season; (b) when peak timing is shifted from the centre of an *a priori* assigned season; and (c) when peak timing aligns with the boundary between 2 seasons. Scenario (a) offers higher precision and accuracy as compared to scenarios (b) and (c).

allow adjusting for additional confounding variables. Differences in season lengths require special attention: researchers must weight differences in the duration of each season. Studies rarely addressed this issue.

The most accurate detection of seasonality occurs when the seasonal peak falls at the centre of an *a priori* assigned season (Fig. 3a). Researchers' ability to detect seasonality reduces with any misalignment between assigned seasons and the actual seasonal curve (Figs 3b and 3c). When the seasonal peak falls near or at the boundary of two seasons, these seasons are indistinguishable. Researchers may then conclude that an infection peaks within a ~6-month period – a substantially reduced precision compared to quarterly seasons. When discrete seasons are defined by exogenous factors, such as ambient temperature or rainfall, misalignments could indicate a lag between infection and exposure (CID 65).

Defining seasonality with four seasons coarsely aggregates time series data, resulting in less precise estimates than daily, weekly or monthly data could allow for. Data aggregation impedes researchers from examining complex temporal behaviours of seasonal curves to inspecting the reliability of peak timing estimates. Quarterly seasons also lack a uniform environmental or biological factor shared across geographic locations. Comparisons between studies are challenging to assess and may cause confusion given seasons' common names worldwide. Even studies in the same location using the same dataset and study period used dissimilar definitions, reducing the precision of peak timing estimates when comparing these studies.

The four-season method somewhat ignores biologically plausible assumptions of temporality. Take the example of comparing springtime incidence to other seasons. The conceptual interpretation of a difference with a preceding season like winter differs from a comparison to an immediately following season like summer. Furthermore, comparisons between spring and fall fail to account for variations in incidence during summer. The use of discrete seasons overlooks the autoregressive nature of time series data and might draw comparisons based on unrealistic assumptions of temporality.

Calendar months

Studies most often used discrete Gregorian calendar months to detect seasonality and estimate peak timing. Researchers applied various statistical methods to monthly time series data (CID 56, 110–113) and estimated peak timing by identifying the calendar month with the highest average incidence or cumulative infections compared to other months (CID 13, 20, 25, 44, 51, 114–

https://doi.org/10.1017/S0950268822000243 Published online by Cambridge University Press

118). Many studies with only 1–3 years of surveillance data warranted this method, as more rigorous inspection of seasonal curves was not possible (Supplementary Table S4; CID 119–128).

Few studies with longer study periods conducted Mann–Whitney rank-sum tests with Bonferroni multiple comparison corrections (CID 129–130). Most studies examined seasonality using a discrete, 12-level categorical variable within logistic regression models. Researchers assessed significant differences using OR and IRR measures of association, which compared average incidence in each calendar month to a reference month (CID 34, 56, 110–113). When reference months had lowest incidence, OR and IRR estimates for the highest incidence month were analogous with the seasonal amplitude.

The international recognition of Gregorian calendar months establishes a common terminology for comparing study results. Many surveillance systems publicly report monthly records, allowing researchers to define seasonality by month and coarser seasons as desired (CID 127, 130). Monthly records are not bound to infection incidence or environmental drivers, easing researchers' examination of shifts in peak timing [13]. However, this discrete method still violates assumptions of temporality and ignores the autoregressive nature of time series data. Furthermore, the Gregorian calendar has month length irregularities [14] and often poorly reflects true climatic, social or biological seasons.

Monthly maximums accurately and precisely detect seasonality and estimate peak timing when infections have one consistent annual peak. However, statistical maximums are susceptible to outliers in the distribution of time series data. As noted earlier, many gastrointestinal infections exhibit irregularities in their seasonal pattern when long periods of low incidence alternate with short bursts of infections. This variability can result in numerous months with high incidence or the appearance of bimodal peaks due to outbreak events. While researchers can likely detect seasonality even with these irregularities, the accuracy and precision of peak timing estimates may reduce dramatically.

Few studies conducted formal comparison tests to determine differences between months (Supplementary Table S4). Yet, many studies used inferential language when reporting summaries of monthly incidence that implied statistical significance. Additionally, few studies conducting regression analyses stated the reference month when reporting results. These omissions inhibit reproducibility of analyses and prevent comparisons of study findings.

Describing seasonality using seasonal curves

Studies more precisely detected seasonality and estimated peak timing when constructing seasonal curves. These methods retained the temporal order of time series data and assumed that incidence at one time point depended on its intensity and variability in preceding time points, also known as autocorrelation (CID 66, 73, 75, 131, 132) [44, 45]. Descriptive studies constructed seasonal curves using various smoothers, spline functions or STL (CID 55, 69, 70, 72, 133–136). SARIMA models, harmonic models and spectral analyses estimated peak timing while adjusting for the periodicity and autoregressive nature of seasonal curves (CID 54, 74, 75, 137–141). Researchers estimated seasonality features and their uncertainty using regression coefficients from fitted models and applications of the δ-methods (CID 49, 50, 53, 61–65, 142, 143). The accuracy and precision of peak timing depended on time series length, white noise and patterns of missing data.

Splines, smoothers and STL

These methods detected seasonality using moving average smoothing and cubic spline modelling techniques (Supplementary Table S5). Average smoothing used a series of averages estimated on sequential time intervals to remove noise from data (CID 55, 136). Researchers specified the length of time intervals referred to as smoothing windows. Broader windows resulted in more filtering, optimal for examining linear trends while narrower windows resulted in less filtering to reveal seasonal patterns. Researchers detected and estimated seasonality by visual inspection of fitted regression values (CID 55, 136).

Models with embedded spline functions filtered white noise by fitting polynomial functions for sequential time intervals of seasonal curves. Researchers determined interval length by defining breakpoints throughout the curve, referred to as knots (CID 69, 70, 72, 133). Higher order polynomials with more knots had greater noise-to-signal ratios and captured more non-linear fluctuations in incidence like seasonality. Lower order polynomials with fewer knots filtered more white noise and created highly smoothed fitted values approaching linear trends. Researchers determined the presence of seasonality using visual inspection (CID 69, 70, 72, 133). Cubic splines captured seasonal peak and nadir timing more effectively than first- or second-degree polynomial functions.

STL attempted to isolate seasonal trends by decomposing data into three components: (i) a trend model of annual fluctuations; (ii) a seasonal model to account for daily, weekly or monthly fluctuations; and (iii) a model describing residual variability (CID 134, 135) [14]. This partitioning allowed researchers to inspect seasonal patterns using sinusoidal and cosinusoidal harmonic terms while filtering out other components (CID 134, 135). Researchers used rank-based Non-parametric Seasonality Tests (NPST) to estimate peak timing [46].

These methods all filter white noise and irregularities in time series data to reveal trends and seasonality features more clearly. Researchers do not need to aggregate daily and weekly records to precisely describe temporal fluctuations, though daily records may have day-of-the-week effects requiring additional attention. These methods retain the temporal order of data, capture the autocorrelative nature of seasonal curves and estimate peak timing using standardised time units comparable across studies. Researchers can also construct smoothers and splines or perform STL as exploratory data analyses to better specify main regression models.

Application of these techniques depends on how researchers select model parameters and visually inspect smoothed or fitted value curves. Researchers objectively define model parameters, decide window size or knot placement, and select the type of smoothed averaging, degree of polynomial order or method for inspecting seasonal components. These decisions influence the signal-to-noise ratio captured by smoothed or fitted values and necessitate researchers to conduct sensitivity analyses to ensure optimal selection of model parameters.

Seasonal ARIMA models, harmonic models and spectral analyses

These methods examined the periodicity of infection seasonality using the concept of harmonic functions in so-called time and frequency domains [47] (Supplementary Table S5). Time domain methods assume a constant periodicity of health outcomes, often annual cycles and include SARIMA models, Fourier series transformations and harmonic regression models. Studies modelled the seasonal curve of infections using a frequency equal to the

https://doi.org/10.1017/S0950268822000243 Published online by Cambridge University Press

number of time units per annual cycle (e.g. 365.25 days, 52.25 weeks or 12 months). Researchers detected seasonality based on the significance of sinusoidal and cosinusoidal regression coefficients (CID 35, 38, 54, 68, 144). Studies using SARIMA models often examined associations between the peak timing of infections and environmental risk factors (CID 57, 66, 73, 75). SARIMA models also adjusted for seasonal autocorrelation, or when infection seasonality depends on its periodic behaviour in previous annual cycles (CID 66, 73, 75, 131, 132). Seasonal autocorrelation emphasised the importance of longer time series lengths and fewer missing records [47].

Studies using harmonic regression models adjusted for Poisson or negative binomial distributions due to the non-negative right skewed behaviour of disease incidence (CID 43, 53, 70, 71, 143, 145). All studies assumed that annual infection seasonality aligned with Gregorian calendar years. Few studies estimated seasonal characteristics and their uncertainty measures by applying the δ-methods to regression coefficients (CID 49, 50, 53, 61, 62, 65, 76, 142, 143, 146). This technique converted trigonometric regression coefficients from a radial to a linear coordinate system to calibrate and estimate peak timing and amplitude [15]. The δ-methods provided both point estimates and confidence intervals for seasonality feature, enabling formal comparisons of estimates across geographic locations, study populations and pathogens (CID 49, 50, 53, 65, 142, 146).

Frequency domain methods do not assume a constant annual cycle and instead examine all possible cycle lengths in a study period (CID 140, 141). Spectral analyses, sometimes referred to as wavelet analyses, estimate peak timing by identifying the cycle length with best model fit (CID 140, 141). This technique was often used in exploratory analyses to determine the optimal cycle length before constructing harmonic regression models (CID 63, 140). Researchers also used spectral analyses to compare the frequency of seasonal gastrointestinal infections with environmental risk factors (CID 141).

Both time and frequency domain methods retain the temporal order, autocorrelative nature and temporal resolution of time series data. Studies reporting peak timing estimates used standardised Gregorian time units, easing comparisons between studies. Trigonometric functions have well-understood harmonic properties that allow for elegant description and estimation of the shape and frequency of seasonal curves. Researchers detected seasonality by the significance of harmonic terms within models and could investigate complex dual peak behaviours or shifts in peak timing by including multiple harmonic terms of varying frequencies.

Time series length and patterns of missing records influence the accuracy and precision of estimating peak timing with these methods. Shorter time series may have case influential observations that distort seasonal patterns of infections. However, researchers using longer time series should adjust for shifts in seasonal peak timing due to surveillance system maturity or changes in environmental drivers of infection over time. The percentage and location of missing data can also distort seasonal curves and bias estimates of seasonality features. Few studies summarised time series length or patterns of missing data.

Recommendations for improving time series reporting

We summarise the advantages and limitations of each time series method discussed above (Table 2). We hope this overview provides general guidelines to inform decision-making processes of researchers for selecting and utilizing time series methods. We encourage academic journal reviewers to use these guidelines when commenting on the appropriateness and completeness of time series methods in submitted manuscripts. Our overview demonstrates that, while discrete methods are computationally straightforward and require minimal statistical training, the use of seasonal curves provide more reliable description of seasonal patterns and estimation of seasonality features.

In addition, we propose a glossary of terms to standardise the reporting of results when using time series analyses (Table 3). As noted above, researchers used terms like *trends*, *seasonal trends* and *seasonal peaks* interchangeably, yet their meaning and interpretation vary dramatically. While results inferred statistical significance, studies often neither conducted nor reported comparison test results. Non-standardised terminology also yields uncertainty of statistical methods, misleading study findings, and potentially inaccurate estimations of peak timing. Terms defined in Table 3 can provide clearer aims, objectives and outcomes of studies using time series methods to describe, compare, explain and predict infection seasonality. Standardised terminology must accompany improved clarity in the reporting of case definitions and date of illness onset, testing and laboratory confirmation, as these differences may lead to unreliable comparisons of seasonality features across surveillance systems. Establishing consensus also invites interdisciplinary collaboration and sharing of methods for modelling surveillance data.

Discussion

In this review, we described time series methods using discrete seasons and seasonal curves to investigate the seasonality of gastrointestinal infections. Discrete seasons are prone to misclassification biases and studies lacked standardised terminology for reporting results and formal comparison tests. Studies constructing seasonal curves used methods that accounted for the temporality and autocorrelation of data. However, these studies often failed to estimate peak timing or thoroughly report on data limitations. We recommend that researchers: (i) use standardised terminology when reporting seasonality features; (ii) utilise more rigorous methods when estimating peak timing; and (iii) provide greater attention to data limitations when applying time series methods.

Our review revealed that a study's selection of time series methods relates closely to its underlying assumptions and rationale. Descriptive studies often estimate peak timing as the season or calendar month of maximal incidence while comparative or explanatory studies use seasonal curves to examine associations between illnesses and their drivers. However, we noted the stringency of selected methods depended not on study intent but rather the availability of usable data, dictating the acquired precision of seasonality estimates. The assumptions are rarely specified, yet they are essential for proper selection of both study design and methods of data analysis. These assumptions refer to researchers' ability to ensure optimal analytic power to determine the relevant mechanisms governing human infections. The first assumption is that a selected seasonal curve (or model) is optimal for describing the observable temporal processes; the ability to meet this assumption dictates the approach of handling noise due to poor fit or outliers when observed data are not aligned or do not lie sufficiently close to a selected curve. An additional assumption is that the selected populations are optimal for both observing and generating a seasonal curve (or model) for a selected pathogen. To test whether a study can meet these assumptions, we need

https://doi.org/10.1017/S0950268822000243 Published online by Cambridge University Press

https://doi.org/10.1017/S0950268822000243 Published online by Cambridge University Press

Table 2. Overview of the advantages (✓) and limitations (✗) of time series methods described in this systematic review

	2 and 4 Seasons	Calendar months	Smoothers, splines, STL	SARIMA, harmonics	Spectral analyses	δ-Methods
Minimal statistical training is required to calculate peak timing estimates	✓	✓	✗	✗	✗	✗
Definitions of seasons and peak timing estimates are easily comprehended by general audiences	✓	✓	✗	✗	✗	✗
Researchers do not need to aggregate surveillance data to perform time series analyses	✗	✓	✓	✓	✓	✓
Statistical results are generalisable using standardised Gregorian calendar time units	✗	✓	✓	✓	✓	✓
Researchers do not define seasons' lengths or reference seasons (i.e. data-driven analyses)	✗	✗	✓	✓	✓	✓
Time series methods adjust for irregularities and temporality of surveillance data	✗	✗	✓	✓	✓	✓
Time series methods do not require long time series to achieve sufficient sample size	✗	✗	✓	✓	✓	✓
Modelling techniques are flexible to adjust for other time-varying risk factors	✗	✗	✓	✓	✓	✓
Modelling techniques are flexible to adjust for dual peak or multi-peak outbreak behaviours	✗	✗	✗	✓	✓	✓
Modelling techniques adjust for harmonic seasonal curves using trigonometric functions	✗	✗	✗	✓	✓	✓
Modelling techniques are reliable at detecting seasonality using regression coefficients	✗	✗	✗	✓	✓	✓
Modelling techniques offer robust peak estimate in the presence of multiple seasonal peaks	✗	✗	✗	✗	✓	✓
Modelling techniques calculate seasonality features with measures of uncertainty	✗	✗	✗	✗	✗	✓
Peak timing estimates can be easily compared across subpopulations, pathogens, locations, etc.	✗	✗	✗	✗	✗	✓

Methods detect seasonality and estimate peak timing using discrete comparisons between seasons (two seasons or four seasons; calendar months) and constructed seasonal curves (smoothing, spline and STL methods; SARIMA, Fourier series transformations and harmonic models without applying the δ-methods; harmonic models with applying the δ-methods; and spectral analyses). We differentiate the advantages and limitations of harmonic models that do and do not apply the δ-methods to emphasise the importance of these methods in infectious disease seasonality research.

Table 3. A summary of terminology for describing time series analyses conducted in infectious disease epidemiology research

Term	Definition
Time series data	A set or a sample of time-referenced observations or records with an identified time period, cycle and unit (e.g. day, week, month extracted from a timestamp as YYYY:MM:DD:HH:mm) often illustrated by dot, line or needle plots with axes reflecting time and an outcome of interest.
Distribution of time series data	A general summary of frequencies in time-referenced data – i.e. how often an outcome of interest reaches a certain level with respect to time units (often illustrated with histograms and density plots).
Time series analyses	A collection of methods to describe, explain and predict temporal processes with time-referenced data for an outcome of interest.
Trend	General temporal behaviour in an outcome of interest that can exhibit steady incremental changes (linear) or varying incremental changes (non-linear) over time.
Season	An interval of time within one time cycle (typically 1 calendar year) defined by a specific biological, environmental, physical, physiological, or other property or feature in a biological or non-biological system [24].
Seasonal pattern	A recurrence of periods in an outcome of interest with alternating values (e.g. high and low) over the course of a time cycle.
Seasonality	A systematic periodic fluctuation in an outcome of interest over the course of one cycle (typically 1 calendar year) as an observable property of a biological or non-biological system.
Seasonal curve	An analytical representation of seasonal periodic fluctuations in an outcome of interest within one time cycle (typically 1 calendar year).
Seasonality features	A set of measurable characteristics to describe seasonality and a seasonal curve within 1 year, including seasonal peak, nadir, intensity, duration, speed at which a seasonal curve reaches its peak and speed at which a seasonal curve declines to its nadir [17].
Peak or nadir timing	A seasonality feature that represents times when a seasonal curve of an outcome reaches its maximum or minimum [17].
Amplitude or intensity	A seasonality feature that represents the difference between seasonal peaks and nadirs [17].
Duration	A seasonality feature that represents the time interval when incidence rises above a specified threshold [17].

Terms specify differences between time series data, distributions and analyses, as well as trends, season, seasonal patterns, seasonality and seasonality features.

rich and solid methodology development aiming to further improve research quality.

Studies often failed to report the lengths and dates of discrete seasons or to state reference seasons or months when reporting results. These omissions reduce the reliability of peak timing estimates, inhibit the reproducibility of analyses and prevent comparisons of study findings. Researchers must comprehensively report season lengths and dates given the variability of environmentally- or culturally-derived seasons by climate zone and geographic location. This is especially pertinent when using four seasons, which lack uniform environmental or biological factors shared across geographic locations.

While we support defining seasons by solstices and equinoxes due their uniformity, we also recognise the natural changes of the photoperiod during those intervals across latitudes [48]. Photoperiod intervals may fail to capture the relevant environmental drivers of disease transmission in all locations. Discrete seasons may also fail to capture seasonal patterns caused by non-seasonal drivers such as extreme weather events, livestock migration or practices around food, water and hygiene [20–22]. The complexity of defining seasons dictates the need for hypothesis-generating exploratory analyses to better choose a seasonal form and a detailed plan for sensitivity analyses assessing these alternatives. Furthermore, detecting the changes in seasonal features are valuable indicators of how circulating strains [30, 49–52], extreme events [53] or seasonal host migration [54] could alter seasonal behaviours. When seasonal peaks differ across subpopulations, it could indicate different underlying environmental mechanisms and interactions and subsequent disease transmission to humans. To detect such differences, granular temporal, spatial and etiological data with capabilities for global standardisation and harmonisation are needed.

High-resolution data maximise the potential of surveillance systems for describing, comparing and explaining changes in disease incidence over time and across species, pathogens, locations and other dimensions. Worldwide, public health agencies routinely collect time-referenced records to monitor the incidence of gastrointestinal infections and outbreaks. Surveillance systems track many common pathogens, such as *Salmonella*, *Campylobacter*, *Listeria* and *E. coli*, which contribute to ~600 million infections worldwide annually [9, 30–33]. Indicator-based surveillance systems (structured data with formal case definitions) reflect the total number of persons infected per unit of time [1, 13]. Event-based surveillance systems (public health emergencies reported using unstructured information) record implicated food and water sources linked to disease outbreaks [1]. The growing accuracy and precision of surveillance data could offer new opportunities for timely detection of changes in seasonal patterns.

The rapid adoption of growing analytical tools helps researchers to better model disease seasonality. Better understanding of how to construct seasonal curves will encourage disease surveillance systems to collect and report data with the highest temporal and spatial resolution possible. Broader utilisation of the modern time series models is needed to improve precision of peak timing estimates. Approaches like the δ-methods simultaneously detect the presence of seasonality and quantify seasonality features [13, 15, 28]. Most importantly, the δ-methods provide confidence intervals, allowing for formal statistical comparisons by location, subpopulation, pathogen, etc. [12, 16, 17].

Our review revealed that researchers underreport data limitations when applying time series methods. Maximum average incidence or cumulative infections can be biased by case influential observations or shifts in peak timing masked by coarse data aggregation. Studies constructing seasonal curves face data

https://doi.org/10.1017/S0950268822000243 Published online by Cambridge University Press

limitations like time series length and patterns of missing records. Time series length influences the effective sample size for regression analyses while the quantity and location of missing records influence the precision of peak timing estimates. Techniques for investigating the patterns of missing records in time series data have been explored for influenza [55]. We recommend that public health agencies and researchers report similar metrics as metadata to accompany the publicly available surveillance data they report and use, respectively.

Reliable estimation of peak timing permits targeted and proactive public health interventions to dampen seasonal infection incidence and prevent widespread outbreaks [12]. Public health agencies have expanded surveillance coverage in recent decades using collaborative networks of testing laboratories and public health agencies [56, 57]. More rigorous investigation of available data can improve: (i) early warning forecast accuracy to reduce socio-economic burdens of disease; (ii) fiscal and personnel resource allocations in medical facilities to treat higher seasonal patient volumes; (iii) laboratory testing supplies management; and (iv) the timeliness and effectiveness of food and water safety inspections [34, 35, 58, 59]. After the influenza pandemic of 2009, we observed an unprecedented growth in testing and reporting capacities worldwide [55]. The global response to the ongoing pandemic of COVID-19 has demonstrated further improvements in tracking infections. These newly acquired skills and partnerships should now be directed toward better monitoring of seasonal infections causing extensive health and economic burdens.

Conclusion

Greater attention to how seasonality is defined, modelled, interpreted and reported is necessary to promote reproducible research. Our review shows that applications of advanced time series analyses are underutilised in epidemiological research on enteric infections. We encourage increased training in these methods to incite more rigorous assessment of disease seasonality. These methods can provide more reliable estimation of infection peak timing while properly adjusting for irregularities of infections' temporal occurrences. Standardised terminology and more informative reporting requirements on data limitations will promote interdisciplinary collaborations in the modelling and forecasting of infectious diseases. A deeper understanding of the utility of time series analyses will encourage more expansive collection of surveillance data and refined temporal and spatial resolution when reporting that data.

Supplementary material. The supplementary material for this article can be found at https://doi.org/10.1017/S0950268822000243

Acknowledgments. The authors thank Maia Tarnas, Emily Sanchez and Dr. Jose Ordovas for their editorial assistance.

Author contributions. R.B.S. contributed to the review of literature, formal analysis, writing, reviewing, conceptualisation of visual aids, visualisation creation and editing. A.V.K. contributed to reviewing and editing. E.N.N. contributed to the conceptualisation of methodology, visual aids, review and editing, supervision, project administration and funding acquisition.

Financial support. This research was supported by the United States Department of Agriculture (USDA) National Institute of Food and Agriculture (NIFA) Cooperative State Research, Education, and Extension Service Fellowship (grant number 2020-38420-30724) and the National Science Foundation's (NSF) Innovations in Graduate Education (IGE) Program's Solution-Oriented, Student-Initiated, Computationally-Enriched (SOLSTICE) training and learning approach (grant number 1855886).

Conflict of interest. None.

Data availability. The data that support the findings of this study are openly available in Supplementary Table S1.

References

1. **World Health Organization** (2008) *Foodborne Disease Outbreaks: Guidelines for Investigation and Control*. Geneva, Switzerland: World Health Organization, WC 260 (ISBN 9789241547222).
2. **World Health Organization** (2017) *Strengthening Surveillance of and Response to Foodborne Diseases: A Practical Manual: Introductory Module*. Geneva, Switzerland: World Health Organization, License: CC BY-NC-SA 3.0 IGO (ISBN 9789241513227).
3. **National Food Safety System Project Outbreak Coordination and Investigation Workgroup** (2001) *Multistate Foodborne Outbreak Investigations: Guidelines for Improving Coordination and Communication*. Atlanta, GA, USA: National Food Safety System Project, Outbreak Coordination and Investigation Workgroup, Food and Drug Association.
4. **National Research Council of the National Academies** (2007) *Drinking Water Distribution Systems: Assessing and Reducing Risks*. Washington, DC: National Academies Press.
5. **Renwick DV *et al.*** (2019) Potential public health impacts of deteriorating distribution system infrastructure. *Journal-American Water Works Association* **111**, 42.
6. **Cann KF *et al.*** (2013) Extreme water-related weather events and waterborne disease. *Epidemiology and Infection* **141**, 671–686.
7. **Todd ECD** (2014) Foodborne diseases: overview of biological hazards and foodborne diseases. *Encyclopedia of Food Safety* **1**, 221–242.
8. **Canadian Paediatric Society** (2008) Foodborne infections. *Journal of Paediatrics and Child Health* **13**, 779–788.
9. **Centers for Disease Control and Prevention, National Center for Emerging and Zoonotic Infectious Diseases, Division of Foodborne, Waterborne, and Environmental Diseases**. Available at https://www.cdc.gov/foodsafety/foodborne-germs.html (Accessed 1 March 2021).
10. **Naumova EN, O'Neil E and MacNeill IB** (2005) INFERNO: a system for early outbreak detection and signature forecasting. *Morbidity and Mortality Weekly Report* **54**, 77–83.
11. **Naumova EN and MacNeill IB** (2005) Signature-forecasting and early outbreak detection system. *Environmetrics* **16**, 749–766.
12. **Naumova EN** (2006) Mystery of seasonality: getting the rhythm of nature. *Journal of Public Health Policy* **27**, 2–12.
13. **Alarcon Falconi TM *et al.*** (2020) Effects of data aggregation on time series analysis of seasonal infections. *International Journal of Environmental Research and Public Health* **17**, 5887.
14. **Cleveland RB *et al.*** (1990) STL: a seasonal-trend decomposition. *Journal of Official Statistics* **6**, 3–73.
15. **Naumova EN and MacNeill IB** (2007) Seasonality assessment for biosurveillance systems. In Balakrishnan N, Auget JL, Mesbah M and Molenberghs G (eds), *Advances in Statistical Methods for the Health Sciences*. Boston: Birkhäuser, pp. 437–450.
16. **Simpson RB, Zhou B and Naumova EN** (2020) Seasonal synchronization of foodborne outbreaks in the United States, 1996–2017. *Scientific Reports* **10**, 17500.
17. **Simpson RB *et al.*** (2020) An analecta of visualizations for foodborne illness trends and seasonality. *Scientific Data* **7**, 346.
18. **Alsova OK, Loktev VB and Naumova EN** (2019) Rotavirus seasonality: an application of singular spectrum analysis and polyharmonic modeling. *International Journal of Environmental Research and Public Health* **16**, 4309.
19. **Ureña-Castro K *et al.*** (2019) Seasonality of rotavirus hospitalizations at Costa Rica's National Children's Hospital in 2010–2015. *International Journal of Environmental Research and Public Health* **16**, 2321.
20. **Cox R *et al.*** (2012) Spatial and temporal patterns in antimicrobial resistance of Salmonella Typhimurium in cattle in England and Wales. *Epidemiology and Infection* **140**, 2062–2073.

https://doi.org/10.1017/S0950268822000243 Published online by Cambridge University Press

21. **Jokinen CC *et al.*** (2012) Spatial and temporal drivers of zoonotic pathogen contamination of an agricultural watershed. *Journal of Environmental Quality* **41**, 242–252.
22. **Kvitsand HM and Fiksdal L** (2010) Waterborne disease in Norway: emphasizing outbreaks in groundwater systems. *Water Science and Technology* **61**, 563–571.
23. **Bhaskaran K *et al.*** (2013) Time series regression studies in environmental epidemiology. *International Journal of Epidemiology* **42**, 1187–1195.
24. **MacNeill IB** (1974) Tests for periodic components in multiple time series. *Biometrika* **61**, 57–70.
25. **Alonso WJ *et al.*** (2007) Seasonality of influenza in Brazil: a traveling wave from the Amazon to the subtropics. *American Journal of Epidemiology* **165**, 1434–1442.
26. **Lofgren E *et al.*** (2007) Influenza seasonality: underlying causes and modeling theories. *Journal of Virology* **81**, 5429–5436.
27. **Simonsen L *et al.*** (2005) Impact of influenza vaccination on seasonal mortality in the US elderly population. *Archives of Internal Medicine* **165**, 265–272.
28. **Wenger JB and Naumova EN** (2010) Seasonal synchronization of influenza in the United States older adult population. *PLoS ONE* **5**, e10187.
29. **United States National Library of Medicine, National Center for Biotechnology Information**. Available at https://www.ncbi.nlm.nih.gov/home/about/mission/ (Accessed 18 July 2019).
30. **Tack DM *et al.*** (2020) Preliminary incidence and trends of infections with pathogens transmitted commonly through food – Foodborne Diseases Active Surveillance Network, 10 U.S. sites, 2016–2019. *Morbidity and Mortality Weekly Report* **69**, 509–514.
31. **Centers for Disease Control and Prevention, Office of Public Health Scientific Services, Center for Surveillance, Epidemiology, and Laboratory Services, Division of Health Informatics and Surveillance**. Available at https://wwwn.cdc.gov/nndss/conditions/ (Accessed 1 March 2021).
32. **United States Food and Drug Association**. Available at https://www.fda.gov/files/food/published/Most-Common-Foodborne-Illnesses-%28PDF%29.pdf (Accessed 1 March 2021).
33. **United States Food and Drug Association**. Available at https://www.fda.gov/food/consumers/what-you-need-know-about-foodborne-illnesses (Accessed 1 March 2021).
34. **World Health Organization**. Available at https://www.who.int/news-room/fact-sheets/detail/food-safety (Accessed 1 March 2021).
35. **World Health Organization** (2015) *WHO Estimates of the Global Burden of Foodborne Disease: Foodborne Disease Burden Epidemiology Reference Group 2007–2015*. Geneva, Switzerland: World Health Organization, Control of Neglected Tropical Diseases, Foodborne Disease Burden Epidemiology Reference Group, Nutrition and Food Safety, WHO/FOS/15.02 (ISBN 9789241565165).
36. **Centers for Disease Control and Prevention, National Center for Emerging and Zoonotic Infectious Diseases, Division of Foodborne, Waterborne, and Environmental Diseases**. Available at https://www.cdc.gov/foodnet/publications/index.html (Accessed 18 July 2019).
37. **National Center for Immunization and Respiratory Diseases, Division of Viral Diseases**. Available at https://www.cdc.gov/nors/publications.html (Accessed 18 July 2019).
38. **Merriam-Webster**. Available at https://www.merriam-webster.com/dictionary/season (Accessed 1 March 2021).
39. **Chao DL *et al.*** (2019) The seasonality of diarrheal pathogens: a retrospective study of seven sites over three years. *PLoS Neglected Tropical Diseases* **13**, e0007211.
40. **Muchiri JM *et al.*** (2009) Seasonality of *Cryptosporidium* oocyst detection in surface waters of Meru, Kenya as determined by two isolation methods followed by PCR. *Journal of Water and Health* **7**, 67–75.
41. **Chambers R** (1983) Seasonality, poverty and nutrition: a professional frontier. In Neelakantan S (ed.), *EFNAG National Workshop on Poverty and Malnutrition*. Coimbatore: Tamil Nadu Agricultural University, pp. 1–16.
42. **Kulinkina AV *et al.*** (2016) Seasonality of water quality and diarrheal disease counts in urban and rural settings in south India. *Scientific Reports* **6**, 20521.
43. **National Geography Society**. Available at https://www.nationalgeographic.org/encyclopedia/season/#:~:text=Powered%20by-,A%20season%20is%20a%20period%20of%20the%20year%20that%20is,on%20December%2021%20or%2022 (Accessed 1 March 2021).
44. **Box GEP and Jenkins GM** (1976) *Time Series Analysis: Forecasting and Control*. Oakland: Holden-Day.
45. **Helfenstein U** (1996) Box-Jenkins modelling in medical research. *Statistical Methods in Medical Research* **5**, 3–22.
46. **Rogerson PA** (1996) A generalization of Hewitt's test for seasonality. *International Journal of Epidemiology* **25**, 644–648.
47. **Shumway RH, Stoffer DS and Stoffer DS** (2000) *Time Series Analysis and its Applications*, Vol. **3**. New York: Springer.
48. **Pio-Abreu JL** (1997) Seasonal variation in bipolar disorder. *The British Journal of Psychiatry* **170**, 483–484.
49. **Lofgren ET *et al.*** (2010) Disproportional effects in populations of concern for pandemic influenza: insights from seasonal epidemics in Wisconsin, 1967–2004. *Influenza and Other Respiratory Viruses* **4**, 205–212.
50. **Sarkar R, Kang G and Naumova EN** (2013) Rotavirus seasonality and age effects in a birth cohort study of southern India. *PLoS ONE* **8**, e71616.
51. **Stashevsky PS *et al.*** (2019) Agglomerative clustering of enteric infections and weather parameters to identify seasonal outbreaks in cold climates. *International Journal of Environmental Research and Public Health* **16**, 2083.
52. **Colston JM *et al.*** (2018) Seasonality and within-subject clustering of rotavirus infections in an eight-site birth cohort study. *Epidemiology and Infection* **146**, 688–697.
53. **Stratton M *et al.*** (2017) A comparative analysis of three vector-borne diseases across Australia using seasonal and meteorological models. *Scientific Reports* **7**, 40186.
54. **Chui KK, Cohen SA and Naumova EN** (2011) Snowbirds and infection – new phenomena in pneumonia and influenza hospitalizations from winter migration of older adults: a spatiotemporal analysis. *BMC Public Health* **11**, 444.
55. **Simpson RB *et al.*** (2021) Completeness of open access FluNet influenza surveillance data for Pan-America in 2005–2019. *Scientific Reports* **11**, 795.
56. **Angulo FJ and Scallan E** (2007) Activities, achievements, and lessons learned during the first 10 years of the Foodborne Diseases Active Surveillance Network: 1996–2005. *Clinical Infectious Diseases* **44**, 718–725.
57. **Jones TF, Scallan E and Angulo FJ** (2007) FoodNet: overview of a decade of achievement. *Foodborne Pathogens and Disease* **4**, 60–66.
58. **United States Government Accountability Office** (2014) *Federal Food Safety Oversight: Additional Actions Needed to Improve Planning and Collaboration*. Washington, DC, USA: Government Accountability Office, Report to Congressional Addressees no. GAO-15–180.
59. **Buzby JC *et al.*** (1996) *Bacterial Foodborne Disease: Medical Costs and Productivity Losses*. Washington, DC, USA: US Department of Agriculture, Economic Research Service, Agricultural Economic Report no. 741.

https://doi.org/10.1017/S0950268822000243 Published online by Cambridge University Press

scientific reports

Check for updates

OPEN

Completeness of open access FluNet influenza surveillance data for Pan-America in 2005–2019

Ryan B. Simpson, Jordyn Gottlieb, Bingjie Zhou, Meghan A. Hartwick & Elena N. Naumova✉

For several decades, the World Health Organization has collected, maintained, and distributed invaluable country-specific disease surveillance data that allow experts to develop new analytical tools for disease tracking and forecasting. To capture the extent of available data within these sources, we proposed a completeness metric based on the effective time series length. Using FluNet records for 29 Pan-American countries from 2005 to 2019, we explored whether completeness was associated with health expenditure indicators adjusting for surveillance system heterogeneity. We observed steady improvements in completeness by 4.2–6.3% annually, especially after the A(H1N1)-2009 pandemic, when 24 countries reached > 95% completeness. Doubling in decadal health expenditure per capita was associated with ~ 7% increase in overall completeness. The proposed metric could navigate experts in assessing open access data quality and quantity for conducting credible statistical analyses, estimating disease trends, and developing outbreak forecasting systems.

Global and national surveillance systems serve two critical functions: monitoring disease trend trajectories to inform health policies and providing early outbreak warnings that require local, regional, or global responses[1]. Extensive time, personnel, and monetary resources are required to collect, process, and maintain time referenced and geographically tagged surveillance data. These data enable a rapid evidence-based response to protect human health, distribute supplies, and mitigate disease outbreaks. Effective surveillance data must be credible to produce reliable alerts, complex to incorporate a variety of data streams, and historically rich to track disease trajectories for early warning detection[2]. Poor-quality surveillance data can lead to policy interventions that are based on inaccurately interpreted patterns resulting in diminished quality of life, less productive societies, and slower global responses[3,4]. High quality data available to a broad range of experts are critical to reliably predict disease trends[2].

The World Health Organization (WHO) has played an instrumental role in regulating the generation of international surveillance data for over 70 years. The WHO has established high standards by using a comprehensive set of monitoring and evaluation (M&E) metrics to routinely collect worldwide records[5,6]. These metrics track the production of surveillance data and provide critical information for effective analysis and interpretation of the data. Some of these metrics like *sensitivity*, *specificity*, and *positive predicted value* measure the accuracy and reliability of testing protocols and mechanisms. Other metrics, like *timeliness* and *representativeness*, provide information on the frequency and comprehensiveness of data incorporated within surveillance systems[6]. Together, these M&E metrics help data users understand the reliability of patterns that are captured, detected, and demonstrated based on the collected data.

The WHO established the Global Influenza Surveillance Network (GISN) in 1952 to raise awareness of the economic impact and public health consequences of influenza[7–9]. In 1997, the standardization of polymerase chain reaction (PCR) technology enabled rapid case identification of influenza infections and improved the ability to definitively diagnose influenza infection. These scientific breakthroughs made global virological influenza surveillance possible and led to a strengthening of the GISN through the creation of FluNet: a system of over 122 national influenza centers (NICs) and 6 international centers interconnected by Internet servers that consistently record population-level influenza in over 170 countries[9–12]. FluNet data is publicly available to encourage wide dissemination and analysis of influenza trends, burdens, and patterns[12]. This public platform supports the broader mission of WHO influenza surveillance: to monitor, plan for, and alert the world on novel influenza epidemiology for seasonal, pandemic, and zoonotic influenza[12].

As the velocity and volume of collected data increased from 1998–2010, so did opportunities to utilize multiple data streams and disseminate surveillance records more broadly. This gave rise to web-based platforms like FluID that actively collect, deposit, and report influenza health records using various influenza case definitions

Tufts University Friedman School of Nutrition Science and Policy, Boston, USA. ✉email: Elena.Naumova@tufts.edu

and surveillance strategies[13]. Information reported by these platforms includes numerous influenza-related case definitions, testing techniques, surveillance strategies, reporting timeliness, and population coverage. Once registered, any certified health center, not just a NIC, is able to participate in this data curation. The information collected by platforms like FluID complement FluNet to improve the accuracy and coverage of estimating true influenza incidence[9]. The merging of multiple data streams has been shown to improve rates of influenza testing and diagnosis, which greatly influence the reporting completeness of surveillance data[3,4,14].

National healthcare infrastructure and public health resources are likely to drive the reliability, completeness, and accuracy of reported data[5]. Thus, FluNet relies on the case identification and collection capacity of each participating country. While several studies examined the association between country wealth and the burden of influenza[15–17], little is known whether country income or health expenditure indicators along with the national surveillance system attributes influence data availability. A broad network of available data streams might facilitate data collection and reporting to FluNet, but does not guarantee data completeness. Furthermore, existing WHO M&E metrics that target surveillance system quality are not embedded into metadata of publicly available records. This questions whether and how external users assess the quality and completeness of available data[18,19]. Yet, the completeness of publicly disseminated surveillance data influences modeled disease trends, seasonal features, outbreak signatures, and forecasts[20–23].

In this communication, we proposed a metric of *completeness* based on the effective time series length (ETSL) to capture the extent of the available time series data within FluNet records. We illustrated the utility of this metric for 29 Pan-American countries across 14 influenza variables (6 testing outcomes and 8 strain subtypes) from 2005 to 2019. We calculated this metric for each country using annual (52–53 weeks), full study (782 weeks), and select interval (470–782 weeks) time period lengths. We ranked countries based on completeness estimates and determined trends across countries. We adjusted completeness estimates for specific strain subtypes (e.g. A(H1N1)pdm09) to isolate only time periods when reporting is meaningful. We applied a mixed effects regression model to evaluate whether national economic indicators could explain the degree of completeness for each influenza variable. Our proposed completeness metric helps external data users understand the amount of data available for analyses and the potential of data to accurately estimate disease trends, detect temporal changes, and develop spot checks in data quality. This metric can also assist data users to recognize data limitations, understand the heterogeneity of primary data sources, and develop strategies for conducting credible statistical analyses using publicly disseminated surveillance data. The presented material is especially important in light of publicly reported time series data for the ongoing coronavirus disease 2019 (COVID-19) pandemic.

Data and methods

FluNet weekly records. We abstracted FluNet weekly records on 24–27 April 2020 for 29 Pan American countries from Week 1 (03 January) 2005 through Week 52 (29 December) 2019. Due to the absence of a public application programming interface (API) and the challenges of the website's dynamic AJAX interface[24], we acquired public data with a custom scraper built using RSelenium[25]. We downloaded each country's records individually and used a scripted pipeline to standardize and merge country-specific datasets. Codes are available in the Supplementary Materials Appendix.

FluNet reports time series data of influenza confirmed cases representing a complex array of data streams. For each country download, we extracted time series data for 6 available testing outcomes: specimens collected, specimens processed (tests), total positives, total negatives, influenza A positives, and influenza B positives. We also extracted time series data for 8 influenza subtypes: A(H1), A(H1N1)pdm09, A(H3), A(H5), A(Unsubtyped), B(Yamataga), B(Victoria), and B(Undetermined). The overall data compilation included 14 variables for 29 countries covering 782 weeks.

Surveillance systems attributes. We compiled FluNet case definitions, surveillance strategies, reporting quota and timeliness, NICs, and reporting facilities using several WHO reports[6,26–28] to assess surveillance attributes associated with completeness (Table 1). Influenza case definitions are not fully standardized: they have subtle but important differences in their evaluation setting and diagnostic criteria. Case definitions for each country include severe acute respiratory illness (SARI), influenza-like-illness (ILI), pneumonia, influenza cases (Influenza), acute respiratory infection (ARI), and deaths (Mortality) (Supplementary Table S1). Mortality was defined as deaths from influenza unless otherwise specified. Six FluNet countries (Chile, Cuba, Dominica, Dominican Republic, El Salvador, and Honduras) have fully adopted the WHO case definitions. We marked countries utilizing non-WHO definitions.

Surveillance strategies include national, sentinel, and universal, which offer different population coverage for each influenza case definition (Supplementary Table S2). NICs are nationally recognized institutions approved by the WHO and responsible for reporting influenza surveillance records to FluNet. Influenza reporting facilities include SARI hospitals, ILI centers, PCR testing facilities, and influenza (IF) testing laboratories, and their number vary by country. Each facility processes tests at different volumes and speeds, resulting in differing reporting quotas and timeframes. Reporting quotas describe the fraction of cases that are reported to FluNet from in-country surveillance systems. They include all cases or a specific number of cases based on each country's health objectives. Reporting timeframe is the difference between when disease cultures are laboratory confirmed and when they are reported by surveillance facilities to a national or global database. Though FluNet publishes weekly records, reporting timeframes range from daily to monthly across countries. We found no resources that compile these surveillance system characteristics to allow for clear side-by-side comparison across continental countries.

Economic and health expenditure indicators. We extracted three economic indicators for each country reported by the World Bank's *World Development Indicators* publicly available database. Indicators included

Country (abbreviation)	Case definition	WHO definition[a]	Surveillance strategy[a]	Reporting quota[b]	Reporting timeframe[c]	NICs	Reporting facilities
Argentina (ARG)	SARI	Yes	Sentinel	All cases	Weekly	3	44
		Yes	Universal	All cases	Weekly		
	Pneumonia	No	NR	NR	NR		
	Mortality	Yes	Universal	All cases	Weekly		
	ILI	Yes	Universal	0	NR		
		Yes	Sentinel	Unknown	Weekly		
Barbados (BRB)	SARI	No	Sentinel	All cases	Daily	0	3
	Influenza	Yes	Sentinel	All cases	NR		
	ARI	No	Sentinel	6	NR		
Belize (BLZ)	SARI	Yes	Sentinel	All cases	NR	0	10
	Influenza	NR	National	All cases	Weekly		
	ILI	Yes	National	0	NR		
Bolivia (BOL)	SARI	Yes	Sentinel	All cases	Weekly	0	11
	Pneumonia	No	National	0	NR		
	Influenza	NR	National	All cases	Weekly		
Brazil (BRA)	SARI	No	Sentinel	All cases	Daily	3	258
	Mortality	Yes	NR	NR	NR		
	Influenza	Yes	National	All cases	Daily		
	ILI	No	Sentinel	All cases	Daily		
Canada (CAN)	SARI	Yes	Sentinel	Varies	Varies	11	147
	Pneumonia	No	National	Varies	Varies		
	Influenza	Yes	National	All cases	Varies		
	ILI	Yes	Sentinel	Varies	Weekly		
	ARI	No	National	Varies	Varies		
Chile (CHL)	SARI	Yes	Sentinel	All cases	Weekly	1	79
	Influenza	Yes	National	All cases	Daily		
	ILI	Yes	Sentinel	10	Weekly		
Colombia (COL)	SARI	Yes	Sentinel	All cases	Weekly	1	32
	Pneumonia	No	National	0	NR		
	Mortality	No	National	All cases	Weekly		
	Influenza	NR	NR	NR	NR		
	ILI	No	Sentinel	All cases	Weekly		
	ARI	No	National	0	NR		
Costa Rica (CRI)	SARI	Yes	Sentinel	5	Weekly	1	21
	Pneumonia	No	Universal	Unknown	NR		
	Mortality	Yes	Universal	Unknown	NR		
	Influenza	NR	Sentinel	5	Daily		
	ILI	Yes	Universal	NR	NR		
	ARI	No	National	Unknown	NR		
Cuba (CUB)	SARI	Yes	National	All cases	Daily	1	154
	Pneumonia	Yes	National	All cases	Daily		
	Mortality	Yes	National	NR	NR		
	ILI	Yes	National	Unknown	Daily		
	ARI	Yes	National	Unknown	Daily		
Dominica (DMA)	SARI	Yes	Sentinel	All cases	Weekly	0	1
	Mortality	Yes	National	0	NR		
	ARI	Yes	National	6	Weekly		
Dominican Republic (DOM)	SARI	Yes	Sentinel	5	Weekly	1	12
	Influenza	Yes	Sentinel	All cases	Weekly		
	ILI	Yes	Sentinel	5	Weekly		
Ecuador (ECU)	SARI	Yes	Sentinel	All cases	Daily	1	18
	Pneumonia	No	Universal	0	NR		
	Influenza	NR	National	NR	NR		
El Salvador (SLV)	SARI	Yes	Sentinel	5	Weekly	1	14
	ILI	Yes	Sentinel	3	Weekly		

Continued

Country (abbreviation)	Case definition	WHO definition[a]	Surveillance strategy[a]	Reporting quota[b]	Reporting timeframe[c]	NICs	Reporting facilities
Guatemala (GTM)	SARI	Yes	Sentinel	6	Weekly	1	9
	Pneumonia	No	Universal	0	NR		
	Influenza	NR	National	NR	NR		
	ILI	Yes	Sentinel	6	Weekly		
	ARI	No	National	0	NR		
Haiti (HTI)	SARI	Yes	Sentinel	10	NR	0	15
	ARI	NR	National	0	NR		
Honduras (HND)	SARI	Yes	Sentinel	All cases	Weekly	1	10
	Pneumonia	Yes	National	NR	NR		
	Mortality	Yes	Sentinel	NR	NR		
		Yes	National	NR	NR		
	Influenza	Yes	Sentinel	All cases	Weekly		
	ILI	Yes	Sentinel	7	Weekly		
	ARI	Yes	National	NR	NR		
		Yes	Sentinel	NR	NR		
Jamaica (JAM)	SARI	Yes	Sentinel	All cases	Weekly	1	6
	Influenza	Yes	National	All cases	Daily		
	ARI	NR	Sentinel	All cases	Daily		
Mexico (MEX)	Influenza	Yes	Sentinel	All cases	Weekly	1	995
	ILI	No	Sentinel	Varies	Weekly		
	ARI	No	Sentinel	All cases	Weekly		
Nicaragua (NIC)	SARI	Yes	Sentinel	All cases	Weekly	1	17
	Pneumonia	No	National	0	NR		
	Mortality	Yes	National	0	NR		
	Influenza	NR	Sentinel	All cases	Weekly		
	ILI	Yes	Sentinel	3	Weekly		
	ARI	No	National	0	NR		
Panamá (PAN)	SARI	Yes	Sentinel	Varies	Weekly	1	24
	Pneumonia	NR	National	NR	NR		
	Influenza	Yes	National	Unknown	Daily		
		Yes	Sentinel	Unknown	Daily		
	ILI	Yes	Sentinel	Varies	Weekly		
	ARI	No	National	NR	NR		
Paraguay (PRY)	SARI	No	Sentinel	All cases	Weekly	1	17
	Pneumonia	No	Universal	0	NR		
	ILI	No	Sentinel	5	Weekly		
	ARI	No	National	0	NR		
Peru (PER)	SARI	Yes	Sentinel	All cases	Daily	1	46
	Pneumonia	NR	Universal	0	NR		
	Mortality	Yes	National	0	NR		
	ILI	Yes	Sentinel	Unknown	Weekly		
St. Lucia (LCA)	SARI	Yes	Sentinel	All cases	Weekly	0	41
	Influenza	Yes	National	6	NR		
	ILI	Yes	Sentinel	6	NR		
	ARI	No	National	All cases	NR		
St. Vincent & the Grenadines (VCT)	SARI	Yes	Sentinel	All cases	Daily	0	1
	ILI	NR	National	NR	NR		
Suriname (SUR)	SARI	Yes	Sentinel	All cases	Daily	0	7
	Pneumonia	NR	National	0	NR		
	Mortality	Yes	National	0	NR		
	ILI	Yes	Sentinel	10	Weekly		
	ARI	No	Sentinel	0	NR		
Uruguay (URY)	SARI	Yes	Sentinel	All cases	Weekly	1	44
	Influenza	NR	Sentinel	All cases	Weekly		

Continued

Country (abbreviation)	Case definition	WHO definition[a]	Surveillance strategy[a]	Reporting quota[b]	Reporting timeframe[c]	NICs	Reporting facilities
United States (USA)	SARI	No	Sentinel	All cases	NR	1	3100
	Influenza	Yes	National	All cases	Weekly		
	ILI	NR	Sentinel	Unknown	Weekly		
Venezuela (VEN)	Influenza	NR	National	All cases	Weekly	1	NR

Table 1. Case definitions, adherence to WHO case definition, surveillance strategies, reporting quotas, reporting timeframes, number of NICs, and reporting facilities for 29 Pan-American FluNet-reporting countries based on WHO and PAHO reports from 2017[10–13]. [a]NR – country case definitions or surveillance systems that were not reported or unavailable within WHO and PAHO reports. [b]Quotas listed as *All Cases* report all surveillance cases to FluNet. Numbers ranging from 0 to 10 list the number of cases per reporting timeframe reported to FluNet. Quotas listed as *Varies* indicates that quotas are a percentage of the total cases reported or that quotas fluctuate depending on case severity. For quotas listed as *Unknown*, a quota exists but values are not provided in WHO and PAHO reports. Quotas listed as *NR* had neither the existence nor the quantity of a quota reported in WHO and PAHO reports. [c]Reporting timeframe indicates the delay between collecting and processing test shipments. Timeframes reported as *Varies* suggests that this process changes over time. Timeframes that are listed as NR were unavailable within WHO and PAHO reports.

Timeframe	Outcomes	ETSL reporting dates	Number of full weeks, L
Annual	All 14 outcomes	1 Jan–31 Dec	$L_1 = 52$ or 53 52: 2005–2008, 2010–2014, 2016–2019 53: 2009, 2015
Average full study period	All 14 outcomes	03 Jan 2005–29 Dec 2019	$L_2 = 782$
Average corrected	A(H1N1)pdm09 and Specimens A(H5) B(Yamataga) and B(Victoria)	31 Dec 2007–29 Dec 2019 31 Dec 2007–01 Jan 2017 01 Jan 2007–29 Dec 2019	$L_3 = 626$ $L_3 = 470$ $L_3 = 678$

Table 2. Number of full weeks included for calculating the completeness metric using annual, full study, and corrected effective time series lengths.

Gross National Income (GNI) per capita (GNIPC), domestic general government health expenditure per capita (DHEPC), and out-of-pocket health expenditure as a percentage of current health expenditure (OOPHE%)[29]. GNIPC was reported in purchasing power parity (PPP) constant 2011 international US dollars (USD). DHEPC was reported in current international USD. OOPHE% is reported as the percentage of current government expenditure (Supplementary Table S3). GNIPC estimates were available for all countries from 2005 to 2018 except Cuba and Venezuela (data available for 2005–2016 and 2005–2014, respectively). DHEPC and OOPHE% records were available from 2005 to 2016 for all countries except Venezuela (data available for 2005–2015).

Completeness metric. We measured *completeness* based on an effective time series length (ETSL), or the extent of time series data that can be used in data analysis. Time series length greatly influenced how and what the completeness metric described. We used an annual ETSL to calculate completeness from Week 1 to Week 52/53 to compare completeness between outcomes and across countries. We used these values to calculate the overall completeness, or the mean across all years from 2005 to 2019. We also calculated the average completeness using the full time series ETSL for the entire 782-week study period. Finally, we calculated the corrected average values and corrected overall completeness by including only years when selected outcomes or subtypes were reported. This prevented the deflating of the completeness metric by including all study years irrespective of whether a country's surveillance records were present or not.

We calculated the annual completeness, $C_{i,j,k}$, as a fraction of the time series length for which reliable data are available to the overall length of the considered time series, or the number of full weeks between the start and end of the time period, multiplied by 100:

$$C_{i,j,k} = \left(n_{i,j,k}/L_1\right) * 100\%$$

where $C_{i,j,k}$ is completeness for i-outcome ($i = 1$–14), j-country ($j = 1$–29), k-year ($k = 1$–15); $n_{i,j,k}$—the number of time units (weeks) in the time series when records are available (e.g. weeks with reported counts ≥ 0) for i-outcome, j-country, k-year; L_1—the number of full weeks (52 or 53) for k-year (Table 2). We calculated the annual completeness by using the total length in weeks for each year.

We calculated the completeness for each outcome and country for the full time series using the total 782-week length covering the study period from Week 1 (03 January) 2005 to Week 52 (29 December) 2019, as:

$$C_{i,j} = \left(n_{i,j}/L_{i,2}\right) * 100\%$$

where $C_{i,j}$ is completeness for i-outcome ($i = 1$–14), j-country ($j = 1$–29); $n_{i,j}$—the number of time units (weeks) in the time series when records are available (e.g. weeks with reported counts ≥ 0) for i-outcome, j-country; L_{i2}—the

number of full weeks (782) or the full study period. To draw comparisons across countries, we calculated the overall completeness as the average completeness across all 14 outcomes for each country.

To more accurately reflect completeness for specific influenza outcomes, we corrected the average estimates to only include the time period when reporting is meaningful. For example, Jamaica, Paraguay, and Mexico were the first Pan American countries to report the new influenza subtype A(H1N1)pdm09 in 2008. All 29 countries have continued reporting this subtype as of 2019. Thus, we estimated the average estimates for A(H1N1)pdm09 to account for the start of pandemic strain reporting in 2008 for all countries. Specimens were also first reported in 2008 by Paraguay with Canada and the United States continuing reporting through 2019; completeness for specimens was similarly estimated for a 626-week time period from Week 1 2008 to Week 52 2019. For A(H5), we estimated average completeness from Week 1 2008 to Week 52 2016 (470 weeks). For B(Yamataga) and B(Victoria), we estimated average completeness for a 678-week time period from Week 1 2007 to Week 52 2019. All analyses of average estimates were performed using values of L_3 as shown in Table 2.

Completeness analysis. We examined trends in annual completeness for all 14 influenza variables and produced heatmaps illustrating the country ranking with respect to completeness. To further examine trends and associations with national economic indicators (GNIPC, DHEPC, and OOPHE%), we selected annual completeness estimates for tests, positives, A(H1N1)pdm09, and overall. We applied loess smoothers with a span of 0.5 to illustrate trends across all years and countries. We transformed the GNIPC and DHEPC values using the natural logarithm function to minimize the effect of skewed distributions in regression models. For each influenza variable, we estimated the change in annual completeness associated with time and national economic indicators using a mixed effects regression model (Model 1):

$$C_{i,j,k} = \beta_0 + \beta_1 * Year_k + \beta_2 * E_{j,k} + \alpha_j * Country_j + \varepsilon_{jk}$$

where $C_{i,j,k}$ is completeness for i-outcome ($i = 1–4$), j-country ($j = 1–29$), k-year; $E_{j,k}$ – one of three national indicators for j-country and k-year; β_1—fixed effects for the annual trend, α_j – random effects for individual countries. The length of the time series used in each regression varied according to the length of available records for the economic or health expenditure indicator in each country.

We expanded the model to adjust for surveillance systems' attributes (Model 2):

$$C_{i,j,k} = \beta_0 + \beta_1 * Year_k + \beta_2 * E_{j,k} + \beta_m * S_{j,m} + \alpha_j * Country_j + \varepsilon_{jk}$$

where $S_{j,m}$—matrix of the national surveillance system attributes as defined in Table 1. Attributes included in the analysis were: case definition type, including ARI, ILI, Influenza, Pneumonia, Mortality, and SARI as the reference category; adherence to WHO definition as a binary variable; surveillance strategy, including Sentinel, National, and Universal as the reference category; reporting quota, including categories for reported quota, varying or unknown quota, and reporting all cases as the reference category; reporting timeframe, as weekly, not reported (NR), and daily reporting as the reference; number of NICs, and the natural log of reporting facilities number (we applied the transformation given the skewed distribution of reporting facilities as fewer countries have many facilities).

To estimate the effect size (ES) from regression model results, we calculated the decadal change between 2005 and 2015 for each economic and health expenditure indicator. For Venezuela, we estimated decadal changes in GNIPC from 2005 through 2014 due to limited data availability. Using the coefficients from Models 1 and 2, we estimated ES and its 95% confidence intervals (CI) associated with time and health expenditure indicators in the completeness of tests, positives, A(H1N1)pdm09, and overall completeness. For GNIPC and DHEPC, the effect size was associated with a doubling in these predictors; the 95% confidence interval was estimated as: $ES = ln(2) * (\beta_2 + 1.96se(\beta_2))$. For OOPHE%, ES was associated with a 10% increase in expenditures; 95%CI was estimated as: $ES = 10 * (\beta_2 + 1.96se(\beta_2))$.

We used Akaike Information Criterion (AIC) to assess model performance. Data management, statistical analyses, and maps were conducted using Stata/SE 15.1 and R versions 1.1.419 and 4.0.0.

Results

Annual completeness, trends, and spot-checking. The annual completeness values for each influenza outcome in each country and year of the 15-year study period are compiled in Supplementary Table S4. Figures 1 and 2 show the completeness values for influenza outcomes along with the trend line for average completeness across all 29 countries presented as a heatmap and a line-plot, respectively. In each country, completeness for tests, positives, influenza A positives, and influenza B positives are almost identical (completeness for positives shown in Fig. 1a). In 2005, these 4 outcomes are nearly 100% complete for nine countries (Argentina, Brazil, Chile, Colombia, Dominican Republic, Mexico, Paraguay, Peru, and the United States). Since the 2009 pandemic, 19 countries reached > 95% completeness with further improvements by 2019 when 24 countries reached > 95% completeness. This annual progression in influenza outcome surveillance illustrates the maturity of FluNet over time.

Jamaica, Paraguay, and Mexico were the first countries with available records starting in 2008 for both influenza A(H1N1)pdm09 and A(H5) (Fig. 1b,c). For A(H1N1)pdm09, completeness across the region reached ~ 70% by 2010 and slowly grew to ~ 80% by 2019. Some countries, including Uruguay, Ecuador and Nicaragua, show a reduction in completeness for A(H1N1)pdm09 after 2014. Some countries such as Suriname, Haiti, and Barbados did not offer surveillance data for A(H1N1)pdm09 until 2015. For influenza A(H5), completeness across countries almost reached 50% in 2010, then declined to 0% by 2016 and has not been reported by any country

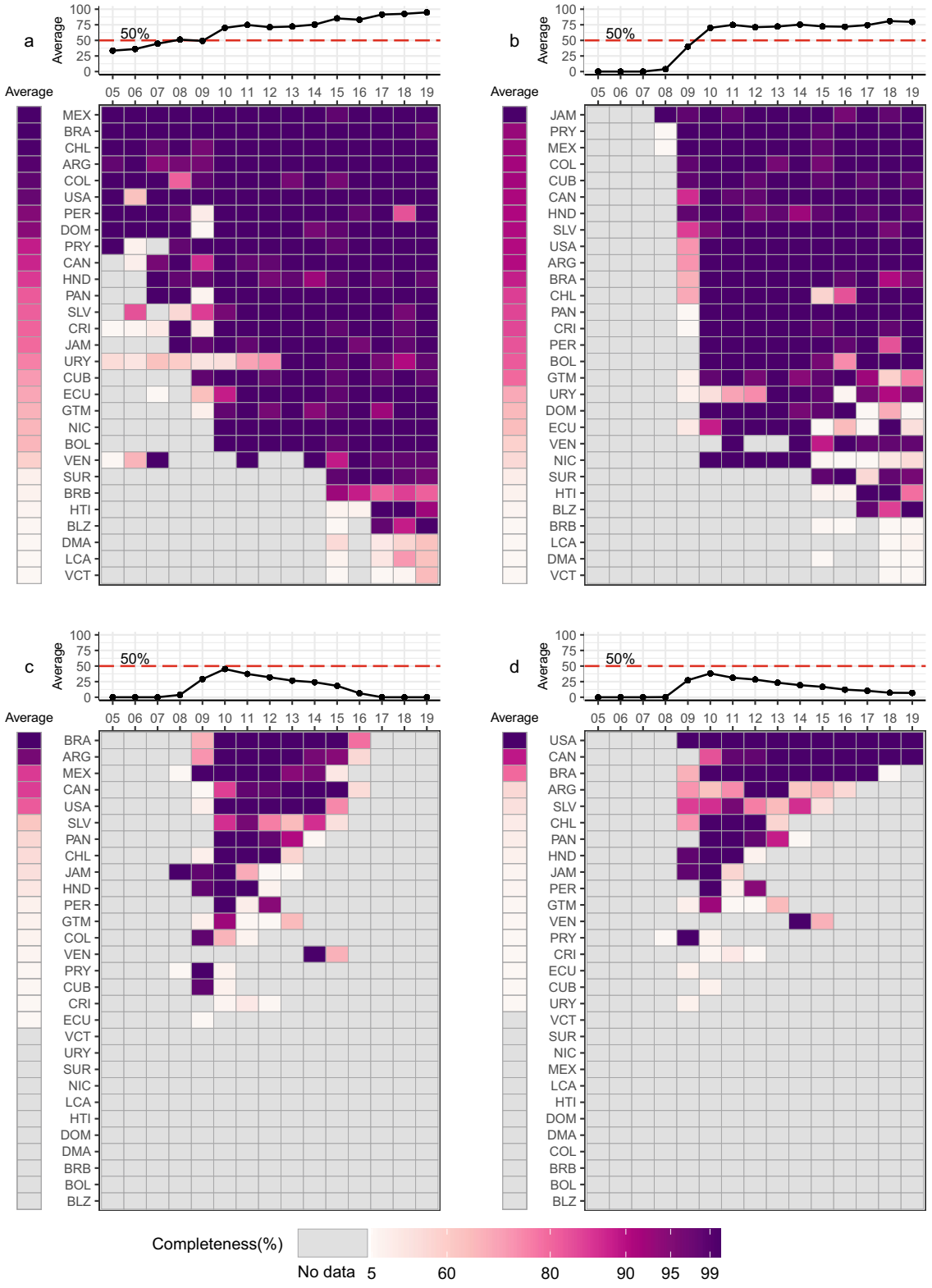


Figure 1. Multi-panel plots of annual completeness of (**a**) positives, (**b**) A(H1N1)pdm09, (**c**) A(H5), and (**d**) specimens for 29 Pan American countries from 2005 through 2019. The top panel provides a line plot of the average completeness across all countries with a dashed red line indicating 50% completeness. The bottom panel provides a heatmap of completeness with grey color indicating no data, white color indicating near 0% completeness, and purple color indicating near 100% completeness. Countries are listed in descending order by corrected average completeness using three letter country abbreviations.

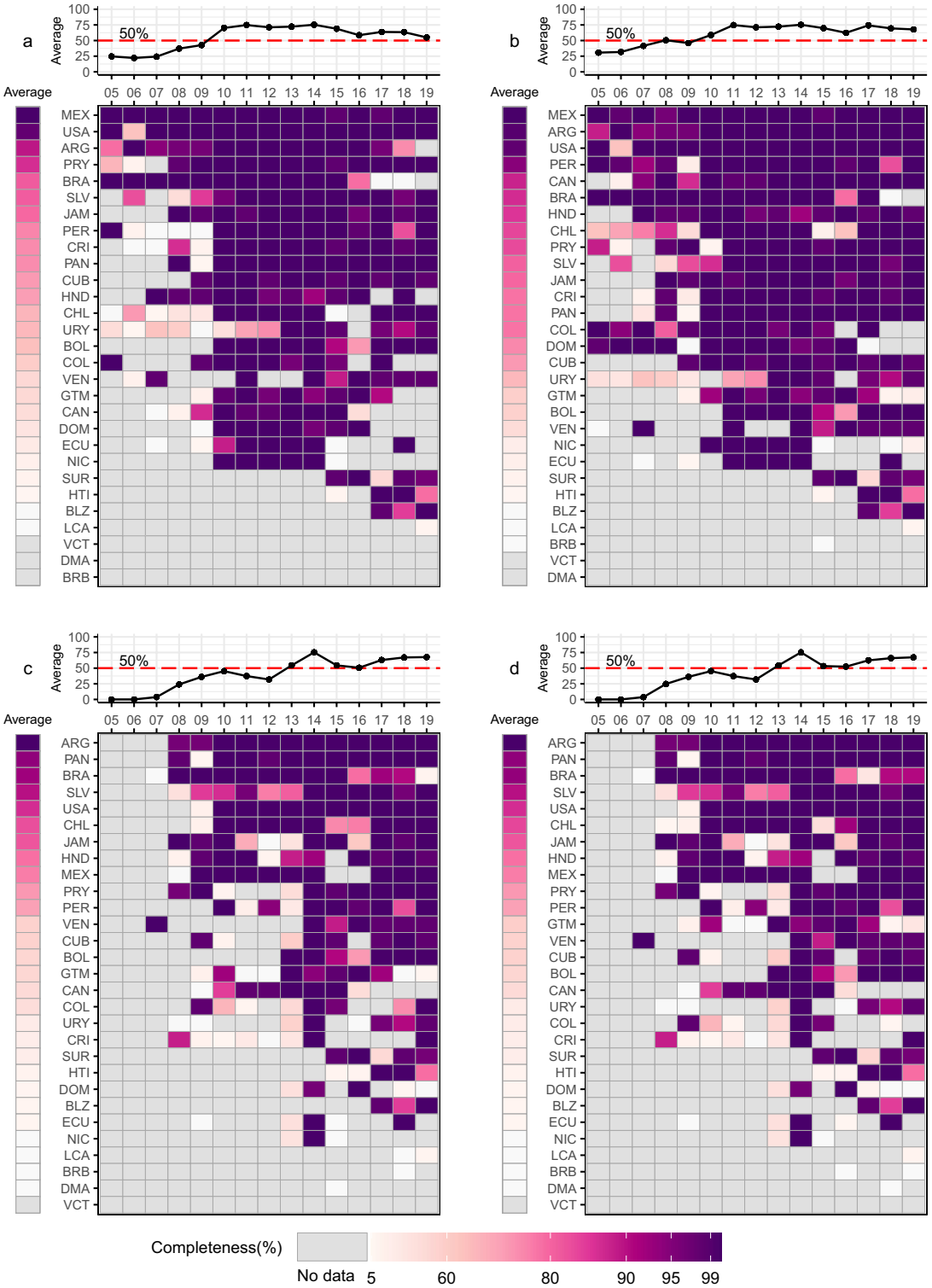


Figure 2. Multi-panel plots of annual completeness of (**a**) A(H1), (**b**) A(Unsubtyped), (**c**) B(Yamataga), and (**d**) B(Victoria) for 29 Pan American countries from 2005 through 2019. The top panel provides a line plot of the average completeness across all countries with a dashed red line indicating 50% completeness. The bottom panel provides a heatmap of completeness with grey color indicating no data, white color indicating near 0% completeness, and purple color indicating near 100% completeness. Countries are listed in descending order by corrected average completeness using three letter country abbreviations.

since. A similar trajectory was seen for specimens though this testing outcome continues to be reported by the United States and Canada as of 2019 (Fig. 1d).

The completeness of influenza A(H1) for the region grew from 43 to 70% between 2009 and 2011 and decreased gradually from 75% in 2014 to 56% as of 2019 (Fig. 2a). The completeness of influenza A(Unsubtyped) increased briefly in 2008 just prior to the A(H1N1)pdm09 pandemic. In 2009, the average completeness across countries increased from 46 to 75% completeness by 2011; it began to decline in 2014, surging back to ~ 70% completeness in 2017 but gradually declining again to 68% completeness as of 2019 (Fig. 2b).

Influenza B(Yamataga) and B(Victoria) subtypes have showed increased trends in completeness since 2012 (Fig. 2c,d). Both subtypes increased in completeness from 2007 to 2010 however the average completeness across countries did not exceed 50% for either subtype. After a brief decline from 2010 to 2011, the average completeness grew for both subtypes from 32% in 2012 to 75% in 2014. While declining from 2014 to 2016, completeness for these influenza B subtypes continuously increased thereafter and reached an average of ~ 67% across the region as of 2019.

In addition to temporal trends, we detected anomalies in annual completeness for influenza subtypes. For example, Fig. 1a showed that the United States, despite having 100% completeness in all other years, had only 63.5% completeness in 2006. During this year, we found that records for total positives are missing from Week 21 (22 May) to Week 49 (10 December). Yet, the United States Centers for Disease Control and Prevention (CDC) reported influenza records during these missing weeks[30]. Though cases are near zero, the national surveillance system does collect data on influenza positives that were not reported in FluNet.

Missing reports for influenza positives in 2018 from Week 30 (23 July) to Week 38 (23 September) in Peru provided another example of using annual completeness for spot-checking data quality (Fig. 1a). Reports from the Pan American Health Organization (PAHO) suggest that Peru reported a surge in influenza A(H1N1)pdm09 and SARI activity during these weeks[31–33]. Despite increased case counts, influenza activity dipped below the alert threshold with pneumonia cases increasing for infants < 5 years of age. Like in the United States, PAHO reported case information on influenza A positives, influenza B positives, and subtypes including A(H1N1)pdm09 and A(Unsubtyped) during these weeks[33] though no data is reported within FluNet.

We also used annual completeness to identify patterns across variables and study years for specific countries. For example, while a surveillance system existed in Venezuela beginning in 2005, annual completeness varied greatly from 2005 to 2019 (Supplementary Table S5). Though surveillance data was reported for 2005–2007, completeness dropped to 0% for all influenza variables for 2008–2010 during the known rise of the A(H1N1)pdm09 pandemic. While 100% completeness was achieved for nearly all influenza outcomes and subtypes in 2011, completeness again dropped to 0% in 2012 and 2013. Since 2014, however, Venezuela maintained > 75% completeness for 5 of 6 influenza outcomes and 7 of 8 influenza subtypes. This fluctuation in annual completeness suggested that attributes related to the surveillance system or factors influencing surveillance performance such as economic stability and health expenditure could be influencing completeness.

Overall completeness ranking and economic and health expenditure indicators. The overall and average completeness values for six influenza outcomes for each country are compiled in Table 3 (all outcomes are reported in Supplementary Table S6). A map of average overall completeness is shown in Fig. 3. The overall completeness was > 80% for 4 countries (Argentina, Brazil, Mexico, United States) and > 70% for an additional 6 countries (Chile, Peru, El Salvador, Paraguay, Honduras, Panama). Completeness for tests, positives, influenza A positives, and influenza B positives were nearly identical for all countries except Brazil, Peru, Honduras, Jamaica, Costa Rica, Venezuela, and Ecuador where test completeness was slightly less than positives completeness. Eight countries (Argentina, Brazil, Mexico, United States, Chile, Peru, Colombia, and the Dominican Republic) had > 90% completeness for tests and total, influenza A, and influenza B positives. The average completeness values for influenza A(H1N1)pdm09 and A(H5) across all countries were 66% and 25%, respectively. Seven countries (Suriname, Haiti, Belize, Barbados, St. Lucia, Dominica, and St. Vincent & Grenadines) had < 40% completeness for all influenza outcomes, subtypes, and overall completeness. Figure 4 demonstrates that high and low overall completeness was likely in countries of mid-range DHEPC and OOPHE%. Given the similarity in completeness for multiple outcomes, we selected tests, positives, A(H1N1)pdm09, and overall completeness for further regression analyses.

Completeness, economic and health expenditure indicators, and surveillance system attributes. Trends in country-specific completeness for tests, positives, A(H1N1)pdm09, and overall and GNIPC, DHEPC, and OOPHE% are shown in Figs. 5 and 6, respectively. The decadal change of economic indicators for each country and averaged across countries (with standard deviation estimates) is provided in Supplementary Table S7. GNIPC and DHEPC almost doubled (2.02 ± 0.67 vs 2.19 ± 0.77, respectively) between 2005 and 2015; and OOPHE% declined by 16 ± 18%.

Table 4 shows the annual change in completeness for four outcome variables estimated from unadjusted (Model 1) and adjusted (Model 2) mixed effects models. All variables exhibited a strong positive trend with an annual increase in completeness from 4.2 to 6.3% on average. Improvements in completeness were most prominent for influenza A(H1N1)pdm09 showing a strong positive relationship with GNIPC. DHEPC was the strongest predictor of completeness across all influenza outcome variables. With the doubling in DHEPC achieved on average in the region, all four variables exhibited an improvement in completeness up to 9.4%. A projected 10% change in OOPHE% had no association with changes in completeness.

The adjusted models also indicated that the high numbers of NICS and reporting facilities were consistently associated with an increase in completeness. For every additional NIC, the completeness for tests, positives, and overall completeness increased by ~ 18–24% irrespective of the economic or expenditure indicator assessed.

Country	Percent completeness for influenza outcomes[a]							Indicators[b]		
	Overall	Tests	Positives	Flu A	Flu B	A(H1N1)	Spec	GNIPC	DHEPC	OOPHE%
All countries	55.59	67.83	68.35	68.35	68.35	65.55	18.44	9.37	0.68	33.25
Completeness > 75%										
Argentina (ARG)	91.27	98.98	98.98	98.98	98.98	89.47	49.46	9.94	1.00	21.03
Brazil (BRA)	90.62	98.46	99.87	99.87	99.87	87.71	72.97	8.99	0.51	39.23
United States (USA)	86.91	97.56	97.56	97.56	97.56	89.47	91.67	52.67	4.67	12.37
Mexico (MEX)	85.83	99.87	99.87	99.87	99.87	91.67	0.00	9.39	0.43	44.72
Chile (CHL)	80.85	99.62	99.62	99.62	99.62	84.09	35.78	11.82	0.80	36.17
Peru (PER)	77.15	94.44	94.56	94.56	94.56	81.73	19.07	4.96	0.27	36.86
Panama (PAN)	75.03	81.64	81.64	81.64	81.64	83.49	33.33	9.11	0.75	30.02
Completeness > 50%										
Honduras (HND)	74.05	85.00	85.13	85.13	85.13	89.91	27.25	1.83	0.14	48.25
Paraguay (PRY)	73.46	88.46	88.46	88.46	88.46	92.15	11.22	4.21	0.24	43.76
Jamaica (JAM)	71.56	72.69	79.36	79.36	79.36	99.20	21.16	4.57	0.25	24.55
Colombia (COL)	71.07	98.08	98.08	98.08	98.08	90.87	0.00	5.83	0.45	20.63
Canada (CAN)	70.82	87.58	87.58	87.58	87.58	90.25	81.57	45.17	3.02	14.99
El Salvador (SLV)	70.69	80.92	80.92	80.92	80.92	89.77	45.46	3.12	0.30	32.70
Costa Rica (CRI)	62.17	78.28	80.33	80.33	80.33	83.17	7.05	8.29	0.72	26.72
Cuba (CUB)	61.92	72.70	72.70	72.70	72.70	90.87	2.56	5.87	1.85	10.90
Dominican Republic (DOM)	59.51	94.08	94.08	94.08	94.08	65.39	0.00	5.59	0.27	45.34
Guatemala (GTM)	57.88	67.52	67.52	67.52	67.52	78.96	16.93	3.08	0.14	58.77
Uruguay (URY)	54.69	76.48	76.48	76.48	76.48	69.18	2.52	11.51	0.93	20.32
Bolivia (BOL)	50.79	66.54	66.54	66.54	66.54	80.94	0.00	2.17	0.19	30.14
Completeness < 50%										
Venezuela (VEN)	49.63	55.27	57.71	57.71	57.71	56.91	13.99	10.01	0.32	38.66
Ecuador (ECU)	46.99	68.17	70.30	70.30	70.30	64.34	2.67	4.82	0.33	48.84
Nicaragua (NIC)	42.14	66.67	66.67	66.67	66.67	52.85	0.00	1.63	0.16	40.52
Suriname (SUR)	25.43	32.82	32.82	32.82	32.82	37.18	0.00	6.71	0.37	21.37
Haiti (HTI)	19.82	22.92	22.92	22.92	22.92	27.52	0.00	0.69	0.02	37.14
Barbados (BRB)	18.78	28.47	28.47	28.47	28.47	4.30	0.00	15.23	0.60	39.53
Belize (BLZ)	15.80	19.48	19.48	19.48	19.48	23.56	0.00	4.09	0.27	26.38
St. Lucia (LCA)	13.47	13.81	13.81	13.81	13.81	2.72	0.00	7.71	0.24	56.06
St. Vincent & the Grenadines (VCT)	7.51	6.28	6.28	6.28	6.28	1.28	0.00	6.27	0.26	21.68
Dominica (DMA)	6.17	14.29	14.29	14.29	14.29	1.91	0.00	6.53	0.32	36.65

Table 3. The overall and average completeness of seven influenza variables and three economic and health expenditure indicators for 2005–2019 time period for 29 Pan American countries and all countries combined. Countries are listed in descending order by overall completeness. [a]Outcomes: total specimens processed (*Test*), total positives (*Pos*), influenza A positives (*Flu A*), influenza B positives (*Flu B*), and total specimens collected (*Spec.*). For tests, total positives, influenza A and B positives, average completeness was calculated from 2005 to 2019. Subtypes of influenza positives: A(H1N1)pdm09 *(A(H1N1)))*. For A(H1N1)pdm09 and specimens collected, average completeness was calculated from 2008 to 2019. *Overall* provides the average completeness across all 14 influenza variables while *All Countries* provides the average completeness for each variable across all 29 countries. [b]Reported values are the average of each indicator from 2005 to 2019. Units: GNIPC and DHEPC are provided in 1000 s USD. OOPHE% is reported as a percentage of current governmental health expenditure.

Similarly, every additional NIC was associated with a 15–20% increase in influenza A(H1N1)pdm09 completeness. A doubling in the number of in-country reporting facilities was associated with a 1.85–5.00% increase in completeness across all influenza outcomes and economic indicators. While some countries use multiple surveillance systems or followed numerous reporting quotas, timeframes, and case definitions, on average there was no difference in completeness values across surveillance system attributes.

Discussion

In this study, we demonstrated the progress made by FluNet over the last decade towards achieving high overall completeness in publicly available influenza surveillance records. The proposed metric shows that influenza surveillance reporting has improved especially after the A(H1N1) 2009 pandemic, highlighting the effort by national systems and the WHO. This metric further demonstrated the substantial increase in completeness after the 2013 WHO guidelines for influenza surveillance[5]. These improvements were practically identical for tests,

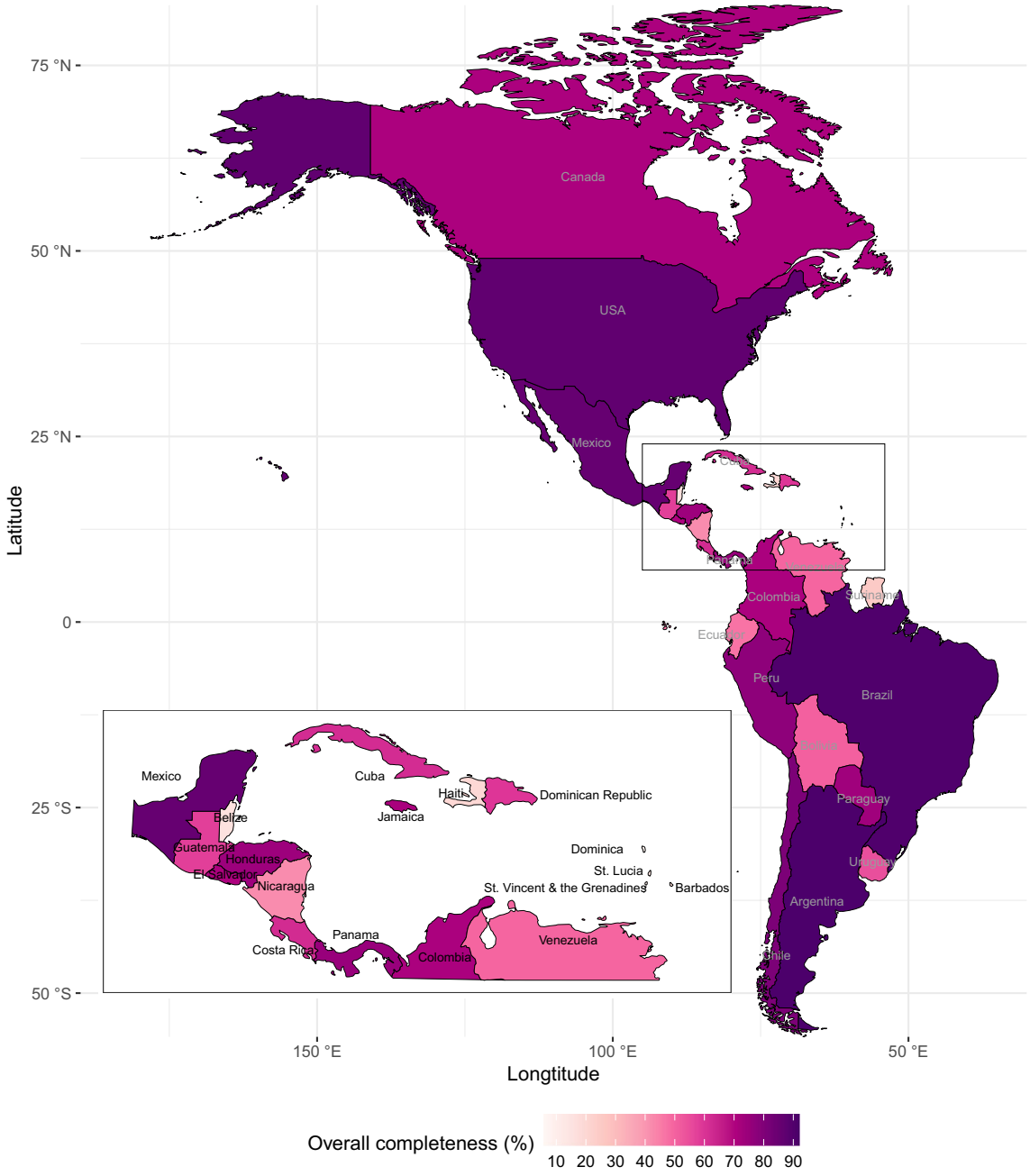


Figure 3. A map of average overall completeness for 29 Pan American countries over the 782-week time series starting from Week 1 (03 January) 2005 to Week 52 (29 December) 2019. A white color indicates near 0% completeness while a purple color indicates near 100% completeness.

total positives, influenza A positives, and influenza B positives indicating the systematic approach taken in their reporting. As of 2019, 24 of 29 Pan-American countries were operating at > 95% of completeness for these key outcomes, though efforts are still needed to ensure consistent surveillance for other indicators. National reporting infrastructures continued to increase in their richness and heterogeneity, which indicates wider in-country surveillance coverage[14]. Annual completeness estimates continue to improve over time by ~ 5% annually and the rates of improvement are similar among countries with different national surveillance systems attributes. Yet, countries with higher numbers of NICs, more reporting facilities, and greater health expenditures showed the best performance. The proposed completeness metric provides essential information on data availability and suitability for statistical analysis and modeling and can improve the utility of existing data for all users.

Our metric is based on the effective time series length and can be computed for any pre-specified time periods. The metric ultimately reflects the fraction of weeks when surveillance reports are missing. We define 'missing' as a week for which case counts are undefined or not reported. This is not to be mistaken with zero reported observations, or the absence of counts for a specific case definition. To further the utility of the completeness

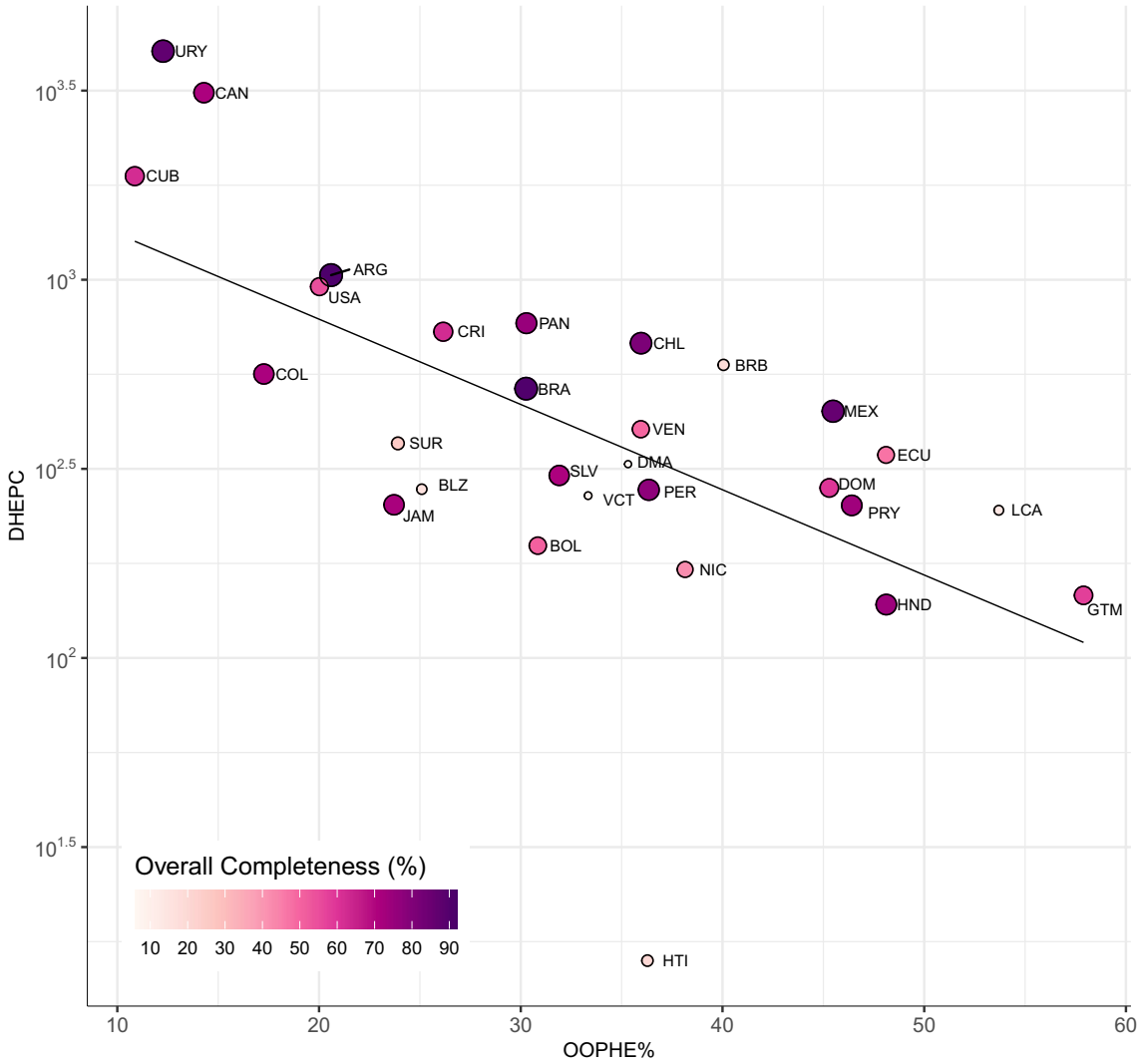


Figure 4. Relationship between overall completeness, domestic general government health expenditure per capita (DHEPC), and percent out-of-pocket health expenditure (OOPHE%) for 29 Pan American countries over the 782-week time series starting from Week 1 (03 January) 2005 to Week 52 (29 December) 2019. DHEPC is reported in current international USD. OOPHE% is reported as the percentage of current government expenditure. A smaller, white-colored marker indicates near 0% completeness while a larger, dark purple-colored marker indicates near 100% completeness.

metric, we recommend supplementing publicly disseminated reports with metadata on *why* data are missing, *what* missing data means, and *how much* missing data are reported.

Although the metric is simple to implement and interpret, the metric could not take into consideration patterns of missingness. Missing records could be distributed randomly or systematically throughout the study period when the data displays structural missingness with records lost in chunks or more frequently during specific times of the year. However, low completeness estimates call for attention to further investigate the pattern of missingness. This was demonstrated above in examples with the United States, Peru, and Venezuela where we identified periods of missing weeks and years using our metric. By knowing the temporal distribution of missing records some correction can be made during the analysis stage, for example by using completeness as an additional variable to reduce the weight of years with incomplete records. Closer inspection into patterns of missingness can also be used for verifying, inspecting, or updating public records within a data source prior to analysis.

The metric provides greater clarity on how a country's surveillance system quality changes over time and helps identify anomalies in surveillance reporting. If an unusual drop in completeness is noted yet the national surveillance records exist for the time period in question, such discrepancies can be curated in a timely manner. Furthermore, such discrepancy calls into question whether external data users could help data curating organizations with checking the fidelity and accuracy of the data they use and their assumptions for handling missing data.

By examining annual completeness estimates, users could determine the study interval with reliable information. In the extracted records from 2005 to 2019, each country-outcome-specific time series had varying numbers and patterns of weeks with missing information. While a longer historical reference period indicates greater

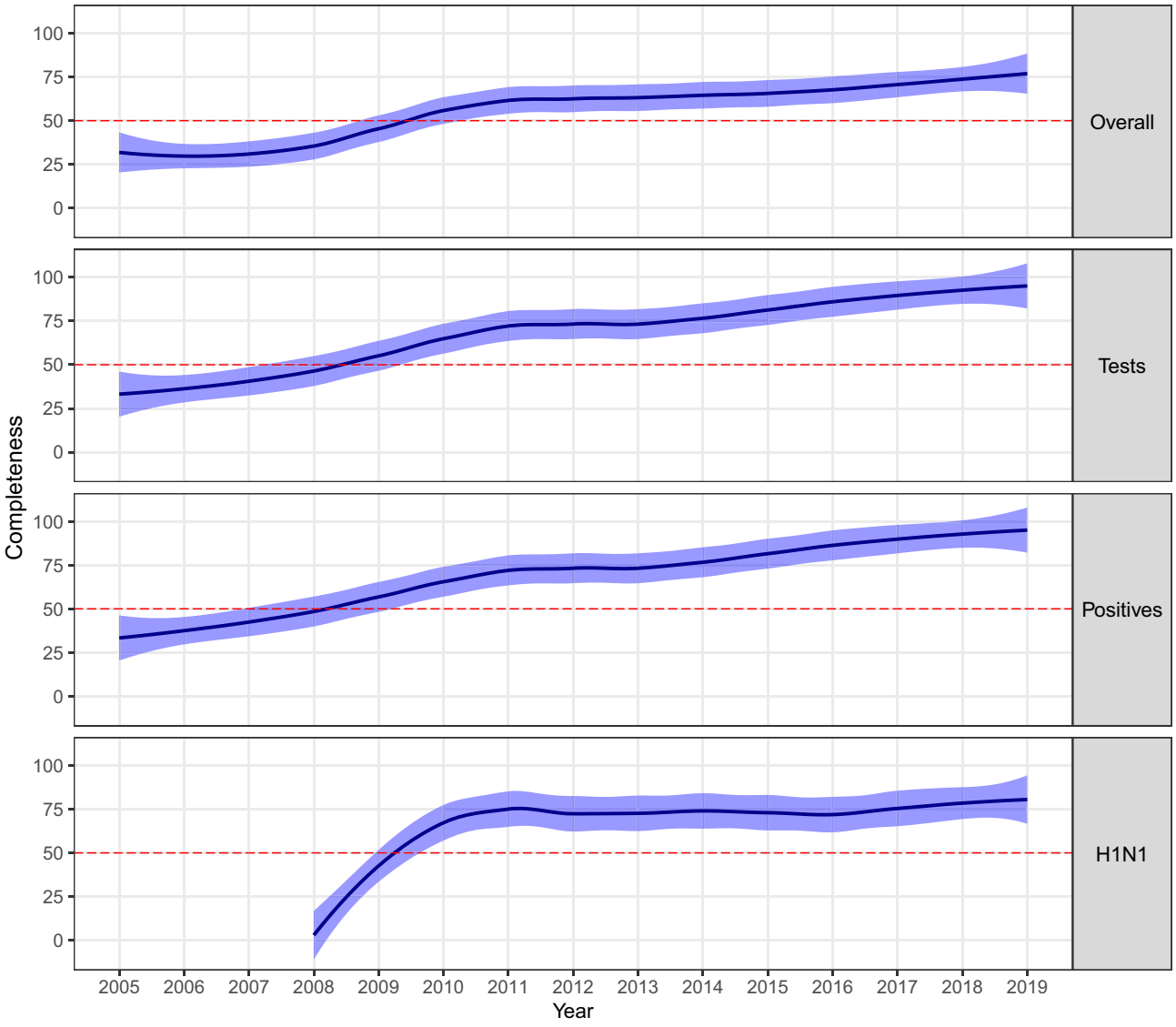


Figure 5. Annual trends presented as loess-smoothed curves along with their confidence intervals in country-specific completeness for four influenza outcome variables (overall, tests, positives, and A(H1N1)pdm09 completeness) for 29 Pan American countries over the 782-week time series starting from Week 1 (03 January) 2005 to Week 52 (29 December) 2019. Horizontal dashed red lines indicate 50% completeness.

statistical power in estimating disease trends, some outcomes are collected over limited time frames. The length of these time series is influenced by the country of interest, outcome of interest, and date of data extraction. For example, positives of A(H1N1)pdm09 showed consistently high completeness across most countries from 2009 to 2019. Yet, for some countries, records were available for a fraction of that period. Based on our findings, we encourage data users to clearly specify the start and end date of their time series, the completeness of that time series, and the date of data extraction.

In recent years, the WHO has taken numerous efforts to evaluate the economic burden associated with seasonal influenza, especially in lower- and middle-income countries[34–36]. These efforts, including a published *Manual for estimating the economic burden of seasonal influenza* in 2016, aim to demonstrate the value of population surveillance by calculating the direct medical, direct non-medical, and indirect costs of influenza illness[34,35]. Studies applying methodologies outlined in this manual confirm that increased country income and health expenditure is associated with increased immunization policies, vaccination coverage, health infrastructure, and surveillance coverage[35,36]. The WHO 2016 manual further recognizes that data validity and completeness can influence assessments of economic burdens related to national income, domestic health expenditure, and out-of-pocket health expenditure[34].

Our study faced several challenges related to data availability and accessibility. First, the FluNet data portal requires country time series to be downloaded individually and merged using a scripted pipeline. This process is both inefficient and prone to human error during data alignment and compilation. While our data extraction and merging code overcomes this challenge, we encourage FluNet curators to allow for multi-country data downloads and improve data accessibility.

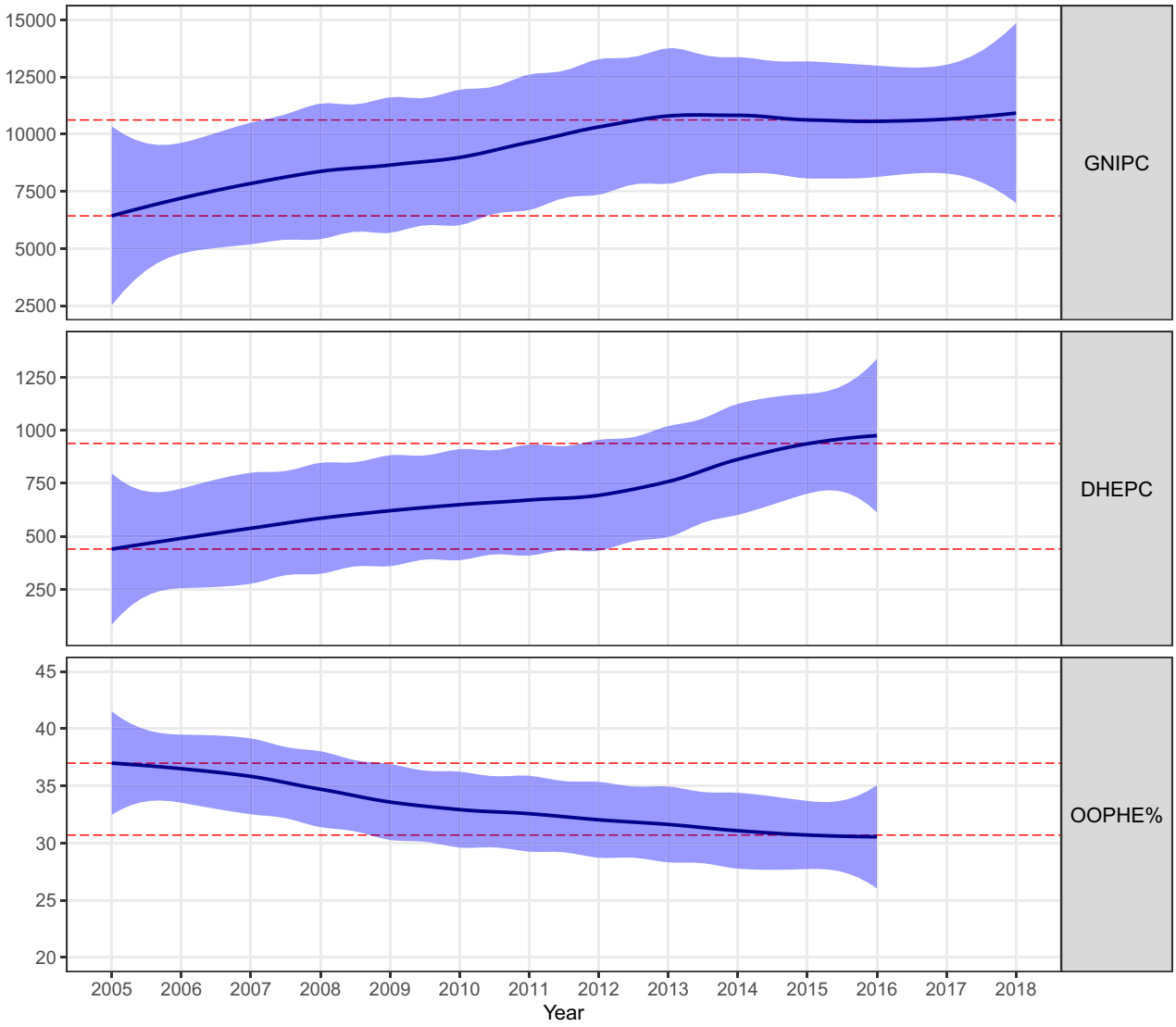


Figure 6. Annual trends presented as loess-smoothed curves along with their confidence intervals for three national economic and health expenditure indicators for 29 Pan American countries for available years between 2005 and 2018. Horizontal lines indicate regional average values for 2005 and 2015. GNIPC was reported in purchasing power parity (PPP) constant 2011 international US dollars (USD). DHEPC was reported in current international USD. OOPHE% is reported as the percentage of current government expenditure.

Next, we examined only the most recent records starting in 2005. Our initial intention was to use all available data from 1995 to 2019. We completed two attempts to extract records: first on 15 December 2019 and second on 26 April 2020 to retrieve data for the final weeks of 2019. Between extraction dates, however, available FluNet data changed dramatically: data originally available from Week 1 1995 to Week 52 2004 were reported as missing at the time of second extraction. No justification is provided regarding this change. Thus, we encourage FluNet curators to provide information on when, by how much, and why retrospective records are modified to ensure accuracy and validity of analyses performed with the open source records.

Finally, we recognize that examined national economic indicators, such as DHEPC and OOPHE% describe all national health expenditures and the fraction of health expenditures dedicated to influenza may vary dramatically each year. During the A(H1N1)pdm09 pandemic, health expenditures may have been quite high for influenza vaccinations and testing. Moving forward, the onset of the coronavirus disease 2019 (COVID-19) pandemic may have decreased this fraction of health expenditures for influenza monitoring much lower. A better tracking of influenza-related expenditures at the national and global levels is needed to confirm or refute our findings.

In prior works, we have developed tools and explored the seasonality of influenza and other infections. In a study of pandemic seasonal epidemics in Wisconsin from 1967 to 2004, we found that seasonal peak timing varied greatly and while viral evolution played an important role, the variability of seasonality estimates was also influenced by the data granularity[23]. The estimates (and their confidence intervals) of seasonal peak timing and intensity could be in part influenced by data aggregation and completeness of surveillance data and thus affect our understanding of deviations in influenza seasonality[21]. Our mini-review of mathematical modeling

Outcome	Unadjusted estimates				Adjusted estimates[a]			
	Effect size	LCI	UCI	*p* value	Effect size	LCI	UCI	*p* value
Estimated annual change in completeness								
Overall	3.948	3.493	4.403	< 0.001	4.251	3.811	4.690	< 0.001
Tests	5.040	4.517	5.563	< 0.001	5.346	4.833	5.858	< 0.001
Positives	4.930	4.408	5.452	< 0.001	5.229	4.717	5.741	< 0.001
A(H1N1)pdm09	5.935	5.174	6.696	< 0.001	6.307	5.541	7.073	< 0.001
Estimated effect associated with doubling in gross national income per capita								
Overall	3.667	− 0.763	8.097	0.105	0.494	− 3.088	4.077	0.787
Tests	1.321	− 3.741	6.383	0.609	− 1.026	− 5.251	3.199	0.634
Positives	1.502	− 3.553	6.557	0.560	− 0.809	− 5.047	3.428	0.708
A(H1N1)pdm09	15.858	8.568	23.149	< 0.001	9.033	2.400	15.666	0.008
Estimated effect associated with doubling in domestic health expenditure per capita								
Overall	12.489	8.050	16.928	< 0.001	6.955	2.978	10.932	0.001
Tests	14.154	9.070	19.239	< 0.001	8.713	3.954	13.472	< 0.001
Positives	14.670	9.575	19.765	< 0.001	9.370	4.567	14.172	< 0.001
A(H1N1)pdm09	12.921	6.742	19.099	< 0.001	7.261	1.258	13.263	0.018
Estimated effect associated with 10% change in out-of-pocket health expenditure								
Overall	− 1.439	− 4.945	2.068	0.421	− 0.061	− 3.217	3.095	0.970
Tests	− 1.880	− 5.919	2.159	0.362	− 0.264	− 4.012	3.484	0.890
Positives	− 0.908	− 4.939	3.123	0.659	0.491	− 3.249	4.231	0.797
A(H1N1)pdm09	− 2.310	− 7.939	3.320	0.421	− 0.522	− 5.798	4.755	0.846

Table 4. Estimated annual change in completeness of four influenza outcome variables and three economic and health expenditure indicators in 29 Pan American countries over the 782-week time series starting from Week 1 (03 January) 2005 to Week 52 (29 December) 2019. The effect size estimation was calculated for a doubling in per capita indicator estimates and a 10% increase in out-of-pocket health expenditure. *LCI* and *UCI* refer to the lower and upper bounds of the 95% confidence interval. [a]Models were adjusted for case definition type, adherence to WHO definition, surveillance strategy, reporting quota, reporting timeframe, number of NICs and reporting facilities.

techniques for influenza transmission highlighted that variations in theories governing seasonal dynamics could also be attributed to data availability limitations[22].

Examining disease trends and seasonal epidemic signatures allows for greater understanding of influenza transmission and developing preparedness strategies at the local, national, and regional levels[2,18–20,36]. The proposed metric of completeness is essential in estimating the statistical power to detect disease trends and temporal changes by providing the effective length of disease surveillance time series data. Further work is needed to understand how completeness influences the reliability of modeling results. The use of the proposed metric will also allow for better assessment of the quality of historical data for tracking disease trends. The continuously updated surveillance records and the ensemble of disease outcomes allows for adaptive modeling to create real-time forecasts and detection of local events with high spatiotemporal granularity[2].

Conclusion

This study provided the first attempt at quantifying the percentage of available data usable for closer examination of disease trends or seasonality analyses. As more surveillance data becomes available for public use, indicators such as completeness should be applied to ensure quality, accuracy, and reliability of trend estimations. The proposed metric of completeness is vital to any secondary time series data analysis where the data user did not curate the data source. This metric can also be estimated and reported by external data users to ensure reliability and improve understanding of data structure. This next step in data sharing can help external data users detect outbreak signatures more accurately and reliably as well as improve health policies, programming, and recommendations. Combined with access to already developed WHO M&E indicators, the completeness metric for publicly disseminated data will strengthen disease surveillance systems.

Received: 14 September 2020; Accepted: 16 December 2020
Published online: 12 January 2021

References

1. World Health Organization (WHO). *Communicable Disease Surveillance and Response Systems: A Guide to Planning (No. WHO/CDS/EPR/LYO/2006.1)*. World Health Organization (2020).
2. Fefferman, N. & Naumova, E. Innovation in observation: a vision for early outbreak detection. *Emerg. Health Threats* **3**, 7103 (2010).

3. Polansky, L. S., Outin-Blenman, S. & Moen, A. C. Improved global capacity for influenza surveillance. *Emerg. Infect. Dis.* **22**, 993–1001 (2016).
4. Johnson, L. E. A. *et al.* Capacity building in national influenza laboratories—use of laboratory assessments to drive progress. *BMC Infect. Dis.* **15**, 501 (2015).
5. World Health Organization (WHO). *Global Influenza Surveillance and Response System*. World Health Organization. https://www.who.int/influenza/gisrs_laboratory/en/ (2020).
6. World Health Organization. *Global Epidemiological Surveillance Standards for Influenza*. World Health Organization (2013).
7. Monto, A. S. Reflections on the global influenza surveillance and response system (GISRS) at 65 years: an expanding framework for influenza detection, prevention and control. *Influenza Other Resp.* **12**, 10–12 (2018).
8. Stöhr, K. The global agenda on influenza surveillance and control. *Vaccine* **21**, 1744–1748 (2003).
9. Brammer, L., Budd, A. & Cox, N. Seasonal and pandemic influenza surveillance considerations for constructing multicomponent systems. *Influenza Other Resp.* **3**, 51–58 (2009).
10. Flahault, A. *et al.* FluNet as a tool for global monitoring of influenza on the Web. *JAMA* **280**, 1330–1332 (1998).
11. World Health Organization (WHO). *Influenza: FluNet*. World Health Organization. https://www.who.int/influenza/gisrs_laboratory/flunet/en/ (2020).
12. World Health Organization (WHO). *Global Influenza Surveillance and Response System (GISRS)*. World Health Organization. https://www.who.int/influenza/gisrs_laboratory/en/ (2019).
13. Flu Informed Decisions (Flu ID). *Pilot Phase—Global Influenza Epidemiological Data Collection Tool*. World Health Organization. (2010).
14. Uyeki, T. M. *et al.* Clinical practice guidelines by the Infectious Diseases Society of America: 2018 update on diagnosis, treatment, chemoprophylaxis, and institutional outbreak management of seasonal influenza. *Clin. Infect. Dis.* **68**, e1–e47 (2019).
15. de Francisco, N., Donadel, M., Jit, M. & Hutubessy, R. A systematic review of the social and economic burden of influenza in low- and middle-income countries. *Vaccine* **33**, 6537–6544 (2015).
16. Saunders-Hastings, P. R. & Krewski, D. Reviewing the history of pandemic influenza: understanding patterns of emergence and transmission. *Pathogens* **5**, 66 (2016).
17. Prager, F., Wei, D. & Rose, A. Total economic consequences of an influenza outbreak in the United States. *Risk Anal.* **37**, 4–19 (2017).
18. Caini, S. *et al.* Temporal patterns of influenza A and B in tropical and temperate countries: what are the lessons for influenza vaccination?. *PLoS ONE* **11**, e0152310 (2016).
19. Caini, S. *et al.* Characteristics of seasonal influenza A and B in Latin America: influenza surveillance data from ten countries. *PLoS ONE.* **12**, e0174592 (2017).
20. Wenger, J. B. & Naumova, E. N. Seasonal synchronization of influenza in the United States older adult population. *PLoS ONE* **5**, e10187 (2010).
21. Moorthy, M. *et al.* Deviations in influenza seasonality: odd coincidence or obscure consequence?. *Clin. Microbiol. Infect.* **18**, 955–962 (2012).
22. Lofgren, E., Fefferman, N. H., Naumov, Y. N., Gorski, J. & Naumova, E. N. Influenza seasonality: underlying causes and modeling theories. *J. Virol.* **81**, 5429–5436 (2007).
23. Lofgren, E. T. *et al.* Disproportional effects in populations of concern for pandemic influenza: insights from seasonal epidemics in Wisconsin, 1967–2004. *Influenza Other Resp.* **4**, 205–212 (2010).
24. World Health Organization (WHO). *FluNet*. World Health Organization. https://apps.who.int/flumart/Default?ReportNo=12 (2020).
25. Harrison, J. *RSelenium: R Bindings for 'Selenium WebDriver'*. R package version 1.7.7. https://CRAN.R-project.org/package=RSelenium (2020).
26. Pan American Health Organization (PAHO) & World Health Organization (WHO). *PAHO/WHO: National Influenza Centers in PAHO Member States*. Pan American Health Organization. www.paho.org/hq/index.php?option=com_content&view=article&id=3360:2010-national-influenza-centers-paho-member-states&Itemid=40295&lang=en (2020).
27. European Centre for Disease Prevention and Control/WHO Regional Office for Europe. *Influenza Surveillance Country, Territory and Area Profiles 2019*. World Health Organization. (2019).
28. Pan American Health Organization (PAHO). *Health Services Preparedness for Pandemic Influenza: Facilitator's Manual*. Pan American Health Organization. (2010).
29. The World Bank. *World Development Indicators*. The World Bank. https://datacatalog.worldbank.org/dataset/world-development-indicators (2020).
30. Centers for Disease Control and Prevention (CDC). *Flu Activity & Surveillance*. Centers for Disease Control and Prevention. https://gis.cdc.gov/grasp/fluview/fluportaldashboard.html (2020).
31. Pan American Health Organization (PAHO). *2018 Weekly Influenza Report EW 28*. Pan American Health Organization. (2018).
32. Pan American Health Organization (PAHO). *2018 Weekly Influenza Report EW 37*. Pan American Health Organization. (2018).
33. Pan American Health Organization (PAHO). *Influenza: Influenza Reports by Year*. Pan American Health Organization. https://www.paho.org/hq/index.php?option=com_topics&view=rdmore&cid=4302&item=influenza&type=statistics&Itemid=40753&lang=en (2020).
34. World Health Organization (WHO). *WHO Manual for Estimating the Economic Burden of Seasonal Influenza*. (2016).
35. Chaiyakunapruk, N., Kotirum, S., Newall, A. T., Lambach, P. & Hutubessy, R. C. Rationale and opportunities in estimating the economic burden of seasonal influenza across countries using a standardized WHO tool and manual. *Influenza Other Resp.* **12**, 13–21 (2018).
36. Ortiz, J. R. *et al.* A global review of national influenza immunization policies: analysis of the 2014 WHO/UNICEF Joint Reporting Form on immunization. *Vaccine* **34**, 5400–5405 (2016).

Acknowledgements

This research is based upon work supported in part by the Office of the Director of National Intelligence (ODNI), Intelligence Advanced Research Projects Activity (IARPA), via 2017-17072100002. The views and conclusions contained herein are those of the authors and should not be interpreted as necessarily representing the official policies, either expressed or implied, of ODNI, IARPA, or the U.S. Government. The U.S. Government is authorized to reproduce and distribute reprints for governmental purposes notwithstanding any copyright annotation therein. The research was also in part supported by the United States Department of Agriculture (USDA) National Institute of Food and Agriculture (NIFA) Cooperative State Research, Education, and Extension Service Fellowship, via grant award 2020-38420-30724, and the Tufts University Data Intensive Studies Center (DISC) COVID-19 Seed Grant. Authors would like to acknowledge Aishwarya Venkat for her early collaborations discussing modeling techniques and approaches for analyzing FluNet data.

Author contributions

R.B.S. assisted with the conceptualization, formal analysis, writing and editing. J.G. assisted with the investigation, validation, and original draft preparation. B.Z. assisted with editing and developing data visualizations. M.A.H. assisted with software, data curation, review and editing, and editing data visualizations. E.N.N. assisted with the conceptualization, writing, editing, supervision, project administration, and funding acquisition.

Competing interests

The authors declare no competing interests.

Additional information

Supplementary Information The online version contains supplementary material available at https://doi.org/10.1038/s41598-020-80842-9.

Correspondence and requests for materials should be addressed to E.N.N.

Reprints and permissions information is available at www.nature.com/reprints.

Publisher's note Springer Nature remains neutral with regard to jurisdictional claims in published maps and institutional affiliations.

Open Access This article is licensed under a Creative Commons Attribution 4.0 International License, which permits use, sharing, adaptation, distribution and reproduction in any medium or format, as long as you give appropriate credit to the original author(s) and the source, provide a link to the Creative Commons licence, and indicate if changes were made. The images or other third party material in this article are included in the article's Creative Commons licence, unless indicated otherwise in a credit line to the material. If material is not included in the article's Creative Commons licence and your intended use is not permitted by statutory regulation or exceeds the permitted use, you will need to obtain permission directly from the copyright holder. To view a copy of this licence, visit http://creativecommons.org/licenses/by/4.0/.

© The Author(s) 2021

scientific reports

Check for updates

OPEN

Seasonal synchronization of foodborne outbreaks in the United States, 1996–2017

Ryan B. Simpson, Bingjie Zhou & Elena N. Naumova✉

Modern food systems represent complex dynamic networks vulnerable to foodborne infectious outbreaks difficult to track and control. Seasonal co-occurrences (alignment of seasonal peaks) and synchronization (similarity of seasonal patterns) of infections are noted, yet rarely explored due to their complexity and methodological limitations. We proposed a systematic approach to evaluate the co-occurrence of seasonal peaks using a combination of L-moments, seasonality characteristics such as the timing (phase) and intensity (amplitude) of peaks, and three metrics of serial, phase-phase, and phase-amplitude synchronization. We used public records on counts of nine foodborne infections abstracted from CDC's FoodNet Fast online platform for the US and ten representative states from 1996 to 2017 (264 months). Based on annualized and trend-adjusted Negative Binomial Harmonic Regression (NBHR) models augmented with the δ-method, we determined that seasonal peaks of *Campylobacter*, *Salmonella*, and Shiga toxin-producing *Escherichia Coli* (STEC) were tightly clustered in late-July at the national and state levels. Phase-phase synchronization was observed between *Cryptosporidium* and *Shigella*, *Listeria*, and *Salmonella* ($\rho = 0.51, 0.51, 0.46$; $p < 0.04$). Later peak timing of STEC was associated with greater amplitude nationally ($\rho = 0.50$, $p = 0.02$) indicating phase-amplitude synchronization. Understanding of disease seasonal synchronization is essential for developing reliable outbreak forecasts and informing stakeholders on mitigation and preventive measures.

Globalization of the food supply adds to the challenge of tracking sources of food contamination. According to the Centers for Disease Control and Prevention (CDC), 1 in 6 Americans (or 48 million) become sick from a foodborne infection annually with 3000 deaths[1]. These illnesses often span multiple states, cause extensive revenue losses for food distributors, and result in millions of pounds of recalled foods[2–7]. The US Foodborne Disease Active Surveillance Network (FoodNet), a collaboration among the CDC, state health departments, U.S. Department of Agriculture's Food Safety and Inspection Service (USDA–FSIS), and the Food and Drug Administration (FDA), monitors the nine most prominent foodborne and waterborne illnesses accounting for over 90% of the 9.4 million cases occurring annually[8]. Established in 1996, this surveillance system maintains records for *Campylobacter, Listeria, Salmonella,* Shiga toxin-producing *E. coli* (STEC)*, Shigella, Vibrio*, and *Yersinia enterocolitica*. *Cryptosporidium* and *Cyclospora* were added in 1997; and in 2000, STEC non-O157 was added to the list of pathogens commonly transmitted through food[8].

In the United States, seasonal increases in cases for *Campylobacter*, STEC, *Listeria*, and *Salmonella* during summer months have been demonstrated using FoodNet records[9–11]. The consistency of foodborne infection seasonality with co-occurring seasonal peaks has inspired the creation of "infection calendars"[12–16]. Better understanding of infection seasonality allows for the identification of environmental and manmade drivers of seasonal infection to improve control measures[15,17–19]. Standardized methods for characterizing seasonality features are needed for effective tracking of how seasonal profiles change over time and across large geographic zones[20–22]. These methods can demonstrate if and how nation-wide policy implementation might delay the onset or dampen the intensity of seasonal outbreaks[12]. Furthermore, comparing seasonality features among infections with a common route of transmission may show whether infections with similar seasonal characteristics (peak timing, amplitude, duration) might proxy for one another[13,15,16] to facilitate the development of new tools for disease forecasting.

The synchronization of seasonal peaks across diseases in the same location or across locations for the same disease is a characteristic of a spatiotemporal pattern of infections with a common route of transmission. The seasonal peaks are merely temporal cumulative clustering of local foodborne outbreaks. In complex system sciences, synchronization is defined as a system's property in which the dynamics of individual elements of a system

Tufts University Friedman School of Nutrition Science and Policy, Boston, USA. ✉email: Elena.Naumova@tufts.edu

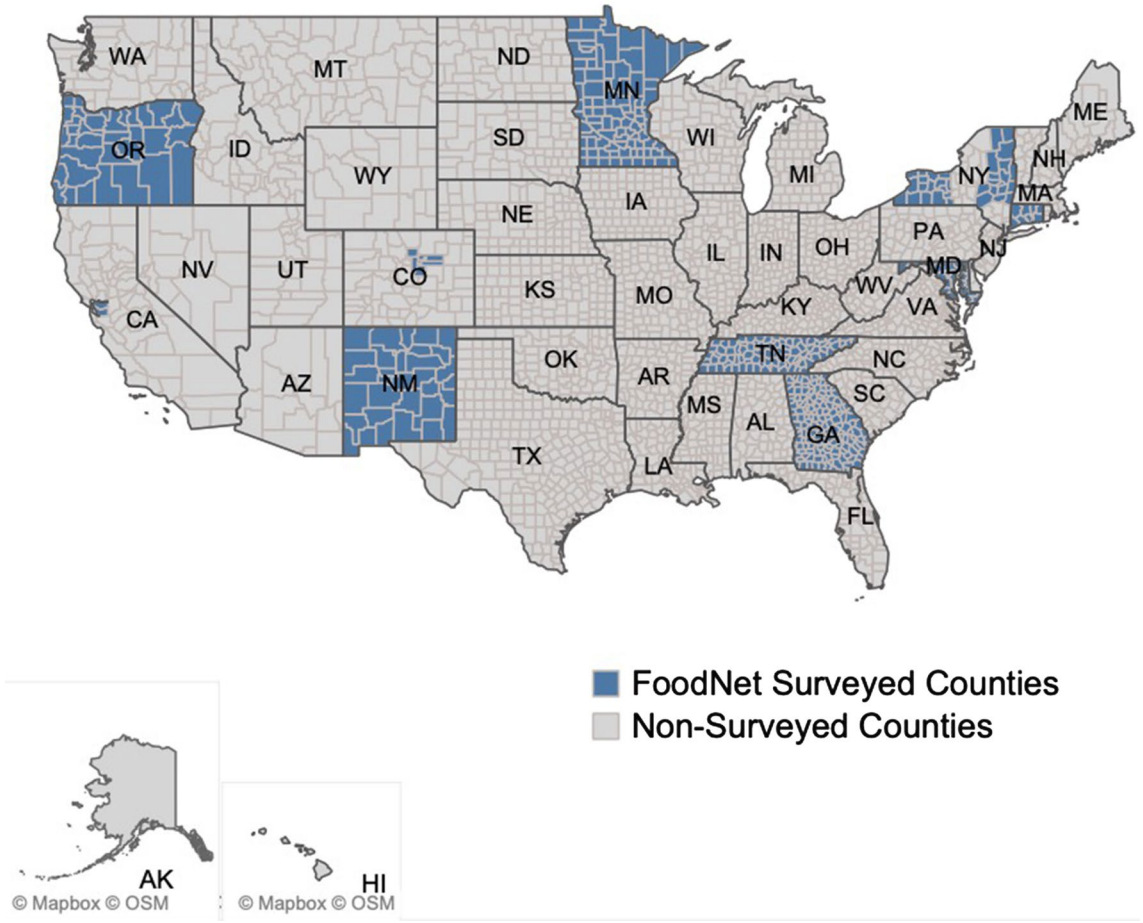


Figure 1. A map of surveyed FoodNet counties as of 2018 (see "Data and methods" section for detail).

are correlated in time due to nonlinear interactions between elements. Many research fields provide illustrations of synchronization, including biology[23], trade and finance[24], mathematics[25], and social sciences[26]. We argue that the synchronization of diseases could be established due to the spatiotemporal alignment of conditions favoring the spread of infections sharing common seasonality features. By extension, infections sharing synchronized seasonal peaks may share similar environmental and manmade drivers of infection associated with food contamination during production and distribution stages.

The synchronization across diseases in a population can be detected and measured. Surveillance systems offer a platform to present time-referenced reported records as an ongoing stream of time series and to assess the properties of these time series, namely the seasonal peak timing and amplitude of seasonal oscillations. The time series of diseases in specific geographic locations can be correlated across infections in a single location or for a single disease across multiple locations. In our earlier works, we illustrated seasonal synchronization between six reported enteric infections in Massachusetts[16] using a systematic approach for estimating the peak timing and amplitude along with their measures of uncertainty[21,27] applied to state surveillance records. We also demonstrated a possible relationship between annual peaks and amplitudes: early peaks in influenza are likely to pair with higher amplitude[22]. These models parallel more recent efforts taken by the CDC and FoodNet surveillance reporting teams[28].

In this study, we further developed techniques for defining, characterizing, and comparing seasonal disease outbreaks. We applied the proposed methodology to monthly rates of nine infections reported by FoodNet public sites in the United States and ten surveyed states (as shown in Fig. 1) and all available years (Supplementary Table S1). First, we demonstrated the use of high order characteristics applied to the distribution of monthly rates, specifically L-skewness and L-kurtosis, to identify infections with periodic and non-periodic outbreaks. Next, we developed annualized and trend-adjusted Negative Binomial Harmonic Regression (NBHR) models to estimate the seasonal characteristics for each infection. We applied the δ-methods to derive peak timing and amplitude estimates and their confidence intervals for each infection. We introduced three metrics of outbreak synchronization: serial synchronization based on serial cross-correlations between time series, phase-phase synchronization based on correlations between peak timing estimates, and phase-amplitude synchronization based on correlations across peak timing and amplitude estimates. These techniques allowed us to characterize seasonal infections in a standardized manner, identify possible multi-state outbreaks, and potentially enhance near-time ensemble forecasting. The proposed standardization of data review and analysis is essential for developing reliable

outbreak forecasts and informing stakeholders on mitigation and prevention measures, and scheduling food contamination inspections.

Results

Monthly rates and sporadic outbreaks. The monthly time series of reported rates for nine foodborne infections (seven bacterial and two protozoal) are shown as a multi-panel plot of stacked time series and rotated frequency histograms for the US from 1996 to 2017 (Fig. 2). The right panel provides a time series for visual inspection of the potential periodic nature of the data. The rotated frequency histogram indicates the right-skewness of the monthly rate distribution, justifying the use of negative binomial regression models. The general summary statistics, including GLM-based average monthly rates and the L-skewness and L-kurtosis coefficients, are provided in Table 1. GLM-based monthly rates properly calculate confidence interval estimates and demonstrate differences in intensity across infections and locations. Coefficients of L-skewness and L-kurtosis identify time series distributions with stable seasonal behaviors or sporadic outbreaks typically reflected by low or high values, respectively.

Nationally, the monthly rates of infections exhibited marked variability of 100-fold difference from ~ 20 to ~ 0.2 cases per month per 1,000,000 persons (cpm). Based on the average monthly rates and their variability we clustered infections in three distinct groups. *Salmonella* and *Campylobacter* infections had the highest average monthly rates of above 10.0 cpm: 12.68 [11.18, 14.37] and 12.17 [10.74, 13.80] cpm, respectively. *Shigella, Cryptosporidium,* and STEC had average monthly rates under 5.0 cpm: 4.84 [4.24, 5.52], 2.04 [1.76, 2.38], and 1.71 [1.47, 1.99] cpm, respectively. *Yersinia, Vibrio*, *Listeria,* and *Cyclospora* had the lowest average monthly rates under 0.5 cpm.

The reported monthly rates of infections vary substantially across states at the magnitude of two to eightfold. For infections with overall high rates the fold increase across states was under 5-folds. For example, *Campylobacter* shows ~ 4.6-fold change with highest average monthly rates in CA and lowest in TN (26.6 [23.5, 30.1] cpm vs 5.70 [4.93, 6.59] cpm). For *Shigella* there was ~ 4.4-fold change with highest rates in CA and lowest in CT (7.55 [6.64, 8.59] vs 1.73 [1.49, 2.02] cpm); *Salmonella* shows ~ twofold change with rates ranging from 17.8 [15.7, 20.1] cpm in GA to 8.56 [7.54, 9.73] cpm in OR. For protozoal infections, *Cryptosporidium* had the highest rates in MN (4.29 [3.74, 4.92] cpm), and lowest rates in MD (0.71 [0.58, 0.86] cpm), yielding sixfold change. *Cyclospora* exhibited the fold increase of 7.4.

As expected, the occurrence of sporadic outbreaks of high intensity was most notable at the state level. The stability of seasonal outbreaks was well detected by L-skewness and L-kurtosis coefficients: low coefficients were found for infections with overall high rates and stable seasonality while high coefficients were found for infections with low monthly rates and sharp sporadic outbreaks. Nationally for *Salmonella*, these coefficients were 0.18 and 0.05, respectively, demonstrating a stable, seasonal pattern. In NM, NY and MN, L-skewness exceeded the national estimate by ~ 1.3 times and in CO, NM, and OR L-kurtosis exceeded the national estimate by ~ 3.0 times, indicating the presence of spikes with increased intensity. For infections with overall low rates, like *Yersinia, Vibrio*, *Cryptosporidium,* and *Cyclospora*, the large values of L-skewness and L-kurtosis coefficients indicate a frequent occurrence of irregular spikes.

Seasonality analysis. As shown in Fig. 2 and supported by L-moments in Table 1, most of the infections exhibited regular periodic increases in incidence indicative of seasonality. Therefore, we estimated peak timing and amplitude based on Model 2 and results are shown in Table 2 (see Supplementary Table S3 for details). Nationwide, all infections except *Yersinia* exhibited summer peaks ranging from early-June (6.43-month for *Cyclospora*) to mid-August (8.59-month for *Shigella*). Four infections: *Campylobacter, Vibrio, Salmonella*, and STEC peaked during mid- to late-July (7.30 [7.08, 7.53]; 7.72 [7.59, 7.84]; 7.79 [7.71, 7.87]; and 7.81 [7.66, 7.96], respectively). The peak in *Campylobacter* was significantly earlier than *Vibrio* ($p = 0.015$), *Salmonella* ($p < 0.001$), and STEC ($p = 0.005$). Three infections: *Cryptosporidium, Listeria*, and *Shigella* peaked during August (8.19 [7.96, 8.43]; 8.35 [8.05, 8.65]; and 8.59 [8.07, 9.11], respectively). Peak timing for *Yersinia* was inconclusive; peak timing of *Cyclospora* was highly variable (6.43 [5.86, 7.01]). Nationally, the amplitude of seasonal peaks varies from 1.27 [1.12, 1.43] for *Yersinia* to 5.56 [3.55, 8.72] for *Cyclospora.*

We compared peak timing estimates to identify seasonal co-occurrences and determine the potential for phase-phase synchronization. At the state level, *Salmonella* peaked during July for all states except GA (8.24 [8.12, 8.35]) while *Campylobacter* had the earliest peak in GA and latest in NM (Table 2). The peak of *Campylobacter* in GA significantly ($p < 0.03$) preceded peaks in six states: CA, CO, MN, NM, NY, and OR. Similarly, the peak of *Campylobacter* in CA significantly ($p < 0.022$) succeeded peaks in seven states: CO, CT, MD, MN, NY, OR, and TN. *Listeria* had far more state-level variability between mid-June in GA to mid-September in MN. STEC also had large state-level variability (early-July in GA to mid-August in CA). *Cryptosporidium* had the least variability across states (from MN (7.97 [7.73, 8.22]) to CA (8.64 [6.11, 11.16]), yet its peak timing in CT significantly succeeded peaks in MN ($p = 0.025$) and OR ($p = 0.048$). Although nationally *Yersinia* peaked at the beginning of January, peaks were spread sporadically across states. Like *Yersinia*, state-specific seasonal peaks for *Cyclospora* were spread over 2 months.

Across states, *Salmonella, Campylobacter, Shigella,* and STEC had the least variability of amplitude estimates, with about 30–70% difference between the highest and lowest amplitudes (Table 2). The high values of peak amplitude for *Salmonella* in GA and for *Campylobacter* in NM tended to co-occur with late peak timing. *Cyclospora* and *Vibrio* had the largest amplitude variability. The large values of peak amplitude co-occur with high values for skewness and kurtosis for *Vibrio* in NY and for *Cyclospora* in OR.

To depict the relationship between peak timing and amplitude simultaneously with annual trend and reoccurrences of seasonal changes for all infections in the US, we combined the traditional time series as a multi-panel

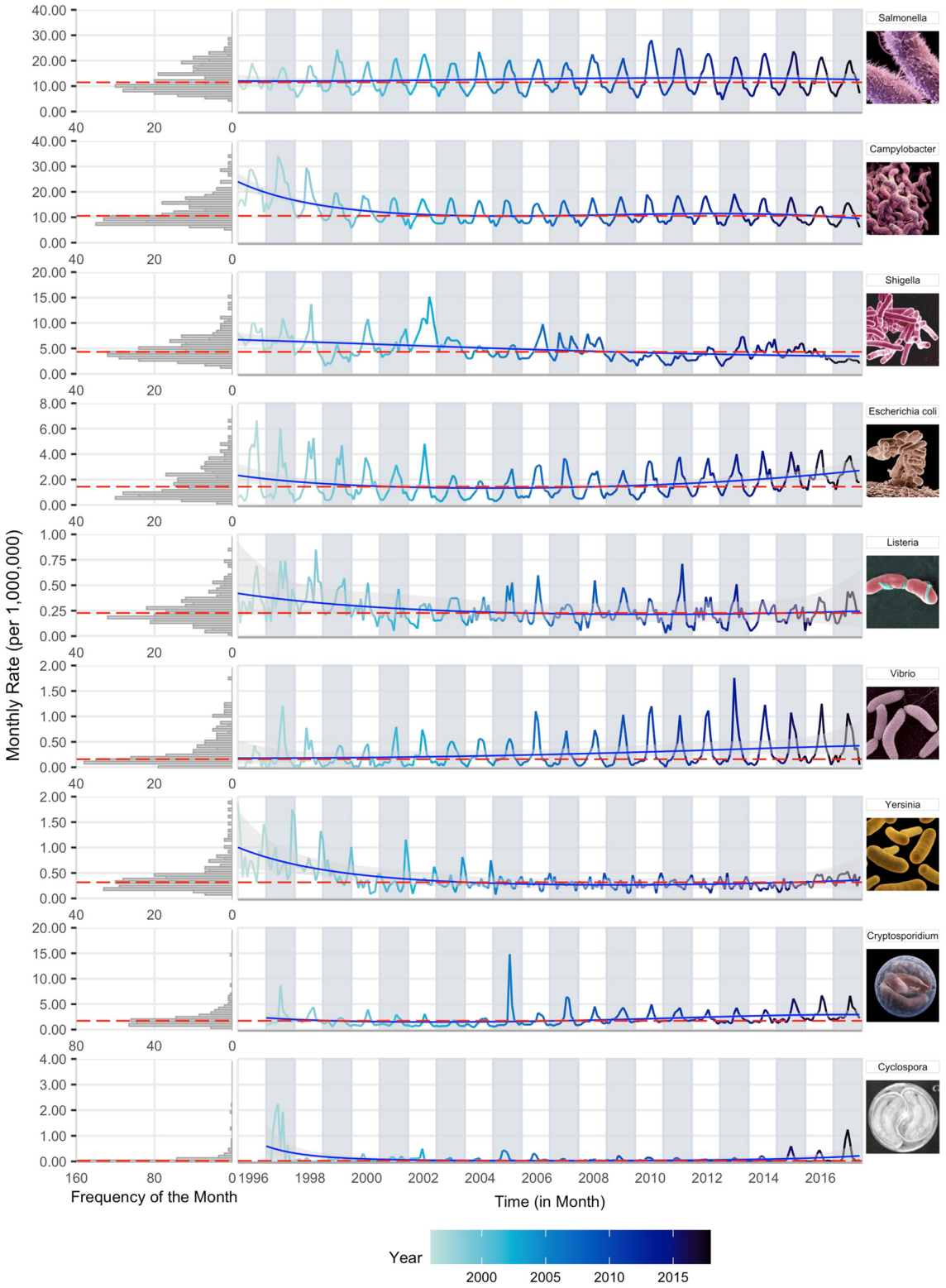


Figure 2. Multi-panel stacked time series plots of monthly reported rates per 1,000,000 persons with median rates (red lines) and predicted trend (blue lines) based on Model 1 and Model 5, respectively, accompanied by the left-rotated frequency histograms for nine FoodNet-reported infections in the United States for available years in 1996–2017. Time series line colour shade indicates more historic vs. more recent data.

	US	CA	CO	CT	GA	MD	MN	NM	NY	OR	TN
Bacteria, > 10.0 cpm											
Salmonella											
LCI	11.18	11.67	8.438	10.22	15.70	11.23	9.976	11.79	8.605	7.537	10.54
Rate	12.68	13.23	9.746	11.59	17.78	12.81	11.31	13.79	9.827	8.562	12.11
UCI	14.37	14.99	11.26	13.14	20.12	14.61	12.83	16.13	11.22	9.726	13.91
L-Skw	0.178	0.197	0.213	0.226	0.228	0.205	0.231	0.256	0.241	0.179	0.193
L-Krt	0.046	0.151	0.163	0.117	0.054	0.097	0.131	0.152	0.144	0.152	0.087
Campylobacter											
LCI	10.74	23.52	10.39	12.66	5.667	6.353	13.57	12.48	10.17	14.20	4.932
Rate	12.17	26.60	11.99	14.34	6.452	7.270	15.37	14.59	11.60	16.08	5.699
UCI	13.80	30.07	13.83	16.25	7.345	8.321	17.40	17.06	13.24	18.21	6.586
L-Skw	0.269	0.175	0.219	0.276	0.264	0.178	0.232	0.181	0.218	0.175	0.147
L-Krt	0.134	0.192	0.153	0.180	0.178	0.108	0.101	0.090	0.115	0.127	0.105
Bacteria, < 5.0 cpm											
Shigella											
LCI	4.235	6.642	2.728	1.489	7.654	2.826	3.470	3.941	1.485	1.799	4.609
Rate	4.835	7.551	3.193	1.733	8.693	3.266	3.972	4.655	1.741	2.083	5.330
UCI	5.520	8.586	3.737	2.016	9.874	3.774	4.545	5.500	2.040	2.413	6.164
L-Skw	0.230	0.314	0.373	0.367	0.302	0.514	0.511	0.297	0.444	0.337	0.384
L-Krt	0.153	0.186	0.251	0.280	0.195	0.395	0.331	0.209	0.313	0.210	0.167
STEC											
LCI	1.470	1.381	2.086	1.428	0.540	0.674	3.155	1.355	1.455	2.243	1.050
Rate	1.711	1.610	2.455	1.663	0.654	0.814	3.616	1.641	1.707	2.585	1.256
UCI	1.992	1.878	2.889	1.938	0.792	0.983	4.144	1.988	2.002	2.980	1.502
L-Skw	0.242	0.330	0.282	0.323	0.234	0.196	0.277	0.215	0.371	0.299	0.254
L-Krt	0.098	0.198	0.161	0.225	0.141	0.119	0.099	0.141	0.267	0.155	0.142
Bacteria, < 0.5 cpm											
Listeria											
LCI	0.196	0.297	0.154	0.376	0.152	0.217	0.098	0.137	0.257	0.189	0.106
Rate	0.256	0.374	0.213	0.466	0.204	0.284	0.138	0.198	0.331	0.248	0.153
UCI	0.334	0.472	0.296	0.577	0.273	0.372	0.196	0.287	0.427	0.325	0.221
L-Skw	0.206	0.255	0.570	0.299	0.229	0.245	0.458	0.640	0.377	0.282	0.268
L-Krt	0.160	0.146	0.276	0.135	0.124	0.108	0.132	0.335	0.179	0.108	0.042
Vibrio											
LCI	0.208	0.515	0.134	0.331	0.166	0.389	0.110	0.044	0.123	0.221	0.085
Rate	0.270	0.625	0.189	0.414	0.221	0.486	0.153	0.078	0.174	0.286	0.126
UCI	0.351	0.759	0.267	0.518	0.293	0.606	0.213	0.140	0.246	0.369	0.188
L-Skw	0.394	0.510	0.540	0.548	0.265	0.399	0.563	0.694	0.539	0.609	0.417
L-Krt	0.198	0.247	0.192	0.280	0.124	0.123	0.265	0.349	0.209	0.306	0.110
Yersinia											
LCI	0.305	0.415	0.173	0.314	0.396	0.147	0.327	0.067	0.275	0.337	0.206
Rate	0.384	0.510	0.237	0.394	0.489	0.200	0.409	0.110	0.352	0.420	0.274
UCI	0.482	0.628	0.324	0.494	0.604	0.272	0.512	0.181	0.451	0.525	0.366
L-Skw	0.366	0.342	0.395	0.274	0.529	0.300	0.258	0.685	0.235	0.207	0.278
L-Krt	0.291	0.195	0.061	0.111	0.407	0.069	0.178	0.352	0.075	0.084	0.170
Protozoa, < 5.0 cpm											
Cryptosporidium											
LCI	1.758	1.564	1.076	0.956	1.850	0.580	3.740	3.118	1.825	2.202	0.974
Rate	2.044	1.824	1.292	1.133	2.164	0.706	4.290	3.697	2.127	2.547	1.168
UCI	2.376	2.127	1.551	1.342	2.532	0.859	4.920	4.384	2.480	2.947	1.401
L-Skw	0.334	0.436	0.385	0.353	0.210	0.322	0.345	0.356	0.619	0.280	0.415
L-Krt	0.236	0.270	0.265	0.225	0.183	0.229	0.210	0.237	0.551	0.100	0.306
Protozoa, < 0.5 cpm											
Cyclospora											
LCI	0.065	0.085	0.071	0.241	0.151	0.039	0.037	0.039	0.026	0.013	0.011
Rate	0.098	0.141	0.133	0.311	0.206	0.068	0.074	0.078	0.055	0.036	0.028
Continued											

	US	CA	CO	CT	GA	MD	MN	NM	NY	OR	TN
UCI	0.148	0.235	0.249	0.400	0.279	0.119	0.146	0.157	0.116	0.106	0.070
L-Skw	0.697	0.853	0.853	0.740	0.724	0.803	0.805	0.802	0.873	0.865	0.810
L-Krt	0.508	0.682	0.680	0.501	0.481	0.587	0.581	0.561	0.715	0.690	0.578

Table 1. GLM-based monthly average rates per 1,000,000 persons accompanied by 95% confidence intervals, L-skewness, and L-kurtosis estimates for the nine FoodNet reported infections for the United States and ten surveyed states from 1996 to 2017. *Note* LCI and UCI are lower and upper boundaries for the 95% confidence interval (CI), respectively; L-Skw represents L-skewness while L-Krt represents L-kurtosis estimates.

calendar plot (Fig. 3). Based on the relationship between peak timing and amplitude, all infections exhibited summer peaks in tightly formed clusters except *Vibrio* and *Yersinia*. The heat map of monthly rates for *Salmonella*, *Campylobacter*, *Shigella,* STEC, and *Cryptosporidium* exhibited distinct seasonal changes in summertime rates.

Trend analysis. The results of trend analyses are shown in Fig. 2 and Supplementary Tables S4–S6. In Fig. 2, the medians and the predicted trends along with their confidence intervals were obtained from Model 1 and Model 5, respectively. The contribution of trend and seasonal components for each infection is shown in Supplementary Table S4. On the national level, seasonality explains a substantial fraction of variability for six infections: *Salmonella*, STEC, *Vibrio*, *Campylobacter*, *Listeria*, and *Cryptosporidium* (64, 43, 43, 29, 20, and 20%, respectively). The contribution of the trend components was most pronounced in *Campylobacter*, *Yersinia*, *Cyclospora*, and *Vibrio* (48, 29, 25, and 20%, respectively). The contributions of linear, quadratic, and cubic trend components are shown in Supplementary Table S5. Overall, an adjustment for linear and non-linear trend components resulted in < 3% fluctuations in average peak timing and amplitude estimates with < 10% fluctuations for *Cyclospora*, *Yersinia,* and *Cryptosporidium* estimates as shown in Supplementary Table S6. This high stability in seasonality estimates irrespective of trend specifications justified the use of Model 1 for calculating annualized seasonality characteristics and conducting phase-phase and phase-amplitude synchronization analyses.

It is expected that infections with strong trend and/or seasonality components have high autocorrelation, e.g. high dependency on the prior month value, which serves as the base for near-term forecasting. We plotted the correlation coefficients across lags of 1–3 months for each infection in each state and all states combined (Fig. 4; Supplementary Table S7). Nationwide, six infections: *Salmonella, Campylobacter, Shigella,* STEC, *Cryptosporidium* and *Vibrio* had strong autocorrelations at 1-month lag ($\rho \geq 0.70$; $p < 0.001$) and moderate autocorrelations at lag of 2 months ($\rho \geq 0.42$; $p < 0.001$). At the state level, GA had the strongest autocorrelation patterns for *Salmonella* and *Shigella*. CA had the strongest patterns for *Campylobacter*, MN had the strongest patterns for STEC, and OR had the strongest patterns for *Cryptosporidium*. In general, autocorrelations across states for *Listeria* and *Vibrio* were low across most lags ($\rho < 0.45$) and thus, support low seasonality and trend contributions as shown in Supplementary Table S4.

Synchronization analysis. It is expected that infections with similar trend and seasonality patterns have high cross-correlations, indicating potential synchronization of the shared temporal behavior. Cross-correlation estimates between diseases at − 3 to + 3 months lags are shown in Fig. 5 and Supplementary Table S8. Nationally, monthly rates of *Campylobacter* were strongly correlated with *Salmonella* at lags − 1 to + 2 ($\rho = 0.59, 0.78, 0.73, 0.50$; $p < 0.001$). *Campylobacter* was also moderately correlated at lags − 1 and 0 with STEC ($\rho = 0.63, 0.66$; $p < 0.001$) and *Vibrio* ($\rho = 0.58, 0.63$; $p < 0.001$), and with *Listeria* at lags − 2 to 0 ($\rho = 0.60, 0.69, 0.63$; $p < 0.001$). *Salmonella* was also strongly correlated from lags − 1 to + 1 with STEC and *Vibrio* as well as moderately correlated with Listeria at lags − 1 and 0. STEC was strongly correlated with *Vibrio* from lags − 1 to + 1 as well as *Cryptosporidium* from lags − 2 to + 1. *Vibrio* was similarly moderately correlated with *Cryptosporidium* from lags − 2 to 0. These results reaffirm strong similarities in the seasonal patterns across infections.

Nationwide, phase-phase synchronization was most pronounced between *Cryptosporidium* and *Shigella* ($\rho = 0.51$, $p = 0.019$), *Listeria* ($\rho = 0.51$, $p = 0.019$), and *Salmonella* ($\rho = 0.46$, $p = 0.036$) (Supplementary Table S9). Strong positive synchronization between *Cryptosporidium* and *Shigella* indicates concordance in their seasonal behavior; when one peaks later, the other does also (Supplementary Fig. S1). In contrast, no significant synchronization was found between *Salmonella* and *Campylobacter* ($\rho = 0.07$) (Supplementary Fig. S2), indicating that the seasonal processes of *Salmonella* and *Campylobacter* peak timing are not associated despite peak co-occurrence in July. At the state level, phase-phase synchronization varies and for one pair the correlation could be significant and positive for one state and negative for another, like *Campylobacter*-STEC in CT and GA, indicative of discordant patterns. The strongest correlations were found between *Salmonella* and STEC in NM ($\rho = 0.62$, $p = 0.018$) and between *Salmonella* and *Campylobacter* in MN ($\rho = 0.60$, $p = 0.003$).

Examining phase-amplitude synchronization, we found positive correlations indicating that the magnitude of seasonal peaks is likely to increase when an infection peaks later in the year for STEC at the national level ($\rho = 0.50$, $p = 0.019$; Fig. 6), as well as in GA ($\rho = 0.58$, $p = 0.005$) (Supplementary Table S10). We also found positive correlations for *Shigella* in CA ($\rho = 0.63$, $p = 0.002$), GA ($\rho = 0.50$, $p = 0.019$), and MN ($\rho = 0.43$, $p = 0.049$) as well as for *Cryptosporidium* in CT ($\rho = 0.48$, $p = 0.029$) indicating the phase-amplitude synchronization.

	US	CA	CO	CT	GA	MD	MN	NM	NY	OR	TN
Bacteria, > 10.0 cpm											
Salmonella											
LCI	7.713	7.339	7.175	7.198	8.124	7.513	7.061	7.536	7.050	6.777	7.700
PT	7.793	7.558	7.528	7.430	8.236	7.649	7.260	7.845	7.226	7.078	7.841
UCI	7.874	7.777	7.881	7.663	8.349	7.784	7.458	8.153	7.402	7.379	7.982
LCI	1.678	1.425	1.317	1.559	2.031	1.712	1.470	1.666	1.710	1.318	1.768
AMP	1.704	1.470	1.377	1.615	2.079	1.757	1.515	1.730	1.776	1.373	1.818
UCI	1.731	1.514	1.438	1.672	2.127	1.802	1.560	1.794	1.841	1.428	1.868
Campylobacter											
LCI	7.077	6.887	7.051	6.989	6.669	7.023	7.253	7.571	7.297	6.986	6.983
PT	7.304	7.528	7.291	7.224	6.973	7.272	7.408	7.809	7.491	7.188	7.196
UCI	7.530	8.168	7.530	7.459	7.277	7.521	7.563	8.048	7.686	7.390	7.410
LCI	1.454	1.152	1.523	1.520	1.401	1.551	1.651	1.734	1.579	1.410	1.476
AMP	1.502	1.211	1.591	1.572	1.463	1.615	1.689	1.794	1.630	1.454	1.525
UCI	1.550	1.270	1.659	1.624	1.524	1.678	1.726	1.854	1.681	1.498	1.575
Bacteria, < 5.0 cpm											
Shigella											
LCI	8.070	7.788	8.450	6.631	7.782	6.550	6.696	8.401	7.308	8.315	7.440
PT	8.589	8.558	8.834	7.629	8.812	7.611	7.824	8.949	8.657	9.221	9.360
UCI	9.108	9.328	9.219	8.627	9.842	8.672	8.953	9.498	10.01	10.13	11.28
LCI	1.236	1.208	1.779	1.141	1.148	1.306	1.156	1.497	1.149	1.219	0.991
AMP	1.305	1.317	1.931	1.296	1.250	1.510	1.369	1.636	1.355	1.355	1.154
UCI	1.374	1.426	2.083	1.451	1.351	1.714	1.582	1.775	1.562	1.491	1.318
STEC											
LCI	7.655	7.800	7.074	6.977	6.817	7.626	7.661	7.262	7.604	7.864	6.916
PT	7.806	8.262	7.429	7.411	7.232	7.942	7.836	7.611	7.995	8.083	7.299
UCI	7.957	8.724	7.784	7.845	7.647	8.257	8.011	7.960	8.385	8.301	7.683
LCI	2.233	1.732	1.802	1.758	1.743	1.939	2.613	1.864	2.198	2.406	1.747
AMP	2.306	1.904	1.968	1.932	1.875	2.066	2.714	2.000	2.396	2.542	1.873
UCI	2.379	2.076	2.133	2.106	2.008	2.194	2.815	2.136	2.594	2.679	2.000
Bacteria, < 0.5 cpm											
Listeria											
LCI	8.048	4.292	8.025	7.794	5.229	7.800	8.736	7.895	8.028	7.755	7.019
PT	8.351	7.027	8.648	8.196	6.481	8.345	9.383	8.755	8.627	8.317	8.624
UCI	8.654	9.762	9.272	8.597	7.733	8.889	10.03	9.614	9.226	8.879	10.23
LCI	1.497	0.937	1.949	1.832	1.092	1.571	1.752	2.034	1.854	1.611	1.052
AMP	1.572	1.118	2.406	2.018	1.257	1.742	2.012	2.596	2.079	1.793	1.263
UCI	1.646	1.298	2.863	2.203	1.423	1.913	2.273	3.158	2.305	1.974	1.475
Vibrio											
LCI	7.592	7.707	7.328	7.560	7.257	7.337	7.178	7.388	7.265	7.652	6.977
PT	7.718	7.914	7.764	7.786	7.667	7.499	7.628	8.648	7.603	7.844	7.459
UCI	7.844	8.121	8.200	8.011	8.076	7.662	8.078	9.907	7.941	8.036	7.940
LCI	3.893	5.540	3.182	4.867	2.113	5.644	2.417	1.697	3.611	8.254	2.227
AMP	4.020	5.817	3.576	5.211	2.269	5.851	2.742	2.258	3.999	8.743	2.508
UCI	4.148	6.095	3.969	5.554	2.426	6.059	3.066	2.818	4.387	9.232	2.789
Yersinia											
LCI	12.34	8.203	5.989	3.295	12.47	12.62	5.906	6.790	1.615	1.835	12.75
PT	1.089	12.51	7.755	7.481	12.84	2.612	7.204	8.648	4.233	3.380	1.461
UCI	1.841	5.814	9.521	11.67	1.222	5.608	8.502	10.51	6.850	4.924	2.173
LCI	1.144	0.862	1.080	0.905	2.185	0.953	1.109	1.000	0.960	1.033	1.460
AMP	1.265	1.069	1.337	1.085	2.433	1.144	1.246	1.558	1.135	1.196	1.654
UCI	1.386	1.277	1.595	1.265	2.681	1.336	1.383	2.117	1.310	1.359	1.847
Protozoa, < 5.0 cpm											
Cryptosporidium											
LCI	7.959	6.110	7.801	7.882	8.004	8.012	7.726	7.625	7.997	7.166	8.001
PT	8.194	8.635	8.256	8.251	8.404	8.531	7.974	8.063	8.318	8.094	8.478
Continued											

	US	CA	CO	CT	GA	MD	MN	NM	NY	OR	TN
UCI	8.430	11.16	8.711	8.619	8.804	9.051	8.223	8.501	8.638	9.023	8.956
LCI	1.724	0.959	1.757	1.935	1.336	1.526	2.013	1.715	2.728	1.206	1.684
AMP	1.833	1.144	1.991	2.107	1.429	1.698	2.121	1.915	3.166	1.352	1.890
UCI	1.942	1.330	2.226	2.278	1.521	1.871	2.229	2.115	3.604	1.498	2.097
Protozoa, < 0.5 cpm											
Cyclospora											
LCI	5.857	5.402	6.142	6.096	6.239	6.422	6.279	5.381	6.247	3.657	5.889
PT	6.432	5.957	6.611	6.386	7.432	7.095	6.792	6.057	6.739	7.145	6.537
UCI	7.007	6.511	7.081	6.676	8.625	7.769	7.306	6.732	7.230	10.63	7.184
LCI	5.114	4.979	37.78	9.872	1.705	4.057	9.172	6.426	9.850	0.578	8.577
AMP	5.563	6.151	40.65	10.45	2.187	4.838	10.35	7.870	11.61	1.651	9.516
UCI	6.012	7.323	43.51	11.12	2.668	5.618	11.54	9.313	13.38	2.723	10.46

Table 2. Average peak timing in months and amplitude and their 95% confidence intervals for monthly rates per 1,000,000 persons for nine infections reported by FoodNet in the United States and ten surveyed states from 1996 to 2017. *Note* LCI and UCI are lower and upper boundaries for the 95% confidence interval (CI), respectively, for peak timing (PT) and amplitude (AMP) estimates.

Discussion

Our results demonstrated how rich and powerful tools of time series analyses could be applied to explore the seasonality and synchronization of foodborne infections between one another and across locations. We urge food safety and public health professionals to make efforts to improve and standardize the analysis of reported infections to allow for a meaningful comparison and actionable inferences derived from this analysis[29]. Measures of L-skewness and L-kurtosis, indicating the degree of departure from a well-defined bell-shaped distribution of cases per selected time unit, could be implemented in routine surveillance system data analysis to quantify the overall degree of outbreak intensity and to distinguish between consistent and thus predictable seasonal behaviors and potentially sporadic outbreaks of foodborne infection. Standardized approaches to quantify seasonal peak timing and intensity (amplitude) along with their uncertainty measures agnostic to infection type or geographic location allow for uniform comparison of seasonal patterns common for all or almost all mandatory or voluntary reported infections.

Detection of foodborne infection outbreaks relies on standardized methods for calculating and comparing infection rates and seasonality features that should be implemented with the highest possible precision. The outdated techniques based on arithmetical means produce meaningless negative values for sporadically occurring infections (as shown in Supplementary Table S2) and must be replaced with GLM-calculated estimates based on the highly skewed nature of time series rates. The commonly used aggregation of daily or weekly counts into monthly values is a substandard solution, because it leads to information loss, coarse resolution, and poor understanding of uncertainties needed for proper trend analysis[30].

By extending the δ-method for systematically estimating the seasonality characteristics, such as peak timing and amplitude, we avoided the traps of using poorly defined seasons, which may vary geographically, climatically, and contextually. When peak timing is calculated as the month with maximal rates using multi-month periods[31–36], this approach, though computationally straightforward, reduces the precision of estimating seasonal characteristics and neglects temporal and geographic variability[37–43]. Our results show that *Campylobacter*, *Vibrio*, *Salmonella*, and STEC peak from mid- to late-July, suggesting co-occurrence based on month of maximal rate calculations. By applying the δ-method and formal statistical testing we demonstrated that, while all infections peak during July, *Campylobacter* significantly precedes *Vibrio*, *Salmonella*, and STEC. Thus, we are able to identify an important feature, missed by the commonly used methods, yet valuable for disease forecasting.

The standardization of analytical tools could substantially improve our understanding of the co-occurrence of infections with respect to each other and across locations. High values of L-skewness and L-kurtosis spotted an outbreak of *Salmonellosis* in NY in 1996 with 5-times the amplitude than any other year following[44,45]. High L-moment estimates in GA for *Yersinia* indicated erratic outbreaks during December and January months and likely reflect reported outbreaks in pork chitterlings for Christmas and New Year celebrations[46,47]. High skewness and kurtosis values for *Cryptosporidium* and *Cyclospora* aligned with well documented outbreaks in NY and CA[46–51]. Unfortunately, cases reported by the FoodNet Fast platform are designated to a single state, heavily aggregated, and no information was available for multistate outbreaks. FoodNet Fast does not provide granular population catchment information within each county and the counties included in FoodNet represent only a fraction of the total state. Drawing spatial relationships for a single infection risks over-stating the association between states, especially when counties in two states share no geographic border. Improved data collection and reporting will enable modeling and forecasting of foodborne infections using complex network analyses to trace supply chain distribution patterns[52–54].

This study provides evidence for potential outbreak synchronization based on several metrics that utilized the complex systems thinking. Serial synchronization examines whether two infections share similar trend and seasonality. Phase-phase and phase-amplitude synchronization evaluate shared seasonal processes between two infections peak timing or a single infection's peak timing and amplitude, respectively. Additionally, these metrics

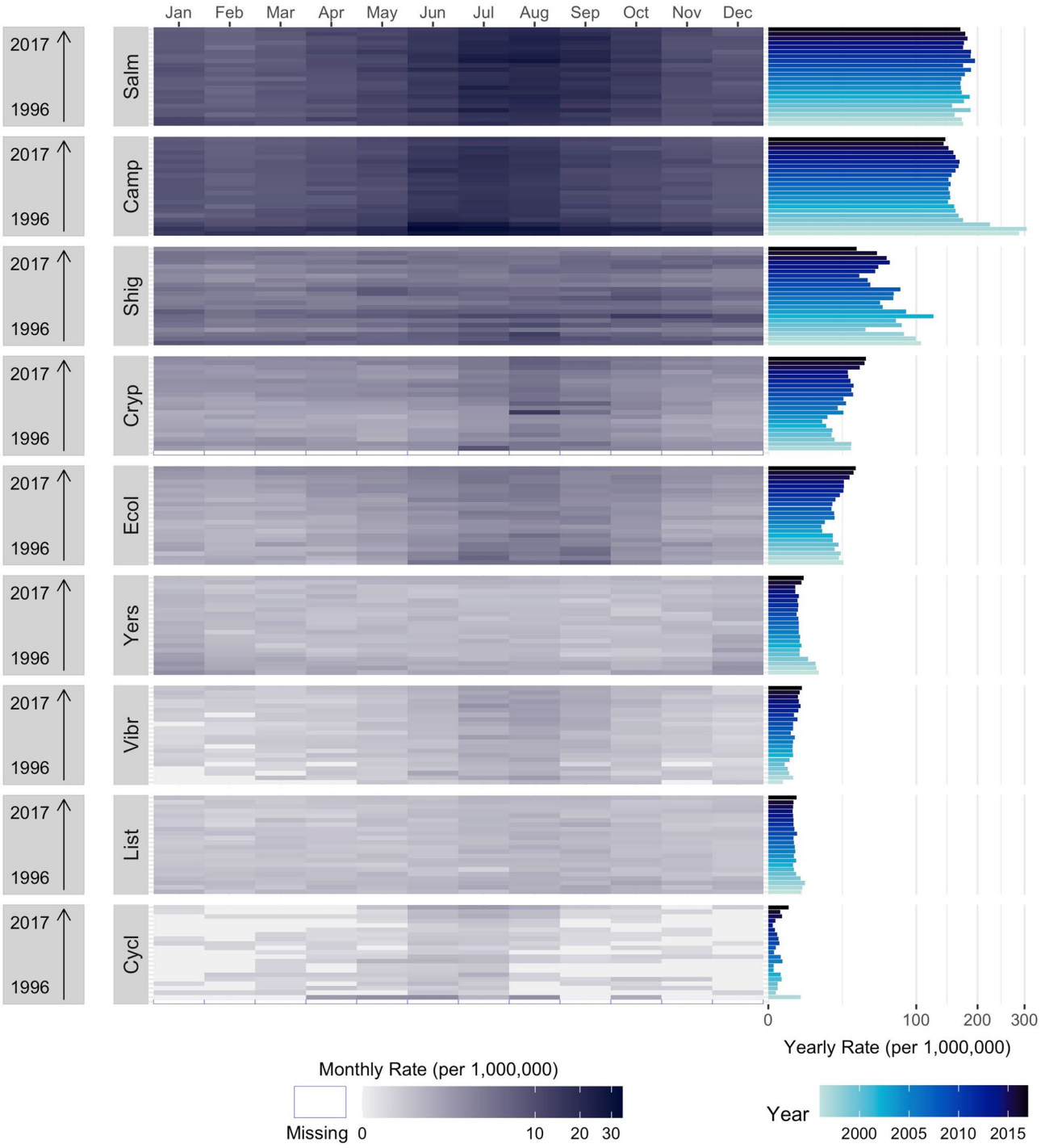


Figure 3. Multi-panel calendar plots of monthly rates combined with yearly rates and peak timing (in month) and amplitude average estimates for nine infections: *Salmonella* (Salm), *Campylobacter* (Camp), *Shigella* (Shig), Shiga Toxin-producing *E. coli* (Ecol), *Listeria* (List), *Vibrio* (Vibr), *Yersinia* (Yers), *Cryptosporidium* (Cryp), and *Cyclospora* (Cycl) as reported by FoodNet in the United States from 1996 to 2017. Average peak timing and amplitude estimates are shown in the top panel, annual trends in rates are shown in the right-rotated bar-charts, and heat maps indicate monthly rates for each infection in the main panel.

can help provide important information for adapting near-term forecasts to more accurately predict, plan for, and prevent seasonal foodborne outbreaks. Surveillance records with more granular temporal resolution and expanded geographic catchment areas can help improve the accuracy and precision of synchronization estimates for creating foodborne infection calendars, inspection schedules, and tracking multistate outbreaks. The public portal automatically compresses data during download, requiring individual year-by-year data extraction. Food recall reports show that a single outbreak is attributable to outbreaks in numerous states for these nine

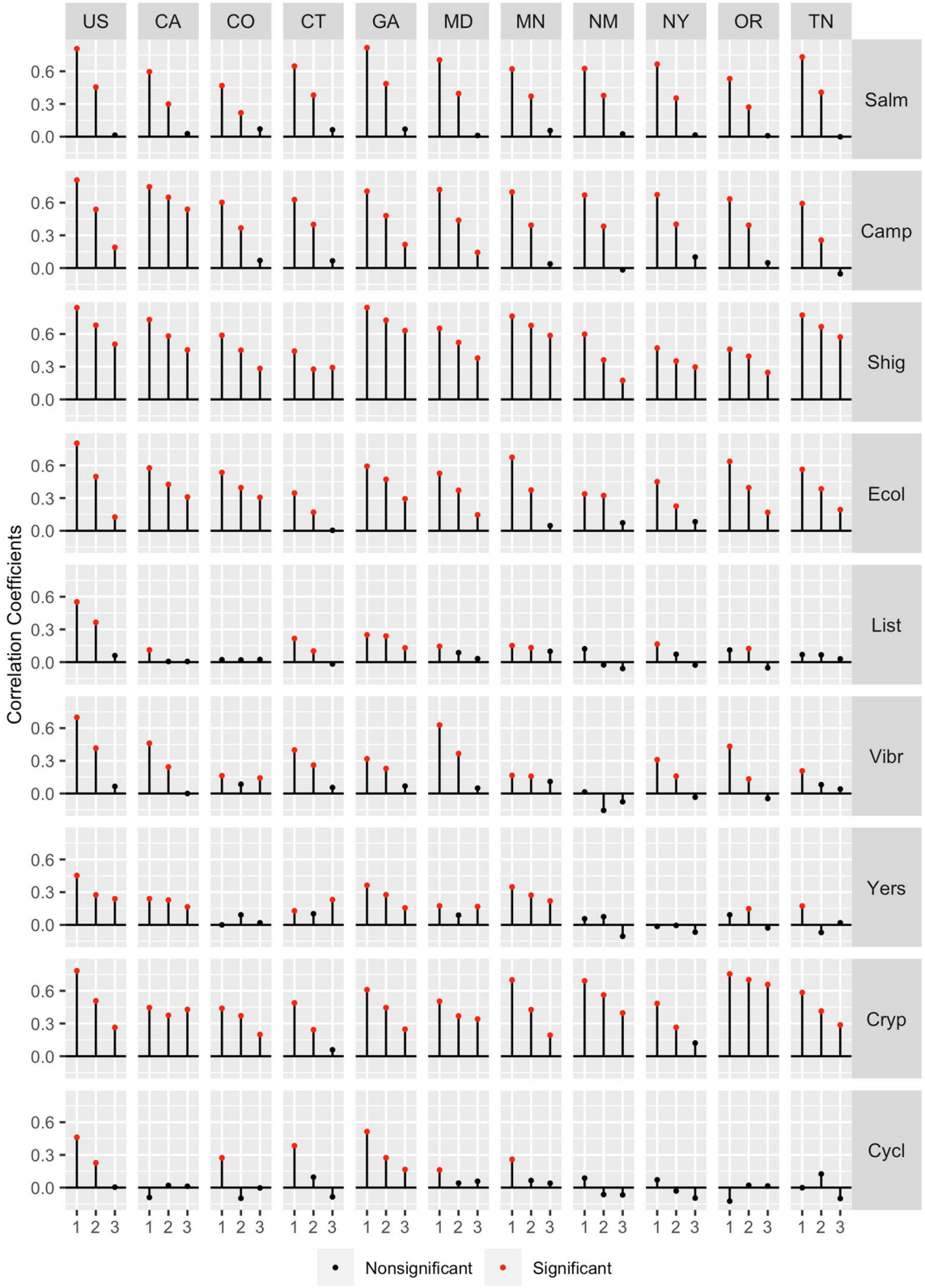


Figure 4. The autocorrelation coefficients across lags of 1–3 months for nine infections: *Salmonella* (Salm), *Campylobacter* (Camp), *Shigella* (Shig), Shiga Toxin-producing *E. coli* (Ecol), *Listeria* (List), *Vibrio* (Vibr), *Yersinia* (Yers), *Cryptosporidium* (Cryp), and *Cyclospora* (Cycl) as reported by FoodNet in the United States and ten surveyed states. Significant values are shown in red.

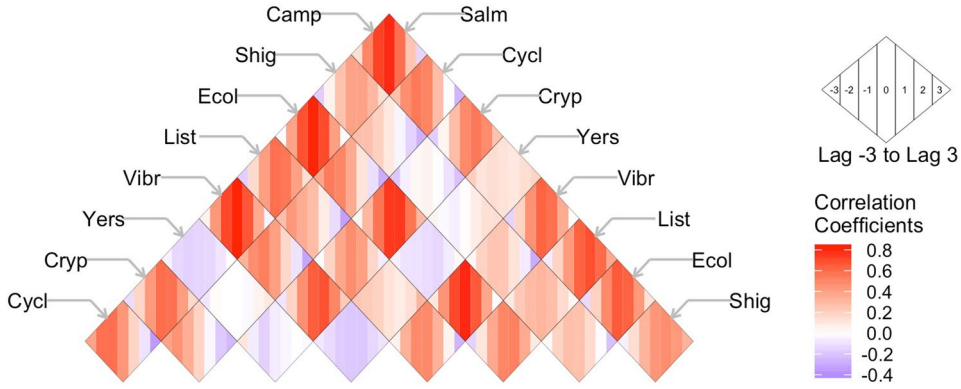


Figure 5. Correlation coefficients across seven lags (− 3 to + 3) between pairs of nine infections *Salmonella* (Salm), *Campylobacter* (Camp), *Shigella* (Shig), Shiga Toxin-producing *E. coli* (Ecol), *Listeria* (List), *Vibrio* (Vibr), *Yersinia* (Yers), *Cryptosporidium* (Cryp), and *Cyclospora* (Cycl) as reported by FoodNet for the US from 1996 to 2017. Infection pairings are found at the intersection of diagonal rows. Shading intensity indicates the strength of correlations ranging from positive (red) to negative (blue) for each lag as a sequence of coloured stripes as shown in the inset.

infections[44]. Failure to consider multistate outbreaks minimizes the utility of assessing cross-state synchronization of infection seasonality.

Given annual fiscal losses and food waste reported annually, our proposed synchronization metrics should be considered in order to mitigate seasonal co-infections, track multi-state outbreaks, and coordinate food inspection scheduling. Further investigation is needed to evaluate how synchronization metrics can identify common manmade drivers of infection during the packaging, processing, and transporting of food products. With thousands hospitalized or dying, millions of pounds of foodstuffs recalled, and billions of dollars lost annually, methods of describing and analyzing the seasonality and synchronization of foodborne infections can lead to important health benefits and cost savings for food producers, food retailers, and public health agencies alike.

Data and methods

Data sources. FoodNet reports confirmed cases from 650 randomly sampled clinical laboratories in select counties that reach roughly 15% of the US population (Supplementary Table S1) using both culture-dependent and culture-independent methods[8,55]. FoodNet Fast provides a publicly available subset of reports for confirmed annual infections, hospitalizations, and deaths as well as the monthly prevalence of confirmed infections. These data are available for seven bacterial infections (*Campylobacter*, *Listeria*, *Salmonella*, *Shigella*, Shiga toxin-producing *E.coli* (STEC), *Vibrio*, and *Yersinia*) and two protozoa (*Cryptosporidium* and *Cyclospora*) in ten select states: California (CA), Colorado (CO), Connecticut (CT), Georgia (GA), Maryland (MD), Minnesota (MN), New Mexico (NM), New York (NY), Oregon (OR), and Tennessee (TN) (Supplementary Fig. S1).

For each state, we downloaded all available annual infection profiles from 1996 to 2017. For each year, we created a monthly time series by multiplying the annual total of confirmed infections by the percentage of confirmed infections for each month of that year. National (US) estimates were generated by summing all ten states' data. To draw comparisons between states, we calculated statewide population estimates by summing all mid-year (July 1st) populations of surveyed counties according to the year of their introduction into FoodNet (Supplementary Table S1). Annual county-level population estimates are made publicly available in the 1990, 2000, and 2010 US Census Bureau reports[56–58]. We calculated monthly rates per 1,000,000 persons by dividing monthly counts by population estimates and multiplying the product by 1,000,000. Results are presented as cases per 1,000,000 persons and abbreviated as 'cpm.'

Summary statistics for reported rates, trend, and seasonality analyses. To perform the synchronization analysis, we generated 99 individual monthly time series of reported rates (9 infections × 11 locations (each state and all states combined)). For each monthly time series of reported rates, we estimated summary statistics, including average rates and coefficients of L-skewness and L-kurtosis, which are superior on detecting spatiotemporal heterogeneity[59]. Estimates of L-skewness and L-kurtosis reflect the degree of departure of an empirical distribution from a symmetrical bell-shaped curve and the extent of extremes, respectively. Large values of L-skewness and L-kurtosis for a distribution of monthly rates are indicative of sporadic spikes, especially for infections with low overall rates. We used these estimates to identify infections with systematic periodic structures and infections with erratic temporal patterns. Infections with systematic periodic structures undergo trend, seasonality, and synchronization analyses based on annualized estimates of peak timing and amplitude. Infections with erratic temporal patterns were examined for trend and seasonality but only serial synchronization estimates were calculated.

To estimate average monthly rates from the compiled time series and adjust for left-skewed distributions, we applied a generalized linear model (GLM) with a negative binomial distribution and log-link function (Model 1). By exponentiating the model's intercept, we calculated average monthly rates, $\exp\{\beta_0\}$, and their 95% confidence

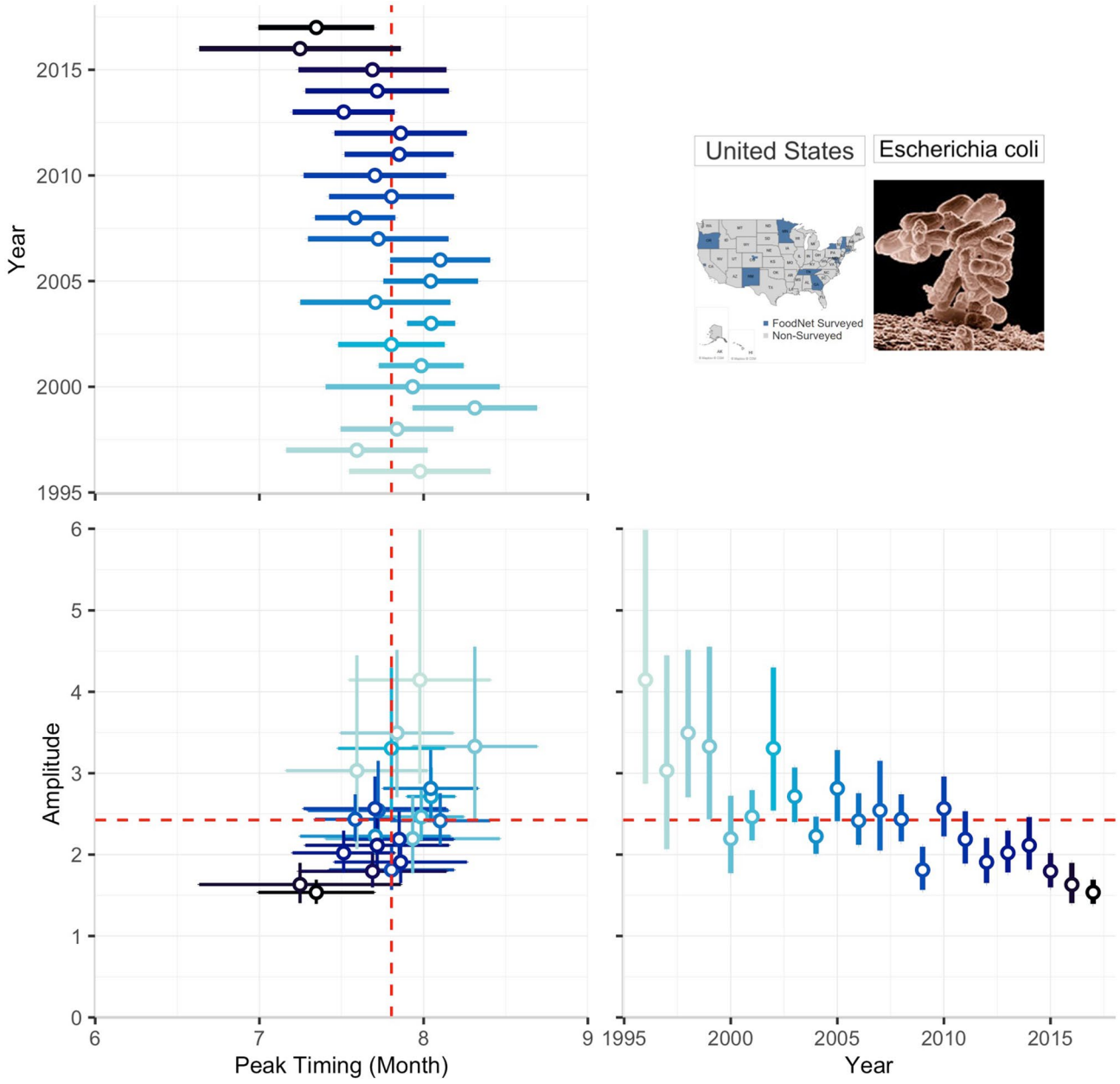


Figure 6. The relationship between annual peak timing and amplitude estimates for Shiga Toxin-producing *E. coli* (STEC) in the US in 1996 to 2017. The multi-panel plot consists of two panels depicting forest plots for peak timing (upper panel) and amplitude (left panel) estimates along with their 95% confidence intervals by year, and the main panel demonstrating the associations between these two seasonality characteristics. Dashed red lines indicate the average peak timing and average amplitude across all years. The colour shade indicates the year of reporting and helps to note the decline in amplitude and the overall tendency to early peak timing that explain the nature of the observed positive correlation and potential synchronization over time.

interval estimates, $\exp\{\beta_0 \pm 1.96se\}$. This unadjusted model avoids biologically implausible, negative rates produced by the traditional arithmetic calculations (Supplementary Table S2).

Next, we developed four Negative Binomial Harmonic Regression (NBHR) models and applied these models for each infection in each state and all 10 states combined (Models 2–5). We explored the effects of linear, quadratic, and cubic trend terms, which were added in a stepwise manner to Model 2 containing solely harmonic seasonal oscillators.

$$\text{Model 1: } \ln[E(Y_{tds})] = \beta_0 \quad (1)$$

$$\text{Model 2: } \ln[E(Y_{tds})] = \beta_0 + \beta_s(\sin(2\pi\omega t)) + \beta_c(\cos(2\pi\omega t)) \quad (2)$$

$$\text{Model 3: } \ln[E(Y_{tds})] = \beta_0 + \beta_s(\sin(2\pi\omega t)) + \beta_c(\cos(2\pi\omega t)) + \beta_1 t \quad (3)$$

$$\text{Model 4: } \ln[E(Y_{tds})] = \beta_0 + \beta_s(\sin(2\pi\omega t)) + \beta_c(\cos(2\pi\omega t)) + \beta_1 t + \beta_2 t^2 \quad (4)$$

$$\text{Model 5: } \ln[E(Y_{tds})] = \beta_0 + \beta_s(\sin(2\pi\omega t)) + \beta_c(\cos(2\pi\omega t)) + \beta_1 t + \beta_2 t^2 + \beta_3 t^3 \quad (5)$$

where Y_{tds}—time series of monthly rates of d-infection for t-month in s-state or all states combined; $\sin(2\pi\omega t)$ and $\cos(2\pi\omega t)$ periodic terms define seasonal oscillations with a frequency of $\omega = 1/M$, where $M = 12$ to represent the length of the annual cycle in months; linear, quadratic, and cubic trend terms are defined by the consecutive month of the study from 1 to L and corresponding regression coefficients. The length of individual time series, L, varied by state according to its introduction into FoodNet: NM was the shortest with 168 months (beginning in 2004) and CA, CT, GA, MN, and OR were the longest being 264 months (beginning in 1996) (Supplementary Table S1).

We estimated peak timing, amplitude, and confidence intervals using the δ-methods (Supplementary Table S3) derived by MacNeill and Naumova[27] with further modifications by Alarcon-Falconi, et al.[21] for each infection in each state and all 10 states combined for the full duration of the study. Confidence intervals for peak timing and amplitude estimates are derived under the assumption of seasonal periodicity. As not all infections had consistent seasonal patterns, peak timing and confidence intervals can reach implausible values. Implausible peak timing estimates (values < 1 or > 13) occur when estimate variance exceeds 6 months for any infection or when peak timing estimates align with the beginning or end of the year (e.g. *Yersinia*). Implausible amplitude estimates (> 20) occur for erratic outbreaks or when estimate variance exceeds the average amplitude estimate (e.g. *Cyclospora*). Peak timing estimates are expressed in continuous month values from 1.0 (beginning of January) to 12.9(9) (end of December) according to the Gregorian calendar. Amplitude estimates are the midpoint of relative intensity reflecting the ratio between the disease rate at the peak (maximum rate) and the disease rate at the midpoint (median rate). Independent sample t-tests were used to determine statistically significant differences of peak timing estimates between states for the same infection and across infections within the same state.

Model goodness-of-fit was evaluated using the Akaike's Information Criterion (AIC), Bayesian Information Criterion (BIC), and Root Mean Squared Error (RMSE). In addition, we assessed the contribution of each trend component by examining regression coefficients for linear, quadratic, and cubic trend terms. Depending on the sign, the linear term indicates overall increases ($\beta_1 > 0$) or decreases ($\beta_1 < 0$) while the quadratic and cubic terms indicate acceleration ($\beta_2 > 0$) or deceleration ($\beta_3 > 0$). We calculated the contribution of each term by multiplying each coefficient by the trend-associated time unit to recover the corresponding predicted rates. The contribution of each trend component (TC) to the overall fit was estimated as follows:

$$TC_k = \beta_k t^k / (|\beta_1 t| + |\beta_2 t^2| + |\beta_3 t^3|) * 100\%, \quad (6)$$

where TC_k is the contribution of k-component (k = 1, linear; k = 2, quadratic; and k = 3, cubic).

We explored the variability of seasonality estimates with respect to trend specification. We evaluated percentage differences of peak timing and amplitude estimates of Models 3–5 compared to Model 2 as follows:

$$\Delta P_m = (P_m - P_1)/(P_1) * 100\% \text{ and } \Delta A_m = (A_m - A_1)/(A_1) * 100\%, \quad (7)$$

where ΔP is percent difference of peak timing, P_m, and amplitude, A_m, estimates of *m*-model (m = 3,4,5) as compared to Model 2 (m = 2).

Synchronization analyses. First, we calculated autocorrelations applied to monthly time series for the full duration of the study using Spearman correlations at 0-, 1-, 2-, and 3-month lags for each infection to confirm the strength of trend and seasonality components. For diseases with marked seasonality and overall trend, the strong serial synchronization reflected the similarities in temporal patterns. In some instances, prolonged periods of low incidence and occasional spikes could drive strong serial synchronization and thus be biased. For infections exhibiting well-marked irregularities, such as *Cyclospora* and *Yersinia*, serial synchronization metrics were likely to be biased, as evidenced by high values of L-skewness and L-kurtosis coefficients.

We then estimated three metrics of synchronization and compared them across infections within the same state and for each infection across states. Serial synchronization captures whether two infections or two locations share a similar temporal pattern. Phase-phase synchronization derives associations between peak timing estimates and identifies co-occurrences of outbreak timing and seasonal processes between infections or locations. Phase-amplitude synchronization examines seasonal behaviors of disease-state pairs and examines how the intensity of a seasonal peak of a foodborne illness varies in relation to its annual peak timing.

In order to conduct phase-phase and phase-amplitude synchronization analyses, we used annualized NBHR model (Model 1) estimates of seasonality characteristics: peak timing, amplitude, and their confidence intervals, using equations shown in Supplementary Table S3. Phase-phase and phase-amplitude synchronization metrics were calculated using Spearman correlations for 7 infections (excluding *Yersinia* and *Cyclospora*) in 11 locations (10 states and US national estimate) across a maximum of 22 years (varying by state). In total, we calculated 77 peak-amplitude pairs spanning a total of 1536 reporting years. Positive correlations for phase-phase synchronization indicate concordance of peak timing estimates between infections or states, e.g. if one infection or state peaks earlier in the calendar year, the other does also. Negative phase-phase synchronization correlations indicate that if one infection or state peaks earlier in the year, the other tends to peak later. Positive phase-amplitude synchronization indicates the magnitude of incidence increases when an infection peaks later

in the year. Negative phase-amplitude synchronization indicates the magnitude of incidence decreases when an infection peaks later in the year. Determination of the association significance is based on the standard test for Spearman correlation at $\alpha < 0.05$.

All statistical analyses were conducted using STATA (SE 15.1) software. All visualizations were designed and created using R Version 3.6.2 and Tableau Desktop 2019.1 software.

Received: 10 March 2020; Accepted: 17 September 2020
Published online: 15 October 2020

References

1. Centers for Disease Control and Prevention (CDC). *Estimates of Foodborne Illness in the United States*. National Center for Emerging and Zoonotic Infectious Diseases (NCEZID), Division of Foodborne, Waterborne, and Environmental Diseases (DFWED) https://www.cdc.gov/foodborneburden/ (2018).
2. McKay, B. *News Release: Mary's Harvest Fresh Foods, Inc. Recalls Wrap and Salad Meat Products due to Possible Salmonella and Listeria monocytogenes Contamination in Corn*. United States Department of Agriculture (USDA) Food Safety and Inspection Service (FSIS) https://www.fsis.usda.gov/wps/portal/fsis/topics/recalls-and-public-health-alerts/recall-case-archive/archive/2018/recall-094-2018-release (2018).
3. Foodborne Outbreak Investigation Outcomes—Response and Prevention. *United States Department of Agriculture (USDA) Food Safety and Inspection Service (FSIS)* https://www.fsis.usda.gov/wps/portal/fsis/topics/recalls-and-public-health-alerts/foodborne-illness-investigations (2020).
4. Shaw, F.L. *The Tremendous Cost of Foodborne Illnesses, and What to Do About It*. QSR https://www.qsrmagazine.com/outside-insights/tremendous-cost-foodborne-illnesses-and-what-do-about-it (2018).
5. Doering, C. Foodborne illness costs $152 billion annually. *Reuters* https://www.reuters.com/article/us-food-safety-study/foodborne-illness-costs-152-billion-annually-idUSTRE6220NO20100304 (2010).
6. A Foodborne Illness Outbreak Could Cost a Restaurant Millions, Study Suggests: Foodborne outbreaks can compromise a restaurant's annual profits, markedly outweighing preventative costs. *John Hopkins Bloomberg School of Public Health* https://www.jhsph.edu/news/news-releases/2018/a-foodborne-illness-outbreak-could-cost-a-restaurant-millions-study-suggests.html (2018).
7. Flynn, D. USDA: U.S. Foodborne Illnesses Cost More Than $15.6 Billion Annually. *Food Safety News (FSN)* https://www.foodsafetynews.com/2014/10/foodborne-illnesses-cost-usa-15-6-billion-annually/ (2014).
8. Centers for Disease Control and Prevention (CDC). FoodNet Surveillance. *National Center for Emerging and Zoonotic Infectious Diseases (NCEZID), Division of Foodborne, Waterborne, and Environmental Diseases (DFWED)* https://www.cdc.gov/foodnet/surveillance.html (2015).
9. Bennion, J. R., Sorvillo, F., Wise, M. E., Krishna, S. & Mascola, L. Decreasing listeriosis mortality in the United States, 1990–2005. *Clin. Infect. Dis.* **47**, 867–874 (2008).
10. Ebel, E. D. W. *et al.* Comparing characteristics of sporadic and outbreak-associated foodborne illnesses, United States, 2004–2011. *Emerg. Infect. Dis.* **22**, 1193–1200 (2016).
11. Crim, S. M. I. *et al.* Incidence and trends of infection with pathogens transmitted commonly through food—foodborne diseases active surveillance Network, 10 U.S. Sites, 2006–2013. *Morb. Mortal. Wkly. Rep.* **63**, 328–332 (2014).
12. Chui, K. K. H., Webb, P., Russell, R. M. & Naumova, E. N. Geographic variations and temporal trends of Salmonella-associated hospitalization in the U.S. elderly, 1991–2004: a time series analysis of the impact of HACCP regulation. *BMC Public Health*. **9**, 447 (2009).
13. Chui, K. K. H., Jagai, J. S., Griffiths, J. K. & Naumova, E. N. Hospitalization of the elderly in the United States for nonspecific gastrointestinal diseases: a search for etiological clues. *Am. J. Public Health*. **101**, 2082–2086 (2011).
14. Chui, K. K. H., Wenger, J. B., Cohen, S. A. & Naumova, E. N. Visual analytics for epidemiologists: understanding the interactions between age, time, and disease with multi-panel graphs. *PLoS ONE* **6**, e14683 (2011).
15. Martinez, M. E. The calendar of epidemics: Seasonal cycles of infectious diseases. *PLoS Pathog.* **14**, e1007327 (2018).
16. Naumova, E. N. *et al.* Seasonality in six enterically transmitted diseases and ambient temperature. *Epidemiol. Infect.* **135**, 281–292 (2007).
17. Williams, M. S., Golden, N. J., Ebel, E. D., Crarey, E. T. & Tate, H. P. Temporal patterns of Campylobacter contamination on chicken and their relationship to campylobacteriosis cases in the United States. *Int. J. Food Microbiol.* **208**, 114–121 (2015).
18. Mark Your Calendar: All Infectious Diseases Are Seasonal. Columbia Mailman School of Public Health https://www.mailman.columbia.edu/public-health-now/news/mark-your-calendar-all-infectious-diseases-are-seasonal (2018).
19. Lee, D., Chang, H. H., Sarnat, S. E. & Levy, K. Precipitation and Salmonellosis Incidence in Georgia, USA: interactions between extreme rainfall events and antecedent rainfall conditions. *Environ. Health Perspect.* **127**, 097005 (2019).
20. Jagai, J. S., Castronovo, D. A., Monchak, J. & Naumova, E. N. Seasonality of cryptosporidiosis: a meta-analysis approach. *Environ. Res.* **109**, 465–478 (2009).
21. Falconi, T. A., Cruz, M. S. & Naumova, E. N. The shift in seasonality of legionellosis in the USA. *Epidemiol. Infect.* **146**, 1824–1833 (2018).
22. Wenger, J. B. & Naumova, E. N. Seasonal synchronization of influenza in the United States older adult population. *PLoS ONE* **5**, e10187 (2010).
23. Acebrón, J. A., Bonilla, L. L., Vicente, C. J. P., Ritort, F. & Spigler, R. The Kuramoto model: a simple paradigm for synchronization phenomena. *Rev. Mod. Phys.* **77**, 137 (2005).
24. Imbs, J. Trade, finance, specialization, and synchronization. *Rev. Econ. Stat.* **86**, 723–734 (2004).
25. Pikovsky, A. S., Rosenblum, M. G., Osipov, G. V. & Kurths, J. Phase synchronization of chaotic oscillators by external driving. *Physica D.* **104**, 219–238 (1997).
26. Morales, A. J., Vavilala, V., Benito, R. M. & Bar-Yam, Y. Global patterns of synchronization in human communications. *J. R. Soc. Interface.* **14**, 20161048 (2017).
27. Naumova, E. N. & MacNeill, I. B. Seasonality assessment for biosurveillance systems. In *Advances in Statistical Methods for the Health Sciences* (eds Mesbah, M. *et al.*) 437–450 (Birkhäuser, Basel, 2007).
28. Tremblay, M. *et al.* Evaluation of the use of zero-augmented regression techniques to model incidence of campylobacter infections in foodnet. *Foodborne Pathog. Dis.* **14**, 587–592 (2017).
29. Fefferman, N. & Naumova, E. Innovation in observation: a vision for early outbreak detection. *Emerg. Health Threats.* **3**, 7103 (2010).
30. Alarcon Falconi, T. M., Estrella, B., Sempértegui, F. & Naumova, E. N. Effects of data aggregation on time series analysis of seasonal infections. *Int. J. Environ. Res. Public Health.* **17**, 5887 (2020).
31. Arsenault, J., Michel, P., Berke, O., Ravel, A. & Gosselin, P. Environmental characteristics associated with campylobacteriosis: accounting for the effect of age and season. *Epidemiol. Infect.* **140**, 311–322 (2012).

32. Chakraborty, A. *et al.* The descriptive epidemiology of yersiniosis: a multistate study, 2005–2011. *Public Health Rep.* **130**, 269–277 (2015).
33. Edge, V. L. *et al.* Syndromic surveillance of norovirus using over-the-counter sales of medications related to gastrointestinal illness. *Can. J. Infect. Dis. Med. Microbiol.* **17**, 235–241 (2006).
34. Hearnden, M., Skelly, C., Eyles, R. & Weinstein, P. The regionality of campylobacteriosis seasonality in New Zealand. *Int. J. Environ. Res. Public Health.* **13**, 337–348 (2003).
35. Jiang, C. *et al.* Climate change, extreme events and increased risk of salmonellosis in Maryland, USA: evidence for coastal vulnerability. *Environ. Int.* **83**, 58–62 (2015).
36. Moffatt, C. R., Glass, K., Stafford, R., D'Este, C. & Kirk, M. D. The campylobacteriosis conundrum: examining the incidence of infection with *Campylobacter* sp. in Australia, 1998–2013. *Epidemiol. Infect.* **145**, 839–847 (2017).
37. Miao, J. *et al.* Total coliforms as an indicator of human enterovirus presence in surface water across Tianjin city, China. *BMC Infect. Dis.* **18**, 542 (2018).
38. Omore, R. *et al.* Epidemiology, seasonality and factors associated with rotavirus infection among children with moderate-to-severe diarrhea in rural Western Kenya, 2008–2012: The Global Enteric Multicenter Study (GEMS). *PLoS ONE* **11**, e0160060 (2016).
39. Osei-Tutu, B. & Anto, F. Trends of reported foodborne diseases at the Ridge Hospital, Accra, Ghana: a retrospective review of routine data from 2009–2013. *BMC Infect. Dis.* **16**, 139 (2016).
40. Saha, S., Halder, M., Mookerjee, S. & Palit, A. Seasonal influence, enteropathogenic microbial load and diarrhoeal enigma in the Gangetic Delta, India: Present scenario and health implications. *J. Infect. Public Health.* **12**, 540–548 (2019).
41. Schmutz, C., Mausezahl, D., Jost, M., Baumgartner, A. & Mausezahl-Feuz, M. Inverse trends of Campylobacter and Salmonella in Swiss surveillance data, 1988–2013. *Euro. Surveill.* **21**, 30130 (2016).
42. Wang, X., Zhou, M., Jia, J., Geng, Z. & Xiao, G. A Bayesian approach to real-time monitoring and forecasting of chinese foodborne diseases. *Int. J. Environ. Res. Public Health.* **15**, 1740 (2018).
43. Zintl, A. *et al.* The prevalence of Cryptosporidium species and subtypes in human faecal samples in Ireland. *Epidemiol. Infect.* **137**, 270–277 (2009).
44. Foodborne Illness Outbreak Database. *About Outbreakdatabase.com*. Marler Clark LLP https://outbreakdatabase.com/about (2020).
45. Foodborne Illness Outbreak Database. 1996 Gastroenteritis Outbreak at a New York State Convenience Store Linked to Potato Salad, Macaroni Salad, and Ziti. *Marler Clark LLP* https://outbreakdatabase.com/details/1996-gastroenteritis-outbreak-at-a-new-york-state-convenience-store-linked-to-potato-salad-macaroni-salad-and-ziti/? (2020).
46. Foodborne Illness Outbreak Database. *Pork Chitterlings 2001*. Marler Clark LLP https://outbreakdatabase.com/details/pork-chitterlings-2001/?outbreak=yersin&organism=other&state=41 (2020).
47. Foodborne Illness Outbreak Database. *Chitterling 2002*. Marler Clark LLP https://outbreakdatabase.com/details/chitterling-2002/?outbreak=yersin&organism=other&state=41 (2020).
48. Foodborne Illness Outbreak Database. *Seneca Lake State Park Spraypark Recreational Water 2005*. Marler Clark LLP https://outbreakdatabase.com/details/chitterling-2002/?outbreak=yersin&organism=other&state=41 (2020).
49. Foodborne Illness Outbreak Database. *2015 Multistate Outbreak of Cyclospora*. Marler Clark LLP https://outbreakdatabase.com/details/2015-multistate-outbreak-of-cyclospora/?organism=Cyclospora&state=3 (2020).
50. Foodborne Illness Outbreak Database. *2013 Multistate Outbreak of Cyclospora cayetanensis*. Marler Clark LLP https://outbreakdatabase.com/details/2013-multistate-outbreak-of-cyclospora-cayetanensis/?organism=Cyclospora&state=3 (2020).
51. Foodborne Illness Outbreak Database. *2008 Outbreak of Cyclosporiasis at a Workplace or Banquet Facility Linked to Mixed Berries, California*. *Marler Clark LLP* https://outbreakdatabase.com/details/2008-outbreak-of-cyclosporiasis-at-a-workplace-or-banquet-facility-linked-to-mixed-berries-california/?organism=Cyclospora&state=1 (2020).
52. Horn, A. L. & Friedrich, H. Locating the source of large-scale outbreaks of foodborne disease. *J. R. Soc. Interface.* **16**, 20180624 (2019).
53. Schlaich, T., Horn, A. L., Fuhrmann, M. & Friedrich, H. A gravity-based food flow model to identify the source of foodborne disease outbreaks. *Int. J. Environ. Res. Public Health.* **17**, 444 (2020).
54. Horn, A. L. & Friedrich, H. The network source location problem in the context of foodborne disease outbreaks. In *Dynamics on and of Complex Networks* 151–165 (Springer, Berlin, 2017).
55. Gilliss, D. *et al.* Incidence and trends of infection with pathogens transmitted commonly through food—foodborne diseases active surveillance network, 10 US sites, 1996–2012. *MMWR. Morb. Mortal. Wkly. Rep.* **62**, 283 (2013).
56. United States Census Bureau. *1990s: County Tables*. https://www.census.gov/data/tables/time-series/demo/popest/1990s-county.html#statelist_6 (2016).
57. United States Census Bureau. *County Intercensal Tables: 2000–2010*. https://www.census.gov/content/census/en/data/tables/time-series/demo/popest/intercensal-2000-2010-counties.html (2017).
58. United States Census Bureau. *Annual Estimates of the Resident Population: April 1, 2010 to July 1, 2017*. https://factfinder.census.gov/faces/tableservices/jsf/pages/productview.xhtml?pid=PEP_2017_PEPANNRES&prodType=table (2018).
59. Hosking, J. L-Moments: analysis and estimation of distributions using linear combinations of order statistics. *J. R. Stat. Soc. B.* **52**, 105–124 (1990).

Acknowledgements

The authors would like to thank Sofia Babool, Paulina Kaminski, Maia Tarnas, Dr. Tania Mercedes Alarcon Falconi, and Dr. Meghan Hartwick for editorial and technical assistance.

Author contributions

R.S. contributed to data extraction, formal analysis, writing, reviewing and editing. B.Z. contributed to data validation, conceptualization of visual aids, and visualization creation, writing, reviewing and editing. E.N. contributed to methodology development, review and editing, supervision, project administration and funding acquisition.

Funding

This research is based upon work supported in part by the Office of the Director of National Intelligence (ODNI), Intelligence Advanced Research Projects Activity (IARPA), via 2017-17072100002. The views and conclusions contained herein are those of the authors and should not be interpreted as necessarily representing the official policies, either expressed or implied, of ODNI, IARPA, or the U.S. Government. The U.S. Government is authorized to reproduce and distribute reprints for governmental purposes notwithstanding any copyright annotation therein. The research was also in part supported by the United States Department of Agriculture (USDA) National Institute of Food and Agriculture (NIFA) Cooperative State Research, Education, and Extension Service Fellowship, via grant award 2020-38420-30724.

Competing interests
The authors declare no competing interests.

Additional information
Supplementary information is available for this paper at https://doi.org/10.1038/s41598-020-74435-9.

Correspondence and requests for materials should be addressed to E.N.N.

Reprints and permissions information is available at www.nature.com/reprints.

Publisher's note Springer Nature remains neutral with regard to jurisdictional claims in published maps and institutional affiliations.

Open Access This article is licensed under a Creative Commons Attribution 4.0 International License, which permits use, sharing, adaptation, distribution and reproduction in any medium or format, as long as you give appropriate credit to the original author(s) and the source, provide a link to the Creative Commons licence, and indicate if changes were made. The images or other third party material in this article are included in the article's Creative Commons licence, unless indicated otherwise in a credit line to the material. If material is not included in the article's Creative Commons licence and your intended use is not permitted by statutory regulation or exceeds the permitted use, you will need to obtain permission directly from the copyright holder. To view a copy of this licence, visit http://creativecommons.org/licenses/by/4.0/.

© The Author(s) 2020

SCIENTIFIC DATA

Check for updates

OPEN

ANALYSIS

An analecta of visualizations for foodborne illness trends and seasonality

Ryan B. Simpson, Bingjie Zhou, Tania M. Alarcon Falconi & Elena N. Naumova ✉

Disease surveillance systems worldwide face increasing pressure to maintain and distribute data in usable formats supplemented with effective visualizations to enable actionable policy and programming responses. Annual reports and interactive portals provide access to surveillance data and visualizations depicting temporal trends and seasonal patterns of diseases. Analyses and visuals are typically limited to reporting the annual time series and the month with the highest number of cases per year. Yet, detecting potential disease outbreaks and supporting public health interventions requires detailed spatiotemporal comparisons to characterize spatiotemporal patterns of illness across diseases and locations. The Centers for Disease Control and Prevention's (CDC) FoodNet Fast provides population-based foodborne-disease surveillance records and visualizations for select counties across the US. We offer suggestions on how current FoodNet Fast data organization and visual analytics can be improved to facilitate data interpretation, decision-making, and communication of features related to trend and seasonality. The resulting compilation, or analecta, of 436 visualizations of records and codes are openly available online.

Introduction

Disease surveillance systems worldwide face increasing pressure to maintain and distribute data in usable formats with clearly communicated visualizations to promote actionable policy and programming responses[1]. Decade-long efforts to sustain surveillance systems improve early outbreak detection, infection containment, and mobilization of health resources[1–4] and create adaptive, near-time forecasts for disease outbreaks[5,6]. Web-based platforms provide access to more accurate, timely, and frequent surveillance data. The World Health Organization's (WHO) FluNet, for example, provides time-referenced data on worldwide influenza[7]. Publicly available downloads increase the flexibility for analyses and enables adaptive research due to frequent and timely reporting.

The pandemic of 2019 novel coronavirus disease (COVID-19) serves as a vivid demonstration of how limited access to publicly available high-quality data can stymy research. As the quantity and diversity of data available for processing, synthesizing, and communicating increases, new visual analytics, including complex multi-panel plots, must be considered to monitor trends, investigate seasonality, and support public health planning[8]. These visualizations, and the methodologies used to generate them, must be standardized to enable comparability across time periods, locations, at-risk populations, and pathogens. However, current surveillance systems, including foodborne disease surveillance in the United States, often compress time series records to simplistic annual trends[9–13] and describe seasonality by the month(s) with the highest cases per year or the first month of outbreak onset[14–19]. Visualizations using these annual trends or broad assessments of seasonality fail to utilize the full complexity of surveillance data and in some cases may be misleading. More specifically, these visualizations fail to provide detailed examination of how long-term trends change over time, how seasonality estimates vary by year or across locations, or how peak timing and amplitude estimates could change over time.

The CDC Foodborne Disease Active Surveillance Network (FoodNet) provides preprocessed population-based foodborne-disease surveillance records and visualizations via FoodNet Fast, a publicly available data portal[20,21]. The FoodNet Fast platform contains rich demographic data, including age group, gender, and ethnic group, valuable for a broad spectrum of analyses. The visualizations aim to aid users in identifying trends of nine laboratory-confirmed foodborne diseases in select counties from ten US states and nationally. However, in the present form and due to substantial data compression, the available data and visualizations provided are limited in scope preventing the

Tufts University Friedman School of Nutrition Science and Policy, Boston, USA. ✉e-mail: elena.naumova@tufts.edu

characterization of inter-annual trends and seasonality characteristics and comparisons across locations, diseases, and time[14,15,17,22–24]. The data portal allows researchers to download time series from a public domain. After downloading, processing, and analyzing the data, we created an analecta of visualization techniques enabling inter-annual and sub-annual comparisons between diseases and locations with respect to long-term trends and seasonal oscillations.

Analects, or analecta, is defined as a compilation of select passages from the work of an author[25]. Our analecta includes two compilations: (1) a collection of FoodNet Fast datasets collated into usable and analyzable time series data, and (2) an anthology of effective and informative visualizations for communicating information on disease trends and seasonality. By merging FoodNet Fast datasets and calculating disease rates from counts, we facilitate the comparison of spatial and temporal patterns of foodborne diseases, and detection of potential outbreaks and their synchronization. The presented anthology eases data interpretation, decision-making, and communication of features related to trend and seasonality and can be replicated for other longitudinal disease surveillance databases to support public health interventions.

In this paper, we describe the process of compiling, organizing, and visualizing surveillance time series data using FoodNet Fast as an example[21]. We demonstrate how current FoodNet Fast visual analytics can be improved to provide a clear yet comprehensive description of trends and seasonality features. We emphasize the utility of multi-panel graphs[8] for describing trends over time and features of seasonality, including disease peak timing and amplitude. We also provide guides on how to explore and compare trends and seasonality between multiple diseases and geographic locations. As surveillance systems offer a time-referenced data repository, analects of data visualizations can show how diseases change over time. Such a tool can help ensure the longevity of data and information to better understand and evaluate the efficacy of public health programming over time. The resulting analecta of 436 visualizations for foodborne diseases, original and processed data, and the codes used to produce visualizations are available at our website (https://sites.tufts.edu/naumovalabs/analecta/).

Methods

FoodNet fast data compilation. The FoodNet Fast platform provides publicly available data for laboratory-confirmed diseases caused by seven bacteria [*Campylobacter*, *Listeria*, *Salmonella*, *Shigella*, Shiga toxin-producing *Escherichia coli* O157 and non-O157 (STEC), *Vibrio*, and *Yersinia enterocolitica*] and two protozoa (*Cryptosporidium* and *Cyclospora*) in counties from 10 states: California (CA), Connecticut (CT), Georgia (GA), Minnesota (MN), and Oregon (OR) since 1996; Maryland (MD) and New York (NY) since 1998; Tennessee (TN) since 2000; Colorado (CO) since 2001; and New Mexico (NM) since 2004. National estimates are generated from the sum of data across these 10 states, which represent approximately 15% of the US population[20,21].

FoodNet Fast allows data download and visualization of these diseases for a user-specified time period. Data downloads include information on the incidence of confirmed cases, monthly percentage of confirmed cases, distribution of cases by pathogen, and totals of cases, hospitalizations, and deaths. For multi-year periods, the portal aggregates totals and monthly percentages into single statistics for the full time period selected rather than showing individual years. This aggregation ensures case anonymity but monthly time units minimize the refinement of trend and seasonality analyses. To calculate monthly percentages of confirmed cases for all diseases in one year and one location, we had to download each state-year combination individually, for a total of 221 files in MS Excel format.

To create a time series of total monthly cases by pathogen and location, we used data from two tables in each data download: annual counts of confirmed cases (long format) and monthly percentage of confirmed cases (wide format). We transposed the monthly percentages of confirmed cases from wide to long format and then multiplied them by the annual counts of confirmed cases (Supplementary Figure S1). Since the provided monthly percentages are rounded to 1 digit in the data download, calculated counts slightly under- or over-estimate annual totals. We did not round non-integer cases in our calculated time series to best preserve the monthly distribution of cases from the original data download. A monthly time series of confirmed cases of hospitalizations or deaths could not be reconstructed as described because no information is provided on their monthly percentages. We next calculated disease rates using confirmed monthly cases and annual population data. Rates are preferred over counts since changes in counts could be a direct result of changes in the population catchment area of a surveillance system. The number of counties and states monitored in FoodNet increased between 1996 and 2004 and has remained constant to date since (Supplementary Table S1).

We downloaded county-level population estimates from the 1990, 2000, and 2010 US Census Bureau inter-annual census reports, which provide annual population estimates[26–28]. We then estimated state-level FoodNet population catchment area by adding all mid-year (July 1st) populations of surveyed counties monitored in each year. Next, we calculated the United States population catchment area by adding all state-level estimates for all surveyed counties for each year. Finally, we developed a time series of monthly rates per 1,000,000 persons for each pathogen and location by dividing monthly counts by annual population estimates and multiplying this quotient by 1,000,000. In addition to monthly rates, we calculated yearly rates by adding all monthly counts each year, dividing by the annual population, and multiplying this quotient by 1,000,000.

Modeling trends and seasonality. We estimated trend and seasonality characteristics using Negative Binomial Harmonic Regression (NBHR) models, which are commonly used to analyse count-based time series records with periodic fluctuations[29–31]. These models include harmonic terms representing sine and cosine functions, which allow us to fit periodic oscillations. The regression parameters for these harmonic terms serve as a base for estimating important characteristics of seasonality: when the maximum rate occurs (peak timing) and the magnitude at that peak (amplitude). We calculated peak timing, amplitude, and their confidence intervals from NBHR model coefficients using the δ-method, which allow us to transform the regression coefficients of the model to seasonality characteristics based on the properties of the basic trigonometric functions (Supplementary

Table S2)[29,30]. To estimate annualized seasonality characteristics, we applied a NBHR model for each study year and location with the length of the time series set to 12 to represent the months of the year. We also estimated seasonality characteristics for the full time period. To show average trends across the entire 22-year period, we fit a NBHR model with three trend terms (linear, quadratic, and cubic) where the length of the time series varied according to when FoodNet began surveying that location from 168 to 264 months. The selection of three polynomial terms was driven by the clarity of interpretation as a monthly increase and the potential for overall acceleration or deceleration, although other ways of assessing the trend such moving averages and spline functions could be also explored.

Plot terminology. We develop multi-panel visualization techniques using the best practices of current data visualization resources[32,33] and our own research[8,34,35]. A multi-panel plot, as defined by our earlier work, "involves the strategic positioning of two or more graphs sharing at least one common axis on a single canvas[8]." These plots can effectively illustrate multiple dimensions of information including different time units (e.g. yearly, monthly), disease statistics (e.g. pathogens, rates, counts), seasonality characteristics (e.g. peak timing, amplitude), and locations (e.g. state-level, national). We use the following common, standardized terminology across visualizations to ensure comprehension:

- Disease – each of the nine reported FoodNet infections, including campylobacteriosis (Camp), listeriosis (List), salmonellosis (Salm), shigellosis (Shig), infection due to Shiga toxin-producing *Escherichia coli* O157 and non-O157 (Ecol), vibriosis (Vibr), infection due to *Yersinia enterocolitica* (Yers), cryptosporidiosis (Cryp) and cyclosporiasis (Cycl)
- Monthly Rate – monthly confirmed cases per 1,000,000 persons
- Yearly Rate – total confirmed cases in a year divided by the mid-year population of all surveyed counties in that location (cases per 1,000,000 persons)
- Frequency – the number of months reporting the disease rates in the same range
- Peak Timing – the time of year according to the Gregorian calendar that a disease reaches its maximal rate; for monthly time series, peak timing ranges in [1, 13[, i.e. from 1.0 (beginning of January) to 12.9 (end of December)
- Amplitude – the mathematical amplitude, or the midpoint of relative intensity; for NBHR models, the amplitude estimate reflects the ratio between the disease rate at the peak (maximum rate) and the disease rate at the midpoint (median rate)
- FoodNet Surveyed County – the counties under FoodNet surveillance as of 2017
- Non-Surveyed County – all remaining counties within a surveillance state as of 2017.

We present our analecta of visualizations allowing to describe trend, examine seasonal signatures, curves depicting characteristic variations in disease incidence over the course of one year, and understand features of seasonality, such as peak timing and amplitude across locations and diseases. We illustrate all visualizations using salmonellosis for the United States from 1996–2017. The full analecta with time series data and code are available on our website (https://sites.tufts.edu/naumovalabs/analecta/) with data and code also available on figshare[36].

Results

Describing trend. The interpretability of trends in a time series plot is greatly affected by the length and units of the time series. FoodNet Fast aggregates data annually, as shown in Supplementary Figure S2, which provides clear, concise information on annual rates. In this example, the rate of salmonellosis remains largely unchanging over time with distinct outbreaks seen in 1999 and 2010. As expected, by compressing data to annual rates, Supplementary Figure S2 masks within-year trends of disease rates. FoodNet reports and publications similarly tend to show only inter-annual changes in disease counts or rates[9–13,37,38]. Without more granular within-year variations, the viewer cannot determine if increased yearly rates are driven by erratic outbreaks in a specific month or higher rates across all months of the year.

To capture within-year trends, we propose a multi-panel plot that combines information on monthly rates, inter-annual trends, and the frequency distribution of rates by utilizing the shared axes of individual plots (Fig. 1). The right panel of Fig. 1 provides a time series of monthly rates with a NBHR model fit with three trend terms (linear, quadratic, and cubic). The inclusion of polynomial terms allows us to capture long-term trends (linear term) and their acceleration and deceleration over time (quadratic and cubic terms). The predicted trend line is shown in blue and its 95% confidence interval is in grey shades. The estimated median monthly rate is shown in red. The left panel depicts a rotated histogram of rate frequencies indicating the right-skewness of the monthly rate distribution. The histogram shares the vertical monthly rate-axis with the time series plot and is essential for connecting two concepts: the distribution of monthly counts on the base of their frequency and the distribution of monthly counts over time. Two pictograms refer to the selected pathogen and location.

Figure 1 shows the stability of seasonal oscillation in salmonellosis over time series with increased rates from 1998–2010 followed by a gradual decrease in rates through 2017. While preserving the within-year seasonal fluctuations, the plot provides additional information. Alternating background colours help distinguish differences in the shape of seasonal curves between adjacent years. An increasingly darker hue for the monthly rate values distinguishes more recent data from more historic data. Contrasting background colours mixed with a gradual intensity of line hues, saturation, brightness, and transparency allow for greater focus and attention to trends in the data[32–34].

The rotated histogram in the left panel of Fig. 1 shows the distribution of monthly rates and its degree of skewness due to months with high counts. We include the red median line to provide the most appropriate measure of central tendency for the skewed distribution. The shared vertical axis helps readers track those high values to a

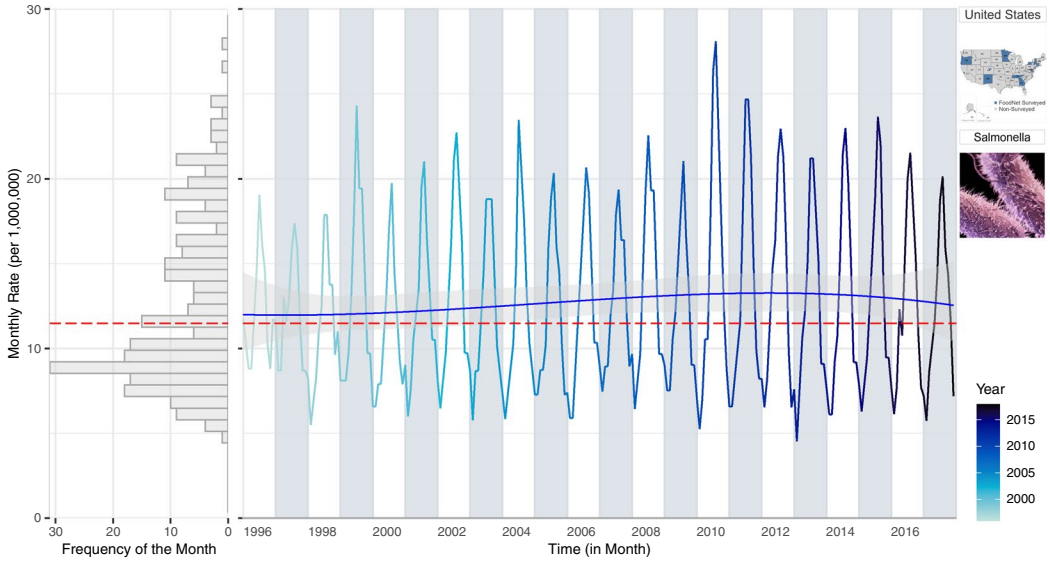


Fig. 1 A multi-panel plot: a rotated histogram of monthly rate frequency (left panel) sharing the vertical monthly rate-axis with the time series of monthly rates (right panel) for salmonellosis in the US from 1996–2017. The red line indicates the median rates while the blue line is a NBHR model fit with seasonal oscillators and three (linear, quadratic, and cubic) trend terms.

specific month in the time series. The distribution also justifies the use of negative binomial regression models to evaluate temporal patterns. By supplementing the time series plot with the distribution of monthly rates, we show a visual rationale for using appropriate analytical tools (negative binomial model, in this case) for calculating inter-annual trends.

Examining seasonal signatures. FoodNet reports describe seasonal patterns with the month with the highest cases per year[13]. Supplementary Figure S3 provides an example of a typical seasonal curve from the FoodNet Fast portal. The estimates are the average percentage of confirmed cases per month for salmonellosis in the US from 1996–2017. This visualization provides easily computed and interpreted information on seasonality: on average, salmonellosis cases peak in August for this 22-year period. However, the data compression and use of relative measurements, such as average percentages, masks variability in monthly values across years. Supplementary Figure S3 leaves certain questions unanswered. Do seasonal patterns vary by year? Is this gradual incline and decline in the signature stable over the 22-years or masking frequent erratic outbreaks? What is the variability in cases at each time of year? What are the actual rates for each month of the year for each year?

To better understand annual differences in seasonal behaviors, we propose a multi-panel plot that incorporates annual seasonal signatures, summary statistics of monthly rates, and radar plots (Fig. 2). Given varying visual perceptions of these three ways of presenting seasonal patterns, we offer side-by-side comparisons that aim to increase comprehension. The top-left panel provides an overlay of all annual seasonal signatures, a set of curves depicting characteristic variations in disease incidence over the course of one year, where line hues become increasingly darker with more recent data and a red line indicates median monthly rates, as in Fig. 1. The bottom-left panel provides a set of box plots for each month that aggregates information over the study period and provides essential summary statistics, including the median rate values and the measures of spread. The shared horizontal axis allows the two plots to be compared across the years using identical scales. To provide visual context, background colours were used to indicate the four seasons (winter, spring, summer and autumn). The right panel provides overlaying monthly rates using a radar plot where time is indicated on the rotational axis and rates are indicated on the radial axis. The radar plot emphasizes the periodic nature of seasonal variations in one continuous line with graduating colours. The colour hue of the lines, background colour, median line colour and the axis scales are uniform across all three panels. We also repeat the pictograms to refer to the selected pathogen and location.

For salmonellosis, disease rates are highest in the summertime (with peaks in July and August) and lowest during the wintertime (with a well-defined February nadir). Rate increases and decreases during equinox periods indicate bacterial growth rates due to more and less favourable climate conditions, respectively.

The top-left panel of Fig. 2 disaggregates annual seasonal signatures to show the stable seasonal peak timing of salmonellosis across all years. This stable behavior reflects the average monthly percentages shown in Supplementary Figure S3. This panel provides the seasonal signatures of salmonellosis rates and helps to better understand the annual variations hidden in Supplementary Figure S3. Supplementary Figures S4 and S5 provide examples of how occasional irregular outbreak behaviors could be identified using this annual overlay plotting technique.

The bottom-left panel of Fig. 2 overcomes another deficiency of Supplementary Figure S3 of masking variations. This panel provides box plots depicting the median monthly rate (red), interquartile range (box), 95%

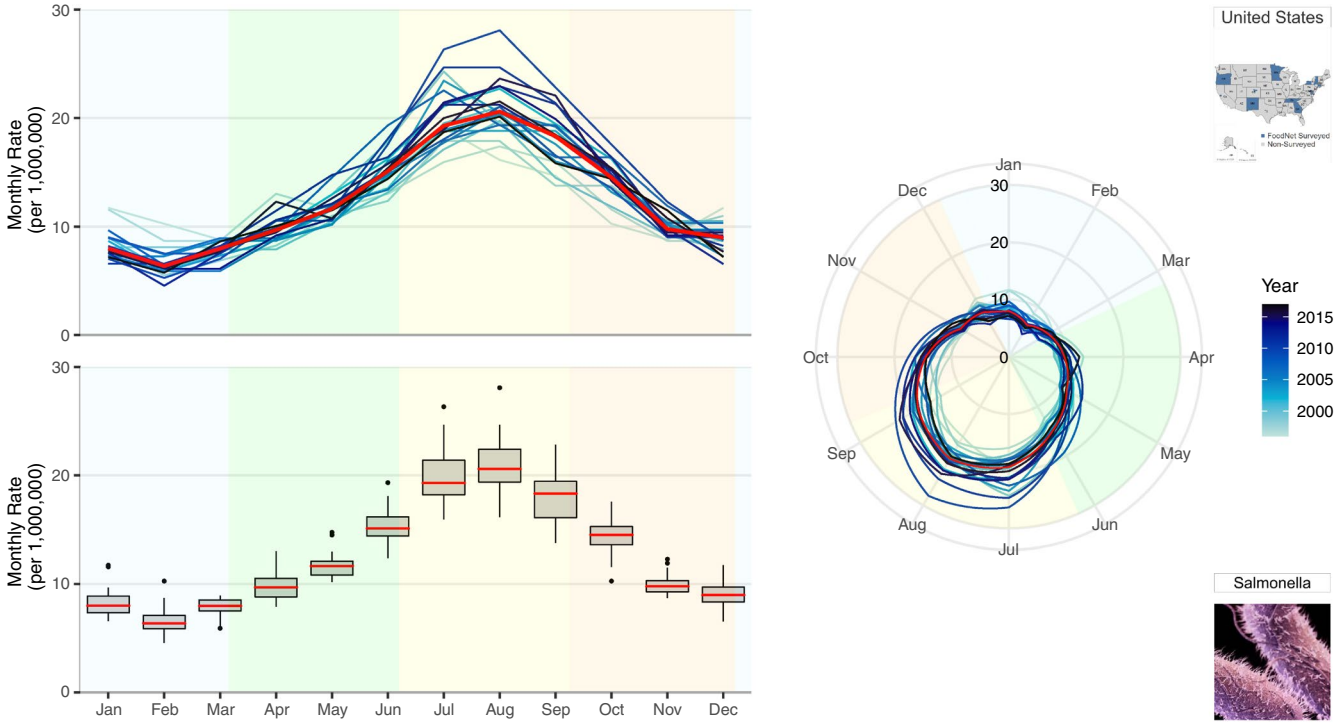


Fig. 2 A multi-panel plot for visualizing seasonal signatures of salmonellosis monthly rates in the US from 1996–2017. This includes overlaid annual time series plots of monthly rates, a box plot of average monthly rates for the 22-year period, and overlaid annual radar plots of monthly rates. Background colours indicate the four seasons defined by solar solstices and equinoxes: winter (blue), spring (green), summer (yellow), and autumn (orange).

confidence interval (whisker), and outliers or potentially influential observations (markers) over the 22-year period. Measures of distribution spread provide an insight for the dispersion of rates in each month: the variability of salmonellosis rates decreases in winter months closer to the February nadir but increases in summer months of July and August closer to the seasonal peak. Unusually high values are indicative of erratic behavior characterized by spikes in specific months and years.

The right-hand panel of Fig. 2 further emphasizes the periodic nature and the positioning of the seasonal peaks and nadirs. Radar or spider plots describe time using a rotational axis where the radial distance from the centre of the plot depicts rate magnitude[39–42]. Radial axes, compared to perpendicular axes, show annual fluctuations as a continuous flow. This more clearly demonstrates declines of salmonellosis rates during nadir months (November to March) without the visual discontinuity of left panel visuals.

To capture the advantage of a multi-panel plot (Fig. 3), we incorporate the boxplot from Fig. 2 (lower left panel) with a calendar heatmap containing 264 monthly rate values. In the heatmap, information for each individual year is shown as stacked rows of width 12 (for each month of the year) where cell colour intensity represents the magnitude of monthly rates. Like Fig. 2, the heatmap illustrates the highest rates (shown as the darker cells) are in July and August. Compared to stacked line plots, however, Fig. 3 provides an individual row for each year of the time series, allowing for greater decomposition, differentiation, and comparison of seasonal signatures across years. In this plot, seasonal changes are shown horizontally from left to right - from January to December and the yearly trend transition can be observed in a vertical view from bottom to top-from year 1996 to 2017 in the right panel.

While Fig. 2 provides the annual variability of seasonal patterns, monthly rate values for each year are difficult to ascertain. Instead, the emphasis is placed on similarities and differences of the seasonal curvature over time. In Fig. 3, the attention shifts to comparing the intensity of rates per month of the year across years. Here, we evaluate which months of the year are most intense across years using the intensity of each cell's colour hue to describe the intensity of rates. The Fig. 3 panel integrates information on both trends and seasonality along with the individual monthly values unlike any of the previously shown visualizations. Yearly rates provide a bar graph for comparing fluctuations in inter-annual rates while the adjacent heatmap indicates the month(s) driving these fluctuations. In doing so, the calendar heatmap identifies whether inter-annual changes are driven by sporadic outbreaks or increased seasonal magnitude of rates. At the same time, the shared axis box plot provides an overview of the average seasonal signature for the entire time series, as emphasized in Fig. 2.

Understanding seasonal features. Detailed characterization of the timing and intensity of seasonal peaks requires a standardized estimation of peak timing and amplitude. This standardization improves upon implemented techniques of comparing months with the highest cases in a given year by applying the δ–methods to

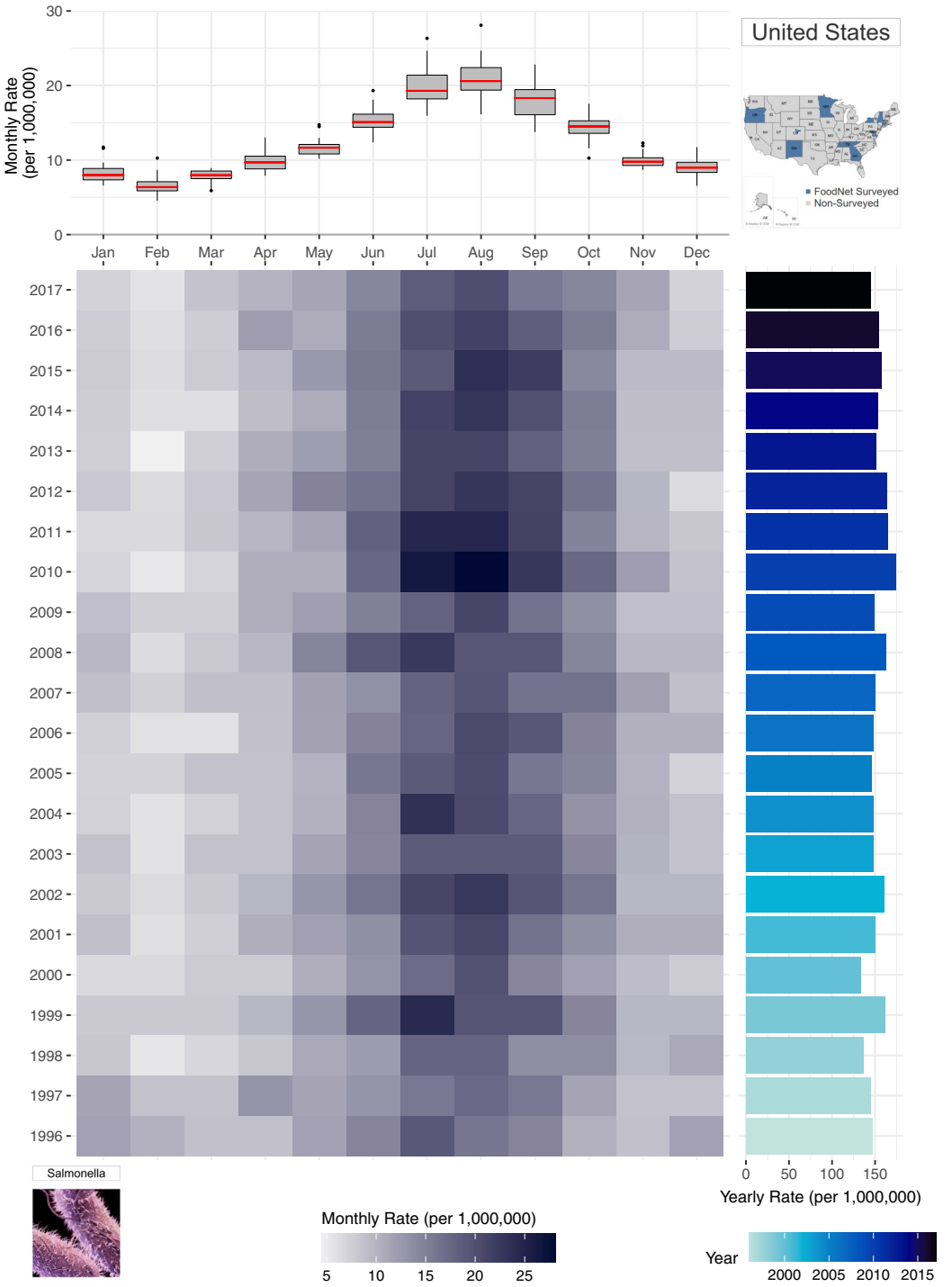


Fig. 3 A multi-panel plot for improved visualization of the annual seasonal signatures of monthly rates of salmonellosis in the US from 1996–2017. The top panel provides a box plot of monthly rates for each month of year. The bottom heatmap shows the distribution of monthly rates for each year where darker hues indicate greater rates. The right panel provides a rotated bar graph of yearly rates.

NBHR model parameters[29,30]. Average seasonality characteristics can be estimated across the full time series while annual estimates allow for more granular comparisons between years. To depict point estimates and confidence intervals of seasonality characteristics, we use forest plots - a technique commonly used in meta-analyses[18,43,44]. We develop a multi-panel forest plot to depict annual peak timing, annual amplitude, and their joint distribution, to better understand the relationship among the seasonal features and how it changes over time (Fig. 4).

Figure 4 is a multi-panel plot that incorporates two forest plots (one each for annual peak timing and amplitude estimates) and one scatterplot (for peak timing and amplitude) to describe seasonality features. The top-left

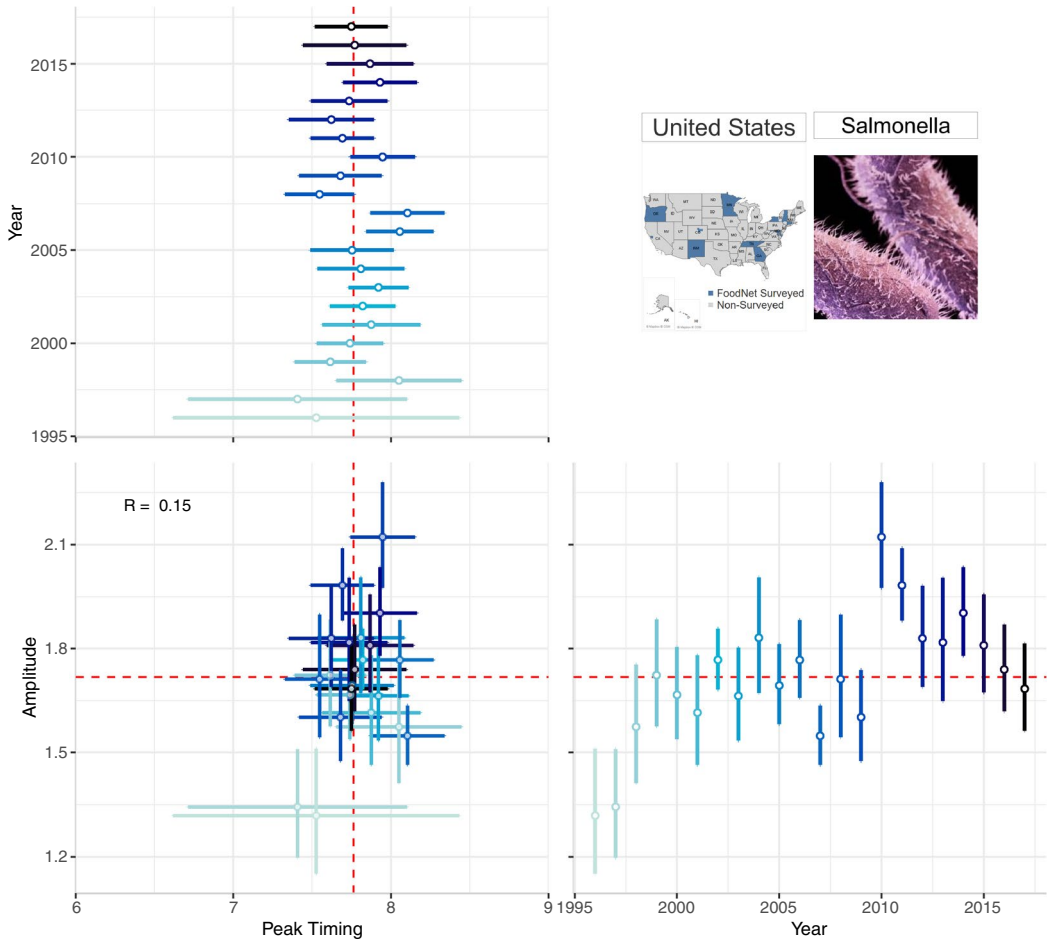


Fig. 4 A multi-panel plot for visualizing the annual peak timing and amplitude of salmonellosis in the US from 1996–2017. The top-left panel shows the peak timing of salmonellosis by year; the bottom-right panel shows the annual amplitude by year. The bottom-left panel shows their combination: a scatterplot between peak timing and amplitude. Marker colour intensity indicates more historic vs. more recent data, horizontal and vertical whiskers provide measures of uncertainty, and red lines indicate median peak timing and amplitude across 22 years.

panel shows peak timing estimates (as month of the year, ranging from 1.0 (beginning of January) to 12.9 (end of December) - horizontal axis) for each study year (vertical axis). The bottom-right panel shows amplitude estimates where the horizontal axis indicates the study year and the vertical axis shows the amplitude (ratio between the disease rate at peak and the median rate). The bottom-left corner shows the scatterplot of peak timing (horizontal axis) and amplitude (vertical axis) with markers representing each pair of annual estimates. Measures of uncertainty (95% confidence intervals) are reflected in error bars of each marker; dashed red lines show median peak timing and amplitude estimates.

Forest plots in Fig. 4 provide a compact, clear, and comprehensive visual describing the stability of peak timing and amplitude, even without showing the entire seasonal signature. For example, salmonellosis peak timing and amplitude vary little each year indicating strong, stable seasonal peaks in July and August. Consistent peak timing means practitioners could time preventive strategies, increase awareness for foodborne illnesses to prevent transmission, and inform food retailers of when food safety inspections should be in higher demand within their supply chains. Consistent amplitude estimates show that the intensity of salmonellosis varies little over time, suggesting that federal food safety regulations have not greatly influenced the number of salmonellosis cases annually. This type of information is likely to benefit FoodNet Fast users.

Supplementary Figure S6 provides an example of how a sporadic outbreak behavior can be depicted by forest plots of peak timing and amplitude estimates for shigellosis in NY. The lack of seasonality for shigellosis is shown by the broad confidence intervals for peak timing, spanning the entire year and beyond.

Drawing comparisons across locations. Supplementary Figure S7 provides an example bar chart showing differences in the average annual incidence of salmonellosis for the ten FoodNet-surveyed states. As with other FoodNet visualizations, data has been compressed to show only average annual estimates. Like in Fig. 1, annual rates mask within-year seasonal variations, calling into question if differences in states are driven by single year outbreaks. The alphabetical organization of the horizontal axis makes states ranking and comparison more difficult than if they were ordered from highest to lowest rates. To ease comparisons of a single disease across

geographic locations, we generated two multi-panel plots (Figs. 5 and 6). These plots mirror the same techniques shown above but include multiple shared axes and multiple locations to draw spatial comparisons.

Supplementary Figure S8 follows the same design as Fig. 3; we replicate this design for salmonellosis in all FoodNet-surveyed states. We present all states in one plot in a descending order by the sum of yearly rates in each state and display all available data so that state level patterns can be compared. The box plot in the top panel provides an overview of the seasonal signature for the entire US. The bottom panel disaggregates the entire US by states. As shown, all states share similar peak timing in July and August for almost every surveillance year from 1996–2017. For some states, like GA and CA, rates are densely concentrated from July to September with rapid decline from September to February and gradual incline from February to July. For other states, like NY and OR, seasonal peaks are much less pronounced and rate differences are smaller between months. Clear indication of missing data provides additional information on differences in reporting completeness not captured by previous figures.

While heatmaps provide information on seasonal signatures, yearly rate bar graphs (right panel) capture state-level trends over time. States are stacked in the order of total cases from 1996–2017, showing differences in the intensity of salmonellosis infection across states. Comparisons within states between years help identify inter-annual rate changes over time. For example, while MD and CA have generally declined in annual rates over the 22-year period, GA rates increased from 1996–2012 and steadily declined from 2012–2017. In combination with heatmaps, yearly rates also allow for detailed assessment of sporadic outbreaks. For example, erratic outbreaks came from two monthly spikes in April and June for CT in 1997 while for NM in 2000 a multi-month outbreak lasted from May to July.

By using shared horizontal and vertical axes, this plot eases the comparison of disease rates across months, years and states. It also helps to determine hotspots and detect potential co-occurrences of infection in different states. Moreover, the plot can be periodically updated by adding new information, offering a sustainable approach to make consistent comparisons between historical data and data captured in the future.

To compare seasonality features across locations, we designed a multi-panel plot similar to Fig. 4 to show average peak timing and amplitude estimates over the 22-year period for each state. In Fig. 6 the top-left panel plots peak timing estimates ordered from the earliest (OR) to latest (GA) peak timing while the bottom-right panel plots amplitude estimates in order of magnitude. Marker and line colours are used to differentiate the seasonality feature estimate and its measure of uncertainty between states. The bottom-left panel shows the relationship between peak timing and amplitude across states.

Comparisons across diseases. Supplementary Figure S8 provides an example of FoodNet Fast bar chart showing differences in the total confirmed infections for each of the nine surveyed pathogens in the US from 1996–2017. The visual shows that infections due to *Campylobacter* and *Salmonella* have the highest cumulative counts of infections while *Cyclospora* has the lowest counts. While depicting these differences clearly, this visual lacks sufficient specificity for drawing more intricate comparisons between infections. How are counts or rates distributed by year? What are the within-year variations of rates by pathogen? How do seasonal signatures and their variability differ by pathogen? Can axes be reordered or recalculated for easier comparisons between pathogen counts or rates? We propose two multi-panel plots (Figs. 7 and 8) that improve the comparisons of multiple diseases for a given geographic location.

Figure 7 replicates the plot design of Fig. 5 but emphasizes comparisons between pathogens for a single location. Instead of a seasonal signature box plot, the top panel provides a scatterplot to illustrate the peak timing and amplitude of each pathogen. In combination with the heatmap in the bottom panel, these plots illustrate the strong seasonality of salmonellosis, campylobacteriosis, and STEC in July and August and cryptosporidiosis in August. These seasonal peaks are consistent across almost all years suggesting a stable seasonal periodicity and strong alignment between infections. In contrast, infections caused by *Yersinia enterocolitica*, vibriosis, listeriosis, and cyclosporiasis have much less pronounced seasonality and monthly rates much lower than salmonellosis or campylobacteriosis. Yearly rates, shown in the right panel, indicate erratic outbreak behaviors for cyclosporiasis. Given sizable differences in rates across diseases we applied a high-order calibration colour scheme.

We also provide the same multi-panel, shared-axis visualization design seen in Fig. 6 for comparisons across pathogens. Figure 8 includes a forest plot of peak timing by disease pathogen (top-left panel), a forest plot of amplitude by pathogen (bottom-right panel), and a scatterplot between peak timing and amplitude estimates (bottom-left panel). As in Fig. 6, average peak timing and amplitude estimates are calculated using NBHR models for the entire 22-year time series. Comparisons between diseases allow for understanding the alignment of seasonal processes across pathogens as well as shared relative magnitudes in a specific location. In our case, most of the pathogens peak during the summertime except cyclosporiasis. However, if the selected diseases peak during winter months, we recommend adjusting the starting and ending months to center these peaks in the figure.

Discussion

In this study we offered ways of thinking on how public data platforms can be improved by using visual analytics to provide a comprehensive description of trends and seasonality features in reported infectious diseases. We emphasize the utility of multi-panel graphs by showing side-by-side different methods of depicting trends over time and features of seasonality, including disease peak timing and amplitude. We provided visual tools to show trends (Fig. 1), examine seasonal signatures (Figs. 2 and 3) and their characteristics (Fig. 4), compare diseases across locations for trends (Fig. 5) and seasonal signatures (Fig. 6), and drawing comparisons across pathogens for trends (Fig. 7) and seasonal signatures (Fig. 8). We also provide guides on how to explore and compare trends and seasonality between multiple diseases and geographic locations using FoodNet Fast data. Given varying visual perceptions, we offer side-by-side comparison of different tools aiming to increase comprehension and faster adoption of efficient graphical depictions.

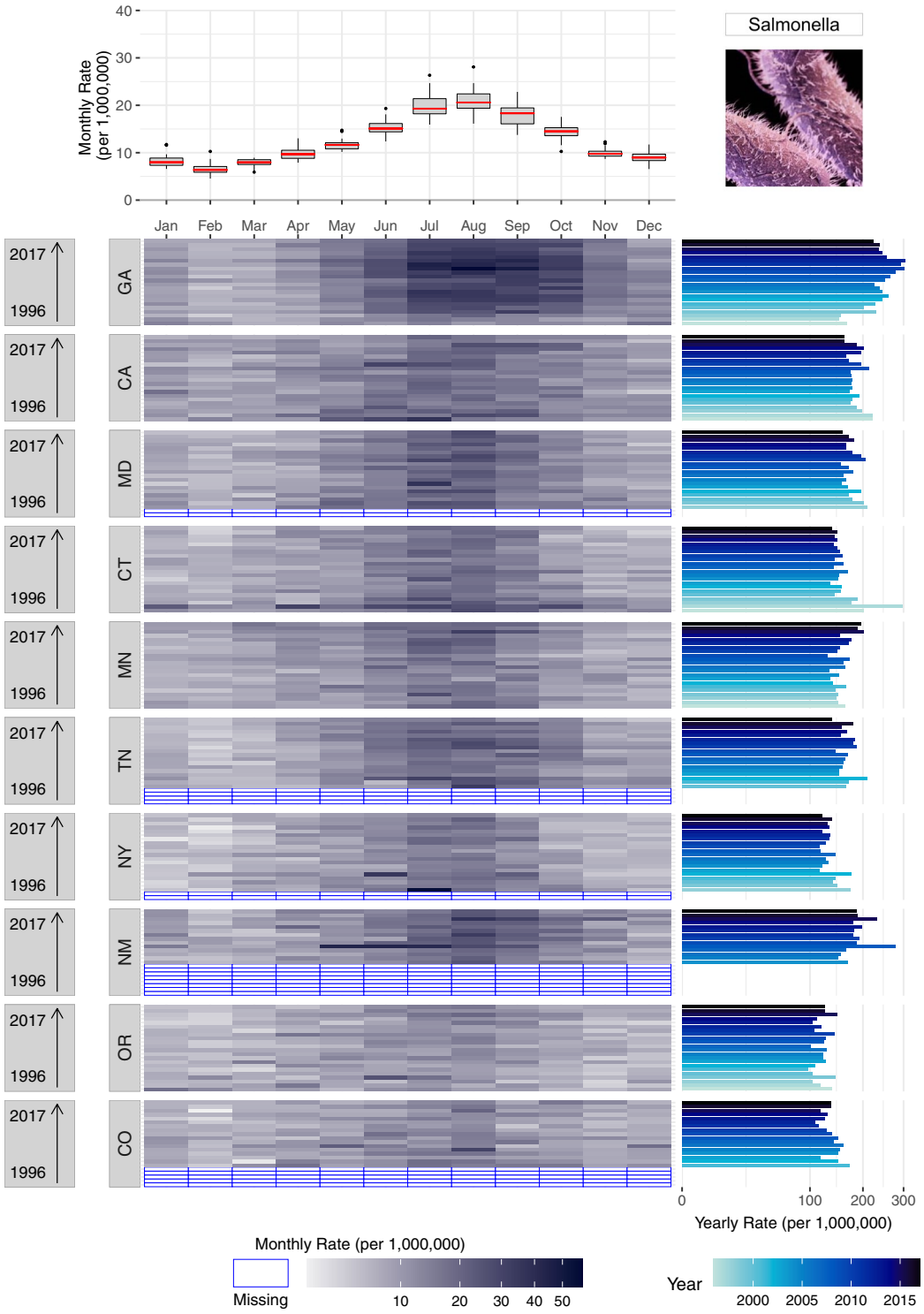


Fig. 5 A multi-panel plot for comparing seasonal signatures and yearly rates of salmonellosis in the US from 1996–2017 disaggregated by the ten FoodNet-surveyed states. The top panel provides a box plot of monthly rates for each month of year for the US. The calendar heatmap uses shared horizontal axes to show the distribution of monthly rates for each year and each state. Darker hues indicate higher rates while empty cells with blue borders indicate years when FoodNet surveillance was not conducted. The right panel provides a rotated bar graph of yearly rates. Given sizable differences in rates across states we applied a high-order calibration colour scheme.

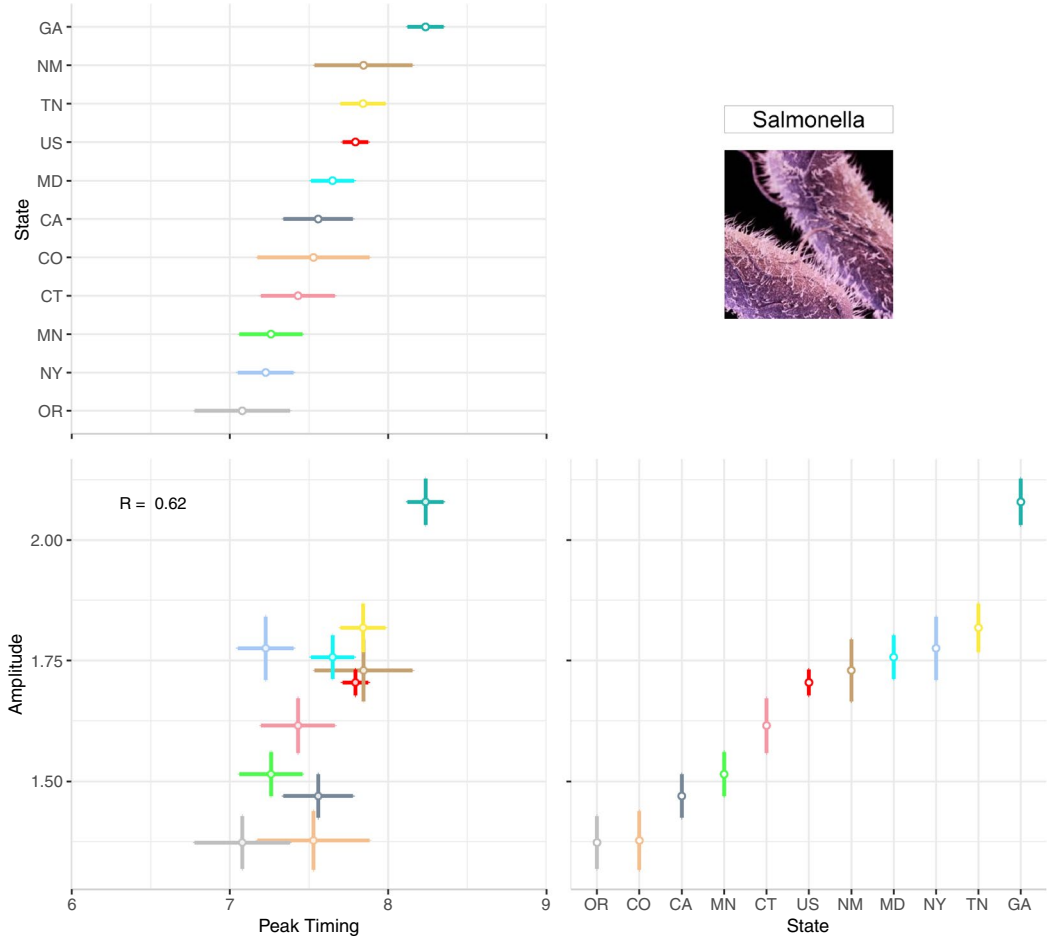


Fig. 6 A multi-panel plot for visualizing the annual peak timing and amplitude of salmonellosis in ten FoodNet-reporting states and the US from 1996–2017. The top-left panel shows the average peak timing of salmonellosis per location while the bottom-right panel shows the average amplitude per location. The bottom-left panel shows a combined scatterplot between peak timing and amplitude estimates.

We developed a time series of monthly rates by reconstructing a time series of monthly counts (see Fig. 1) then dividing counts by the sum of all FoodNet-surveyed counties' mid-year populations per state per 1,000,000 persons. In this calculation, we recognize that average monthly percentages are rounded in the raw data file and do not sum to 100% annually for downloaded years. This rounding resulted in obtaining non-integer counts within our time series. To prevent modification of raw data files, we did not round counts to integers before or after calculating rates. No information is provided on the FoodNet Fast website for the definition of confirmed cases, and data downloads provide no metadata for distinguishing cases from hospitalizations and deaths. Although the case definition is provided on the CDC website as "laboratory-confirmed cases (defined as isolation for bacteria or identification for parasites of an organism from a clinical specimen) and cases diagnosed using culture-independent methods"[45], it forces the user to assume that a confirmed case is any person with laboratory confirmed cultures of a specific pathogen who may or may not have been hospitalized or died from infection. FoodNet also collects information on hospitalizations and deaths, but does not provide information on the monthly percentage of hospitalizations or deaths, so users are unable to reconstruct a monthly time series for deaths or hospitalizations.

The FoodNet Fast platform states all confirmed diseases as "incidence" calculations. Technical documentation on the FoodNet website shows that the term incidence reflects cases per 100,000 persons (used interchangeably with a disease rate) with no distinction of whether these are newly introduced within the population (i.e. incidence) or the total persons diagnosed with a disease (i.e. prevalence)[46]. We found that monthly rates can similarly be calculated by multiplying annual incidence rates and the monthly percentage of confirmed cases for each disease-state pair. Differences between our calculations and this alternative method are no more than ± 2%. We suspect that rounding errors of average monthly percentages and differential population catchment areas for rate calculations cause these differences. As shown in Supplemental Table S1, population of the surveillance catchment area is changing over time. Oftentimes, publicly available surveillance datasets, including FoodNet Fast, do not include location- and year-specific population catchment area estimates, which are needed for calculating rates from diseases counts. As FoodNet does not provide population catchment areas for calculating rates, it

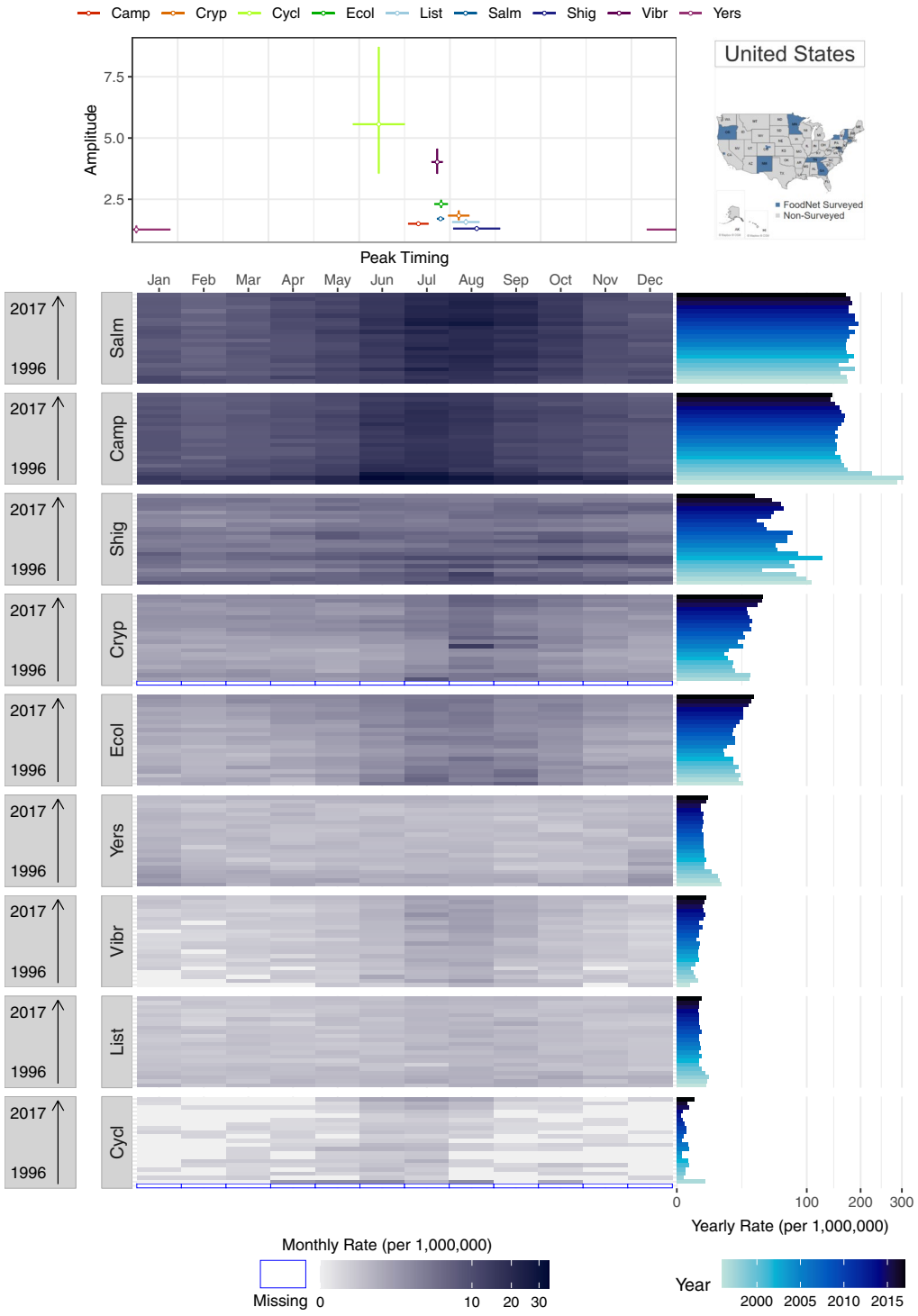


Fig. 7 A multi-panel plot for comparing seasonal signatures and yearly rates of nine FoodNet-reported infections in the US from 1996–2017. The top panel provides a scatterplot of average peak timing and amplitude estimates per pathogen across the 22-year period. The bottom heatmap uses shared horizontal axes to show the distribution of monthly rates for each year and each disease (campylobacteriosis (Camp), listeriosis (List), salmonellosis (Salm), shigellosis (Shig), infections caused by Shiga toxin-producing *Escherichia coli* O157 and non-O157 (Ecol), vibriosis (Vibr), infections caused by *Yersinia enterocolitica* (Yers), cryptosporidiosis (Cryp) and cyclosporiasis (Cycl)). Darker hues indicate greater rates while empty cells with blue borders indicate years when FoodNet surveillance was not conducted. The right panel provides a rotated bar graph of yearly rates.



Fig. 8 A multi-panel plot for visualizing the average peak timing and amplitude of nine FoodNet-reported pathogens in the US from 1996–2017. The top-left panel shows the average peak timing of each disease while the bottom-right panel shows the average amplitude per disease (campylobacteriosis (Camp), listeriosis (List), salmonellosis (Salm), shigellosis (Shig), infections caused by Shiga toxin-producing *Escherichia coli* O157 and non-O157 (Ecol), vibriosis (Vibr), infections caused by *Yersinia enterocolitica* (Yers), cryptosporidiosis (Cryp) and cyclosporiasis (Cycl)). The bottom-left panel shows a combined scatterplot between peak timing and amplitude estimates.

forces the user to assume that FoodNet surveillance reaches the total population of a surveyed county (likely an overestimate), yet such oversight is easy to fix. Three collaborators confirmed our monthly rate calculations for quality control.

We applied the negative binomial harmonic regression NBHR models, commonly used in the time series analysis of counts and cases. While the use of NBHR models, specifically the inclusion of trigonometric harmonic oscillations, is similar to existing works on foodborne illnesses, these studies often incorporate harmonic oscillators only to adjust for or remove seasonal oscillations[47–55]. We have extended the use of harmonic terms and develop the tools to estimate peak timing and amplitude[8,29,30]. The developed δ-method provides a systematic calculation of confidence intervals for peak timing and amplitude estimates based on the results of harmonic regression models. In the proposed approach, we present the amplitude as the ratio of seasonal peak to seasonal median, which offers robust estimation even for rare or highly sporadic infections. These features are not available when traditional models, like Auto-Regressive Integrated Moving Average (ARIMA), are applied[56]. Measures of uncertainty enable formal testing and comparisons across diseases in the same location or locations for the same disease. In our previous works, we have demonstrated the broad utility of the δ-method and applications of peak timing and amplitude estimation in the context of epidemiological studies[6,29,56–62].

We evaluate each state's cases individually as well as all national cases as the sum of all states' cases. Our analysis evaluated all cases reported to FoodNet Fast irrespective of demographic factors such as age group, sex, or ethnic group. Future analyses can consider conducting analyses using demographic factors available on the FoodNet Fast platform such as age group (<5, 5–9, 10–19, 20–29, 30–39, 40–49, 50–59, 60–69, 70 + years), sex (male and female), and ethnic group (American Indian and Alaskan Native, Asian and Pacific Islander, Black, Multiple, White). To incorporate this information, our methodology for data extraction would need to be repeated for each subcategory or combination of categories desired (e.g. download 221 files for males and 221 files for females).

Future analyses can also consider differences in pathogen strain, which can only be obtained if extracting data for each pathogen-location-year combination (e.g. 221 files for each of the 9 diseases for each of 11 locations or 21,879 files).

FoodNet Fast, like many global disease surveillance databases, has no metadata describing missing data. FoodNet Fast reports missing counts using "N/A" for years when pathogens or locations were not under surveillance. However, there are also years when FoodNet surveillance was live in a state, but a pathogen is missing from the data download. We believe that this missing data comes when, for a given year, a pathogen has 0 total cases. However, we cannot specify whether absences of surveillance reporting came due to a breakdown in reporting or 0 annual counts. Without specification, we have set any year with "N/A" as missing due to no reported case information.

When calculating peak timing and amplitude using the δ-methods, we applied NBHR models adjusted for harmonic seasonal oscillators and three trends (linear, quadratic, and cubic). We selected the polynomial terms as an example, yet researchers can consider alternative techniques for measuring seasonality such as splines, non-parametric regression, ARIMA models, or their extensions. Additionally, the CDC recommends using a mixed effects model when conducting time series analyses on FoodNet Fast data to account for differential population catchment areas and laboratory culture confirmation techniques pre- and post-2004[1,2,46]. We focus on the analysis of individual states and diseases and adjust for population catchment variations by calculating monthly rates using county-level population estimates. Future analyses could include detailed assessments between peak timing and amplitude across diseases, locations, and time periods. Such analyses will help determine whether a synchronization of outbreak peaks occurs or if social, economic, or environmental factors influence peak timing and amplitude.

Future applications. This analecta of visualizations intends to communicate detailed information on foodborne outbreak trends and seasonality suitable for a general audience, public health professionals, stakeholders, and policymakers. Future applications would involve the development of an interactive web-based platform allowing users to select the outcome, timeframe, and location of interest for educational training and research purposes. For example, public health researchers and practitioners could use this tool to generate insights related to long-term trends, changes in disease dynamics, or changes in populations at risk[62]. Information on when and where outbreaks are most common enable producers, distributors, and retailers to improve food safety practices to prevent these outbreaks. Finally, this platform could aid policymakers in shaping public understanding of outbreak dynamics and using scientific evidence to refine public health policies.

Data availability

The analecta of our time series of monthly rates, 436 data visualizations, and code used for all calculations and visualizations are available on our website (https://sites.tufts.edu/naumovalabs/analecta/). Data and code can be directly downloaded from the website while visualizations are linked on the website to an external visualization repository. Time series data and code are also available on figshare[36]. Visualizations on our website are provided in the same order as presented here: describing trends (Fig. 1), examining seasonal signatures with the three standard techniques: line graphs, boxplots, and radar plots (Fig. 2) and heatmaps (Fig. 3), characterizing features of seasonality (Fig. 4), drawing comparisons across locations for trends (Fig. 5) and seasonal signatures (Fig. 6), and drawing comparisons across pathogens for trends (Fig. 7) and seasonal signatures (Fig. 8). File downloads are available for trend, seasonal signature, and annual time series visualizations. For images examining a single disease in a single location, downloads are formatted where the prefix abbreviates the location and the suffix abbreviates the pathogen (see Supplementary Table S3). For visualizations comparing multiple locations or diseases, the prefix "LOC" indicates comparisons across locations while the prefix "DIS" indicates comparisons across pathogens (see Supplementary Tables S4,S5).

Code availability

All statistical analyses were conducted using STATA (SE 15.1) software. All visualizations were created using R Version 3.6.2 and Tableau Professional 2019.1 software. All software code is open access on our website (https://sites.tufts.edu/naumovalabs/analecta/) and figshare, and is available for public reuse with proper citation of this manuscript[36].

Received: 30 March 2020; Accepted: 16 September 2020;
Published online: 13 October 2020

References

1. Choi, J., Cho, Y., Shim, E. & Woo, H. Web-based infectious disease surveillance systems and public health perspectives: a systematic review. *BMC Public Health.* **16**, 1238 (2016).
2. Ginsberg, J. *et al*. Detecting influenza epidemics using search engine query data. *Nature.* **457**, 1012–1014 (2009).
3. Fefferman, N. & Naumova, E. N. Innovation in observation: a vision for early outbreak detection. *Emerg. Health Threat. J.* **3**, 7103 (2010).
4. Keller, M. *et al*. Use of unstructured event-based reports for global infectious disease surveillance. *Emerg. Infect. Dis.* **15**, 689 (2009).
5. Buckeridge, D. L., Burkom, H., Campbell, M., Hogan, W. R. & Moore, A. W. Algorithms for rapid outbreak detection: a research synthesis. *J. Biomed. Inform.* **38**, 99–113 (2005).
6. Lofgren, E., Fefferman, N. H., Naumov, Y. N., Gorski, J. & Naumova, E. N. Influenza seasonality: underlying causes and modeling theories. *J. Virol.* **81**, 5429–5436 (2007).
7. World Health Organization (WHO). FluNet. *Global Influenza Surveillance and Response Systems (GISRS)* https://www.who.int/influenza/gisrs_laboratory/flunet/en/ (2020).
8. Chui, K. K., Wenger, J. B., Cohen, S. A. & Naumova, E. N. Visual analytics for epidemiologists: understanding the interactions between age, time, and disease with multi-panel graphs. *PLoS One.* **6**, e14683 (2011).

9. Crim, S. M. *et al*. Incidence and trends of disease with pathogens transmitted commonly through food — Foodborne Diseases Active Surveillance Network, 10 U.S. sites, 2006–2013. *Morb. Mortal. Wkly. Rep.* **63**, 328–332 (2014).
10. Crim, S. M. *et al*. Preliminary incidence and trends of disease with pathogens transmitted commonly through food—Foodborne Diseases Active Surveillance Network, 10 US sites, 2006–2014. *Morb. Mortal. Wkly. Rep.* **64**, 495–499 (2015).
11. Marder, E. P. *et al*. Incidence and trends of diseases with pathogens transmitted commonly through food and the effect of increasing use of culture-independent diagnostic tests on surveillance—Foodborne Diseases Active Surveillance Network, 10 U.S. sites, 2013–2016. *Morb. Mortal. Wkly. Rep.* **66**, 397–403 (2017).
12. Huang, J. Y. *et al*. Disease with pathogens transmitted commonly through food and the effect of increasing use of culture-independent diagnostic tests on surveillance — Foodborne Diseases Active Surveillance Network, 10 U.S. sites, 2012–2015. *Morb. Mortal. Wkly. Rep.* **65**, 368–371 (2016).
13. Centers for Disease Control and Prevention (CDC). Foodborne Diseases Active Surveillance Network: FoodNet 2013 surveillance report. *National Center for Emerging and Zoonotic Diseases* https://www.cdc.gov/foodnet/pdfs/508-Compliant-2013-FoodNet-Annual-Report.pdf (2013).
14. Bennett, S. D. *et al*. Produce-associated foodborne disease outbreaks, USA, 1998-2013. *Epidemiol. Infect.* **146**, 1397–1406 (2018).
15. Ebel, E. D. W. *et al*. Comparing characteristics of sporadic and outbreak-associated foodborne illnesses, United States, 2004–2011. *Emerg. Infect. Dis.* **22**, 1193–1200 (2016).
16. Geissler, A. L., *et al*. Increasing Campylobacter infections, outbreaks, and antimicrobial resistance in the United States, 2004-2012. *Clin. Infect. Dis*. 65, 1624-1631 (2017).
17. Jiang, C. *et al*. Climate change, extreme events and increased risk of salmonellosis in Maryland, USA: Evidence for coastal vulnerability. *Environ. Int.* **83**, 58–62 (2015).
18. Keithlin, J., Sargeant, J., Thomas, M. K. & Fazil, A. Systematic review and meta-analysis of the proportion of Campylobacter cases that develop chronic sequelae. *BMC Public Health* **14**, 1203 (2014).
19. Moffatt, C. R., Glass, K., Stafford, R., D'Este, C. & Kirk, M. D. The campylobacteriosis conundrum - examining the incidence of infection with Campylobacter sp. in Australia, 1998-2013. *Epidemiol. Infect.* **145**, 839–847 (2017).
20. Centers for Disease Control and Prevention (CDC). FoodNet Fast: pathogen surveillance tool. *Atlanta, Georgia: U.S. Department of Health and Human Services* http://wwwn.cdc.gov/foodnetfast (2020).
21. Centers for Disease Control and Prevention (CDC). FoodNet surveillance. *U.S. Department of Health and Human Services* https://www.cdc.gov/foodnet/surveillance.html (2020).
22. Scallan, E. *et al*. Bacterial enteric diseases among older adults in the United States: Foodborne Diseases Active Surveillance Network, 1996-2012. *Foodborne Pathog. Dis.* **12**, 492–499 (2015).
23. Taylor, E. V. *et al*. Common source outbreaks of Campylobacter disease in the USA, 1997-2008. *Epidemiol. Infect.* **141**, 987–996 (2013).
24. Williams, M. S., Golden, N. J., Ebel, E. D., Crarey, E. T. & Tate, H. P. Temporal patterns of Campylobacter contamination on chicken and their relationship to campylobacteriosis cases in the United States. *Int. J. Food Microbiol.* **208**, 114–121 (2015).
25. Merriam-Webster Dictionary. *Analects. Merriam-Webster* https://www.merriam-webster.com/dictionary/analecta (2020).
26. United States Census Bureau. 1990s: county tables. *United States Department of Commerce* https://www.census.gov/data/tables/time-series/demo/popest/1990s-county.html#statelist_6 (2016)
27. United States Census Bureau. County intercensal tables: 2000-2010. *United States Department of Commerce* https://www.census.gov/content/census/en/data/tables/time-series/demo/popest/intercensal-2000-2010-counties.html (2017).
28. United States Census Bureau. Annual estimates of the resident population: April 1, 2010 to July 1, 2017. *United States Department of Commerce* https://factfinder.census.gov/faces/tableservices/jsf/pages/productview.xhtml?pid=PEP_2017_PEPANNRES&prodType=table (2018).
29. Simpson, R. B. *et al*. Incorporating calendar effects to predict influenza seasonality in Milwaukee, Wisconsin. *Epidemiol. Infect.* **147**, 1–13 (2019).
30. Falconi, T. A., Cruz, M. S. & Naumova, E. N. The shift in seasonality of legionellosis in the USA. *Epidemiol. Infect.* **146**, 1824–1833 (2018).
31. Davis, R. A. & Rongning, W. A negative binomial model for time series of counts. *Biometrika.* **96**, 735–749 (2009).
32. Munzner, T. Visualization analysis and design. *CRC press* (2014).
33. Fey, S. Information Dashboard Design: The Effective Visual Communication of Data. *O'Reilly* (2006).
34. Castronovo, D. A., Chui, K. K. H. & Naumova, E. N. Dynamic maps: a visual-analytic methodology for exploring spatio-temporal disease patterns. *J. Environ. Health.* **8**, 1–9 (2009).
35. Alarcon Falconi, T. M., Estrella, B., Sempértegui, F. & Naumova, E. N. Effects of Data Aggregation on Time Series Analysis of Seasonal Infections. *Int. J. Environ. Res. Public Health.* **17**, 5887 (2020).
36. Simpson, R. B., Zhou, B., Alarcon Falconi, T. M., & Naumova, E. N. An analecta of visualizations for foodborne illness trends and seasonality. *figshare* https://doi.org/10.6084/m9.figshare.c.4904736 (2020).
37. Henao, O. L., Jones, T. F., Vugia, D. J. & Griffin, P. M. Foodborne Diseases Active Surveillance Network - 2 decades of achievements, 1996–2015. *Emerg. Infect. Dis.* **21**, 1529–1536 (2015).
38. Scallan, E. Activities, achievements, and lessons learned during the first 10 years of the Foodborne Diseases Active Surveillance Network: 1996–2005. *Clin. Infect. Dis.* **44**, 718–725 (2007).
39. Smallman-Raynor, M. & Trevelyan, B. The spatial structure of epidemic emergence: geographical aspects of poliomyelitis in north-eastern USA, July –October 2016. *J. R. Stat. Soc. Ser. A. Stat. Soc.* **168**, 701–722 (2006).
40. Tunstall-Pedoe, H. *et al*. Prime mover or fellow traveller: 25-hydroxy vitamin D's seasonal variation, cardiovascular disease and death in the Scottish Heart Health Extended Cohort (SHHEC). *Int. J. Epidemiol.* **44**, 1602–1612 (2015).
41. Su, D. *et al*. Season and outdoor temperature in relation to detection and control of hypertension in a large rural Chinese population. *Int. J. Epidemiol.* **43**, 1835–1845 (2014).
42. Semenza, J. C. *et al*. Climate change impact assessment of food- and waterborne diseases. *Crit. Rev. Environ. Sci. Technol.* **42**, 857–890 (2012).
43. Pintar, K. D. *et al*. A systematic review and meta-analysis of the Campylobacter spp. prevalence and concentration in household pets and petting zoo animals for use in exposure assessments. *PLoS One.* **10**, e0144976 (2015).
44. Qi, R. *et al*. Global prevalence of asymptomatic norovirus disease: a meta-analysis. *EClinicalMedicine.* **2**, 50–58 (2018).
45. Centers for Disease Control and Prevention (CDC). FoodNet Surveillance. *U.S. Department of Health and Human Services* https://www.cdc.gov/foodnet/surveillance.html#:~:text=FoodNet%20collects%20information%20on%20laboratory,diagnosed%20using%20culture-independent%20methods (2015).
46. Centers for Disease Control and Prevention (CDC). FoodNet Fast: pathogen surveillance tool FAQ. *U.S. Department of Health and Human Services* https://www.cdc.gov/foodnet/foodnet-fast/faq-pathogen-surveillance.html (2019).
47. Brankston, G. *et al*. Assessing the impact of environmental exposures and Cryptosporidium disease in cattle on human incidence of cryptosporidiosis in southwestern Ontario, Canada. *PLoS One.* **13**, e0196573 (2018).
48. David, J. M. *et al*. Do contamination of and exposure to chicken meat and water drive the temporal dynamics of Campylobacter cases? *Epidemiol. Infect.* **145**, 3191–3203 (2017).
49. De Roos, A. J. *et al*. Review of epidemiological studies of drinking-water turbidity in relation to acute gastrointestinal illness. *Environ. Health Perspect.* **125**, 086003 (2017).

50. Djennad, A. *et al*. Seasonality and the effects of weather on Camylobacter diseases. *BMC Infect. Dis.* **19**, 255 (2019).
51. Hulland, E. *et al*. Increase in reported cholera cases in Haiti following Hurricane Matthew: an interrupted time series model. *Am. J. Trop. Med. Hyg.* **100**, 368–373 (2019).
52. Morris, A. *et al*. Complex temporal climate signals drive the emergence of human water-borne disease. *Emerg. Microbes Infect.* **3**, e56 (2014).
53. Rosenberg Goldstein, R. E. *et al*. Association between community socioeconomic factors, animal feeding operations, and campylobacteriosis incidence rates: Foodborne Diseases Active Surveillance Network (FoodNet), 2004–2010. *BMC Infect. Dis.* **16**, 354 (2016).
54. Rushton, S. P. *et al*. Climate, human behaviour or environment: individual-based modelling of Campylobacter seasonality and strategies to reduce disease burden. *J. Transl. Med.* **17**, 34 (2019).
55. Louis, V. R. *et al*. Temperature-driven Campylobacter seasonality in England and Wales. *Appl. Environ. Microbiol.* **71**, 85–92 (2005).
56. Alsova, O. K., Loktev, V. B. & Naumova, E. N. Rotavirus seasonality: an application of singular spectrum analysis and polyharmonic modeling. *Int. J. Environ. Res. Public Health.* **16**, 4309 (2019).
57. Naumova, E. N. Mystery of seasonality: getting the rhythm of nature. *J. Public Health Policy.* **27**, 2–12 (2006).
58. Wenger, J. B. & Naumova, E. N. Seasonal synchronization of influenza in the United States older adult population. *PLoS One.* **5**, e10187 (2010).
59. Chui, K. K., Webb, P., Russell, R. M. & Naumova, E. N. Geographic variations and temporal trends of Salmonella-associated hospitalization in the U.S. elderly, 1991–2004: a time series analysis of the impact of HACCP regulation. *BMC Public Health.* **9**, 447 (2009).
60. Chui, K. K., Jagai, J. S., Griffiths, J. K. & Naumova, E. N. Hospitalization of the elderly in the United States for nonspecific gastrointestinal diseases: a search for etiological clues. *Am. J. Public Health.* **101**, 2082–2086 (2011).
61. Ramanathan, K. *et al*. Assessing seasonality variation with harmonic regression: accommodations for sharp peaks. *Int. J Environ. Res. Public Health.* **17**, 1318 (2020).
62. Stratton, M., Ehrlich, H., Mor, S. & Naumova, E. N. A comparative analysis of three vector-borne diseases across Australia using seasonal and meteorological models. *Sci. Rep.* **7**, 40186 (2017).

Acknowledgements

This research is based upon work supported in part by the Office of the Director of National Intelligence (ODNI), Intelligence Advanced Research Projects Activity (IARPA), via 2017-17072100002. The views and conclusions contained herein are those of the authors and should not be interpreted as necessarily representing the official policies, either expressed or implied, of ODNI, IARPA, or the U.S. Government. The U.S. Government is authorized to reproduce and distribute reprints for governmental purposes notwithstanding any copyright annotation therein. The research was in part supported by the National Science Foundation (NSF) Innovations in Graduate Education (IGE) Program, via grant award 1855886 and by the United States Department of Agriculture (USDA) National Institute of Food and Agriculture (NIFA) Cooperative State Research, Education, and Extension Service Fellowship, via grant award 2020-38420-30724. The authors would also like to thank Dr. Meghan Hartwick for editorial and technical assistance.

Author contributions

R.S. contributed to data extraction, formal analysis, and writing. B.Z. contributed to data validation, conceptualization of visual aids, and visualization creation. T.M.A.F. contributed to data validation, review, and editing. E.N.N. contributed to methodology development, review and editing, supervision, project administration and funding acquisition.

Competing interests

The authors declare no competing interests.

Additional information

Supplementary information is available for this paper at https://doi.org/10.1038/s41597-020-00677-x.

Correspondence and requests for materials should be addressed to E.N.N.

Reprints and permissions information is available at www.nature.com/reprints.

Publisher's note Springer Nature remains neutral with regard to jurisdictional claims in published maps and institutional affiliations.

Open Access This article is licensed under a Creative Commons Attribution 4.0 International License, which permits use, sharing, adaptation, distribution and reproduction in any medium or format, as long as you give appropriate credit to the original author(s) and the source, provide a link to the Creative Commons license, and indicate if changes were made. The images or other third party material in this article are included in the article's Creative Commons license, unless indicated otherwise in a credit line to the material. If material is not included in the article's Creative Commons license and your intended use is not permitted by statutory regulation or exceeds the permitted use, you will need to obtain permission directly from the copyright holder. To view a copy of this license, visit http://creativecommons.org/licenses/by/4.0/.

© The Author(s) 2020

Journal of Public Health Policy
https://doi.org/10.1057/s41271-022-00345-x

ORIGINAL ARTICLE

Dynamic mapping of cholera outbreak during the Yemeni Civil War, 2016–2019

Ryan B. Simpson[1] · Sofia Babool[2] · Maia C. Tarnas[3] · Paulina M. Kaminski[1] · Meghan A. Hartwick[1] · Elena N. Naumova[1]

Accepted: 5 February 2022
© The Author(s) 2022

Abstract

Widespread destruction from the Yemeni Civil War (2014–present) triggered the world's largest cholera outbreak. We compiled a comprehensive health dataset and created dynamic maps to demonstrate spatiotemporal changes in cholera infections and war conflicts. We aligned and merged daily, weekly, and monthly epidemiological bulletins of confirmed cholera infections and daily conflict events and fatality records to create a dataset of weekly time series for Yemen at the governorate level (subnational regions administered by governors) from 4 January 2016 through 29 December 2019. We demonstrated the use of dynamic mapping for tracing the onset and spread of infection and manmade factors that amplify the outbreak. We report curated data and visualization techniques to further uncover associations between infectious disease outbreaks and risk factors and to better coordinate humanitarian aid and relief efforts during complex emergencies.

Keywords Cholera · Conflict · Data alignment · Dynamic mapping · Time series · Yemen

✉ Elena N. Naumova
elena.naumova@tufts.edu

Ryan B. Simpson
ryan.simpson@tufts.edu

[1] Nutrition Epidemiology and Data Science Division, Tufts University Friedman School of Nutrition Science and Policy, 150 Harrison Avenue, Boston, MA 02111, USA

[2] Neuroscience Department, The University of Texas at Dallas, Richardson, TX, USA

[3] Community Health Department, Tufts University School of Arts and Sciences, Medford, MA, USA

Published online: 25 May 2022

Key messages

- We implore the global public health community to harmonize data collection and reporting protocols and to improve the spatiotemporal resolution of time-referenced data. This will allow external users to trace the onset, spread, and amplification of disease outbreaks.
- We recommend public health professionals use advanced data visualization techniques when investigating complex spatiotemporal patterns of infectious outbreaks.
- Our dynamic maps suggested that the cholera outbreak "travelled" from Sana'a and Sana'a City, the epicentre of the national outbreak, to surrounding governorates, including Al-Hudaydah, characterized as a persistent cluster of conflict events.

Introduction

During complex humanitarian emergencies such as war, detailed analyses of health outcomes and related factors are difficult to conduct. High risk of disease morbidity and mortality impedes primary data collection and severely limit medical resources, personnel, and hospital bed capacity [1]. Real-time analyses are also hindered by limited available data, reduced laboratory testing capacity, and impaired or non-existent health infrastructure due to wartime events such as bombings and explosions. [2, 3]. As data collection and processing capabilities grow, the demand for use of novel approaches to integrate, examine, and present data from multiple sources to broad audiences also grows. These needs promote a new era of precision public health that prioritizes transparency in discussions of data quality, standardizes reporting of statistical methods, and uses advanced data visualization techniques to capture complex spatiotemporal patterns of diseases. Better understanding of these patterns can assist in predictive modelling for early warning outbreak systems and timely, pre-emptive medical resource and personnel mobilization to expected geographic hotspots of infection.

For example, the Yemeni Civil War (2014–present) has led to widespread destruction that has triggered the world's largest cholera outbreak [1, 4]. Even before the war, Yemen was one of the poorest countries in the Arabian Peninsula with limited access to clean and affordable drinking water [5, 6]. High rates of malnourished and immuno-compromised persons have increased cholera infection risks particularly in infants and children [6]. Limited access to sanitation and hygiene supplies has further amplified cholera transmission, mortality, and morbidity. This especially holds true in western, mountainous, densely populated governorates, such as Sana'a and Sana'a City (nation's capital), compared to eastern, arid, sparsely populated governorates, such as Hadhramaut and Al-Maharah [1, 3]. Frequent skirmishes between a Saudi Arabian military coalition,



the Yemeni government, and the armed Houthi movement further stress health infrastructure and medical supplies, particularly after the blockade on the Port of Al-Hudaydah, which has limited imports of food, water, and medical resources like cholera vaccinations [7].

New ways of analysing and presenting data are critical for linking conflict events and fatalities with disastrous health outcomes, as with the current humanitarian emergency in Yemen. However, few studies have investigated associations between illness rates and conflict in Yemen or elsewhere perhaps due to limited publicly available data [8–12]. Some publications have used privately acquired datasets that cannot be replicated or further examined due to data usage limitations [13, 14]. Other publications have referred to humanitarian situation reports built on qualitative findings and observations from health workers [15–17]. In our prior work, we curated a weekly time series dataset of confirmed cholera infections using publicly reported World Health Organization (WHO) epidemiological bulletins from 2016 through 2019 [18]. This provided a foundation for aligning and integrating other spatiotemporal data to create publicly available datasets for further analyses.

Time-referenced conflict databases disseminate publicly available records for reuse. One example is the Armed Conflict Location and Event Data (ACLED) Project, which provides geocoded data on conflict events and fatalities for various types of violence across Asia, the Middle East, Europe, and Latin America [19–22]. Datasets compiled during wartime, such as during the Syrian Conflict (2011–present) and Somali Civil War (1991–present), have proved invaluable as sources of information for coordinating international humanitarian relief [12, 23]. Yet, these data sources reflect the deficiencies of primary data collection such as inconsistent reporting frequency, limited spatial and temporal alignment, insufficient information on reporting practices, and unclear population catchment areas, all of which create challenges in using health data for analysis, inference, and decision-making [12, 23].

Targeted efforts to standardize the preparation, reporting, and visualization of data collected over time can substantially improve the quality of public health research. Given the complexity of global health crises, dynamic maps can condense spatial and temporal information of health records into a single animated image. Dynamic maps can assist researchers in examining the seasonality of infectious disease outbreaks, the synchronization between exposure events and outbreaks, and the geographic variability of these processes [24–28]. Researchers can also investigate temporal and spatial relationships between disease outbreaks and potential underlying processes when overlaying exposure and health outcome data on a single map. In emergency settings, the ability to visualize these spatiotemporal relationships between exposure events and disease outbreak signatures can help inform the timing and type of emergency interventions needed such as food aid delivery, natural disaster relief packages, or peacekeeping operations.

In our prior work, we outlined key principles for consideration when creating dynamic maps and ways to explore them [25]. We also applied dynamic maps to evaluate persistent clusters and travelling waves of influenza in the United States' elderly population for four influenza seasons (Fig. 1; Movie 1) [27]. This series of dynamic maps demonstrated the spatial heterogeneity and emergence of seasonal influenza outbreaks. Understanding factors that drive complex infectious disease



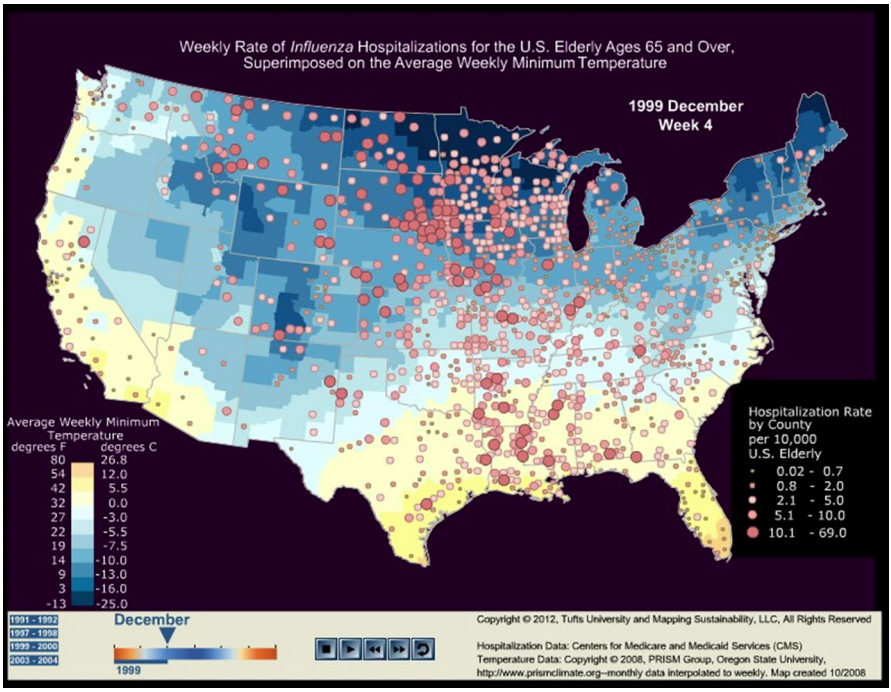


Fig. 1 A snapshot of Movie 1, a moving set of images showing weekly rates of elderly (aged ≥ 65 years) influenza hospitalizations per 10,000 persons and average weekly minimum temperature in the United States for the 1991–1992, 1997–1998, 1999–2000, and 2003–2004 influenza seasons [27]. The size and darkness of red colour indicates more intense influenza outbreaks. Weekly minimum temperatures ranged from − 25 °C (− 13°F, dark blue colour) to ~ + 27 °C (+ 80°F, dark orange colour). The superimposition of weekly minimum temperature and elderly hospitalization rates illustrates travelling waves of infection in the United States and their association to fluctuations in temperature. To watch and download Movie 1, please see the https://doi.org/10.1057/s41271-022-00345-x

dynamics allows for more targeted response recommendations to effectively control seasonal outbreaks or epidemics [27].

In this study, we demonstrated the process of creating a weekly time series dataset that integrated data streams of Yemeni conflict events and fatalities with confirmed cholera infections and rates in 2016–2019. We used the WHO Eastern Mediterranean Regional Office's (EMRO) daily, weekly, and monthly bulletins following the first confirmed cholera case in Sana'a on 1 October 2016 [29]. Our comprehensive dataset allowed for examination of persistent clusters and travelling waves of cholera outbreaks and conflict events. We included visualizing cholera outbreaks and conflict events in complex emergency settings. Dynamic maps allowed us to investigate when outbreaks and conflict events occurred, how long they persisted, how they differed across geographic locations, and the utility and usability of harmonized global health datasets in public health applications. Our findings can also help identify geographic hotspots experiencing both intense cholera outbreaks and persistent conflict events, and thus most in need of cholera reduction strategies such



as restoring infrastructure, improving water sanitation, and increasing access to cholera vaccines. With advanced technological platforms to support big datasets and animated maps, the global health community can move forward solutions to improve open-source surveillance systems and inform targeted health policies.

Data and methods

Conflict fatalities and events

We extracted daily conflict fatalities and events from ACLED reports [30]. ACLED partners with the Yemen Data Project (YDP) to collate and disseminate data on Yemeni war conflicts to improve transparency and promote actor accountability [30]. ACLED cross-references reports with daily and weekly Arabic and English news articles from 450 local, national, and international media agencies [30, 31]. ACLED reported on violent (for example, battles, explosions, violence against civilians) and non-violent (for example, protests, riots, strategic developments) political events, and estimated fatalities when possible [32, 33]. Reports cover ~ 70% of all urban and remote locations within Yemen. However, Houthi- and other warring party-controlled areas strongly censored conflict and political information, resulting in lesser coverage for Al-Jawf and Hajjah governorates [34, 35]. ACLED reported conflict events as discrete, daily, geocoded observations that repeated if multiple events occurred on the same day [34, 35]. We extracted daily records from 4 January 2016 through 29 December 2019, summed all-cause fatalities and events per day, and aggregated daily counts by week and governorate (0% missing data).

Compilation of weekly cholera records

We extracted confirmed cholera infections from the WHO EMRO epidemiological bulletins for all Yemeni governorates. However, analysed only 20 of 21 governorates, as the WHO did not consistently report records for the Hadhramaut governorate within our study period. The EMRO began publishing these reports on 04 September; no data were available for the first 35 calendar weeks of 2016 [29, 36–38]. We assumed weekly counts of 0 infections for these weeks. We extracted, aggregated, and interpolated all reported daily, weekly, and monthly data from Week 36 of 2016 through Week 52 of 2019. To harmonize temporal and spatial resolution into a final curated dataset, we aggregated data by WHO-defined epidemiological weeks, an international standard defining weeks from Monday through Sunday starting with the full week of the year [18, 39].

Daily data from Weeks 36–45 of 2016 included cumulative counts of confirmed cholera infections for each governorate. However, EMRO epidemiological bulletins reported infections nationally from Week 46 of 2016 to Week 12 of 2017. For both time periods, we estimated average daily infections by subtracting cumulative totals from consecutive reports and dividing by the multi-day reporting length. We did not round fractional daily estimates to best estimate the distribution of infections in the

absence of consistently-reported daily records. We distributed national daily average infections across governorates according to their relative population sizes using 2017 estimates, then aggregated daily averages by week [40]. While the spatial distribution of infections was likely a function of more than just population size, we found no additional data on risk factors like hygiene conditions or population displacement for estimating governorate-level case distributions. We assumed relative differences in population size adequately reflected relative differences in the transmissibility of incident infections. The WHO reported only 112 infections nationally during this 18-week period.

As the epidemic progressed, the WHO revised the EMRO epidemiological bulletin into weekly situation reports. These reports provided records of weekly cholera infections and deaths by governorate [38]. From Week 29 of 2017 to Week 26 of 2018, the WHO used a standardized reporting format that provided records for the week of publication and 3 weeks of historic records prior to the publication week (0–3-week lags). With each successive report, the WHO revised records within prior weeks to provide more accurate estimates of cholera infections adjusted for testing and reporting delays. For our analysis, we compiled the most updated records of confirmed case estimates available from each report.

Situation reports transitioned from weekly to monthly temporal aggregation in mid-2018. We extracted monthly data from Week 27 of 2018 through Week 52 of 2019. These reports provided cumulative confirmed infections per governorate from 27 April 2017 until the last day of the reporting month. We subtracted monthly totals of cholera infections from consecutive reports to estimate the cumulative total incidence of confirmed cholera infections. We divided this total by the number of days within that month to approximate average daily counts. Though daily reported infections are expected to fluctuate over a month's time, no data with greater temporal granularity were available. We aggregated daily estimates by WHO-defined weeks to estimate weekly counts.

Irregular WHO bulletin-reporting frequency resulted in numerous weeks with missing records, or a time point when we could not find confirmed cholera case information. These reporting gaps occurred when the WHO transitioned from daily to weekly or weekly to monthly reporting formats. We had missing data for Weeks 13–16 of 2017, Week 8 of 2018, and Weeks 27–30 of 2018. To enhance the usability of our curated dataset, we handled missing data in two ways. First, we created a variable of reported infections that preserved missing data to allow data users to interpolate data if and how they may wish. Second, we created a variable with interpolated missing records using a linear approximation of reported adjacent weeks, as the most conservative representation of the epidemic curve.

Calculating cholera rates

We created a weekly time series of population estimates, adjusted for population growth and conflict fatalities, to calculate weekly cholera rates [18]. First, we calculated each governorate's population in Week 1 of 2017 using the average from multiple sources [38, 40, 41]. Next, we prorated an annual birth rate (≈ 0.024) from the



2004 Yemeni Population Census to reflect the low-fertility and moderate-mortality expected during the Yemeni Civil War [40]. We found no additional information on population growth rate in the 2014 Yemeni Census [42]. For weeks preceding Week 1 of 2017, we added conflict fatalities and divided the sum by the annual prorated growth rate. For weeks succeeding Week 1 of 2017, we subtracted conflict fatalities and multiplied the difference by the annual prorated growth rate.

We estimated national rates by summing infections for all governorates and dividing by the summed weekly population estimates. We report cholera rates per 100,000 persons (abbreviated as 'cph'), calculated by dividing weekly infections by population estimates with a multiplier of 100,000.

Examining persistent outbreak and conflict clusters

We examined persistent clusters of cholera rates and conflict events using Spearman autocorrelations. We assessed autocorrelations for all available lags in our time series (207 weeks) where high autocorrelation values suggested strong temporal trends. We determined governorates with persistent clusters by identifying long streaks of consecutively strong ($\rho > 0.70$) and moderate ($\rho > 0.40$) lagged positive autocorrelations using heatmaps. We defined significant correlations as $\alpha < 0.05$.

Metadata reporting and software usage

We share metadata to provide information needed to replicate the process of data curation and to understand the benefits and limitations of this data upon reuse. Metadata consist of a codebook with variable names, definitions, value types, value units, coding schemes, and the original variable's data sources. We performed all population prorating calculations using Excel (14.3.6) software and calculation equations are visible within the curated dataset. We provide epidemiological bulletins used to create cholera data and R code used for developing and exporting dynamic maps and figures on our *figshare* repository [39].

Results

We created Movie 2 for cholera rates and Movie 3 for conflict events to illustrate the use of dynamic mapping for curated global health datasets. Movie 2 provides a dynamic map of governorate-level rates over the 208-week study period. With this dynamic map, we provided the desired data visualization experience using an optimized frame speed of 1 second per frame to give enough time for the viewer to identify clusters of infections, store this pattern into short-term memory, and compare older clusters to newer clusters when examining the following frame [25]. We also provided an interactive user interface to enable viewers to replay frames at their discretion using a sliding calendar bar that traced the national time series of cholera rates.



We standardized mapping properties to ease the examination of spatiotemporal disease dynamics including when outbreaks occurred, how long they persisted, and differences by governorate [25]. For example, we converted daily and monthly records into weekly estimates to reduce 'noise' and sporadic fluctuations typical for daily records while preventing the over-smoothing typical for monthly records. We applied a complimentary colour gradation to emphasize differences over time and location. As seen in Movie 2 (Fig. 2), infection rates varied from ~ 0.01 cph during outbreak nadirs to ~ 772.35 cph at outbreak peaks. We used a logarithmic transformation to extend the

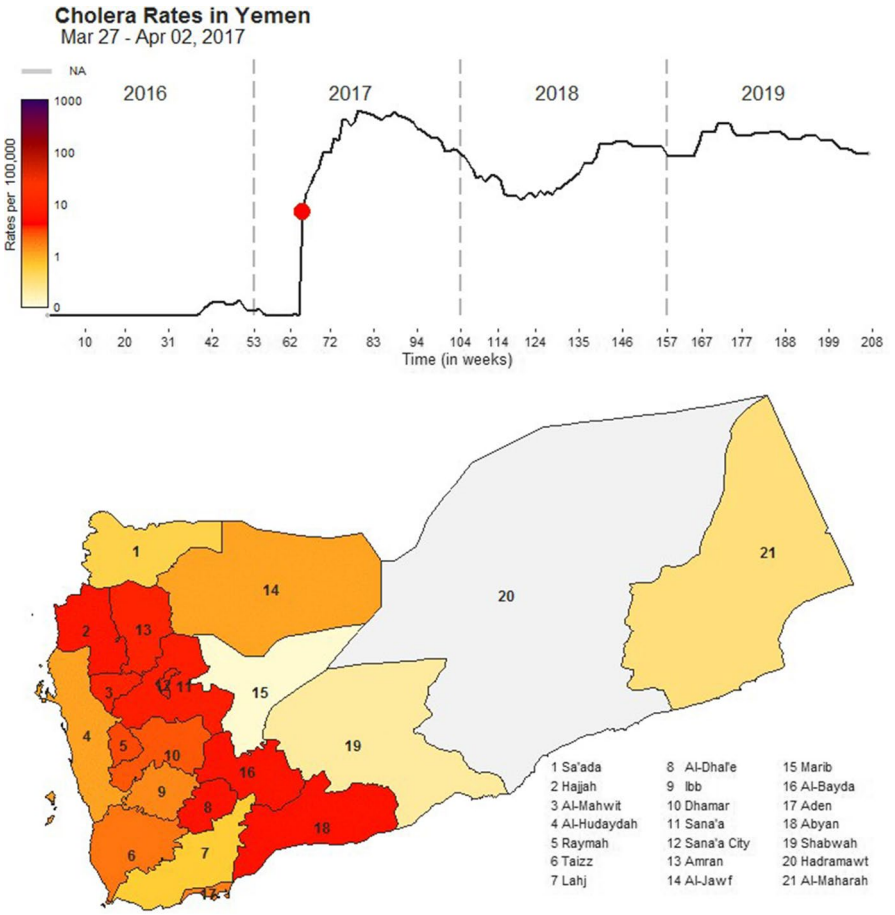


Fig. 2 A snapshot of Movie 2, a dynamic movie showing weekly rates of confirmed cholera infections per 100,000 (cph) persons in 20 of 21 Yemeni governorates from Week 1 of 2016 through Week 52 of 2019 (208 weeks total). The top panel provides a time series of national cholera rates. Below, a governorate-level map illustrates the distribution of cholera rates per governorate. A light-yellow colour indicates rates of 0.00 cph while a deep purple colour indicates rates of 1000.00 cph. We used a logarithmic scale to properly correct the colour scheme for the variability of rates across governorates. We used a grey colour to indicate the Hadhramaut governorate for which no data were consistently reported for analysis. To watch and download Movie 2, please see the https://doi.org/10.1057/s41271-022-00345-x

colour gradation evenly across this range. We selected complimentary colours (yellow and purple) of varying hues so that viewers with colour-blindness could distinguish variations in outbreak intensity.

Nationally, cholera rates had moderate-to-strong positive autocorrelation values for lags 1–14 ($p < 0.001$; Supplementary Figure S1). The length of these consistently moderate-to-strong correlations reflects the persistent national cholera outbreak throughout our study period. We used Movie 2 to identify possible travelling waves of infection from Sana'a, Sana'a City, Al-Mahwit, and Amran to surrounding areas. These governorates demonstrated high rates starting on 22–28 May 2017 (Supplementary Figure S2A). In the 14 weeks that followed (Supplementary Figures S2B-S2D), rates of infection increased rapidly in surrounding governorates suggesting a wave of infection outward to remote governorates of the country (Supplementary Figure S2). While Amran and Al-Mahwit had persistently high rates of infection, rates decreased for Sana'a and Sana'a City from 19–25 June to 17–23 July 2017. At the same time, cholera rates increased for Al-Dhale'e, Dhamar, Al-Bayda, Lahj, and Abyan, which all reached near-peak rates in 21–27 August 2017.

We also used Movie 2 to identify persistent clusters of high rates in Sa'ada, Sana'a, and Sana'a City throughout our study period (Supplementary Figure S3). These governorates had moderate-to-strong positive correlations for ~ 20 lags ($p < 0.001$) indicating persistent temporal trends. While cholera rates remained moderate in Sa'ada, rates were persistently high in Sana'a and Sana'a City even when national rates decreased to a local minimum in 16–22 April 2018 (Supplementary Figure S3A). When national rates reached a third and fourth local maximum in 01–07 October 2018 and 08–14 April 2019, rates remained elevated in Sana'a and Sana'a City compared to other governorates (Supplementary Figures S3B–S3C). Rates decreased little for these governorates by the conclusion of our study period (23–29 December 2019; Supplementary Figure S3D).

Movie 3 provided a dynamic map of governorate-level conflict events to show spatiotemporal fluctuations of exposure factors influencing cholera outbreaks (Fig. 3). We emphasized governorate-level variability in conflict events by providing a bubble plot below the time series line plot that reflects national conflict events. National conflict events had moderate-to-strong positive autocorrelation values for a 1–8-week lag period ($p < 0.001$; Supplementary Figure S4). This shorter lag interval compared to cholera rates illustrates the increased variability of conflict events during the Yemeni Civil War in 2016–2019. When inspecting autocorrelation values across governorates, we found that Al-Hudaydah had persistently moderate-to-strong positive autocorrelation values in lags 1–38 ($p < 0.001$). This illustrates a regional hotspot of conflict events clearly visualized using Movie 3. Al-Hudaydah conflict events rose sharply in June of 2018 (Supplementary Figure S5A) and accounted for nearly all events near and at the national peak in 2019 (Supplementary Figure S5B–S5C). Even as national events declined in October of 2019, Al-Hudaydah remained a persistent cluster of conflict events (Supplementary Figure S5D).

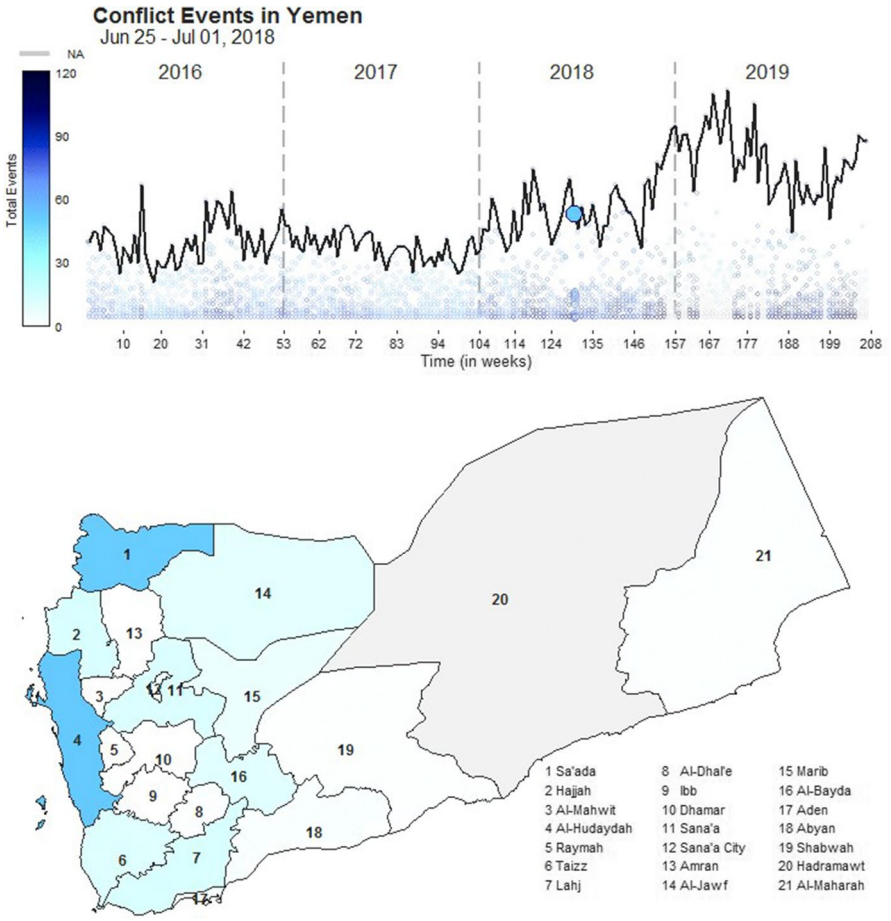


Fig. 3 A snapshot of Movie 3, a dynamic movie showing the weekly sum of conflict events in 20 Yemeni governorates and nationally from Week 1 of 2016 through Week 52 of 2019. The top panel provides a bubble plot and time series of the national conflict events. Below, conflict event intensity is illustrated by governorate using a shaded map. A white colour indicates 0 events while a deep purple colour indicates 120 events. We selected the colour scheme to properly correct for the variability of conflict events across governorates. We used a grey colour to indicate the Hadhramaut governorate for which the WHO did not consistently report data for analysis. To watch and download Movie 3, please see https://doi.org/10.1057/s41271-022-00345-x

Discussion

Our research demonstrated the importance of public data sharing using a standardized approach for extracting, aligning, and integrating spatiotemporal data. Our curated dataset enabled the creation of dynamic maps to investigate travelling waves and persistent clusters of infection rates and conflict events during the Yemeni Civil War in 2016–2019. Movie 2 illustrated a persistent cluster of rates in Sana'a and Sana'a City supported by moderate-to-strong positive autocorrelation values for



a ~ 20-week lag period. This movie also allowed us to identify a possible travelling wave of infection from this cluster to surrounding governorates in May–August of 2017.

We found a shorter lag period of moderate-to-strong positive autocorrelation values nationally for conflict events reflecting greater variability of conflict events in most governorates. However, Al-Hudaydah demonstrated persistent correlations across ~ 40-week lag period. Movie 3 showed that Al-Hudaydah's conflict events were greatest from June of 2018 through December of 2019. This increase coincided with assaults on Al-Hudaydah by pro-government forces, backed by the Saudi-led coalition, in June–November of 2018 [43]. These forces installed a blockade in Al-Hudaydah port, which continued to restrict both humanitarian medical supplies and food aid to the entire country the end of our study period [44].

Our findings illustrate the possibility of conducting early outbreak warnings if timely surveillance data are available and accessible. These efforts can help to develop humanitarian assistance strategies amidst ongoing public health emergencies. The cholera epidemic's origin and persistence within Sana'a and Sana'a City suggests the importance of monitoring these governorates as markers for future outbreaks. Evidence of travelling waves from this epicentre necessitates the strengthening of health and environmental infrastructure and implementation of preventative infections' mitigation strategies in surrounding governorates. These measures will reduce the likelihood of a national epidemic. Movie 3 also demonstrates the direct effect of war conflict in specific governorates, and therefore, challenges to implementing public health interventions. The persistent cluster of conflict events within Al-Hudaydah illustrates the extent of these challenges in complex emergency settings.

We encourage researchers to replicate dynamic mapping techniques for other data streams such as environment- or nutrition-related variables if properly aligned and integrated with our dataset. This will allow for data modellers to spatiotemporal associations between conflict-, environment-, or nutrition-related factors and cholera rates using our curated dataset. Many recent studies have explored factors associated with cholera transmission dynamics using granular remote sensing, climate-related spatial data, and conflict information [14, 45–51]. By improving data collection and processing capabilities, public health professionals will be well equipped with the data and tools to embrace a new era of precision health that prioritizes the sharing of granular temporal and spatial information and creation of high-quality data visualizations that capture complex spatiotemporal patterns of disease outbreaks. We recommend that future research use modelling approaches that properly account for complex, non-linear, and spatially-autocorrelated relationships between these variables.

Modern surveillance systems must improve to reflect both how internal data curators collect, store, monitor, and manage data—and how external data users extract, process, and analyse these data. Such systems can offer near- and real-time forecasts, long-term trend analyses, and outbreak modelling to develop early outbreak warnings and inform timely aid resource deployment. Disease surveillance systems should ensure data transparency and longevity by developing strong protocols for metadata standardization [52]. Improving data quality and availability corresponds

with a greater need for prioritizing information management within and across national and international public health, environmental, and humanitarian emergency agencies and organizations. A lack of coordination in data collection and sharing reduces the availability of granular temporal and spatial data for public use. In turn, this forces efforts and decision-making to occur at coarser spatial and temporal scales, reducing the efficacy and refinement of public health and humanitarian interventions.

Study limitations

From Week 46 of 2016 to Week 12 of 2017, we distributed national daily average cholera infections across governorates according to relative population estimates. We made this approximation by assuming that cholera outbreaks followed specific population transmission dynamics with higher incidence in more densely populated locations [53]. Additionally, we reported missing weeks only if all days within that week had a missing estimate. Though sensitive to underestimation, this approach maximized the utility of available surveillance data for conducting time series analyses in the absence of additional information to estimate weekly rates. We stress the need for national public health agencies, international health organizations, and the global health community at large to dedicate more resources and funds to implement thorough infectious disease outbreak investigations worldwide [54].

ACLED methodological codebooks noted that fatalities were not easily verified and prone to manipulation by armed groups [32]. Even so, these estimates provided the most accurate and reliable approximation of all-cause conflict fatalities during the Yemeni Civil War (neither civilian nor bystander causalities reported) [31]. Furthermore, ACLED and YDP validated all fatality and conflict event information using a combination of health reports, news articles, field surveys, and media stories [31, 32]. While population estimates fluctuate dramatically during conflict due to rapid internal displacement and external migration, we lacked sufficient temporally granular displacement and migration data to improve our adjusted population rate calculations [55].

We used a 2017 population estimate calculated as the average of the WHO EMRO epidemiological bulletins (from which we extracted cholera infections), Yemeni Central Statistical Organization (in-country reporting), and the International Organization of Migration's Displacement Tracking Matrix (monitoring migration during humanitarian emergencies) reports [38, 40, 41]. Together, these estimates provided the best approximation for governorate-level population. We prorated weekly population estimates using a low-fertility and moderate-mortality birth rate estimate and ACLED fatalities to favour under-reporting of infection rates during the Yemeni Civil War [56]. We found no alternative calculation technique for describing population estimation during conflict events or humanitarian emergencies.

We used various data sources to harmonize this dataset including health reports, news articles, and field surveys. We believe these reports provided accessible, usable, and timely documentation of information related to Yemeni cholera infections and conflict-related outcomes in 2016–2019. While encouraged by this



harmonization process, researchers must recognize that all estimates were only as accurate as the reports from which data were extracted. We strove for clarity and transparency in the applied methods, yet we acknowledge that metadata on the pre-processing of publicly available data from international organizations was extremely limited. Where possible, we compiled the metadata or raw text files for the extracted records used to create this dataset and uploaded files to our *figshare* repository [39].

Future directions

The essence of an informative dynamic map is strong data structure and a rigorous process of compilation. In this study, we demonstrated that the curation of comprehensive global health repositories enabled the creation of dynamic maps for tracking, recognizing, and visualizing complex spatiotemporal processes. The standardization and harmonization of reporting publicly available data ensures the longevity of data usability even as the platforms used to store, analyse, and communicate data change over time. Curated global health datasets and web-based dashboards with built-in dynamic mapping tools improve the reporting and understanding of associations between diseases and manmade or natural risk factors. Both dynamic maps and the process of data extraction, aggregation, and alignment emphasize the importance of long-term surveillance data collection in usable time series data formats. Only with these tools can surveillance records and dynamic mapping be used effectively and efficiently to plan for and respond to complex emergencies with medical, fiscal, and humanitarian supplies and aid resources [57].

Our data curation techniques can be applied to updated cholera data when it becomes publicly available for the Yemeni outbreak. Researchers can also apply our data extraction, alignment, and compilation techniques for other infectious disease outbreaks worldwide, as many WHO globally monitored infections share similar epidemiological bulletin reporting formats. We encourage researchers to harmonize and integrate more global public health data streams within this dataset, especially those from the WHO and World Food Programme (WFP) [58–63]. Research has documented how environmental risk factors amplify cholera infection rates at the district level, though few studies have explored these factors in combination with other conflict- or nutrition-related risk factors [13]. While key informant interviews have noted increased cholera morbidity and mortality in individuals with poor nutrition status, we found no studies investigating temporal relationships between cholera infection rates and risk factors related to food access, purchasing power, or insecurity [2, 3, 64]. Future research must be translational; we encourage researchers to standardize and harmonize data at granular spatial scales to inform and empower local actors to promote public health programming under constrained resource circumstances.

We reported confirmed cholera infections as weekly time series in two ways: with and without interpolating missing data. We urge the global health community to standardize reporting of missing with respect to reasons for, quantity of, and location where missing data occur within a time series. Metadata reports can include information describing the completeness of time series data over time and



by geographic location [52]. These reports inform data users how interpolation techniques impact time series analyses and forecasts [65]. Our attempts at interpolating missing data demonstrated the difficulties and ambiguity of using publicly reported time-referenced data when no metadata or standardized reporting protocol exists. These concerns and difficulties also occurred when extracting and aligning conflict-related time series data.

Conclusions

The global public health community needs comprehensive interdisciplinary data repositories and platforms supported by standardized data collection protocols. Modern surveillance systems should seek to harmonize the spatial and temporal resolution of time-referenced data so external users can effectively trace the onset, spread, and amplification of infections. We implore data-curating organizations to collect public health records in a way that ensures their long-term usability and should be treated as public health investments. We demonstrated how to curate public records in this way and used dynamic maps to trace the onset and spread of infection and conflict events that amplified the cholera outbreak in Yemen. Our dynamic maps suggest travelling waves of infection from Sana'a and Sana'a City to surrounding governorates as well as a persistent cluster of conflict events in Al-Hudaydah from June of 2018 through December of 2019. Future research must integrate additional global health data streams and utilize this visualization technique to uncover more associations between the cholera outbreaks and conflict-, environment-, and nutrition-related risk factors driving infection.

Supplementary Information The online version contains supplementary material available at https://doi.org/10.1057/s41271-022-00345-x. All movies are available for download at: https://tufts.box.com/v/Simpson-2022-CholeraDynamicMap.

Acknowledgements This research was based upon work supported in part by the Office of the Director of National Intelligence (ODNI), Intelligence Advanced Research Projects Activity (IARPA), via 2017-17072100002 (Naumova – PI). The views and conclusions contained herein are those of the authors and should not be interpreted as necessarily representing the official policies, either expressed or implied, of ODNI, IARPA, or the U.S. Government. The U.S. Government is authorized to reproduce and distribute reprints for governmental purposes notwithstanding any copyright annotation therein. The United States Department of Agriculture (USDA) National Institute of Food and Agriculture (NIFA) Cooperative State Research, Education, and Extension Service Fellowship supported Ryan B. Simpson via grant award number 2020-38420-30724. This work in part was supported by the STOP Spillover project through the United States Agency for International Development (USAID). The contents are the responsibility of STOP Spillover and do not necessarily reflect the views of USAID or the United States Government. The Tufts School of Medicine Building Diversity Biomedical Sciences Program supported Sofia Babool via award number R25-HL007785. The Tufts University Data Intensive Studies Center (DISC) Seed Grant also supported this research. Authors would like to acknowledge Alissa Ebel and Sirjana Shakya for their support in compiling ACLED data and Steff Rahaim of Tufts Technology Services for converting and re-mastering SWF files to MP4 formats.

Author Contributions M.C.T. contributed to data validation, the extraction of data from grey literature sources, and original conception of this research. R.B.S. and M.C.T. provided the original draft preparation and contributed to reviewing and editing the manuscript. R.B.S., S.B., and P.M.K. contributed to data extraction. R.B.S. conducted all spatial and temporal alignment. S.B. and P.M.K. validated spatial



and temporal alignment for all data sources. M.A.H. created dynamic map visualizations. E.N.N. contributed to methodology development, writing, reviewing, and editing the manuscript, supervision, project administration, and funding acquisition.

Declarations

Conflict of interest: Drs. Elena N. Naumova and Meghan A. Hartwick serve as the editor-in-chef and assistant to the editor for the Journal of Public Health Policy. They were not part of the review process for this article, which was handled by a member of the Editorial Board.

Open Access This article is licensed under a Creative Commons Attribution 4.0 International License, which permits use, sharing, adaptation, distribution and reproduction in any medium or format, as long as you give appropriate credit to the original author(s) and the source, provide a link to the Creative Commons licence, and indicate if changes were made. The images or other third party material in this article are included in the article's Creative Commons licence, unless indicated otherwise in a credit line to the material. If material is not included in the article's Creative Commons licence and your intended use is not permitted by statutory regulation or exceeds the permitted use, you will need to obtain permission directly from the copyright holder. To view a copy of this licence, visit http://creativecommons.org/licenses/by/4.0/.

References

1. Al-Mekhlafi HM. Yemen in a time of cholera: current situation and challenges. Am J Trop Med Hyg. 2018;98:1558–62.
2. Spiegel P, et al. Responding to epidemics in large-scale humanitarian crises: a case study of the cholera response in Yemen, 2016–2018. BMJ Glob Health. 2019;4:e001709.
3. Federspiel F, Ali M. The cholera outbreak in Yemen: lessons learned and way forward. BMC Public Health. 2018;18:1338.
4. Al-Awlaqi S, Dureab F, Annuzaili D, Al-Dheeb N. COVID-19 and conflict: The devastating impact of withdrawing humanitarian support on universal health coverage in Yemen. Public Health in Practice. 2020;1:100015.
5. Biggs, M. Yemen was poor before, but 'the war just finished us'. PBS NewsHour. 2018. https://www.pbs.org/newshour/show/yemen-was-poor-before-but-the-war-just-finished-us. Accessed 02 Feb 2022.
6. Hove-Musekwa SD, Nyabadza F, Chiyaka C, Das P, Tripathi A, Mukandavire Z. Modelling and analysis of the effects of malnutrition in the spread of cholera. Math Comput Model. 2011;53:1583–95.
7. Michael, M. Vaccines blocked as deadly cholera raged across Yemen. Associated Press News. https://apnews.com/article/health-united-nations-yemen-cholera-international-news-b821a9b1811d4b4d803fffd4fe132b4e. Accessed 02 Feb 2022.
8. Abbara A, et al. The challenges of tuberculosis control in protracted conflict: the case of Syria. Int J Infect Dis. 2020;90:53–9.
9. Alawieh A, et al. Revisiting leishmaniasis in the time of war: the Syrian conflict and the Lebanese outbreak. Int J Infect Dis. 2014;29:115–9.
10. Khwaif JM, Hayyawi AH, Yousif TI. Cholera outbreak in Baghdad in 2007: an epidemiological study. East Mediterr Health J. 2010;16:584–9.
11. Azman AS, Moore SM, Lessler J. Surveillance and the global fight against cholera: setting priorities and tracking progress. Vaccine. 2020;38:A28.
12. Sparrow A, Almilaji K, Tajaldin B, Teodoro N, Langton P. Cholera in the time of war: implications of weak surveillance in Syria for the WHO's preparedness—a comparison of two monitoring systems. BMJ Glob Health. 2016;1:e000029.
13. Camacho A, et al. Cholera epidemic in Yemen, 2016–18: an analysis of surveillance data. Lancet Glob Health. 2018;6:e680–90.

14. Dureab F, Ismail O, Mueller O, Jahn A. Cholera outbreak in Yemen: timeliness of reporting and response in the National Electronic Disease Early Warning System. Acta Inform Med. 2019;2:85.
15. Craig I. 'Only God can save us': Yemeni children starve as aid is held at border. *The Guardian*. 2017. https://www.theguardian.com/world/2017/nov/12/millions-on-brink-of-famine-in-yemen-as-saudi-arabia-tightens-blockade. Accessed 02 Jun 2021.
16. Ghebreyesus TA, Lake A, Beasley D. UN leaders appeal for immediate lifting of humanitarian blockade in Yemen – lives of millions are at risk. UNICEF. 2017. https://www.unicef.org/media/media_101496.html. Accessed 02 Jun 2021.
17. Médecins Sans Frontières (MSF) International. Yemen: MSF statement on Saudi-led coalition blockage. MSF. 2017. https://www.msf.org/yemen-msf-statement-saudi-led-coalition-blockage. Accessed 02 Jun 2021.
18. Simpson RB, Babool S, Tarnas MC, Kaminski PM, Hartwick MA, Naumova EN. Signatures of cholera outbreak during the Yemeni Civil War, 2016–2019. Int J Environ Res Public Health. 2022;19:378.
19. Armed Conflict Location & Event Data Project (ACLED). About ACLED. ACLED. 2021. https://www.acleddata.com/about-acled/. Accessed 01 Jun 2019.
20. Hegre H, Østby G, Raleigh C. Poverty and Civil war events: a disaggregated study of Liberia. J Conflict Resolut. 2009;53:598–623.
21. Raleigh C, Hegre H. Population size, concentration, and civil war. A geographically disaggregated analysis. Political Geogr. 2009;28:224–38.
22. Raleigh C, Linke A, Hegre H, Karlsen J. Introducing ACLED: an armed conflict location and event dataset. J Peace Res. 2010;47:651–60.
23. Ismail SA, et al. Communicable disease surveillance and control in the context of conflict and mass displacement in Syria. Int J Infect Dis. 2016;47:15–22.
24. Blok C, Kobben B, Cheng T, Kuterma A. Visualization of relationships between spatial patterns in time by cartographic animation. Cartogr Geogr Inf Sci. 1999;26:139–51.
25. Castronovo DA, Chui KK, Naumova EN. Dynamic maps: a visual-analytic methodology for exploring spatio-temporal disease patterns. Environ Health. 2009;8:1–9.
26. Harrower M, Fabrikant SI. The role of map animation for geographic visualization. In: Dodge M, McDerby M, Turner M, editors. Geographic visualization. Hoboken: Wiley; 2008. p. 49–65.
27. Moorthy M, et al. Deviations in influenza seasonality: odd coincidence or obscure consequence? Clin Microbiol Infect. 2012;18:955–62.
28. Yattaw NJ. Conceptualizing space and time: a classification of geographic movement. Cartogr Geogr Inf Sci. 1999;26:85–98.
29. Eastern Mediterranean Regional Office (EMRO): World Health Organization. Archived epidemiology bulletins. WHO. 2021. http://www.emro.who.int/yem/information-resources/epidemiology-bulletins-archive.html. Accessed 01 Jun 2019.
30. Armed Conflict Location & Event Data Project (ACLED). Data Export Tool. ACLED. 2021. https://www.acleddata.com/data/. Accessed 01 Jun 2019.
31. Armed Conflict Location & Event Data Project (ACLED). ACLED Methodology and Coding Decisions around the Yemen Civil War. ACLED. 2021. https://acleddata.com/acleddatanew/wp-content/uploads/dlm_uploads/2019/01/YemenMethodology_2020_ACLED.pdf. Accessed 01 Jun 2019.
32. Armed Conflict Location & Event Data Project (ACLED). ACLED Codebook. ACLED. 2021. https://acleddata.com/acleddatanew/wp-content/uploads/dlm_uploads/2019/04/ACLED_Codebook_2019FINAL_pbl.pdf. Accessed 01 Jun 2019.
33. Armed Conflict Location & Event Data Project (ACLED). ACLED Definitions of Political Violence and Protest. ACLED. 2021. https://acleddata.com/acleddatanew/wp-content/uploads/dlm_uploads/2019/04/ACLED-Event-Definitions_Final.pdf. Accessed 01 Jun 2019.
34. Armed Conflict Location & Event Data Project (ACLED). ACLED Methodology. ACLED. 2021. https://acleddata.com/acleddatanew/wp-content/uploads/dlm_uploads/2019/04/Methodology-Overview_FINAL.pdf. Accessed 01 Jun 2019.
35. Armed Conflict Location & Event Data Project (ACLED). ACLED General Quick User Guide. ACLED. 2021. https://acleddata.com/acleddatanew/wp-content/uploads/dlm_uploads/2019/04/General-User-Guide_FINAL-1.pdf. Accessed 01 Jun 2019.
36. Eastern Mediterranean Regional Office (EMRO): World Health Organization. Cholera Outbreaks. WHO. 2021. http://www.emro.who.int/health-topics/cholera-outbreak/cholera-outbreaks.html. Accessed 01 Jun 2019.



37. Eastern Mediterranean Regional Office (EMRO): World Health Organization. Epidemic and pandemic-prone diseases. WHO. 2021. http://www.emro.who.int/pandemic-epidemic-diseases/cholera/index.html. Accessed 01 Jun 2019.
38. Eastern Mediterranean Regional Office (EMRO): World Health Organization. Yemen Situation Reports: Weekly cholera bulletins. WHO. 2021. http://www.emro.who.int/yem/yemeninfocus/situation-reports.html. Accessed 01 Jun 2019.
39. Simpson RB. et al. Dynamic mapping of cholera spread and conflict severity during the Yemeni Civil War, 2016-2019. figshare. 2021. https://figshare.com/s/3b2882c020ae9ed2e576. Accessed 17 Feb 2021.
40. Central Statistical Organization (CSO). Summary table of the main results of population projection data and indicators (2005–2025) according to different hypotheses and alternatives. Yemeni Central Bureau of Statistics. 2010. http://www.cso-yemen.com/content.php?lng=arabic&id=553. Accessed 01 Jun 2019.
41. Displacement Tracking Matrix (DTM). Yemen. International Organization of Migration. 2019. https://dtm.iom.int/yemen. Accessed 01 Jun 2019.
42. Central Statistical Organization (CSO). The General Census of Population, Housing, and Establishments 2014. Yemeni Central Bureau of Statistics. 2012. http://www.cso-yemen.com/content.php?lng=arabic&id=593. Accessed 01 Jun 2019.
43. British Broadcasting Corporation (BBC). Yemen war: Battle for vital port of Hudaydah intensifies. BBC News. 2018. https://www.bbc.com/news/world-middle-east-46125858. Accessed on 15 August 2021.
44. Human Rights Watch (HRW). Deadly Consequences: Obstruction of aid in Yemen during COVID-19. Human Rights Watch. 2020. https://www.hrw.org/report/2020/09/14/deadly-consequences-obstruction-aid-yemen-during-covid-19. Accessed on 15 August 2021.
45. Jutla A, et al. Environmental factors influencing epidemic cholera. Am J Trop Med Hyg. 2013;89:597–607.
46. Richterman A, Azman AS, Constant G, Ivers LC. The inverse relationship between national food security and annual cholera incidence: a 30-country analysis. BMJ Glob Health. 2019;4:e001755.
47. Von Seidlein L, Deen JL. Preventing cholera outbreaks through early targeted interventions. PLoS Med. 2018;15:e1002510.
48. De Magny GC, et al. Environmental signatures associated with cholera epidemics. Proc Natl Acad Sci USA. 2008;105:17676–81.
49. Grad YH, Miller JC, Lipsitch M. Cholera modeling: challenges to quantitative analysis and predicting the impact of interventions. Epidemiology. 2012;23:523.
50. Norris A, Hachey K, Curtis A, Bourdeaux M. Crippling violence: conflict and incident polio in Afghanistan. PLoS ONE. 2016;11:e0149074.
51. Verma AA, Jimenez MP, Tangermann RH, Subramanian SV, Razak F. Insecurity, polio vaccination rates, and polio incidence in northwest Pakistan. Proc Natl Acad Sci USA. 2018;115:1593–8.
52. Simpson RB, Gottlieb J, Zhou B, Hartwick MA, Naumova EN. Completeness of open access FluNet influenza surveillance data for Pan-America in 2005–2019. Sci Rep. 2021. https://doi.org/10.1038/s41598-020-80842-9.
53. Tarwater PM, Martin CF. Effects of population density on the spread of disease. Complexity. 2001;6:29–36.
54. The WHO. deserves more money for its core mission—and more respect. Nature. 2022;602:7–8.
55. International Organization for Migration's (IMO) Global Migration Data Analysis Center: Migration Data Portal. Themes: Forced migration or displacement. IOM. 2021. http://migrationdataportal.org/themes/forced-migration-or-displacement. Accessed 01 Jun 2019.
56. Cockburn P. The Yemen war death toll is five times higher than we think – we can't shrug off our responsibilities any longer. The Independent. 2018. https://www.independent.co.uk/voices/yemen-war-death-toll-saudi-arabia-allies-how-many-killed-responsibility-a8603326.html. Accessed 01 Jun 2019.
57. Jain V. Financing global health emergency response: outbreaks, not agencies. J Public Health Policy. 2019;41:1–10.
58. World Food Program (WFP). Vulnerability and Mapping Assessment Food Security Analysis: Seasonal Explorer. WFP. 2021. https://dataviz.vam.wfp.org/seasonal_explorer/rainfall_vegetation/visualizations. Accessed 01 Jun 2019.

59. World Food Program (WFP). Vulnerability and Mapping Assessment Food Security Analysis: Yemen mVAM Methodology. WFP. 2021. https://vam.wfp.org/sites/mvam_monitoring/Methodology/read_me_yemen.pdf. Accessed 01 Jun 2019.
60. World Food Program (WFP). Vulnerability and Mapping Assessment Food Security Analysis: Technical Guidance Sheet, Food Consumption Analysis. WFP. 2021. https://documents.wfp.org/stellent/groups/public/documents/manual_guide_proced/wfp197216.pdf. Accessed 01 Jun 2019.
61. Maxwell D, Caldwell R. The Coping Strategies Index: A tool for rapid measurement of household food security and the impact of food aid programs in humanitarian emergencies. World Food Programme (WFP). 2008. https://documents.wfp.org/stellent/groups/public/documents/manual_guide_proced/wfp211058.pdf. Accessed 01 Jun 2019.
62. World Food Program (WFP). Vulnerability and Mapping Assessment Food Security Analysis: Economic Explorer. WFP. 2021. https://dataviz.vam.wfp.org/economic_explorer/prices. Accessed 01 Jun 2019.
63. World Food Program (WFP). Vulnerability and Mapping Assessment Food Security Analysis: Seasonal Explorer, How It Works. WFP. 2021. https://dataviz.vam.wfp.org/seasonal_explorer/rainfall_vegetation/help. Accessed 01 Jun 2019.
64. Legros D. Global cholera epidemiology: opportunities to reduce the burden of cholera by 2030. J Infect Dis. 2018;218:S137–40.
65. Fefferman N, Naumova E. Innovation in observation: a vision for early outbreak detection. Emerg Health Threats J. 2010;3:7103.

Publisher's Note Springer Nature remains neutral with regard to jurisdictional claims in published maps and institutional affiliations.

Ryan B. Simpson is a Ph.D. candidate in the Nutrition Epidemiology and Data Science Division at the Tufts University Friedman School of Nutrition Science and Policy, Boston, MA, USA.

Sofia Babool is a Bachelor of Arts student in the Neuroscience Department at the University of Texas at Dallas, Richardson, TX, USA.

Maia C. Tarnas was an undergraduate student in the Community Health Department at Tufts University School of Arts and Sciences, Medford, MA, USA at the time of paper preparation. She is now a Ph.D. student at the University of California Irvine, Irvine, CA, USA.

Paulina M. Kaminski was a fellow at the Tufts Initiative for the Forecasting and Modeling of Infectious Diseases (InForMID, Friedman School of Nutrition Science and Policy, Tufts University, Boston, MA, USA at the time of paper preparation. She is now a Senior Associate at Oxeon Partners, New York City, NY, USA.

Meghan A. Hartwick was a fellow at the Tufts Initiative for the Forecasting and Modeling of Infectious Diseases (InForMID, Friedman School of Nutrition Science and Policy, Tufts University, Boston, MA, USA at the time of paper preparation. She is now a Data Science Fellow at the National Institutes of Health, Bethesda, MD, USA.

Elena N. Naumova is a Professor and the Chair of the Nutrition Epidemiology and Data Science Division at the Friedman School of Nutrition Science and Policy, Tufts University, Boston, MA, USA.

International Journal of
Environmental Research and Public Health

MDPI

Article

Signatures of Cholera Outbreak during the Yemeni Civil War, 2016–2019

Ryan B. Simpson [1,*], Sofia Babool [2], Maia C. Tarnas [3], Paulina M. Kaminski [1], Meghan A. Hartwick [1] and Elena N. Naumova [1,*]

[1] Division of Nutrition Epidemiology and Data Science, Friedman School of Nutrition Science and Policy, Tufts University, 150 Harrison Avenue, Boston, MA 02111, USA; paulina.kaminski13@gmail.com (P.M.K.); meghartwick@gmail.com (M.A.H.)
[2] Department of Neuroscience, The University of Texas at Dallas, 800 W Campbell Road, Richardson, TX 75080, USA; sfb170000@utdallas.edu
[3] Department of Community Health, School of Arts and Sciences, Tufts University, 574 Boston Avenue, Medford, MA 02155, USA; maia.tarnas@gmail.com
* Correspondence: ryan.simpson@tufts.edu (R.B.S.); elena.naumova@tufts.edu (E.N.N.); Tel.: +1-978-697-1037 (R.B.S.); +1-617-636-2927 (E.N.N.)

Abstract: The Global Task Force on Cholera Control (GTFCC) created a strategy for early outbreak detection, hotspot identification, and resource mobilization coordination in response to the Yemeni cholera epidemic. This strategy requires a systematic approach for defining and classifying outbreak signatures, or the profile of an epidemic curve and its features. We used publicly available data to quantify outbreak features of the ongoing cholera epidemic in Yemen and clustered governorates using an adaptive time series methodology. We characterized outbreak signatures and identified clusters using a weekly time series of cholera rates in 20 Yemeni governorates and nationally from 4 September 2016 through 29 December 2019 as reported by the World Health Organization (WHO). We quantified critical points and periods using Kolmogorov–Zurbenko adaptive filter methodology. We assigned governorates into six clusters sharing similar outbreak signatures, according to similarities in critical points, critical periods, and the magnitude of peak rates. We identified four national outbreak waves beginning on 12 September 2016, 6 March 2017, 28 May 2018, and 28 January 2019. Among six identified clusters, we classified a core regional hotspot in Sana'a, Sana'a City, and Al-Hudaydah—the expected origin of the national outbreak. The five additional clusters differed in Wave 2 and Wave 3 peak frequency, timing, magnitude, and geographic location. As of 29 December 2019, no governorates had returned to pre-Wave 1 levels. The detected similarity in outbreak signatures suggests potentially shared environmental and human-made drivers of infection; the heterogeneity in outbreak signatures implies the potential traveling waves outwards from the core regional hotspot that could be governed by factors that deserve further investigation.

Keywords: cholera; critical periods; Kolmogorov–Zurbenko filter; outbreak signature; time series; Yemen

check for updates

Citation: Simpson, R.B.; Babool, S.; Tarnas, M.C.; Kaminski, P.M.; Hartwick, M.A.; Naumova, E.N. Signatures of Cholera Outbreak during the Yemeni Civil War, 2016–2019. *Int. J. Environ. Res. Public Health* **2022**, *19*, 378. https://doi.org/10.3390/ijerph19010378

Academic Editor: Paul B. Tchounwou

Received: 29 November 2021
Accepted: 27 December 2021
Published: 30 December 2021

Publisher's Note: MDPI stays neutral with regard to jurisdictional claims in published maps and institutional affiliations.

Copyright: © 2021 by the authors. Licensee MDPI, Basel, Switzerland. This article is an open access article distributed under the terms and conditions of the Creative Commons Attribution (CC BY) license (https://creativecommons.org/licenses/by/4.0/).

1. Introduction

The ongoing cholera epidemic in Yemen is the largest in recorded history, with over 1 million suspected cholera cases since 2016 [1,2]. The inability of the Yemeni government, Houthi forces, and other involved actors and international agencies to mitigate this epidemic demonstrates the challenges that many countries face when trying to manage infectious disease outbreaks amidst other humanitarian emergencies [1–5]. The ongoing outbreak coincides with the Yemeni Civil War (2015–ongoing), which has crippled existing health infrastructure and depleted medical resource stockpiles [5,6]. Even before these crises, Yemen was one of the poorest countries in the Arabian Peninsula, with widespread malnutrition and rampant poverty [5].

Limited access to safe and affordable water has increased the number of individuals exposed to cholera, a waterborne disease, while a growing malnourished and immunocompromised population has increased the risk of infection [5,7]. This, coupled with limited access to health care, has severely decreased the efficacy of existing prevention and control measures. The variety of human-made and environmental drivers of the outbreak complicates what resources international aid organizations distribute and how, when, and where these resources are disseminated. The response to the ongoing cholera outbreak in Yemen differed from those in other countries, with factors governing transmission still unclear. The response is now aggravated by the COVID-19 pandemic, forcing public health professionals to rethink the ways to handle large-scale outbreaks.

The World Health Organization's (WHO) Global Task Force on Cholera Control (GTFCC) created a global roadmap for country-level cholera mitigation in October 2017 [8,9]. The report emphasized the need for data-driven recommendations to (1) improve early outbreak detection; (2) identify regional hotspots with recurrent outbreaks; and (3) coordinate medical resource mobilization in 47 countries worldwide [8,9]. The GTFCC stressed that improved analyses of available surveillance data can improve outbreak characterization and identification of transmission patterns to create national prevention programs [8]. This included conducting routine vulnerability assessments of at-risk populations and monitoring environmental and human-made drivers of the cholera outbreak for early detection and response [8]. Once outbreak signatures are defined, public health professionals can detect common risk factors, inform the appropriate aid organizations, and improve outbreak response efforts [8,10,11].

In our early works, we explored the concept of outbreak signatures, defined as the shape of an epidemic curve in combination with its temporal features including critical points (onset, peak, resolution) and critical periods (acceleration, deceleration, steady state) [12–14]. We applied this concept to modeling waterborne infections and emphasized the importance of characterizing outbreak signatures for early detection and mitigation [12–15]. We also provided a methodology for estimating the peak timing and amplitude of seasonal enteric infections and used these features to assess the synchronization of infections across geographic regions [16–24].

While researchers agree on a general definition of an outbreak and its features, such as onset, peak intensity, and resolution, there are no widely accepted systematic approaches to estimate such features from historic data. The onset and resolution timing are often declared (and occasionally revised) by local, national, or international officials. The common approach to defining the outbreak signature is solely based on the visual inspection of an epidemic curve or basic agreements [25]. We expanded on our early works by proposing a methodology for systematically defining outbreak signatures and classifying regional hotspots to explore the potential of traveling waves of infection outwards from regional hotspots.

In this study, we quantified outbreak features, including critical points (onset, peak, and resolution) and critical periods (acceleration, deceleration, and steady state), of the ongoing cholera epidemic in Yemen and clustered governorates according to these features. We compiled publicly available data from the WHO's Eastern Mediterranean Regional Office's (EMRO) epidemiological bulletins and created a weekly time series of cholera rates for 20 of 21 governorates in the period 2016–2019. We defined critical points and periods using a non-parametric Kolmogorov–Zurbenko adaptive filter and classified governorates according to similarities of these features. Our curated time series dataset and applied methodology could offer technical guidance to supplement the GTFCC cholera mitigation roadmap and can be used to further investigate human-made and environmental drivers of cholera outbreaks in conflict areas.

2. Materials and Methods

2.1. Data Sources

The WHO, in collaboration with the Yemeni Ministry of Health (MOH), has collected records of laboratory-confirmed cholera infections in Yemen as part of the electronic Disease Early Warning System (eDEWS) since 2013 [26]. This database contains public and private health facility records compiled into a district-level time series dataset based on the time of hospital admission [26,27]. The MOH and the WHO reported governorate-level aggregated eDEWS data via the WHO's Eastern Mediterranean Regional Office's (EMRO) epidemiological bulletins for public use in the period 2016–2019 [28–30].

These bulletins changed reporting formats multiple times during the study period, specifically its temporal resolution (as daily, weekly, and monthly cumulative counts) and spatial granularity (at the governorate and national levels). No epidemiological bulletins were available prior to Week 36 of 2016. We had only 9 weeks (5% of 172) with missing data. Records were missing for 4 consecutive weeks in 2017 (Week 13–16 (27-March to 23-April)), 1 week in February of 2018 (Week 8 (19–25 February)) and 4 consecutive weeks in July of 2018 (Week 27–30 of 2018 (2–29 July)). We excluded Hadramaut and Socotra island from our analysis as the EMRO inconsistently reported data for these locations. The EMRO did not report cholera data for 2020 or 2021. All discovered bulletins along with the raw and curated records were uploaded to figshare [31].

2.2. Time Series Compilation

To conduct our analyses, we compiled all abstracted records in a uniform format. We aggregated data by WHO-defined epidemiological weeks as performed for other WHO-monitored infections [32]. Daily case reports were available for 29 weeks (17% of study period) from Week 36 of 2016 (4 September 2016) to Week 12 of 2017 (21 March 2017). Weekly reports were available for 62 weeks (36%) from Week 17 of 2017 (24 April 2017) through Week 26 of 2018 (1 July 2018). Monthly reports were available for 74 weeks (43%) from July 2018 through December 2019. We describe the procedure for time series compilation below.

We extracted daily case data from irregularly reported WHO EMRO daily epidemiological bulletins and aggregated cases by WHO-defined weeks. Bulletins provided updates on the number of cumulative confirmed infections occurring during multi-day reporting periods based on time of hospital admission [26,27]. We estimated average daily cases by subtracting total cases from consecutive reports and dividing by the number of days in the reporting period. We prorated weekly case counts for Week 12 of 2017 as records were incomplete (5 of 7 days had missing records). We interpolated records for 4 consecutive weeks (14% out of 29) using linear approximation based on information from adjacent weeks (before and after the missing week) capturing the overall seasonal behavior.

We extracted weekly records from epidemiological bulletins available from Week 17 of 2017 (24 April 2017) through Week 26 of 2018 (1 July 2018). Weekly data were reported using a governorate-level spreadsheet containing cumulative confirmed cholera cases for the WHO-defined "Second Wave" of the epidemic. In these bulletins, weekly cases were provided for the week of the report, including both provisional and confirmed cases, and for each of the prior three weeks, which included only confirmed cases. We reviewed each weekly bulletin in chronological order and extracted the 3 week lagged confirmed case estimate that presumably contained most accurate information. For 5 incomplete bulletins (8% out of 62), we estimated weekly cases using 2 week and 1 week lagged case estimates. We interpolated cases for Week 8 of 2018 (19–25 February) using adjacent weeks' values.

We used monthly records from the WHO EMRO monthly situation reports available from July 2018 through December 2019. These bulletins provided cumulative confirmed cases from Week 17 of 2017 to the final day of the reporting month. We converted monthly cumulative counts to weekly case counts in two steps. First, we subtracted consecutive monthly bulletins to estimate newly reported cases in that month. Next, we estimated average cases for each day within a given month by dividing these new cases by the number

of days within the month, and aggregated cases according to WHO-defined epidemiological weeks. We interpolated missing records for 4 consecutive weeks (5.6% out of 72) using linear approximation based on information from adjacent weeks.

We estimated national cases by summing all governorate-level cases for each week of the 172 week study. We conducted all analyses according to study week (ranging 1–172) and reported all results using a combination of WHO-defined epidemiological weeks (ranging 1–52 per year) and Gregorian calendar dates (formatted DD-Month-YYYY).

2.3. Rate Calculations

To compare outbreak signatures across governorates, we calculated weekly rates of infection using fatality-adjusted, pro-rated weekly population estimates. We extracted data on conflict fatalities using the Armed Conflict Location and Event Data (ACLED) project, which reported on both violent and non-violent political events [33,34]. We summed all fatalities from all political events on each day per governorate and then aggregated daily totals by WHO-defined epidemiological week. We used fatality counts to correct the population estimates. We also applied a low-to-moderate population growth rate (≈ 0.024) reported by the Yemeni Central Bureau of Statistics to approximate population changes during the civil war [35] and prorated this growth rate for the annual cycle in weeks (e.g., 0.024/52.25 = 0.00045933).

We estimated weekly governorate-level population in several steps. First, we calculated the population for Week 1 of 2017 as the average of population estimates from multiple sources including the WHO EMRO, the 2004 Yemeni Central Statistical Organization (CSO) population projection for 2005–2025, and the International Organization for Migration (IOM) Displacement Tracking Matrix's (DTM) 2017 Population Estimate [30,35,36]. Next, for Week 2 of 2017 through Week 52 of 2019, we estimated weekly governorate-level population iteratively forwards by subtracting conflict fatalities from the prior week and multiplying the difference by the prorated annual growth rate (Equation (1)). Finally, to correct for fatalities occurring between Week 36 of 2016 and Week 1 of 2017, we estimated weekly population by adding conflict fatalities and dividing the sum by the weekly-adjusted population growth rate (Equation (2)).

$$P_{s,t} = (P_{s,t-1} - F_{s,t-1}) * (1 + \frac{0.024}{52.25}) \text{ if } t > \text{ Week 1 of 2017} \quad (1)$$

$$P_{s,t} = (P_{s,t+1} + F_{s,t+1}) * (1 - \frac{0.024}{52.25}) \text{ if } t < \text{ Week 1 of 2017} \quad (2)$$

where $P_{s,t}$—the population for s-governorate in t-week; and $F_{s,t}$—the all-cause war conflict fatalities for s-governorate in t-week.

We calculated weekly rates of confirmed cholera infections (cases per 100,000 persons or cph) by dividing weekly cases by population estimates and multiplying by 100,000. We provide the curated weekly time series of case and rate estimates with and without interpolated values (Supplementary Excel Table S1).

2.4. Defining Outbreak Signatures and Features

We defined outbreak signatures using the timing of critical points, the duration of critical periods, and the magnitude of smoothed peak rates (example shown in Figure 1; Supplementary Excel Table S2). Critical points included the onset (O) of an outbreak when weekly rates began increasing, an outbreak peak (P) when weekly rates reached local maxima, and the return-from-peak or resolution (R) of an outbreak when weekly rates returned to steady-state levels, if this occurred.

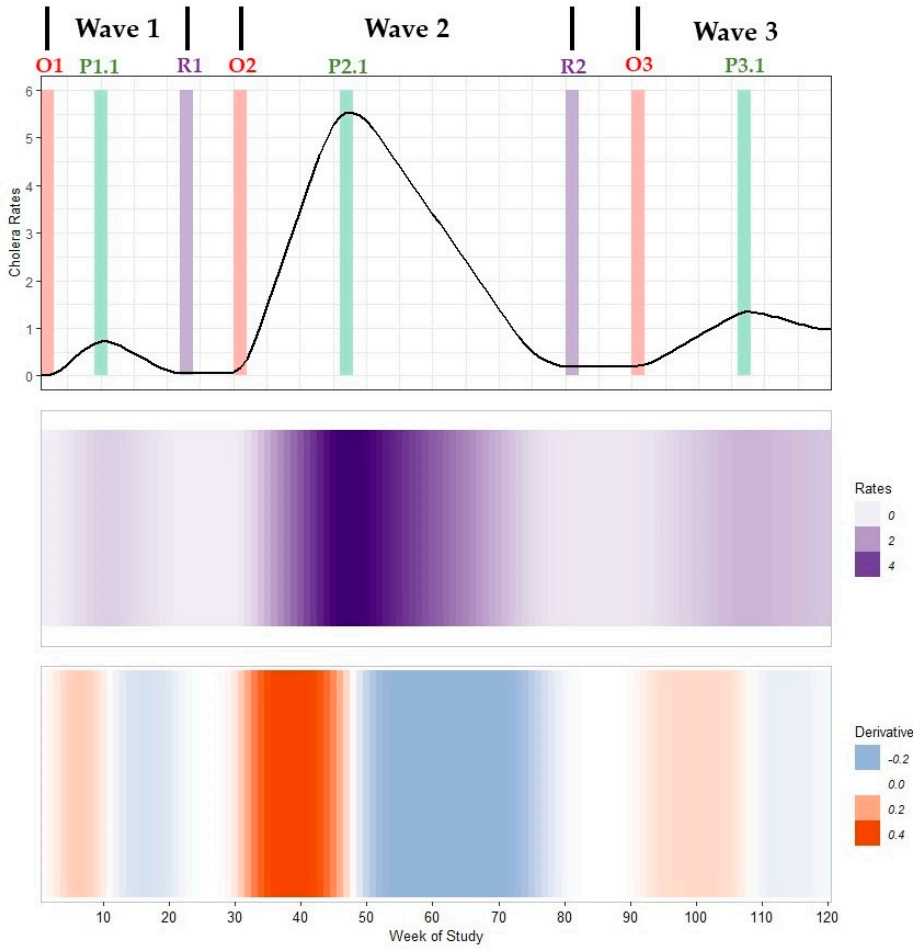


Figure 1. A multi-panel plot of an example cholera outbreak signature with three waves. Top panel: a time series of smoothed average rates of cholera infection (an epidemic curve). Middle panel: a heatmap that compactly reports weekly rates (outbreak magnitude) where light purple represents low values and dark purple represents high values. Bottom panel: a heatmap of the change in rates (trivial derivative) where acceleration periods are shown by the orange gradient, deceleration periods are shown by the blue gradient, and steady-state periods or critical change points near peaks are shown in grey. All panels share the common horizontal axis of time (study week). The timing of outbreak onset (O_n), peak ($P_{n.i}$), and resolution (R_n) are marked with red, green and purple bars, respectively, for the nth wave and the ith peak within that wave. If no resolution period occurs, the outbreak remains ongoing until reaching resolution or the next wave's onset (shown in Wave 3). Data used to develop this visualization are reported in Supplementary Excel Table S2.

Critical periods included the acceleration period from onset to peak, the deceleration period from peak to resolution (or next outbreak onset if no resolution occurred), and the steady-state period from resolution to onset. Each period had a distinct behavior: acceleration periods indicated times when weekly rates steadily increased, deceleration periods indicated when rates steadily decreased, and steady-state periods indicated when rates plateaued. We also calculated the pace of increase (proxy to basic reproduction number) and pace of decline as the linear approximation from onset timing to peak timing and peak timing to resolution timing or next wave onset timing, respectively. We reported critical period duration in weeks and pace of increase or decline in cph per week (cph/week). By comparing the timing of critical points, duration of critical periods, and magnitude of smoothed peak rate times in different locations, we defined regional hotspots and explored the potential of traveling waves of infection outwards from regional hotspots.

To produce smoothed outbreak signatures and detect change points in the time series (including the time periods when the absolute change increased, decreased, or approached near-zero values), we applied a modified version of the Kolmogorov–Zurbenko (KZ) adaptive filter [37–40]. The KZ filter is a non-parametric smoothing technique used to detect distinct changes in a highly noisy time series [37–40]. This technique used a real-values time series $X(t)$, $t = 0, \pm1, \pm2, \pm3 \ldots$ to generate a set of moving averages (MA) for windows of various sizes (Equation (3)):

$$Z(t,q) = \frac{1}{2q+1} \sum_{l=-q}^{q} X(t,l) \quad (3)$$

where q was the half length of a MA window, so $Z(t,q)$ were the smoothed values of $X(t)$ with a different degree of reduced noise.

We created a set of time series of natural logarithm (ln)-transformed corrected rates (Equation (4)), estimated as:

$$Y^*_{t,s} = \ln\left(\frac{C_{t,s} + \alpha}{P_{t,s}} * M\right) \quad (4)$$

where $C_{t,s}$ were weekly counts for t-week and s-location corrected by a = 1 case and adjusted for estimated weekly population ($P_{t,s}$) estimates, per M = 100,000 persons. Natural logarithm transformations addressed the right skewed distribution of weekly rates due to short bursts of high values during epidemic peaks and prolonged periods of low reported rates in the beginning of the epidemic. We then created a set of time series of the trivial derivatives, which were estimated as the absolute change in weekly ln-transformed rates: $Y^{*\prime}_{t,s} = Y^*_{t+1,s} - Y^*_{t,s}$.

We applied the KZ filter iteratively and generated a set of MA for both sets (Equations (5) and (6)), as:

$$Z^*_{t,s,q} = \frac{1}{2q+1} \sum_{l=-q}^{q} Y^*_{t,s,l} \quad (5)$$

$$Z^{*\prime}_{t,s,q} = \frac{1}{2q+1} \sum_{l=-q}^{q} Y^{*\prime}_{t,s,l} \quad (6)$$

for q = 1–25, to cover various window sizes $\omega = 2q + 1$, from 3 to 51 weeks to depict the outbreak signature and to reflect the temporal changes from about one month to about one year. We then examined each set of select windows that sufficiently reduced noise yet maintained inflection points within the trivial derivative, as a verification step. By comparing the fit with sum of squares criteria, we selected candidates averaging across four windows: q = 1–15, q = 1–11, q = 1–7, and q = 3–5. We selected the best performing smoother (q = 3–5) to assess the similarities across governorate-specific outbreak signatures and to estimate the absolute change in weekly smoothed rates, as: $Z'_{t,s,3\text{–}5} = (Z^*_{t+1,s,3} + Z^*_{t+1,s,5})/2 - (Z^*_{t,s,3} + Z^*_{t,s,5})/2$. The fit of this smoother for each governorate and nationally is shown in Figures S1–S6 (data in Supplementary Excel Table S3).

We estimated local maximums and minimums in $Y^*_{t,s}$, $Z^*_{t,s,3\text{–}5}$, $Z^*_{t,s,0\text{–}7}$, $Z^*_{t,s,0\text{–}11}$, $Z^*_{t,s,0\text{–}15}$, to identify time points and periods of high and low disease rates, respectively. To confirm maximums and minimums detected in the smoothed values of rates, we identified weeks when $Y^{*\prime}_{t,s}$, $Z^{*\prime}_{t,s,3\text{–}5}$, $Z^{*\prime}_{t,s,0\text{–}7}$, $Z^{*\prime}_{t,s,0\text{–}11}$, and $Z^{*\prime}_{t,s,0\text{–}15}$ approached zero. We defined outbreak onset as the beginning of a rapid rise of rates ($Z^*_{t,s,3\text{–}5}$) and inflection of the trivial derivative ($Z'_{t,s,3\text{–}5}$) from near-zero to high positive values. We defined outbreak peak as the time when rates were reaching a local maximum of $Z^*_{t,s,3\text{–}5}$ with the inflection point of $Z'_{t,s,3\text{–}5}$ at near-zero or negative values. We defined outbreak resolution time as when rates $Z^*_{t,s,3\text{–}5}$ were low or near a local minimum and $Z'_{t,s,3\text{–}5}$ approached near-zero values. We expressed critical time points and periods in WHO-defined epidemiological weeks along with its plausible range.

We defined outbreak waves as either the duration from onset to resolution critical points or the duration between two onset critical points if no definite resolution occurred using the most refined window of 3–5 weeks. If no resolution occurred, we differentiated between waves by identifying weeks when rates $Z^*_{t,s,3–5}$ plateau for 4–6 weeks followed by 3–5 weeks of a steady increase in rates when the trivial derivative ($Z'_{t,s,3–5}$) increased from near-zero to high positive values. When possible, we identified primary and secondary outbreak peaks for specific waves based on our ability to detect local minimums and maximums. Secondary peaks referred to times when rates reached a local maximum of $Z^*_{t,s,3–5}$ after a burst of $Z'_{t,s,3–5}$ from high negative to high positive values. To confirm the potential for a secondary peak, we calculated the acceleration period and pace of increase from wave onset to each peak timing and calculated the deceleration period and pace of decline from each peak timing to the conclusion of the wave (resolution or following wave onset) that are characteristic for an ongoing outbreak.

2.5. Clustering of Outbreak Signatures

We applied pairwise Spearman cross-correlation estimates, covering six lead and six lag weeks (or lead-lag of +6 to −6 weeks) to examine similarities across governorate-specific outbreak signatures using the best performing smoother (Supplementary Table S1). We selected this lead-lag structure because governorate critical points varied by approximately six weeks. We assigned governorates with strong serial cross-correlations, close spatial proximity to each other, and similarities across outbreak signature features including the timing of critical points, duration of critical periods, and magnitude of peak rates into the same cluster (six clusters in all).

We performed all statistical analyses and visualizations using Excel (14.3.6), Stata (SE 15.1), and R (3.6.3) software. We created all maps using publicly available shapefiles reported by the United Nations (UN) Office for the Coordination of Humanitarian Affairs (OCHA) and published on the Humanitarian Data Exchange (HumData) [41]. The data and R codes used to create maps and illustrations in this study are available in Supplementary Materials.

3. Results

We presented results starting with quantifying outbreak features for Yemen nationally and by governorate using smoothed rates and trivial derivatives. We then examined similarities in outbreak features (critical points, critical periods, spatial proximity, and smoothed rate magnitudes) to define clusters. Finally, we analyzed similarities within and differences between clusters on a one-by-one basis in all subsequent subsections.

3.1. Four Waves of Cholera Outbreak Signatures

Over our 172 week study period, we identified ~2.1 million confirmed cholera infections among the ~28.6 million estimated inhabitants of Yemen. Based on the estimated onset, peak, and resolution critical points and acceleration, deceleration, and steady-state period durations for the Yemeni cholera outbreak from 4 September 2016 through 29 December 2019, we identified four distinct national outbreak waves (Figure 2, Tables 1 and 2; Supplementary Excel Tables S3 and S4). Wave 1 began in 12–18 September 2016 with a peak in 7–13 November 2016 and resolution in 2–8 January 2017. Peak rates were low during this wave (peak rate ~0.06 cph) and the outbreak only affected 15 governorates. Wave 2, the largest outbreak wave nationwide, began approximately nine weeks after the conclusion of Wave 1 (6–12 March-2017). We identified two peaks in Wave 2: the first in 24–30 July 2017 (peak rate ~151.3 cph) and the second in 18–24 September 2017 (peak rate ~141.1), with a sharp decline in rates between peaks (~20% of peak rate values). The speed of increase for the primary and secondary peaks was 1.88–2.32 cph/week and 1.05–1.76 cph/week greater than the speed of decline, respectively. The prolonged decline from the second peak to the time of resolution (2–8 April 2018) lasted 28 weeks. For both Waves 1 and 2, the acceleration

period from the onset to the peak was 1.5–2.2-fold shorter than the deceleration period from the peak to the onset of the next wave (Table 2).

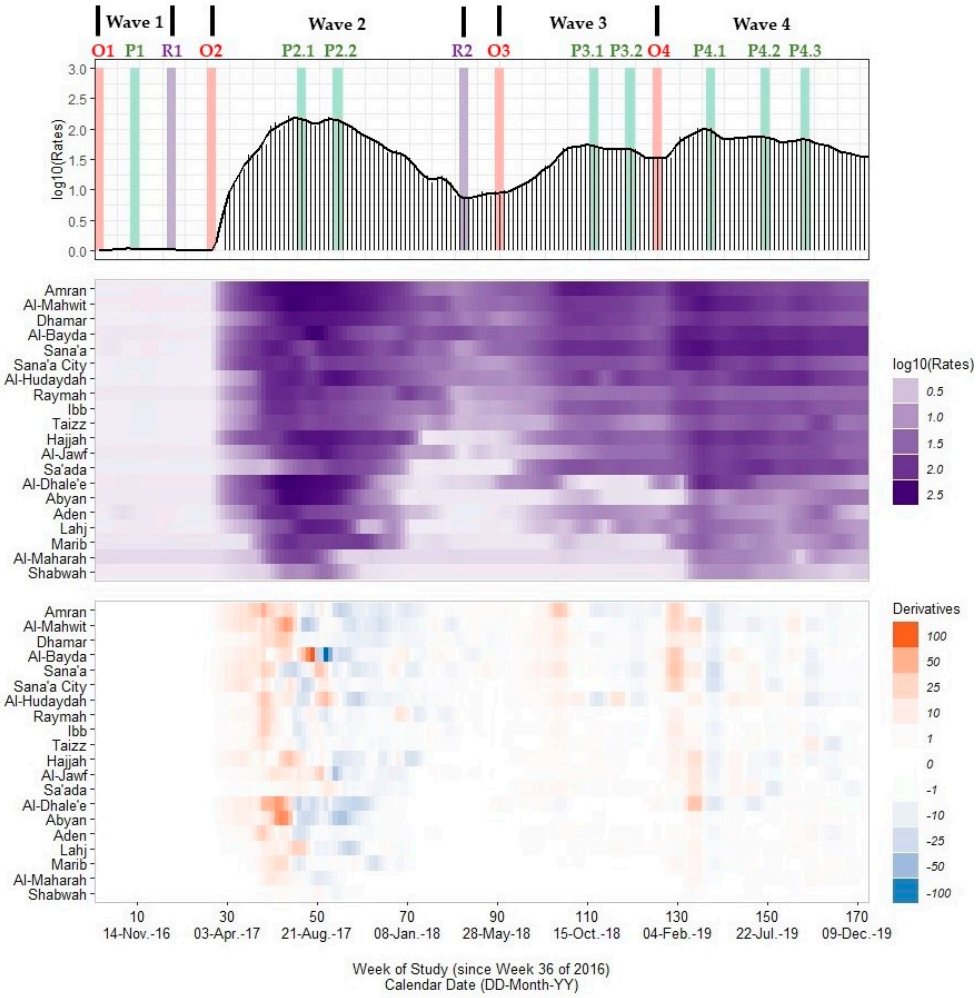


Figure 2. A multi-panel plot of the national Yemeni cholera outbreak signature (top panel), a heatmap of rate values across 20 governorates (middle panel; excludes the Hadramaut and Socotra island governorate), and a heatmap of differences in rates or trivial derivative values (bottom panel). Cholera rates (cases per 100,000 persons, or cph) are presented as a spike plot using a log10-transformed scale for 172 study weeks (all missing data imputed with linear approximations). A smoothed time series line plot is superimposed on this spike plot, which was calculated using Kolmogorov–Zurbenko adaptive filters from Week 36 (4–11 September) of 2016 through Week 52 (23–29 December) of 2019. Smoothed rates (laboratory-confirmed cholera cases per 100,000 persons) were estimated using the best performing smoother. Vertical bars represent the onset timing (red) for each wave (O1, O2, O3, O4), the peak timing (green) including one peak for Wave 1 (P1), two peaks for Wave 2 (P2.1, P2.2) and Wave 3 (P3.1, P3.2), and three peaks for Wave 4 (P4.1, P4.2, P4.3), and the resolution timing (purple) for Waves 1 and 2 (R1, R2). The heatmap of rates uses a purple gradient scale (lighter hues ~0.0 cph and darker hues ~400 cph) while the heatmap of derivative values uses a diverging scale ranging from −100 (dark blue) to +100 (dark orange) with values near zero in grey. All plots share a common horizontal axis of time reported in weeks since Week 36 of 2016 (defined as study Week 0). Governorates are grouped by assigned outbreak clusters: the core outbreak (Sana'a, Sana'a City, and Al-Hudaydah), immediate neighboring I (Amran, Al-Mahwit, Dhamar, and Al-Bayda), immediate neighboring II (Raymah, Ibb, and Taizz), northern (Hajjah, Al-Jawf, and Sa'ada), southern (Al-Dhale'e, Abyan, Aden, and Lahj), and eastern (Marib, Al-Maharah, and Shabwah) clusters. Data used to develop this visualization are reported in Tables 1 and 2 and Supplementary Excel Tables S3 and S4.

Table 1. Timing and magnitude of smoothed rate values at the onset, peak, and resolution critical points for four outbreak waves in Yemen from Week 36 (4–11 September) of 2016 through Week 52 (23–29 December) of 2019.

Location	Metric	O1	P1	R1	O2.1	P2.1	O2.2	P2.2	O2.3	P2.3	R2	O3.1	P3.1	O3.2	P3.2	R3	O4.1	P4.1	O4.2	P4.2	O4.3	P4.3
Yemen	Timing	1	9	17	26	46	50	54			82	90	111	116	119		125	137	142	149	154	158
Yemen	Rate	0.01	0.06	0.03	0.01	151.33	122.17	141.13			6.34	7.89	53.12	44.42	45.59		31.84	99.65	66.79	73.41	59.91	66.08
Sana'a	Timing	1	5	17	26	42	49	54	65	69		83	107	111	115		127	136	142	150		
Sana'a	Rate	0.07	0.29	0.10	0.08	172.81	58.29	154.88	47.06	66.78		6.71	111.35	108.16	112.59		58.12	228.81	150.93	170.86		
Sana'a City	Timing	3	9	17	26	46	50	54			83	92	107	111	115		124	136	145	150	155	158
Sana'a City	Rate	0.03	0.14	0.06	0.04	131.36	49.80	82.07			9.23	6.82	50.96	50.24	51.07		34.71	146.37	67.45	86.48	54.42	61.33
Al-Hudaydah	Timing	3	7	17	26	45	50	55			80	94	110	115	120		132	137	141	158		
Al-Hudaydah	Rate	0.03	0.10	0.06	0.04	157.26	91.28	215.79			12.29	9.87	81.55	29.26	81.77		47.25	74.25	56.16	131.58		
Amran	Timing	5	13	17	26	46	77	79				82	110				128	133	154	159		
Amran	Rate	0.09	0.16	0.12	0.09	347.50	17.30	17.97				12.67	188.36				65.22	166.90	58.39	70.71		
Al-Mahwit	Timing				27	46	75	78				83	107				127	137	154	159		
Al-Mahwit	Rate				0.14	397.67	42.16	49.68				18.50	90.84				41.36	208.86	70.65	99.38		
Dhamar	Timing	8	13	17	26	46	77	80	84	88		92	110				127	137	155	158		
Dhamar	Rate	0.05	0.12	0.08	0.05	216.32	22.95	27.49	14.35	19.02		9.44	93.51				38.23	112.44	53.09	58.28		
Al-Bayda	Timing	2	6	17	26	50	67	72	75	81		93	107	111	115		124	133	141	146	154	158
Al-Bayda	Rate	0.13	0.28	0.16	0.14	391.53	29.84	52.82	39.38	54.40		25.95	68.28	60.67	63.07		33.13	166.26	108.80	135.80	112.76	125.31
Raymah	Timing	8	13	17	26	42	67	71			82	98	107				124	133	141	146	154	158
Raymah	Rate	0.17	0.24	0.19	0.17	125.58	28.60	70.79			3.56	8.59	22.26				21.98	48.00	29.76	33.78	30.44	32.10
Ibb	Timing	3	9	17	26	43	74	78			83	90	115				125	136	145	150	154	158
Ibb	Rate	0.04	0.12	0.06	0.04	113.44	14.45	19.22			2.45	4.12	47.16				27.81	81.19	50.29	54.41	48.52	57.77
Taizz	Timing	3	10	17	26	45	75	78			83	99	111				124	137	141	150	158	163
Taizz	Rate	0.03	0.12	0.06	0.04	85.69	5.04	9.25			2.92	3.54	23.40				8.40	51.69	33.98	45.95	30.86	65.77
Hajjah	Timing	3	13	17	26	53					74	90	107	111	115		127	137	141	145	154	158
Hajjah	Rate	0.05	0.12	0.07	0.05	208.08					0.24	0.58	38.23	0.17	0.41		27.33	121.84	89.32	103.53	59.54	69.61
Al-Jawf	Timing	10	15	17	26	52					81	91	120				127	137	141	145	155	159
Al-Jawf	Rate	0.17	0.22	0.20	0.18	192.51					0.77	0.78	23.95				22.20	91.12	65.35	80.27	49.93	53.51
Sa'ada	Timing				27	56					72	92	110				128	137	141	149	155	158

Table 1. *Cont.*

Location	Metric	O1	P1	R1	O2.1	P2.1	O2.2	P2.2	O2.3	P2.3	R2	O3.1	P3.1	O3.2	P3.2	R3	O4.1	P4.1	O4.2	P4.2	O4.3	P4.3
Sa'ada	Rate				0.10	72.96					0.19	0.10	48.94				33.86	87.60	72.49	111.12	64.63	72.69
Al-Dhale'e	Timing	5	9	13	27	45					72	95	102			111	123	128	132	137		
Al-Dhale'e	Rate	0.14	0.25	0.14	0.14	394.66					0.32	9.53	20.62			0.17	0.28	13.08	2.31	133.76		
Abyan	Timing	8	13	17	26	45					72	93	110			115	128	137	141	146	154	167
Abyan	Rate	0.18	0.25	0.20	0.18	358.26					0.17	0.17	2.96			0.40	0.20	18.60	7.71	13.60	7.67	21.13
Aden	Timing	3	8	17	26	45					79	94	115				127	136	154	163		
Aden	Rate	0.11	0.56	0.14	0.11	134.95					0.15	0.39	11.69				5.32	28.10	6.40	27.46		
Lahj	Timing	3	9	17	26	49	64	68			72	93	111	115	120		124	128	132	137	154	163
Lahj	Rate	0.10	0.17	0.13	0.10	164.88	2.63	10.37			0.13	0.10	7.26	1.13	10.99		6.56	11.85	7.85	30.16	6.83	17.10
Marib	Timing				27	45	58	61			73	101	106				124	137	146	149	155	167
Marib	Rate				0.29	110.22	75.11	83.20			0.41	0.28	2.14				0.40	33.00	9.34	11.47	6.43	17.72
Al-Maharah	Timing				27	47					69						132	137	158	163		
Al-Maharah	Rate				0.66	72.63					0.65						0.63	17.68	1.24	8.48		
Shabwah	Timing				27	52					67						127	145				
Shabwah	Rate				0.16	22.14					0.26						0.16	10.21				

All critical points were estimated using smoothed rates (laboratory-confirmed cholera cases per 100,000 persons) and trivial derivative values (Δ rates per epidemiological week) produced with Kolmogorov–Zurbenko (KZ) adaptive filters. We selected the best performing smoother ($Z^*_{t,s,3\text{–}5}$) as the average of a 3 week ($Z^*_{t+1,s,3}$) and 5 week ($Z^*_{t+1,s,5}$) window size and trivial derivative as the absolute change in weekly smoothed rates calculated as: $Z'_{t,s,3\text{–}5} = (Z^*_{t+1,s,3} + Z^*_{t+1,s,5})/2 - (Z^*_{t,s,3} + Z^*_{t,s,5})/2$. Onset ($O_{n.i}$) critical points marked a rapid rise in $Z^*_{t,s,3\text{–}5}$ and near-zero to high positive values of $Z'_{t,s,3\text{–}5}$. Peak ($P_{n.i}$) critical points marked local maximum of $Z^*_{t,s,3\text{–}5}$ and inflection of $Z'_{t,s,3\text{–}5}$ at near-zero or negative values. Resolution (R_n) critical points defined times when $Z^*_{t,s,3\text{–}5}$ were near local minimum values and $Z'_{t,s,3\text{–}5}$ approached near-zero values. All critical points are listed for each of the nth outbreak waves and ith occurrences per wave. No resolution critical point for Wave 4 was found by the conclusion of the study period. Critical points are reported in weeks since Week 36 of 2016 (defined as study Week 0). Smoothed rates are reported for the week of each critical point and were estimated for each governorate and nationally using 172 weeks of data. All weeks with missing data were imputed using linear approximation. Governorates are grouped by assigned outbreak clusters (separated by double solid lines) and include: the core outbreak (Sana'a, Sana'a City, and Al-Hudaydah), immediate neighboring I (Amran, Al-Mahwit, Dhamar, and Al-Bayda), immediate neighboring II (Raymah, Ibb, and Taizz), northern (Hajjah, Al-Jawf, and Sa'ada), southern (Al-Dhale'e, Abyan, Aden, and Lahj), and eastern (Marib, Al-Maharah, and Shabwah) clusters. Data summarized in this table are graphically presented in Figures 2–9 and Supplementary Figures S1–S6.

Table 2. Summary of the acceleration, deceleration, and steady-state critical period durations and the pace of increase and decline for four outbreak waves in Yemen from Week 36 (4–11-September) of 2016 through Week 52 (23–29-December) of 2019.

	From	**O1**	**P1**	**P1**	**R1**	**O2.1**	**O2.1**	**O2.1**	**P2.1**	**P2.2**	**P2.3**	**P2.1**	**P2.2**	**P2.3**	**R2**	**O3.1**	**O3.1**	**P3.1**	**P3.1**	**P3.2**	**R3**	**O4.1**	**O4.1**	**O4.1**
Location	To	P1	R1	O2.1	O2.1	P2.1	P2.2	P2.3	R2	R2	R2	O3.1	O3.1	O3.1	O3.1	P3.1	P3.2	R3	O4.1	O4.1	O4.1	P4.1	P4.2	P4.3
Yemen	Duration	8	8	17	9	20	28		36	28		44	36		8	21	29		14	6		24	29	33
Yemen	Pace	0.01	0.00	0.00	0.00	7.57	5.04		−4.03	−4.81		−3.26	−2.86		0.19	2.15	1.30		−1.52	−2.29		5.65	1.73	1.04
Sana'a	Duration	4	12	21	9	16	28	43				41	29	14		24	32		20	12		9	23	
Sana'a	Pace	0.07	−0.02	−0.01	0.00	10.80	5.53	1.55				−4.05	−5.11	−4.29		4.36	3.31		−2.66	−4.54		18.97	4.90	
Sana'a City	Duration	6	8	17	9	20	28		37	29		46	38		9	15	23		17	9		26	31	34
Sana'a City	Pace	0.03	−0.01	−0.01	0.00	6.57	2.93		−3.30	−2.51		−2.71	−1.98		−0.27	2.94	1.92		−0.96	−1.82		9.31	1.99	0.78
Al-Hudaydah	Duration	4	10	19	9	19	29		35	25		49	39		14	16	26		22	12		5	26	
Al-Hudaydah	Pace	0.03	0.00	0.00	0.00	8.27	7.44		−4.14	−8.14		−3.01	−5.28		−0.17	4.48	2.77		−1.56	−2.88		5.40	3.24	
Amran	Duration	8	4	13	9	20	53					36	3			28			18			5	31	
Amran	Pace	0.09	−0.01	−0.01	0.00	17.37	0.34					−9.30	−1.77			6.27			−6.84			20.34	0.18	
Al-Mahwit	Duration					19	51					37	5			24			20			10	32	
Al-Mahwit	Pace					20.92	0.97					−10.25	−6.24			3.01			−2.47			16.75	1.81	
Dhamar	Duration	5	4	13	9	20	54	62				46	12	4		18			17			10	31	
Dhamar	Pace	0.01	−0.01	−0.01	0.00	10.81	0.51	0.31				−4.50	−1.50	−2.40		4.67			−3.25			7.42	0.65	
Al-Bayda	Duration	4	11	20	9	24	46	55				43	21	12		14	22		17	9		9	22	34
Al-Bayda	Pace	0.04	−0.01	−0.01	0.00	16.31	1.15	0.99				−8.50	−1.28	−2.37		3.02	1.69		−3.25	0.30		14.79	4.67	2.71
Raymah	Duration	5	4	13	9	16	45		40	11		56	27		16	9			17			9	22	34
Raymah	Pace	0.01	−0.01	−0.01	0.00	7.84	1.57		−3.05	−6.11		−2.09	−2.30		0.31	1.52			−0.02			2.89	0.54	0.30
Ibb	Duration	6	8	17	9	17	52		40	5		47	12		7	25			10			11	25	33
Ibb	Pace	0.01	−0.01	0.00	0.00	6.67	0.37		−2.77	−3.35		−2.33	−1.26		0.24	1.72			−1.94			4.85	1.06	0.91
Taizz	Duration	7	7	16	9	19	52		38	5		54	21		16	12			13			13	26	39
Taizz	Pace	0.01	−0.01	−0.01	0.00	4.51	0.18		−2.18	−1.27		−1.52	−0.27		0.04	1.66			−1.15			3.33	1.44	1.47
Hajjah	Duration	10	4	13	9	27			21			37			16	17	25		20	12		10	18	31
Hajjah	Pace	0.01	−0.01	−0.01	0.00	7.70			−9.90			−5.61			0.02	2.21	−0.01		−0.55	2.24		9.45	4.23	1.36

Table 2. *Cont.*

	From	O1	P1	P1	R1	O2.1	O2.1	O2.1	P2.1	P2.2	P2.3	P2.1	P2.2	P2.3	R2	O3.1	O3.1	P3.1	P3.1	P3.2	R3	O4.1	O4.1	O4.1
Al-Jawf	Duration	5	2	11	9	26			29			39			10	29			7			10	18	32
Al-Jawf	Pace	0.01	−0.01	0.00	0.00	7.40			−6.61			−4.92			0.00	0.80			−0.25			6.89	3.23	0.98
Sa'ada	Duration					29			16			36			20	18			18			9	21	30
Sa'ada	Pace					2.51			−4.55			−2.02			0.00	2.71			−0.84			5.97	3.68	1.29
Al-Dhale'e	Duration	4	4	18	14	18			27			50			23	7		9	21		12	5	14	
Al-Dhale'e	Pace	0.03	−0.03	−0.01	0.00	21.92			−14.61			−7.70			0.40	1.58		−2.27	−0.97		0.01	2.56	9.53	
Abyan	Duration	5	4	13	9	19			27			48			21	17		5	18		13	9	18	39
Abyan	Pace	0.01	−0.01	−0.01	0.00	18.85			−13.26			−7.46			0.00	0.16		−0.51	−0.15		−0.02	2.04	0.74	0.54
Aden	Duration	5	9	18	9	19			34			49			15	21			12			9	36	
Aden	Pace	0.09	−0.05	−0.03	0.00	7.10			−3.96			−2.75			0.02	0.54			−0.53			2.53	0.62	
Lahj	Duration	6	8	17	9	23	42		23	4		44	25		21	18	27		13	4		4	13	39
Lahj	Pace	0.01	−0.01	0.00	0.00	7.16	0.24		−7.16	−2.56		−3.75	−0.41		0.00	0.40	0.40		−0.05	−1.11		1.32	1.82	0.27
Marib	Duration					18	34		28	12		56	40		28	5			18			13	25	43
Marib	Pace					6.11	2.44		−3.92	−6.90		−1.96	−2.07		0.00	0.37			−0.10			2.51	0.44	0.40
Al-Maharah	Duration					20			22													5	31	
Al-Maharah	Pace					3.60			−3.27													3.41	0.25	
Shabwah	Duration					25			15													18		
Shabwah	Pace					0.88			−1.46													0.56		

Deceleration periods are reported for both the duration from a wave's peak to resolution and from a wave's peak to the following wave's onset. Acceleration periods indicated times when weekly rates were steadily increasing (onset to peak), deceleration periods indicated times when weekly rates were steadily decreasing (peak to resolution or peak to onset), and steady-state periods indicated times when the weekly rates plateaued (resolution to onset). The pace of increase or decline is measured as a linear slope (rates per week) and estimated simply as the smoothed rate at one critical point minus the smoothed rate at the following critical point and divided by the duration between critical points. Duration between critical points ranged 2–56 weeks. Critical periods are denoted from their starting and ending onset ($O_{n.i}$), peak ($P_{n.i}$), and resolution (R_n) critical points for the nth outbreak wave and ith occurrence per wave. No resolution critical point for Wave 4 was found by the conclusion of the study period. As a result, we found no deceleration or steady-state periods for Wave 4. Critical period duration is reported in weeks since Week 36 of 2016 (defined as study Week 0). The pace of increase and decline are reported in laboratory-confirmed cholera cases per 100,000 persons per week. Critical points used to define critical periods were estimated using smoothed rates (laboratory-confirmed cholera cases/100,000 persons) and trivial derivative values (Δ rates/week) produced with Kolmogorov–Zurbenko (KZ) adaptive filters (see Table 1). Governorates are grouped by assigned outbreak clusters indicated with double solid lines and include: the core outbreak (Sana'a, Sana'a City, and Al-Hudaydah), immediate neighboring I (Amran, Al-Mahwit, Dhamar, and Al-Bayda), immediate neighboring II (Raymah, Ibb, and Taizz), northern (Hajjah, Al-Jawf, and Sa'ada), southern (Al-Dhale'e, Abyan, Aden, and Lahj), and eastern (Marib, Al-Maharah, and Shabwah) clusters. Data summarized in this table are, in part, graphically presented in Figure 2 and Supplementary Figures S1–S6.

We also identified two additional waves: Wave 3 from 28 May 2018 through 27 January 2019 and Wave 4 from 28 January 2019 through 29 December 2019. In Wave 3, we identified two peaks: the first in 22–28 October 2018 (peak rate ~53.1 cph) and the second in 17–23 December 2018 (peak rate ~45.6 cph). These peaks were approximately 66% lower than the peak rate values for Wave 2, declined briefly (~10 cph) in rate values between peaks, and had a speed of increase/decline of ~2 cph/week. For Wave 3, the acceleration period from the onset to the peak was >1.5-fold longer than the deceleration period from the peak of Wave 3 to the onset of Wave 4. For Wave 4, we identified three peaks (22–28 April 2019, 15–21 July 2019, 16–22 September 2019). These peaks declined in magnitude throughout the outbreak wave (~99.7 cph, ~73.4 cph, ~66.1 cph) and occurred approximately 12 weeks apart. We did not identify a resolution critical point for Wave 4 by the end of our study.

3.2. Governorate-Level Signature Variability

In our study period, Al-Hudaydah governate had the most reported cases cumulatively (n = 318,969) followed by Sana'a City (n = 230,577), Dhamar (n = 205,179), and Sana'a (200,003). Both Al-Hudaydah and Sana'a City were among the most populated governorates during this period (average weekly population of ~3.3 million and ~3.0 million persons, respectively) as well as Taizz (~3.1 million persons) and Ibb (~3.0 million persons). In the center and bottom panels of Figure 2, we provide a heatmap of smoothed rate values and their trivial derivative estimates for each governorate, respectively. Both heatmaps show that outbreak signatures varied substantially across governorates. The Wave 1 onset timing spanned from 12 to 18 September 2016 in Sana'a to 14–20 November 2016 in Al-Jawf with peak rates <1 cph in all governorates. Yet, in all 15 affected governorates, Wave 1 was resolved by 2–8 January 2017.

We identified a uniform Wave 2 onset in 6–19 March 2017 for all 20 governorates. Eight governorates had one outbreak peak during Wave 2, which occurred from 17 July 2017 to 8 October 2017. Nine governorates had two outbreak peaks with the secondary peak occurring either from 18 September 2017 to 31 December 2017 or from 22 January 2018 to 25 March 2018. Three governorates (Dhamar, Al-Bayda, and Sana'a) had three outbreak peaks. We also found variation in the number and timing of peaks for Wave 3 (12 governorates with one peak, 6 governorates with two peaks) and Wave 4 (1 governorate with one peak, 8 governorates with two peaks, and 11 governorates with three peaks).

We found groups of governorates that were strongly correlated with one another according to Spearman correlation estimates. Sana'a and Sana'a City were strongly correlated with Al-Hudaydah (ρ = 0.82–0.90; $p < 0.001$) for a lag of +1–5 weeks and with each other (ρ = 0.86–0.88; $p < 0.001$) for a lead-lag of -3 to +1 weeks. We found even stronger correlations between Amran, Al-Mahwit, and Dhamar (ρ = 0.87–0.96; $p < 0.001$) for a lead-lag of -2 to +4 weeks. We also found strong correlations between Raymah and Ibb (ρ = 0.82–0.84; $p < 0.001$), Raymah and Taizz (ρ = 0.86–0.88; $p < 0.001$), Ibb and Taizz (ρ = 0.88–0.94; $p < 0.001$) for a lead-lag of -2 to +2 weeks.

3.3. Six Clusters of Outbreak Signatures

Based on the combination of correlation estimates, timing of critical points, and geographic proximity, we assigned all governorates into one of six clusters including a core outbreak cluster, two immediately neighboring clusters, and three remote clusters in northern, southern and eastern regions of Yemen (Figure 3; Supplementary Excel Table S3).

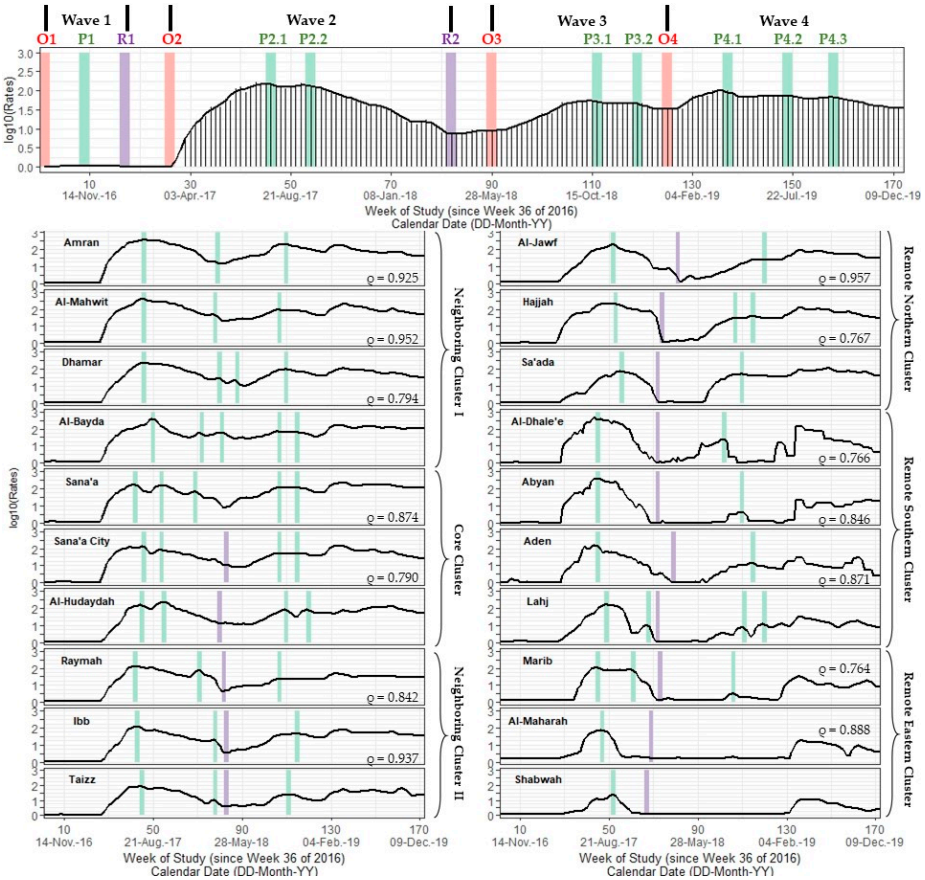


Figure 3. A multi-panel plot of the national Yemeni cholera outbreak signature and signatures for 20 Yemeni governorates (excludes the Hadramaut and Socotra island governorate). Top panel: the national signature includes a spike plot of log10-transformed cholera rates (in cases per 100,000 persons) and a time series line plot of smoothed rates calculated using Kolmogorov–Zurbenko adaptive filters from Week 36 (4–11 September) of 2016 through Week 52 (23–29 December) of 2019. Smoothed rates (laboratory-confirmed cholera cases per 100,000 persons) were estimated using the best performing smoother. Vertical red, green, and purple lines depict the timing of onset, peak, and resolution critical point (s), respectively, for each of the four outbreak waves. Bottom panels: governorate-level signatures are shown in two columns of stacked multi-panel time series plots that share a common vertical axis between columns (log10-transformed rates (cph)) and a common horizontal axis within columns (weeks since Week 36 of 2016, defined as study Week 0). Vertical green and purple bars depict the timing of the Wave 2 peak, Wave 2 resolution, and Wave 3 peak, which were important signature features for defining outbreak clusters. Spearman cross correlation estimates (ρ) are at lag 0 between adjacently reported governorates within the same cluster based on 172 weeks (all correlation coefficients are significant at $\alpha < 0.001$). Data used to develop this visualization are reported in Table 1, Supplementary Table S1, and Supplementary Excel Table S3.

3.4. Core Cluster

We identified Sana'a, Sana'a City, and Al-Hudaydah governorates as the core outbreak cluster (Figure 4; Supplementary Excel Table S5). We used the term 'core' as these governorates were located centrally in Yemen, contained or surrounded the nation's capital, housed a large percentage of the population, and had the earliest timing of onset and peak critical points in Wave 1. These governorates had closely aligned primary and secondary peaks in Wave 2 from 26 June 2017 to 30 July 2017 (131.4–172.8 cph) and from 18 September 2017 to 1 October 2017 (82.1–215.8 cph). Pace of increase for primary peaks were 2.43–2.75-fold greater than pace of decline for all governorates. After a long deceleration period of ~30 weeks, cholera rates never returned to pre-Wave 2 baseline levels for any

of these three governorates. Rates decreased by ~40–66% for these governorates during the ~6 weeks between peaks. While Sana'a had a smaller third peak (66.8 cph) in 1–7 January 2018, Sana'a City and Al-Hudaydah had a brief (9–14 weeks) resolution period from 19 March 2018 to 1 July 2018.

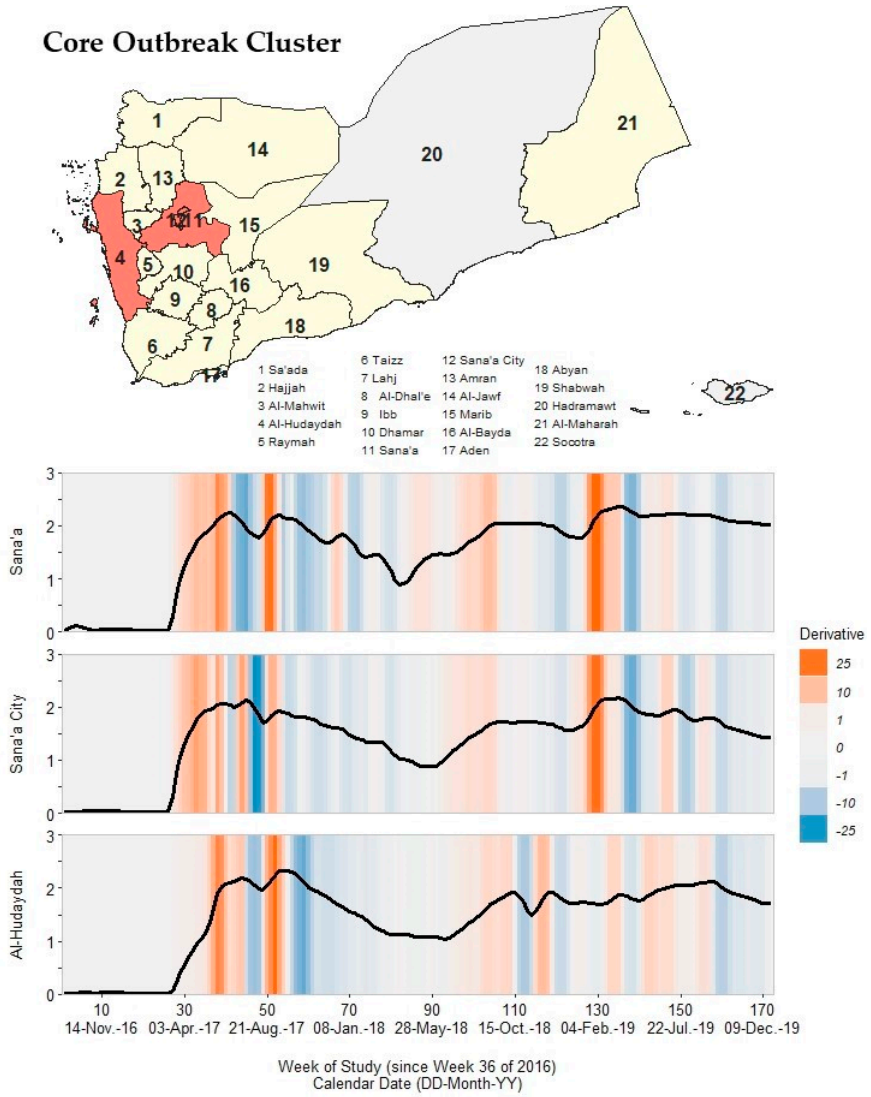


Figure 4. A map of Yemen with a shaded outbreak cluster including Sana'a, Sana'a City, and Al-Hudaydah, and a stacked time series plot and heatmap for each governorate's outbreak signature. Top panel: the governorate-level map indicates governorates within the cluster in orange, remaining governorates within our study in yellow, and excluded governorates in grey (the Hadramaut and Socotra island governorate). Bottom panel: stacked time series plots for each governorate within the cluster. All plots show log10-transformed smoothed rates produced using Kolmogorov–Zurbenko adaptive filters from Week 36 (4–11 September) of 2016 through Week 52 (23–29 December) of 2019. Smoothed rates (laboratory-confirmed cholera cases per 100,000 persons) were estimated using the best performing smoother. Backgrounds for each plot are heatmaps of trivial derivative values, ranging from −25 (dark blue) to +25 (dark orange) with values near zero in grey. Time series plots have a common horizontal axis of time reported in weeks since Week 36 of 2016 (defined as study Week 0). Data used to develop this visualization are reported in Table 1 and Supplementary Excel Table S5.

In Wave 3, all three governorates had two peaks: from 24 September 2018 to 21 October 2018 and from 19 November 2018 to 30 December 2018. For each governorate, primary and

secondary peak rate values were nearly identical (Sana'a: ~112 cph; Sana'a City: ~51 cph; Al-Hudaydah: ~81 cph). In Wave 4, these governorates had the same first peak timing in 15–28 April 2019. However, the second peak in Sana'a and Sana'a City occurred in 22–28 July 2019, approximately two months prior to the third peak of Sana'a City and second peak of Al-Hudaydah in 16–22 September 2019. Differences in the alignment of peak timing supported Sana'a and Sana'a City's strong association (ρ = 0.82–0.89; $p < 0.001$) with Al-Hudaydah for lags from 1 to 5 weeks.

3.5. Immediate Neighboring Cluster I

We identified four governorates, Amran, Al-Mahwit, Dhamar, and Al-Bayda, that formed a cluster immediately neighboring the core cluster (Figure 5; Supplementary Excel Table S5). This neighboring cluster had similar critical points but higher peak rates in Wave 2 compared to the core cluster.

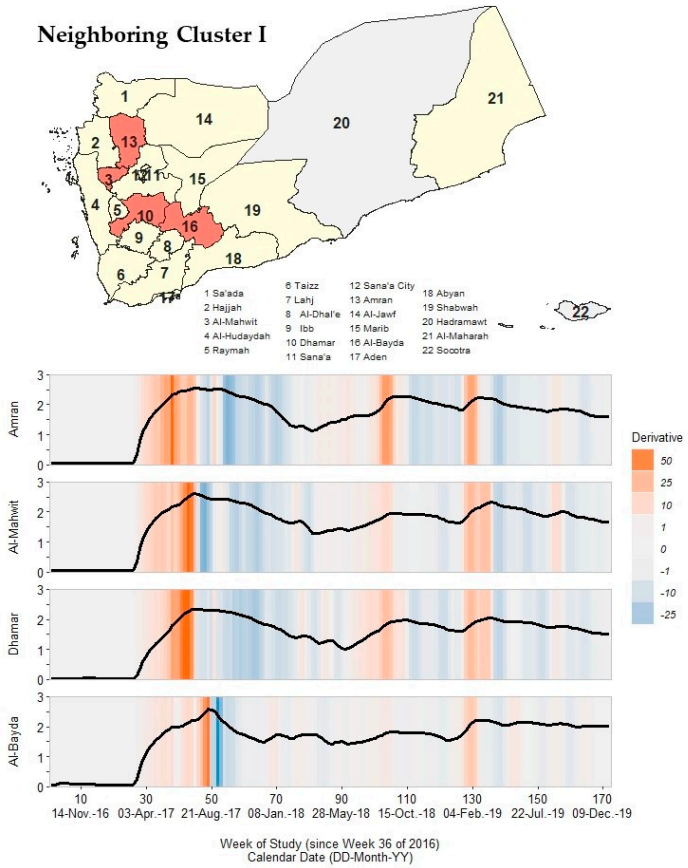


Figure 5. A map of Yemen with a shaded outbreak cluster including Amran, Al-Mahwit, Dhamar, and Al-Bayda, and a stacked time series plot and heatmap for each governorate's outbreak signature. Top panel: the governorate-level map indicates governorates within the cluster in orange, remaining governorates within our study in yellow, and excluded governorates in grey (the Hadramaut and Socotra island governorate). Bottom panel: stacked time series plots for each governorate within the cluster. All plots show log10-transformed smoothed rates produced using Kolmogorov–Zurbenko adaptive filters from Week 36 (4–11 September) of 2016 through Week 52 (23–29 December) of 2019. Smoothed rates (laboratory-confirmed cholera cases per 100,000 persons) were estimated using the best performing smoother. Backgrounds for each plot are heatmaps of trivial derivative values, ranging from −25 (dark blue) to +50 (dark orange) with values near zero in grey. Time series plots have a common horizontal axis of time reported in weeks since Week 36 of 2016 (defined as study Week 0). All rates and trivial derivates were calculated for the 172 weeks of time series. Data used to develop this visualization are reported in Table 1 and Supplementary Excel Table S5.

Though the early primary peak (24 July 2017 to 27 August 2017) was similar to the core cluster, the neighboring cluster had a later secondary peak from 5 March 2018 to 1 April 2018 that fell ~10 weeks after the core cluster. Additionally, Al-Mahwit, Al-Bayda, and Amran had peak rates of ~400 cph, roughly twice the magnitude of peak rates in the core cluster. The pace of increase for primary peaks ranged from 10.8 to 20.9 cph/week, which was on average twice as large compared to the core cluster (6.6–10.8 cph/week). Unlike the core cluster, none of the governorates in this neighboring cluster had a Wave 2 resolution, though rate values declined to ~20 cph (roughly twice the magnitude of the core cluster) by the onset timing of Wave 3.

In Wave 3, Amran, Al-Mahwit, and Dhamar had only one peak, which occurred from 24 September 2018 to 21 October 2018. Al-Bayda had a secondary peak in 19–25 November 2018, which was identical in timing to governorates in the core cluster. As in Wave 2, Wave 3 peak rate values for the neighboring cluster were, on average, higher than the peak rates for core cluster governorates (63.1–188.4 cph).

In Wave 4, all governorates peaked twice (except Al-Bayda, which peaked three times). All four governorates shared a secondary peak in 16–29 September 2019, which aligns with the later peak timing for Sana'a City and Al-Hudaydah.

3.6. Immediate Neighboring Cluster II

Raymah, Ibb, and Taizz formed a second cluster that immediately neighbored the core cluster. This second neighboring cluster had two well-aligned peaks in Wave 2, one well-aligned peak in Wave 3, three peaks in Wave 4, and low peak rate magnitudes compared to previously described clusters (Figure 6; Supplementary Excel Table S5).

In Wave 2, the primary peak occurred from 26 June 2017 to 23 July 2017 (like the core cluster) and the secondary peak occurred from 15 January 2018 to 11 March 2018 (like the first neighboring cluster). Wave 2 peak rates ranged from 9.25 to 125.6 cph, which were approximately half the magnitude of the first neighboring cluster (216.3–397.7 cph). All governorates in this second neighboring cluster reached resolution timing for Wave 2 in 2–15 April 2018, when rates nearly returned to pre-Wave 2 levels (~2.45–3.56 cph).

In Wave 3, the governorates in this neighboring cluster had only one outbreak peak, which occurred from 24 September 2018 to 25 November 2018 (same as core cluster). However, peak rates had low magnitudes, ranging from 22.3 to 47.2 cph, which were less than half the peak rate magnitudes for governorates in the core and first neighboring clusters. In Wave 4, this neighboring cluster had similar peak timing as the core cluster for all three identified peaks.

3.7. Remote Clusters: Northern, Southern, and Eastern

The ten remaining governorates had outbreak signatures that differed from the governorates in the core and neighboring clusters, forming three geographically distinct clusters in the northern (Hajjah, Al-Jawf, and Sa'ada), southern (Al-Dhale'e, Abyan, Aden, and Lahj), and eastern (Marib, Al-Maharah, and Shabwah) regions of Yemen. Governorates within these remote clusters had one peak in Waves 2 and 3, a short Wave 2 deceleration period duration, and an early arrival of Wave 2 resolution critical points compared to the other three clusters.

In the northern cluster (Figure 7; Supplementary Excel Table S5), governorates had Wave 2 peak timing from 4 September 2017 to 8 October 2017. Rate values reached magnitudes like those in the core outbreak cluster (73.0–208.1 cph). However, the pace of increase to and pace of decline from Wave 2 peak timing were approximately the same and occurred ~6–10 weeks after the primary peak timing of governorates in the first neighboring cluster. Cholera rates declined to pre-Wave 2 magnitudes (<1 cph) 16–30 weeks after the primary peak. Governorates within this northern cluster had Wave 3 peak rate magnitudes (24.0–49.0 cph) like those in the second neighboring cluster governorates.

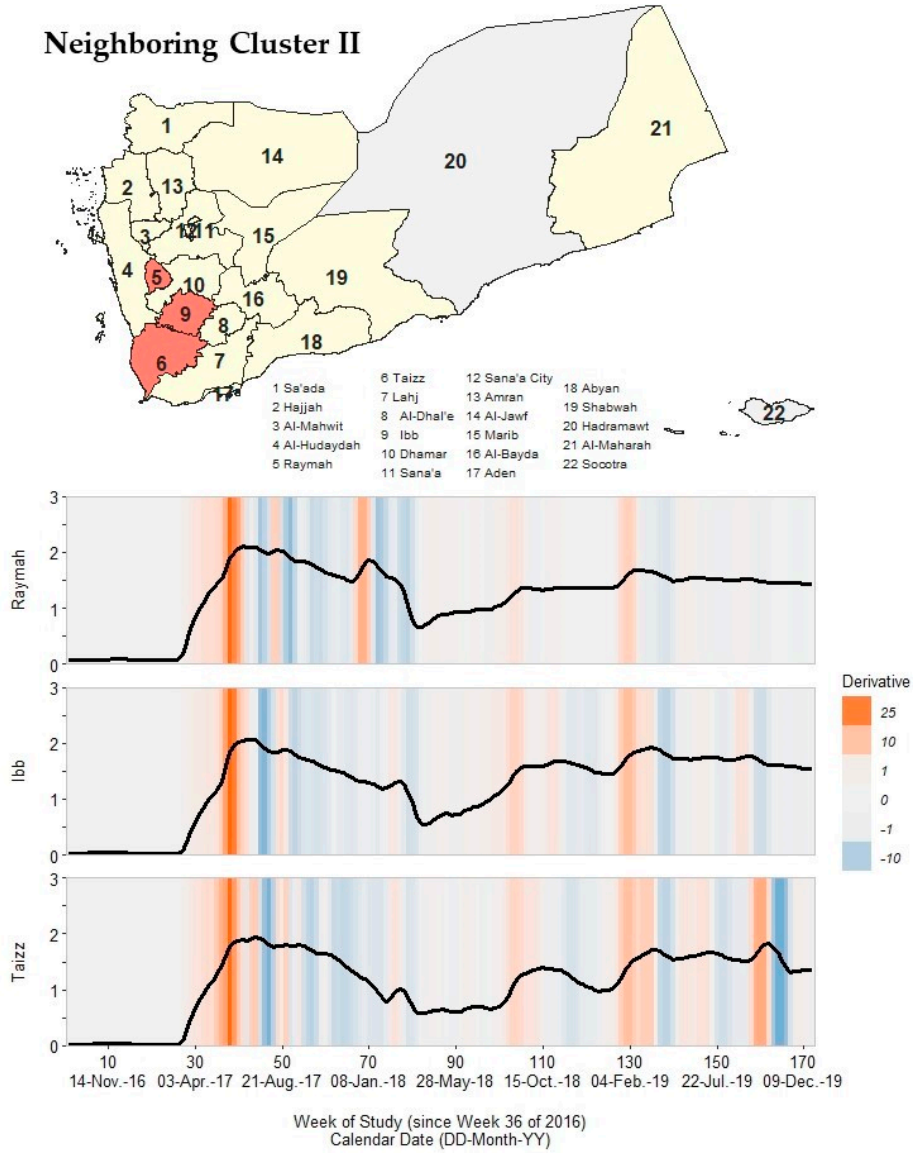


Figure 6. A map of Yemen with a shaded outbreak cluster including Raymah, Ibb, and Taizz, and a stacked time series plot and heatmap for each governorate's outbreak signature. Top panel: the governorate-level map indicates governorates within the cluster in orange, remaining governorates within our study in yellow, and excluded governorates in grey (the Hadramaut and Socotra island governorate). Bottom panel: stacked time series plots for each governorate within the cluster. All plots show log10-transformed smoothed rates produced using Kolmogorov–Zurbenko adaptive filters from Week 36 (4–11 September) of 2016 through Week 52 (23–29 December) of 2019. Smoothed rates (laboratory-confirmed cholera cases per 100,000 persons) were estimated using the best performing smoother. Backgrounds for each plot are heatmaps of trivial derivative values, ranging from −10 (dark blue) to +25 (dark orange) with values near zero in grey. Time series plots have a common horizontal axis of time reported in weeks since Week 36 of 2016 (defined as study Week 0). All rates and trivial derivates were calculated for the 172 weeks of time series. Data used to develop this visualization are reported in Table 1 and Supplementary Excel Table S5.

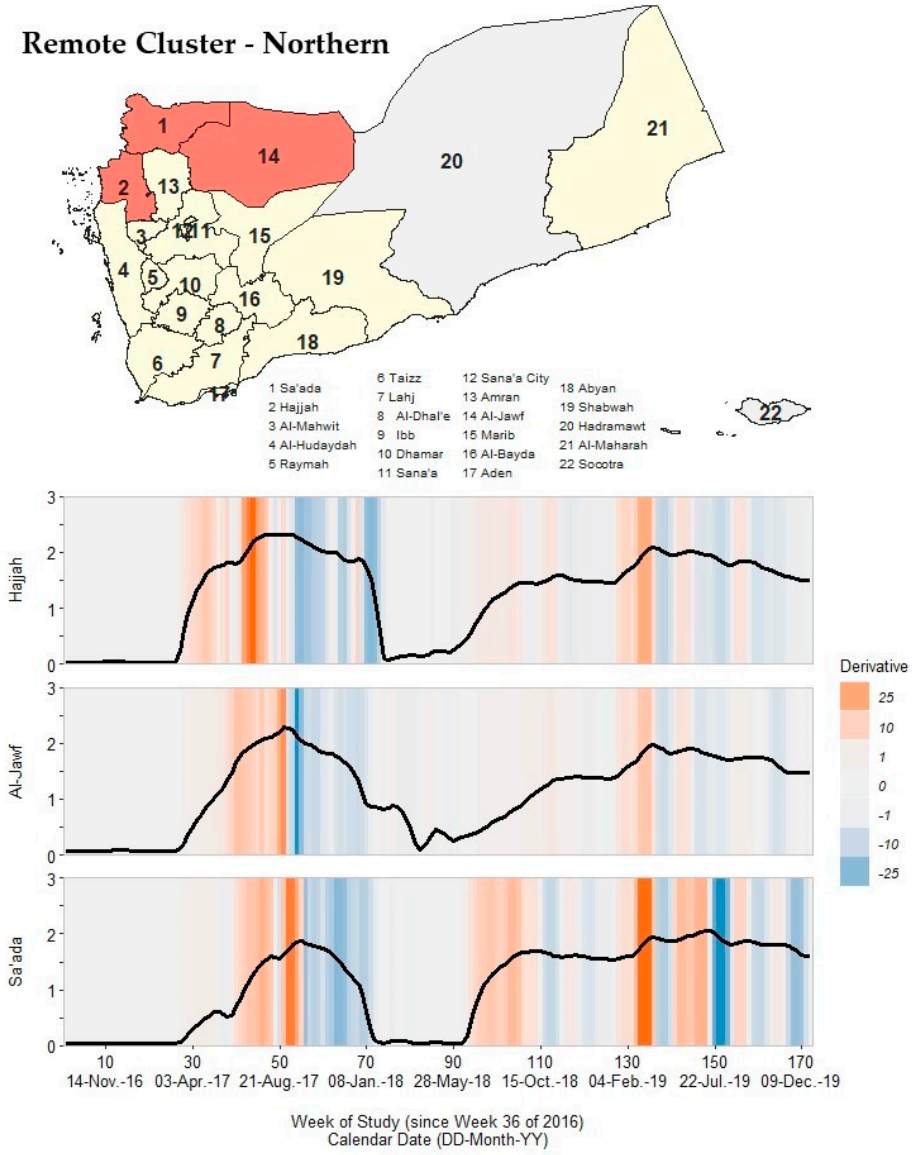


Figure 7. A map of Yemen with a shaded outbreak cluster including Hajjah, Al-Jawf, and Sa'ada, and a stacked time series plot and heatmap for each governorate's outbreak signature. Top panel: the governorate-level map indicates governorates within the cluster in orange, remaining governorates within our study in yellow, and excluded governorates in grey (the Hadramaut and Socotra island governorate). Bottom panel: stacked time series plots for each governorate within the cluster. All plots show log10-transformed smoothed rates produced using Kolmogorov–Zurbenko adaptive filters from Week 36 (4–11 September) of 2016 through Week 52 (23–29 December) of 2019. Smoothed rates (laboratory-confirmed cholera cases per 100,000 persons) were estimated using the best performing smoother. Backgrounds for each plot are heatmaps of trivial derivative values, ranging from −25 (dark blue) to +25 (dark orange) with values near zero in grey. Time series plots have a common horizontal axis of time reported in weeks since Week 36 of 2016 (defined as study Week 0). All rates and trivial derivates were calculated for the 172 weeks of time series. Data used to develop this visualization are reported in Table 1 and Supplementary Excel Table S5.

In the southern cluster (Figure 8; Supplementary Excel Table S5), Al-Dhale'e, Abyan, and Aden had only one Wave 2 peak that occurred in 17–23 July 2017. Lahj had two Wave 2 peaks: the primary occurred in 14–20 August 2017 and the secondary occurred in 25–31 December 2017. Irrespective of peak timing, all governorates had a prolonged deceleration period of ~30 weeks and reached Wave 2 resolution from 22 January 2018 to 18 March 2018.

By the conclusion of Wave 2, governorates within this cluster had returned to pre-Wave 2 rate magnitudes (<1 cph).

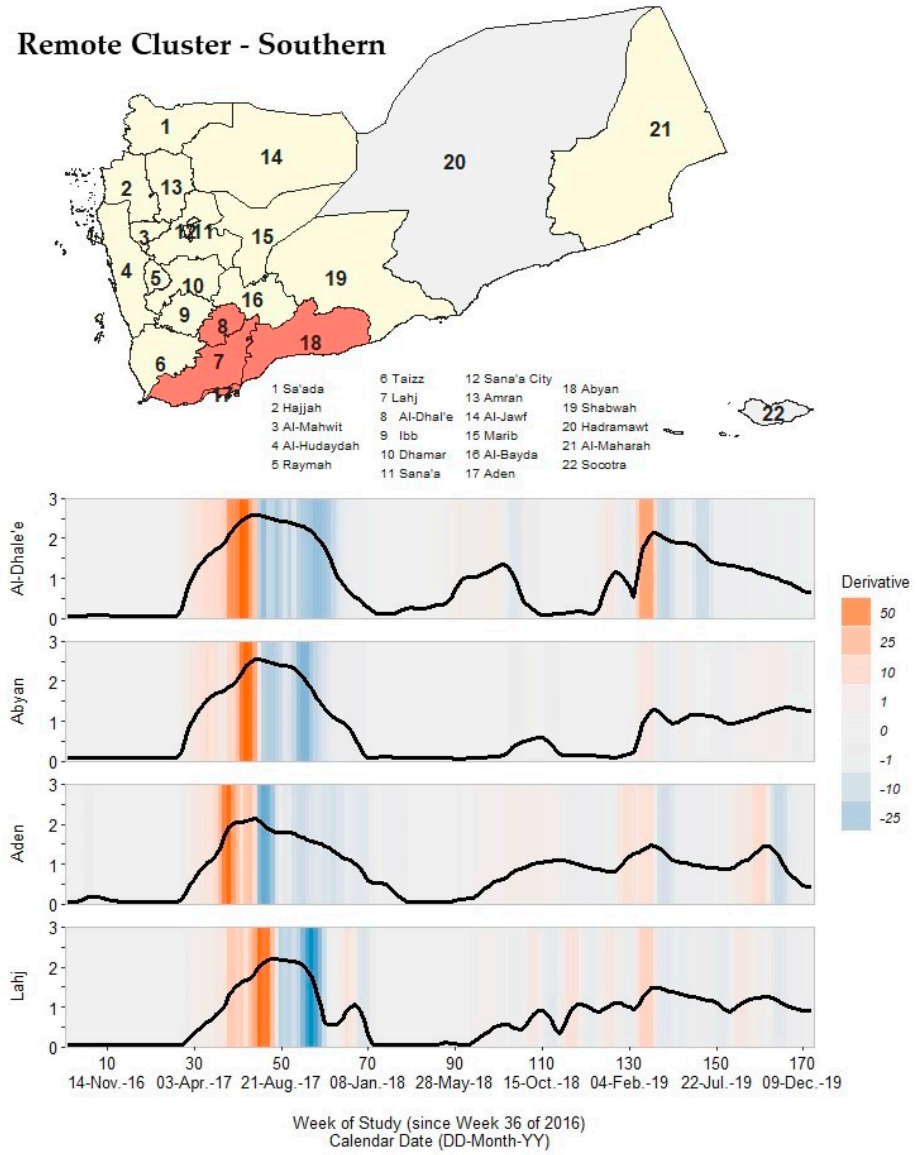


Figure 8. A map of Yemen with a shaded outbreak cluster including Al-Dhale'e, Abyan, Aden, and Lahj, and a stacked time series plot and heatmap for each governorate's outbreak signature. Top panel: the governorate-level map indicates governorates within the cluster in orange, remaining governorates within our study in yellow, and excluded governorates in grey (the Hadramaut and Socotra island governorate). Bottom panel: stacked time series plots for each governorate within the cluster. All plots show log10-transformed smoothed rates produced using Kolmogorov–Zurbenko adaptive filters from Week 36 (4–11 September) of 2016 through Week 52 (23–29 December) of 2019. Smoothed rates (laboratory-confirmed cholera cases per 100,000 persons) were estimated using the best performing smoother. Backgrounds for each plot are heatmaps of trivial derivative values, ranging from −25 (dark blue) to +50 (dark orange) with values near zero in grey. Time series plots have a common horizontal axis of time reported in weeks since Week 36 of 2016 (defined as study Week 0). All rates and trivial derivates were calculated for the 172 weeks of time series. Data used to develop this visualization are reported in Table 1 and Supplementary Excel Table S5.

Governorates in the eastern cluster (Figure 9; Supplementary Excel Table S5) had no reported cases of cholera during Wave 1 and no well-defined critical points in Wave 3. In

fact, cholera rates did not exceed 5 cph between the resolution of Wave 2 (as early as 18–24 December 2017) and the onset of Wave 4 (as late as 18–24 March 2019) for any eastern cluster governorate. In Wave 2, these governorates had a wide range of peak rate magnitudes, from Shabwah at ~22.1 cph to Marib at ~110.2 cph. Shabwah and Al-Maharah had the earliest resolution timing, which occurred from 18 December 2017 to 4 February 2018. As with governorates in the southern cluster, all governorates in the eastern cluster had Wave 4 peak rate magnitudes of <35 cph.

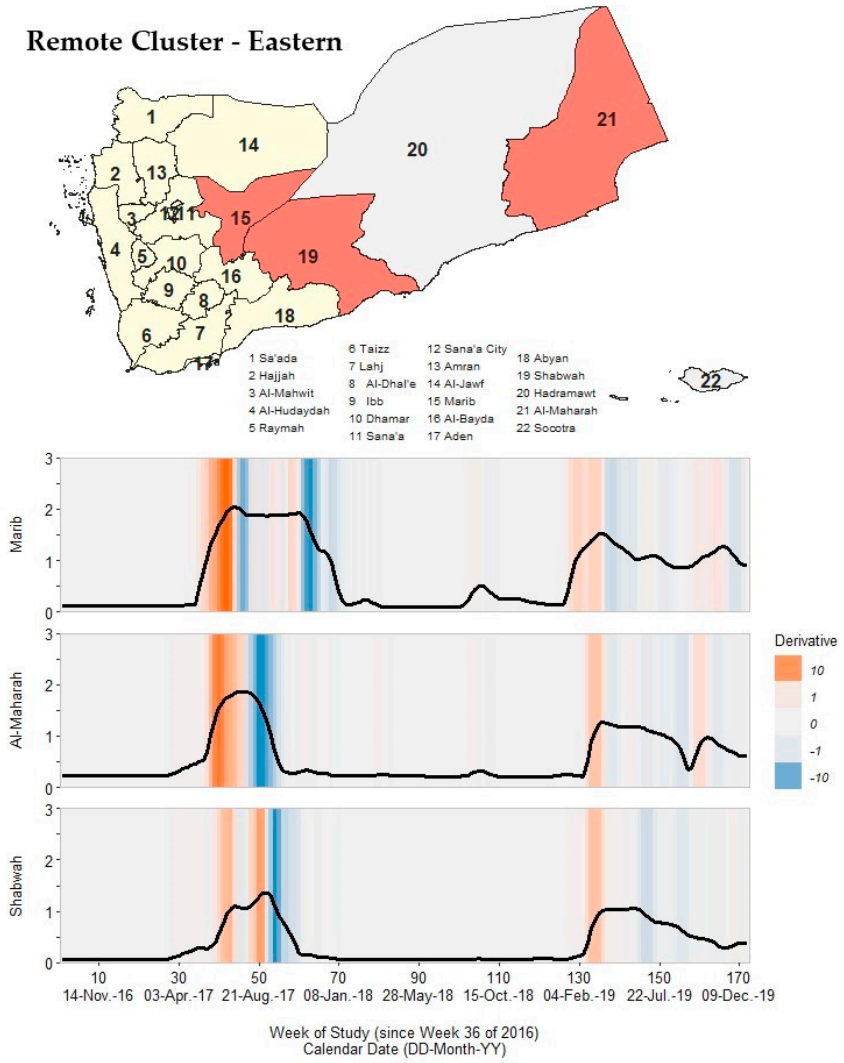


Figure 9. A map of Yemen with a shaded outbreak cluster including Marib, Al-Maharah, and Shabwah, and a stacked time series plot and heatmap for each governorate's outbreak signature. Top panel: the governorate-level map indicates governorates within the cluster in orange, remaining governorates within our study in yellow, and excluded governorates in grey (the Hadramaut and Socotra island governorate). Bottom panel: stacked time series plots for each governorate within the cluster. All plots show log10-transformed smoothed rates produced using Kolmogorov–Zurbenko adaptive filters from Week 36 (4–11 September) of 2016 through Week 52 (23–29 December) of 2019. Smoothed rates (laboratory-confirmed cholera cases per 100,000 persons) were estimated using the best performing smoother. Backgrounds for each plot are heatmaps of trivial derivative values, ranging from −10 (dark blue) to +10 (dark orange) with values near zero in grey. Time series plots have a common horizontal axis of time reported in weeks since Week 36 of 2016 (defined as study Week 0). All rates and trivial derivates were calculated for the 172 weeks of time series. Data used to develop this visualization are reported in Table 1 and Supplementary Excel Table S5.

4. Discussion

Our study demonstrated the utility of publicly reported surveillance data to characterize, classify, and compare infectious disease outbreak signatures. We proposed an application of non-parametric KZ adaptive filters to define outbreak signatures and identified regional hotspots of cholera outbreaks. We used this data-driven approach to define outbreak critical points (onset, peak timing, and resolution) and critical periods (acceleration, deceleration, and steady state) to examine spatiotemporal patterns in cholera outbreak signatures. This methodology introduced a protocol for routine vulnerability mapping of outbreak hotspots to improve resource management and mobilization during humanitarian aid responses.

Application of KZ filter methodology permitted closer inspection of subtle differences between governorates' outbreak signatures considering several investigated features. Using the proposed methodology, we defined a core outbreak hotspot of Sana'a, Sana'a City, and Al-Hudaydah, which was the expected origin of the national outbreak [42–45]. These governorates shared nearly identical features as the national outbreak signature in all four waves, including onset and peak timing critical points, peak rate magnitudes, and durations of acceleration and deceleration periods. While key informant interviews and trend analyses elsewhere suggested that Wave 1 peak timing occurred in 5–31 December 2016, we identified earlier peak timing for the core cluster and nationally ranging from 10 October 2016 to 13 November 2016 [26,27,46]. Additionally, various sources including the WHO declared that Wave 1 concluded for all governorates and nationally in 13–27 April 2017 [26,27,46,47]. However, we identified a resolution period for all affected governorates ranging from 2 January 2017 to 5 March 2017.

Our results for Wave 2 outbreak signatures closely aligned with those of Dureab et al. and Camacho et al., whose descriptive trend analyses were based on the Yemeni National Electronic Disease Early Warning System (eDEWS) [26,27]. While Camacho et al. reported a Wave 2 peak at the end of June 2017, Dureab et al. reported a first outbreak peak in 17–23 July 2017 and a second peak of lesser magnitude 3 months later in 18–24 September 2017 [26,27]. We identified two outbreak peaks with similar timing (24–30 July 2017 and 25 September 2017 to 01 October 2017), shared by most governorates. However, we also identified a third peak found in the two neighboring clusters (Amran, Al-Mahwit, Dhamar, Al-Bayda, Raymah, Ibb, and Taizz) surrounding the core outbreak cluster (Sana'a, Sana'a City, and Al-Hudaydah) from 5 March 2018 to 1 April 2018. Similarities in our findings suggested consistency in the reporting of district-level and governorate-level data.

These findings potentially suggested traveling waves from the core outbreak cluster, whose earlier second peak timing (18 September 2017 to 1 October 2017) preceded the later peak timing (1 January 2018 to 20 May 2018) in neighboring governorates. The core cluster reflected a persistent cluster of infections due to consistently high peak rates, early peak timing, and large population density in these governorates. The later peak timing of governorates within close spatial proximity suggested a high degree of percolation to other clusters, though these variations may have been dictated by differences in the spatial distribution of conflict, environmental, and socioeconomic factors within each governorate. Further research is needed to describe patterns of disease spread and differences in drivers of infection in each governorate.

Our findings also suggest a possible second traveling wave from the first neighboring cluster (Amran, Al-Mahwit, Dhamar, and Al-Bayda) to the northern, southern, and eastern remote clusters. The four governorates in this neighboring cluster bordered governorates in each of the three remote clusters. As described earlier, this neighboring cluster is characterized by extremely high peak rate magnitudes (216.3–397.7 cph) for the first peak timing (24 July 2017 to 27 August 2017) in Wave 2 with equally high paces of increase to the peak (10.8–20.9 cph/week). In contrast, most remote clusters had a single peak whose timing was slightly later than the neighboring cluster (24 July 2017 to 17 September 2017) and whose magnitude was lower (22.14–164.88 cph) in most governorates. This suggested that larger outbreaks in this neighboring cluster could have resulted in percolation of

the outbreak to the remote clusters, which experienced a short, intense Wave 2 outbreak before quickly returning to pre-outbreak rate values (<4 cph) from 18 December 2017 to 1 April 2018.

While WHO epidemiological surveillance bulletins suggested that Wave 2 persisted from April 2017 through January 2020, we identified two national outbreak waves with onsets in May 2018 and January 2019 [47]. These waves suggest that the epidemic remains ongoing with numerous onsets of outbreak events rather than one prolonged outbreak period. For Waves 1 and 2, the acceleration period from the onset to the peak was 1.5–2.2-fold shorter than the deceleration period from the peak timing to the onset of the next wave. Furthermore, for Wave 3, the acceleration period from the onset to peak was >1.5-fold longer than the deceleration period from the peak of Wave 3 to the onset of Wave 4. As with Waves 1 and 2, we found great heterogeneity in the onset, peak timing, and duration of outbreaks across governorates for Wave 3 and Wave 4. Differences in patterns of outbreak signatures across waves may suggest that drivers of disease transmission varied over time and location. These differences must be inspected individually for each wave and may have required different types of humanitarian relief according to the conflict-, environmental-, and socioeconomic-related drivers of infection.

Discrepancies in outbreak signatures can significantly influence reported associations between cholera rates and human-made or environmental drivers of transmission. For example, Wave 3 began nationally from 28 May 2018 to 3 June 2018, though onset timing ranged from 2 April 2018 to 8 July 2018. The Wave 3 onset timing for southern cluster governorates closely aligned with the arrival of the Mekunu cyclone, which made landfall in Oman and Yemen on 25 May 2018 and resulted in severe flooding [48–50]. In contrast, the Battle of Al-Hudaydah from 13 to 22 June 2018 left governorates in the core, neighboring, and remote northern clusters with severe health infrastructure destruction [51]. These natural disaster and conflict events, whose repercussions persisted through December 2019, may explain the shorter acceleration periods and more frequent outbreak peaks in Waves 3 and 4. Future research using our defined outbreak signatures is needed to examine how environmental and human-made risk factors varied both across and within outbreak clusters on a wave-by-wave basis.

Our study could shed light on previous research examining associations between cholera incidence and environmental risk factors for Wave 2 of the Yemeni cholera outbreak. Camacho et al. used district-level surveillance records and high-resolution rainfall data to show that within 10 days of a 10 mm rainfall event the likelihood of cholera infection increased by 21% compared to a week of no rainfall [26]. However, results assumed that each district followed identical outbreak onset and peak timing according to national-level, WHO-defined outbreak wave critical points [26]. Other studies aimed at modeling cholera outbreak signatures similarly did so with pre-defined national-level characteristics, preventing exploration of regional hotspots [27,46,52]. Our results provided more refined estimates of critical points and helped account for the variability of outbreak signatures or differences in outbreak duration across governorates, which faced differing intensities of wartime conflicts, food insecurity, and malnutrition. If more spatially granular time series data were reported at the district level, we could further refine how governorates were assigned to outbreak clusters.

Our study had several limitations. Firstly, the reliability of case data may be impacted by the scattered dispersal of public technical reports and their inconsistent, infrequent, and sometimes non-overlapping time periods. Furthermore, data collection and reporting were expected to be limited by health care services/capacity, utilization of health services, and reporting ability in combination with the ruralness and governing stability of each governorate. The WHO provided no metadata explaining limitations in data quality and coverage after data were aggregated from district-level eDEWS reports to governorate-level WHO bulletins. Dureab et al., who used eDEWS data reports, found only ~1 week lag between the time of infection and reporting of time series records suggesting consistent reporting despite ongoing conflict events [27]. However, key informant interviews in Yemen

noted significant destruction of emergency health facilities in Sana'a City and low capacity for routine and reliable laboratory culture testing in Sana'a and Al-Hudaydah [3,5,46]. This suggests possible under-reporting in these governorates, especially during the second wave of the epidemic between March 2017 and April 2018.

We compiled data presented in various formats to the best of our knowledge and abilities and are unaware of alternative methods that could have better validated the compiled data, given the inconsistent reporting and availability of case reports. Similarly, data were only available at the governorate level, which prevented more refined cluster assignments that would account for district-level differences in topography, climate, health infrastructure, etc. While district-level data would improve the granularity of classified outbreak clusters, our use of governorate-level data reflected both the usability of publicly reported data and the reality of the data landscape in Yemen. That said, we found similar critical point timing and magnitudes in our national outbreak signature to the study performed by Dureab et al. (which used eDEWS data), which suggested that our estimation techniques retained the features of reported data [27].

Secondly, population estimates used to calculate weekly rates only accounted for possible changes in population growth rate and conflict fatalities. This growth rate was retrieved from the 2004 Yemeni Census as no additional population estimates or growth rates were provided in the 2014 Census [35,53]. ACLED fatality data used to adjust for violent and non-violent political events were retrieved from a variety of media sources and may not be reliable [54–57]. Additionally, we were unable to adjust for possible population migration from Yemen or internal displacement within Yemen, as these data were not reported consistently at the monthly or weekly levels [36]. While a substantial proportion (~15%) of Yemen's population has been internally displaced throughout the Yemeni Civil War, neither ACLED nor any other dataset we explored provided data on migration or internal displacement with sufficient temporal resolution, spatial granularity, or consistent reporting to use in adjusting population estimates. Furthermore, data lacked sufficient spatial resolution to consider examining rates by population density, as most governorates included both urban cities and rural mountainous areas. Because we used a prorated weekly population estimate to account for possible population growth over time in the absence of more refined population data, we likely underestimated the rate of infection.

Finally, data from this study were reported through 29 December 2019. We were unable to extend our time series through 2020 or 2021 due to a lack of epidemiological bulletins for this year [29,47]. Understandably, resources could have been diverted to mitigate and manage the ongoing SARS-CoV-2 pandemic. While weekly updates were provided on the current cholera crisis in Yemen, these reports provided insufficient temporal and spatial granularity for recreating weekly time series of cases. However, various reports suggested, as found in our study, that the cholera epidemic within Yemen remains ongoing with rates like those reported in 2019 [58–62]. Thus, coordinated efforts for mitigating and preventing the spread of cholera are still needed [62–66].

While we detected potential traveling waves for governate-specific outbreaks, there could be many reasons for observed spatiotemporal patterns. The differences in outbreak signatures could be governed by variations in environmental factors, such as rainfall, flooding, and water contamination, conflicts and social unrest, depleted health infrastructure, food insecurity, and many other factors that deserve further investigations. Any such investigation should start with better understanding the spatiotemporal behaviors of infection across clusters and synchronicity between exposure events and outbreaks, that could be explored with dynamic mapping. Dynamic or animated maps are an emerging data visualization technique that compresses large amounts of spatially and temporally aligned records into visuals. We have demonstrated the utility of this visualization technique to identify persistent and percolating clusters of *Salmonella* outbreaks and traveling waves of influenza in the United States [18,67]. Our curated dataset provides the foundation for aligning and integrating other spatiotemporal data on conflict-, environmental-, and socioeconomic-related factors to conduct these future analyses. This expanded dataset can

then be used for evaluating the drivers and consequences of disease outbreaks during the Yemeni Civil War.

To increase the usability and transparency of valuable epidemiological records collected by many national and international organizations, public access and dissemination of information are critical. Publicly available data and information could assist in preventing or mitigating humanitarian crises such as this one in Yemen. We encourage the holders of epidemiological records to share data and metadata with the broader scientific community at the highest temporal and spatial granularity possible to ease the extraction, understanding, and utilization of publicly disseminated data. We also encourage future applications of the novel methods for early outbreak detection, regional hotspot identification, and resource distribution coordination in accordance with the global mandate of the WHO's GTFCC [8–11]. Our findings, in conjunction with future research, could support the GTFCC roadmap and provide solid methodology to define outbreak signatures, classify regional hotspots, evaluate risk factors contributing to outbreak transmission, and establish an early outbreak warning system [10,11].

5. Conclusions

Our study provided a data-driven approach to describe and compare outbreak signatures of governorate-level cholera outbreaks in Yemen. These techniques utilized time series surveillance data and were not unique to the temporal resolution, spatial granularity, or infectious disease examined. Though our analysis evaluated data retrospectively, the proposed methodology can be adapted and applied for real-time forecasting to determine outbreak signatures of ongoing epidemics. Furthermore, our approach demonstrated how data published publicly by humanitarian organizations can be retrieved, harmonized, and utilized for modeling outbreak signatures. The detected heterogeneity in outbreak signatures associated with spatial proximity suggested possible traveling waves of infection outwards from the core cluster. Further research is needed to investigate if these differences are due to impacts of conflict, environmental, social, and economic factors across governorates. Similarities in outbreak signatures also suggested potentially shared environmental and human-made drivers of infection. By identifying and grouping governorates with similar critical points, periods, and rate magnitudes, we provided the context for identifying and comparing human-made and environmental drivers of disease transmission. These methods can help to parse out associations between infectious disease outbreaks and wartime conflict, rainfall, food insecurity, and consumer price risk factors to assist in coordinating humanitarian relief efforts.

Supplementary Materials: The following supporting information can be downloaded at: https://www.mdpi.com/article/10.3390/ijerph19010378/s1, Supplementary Excel File: This file provides Excel Tables S1–S5, which publicly report datasets used for statistical analyses and visualizations within this study; Figures S1–S6: Stacked multi-panel time series plots of the national Yemeni cholera outbreak signature and the governorate-level signatures of each outbreak cluster; Table S1: weak serial synchronization of confirmed cholera rates in 20 Yemeni governorates from Week 36 of 2016 through Week 52 of 2019; Supplementary R software files: these files provide scripts for re-creating all illustrations in both the main text and supplementary text files.

Author Contributions: M.C.T. contributed to data validation, the extraction of data from grey literature sources, and original conception of this research. R.B.S. and M.C.T. provided the original draft preparation and contributed to reviewing and editing the manuscript. R.B.S., S.B. and P.M.K. contributed to data extraction. R.B.S. conducted all spatial and temporal alignment. S.B. and P.M.K. validated spatial and temporal alignment for all data sources. M.A.H. and R.B.S. created all data visualizations using R software. E.N.N. contributed to methodology development, writing, reviewing, and editing the manuscript, supervision, project administration, and funding acquisition. All authors have read and agreed to the published version of the manuscript.

Funding: This research is based upon work supported in part by the Office of the Director of National Intelligence (ODNI), Intelligence Advanced Research Projects Activity (IARPA), via 2017-17072100002

(Naumova-PI). The views and conclusions contained herein are those of the authors and should not be interpreted as necessarily representing the official policies, either expressed or implied, of ODNI, IARPA, or the U.S. Government. The U.S. Government is authorized to reproduce and distribute reprints for governmental purposes notwithstanding any copyright annotation therein. The United States Department of Agriculture (USDA) National Institute of Food and Agriculture (NIFA) Cooperative State Research, Education, and Extension Service Fellowship supported Ryan B. Simpson via grant award number 2020-38420-30724. The Tufts School of Medicine Building Diversity Biomedical Sciences Program supported Sofia Babool via award number R25-HL007785. This research was also supported by the Tufts University Data Intensive Studies Center (DISC) Seed Grant.

Institutional Review Board Statement: Not applicable.

Informed Consent Statement: Not applicable.

Data Availability Statement: All data and visualization coding resources are reported in Supplementary Materials.

Acknowledgments: Authors would like to acknowledge Alissa Ebel and Sirjana Shakya for their support in compiling ACLED data and Erin Boyd from Tufts Feinstein International Center for her insights on data sharing, disease modelling, and humanitarian assistance in the current Yemen crisis.

Conflicts of Interest: The authors declare no conflict of interest.

References

1. Potter, C. Largest Cholera Outbreak on Record Continues. John Hopkins Bloomberg School of Public Health, Center for Health Security, 16 January 2020. Available online: https://www.outbreakobservatory.org/outbreakthursday-1/1/16/2020/large-cholera-outbreak-on-record-continues-in-yemen (accessed on 12 March 2020).
2. Sifferlin, A. What to Know about the Massive Cholera Outbreak in Yemen. *TIME*, 26 July 2017. Available online: https://time.com/4874345/yemen-cholera-outbreak/ (accessed on 12 March 2020).
3. Al-Mekhlafi, H.M. Yemen in a time of cholera: Current situation and challenges. *Am. J. Trop. Med. Hyg.* **2018**, *98*, 1558–1562. [CrossRef] [PubMed]
4. Eastern Mediterranean Regional Office: World Health Organization. Cholera Outbreaks. Available online: http://www.emro.who.int/health-topics/cholera-outbreak/cholera-outbreaks.html (accessed on 1 June 2018).
5. Federspiel, F.; Ali, M. The cholera outbreak in Yemen: Lessons learned and way forward. *BMC Public Health* **2018**, *18*, 1338. [CrossRef] [PubMed]
6. Biggs, M. Yemen Was Poor Before, But 'the War Just Finished Us'. *PBS News Hour*, 16 May 2018. Available online: https://www.pbs.org/newshour/show/yemen-was-poor-before-but-the-war-just-finished-us (accessed on 12 March 2020).
7. Hove-Musekwa, S.D.; Nyabadza, F.; Chiyaka, C.; Das, P.; Tripathi, A.; Mukandavire, Z. Modelling and analysis of the effects of malnutrition in the spread of cholera. *Math Comput. Model.* **2011**, *53*, 1583–1595. [CrossRef]
8. Global Task Force on Cholera Control: World Health Organization. Ending Cholera: A Global Roadmap to 2030. Available online: https://www.who.int/cholera/publications/global-roadmap.pdf?ua=1 (accessed on 8 December 2020).
9. Legros, D. Global cholera epidemiology: Opportunities to reduce the burden of cholera by 2030. *J. Infect. Dis.* **2018**, *218*, S137–S140. [CrossRef]
10. Global Task Force on Cholera Control: World Health Organization. Guidance and Tool for Countries to Identify Priority Areas for Intervention: September 2019. Available online: https://www.gtfcc.org/wp-content/uploads/2019/11/guidance-and-tool-for-countries-to-identify-priority-areas-for-intervention1.pdf (accessed on 8 December 2020).
11. Global Task Force on Cholera Control: World Health Organization. Interim Guiding Document to Support Countries for the Development of their National Cholera Plan: Advanced Copy. Available online: https://www.gtfcc.org/wp-content/uploads/2020/11/gtfcc-Interim-guiding-document-to-support-countries-for-the-development-of-their-national-cholera-plan.pdf (accessed on 8 December 2020).
12. Fefferman, N.H.; Naumova, E.N. Combinatorial decomposition of an outbreak signature. *Math. Biosci.* **2006**, *202*, 269–287. [CrossRef]
13. Naumova, E.N.; O'Neil, E.; MacNeill, I. INFERNO: A system for early outbreak detection and signature forecasting. *MMWR Morb. Mortal. Wkly. Rep.* **2005**, *54*, 77–83.
14. Naumova, E.N.; MacNeill, I.B. Signature-forecasting and early outbreak detection system. *Environmetrics* **2005**, *16*, 749–766. [CrossRef]
15. Fefferman, N.; Naumova, E.N. Innovation in observation: A vision for early outbreak detection. *Emerg. Health Threats J.* **2010**, *3*, 7103. [CrossRef]
16. Chui, K.K.; Jagai, J.S.; Griffiths, J.K.; Naumova, E.N. Hospitalization of the elderly in the United States for nonspecific gastrointestinal diseases: A search for etiological clues. *Am. J. Public Health* **2011**, *101*, 2082–2086. [CrossRef]

17. Chui, K.K.; Cohen, S.A.; Naumova, E.N. Snowbirds and infection–new phenomena in pneumonia and influenza hospitalizations from winter migration of older adults: A spatiotemporal analysis. *BMC Public Health* **2011**, *11*, 444. [CrossRef]
18. Moorthy, M.; Castronovo, D.; Abraham, A.; Bhattacharyya, S.; Gradus, S.; Gorski, J.; Naumov, Y.N.; Fefferman, N.H.; Naumova, E.N. Deviations in influenza seasonality: Odd coincidence or obscure consequence? *Clin. Microbiol. Infect.* **2012**, *18*, 955–962. [CrossRef] [PubMed]
19. Naumova, E.N.; Jagai, J.S.; Matyas, B.; DeMaria, A.; MacNeill, I.B.; Griffiths, J.K. Seasonality in six enterically transmitted diseases and ambient temperature. *Epidemiol. Infect.* **2007**, *135*, 281–292. [CrossRef] [PubMed]
20. Naumova, E.N.; MacNeill, I.B. Time-distributed effect of exposure and infectious outbreaks. *Environmetrics* **2009**, *20*, 235–248. [CrossRef]
21. Simpson, R.B.; Falconi, T.M.A.; Venkat, A.; Chui, K.H.; Navidad, J.; Naumov, Y.N.; Gorski, J.; Bhattacharyya, S.; Naumova, E.N. Incorporating calendar effects to predict influenza seasonality in Milwaukee, Wisconsin. *Epidemiol. Infect.* **2019**, *147*, e268. [CrossRef]
22. Simpson, R.B.; Zhou, B.; Naumova, E.N. Seasonal synchronization of foodborne outbreaks in the United States, 1996–2017. *Sci. Rep.* **2020**, *10*, 17500. [CrossRef]
23. Simpson, R.B.; Zhou, B.; Falconi, T.M.A.; Naumova, E.N. An analecta of visualizations for foodborne illness trends and seasonality. *Sci. Data* **2020**, *7*, 346. [CrossRef]
24. Wenger, J.B.; Naumova, E.N. Seasonal synchronization of influenza in the United States older adult population. *PLoS ONE* **2010**, *5*, e10187. [CrossRef] [PubMed]
25. National Center for Emerging and Zoonotic Infectious Diseases: Division of Foodborne, Waterborne, and Environmental: Centers for Disease Control and Prevention. 7. Decide Outbreak Is over. Available online: https://www.cdc.gov/healthywater/emergency/waterborne-disease-outbreak-investigation-toolkit/outbreak-over.html (accessed on 12 March 2020).
26. Camacho, A.; Bouhenia, M.; Alyusfi, R.; Alkohlani, A.; Naji, M.A.M.; de Radiguès, X.; Abubakar, A.M.; Almoalmi, A.; Seguin, C.; Sagrado, M.J.; et al. Cholera epidemic in Yemen, 2016–2018: An analysis of surveillance data. *Lancet Glob. Health* **2018**, *6*, e680–e690. [CrossRef]
27. Dureab, F.; Ismail, O.; Mueller, O.; Jahn, A. Cholera outbreak in Yemen: Timeliness of reporting and response in the National Electronic Disease Early Warning System. *Acta Inform. Med.* **2019**, *2*, 85. [CrossRef] [PubMed]
28. Eastern Mediterranean Regional Office: World Health Organization. Epidemic and Pandemic-Prone Diseases. Available online: http://www.emro.who.int/pandemic-epidemic-diseases/cholera/index.html (accessed on 1 June 2018).
29. Eastern Mediterranean Regional Office: World Health Organization. Yemen Situation Reports: Weekly Cholera Bulletins. Available online: http://www.emro.who.int/yem/yemeninfocus/situation-reports.html (accessed on 1 June 2018).
30. Eastern Mediterranean Regional Office: World Health Organization. Archived Epidemiology Bulletins. Available online: http://www.emro.who.int/yem/information-resources/epidemiology-bulletins-archive.html (accessed on 1 June 2018).
31. Simpson, R.B.; Babool, S.; Tarnas, M.C.; Kaminski, P.M.; Hartwick, M.A.; Naumova, E.N. Dynamic Mapping of Cholera Spread and Conflict Severity During the Yemeni Civil War, 2016–2019. Figshare, 2021. Available online: https://figshare.com/s/3b2882c020ae9ed2e576 (accessed on 12 March 2021).
32. World Health Organization. Global Influenza Surveillance and Response Systems. FluNet. Available online: https://www.who.int/influenza/gisrs_laboratory/flunet/en/ (accessed on 1 June 2018).
33. Armed Conflict Location and Event Data Project. Data Export Tool. Available online: https://www.acleddata.com/data/ (accessed on 1 July 2018).
34. Armed Conflict Location and Event Data Project. ACLED Methodology and Coding Decisions around the Yemen Civil War. Available online: https://acleddata.com/acleddatanew/wp-content/uploads/dlm_uploads/2019/01/YemenMethodology_2020_ACLED.pdf (accessed on 1 July 2018).
35. Central Statistical Organization: Yemeni Central Bureau of Statistics. Summary Table of the Main Results of Population Projection Data and Indicators (2005–2025) According to Different Hypotheses and Alternatives. Available online: http://www.cso-yemen.com/content.php?lng=arabic&id=553 (accessed on 1 July 2018).
36. International Organization of Migration. Displacement Tracking Matrix: Yemen. Available online: https://dtm.iom.int/yemen (accessed on 1 July 2018).
37. Tukey, J.W. *Thinking about Non-Linear Smoothers*; Report #ARO-23360.4-MA; Department of Statistics, Princeton University; United States Army Research Office: Princeton, NJ, USA, 1986.
38. Yang, W.; Zurbenko, I. Kolmogorov–Zurbenko filters. *Wiley Interdiscip. Rev. Comput. Stat.* **2010**, *2*, 340–351. [CrossRef]
39. Zurbenko, I.G.; Sun, M. Applying Kolmogorov-Zurbenko Adaptive R-Software. *Int. J. Probab. Stat.* **2017**, *6*, 110. [CrossRef]
40. Zurbenko, I.G.; Smith, D. Kolmogorov–Zurbenko filters in spatiotemporal analysis. *Wiley Interdiscip. Rev. Comput. Stat.* **2018**, *10*, e1419. [CrossRef]
41. Humanitarian Data Exchange. Yemen—Subnational Administrative Boundaries. Available online: https://data.humdata.org/dataset/yemen-admin-boundaries (accessed on 1 November 2020).
42. Eastern Mediterranean Regional Office: World Health Organization. Media Centre: The Ministry of Public Health and Population Announces Cholera Cases in Yemen. Available online: http://www.emro.who.int/media/news/the-ministry-of-health-announces-cholera-cases-in-yemen.html (accessed on 1 June 2018).

43. Eastern Mediterranean Regional Office: World Health Organization. Situation Report: Acute Watery Diarrhea/Cholera Outbreak—Yemen (26 October 2016). Available online: http://www.emro.who.int/images/stories/yemen/situation_report_cholera_in_yemen_2.pdf (accessed on 1 June 2018).
44. Eastern Mediterranean Regional Office: World Health Organization. Yemen: Cholera Outbreak: Situation Report No. 2 (as of 1 November 2016). Available online: https://reliefweb.int/sites/reliefweb.int/files/resources/OCHA%20Cholera%20Situation%20Report%202-%20For%20Publication%20.pdf (accessed on 1 June 2018).
45. United Nations Office for the Coordination of Humanitarian Affairs. Yemen: Cholera Outbreak—Oct 2016. Available online: https://www.humanitarianresponse.info/en/disaster/ep-2016-000107-yem (accessed on 8 December 2020).
46. Spiegel, P.; Ratnayake, R.; Hellman, N.; Ververs, M.; Ngwa, M.; Wise, P.H.; Lantagne, D. Responding to epidemics in large-scale humanitarian crises: A case study of the cholera response in Yemen, 2016–2018. *BMJ Glob. Health* **2019**, *4*, e001709. [CrossRef] [PubMed]
47. Eastern Mediterranean Regional Office: World Health Organization. Cholera Situation in Yemen: January 2020. Available online: https://applications.emro.who.int/docs/EMCSR252E.pdf (accessed on 8 December 2020).
48. Almasmari, H.; Smith-Spark, L. Cyclone Pounds Yemeni Island Ahead of Landfall on Yemen, Oman Coast. *Cable News Network World*. 25 May 2018. Available online: https://www.cnn.com/2018/05/25/middleeast/yemen-oman-cyclone-mekunu-wxc-intl/index.html (accessed on 12 March 2020).
49. The Weather Channel. Tropical Cyclone Mekunu Slams Oman and Yemen, Killing at Least 13. 30 May 2018. Available online: https://weather.com/safety/news/2018-05-26-tropical-cyclone-mekunu-oman-yemen-socotra-impacts (accessed on 12 March 2020).
50. World Meteorological Organization. Extremely Severe Cyclonic Storm Mekunu Impacts Oman and Yemen. 25 May 2018. Available online: https://public.wmo.int/en/media/news/extremely-severe-cyclonic-storm-mekunu-impacts-oman-and-yemen (accessed on 12 March 2020).
51. British Broadcasting Corporation. Yemen War: Battle for Vital Port of Hudaydah Intensifies. *BBC News*, 7 November 2018. Available online: https://www.bbc.com/news/world-middle-east-46125858 (accessed on 12 March 2020).
52. Nishiura, H.; Tsuzuki, S.; Yuan, B.; Yamaguchi, T.; Asai, Y. Transmission dynamics of cholera in Yemen, 2017: A real time forecasting. *Theor. Biol. Med. Model.* **2017**, *14*, 14. [CrossRef] [PubMed]
53. Central Statistical Organization: Yemeni Central Bureau of Statistics. The General Census of Population, Housing, and Establishments 2014. Available online: http://www.cso-yemen.com/content.php?lng=arabic&id=593 (accessed on 1 June 2018).
54. Armed Conflict Location and Event Data Project. About ACLED. Available online: https://www.acleddata.com/about-acled/ (accessed on 8 December 2020).
55. Armed Conflict Location and Event Data Project. ACLED Definitions of Political Violence and Protest. Available online: https://acleddata.com/acleddatanew/wp-content/uploads/dlm_uploads/2019/04/ACLED-Event-Definitions_Final.pdf (accessed on 8 December 2020).
56. Armed Conflict Location and Event Data Project. ACLED Methodology. Available online: https://acleddata.com/acleddatanew/wp-content/uploads/dlm_uploads/2019/04/Methodology-Overview_FINAL.pdf (accessed on 8 December 2020).
57. Armed Conflict Location and Event Data Project. ACLED General Quick User Guide. Available online: https://acleddata.com/acleddatanew/wp-content/uploads/dlm_uploads/2019/04/General-User-Guide_FINAL-1.pdf (accessed on 8 December 2020).
58. Eastern Mediterranean Regional Office: World Health Organization. Epidemic and Pandemic-Prone Diseases: Outbreak Update—Cholera in Yemen, 16 August 2020. Available online: http://www.emro.who.int/pandemic-epidemic-diseases/cholera/outbreak-update-cholera-in-yemen-16-august-2020.html (accessed on 8 December 2020).
59. Eastern Mediterranean Regional Office: World Health Organization. WHO in Yemen: Situation Reports. Available online: http://www.emro.who.int/yemen/information-resources/situation-reports.html (accessed on 8 December 2020).
60. Eastern Mediterranean Regional Office: World Health Organization. Situation Report: February 2020, Issue No.2, Yemen Update. Available online: http://www.emro.who.int/images/stories/somalia/yemen-situation_report-feb2020.pdf?ua=1&ua=1 (accessed on 8 December 2020).
61. Eastern Mediterranean Regional Office: World Health Organization. Situation Report: June 2020, Issue No. 6, Yemen Update. Available online: http://www.emro.who.int/images/stories/yemen/who_situation_report_june2020.pdf?ua=1 (accessed on 8 December 2020).
62. Eastern Mediterranean Regional Office: World Health Organization. Situation Report: October 2020, Issue No. 10, Yemen Update. Available online: http://www.emro.who.int/images/stories/yemen/who_situation_report_october2020.pdf?ua=1 (accessed on 8 December 2020).
63. Al-Arshani, S. Aid Agencies in Yemen Are Worried that Cholera Is Being Overlooked as COVID-19 Overwhelms the Countries Already Fragile Healthcare System after 5 Years of Crisis. *Insider*. 31 July 2020. Available online: https://www.insider.com/aid-groups-yemen-worry-cholera-overlooked-covid-19-cases-rise-2020-7 (accessed on 12 March 2020).
64. Beaumont, P.; Wintour, P. Agencies Fear Hidden Cholera Deaths in Yemen as COVID-19 Overwhelms Clinics. *The Guardian News and Media*. 28 July 2020. Available online: https://www.theguardian.com/global-development/2020/jul/28/agencies-fear-hidden-cholera-deaths-in-yemen-as-covid-19-overwhelms-clinics (accessed on 12 March 2020).

65. Hartnett, L. Yemen Facing Hidden Cholera Crisis as COVID Cases Set to Peak in Coming Weeks. *Oxfam America*, 27 July 2020. Available online: https://www.oxfamamerica.org/press/yemen-facing-hidden-cholera-crisis-as-covid-cases-set-to-peak-in-coming-weeks-oxfam/ (accessed on 12 March 2020).
66. Patel, K. Predicting Cholera Risk in Yemen. NASA Earth Observatory, 23 February 2020. Available online: https://earthobservatory.nasa.gov/images/147101/predicting-cholera-risk-in-yemen (accessed on 12 March 2020).
67. Castronovo, D.A.; Chui, K.K.; Naumova, E.N. Dynamic maps: A visual-analytic methodology for exploring spatio-temporal disease patterns. *Environ. Health* **2009**, *8*, 61. [CrossRef]

International Journal of
Environmental Research and Public Health

MDPI

Article

Critical Periods, Critical Time Points and Day-of-the-Week Effects in COVID-19 Surveillance Data: An Example in Middlesex County, Massachusetts, USA

Ryan B. Simpson †, Brianna N. Lauren †, Kees H. Schipper, James C. McCann, Maia C. Tarnas and Elena N. Naumova *

Division of Nutrition Epidemiology and Data Science, Friedman School of Nutrition Science and Policy, Tufts University, 150 Harrison Avenue, Boston, MA 02111, USA; ryan.simpson@tufts.edu (R.B.S.); brianna.lauren@tufts.edu (B.N.L.); kschipper0430@comcast.net (K.H.S.); james.mccann@tufts.edu (J.C.M.); maia.tarnas@gmail.com (M.C.T.)

* Correspondence: elena.naumova@tufts.edu; Tel.: +1-617-636-2927

† These authors contributed equally to this work.

Abstract: Critical temporal changes such as weekly fluctuations in surveillance systems often reflect changes in laboratory testing capacity, access to testing or healthcare facilities, or testing preferences. Many studies have noted but few have described day-of-the-week (DoW) effects in SARS-CoV-2 surveillance over the major waves of the novel coronavirus 2019 pandemic (COVID-19). We examined DoW effects by non-pharmaceutical intervention phases adjusting for wave-specific signatures using the John Hopkins University's (JHU's) Center for Systems Science and Engineering (CSSE) COVID-19 data repository from 2 March 2020 through 7 November 2021 in Middlesex County, Massachusetts, USA. We cross-referenced JHU's data with Massachusetts Department of Public Health (MDPH) COVID-19 records to reconcile inconsistent reporting. We created a calendar of statewide non-pharmaceutical intervention phases and defined the critical periods and timepoints of outbreak signatures for reported tests, cases, and deaths using Kolmogorov-Zurbenko adaptive filters. We determined that daily death counts had no DoW effects; tests were twice as likely to be reported on weekdays than weekends with decreasing effect sizes across intervention phases. Cases were also twice as likely to be reported on Tuesdays-Fridays (RR = 1.90–2.69 [95%CI: 1.38–4.08]) in the most stringent phases and half as likely to be reported on Mondays and Tuesdays (RR = 0.51–0.93 [0.44, 0.97]) in less stringent phases compared to Sundays; indicating temporal changes in laboratory testing practices and use of healthcare facilities. Understanding the DoW effects in daily surveillance records is valuable to better anticipate fluctuations in SARS-CoV-2 testing and manage appropriate workflow. We encourage health authorities to establish standardized reporting protocols.

Keywords: COVID-19; data reliability; day-of-the-week effects; Kolmogorov-Zurbenko filters; nonpharmaceutical interventions; precision public health; stringency

check for updates

Citation: Simpson, R.B.; Lauren, B.N.; Schipper, K.H.; McCann, J.C.; Tarnas, M.C.; Naumova, E.N. Critical Periods, Critical Time Points and Day-of-the-Week Effects in COVID-19 Surveillance Data: An Example in Middlesex County, Massachusetts, USA. *Int. J. Environ. Res. Public Health* **2022**, *19*, 1321. https://doi.org/10.3390/ijerph19031321

Academic Editor: Paul B. Tchounwou

Received: 25 December 2021
Accepted: 19 January 2022
Published: 25 January 2022

Publisher's Note: MDPI stays neutral with regard to jurisdictional claims in published maps and institutional affiliations.

Copyright: © 2022 by the authors. Licensee MDPI, Basel, Switzerland. This article is an open access article distributed under the terms and conditions of the Creative Commons Attribution (CC BY) license (https://creativecommons.org/licenses/by/4.0/).

1. Introduction

One of the most important lessons of the novel coronavirus 2019 pandemic (COVID-19) has been the importance and utility of real-time infectious disease surveillance for monitoring, tracking, and reducing emerging infectious outbreaks [1–3]. Worldwide, and in the United States, SARS-CoV-2 surveillance has been made possible by collaborations between governmental agencies, public health authorities, healthcare systems, academic institutions, and media outlets to collect, curate, distribute, and communicate spatially and temporally refined health surveillance records [4,5]. Unlike most publicly available infectious disease surveillance data, SARS-CoV-2 reported tests, cases, and deaths have been curated at a daily temporal resolution and state- and county-level geographic areas. These reporting protocols create unique opportunities for public health professionals to

explore the patterns associated with broad intervention measures or often common yet overlooked patterns in reported data. The systematic changes in COVID-19 outcomes triggered by various interventions are under ongoing investigations by many research groups, yet a more granular and less obvious weekly variations are less explored.

One such pattern is day-of-the-week (DoW) effects, which describe differences in the reporting of health outcomes for some weekdays compared to a single reference day. To date, few studies have aimed to describe and quantify DoW effects in daily SARS-CoV-2 surveillance data. Instead, many studies aggregate or average daily records into weekly counts or rates or adjust for the DoW effects with various statistical techniques and thus ignore the potentially substantial and informative variations and differences between weekday or weekend reporting or their changes over time [6–9]. However, DoW effects reflect important patterns in the availability and capacity of laboratory testing facilities as well as popular preferences for seeking testing. The presence of DoW effects help to inform public health testing facilities and laboratories which days of the week have the highest or lowest demands for testing. In doing so, these facilities and public health agencies can better collaborate, anticipate, and manage laboratory testing resources and the scheduling of personnel to accommodate higher testing demands [10–13]. By examining how DoW effect sizes change over time, public health professionals can also monitor changes in popular preferences throughout the year, such as before and during times of federal or religious holidays or after the relaxation of non-pharmaceutical interventions [14–17]. This real-time surveillance improves the timeliness of test stockpiling and improves testing availability using mobile testing, the opening of additional test clinics, or subsidizing at-home, low-cost testing kits.

Examination of DoW effects has proven extremely beneficial in public health planning and programming for other respiratory illnesses and burdens. For example, influenza and influenza-like-illnesses have demonstrated clear increases in the reporting of tests and cases on weekdays compared to weekends due to laboratory testing capacity [18,19]. These findings have informed patterns of seasonal vaccination rollout and preparations for increased influenza testing capacity to accommodate increased volumes of seasonal influenza cases. Other calendar effects, including holiday effects, have identified amplification and dampening of influenza incidence due to social holidays and school closures, respectively [19–21]. Within environmental health sciences, DoW effects have been recognized for a long time in both the exposure and outcome variables [22,23].

One of the challenges of studying DoW effects is the need for assuring data quality, the absence of structural missingness or spikes (say during weekends or holidays), and consistency in reporting of time-referenced records. Now almost 2 years into the ongoing pandemic, several reports and commentaries have discussed limitations of publicly available COVID-19 surveillance data and the need for improvement as the pandemic persists [24–31]. For example, many statewide agencies use a variety of dates for reported cases such that a positive test result could be reported by the date of symptom onset, specimen collection, positively identified culture, or date of reporting [27,31]. Similarly, the definition of SARS-CoV-2 deaths may rely on a positive test shortly before or after death (which would underestimate deaths depending on testing availability) or include individuals who were not tested but were suspected of having SARS-CoV-2 (likely overestimating deaths) [29]. Despite these criticisms, few studies have quantified patterns to reporting inconsistencies or missing data in commonly used publicly available surveillance data [32,33].

In this study, we examined DoW effects using publicly available SARS-CoV-2 surveillance data reported from 2 March 2020 through 7 November 2021. We used John Hopkins University's (JHU's) Center for Systems Science and Engineering (CSSE) COVID-19 data repository in Middlesex County, Massachusetts, USA. We inspected and cross-referenced JHU data with the records of the Massachusetts Department of Public Health (MDPH) COVID-19 data dashboard. We defined major waves, their critical periods and points—constituting so-called outbreak signatures—for reported tests, cases, and deaths using Kolmogorov-Zurbenko adaptive filters with a 21-day smoothing window. We modeled

DoW effects using segmented time series analyses that adjusted for linear and quadratic trends within outbreak signatures' critical periods. We evaluated differences in DoW effects by Massachusetts non-pharmaceutical intervention phases and their stringency. By exploring DoW effects, public health professionals can identify patterns of reporting and begin to speculate testing capacity limitations and popular testing preferences to precisely model outbreak signatures.

2. Methods

2.1. Data Extraction and Management

In December 2019, JHU CSSE designed an online interactive dashboard to curate and report cumulative incidence of SARS-CoV-2 cases, deaths, and recoveries [34]. Scraping electronic health records from city, state, and national health agencies, this publicly available data repository provided the most extensive reporting of SARS-CoV-2 information in the United States [35,36]. We extracted cumulative counts of cases and deaths for all US counties from Monday, 2 March 2020 through Sunday, 7 November 2021 [37].

Upon extraction, we subset data for Middlesex County, Massachusetts as a case study to explore DoW effects in publicly available surveillance data. We selected Massachusetts as it ranked 2nd nationwide in healthcare access and 4th nationwide in public health spending throughout our study period [38]. These rankings suggested that Massachusetts would have highly reliable and complete SARS-CoV-2 surveillance data. We selected Middlesex County as it was the most populous county in the state (~25% of residents) and the New England region [39].

JHU metadata reported several modifications in historic records as of 10 November 2021 (data download date) [40]. First, JHU back-distributed probable cases previously reported on 12 June 2020 across 15 April through 11 June 2020 in accordance with revised MDPH records. Second, MDPH revised reporting methodology of cumulative cases and deaths on 19 August 2020. New guidelines transitioned from aggregating probable and confirmed cases to reporting confirmed cases only. Reporting methodology changed again on 3 September 2020 when MDPH revised definitions of probable cases to exclude antibody tests, resulting in the removal of 8051 historic reported cases statewide [40].

Similarly, JHU reported that 680 positive cases prior to 1 December 2020 were not reported by MDPH due to technical issues at laboratory testing facilities [40]. JHU redistributed historic cases, yet no metadata described how such redistribution occurred. Finally, JHU uploaded electronic records from MDPH weekly on Monday-Friday only; metadata provided no information on how weekend records were reported. While JHU reported state and county level test data nationwide from 2 March 2020 through 1 August 2021, no records were available for Middlesex County or Massachusetts [41].

We extracted MDPH cumulative reports for SARS-CoV-2 cases and deaths to validate JHU records [42,43]. MDPH reported cumulative cases starting 17 April 2020 while cumulative deaths were reported starting 1 June 2020. Neither cases nor deaths were reported from 12–18 August 2020, one week prior to changes in statewide case reporting guidelines. We extracted cases and deaths for Middlesex County, however no county-level reported tests were available [42,43]. Instead, we extracted state-level reported tests to approximate DoW effects in Middlesex County.

We estimated daily tests, cases, and deaths by subtracting cumulative counts of health outcomes from successive days. We estimated daily rates as the ratio of daily counts to annual population estimates (drawn from the 2010 US Census) and multiplied by 1,000,000. We reported tests, cases, and deaths per 1,000,000 persons ('tpm', 'cpm', and 'dpm', respectively).

2.2. Inspection of Data Reliability

We examined JHU data reliability for health outcomes using 3 metrics. First, we explored quantities and patterns of completeness, defined as the number of time points with non-missing records [44]. Completeness reflected the number of days with usable

health records in our study period. We differentiated incomplete records (i.e., blanks) from days with 0 counts and examined patterns of completeness by DoW and Gregorian calendar date.

Next, we examined data precision, defined as the plausibility of case information (e.g., negative counts). Data imprecision suggested inaccurately reported or modified records. We corrected negative counts by replacing negative values with 0 counts and subtracting 1 test, case, or death from as many days as the absolute value of negative counts.

Finally, we explored data interoperability, defined as the concordance between surveillance systems' records. As JHU extracted data directly from MDPH, we expected strong concordance between systems for cases and deaths. We identified days with concordant and discordant data to clarify discrepancies between surveillance systems.

2.3. Defining Outbreak Signatures

By defining outbreak signatures, or the profile of an epidemic curve and its features, modelers can precisely quantify and adjust for complex temporal trends [45–47]. Signatures consist of 3 features: (i) rate magnitudes, (ii) critical points (e.g., onset, peak, resolution), and (iii) critical periods (e.g., acceleration, deceleration, steady state). Critical points represent time points when rate magnitudes reach local minima and maxima. These time points define key features of an epidemic curve such as the onset, peak, or resolution of an outbreak wave. Furthermore, these points reflect transitions between waves of persistent outbreaks or primary and secondary peaks within a single outbreak wave. Critical periods, defined as the duration between consecutive critical points, reflect intervals when the pace of rates accelerate, decelerate, or remain unchanged over time. These periods represent well-defined linear and non-linear temporal trends of rates.

We estimated rate magnitudes using a version of Kolmogorov-Zurbenko (KZ) adaptive filters. This smoothing technique delineates trends in noisy time series by generating average estimates across a moving window of time points [48–51]. We used a 21-day smoother, which ensured sufficient reduction of daily noise without overly aggregating daily records (as with monthly smoothers). Furthermore, this smoother ensured low probability of erroneous critical points (more probable with 7- or 14-day smoothers) and ensured equal weighting of DoW observations compared to non-7-day smoothing windows.

We defined critical points using rate magnitudes and their trivial derivatives, calculated as the difference between rates of successive days. We identified peaks as days with maximum rate magnitudes and low or near-zero trivial derivative values. We identified onset points as days with local minimum rate magnitudes when trivial derivatives began increasing from near-zero to highly positive values, marking the beginning of an outbreak wave. We identified resolution points as days with local minimum rate magnitudes when trivial derivatives declined from highly positive to near-zero or near-minimum values, marking the conclusion of an outbreak wave.

With respect to critical periods, we defined acceleration periods from outbreak onset points to peaks when the pace of rates steadily increased. In contrast, we defined deceleration periods from outbreak peaks to resolution or next wave onset points when the pace of rates steadily decreased. We defined steady state periods as the duration between the resolution of one outbreak wave and the onset of another when rates remain near-constant and trivial derivatives were consistently near-zero values.

Outbreak waves reflected the duration from onset to resolution critical points. For many waves, no resolution occurred; the conclusion of one wave marked the onset of the next. As such, outbreak waves were also defined as the duration between 2 onset points if no resolution occurred. We identified primary and secondary outbreak peaks for specific waves when rates reached 2 local maxima after abrupt changes in the trivial derivative from systematically high negative to systematically high positive values.

2.4. Defining Intervention Stringency Phases

Stepwise implementation of statewide non-pharmaceutical interventions intended to improve SARS-CoV-2 testing and reduce disease transmission beginning 15 March 2020 [52]. These interventions included stay-at-home advisories and business closures and reopening restrictions to reduce SARS-CoV-2 transmission. Statewide policies closely aligned with county-level mask mandates, business curfews, lock-down restrictions, and school closures also intending to disrupt SARS-CoV-2 transmission (Supplementary Table S1). As case and death counts increased and declined, intervention mandates gradually became more stringent or relaxed their stringency, respectively.

Changes in statewide advisories defined 9 intervention phases beginning 22 January 2020 through 28 May 2021 (Table 1). We scored phases by the stringency of policies for restricting social mobility and reducing disease transmission. Scores of 5 represented most stringent policies (e.g., school closures, stay-at-home order) while scores of 0 represented least stringent policies (e.g., prior to and after the Massachusetts state of emergency). We examined differences in DoW effects by phase, as statewide mandates influenced reporting patterns, laboratory testing capacity, and testing preferences. We also compared the alignment of outbreak signature critical points and intervention phases to better understand delays in health policy implementation.

Table 1. Non-pharmaceutical intervention phases in accordance with Massachusetts statewide COVID-19 health advisories. We defined intervention phases according to the Massachusetts shelter in place order on 15 March 2020 and subsequent reopening of businesses and public venues thereafter [52]. We assigned a stringency score for each phase where 5 reflects the most stringent mandates to reduce social mobility and disease transmission while 0 reflects periods before and after the statewide state of emergency. We report the duration of each phase in days. Phase I duration is reported from the termination of the state of emergency to the end of our study period (7 November 2021).

Phase	Start Date	Duration (Days)	Description	Stringency
A	22 January 2020	53	Period before COVID-19 widespread in the United States	0
B	15 March 2020	64	Closures of public and private elementary and secondary schools; prohibited gatherings of more than 25 people	5
C	18 May 2020	45	Phases I and II reopening	4
D	2 July 2020	89	Phase III-Step 1 reopening	3
E	29 September 2020	70	Phase III-Step 2 reopening	2
F	8 December 2020	79	Return to Phase III-Step 1	3
G	25 February 2021	21	Reentering Phase III-Step 2 reopening	2
H	18 March 2021	71	Phase IV reopening	1
I	28 May 2021	163	Termination of State of Emergency	0

2.5. Modeling DoW Effects

We estimated average (with 95% confidence intervals) and median (with interquartile range) daily rates and product moments by DoW. We selected L-skewness and L-kurtosis given their sensitivity for distributions of low rates and smaller sample size [53]. High values of L-moments indicate a possible surge in tests, cases, or deaths and are necessary for justifying the use of negative binomial distributions when modeling count-based distributions. We estimated average rates using generalized linear models adjusted for a negative binomial distribution and log-link function to accommodate moderately skewed count-based data:

$$\ln\left[E\left(Y_j\right)\right] = \beta_1(D_t) \quad (1)$$

where $Y_{j,d}$—daily rates of j-outcome (e.g., tests, cases, deaths) for d-DoW. We estimated average and confidence interval values by exponentiating model coefficients ($\exp(\beta_0)$ and $\exp(\beta_0 \pm 1.96se)$, respectively).

Next, we compared DoW effects adjusting for linear (t) and quadratic (t^2) trends in outbreak signature critical periods. This adjustment captured general increases and decreases in rate magnitudes as well as acceleration and deceleration in the pace of rates. We used a segmented negative binomial regression model, such that:

$$\ln\left[E\left(Y_{j,t}\right)\right] = \beta_0 + \beta_1(D_t) + \sum_{k=1}^{q}\left[\beta_{2k}(t - t_k) + \beta_{2k+1}(t - t_k)^2\right] \quad (2)$$

where $Y_{j,t}$—daily rates for j-outcome on t-day; D_t—categorical variable for DoW on t-day (Reference: Sunday); and $(t - t_k)$—continuous time series variables (in days) for k-critical period of j-outcome. Here, q corresponded to the total number of critical periods for tests (10), cases (8), and deaths (8), as defined by our study period and KZ adaptive filters.

We estimated DoW effects for each intervention phase using a similar model:

$$\ln\left[E\left(Y_{j,t,p}\right)\right] = \beta_0 + \beta_1(D_{t,p}) + \sum_{k=r}^{q}\left[\beta_{2k}(t - t_k) + \beta_{2k+1}(t - t_k)^2\right] \quad (3)$$

where p—policy intervention phase ranging from A–I as reported in Table 1. Here, r corresponded to the first outbreak critical period occurring within p-intervention phase.

We compared model fit using Akaike's Information Criterion (AIC) estimates. We defined statistical significance as $\alpha < 0.05$. We performed data extraction, alignment, management, and cleaning using Excel 2016 Version 2103 and R (4.0.0) software. We conducted statistical analyses and created data visualizations using SE/16.1 and R (4.0.0) software. We share all R software codes as Supplementary Materials.

3. Results

3.1. JHU and MDPH Data Cross-Referensing

While JHU data had 100% completeness, we found several discrepancies in daily counts including 3 days with negative values in cases (3 September 2020, 2 March 2021, and 27 June 2021) and 4 days with negative values in deaths (30 June 2020, 21 July 2020, 2 September 2020, and 9 July 2021). Negative values ranged from −16 to −69 for cases and −1 to −11 for deaths. Negative values in September 2020 coincided with revisions in MDPH guidelines to exclude probable cases with positive antibody tests and were found in JHU data only. Negative values for cases and deaths in March–July of 2020 and 2021 were reported by both JHU and MDPH. We detected no negative values for state-level tests.

JHU systematically reported 0 (zero) counts for cases and deaths on federal and religious holidays. These included Thanksgiving (26 November 2020), Christmas (25 December 2020), New Year's (1 January 2021), Easter (4 April 2021), Memorial Day (31 May 2021), Independence Day (5 July 2021), Labor Day (6 September 2021), and Columbus/Indigenous People's Day (11 October 2021). Similarly, JHU systematically reported 0 counts on all weekend days beginning 3 July 2021. When compared to MDPH, we found incomplete records (blanks) on these holidays and weekends suggesting no statewide reporting. Thus, JHU reported 0 counts on these holidays and weekends as cumulative counts remained unchanged in the absence of MDPH reporting.

We assessed the interoperability between JHU and MDPH beginning 17 April 2020 for cases and 1 June 2020 for deaths. JHU case records were systematically discordant with MDPH records from 17 April 2020 through 3 September 2020. On 3 September 2020, JHU reported negative counts, which reflected the correction of cumulative counts needed to achieve the concordance of JHU records with MDPH records for the remainder of our study period. The death records for JHU and MDPH were the same for the study period.

3.2. Outbreak Signatures and Their Features

We identified 5 distinct outbreak waves for statewide reported tests with the highest peak values on 6 December 2020 (Wave 3; 3213.94 tpm) and 15 September 2021 (Wave 5; 4412.13 tpm) (Tables 2 and 3, Figure 1). Wave 3 peak timing aligned with the onset of non-pharmaceutical intervention Phase F, which returned to more stringent health mandates after an outbreak in reported cases. Tests reached a global minimum at Wave 5 onset (27 June 2021; 886.56 tpm), with rate magnitudes paralleling Wave 2 onset a year prior (4 June 2021; 1171.02 tpm). Wave 3 onset (25 September 2021) aligned closely with intervention Phase E (29 September 2020), which relaxed the stringency of health mandates most compared to prior phases (Figure 2). Wave 5 onset came ~1 month after lifting the Massachusetts State of Emergency (Phase I; 28 May 2021) and peaked on 15 September 2021.

Table 2. Dates of outbreak signature critical points for reported tests in Massachusetts and reported cases and deaths in Middlesex County, Massachusetts, USA from 2 March 2020 through 7 November 2021. We identified critical points using rate magnitudes and trivial derivatives defined using 21-day Kolmogorov-Zurbenko adaptive filter average smoothers. We extracted data from the John Hopkin's University's Center for Systems Science and Engineering (CSSE) COVID-19 data repository and Massachusetts Department of Public Health COVID-19 data dashboard. Critical points included the timing of wave onset, the peak of rate magnitudes, and when applicable, the resolution of outbreak waves.

Tests			Cases			Deaths		
Wave	**Critical Point**	**Date**	**Wave**	**Critical Point**	**Date**	**Wave**	**Critical Point**	**Date**
1	Onset	2 March 2020	1	Onset	2 March 2020	1	Onset	2 March 2020
1	Peak	8 May 2020	1	Peak	20 April 2020	1	Peak	30 April 2020
2	Onset	4 June 2020	2	Onset 1	4 July 2020	1	Resolution	8 August 2020
2	Peak	25 August 2020	2	Peak 1	2 January 2021	2	Onset	12 September 2020
3	Onset	25 September 2020	2	Onset 2	2 March 2021	2	Peak	15 January 2021
3	Peak	6 December 2020	2	Peak 2	1 April 2021	2	Resolution	7 July 2021
4	Onset	10 March 2021	3	Onset	23 June 2021	3	Onset	1 August 2021
4	Peak	4 April 2021	3	Peak	12 September 2021	3	Peak	1 October 2021
5	Onset	27 June 2021						
5	Peak	15 September 2021						

Table 3. Dates of outbreak signature critical periods for reported tests in Massachusetts and reported cases and deaths in Middlesex County, Massachusetts, USA from 2 March 2020 through 7 November 2021. We identified critical points using rate magnitudes and trivial derivatives defined using 21-day Kolmogorov-Zurbenko adaptive filter average smoothers. We extracted data from the John Hopkin's University's Center for Systems Science and Engineering (CSSE) COVID-19 data repository and Massachusetts Department of Public Health COVID-19 data dashboard. We defined critical periods, including acceleration, deceleration, and steady state, as the duration between 2 consecutive critical points. We report the start date for each period, as the end date was defined by the following start date. We list the number of periods defined for each outcome, which were used in segmented time series analyses for modeling day-of-the-week effects.

Tests			Cases			Deaths		
Period	**Period Type**	**Start Date**	**Period**	**Critical Point**	**Start Date**	**Period**	**Critical Point**	**Start Date**
1	Acceleration	2 March 2020	1	Acceleration	2 March 2020	1	Acceleration	2 March 2020
2	Deceleration	8 May 2020	2	Deceleration	20 April 2020	2	Deceleration	30 April 2020
3	Acceleration	4 June 2020	3	Acceleration	4 July 2020	3	Steady State	8 August 2020

Table 3. *Cont.*

4	Deceleration	25 August 2020	4	Deceleration	2 January 2021	4	Acceleration	12 September 2020
5	Acceleration	25 September 2020	5	Acceleration	2 March 2021	5	Deceleration	15 January 2021
6	Deceleration	6 December 2020	6	Deceleration	1 April 2021	6	Steady State	7 July 2021
7	Acceleration	10 March 2021	7	Acceleration	23 June 2021	7	Acceleration	1 August 2021
8	Deceleration	4 April 2021	8	Steady State	12 September 2021	8	Deceleration	1 October 2021
9	Acceleration	27 June 2021						
10	Deceleration	15 September 2021						

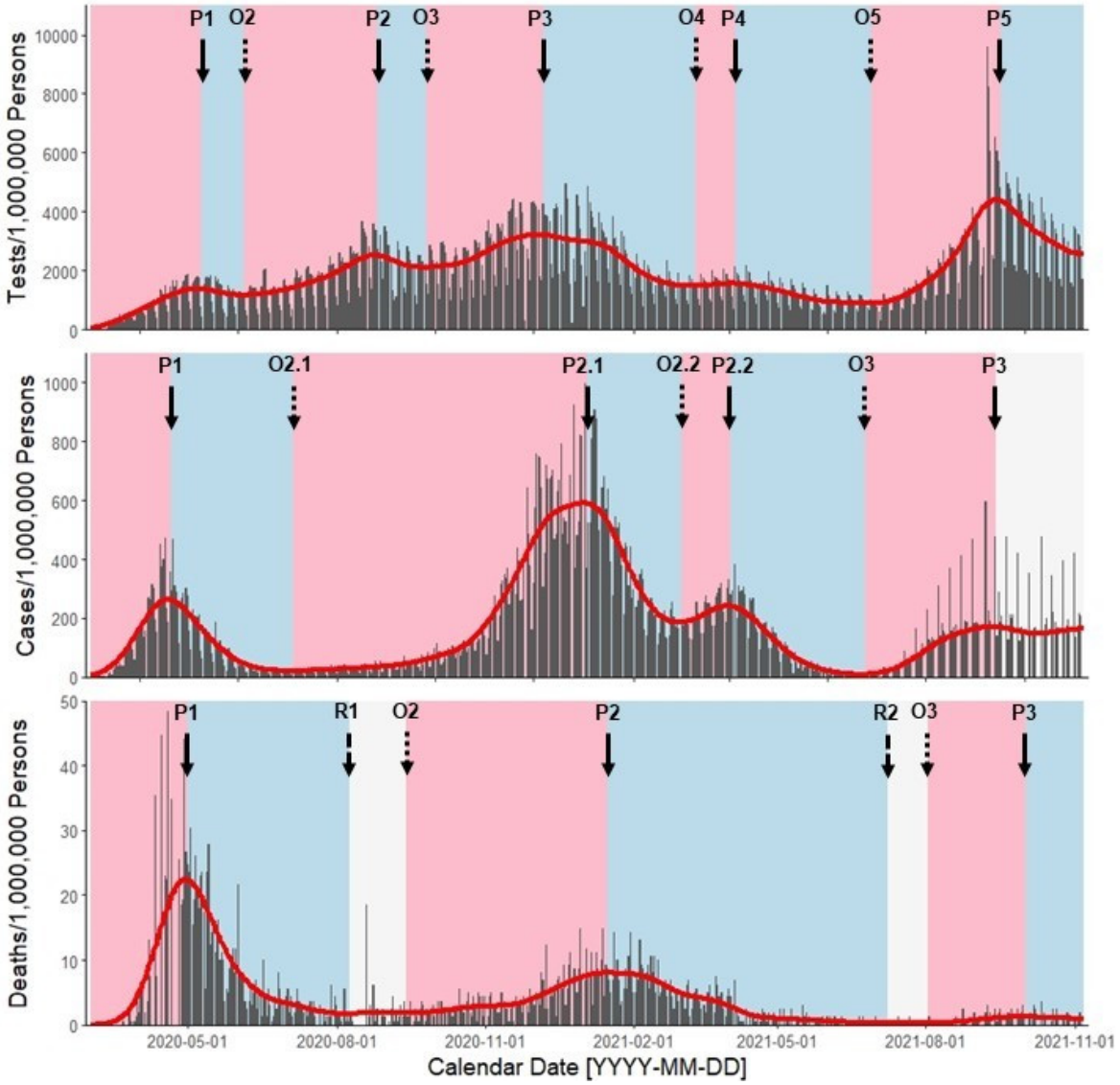


Figure 1. Multi-panel, shared-axis time series plots of MDPH-reported Massachusetts statewide tests (**top** panel) and JHU-reported Middlesex County cases and deaths (**middle** and **bottom** panels, respectively) from 2 March 2020 through 7 November 2021. Within each plot, we provide estimated rates (grey bars) from reported data and 21-day average smoothers (red lines) estimated using Kolmogorov-Zurbenko adaptive filters. Background colors depict acceleration periods (pink), deceleration periods (blue), and steady-state periods (grey) defined independently for each health outcome. We embedded text and arrows at the top of each plot to signify the onset timing (O1–O5, short dashed arrow), peak timing (P1–P5, solid arrow), and resolution timing (R1–R2, long dashed arrow) across outbreak waves. We report rates as tests, cases, and deaths per 1,000,000 persons.

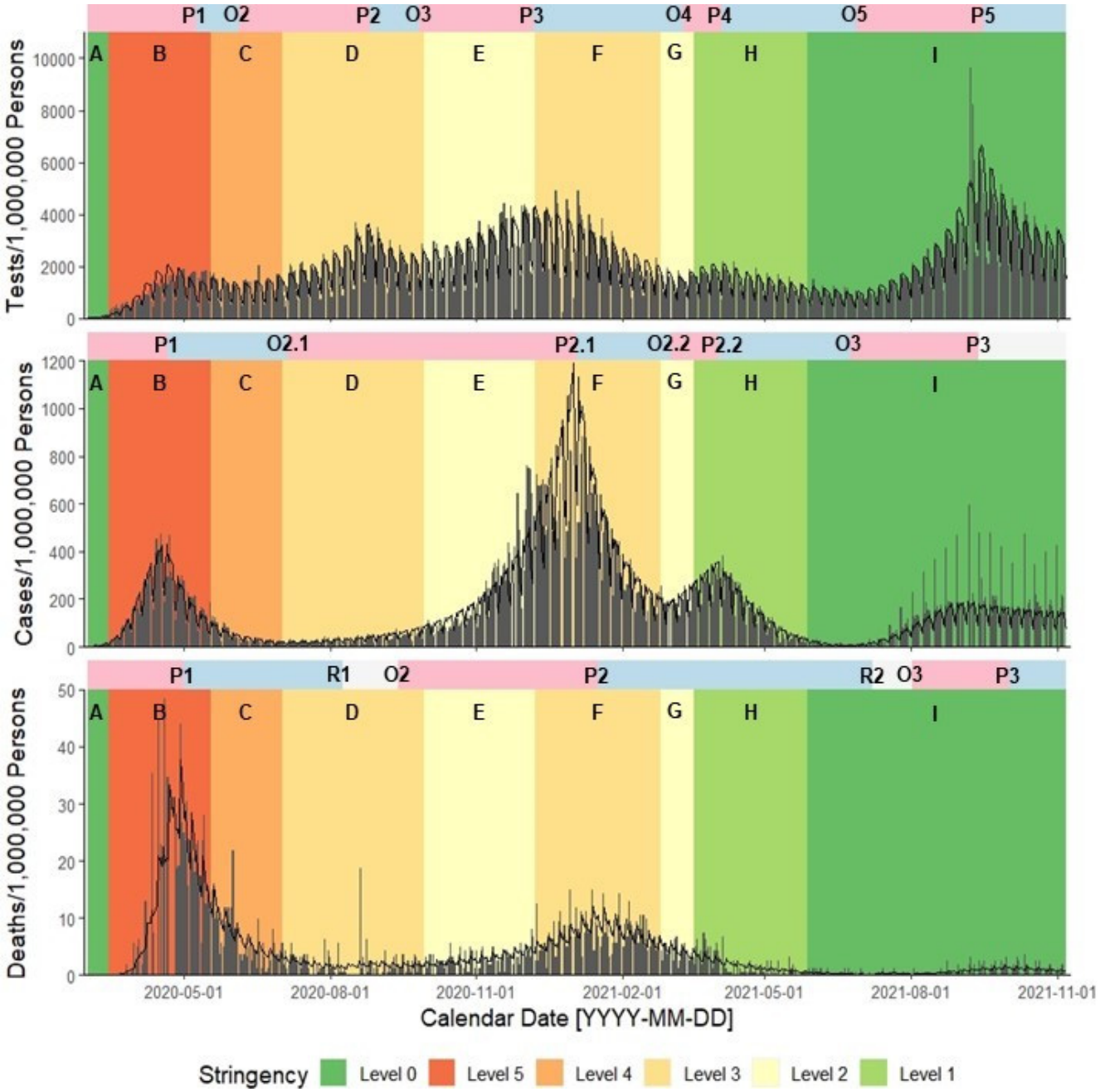


Figure 2. Multi-panel, shared-axis time series plots of MDPH-reported Massachusetts statewide tests (**top** panel) and JHU-reported Middlesex County cases and deaths (**middle** and **bottom** panels, respectively) by outbreak critical period and non-pharmaceutical intervention phase from 2 March 2020 through 7 November 2021. Within each plot, we provide estimated rates (grey bars) from reported data with fitted model results (black lines) from segmented negative binomial regression models adjusted for linear and quadratic trends for each outbreak critical period as defined by Kolmogorov-Zurbenko adaptive filters. Colored bars above each plot depict acceleration (pink), deceleration (blue), and steady-state (grey) periods as reported in Table 3 and Figure 1. We embedded text to signify the onset timing (O1–O5), peak timing (P1–P5), and resolution timing (R1–R2) of critical periods across outbreak waves. Background colors depict phases of Massachusetts non-pharmaceutical interventions from most stringent (red) to least stringent (dark green). We label each intervention phase in accordance with Table 1 (A–I). We report incidence as tests, cases, and deaths per 1,000,000 persons.

We identified a global maximum of cases for the primary peak of Wave 2 (2 January 2021; 591.37 cpm), which trailed peak tests and a return to more-stringent intervention Phase F by ~1 month. We also identified a Wave 2 secondary peak on 1 April 2020 (242.55 cpm), which trailed the relaxation to less-stringent intervention Phases G and H (25 February 2021 and 18 March 2021, respectively) by ~1 month. Rate magnitudes of the Wave 2 secondary peak paralleled Wave 1 peak (264.01 cpm). Similarly, Wave 3 onset (23 June 2021; 9.80 cpm) returned to similar magnitudes as Wave 2 onset (4 July 2020; 21.29 cpm) ~1 year later. Rates of reported cases reached steady state at ~165 cpm after peaking for Wave 3 on 12 September 2021, which aligned with the global maxima in reported tests.

Wave 1 peak had the highest reported rates of death (22.51 dpm), which were ~3-times higher than Wave 2 peak rate magnitudes (8.00 dpm). Peaks in reported deaths (30 April 2020, 15 January 2021, 1 October) trailed peaks in reported cases (20 April 2020, 2 January 2021, 12 September 2021) by ~10–20 days. Resolution critical points of similar magnitudes for reported deaths were observed in Wave 1 (8 August 2020; 1.72 dpm) and Wave 2 (7 July 2021; 0.30 dpm). Like with reported cases, these resolution critical points separated consecutive outbreak waves by ~1 year.

3.3. Day-of-the-Week Effects

The estimated median values for reported tests, cases, and deaths along with their confidence intervals and coefficients of skewness and kurtosis are shown in Table 4. As expected for each death there were about 30 cases of infections, and for each reported case there were about 10 reported tests. Median rates were high on weekdays for tests and cases yet low on weekends; we found little differences between mean or median rates of deaths across all days of the week. Relatively high values of L-skewness and L-kurtosis for daily death cases suggested the potential for high temporal variability.

Table 4. Descriptive summaries of rates for reported tests, cases, and deaths by DoW from 2 March 2020 through 7 November 2021. We extracted data on state-level tests from the Massachusetts Department of Public Health COVID-19 data dashboard and data on county-level cases and deaths from John Hopkin's University's COVID-19 data dashboard. We estimated average rates (with 95% confidence intervals) using negative binomial regression models adjusted for log-link functions. We also report median rates (with interquartile range), L-skewness values, and L-kurtosis values by DoW and health outcome.

Day-of-Week	Mean [LCI, UCI]	Median [LQR, UQR]	L-Skewness	L-Kurtosis
		Tests		
Sunday	103.28 [83.73, 127.41]	90.89 [63.90, 145.34]	0.16	0.09
Monday	239.26 [194.06, 294.98]	207.89 [146.08, 332.57]	0.14	0.11
Tuesday	248.50 [201.56, 306.37]	195.28 [149.10, 339.75]	0.23	0.17
Wednesday	233.35 [189.27, 287.71]	199.93 [142.05, 307.45]	0.19	0.17
Thursday	213.99 [173.56, 263.85]	183.75 [135.65, 281.46]	0.18	0.17
Friday	199.09 [161.46, 245.48]	179.83 [129.81, 268.36]	0.14	0.13
Saturday	129.26 [104.80, 159.42]	114.61 [78.54, 173.63]	0.13	0.09
		Cases		
Sunday	11.69 [9.40, 14.54]	3.85 [0.56, 17.25]	0.47	0.17
Monday	17.06 [13.76, 21.15]	12.69 [3.23, 28.39]	0.25	0.00
Tuesday	14.78 [11.91, 18.34]	12.25 [3.20, 19.33]	0.34	0.17
Wednesday	18.50 [14.93, 22.92]	15.20 [4.25, 24.07]	0.35	0.18
Thursday	18.58 [14.99, 23.02]	14.70 [3.66, 24.23]	0.36	0.19

Table 4. *Cont.*

Day-of-Week	Mean [LCI, UCI]	Median [LQR, UQR]	L-Skewness	L-Kurtosis
Friday	17.77 [14.34, 22.03]	13.96 [3.66, 23.92]	0.35	0.19
Saturday	15.45 [12.46, 19.17]	5.96 [1.18, 22.03]	0.49	0.21
		Deaths		
Sunday	0.40 [0.27, 0.59]	0.12 [0.00, 0.47]	0.57	0.32
Monday	0.30 [0.20, 0.47]	0.19 [0.06, 0.37]	0.44	0.26
Tuesday	0.32 [0.21, 0.49]	0.12 [0.06, 0.37]	0.53	0.32
Wednesday	0.50 [0.35, 0.72]	0.28 [0.06, 0.59]	0.50	0.32
Thursday	0.37 [0.25, 0.55]	0.25 [0.06, 0.50]	0.43	0.27
Friday	0.36 [0.24, 0.54]	0.19 [0.06, 0.43]	0.46	0.25
Saturday	0.53 [0.37, 0.75]	0.25 [0.00, 0.56]	0.64	0.47

For the entire study period, reported tests were ~2.00–2.30-times more likely to be reported on weekdays compared to Sunday (Table 5). For all weekdays, the size of this effect decreased consistently from more stringent Phase C (RR = 2.45–2.88 [2.01, 3.53]) to less stringent Phase G (RR = 1.72–2.24 [1.63, 2.35]). Effect sizes slightly increased for Tuesdays-Thursdays in Phases H–I, which aligned with the global maxima of reported tests in outbreak Wave 5. In contrast to weekdays, tests were only 1.26-times [1.17, 1.35] more likely to be reported on Saturday compared to Sunday. We found lower effect sizes for reported tests on Saturday compared to Sunday in least stringent Phases G (RR = 1.19 [1.13, 1.25]) and H (RR = 1.19 [1.12, 1.27]). In the last Phase I, there were substantial drops in testing on weekends and no significant differences in reported tests on Saturday compared to Sunday. Analyses for individual intervention phases largely support the findings observed for the entire study period (Figure 3).

Like statewide tests, county-level cases were ~1.75–2.00-times more likely to be reported on weekdays compared to Sunday; cases reported on Saturday were only 1.32-times [1.04, 1.67] higher as compared to Sunday. For all weekdays, the effect size decreased consistently from more stringent Phase B (RR = 2.06–2.25 [1.81, 2.56]) to less stringent Phase D (RR = 1.53–1.87 [1.13, 2.54]). However, DoW effects changed substantially in less stringent Phases E–H, which aligned with the overall testing and case reporting. Furthermore, cases were significantly less likely to be reported on Mondays (RR: 0.66–0.93 [0.47, 0.97]) in Phases E–G and Tuesdays (RR: 0.51–0.85 [0.44, 0.88]) in Phases F–G during the large second wave.

Overall, we found minimal or no significant differences in reported deaths between any days of the week, especially in the most stringent Phases B–C. As later intervention phases had many weeks without reported deaths, confidence intervals were exaggerated in regression analyses. The observed increase in reported deaths on Wednesdays and Thursdays (1.46-times [1.15, 1.85], $p = 0.002$) and 1.28-times ([1.00, 1.64], $p = 0.047$, respectively) were driven by spikes in deaths in individual critical periods and intervention phases.

Table 5. Rate ratios (with 95% confidence intervals) of DoW effects relative to Sunday for the full study period (Overall) and by public health policy intervention phase from 2 March 2020 through 7 November 2021. We examined DoW effects using segmented negative binomial regression models adjusted for log-link functions. We adjusted each model with linear and quadratic trends for the outbreak signature critical periods occurring within each intervention phase. We supplement model findings with Akaike's Information Criterion (AIC) values used to assess model fit. We report results beginning in Phase B, as this marks the first complete phase aligning with our study period. We exclude Phase I for cases and deaths, as no weekend reporting occurred during this phase.

Phase	Monday	Tuesday	Wednesday	Thursday	Friday	Saturday	AIC
Tests							
Overall	2.27 [2.11, 2.45] [a]	2.33 [2.16, 2.51] [a]	2.20 [2.05, 2.37] [a]	2.05 [1.90, 2.21] [a]	1.94 [1.80, 2.09] [a]	1.26 [1.17, 1.35] [a]	9188.30
B	2.26 [2.04, 2.52] [a]	2.45 [2.20, 2.72] [a]	2.50 [2.25, 2.78] [a]	2.41 [2.17, 2.68] [a]	2.59 [2.34, 2.88] [a]	1.48 [1.34, 1.65] [a]	790.47
C	2.45 [2.01, 2.98] [a]	2.73 [2.24, 3.32] [a]	2.88 [2.35, 3.53] [a]	2.72 [2.22, 3.33] [a]	2.51 [2.05, 3.08] [a]	1.33 [1.08, 1.63] [b]	627.75
D	2.56 [2.25, 2.91] [a]	2.60 [2.28, 2.96] [a]	2.45 [2.15, 2.79] [a]	2.30 [2.03, 2.62] [a]	2.16 [1.90, 2.45] [a]	1.29 [1.14, 1.47] [a]	1298.50
E	2.58 [2.12, 3.14] [a]	2.63 [2.16, 3.21] [a]	2.46 [2.02, 3.00] [a]	2.25 [1.84, 2.74] [a]	2.17 [1.79, 2.65] [a]	1.43 [1.17, 1.74] [a]	1107.60
F	2.32 [1.82, 2.97] [a]	2.23 [1.75, 2.83] [a]	2.10 [1.65, 2.66] [a]	1.79 [1.40, 2.28] [a]	1.61 [1.26, 2.06] [a]	1.35 [1.05, 1.72] [c]	1276.10
G	2.24 [2.14, 2.35] [a]	2.01 [1.92, 2.11] [a]	1.91 [1.82, 2.01] [a]	1.83 [1.74, 1.92] [a]	1.72 [1.63, 1.80] [a]	1.19 [1.13, 1.25] [a]	223.09
H	2.27 [2.14, 2.42] [a]	2.06 [1.93, 2.19] [a]	1.93 [1.82, 2.06] [a]	1.79 [1.68, 1.90] [a]	1.74 [1.63, 1.85] [a]	1.19 [1.12, 1.27] [a]	868.16
I	2.07 [1.84, 2.32] [a]	2.27 [2.02, 2.54] [a]	2.07 [1.85, 2.33] [a]	1.96 [1.75, 2.20] [a]	1.74 [1.55, 1.95] [a]	1.10 [0.98, 1.23]	2429.90
Cases							
Overall	2.00 [1.56, 2.57] [a]	1.74 [1.36, 2.22] [a]	1.94 [1.53, 2.47] [a]	1.91 [1.50, 2.43] [a]	1.98 [1.56, 2.53] [a]	1.32 [1.04, 1.67] [c]	6783.20
B	2.06 [1.81, 2.35] [a]	2.24 [1.97, 2.56] [a]	2.24 [1.97, 2.56] [a]	2.24 [1.97, 2.55] [a]	2.25 [1.97, 2.56] [a]	1.41 [1.23, 1.61] [a]	587.67
C	2.04 [1.50, 2.79] [a]	2.20 [1.62, 3.00] [a]	2.18 [1.60, 2.97] [a]	2.11 [1.54, 2.90] [a]	2.01 [1.46, 2.77] [a]	1.13 [0.81, 1.59]	343.92
D	1.53 [1.13, 2.07] [b]	1.58 [1.16, 2.16] [b]	1.87 [1.38, 2.54] [a]	1.66 [1.22, 2.26] [b]	1.84 [1.35, 2.50] [a]	1.21 [0.90, 1.64]	713.90
E	0.66 [0.47, 0.92] [c]	0.82 [0.58, 1.15]	0.99 [0.70, 1.39]	0.92 [0.65, 1.29]	1.14 [0.81, 1.60]	1.07 [0.76, 1.50]	811.69
F	0.93 [0.89, 0.97] [b]	0.85 [0.81, 0.88] [a]	1.23 [1.19, 1.28] [a]	1.32 [1.27, 1.37] [a]	1.00 [0.96, 1.04]	1.42 [1.36, 1.47] [a]	4204.20
G	0.81 [0.71, 0.92] [b]	0.51 [0.44, 0.59] [a]	1.17 [1.03, 1.33] [c]	1.11 [0.97, 1.27]	1.14 [1.02, 1.29] [c]	1.03 [0.91, 1.15]	365.18
H	0.89 [0.65, 1.22]	0.75 [0.55, 1.03]	1.37 [1.01, 1.87] [c]	1.29 [0.95, 1.75]	1.30 [0.95, 1.77]	1.37 [1.01, 1.87] [c]	766.20
Deaths							
Overall	0.98 [0.77, 1.27]	0.92 [0.72, 1.19]	1.46 [1.15, 1.85] [b]	1.28 [1.00, 1.64] [c]	1.13 [0.89, 1.45]	1.24 [0.98, 1.57]	2356.60
B	0.44 [0.14, 1.41]	0.96 [0.32, 2.96]	1.08 [0.37, 3.15]	0.76 [0.25, 2.38]	0.70 [0.24, 2.09]	1.43 [0.50, 4.06]	399.09
C	1.29 [0.74, 2.27]	0.90 [0.50, 1.63]	1.50 [0.87, 2.64]	1.18 [0.66, 2.13]	1.36 [0.77, 2.43]	1.17 [0.65, 2.12]	238.51
D	1.45 [0.67, 3.19]	0.87 [0.36, 2.08]	2.05 [0.97, 4.46]	3.02 [1.48, 6.36] [c]	1.30 [0.59, 2.90]	2.20 [1.06, 4.68] [c]	342.27
E	0.72 [0.43, 1.18]	0.39 [0.20, 0.72] [b]	1.04 [0.66, 1.66]	0.88 [0.54, 1.41]	0.99 [0.62, 1.57]	0.69 [0.41, 1.13]	264.52
F	0.69 [0.49, 0.96] [c]	0.84 [0.61, 1.14]	1.32 [1.00, 1.75] [c]	0.77 [0.56, 1.06]	0.90 [0.66, 1.23]	1.05 [0.78, 1.42]	401.37
G	0.47 [0.18, 1.08]	0.67 [0.30, 1.45]	0.81 [0.38, 1.70]	0.87 [0.42, 1.80]	0.65 [0.29, 1.39]	0.99 [0.49, 1.99]	92.87
H	2.93 [1.47, 6.37] [b]	0.81 [0.30, 2.10]	2.47 [1.20, 5.49] [c]	1.70 [0.81, 3.81]	2.06 [1.00, 4.56]	1.68 [0.78, 3.80]	216.62

Asterisks indicate statistical significance at $p < 0.001$ ([a]), $p < 0.01$ ([b]), and $p < 0.05$ ([c]).

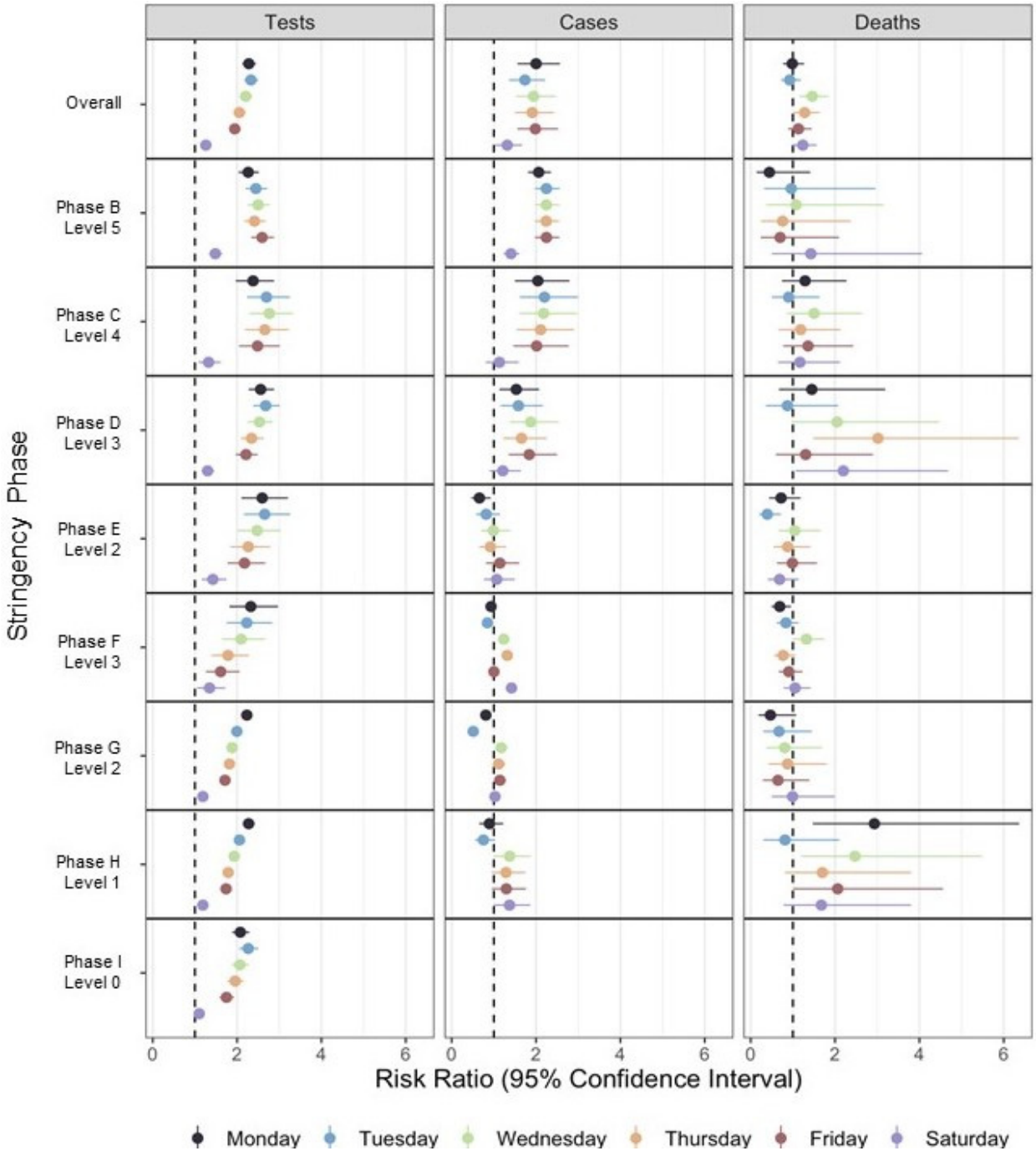


Figure 3. Shared axis, multi-panel forest plot diagrams describing day-of-the-week (DoW) effects for reported tests (**left**), cases (**middle**), and deaths (**right**) by Massachusetts non-pharmaceutical intervention phase. We report DoW effects for the entire study period (Overall, top panels) and by intervention phase from most historic (Phase B) to most recent (Phase I). We used embedded text to list the stringency level (ranging 0–5) for each policy phase. We estimated these effects using segmented negative binomial regression models adjusted for linear and quadratic trends in outbreak critical periods as defined by Kolmogorov-Zurbenko adaptive filters. We denote each day of the week from Monday to Saturday (Reference: Sunday). We report effects as risk ratio (RR) estimates (markers) and 95% confidence intervals (horizontal error bars) denoting RR = 1 with a vertical dashed line across all panels. We report results beginning in Phase B, as this marks the first complete phase aligning with our study period. We exclude Phase I for cases and deaths, as no weekend reporting occurred during this phase.

4. Discussion

The presented investigation described and compared patterns in the reporting of publicly available statewide SARS-CoV-2 tests and Middlesex County reported cases and deaths from 2 March 2020 through 7 November 2021. First, we identified distinct waves with their critical periods using a novel application of Kolmogorov-Zurbenko adaptive filters that allowed us to define, describe, and compare features of outbreak signatures. We found patterns in the timing of wave onset, peak, and resolution critical points compared to non-pharmaceutical intervention phases. Given such characterization, we identified significant DoW effects for Massachusetts statewide tests and Middlesex County cases with distinct patterns across intervention phases. We also identified and reconciled systematic reporting inconsistencies between JHU and MDPH surveillance systems, including dissimilar missing data reporting protocols and the reporting of negative counts to correct historic records. These findings provide critical insight on the systematic features in daily patterns of major pandemic outcomes, such as tests, cases, and deaths. These findings help to understand the utilization of laboratory capacity and popular preferences of testing that can assist public health agencies in effectively distributing testing resources and managing laboratory personnel. The combination of these findings indicates health professionals must place greater attention to investigating DoW effects and other reporting inconsistencies in public surveillance data.

In Massachusetts, the signature of statewide reported tests aligned closely with the transition between non-pharmaceutical intervention phases. Wave 3 onset timing (25 September 2021) aligned with the relaxation to less-stringent Phase E (29 September 2020) while Wave 3 peak timing (6 December 2020) aligned with the return to more-stringent Phase F (8 December 2020). Similarly, Wave 4 onset timing (10 March 2021) aligned closely with the relaxation to less-stringent Phase H (18 March 2021). The acceleration of reported tests after phase stringency relaxation reflects increased anxiety of disease transmission with greater social mobility or necessity for pooled testing in schools or workplaces and inpatient testing even among those without presenting symptoms [54–59].

Alternatively, increased testing may reflect premature relaxation in the stringency of non-pharmaceutical intervention phases. We found that the onset timing of reported cases in Wave 2 (4 July 2020 and 2 March 2021) aligned closely with the relaxation to intervention Phase D (2 July 2020) and Phase G (25 February 2021). We also found that the peak timing of reported deaths trailed the peak timing of reported cases by ~10–20 days. Thus, increases in social mobility and business/workplace re-openings resulted in almost immediate increases in reported cases of high morbidity/mortality [60,61].

Shared signatures of reported tests and cases also reflect potential seasonal patterns of testing behaviors. Tests peak timing in December 2020 preceded cases peak timing in January 2021 by ~1 month. Yet, both health outcomes peaked at nearly the same time in April and September 2021. These changes reflect increased testing volumes in anticipation of seasonal travel in December as well as increased cases after wintertime social mixing [62–66]. Additionally, reported tests and cases reached near-identical rate magnitudes in June/July 2020 as June/July 2021 after their wintertime peaks. These signatures resemble seasonal patterns of influenza, which are often associated with patterns of school openings and increased social mixing [20,67,68]. While research already suggests an underlying endemic seasonality of SARS-CoV-2 [69,70], no definitive seasonal pattern can be determined without further research across a longer time series length.

DoW effects in reported tests reflect a combination of laboratory testing capacity and popular testing preferences. Tests were more likely to be reported on weekdays than on Saturday or Sunday. These patterns reflect the limited testing and reporting capacity, particularly at the beginning of the COVID-19 pandemic [71,72]. Greater DoW effects across weekdays also reflects greater required or preferred testing during weekdays. Furthermore, we found changes in testing across intervention phases that likely reflect changes in health safety precautions throughout the pandemic, such as preparation for

weekend social activities and travel [73] or mandates for testing in workplaces, schools, and other transmission-prone environments [74,75].

We found similar patterns in county-level reported cases as with statewide tests. Like tests, DoW effect sizes for reported cases decreased consistently from more stringent Phase B to less stringent Phase D. Changes in weekday DoW effects for reported cases might reflect changes in hospitalization patterns, severity of infections, and potential delays due to high testing volumes earlier in the week or during wave peaks. DoW effects for tests and cases may also reflect changes in transmission and social mixing when stay-at-home policies and business and retailer closures were relaxed in 2021. Alternatively, we found no DoW effects for deaths, as the likelihood of death was equally probable on any day of the week. Yet, we found several spikes in death counts we can't explain; those spikes triggered occasional significant effects. These spikes are supported by high values of L-skewness and L-kurtosis suggesting temporal variability of deaths within our time series. Future studies must examine compound effects of additional contributors, like local air quality [76], extreme weather [77], specific calendar events (see Supplementary Table S1), an introduction of rapid over-the-counter tests [11] influencing viral transmission and thus, daily COVID-19 outcomes. Studies may also consider more exhaustive adjustment of confounding factors expected to influence case or death onset such as age, chronic health conditions, body mass index, etc.

Our findings demonstrate serious concerns over how longitudinal public health surveillance death records are curated and reported. This largely stems from discrepancies in how dates are reported, such as the date of death or the date of reporting SARS-CoV-2 as the cause of death, and potential weekly batch reporting rather than consistent reporting throughout every week [78]. These reporting patterns question the reliability and usability of SARS-CoV-2 death records for examining temporal patterns in case severity. We encourage the public health community to incorporate how test, case, and death dates are reported in standardized case definitions of infectious disease health outcomes.

One of the major advantages of publicly available SARS-CoV-2 surveillance data are their temporal and spatial granularity that allow not only a more precise estimation of outbreak signatures but also highlights the need for improved standardization of reporting protocols for publicly available infectious disease surveillance data. We found that both JHU and MDPH reports of cumulative counts produce biologically implausible negative values that aligned closely with historical record modifications in September 2020 [40]. After negative value corrections on 3 September 2020, JHU reported cases were concordant with MDPH records. While metadata report the presence of historic changes, neither database thoroughly explains techniques used to make these corrections. The appearance of negative values creates well justified distrust, which can lead data users to question the reliability and precision of highly granular public data for reuse. As inconsistencies might occur in any system, data curators and modelers should better communicate the techniques used to correct unplausible values and thus improve the reproducibility and generalizability of results. We encourage health and media agencies responsible for curating public data to report daily records in a standardized form, avoid using cumulative trend that often masks discrepancies, and provide documentation on the applied corrections of historic records.

We found systematic reporting of 0 counts for federal holidays and weekends throughout our study period. Zero counts corresponded to missing MDPH records. This demonstrates the limitations of cumulative count surveillance reporting: unchanging totals between days will mistake records with missing data as 0 counts. This discrepancy reflects a broader systematic flaw of non-standardized surveillance reporting protocols for infectious disease data repositories [79]. Replacing missing records with 0 counts underreports health outcomes and reduces the precision of near-term forecasts for early outbreak detection. Furthermore, these anomalies introduce greater noise within daily time series that can distort the detection of outbreak events. We implore the scientific community to create standardized protocols and metadata explaining when, why, and how much missing data are present within publicly available records.

Our study did not explore differences in DoW effects according to the introduction and availability of COVID-19 vaccines. We believe that this topic deserves special attention; future research should explore temporal trends and DoW effects for health outcomes including hospitalization, intensive care unit, and vaccination rates. This analysis can utilize the analytic approach demonstrated here to explore segmented temporal trends in DoW effects according to the timing of vaccination rollout by vaccine-accessible subpopulation, type of vaccine, and COVID-19 strain.

In this study we demonstrated applications of adaptive filters as a standardized data-driven approach for defining and comparing outbreak signatures. Public health professionals can apply average smoothers in real-time to monitor the spread, speed, and severity of infectious outbreaks. Rate magnitudes and their trivial derivatives can identify critical points in outbreak signatures so that health professionals might anticipate the acceleration or deceleration in rates of health outcomes. Using these findings, local, state, and national health agencies can identify geographic hotspots of infection, build laboratory testing capacity in locations with emerging outbreak threats, and improve the timeliness of mobilizing medical supplies and personnel to reduce peak rate magnitudes.

5. Conclusions

The systematic DoW effects in major outcomes of the COVID-19 pandemic at the different stages of interventions highlight important features of public health responses. The observed patterns across non-pharmaceutical intervention phases reflect the changes in testing capacities, access to healthcare, and preferences imperative for efficiently managing laboratory supplies and public health personnel. Using real-time surveillance and presented methodology, public health agencies can better anticipate testing demands as the COVID-19 pandemic persists. Furthermore, exploration of outbreak signatures can improve the timeliness of mobilizing testing resources and laboratory personnel in anticipation of increased rates of testing and infection. The study also revealed underlying discrepancies in publicly reported health data threatening to underreport SARS-CoV-2 cases and reduce the reproducibility of time series modeling analyses. Public health agencies curating publicly disseminated data must devise universal standards for reporting missing data, correcting historical records, and further improve the reporting infrastructure.

Supplementary Materials: The following supporting information can be downloaded at: https://www.mdpi.com/article/10.3390/ijerph19031321/s1, Table S1: Non-pharmaceutical intervention phases in accordance with Massachusetts state and Middlesex County, Massachusetts COVID-19 health advisories identified from numerous sources; R software script (with Excel files) used to estimate critical points and periods, conduct segmented time series analyses, and create visualizations in this manuscript.

Author Contributions: M.C.T. and J.C.M. contributed to the extraction of data from grey literature sources and editing of the manuscript. B.N.L., R.B.S. and K.H.S. contributed to the data extraction, validation, formal analysis, original draft preparation, reviewing and editing, and creation of data visualizations for the manuscript. E.N.N. contributed to methodology development, writing, reviewing, and editing the manuscript, supervision, project administration, and funding acquisition. All authors have read and agreed to the published version of the manuscript.

Funding: This research is based upon work supported in part by the Office of the Director of National Intelligence (ODNI), Intelligence Advanced Research Projects Activity (IARPA), via 2017-17072100002 (Naumova–PI). The views and conclusions contained herein are those of the authors and should not be interpreted as necessarily representing the official policies, either expressed or implied, of ODNI, IARPA, or the U.S. Government. The U.S. Government is authorized to reproduce and distribute reprints for governmental purposes notwithstanding any copyright annotation therein. The United States Department of Agriculture (USDA) National Institute of Food and Agriculture (NIFA) Cooperative State Research, Education, and Extension Service Fellowship supported Ryan B. Simpson via grant award number 2020-38420-30724. This research was also supported by the Tufts University Data Intensive Studies Center (DISC) Seed Grant. This manuscript was completed for a course enrolled in the National Science Foundation Innovations in Graduate Education Program

grant (Award #1855886) entitled SOLution-oriented, STudent-Initiated, Computationally-Enhanced (SOLSTICE) Training.

Institutional Review Board Statement: Not applicable.

Informed Consent Statement: Not applicable.

Data Availability Statement: We provide Excel files with data used to estimate critical points and periods, conduct segmented time series analyses, and create visualizations within our Supplementary Materials. Raw data is publicly accessible on state-level tests from the Massachusetts Department of Public Health COVID-19 data dashboard [42,43] and on county-level cases and deaths from John Hopkin's University's COVID-19 data dashboard [37].

Acknowledgments: Authors acknowledge the support of Abigail Larson and Clea Bell for their support in the background literature search and data analysis performed in this study.

Conflicts of Interest: The authors declare no conflict of interest.

References

1. Holtgrave, D.R.; Vermund, S.H.; Wen, L.S. Potential Benefits of Expanded COVID-19 Surveillance in the US. *JAMA* **2021**, *326*, 381–382. [CrossRef]
2. World Health Organization. Public Health Surveillance for COVID-19: Interim Guidance. 16 December 2020. Available online: https://apps.who.int/iris/bitstream/handle/10665/337897/WHO-2019-nCoV-SurveillanceGuidance-2020.8-eng.pdf (accessed on 20 December 2021).
3. Ibrahim, N.K. Epidemiologic surveillance for controlling COVID-19 pandemic: Challenges and implications. *J. Infect. Public Health* **2020**, *13*, 1630–1638. [CrossRef]
4. Bernardo, T.; Sobkowich, K.E.; Forrest, R.O.; Stewart, L.S.; D'Agostino, M.; Gutierrez, E.P.; Gillis, D. Collaborating in the time of COVID-19: The scope and scale of innovative responses to a global pandemic. *JMIR Public Health Surveill.* **2021**, *7*, e25935. [CrossRef] [PubMed]
5. United States White House. National Strategy for the COVID-19 Response and Pandemic Preparedness: January 2021. Available online: https://www.whitehouse.gov/wp-content/uploads/2021/01/National-Strategy-for-the-COVID-19-Response-and-Pandemic-Preparedness.pdf (accessed on 20 December 2021).
6. Perski, O.; Herbeć, A.; Shahab, L.; Brown, J. Influence of the SARS-CoV-2 outbreak on the uptake of a popular smoking cessation app in UK smokers: Interrupted time series analysis. *JMIR mHealth uHealth* **2020**, *8*, e19494. [CrossRef] [PubMed]
7. Karaca-Mandic, P.; Sen, S.; Georgiou, A.; Zhu, Y.; Basu, A. Association of COVID-19-related hospital use and overall COVID-19 mortality in the USA. *J. Gen. Intern. Med.* **2020**, 1–3. [CrossRef] [PubMed]
8. Slater, J.J.; Brown, P.E.; Rosenthal, J.S. Forecasting subnational COVID-19 mortality using a day-of-the-week adjusted Bayesian hierarchical model. *Stat* **2021**, *10*, e328. [CrossRef]
9. Bo, Y.; Guo, C.; Lin, C.; Zeng, Y.; Li, H.B.; Zhang, Y.; Hossain, M.S.; Chan, J.W.; Yeung, D.W.; Kwok, K.O.; et al. Effectiveness of non-pharmaceutical interventions on COVID-19 transmission in 190 countries from 23 January to 13 April 2020. *Int. J. Infect. Dis.* **2021**, *102*, 247–253. [CrossRef]
10. Nam, S. St. Lucie County Offering COVID-19 Testing Every Day of the Week. *25 WPBF News*, 24 August 2021. Available online: https://www.wpbf.com/article/st-lucie-county-covid-19-tests-vaccine-cases/37385079# (accessed on 20 December 2021).
11. Moraes, M.M.; Badea, A.; Reddy, A.; Bosch, M.; Salcedo, N.; Gomez, A.R. Validating and Modeling the Impact of High-Frequency Rapid Antigen Screening on COVID-19 Spread and Outcomes. *J. Clin. Trials* **2021**, *11*, 483.
12. Wingerter, M. State Pushes COVID Testing, but It's Hard to Find Some Parts of Colorado. *The Denver Post*, 3 September 2021. Available online: https://www.denverpost.com/2021/09/03/colorado-covid-testing-denver-rural/ (accessed on 20 December 2021).
13. Alltucker, K. The Demand for COVID-19 Testing Is Up, Stressing Labs and Delaying Results. *USA Today*, 26 November 2020. Available online: https://www.usatoday.com/story/news/health/2020/11/26/covid-19-testing-delays-record-demand-thanksgiving/6417506002/ (accessed on 20 December 2021).
14. Cunningham, K. RDU Prepares for Crowds This Week as Doctors Share Travel Concerns. *WRAL.COM*, 20 December 2021. Available online: https://www.wral.com/coronavirus/rdu-prepares-for-crowds-this-week-as-doctors-share-travel-concerns/20043724/ (accessed on 20 December 2021).
15. Moran, J. COVID-19 Testing Demand in New Hampshire Expected to Remain High after Holiday Season. *WMUR9*, 20 December 2021. Available online: https://www.wmur.com/article/new-hampshire-covid-testing-demand-12-20-2021/38573850# (accessed on 20 December 2021).
16. Buckley, M.; Schencker, L.; Petrella, D. COVID-19 Testing Demand Is Up as Holiday Looms and Illinois Sees Most Single-Day Cases Since 1 December 2020. *Chicago Tribune*, 20 December 2021. Available online: https://www.chicagotribune.com/coronavirus/ct-covid-testing-demand-20211221-oqjwdnk2n5gq3iebooqovnhc2m-story.html (accessed on 20 December 2021).

17. Keithley, J. COVID-19 Testing Demand Skyrockets Ahead of the Christmas Holiday. *WMTW8*, 20 December 2021. Available online: https://www.wmtw.com/article/covid-19-testing-demand-skyrockets-ahead-of-the-christmas-holiday/38571687 (accessed on 20 December 2021).
18. Jiang, L.; Lee, V.J.; Lim, W.Y.; Chen, M.I.; Chen, Y.; Tan, L.; Lin, R.T.; Leo, Y.S.; Barr, I.; Cook, A.R. Performance of case definitions for influenza surveillance. *Eurosurveillance* **2015**, *20*, 21145. [CrossRef]
19. De Luca, G.; Van Kerckhove, K.; Coletti, P.; Poletto, C.; Bossuyt, N.; Hens, N.; Colizza, V. The impact of regular school closure on seasonal influenza epidemics: A data-driven spatial transmission model for Belgium. *BMC Infect. Dis.* **2018**, *18*, 29.
20. Simpson, R.B.; Falconi, T.M.A.; Venkat, A.; Chui, K.H.; Navidad, J.; Naumov, Y.N.; Gorski, J.; Bhattacharyya, S.; Naumova, E.N. Incorporating calendar effects to predict influenza seasonality in Milwaukee, Wisconsin. *Epidemiol. Infect.* **2019**, *147*, e268. [CrossRef] [PubMed]
21. Sugisaki, K.; Seki, N.; Tanabe, N.; Saito, R.; Sasaki, A.; Sasaki, S.; Suzuki, H. Effective School Actions for Mitigating Seasonal Influenza Outbreaks in Niigata, Japan. *PLoS ONE* **2013**, *8*, e74716. [CrossRef] [PubMed]
22. Breitner, S.; Stölzel, M.; Cyrys, J.; Pitz, M.; Wölke, G.; Kreyling, W.; Küchenhoff, H.; Heinrich, J.; Wichmann, H.E.; Peters, A. Short-term mortality rates during a decade of improved air quality in Erfurt, Germany. *Environ. Health Perspect.* **2009**, *117*, 448–454. [CrossRef] [PubMed]
23. Morris, R.D.; Naumova, E.N.; Munasinghe, R.L. Ambient air pollution and hospitalization for congestive heart failure among elderly people in seven large US cities. *Am. J. Public Health* **1995**, *85*, 1361–1365. [CrossRef] [PubMed]
24. United States Government Accountability Office. Technology Assessment, COVID-19: Data Quality and Considerations for Modeling and Analysis. Available online: https://www.gao.gov/assets/gao-20-635sp.pdf (accessed on 20 December 2021).
25. Morgan, O.W.; Aguilera, X.; Ammon, A.; Amuasi, J.; Fall, I.S.; Frieden, T.; Heymann, D.; Ihekweazu, C.; Jeong, E.K.; Leung, G.M.; et al. Disease Surveillance for the COVID-19 era: Time for bold changes. *Lancet* **2021**, *397*, 2317–2319. [CrossRef]
26. Pearce, N.; Vandenbroucke, J.P.; VanderWeele, T.J.; Greenland, S. Accurate Statistics on COVID-19 Are Essential for Policy Guidance and Decisions. *Am. J. Public Health* **2020**, *110*, 949–951. [CrossRef]
27. Arvisais-Anhalt, S.; Lehmann, C.U.; Park, J.Y.; Araj, E.; Holcomb, M.; Jamieson, A.R.; McDonald, S.; Medford, R.J.; Perl, T.M.; Toomay, S.M.; et al. What the Coronavirus Disease 2019 (COVID-19) Pandemic Has Reinforced: The Need for Accurate Data. *Clin. Infect. Dis. Off. Publ. Infect. Dis. Soc. Am.* **2021**, *72*, 920–923. [CrossRef]
28. Yiannakoulias, N.; Slavik, C.E.; Sturrock, S.L.; Darlington, J.C. Open government data, uncertainty and coronavirus: An infodemiological case study. *Soc. Sci. Med.* **2020**, *265*, 113549. [CrossRef]
29. Cavataio, J.; Schnell, S. Interpreting SARS-CoV-2 seroprevalence, deaths, and fatality rate—Making a case for standardized reporting to improve communication. *Math. Biosci.* **2021**, *333*, 108545. [CrossRef]
30. Rosenbaum, J.E.; Stillo, M.; Graves, N.; Rivera, R. Timeliness of provisional United States mortality data releases during the COVID-19 pandemic: Delays associated with electronic death registration system and weekly mortality. *J. Public Health Policy* **2021**, *42*, 536–549. [CrossRef]
31. Galaitsi, S.E.; Cegan, J.C.; Volk, K.; Joyner, M.; Trump, B.D.; Linkov, I. The challenges of data usage for the United States' COVID-19 response. *Int. J. Inf. Manag.* **2021**, *59*, 102352. [CrossRef] [PubMed]
32. Costa-Santos, C.; Neves, A.L.; Correia, R.; Santos, P.; Monteiro-Soares, M.; Freitas, A.; Ribeiro-Vaz, I.; Henriques, T.S.; Rodrigues, P.P.; Costa-Pereira, A.; et al. COVID-19 surveillance data quality issues: A national consecutive case series. *BMJ Open* **2021**, *11*, e047623. [PubMed]
33. Clare, T.; Twohig, K.A.; O'Connell, A.M.; Dabrera, G. Timeliness and completeness of laboratory-based surveillance of COVID-19 cases in England. *Public Health* **2021**, *194*, 163–166. [CrossRef] [PubMed]
34. Dong, E.; Du, H.; Gardner, L. An interactive web-based dashboard to track COVID-19 in real time. *Lancet Infect. Dis.* **2020**, *20*, 533–534. [CrossRef]
35. Rogers, K. John Hopkins' Dashboard: The People behind the Pandemic's Most Visited Site. *CNN Health*, 11 July 2020. Available online: https://www.cnn.com/2020/07/11/health/johns-hopkins-covid-19-map-team-wellness-trnd/index.html (accessed on 20 December 2021).
36. Swenson, K. Millions Track the Pandemic on John Hopkin's Dashboard. Those Who Built It Say Some Miss the Real Story. *The Washington Post*, 29 June 2020. Available online: https://www.washingtonpost.com/local/johns-hopkins-tracker/2020/06/29/daea7eea-a03f-11ea-9590-1858a893bd59_story.html (accessed on 20 December 2021).
37. Johns Hopkins University. Time Series Summary (Csse_COVID_19_Time_Series). Available online: https://github.com/CSSEGISandData/COVID-19/tree/master/csse_covid_19_data/csse_covid_19_time_series (accessed on 9 November 2020).
38. Ziegler, B. Health Care Rankings: Measuring How Well States Are Meeting Citizens' Healthcare Needs. *U.S. News*. 2021. Available online: https://www.usnews.com/news/best-states/rankings/health-care (accessed on 9 November 2021).
39. United States Census Bureau. Middlesex County, Massachusetts. Available online: https://data.census.gov/cedsci/profile?g=0500000US25017 (accessed on 9 November 2021).
40. John Hopkins University. JHU CSSE COVID-19 Dataset. Available online: https://github.com/CSSEGISandData/COVID-19/tree/master/csse_covid_19_data (accessed on 9 November 2021).
41. John Hopkins University. U.S. Testing Data. Available online: https://github.com/govex/COVID-19/tree/master/data_tables/testing_data (accessed on 9 November 2021).

42. Massachusetts Department of Public Health. COVID-19 Response Reporting. Available online: https://www.mass.gov/info-details/covid-19-response-reporting#covid-19-interactive-data-dashboard (accessed on 9 November 2021).
43. Massachusetts Department of Public Health. Archive of COVID-19 Cases in Massachusetts. Available online: https://www.mass.gov/info-details/archive-of-covid-19-cases-in-massachusetts (accessed on 9 November 2021).
44. Simpson, R.B.; Gottlieb, J.; Zhou, B.; Hartwick, M.A.; Naumova, E.N. Completeness of open access FluNet influenza surveillance data for Pan-America in 2005–2019. *Sci. Rep.* **2021**, *11*, 795. [CrossRef] [PubMed]
45. Fefferman, N.H.; Naumova, E.N. Combinatorial decomposition of an outbreak signature. *Math. Biosci.* **2006**, *202*, 269–287. [CrossRef] [PubMed]
46. Naumova, E.N.; O'Neil, E.; MacNeill, I. INFERNO: A system for early outbreak detection and signature forecasting. *MMWR Morb. Mortal. Wkly. Rep.* **2005**, *54*, 77–83.
47. Naumova, E.N.; MacNeill, I.B. Signature-forecasting and early outbreak detection system. *Environmetrics* **2005**, *16*, 749–766. [CrossRef]
48. Tukey, J.W. *Thinking about Non-Linear Smoothers*; Report # ARO-23360.4-MA; Princeton University Department of Statistics: Princeton, NJ, USA; United States Army Research Office: Durham, NC, USA, 1986.
49. Yang, W.; Zurbenko, I. Kolmogorov–Zurbenko Filters. *Wiley Interdiscip. Rev. Comput. Stat.* **2010**, *2*, 340–351. [CrossRef]
50. Zurbenko, I.G.; Sun, M. Applying Kolmogorov-Zurbenko Adaptive R-Software. *Int. J. Probab. Stat.* **2017**, *6*, 110. [CrossRef]
51. Zurbenko, I.G.; Smith, D. Kolmogorov–Zurbenko Filters in Spatiotemporal Analysis. *Wiley Interdiscip. Rev. Comput. Stat.* **2018**, *10*, e1419. [CrossRef]
52. Massachusetts Department of Public Health. COVID-19 State of Emergency. Available online: https://www.mass.gov/info-details/covid-19-state-of-emergency (accessed on 9 November 2021).
53. Hosking, J.R. L-moments: Analysis and estimation of distributions using linear combinations of order statistics. *J. R. Stat. Soc. Ser. B. Stat. Methodol.* **1990**, *52*, 105–124. [CrossRef]
54. Massachusetts Lab to Be Among First to Use New Pooled Testing Method for COVID-19. *WCVB5*, 20 June 2020. Available online: https://www.wcvb.com/article/massachusetts-lab-to-be-among-first-to-use-new-pooled-testing-method-for-covid-19/33365999 (accessed on 19 December 2021).
55. Loncich, J. Coronavirus Concerns Growing in Massachusetts Due to Delayed Test Results. *WCVB5*, 3 August 2020. Available online: https://www.wcvb.com/article/coronavirus-concerns-growing-in-massachusetts-due-to-delayed-covid-19-test-results/33503683# (accessed on 19 December 2021).
56. Chen, A. If a Second COVID-19 Wave Is on the Horizon in Mass., Experts Say There's a Good chance We'll See it Coming. *Wbur*, 5 August 2020. Available online: https://www.wbur.org/news/2020/08/05/second-wave-covid-coming (accessed on 19 December 2021).
57. Kashinsky, L. 20 Massachusetts Cities and Towns at High Risk for Coronavirus, First Increase in Weeks. *Boston Herald*, 19 March 2021. Available online: https://www.bostonherald.com/2021/03/18/20-massachusetts-cities-and-towns-at-high-risk-for-coronavirus-first-increase-in-weeks/ (accessed on 19 December 2021).
58. Hanson, M. Pooled COVID Testing in Massachusetts Schools Showing Low Prevalence of Virus among Students, Staff. *Mass LIVE*, 17 March 2021. Available online: https://www.masslive.com/coronavirus/2021/03/pooled-covid-testing-in-massachusetts-schools-showing-low-prevalence-of-virus-among-students-staff.html (accessed on 19 December 2021).
59. Dwinell, J. Charlie Baker Urges all Massachusetts Schools to Jump into Pooled Coronavirus Testing. *Boston Herald*, 26 February 2021. Available online: https://www.bostonherald.com/2021/02/26/charlie-baker-urges-all-massachusetts-schools-to-jump-into-pooled-coronavirus-testing/ (accessed on 19 December 2021).
60. State House News Service. Mass. COVID-19 Case Counts on the Rise Again. *Wbur*, 27 July 2020. Available online: https://www.wbur.org/news/2020/07/27/massachusetts-coronavirus-cases-positives-up (accessed on 19 December 2021).
61. Young, C.A. Baker Expands Hot Spot Testing to 8 More Mass. Communities. *Wbur*, 27 July 2020. Available online: https://www.wbur.org/news/2020/07/27/massachusetts-charlie-baker-testing-expanded-covid-19-coronavirus (accessed on 19 December 2021).
62. Congi, S. Massachusetts Experiencing Rush on COVID-19 Testing before Holidays. *WCVB5*, 22 December 2020. Available online: https://www.wcvb.com/article/massachusetts-experiencing-rush-on-covid-19-coronavirus-testing-before-holidays/35049752 (accessed on 19 December 2021).
63. Rosenfield, M. Long Lines Keep People Waiting for Pre-Christmas COVID Testing. *10 Boston*, 23 December 2020. Available online: https://www.nbcboston.com/news/coronavirus/long-lines-keep-people-waiting-for-pre-christmas-covid-testing/2264398/ (accessed on 19 December 2021).
64. Klein, A.; Pescaro, M. 190 Mass. Communities, Including Boston, Are at High Risk for COVID-19 Transmission. *10 Boston*, 31 December 2020. Available online: https://www.nbcboston.com/news/coronavirus/190-mass-communities-including-boston-are-at-high-risk-for-covid-19-transmission/2269622/ (accessed on 19 December 2021).
65. 4358 New COVID-19 Cases, 60 Additional Deaths Reported in Massachusetts. *WCVB5*, 4 January 2021. Available online: https://www.wcvb.com/article/massachusetts-covid-19-cornonavirus-numbers-daily-update-january-4-2021/35121269 (accessed on 19 December 2021).

66. Enos, C. Dozens of COVID-19 Cases Linked to Christmas Eve Gatherings at Woburn Church. *Boston Globe*, 2 January 2021. Available online: https://www.bostonglobe.com/2021/01/02/metro/dozens-covid-19-cases-linked-christmas-eve-gatherings-woburn-church/ (accessed on 19 December 2021).
67. Shi, P.; Keskinocak, P.; Swann, J.L.; Lee, B.Y. The impact of mass gatherings and holiday traveling on the course of an influenza pandemic: A computational model. *BMC Public Health* **2010**, *10*, 778. [CrossRef] [PubMed]
68. Ewing, A.; Lee, E.C.; Viboud, C.; Bansal, S. Contact, travel, and transmission: The impact of winter holidays on influenza dynamics in the United States. *J. Infect. Dis.* **2017**, *215*, 732–739. [CrossRef] [PubMed]
69. Liu, X.; Huang, J.; Li, C.; Zhao, Y.; Wang, D.; Huang, Z.; Yang, K. The role of seasonality in the spread of COVID-19 pandemic. *Environ. Res.* **2021**, *195*, 110874. [CrossRef] [PubMed]
70. Audi, A.; AlIbrahim, M.; Kaddoura, M.; Hijazi, G.; Yassine, H.M.; Zaraket, H. Seasonality of respiratory viral infections: Will COVID-19 follow suit? *Front. Public Health* **2020**, *8*, 576. [CrossRef] [PubMed]
71. De Simoni, G. Drive-through COVID-19 Testing Site to Open in Medford. *10 Boston*, 30 March 2020. Available online: https://www.nbcboston.com/news/coronavirus/drive-thru-covid-19-testing-site-to-open-in-medford-mass/2099463/ (accessed on 19 December 2021).
72. Lee, T.B. America's COVID-19 Testing Has Stalled, and That's a Big Problem. *Ars Technica*, 2 April 2020. Available online: https://arstechnica.com/tech-policy/2020/04/americas-covid-19-testing-has-stalled-and-thats-a-big-problem/ (accessed on 19 December 2021).
73. Becker, K.M. Baker Closes Mass. Schools, Bans Mid-Size Gatherings, Eating at Restaurants over Coronavirus. *10 Boston*, 16 March 2020. Available online: https://www.nbcboston.com/news/local/26-new-coronavirus-cases-in-massachusetts-164-total/2091478/ (accessed on 19 December 2021).
74. More than 900 Massachusetts Schools Participating in COVID-19 Pool Testing. *WCVB5*, 26 February 2021. Available online: https://www.wcvb.com/article/covid-19-pool-testing-underway-at-massachusetts-schools-1614337230/35642430 (accessed on 19 December 2021).
75. Krantz, L. Surveillance Pool Testing for COVID-19 Offers New Way to Catch Outbreaks Quickly. *Boston Globe*, 22 January 2021. Available online: https://www.bostonglobe.com/2021/01/22/nation/strength-numbers-future-covid-19-testing-may-depend-it/ (accessed on 19 December 2021).
76. Simon, M.C.; Patton, A.P.; Naumova, E.N.; Levy, J.I.; Kumar, P.; Brugge, D.; Durant, J.L. Combining measurements from mobile monitoring and a reference site to develop models of ambient ultrafine particle number concentration at residences. *Environ. Sci. Technol.* **2018**, *52*, 6985–6995. [CrossRef]
77. Liss, A.; Wu, R.; Chui, K.K.H.; Naumova, E.N. Heat-related hospitalizations in older adults: An amplified effect of the first seasonal heatwave. *Sci. Rep.* **2017**, *7*, 39581. [CrossRef]
78. Hoffman, H. How Day-of-the-Week Effects Impact COVID-19 Data. *The Atlantic*, 22 February 2021. Available online: https://covidtracking.com/analysis-updates/how-day-of-week-effects-impact-covid-19-data (accessed on 19 December 2021).
79. Aliabadi, A.; Sheikhtaheri, A.; Ansari, H. Electronic health record–based disease surveillance systems: A systematic literature review on challenges and solutions. *J. Am. Med. Inform. Assoc.* **2020**, *27*, 1977–1986. [CrossRef]